VOLUME 27 / NUMBER 9
MAY 8, 1989
ACC. NOS. N89-16718 TO N89-17563

STAR
AN ABSTRACT JOURNAL

Scientific and Technical Aerospace Reports

PRODUCED BY THE
SCIENTIFIC AND TECHNICAL
INFORMATION
DIVISION

NASA

NATIONAL AERONAUTICS AND SPACE ADMINISTRATION

WHAT YOU CAN DO FOR *STAR*

All users of this abstract service are urged to forward reports to be considered for announcement in *STAR*. This will aid NASA in its efforts to provide the fullest possible coverage of all scientific and technical publications that might support aeronautics and space research and development. If you have prepared relevant reports (other than those that you will transmit to NASA, DoD, or DOE through the usual contract- or grant-reporting channels), please send them for consideration to the NASA Scientific and Technical Information Facility, P.O. Box 8757, BWI Airport, Maryland 21240.

Reprints of journal articles, book chapters, and conference papers are also welcome. These will be considered for announcement in *STAR's* companion journal, *International Aerospace Abstracts*.

You may specify a particular source to be included in a report announcement if you wish; otherwise the report will be placed on public sale at the National Technical Information Service. Copyrighted publications will be announced but not distributed or sold.

PURCHASE OF *STAR*

The semimonthly issues are available to registered users on annual subscription for $99.00 from the NASA Scientific and Technical Information Facility, ATTN: Registration Services, P.O. Box 8757, BWI Airport, MD 21240. *STAR* is publically available on annual subscription for $99.00 from the Superintendent of Documents, U.S. Government Printing Office, Washington, DC 20402.

PUBLISHED BY:

UNITED STATES GOVERNMENT
NATIONAL AERONAUTICS AND SPACE ADMINISTRATION
SCIENTIFIC AND TECHNICAL INFORMATION DIVISION
Scientific and Technical Aerospace Reports, Volume 27, is prepared by the NASA Scientific and Technical Information Facility operated for the National Aeronautics and Space Administration by RMS Associates.

The Administrator of the National Aeronautics and Space Administration has determined that the publication of this periodical is necessary in the transaction of the public business required by law of this Agency. Use of funds for printing this periodical has been approved by the Director of the Office of Management and Budget through March 22, 1990.

US ISSN 0036-8741

INTRODUCTION

Scientific and Technical Aerospace Reports (STAR) is a major component of a comprehensive National Aeronautics and Space Administration information system covering aeronautics, space, and supporting disciplines. *STAR* is issued on the 8th and 23rd of each month and announces current publications of the following types:

- NASA, NASA contractor, and NASA grantee reports
- Reports issued by other U.S. Government Agencies, domestic and foreign institutions, universities, and private firms
- Translations in report form
- NASA-owned patents and patent applications
- Other U.S. Government Agency and foreign patents and patent applications
- Domestic and foreign dissertations and theses

Journal, book, and conference literature, cover-to-cover journal translations, and certain foreign dissertations are announced in a companion journal, *International Aerospace Abstracts (IAA),* available on subscription from the American Institute of Aeronautics and Astronautics, Technical Information Service, 555 West 57th Street, 12th Floor, New York, New York 10019.

SUBJECT SCOPE

Subject scope of *STAR,* and *IAA* includes all aspects of aeronautics and space research and development, supporting basic and applied research, and applications. Aerospace aspects of earth resources, energy development, conservation, oceanography, environmental protection, urban transportation, and other topics of high national priority are also covered.

OTHER NASA PUBLICATIONS

Other NASA publications and information services are described in the publication, *The NASA Scientific and Technical Information System ... and How to Use It,* available without charge from the NASA Scientific and Technical Information Facility, P.O. Box 8757, BWI Airport, Maryland 21240.

HOW TO USE *STAR* SUBJECT CATEGORIES

STAR is categorized by 10 major subject divisions divided into 76 specific subject categories and one general category/division. The major subject divisions are listed in the Table of Contents, together with a note for each that defines its scope and provides any cross-references. For example:

AERONAUTICS

Includes aeronautics (general); aerodynamics; air transportation and safety; aircraft communications and navigation; aircraft design, testing and performance; aircraft instrumentation; aircraft propulsion and power; aircraft stability and control; and research and support facilities (air).

For related information see also *Astronautics.*

Each major division is further divided into as many as nine specific categories, which are identified by category numbers.

Abstracts in *STAR* are grouped by specific category, the categories appearing in sequential order. Category breaks in the abstract section are identified by the category number and title, and a scope note. Cross-references to other categories are provided as appropriate. For example:

02 AERODYNAMICS

Includes aerodynamics of bodies, combinations, wings, rotors, and control surfaces; and internal flow in ducts and turbomachinery.

For related information see also *34 Fluid Mechanics and Heat Transfer.*

CROSS-REFERENCES

Individual *STAR* abstracts are not ordinarily cross-referenced, except for certain conference reports or book translations that have had separate abstracts written for their component papers or chapters. Citations and abstracts of the components follow immediately after those of the parent document. When the subject content of a component differs sufficiently from the general content of the parent, a cross-reference citation also is printed at the end of the category to which it normally would have been assigned if it were independent.

DOCUMENTS ON MICROFICHE

Documents on microfiche(1) are designated by a pound sign (#) following the accession number. The pound sign is used without regard to the source or quality of the microfiche.

AVAILABILITIES

One or more sources from which a document announced in *STAR* is available to the public is given in each citation. The most commonly indicated sources and their acronyms or abbreviations are listed below. If the publication is available from a source other than those listed, the publisher and his address will be displayed on the availability line or in combination with the corporate source line.

Avail: NTIS. Sold by the National Technical Information Service. Prices for hard copy (HC) and microfiche (MF) are indicated by a price code following the letters HC or MF in the *STAR* citation. Current values for the price codes are given in the tables on page vii.

Initially distributed microfiche under the NTIS SRIM (Selected Research in Microfiche) is available at greatly reduced unit prices. For this service and for information concerning subscription to NASA printed reports, consult the NTIS Subscription Section, Springfield, Va. 22161.

NOTE ON ORDERING DOCUMENTS: When ordering NASA publications (those followed by the * symbol), use the N accession number. NASA patent applications (only the specifications are offered) should be ordered by the US-Patent-Appl-SN number. Non-NASA publications (no asterisk) should be ordered by the AD, PB, or other *report number* shown on the last line of the citation, not by the N accession number. It is also advisable to cite the title and other bibliographic identification.

Avail: SOD (or GPO). Sold by the Superintendent of Documents, U.S. Government Printing Office, in hard copy. The current price and order number are given following the availability line. (NTIS will fill microfiche requests, as indicated above, for those documents identified by a # symbol.)

(1) A microfiche is a transparent sheet of film, 105 by 148 mm in size, containing as many as 60 to 98 pages of information reduced to micro images (not to exceed 26:1 reduction).

Avail: BLL (formerly NLL): British Library Lending Division, Boston Spa, Wetherby, Yorkshire, England. Photocopies available from this organization at the price shown. (If none is given, inquiry should be addressed to the BLL.)

Avail: DOE Depository Libraries. Organizations in U.S. cities and abroad that maintain collections of Department of Energy reports, usually in microfiche form, are listed in *Energy Research Abstracts*. Services available from the DOE and its depositories are described in a booklet, *DOE Technical Information Center - Its Functions and Services* (TID-4660), which may be obtained without charge from the DOE Technical Information Center.

Avail: ESDU. Pricing information on specific data, computer programs, and details on ESDU topic categories can be obtained from ESDU International Ltd. Requesters in North America should use the Virginia address while all other requesters should use the London address, both of which are on page vi.

Avail: Fachinformationszentrum, Karlsruhe. Sold by the Fachinformationszentrum Energie, Physik, Mathematik GMBH, Eggenstein Leopoldshafen, Federal Republic of Germany, at the price shown in deutschmarks (DM).

Avail: HMSO. Publications of Her Majesty's Stationery Office are sold in the U.S. by Pendragon House, Inc. (PHI), Redwood City, California. The U.S. price (including a service and mailing charge) is given, or a conversion table may be obtained from PHI.

Avail: NASA Public Document Rooms. Documents so indicated may be examined at or purchased from the National Aeronautics and Space Administration, Public Documents Room (Room 126), 600 Independence Ave., S.W., Washington, D.C. 20546, or public document rooms located at each of the NASA research centers, the NASA Space Technology Laboratories, and the NASA Pasadena Office at the Jet Propulsion Laboratory.

Avail: Univ. Microfilms. Documents so indicated are dissertations selected from *Dissertation Abstracts* and are sold by University Microfilms as xerographic copy (HC) and microfilm. All requests should cite the author and the Order Number as they appear in the citation.

Avail: US Patent and Trademark Office. Sold by Commissioner of Patents and Trademarks, U.S. Patent and Trademark Office, at the standard price of $1.50 each, postage free. (See discussion of NASA patents and patent applications below.)

Avail: (US Sales Only). These foreign documents are available to users within the United States from the National Technical Information Service (NTIS). They are available to users outside the United States through the International Nuclear Information Service (INIS) representative in their country, or by applying directly to the issuing organization.

Avail: USGS. Originals of many reports from the U.S. Geological Survey, which may contain color illustrations, or otherwise may not have the quality of illustrations preserved in the microfiche or facsimile reproduction, may be examined by the public at the libraries of the USGS field offices whose addresses are listed in this Introduction. The libraries may be queried concerning the availability of specific documents and the possible utilization of local copying services, such as color reproduction.

Avail: Issuing Activity, or Corporate Author, or no indication of availability. Inquiries as to the availability of these documents should be addressed to the organization shown in the citation as the corporate author of the document.

NASA PATENTS AND PATENT APPLICATIONS

Patents and patent applications owned by NASA are announced in *STAR* under appropriate subject categories and are referenced in the *STAR* indexes. In the Report/Accession Number Index, patents are indexed by the NASA Case Number (which appears in lieu of the report number in other indexes), the U.S. Patent Number, the U.S. Patent Application Serial Number, and the U.S. Patent Class. Patent applications for which patents have not yet been issued are indexed by the NASA Case Number and the U.S. Patent Application Serial Number.

NASA *patent application specifications* are sold in paper copy by the National Technical Information Service at price code A02. Microfiche are sold at price code A01. The US-Patent-Appl-SN- number should be used in ordering either paper copy or microfiche from NTIS. Printed copies of *patents* (which are not microfiched) are available for purchase at $1.50 per copy from:

Commissioner of Patents and Trademarks
U.S. Patent and Trademark Office
Washington, D.C. 20231

When ordering patents, the U.S. Patent Number should be used, and payment must be remitted in advance, preferably by money order or check payable to the Commissioner of Patents and Trademarks. Prepaid purchase coupons for ordering are also available from the Patent and Trademark Office. The patents and patent applications announced in *STAR* are owned by NASA and are available for royalty-free licensing. Requests for licensing terms and further information should be addressed to:

Associate General Counsel for Intellectual Property/Code GP
National Aeronautics and Space Administration
Washington, D.C. 20546

ELIGIBILITY AND REGISTRATION FOR NASA INFORMATION PRODUCTS AND SERVICES

A variety of services is available to organizations of the following types that have registered with NASA to receive specific services or products:

1. NASA offices, research centers, contractors, subcontractors, grantees, and consultants;
2. Other U.S. Government agencies and their contractors;
3. Libraries in the United States that have arrangements with NASA to maintain collections of NASA documents for public reference;
4. Other organizations in the United States having a need for NASA documents in work related to aeronautics and space research;
5. Organizations abroad that have established reciprocal document exchange arrangements with NASA.

Only the central service points or central points of document acquisition and control within qualified organizations are eligible to register for NASA products and services. Domestic organizations that may be eligible to receive various classes of NASA publications and services should address their requests for registration or for further information to:

NASA Scientific and Technical Information Facility
ATTN: Registration Services
Post Office Box 8757
BWI Airport, Maryland 21240

Organizations abroad should direct requests to Manager, International STI Activities, NTT, NASA Headquarters, Washington, D.C. 20546.

AVAILABILITY OF *STAR* ABSTRACTS ON MICROFICHE

Microfiche of the abstract sections of this issue and other issues of *STAR* are available on annual subscription from NTIS as PB89-911300, Attn: Subscriptions, 5285 Port Royal Road, Springfield, Virginia 22161. Annual subscription rates are $70.00 North America; $140.00 foreign. Abstract sections for previous years retroactive to 1964 are available at the current rates. Microfiche for individual *STAR* issue abstract sections are not available.

PUBLIC COLLECTIONS OF NASA DOCUMENTS

DOMESTIC: NASA and NASA-sponsored documents and a large number of aerospace publications are available to the public for reference purposes at the library maintained by the American Institute of Aeronautics and Astronautics, Technical Information Service, 555 West 57th Street, 12th Floor, New York, New York 10019

EUROPEAN: An extensive collection of NASA and NASA-sponsored publications is maintained by the British Library Lending Division, Boston Spa, Wetherby, Yorkshire, England for public access. The British Library Lending Division also has available many of the non-NASA publications cited in *STAR*. European requesters may purchase facsimile copy or microfiche of NASA and NASA-sponsored documents, those identified by both the symbols # and • from ESA - Information Retrieval Service European Space Agency, 8-10 rue Mario-Nikis, 75738 Paris CEDEX 15, France.

FEDERAL DEPOSITORY LIBRARY PROGRAM

In order to provide the general public with greater access to U.S. Government publications, Congress established the Federal Depository Library Program under the Government Printing Office (GPO), with 50 regional depositories responsible for permanent retention of material, inter-library loan, and reference services. At least one copy of nearly every NASA and NASA-sponsored publication, either in printed or microfiche format, is received and retained by the 50 regional depositories. A list of the regional GPO libraries, arranged alphabetically by state, appears on the inside back cover. These libraries are *not* sales outlets. A local library can contact a Regional Depository to help locate specific reports, or direct contact may be made by an individual.

ADDRESSES OF ORGANIZATIONS

American Institute of Aeronautics and Astronautics
Technical Information Service
555 West 57th Street, 12th Floor
New York, New York 10019

British Library Lending Division,
Boston Spa, Wetherby, Yorkshire,
England

Commissioner of Patents and Trademarks
U.S. Patent and Trademark Office
Washington, D.C. 20231

Department of Energy
Technical Information Center
P.O. Box 62
Oak Ridge, Tennessee 37830

ESA-Information Retrieval Service
ESRIN
Via Galileo Galilei
00044 Frascati (Rome) Italy

ESDU International
P.O. Box 1633
Manassas, Virginia 22110

ESDU International, Ltd.
251-259 Regent Street
London, W1R 7AD, England

Fachinformationszentrum Energie, Physik, Mathematik GMBH
7514 Eggenstein Leopoldshafen
Federal Republic of Germany

Her Majesty's Stationery Office
P.O. Box 569, S.E. 1
London, England

NASA Scientific and Technical Information Facility
P.O. Box 8757
B.W.I. Airport, Maryland 21240

National Aeronautics and Space Administration
Scientific and Technical Information Division (NTT)
Washington, D.C. 20546

National Technical Information Service
5285 Port Royal Road
Springfield, Virginia 22161

Pendragon House, Inc.
899 Broadway Avenue
Redwood City, California 94063

Superintendent of Documents
U.S. Government Printing Office
Washington, D.C. 20402

University Microfilms
A Xerox Company
300 North Zeeb Road
Ann Arbor, Michigan 48106

University Microfilms, Ltd.
Tylers Green
London, England

U.S. Geological Survey Library
National Center - MS 950
12201 Sunrise Valley Drive
Reston, Virginia 22092

U.S. Geological Survey Library
2255 North Gemini Drive
Flagstaff, Arizona 86001

U.S. Geological Survey
345 Middlefield Road
Menlo Park, California 94025

U.S. Geological Survey Library
Box 25046
Denver Federal Center, MS914
Denver, Colorado 80225

NTIS PRICE SCHEDULES

(Effective January 1, 1989)

Schedule A
STANDARD PRICE DOCUMENTS AND MICROFICHE

PRICE CODE	NORTH AMERICAN PRICE	FOREIGN PRICE
A01	$ 6.95	$13.90
A02	10.95	21.90
A03	13.95	27.90
A04-A05	15.95	31.90
A06-A09	21.95	43.90
A10-A13	28.95	57.90
A14-A17	36.95	73.90
A18-A21	42.95	85.90
A22-A25	49.95	99.90
A99	*	*
NO1	55.00	70.00
NO2	55.00	80.00

Schedule E
EXCEPTION PRICE DOCUMENTS AND MICROFICHE

PRICE CODE	NORTH AMERICAN PRICE	FOREIGN PRICE
E01	$ 9.00	18.00
E02	11.50	23.00
E03	13.00	26.00
E04	15.50	31.00
E05	17.50	35.00
E06	20.50	41.00
E07	23.00	46.00
E08	25.50	51.00
E09	28.00	56.00
E10	31.00	62.00
E11	33.50	67.00
E12	36.50	73.00
E13	39.00	78.00
E14	42.50	85.00
E15	46.00	92.00
E16	50.50	101.00
E17	54.50	109.00
E18	59.00	118.00
E19	65.50	131.00
E20	76.00	152.00
E99	*	*

*Contact NTIS for price quote.

IMPORTANT NOTICE

NTIS Shipping and Handling Charges

U.S., Canada, Mexico — ADD $3.00 per TOTAL ORDER

All Other Countries — ADD $4.00 per TOTAL ORDER

Exceptions — Does NOT apply to:

ORDERS REQUESTING NTIS RUSH HANDLING

ORDERS FOR SUBSCRIPTION OR STANDING ORDER PRODUCTS *ONLY*

NOTE: Each additional delivery address on an order requires a separate shipping and handling charge.

VOLUME 27 NUMBER 9 / MAY 8, 1989

TABLE OF CONTENTS

AERONAUTICS

Includes aeronautics (general); aerodynamics; air transportation and safety; aircraft communications and navigation; aircraft design, testing and performance; aircraft instrumentation; aircraft propulsion and power; aircraft stability and control; and research and support facilities (air).

For related information see also *Astronautics.*

01 AERONAUTICS (GENERAL) 1171

02 AERODYNAMICS 1171

Includes aerodynamics of bodies, combinations, wings, rotors, and control surfaces; and internal flow in ducts and turbomachinery.

For related information see also *34 Fluid Mechanics and Heat Transfer*

03 AIR TRANSPORTATION AND SAFETY 1178

Includes passenger and cargo air transport operations; and aircraft accidents.

For related information see also *16 Space Transportation* and *85 Urban Technology and Transportation.*

04 AIRCRAFT COMMUNICATIONS AND NAVIGATION 1179

Includes digital and voice communication with aircraft; air navigation systems (satellite and ground based); and air traffic control.

For related information see also *17 Space Communications, Spacecraft Communications, Command and Tracking* and *32 Communications and Radar.*

05 AIRCRAFT DESIGN, TESTING AND PERFORMANCE 1180

Includes aircraft simulation technology.

For related information see also *18 Spacecraft Design, Testing and Performance* and *39 Structural Mechanics.* For land transportation vehicles see *85 Urban Technology and Transportation.*

06 AIRCRAFT INSTRUMENTATION 1181

Includes cockpit and cabin display devices; and flight instruments.

For related information see also *19 Spacecraft Instrumentation* and *35 Instrumentation and Photography.*

07 AIRCRAFT PROPULSION AND POWER 1188

Includes prime propulsion systems and systems components, e.g., gas turbine engines and compressors; and onboard auxiliary power plants for aircraft.

For related information see also *20 Spacecraft Propulsion and Power, 28 Propellants and Fuels,* and *44 Energy Production and Conversion.*

08 AIRCRAFT STABILITY AND CONTROL 1193

Includes aircraft handling qualities; piloting; flight controls; and autopilots.

For related information see also *05 Aircraft Design, Testing and Performance.*

09 RESEARCH AND SUPPORT FACILITIES (AIR) 1193

Includes airports, hangars and runways; aircraft repair and overhaul facilities; wind tunnels; shock tubes; and aircraft engine test stands.

For related information see also *14 Ground Support Systems and Facilities (Space).*

ASTRONAUTICS

Includes astronautics (general); astrodynamics; ground support systems and facilities (space); launch vehicles and space vehicles; space transportation; space communications, spacecraft communications, command and tracking; spacecraft design, testing and performance; spacecraft instrumentation; and spacecraft propulsion and power.

For related information see also *Aeronautics*

12 ASTRONAUTICS (GENERAL) 1199

For extraterrestrial exploration see *91 Lunar and Planetary Exploration.*

13 ASTRODYNAMICS 1200

Includes powered and free-flight trajectories; and orbital and launching dynamics.

14 GROUND SUPPORT SYSTEMS AND FACILITIES (SPACE) 1200

Includes launch complexes, research and production facilities; ground support equipment, e.g., mobile transporters; and simulators.

For related information see also *09 Research and Support Facilities (Air).*

15 LAUNCH VEHICLES AND SPACE VEHICLES 1201

Includes boosters; operating problems of launch/space vehicle systems; and reusable vehicles.

For related information see also *20 Spacecraft Propulsion and Power.*

16 SPACE TRANSPORTATION 1201

Includes passenger and cargo space transportation, e.g., shuttle operations; and space rescue techniques.

For related information see also *03 Air Transportation and Safety* and *18 Spacecraft Design, Testing and Performance.* For space suits see *54 Man/System Technology and Life Support.*

17 SPACE COMMUNICATIONS, SPACECRAFT COMMUNICATIONS, COMMAND AND TRACKING 1201

Includes telemetry; space communications networks; astronavigation and guidance; and radio blackout.

For related information see also *04 Aircraft Communications and Navigation* and *32 Communications and Radar.*

18 SPACECRAFT DESIGN, TESTING AND PERFORMANCE 1202

Includes satellites; space platforms; space stations; spacecraft systems and components such as thermal and environmental controls; and attitude controls.

For life support systems see *54 Man/System Technology and Life Support.* For related information see also *05 Aircraft Design, Testing and Performance, 39 Structural Mechanics,* and *16 Space Transportation.*

19 SPACECRAFT INSTRUMENTATION N.A.

For related information see also *06 Aircraft Instrumentation* and *35 Instrumentation and Photography.*

20 SPACECRAFT PROPULSION AND POWER 1203

Includes main propulsion systems and components, e.g. rocket engines; and spacecraft auxiliary power sources.

For related information see also *07 Aircraft Propulsion and Power, 28 Propellants and Fuels, 44 Energy Production and Conversion,* and *15 Launch Vehicles and Space Vehicles.*

CHEMISTRY AND MATERIALS

Includes chemistry and materials (general); composite materials; inorganic and physical chemistry; metallic materials; nonmetallic materials; propellants and fuels; and materials processing.

23 CHEMISTRY AND MATERIALS (GENERAL) N.A.

24 COMPOSITE MATERIALS 1205

Includes physical, chemical, and mechanical properties of laminates and other composite materials.

For ceramic materials see *27 Nonmetallic Materials.*

25 INORGANIC AND PHYSICAL CHEMISTRY 1208

Includes chemical analysis, e.g., chromatography; combustion theory; electrochemistry; and photochemistry.

For related information see also *77 Thermodynamics and Statistical Physics.*

26 METALLIC MATERIALS 1213

Includes physical, chemical, and mechanical properties of metals, e.g., corrosion; and metallurgy.

27 NONMETALLIC MATERIALS 1217

Includes physical, chemical, and mechanical properties of plastics, elastomers, lubricants, polymers, textiles, adhesives, and ceramic materials.

For composite materials see *24 Composite Materials.*

28 PROPELLANTS AND FUELS 1221

Includes rocket propellants, igniters and oxidizers; their storage and handling procedures; and aircraft fuels.

For related information see also *07 Aircraft Propulsion and Power, 20 Spacecraft Propulsion and Power,* and *44 Energy Production and Conversion.*

29 MATERIALS PROCESSING 1222

Includes space-based development of products and processes for commercial application.

For biological materials see *55 Space Biology.*

ENGINEERING

Includes engineering (general); communications and radar; electronics and electrical engineering; fluid mechanics and heat transfer; instrumentation and photography; lasers and masers; mechanical engineering; quality assurance and reliability; and structural mechanics.

For related information see also *Physics.*

31 ENGINEERING (GENERAL) 1226

Includes vacuum technology; control engineering; display engineering; cryogenics; and fire prevention.

32 COMMUNICATIONS AND RADAR 1228

Includes radar; land and global communications; communications theory; and optical communications.

For related information see also *04 Aircraft Communications and Navigation* and *17 Space Communications, Spacecraft Communications, Command and Tracking.* For search and rescue see *03 Air Transportation and Safety,* and *16 Space Transportation.*

33 ELECTRONICS AND ELECTRICAL ENGINEERING 1231

Includes test equipment and maintainability; components, e.g., tunnel diodes and transistors; microminiaturization; and integrated circuitry.

For related information see also *60 Computer Operations and Hardware* and *76 Solid-State Physics.*

34 FLUID MECHANICS AND HEAT TRANSFER 1239

Includes boundary layers; hydrodynamics; fluidics; mass transfer and ablation cooling.

For related information see also *02 Aerodynamics* and *77 Thermodynamics and Statistical Physics.*

35 INSTRUMENTATION AND PHOTOGRAPHY 1247

Includes remote sensors; measuring instruments and gages; detectors; cameras and photographic supplies; and holography.

For aerial photography see *43 Earth Resources and Remote Sensing.* For related information see also *06 Aircraft Instrumentation* and *19 Spacecraft Instrumentation.*

36 LASERS AND MASERS 1249

Includes parametric amplifiers.

For related information see also *76 Solid-State Physics.*

37 MECHANICAL ENGINEERING 1252

Includes auxiliary systems (nonpower); machine elements and processes; and mechanical equipment.

38 QUALITY ASSURANCE AND RELIABILITY 1256

Includes product sampling procedures and techniques; and quality control.

39 STRUCTURAL MECHANICS 1258

Includes structural element design and weight analysis; fatigue; and thermal stress.

For applications see *05 Aircraft Design, Testing and Performance* and *18 Spacecraft Design, Testing and Performance.*

GEOSCIENCES

Includes geosciences (general); earth resources and remote sensing; energy production and conversion; environment pollution; geophysics; meteorology and climatology; and oceanography.

For related information see also *Space Sciences.*

42 GEOSCIENCES (GENERAL) **N.A.**

43 EARTH RESOURCES AND REMOTE SENSING **1269**

Includes remote sensing of earth resources by aircraft and spacecraft; photogrammetry; and aerial photography.

For instrumentation see *35 Instrumentation and Photography.*

44 ENERGY PRODUCTION AND CONVERSION **1270**

Includes specific energy conversion systems, e.g., fuel cells; global sources of energy; geophysical conversion; and windpower.

For related information see also *07 Aircraft Propulsion and Power, 20 Spacecraft Propulsion and Power,* and *28 Propellants and Fuels.*

45 ENVIRONMENT POLLUTION **1273**

Includes atmospheric, noise, thermal, and water pollution.

46 GEOPHYSICS **1274**

Includes aeronomy; upper and lower atmosphere studies; ionospheric and magnetospheric physics; and geomagnetism.

For space radiation see *93 Space Radiation.*

47 METEOROLOGY AND CLIMATOLOGY **1276**

Includes weather forecasting and modification.

48 OCEANOGRAPHY **1278**

Includes biological, dynamic, and physical oceanography; and marine resources.

For related information see also *43 Earth Resources and Remote Sensing.*

LIFE SCIENCES

Includes life sciences (general); aerospace medicine; behavioral sciences; man/system technology and life support; and space biology.

51 LIFE SCIENCES (GENERAL) **1278**

52 AEROSPACE MEDICINE **1279**

Includes physiological factors; biological effects of radiation; and effects of weightlessness on man and animals.

53 BEHAVIORAL SCIENCES **1281**

Includes psychological factors; individual and group behavior; crew training and evaluation; and psychiatric research.

54 MAN/SYSTEM TECHNOLOGY AND LIFE SUPPORT **1281**

Includes human engineering; biotechnology; and space suits and protective clothing.

For related information see also *16 Space Transportation.*

55 SPACE BIOLOGY **N.A.**

Includes exobiology; planetary biology; and extraterrestrial life.

MATHEMATICAL AND COMPUTER SCIENCES

Includes mathematical and computer sciences (general); computer operations and hardware; computer programming and software; computer systems; cybernetics; numerical analysis; statistics and probability; systems analysis; and theoretical mathematics.

59 MATHEMATICAL AND COMPUTER SCIENCES (GENERAL) **N.A.**

60 COMPUTER OPERATIONS AND HARDWARE **1282**

Includes hardware for computer graphics, firmware, and data processing.

For components see *33 Electronics and Electrical Engineering.*

61 COMPUTER PROGRAMMING AND SOFTWARE **1282**

Includes computer programs, routines, algorithms, and specific applications, e.g., CAD/CAM.

62 COMPUTER SYSTEMS **1284**

Includes computer networks and special application computer systems.

63 CYBERNETICS **1285**

Includes feedback and control theory, artificial intelligence, robotics and expert systems.

For related information see also *54 Man/System Technology and Life Support.*

64 NUMERICAL ANALYSIS **1286**

Includes iteration, difference equations, and numerical approximation.

65 STATISTICS AND PROBABILITY **1288**

Includes data sampling and smoothing; Monte Carlo method; and stochastic processes.

66 SYSTEMS ANALYSIS **1289**

Includes mathematical modeling; network analysis; and operations research.

67 THEORETICAL MATHEMATICS **1290**

Includes topology and number theory.

PHYSICS

Includes physics (general); acoustics; atomic and molecular physics; nuclear and high-energy physics; optics; plasma physics; solid-state physics; and thermodynamics and statistical physics.

For related information see also *Engineering.*

70 PHYSICS (GENERAL) **1290**

For precision time and time interval (PTTI) see *35 Instrumentation and Photography;* for geophysics, astrophysics or solar physics see *46 Geophysics, 90 Astrophysics,* or *92 Solar Physics.*

71 ACOUSTICS 1291
Includes sound generation, transmission, and attenuation.
For noise pollution see *45 Environment Pollution.*

72 ATOMIC AND MOLECULAR PHYSICS 1292
Includes atomic structure, electron properties, and molecular spectra.

73 NUCLEAR AND HIGH-ENERGY PHYSICS 1295
Includes elementary and nuclear particles; and reactor theory.
For space radiation see *93 Space Radiation.*

74 OPTICS 1295
Includes light phenomena and optical devices.
For lasers see *36 Lasers and Masers.*

75 PLASMA PHYSICS 1297
Includes magnetohydrodynamics and plasma fusion.
For ionospheric plasmas see *46 Geophysics.* For space plasmas see *90 Astrophysics.*

76 SOLID-STATE PHYSICS 1300
Includes superconductivity.
For related information see also *33 Electronics and Electrical Engineering* and *36 Lasers and Masers.*

77 THERMODYNAMICS AND STATISTICAL PHYSICS 1305
Includes quantum mechanics; theoretical physics; and Bose and Fermi statistics.
For related information see also *25 Inorganic and Physical Chemistry* and *34 Fluid Mechanics and Heat Transfer.*

SOCIAL SCIENCES

Includes social sciences (general); administration and management; documentation and information science; economics and cost analysis; law, political science, and space policy; and urban technology and transportation.

80 SOCIAL SCIENCES (GENERAL) N.A.
Includes educational matters.

81 ADMINISTRATION AND MANAGEMENT N.A.
Includes management planning and research.

82 DOCUMENTATION AND INFORMATION SCIENCE 1306
Includes information management; information storage and retrieval technology; technical writing; graphic arts; and micrography.
For computer documentation see *61 Computer Programming and Software.*

83 ECONOMICS AND COST ANALYSIS N.A.
Includes cost effectiveness studies.

84 LAW, POLITICAL SCIENCE AND SPACE POLICY N.A.
Includes NASA appropriation hearings; aviation law; space law and policy; international law; international cooperation; and patent policy.

85 URBAN TECHNOLOGY AND TRANSPORTATION 1307
Includes applications of space technology to urban problems; technology transfer; technology assessment; and surface and mass transportation.
For related information see *03 Air Transportation and Safety, 16 Space Transportation,* and *44 Energy Production and Conversion.*

SPACE SCIENCES

Includes space sciences (general); astronomy; astrophysics; lunar and planetary exploration; solar physics; and space radiation.
For related information see also *Geosciences.*

88 SPACE SCIENCES (GENERAL) N.A.

89 ASTRONOMY 1307
Includes radio, gamma-ray, and infrared astronomy; and astrometry.

90 ASTROPHYSICS 1308
Includes cosmology; celestial mechanics; space plasmas; and interstellar and interplanetary gases and dust.
For related information see also *75 Plasma Physics.*

91 LUNAR AND PLANETARY EXPLORATION 1309
Includes planetology; and manned and unmanned flights.
For spacecraft design or space stations see *18 Spacecraft Design, Testing and Performance.*

92 SOLAR PHYSICS 1309
Includes solar activity, solar flares, solar radiation and sunspots.
For related information see *93 Space Radiation.*

93 SPACE RADIATION 1309
Includes cosmic radiation; and inner and outer earth's radiation belts.
For biological effects of radiation see *52 Aerospace Medicine.* For theory see *73 Nuclear and High-Energy Physics.*

GENERAL

Includes aeronautical, astronautical, and space science related histories, biographies, and pertinent reports too broad for categorization; histories or broad overviews of NASA programs.

99 GENERAL N.A.

Note: N.A. means that no abstracts were assigned to this category for this issue.

SUBJECT INDEX I-1
PERSONAL AUTHOR INDEX I-49
CORPORATE SOURCE INDEX I-57
CONTRACT NUMBER INDEX I-69
REPORT/ACCESSION NUMBER INDEX I-71

TYPICAL CITATION AND ABSTRACT

NASA SPONSORED
ON MICROFICHE
ACCESSION NUMBER
N89-11793*#
Draper (Charles Stark) Lab., Inc., Cambridge, Mass.
CORPORATE SOURCE
TITLE
CONTROL OF FLEXIBLE STRUCTURES-2 (COFS-2) FLIGHT CONTROL, STRUCTURE AND GIMBAL SYSTEM INTERACTION STUDY Final Report
AUTHORS
Stanley Fay, Stephen Gates, Timothy Henderson, Lester Sackett, Kim Kirchwey, Isaac Stoddard, and Joel Storch
Sep. 1988
PUBLICATION DATE
205 p
CONTRACT OR GRANT
(Contract NAS9-17560)
REPORT NUMBERS
(NASA-CR-172095; R-2088; NAS 1.26:172095)
Avail: NTIS HC
AVAILABILITY SOURCE
PRICE CODE
A10/MF A01 CSCL 22B
COSATI CODE
The second Control Of Flexible Structures Flight Experiment (COFS-2) includes a long mast as in the first flight experiment, but with the Langley 15-m hoop column antenna attached via a gimbal system to the top of the mast. The mast is to be mounted in the Space Shuttle cargo bay. The servo-driven gimbal system could be used to point the antenna relative to the mast. The dynamic interaction of the Shuttle Orbiter/COFS-2 system with the Orbiter on-orbit Flight Control System (FCS) and the gimbal pointing control system has been studied using analysis and simulation. The Orbiter pointing requirements have been assessed for their impact on allowable free drift time for COFS experiments. Three fixed antenna configurations were investigated. Also simulated was Orbiter attitude control behavior with active vernier jets during antenna slewing. The effect of experiment mast dampers was included. Control system stability and performance and loads on various portions of the COFS-2 structure were investigated. The study indicates possible undesirable interaction between the Orbiter FCS and the flexible, articulated COFS-2 mast/antenna system, even when restricted to vernier reaction jets. Author

VOLUME 27 NUMBER 9 / MAY 8, 1989

Scientific and Technical Aerospace Reports

A Semimonthly Publication of the National Aeronautics and Space Administration

01 AERONAUTICS (GENERAL)

N89-16718# Air Command and Staff Coll., Maxwell AFB, AL.
EVENT-CENTERED SCHEDULING PROGRAM: THE NEED FOR PERT (PROGRAM EVALUATION REVIEW TECHNIQUE) IN C-141 ISO INSPECTION MANAGEMENT
Kent A. Mueller Apr. 1988 74 p
(AD-A200094; ACSC-88-1925) Avail: NTIS HC A04/MF A01 CSCL 05A

Scheduled inspections, specifically the C-141 Isochronal Major, consume a significant amount of time as currently managed. The study proposes that Program Evaluation Review Technique (PERT) methods be applied to this flow management process to produce optimized inspection flow plans. Harvard Total Project Manager (HTPM) software is used to build an optimized flow which demonstrates the potential for flow day savings if attention is shifted from scheduling within a block of time to resequencing of events. The study concludes that current desktop project planning software can be integrated into the ISO flow management process. GRA

N89-16719# RAND Corp., Santa Monica, CA.
AIRCRAFT AIRFRAME COST ESTIMATING RELATIONSHIPS: ALL MISSION TYPES Interim Report
R. W. Hess and H. P. Romanoff Dec. 1987 147 p
(Contract F49620-86-C-0008)
(AD-A200262; RAND/N-2283/1-AF) Avail: NTIS HC A07/MF A01 CSCL 05C

This Note is part of a series of Notes that derive a set of equations suitable for estimating the acquisition costs of various types of aircraft airframes in the absence of detailed design and manufacturing information. A single set of equations was selected as being the most representative and applicable to the widest range of estimating situations. For all mission types, the equation set used empty weight types and speed as the basic size-performance variable combination. GRA

N89-16720# RAND Corp., Santa Monica, CA.
AIRCRAFT AIRFRAME COST ESTIMATING RELATIONSHIPS: FIGHTERS Interim Report
R. W. Hess and H. P. Romanoff Dec. 1987 151 p
(Contract F49620-86-C-0008)
(AD-A200263; RAND/N-2283/2-AF) Avail: NTIS HC A08/MF A01 CSCL 05C

This note is part of a series of notes that derive a set of equations suitable for estimating the acquisition costs of various types of aircraft airframes in the absence of detailed design and manufacturing information. A single set of equations was selected as being the most representative and applicable to the widest range of estimating situations. For fighters, the equation set uses airframe unit weight as the variable. GRA

N89-16721# RAND Corp., Santa Monica, CA.
AIRCRAFT AIRFRAME COST ESTIMATING RELATIONSHIPS: BOMBERS AND TRANSPORTS Interim Report
R. W. Hess and H. P. Romanoff Dec. 1987 63 p
(Contract F49620-86-C-0008)
(AD-A200264; RAND/N-2283/3-AF) Avail: NTIS HC A04/MF A01 CSCL 05C

This note is part of a serious of notes that derive a set of equations suitable for estimating the acquisition costs of various types of aircraft airframes in the absence of detailed design and manufacturing information. A single set of equations was selected as being the most representative and applicable to the widest range of estimating situations. For bombers and transports, no single acceptable estimating relationship could be identified. Estimates for these aircraft should be developed by analogy or by using the equation set developed for all mission types. GRA

N89-16722# RAND Corp., Santa Monica, CA.
AIRCRAFT AIRFRAME COST ESTIMATING RELATIONSHIPS: ATTACK AIRCRAFT Interim Report
R. W. Hess and H. P. Romanoff Dec. 1987 60 p
(Contract F49620-86-C-0008)
(AD-A200265; RAND/N-2283/4-AF) Avail: NTIS HC A04/MF A01 CSCL 05C

This note is part of a series of notes that derive a set of equations suitable for estimating the acquisition costs of various types of aircraft airframes in the absence of detailed design and manufacturing information. A single set of equations was selected as being the most representative and applicable to the widest range of estimating situations. For attack aircraft, no single acceptable estimating relationship could be identified because sample sizes were small and not homogeneous. Estimates for these aircraft should be developed by analogy or by using the equation set developed for all mission types. GRA

02 AERODYNAMICS

Includes aerodynamics of bodies, combinations, wings, rotors, and control surfaces; and internal flow in ducts and turbomachinery.

For related information see also *34 Fluid Mechanics and Heat Transfer.*

N89-16723 Stanford Univ., CA.
TRANSONIC AEROELASTIC ANALYSIS OF LAUNCH VEHICLE CONFIGURATIONS Ph.D. Thesis
Joao Luiz Filgueiras deAzevedo 1988 170 p
Avail: Univ. Microfilms Order No. DA8814978

A numerical study of the aeroelastic stability of typical launch vehicle configurations in transonic flight is performed. Recent computational fluid dynamics techniques are used to simulate the transonic aerodynamic flowfield, as opposed to relying on experimental data for the unsteady aerodynamic pressures. The flow solver is coupled to an appropriate structural-dynamic representation of the vehicle. The aerodynamic formulation is based on the thin layer approximation to the Reynolds-Averaged Navier-Strokes equations, where the account for turbulent mixing is done by the two-layer Baldwin and Lomax algebraic eddy viscosity model. The structural-dynamic equations are developed considering free-free fluxural vibration of an elongated beam with variable properties and are cast in moldal form. Aeroelastic analyses are performed by integrating simultaneously in time the two sets of equations. By tracing the growth or decay of a perturbed

oscillation, the aeroelastic stability of a given configuration can be ascertained. The method is described in detail, and results that indicate its application are presented. Dissert. Abstr.

N89-16724 Stanford Univ., CA.
ON THE AEROACOUSTICS, AERODYNAMICS AND AEROELASTICITY OF LIFTING SURFACES Ph.D. Thesis
Mauricio Pazini Brandao 1988 228 p
Avail: Univ. Microfilms Order No. DA8814982

A aeroacoustic theory is studied and applied to aerodynamics. The method can be used to determine the pressure distribution on the surface of bodies of general geometry in arbitrary motion. Bodies may be perfectly rigid or may undergo deformation while moving. Therefore, the theory may be applicable to any of the three interdisciplinary areas quoted in the title. The conservation laws of mass and monentum are cast in the form of an inhomogeneous wave equation for the compressible case and of an inhomogeneous Laplacian equation for the incompressible case. Both differential equations are transformed into singular integral equations using the standard Green's function technique. The resulting kernels account for three-dimensional, nonlinear, unsteady and viscous effects that stem from the exact conservation equations. To allow validation of the theoretical approach, the formulation is simplified for the case of inviscid fluids. In addition, the nonlinear free-field quadrupole term is neglected. After these simplifications, the formulation should be considered as valid only for small disturbance problems. Dissert. Abstr.

N89-16725# Princeton Univ., NJ. Dept. of Mechanical and Aerospace Engineering.
DEVELOPMENT AND APPLICATION OF OXYGEN FLOW TAGGING FOR VELOCITY MEASUREMENTS AND FLOW VISUALIZATION IN TURBULENT THREE-DIMENSIONAL SUPERSONIC FLOWS Annual Technical Report, 1 Jun. 1987 - 31 May 1988
Richard B. Miles 14 Sep. 1988 39 p
(Grant AF-AFOSR-0191-86; AF Proj. 2307)
(AD-A200119; AFOSR-88-1153TR) Avail: NTIS HC A03/MF A01 CSCL 20D

A demonstration is presented of the oxygen flow tagging under conditions which duplicate the Mach 3 facility. These tests were done in an underexpanded axisymmetric jet up to Mach 4. Velocity data was taken through the core and across the free shear layer of this jet and images were generated of instantaneous flow structure from which are computed the average velocity profiles, turbulence intensity, and the axial velocity correlations. Simultaneous two-line flow tagging was done. That data was used to generate stream-wise velocity correlations in the same axisymmetric jet. The data which has been generated has been compared with a high-speed subsonic jet to give us a quantitative measure of the difference between supersonic and subsonic turbulence. GRA

N89-16726# Continuum Dynamics, Inc., Princeton, NJ.
VORTEX DYNAMICS FOR ROTORCRAFT INTERACTIONAL AERODYNAMICS
Todd R. Quackenbush and Donald B. Bliss (Duke Univ., Durham, NC.) Mar. 1988 65 p Prepared in cooperation with Duke University, Durham, NC
(Contract DAAL03-87-C-0013)
(AD-A200128; ARO-25093.1-EG-SBI) Avail: NTIS HC A04/MF A01 CSCL 01A

Promising results were obtained that indicate that new techniques in the analysis of vortex dynamics could be used as the foundation of a general analysis of rotor/airframe interactions. Prediction of the velocity field downstream of helicopter rotors was addressed first. Using a novel, full-span rotor wake representation constructed of curved vortex elements, accurate qualitative and quantitative predictions of wake velocity data were achieved for rotors in both low- and high-speed forward flight. The flow field predictions illustrated the radical changes that take place in the wake velocity field as speed increases and demonstrated the success of this approach in capturing these variations. New methods for analyzing close interactions between vortices and fixed surfaces were developed. The basis of this new approach is the inclusion of the special treatment of the vortex velocity field for close interactions with paneled surfaces which obviates the need for high local panel density. Model problems were solved featuring vortices in close proximity to flat surfaces and cylinders that amply illustrate the accuracy and efficiency of the new method. GRA

N89-16727# Naval Postgraduate School, Monterey, CA.
TURBULENCE EFFECTS ON THE HIGH ANGLE OF ATTACK AERODYNAMICS OF A VERTICALLY LAUNCHED MISSILE M.S. Thesis
M. Peter Rabang Jun. 1988 165 p
(AD-A200418) Avail: NTIS HC A08/MF A01 CSCL 20D

A subsonic wind tunnel investigation was conducted at the Naval Postgraduate School Wind Tunnel Test Facility to examine the effects of grid generated turbulence on the high angle of attack aerodynamics of a vertically launched missile. Four turbulence generating grids produced turbulence with length scale to missile and model diameter ratios of 1.05, 0.89, 0.62, and 0.15 with respective turbulence intensities of 3.31 percent, 2.78 percent, 1.88 percent, and 0.47 percent. The test model is representative of current cruciform wing missiles with low aspect ratio wings and long root chords. The tangent ogive nose has a nose fineness ratio of 2.29. Three separate body configurations were tested with and without the turbulence generating grids. One configuration was a body in isolation and the other two were wing and tail configurations at 0 deg and 45 deg and roll angles. All test runs were conducted over an angle of attack range of -5 deg to 95 deg. Results indicate that as turbulence length scales approach body diameter size, the angle of attack for the onset of asymmetric vortices was delayed and the side force magnitude was reduced. The vortices generated by the nose of the missile continue to dominate the afterbody vortices for body configurations with and without wings regardless of the turbulence conditions. GRA

N89-16728# Naval Postgraduate School, Monterey, CA.
AERODYNAMIC PERFORMANCE OF WINGS OF ARBITRARY PLANFORM IN INVISCID, INCOMPRESSIBLE, IRROTATIONAL FLOW M.S. Thesis
Chris L. Holm Sep. 1988 200 p
(AD-A200436) Avail: NTIS HC A09/MF A01 CSCL 01A

This thesis contains discussion, theory and program code for a computational fluid dynamics (CFD) model of a wing of arbitrary planform. The mathematical model assumes incompressible, inviscid, irrotational flow. The program computes forces acting on the wing by modeling the flow with a set of horseshoe vortex elements. It models the flow over an arbitrary wing using two solutions. One solution is the ideal lift, associated with a cambered and twisted wing. The other solution is the additional lift associated with a flat wing. The program computes wing camber and twist using an elliptic loading distribution. The thesis includes the FORTRAN source code, a separable user's manual for the VORTEX program, discussion of the theory applied in the model, and instructions for operating the program. It shows a sample wing planform with tabular and graphic results. Two other CFD models are also discussed, based on circulation and pressure difference, along with some of the problems and solutions in grid generation. Computer programs. Theses. (edc) GRA

N89-16729 Maryland Univ., College Park.
NUMERICAL SOLUTIONS TO THREE-DIMENSIONAL SHOCK WAVE/VORTEX INTERACTION AT HYPERSONIC SPEEDS Ph.D. Thesis
Griffin Pat Corpening 1988 301 p
Avail: Univ. Microfilms Order No. DA8818380

A recent study was undertaken to solve the interaction flow field between a helical type vortex and an oblique shock wave. Two solutions were developed to three-dimensional shock wave vortex interaction at two Mach numbers, Mach 2.28 and 5.00. The numerical model used is based on finite volume, implicit upwind differening method which is used to solve the integral form of the

Euler equations. In each case, a vortex was input into a flow field containing a 46.4 degree shock wave. These solutions showed several interesting results. These results are discussed.
Dissert. Abstr.

N89-16730 ESDU International Ltd., London (England).
ESTIMATION OF DRAG ARISING FROM ASYMMETRY IN THRUST OR AIRFRAME CONFIGURATION
Dec. 1988 40 p
(ESDU-88006; ISBN-0-85679-638-7; ISSN-0141-4054) Avail: ESDU

This data item 88006, an addition to the Sub-series on Aircraft Performance, gives a simple method, based on a correlation of established for a range of propeller and turbo-jet and turbo-fan powered aircraft, for predicting approximately the drag increment in flight with one or more engines inoperative (including the drag of the failed engine(s)). The derivation of the parameters used in that non-dimensional presentation is also considered and methods of estimating asymmetric flight is also considered and methods of estimating some of them are provided together with a list of sources of data for the others. The force and moment equations used to determine equilibrium flight conditions are given for use with either estimated or wind-tunnel aerodynamic data and an example of their application to a transport aeroplane is included. There is also a detailed discussion of alternative ways in which an aircraft may be flown in steady straight flight with thrust or other airframe asymmetries. ESDU

N89-16731 ESDU International Ltd., London (England).
ROLLING MOMENT DERIVATIVE Lxi, FOR PLAIN AILERONS AT SUBSONIC SPEEDS
Aug. 1988 18 p Supersedes ESDU Aero C.06.01.01
(ESDU-88013; ISBN-0-85679-645-X; ISSN-0141-397X) Avail: ESDU

This Data Item 88013, an addition to the Sub-series on Aerodynamics, presents a semi-empirical method that improves the traditional approach based on Weissinger's simplified lifting-surface theory which drew parallels with the dihedral contribution to the rolling moment due to sideslip. The method relies on ESDU 74011 to estimate the lift increment due to control deflection (in conjunction with the wing lift-curve slope from ESDU 70011), assumes that it acts at the mid-span of the aileron, and corrects the rolling moment so derived by an empirical factor that allows for the aileron effectiveness. The ranges of wing and control geometry for which the method is validated are given, and it is found to predict the derivative to within 20 percent for values up to -0.15 and to within 0.03 for numerically higher values. ESDU

N89-16732 ESDU International Ltd., London (England).
DERIVATION OF PRIMARY AIR-DATA PARAMETERS FOR HYPERSONIC FLIGHT
Dec. 1988 48 p
(ESDU-88025; ISBN-0-85679-657-3; ISSN-0141-4054) Avail: ESDU

This Data Item 88025, an addition to the Sub-series on Aircraft Performance, gives data and methods of analysis for deriving true airspeed, Mach number, pressure height and ambient air temperature from registered values of total pressure and temperature, and static pressure. The methods apply for Mach numbers between approximately 4 and 10 and for heights up to 65 km (210,000 ft). Such air data are of particular importance where they are used to control an air-breathing propulsion unit. The assuptions and limitations of the methods are clearly stated and explaned, and a worked example illustrates the use of graphs and tables for the properties of equilibrium air behind a normal shock which are then used with the Rankine-Hugoniot relationships to devise the required data. ESDU

N89-16733 ESDU International Ltd., London (England).
NORMAL-FORCE-CURVE AND PITCHING-MOMENT-CURVE SLOPES FOR TANGENT-OGIVE FOREBODY-CYCLINDER COMBINATIONS AT ZERO ANGLE OF ATTACK
Nov. 1988 16 p Supersedes in part ESDU-86029
(ESDU-88026; ISBN-0-85679-658-1; ISSN-0141-397X) Avail: ESDU

This Data Item 88026, an addition to the Sub-series on Aerodynamics, provides a semi-empirical prediction method that incorporates corrections for the effects of boundary layer displacement thickness and skin friction; curves are included for the prediction of those quantities. It applies over the complete Mach number range from subsonic through to a value of 5. The method was validated against a large quantity of unpublished wing-tunnel test results covering a Reynolds number range of 1E+5 to 4.7E+7 and geometries with forebody length/diameter ratios from 1.5 to 7 and cylinder length/diameter ratios of 0 to 20. It is suggested, however, that the method applies over the Reynolds number range (based on body length) of 1E+5 to 1E+9. The method predicted normal-force curve slope to within 10 percent and center of pressure position as incidence tended to zero to within 5 percent of body length increasing to 10 percent on short bodies. ESDU

N89-16734 ESDU International Ltd., London (England).
YAWING MOMENT COEFFICIENT FOR PLAIN AILERONS AT SUBONIC SPEEDS
Dec. 1988 16 p
(ESDU-88029; ISBN-0-85679-661-1; ISSN-0141-397X) Avail: ESDU

This data item 88029, an addition to the Sub-series on Aerodynamics, predicts the adverse yawing moment accompanying aileron deflection as two components, an induced drag contribution due to the differential setting and a profile drag component. For the first component a semi-empirical correlation procedure is developed while for the second the method of ESDU 87024, which deals with the profile drag due to deflection of plain flaps, is used. The method applies to sealed controls (or controls with small gaps) and allows for differential operation and flap deployment. The experimental data drawn from the literature (with some unpublished wind-tunnel measurements) covered a wide range of wing and aileron geometry which is specified. The method predicted the change of yawing moment coefficient per unit control deflection to within 0.003/rad at zero lift and without deployed flaps. ESDU

N89-16735 ESDU International Ltd., London (England).
BOUNDARIES OF LINEAR CHARACTERISTICS OF CAMBERED AND TWISTED WINGS AT SUBCRITICAL MACH NUMBERS
Nov. 1988 43 p
(ESDU-88030; ISBN-0-85679-662-X; ISSN-0141-397X) Avail: ESDU

This Data Item 88030, an addition to the Sub-series on Aerodynamics, estimates the onset of non-linear aerodynamic characteristics by giving an empirical method for predicting the incidence and corresponding lift coefficient for either initial leading- or trailing-edge separation. The method developed treats the incidence as contributed to by three components: one from a datum plane wing, and one each from the superimposed aerodynamically smooth wings provided that the local effective twist does not exceed 10 degrees and will not apply when the ranges of planform and flow conditions are covered by the method (including aspect ratios from 1.4 to 13 and leading-edge sweeps from zero to 62 degrees). The method applies to any camber line slope, which may vary spanwise, as may the thickness chord ratio, and comparisons are shown between predicted lift coefficient for the onset of separation for both leading- and trailing-edge types which show it is predicted to within 15 percent. Comprehensive practical worked examples illustrate the use of the method, and a calculation summary sheet guides the user step-by-step through the procedure. ESDU

N89-16736 ESDU International Ltd., London (England).
LIFT AND LONGITUDINAL FORCES ON PROPELLER/NACELLE/WING/FLAP SYSTEMS

Dec. 1988 41 p
(ESDU-88031; ISBN-0-85679-663-8; ISSN-0141-397X) Avail: ESDU

This Data Item 88031, an addition to the Sub-series on Aerodynamics, provides a simple semi-empirical method for estimating the free air low-speed values of these forces for an unswept wing/flap system submerged in the slipstream from multiple propellers. It provides for the separate estimation of forces on the propeller and on the nacelle/wing/flap and requires a knowledge of the geometry and of the power-off lift and drag for the nacelle/wing/flap. There is a basic method, developed using simple momentum theory, which applies to flaps continuous across the slipstream, circular section nacelles of diameter equal to that of the spinner, and propellers that do not overlap. Guidance is then provided on the effect of flap cut-out, nacelle size and propeller overlap. The wing may be fitted with any of a wide range of single- or multi-element flaps, provided the flow is fully attached. Estimates are provided over the full range of thrust coefficients (based on slipstream kinetic pressure and propeller disc area) from zero to unity and predictions of the lift and longitudinal force on the nacelle/wing/flap system are within 10 and 15 percent respectively. ESDU

N89-16737# Sandia National Labs., Albuquerque, NM. Computational Aerodynamics Div.
VERIFICATION OF A NAVIER-STOKES CODE FOR SOLVING THE HYPERSONIC BLUNT BODY PROBLEM
Frederick G. Blottner 1988 12 p Presented at the 4th Symposium on Numerical and Physical Aspects of Aerodynamic Flows, Long Beach, CA, 16 Jan. 1989
(Contract DE-AC04-76DP-00789)
(DE89-003169; SAND-88-0917C; CONF-890151-1) Avail: NTIS HC A03/MF A01

Computational results obtained from a Navier-Stokes code for the subsonic nose region flow on blunt bodies in supersonic flow have been evaluated for accuracy. The unsteady thin-layer form of the governing equations for a perfect gas are solved with a linearized block Alternating-Directions Implicit finite-difference solution procedure. A modification to the usual numerical scheme is required near the stagnation point to obtain satisfactory heat transfer results in this region. Sensitivity of the solutions to code input parameters is investigated. Predictions obtained from the code are presented an compared to numerical and experimental results. This study indicates that very accurate surface pressures and reasonably accurate heat transfer predictions are obtained from the code. DOE

N89-16738# Von Karman Inst. for Fluid Dynamics, Rhode-Saint-Genese (Belgium).
INTAKE AERODYNAMICS, VOLUME 1
1988 333 p Lecture series held in Rhode-Saint-Genese, Belgium, 22-26 Feb. 1988
(VKI-LS-1988-04-Vol-1; ISSN-0377-8312; ETN-89-93592) Avail: NTIS HC A15/MF A01

Tactical fighter inlets; inlet-engine compatibility; intake swirl and simplified methods for dynamic pressure distortion assessment; Jaguar/Tornado intake design; intake-airframe integration; intakes for high angle of attack; transonic cowl design; and intake drag were discussed. For individual titles, see N89-16739 through N89-16747.

N89-16739# Von Karman Inst. for Fluid Dynamics, Rhode-Saint-Genese (Belgium).
INTRODUCTION TO INTAKE AERODYNAMICS
J. Seddon *In its* Intake Aerodynamics, Volume 1 1988 28 p (For primary document see N89-16738 09-02)
Avail: NTIS HC A15/MF A01

Pressure recovery in axial flow engines, with subsonic or supersonic inlets; boundary layers around inlets; inlet drag; and variable geometry inlets are introduced. ESA

N89-16740# Air Force Wright Aeronautical Labs., Wright-Patterson AFB, OH. Flight Dynamics Lab.
TACTICAL FIGHTER INLETS
Lewis E. Surber and Keith E. Numbers *In* VKI, Intake Aerodynamics, Volume 1 1988 34 p (For primary document see N89-16738 09-02)
Avail: NTIS HC A15/MF A01

It is shown that the design of a tactical fighter air intake results from a compromise of performance and stability against complexity and weight, driven by overall aircraft mission requirements. Intake design requires thorough understanding of the various facets of inlet performance and the flow field phenomena which affect them. The basic measures of performance and the primary flow field phenomena which must be controlled are introduced. Design considerations involved in maximizing pressure recovery, minimizing drag, and controlling the flow for improved uniformity and steadiness are discussed. Given the design techniques available and their implementation in current aircraft it is shown that the inlet configuration itself can reveal much about the intended aircraft mission application and the overall system design philosophy. ESA

N89-16741# Air Force Wright Aeronautical Labs., Wright-Patterson AFB, OH. Flight Dynamics Lab.
INLET-ENGINE COMPATIBILITY **c05**
Lewis E. Surber and Clay Fujimara *In* VKI, Intake Aerodynamics, Volume 1 1988 32 p (For primary document see N89-16738 09-02)
Avail: NTIS HC A15/MF A01

Inlet-engine compatibility is reviewed to show how inlet spatial flow distortion relates to the compatibility problem in turbine-engine powered supersonic fighter aicraft. It is shown that flow distortion is actually experienced as off-design flow incidence by compressor airfoils, but may be characterized and treated as flow field total pressure distortion in the development process. Axial compressor engines respond to time-variant spatial distortion up to the range of the blade passing frequency. Therefore, any accurate compatibility analysis must deal with dynamic distortion. Information is presented to show that accurate distortion parameter values and pressure distortion maps can be produced for low and moderate inlet turbulence levels with as few as eight turbulence measurements. Advanced fighter inlets with compact offset diffusers may experience turbulence levels in the 5 plus percent range where probe-to-probe signal coherence violates the basic premise of statistical analysis. In cases where highly accurate compatibility assessments are required for high turbulence inlet flows, deterministic methods are employed. ESA

N89-16742# Messerschmitt-Boelkow-Blohm G.m.b.H., Munich (Germany, F.R.). Military Aircraft Div.
INTAKE SWIRL AND SIMPLIFIED METHODS FOR DYNAMIC PRESSURE DISTORTION ASSESSMENT
F. Aulehla and D. M. Schmitz *In* VKI, Intake Aerodynamics, Volume 1 1988 58 p (For primary document see N89-16738 09-02)
Avail: NTIS HC A15/MF A01

It is shown that all supersonic intakes of present combat aircraft produce essentially two types of swirl components of varying magnitude, i.e., bulk and twin swirl. Depending on the sensitivity of the engine towards such disturbances serious engine/intake compatibility problems may arise, for example engine surge and fan vibration. The remedial measures to overcome this problem are described and the solution of fenced intakes selected for Tornado is discussed. A similar problem solution for the Airbus A300 is also presented. The relevance of dynamic total pressure distortion as the prime compatibility parameter for engines without inlet guide vanes is questioned and a proposal for an improved intake disturbance simulation in engine bench tests is made. It is suggested that fully dynamic distortion measurements can be replaced by simplified methods at least in the early stage of a project. ESA

N89-16743# British Aerospace Aircraft Group, Preston (England). Military Aircraft Div.
JAGUAR/TORNADO INTAKE DESIGN
D. C. Leyland *In* VKI, Intake Aerodynamics, Volume 1 1988 25 p (For primary document see N89-16738 09-02)
Avail: NTIS HC A15/MF A01

The assessment of aerodynamic features that led to the chosen intake configurations and particular aspects that had to be taken into account in overall design of the Jaguar and Tornado intakes are summarized. Intake sizing and profiles; pressure recovery; boundary layers; intake control; supersonic characteristics; and vortex-incidence aspects are discussed. ESA

N89-16744# Air Force Wright Aeronautical Labs., Wright-Patterson AFB, OH. Flight Dynamics Lab.
INTAKE-AIRFRAME INTEGRATION **c05**
Lewis E. Surber *In* VKI, Intake Aerodynamics, Volume 1 1988 66 p (For primary document see N89-16738 09-02)
Avail: NTIS HC A15/MF A01

Intake-airframe integration of tactical aircraft is reviewed. It is shown that the stream flow approaching a side-mounted inlet is substantially distorted by the presence of the fuselage in maneuvering flight. This flow distortion has a generally adverse effect on inlet total pressure recovery and inlet-engine compatibility. Supersonic maneuvering flight can lead to substantial performance degradation in a side-mounted leeward 2-D inlet due to flow separation at the inboard sideplate. Performance degradation in side-mounted half-axisymmetric inlets in supersonic maneuvers results from flow separation in the upper portion of the throat followed by choking of the rest of the throat. Flow field studies show dramatic potential performance advantages for shielding supersonic maneuvering inlets. Fuselage-shielding, however, is the only technique which retains all the advantages for 2-D inlets when alpha/Beta combinations were explored. Half-axisymmetric inlets show substantial performance advantages over 2-D inlets in supersonic wing-shielded flow fields when considering the entire maneuver envelope. Experiments demonstrate limited tailoting of top-mounted inlet flow fields through careful design of wing leading-edge strakes which control the vortex pattern over an aircraft's upper surface. Such designs may be able to facilitate an acceptable inlet environment for limited maneuver conditions. ESA

N89-16745# British Aerospace Aircraft Group, Preston (England). Military Aircraft Div.
INTAKES FOR HIGH ANGLE OF ATTACK **c05**
D. C. Leyland *In* VKI, Intake Aerodynamics, Volume 1 1988 26 p (For primary document see N89-16738 09-02)
Avail: NTIS HC A15/MF A01

Intake design and location for combat aircraft are reviewed. Experience of operation at moderate angles-of-attack was obtained from testing of models of existing aircraft, to the extent of showing what features and characteristics require investigation. Shielding to provide preturning of entry flow is desirable and the chin location chosen for EAP and EFA proves very effective. Research studies, however, included other locations to determine what can be expected and accepted. The chin intake is not always the best overall configuration choice; it constrains fuselage stores carriage in smaller aircraft and is likely to be unacceptable in STOVL aircraft because of hot gas reingestion. Results from research testing, mostly on fuselage integrated intakes, are given to show what flow changes take place with increasing angle-of-attack and what configuration choices can be made to give acceptable characteristics. ESA

N89-16746# Von Karman Inst. for Fluid Dynamics, Rhode-Saint-Genese (Belgium).
TRANSONIC COWL DESIGN **c05**
J. Seddon *In its* Intake Aerodynamics, Volume 1 1988 23 p (For primary document see N89-16738 09-02)
Avail: NTIS HC A15/MF A01

Transonic cowl design is discussed in the context of external drag of engine nacelles on high-subsonic transport aircraft. The principal concern arises because at high subsonic speeds the airflow over the intake cowl, and in other regions of an overall podded installation, becomes locally supersonic, giving rise to shock waves and possible boundary layer separation. Both these features can lead to substantial increases in aircraft drag. Drag below the critical Mach number (where flow locally reaches sonic speed) and subcritical cowl design are treated. Supercritical cowl design and installation drag are discussed. ESA

N89-16747# British Aerospace Aircraft Group, Preston (England). Military Aircraft Div.
INTAKE DRAG
D. C. Leyland *In* VKI, Intake Aerodynamics, Volume 1988 28 p (For primary document see N89-16738 09-02)
Avail: NTIS HC A15/MF A01

Intake drag associated with location and external geometry at full mass flow and that due to reduction in entry flow from the maximum or datum value, the engine throttle dependent term, is discussed. General methods for estimating intake spillage drag are given but there is considerable installation geometry dependence and it is preferable to use test data for a similar configuration. The need for a correct understanding of the origin of propulsion related forces and of the requirements for proper book keeping of thrust and drag terms is emphasized. The use of part models in propulsion installation analysis is reviewed, and it is suggested that distinction needs to be made between the contributions to axial force from potential flow and real flow, only the latter part being strictly drag and contributing to overall aircraft drag. The use of data from part models is indicated, in support of the usual book keeping arrangement for throttle dependent terms to be taken into the engine installation account. ESA

N89-16748# Von Karman Inst. for Fluid Dynamics, Rhode-Saint-Genese (Belgium).
INTAKE AERODYNAMICS, VOLUME 2
1988 302 p Lecture series held in Rhode-Saint-Genese, Belgium, 22-26 Feb. 1988
(VKI-LS-1988-04-Vol-2; ISSN-0377-8312; ETN-89-93593) Avail: NTIS HC A14/MF A01

Transport aircraft intake design; missile intakes; wind tunnel air intake test techniques; computational methods for inlet airframe integration; computational fluid dynamics (CFD) application to subsonic inlet airframe integration; and CFD application to supersonic/hypersonic inlet airframe integration were discussed. For individual titles, see N89-16749 through N89-16754.

N89-16749# Office National d'Etudes et de Recherches Aerospatiales, Paris (France).
TRANSPORT AIRCRAFT INTAKE DESIGN **c05**
Jacky Leynaert *In* VKI, Intake Aerodynamics, Volume 2 1988 28 p (For primary document see N89-16748 09-02)
Avail: NTIS HC A14/MF A01

Subsonic air intake, Mach 2+ transport aircraft intake, and Mach 3 are considered. Hypersonic cruise intakes are mentioned. The problem of supersonic intake adaptation to the intermediate flight Mach number range is reviewed. Future multicycle engine design is discussed. ESA

N89-16750# Office National d'Etudes et de Recherches Aerospatiales, Paris (France).
MISSILE INTAKES **c05**
Gerard Laruelle *In* VKI, Intake Aerodynamics, Volume 2 1988 76 p (For primary document see N89-16748 09-02)
Avail: NTIS HC A14/MF A01

General intake principles are applied to air-breathing missiles. The operational constraints are reviewed and explain the evolution of the configurations over 30 yr. The fuselage flow field and isolated intake characteristics are analyzed. Missile configurations are discussed. Explanations concerning performance prediction and test facilities are given. Suggestions for design of air-breathing missiles are proposed. ESA

N89-16751# Office National d'Etudes et de Recherches Aerospatiales, Paris (France).
WIND TUNNEL AIR INTAKE TEST TECHNIQUES
Jacky Leynaert *In* VKI, Intake Aerodynamics, Volume 2 1988 30 p (For primary document see N89-16748 09-02)
Avail: NTIS HC A14/MF A01

The general concept and validation of wind tunnel intake test setups are reviewed. The main intake test parameters are defined. Test rigs adapted to subsonic transport intakes, and to supersonic or combat aircraft intakes at supersonic Mach number, at transonic, and low speed are discussed. Devices for unsteady flow analysis, and for detailed inner flow probing are mentioned. ESA

N89-16752*# National Aeronautics and Space Administration. Lewis Research Center, Cleveland, OH.
COMPUTATIONAL METHODS FOR INLET AIRFRAME INTEGRATION
Charles E. Towne *In* VKI, Intake Aerodynamics, Volume 2 1988 43 p (For primary document see N89-16748 09-02)
Avail: NTIS HC A14/MF A01

Fundamental equations encountered in computational fluid dynamics (CFD), and analyses used for internal flow are introduced. Irrotational flow; Euler equations; boundary layers; parabolized Navier-Stokes equations; and time averaged Navier-Stokes equations are treated. Assumptions made and solution methods are outlined, with examples. The overall status of CFD in propulsion is indicated. ESA

N89-16753*# National Aeronautics and Space Administration. Lewis Research Center, Cleveland, OH.
CFD APPLICATION TO SUBSONIC INLET AIRFRAME INTEGRATION
Bernhard H. Anderson *In* VKI, Intake Aerodynamics, Volume 2 1988 59 p (For primary document see N89-16748 09-02)
Avail: NTIS HC A14/MF A01

The fluid dynamics of curved diffuser duct flows of military aircraft is discussed. Three-dimensional parabolized Navier-Stokes analysis, and experiment techniques are reviewed. Flow measurements and pressure distributions are shown. Velocity vectors, and the effects of vortex generators are considered. ESA

N89-16754*# National Aeronautics and Space Administration. Lewis Research Center, Cleveland, OH.
CFD APPLICATION TO SUPERSONIC/HYPERSONIC INLET AIRFRAME INTEGRATION
Thomas J. Benson *In* VKI, Intake Aerodynamics, Volume 2 1988 62 p (For primary document see N89-16748 09-02)
Avail: NTIS HC A14/MF A01

Supersonic external compression inlets are introduced, and the computational fluid dynamics (CFD) codes and tests needed to study flow associated with these inlets are outlined. Normal shock wave turbulent boundary layer interaction is discussed. Boundary layer control is considered. Glancing sidewall shock interaction is treated. The CFD validation of hypersonic inlet configurations is explained. Scramjet inlet modules are shown. ESA

N89-16755# Imperial Coll. of Science and Technology, London (England). Dept. of Aeronautics.
A STATISTICAL THEORY FOR GAS SURFACE INTERACTIONS IN RAREFIED HYPERSONIC FLOWS
A. A. Agbormbai Jul. 1988 65 p
(IC-Aero-88-01; ISSN-0308-7247; ETN-89-93297) Avail: NTIS HC A04/MF A01

The phenomenological approach to the modelling of gas surface interactions is generalized to include an arbitrary number of internal modes as well as an arbitrary number of solid atoms. A transition probability is introduced to characterize the interaction, so that the interaction potential is bypassed. A generalized reciprocity/detailed balance equation is constructed and symmetrized by casting the transition probability in a suitable form with respect to the forward and reverse process. This symmetrization permits models to be constructed via methods suggested by the calculus of distributions. The models consist of a series of statistical transformations simulating the contact transformation in analytical dynamics. The models also permit a continuous variation between specular and diffuse reflection. A gas surface interaction integral is proposed and used to demonstrate accordance with the H-theorem; equilibrium distributions are also constructed. The approach appears to be physically and mathematically plausible. ESA

N89-16756# Centre Aeroporte de Toulouse (France).
STUDY OF THE AERODYNAMIC SITUATION ALONG THE C 160 AIRCRAFT IN PARACHUTING CONFIGURATION [ETUDE DE LA SITUATION AERODYNAMIQUE LE LONG DU C 160 EN CONFIGURATION DE PARACHUTAGE]
M. Carol May 1988 97 p In FRENCH
(DAT-88-06; ETN-89-93610) Avail: NTIS HC A05/MF A01

Wind tunnel tests and flight tests were carried out to characterize the aerodynamic flow along and behind the C 160 aircraft when proceeding to a parachuting operation. The study gives indications to improve the aircraft design and the understanding of parachute behavior after leaving the aircraft. The test results, associated to a theoretical analysis show that the aerodynamical effect on the torsion of a parachute in automatic operation is negligible. ESA

N89-16757# National Aeronautical Lab., Bangalore (India). Fluid Mechanics Div.
NUMERICAL SOLUTION OF FLOW FIELDS AROUND DELTA WINGS USING EULER EQUATIONS METHOD
Anand Kumar and A. Das (Deutsche Forschungs- und Versuchsanstalt fuer Luft- und Raumfahrt, Brunswick, Germany, F.R.) Jan. 1987 15 p Presented at the International Vortex Flow Symposium on Euler Code Validation, Stockholm, Sweden, 1-3 Oct. 1986
(NAL-TM-FM-8701) Avail: NTIS HC A03/MF A01

Flow over cropped delta wings having a leading edge sweep of 65 deg and an aspect ratio of 1.38 are computed using the DFVLR Euler code. Both sharp and round leading edges are considered. Calculations are performed for angles of incidence of 10, 20 and 24 deg for free-stream Mach number of 0.85, and for angles of incidence of 2, 10, to 30 deg (5 deg) for free-stream Mach number of 0.4. Influence of grid refinement and surface pressure evaluation on the solution are also studied. Author

N89-16758*# Old Dominion Univ., Norfolk, VA. Dept. of Mechanical Engineering and Mechanics.
AN EXPERIMENTAL INVESTIGATION OF THE AERODYNAMIC CHARACTERISTICS OF SLANTED BASE OGIVE CYLINDERS USING MAGNETIC SUSPENSION TECHNOLOGY Progress Report, 1 Apr. - 30 Sep. 1988
Charles W. Alcorn and Colin Britcher Aug. 1988 90 p
(Grant NAG1-716)
(NASA-CR-184624; NAS 1.26:184624) Avail: NTIS HC A05/MF A01 CSCL 01A

An experimental investigation is reported on slanted base ogive cylinders at zero incidence. The Mach number range is 0.05 to 0.3. All flow disturbances associated with wind tunnel supports are eliminated in this investigation by magnetically suspending the wind tunnel models. The sudden and drastic changes in the lift, pitching moment, and drag for a slight change in base slant angle are reported. Flow visualization with liquid crystals and oils is used to observe base flow patterns, which are responsible for the sudden changes in aerodynamic characteristics. Hysteretic effects in base flow pattern changes are present in this investigation and are reported. The effects of a wire support attachment on the zero degree slanted base model is studied. Computational drag and transition location results using VSAERO and SANDRAG are presented and compared with experimental results. Base pressure measurements over the slanted bases are made with an onboard pressure transducer using remote data telemetry. Author

N89-16759*# National Aeronautics and Space Administration. Lewis Research Center, Cleveland, OH.
THREE DIMENSIONAL VISCOUS ANALYSIS OF A HYPERSONIC INLET
D. R. Reddy, G. E. Smith, M.-F. Liou, and Thomas J. Benson Jan. 1989 9 p Presented at the 27th Aerospace Sciences Meeting, Reno, NV, 9-12 Jan. 1989; sponsored in part by AIAA Prepared in cooperation with Sverdrup Technology Inc., Cleveland, OH
(NASA-TM-101474; E-4592; NAS 1.15:101474; AIAA-89-0004)
Avail: NTIS HC A02/MF A01 CSCL 01A

The flow fields in supersonic/hypersonic inlets are currently being studied at NASA Lewis Research Center using 2- and 3-D full Navier-Stokes and Parabolized Navier-Stokes solvers. These tools have been used to analyze the flow through the McDonnell Douglas Option 2 inlet which has been tested at Calspan in support of the National Aerospace Plane Program. Comparisons between the computational and experimental results are presented. These comparisons lead to better overall understanding of the complex flows present in this class of inlets. The aspects of the flow field emphasized in this work are the 3-D effects, the transition from laminar to turbulent flow, and the strong nonuniformities generated within the inlet. Author

N89-16760# Advisory Group for Aerospace Research and Development, Neuilly-Sur-Seine (France). Fluid Dynamics Panel.
REYNOLDS NUMBER EFFECTS IN TRANSONIC FLOW
A. Elsenaar, T. W. Binion, Jr., E. Stanewsky, and H. C. Hornung, ed. (California Inst. of Tech., Pasadena.) Mar. 1989 92 p
(AGARD-AG-303) Copyright Avail: NTIS HC A05/MF A01

Reynolds number effects in transonic flow are critically reviewed. A discussion is presented of the viscous effects observed on realistic configurations. The following geometries are considered: Airfoils and high aspect ratio wings typical of transport aircraft, fighter-type low aspect ratio delta wings, two- and three-dimensional bodies characteristic of missiles and combat aircraft fuselages, and afterbodies. Pseudo-Reynolds number effects are identified which may arise, for instance due to the influence of the Reynolds number on the wind tunnel environment and in turn affect the flow about a model. As an introduction, a brief retrospect of the history of Reynolds number effect is presented. Author

N89-16761*# Texas A&M Univ., College Station. Dept. of Aerospace Engineering.
DEVELOPMENT OF DIRECT-INVERSE 3-D METHODS FOR APPLIED TRANSONIC AERODYNAMIC WING DESIGN AND ANALYSIS Semiannual Progress Report, 1 Jul. - 31 Dec. 1988
Leland A. Carlson Feb. 1989 85 p
(Grant NAG1-619)
(NASA-CR-184788; NAS 1.26:184788; TAMRF-5373-89-01)
Avail: NTIS HC A05/MF A01 CSCL 01A

Progress in the direct-inverse wing design method in curvilinear coordinates has been made. This includes the remedying of a spanwise oscillation problem and the assessment of grid skewness, viscous interaction, and the initial airfoil section on the final design. It was found that, in response to the spanwise oscillation problem that designing at every other spanwise station produced the best results for the cases presented, a smoothly varying grid is especially needed for the accurate design at the wing tip, the boundary layer displacement thicknesses must be included in a successful wing design, the design of high and medium aspect ratio wings is possible with this code, and the final airfoil section designed is fairly independent of the initial section. Author

N89-16762*# California Univ., Berkeley. Dept. of Mechanical Engineering.
SUPERCRITICAL FLOW PAST A SYMMETRICAL BICIRCULAR ARC AIRFOIL
Maurice Holt and Khoy Chuah Yew 13 Feb. 1989 27 p
(Grant NAG1-725)
(NASA-CR-184787; NAS 1.26:184787) Avail: NTIS HC
A03/MF A01 CSCL 01A

A numerical scheme is developed for computing steady supercritical flow about symmetrical airfoils, applying it to an ellipse for zero angle of attack. An algorithmic description of this new scheme is presented. Application to a symmetrical bicircular arc airfoil is also proposed. The flow field before the shock is region 1. For transonic flow, singularity can be avoided by integrating the resulting ordinary differential equations away from the body. Region 2 contains the shock which will be located by shock fitting techniques. The shock divides region 2 into supersonic and subsonic regions and there is no singularity problem in this case. The Method of Lines is used in this region and it is advantageous to integrate the resulting ordinary differential equation along the body for shock fitting. Coaxial coordinates have to be used for the bicircular arc airfoil so that boundary values on the airfoil body can be taken with one direction of the coaxial coordinates fixed. To avoid taking boundary values at + or - infinity in the coaxial co-ordinary system, approximate analytical representation of the flow field near the tips of the airfoil is proposed. Author

N89-16763*# National Aeronautics and Space Administration. Ames Research Center, Moffett Field, CA.
GENERATION OF THREE-DIMENSIONAL BODY-FITTED GRIDS BY SOLVING HYPERBOLIC AND PARABOLIC PARTIAL DIFFERENTIAL EQUATIONS
Joseph L. Steger Jan. 1989 12 p
(NASA-TM-101069; A-89022; NAS 1.15:101069) Avail: NTIS
HC A03/MF A01 CSCL 01A

Hyperbolic grid generation procedures are described which have been used in external flow simulations about complex configurations. For many practical applications a single well-ordered (i.e., structured) grid can be used to mesh an entire configuration, in other problems, composite or unstructured grid procedures are needed. Although the hyperbolic partial differential equation grid generation procedure has mainly been utilized to generate structured grids, extension of the procedure to semiunstructured grids is briefly described. Extensions of the methodology are also described using two-dimensional equations. Author

N89-16764*# General Dynamics Corp., Fort Worth, TX.
PROPULSIVE-JET FLOW FIELD ANALYSIS USING THE THREE-DIMENSIONAL NAVIER-STOKES EQUATIONS Contract Report, Jul. 1985 - Mar. 1987
C. L. Reed Oct. 1988 30 p
(NASA Order A-30142-C)
(NASA-CR-177508; NAS 1.26:177508) Avail: NTIS HC
A03/MF A01 CSCL 01A

A three-dimensional Navier-Stokes code has been applied to the analysis of flow fields containing propulsive jets. Specifically, the application was made to a flow field containing a supersonic jet injected at an angle of 90 degrees to a subsonic free stream. Although wind tunnel data were available, the computational results were not readily comparable to the experimental data because of significant differences between the two plume trajectories. Reasons for the differences are suggested in the report and include: (1) incomplete convergence, (2) inadequate grid resolution in the high gradient regions, and (3) use of a low-order turbulence closure model. Author

N89-16765*# Aerometrics, Inc., Sunnyvale, CA.
EVALUATION AND APPLICATION OF A NEW INTERFEROMETRY TECHNIQUE FOR COMPRESSIBLE FLOW RESEARCH
William D. Bachalo and Michael C. Houser Oct. 1988 58 p
(Contract NAS2-11575)
(NASA-CR-177467; NAS 1.26:177467) Avail: NTIS HC
A04/MF A01 CSCL 01A

A new method for obtaining large scale interferograms of flow fields in real time was investigated. The method was based on the point diffraction interferometry technique. The method was modified to accommodate the higher laser power required in recording transonic and supersonic flow fields. Basic tests were conducted in unsteady flows and flows about circulation control airfoils at transonic speeds. It was found that vibration was not a significant factor in the application of the system. In the case of

the circulation control airfoils, the real-time viewing allowed the identification of the Coanda jet interaction with the external flow and the shedding of large scale vortices. The method proved to be very sensitive to the optical quality of the wind tunnel windows. The results obtained were compared with earlier interferograms obtained using interferometry. These results were in qualitative agreement. Author

N89-16847*# Army Aviation Systems Command, Moffett Field, CA.
A CRITICAL ASSESSMENT OF WIND TUNNEL RESULTS FOR THE NACA 0012 AIRFOIL
W. J. McCroskey *In* AGARD, Aerodynamic Data Accuracy and Quality: Requirements and Capabilities in Wind Tunnel Testing Jul. 1988 21 p Previously announced as N88-11636 (For primary document see N89-16846 09-09)
Copyright Avail: NTIS HC A22/MF A01 CSCL 01A

N89-16849# Office National d'Etudes et de Recherches Aeronautiques, Paris (France).
COMPARISON OF THE RESULTS OF TESTS ON A300 AIRCRAFT IN THE RAE 5 METRE AND THE ONERA F1 WIND TUNNELS
C. Quemard and P. B. Earnshaw (Royal Aircraft Establishment, Farnborough, England) *In* AGARD, Aerodynamic Data Accuracy and Quality: Requirements and Capabilities in Wind Tunnel Testing Jul. 1988 16 p (For primary document see N89-16846 09-09)
Copyright Avail: NTIS HC A22/MF A01

N89-16850# Boeing Vertol Co., Philadelphia, PA. Advanced Aircraft Aerodynamics.
ANALYTICAL AND EXPERIMENTAL METHODS USED TO RESOLVE THE AERODYNAMIC RESULTS OF TESTS CONDUCTED IN THREE TEST FACILITIES
Ross D. Clark and H. J. Rosenstein *In* AGARD, Aerodynamic Data Accuracy and Quality: Requirements and Capabilities in Wind Tunnel Testing Jul. 1988 15 p (For primary document see N89-16846 09-09)
Copyright Avail: NTIS HC A22/MF A01

N89-16858# Office National d'Etudes et de Recherches Aerospatiales, Modane (France).
PRECISION IMPROVEMENT OF TRANSPORT AIRCRAFT DRAG MEASUREMENTS [AMELIORATION DE LA PRECISION DE LA MESURE DE LA TRAINEE D'UN AVION DE TRANSPORT]
C. Armand and C. Pujol (Societe Nationale Industrielle Aerospatiale, Toulouse, France) *In* AGARD, Aerodynamic Data Accuracy and Quality: Requirements and Capabilities in Wind Tunnel Testing Jul. 1988 14 p In FRENCH Previously announced in IAA as A88-22597 (For primary document see N89-16846 09-09)
Copyright Avail: NTIS HC A22/MF A01

N89-16866# National Aerospace Lab., Amsterdam (Netherlands).
ON REYNOLDS NUMBER EFFECTS AND SIMULATION
A. Elsenaar *In* AGARD, Aerodynamic Data Accuracy and Quality: Requirements and Capabilities in Wind Tunnel Testing Jul. 1988 22 p (For primary document see N89-16846 09-09)
Copyright Avail: NTIS HC A22/MF A01

N89-16868# Naples Univ. (Italy). Inst. of Aerodynamics 'Umberto Nobile'.
EXPERIMENTS ON BOUNDARY LAYER TRANSITION TRIPPING AT LOW REYNOLDS NUMBERS
Giuseppe P. Russo *In* AGARD, Aerodynamic Data Accuracy and Quality: Requirements and Capabilities in Wind Tunnel Testing Jul. 1988 13 p (For primary document see N89-16846 09-09)
Copyright Avail: NTIS HC A22/MF A01

N89-16869# Office National d'Etudes et de Recherches Aeronautiques, Paris (France).
SOME DIFFICULTIES IN THE WIND TUNNEL PREDICTION OF MODERN CIVIL AIRCRAFT BUFFETING: PROPOSED REMEDIES
R. Destuynder, V. Schmitt, J. Berger, and R. Barreau (Societe Nationale Industrielle Aerospatiale, Toulouse, France) *In* AGARD, Aerodynamic Data Accuracy and Quality: Requirements and Capabilities in Wind Tunnel Testing Jul. 1988 14 p In FRENCH; ENGLISH summary (For primary document see N89-16846 09-09)
Copyright Avail: NTIS HC A22/MF A01

N89-16875# MATRA Service Aerodynamique, Velizy-Villacoublay (France).
ACCURACY OF LIFT AND CENTER-OF-THRUST MEASUREMENTS AT MISSILE CONTROL SURFACES
J. Perinelle and M. Ribadeau Dumas *In* AGARD, Aerodynamic Data Accuracy and Quality: Requirements and Capabilities in Wind Tunnel Testing Jul. 1988 17 p In FRENCH; ENGLISH summary (For primary document see N89-16846 09-09)
Copyright Avail: NTIS HC A22/MF A01

N89-16876# Naples Univ. (Italy). Inst. of Aerodynamics 'Umberto Nobile'.
COMPUTERIZED THERMOGRAPHIC TECHNIQUE FOR THE DETECTION OF BOUNDARY LAYER SEPARATION
R. Monti and G. Zuppardi *In* AGARD, Aerodynamic Data Accuracy and Quality: Requirements and Capabilities in Wind Tunnel Testing Jul. 1988 15 p (For primary document see N89-16846 09-09)
Copyright Avail: NTIS HC A22/MF A01

03 AIR TRANSPORTATION AND SAFETY

Includes passenger and cargo air transport operations; and aircraft accidents.

For related information see also *16 Space Transportation* and *85 Urban Technology and Transportation.*

N89-16766# Sandia National Labs., Albuquerque, NM. Systems Engineering Div.
AVIATION SECURITY: A SYSTEM'S PERSPECTIVE
James P. Martin 1988 35 p Presented at the 5th FAA International Civil Aviation Security Conference, Washington, DC, 24 Oct. 1988
(Contract DE-AC04-76DP-00789)
(DE89-002020; SAND-88-2629C; CONF-8810219-1) Avail: NTIS HC A03/MF A01

For many years the aviation industry and airports operated with security methods and equipment common to most other large industrial complexes. At that time, the security systems primarily provided asset and property protection. However, soon after the first aircraft hijacking the focus of security shifted to emphasize the security requirements necessary for protecting the traveling public and the one feature of the aviation industry that makes it unique---the airplane. The airplane and its operation offered attractive opportunities for the homesick refugee, the mentally unstable person and the terrorist wanting to make a political statement. The airport and its aircraft were the prime targets requiring enhanced security against this escalated threat. In response, the FAA, airport operators and air carriers began to develop plans for increasing security and assigning responsibilities for implementation. DOE

N89-16767# Dunlap and Associates, Inc., Norwalk, CT.
TECHNOLOGY ASSESSMENT FOR AIRCRAFT COMMAND IN EMERGENCY SITUATIONS Final Report, 28 Apr. 1987 - 31 May 1988
Richard D. Blomberg, Edward W. Bishop, John W. Hamilton, and Richard L. P. Custer (Worcester Polytechnic Inst., MA.) Oct. 1988 134 p Prepared in cooperation with Federal Aviation

Agency, Atlantic City, NJ
(Contract DTFA03-87-C-00020)
(DOT/FAA/CT-88/20; DA88-1) Avail: NTIS HC A07/MF A01

This technology assessment determined the feasibility of FAA support for development of a computer-based system to supplement crew function during in-flight fire/smoke incidents. The system is called Aircraft Command in Emergency Situations (ACES). It is limited to fire/smoke incidents in areas other than power-plant or lifting and control surfaces. It is to be used in large commercial air transports. Thirteen scenarios of in-flight fire/smoke incidents which had occurred or were likely to occur were written to define the events to which a flight crew might have to respond. The responses to each scenario, based on current practice, are described and presented on a timeline. The development of each incident is described as are the significant operational and environmental features. An analysis of each scenario is then made to identify problems encountered in detection and management of the incident. Separate analyses of current sensor technology, aircraft computer/display technology, and of human factors led to a hypothetical ACES system using smoke/heat sensing with determination of rate and extent of change in both. The postulated ACES was incorporated into the master warning concept with advisory displays forced to the cockpit. The scenarios were reanalyzed using the ACES and results compared to the first scenario analysis. It is concluded that an ACES is technologically feasible and can be used in and facilitate air crew emergency procedures. Training will be needed but crew workload will not be negatively affected. In almost every incident the ACES concept significantly reduced reaction time and severity. Author

N89-16768# National Transportation Safety Board, Washington, DC.
AIRCRAFT ACCIDENT/INCIDENT SUMMARY REPORT, TRAVIS AIR FORCE BASE, CALIFORNIA, 8 APRIL 1987
31 Dec. 1988 16 p
(PB88-910414; NTSB-AAR-88-03-SUM) Avail: NTIS HC A03/MF A01 CSCL 01C

This report is a summary of an aircraft accident investigated by the National Transportation Safety Board. The accident location and date is Travis Air Force Base, California, April 8, 1987. Author

N89-16769*# Battelle Columbus Labs., Mountain View, CA.
HUMAN FACTORS IN AVIATION OPERATIONS: THE HEARBACK PROBLEM
William P. Monan Nov. 1988 36 p
(Contract NAS2-11934)
(NASA-CR-177398; A-89108; NAS 1.26:177398) Avail: NTIS HC A03/MF A01 CSCL 01C

This report covers a study of ASRS reports wherein ATC controllers failed to monitor adequately (hearback) incorrect readbacks of ATC clearances. A total of 417 reports received over a period of 29 months from April 1981 through July 1983 comprised the study data set. Factors examined were: the reasons for a flight crew's getting clearances incorrectly, the operating factors that caused controllers to mishear or not hear the correct readbacks, and consequences of the various types of hearback misses. The principle conclusion of the study takes the form of a precaution to flight crews that a controller's not challenging a readback does not necessarily mean the readback is correct and that flight crews must explicitly question any doubtful or unusual aspects of clearances rather than depending on controllers to detect readback errors. Author

04 AIRCRAFT COMMUNICATIONS AND NAVIGATION

Includes digital and voice communication with aircraft; air navigation systems (satellite and ground based); and air traffic control.

For related information see also *17 Space Communications, Spacecraft Communications, Command and Tracking* and *Communications and Radar.*

N89-16770# Defence Science and Technology Organization, Salisbury (Australia).
GPS (GLOBAL POSITIONING SYSTEM) USER EQUIPMENT EVALUATION TECHNIQUES USING A ROTOR MOUNTED ANTENNA
J. S. Gubbay Aug. 1988 20 p
(AD-A200515; SRL-0018-TM; DODA-AR-005-416) Avail: NTIS HC A03/MF A01 CSCL 09A

The accuracy of the NAVSTAR Global Positioning System (GPS) permits evaluation of dynamic performance of user equipments by mounting the antenna on a rotor of practical dimension. The reported diameter of the circular path described by the antenna phase center will depend on Kalman filter characteristics and will tend Rayleigh statistics through measurement delay intervals up to 1 min. This characteristic of system noise and the development of symmetry techniques permits delayed difference measurement of reported diameter of antenna path to an accuracy of better than 0.5 m over 30 min. This method of Kalman error measurement provides a means for establishing a benchmark for integration filter design software simulation. GRA

N89-16771# Carnegie-Mellon Univ., Pittsburgh, PA. Software Engineering Inst.
INERTIAL NAVIGATION SYSTEM SIMULATOR: BEHAVIORAL SPECIFICATION Final Technical Report
Stefan F. Landherr and Mark H. Klein Oct. 1987 48 p
(Contract F19628-85-C-0003)
(AD-A200604; CMU/SEI-87-TR-33; ESD-TR-87-196) Avail: NTIS HC A03/MF A01 CSCL 12E

The Ada Embedded Systems Testbed Project at the Software Engineering Institute is specifying and developing a representative real-time application. This document augments an original set of specifications written by a Navy affiliate. The purpose of this behavioral specification is to clarify and augment the original. GRA

N89-16772# Carnegie-Mellon Univ., Pittsburgh, PA. Software Engineering Inst.
INERTIAL NAVIGATION SYSTEM SIMULATOR PROGRAM: TOP-LEVEL DESIGN Final Technical Report
Stefan F. Landherr and Mark H. Klein Oct. 1987 49 p
(Contract F19628-85-C-0003)
(AD-A200605; CMU/SEI-87-TR-34; ESD-TR-87-197) Avail: NTIS HC A03/MF A01 CSCL 12E

A real-time Ada application, an Inertial Navigation System (INS) simulator, is being developed by the Ada Embedded Systems Testbed Project as a vehicle to analyze issues regarding the use of Ada in the real-time embedded domain and to provide a context for future experimentation. The technical philosophy behind developing a real-time Ada artifact is to: (1) select a representative (e.g., strict timing demands, multiple concurrent activities, low-level I/O error handling, interrupts, and periodic activities) real-time application; (2) use Ada tasks as the unit on concurrency for the real-time scheduling research community. In particular, the INS simulator most satisfy a set of timing requirements that are similar to an INS with respect to data updating, message transmission, and message reception. This document discusses the top-level design of this application from three points of view: data flow perspective, the concurrency and control perspective, and the Ada module perspective. GRA

05 AIRCRAFT DESIGN, TESTING AND PERFORMANCE

Includes aircraft simulation technology.

For related information see also *18 Spacecraft Design, Testing and Performance* and *39 Structural Mechanics*.For land transportation vehicles see *85 Urban Technology and Transportation*.

N89-16773 Cranfield Inst. of Tech., Bedford (England).
THE DESIGN, CONSTRUCTION AND TEST OF A POSTBUCKLED, CARBON FIBRE REINFORCED PLASTIC WING BOX Ph.D. Thesis
W. G. Brooks 1987 290 p
Avail: Univ. Microfilms Order No. BRDX82023

Methods of analysis have been evaluated including: (1) non-linear finite element analysis for the prediction of panel postbuckling; (2) a simpler technique based on an effective width method (forming the core of a design program, OPTIMIST, it predicts buckling loads, postbuckled reduced stiffness and overall column failure of co-cured hat stiffened panels; and (3) the use of the effective width method allied to a large scale, linear finite element analysis. The work includes the development of a new method of construction for composite box structures. The wing skin, stiffeners and rib flanges are co-cured together. Integral slotted joint features are formed in each part. The structure is then adhesively bonded together. A full description of the manufacture of the wing box is included. Dissert. Abstr.

N89-16774# Texas A&M Univ., College Station. Dept. of Mechanical Engineering.
NONLINEAR DYNAMIC RESPONSES OF COMPOSITE ROTOR BLADES Final Technical Report, 1 Dec. 1985 - Jun. 1988
John J. Engblom and Ozden O. Ochoa Aug. 1988 72 p
(Contract F49620-86-K-0003)
(AD-A200145; ME-5375-88; AFOSR-88-1018TR) Avail: NTIS HC A04/MF A01 CSCL 01C

Summarized are research activities related to Nonlinear Dynamic Response of Composite Rotor Blades. Fundamental to the analysis is the development of a continuum formulation that can accurately account for the effects of interlaminar shear and interlaminar normal stress variation through-the-thickness of a laminate. Technical highlights of the research efforts to date are presented for each of the proposed tasks; namely, Nonlinear Displacement Formulation for Composite Media, Incorporate Damage Mechanisms into Dynamic Response Formulation and Correlation of Formulated Response Model with Experimental data. GRA

N89-16775# Analytical Methods, Inc., Redmond, WA.
DEVELOPMENT OF A PANEL METHOD FOR MODELING CONFIGURATIONS WITH UNSTEADY COMPONENT MOTIONS, PHASE 1 Final Report, 1 Jul. 1987 - 31 Jan. 1988
David R. Clark and Brian Maskew 15 Apr. 1988 35 p
(Contract DAAL03-87-C-0011)
(AD-A200255; AMI-8801; ARO-25090.1-EG-SBI) Avail: NTIS HC A03/MF A01 CSCL 01C

This report reviews the background to the calculation of unsteady rotor and fuselage loads and presents results from an analysis of a typical helicopter configuration made using a panel method operated in a time-stepping mode. The method models the fuselage and blades using surface singularities and the shed and trailing wakes with doublet lattice sheets. Unsteady local pressures and component forces are presented and the ability of the analysis to determine dynamic phenomena such as fuselage/blade-passage events and blade/vortex interactions is demonstrated. GRA

N89-16776# Anamet Labs., Inc., Hayward, CA.
FINITE ELEMENT ANALYSIS OF F-16 BALLISTIC TESTS Interim Report, Aug. 1986 - Aug. 1987
Gordon R. Negaard Jul. 1988 231 p
(Contract F33615-84-C-3216)
(AD-A200289; Rept-887.1C; AFWAL-TR-88-3041) Avail: NTIS HC A11/MF A01 CSCL 01C

The results of finite element analyses of an F-16 wing is presented. The analysis includes modeling of damage cases based on test results, modeling of patches to repair the damage, and NASTRAN static and dynamic analyses from which stresses, displacements, and natural frequencies were obtained. GRA

N89-16777# Naval Postgraduate School, Monterey, CA.
A MODEL OF THE EFFECT OF SPARING AND REPAIR TURNAROUND TIME OF THE INERTIAL NAVIGATION SYSTEM ON AIRCRAFT READINESS FOR THE F/A-18 M.S. Thesis
Christopher A. Hase Jun. 1988 65 p
(AD-A200317) Avail: NTIS HC A04/MF A01 CSCL 15E

Modern aircraft design allows for short turnaround times by removing the failed component and installing an operational one. The defective component is then either repaired in the squadron or turned in to supply which then sends the defective component to an Intermediate Maintenance Activity (IMA) for repair. The aircraft is unable to be turned around for another flight if supply is out of stock of that component without resorting to additional maintenance measures. This is when aircraft readiness experiences a measureable deterioration due to supply not having the part on hand. Aircraft readiness, as defined in this thesis, is the ability of a specific F/A-18 to perform all of its missions. A simulation model which measures the time that an aircraft is not ready (downtime) was developed to relate the turnaround time at the IMA and the quantity of spare parts maintained by the supply system to this lack of readiness. The model developed showed that a decrease in the turnaround time of a part at the IMA, the increase in quantity of spare parts maintained by the supply system cause a nonlinear reduction in aircraft readiness. This model could be used to aide decision makers in determining the effect changes in spare parts quantities and IMA turnaround times could have on aircraft readiness. GRA

N89-16778 Maryland Univ., College Park.
AEROELASTIC OPTIMIZATION OF A HELICOPTER ROTOR Ph.D. Thesis
Joon Won Lim 1988 232 p
Avail: Univ. Microfilms Order No. DA8818424

Structural optimization of a hingeless rotor is investigated to reduce oscillatory hub loads while maintaining aeroelastic stability in forward flight. Design variables include spanwise distribution of nonstructural mass, chordwise location of blade center of gravity and blade bending stiffnesses. The objective function is expressed as a function of one or more components of oscillatory hub loads with suitable weighting functions. For inequality constraints, the aeroelastic stability of the blade in forward flight is selected to keep the blade aeroelastically stable. An aeroelastic analysis of rotors, based on a finite element method in space and time, is linked with optimization algorithms to perform optimization of rotor blades. The vehicle trim and blade steady response are calculated iteratively as one coupled solution using a modified Newton method. Eigenvalues corresponding to different blade modes are calculated using Floquet transition matrix theory. For the optimization process, a new methodology, direct analytical approach for calculation of sensitivity derivatives of blade response, hub loads and eigenvalues with respect to design variable is proposed. Dissert. Abstr.

N89-16779*# Planning Research Corp., Hampton, VA. Aerospace Technologies Div.
AN INDIRECT METHOD FOR NUMERICAL OPTIMIZATION USING THE KREISSELMEIR-STEINHAUSER FUNCTION Final Report
Gregory A. Wrenn Washington NASA [1989] 82 p
(Contract NAS1-18000)
(NASA-CR-4220; NAS 1.26:4220) Avail: NTIS HC A05/MF A01 CSCL 01C

A technique is described for converting a constrained optimization problem into an unconstrained problem. The technique transforms one of more objective functions into reduced objective

functions, which are analogous to goal constraints used in the goal programming method. These reduced objective functions are appended to the set of constraints and an envelope of the entire function set is computed using the Kreisselmeir-Steinhauser function. This envelope function is then searched for an unconstrained minimum. The technique may be categorized as a SUMT algorithm. Advantages of this approach are the use of unconstrained optimization methods to find a constrained minimum without the draw down factor typical of penalty function methods, and that the technique may be started from the feasible or infeasible design space. In multiobjective applications, the approach has the advantage of locating a compromise minimum design without the need to optimize for each individual objective function separately. Author

N89-16741# Air Force Wright Aeronautical Labs., Wright-Patterson AFB, OH. Flight Dynamics Lab.
INLET-ENGINE COMPATIBILITY
Lewis E. Surber and Clay Fujimara *In* VKI, Intake Aerodynamics, Volume 1 1988 32 p (For primary document see N89-16738 09-02)
Avail: NTIS HC A15/MF A01

N89-16744# Air Force Wright Aeronautical Labs., Wright-Patterson AFB, OH. Flight Dynamics Lab.
INTAKE-AIRFRAME INTEGRATION
Lewis E. Surber *In* VKI, Intake Aerodynamics, Volume 1 1988 66 p (For primary document see N89-16738 09-02)
Avail: NTIS HC A15/MF A01

N89-16745# British Aerospace Aircraft Group, Preston (England). Military Aircraft Div.
INTAKES FOR HIGH ANGLE OF ATTACK
D. C. Leyland *In* VKI, Intake Aerodynamics, Volume 1 1988 26 p (For primary document see N89-16738 09-02)
Avail: NTIS HC A15/MF A01

N89-16746# Von Karman Inst. for Fluid Dynamics, Rhode-Saint-Genese (Belgium).
TRANSONIC COWL DESIGN
J. Seddon *In its* Intake Aerodynamics, Volume 1 1988 23 p (For primary document see N89-16738 09-02)
Avail: NTIS HC A15/MF A01

N89-16749# Office National d'Etudes et de Recherches Aerospatiales, Paris (France).
TRANSPORT AIRCRAFT INTAKE DESIGN
Jacky Leynaert *In* VKI, Intake Aerodynamics, Volume 2 1988 28 p (For primary document see N89-16748 09-02)
Avail: NTIS HC A14/MF A01

N89-16750# Office National d'Etudes et de Recherches Aerospatiales, Paris (France).
MISSILE INTAKES
Gerard Laruelle *In* VKI, Intake Aerodynamics, Volume 2 1988 76 p (For primary document see N89-16748 09-02)
Avail: NTIS HC A14/MF A01

N89-17278# Fraunhofer-Inst. fuer Betriebsfestigkeit, Darmstadt (Germany, F.R.).
DAMAGE TOLERANCE BEHAVIOR OF FIBER REINFORCED COMPOSITE AIRFRAMES [ZUM SCHADENSTOLERANZVERHALTEN VON LUFTFAHRZEUGKONSTRUKTIONEN AUS FASERVERBUNDWERKSTOFFEN]
J. J. Gerharz and H. Huth *In its* Papers of the 5th LBF Colloquium 1988 p 93-110 In GERMAN (For primary document see N89-17272 09-39)
Avail: NTIS HC A12/MF A01

06 AIRCRAFT INSTRUMENTATION

Includes cockpit and cabin display devices; and flight instruments.

For related information see also *19 Spacecraft Instrumentation* and *35 Instrumentation and Photography.*

N89-16780# Advisory Group for Aerospace Research and Development, Neuilly-Sur-Seine (France). Propulsion and Energetics Panel.
ENGINE CONDITION MONITORING: TECHNOLOGY AND EXPERIENCE
Oct. 1988 462 p In ENGLISH and FRENCH Symposium held in Quebec City, Quebec, 30 May - 3 Jun. 1988
(AGARD-CP-448; ISBN-92-835-0481) Copyright Avail: NTIS HC A20/MF A01

Topics addressed include: military operations; civil experience; manufacturer's perspective; turboprops and turboshafts; systems; diagnostic methods; and advanced technologies. Questions and answers of the discussions follow each paper. For individual titles, see N89-16781 through N89-16819.

N89-16781# NATO European Fighter Management Agency, Munich (Germany, F.R.).
OPERATIONAL REQUIREMENTS FOR ENGINE CONDITION MONITORING FROM THE EFA VIEWPOINT **c07**
J. V. Goodfellow *In* AGARD, Engine Condition Monitoring: Technology and Experience Oct. 1988 4 p (For primary document see N89-16780 09-06)
Copyright Avail: NTIS HC A20/MF A01

The Engine Health Monitoring (EHM) System for the European Fighter Aircraft (EFA) is to be an integral part of the overall Weapons Systems Integrated Monitoring and Recording System. This will include both an on-aircraft element and a ground-based station which will have to interface with the different logistics ADP systems being developed. By means of measurements and analyses the EHM is required to automatically and continuously monitor the condition of the engine and to detect and accurately diagnose any need for immediate and future maintenance actions. The purpose is to provide for a rapid turn-around at the flight line and to reduce both the need and the time required for all maintenance thereby increasing the overall availability for operational use. The intention is that this shall contribute to the significant improvement in weapon system cost effectiveness that is believed to be achieveable through greater attention to reliability, maintainability, and testability. Author

N89-16782# Naval Air Systems Command, Washington, DC.
AN OVERVIEW OF US NAVY ENGINE MONITORING SYSTEM PROGRAMS AND USER EXPERIENCE **c07**
Andrew J. Hess *In* AGARD, Engine Condition Monitoring: Technology and Experience Oct. 1988 16 p (For primary document see N89-16780 09-06)
Copyright Avail: NTIS HC A20/MF A01

The Naval Air System Command (NAVAIR) has made a commitment to require inflight engine monitoring capabilities and Engine Monitoring Systems (EMS) on all new aircraft and engine programs. The current EMS requirement and system design concepts are the end result of over 15 years of developing system capabilities and justifying system benefits. These requirements and system design concepts are based on the lessons learned from the F/A-18 and A-7E Inflight Engine Condition Monitoring System (IECMS) program. The highly successful A-7E IECMS is the cornerstone on which all Navy EMS are based today. NAVAIR has revised the general engine specifications to contain detailed requirements for a comprehensive EMS. These requirements were included for flight safety, maintenance, engineering management, and operational support benefits. These specification requirements were used on all new aircraft/engine programs (e.g., F-14A+, F-14D, A-6F, AV-8B, E-2C re-engine, and V-22). When justifiable, EMS is also being considered for retrofit on several older aircraft/engine applications. An overview is given of the U.S. Navy EMS program status. Established EMS functional capabilities and requirements are discussed and detailed specification items are

reviewed. Current EMS projects are examined with respect to system description, program status and individual peculiarities. Finally, conclusions are given on EMS projected benefits, user experience, lessons learned, and future directions of this technology. Author

N89-16783# Royal Air Force, London (England).
ENGINE USAGE CONDITION AND MAINTENANCE MANAGEMENT SYSTEMS IN THE UK ARMED FORCES **c07**
W. D. M. Fletcher and N. A. Bairsto *In* AGARD, Engine Condition Monitoring: Technology and Experience Oct. 1988 5 p (For primary document see N89-16780 09-06)
Copyright Avail: NTIS HC A20/MF A01

The cost effectiveness of engine condition monitoring is often questioned. The Royal Air Force (RAF) has considerable experience in engine condition monitoring based on a series of trials. Recently aircraft were introduced with comprehensive monitoring systems. Previous condition usage monitoring trials are outlined together with the reasons for changing from scheduled based maintenance to condition based maintenance. The cost effectiveness of various methods is revealed and the difficulty of justifying the retrofit of equipment fleetwide is discussed. Finally, some of the current activities in the RAF on condition monitoring are presented. Author

N89-16784# National Defence Headquarters, Ottawa (Ontario). Directorate of Transport and Helicopter Engineering and Maintenance.
CANADIAN FORCES AIRCRAFT CONDITION/HEALTH MONITORING: POLICY, PLANS AND EXPERIENCE **c07**
Christopher Schofield, Ross LaGrandeur, Francois Dube, Thomas Harris, Robert W. Cue, and Alain LeBlanc *In* AGARD, Engine Condition Monitoring: Technology and Experience Oct. 1988 10 p (For primary document see N89-16780 09-06)
Copyright Avail: NTIS HC A20/MF A01

Current Canadian Forces (CF) policy with respect to aircraft Engine Condition/Health Monitoring (ECM/EHM) is highlighted. In doing so, a summary of CF aircraft types and the ECM/EHM techniques applied to each is presented. The CF's experience to date with the development and application of ECM/EHM is reviewed. This includes an examination of the effectiveness of the CF Spectrometric Oil Analysis Program and the use of magnetic particle detectors and manual performance trending. Present plans for further development and implementation of policy; methodologies and techniques; and for the integration of these into an effective ECM/EHM capability that will pay benefits both in terms of life cycle costs and operational availability, are presented. Author

N89-16785# German Air Force Air Armament Directorate, Cologne (Germany, F.R.).
ON BOARD LIFE MONITORING SYSTEM TORNADO (OLMOS)
J. H. Kunz and U. Schulz (Dornier-Werke G.m.b.H., Friedrichshafen, Germany, F.R.) *In* AGARD, Engine Condition Monitoring: Technology and Experience Oct. 1988 6 p (For primary document see N89-16780 09-06)
Copyright Avail: NTIS HC A20/MF A01

The development of the onboard life monitoring system (OLMOS) of the GE Tornado proved, that on-board monitoring is possible, and the received data can be used in the logistic system. The Tornado OLMOS is a system which serves engine, structure, and functional equipment. The level of integration is high, but due to the structured software approach the system can be handled. The software was developed by four companies, and in the using phase the same companies are sharing the SW maintenance. High integrated systems definitely do need a very close management on both sides, the government and the industry. The OLMOS proves that even commercial and proprietary aspects can be worked out. Author

N89-16786# Royal Air Force, London (England).
INFORMATION MANAGEMENT SYSTEMS FOR ON-BOARD MONITORING SYSTEMS
P. J. Jenkins *In* AGARD, Engine Condition Monitoring: Technology and Experience Oct. 1988 8 p (For primary document see N89-16780 09-06)
Copyright Avail: NTIS HC A20/MF A01

With the advent of microprocessors is a phase which has heralded a host of advances in aircraft mounted equipment. It promises to yield rich dividends for the hard pressed maintenance engineer by providing detailed information on equipment performance to enable defects to be accurately and rapidly diagnosed. Latest develpments in the propulsion field show the potential of being able to anticipate certain types of defects and thus achieve true on-condition maintenance in these cases. The aim is to highlight the vitally important role played by maintenance information management systems in storing, analyzing, and displaying the data captured by on-board monitoring systems and to make recommendations for a code of practice for the successful implementation of such systems. Author

N89-16787# GasTOPS Ltd., Ottawa (Ontario).
CF-18 ENGINE PERFORMANCE MONITORING **c07**
D. E. Muir, D. M. Rudnitski, and Robert W. Cue (National Defence Headquarters, Ottawa, Ontario) *In* AGARD, Engine Condition Monitoring: Technology and Experience Oct. 1988 20 p (For primary document see N89-16780 09-06)
Copyright Avail: NTIS HC A20/MF A01

The Canadian Forces (CF) have adopted a conditional maintenance concept for the engines of the CF-18 fighter aircraft. In support of this concept, advanced engine performance monitoring procedures are being developed to track the general performance level of each engine and identify problematic engine components. The procedures are based on takeoff ground roll data recorded by the aircraft In-Flight Engine Condition Monitoring System and steady-state data obtained from automated Engine Test Facilities. The development and field evaluation of these procedures is described. A discussion of future development work and related research activities is also included. Author

N89-16788# Rockwell International Corp., Lakewood, CA.
B-1B CITS ENGINE MONITORING
B. Laine and K. Derbyshire *In* AGARD, Engine Condition Monitoring: Technology and Experience Oct. 1988 12 p (For primary document see N89-16780 09-06)
Copyright Avail: NTIS HC A20/MF A01

The Central Integrated Test Systems (CITS) is a real-time tests system which continually monitors the performance of the 34 principal systems, onboard the B-1B aircraft, including the four General Electric F101 turbofan engines. The CITS consists of an onboard computer, four data acquisition units, a data conversion unit, a printer, a magnetic tape recorder, and a control and display panel. Approximately 19,000 parameters are available for recording and display purposes. The engine diagnostic algorithm was designed in close coordination with General Electric. Information obtained from early test cell runs was utilized in the original logic design. Many modifications were made as a result of flight test experience, but the overall test sequence has remained unchanged. The engine diagnostic software utilizes approximately 100 parameters per engine. The test logic is exercised four time per second and a fault is declared is a failure condition occurs for six consecutive passes. Every effort is made to ensure that a single failure will result in only one fault code out of 154 possible codes per engine. The B-1B engine diagnostic program is the most advanced flying test algorithm. Its inherent complexities are due to calculations of test limits based on aircraft flight mode, environmental conditions, and engine control schedules. These limits are then compared to actual engine readings, and if established limits are exceeded, a fault code is annunciated. Author

N89-16789# Motoren- und Turbinen-Union Muenchen G.m.b.H. (Germany, F.R.).
ENGINE LIFE CONSUMPTION MONITORING PROGRAM FOR RB199 INTEGRATED IN THE ON-BOARD LIFE MONITORING SYSTEM

J. Broede *In* AGARD, Engine Condition Monitoring: Technology and Experience Oct. 1988 11 p (For primary document see N89-16780 09-06)
Copyright Avail: NTIS HC A20/MF A01

The On-board Life Monitoring System (OLMOS) of the GE Tornado consists of on-board equipment (data acquisition unit, DAU) where the majority of the data processing is carried out, and of ground equipment (OLMOS Ground Station, OGS, connected to the Central Logistic Support System, BMS) where the majority of the data management tasks are carried out. The Engine Life Consumption Monitoring Program (ELCMP) is part of OLMOS. Its main task is LCF life consumption calculation, which consists of data acquisition and data checking, calculation of temperatures and stresses, as well as damage assessment. A general view of the calculation path within ELCMP is given, and the hardware structure of the system is presented. Some advantages of individual and complete engine monitoring are pointed out. Author

N89-16790# Ministry of Defence, London (England). Directorate of Engines.
RECENT UK TRIALS IN ENGINE HEALTH MONITORING: FEEDBACK AND FEEDFORWARD **c07**
M. J. Sapsard *In* AGARD, Engine Condition Monitoring: Technology and Experience Oct. 1988 8 p (For primary document see N89-16780 09-06)
Copyright Avail: NTIS HC A20/MF A01

Engine health monitoring effectiveness had to be quantified prior to large scale commitment by the UK Services. Some of the activities undertaken in Air Staff Target 603 are described. A program was set up to assess that effectiveness. Also described are some of the incidental lessons learned from this and other related health monitoring exercises. Author

N89-16791# Turkish Air Force, Ankara. Aircraft Engines Branch.
F110 ENGINE MONITORING AND MAINTENANCE MANAGEMENT SYSTEMS FOR F-16 C/D **c07**
F. Algun *In* AGARD, Engine Condition Monitoring: Technology and Experience Oct. 1988 12 p (For primary document see N89-16780 09-06)
Copyright Avail: NTIS HC A20/MF A01

The engine monitoring and management systems employed by the Turkish Air Force for F110-GE-100 engines of F-16 C/D aircraft are described. These systems include the Engine Monitoring System (EMS) and the Minimum Essential Engine Tracking System (MEETS). The EMS performs the acquisition, transfer and processing of engine data for maintenance use. The systems monitors engine operation, and determines engine exceedances and faults; isolates faults to appropriate level and processes data to interface with other data systems. The MEETS provides an automated means of managing on-condition maintenance of fighter engines. This system tracks engines and components in terms of operation time, temperature, and cycle limits, and also forecasts remaining flying and engine operation hours for an individual engine, aircraft, or the whole fleet. The operation of the systems and future plans to develop and implement a unique data automation systems are discussed. This automated data system will be capable of supporting all the base level functions of aircraft, engines, trainers, support equipment, test equipment, missiles, munitions and communications/electronics. Author

N89-16792# Deutsche Lufthansa A.G., Hamburg (Germany, F.R.). Maintenance Systems and Reliability.
ENGINE CONDITION MONITORING: STATE-OF-THE-ART CIVIL APPLICATION
Heinrich Schlueter and Rolf Schoeddert *In* AGARD, Engine Condition Monitoring: Technology and Experience Oct. 1988 8 p (For primary document see N89-16780 09-06)
Copyright Avail: NTIS HC A20/MF A01

With the introduction of the AIRBUS A-310, an enhanced ECM concept was established at Lufthansa. Highlights of the theme include application areas and the economic aspects of everyday airline operation. The ECM information system supports maintenance personnel in detecting incipient engine failures, in carrying out optimum adjustment of engine controls, and in cutting down the number of engine run-ups. It also assists overhaul personnel in removal planning and overhaul planning. All data are acquired by an aircraft integrated data system through expanded engine instrumentation and are periodically reported through an on-board printer. Data printouts are entered into the Lufthansa computer network from each flight destination station. A high degree of actuality data are processed on-line in the central computer at the Frankfurt maintenance base. In addition to engine modular performance and mechanical parameter analysis, data processing also performs automatic trend recognition and alert report generation. Author

N89-16793# Air France, Paris. Direction du Materiel.
THE CFM 56-5 ON THE A-320 AT AIR FRANCE [LE CFM 56-5 SUR A320 A AIR FRANCE]
P. Chetail *In* AGARD, Engine Condition Monitoring: Technology and Experience Oct. 1988 19 p In FRENCH (For primary document see N89-16780 09-06)
Copyright Avail: NTIS HC A20/MF A01

A brief history of engine monitoring strategies used by Air France is presented and the systems limitations encountered in service are discussed. The engine monitoring system to be used for the A-320 aircraft is described. The use of the AIRCOM system, the automatic alert function, and the use of the GEM (Ground based Engine Monitoring) program for data analysis are discussed. M.G.

N89-16794# Aerospatiale Usines de Toulouse (France). Aircraft Div.
IMPLICATION OF ENGINE PERFORMANCE MONITORING FOR THE AIRCRAFT MANUFACTURER [IMPLICATION DE L'AVIONNEUR DANS LE SUIVI DES PERFORMANCES DU MOTEUR]
A. Vieillard *In* AGARD, Engine Condition Monitoring: Technology and Experience Oct. 1988 6 p In FRENCH (For primary document see N89-16780 09-06)
Copyright Avail: NTIS HC A20/MF A01

The experience acquired by Aerospatiale in the Airbus and ATR programs has highlighted the necessity for the aircraft manufacturers to be associated with Engine Conditioning Monitoring (ECM) system implementation. The aircraft manufacturer will thus be more involved as regards: the acquisition of information on the design of airborne systems and validation of measurement systems on the basis of flight tests; and the use of information to ensure the consistency of and engine models used by the aircraft in engine monitoring systems and familiarity with the ECM system. The predictable growth of this performance monitoring activity will necessitate closer coordination with the engine manufacturers and airlines, the objective still being to quantify the deterioration of each aircraft subassembly, i.e., the engines, the airframe and their respective components. Author

N89-16795# Pratt and Whitney Aircraft, West Palm Beach, FL.
F100-PW-220 ENGINE MONITORING SYSTEM
Dennis A. Myers and G. William Hogg *In* AGARD, Engine Condition Monitoring: Technology and Experience Oct. 1988 9 p (For primary document see N89-16780 09-06)
Copyright Avail: NTIS HC A20/MF A01

The development and operational experience is reviewed of the F100-PW-220 Engine Monitoring System currently in service with the U.S.A.F. and other national defense air forces utilizing the F100-PW-220 engine and its derivatives. The F100-PW-220 Engine Monitoring System (EMS) is an advanced logistics support tools in production for the Pratt and Whitney F100 family of gas turbine engines. The introduction of the PW-220 EMS represents over 10 yrs of diagnostic system and maintenance technology development using aerospace electronic component design and digital engine control system implementation. The PW-220 EMS is a comprehensive engine support system that is fully integrated

with in-flight aircraft operating systems, as well as, ground based maintenance and logistics systems. Author

N89-16796# Societe Nationale d'Etude et de Construction de Moteurs d'Aviation, Evry Cedex (France).
SERVICE LIFE CALCULATOR FOR THE M53 TURBOFAN ENGINE [LE CALCULATEUR DE POTENTIEL SUR LE REACTEUR M53] **c07**
Claude Sprung *In* AGARD, Engine Condition Monitoring: Technology and Experience Oct. 1988 15 p In FRENCH (For primary document see N89-16780 09-06)
Copyright Avail: NTIS HC A20/MF A01

The functional requirements for a service life calculator are defined and the flight and ground equipment comprising such a system are described. A system utilization philosophy is defined and preliminary results from studies considering the application of service life calculators are presented. Author

N89-16797# Rolls-Royce Ltd., Bristol (England). Engine Data Systems.
MILITARY ENGINE CONDITION MONITORING SYSTEMS: THE UK EXPERIENCE
C. M. OConnor *In* AGARD, Engine Condition Monitoring: Technology and Experience Oct. 1988 8 p (For primary document see N89-16780 09-06)
Copyright Avail: NTIS HC A20/MF A01

The monitoring of engine usage is probably as old as the gas turbine engine itself. However, it was not until the mid-seventies that the concept of engine monitoring became viable following the appearance and general availability of digital electronics, including the minicomputer. Since, the proliferation of engine condition monitoring has resulted in the development of many different systems and it is now customary for defense organizations to include it among their requirements for new military aircraft. The functional requirements for engine condition monitoring are usually defined in general terms, except for the life usage monitoring of major rotating components, these being the discs and the turbines. The level of importance afforded to the monitoring of these components is attributable to safety and economic factors. Engine condition monitoring in the UK military has been built on the foundations of usage monitoring. It is interesting that except for vibration and oil system monitoring, the engine parameters required for usage monitoring can provide enough data for many other condition monitoring functions. This idea is further expanded and detailed. Author

N89-16798# General Electric Co., Cincinnati, OH. Monitoring Systems Engineering.
MILITARY ENGINE MONITORING STATUS AT GE AIRCRAFT ENGINES, CINCINNATI, OHIO
R. J. E. Dyson and M. J. Ashby *In* AGARD, Engine Condition Monitoring: Technology and Experience Oct. 1988 11 p (For primary document see N89-16780 09-06)
Copyright Avail: NTIS HC A20/MF A01

The design and development of GE Aircraft engines of recent military engine monitoring systems is described. In particular, the systems for the F101-GE-102 engine in the B-1B aircraft and the F110-GE-100 engine in the F-16C/D are used as examples. Since both of these systems have recently been introduced into service, this experience is discussed together with operational status. These present systems are compared with future evolutionary trends which are affected by the development of miniaturized, rugged electronics and by the desire to minimize the unique hardware and software required for engine monitoring. A discussion of interfaces, both airborne to the flight crew, and, through support equipment and ground analysis programs, to the ground crew, is included. Author

N89-16799# General Electric Co., Cincinnati, OH. Monitoring Systems Engineering.
COMMERCIAL ENGINE MONITORING STATUS AT GE AIRCRAFT ENGINES, CINCINNATI, OHIO
R. J. E. Dyson and J. E. Paas *In* AGARD, Engine Condition Monitoring: Technology and Experience Oct. 1988 12 p (For primary document see N89-16780 09-06)
Copyright Avail: NTIS HC A20/MF A01

The design, introduction and development of expanded commercial engine monitoring systems by GE Aircraft Engine is described. The history of present systems is outlined, starting from the introduction of the CF6-80A3 engine for the A310 aircraft of the Propulsion Multiplexer (PMUX) which has led to similar systems on the CF6-80C2 engine. The impact of the full authority digital control on future systems is also discussed. The introduction and application of the Ground-based Engine Monitoring (GEM) software developed by GE in conjunction with several airline users is recounted. The original software development occurred in parallel with the expanded sensor complement and digitization of data. A description of the functions of a typical ground software program is provided together with proposed improvements and future directions. Author

N89-16800# Motoren- und Turbinen-Union Muenchen G.m.b.H. (Germany, F.R.).
THE ADVANTAGE OF A THRUST RATING CONCEPT USED ON THE RB199 ENGINE **c07**
P. Theimer *In* AGARD, Engine Condition Monitoring: Technology and Experience Oct. 1988 15 p (For primary document see N89-16780 09-06)
Copyright Avail: NTIS HC A20/MF A01

The control system of the RB199 engine was designed for a rating, using the HP-turbine inlet temperature as a limiter. The engine has now been in service for 7 years and still uses the original concept throughout all fleets in the UK, Italy and Germany, although new digital engine control units are being introduced which will allow considerable improvements. For some fleets a thrust rating concept based on the original control system design has been installed recently. The concept is described and the procedure explained. A comparison is made between the existing full thrust concept at the maximum cleared HP turbine temperature and the applied thrust rating concept. Besides the basic behavior of seal gaps, the influence of thrust rating in view of the life usage of life-limited parts as well as in the change of the maintenance material costs is explained. The assumptions for the comparison with their background are described. Finally, a refined thrust rating concept is introduced. Author

N89-16801# Bureau Veritas, Paris (France).
TREND MONITORING OF A TURBOPROP ENGINE AT LOW AND MEAN POWER [TREND-MONITORING DES TURBO-PROPULSEUR DE PETITE ET MOYENNE PUISSANCE]
Philippe Vaquez *In* AGARD, Engine Condition Monitoring: Technology and Experience Oct. 1988 9 p In FRENCH (For primary document see N89-16780 09-06)
Copyright Avail: NTIS HC A20/MF A01

Trend monitoring relates to the observation, between two maintenance periods, of changes in certain parameters that represent the physical state of an engine. The experiences of French engineers with the use of this method are discussed. Specifically, the application of trend monitoring to the Pratt and Whitney PT6 A and PW 120, and the General Electric CT 7 turboprop engines is discussed. The engines were mounted on various single and twin engine aircraft. Author

N89-16802# Aeronautical Research Labs., Melbourne (Australia).
GAS PATH ANALYSIS AND ENGINE PERFORMANCE MONITORING IN A CHINOOK HELICOPTER **c07**
D. E. Glenny *In* AGARD, Engine Condition Monitoring: Technology and Experience Oct. 1988 14 p (For primary document see N89-16780 09-06)
Copyright Avail: NTIS HC A20/MF A01

Periodic and consistent assessment of engine performance in military heicopters is essential if in-service operating margins are not to be eroded by harsh environmental conditions. Manually initiated GO-NO-GO pre-flight checks (HIT, etc.) or ad-hoc in-flight performance checks rarely provide sufficiently reliable data for

maintenance or diagnostic purposes. In contrast, performance assessment methods based on gas path analysis principles and engine/aircraft data, automatically recorded during flight, offer a potentially attractive alternative. ARL has investigated a number of these alternatives, and has carried out an in-service trial on a Boeing CH47C Chinook helicopter operated by the RAAF. In the trial existing aircraft/engine instrumentation was complemented by specially designed probes located at module interfaces while the data was recorded on an ARL designed acquisition system. The performance-fault algorithms used in the analyses were configured for a range of engine operating speeds. Results for the trial are presented in terms of deviations from pre-established baseline conditions. Statistical analyses using linear regression fits and Kalman filtering techniques have been investigated to minimize the effects of data uncertainty. The applicability of the procedures, including thermodynamic analyses and equipment are discussed in terms of fleetwide adoption of the Chinook. Author

N89-16803# National Research Council of Canada, Ottawa (Ontario).
THE EFFECTS OF A COMPRESSOR REBUILD ON GAS TURBINE ENGINE PERFORMANCE **c07**
J. D. MacLeod and J. C. G. Laflamme (Canadian Forces Base, Baden-Soellingen, Germany, F.R.) *In* AGARD, Engine Condition Monitoring: Technology and Experience Oct. 1988 14 p (For primary document see N89-16780 09-06)
Copyright Avail: NTIS HC A20/MF A01

The Canadian Department of Defence, in conjunction with the Engine Laboratory of the National Research Council Canada, initiated a project for the evaluation of gas path coatings on the Allison T56 engine. The objective of this work was to evaluate blade coatings in terms of engine performance effects and material durability. The project included a study of the influence of rebuilding the compressor on performance, since dismantling and rebuilding was required in the coating process. Described is the compressor rebuild study, including the overall objectives, the test set-up, the performance effects, and the uncertainty of the measured results. The impact of this work on the coatings project is also documented. Author

N89-16804# GEC Avionics Ltd., Rochester (England). Future Systems Group.
SYSTEM CONSIDERATIONS FOR INTEGRATED MACHINERY HEALTH MONITORING **c07**
R. M. Tester *In* AGARD, Engine Condition Monitoring: Technology and Experience Oct. 1988 14 p (For primary document see N89-16780 09-06)
Copyright Avail: NTIS HC A20/MF A01

Aircraft engine health monitoring, and other related machinery condition monitoring, has been gaining in credibility and implementation over recent years. It is destined to become standard fit on all new major aircraft programs in the near future. To date the monitoring systems have mainly been stand-alone in form, and have been treated as separate functions. This paper discusses the considerations for integrating health monitoring into other aircraft systems, and reviews the potential benefits to be gained by such integration. In conclusion, the paper presents two products from both ends of the spectrum, representing a simple single unit integration, and a full aircraft-wide implementation. Author

N89-16805# Societe de Fabrication d'Instruments de Mesure, Massy (France). Measurement and Flight Test Dept.
MAINTENANCE AID SYSTEM FOR WIDE BODY AIRCRAFT **c07**
Albert Levionnois *In* AGARD, Engine Condition Monitoring: Technology and Experience Oct. 1988 7 p (For primary document see N89-16780 09-06)
Copyright Avail: NTIS HC A20/MF A01

Aircraft maintenance personnel, when troubleshooting aircraft failures, must first acquire a great deal of information about the aircraft's engines before being able to arrive at any kind of diagnosis. Computerized modern aircraft provide all necessary parameters with good precision. Aircraft condition monitoring systems centralize information from data buses, compute flight phases, determine the reports to be made per flight phase and function, and carry out automatic parameter identification. Should an incident occur, then the parameter's history is stored before and after the incident, together with its evolution. All this information is stored in static memory for transmission by data link, is printed during or after the flight, or downloaded when the aircraft is back at its base. Today between 35 and 40 reports are currently produced by wide body aircraft. This technology is easily adaptable to combat aircraft. Author

N89-16806# Computing Devices Co., Ottawa (Ontario).
INSTALLED THRUST AS A PREDICTOR OF ENGINE HEALTH FOR JET ENGINES **c07**
G. B. Mackintosh and M. J. Hamer *In* AGARD, Engine Condition Monitoring: Technology and Experience Oct. 1988 10 p (For primary document see N89-16780 09-06)
Copyright Avail: NTIS HC A20/MF A01

Extensive installed and uninstalled gross thrust measurements were made over one complete maintenance cycle on 19 afterburning turbojet engines. Installed measurements utilized a sensor which can compute the thrust in real time from engine tailpipe pressure measurements. Correlation of installed thrust with maintenance history indicated a maximum degradation below which engines were removed from service. The engines were trimmed uninstalled, using lapse rate charts to produce a specific value of uninstalled thrust, corrected to standard conditions. Significant variations in installed corrected thrust resulted. Higher initial values of installed corrected thrust resulted in more rapid engine degradation and a shorter time before maintenance was required. Author

N89-16807# Stewart Hughes Ltd., Southhampton (England).
GETTING MORE FROM VIBRATION ANALYSIS
R. M. Stewart, I. C. Cheeseman, and K. Librowski *In* AGARD, Engine Condition Monitoring: Technology and Experience Oct. 1988 12 p (For primary document see N89-16780 09-06)
Copyright Avail: NTIS HC A20/MF A01

Traditional vibration monitoring of gas turbines has been restricted to activation of alarms from overall levels and shaft orders. Use of more of the information contained in the signal could improve fault coverage and diagnostics. The practical problem is one of being able to model the vibration of an engine in sufficient detail. Furthermore, some problems experienced in the field have origins that no designer could be expected to predict, i.e., module mismatch. How then to proceed. Any practical system must incorporate an evolutionary mechanism that feeds skilled field operator experience to a computer based monitoring system. This is based on the machine designer's knowledge and improves its performance by this feedback. Fortunately, there is a growing body of technology on the vibration produced by gas turbine engines, both to do with its interpretation and signal processing which make such a system feasible. Two areas of application are dealt with, the first connected with engine module roughness diagnostics and the second with fault identification of individual components such as main line bearings and accessory drive gears. For both, much of the hardware required to gather the necessary data is being specified and constructed, so overcoming a major objection to furtherance of this technology. Author

N89-16808# Rolls-Royce Ltd., Bristol (England). Mechanical Technology (Military) Dept.
A JOINT STUDY ON THE COMPUTERISATION OF IN-FIELD AERO ENGINE VIBRATION DIAGNOSIS **c07**
H. R. Carr, G. J. Ives, and P. Jenkins (Ministry of Defence, London, England) *In* AGARD, Engine Condition Monitoring: Technology and Experience Oct. 1988 13 p Sponsored by Ministry of Defence Procurement Executive, London, United Kingdom (For primary document see N89-16780 09-06)
Copyright Avail: NTIS HC A20/MF A01

Test House methods used by the RAF for diagnosing causes of excessive vibration in Military Engines are based on a visual comparison of the test signatures with those from buillt-in-fault

tests. Interpretation depends largely on operator experience. A joint program was launched in 1984 to develop a software-based analyzer to diagnose a range of mechanical abnormalities including unbalance, malalignment of bearings and shafts, and squeeze film bearing functions. The analyzer would handle a variety of engine types and would be suitable for inexperienced operators. The ensuing program between MOD and RR plc developed data acquisition and interpretive routines, and provided recorded engine signatures from both the RAF and Rolls-Royce plc test beds. Important aspects were the essential combination of intuitive operator experience, detailed, strip and inspection of problem engines, and an engineering understanding from Rolls-Royce plc. The current intention is to install an Automatic Data Processing system by 1990/1991. This paper reviews the successes achieved and problems encountered. Author

N89-16809# Pratt and Whitney Aircraft of Canada Ltd., Longueuil (Quebec).

FAULT MANAGEMENT IN AIRCRAFT POWER PLANT CONTROLS **c07**

S. Mazareanu and A. Nobre *In* AGARD, Engine Condition Monitoring: Technology and Experience Oct. 1988 16 p (For primary document see N89-16780 09-06)

Copyright Avail: NTIS HC A20/MF A01

The advent of Digital Electronics in aviation has opened new doors to fault management as a tool to enhance aircraft operability and safety in flight. Today it is possible to integrate flight control systems with power plant management systems. Operability of a battle-damaged aircraft can be enhanced under certain conditions through sophisticated fault management systems. This paper reviews some of the considerations applicable to engine control fault management systems in commercial aviation. Engine control systems have evolved in the last decade from being primarily hydromechanical to being primarily electronics. This rapid growth in acceptance of the electronic systems by the aviation industry was due to the improvement in reliability of the digital system over analog systems previously in use. The fault management system is a powerful tool to organize and optimize maintenance logistics. Operating costs can be significantly reduced with an appropriate fault management system on board. The paper presents: (1) a brief review of the evolution of engine controls; (2) the emergence of fault management systems (as part of engine control systems); (3) maturity of fault management systems (still evolving); and (4) future potential. Author

N89-16810# National Technical Univ., Athens (Greece). Lab. of Thermal Turbomachines.

DISCRETE OPERATING CONDITIONS GAS PATH ANALYSIS

A. Stamatis and K. D. Papailiou *In* AGARD, Engine Condition Monitoring: Technology and Experience Oct. 1988 10 p (For primary document see N89-16780 09-06)

Copyright Avail: NTIS HC A20/MF A01

The implementation of a reliable Diagnostic System based on a Gas Path Analysis (GPA) approach is not always feasible. Extra instrumentation is required in order to predict, detect, and isolate failures. Discrete Operating Conditions Gas Path Analysis (DOCGPA), presented here, is an extended version of the conventional GPA algorithm, providing the capability of increased reliability when using only existing sensors for estimating engine malfunctions. Author

N89-16811# Hochschule der Bundeswehr, Hamburg (Germany, F.R.).

GAS PATH MODELLING, DIAGNOSIS AND SENSOR FAULT DETECTION

R. Lunderstaedt and K. Fiedler *In* AGARD, Engine Condition Monitoring: Technology and Experience Oct. 1988 13 p (For primary document see N89-16780 09-06)

Copyright Avail: NTIS HC A20/MF A01

The gas path analysis (GPA) becomes more and more an important method for the diagnosis of jet engines. Here, a fundamental way of finding the mathematical engine model is shown, especially with regard to the adaptation of the coefficients of the system matrix to the gradients of the characteristic curves of the turbomachines. The theoretical fundamentals are applied to a two-shaft jet engine. In order to test the method some faults in the engine are simulated. All faults are detected very accurately and the method shows by this its efficiency. For practical use of the method, the faults of the measuring device (sensors) are to be taken into consideration. Therefore filter algorithms are outlined to diminish the stochastic parts of these faults. For the systematic parts (offsets), a special and new theory is developed for compensation. For both, simulation results are given based on actual test stand data. Author

N89-16812# Technische Univ., Munich (Germany, F.R.). Inst. fuer Luft-und Raumfahrt/Flugantriebe.

SYSTEM-THEORETICAL METHOD FOR DYNAMIC ON-CONDITION MONITORING OF GAS TURBINES

F. Hoerl, G. Kappler, and H. Rick *In* AGARD, Engine Condition Monitoring: Technology and Experience Oct. 1988 17 p (For primary document see N89-16780 09-06)

Copyright Avail: NTIS HC A20/MF A01

In order to ensure reliability and safety of such complex technical systems as aero-engines, model-related diagnostic techniques must be applied. The basis for this is a linear, time-invariant, dynamic engine state space model derived from system analysis. Due to the model order and the associated difficulties, order reduction procedures are used. The diagnostic parameters to be taken into account are integrated into a dynamic disturbance model. This disturbance model and the reduced engine model form the extended dynamic engine state space model. A detailed investigation of the dynamic system for observability and disturbability is essential. Because of measuring/process noise and other system disturbances, dynamic state estimation methods are applied in the diagnosis, whereby the synthesis of such observer systems is a crucial point. The usefulness of the dynamic monitoring method is demonstrated on the example of the helicopter engine using computed simulations. A sensitivity analysis allows the accuracy of the diagnostic results to be estimated. Author

N89-16813# Aeronautical Research Labs., Melbourne (Australia).

IDENTIFICATION OF DYNAMIC CHARACTERISTICS FOR FAULT ISOLATION PURPOSES IN A GAS TURBINE USING CLOSED-LOOP MEASUREMENTS **c07**

G. L. Merrington *In* AGARD, Engine Condition Monitoring: Technology and Experience Oct. 1988 13 p (For primary document see N89-16780 09-06)

Copyright Avail: NTIS HC A20/MF A01

Combat aircraft, because of the mission profiles involved, tend to rarely operate with their engines in a steady-state condition for extended periods. Furthermore, current generation aircraft contain Engine Monitoring Systems (EMS) which automatically capture a record of important engine parameters when a parameter exceedance is detected. It follows then that any subsequent post-flight data analysis for fault isolation purpose will often necessitate the extraction of the required diagnostic information from transient data records. This generally contrasts with past practice where most of the available fault diagnostic procedures have been derived from steady-state information. In an attempt to overcome this, and thereby provide effective tools for diagnosing faults from transient data records, a procedure is outlined to extract information about the dynamic characteristics of gas turbines from input/output measurements. The parameter estimator technique involved has the potential to provide a means of detecting changes in some unmeasured/unrecorded parameter, such as shifts in variable geometry schedules. Thus in essence, it provides a tool for identifying problems from simple transient test data which were previously inaccessible or difficult to obtain. Author

N89-16814# Canadian Forces Base Trenton, Astra (Ontario). Aerospace Maintenance Development Unit.

CF-18/F404 TRANSIENT PERFORMANCE TRENDING **c07**

J. R. Henry *In* AGARD, Engine Condition Monitoring: Technology and Experience Oct. 1988 13 p (For primary document see

N89-16780 09-06)
(Contract FE220786FRMC4; ARP-3610-147)
Copyright Avail: NTIS HC A20/MF A01

The on condition concept of aircraft engine maintenance has led to intensive analysis of the data recorded by Engine Health Monitoring systems during steady-state operation of the engine. To date however the transient data acquired during take-off or in-flight have received far less attention. Presented here are the results of an investigation into the feasibility of utilizing engine data acquired during take-off to trend the performance of a modern turbofan engine (GE-F404). Factors influencing the repeatability of take-off data such as throttle rate, variable geometry and instrumentation effects are discussed. Using engine data from operational aircraft, various trending parameters are evaluated using a data capture window developed to minimize the scatter of nominal engine performance. A statistical tool to identify performance shifts is briefly described, and is shown to successfully detect a shift in the take-off performance of a recently repaired engine. It is concluded that the trending of transient performance data is a viable means of detecting certain engine faults and recommendations are made concerning the implementation of such a program for the F404 engine. Author

N89-16815*# National Aeronautics and Space Administration. Marshall Space Flight Center, Huntsville, AL.
SPACE SHUTTLE MAIN ENGINE MONITORING EXPERIENCE AND ADVANCED MONITORING SYSTEMS DEVELOPMENT **c20**
Harry A. Cikanek *In* AGARD, Engine Condition Monitoring: Technology and Experience Oct. 1988 20 p (For primary document see N89-16780 09-06)
Copyright Avail: NTIS HC A20/MF A01 CSCL 21H

Advanced space transportation systems must provide improved availability, reliability, safety, and reduced cost in order to make a new, more vigorous level of space activity economically feasible. Earth-to-Orbit (ETO) propulsion monitoring systems are a major factor in progress toward these improvements, and in the success of current systems. Operational experience with the Space Shuttle Main Engine (SSME), the first reusable ETO rocket engine, is valuable for examining current rocket engine monitoring capability and technology developments. Here, Space Shuttle Main Engine (SSME) monitoring practice and experience are surveyed. Unique aspects of rocket engine mission requirements are highlighted to provide improved understanding of engine monitoring practices and technology needs. Current ETO engine transportation systems mission needs are outlined. With this foundation, the techniques and components addressed within current technology programs are discussed to complete a picture of ETO propulsion monitoring status and development. Author

N89-16816*# National Aeronautics and Space Administration. Marshall Space Flight Center, Huntsville, AL.
PLUME SPECTROMETRY FOR LIQUID ROCKET ENGINE HEALTH MONITORING **c20**
William T. Powers, F. G. Sherrell, J. H. Bridges, III, and T. W. Bratcher (Sverdrup Technology, Inc., Arnold Air Force Station, TN.) *In* AGARD, Engine Condition Monitoring: Technology and Experience Oct. 1988 10 p (For primary document see N89-16780 09-06)
Copyright Avail: NTIS HC A20/MF A01 CSCL 21H

An investigation of Space Shuttle Main Engine (SSME) testing failures identified optical events which appeared to be precursors of those failures. A program was therefore undertaken to detect plume trace phenomena characteristic of the engine and to design a monitoring system, responsive to excessive activity in the plume, capable of delivering a warning of an anomalous condition. By sensing the amount of extraneous material entrained in the plume and considering engine history, it may be possible to identify wearing of failing components in time for a safe shutdown and thus prevent a catastrophic event. To investigate the possibilities of safe shutdown and thus prevent a monitor to initiate the shutdown procedure, a large amount of plume data were taken from SSME firings using laboratory instrumentation. Those data were used to design a more specialized instrument dedicated to rocket plume diagnostics. The spectral wavelength range of the baseline data was about 220 nanometers (nm) to 15 microns with special attention given to visible and near UV. The data indicates that a satisfactory design will include a polychromator covering the range of 250nM to 1000nM, along with a continuous coverage spectrometer, each having a resolution of at least 5A degrees. The concurrent requirements for high resolution and broad coverage are normally at odds with one another in commercial instruments, therefore necessitating the development of special instrumentation. The design of a polychromator is reviewed herein, with a detailed discussion of the continuous coverage spectrometer delayed to a later forum. The program also requires the development of applications software providing detection, variable background discrimination, noise reduction, filtering, and decision making based on varying historical data. Author

N89-16817# Stewart Hughes Ltd., Southhampton (England). Centre for Advanced Technology.
GAS PATH CONDITION MONITORING USING ELECTROSTATIC TECHNIQUES
Celia Fisher *In* AGARD, Engine Condition Monitoring: Technology and Experience Oct. 1988 10 p Sponsored by Ministry of Defence Procurement Executive, London, United Kingdom (For primary document see N89-16780 09-06)
Copyright Avail: NTIS HC A20/MF A01

The concept of condition monitoring using electrostatics offers the opportunity to monitor gas path faults as they occur. It is based on the assumption that gas path distresses, such as blade rubs and combustor burns, cause the production of minute particles of debris, which carry electrostatic charge, and can be monitored on suitable sensors mounted in the engine. The engine has a normal level of charge, which produces a background signal. The debris produced by distresses causes a change in the signal which can be monitored using suitable signal processing techniques. Described here is the research work which was necessary to provide an understanding of the mechanisms involved. This forms the basis of the technique which is described, with examples of the application of the systems to various engines. Author

N89-16818# Atomic Energy of Canada Ltd., Pinawa (Manitoba).
AN INTELLIGENT SENSOR FOR EQUIPMENT HEALTH MONITORING OF FERROMAGNETIC WEAR DEBRIS CONCENTRATION IN FLUIDS
K. W. Chambers, M. C. Arneson, J. L. Montin, W. Dueck, and C. A. Waggoner (Defence Research Establishment Pacific, Victoria, British Columbia) *In* AGARD, Engine Condition Monitoring: Technology and Experience Oct. 1988 10 p (For primary document see N89-16780 09-06)
Copyright Avail: NTIS HC A20/MF A01

FERROSCAN R is a device that has been developed for the Canadian Department of National Defence by Atomic Energy of Canada Limited (AECL) for monitoring the relative concentration of ferromagnetic wear debris in fluid systems. FERROSCAN R generates a wear profile in real time and uses it to detect the onset of an increase in the rate of wear of ferromagnetic components. Described here are the background, development and operating principles of the sensor. Some engineering test results are given. Author

N89-16819# Rolls-Royce Ltd., Derby (England).
COMPASS (TRADEMARK): A GENERALIZED GROUND-BASED MONITORING SYSTEM
M. J. Provost *In* AGARD, Engine Condition Monitoring: Technology and Experience Oct. 1988 13 p (For primary document see N89-16780 09-06)
Copyright Avail: NTIS HC A20/MF A01

Condition monitoring has developed from simple hand recording and analysis of cockpit instrumentation to the use of electronic systems selecting and recording a multitude of measurements for transmission to ground-based computer systems, which store and analyze data from an entire fleet. COMPASS (Condition Monitoring and Performance Analysis Software System) is a ground-based

computer system, currently being developed by Rolls-Royce plc for application on the Rolls-Royce RB211 and Tay and International Aero Engines (IAE) V2500 turbofans. After discussing the benefits of monitoring system, COMPASS, its sources of data and its analytical functions, including details of new techniques developed to improve the usefulness of the analysis that is done are described. Also shown is how COMPASS is designed in two parts: - analytical functions specific to a given application and general host routines, providing all the housekeeping functions required in any monitoring system, including smoothing and trending, alert generation, fleet averaging, compression, data management and data plotting. The use of the general host routines could be extended to cover any operation. The approach Rolls-Royce plc is adopting to enable the COMPASS host to be made available for widespread application is discussed. Author

N89-16820*# National Aeronautics and Space Administration. Langley Research Center, Hampton, VA.
PILOTED-SIMULATION EVALUATION OF ESCAPE GUIDANCE FOR MICROBURST WIND SHEAR ENCOUNTERS M.S. Thesis - George Washington Univ.
David A. Hinton Washington, DC Mar. 1989 57 p Sponsored in part by FAA, Washington, DC
(NASA-TP-2886; L-16498; NAS 1.60:2886; DOT/FAA/DS-89/06) Avail: NTIS HC A04/MF A01 CSCL 01D

Numerous air carrier accidents and incidents result from encounters with the atmospheric wind shear associated with microburst phenomena, in some cases resulting in heavy loss of life. An important issue in current wind shear research is how to best manage aircraft performance during an inadvertent wind shear encounter. The goals of this study were to: (1) develop techniques and guidance for maximizing an aircraft's ability to recover from microburst encounters following takeoff, (2) develop an understanding of how theoretical predictions of wind shear recovery performance might be achieved in actual use, and (3) gain insight into the piloting factors associated with recovery from microburst encounters. Three recovery strategies were implemented and tested in piloted simulation. Results show that a recovery strategy based on flying a flight path angle schedule produces improved performance over constant pitch attitude or acceleration-based recovery techniques. The best recovery technique was initially counterintuitive to the pilots who participated in the study. Evidence was found to indicate that the techniques required for flight through the turbulent vortex of a microburst may differ from the techniques being developed using classical, nonturbulent microburst models. Author

07 AIRCRAFT PROPULSION AND POWER

Includes prime propulsion systems and systems components, e.g., gas turbine engines and compressors; and onboard auxilliary power plants for aircraft.

For related information see also *20 Spacecraft Propulsion and Power, 28 Propellants and Fuels,* and *44 Energy Production and Conversion.*

N89-16821# Naval Postgraduate School, Monterey, CA. Dept. of Aeronautics and Astronautics.
MEASUREMENTS OF GAS TURBINE COMBUSTOR AND ENGINE AUGMENTOR TUBE SOOTING CHARACTERISTICS Final Report, Oct. 1986 - Sep. 1987
M. F. Young, T. A. Grafton, H. Conner, and David W. Netzer Jul. 1988 57 p
(AD-A199768; NPS67-88-002) Avail: NTIS HC A04/MF A01 CSCL 21B

An experimental investigation was conducted to determine the changes in soot mean diameter across the combustor and exhaust nozzle of a T63 gas turbine engine, and across an exhaust augmentor tube. D32 within the combustor varied between 0.16 and 0.25 microns, depending upon fuel composition. Data correlation was most successful in this location using an index of refraction of 1.95 -0.66i with sigma = 1.5. In the aft can location (ahead of the exhaust nozzle) D32 was between 0.35 and 0.45 microns, depending upon the fuel-air ratio. Increasing fuel-air ratios decreased D32, also in agreement with the results presented in reference 1. Using NAPC 9 high aromatic fuel, D32 increased across the exhaust nozzle (0.35 to 1.2 microns) and across the augmentor tube (1.2 to 1.5 = 1.9 microns). Malvern data were in good agreement with the results obtained using larger scattering angles. GRA

N89-16822# Vatell Corp., Christiansburg, VA.
TIP CLEARANCE SIGNAL PROCESSOR DEVELOPMENT Final Report, 31 Jul. 1987 - 24 May 1988
Lawrence W. Langley Oct. 1988 54 p
(Contract F33615-87-C-2802)
(AD-A199830; AFWAL-TR-88-2089) Avail: NTIS HC A04/MF A01 CSCL 14B

A signal processing system was designed and constructed to detect peaks of the Vatell eddy current clearance sensor signal, measure their amplitude and timing, and compute a correction for machine speed to indicate clearance and time arrival for individual blades of a turbomachine. The system is based on an ADPIBM301 plug-in for the PC/XT, and consists of a second plug-in, along with software for signal detection and processing. GRA

N89-16823 Texas Univ., Arlington.
THE SYNCHRONOUS INJECTION IGNITION VALVELESS PULSEJET Ph.D. Thesis
Dudley Edington Smith 1987 155 p
Avail: Univ. Microfilms Order No. DA8812834

An unsteady, quasi-one-dimensional channel flow code has been developed for the purpose of analyzing transient flow phenomena associated with the operation of valveless pulsejets. The method employs a real gas method-of-characteristics analysis, with discrete tracking of shock waves and other discontinuities. Frictional and heat transfer effects, as well as spatially varying cross sectional area are included in the analysis. The combustion transient is based on a hybrid, quasi-one-dimensional mixing, constant volume combustion model. The pulsed combustion model incorporates empirical turbulent mixing lengths of the injected fuel and a simple heat release model for the constant volume combustion process. Comparisons of performance calculations and experimental data are presented for a selection of valveless pulsejet configurations. Calculations of mass flows, temperatures, pressures, fuel consumption, thrust developed, and fuel air ratios as a function of the various geometries and fuel injection methods are in excellent agreement with existing experimental data. Dissert. Abstr.

N89-16824# Vatell Corp., Christiansburg, VA.
TIP SENSOR DEVELOPMENT Final Report, Jul. 1987 - Jan. 1988
Lawrence W. Langley Oct. 1988 43 p
(Contract F33615-87-C-2801)
(AD-A200080; VTR-88-01; AFWAL-TR-88-2088) Avail: NTIS HC A03/MF A01 CSCL 14B

Turbomachinery blade clearance and time of arrival sensors based on the Vatell eddy current principle, and suitable for operation at temperatures up to 200 C, were designed, built and tested on the first fan stage of a JT15-D. The sensors produced robust, low noise signals whose general shape is virtually independent of speed, and whose amplitudes are related to speed and clearance. The signals of individual blades were readily resolved and identified. A model equation which predicts sensor signal amplitude, given values of clearance and speed, was developed, and coefficients derived to fit the experimental data. The engine was equipped with an optical once/revolution sensor. GRA

N89-16825# Von Karman Inst. for Fluid Dynamics, Rhode-Saint-Genese (Belgium).
TRANSONIC COMPRESSORS, VOLUME 1
1988 240 p Lecture series held in Rhode-Saint-Genese, Belgium,

1-4 Feb. 1988
(VKI-LS-1988-03-Vol-1; ISSN-0377-8312; ETN-89-93590) Avail: NTIS HC A11/MF A01

Loss development in transonic compressor cascades; incidence angle rules in supersonic cascades; exit angle rules in supersonic cascades; shock losses in transonic and supersonic compressor cascades; axial velocity density ratio influence on exit flow angle in transonic/supersonic cascades; analysis of 3D viscous flows in transonic compressors; and inverse methods for blade design, controlled diffusion blading for supercritical compressor flow were discussed. For individual titles, see N89-16826 through N89-16832.

N89-16826# Deutsche Forschungs- und Versuchsanstalt fuer Luft- und Raumfahrt, Porz (Germany, F.R.). Inst. fuer Strahlantrieb.

LOSS DEVELOPMENT IN TRANSONIC COMPRESSOR CASCADES

Hans Starken *In* Von Karman Institute for Fluid Dynamics, Transonic Compressors, Volume 1 1988 17 p (For primary document see N89-16825 09-07)
Avail: NTIS HC A11/MF A01

Loss in a supercritical cascade is discussed. It is argued that efficient transition of a compressor cascade to supersonic velocities requires a limitation of the suction surface Mach number to values below 1.3. This, in turn, limits pitch-chord ratio, front suction surface camber, and leading edge radius as the responsible parameters. In order to elucidate this, the influence of the blade suction surface and the pitch chord ratio is demonstrated by test results obtained at subsonic and low supersonic velocities. ESA

N89-16827# Deutsche Forschungs- und Versuchsanstalt fuer Luft- und Raumfahrt, Porz (Germany, F.R.). Inst. fuer Strahlantriebe.

INCIDENCE ANGLE RULES IN SUPERSONIC CASCADES

Hans Starken *In* Von Karman Institute for Fluid Dynamics, Transonic Compressors, Volume 1 1988 31 p (For primary document see N89-16825 09-07)
Avail: NTIS HC A11/MF A01

Supersonic inlet flow of flat plate cascades, and blades having cambered suction surfaces is analyzed. The whole flow field is computed with the method of characteristics in cases where supersonic velocity is assumed everywhere in the entrance region. Where the flow field contains local subsonic regions, approximations can be applied, if the subsonic regions are small enough. Calculations were performed for a straight flat plate profile. The maximum mass-flow of a two dimensional cascade is shown to be limited by the ratio of leading edge over blade pitch. The strong influence of leading edge radius, and the minor influence of stagger angle on the maximum axial Mach number are noted. ESA

N89-16828# Deutsche Forschungs- und Versuchsanstalt fuer Luft- und Raumfahrt, Porz (Germany, F.R.). Inst. fuer Strahlantriebe.

EXIT ANGLE RULES IN SUPERSONIC CASCADES

Hans Starken *In* Von Karman Institute for Fluid Dynamics, Transonic Compressors, Volume 1 1988 19 p (For primary document see N89-16825 09-07)
Avail: NTIS HC A11/MF A01

The infinitely thin flat plate cascade is used to describe the fundamental flow phenomena which apply to compressor and turbine cascades. With increasing flow angle at the blade trailing edges, which is equivalent to an increase in back pressure, left running oblique shock waves occur at the suction sides of the trailing edges and are reflected at the pressure sides of the adjacent blades. Up to these left running trailing edge shock waves the supersonic flow field in front and within the cascade remains unchanged. For the calculation of the exit flow field behind these shock waves it is necessary to realize that all left running characteristics emanate from the uniform flow field infinitely far downstream. Therefore, the exit flow field can be assumed, in first approximation, to be of the simple wave type, which means that the right running characteristics are straight lines with constant properties. In order to calculate the neutral exit characteristic, it would be necessary to continue the computation up to infinity downstream. But if the knowledge of the complete flow field behind the cascade is not required, a method based upon the simple wave approximation can be used. ESA

N89-16829# Deutsche Forschungs- und Versuchsanstalt fuer Luft- und Raumfahrt, Porz (Germany, F.R.). Inst. fuer Strahlantriebe.

SHOCK LOSSES IN TRANSONIC AND SUPERSONIC COMPRESSOR CASCADES

H. A. Schreiber *In* Von Karman Institute for Fluid Dynamics, Transonic Compressors, Volume 1 1988 58 p (For primary document see N89-16825 09-07)
Avail: NTIS HC A11/MF A01

Flow phenomena and the associated losses of transonic blade sections for upstream Mach numbers of 0.8 to 1.2 are described. Shock losses of two supersonic blade sections of the so-called precompression type are analyzed. Theoretical results of a shock loss model are discussed, showing the influence of inlet Mach number and inlet flow angle. The shock structure and strength within the blade passage of a supersonic blade section is studied, and an insight into the problem of strong shock wave boundary layer interaction with turbulent boundary layer separation is given. Depending on inlet Mach number, inlet flow angle, and back pressure the shock loss level reaches 40 to 70 percent of the overall losses. The data show that shock loss calculations should not be oversimplified but should be carefully modeled according to the real flow conditions. The overall losses have their origins in the leading edge bow shock of supersonic blades that contributes up to 30 percent to the shock losses; the main compression shock or strong passage shock; and viscous losses related to the boundary layer evolution including regions of shock/boundary layer interactions. ESA

N89-16830# Deutsche Forschungs- und Versuchsanstalt fuer Luft- und Raumfahrt, Porz (Germany, F.R.). Inst. fuer Strahlantriebe.

AXIAL VELOCITY DENSITY RATIO INFLUENCE ON EXIT FLOW ANGLE IN TRANSONIC/SUPERSONIC CASCADES

H. A. Schreiber *In* Von Karman Institute for Fluid Dynamics, Transonic Compressors, Volume 1 1988 22 p (For primary document see N89-16825 09-07)
Avail: NTIS HC A11/MF A01

Axial velocity density ratio (AVDR) influence on the cascade exit flow angle Beta sub 2 is discussed. A simple relationship between AVDR and Beta sub 2 is outlined. The AVDR influence on the exit flow properties of supersonic cascades which operate with started supersonic flow at cascade entrance is reviewed. ESA

N89-16831# Cambridge Univ. (England).

ANALYSIS OF 3D VISCOUS FLOWS IN TRANSONIC COMPRESSORS

W. N. Dawes *In* Von Karman Institute for Fluid Dynamics, Transonic Compressors, Volume 1 1988 27 p (For primary document see N89-16825 09-07)
Avail: NTIS HC A11/MF A01

A computer code to solve the 3D Reynolds averaged compressible Navier-Stokes equations was applied to a linear cascade of compressor blades and the effect of mesh refinement on profile loss prediction studied. Secondary flow development in a cascade of compressor stator blades is predicted and compared with measurement. The code was applied to the study of the flow field in a transonic axial compressor rotor at design speed and maximum efficiency. The first test case shows that near grid independent predictions could be achieved for profile loss. The second case shows predictions of secondary flow development in a cascade of compressor stator blades comparing well with measurement. The third case shows predictions for the flow in a transonic compressor rotor with clearance. Good agreement with

experimental evidence is achieved and valuable insight obtained into the loss production mechanisms associated with clearance flows. ESA

N89-16832# Stuttgart Univ. (Germany, F.R.). Inst. fuer Aerodynamik und Gasdynamik.
INVERSE METHODS FOR BLADE DESIGN, CONTROLLED DIFFUSION BLADING FOR SUPERCRITICAL COMPRESSOR FLOW
E. Schmidt *In* Von Karman Institute for Fluid Dynamics, Transonic Compressors, Volume 1 1988 56 p (For primary document see N89-16825 09-07)
Avail: NTIS HC A11/MF A01

Cascade design methods are reviewed, and an inverse cascade design method on stream surfaces of revolution is presented. The method seems to be an effective procedure to design highly loaded axial compressor cascades on stream surfaces of revolution. It produces accurate results compared with complete flow field measurements and computations from other methods. It was applied to cascade and multisection compressor blade design. Lower losses are obtained, compared with conventional NACA blading. ESA

N89-16833# Von Karman Inst. for Fluid Dynamics, Rhode-Saint-Genese (Belgium).
TRANSONIC COMPESSORS, VOLUME 2
1988 390 p Lecture series held in Rhode-Saint-Genese, Belgium, 1-4 Feb. 1988
(VKI-LS-1988-03-Vol-2; ISSN-0377-8312; ETN-89-93591) Avail: NTIS HC A17/MF A01

The design and development of transonic multistage compressors; design of critical compressor stages; supersonic compressors; supersonic throughflow fans; variable geometry in supersonic compressors; axial supersonic inlet components; design methodology for high pressure compressors; and holographic inteferometry for flow visualization studies in high speed fans, and in vibration and flutter study of fans were discussed. For individual titles, see N89-16834 through N89-16842.

N89-16834*# National Aeronautics and Space Administration. Lewis Research Center, Cleveland, OH.
THE DESIGN AND DEVELOPMENT OF TRANSONIC MULTISTAGE COMPRESSORS
C. L. Ball, R. J. Steinke, and F. A. Newman *In* Von Karman Institute for Fluid Dynamics, Transonic Compressors, Volume 2 1988 97 p (For primary document see N89-16833 09-07)
Avail: NTIS HC A17/MF A01

The development of the transonic multistage compressor is reviewed. Changing trends in design and performance parameters are noted. These changes are related to advances in compressor aerodynamics, computational fluid mechanics and other enabling technologies. The parameters normally given to the designer and those that need to be established during the design process are identified. Criteria and procedures used in the selection of these parameters are presented. The selection of tip speed, aerodynamic loading, flowpath geometry, incidence and deviation angles, blade/vane geometry, blade/vane solidity, stage reaction, aerodynamic blockage, inlet flow per unit annulus area, stage/overall velocity ratio, and aerodynamic losses are considered. Trends in these parameters both spanwise and axially through the machine are highlighted. The effects of flow mixing and methods for accounting for the mixing in the design process are discussed. ESA

N89-16835# Air Force Wright Aeronautical Labs., Wright-Patterson AFB, OH.
DESIGN OF CRITICAL COMPRESSOR STAGES
A. J. Wennerstrom *In* Von Karman Institute for Fluid Dynamics, Transonic Compressors, Volume 2 1988 32 p (For primary document see N89-16833 09-07)
Avail: NTIS HC A17/MF A01

The through blade design approach to axial compresor stages for which high performance is critical as to thermodynamic cycle, and difficult due to high aerodynamic loading and/or Mach number is introduced. The mathematical models used, and the treatment of empirical inputs and shock losses are outlined. Design control and optimization are explained. Other major design factors, including mass flow, solidity, ramp angle, flow distribution, airfoil stacking, and structural parameters are reviewed. Design system weaknesses and trends are indicated, and computational goals are mentioned. ESA

N89-16836# Air Force Wright Aeronautical Labs., Wright-Patterson AFB, OH.
SUPERSONIC COMPRESSORS
A. J. Wennerstrom *In* Von Karman Institute for Fluid Dynamics, Transonic Compressors, Volume 2 1988 54 p (For primary document see N89-16833 09-07)
Avail: NTIS HC A17/MF A01

The analysis of shock losses and tip clearance losses in supersonic compressors is introduced. Boundary layer control, including rotor vortex generators, casing vortex generators, and stator slots is reviewed. Unconventional design concepts such as splitter vanes, counterswirl, and nonsteady flow are discussed. ESA

N89-16837*# National Aeronautics and Space Administration. Lewis Research Center, Cleveland, OH.
SUPERSONIC THROUGHFLOW FANS
C. L. Ball and R. D. Moore *In* Von Karman Institute for Fluid Dynamics, Transonic Compressors, Volume 2 988 30 p (For primary document see N89-16833 09-07)
Avail: NTIS HC A17/MF A01

Supersonic throughflow fan research, and technology needs are reviewed. The design of a supersonic throughflow fan stage, a facility inlet, and a downstream diffuser is described. The results from the analysis codes used in executing the design are shown. An engine concept intended to permit establishing supersonic throughflow within the fan on the runway and maintaining the supersonic throughflow condition within the fan throughout the flight envelope is presented. ESA

N89-16838# Von Karman Inst. for Fluid Dynamics, Rhode-Saint-Genese (Belgium). Turbomachinery Dept.
VARIABLE GEOMETRY IN SUPERSONIC COMPRESSORS
F. A. E. Breugelmans *In its* Transonic Compressors, Volume 2 1988 23 p Sponsored in part by the European Office of Aerospace Research (For primary document see N89-16833 09-07)
Avail: NTIS HC A17/MF A01

A flexible inlet guide vane was designed for an independent control of the pre- or counterswirl condition over the blade height. The model was investigated with a Mach 2 supersonic rotor. The vertical supersonic compressor characteristic can be adapted to important mass flow variations by introducing a limited amount of inlet swirl. The matching and flow problems of the rotor supersonic inlet conditions and the variable inlet guide vanes are demonstrated. Large changes in the rotor exit flow field are observed when operating the variable guide vane. The classical variable stagger stator vanes are not the solution to the large angle variations at high subsonic Mach numbers. A flexible blade is also proposed in the exit flow field. ESA

N89-16839# Von Karman Inst. for Fluid Dynamics, Rhode-Saint-Genese (Belgium). Turbomachinery Dept.
AXIAL SUPERSONIC INLET COMPOUND
F. A. E. Breugelmans *In its* Transonic Compressors, Volume 2 1988 25 p Sponsored in part by the European Office of Aerospace Research (For primary document see N89-16833 09-07)
Avail: NTIS HC A17/MF A01

A prototype rotor was designed to investigate the supersonic axial component at the inlet face of a compressor. A flexible inflatable nozzle is installed in the inlet duct in order to simulate a continuously variable inlet Mach number up to 1.5. A relative inlet Mach number of 2.4 is achieved at 90 percent of the design

speed. The transition from the subsonic to the supersonic axial component is explored. A blade failure prevented completion of the research on the dynamic response of the compressor to throttle valve, speed, and inlet nozzle variations. ESA

N89-16840# Societe Nationale d'Etude et de Construction de Moteurs d'Aviation, Villaroche (France).
DESIGN METHODOLOGY FOR ADVANCED HIGH PRESSURE (HP) COMPRESSOR FIRST STAGE
Marius Goutines *In* Von Karman Institute for Fluid Dynamics, Transonic Compressors, Volume 2 1988 36 p (For primary document see N89-16833 09-07)
Avail: NTIS HC A17/MF A01

The design methodology used for the first stage of a one stage high pressure compressor whose rotor blades are supersonic (relative Mach number varies from 1.1 at hub to 1.3 at tip) is outlined. Improvements brought by three-dimensional Euler calculations and secondary flow prediction method are discussed. Theoretical computations and experimental data are compared. The method can be improved by full 3-D aerodynamic calculations on the blade rows, particularly on the supersonic rotor. A 3-D Euler solver is necessary to give the correct shock shape. This method cancels the spanwise compatibility problem between the different 3-D profiles that occurs on classical quasi three-dimensional design methods. Spanwise detailed secondary flow calculation method provides inlet axisymetric aerodynamic conditions of the various blade rows which are useful for the upstream end adaptations. This method can also give the outlet end adaptation effects on secondary losses and on the downstream row inlet conditions. ESA

N89-16841# Rolls-Royce Ltd., Derby (England). Advanced Research Lab.
HOLOGRAPHIC INTERFEROMETRY FOR FLOW VISUALIZATION STUDIES IN HIGH SPEED FANS c35
R. K. Parker *In* Von Karman Institute for Fluid Dynamics, Transonic Compressors, Volume 2 1988 45 p Previously announced as N88-28072 (For primary document see N89-16833 09-07)
Avail: NTIS HC A17/MF A01

The versatility of holography as an optical diagnostic technique is discussed. In the study of rotating aero-engine fans it allows the aerodynamic behavior to be investigated. Holography provides useful data for the verification of three-dimensional time marching models of the flow field. When coupled with other optical diagnostic techniques, e.g., laser anemometry, holography can be used to provide rapid assessment of the whole flow field. It can be used to direct other, slower techniques to areas of interest within the flow field. The extraction of three-dimensional data from transonic flow holograms recorded in rotating fans is demonstrated. Digitizing equipment allows accurate measurement of data from holographic images. The extracted data can be transferred to a mainframe computer, manipulated, and combined with blade design data. It is possible to section the data so that other required information may be extracted. The engineer can thus compare aerodynamic performance and design intent in the computer. ESA

N89-16842# Rolls-Royce Ltd., Derby (England).
USE OF HOLOGRAPHY IN VIBRATION AND FLUTTER STUDY OF FANS c35
R. J. Parker *In* Von Karman Institute for Fluid Dynamics, Transonic Compressors, Volume 2 1988 44 p Previously announced as N88-30098 (For primary document see N89-16833 09-07)
Avail: NTIS HC A17/MF A01

The versatility of holography as an optical diagnostic technique is demonstrated. In can be used on small components and large assemblies to masure the mode shape and vibration amplitude. In the study of rotating aero-engine fans it allows mechanical behavior to be investigated in aerodynamic test facilities. Holography provides useful data for the verification of finite element models of the vibration of stationary components and rotating fans. ESA

N89-16843*# United Technologies Research Center, East Hartford, CT.
SUPERSONIC THROUGH-FLOW FAN ASSESSMENT
Contractural Report, Jan. 1986 - Nov. 1988
C. E. Kepler and G. A. Champagne Nov. 1988 166 p
(Contract NAS3-24843)
(NASA-CR-182202; NAS 1.26:182202; UTRC-R88-957367-31)
Avail: NTIS HC A08/MF A01 CSCL 21E

A study was conducted to assess the performance potential of a supersonic through-flow fan engine for supersonic cruise aircraft. It included a mean-line analysis of fans designed to operate with in-flow velocities ranging from subsonic to high supersonic speeds. The fan performance generated was used to estimate the performance of supersonic fan engines designed for four applications: a Mach 2.3 supersonic transport, a Mach 2.5 fighter, a Mach 3.5 cruise missile, and a Mach 5.0 cruise vehicle. For each application an engine was conceptualized, fan performance and engine performance calculated, weight estimates made, engine installed in a hypothetical vehicle, and mission analysis was conducted. Author

N89-16781# NATO European Fighter Management Agency, Munich (Germany, F.R.).
OPERATIONAL REQUIREMENTS FOR ENGINE CONDITION MONITORING FROM THE EFA VIEWPOINT
J. V. Goodfellow *In* AGARD, Engine Condition Monitoring: Technology and Experience Oct. 1988 4 p (For primary document see N89-16780 09-06)
Copyright Avail: NTIS HC A20/MF A01

N89-16782# Naval Air Systems Command, Washington, DC.
AN OVERVIEW OF US NAVY ENGINE MONITORING SYSTEM PROGRAMS AND USER EXPERIENCE
Andrew J. Hess *In* AGARD, Engine Condition Monitoring: Technology and Experience Oct. 1988 16 p (For primary document see N89-16780 09-06)
Copyright Avail: NTIS HC A20/MF A01

N89-16783# Royal Air Force, London (England).
ENGINE USAGE CONDITION AND MAINTENANCE MANAGEMENT SYSTEMS IN THE UK ARMED FORCES
W. D. M. Fletcher and N. A. Bairsto *In* AGARD, Engine Condition Monitoring: Technology and Experience Oct. 1988 5 p (For primary document see N89-16780 09-06)
Copyright Avail: NTIS HC A20/MF A01

N89-16784# National Defence Headquarters, Ottawa (Ontario). Directorate of Transport and Helicopter Engineering and Maintenance.
CANADIAN FORCES AIRCRAFT CONDITION/HEALTH MONITORING: POLICY, PLANS AND EXPERIENCE
Christopher Schofield, Ross LaGrandeur, Francois Dube, Thomas Harris, Robert W. Cue, and Alain LeBlanc *In* AGARD, Engine Condition Monitoring: Technology and Experience Oct. 1988 10 p (For primary document see N89-16780 09-06)
Copyright Avail: NTIS HC A20/MF A01

N89-16787# GasTOPS Ltd., Ottawa (Ontario).
CF-18 ENGINE PERFORMANCE MONITORING
D. E. Muir, D. M. Rudnitski, and Robert W. Cue (National Defence Headquarters, Ottawa, Ontario) *In* AGARD, Engine Condition Monitoring: Technology and Experience Oct. 1988 20 p (For primary document see N89-16780 09-06)
Copyright Avail: NTIS HC A20/MF A01

N89-16790# Ministry of Defence, London (England). Directorate of Engines.
RECENT UK TRIALS IN ENGINE HEALTH MONITORING: FEEDBACK AND FEEDFORWARD
M. J. Sapsard *In* AGARD, Engine Condition Monitoring: Technology and Experience Oct. 1988 8 p (For primary document see N89-16780 09-06)
Copyright Avail: NTIS HC A20/MF A01

N89-16791# Turkish Air Force, Ankara. Aircraft Engines Branch.
F110 ENGINE MONITORING AND MAINTENANCE MANAGEMENT SYSTEMS FOR F-16 C/D
F. Algun *In* AGARD, Engine Condition Monitoring: Technology and Experience Oct. 1988 12 p (For primary document see N89-16780 09-06)
Copyright Avail: NTIS HC A20/MF A01

N89-16796# Societe Nationale d'Etude et de Construction de Moteurs d'Aviation, Evry Cedex (France).
SERVICE LIFE CALCULATOR FOR THE M53 TURBOFAN ENGINE [LE CALCULATEUR DE POTENTIEL SUR LE REACTEUR M53]
Claude Sprung *In* AGARD, Engine Condition Monitoring: Technology and Experience Oct. 1988 15 p In FRENCH (For primary document see N89-16780 09-06)
Copyright Avail: NTIS HC A20/MF A01

N89-16800# Motoren- und Turbinen-Union Muenchen G.m.b.H. (Germany, F.R.).
THE ADVANTAGE OF A THRUST RATING CONCEPT USED ON THE RB199 ENGINE
P. Theimer *In* AGARD, Engine Condition Monitoring: Technology and Experience Oct. 1988 15 p (For primary document see N89-16780 09-06)
Copyright Avail: NTIS HC A20/MF A01

N89-16802# Aeronautical Research Labs., Melbourne (Australia).
GAS PATH ANALYSIS AND ENGINE PERFORMANCE MONITORING IN A CHINOOK HELICOPTER
D. E. Glenny *In* AGARD, Engine Condition Monitoring: Technology and Experience Oct. 1988 14 p (For primary document see N89-16780 09-06)
Copyright Avail: NTIS HC A20/MF A01

N89-16803# National Research Council of Canada, Ottawa (Ontario).
THE EFFECTS OF A COMPRESSOR REBUILD ON GAS TURBINE ENGINE PERFORMANCE
J. D. MacLeod and J. C. G. Laflamme (Canadian Forces Base, Baden-Soellingen, Germany, F.R.) *In* AGARD, Engine Condition Monitoring: Technology and Experience Oct. 1988 14 p (For primary document see N89-16780 09-06)
Copyright Avail: NTIS HC A20/MF A01

N89-16804# GEC Avionics Ltd., Rochester (England). Future Systems Group.
SYSTEM CONSIDERATIONS FOR INTEGRATED MACHINERY HEALTH MONITORING
R. M. Tester *In* AGARD, Engine Condition Monitoring: Technology and Experience Oct. 1988 14 p (For primary document see N89-16780 09-06)
Copyright Avail: NTIS HC A20/MF A01

N89-16805# Societe de Fabrication d'Instruments de Mesure, Massy (France). Measurement and Flight Test Dept.
MAINTENANCE AID SYSTEM FOR WIDE BODY AIRCRAFT
Albert Levionnois *In* AGARD, Engine Condition Monitoring: Technology and Experience Oct. 1988 7 p (For primary document see N89-16780 09-06)
Copyright Avail: NTIS HC A20/MF A01

N89-16806# Computing Devices Co., Ottawa (Ontario).
INSTALLED THRUST AS A PREDICTOR OF ENGINE HEALTH FOR JET ENGINES
G. B. Mackintosh and M. J. Hamer *In* AGARD, Engine Condition Monitoring: Technology and Experience Oct. 1988 10 p (For primary document see N89-16780 09-06)
Copyright Avail: NTIS HC A20/MF A01

N89-16808# Rolls-Royce Ltd., Bristol (England). Mechanical Technology (Military) Dept.
A JOINT STUDY ON THE COMPUTERISATION OF IN-FIELD AERO ENGINE VIBRATION DIAGNOSIS
H. R. Carr, G. J. Ives, and P. Jenkins (Ministry of Defence, London, England) *In* AGARD, Engine Condition Monitoring: Technology and Experience Oct. 1988 13 p Sponsored by Ministry of Defence Procurement Executive, London, United Kingdom (For primary document see N89-16780 09-06)
Copyright Avail: NTIS HC A20/MF A01

N89-16809# Pratt and Whitney Aircraft of Canada Ltd., Longueuil (Quebec).
FAULT MANAGEMENT IN AIRCRAFT POWER PLANT CONTROLS
S. Mazareanu and A. Nobre *In* AGARD, Engine Condition Monitoring: Technology and Experience Oct. 1988 16 p (For primary document see N89-16780 09-06)
Copyright Avail: NTIS HC A20/MF A01

N89-16813# Aeronautical Research Labs., Melbourne (Australia).
IDENTIFICATION OF DYNAMIC CHARACTERISTICS FOR FAULT ISOLATION PURPOSES IN A GAS TURBINE USING CLOSED-LOOP MEASUREMENTS
G. L. Merrington *In* AGARD, Engine Condition Monitoring: Technology and Experience Oct. 1988 13 p (For primary document see N89-16780 09-06)
Copyright Avail: NTIS HC A20/MF A01

N89-16814# Canadian Forces Base Trenton, Astra (Ontario). Aerospace Maintenance Development Unit.
CF-18/F404 TRANSIENT PERFORMANCE TRENDING
J. R. Henry *In* AGARD, Engine Condition Monitoring: Technology and Experience Oct. 1988 13 p (For primary document see N89-16780 09-06)
(Contract FE220786FRMC4; ARP-3610-147)
Copyright Avail: NTIS HC A20/MF A01

N89-16853# National Aerospace Lab., Amsterdam (Netherlands).
MEASUREMENT UNCERTAINTY OF THE AGARD/PEP UNIFORM ENGINE TEST PROGRAM
J. P. K. Vleghert *In* AGARD, Aerodynamic Data Accuracy and Quality: Requirements and Capabilities in Wind Tunnel Testing Jul. 1988 12 p (For primary document see N89-16846 09-09)
Copyright Avail: NTIS HC A22/MF A01

N89-16854# Sverdrup Technology, Inc., Arnold Air Force Station, TN. Instrumentation and Controls.
AN OVERVIEW OF THE APPLICATION OF STANDARD MEASUREMENT UNCERTAINTY METHODOLOGY TO PROPULSION TESTING
J. W. Thompson, Jr., W. F. Kimzey, and W. O. Boals, Jr. *In* AGARD, Aerodynamic Data Accuracy and Quality: Requirements and Capabilities in Wind Tunnel Testing Jul. 1988 15 p Prepared in cooperation with Arnold Engineering Development Center, Arnold Air Force Station, TN (For primary document see N89-16846 09-09)
Copyright Avail: NTIS HC A22/MF A01

N89-16996# Rolls-Royce Ltd., Derby (England). Non-Metal and Composite Manufacturing Technology.
LIMITATIONS AT HIGH TEMPERATURES OF PRESENT DAY ENGINEERING MATERIALS
G. W. Meetham *In* Office of Naval Research, Engineering Materials for Very High Temperatures. An ORNL Workshop 1988 p 35-42 (For primary document see N89-16992 09-27)
Avail: NTIS HC A05/MF A01

08 AIRCRAFT STABILITY AND CONTROL

Includes aircraft handling qualities; piloting; flight controls; and autopilots.

For related information see also *05 Aircraft Design, Testing and Performance.*

N89-16844*# National Aeronautics and Space Administration. Ames Research Center, Moffett Field, CA.
R-PARAMETERIZATION AND ITS ROLE IN CLASSIFICATION OF LINEAR MULTIVARIABLE FEEDBACK SYSTEMS
Robert T. N. Chen Dec. 1988 24 p
(NASA-TM-101066; A-89030; NAS 1.15:101066) Avail: NTIS HC A03/MF A01 CSCL 01C

A classification of all the compensators that stabilize a given general plant in a linear, time-invariant multi-input, multi-output feedback system is developed. This classification, along with the associated necessary and sufficient conditions for stability of the feedback system, is achieved through the introduction of a new parameterization, referred to as R-Parameterization, which is a dual of the familiar Q-Parameterization. The classification is made to the stability conditions of the compensators and the plant by themselves; and necessary and sufficient conditions are based on the stability of Q and R themselves. Author

N89-16845*# National Aeronautics and Space Administration. Ames Research Center, Moffett Field, CA.
MODAL CONTROL OF AN OBLIQUE WING AIRCRAFT
James D. Phillips Jan. 1989 49 p
(NASA-TP-2898; A-88250; NAS 1.60:2898) Avail: NTIS HC A03/MF A01 CSCL 01C

A linear modal control algorithm is applied to the NASA Oblique Wing Research Aircraft (OWRA). The control law is evaluated using a detailed nonlinear flight simulation. It is shown that the modal control law attenuates the coupling and nonlinear aerodynamics of the oblique wing and remains stable during control saturation caused by large command inputs or large external disturbances. The technique controls each natural mode independently allowing single-input/single-output techniques to be applied to multiple-input/multiple-output systems. Author

09 RESEARCH AND SUPPORT FACILITIES (AIR)

Includes airports, hangars and runways; aircraft repair and overhaul facilities; wind tunnels; shock tubes; and aircraft engine test stands.

For related information see also *14 Ground Support Systems and Facilities (Space).*

N89-16846# Advisory Group for Aerospace Research and Development, Neuilly-Sur-Seine (France). Fluid Dynamics Panel.
AERODYNAMIC DATA ACCURACY AND QUALITY: REQUIREMENTS AND CAPABILITIES IN WIND TUNNEL TESTING
Jul. 1988 516 p In ENGLISH and FRENCH Symposium held in Naples, Italy, 28 Sep. - 1 Oct. 1988
(AGARD-CP-429; ISBN-92-835-0469-0) Copyright Avail: NTIS HC A22/MF A01

The wind tunnel is the main instrument for providing experimental aerodynamic data to the aerospace industry and researcher for the purpose of load and performance evaluation and for verification of theoretical results. In both cases, it is imperative that the user has confidence in the quality of the results, which means that he must have information on what accuracy to attach to the data. The quality of wind tunnel results depends upon both the accuracy of measurements and the imperfections provided by the wind tunnel environment. Great strides have been made on measurement accuracy and as a rule this need no longer be of much concern if properly attended to. However, imperfections provided by the wind tunnel are still extant and these are the main sources affecting the quality and accuracy of aerodynamic wind tunnel data. The capabilities of wind tunnels are compared with the demands of the user. For individual titles, see N89-16847 through N89-16880.

N89-16847*# Army Aviation Systems Command, Moffett Field, CA.
A CRITICAL ASSESSMENT OF WIND TUNNEL RESULTS FOR THE NACA 0012 AIRFOIL **c02**
W. J. McCroskey *In* AGARD, Aerodynamic Data Accuracy and Quality: Requirements and Capabilities in Wind Tunnel Testing Jul. 1988 21 p Previously announced as N88-11636 (For primary document see N89-16846 09-09)
Copyright Avail: NTIS HC A22/MF A01 CSCL 01A

A large body of experimental results, obtained in more than 40 wind tunnels on a single, well known two-dimensional configuration, was critically examined and correlated. An assessment of some of the possible sources of error was made for each facility, and data which are suspect were identified. It was found that no single experiment provided a complete set of reliable data, although an investigation stands out as superior in many respects. However, from the aggregate of data the representative properties of the NACA 0012 airfoil can be identified with reasonable confidence over wide range of Mach numbers, Reynolds number, and angles of attack. This synthesized information can now be used to assess and validate existing and future wind tunnel results and to evaluate advanced Computational Fluid Dynamics codes. Author

N89-16848# Deutsche Forschungs- und Versuchsanstalt fuer Luft- und Raumfahrt, Brunswick (Germany, F.R.).
EXPERIMENTS ON THE DFVLR-F4 WING BODY CONFIGURATION IN SEVERAL EUROPEAN WINDTUNNELS
G. Redeker, R. Mueller, P. R. Ashill, A. Elsenaar, and V. Schmitt (Office National d'Etudes et de Recherches Aeronautiques, Paris, France) *In* AGARD, Aerodynamic Data Accuracy and Quality: Requirements and Capabilities in Wind Tunnel Testing Jul. 1988 15 p (For primary document see N89-16846 09-09)
Copyright Avail: NTIS HC A22/MF A01

Attempts are made to improve design methods for three-dimensional configurations in transonic flow and to increase the confidence in wind tunnel data. The selected configuration was the DFVLR-F4 wing-body combination incorporating a transonic wing of high aspect ratio and a fuselage of Airbus type. The experimental part of the exercise is examined, where the same model of the wing-body configuration was tested in three European Transonic wind tunnels. The tests followed an agreed test program comprised of force and moment measurement as well as measurements of pressure distribution on wing and fuselage. Selected test results from the three wind tunnel tests are compared, the main emphasis being placed on the comparison of results from different wind tunnels on physically the same model. The results show that the data of the three wind tunnels are in reasonable agreement, although the severe accuracy requirements of industry for judging performance data from different wind tunnels could not be met. Author

N89-16849# Office National d'Etudes et de Recherches Aeronautiques, Paris (France).
COMPARISON OF THE RESULTS OF TESTS ON A300 AIRCRAFT IN THE RAE 5 METRE AND THE ONERA F1 WIND TUNNELS **c02**
C. Quemard and P. B. Earnshaw (Royal Aircraft Establishment, Farnborough, England) *In* AGARD, Aerodynamic Data Accuracy and Quality: Requirements and Capabilities in Wind Tunnel Testing Jul. 1988 16 p (For primary document see N89-16846 09-09)
Copyright Avail: NTIS HC A22/MF A01

Studies of the A300 Airbus were carried out in the pressurized low speed wind tunnel at RAE and ONERA. Initially comparison of the results from the same model mounted on an identical three strut support, showed discrepancies which in the case of lift coefficient amounted to about 2.5 pct. A systematic comparison was made of the measurement techniques together with the

methods used in the reduction of the resulting data. The production of uncorrected aerodynamic coefficients required the measurement of loads by means of underfloor balances and of the reference pressure. Checks were carried out on the balance calibrations confirming their accuracy after which an attempt was made in both facilities to assess and refine the accuracy of the reference pressure measurement. As a result, corrections were applied to the measurements made in both wind tunnels which reduced but did not eliminate the differences between the two sets of results. The data reduction relies on corrections to be applied for tunnel wall interference as well as that from the strut support system. Author

N89-16850# Boeing Vertol Co., Philadelphia, PA. Advanced Aircraft Aerodynamics.

ANALYTICAL AND EXPERIMENTAL METHODS USED TO RESOLVE THE AERODYNAMIC RESULTS OF TESTS CONDUCTED IN THREE TEST FACILITIES **c02**

Ross D. Clark and H. J. Rosenstein *In* AGARD, Aerodynamic Data Accuracy and Quality: Requirements and Capabilities in Wind Tunnel Testing Jul. 1988 15 p (For primary document see N89-16846 09-09)

Copyright Avail: NTIS HC A22/MF A01

The V-22 aerodynamic drag and stability data base developed through extensive wind tunnel testing is examined. Early drag and stability aerodynamic testing showed differences in characteristics when comparing results from different tests facilities. A joint Bell-Boeing/Navy plan involving a thorough understanding/ refinement of test techniques, facility calibrations and application of computational methods resolved these issues and permitted validation of the data base. Author

N89-16851# Calspan Field Services, Inc., Arnold AFS, TN. Aerodynamics Sect.

HIERARCHY OF UNCERTAINTY SOURCES IN TRANSONIC WIND TUNNEL TESTING

James M. Whoric and Randy W. Hobbs *In* AGARD, Aerodynamic Data Accuracy and Quality: Requirements and Capabilities in Wind Tunnel Testing Jul. 1988 13 p Prepared in cooperation with Arnold Engineering Development Center, Arnold Air Force Station, TN (For primary document see N89-16846 09-09)

Copyright Avail: NTIS HC A22/MF A01

A numerical perturbation technique was employed to compute the aerodynamic coefficient uncertainties attributable to uncertainty sources associated with transonic wind tunnel testing. A force accounting system which included data from an aerodynamic reference system, a nozzle afterbody test, and an inlet test was established to develop a system of equations by which to compute nominal flight values of lift, drag, and pitching moment coefficient uncertainties. Uncertainty estimates included standard instrumentation uncertainties for such sources as wall interference, specific humidity, and viscous simulation which were based on combinations of CFD calculations and experimental data. Author

N89-16852# Naval Air Systems Command, Washington, DC. Aerodynamics and Flight Controls.

WIND TUNNEL PREDICTED AIR VEHICLE PERFORMANCE: A REVIEW OF LESSONS LEARNED

E. C. Rooney and R. F. Lauer, Jr. (Calspan Field Services, Inc., Arnold AFS, TN.) *In* AGARD, Aerodynamic Data Accuracy and Quality: Requirements and Capabilities in Wind Tunnel Testing Jul. 1988 11 p (For primary document see N89-16846 09-09)

Copyright Avail: NTIS HC A22/MF A01

Air vehicle development programs continue to experience difficulty in preformacne prediction of new aircraft configurations. Advances in the state-of-the-art in wind tunnel simulation techniques, flight performance measurements and computational fluid dynamics have provided the basis for investigating the accuracy of the aerodynamic element used in the performance prediction process. The force accounting procedures, model and wind tunnel simulation techniques and correction procedures are reviewed, along with full scale adjustments used to predict the performance of air vehicles. The lesson learned in this review should enhance the capability to predict aircraft performance for future air vehicle development programs. Author

N89-16853# National Aerospace Lab., Amsterdam (Netherlands).

MEASUREMENT UNCERTAINTY OF THE AGARD/PEP UNIFORM ENGINE TEST PROGRAM **c07**

J. P. K. Vleghert *In* AGARD, Aerodynamic Data Accuracy and Quality: Requirements and Capabilities in Wind Tunnel Testing Jul. 1988 12 p (For primary document see N89-16846 09-09)

Copyright Avail: NTIS HC A22/MF A01

In the AGARD/PEP Uniform Engine Test Program (UETP) two engines were tested in 8 facilities in 5 different countries to compare measuring practices and results. An overview is given of the UTEP with the emphasis on Uncertainty Assessment according to the method proposed by Dr. Abernethy, in which the total uncertainty is split in a random error (scatter, precision) and a bias error or offset. The results show that the random error is small but that appreciable bias error exists between participants. Author

N89-16854# Sverdrup Technology, Inc., Arnold Air Force Station, TN. Instrumentation and Controls.

AN OVERVIEW OF THE APPLICATION OF STANDARD MEASUREMENT UNCERTAINTY METHODOLOGY TO PROPULSION TESTING **c07**

J. W. Thompson, Jr., W. F. Kimzey, and W. O. Boals, Jr. *In* AGARD, Aerodynamic Data Accuracy and Quality: Requirements and Capabilities in Wind Tunnel Testing Jul. 1988 15 p Prepared in cooperation with Arnold Engineering Development Center, Arnold Air Force Station, TN (For primary document see N89-16846 09-09)

Copyright Avail: NTIS HC A22/MF A01

In the past several years, a standard measurement uncertainty methodology has been adopted by the SAE, ASME, AIAA, ISA, JANNAF, and ISO. This standard methodology has significantly improved the ability to resolve and understand measurement systems accuracies in the engine test facility at AEDC. The measurement accuracy assessment methodology and its development background is examined. The procedural steps in making an uncertainty analysis are reviewed, and typical results of an analysis effort are illustrated by reviewing the elemental errors and uncertainties for state-of-the-art measurement systems used in simulated altitude tests of air breathing engine propulsion systems. Typical elemental and combined uncertainties for measured values of pressure, force, flow, and temperature and uncertainties of propulsion system thrust and specific fuel consumption performance parameters are included. Author

N89-16855# Royal Aircraft Establishment, Bedford (England).

THE ACCURATE MEASUREMENT OF DRAG IN THE 8 FT X 8 FT TUNNEL

M. N. Wood and D. S. Capps *In* AGARD, Aerodynamic Data Accuracy and Quality: Requirements and Capabilities in Wind Tunnel Testing Jul. 1988 9 p Previously announced as X88-72373 (For primary document see N89-16846 09-09)

Copyright Avail: NTIS HC A22/MF A01

The techniques currently adopted in the 8 ft by 8 ft wind tunnel at RAE for the accurate measurement of drag are described in detail. Data are presented from three series of tests on a model of the A-310 aircraft and these demonstrate the level of accuracy which can be achieved. Author

N89-16856# British Aerospace Public Ltd. Co., Preston (England).

ACCURATE DRAG ESTIMATION USING A SINGLE COMPONENT DRAG MODEL TECHNIQUE

A. M. Cassie *In* AGARD, Aerodynamic Data Accuracy and Quality: Requirements and Capabilities in Wind Tunnel Testing Jul. 1988 16 p (For primary document see N89-16846 09-09)

Copyright Avail: NTIS HC A22/MF A01

The design, development and operation of an advance afterbody drag rig at the high speed wind tunnel at Warton is reviewed. The

rig has been extensively used over a 16 year period for minimization of modern combat aircraft afterbody drag. Accurate incremental drag data is produced by measurement of the axial force on a fully representative metric afterbody section. A full description of the rig is given along with techniques for data correction and presentation of typical data. Author

N89-16857# Aircraft Research Association Ltd., Bedford (England).
DEVELOPMENT OF TESTING TECHNIQUES IN A LARGE TRANSONIC WIND TUNNEL TO ACHIEVE A REQUIRED DRAG ACCURACY AND FLOW STANDARDS FOR MODERN CIVIL TRANSPORTS
E. C. Carter and K. C. Pallister *In* AGARD, Aerodynamic Data Accuracy and Quality: Requirements and Capabilities in Wind Tunnel Testing Jul. 1988 20 p (For primary document see N89-16846 09-09)
Copyright Avail: NTIS HC A22/MF A01

Experience and results obtained in the ARA 9 ft by 8 ft transonic wind tunnel are used to address the questions of measurement and flow quality, data accuracy and achieved performance. The discussions relate primarily to experience with civil transports for which accurate drag prediction and efficient drag reduction through reliable experimental techniques is of major importance. The quality of results is studied via the definition of the problem areas, the correction methods and analysis of dynamics of the flow and the associated measurements. Techniques specific to a large development transonic tunnel are discussed in detail with a constant awareness of the cost and efficiency in relation to the required accuracy and repeatability standards. Author

N89-16858# Office National d'Etudes et de Recherches Aerospatiales, Modane (France).
PRECISION IMPROVEMENT OF TRANSPORT AIRCRAFT DRAG MEASUREMENTS [AMELIORATION DE LA PRECISION DE LA MESURE DE LA TRAINEE D'UN AVION DE TRANSPORT] **c02**
C. Armand and C. Pujol (Societe Nationale Industrielle Aerospatiale, Toulouse, France) *In* AGARD, Aerodynamic Data Accuracy and Quality: Requirements and Capabilities in Wind Tunnel Testing Jul 1988 14 p In FRENCH Previously announced in IAA as A88-22597 (For primary document see N89-16846 09-09)
Copyright Avail: NTIS HC A22/MF A01

Methods used in the ONERA S1MA and S2MA wind tunnels for attaining the desired absolute precision of 0.0002 in drag measurements of Airbus type transport aircraft are discussed. Factors considered include the quality of the balances, the precision of the incidence measurements, and the effects of friction and extreme temperatures. It is also noted that in order to obtain accurate drag measurements the airfoil geometry and the pressure distribution on the airfoil must be known to a high degree of precision. The results are corrected for the pressure fields in the test section and for the effects of the wall and the sting. E.R.

N89-16859# Deutsche Forschungs- und Versuchsanstalt fuer Luft- und Raumfahrt, Berlin (Germany, F.R.).
FLOW UNSTEADINESS IN THREE LOW-SPEED WIND TUNNELS
U. Michel and E. Froebel *In* AGARD, Aerodynamic Data Accuracy and Quality: Requirements and Capabilities in Wind Tunnel Testing Jul. 1988 10 p (For primary document see N89-16846 09-09)
Copyright Avail: NTIS HC A22/MF A01

The velocity unsteadiness in 6 test sections of 3 low speed wind tunnels is discussed. Large differences of the root-mean-square velocity or turbulence levels are observed in these tunnels. It is shown that these differences can be explained with the two independent contributions to the velocity unsteadiness in a wind tunnel: (1) vorticity which is convected into the test section from upstream, and (2) pressure waves which have many origins but the important ones for low speed wind tunnels are the free shear layers of open test sections and slotted wall test sections. It is further shown that the turbulence level is not sufficient to describe the effect of velocity unsteadiness on the quality of data measured in a wind tunnel and it is demonstrated with the example of boundary layer transition that the distribution of the fluctuating energy in the frequency domain is more important. Author

N89-16860# DSMA International, Inc., Toronto (Ontario).
IMPACT OF NOZZLE DESIGN CONSTRAINTS ON TEST SECTION FLOW QUALITY
D. VanEvery, S. Raimondo, and G. M. Elfstrom *In* AGARD, Aerodynamic Data Accuracy and Quality: Requirements and Capabilities in Wind Tunnel Testing Jul. 1988 11 p (For primary document see N89-16846 09-09)
Copyright Avail: NTIS HC A22/MF A01

A procedure is described which allows the design of relatively short adjustable nozzles without resorting to the assumption of radial flow upstream of the nozzle inflection point. This design procedure is used to generate a number of fully flexible nozzle designs for a design Mach number of 1.4. Flexible nozzle parameters such as pressure loading, number of actuators and nozzle length are varied in order that the influence of these parameters on test section flow quality may be evaluated. The influence of nozzle actuator setting accuracy is also estimated. The parametric study shows that high flow quality can be achieved for the shortest nozzle considered. The examination of jack setting errors shows that for well designed nozzles, jack setting error will be a significant source of test section flow nonuniformities. Author

N89-16861# McDonnell Aircraft Co., St. Louis, MO. Aerodynamics and Propulsion Labs.
TRANSONIC WIND TUNNEL BOUNDARY INTERFERENCE: A CORRECTION PROCEDURE
R. C. Crites *In* AGARD, Aerodynamic Data Accuracy and Quality: Requirements and Capabilities in Wind Tunnel Testing Jul. 1988 16 p (For primary document see N89-16846 09-09)
Copyright Avail: NTIS HC A22/MF A01

An effort to develop a transonic wind tunnel boundary correction procedure is examined. The goal is a boundary correction procedure applicable to ventilated test sections from subsonic through transonic Mach numbers. Boundary correction is distinguished from wall correction. Boundary corrections contain wall corrections, but also contain model support, and other tunnel dependent corrections. The approach taken uses computational fluid dynamics with measured boundary conditions to provide corrections at a few points in the test envelope. Conventional similiarity principles and regression techniques are used to extend these corrections over the full test range. To provide experimental data needed for development and validation, a wind tunnel test program was initiated. A set of 4 wing-body model were built. Model size was varied while maintaining precise geometric similarity. The 3 smallest models were tested from Mach 0.5 to 1.2 in a small transonic tunnel. Preliminary testing of 2 of the largest models was made in a larger tunnel. Extensive boundary pressure data were measured in both tunnels. Typical results of these tests are reviewed. Author

N89-16862# Aircraft Research Association Ltd., Bedford (England).
THE USE OF COMPUTATIONAL FLUID DYNAMIC METHODS TO ASSESS THE EFFECTS OF MODEL SUPPORT SYSTEMS AND WORKING SECTION MODIFICATIONS ON THE FLOW AROUND WIND TUNNEL MODELS
D. R. Stanniland *In* AGARD, Aerodynamic Data Accuracy and Quality: Requirements and Capabilities in Wind Tunnel Testing Jul. 1988 16 p (For primary document see N89-16846 09-09)
Copyright Avail: NTIS HC A22/MF A01

The continuing development of computer codes and power means that computational fluid dynamic methods can be used, in conjunction with test techniques, to provide a more thorough knowledge of measured flow phenomena. The use of various programs is demonstated to evaluate the magnitude of the interference due to model support and flow measurement

installations and to guide the design of an acoustic liner for the ARA transonic wind tunnel. Various simplifications are necessary to permit the representation of the complex geometry within the constraints imposed by the programs, and hence, care is needed in using the computed results. Within this limitation, the methods can provide a valuable aid to the interpretation of experimental results and to guide the design of wind tunnel installations. Calculations are described using various theoretical methods, carried out in support of tests on five different wind tunnel installations. Author

N89-16863# National Aerospace Lab., Amsterdam (Netherlands).
ACCURACY OF VARIOUS WALL-CORRECTION METHODS FOR 3D SUBSONIC WIND-TUNNEL TESTING
R. A. Maarsingh, Th. E. Labrujere, and J. Smith *In* AGARD, Aerodynamic Data Accuracy and Quality: Requirements and Capabilities in Wind Tunnel Testing Jul. 1988 13 p (For primary document see N89-16846 09-09)
Copyright Avail: NTIS HC A22/MF A01

On the basis of wind-tunnel measurements on a (simple, unpowered, but complete) transport aircraft model in a small and a very large solid-wall test section the accuracy of four measured-boundary-condition (MEC) methods, as well as two classical methods, was analyzed at low-speed conditions. Large reductions in the amount of in situ measured data are shown to be possible, yet yielding results which match almost with those of calculations using multiples of input data. Classical methods need not be abandoned at once in low-speed solid-wall testing. Higher priority should be given to the well-known interpretation problem: the determination of the actual model reaction upon the wall-induced flow field. Author

N89-16864*# National Aeronautics and Space Administration. Langley Research Center, Hampton, VA.
WIND TUNNEL-SIDEWALL-BOUNDARY-LAYER EFFECTS IN TRANSONIC AIRFOIL TESTING-SOME CORRECTABLE, BUT SOME NOT
F. T. Lynch (Douglas Aircraft Co., Inc., Long Beach, CA.) and C. B. Johnson *In* AGARD, Aerodynamic Data Accuracy and Quality: Requirements and Capabilities in Wind Tunnel Testing Jul. 1988 16 p (For primary document see N89-16846 09-09)
Copyright Avail: NTIS HC A22/MF A01 CSCL 14B

The need to correct transonic airfoil wind tunnel test data for the influence of the tunnel sidewall boundary layers, in addition to the wall accepted corrections for the analytical investigation was carried out in order to evaluate sidewall boundary layer effects on transonic airfoil characteristics, and to validate proposed correction and the limit to their applications. This investigation involved testing of modern airfoil configurations in two different transonic airfoil test facilities, the 15 x 60 inch two-dimensional insert of the National Aeronautical Establishment (NAE) 5 foot tunnel in Ottawa, Canada, and the two-dimensional test section of the NASA Langley 0.3 m Transonic Cryogenic Tunnel (TCT). Results presented included effects of variations in sidewall-boundary layer bleed in both facilities, different sidewall boundary layer correction procedures, tunnel-to tunnel comparisons of correcte results, and flow conditions with and without separation. Author

N89-16865# Deutsche Forschungs- und Versuchsanstalt fuer Luft- und Raumfahrt, Goettingen (Germany, F.R.). Inst. fuer Experimentelle Stroemungsmechanik.
PHYSICAL ASPECTS OF VISCOUS SIMULATION AND ASSOCIATED RESEARCH REQUIREMENTS Summary Report
E. Stanewsky *In* AGARD, Aerodynamic Data Accuracy and Quality: Requirements and Capabilities in Wind Tunnel Testing Jul. 1988 16 p (For primary document see N89-16846 09-09)
Copyright Avail: NTIS HC A22/MF A01

Boundary layer development and transition; nonequilibrium boundary layers; shock boundary layer interaction; classical separation, trailing edge flow and buffet; vortex flows; environmental effects on the boundary layer development and transition; and boundary layer manipulation are examined. Some selected results are presented and summarized with respect to the dominant viscous and outer inviscid flow parameters and most urgently needed research. B.G.

N89-16866# National Aerospace Lab., Amsterdam (Netherlands).
ON REYNOLDS NUMBER EFFECTS AND SIMULATION **c02**
A. Elsenaar *In* AGARD, Aerodynamic Data Accuracy and Quality: Requirements and Capabilities in Wind Tunnel Testing Jul. 1988 22 p (For primary document see N89-16846 09-09)
Copyright Avail: NTIS HC A22/MF A01

The change in flow development with Reynolds number, commonly referred to as the Reynolds number effect, has both attracted and annoyed the aerodynamic community. A misjudgment of the magnitude of the Reynolds number effect may lead to an over- or underestimation of flight performance resulting in economic loss. In the worst case a costly redesign is required during the period of flight testing. The question of Reynolds number effects is crucial because of its very fundamental nature: a thorough understanding of viscous flow phenomena and their interactions with the inviscid flow field is required to explain the Reynolds number effects. As long as routine wind tunnel testing at the actual flight Reynolds number is not possible, other ways must be found to close the experimental Reynolds number gap. Basically, Reynolds number effects originate from a Reynolds number dependency of a viscous shear layer close to the body surface and its interaction with the outer inviscid flow field. If the boundary layer can be manipulated in the wind tunnel such that its development at flight Reynolds number is closely approximated, the inviscid flow senses the proper boundary condition and the overall flow development will then be very similar. The fundamental aspects of the Reynolds number effects are reviewed. Author

N89-16867# Case Western Reserve Univ., Cleveland, OH.
A PROPOSED BOUNDARY LAYER SIMULATION METHODOLOGY FOR WIND TUNNEL TESTING
Eli Reshotko, C. Armand, Y. Y. Chan, A. Elsenaar, A. B. Haines, J. L. Potter, and Giuseppe P. Russo *In* AGARD, Aerodynamic Data Accuracy and Quality: Requirements and Capabilities in Wind Tunnel Testing Jul. 1988 12 p (For primary document see N89-16846 09-09)
Copyright Avail: NTIS HC A22/MF A01

While wind tunnels were used for about a century to obtain performance data for vehicles to be used in atmospheric flight, these are still numerous uncertainties and ambiguities in the interpretation of the data and in reliably extrapolating them to flight conditions. These issues were recently addressed. The development of a boundary layer simulation/extrapolation methodology is examined. Author

N89-16868# Naples Univ. (Italy). Inst. of Aerodynamics 'Umberto Nobile'.
EXPERIMENTS ON BOUNDARY LAYER TRANSITION TRIPPING AT LOW REYNOLDS NUMBERS **c02**
Giuseppe P. Russo *In* AGARD, Aerodynamic Data Accuracy and Quality: Requirements and Capabilities in Wind Tunnel Testing Jul. 1988 13 p (For primary document see N89-16846 09-09)
Copyright Avail: NTIS HC A22/MF A01

A systematical experimental investigation was undertaken with the aim of obtaining sound results on the effectiveness of distributed roughnesses in tripping transition on a flat plate at low Reynolds numbers. A 2.5 mm band of double stick scotch tape dusted with sparse carborundum grains was used as a tripping element at various speeds, ranging from 11 to 17 m/s. Transition location was detected by streamwise traversing, at a fixed height from the flat plate, both a Pitot tube and a hot-wire probe; also relevant velocity profiles in the boundary layer were measured. When needed surface flow visualization was used to confirm the transition position. A good correlation was found, in terms of the critical roughness Reynolds number needed to fix transition at the roughness, with the results found in the open literature. Author

N89-16869# Office National d'Etudes et de Recherches Aeronautiques, Paris (France).
SOME DIFFICULTIES IN THE WIND TUNNEL PREDICTION OF MODERN CIVIL AIRCRAFT BUFFETING: PROPOSED REMEDIES **c02**
R. Destuynder, V. Schmitt, J. Berger, and R. Barreau (Societe Nationale Industrielle Aerospatiale, Toulouse, France) *In* AGARD, Aerodynamic Data Accuracy and Quality: Requirements and Capabilities in Wind Tunnel Testing Jul. 1988 14 p In FRENCH; ENGLISH summary (For primary document see N89-16846 09-09)
Copyright Avail: NTIS HC A22/MF A01

The prediction of transport aircraft buffet response still remains a challenge despite recent progress in understanding of the phenomenon. The prediction is up to now inaccessible to a purely theoretical approach and so is mainly based on wind tunnel investigations. After a review of experimental methods currently used to determine model buffeting and a short description of full scale application techniques, the simulation problems that appear are presented. The next point deals with a number of improvements concerning models and experimental methodology with the final objective to provide more reliable buffeting predictions on large transport aircrafts. Author

N89-16870# Messerschmitt-Boelkow-Blohm G.m.b.H., Bremen (Germany, F.R.).
ACCURACY REQUIREMENTS FOR HIGH-SPEED TEST WITH ENGINE SIMULATION ON TRANSPORT AIRCRAFT MODELS IN THE NLR-HST
W. Burgsmueller, J. W. Kooi, and K Moeller, W. (National Aerospace Lab., Amsterdam, Netherlands) *In* AGARD, Aerodynamic Data Accuracy and Quality: Requirements and Capabilities in Wind Tunnel Testing Jul. 1988 16 p (For primary document see N89-16846 09-09)
Copyright Avail: NTIS HC A22/MF A01

Air-driven turbo-powered simulators, so-called TPS units, are being used in wind tunnel testing to simulate the engine flow for an aircraft model. These simulators provide substantial improvement in testing as compared to simple through-flow nacelles used earlier. In order to fully explore the improvement potential in aerodynamic simulation it is mandatory to assure a high level of accuracy or in case of increment testing a good repeatability because the effects of engine interference drag are of the order of a few counts. For increment testing a repeatability of at least + or - 1 drag count must be achieved. The efforts made to demonstrate that this repeatability can be achieved in the NLR high speed wind tunnel (HST) for a half model with a wing-mounted TPS engine are described. The test was performed in a joint program of NLR and MBB-UT, where MBB delivered the model and TPS unit with engine cowlings, while NLR was responsible for engine calibration, wind tunnel instrumentation, and the test. To obtain the desired quality of the final test results the investigation was subdivided into several steps. These steps and the technical problems and questions encountered will be described in detail. Author

N89-16871# Deutsche Forschungs- und Versuchsanstalt fuer Luft- und Raumfahrt, Goettingen (Germany, F.R.).
ENGINE SIMULATOR TESTS: COMPARISON OF CALIBRATION AND WIND TUNNEL RESULTS
W. Baumert, B. Binder, and W. Staeger *In* AGARD, Aerodynamic Data Accuracy and Quality: Requirements and Capabilities in Wind Tunnel Testing Jul. 1988 11 p (For primary document see N89-16846 09-09)
Copyright Avail: NTIS HC A22/MF A01

A turbine powered simulator (TPS) was tested with a bellmouth inlet in the calibration tank and with a flight inlet in the low speed wind tunnel at DFVLR Gottingen. Local Mach number distribution shows good agreement in both facilities. The Pitot pressure distribution behind the fan however is different. This is probably due to the different inlet configurations. The nozzle coefficients obtained in the calibration tank are used to calculate the thrust of the simulator in the wind tunnel. The comparison with the thrust measured in the wind tunnel shows that additional corrections have to be applied when evaluating wind tunnel measurements with TPS. Author

N89-16872# Office National d'Etudes et de Recherches Aerospatiales, Modane (France).
INSTANTANEOUS FORCE MEASUREMENT ON A MODEL SUBJECTED TO RAPID CONTROL VARIATIONS
J. P. Drever and M. Robert *In* AGARD, Aerodynamic Data Accuracy and Quality: Requirements and Capabilities in Wind Tunnel Testing Jul. 1988 20 p In FRENCH; ENGLISH summary Original language document was announced in IAA as A88-22599 (For primary document see N89-16846 09-09)
Copyright Avail: NTIS HC A22/MF A01

The development of a wind-tunnel model using a lateral-jet system to enact rapid control variations is discussed, and the results of instantaneous force measurements obtained with the model without wind in the supersonic test section of the ONERA S2MA facility are reported. The range of frequencies to be avoided in controlling the generator are identified, and a mathematical model for calculating the model motion is developed. Torsion applied to the model is measured with a precision of + or - 5 percent in roll and + or - 10 percent in pitch and yaw over a range of frequencies from 0 to 60 Hz. Good correlation is found between the applied and measured forces. Author

N89-16873# Technische Univ., Darmstadt (Germany, F.R.).
BALANCE ACCURACY AND REPEATABILITY AS A LIMITING PARAMETER IN AIRCRAFT DEVELOPMENT FORCE MEASUREMENTS IN CONVENTIONAL AND CRYOGENIC WIND TUNNELS
B. Ewald *In* AGARD, Aerodynamic Data Accuracy and Quality: Requirements and Capabilities in Wind Tunnel Testing Jul. 1988 12 p (For primary document see N89-16846 09-09)
Copyright Avail: NTIS HC A22/MF A01

The success of a commercial transport development is heavily influenced by the accuracy of drag measurements during the aerodynamic development in the wind tunnel. It is shown, that the internal balance in one limiting factor of accuracy. The accuracy standard of modern internal balances is compared to the accuracy and repeatability requirement of the aerodynamicist. The comparison with high precision single component load cells promises a large improvement potential in multi-component balance design and calibration. The following fields of improvement are discussed: balance design, balance material selection and treatment, calibration methods, calibration software, and thermal effects. Perfect correction of the thermal effects is the key to the successful use of cryogenic tunnels. An approach for the crucial problem of balance body distortion due to temperature gradients is demonstrated. Author

N89-16874# Arnold Engineering Development Center, Arnold Air Force Station, TN.
CHARACTERIZATION OF HYPERSONIC WIND TUNNEL FLOW FIELDS FOR IMPROVED DATA ACCURACY
Albert H. Boudreau *In* AGARD, Aerodynamic Data Accuracy and Quality: Requirements and Capabilities in Wind Tunnel Testing Jul. 1988 9 p (For primary document see N89-16846 09-09)
Copyright Avail: NTIS HC A22/MF A01

Hypersonic test facilities produce flow fields which are difficult to characterize. In the past, many hypersonic facilities were reputed to produce test data of inferior quality, when, in fact, it was poor characterization of the flow field principally at fault. With the renaissance in hypersonics at hand, experimentalists face anew the challenge of accurately characterizing flow fields. The U.S. Air Force's Arnold Engineering Development Center has faced these complex problems and developed techniques to accurately determine free-stream conditions. Those tools of characterization are highlighted and a standard by which all hypersonic wind tunnels should be compared. Author

N89-16875# MATRA Service Aerodynamique, Velizy-Villacoublay (France).
ACCURACY OF LIFT AND CENTER-OF-THRUST MEASUREMENTS AT MISSILE CONTROL SURFACES c02
J. Perinelle and M. Ribadeau Dumas *In* AGARD, Aerodynamic Data Accuracy and Quality: Requirements and Capabilities in Wind Tunnel Testing Jul. 1988 17 p In FRENCH; ENGLISH summary (For primary document see N89-16846 09-09)
Copyright Avail: NTIS HC A22/MF A01

During the study of aerodynamically piloted missiles it is necessary to estimate the forces and moments applied to the control surfaces. These qualities are difficult to evaluate by numerical methods and the study is performed in the wind tunnel experimentally. After a first evaluation of an optimal position of the axis of rotation and of the planform, the efforts, and moments are measured in the whole flight envelope. An accurate knowledge of the moments about the axis (hinge moment) is required for guidance and control studies. The influence of various experimental parameters on the accuracy of such measurements is assessed. Author

N89-16876# Naples Univ. (Italy). Inst. of Aerodynamics 'Umberto Nobile'.
COMPUTERIZED THERMOGRAPHIC TECHNIQUE FOR THE DETECTION OF BOUNDARY LAYER SEPARATION c02
R. Monti and G. Zuppardi *In* AGARD, Aerodynamic Data Accuracy and Quality: Requirements and Capabilities in Wind Tunnel Testing Jul. 1988 15 p (For primary document see N89-16846 09-09)
Copyright Avail: NTIS HC A22/MF A01

The computerized unsteady thermographic methodology was used as a noninvasive technique to analyze the boundary layer development and to detect the transition lines and the separation regions on airfoil surfaces in the wind tunnel. The method is based on the strong depencence of the heat transfer coefficient upon the flow field condition at the airfoil surface. This noninvasive technique has proved to be very appropriate when studying the boundary layer behavior at very low Reynolds numbers in incompressible flow because at these conditions the boundary layer is very unstable and cannot tolerate any disturbance induced by intrusive techniques. The experimental diagnostic equipment consists of a thermograph (AGA 680), and A/D conversion unit (AVIORRADIO DIGIMEN) and a microcomputer (APPLE IIe). The tests were performed on an elliptic cylinder, on a WORTMANN FX-63-137 and on a Miley MO6-13-128 airfoil. The experimental results compare favorably with those obtained by other authors that ultilized conventional techniques. Author

N89-16877# Messerschmitt-Boelkow-Blohm G.m.b.H., Bremen (Germany, F.R.).
ACCURACY PROBLEMS IN WIND TUNNELS DURING TRANSPORT AIRCRAFT DEVELOPMENT
Guenter Krenz *In* AGARD, Aerodynamic Data Accuracy and Quality: Requirements and Capabilities in Wind Tunnel Testing Jul. 1988 9 p (For primary document see N89-16846 09-09)
Copyright Avail: NTIS HC A22/MF A01

Wind tunnel test data accuracy requirements for transport aircraft are derived. Airline performance guarantees, model and tunnel test techniques available and the quality of prediction methods used form the concept for wind tunnel test programs and set accuracy requirements for test data. Procedures which were followed in high speed cruise and low speed takeoff and landing are described. The accuracy of the wind tunnel tests is limited by several parameters, the most important being flow quality, model and model suspension quality, and balance accuracy. Problems which occurred during the test with small models in the transonic regime led to the concepts presented: the use of large models on a specific suspension with a range-limited balance and the improvement of small model test techniques in connection with the requirements for measurements in cryogenic facilities. Low speed tests are ambitious and extensive due to the many configurations at takeoff and landing. Furthermore, the work is complicated by the many details like closing plates and shutters, which can have a strong effect on the performance data. Some examples are presented. Author

N89-16878# National Aerospace Lab., Amsterdam (Netherlands).
REQUIREMENTS AND CAPABILITIES IN UNSTEADY WINDTUNNEL TESTING
R. D. denBoer, R. Houwink, and R. J. Zwaan *In* AGARD, Aerodynamic Data Accuracy and Quality: Requirements and Capabilities in Wind Tunnel Testing Jul. 1988 18 p (For primary document see N89-16846 09-09)
Copyright Avail: NTIS HC A22/MF A01

The accuracy required for aeroelastic applications concerning full-scale aircraft is discussed, after which the accuracy in current unsteady wind tunnel testing is considered. Author

N89-16879# Institut de Mecanique des Fluides de Lille (France).
PARTICULAR FLIGHT MECHANICS SPECIFICATIONS RELATED TO WIND TUNNEL TEST RESULTS [SPECIFICATIONS PARTICULIERES CONCERNANT LES RESULTATS DES ESSAIS EN SOUFFLERIE POUR LA MECANIQUE DU VOL]
Marc Pianko *In* AGARD, Aerodynamic Data Accuracy and Quality: Requirements and Capabilities in Wind Tunnel Testing Jul. 1988 19 p In FRENCH Original language document was announced in IAA as A88-28859 (For primary document see N89-16846 09-09)
Copyright Avail: NTIS HC A22/MF A01

A flight mechanics analysis of requirements and recommendations for the quality and precision of wind tunnel measurements is presented. The effect of imprecision in modeling flight behavior is examined in order to determine the sensitivity of the individual aerodynamic coefficients. Problems in the characterization of flight at large angles of incidence and sideslip, where unsteady phenomena and perturbations play a large role, are considered. Difficulties in the use of the wind tunnel for aircraft design are also reviewed. Author

N89-16880*# National Aeronautics and Space Administration. Ames Research Center, Moffett Field, CA.
WIND TUNNEL REQUIREMENTS FOR COMPUTATIONAL FLUID DYNAMICS CODE VERIFICATION
Joseph G. Marvin *In* AGARD, Aerodynamic Data Accuracy and Quality: Requirements and Capabilities in Wind Tunnel Testing Jul. 1988 13 p Previously announced as N87-27150 (For primary document see N89-16846 09-09)
Copyright Avail: NTIS HC A22/MF A01 CSCL 14B

The role of experiment in the development of computational fluid dynamics (CFD) for aerodynamic flow field prediction is discussed. Requirements for code verification from two sources that pace the development of CFD are described for: (1) development of adequate flow modeling, and (2) establishment of confidence in the use of CFD to predict complex flows. The types of data needed and their accuracy differes in detail and scope and leads to definite wind tunnel requirements. Examples of testing to assess and develop turbulence models, and to verify code development, are used to establish future wind tunnel testing requirements. Versatility, appropriate scale and speed range, accessibility for nonintrusive instrumentation, computerized data systems, and dedicated use for verification were among the more important requirements identified. Author

N89-16881# Carnegie-Mellon Univ., Pittsburgh, PA. Software Engineering Inst.
FUNCTIONAL PERFORMANCE SPECIFICATION FOR AN EXTERNAL COMPUTER SYSTEM SIMULATOR Final Technical Report
B. C. Meyers and Hans Mumm Aug. 1988 25 p
(Contract F19628-85-C-0003)
(AD-A200611; CMU/SEI-88-TR-25; ESD-TR-88-026) Avail: NTIS HC A03/MF A01 CSCL 12E

This document defines the functional and performance

requirements for the external computer system (ECS) simulator that interfaces with the inertial navigation system simulator. Both the ECS simulator and the INS Inertial Navigation System simulator are being developed in Ada by the Real-Time Embedded Systems Testbed Project at the Software Engineering Institute. The ECS simulator is similar to a real-world ECS, but has reduced functionality. This document provides specifications for the major functions of the ECS simulator. In the real world the INS provides accurate information about ship position and motion on a time-critical basis to the ECS. The ECS interfaces with the INS and is capable of receiving and transmitting messages to the INS. The ECS also has functional requirements for providing information to launch controllers (such as missile guidance sets) and other shipboard systems. This document specifies the functional and timing requirements for the ECS simulator. Thus, this program is developed to interface with the INS simulator. However, the scope of this document is to present message processing functions and the operator interaction. Detailed processing, such as missile guidance set alignment, is not considered in this document. GRA

N89-16882*# Sverdrup Technology, Inc., Cleveland, OH.
NASA POWERED LIFT FACILITY INTERNALLY GENERATED NOISE AND ITS TRANSMISSION TO THE ACOUSTIC FAR FIELD Final Report
Ronald G. Huff Nov. 1988 219 p
(Contract NAS3-25266)
(NASA-CR-182217; E-4474; NAS 1.26:182217) Avail: NTIS HC A10/MF A01 CSCL 14B

Noise tests of NASA Lewis Research Center's Powered Lift Facility (PLF) were performed to determine the frequency content of the internally generated noise that reaches the far field. The sources of the internally generated noise are the burner, elbows, valves, and flow turbulence. Tests over a range of nozzle pressure ratios from 1.2 to 3.5 using coherence analysis revealed that low frequency noise below 1200 Hz is transmitted through the nozzle. Broad banded peaks at 240 and 640 Hz were found in the transmitted noise. Aeroacoustic excitation effects are possible in this frequency range. The internal noise creates a noise floor that limits the amount of jet noise suppression that can be measured on the PLF and similar facilities. Author

12 ASTRONAUTICS (GENERAL)

For extraterrestrial exploration see *91 Lunar and Planetary Exploration.*

N89-16883# Deutsche Forschungs- und Versuchsanstalt fuer Luft- und Raumfahrt, Oberpfaffenhofen (West Germany).
PROCEEDINGS OF THE COLLOQUIUM ABOUT JOINT PROJECTS WITHIN THE DFVLR/ISRO COOPERATION
Jun. 1988 119 p Colloquium held in Bangalore, India, 20 Jan. 1987
(DFVLR-Mitt-88-19; ISSN-0176-7739; ETN-89-93522) Avail: NTIS HC A06/MF A01; DFVLR, VB-PL-DO, Postfach 90 60 58, 5000 Cologne, Fed. Republic of Germany, 34.50 Deutsche marks

Joint activities discussed include analysis of meteorite and lunar samples, microwave remote sensing, Indian launcher program, Indian space programs, German spaceborne remote sensing, monocular electro-optical stereo experiments and the autonomous payload control experiment. For individual titles, see N89-16884 through N89-16891.

N89-16884# Indian Space Research Organization, Ahmedabad. Physical Research Lab.
ISRO-DFVLR COLLABORATION IN SPACE SCIENCES
B. H. Subbaraya *In* DFVLR, Proceedings of the Colloquium about Joint Projects Within the DFVLR/ISRO Cooperation Jun. 1988 p 13-25 (For primary document see N89-16883 09-12)
Avail: NTIS HC A06/MF A01; DFVLR, VB-PL-DO, Postfach 90 60 58, 5000 Cologne, Fed. Republic of Germany, 34.50 Deutsche marks

The programs made in cooperation are discussed, including the study of equatorial spread-F using RH-560 rockets from SHAR, nitric oxide measurements in the equatorial mesosphere and lower thermosphere, balloon programs for trace gas measurements, ozone concentration profiles from balloon experiments using a multichannel suntracking photometer, and radiation/aerosol studies. ESA

N89-16885# Indian Space Research Organization, Ahmedabad.
METEORITES AND LUNAR SAMPLES AS SPACE PROBES **c91**
M. N. Rao *In* DFVLR, Proceedings of the Colloquium about Joint Projects Within the DFVLR/ISRO Cooperation Jun. 1988 p 27-38 (For primary document see N89-16883 09-12)
Avail: NTIS HC A06/MF A01; DFVLR, VB-PL-DO, Postfach 90 60 58, 5000 Cologne, Fed. Republic of Germany, 34.50 Deutsche marks

Lunar and meteorite material were analyzed in order to study the long term variation of the fluxes and spectral energies of solar flare associated energetic particles (solar cosmic rays) and galactic cosmic rays. A 1 kg fragment of the Dhursmala meteorite was fractioned in six samples to measure cosmogenic noble gases, radionuclides, and particle tracks. Data indicates that the sample was inside a large meteoroid where the production profiles of cosmogenic isotopes are flat. It is demonstrated that solar flare neon composition is different from solar wind neon composition, and that lunar soil samples yield consistant solar cosmic ray ages with those determined independently by particle track methods. ESA

N89-16886# National Remote Sensing Agency, Hyderabad (India).
INDIAN ACTIVITIES IN REMOTE SENSING APPLICATIONS: MICROWAVE REMOTE SENSING **c43**
B. L. Deekshatulu *In* DFVLR, Proceedings of the Colloquium about Joint Projects Within the DFVLR/ISRO Cooperation Jun. 1988 p 39-56 (For primary document see N89-16883 09-12)
Avail: NTIS HC A06/MF A01; DFVLR, VB-PL-DO, Postfach 90 60 58, 5000 Cologne, Fed. Republic of Germany, 34.50 Deutsche marks

Indian and Indo-German programs concerning airborne and spaceborne multispectral scanning and microwave remote sensing are reviewed, including LANDSAT and Meteosat data processing, development of the Rohini satellite, design and development of a six channel chlorophyll scanner, IRS Sun synchronous spaceborne mission for optical remote sensing, SPOT date reception and processing, and microwave signature studies. ESA

N89-16887# Deutsche Forschungs- und Versuchsanstalt fuer Luft- und Raumfahrt, Oberpfaffenhofen (West Germany).
GERMAN SPACEBORNE REMOTE SENSING ACTIVITIES **c43**
H. Oettl *In its* Proceedings of the Colloquium about Joint Projects Within the DFVLR-ISRO Cooperation Jun. 1988 p 57-67 (For primary document see N89-16883 09-12)
Avail: NTIS HC A06/MF A01; DFVLR, VB-PL-DO, Postfach 90 60 58, 5000 Cologne, Fed. Republic of Germany, 34.50 Deutsche marks

Metric camera, which is a modified version of a classical airborne camera for spaceborne use, a modular optoelectronic multispectral scanner implemented with charge coupled device (CCD) technology and already flown twice in shuttle missions, and a LIDAR system to study the backscattering properties of low and high atmosphere aerosols are discussed. ESA

N89-16888# Deutsche Forschungs- und Versuchsanstalt fuer Luft- und Raumfahrt, Oberpfaffenhofen (West Germany).
PRESENTATION OF THE STATUS OF THE EXPERIMENT AND MISSION ACTIVITIES OF THE MONOCULAR ELECTRO-OPTICAL STEREO SCANNER (MEOSS) **c74**
F. Lanzl *In its* Proceedings of the Colloquium about Joint Projects Within the DFVLR/ISRO Cooperation Jun. 1988 p 69-79 (For primary document see N89-16883 09-12)

Avail: NTIS HC A06/MF A01; DFVLR, VB-PL-DO, Postfach 90 60 58, 5000 Cologne, Fed. Republic of Germany, 34.50 Deutsche marks

The design and implementation of a charge coupled device (CCD) camera; the development of evaluation software for orbit and attitude data; and Weilheim ground station receiving experiment are reviewed. The reception test included five consecutive orbits. A map illustrating the covering area is presented. The scientific applications are discussed. ESA

N89-16889# Indian Space Research Organization, Bangalore.
MISSION UNDER SROSS PROGRAM AND POSITION PAPER ON SROSS-2 WITH MEOSS PAYLOAD **c15**
Tarsem Singh *In* DFVLR, Proceedings of the Colloquium about Joint Projects Within the DFVLR/ISRO Cooperation Jun. 1988 p 81-101 (For primary document see N89-16883 09-12)
Avail: NTIS HC A06/MF A01; DFVLR, VB-PL-DO, Postfach 90 60 58, 5000 Cologne, Fed. Republic of Germany, 34.50 Deutsche marks

The SVL3 launcher was boosted to carry 150 kg satellites to low orbits. The new launcher, called ASLV, is used by the SROSS program which includes gamma ray burst detector experiments, optical tracking experiments, and remote sensing payloads with monocular electro-optical stereo scanner. Mission status is summarized. ESA

N89-16890# Deutsche Forschungs- und Versuchsanstalt fuer Luft- und Raumfahrt, Oberpfaffenhofen (West Germany).
STATUS OF SABREX **c35**
H. Goessl and W. Keydel *In its* Proceedings of the Colloquium about Joint Projects Within the DFVLR/ISRO Cooperation Jun. 1988 p 103-109 (For primary document see N89-16883 09-12)
Avail: NTIS HC A06/MF A01; DFVLR, VB-PL-DO, Postfach 90 60 58, 5000 Cologne, Fed. Republic of Germany, 34.50 Deutsche marks

An airborne radiometer experiment was designed to study the 90 GHz radiometer included in the SROSS-5 mission planning. The technological requirements were examined. Sensor and onboard processor were designed. All components are ordered. Test equipment is built. ESA

N89-16891# Deutsche Forschungs- und Versuchsanstalt fuer Luft- und Raumfahrt, Oberpfaffenhofen (West Germany).
AUTONOMOUS PAYLOAD CONTROL EXPERIMENT ON SROSS-3, A STATUS REVIEW
J. Beck and G. Mayer *In its* Proceedings of the Colloquium about Joint Projects Within the DFVLR/ISRO Cooperation Jun. 1988 p 111-115 (For primary document see N89-16883 09-12)
Avail: NTIS HC A06/MF A01; DFVLR, VB-PL-DO, Postfach 90 60 58, 5000 Cologne, Fed. Republic of Germany, 34.50 Deutsche marks

The study of the autonomous payload control experiment is part of the autonomous onbord data processing and transmission program, bound to the Germain space technology program. The aim is to develop and test advanced communication techniques to enable control of future space experiments. The study progress is reported and the planning is detailed. ESA

N89-16892# Centre National d'Etudes Spatiales, Toulouse (France).
SATELLITE-GROUND DATING AND SYNCHRONIZATION TECHNIQUE [TECHNIQUES DE DATATION ET DE SYNCHRONISATION BORD SOL]
Pierre Virlogeux 14 Jan. 1986 123 p In FRENCH; ENGLISH summary
(CNES-CT/DRT/TIT/TB-040-T; ETN-89-93617) Avail: NTIS HC A06/MF A01

The needs of different projects to synchronize the ground and on-board times are described. The projects discussed include Ariane launcher, telecom satellites, scientific missions, and remote sensing missions. The different solutions adopted by the projects to realize the on board - ground synchronization are presented. Other feasible methods to carry out the synchronization with the telecommand and telemetry packets from the consultative committee for space data systems are also examined. ESA

13 ASTRODYNAMICS

Includes powered and free-flight trajectories; and orbital and launching dynamics.

N89-16893*# Eagle Engineering, Inc., Houston, TX.
USER AND TECHNICAL DOCUMENTATION
30 Sep. 1988 56 p
(Contract NAS9-17878)
(NASA-CR-172087; NAS 1.26:172087; EEI-88-208) Avail: NTIS HC A04/MF A01 CSCL 22C

The program LIBRATE calculates velocities for trajectories from low earth orbit (LEO) to four of the five libration points (L2, L3, L4, and L5), and from low lunar orbit (LLO) to libration points L1 and L2. The flight to be analyzed departs from a circular orbit of any altitude and inclination about the Earth or Moon and finishes in a circular orbit about the Earth at the desired libration point within a specified flight time. This program produces a matrix of the delta V's needed to complete the desired flight. The user specifies the departure orbit, and the maximum flight time. A matrix is then developed with 10 inclinations, ranging from 0 to 90 degrees, forming the columns, and 19 possible flight times, ranging from the flight time (input) to 36 hours less than the input value, in decrements of 2 hours, forming the rows. This matrix is presented in three different reports including the total delta V's, and both of the delta V components discussed. The input required from the user to define the flight is discussed. The contents of the three reports that are produced as outputs are also described. The instructions are also included which are needed to execute the program. Author

14 GROUND SUPPORT SYSTEMS AND FACILITIES (SPACE)

Includes launch complexes, research and production facilities; ground support equipment, e.g., mobile transporters; and simulators.

For related information see also *09 Research and Support Facilities (Air).*

N89-16894# Toronto Univ. (Ontario). Inst. for Aerospace Studies.
NUMERICAL STUDY OF TWO-STAGE LIGHT-GAS HYPERVELOCITY PROJECTILE LAUNCHERS
C. P. T. Groth and J. J. Gottlieb Oct. 1988 227 p
(UTIAS-327; ISSN-0082-5255) Avail: NTIS HC A11/MF A01

A comprehensive theoretical and numerical analysis is presented for predicting the performance and operation of two-stage light-gas hypervelocity model launchers with deformable pistons. Such launchers are often used in aeroballistic and terminal ballistic ranges. This analyis includes a lumped-parameter interior-ballistics model for simulating the burning of the solid propellant in the combustion chamber, a generalized one-dimensional unsteady gas dynamic model for predicting the flow of the light gas, an ideal-viscoplastic extrusion model for representing the piston deformation process, and a friction model for determining the motions of the piston and projectile/sabot package in the pump and launch tubes. The random-choice method (RCM) with operator splitting, non-staggered gridding, variable node spacing, and local-time stepping is used to solve numerically the one-dimensional flow equations. A comparison of numerical results to light-gas gun experimental data demonstrates that the theoretical analysis is valid and capable of simulating the complicated physical processes that occur in these two-stage projectile launchers. Author

N89-16895# Brookhaven National Lab., Upton, NY.
MECHANICAL DESIGN OF A RF ELECTRON GUN
M. H. Woodle, K. Batchelor, and J. Sheehan 1988 2 p Presented at the Linear Accelerator Conference,, Williamsburg, VA, 2-7 Oct. 1988
(Contract DE-AC02-76CH-00016)
(DE89-004890; BNL-42001; CONF-881049-52) Avail: NTIS HC A02/MF A01

Brookhaven National Laboratory is building an Accelerator Test Facility at which we plan to study laser acceleration of electrons inverse free electron lasers and the production of X-rays by non-linear Compton scattering. The facility contains an electron gun, linac, lasers and ancillary systems which will enable the production of 6 ps duration pulses of 50 to 100 MeV electrons. The electron source is a one and one half cell RF Electron gun which utilizes either a thermionic or photoemissive cathode to produce 5 MeV electrons. This paper discusses how gun mechanical design considerations such as material, vacuum maintenance, surface finish, fabrication methods, cavity tuning, and cathode replacement were reconciled to arrive at the final design. DOE

N89-16896*# Sterling Federal Systems, Inc., Palo Alto, CA.
MODIFICATIONS TO THE NASA AMES SPACE STATION PROXIMITY OPERATIONS (PROX OPS) SIMULATOR
Adam Brody Oct. 1988 10 p
(Contract NAS2-11555)
(NASA-CR-177510; NAS 1.26:177510) Avail: NTIS HC A02/MF A01 CSCL 14B

As the United States is approaching an operational space station era, flight simulators are required to investigate human design and performance aspects associated with orbital operations. Among these are proximity operations (PROX OPS), those activities occurring within a 1-km sphere of Space Station including rendezvous, docking, rescue, and repair. The Space Station Proximity Operations Simulator at NASA Ames Research Center was modified to provide the capability for investigations into human performance aspects of proximity operations. Accurate flight equations of motion were installed to provide the appropriate visual scene to test subjects performing simulated missions. Also, the flight control system was enhanced by enabling pilot control over thruster acceleration values. Currently, research is under way to examine human performance in a variety of mission scenarios. Author

15 LAUNCH VEHICLES AND SPACE VEHICLES

Includes boosters; operating problems of launch/space vehicle systems; and reusable vehicles.

For related information see also *20 Spacecraft Propulsion and Power.*

N89-16889# Indian Space Research Organization, Bangalore.
MISSION UNDER SROSS PROGRAM AND POSITION PAPER ON SROSS-2 WITH MEOSS PAYLOAD
Tarsem Singh *In* DFVLR, Proceedings of the Colloquium about Joint Projects Within the DFVLR/ISRO Cooperation Jun. 1988 p 81-101 (For primary document see N89-16883 09-12)
Avail: NTIS HC A06/MF A01; DFVLR, VB-PL-DO, Postfach 90 60 58, 5000 Cologne, Fed. Republic of Germany, 34.50 Deutsche marks

N89-17039# Blaber (A.) and Blaber (P.), Hamilton (Ontario).
A CANADIAN LOW EARTH ORBIT LAUNCH VEHICLE: LAUNCH VEHICLE PERFORMANCE ANALYSIS OF BLACK BRANT VC AND NIHKA ROCKET MOTOR CONFIGURATIONS
A. Blaber, J. S. Bullard (Bullard, J. S., Brandtford, Ontario), and P. Blaber *In* National Research Council of Canada, Workshop on Microgravity Experimentation in Aircraft and Rockets 1988 p 119-121 (For primary document see N89-17019 09-29)
Avail: NTIS HC A07/MF A01; also available from Publication Sales and Distribution, National Research Council of Canada, Ottawa, ON, Canada K1A OR6

16 SPACE TRANSPORTATION

Includes passenger and cargo space transportation, e.g., shuttle operations; and space rescue techniques.

For related information see also *03 Air Transportation and Safety* and *18 Spacecraft Design, Testing and Performance.* For space suits see *54 Man/System Technology and Life Support.*

N89-16897# Technische Univ., Berlin (Germany, F.R.). Fachgebiet Raumfahrt.
ANALYSIS AND DESIGN OF A UNIVERSAL SHUTTLE FOR ROCKETS [ANALYSE UND ENTWURF EINER UNIVERSELLEN RAUMFAEHRE FUER GROSSE FRACHTRAKETEN]
Zeljko Matijevic May 1988 182 p In GERMAN; ENGLISH summary
(ILR-Mitt-199; ETN-89-93482) Avail: NTIS HC A09/MF A01

A universally applicable orbital ferry as the third stage of the heavy-load rocket Neptune was designed. The shuttle was analyzed in terms of payload capacity and specific transportation costs for missions within the cislunar orbit. A conventional chemical propulsion system on the basis of LOx and LH2 was considered. It is shown that payloads between 88 and 110 metric tons can be transported from the 150 km low Earth orbit to a 100 km lunar orbit. The 110 metric tons can be carried to the geostationary orbit by the cargo model of this orbital transfer vehicle with an initial mass below 370 metric tons. The specific transportation costs are estimated at 364 $/kg to geostationary orbit, given a transportation volume equivalent to that required to install giant space power satellites in the geostationary orbit. ESA

17 SPACE COMM., SPACECRAFT COMM., COMMAND & TRACKING

Includes telemetry; space communications networks; astronavigation and guidance; and radio blackout.

For related information see also *04 Aircraft Communications and Navigation* and *32 Communications and Radar.*

N89-16898# Sandia National Labs., Albuquerque, NM. Telemetry Systems Div.
CONTROLLER-PROGRAMMER FOR TELEMETRY SYSTEMS
R. Michael Daniels Oct. 1988 56 p
(Contract DE-AC04-76DP-00789)
(DE89-002539; SAND-88-9003) Avail: NTIS HC A03/MF A01

The development, testing, and implementation of modern, sophisticated telemetry systems requires a controller capable of adequately exercising the telemeter. A flight test requires a programmer to cycle through the flight events. This report describes an adaptable, programmable system that encompasses both of these requirements. DOE

18 SPACECRAFT DESIGN, TESTING AND PERFORMANCE

Includes satellites; space platforms; space stations; spacecraft systems and components such as thermal and environmental controls; and attitude controls.

For life support systems see *54 Man/System Technology and Life Support.* For related information see also *05 Aircraft Design, Testing and Performance, 39 Structural Mechanics,* and *16 Space Transportation.*

N89-16899# Iowa State Univ. of Science and Technology, Ames. Engineering Research Inst.
INVESTIGATION OF LIQUID SLOSHING IN SPIN-STABILIZED SATELLITES Annual Report, 1 Jan. 1987 - 31 Dec. 1987
31 Jan. 1988 46 p
(Grant AF-AFOSR-0080-86; AF Proj. 2302)
(AD-A199629; ISU-ERI-AMES-88175; AFOSR-88-1141TR) Avail: NTIS HC A03/MF A01 CSCL 22C

A vorticity, stream function approach has resulted in a formulation and numerical algorithm for the two-dimensional viscous sloshing problem. A key feature of the formulation is the use of a coordinate transformation that maps the fluid body into a fixed geometric shape. The formulation also removes an initial singularity from the governing equations that would otherwise cause the numerical method to diverge. An experimental test rig has been designed and built to study the interaction of the sloshing fluid and spinning structure. The test rig has been instrumented to monitor the motion of several rotating configurations. In addition, a computer simulation model of the test rig is presently under development. GRA

N89-16900# Sandia National Labs., Albuquerque, NM. Computatinal Aerodynamics Div.
INVISCID FLOW FIELD ANALYSIS OF COMPLEX REENTRY VEHICLES. VOLUME 1: DESCRIPTION OF NUMERICAL METHODS
R. W. Noack and A. R. Lopez Oct. 1988 109 p
(Contract DE-AC04-76DP-00789)
(DE89-002814; SAND-87-0776/1) Avail: NTIS HC A06/MF A01

This is the first of two volumes concerning the SANDia Inviscid Afterbody Code. The SANDIAC computer code predicts the supersonic and hypersonic inviscid flow field about reentry vehicles. The theory, formulation, and results of the code are described in Volume 1, and the inputs and usage are described in Volume 2. The code solves the three-dimensional, steady-state, Euler equations in finite difference form. The equations are solved in a transformed computational plane. A parabolic grid generation scheme is used to provide body normal grids for complex configurations. The code has options to solve the conservative and nonconservative Euler equations using either upwind differencing or standard centered differencing. The calculations may use either equilibrium or ideal gas chemistry. The code provides the complete flow field in addition to integrated force and moment data as output. DOE

N89-16901# Integrated Systems, Inc., Santa Clara, CA.
ADAPTIVE CONTROL TECHNIQUES FOR LARGE SPACE STRUCTURES Annual Technical Report, 1 Jun. 1986 - 31 May 1987
Robert L. Kosut 23 Dec. 1987 91 p
(Contract F49620-85-C-0094)
(AD-A200208; ISI-110; AFOSR-88-0848TR) Avail: NTIS HC A05/MF A01 CSCL 22B

This report summarizes the research performed on adaptive control techniques for Large Space Structures (LSS). The research effort concentrated on two areas: (1) on-line robust design from identified models - what is referred to here as adaptive calibration; and (2) an analysis of slow-adaptation for adaptive control of LSS. The report summarizes the results obtained in these areas and also includes Appendices which contain technical articles: (1) Adaptive Control of Large Space Structures; (2) Adaptive Control Via Finite Modeling and Robust Control; (3) On the use of the Method of Averaging for the Stability analysis of Adaptive Linear Control Systems; and (4) Conditions for the Convergence and Divergence of Parameter Adaptive Linear Systems. GRA

N89-16902 Virginia Polytechnic Inst. and State Univ., Blacksburg.
SPILLOVER STABILIZATION IN THE CONTROL OF LARGE FLEXIBLE SPACE STRUCTURES Ph.D. Thesis
Eva A. Czajkowski 1988 285 p
Avail: Univ. Microfilms Order No. DA8817403

Active control of large flexible space structures is typically implemented to control only a few known elastic modes. Linear Quadratic Regulators (LQR) and Kalman-Bucy Filter (KBF) observers are usually designed to control the desired modes of vibration. Higher modes, referred to as residual modes, are generally ignored in the analysis and may be excited by the controller to cause a net destablizing effect on the system. This is referred to as spillover phenomenon. The stabilization of the neglected dynamics of the higher modes of vibration are considered. Modal controllers are designed with improved spillover stability properties. The proposed method calls for designing the observer so as to improve spillover stability with minimum loss in performance. Two formulations are pursued. The first is based on optimizing the noise statistics used in the design of the KBF. The second optimizies directly the gain matrix of the observer.
Dissert. Abstr.

N89-16903# Instituto de Pesquisas Espaciais, Sao Jose dos Campos (Brazil).
CONTROL OF REACTION WHEELS THROUGH DIGITAL TECHNIQUES USING REFERENCE MODELS M.S. Thesis
Gilberto daCunhaTrivelato Oct. 1988 200 p In PORTUGUESE; ENGLISH summary
(INPE-4618-TDL/335) Avail: NTIS HC A09/MF A01

The study and the development of digital control systems for reaction wheel torques (used in the attitude control of artificial satellites) are considered. Model-following control techniques are used to reduce the effects of: (1) wheel disturbing torques, and (2) wheel sensor noises, on wheel torque. Initially, it presents the formulation of the problem, the simplifications done, the reference model and the real model of the reaction wheel used. Then it selects the candidate controllers and the criteria for choosing their parameters. Finally, two of the selected controllers (proportional - P - and proportional plus integral - PI - with velocity feedback) are tested by digital simulation and hardware implementation. These tests show that: (1) the model-following technique is adequate to the problem' (2) both controllers satisfy those objectives; (3) the P controller is better than the PI in this case; (4) the adopted criteria are satisfactory; and (5) the digital simulation of the reaction wheel is qualified for digital simulations of attitude control systems. Author

N89-16904*# Naval Academy, Annapolis, MD.
PROJECT LONGSHOT: AN UNMANNED PROBE TO ALPHA CENTAURI Program Project Report, 1987 - 1988
Keith A. Beals, Martin Beaulieu, Frank J. Dembia, Joseph Kerstiens, Daniel L. Kramer, Jeffrey R. West, and James A. Zito 1988 74 p
(Grant NGT-21-002-080)
(NASA-CR-184718; NAS 1.26:184718) Avail: NTIS HC A04/MF A01 CSCL 22B

A preliminary design is presented for an unmanned probe to Alpha Centauri with a planned launch early in the 21st century. The probe would be assembled at the space station and take approx. 100 yrs to reach the nearest star. Several technologies must be developed in order for this mission to be possible. A pulsed fusion microexplosion drive with 1,000,000 secs of specific impulse is the primary enabling technology. A large, long life fission reactor with 300 kW power output is also required. Communications lasers would use a 0.532 micrometer wavelength since there is minimal power output by the stars in that frequency band. A laser with an input power of 250 kW would allow for a data rate of

1000 bits per second at maximum range. There are 3 types of information to be gathered by the probe: properties of the interstellar medium, characteristics of the three star Alpha Centauri system, and astrometry. Author

N89-16905*# National Aeronautics and Space Administration. Lewis Research Center, Cleveland, OH.
A MODIFIED VAPEPS METHOD FOR PREDICTING VIBROACOUSTIC RESPONSE OF UNREINFORCED MASS LOADED HONEYCOMB PANELS
Mark E. McNelis 1989 12 p Prepared for presentation at the 35th Technical Meeting of the Inst. of Environmental Sciences, Anaheim, CA, 1-5 May 1989
(NASA-TM-101467; E-4579; NAS 1.15:101467) Avail: NTIS HC A03/MF A01 CSCL 22B

VAPEPS (VibroAcoustic Payload Environment Prediction System) is a computer program used to predict the vibroacoustic response of a structure. An alternate VAPEPS modeling technique, the Modified NASA Lewis Method, is an improvement for modeling unreinforced mass loaded honeycomb panels. The Modified NASA Lewis Method prediction is compared to the standard ASMS VAPEPS prediction, and the acoustic test data for three spacecraft panels. An analytical method of computing variance is presented and used to compute 95 percent confidence levels. These levels are compared to the standard VAPEPS confidence levels and to the envelope of the test data. As a result of using the new methodology suggested in the paper, both the mean prediction and the 95 percent confidence level prediction agree well with the test data in both spectral shape and magnitude. Therefore, the Modified NASA Lewis Method prediction methodology may be used to define more realistic random vibration test levels. Author

19 SPACECRAFT INSTRUMENTATION

For related information see also *06 Aircraft Instrumentation* and *35 Instrumentation and Photography.*

No abstracts in this category.

20 SPACECRAFT PROPULSION AND POWER

Includes main propulsion systems and components, e.g., rocket engines; and spacecraft auxilliary power sources.

For related information see also *07 Aircraft Propulsion and Power, 28 Propellants and Fuels, 44 Energy Production and Conversion,* and *15 Launch Vehicles and Space Vehicles.*

N89-16906# Advisory Group for Aerospace Research and Development, Neuilly-Sur-Seine (France). Propulsion and Energetics Panel.
DESIGN METHODS IN SOLID ROCKET MOTORS
Apr. 1988 243 p In ENGLISH and FRENCH Lecture series held in London, United Kingdom, 18-19 Apr. 1988, in Saint-Aubin de Medoc, France, 21-22 Apr. 1988, in Neubiberg, Fed. Republic of Germany, 25-26 Apr. 1988, and in Rome, Italy, 28-29 Apr. 1988 Revised
(AGARD-LS-150-Rev; ISBN-92-835-0454-2) Copyright Avail: NTIS HC A11/MF A01

The current state of the art in designing solid rocket motors and their components are summarized. The aim is to collect the experience of several countries in using new technologies and new methods which have been developed over the past ten years. Specific sessions dealt with propellant grain, cases, nozzles, internal thermal insulations. The question of the general optimization of a solid rocket motor is emphasized. For individual titles, see N89-16907 through N89-16916.

N89-16907# Air Force Rocket Propulsion Lab., Edwards AFB, CA.
ADVANCES IN SOLID ROCKET NOZZLE DESIGN AND ANALYSIS TECHNOLOGY IN THE UNITED STATES SINCE 1970
Joseph H. Hildrath *In* AGARD, Design Methods in Solid Rocket Motors Apr. 1988 15 p (For primary document see N89-16906 09-20)
Copyright Avail: NTIS HC A11/MF A01

The evolution of the nozzle design and analysis in the U.S. in the past decade is examined. A brief summary is given of generalized design requirements along with a description of the design evolution from tungsten and graphite based designs to the current carbon-carbon designs. The main caused for the incorporation of new technologies in the design are identified. A technical description of the analysis processes that are employed in the design cycle is given. The verification of the analysis procedure is a vital aspect of improving the analysis capabilities. A description is also given of some of the activities which have occurred to demonstrate the validity of the new analysis technology. These activities include code vs. code comparisons as well as code vs. lab measurement efforts. The code vs. measurement efforts include investigations into threaded interfaces between the throat and exit cone parts and the behavior of carbon-carbon involute exit cones subjected to mulitaxial loads. Author

N89-16908# European Space Agency, Paris (France).
DESIGN AND ANALYSIS OF SOLID ROCKET MOTOR NOZZLE
A. Truchot *In* AGARD, Design Methods in Solid Rocket Motors Apr. 1988 22 p (For primary document see N89-16906 09-20)
Copyright Avail: NTIS HC A11/MF A01

The different methods are presented which are used to design and analyze solid rocket motor nozzles. In a preliminary phase, the typical requirements and parameters required to design a nozzle are discussed. Afterwards, the general process of the design is detailed: nozzle configuration, aerodynamic contour design, selection and sizing of liners and insulators, etc. In a second step, the different systems used to control the motor thrust or to improve the performance, such as extendible exit cones, are presented. For each step (aerodynamic, thermal and structural) the different computer programs used are presented. Author

N89-16909# Hercules, Inc., Rocket Center, WV. Aerospace Products Group.
COMPOSITE MOTOR CASE DESIGN
P. R. Evans *In* AGARD, Design Methods in Solid Rocket Motors Apr. 1988 11 p Previously announced as N87-28592 (For primary document see N89-16906 09-20)
Copyright Avail: NTIS HC A11/MF A01

Information is presented on the design of composite cases for rocket motors. Typical design requirements are discussed, including pressure, axial and bending loads and thermal loading. Material technology discussed include filament winding resins and glass, Kevlar and graphite fibers. Design features discussed include the pressure vessel body, skirts, polar adapters and other attachments. Typical qualification testing and inspection techniques are presented. Author

N89-16910# Societe Nationale Industrielle Aerospatiale, Saint-Medard-en-Jalles (France). Programs for Filament-Wound Structures.
DESIGN OF FILAMENT-WOUND ROCKET CASES
J. P. Denost *In* AGARD, Design Methods in Solid Rocket Motors Apr. 1988 22 p (For primary document see N89-16906 09-20)
Copyright Avail: NTIS HC A11/MF A01

Aerospatiale began developing methods for design and sizing of filament-wound rocket cases in the early 1970's. Such methods have since evolved to the extent that rapid design and precise

verification means are now available. These two approaches are outlined, criticized, and their complementarity is determined. The principle rules are outlined. The theory is completed by considerations relating to materials, their implementation and performances, and by a description of the major principles of fabrication of this type of structure. Author

N89-16911# IMI Summerfield, Kidderminster (England). Rocket Motor Design and Development.
CONSIDERATIONS FOR DESIGNERS OF CASES FOR SMALL SOLID PROPELLANT ROCKET MOTORS
H. Badham and G. P. Thorp *In* AGARD, Design Methods in Solid Rocket Motors Apr. 1988 20 p Previously announced as N87-28594 (For primary document see N89-16906 09-20)
Copyright Avail: NTIS HC A11/MF A01

When manufacturing the initial design of the case or load bearing components for a solid propellant rocket motor, a number of possible solutions may be apparent and many factors need consideration before the design of the individual components can be finalized. The process of optimization involves consideration of material properties, methods of manufacturing, inspection and proof as well as interactions with other rocket motor and missile components. The various factors are considered and indications are given of the interactions to be taken into account. Particular emphasis is given to the design of metallic motor cases. Both homogeneous and nonhomogeneous body structures are considered, the latter being fiber overwound metallic and strip laminate structures. The relatively recent requirement of munitions insensitivity (resistance to fragment attack and fuel fire) is also discussed in relation to body construction. Author

N89-16912# Bombrini Parodi-Delfino S.p.A., Colleferro (Italy). Defense and Space Div.
PROPELLANT GRAIN DESIGN **c28**
S. Scippa *In* AGARD, Design Methods in Solid Rocket Motors Apr. 1988 20 p Previously announced as N87-28595 (For primary document see N89-16906 09-20)
Copyright Avail: NTIS HC A11/MF A01

A general overview of the current methodologies used at SNIA BPD in designing solid rocket motor propellant grains is presented. The internal ballistics aspect of grain design is emphasized. The general requirements (thrust vs. time curve, volumetric constraints, etc.), the available technologies (propellant types, manufacturing processes, etc.), and the methodology for the selection of the most appropriate technology are described. In particular, propellant characterization, design of internal geometry, and methods for propellant formulation choice are discussed. An analysis of the predictability factors and how they can be taken into account for contingency planning is reported. Finally, the experimental tests commonly used for grain design validation are summarized. Author

N89-16913# Societe Nationale des Poudres et Explosifs, Vert-Le-Petit (France). Direction Technique Autopropulsion.
SOLID PROPELLANT GRAIN DESIGN **c28**
Bernard Zeller *In* AGARD, Design Methods in Solid Rocket Motors Apr. 1988 29 p (For primary document see N89-16906 09-20)
Copyright Avail: NTIS HC A11/MF A01

To design a solid propellant grain is to conceive and to define a grain which satisfies various requirements. The methods and procedures are described which are used today in France to design propellant grains. Described and analyzed are: (1) the various types of grain and the various families of propellant which are available and used today; (2) the detailed requirements that a solid propellant grain must satisfy; (3) the methods which are used to precisely define the propellant, the architecture and the configuration of the grain, and more specifically the methods used in order to ensure required ballistic performance though maintaining structural integrity of the grain; and (4) an overview on a method of solid propellant grain reliability assessment. The improvements needed in the area of grain design analysis and the related technical breakthroughs are briefly presented. Author

N89-16914# Air Force Rocket Propulsion Lab., Edwards AFB, CA.
STATE OF THE ART OF SOLID PROPELLANT ROCKET MOTOR GRAIN DESIGN IN THE UNITED STATES **c28**
Durwood I. Thrasher *In* AGARD, Design Methods in Solid Rocket Motors Apr. 1988 21 p (For primary document see N89-16906 09-20)
Copyright Avail: NTIS HC A11/MF A01

A brief disscussion is presented of the basic ground rules and overall considerations in solid rocket motor design. This discussion includes ballistic design considerations, grain features related to ballistic design and their purposes, primary factors which determines stress and strain with solid rocket motor propellant grain structural integrity assurance, including materials characterization, structural analysis, and structural capability verification. The topics addressed include viscoelastic material behavior and the requisite thermomechanical analysis testing and approaches; failure criteria and the appropriate testing approaches; experimental structural methods, including in situ stress and strain measurement technology; and service life considerations. Author

N89-16915# European Space Agency, Paris (France).
DESIGN AND ANALYSIS OF SOLID ROCKET MOTOR INTERNAL INSULATION
A. Truchot *In* AGARD, Design Methods in Solid Rocket Motors Apr. 1988 13 p (For primary document see N89-16906 09-20)
Copyright Avail: NTIS HC A11/MF A01

The main purpose of internal insulation is to protect the motor case from the thermal environment of propellant combustion products. Several secondary objectives must also be met. Internal insulation must bond to propellant and case, transmit case strain into propellant and sometimes seal the case. In the first step, the general process of internal insulation is presented: evaluation of thermal environment, selection of material, thermal and structural analyses. For each phase, the different analysis methods are described: aerodynamic, thermal and structural. Also the different phases of internal insulation fabrication are presented: elastomer formulation, fabrication of parts and integration into the motor case. Author

N89-16916# European Space Agency, Paris (France).
OVERALL OPTIMIZATION OF SOLID ROCKET MOTOR
A. Truchot *In* AGARD, Design Methods in Solid Rocket Motors Apr. 1988 10 p (For primary document see N89-16906 09-20)
Copyright Avail: NTIS HC A11/MF A01

The overall optimization of a solid rocket motor consists of determining the most efficient configuration of the motor in terms of range or payload of the vehicle. After a presentation of the general requirements of a solid rocket motor, the different design parameters are detailed: operating conditions, geometric parameters and technologies used for each component. In order to achieve parametric studies, a computer program was developed by SEP. The principle and main characteristics of this program are presented and two examples of application are given in order to illustrate the possibilities of the program. Author

N89-16917*# National Aeronautics and Space Administration. Lewis Research Center, Cleveland, OH.
NASA PHOTOVOLTAIC RESEARCH AND TECHNOLOGY
Dennis J. Flood Dec. 1988 12 p Prepared for the Annual Meeting of the American Institute of Chemical Engineers, Washington, DC, 28 Nov. - 2 Dec. 1988
(NASA-TM-101422; E-4522; NAS 1.15:101422) Avail: NTIS HC A03/MF A01 CSCL 10B

NASA photovoltaic R and D efforts address future Agency space mission needs through a comprehensive, integrated program. Activities range from fundamental studies of materials and devices to technology demonstrations of prototype hardware. The program aims to develop and apply an improved understanding of photovoltaic energy conversion devices and systems that will increase the performance, reduce the mass, and extend the lifetime

of photovoltaic arrays for use in space. To that end, there are efforts aimed at improving cell efficiency, reducing the effects of space particulate radiation damage (primarily electrons and protons), developing ultralightweight cells, and developing advanced ray component technology for high efficiency concentrator arrays and high performance, ultralightweight arrays. Current goals that have been quantified for the program are to develop cell and array technology capable of achieving 300 watts/kg for future missions for which mass is a critical factor, or 300 watts/sq m for future missions for which array size is a major driver (i.e., Space Station). A third important goal is to develop cell and array technology which will survive the GEO space radiation environment for at least 10 years. Author

N89-16918*# Pratt and Whitney Aircraft, West Palm Beach, FL. Government Engine Business.
DESIGN AND ANALYSIS REPORT FOR THE FLIGHT WEIGHT 20-INCH COLUMBIUM SECONDARY NOZZLE FOR THE RL10 ENGINE Final Report
J. H. Castro Feb. 1989 57 p
(Contract NAS3-24238)
(NASA-CR-179612; NAS 1.26:179612) Avail: NTIS HC A04/MF A01 CSCL 21H

Pratt & Whitney (P and W) is currently under contract to NASA-LeRC for a multi-year program to evaluate the feasibility of the RL10-IIB/IIC engine models and the various improvements which broaden the engine capabilities and range of applications. The features being evaluated include the operation of the RL10 engine at low thrust levels and/or high mixture ratio levels and the addition of a high area ratio (250:1) translating nozzle to the engine to increase its specific impulse while shortening the installed engine length. The translating nozzle for the RL10-IIB/IIC engine is approximately 55 inches long with an exit plane diameter of 71 inches and an inlet plane diameter of 40 inches. This report documents the design and analysis work done investigating a small subscale Columbium nozzle which could be built and tested to provide findings which then could be incorporated into the high area ratio nozzle final design for the RL10-IIB/IIC engine. This report documents the design and analysis work done investigating a small subscale Columbium nozzle which could be built and tested to provide findings which then could be incorporated into the high area ratio nozzle final design for the RL10-IIB/IIC engine. The length of the subscale nozzle is 20 in.; its exit diameter is 46 in. With the nozzle in the stowed position, an RL10A-3-3A engine system is 70 inches long (Area Ratio = 61:1); with the nozzle deployed the engine length and area ratio are increased to 90 inches and 83:1 respectively. The increase in area ratio provides a calculated increase of 7 + or - 1 second of specific impulse. Author

N89-16815*# National Aeronautics and Space Administration. Marshall Space Flight Center, Huntsville, AL.
SPACE SHUTTLE MAIN ENGINE MONITORING EXPERIENCE AND ADVANCED MONITORING SYSTEMS DEVELOPMENT
Harry A. Cikanek *In* AGARD, Engine Condition Monitoring: Technology and Experience Oct. 1988 20 p (For primary document see N89-16780 09-06)
Copyright Avail: NTIS HC A20/MF A01 CSCL 21H

N89-16816*# National Aeronautics and Space Administration. Marshall Space Flight Center, Huntsville, AL.
PLUME SPECTROMETRY FOR LIQUID ROCKET ENGINE HEALTH MONITORING
William T. Powers, F. G. Sherrell, J. H. Bridges, III, and T. W. Bratcher (Sverdrup Technology, Inc., Arnold Air Force Station, TN.) *In* AGARD, Engine Condition Monitoring: Technology and Experience Oct. 1988 10 p (For primary document see N89-16780 09-06)
Copyright Avail: NTIS HC A20/MF A01 CSCL 21H

23 CHEMISTRY AND MATERIALS (GENERAL)

No abstracts in this category.

24 COMPOSITE MATERIALS

Includes physical, chemical, and mechanical properties of laminates and other composite materials.
For ceramic materials see *27 Nonmetallic Materials.*

N89-16919 New South Wales Univ., Kensington (Australia). School of Chemical Engineering and Industrial Chemistry.
SYNTHESIS AND ANALYSIS OF EPICHLOROHYDRIN BASED WET STRENGTH RESINS FOR PAPER M.S. Thesis
T. F. Muir Nov. 1987 3 p
Avail: Issuing Activity

The addition of various polymeric materials to paper, which incurs extraordinary resistance to rupture or disintegration of the paper sheet when saturated with water, has been performed on a commercial basis since the mid 1930's. Polyamide epichlorohydrin type resins are currently employed as wet-end additives to paper for this purpose. A polyester modified wet strength resin was examined as a viable alternative to commercially available resins. The examination included a comparison of various performance criteria and the analysis of both the commercial and laboratory synthesized resin systems. While the polyester modified resin treated paper possesses a lower wet strength than its commercial counterpart, the repulpability characteristics were significantly improved. The analysis of the various resins by Carbon-13 N.M.R. spectroscopy suggests the existence of chlorine containing groups pendant to the polyamide backbone, which had previously been discounted. Fusion-gas chromatography of polyamide epichlorohydrin type resins which had not been previously investigated, supports the presence of azetidinium groups as well as unreacted epichlorohydrin as resinous components. Author

N89-16920# Naval Ocean Systems Center, San Diego, CA.
A MULTIAXIAL STRENGTH CRITERION FOR COMPOSITES Final Report, Oct. 1987 - Apr. 1988
P. Y. Tang Jul. 1988 13 p
(AD-A199610; NOSC/TD-1295) Avail: NTIS HC A03/MF A01 CSCL 11D

The document presents the development of a piecewise quadratic strength tensor theory for composites with orthogropic, transversely isotropic, and isotropic material symmetries. The proposed strength criterion improves the best available quadratic failure theory for such composites, the Tsai and Wu quadratic strength tensor theory, by including stress terms that can reflect different failure mechanisms of the composites under tension and compression. To demonstrate the applicability of the proposed theory to composites, extensive and good correlations are shown between the theory and the biaxial fracture data of five composite material systems: graphite/epoxy, graphite particulate, graphite/aluminum, glass/epoxy, and organic textolite composites. GRA

N89-16921# University of Southern Mississippi, Hattiesburg. Dept. of Polymer Science.
THE 15N CP/MAS NMR OF ARAMIDS: A TOOL FOR CHARACTERIZATION OF THE MORPHOLOGY OF HIGH MODULUS FIBERS FOR COMPOSITES Technical Report, No. 11, Aug. 1987 - Jul. 1988
Lon J. Mathias and Douglas G. Powell 15 Jul. 1988 11 p
Submitted for publication
(Contract N00014-86-K-0659)
(AD-A199656) Avail: NTIS HC A03/MF A01 CSCL 11I

Natural abundance 15N solid state NMR was found to provide

unique molecular and microscopic level information on aramids and aramid-containing copolymers. Poly(p-phenyleneterephthalamide) (PPTA) coagulated from H2SO4 into water displayed a broad envelope of overlapping peaks between 90 and 100 ppm (relative to solid glycine). Annealing significantly reduced the width of this envelope although not to the level of the commercial Kevlar fiber spectrum. Molecular level composites of PPTA grafted with nylon 3 in a nylon 3 matrix showed broad peaks for the aramid components up to 30 percent by weight content. Peak widths were comparable to that of the precipitated PPTA. Above 30 percent PPTA, phase separation (confirmed by IR, X-ray and SEM) is observed by solid state NMR as narrow peaks for the aramid nitrogens. GRA

N89-16922# Stanford Univ., CA. Dept. of Aeronautics and Astronautics.
MANUFACTURING THERMOPLASTIC MATRIX COMPOSITES Final Report, Oct. 1985 - Apr. 1988
George S. Springer Jul. 1988 110 p
(Contract F33615-84-C-5049)
(AD-A199724; AFWAL-TR-88-4115) Avail: NTIS HC A06/MF A01 CSCL 11D

A model is presented of the steps involved in the manufacturing process of semicrystalline thermoplastic matrix composites. The model relates the temperature and pressure applied during processing to : (1) the flow of the matrix into the fiber tow: (2) the formation of contact and bond between adjacent plies, and (3) the crystallinity. The results of the model were verified by tests performed with PEEK 150P polymer and APC-2 graphite/PEEK composite. In addition the mechanical properties of PEEK 150P polymer and APC 2 graphite/PEEK composite were measured at different crystallinites, from 0 to 40 weight percent. For PEEK 150P the tensile, compressive, and shear properties and the fracture toughness were measured. For APC-2 the Mode 1 and Mode 2 fracture toughnesses and fracture energies as well as the mixed mode stress intensity factors were determined. GRA

N89-16923# Sandia National Labs., Albuquerque, NM.
SYNTHESIS AND PROPERTIES OF LOW CARBON BORON CARBIDES
C. L. J. Adkins, A. N. Campbell, and T. J. Headley 1988 12 p Presented at the 41st Pacific Coast Regional Meet of American Ceramic Society, San Francisco, CA, 24 Oct. 1988
(Contract DE-AC04-76DP-00789)
(DE89-002184; SAND-88-2976C; CONF-8810195-2) Avail: NTIS HC A03/MF A01

Boron carbides of low carbon content (less than 10 percent) were produced from BCl3 and CCl4 at 1273 - 1673 K in a CVD reactor. TEM revealed that tetragonal boron carbide and beta-boron formed under the most carbon depleted gas-phase conditions. Interactions have been observed between the graphite substrates and the deposits at elevated temperatures. The microstructure of the deposits will be discussed. DOE

N89-16924 Stanford Univ., CA.
HYGROTHERMAL DEFORMATIONS OF LAMINATED COMPOSITE SHELLS Ph.D. Thesis
Lawrence Edward Doxsee, Jr. 1988 228 p
Avail: Univ. Microfilms Order No. DA8814998

A method was developed for determining the deformation of laminated fiber-reinforced composite plates and shells subjected to changes in temperature and moisture concentration. The method consists of two parts: the mathematical model, which describes the physics of the system, and a numerical procedure based on this model, which is used to obtain numerical solutions to specific problems. The mathematical model is a two-dimensional shell theory which includes the effects of transverse shear and normal strains and is valid for composite shells of any shape with arbitrary temperature and moisture distributions. The numerical procedure is a displacement-based finite element program for shells of revolution with axisymmetric temperature and moisture distributions. The shell theory and the finite element program were verified by obtaining solutions to a wide variety of problems using the finite element program. These numerical solutions were then compared to existing analytical solutions to experimental data generated during the course of this investigation. Dissert. Abstr.

N89-16925# Virginia Univ., Charlottesville. Dept. of Materials Science.
INVESTIGATION OF MICROSTRUCTURAL FACTORS THAT CAUSE LOW FRACTURE TOUGHNESS IN SILICON CARBIDE WHISKER/Al ALLOY COMPOSITES Annual Report, 1 Sep. 1987 - 30 Sep. 1988
F. E. Wawner and R. D. Schueller Oct. 1988 56 p
(Contract N00014-85-K-0179)
(AD-A200147; UVA/525398/MS89/103) Avail: NTIS HC A04/MF A01 CSCL 11D

This program deals with determining factors that influence strength, ductility, fracture toughness, and elongation to failure in Silicon Carbon Whisker/Aluminum alloy composites. Specifically, a microstructural study is being made in an attempt to define extrinsic and intrinsic factors that control fracture and thus influence properties. One of the more important products produced by ACMC from SiCw/Al composites has been the rolled sheet. The response of the material to secondary processing and thermo-mechanical treatment is of utmost importance with respect to material quality. The present study emphasizes microstructural-mechanical property characterization of the rolled material GRA

N89-16926# National Academy of Sciences - National Research Council, Washington, DC.
NATIONAL RESEARCH COUNCIL RESIDENT RESEARCH ASSOCIATESHIP (NRC-RRA) PROGRAM Annual Report, 1 Jul. 1987 - 30 Jun. 1988
Aug. 1988 77 p
(Contract F49620-85-C-0124)
(AD-A200183; AFOSR-88-1142TR) Avail: NTIS HC A05/MF A01 CSCL 05A

We report here on all Associateship Programs for the Air Force Systems Command. In addition to reporting on activities specifically sponsored under this contract, we also summarize any other current activities of the Air Force Associateship Program such as the termination of Associates who were sponsored under the previous year's contract. Furthermore, after each review of Air Force applicants, we have supplied a listing of all applicants who have passed the panel review. GRA

N89-16927# Connecticut Univ., Storrs. Liquid Crystalline Polymer Research Center.
ISOTROPIC KEVLAR AND PBA (POLY 1,4-BENZAMIDE) REINFORCEMENTS FOR COMPOSITES Interim Report
Maria A. Alonso and M. T. Shaw 27 Sep. 1988 8 p Presented at the 3rd Chemical Congress of North America, Toronto, Ontario, Jun. 1988 Submitted for publication
(Contract N00014-86-K-0772)
(AD-A200239; TR-25) Avail: NTIS HC A02/MF A01 CSCL 07F

Kevlar and PBA (Poly 1,4-benzamide) reinforcements were prepared in 96 percent H2 SO4. Water/methanol mixtures were used as the extracting solvent. Other solvent combinations were tried, but with less success. The structure obtained by SEM (scanning electron micrograph) showed small cell size but a non-uniform structure. Composites were made from these reinforcements using as matrices a variety of epoxy resins and acrylates. The curing times varied according to the matrix used. Structure and penetration of the matrix into the reinforcements was studied by optical microscopy. GRA

N89-16928# West Virginia Univ., Morgantown. Dept. of Physics.
HIGH TEMPERATURE PROPERTIES OF CERAMIC/CARBON SYSTEMS IN AN OXIDIZING ENVIRONMENT Annual Technical Report, 1 Jun. 1987 - 31 May 1988
Bernard R. Cooper and Pedro A. Montano 31 May 1988 18 p

(Grant AF-AFOSR-0251-87; AF Proj. 2306)
(AD-A200254; AFOSR-88-1078TR) Avail: NTIS HC A03/MF A01 CSCL 11B

The objective of our research is to identify and learn to constructively modify the features of the bonding interactions that lead to brittleness in carbon-based ceramic materials. We have been examining the titanium/carbon and tungsten/carbon systems, both the naturally occurring carbides and artificially constructed superlattices. We are examining the question of whether artificially constructed multilayer (superlattices) structures offer an advantage over the naturally occurring crystalline structures in maintaining high temperature mechanical stability in an oxygen-containing environment. This related to the modification of the type of bonding, metallic versus covalent, possible by making artificial structures and how this affects brittleness and hence fracture behavior. GRA

N89-16929 Maryland Univ., College Park.
TENSILE STRENGTH OF COMPOSITE STRUCTURES WITH INTERNAL PLY DROPS AND FREE-EDGE EFFECTS Ph.D. Thesis
John Cristopher Fish 1988 290 p
Avail: Univ. Microfilms Order No. DA8818395

Experimental and numerical analyses were conducted to determine the tensile strength of glass epoxy composite laminates with internal ply drops, and free edge effects. The experimental program consisted of manufacturing and testing five different tapered layups, incorporating internal ply drops, and flat layups representing the thin section of the tapered laminates. Free edge effects were significant in some of the laminates and negligible in others. Finite element models were used to examine the out of plane stress states created by the internal ply drops and the free edge effect. In addition to the plies, the interply resin was simulated in the critical ply interfaces in some of the finite element models. Both ply failure and interply resin failure were examined as methods for predicting laminate strength. Dissert. Abstr.

N89-16930 ESDU International Ltd., London (England).
ELASTIC WRINKLING OF SANDWICH PANELS WITH LAMINATED FIBRE REINFORCED FACE PLATES (FACE PLATES OF AsBoDs, AsDIDs AND AsBsDs TYPES). (COMPUTER PROGRAM)
Dec. 1988 63 p
(ESDU-88015; ISBN-0-85679-647-6; ISSN-0141-4097) Avail: ESDU

This Data Item 88015, an addition to the Sub-series on Structures and on Composites, provides a program listing in FORTRAN for calculating the wrinkling loads of balanced, and two classes of unbalanced, laminated faceplates under uniaxial or biaxial loading. Symmetric or antisymmetric wrinkling modes are considered and account is taken of the two orthogonal shear moduli and the through-thickness modulus of the core, together with the panel dimensions. The input to the program is detailed, and the faceplate properties can be provided as layer properties with a stacking sequence or directly as faceplate stiffness matrix along and across the panel. Graphs are included to illustrate the influence of the major variables on wrinkling loads. The faceplate/core adhesive layer can significantly affect the wrinkling load, and that effect is allowed for in the program. The program checks that input values comply with the limits to the analysis and the program terminates, providing an appropriate explanation, when those limits are not met. Program testing is briefly outlined, and several worked examples illustrate its use. The program is available on magnetic media as ESDUpac 88015. ESDU

N89-16931 ESDU International Ltd., London (England).
WRINKLING OF SANDWICH PANEL FACE PLATES (ISOTROPIC FACE PLATES ON ORTHOTROPIC CORES, IN-PLANE LOADING OR BENDING)
Dec. 1988 25 p
(ESDU-88032; ISBN-0-85679-664-6; ISSN-0141-4097) Avail: ESDU

This Data Item 88032, an addition to the Sub-series on Structures, provides comprehensive data for estimating the wrinkling stress of the faceplates. The effect is taken into account of the faceplate properties and dimensions, the core shear moduli and through-thickness modulus, and the core dimensions. For in-plane loads (any combination of direct and shear) both symmetric and antisymmetric wrinkling modes are considered. The effect of material plasticity can be allowed for and comprehensive example calculations illustrate that. The implications of the theoretical models used are considered and guidance is provided on conditions where they may lead to an under- or over-estimate of the wrinkling stress of real structures. A method is given for estimating the reduction in wrinkling stress due to initial faceplate irregularities. Notes discuss the effects of variations in core properties and the possible influence of the faceplate/core adhesive layer. ESDU

N89-16932# Oak Ridge National Lab., TN. Metals and Ceramics Div.
MICROANALYTICAL CHARACTERIZATION OF WEAR DAMAGE IN AN ALUMINA-SILICON CARBIDE WHISKER COMPOSITE
C. S. Yust and L. F. Allard 1988 17 p Presented at the 3d International Symposium on Ceramic Materials and Components for Engines, Las Vegas, NV, 27 Nov. 1988
(Contract DE-AC05-84OR-21400)
(DE89-003149; CONF-881125-2) Avail: NTIS HC A03/MF A01

Wear damage in a silicon carbide whisker-reinforced alumina composite resulting from unlubricated, self-mated, pin-on-disk sliding in air at 800 C has been characterized using scanning Auger spectroscopy, transmission electron microscopy, and energy dispersive X-ray analysis. Using constant bearing pressure and sliding velocity, sliding for 2 km resulted in mild wear of the disk surface on which regions of silicon oxide were formed. At a sliding distance of 5 km, the wear rates measured still indicated mild wear, but pitting at the center of the disk wear track was observed. Subsurface damage of the alumina matrix beneath the disk wear track at 5 km sliding distance was characterized by transmission electron microscopy of cross sections. Wear debris observed on the wear surface was comprised of fine particulates of composition similar to that of the bulk material. The implications of the observations regarding wear mode and wear lifetime are discussed. DOE

N89-16933# Los Alamos National Lab., NM.
MECHANICAL CHARACTERIZATION OF SiC WHISKER-REINFORCED MoSi
David H. Carter, W. Scott Gibbs, and John J. Petrovic 1988 11 p Presented at the 3rd International Symposium on Ceramic Materials and Components for Engines, Las Vegas, NV, 27 Nov. 1988
(Contract W-7405-eng-36)
(DE89-003486; LA-UR-88-3776; CONF-881125-3) Avail: NTIS HC A03/MF A01

The mechanical characteristics of an intermetallic matrix with two different reinforcements were studied. The matrix material was MoSi2, with either Los Alamos VLS SiC whiskers or Huber VS SiC whiskers. The purpose of the reinforcement was to provide toughening at ambient temperature and strengthening at elevated temperatures. The VLS whiskers greatly improved the yield strength of the matrix at 1200 C, and also increased the room temperature fracture toughness of the matrix. The VS whiskers were added because they are much smaller in length and diameter, and therefore decreased the mean free path between whiskers, at the same volume fraction. The VS whiskers improved the toughness of the matrix at ambient temperature, and increased the yield strength of MoSi2 at 1400 C by 470 percent. The high strength of this new composite places this material in the realm of attractive engineering materials for high-temperature applications. DOE

N89-16934# Centre d'Essais Aeronautique Toulouse (France). Lab. des Materiaux Composites et Organiques.
QUALIFICATION TESTS OF PREIMPREGNATED CARBON EPOXY T800H/DA 0506 FROM STRUCTIL. TEST REPORT M6-570500 Final Report [PROGRAMME CSPC: ESSAIS DE QUALIFICATION DU PREIMPREGNE CARBONE/EPOXY T800H/DA 0506 DE STRUCTIL. PROCES VERBAL M6-570500]
M. Loriot 15 Dec. 1987 75 p In FRENCH
(Contract STPA-83-96-003)
(Rept-M6-570500; ETN-89-93611) Copyright Avail: NTIS HC A04/MF A01

The results obtained by infrared spectrophotometry, liquid chromatography, differential microcalorimetry and thermogravimetric analysis of a carbon epoxy are given. They are similar to results obtained previously with the DA0560 resin. The mechanical tests were carried out on 8, 28, and 80 ply specimen geometry. The 8 ply tensile tests show a breaking strength increase of 10 percent The compression results with 28 ply are improved, but a larger sensitivity to a hole in the tensile tests is observed. ESA

N89-16935# Aerospatiale, Suresnes (France). Direction Centrale de la Qualite.
EVALUATION OF PHYSICAL CHEMICAL TEST METHODS FOR CHARACTERIZING POLYMERIZED COMPOSITES OR POLYMERIZING COMPOSITES: LITERATURE REVIEW [EVALUATION DE METHODES D'ESSAIS PHYSICO-CHIMIQUES POUR LA CARACTERISATION DES COMPOSITES POLYMERISES OU EN COURS DE POLYMERISATION: ETUDE BIBLIOGRAPHIQUE]
P. Abjean, B. Costes, D. Lairez, and B. Hilaire 3 May 1988 114 p In FRENCH
(Contract STPA-86-96-031-00-471-75-86)
(Rept-49-438/F; ETN-89-93651) Avail: NTIS HC A06/MF A01

Epoxy resin matrix composites are discussed. A distinction is made between macroscopic methods such as ultrasonic detection, fractal analysis, and dielectrometry which allow a global measurement of reaction progress, and the microscopic methods such as the nuclear magnetic resonance and infrared photometry which allow access to structural details of the materials. ESA

N89-16936# Lawrence Livermore National Lab., CA. Chemistry and Materials Lab.
INTERFACIAL BONDING IN W/C AND W/B4C MULTILAYERS
A. F. Jankowski, L. R. Schrawyer, M. A. Wall, W. W. Craig, R. I. Morales, and D. M. Makowiecki Oct. 1988 17 p Presented at the Topical Conference on Probing the Nanometer Scale Properties of Surfaces and Interfaces, Atlanta, GA, 3 Oct. 1988
(Contract W-7405-eng-48)
(DE89-002931; UCRL-99378; CONF-8810230-1) Avail: NTIS HC A03/MF A01

The nature of carbon bonding in W/C and W/B4C multilayer structures is investigated by Auger electron spectroscopy (AES). The interfacial roughness in these X-ray mirrors directly affects their use as efficient optical elements. A significant contribution to interfacial roughness is the possible presence of second phases, WC in particular for the W/C and W/B4C combinations. AES depth profiling of the multilayer interfaces is used as a direct method to probe for the existence of WC. DOE

N89-16994# Office National d'Etudes et de Recherches Aeronautiques, Paris (France). Materials Dept.
CERAMIC-CERAMIC COMPOSITES FOR USE AT HIGH TEMPERATURE
J. F. Jamet *In* Office of Naval Research, Engineering Materials for Very High Temperatures. An ORNL Workshop 1988 p 13-25 (For primary document see N89-16992 09-27)
Avail: NTIS HC A05/MF A01

N89-16995# Technische Hogeschool, Eindhoven (Netherlands). Dept. of Physical Chemistry.
DEVELOPMENT OF COMPOSITE HIGH TEMPERATURE MATERIALS FOR FUTURE ENERGY CONVERSION APPLICATIONS
R. Metselaar and L. R. Wolff *In* Office of Naval Research, Engineering Materials for Very High Temperatures. An ORNL Workshop 1988 p 27-34 (For primary document see N89-16992 09-27)
Avail: NTIS HC A05/MF A01

25 INORGANIC AND PHYSICAL CHEMISTRY

Includes chemical analysis, e.g., chromatography; combustion theory; electrochemistry; and photochemistry.

For related information see also *77 Thermodynamics and Statistical Physics.*.

N89-16937# Indiana Univ., Bloomington. Dept. of Chemistry.
EVALUATION OF A SUPERCRITICAL FLUID CHROMATOGRAPH COUPLED TO A SURFACE-WAVE-SUSTAINED MICROWAVE-INDUCED PLASMA DETECTOR
Debra R. Luffer, Leonard J. Galante, Paul A. David, Milos Novotny, and Gary M. Hieftje 11 Jul. 1988 27 p
(Contract N00014-86-K-0366)
(AD-A198728; INDU/DC/GMH/TR-88-31) Avail: NTIS HC A03/MF A01 CSCL 17H

A capillary supercritical fluid chromatograph was coupled to a surface-wave-sustained microwave-induced plasma (MIP) sustained with a surfatron. The chromatographic system, interface, and plasma source are described. The plasma was optimized for sulfur emission at 921.3 nm and used to detect a mixture of sulfur-containing polycyclics that had been separated by SFC. The linear dynamic range for these compounds is 3 orders of magnitude with detection limits of 25 pg/sec of sulfur for thiophene. The relative standard deviations for repetitive injections are typically 1 to 5 percent at concentrations well above the detection limit. GRA

N89-16938# Chemical Research and Development Center, Aberdeen Proving Ground, MD.
LIGHT-OFF TEMPERATURE DETERMINATION OF OXIDATION CATALYST USING FOURIER TRANSFORM INFRARED TECHNIQUE Technical Report, Jul. - Dec. 1987
Chen C. Hsu Aug. 1988 13 p
(AD-A199596; CRDEC-TR-88160) Avail: NTIS HC A03/MF A01 CSCL 07B

Light off temperatures of oxidation catalysts are considered as one of the important parameters for catalyst performance evaluation. In this study, the in situ Fourier Transform IR technique was developed and used to determine the light-off temperatures and reaction products of three three-way automotive catalysts with 20 torr monomethylamine in air at 0.5 L/min flow rate. Light-off temperatures were 140, 143, and 170 C for Davison, Allied-Signal, and Degussa oxidation catalysts, respectively. CO, CO2, H2O, and nitric acid were the major oxidation products. The activation energies of formation of CO and CO2 on the catalysts were also determined. GRA

N89-16939# Manchester Coll. of Science and Technology (England). Dept. of Chemistry.
THE KINETICS AND DYNAMICS OF IODINE MONOFLUORIDE FORMATION IN GAS-PHASE COLLISIONS Final Report, 1 Dec. 1984 - 31 May 1988
J. C. Whitehead 15 Sep. 1988 9 p
(Grant AF-AFOSR-0039-85; AF Proj. 2303)
(AD-A199622; AFOSR-88-1034TR) Avail: NTIS HC A02/MF A01 CSCL 07B

The production of IF(B) in gas phase collisions of fluorine atoms with various organic and inorganic iodides has been investigated

to determine methods of efficient production. The key role of electronically excited iodine atoms has been identified. Excimer laser photolysis of mixtures of molecular fluorine and organic iodides is shown to yield high pulse intensities of IF(B). GRA

N89-16940# Chemical Research and Development Center, Aberdeen Proving Ground, MD.
ION CONTENT OF MOIST ATMOSPHERIC AIR AND THE MOLECULAR STRUCTURE OF WATER VAPOR THUS INFERRED Technical Report, May 1986 - May 1987
Hugh R. Carlon Jul. 1988 46 p
(AD-A199732; CRDEC-TR-88088) Avail: NTIS HC A03/MF A01 CSCL 07B

A great deal of multidisciplinary research, reported in the open literature, suggests that even the cleanest water vapor is not simply a collection of single water molecules (monomers) as is popularly supposed, but also contains vast populations of molecular aggregates of clusters especially under conditions of high humidity. These water clusters include not only collision-induced, Boltzmann-distributed dimers, trimers, etc., but also a preponderance of much larger evaporatively-produced clusters that are extensively hydrogen bonded and thus form equilibrium populations in the vapor. The question of the extent of such clustering in the vapor versus temperature and humidity has been investigated in rigorous new measurements of the electrical conductivity of moist air. The ion populations measured in the vapor give excellent agreement with those predicted by equations developed from first principles of kinetic theory. These ion populations are dissociative products of the large clusters. GRA

N89-16941# Chemical Research and Development Center, Aberdeen Proving Ground, MD.
GAS CHROMATOGRAPHIC METHOD FOR THE DETERMINATION OF TRACE QUANTITIES OF DIETHYL MALONATE IN ETHANOL Technical Report, Dec. 1985 - Apr. 1986
Juan D. Lopez Jul. 1988 13 p
(AD-A199733; CRDEC-TR-88117) Avail: NTIS HC A03/MF A01 CSCL 07C

This report presents an experimental study conducted to determine a method for analytically detecting and determining trace quantities of diethyl malonate (DEM) in ethyl alcohol using a gas chromatograph equipped with a flame ionization detector. The method developed proved to be effective for determining trace quantities at a concentration (mean) range of 21-840 ng. A linear fit was obtained at this range with an average slope of 1.4032 + or - 0.0063 x 10 to the -7th micro g/au and an intercept of 0.0359 + or - 0.0359 micro g. The correlation coefficient was 0.9996 + or - 0.0009. Based on replicate injections, the accuracy of this method was within + or - 2.4 percent. GRA

N89-16942# Smithsonian Astrophysical Observatory, Cambridge, MA.
ABSOLUTE ABSORPTION CROSS SECTION MEASUREMENTS OF OZONE AND THE TEMPERATURE DEPENDENCE AT FOUR REFERENCE WAVELENGTHS LEADING TO RENORMALIZATION OF THE CROSS SECTION BETWEEN 240 AND 350 nm Final Report, 24 Jul. 1985 - 31 Dec. 1987
W. H. Parkinson, K. Yoshino, and D. E. Freeman Mar. 1988 36 p
(Contract F19628-85-K-0049)
(AD-A199737; AFGL-TR-88-0161) Avail: NTIS HC A03/MF A01 CSCL 07B

We have developed techniques for the preparation and preservation of pure ozone which have enabled its absolute cross section at important mercury-line reference wavelength 253.7 nm and at iron line wavelengths 283.3, 245.8 and 26.7 nm to be determined at the temperatures 293, 228 and 195 k. Specially constructed absorption cells are used together with existing spectrometers and associated equipment and light sources which have already been employed successfully to study the absolute cross section of ozone at longer wavelengths. This determination of the temperature dependence of the absolute cross section at 238.3, 245.8, 253.7 and 263.7 nm permit renormalization of the full relative cross sections for ozone between 240nm and 350nm. A tabular and computer accessible form of the ozone cross sections data has been made at 5/cm intervals. These absolute cross sections and their temperature dependence are needed for accurate calculations of the atmospheric transmission in the visible and near ultraviolet regions. GRA

N89-16943# Ementeck, Inc., College Station, TX.
AN INVESTIGATION OF THE RECHARGEABILITY OF CERTAIN MODIFIED FORMS OF MnO2 Final Report
John O. Brockris Sep. 1988 29 p
(Contract N00014-87-C-0662)
(AD-A199885) Avail: NTIS HC A03/MF A01 CSCL 07B

The modified form of MnO2 prepared through doping with bismuth or lead possesses rechargeable properties. The work performed under this project was to investigate these properties. The bismuth modified MnO2 (designated as MnO2) was prepared by coprecipitation of hydroxides from the aqueous solutions of nitrates of Mn and Bi and subsequent oxidation of the hydroxides to the MnO2. Preliminary investigations of the Zn-MnO2 system in the presence of selected membranes were aimed at determining ways to prevent migration of the soluble zincate anion to the MnO2 electrode. Selected membranes and additives were tested. An improvement in the cyclability of the MnO2 electrode was achieved under certain circumstances. Extensive testings of the Zn-MnO2 systems are needed. GRA

N89-16944# Northwestern Univ., Evanston, IL.
THINNING AND RUPTURE OF A THIN LIQUID FILM ON A HORIZONTAL HEATED SOLID SURFACE Progress Report, 16 Jun. 1987 - 31 Jul. 1988
S. G. Bankoff and S. H. Davis Aug. 1988 10 p
(Contract DE-FG02-86ER-13641)
(DE89-001792; DOE/ER-13641/1) Avail: NTIS HC A02

The analysis of the nonlinear stability and rupture of a thin liquid film on a heated horizontal plate has been completed. Extensions to condensing films, films subjected to constant heat fluxes and films with three-dimensional waves have been obtained. Multiple time scales were introduced in order to determine the effects of the initial conditions, and to clarify the behavior just before rupture. The general evolution equation has been derived for the case where both the viscosity and the surface tension are linear functions of temperature. The thinning and rupture of a thin film of an organic liquid on a non-uniformly heated Invar plate has been measured. Analysis of the data is in progress. DOE

N89-16945# Altex Technologies Corp., Los Gatos, CA.
CHARACTERIZATION OF NONPREMIXED TURBULENT BLUFF-BODY BURNER FLAMES Annual Report, Jan. - Dec. 1987
J. Kelly, M. Namazian, and R. Schefer (Sandia National Labs., Albuquerque, NM.) 22 Jan. 1988 221 p
(Contract GRI-5086-260-1250)
(PB89-100507; GRI-88/0168) Avail: NTIS HC A10/MF A01 CSCL 21B

Detailed laser based diagnostics were used to characterize bluff body burner flames for a range of fuel to air velocity ratios and bluff body to fuel jet diameter ratios. In support of data analysis, flamelet and dissipative eddy flame structure models were developed and applied. For large fuel to air flow momentum ratios, the fuel jet penetrates the recirculation zone and flow patterns, entrainment and flame patterns are similar to those in jet flames. At small ratios, the fuel jet is stagnated and dispersed within the recirculation zone, entrainment increases by an order of magnitude and flames are drastically shortened. Turbulence, particularly near the flame surface, exhibits a large scale time varying component which cannot be modeled by current time averaged techniques. Author

N89-16946# Schmitt Technology Associates, New Haven, CT.
GAS JET DEPOSITION OF MULTICOMPONENT ULTRAFINE MICROSTRUCTURES Final Report, 30 Sep. 1987 - 31 Mar. 1988
Bret L. Halpern and Jerome J. Schmitt 28 Jun. 1988 14 p
(Contract N00014-87-C-0840)
(AD-A200101; Rept-03/ONR-F1) Avail: NTIS HC A03/MF A01 CSCL 07B

The potential importance of multicomponent ultrafine microstructures makes it essential to develop methods of formation which permit both higher growth rates and improved control over material properties. During the course of the Phase 1 research effort, it was shown that the new proprietary technique, Gas Jet Deposition, has these capabilities and other advantages over established methods. In this technique, depositing atoms, molecules or clusters are seeded into a free jet which is directed at a substrate at low temperature in a high background pressure. The deposition rates can be exceptionally large; the high pressure, low temperature conditions permit the processing of new types of surfaces; and deposition can occur in a reactive mode for production of oxide and nitride materials. Phase 1 achievements include: (1) fabrication of uniform 100 layer alternating gold/copper thin film multilayer microstructures with 5 nm individual layer thickness; (2) fabrication of 3 nm gold particles; (3) deposition of copper oxide, gold oxide, silicon oxide and silicon nitride thin films. These results were confirmed using stylus profilometry, X-ray diffraction, auger profiling and electron microscopy. Author

N89-16947# Air Force Systems Command, Wright-Patterson AFB, OH. Foreign Technology Div.
LAMINAR FLAME IN A TURBULENT FLOW
A. M. Klimov 18 Nov. 1988 28 p Transl. into ENGLISH from Prikladnoy Mekhaniki i Tekhnicheskoy Fiziki Zhurnal (USSR), no. 3, May - Jun. 1963 p 49-58
(AD-A200241; FTD-ID(RS)T-0642-88) Avail: NTIS HC A03/MF A01 CSCL 20D

Are obtained equations, which describe laminar flame in heterogeneous hydrodynamic field if curvature of flame front can be disregarded (action of large-scale turbulence). The basic properties of this flame are clarified. The possible mechanism of extinguishing of flame is obtained. The mechanism of turbulent combustion is considered. GRA

N89-16948# United Technologies Research Center, East Hartford, CT.
INVESTIGATION OF FUEL ADDITIVE EFFECTS ON SOOTING FLAMES Annual Technical Report, 1 Jun. 1987 - 31 May 1988
Paul A. Bonczyk 30 Jun. 1988 16 p
(Contract F49620-86-C-0054)
(AD-A200273; UTRC-R88-957464-A; AFOSR-88-0801TR) Avail: NTIS HC A03/MF A01 CSCL 21D

The objective of this research is to clarify the mechanisms responsible for the suppression of soot in flames by fuel additives. Measurements are limited to well-defined hydrocarbon air prevaporized liquid- and gaseous-fueled flames. Gas-phase hydrocarbon species measurements have been made in an axisymmetric prevaporized iso-octane/air diffusion flame with and without ferrocene present as a fuel additive. The concentrations have been determined using quartz probe sampling and chromatographic analysis. Of the roughly twenty species detected, most were unaffected by the ferrocene. Expections were C2H2 and H2 which showed a decrease and increase, respectively, with ferrocene seeding. Solid effluent has been collected and analyzed by ESCA (Electron Scattering for Chemical Analysis) for the seeded flame. For seeding levels sufficient to suppress a soot plume, the effluent was hematite. GRA

N89-16949# Utah Univ., Salt Lake City. Dept. of Chemistry.
IN-SITU VIBRATIONAL SPECTROELECTROCHEMISTRY Technical Report No. 95, Sep. 1987 - Jul. 1988
B. Stanley Pons 15 Jul. 1988 26 p Submitted for publication
(Contract N00014-83-K-0470)
(AD-A200303) Avail: NTIS HC A03/MF A01 CSCL 07D

The use of infrared and Raman spectroscopies for the investigation of the electrode-solution interface as described. Applications for the studies of adsorbates, surface reactions, electron transfer reactions, and recently developed models that treat the potential dependency of vibrational bands of adsorbed species are discussed. GRA

N89-16950# Utah Univ., Salt Lake City. Dept. of Chemistry.
AN IN SITU SURFACE FOURIER TRANSFORM STUDY OF COMPLEXES OF LITHIUM, MAGNESIUM POTASSIUM AND LANTHANUM FERROCYANIDE AT PLATINUM AND GOLD ELECTRODES Technical Report No. 102, Sep. 1987 - Jul. 1988
D. J. Blackwood and B. Stanley Pons 15 Jul. 1988 10 p Submitted for publication
(Contract N00014-83-K-0470)
(AD-A200305) Avail: NTIS HC A02/MF A01 CSCL 09A

The working electrode was either a platinum or gold disk (1 cm diameter), which had been polished to a mirror finish using progressively smaller diameters of alumina down to 0.05 micro meters. The disk was mounted on the end of a glass syringe barrel designed to fit the infrared cell. The cell construction was of the thin layer type and has been described previously. A platinum wire quasi-reference electrode was used throughout these experiments. The spectrometer employed was a vacuum bench Brucker-IBM model IR/98 FTIR on which subtractively normalized interfacial Fourier transform infrared spectroscopy (SNIFTIRS9) could be performed. In SNIFTIRS difference spectra, the data are displayed so that bands extending to positive (upwards) values of relative reflectance are due to species at the base reference potential (reactants in the unperturbed system), while negative bands denote species formed when the potential is stepped to a new value (the products of the electrochemical reaction). GRA

N89-16951# Utah Univ., Salt Lake City. Dept. of Chemistry.
THE BEHAVIOR OF MICRODISKS AND MICRORING ELECTRODES. APPLICATIONS OF NEUMANN'S INTEGRAL THEOREM Technical Report No. 129, Sep. 1987 - Jul. 1988
Martin Fleischmann, John Daschbach, and B. Stanley Pons 15 Jul. 1988 37 p Submitted for publication
(Contract N00014-83-K-0470)
(AD-A200307; TR-129) Avail: NTIS HC A03/MF A01 CSCL 07D

In a series of papers we have recently discussed the steady state behavior of microdisk and microring electrodes as well as the chronopotentiometric, chronoamperometric, and A.C. responses of microdisk electrodes and the determination of the rates of homogeneous reactions coupled to electrode processes at these electrodes. Our approach has been based on the use of discontinuous integrals of Bessel functions (for comparable solutions in heat conduction). It is shown that Neumann's integral theorem can be used to derive the steady-state behavior of microdisk electrodes. Results obtained previously using other methods for uniform surface concentration and uniform flux boundary conditions are derived as limiting cases of a general equation which describes irreversible and quasi-reversible reaction kinetics. It is shown that the approach can be used to assess the effects of the tertiary current distribution and to predict the behavior for electrode reactions which are non-linear in the concentration terms. GRA

N89-16952# Utah Univ., Salt Lake City. Dept. of Chemistry.
THE BEHAVIOR OF MICRODISKS AND MICORING ELECTRODES. PREDICTION OF THE AMPEROMETRIC RESPONSE OF MICRODISKS AND OF THE STEADY STATE FOR CE AND EC CATALYTIC REACTIONS BY APPLICATION OF NEUMANN'S INTEGRAL THEOREM Technical Report No. 130, Sep. 1987 - Jul. 1988
Martin Fleischmann, Derek Pletcher, Guy Denault (Southampton Univ., England), John Daschbach, and B. Stanley Pons 15 Jul. 1988 35 p
(Contract N00014-83-K-0470)
(AD-A200415) Avail: NTIS HC A03/MF A01 CSCL 07D

It is shown that the chronoamperometric response at microdisk electrodes can be derived from Neumann's integral theorem of two parameters. The form of the transients can be predicted for a wide range of boundary conditions and this is illustrated by the relaxation behavior of irreversible reactions in addition to that of the widely investigated example of zero surface concentration of the reactant. Corrections to the transients due to the tertiary current distribution are derived for relaxation experiments and it is shown that the methods developed can also be applied to linear sweep voltammetry. The steady state behavior of c.e. and e.c. catalytic reactions is formally similar to the chronoamperometry of irreversible electrode reactions and it is shown that complete descriptions can be obtained for the voltammetry of such systems. GRA

N89-16953# Utah Univ., Salt Lake City. Dept. of Chemistry.
THE BEHAVIOR OF MICRODISK AND MICRORING ELECTRODES. MASS TRANSPORT TO THE DISK IN THE UNSTEADY STATE: CHRONOPOTENTIOMETRY Technical Report, Sep. 1987 - Jul. 1988
B. Stanley Pons and Martin Fleischmann (Southampton Univ., England) 15 Jul. 1988 24 p Submitted for publication
(Contract N00014-83-K-0470)
(AD-A200421; TR-110) Avail: NTIS HC A03/MF A01 CSCL 09A

We describe the time dependent response of a finite disk electrode under conditions of constant applied flux (chronopotentiometry). The exact solution is recovered by solving the differential equations in the circular cylindrical coordinate system with the use of suitable discontinuous integrals. In addition, we present the results for the case of linear sweep amperometry, which will generally be more useful for controlled current experiments with microelectronics. Author

N89-16954# Utah Univ., Salt Lake City. Dept. of Chemistry.
THE BEHAVIOR OF MICRODISK AND MICRORING ELECTRODES. MASS TRANSPORT TO THE DISK IN THE UNSTEADY STATE: COUPLED CHEMICAL REACTIONS Technical Report, Sep. 1987 - Jul. 1988
B. Stanley Pons and Martin Fleischmann (Southampton Univ., England) 15 Jul. 1988 24 p Submitted for publication
(Contract N00014-83-K-0470)
(AD-A200422; TR-113) Avail: NTIS HC A03/MF A01 CSCL 09A

In this work, we discuss the solution of the differential equations in the cylindrical coordinate system for the case of a coupled CE reaction mechanism at a finite disk electrode. We use the properties of discontinuous integrals of Bessel functions to treat the mixed boundary conditions at the electrode surface and the surrounding insulator. The results are compared to previous analyses and we also make comparisons of various estimates of the chronoamperometric response for constant surface concentration conditions. GRA

N89-16955# Utah Univ., Salt Lake City. Dept. of Chemistry.
THE USE OF NARROW GAP LINE MICROELECTRODES AS SENSITIVE AND SPECIES SELECTIVE GAS CHROMATOGRAPHIC DETECTORS Technical Report, Sep. 1987 - Jul. 1988
Rossella Brina and B. Stanley Pons 15 Jul. 1988 24 p
(Contract N00014-83-K-0470)
(AD-A200424; TR-116) Avail: NTIS HC A03/MF A01 CSCL 07D

In this work we describe a new microelectrode assembly and its use as a sensitive electrochemical gas chromatographic detector. The conditions of operation of this device, i.e., pretreatment of the microelectrode surface, applied potential, and signal-to-noise ratio were studied in order to achieve maximum sensitivity and reproducibility. Condensation of the analyte in a thin gap between two parallel line microelectrodes comprising the electrochemical cell is considered to be the factor determining the sensitivity of the device. GRA

N89-16956# Naval Postgraduate School, Monterey, CA.
MECHANICAL-CHEMICAL ENERGY TRANSFER OBSERVATIONS OF VAPORIFIC EXPLOSIONS M.S. Thesis
Gilberto Rodriguez Jun. 1988 60 p
(AD-A200428) Avail: NTIS HC A04/MF A01 CSCL 15F

This thesis incorporates an experiment performed with the objective of expanding the existing knowledge about Vaporific Explosions. This phenomenon, known to produce extensive damage to targets, is studied for a possible energy transfer mechanism occurring during the projectile-target impact interaction. This investigation is concentrated mainly to observe the distribution and combustion of fragments (aluminum particles) within the fragment beam and the transfer of kinetic energy to surfaces on the target. The results indicated no evidence of combustion for the selected target. GRA

N89-16957# Akron Univ., OH. Inst. of Polymer Science.
ADSORPTION OF PHOSPHORUS ACIDS ON ALUMINA
R. D. Ramsier, P. N. Henriksen, and A. N. Gent Oct. 1988 44 p
(Contract N00014-85-K-0222)
(AD-A200548; TR-17) Avail: NTIS HC A03/MF A01 CSCL 11C

Penetration of moisture into adhesively bonded aluminum structures can and often does lead to deterioration and ultimate failure of the bonds. Methods of retarding moisture penetration into these systems are therefore desirable. One successful method consists of treating the oxidized aluminum (alumina) surface with an hydration inhibitor prior to application of the adhesive. In a comprehensive study of the use of hydration inhibitors to improve the durability of aluminum joints, Davis et al. found that alumina surfaces treated with certain amino phosphonates exhibited a much higher resistance to hydration than untreated surfaces. There it was proposed that phosphonic acids absorb on alumina by a condensation reaction involving hydroxyl groups of the acid and those on alumina, resulting in the formation of P-O-Al bonds. GRA

N89-16958# Brookhaven National Lab., Upton, NY.
CONVERSION OF NATURAL GAS TO METHANOL
T. E. OHare, R. S. Sapienza, D. Mahajan, and G. T. Skaperdas Aug. 1988 18 p Presented at the Offshore Northern Seas Conference and Exhibition, Stavanger, Norway, 23 Aug. 1988
(Contract DE-AC02-76CH-00016)
(DE89-001088; BNL-41701; CONF-8808151-1) Avail: NTIS HC A03/MF A01

The penetration of natural gas into distant markets can be substantially increased by a new methanol synthesis process under development at the Brookhaven National Laboratory. The new methanol process is made possible by the discovery of a catalyst that drops synthesis temperatures from about 275 F to about 125 C. Furthermore, the new catalyst is a liquid phase system, which permits the synthesis reaction to proceed at fully isothermal conditions, in contrast to the hot spots that prevent currently available pelleted, solid catalysts from operating efficiently. In contrast, the new low temperature liquid catalyst can convert synthesis gas completely to methanol in a single pass through the methanol synthesis reactor. This characteristic leads to a further major improvement in the methanol plant. Atmospheric nitrogen can be tolerated in the synthesis gas, and still the volume of gas fed to the reactor can be smaller than the volume of gas that must be fed to the reactor when accommodating the very low conversions furnished by the best of currently available catalysts. DOE

N89-16959# Brookhaven National Lab., Upton, NY.
MODERN AND PROSPECTIVE TECHNOLOGIES FOR HYDROGEN PRODUCTION FROM FOSSIL FUELS
M. Steinberg and Hsing C. Cheng May 1988 48 p Presented at the Hydrogen Today, Moscow, (USSR) 25 Sep. 1988
(Contract DE-AC02-76CH-00016)
(DE89-001270; BNL-41633; CONF-880925-2) Avail: NTIS HC A03/MF A01

A study is presented assessing the technology and economics of hydrogen production by conventional and advanced processes. Six conventional processes are assessed including: (1) steam reforming of natural gas, (2) partial oxidation of residual oil, (3) gasification of coal by Texaco process, (4) gasification of coal by Koppers-Totzek process, (5) steam-iron process, and (6) water electrolysis. The advanced processes include: (1) high temperature electrolysis of steam, (2) coal gasification and electrochemical shift, (3) integrated coal gasification and high temperature electrolysis, (4) thermal cracking of natural gas, and (5) the HYDROCARB thermal conversion of coal. By-product hydrogen, thermochemical water splitting and high energy radiation, plasma and solar photovoltaic-water electrolysis production of H2 are discussed.
DOE

N89-16960# Colorado Univ., Boulder. Dept. of Chemistry.
STUDIES OF METAL/CARBON SURFACE CHEMISTRY Final Report, 1 Sep. 1984 - 31 Aug. 1987
Bruce E. Koel 25 May 1988 9 p
(Contract DE-FG22-84PC-70779)
(DE88-011264; DOE/PC-70779/16) Avail: NTIS HC A02/MF A01

The purpose of this research is to identify stable surface species formed from molecular adsorption and reaction on metal/carbon surfaces. This research has practical application in improving the fundamental understanding of catalytic coal gasification. Well-defined model catalysts for carbon gasification have been studied by vapor depositing alkali and transition metal atoms on carbon surfaces. Vibrational spectroscopy using high resolution electron energy loss spectroscopy (HREELS) and photoelectron spectroscopy of these surfaces are being used to develop an atomic-level understanding of the chemical bonding, structure, and reactivity of the metal/carbon surface and of the adsorbed molecular species.
DOE

N89-16961# National Inst. of Standards and Technology, Gaithersburg, MD. Thermophysics Div.
THERMOPHYSICAL PROPERTY MEASUREMENTS IN FLUID MIXTURES Final Report, period ending 31 Oct. 1987
20 Sep. 1988 6 p
(Contracts DE-AI01-76PR-06010; DE-AT01-82ER-12045)
(DE89-003281; DOE/PR-06010/T37) Avail: NTIS HC A02/MF A01

Five years ago, the Center for Chemical Engineering of the National Bureau of Standards began a major program to upgrade its experimental capability in fluid property measurement. During the past five years great strides have been taken in improving and upgrading measurement capability at the two NBS sites. The apparatus that have been built under DOE sponsorship and that are now in routine operation are listed.
DOE

N89-16962 ESDU International Ltd., London (England).
VAPOUR PRESSURES AND CRITICAL POINTS OF LIQUIDS. C7 TO C20 ALKANOLS
Aug. 1988 34 p Supersedes in part ESDU-74023
(ESDU-88012; ISBN-0-85679-644-1; ISSN-0141-4062) Avail: ESDU

This Data Item 88012, an addition to the Sub-series on Physical Data, gives vapor pressure for 23 alkyl alcohols. The data were obtained by a method described in ESDU 84021 involving a critical evaluation of experimental results in the literature, extrapolated by recent reliable method into the low pressure region, and fitted by a Wagner equation applying over the full liquid range from the freezing to the critical point. The coefficients for the equation are given for each compound and three tables of vapor pressure are included: in SI units at 5 K intervals, in atmospheres at 5 C intervals, in lbf/sq in at 10 F intervals. The sources of the data used are listed, and a table gives likely uncertanties in values predicted by the equation that should be allowed for in any critical situation.
ESDU

N89-16963 ESDU International Ltd., London (England).
VAPOUR PRESSURES AND CRITICAL POINTS OF LIQUIDS. ORGANIC OXYGEN COMPOUNDS
Nov. 1988 42 p
(ESDU-88017; ISBN-0-85679-649-2; ISSN-0141-4062) Avail: ESDU

This Data Item 88017, an addition to the Sub-series on Physical Data, Chemical Engineering, gives vapor pressure for 18 compounds. The data were obtained by a method described in ESDU 84021 involving a critical evaluation of experimental results in the literature, extrapolated by a recent reliable method into the low pressure region, and fitted by a Wagner equation applying over the full liquid range from the freezing to the critical point. The coefficients of the equation are given for each compound and three tables of vapor pressure are included: in SI units at 5 K intervals, in atmospheres at 5 C intervals, in lbf/sq in at 10 F intervals. For each compound the sources of the data are listed and a table is given of likely uncertainties in values predicted by the equation that should be allowed for in any critical situation.
ESDU

N89-16964# Direction des Recherches Etudes et Techniques, Paris (France). Direction Scientifique Veille et Recherche Scientifique.
DEVELOPMENT OF A LATTICE GAS MODEL FOR THE STUDY OF COMBUSTION Final Report [DEVELOPPEMENT DE MODELE DE GAZ SUR RESEAU POUR L'ETUDE DE LA COMBUSTION]
G. Searby (Centre National de la Recherche Scientifique, Marseilles, France) 1986 42 p In FRENCH
(Contract PES-86/1359/DRET/DS/SR2)
(ETN-89-93612) Avail: NTIS HC A03/MF A01

Models are developed in which two distinct particle species interact on the same lattice. Adapting the type of interaction (elastic, inelastic, reactive) and intrinsic properties of each kind (mass, velocity), it is possible to simulate a mixing layer, the propagation of a chemical reaction front at constant density, or the propagation of a reaction front with heat production and density changes. The simulation is two-dimensional. The examples include a Kelvin Helmholtz instability with formation of coherent structures and vortex coalescence.
ESA

N89-16965*# San Diego State Univ., CA. Dept. of Electrical and Computer Engineering.
PHOTOABSORPTION AND PHOTODISSOCIATION OF MOLECULES IMPORTANT IN THE INTERSTELLAR MEDIUM Annual Report, 15 Jan. 1988 - 14 Jan. 1989
Long C. Lee and Masako Suto 6 Feb. 1989 54 p
(Grant NAGw-319)
(NASA-CR-184771; NAS 1.26:184771) Avail: NTIS HC A04/MF A01 CSCL 07D

Photoabsorption and fluorescence cross sections of molecules important in the interstellar medium were measured in the 90 to 200 nm region using synchrotron radiation, excimer laser, and condensed discharge lamps as light sources. The quantitative spectroscopic data are currently needed for the modeling of formation and destruction rates of molecules by the interstellar radiation field. Fluorescences from excited photofragments produced by vacuum ultraviolet radiation of molecules are dispersed to identify the emitting species. The fluorescence data are useful for the identification of emission sources in interstellar clouds.
Author

N89-16966# Brookhaven National Lab., Upton, NY.
KINETICS OF THE ISOTHERMAL DECOMPOSITION OF LANTHANUM NICKEL HYDRIDE
J. J. Reilly, Y. Josephy, and J. R. Johnson 1988 8 p Presented at the Metal Hydrogen Systems Fundamentals and Applications Conference, Stuttgart, Fed. Republic of Germany, 4 Sep. 1988
(Contract DE-AC02-76CH-00016)
(DE89-002905; BNL-41784; CONF-880969-5) Avail: NTIS HC A02/MF A01

The kinetics of the decomposition of the beta hydride to the

saturated alpha phase of LaNi5H(x) were determined under isothermal conditions using an agitated suspension of the alloy hydride in n-undecane and n-octane. The kinetics are well described by a shrinking core model where the rate limiting process is the solid state transformation taking place at the beta/alpha interface. The activation energy for the transformation is 40 kJ/mol. The excellent correspondence between the data and the model leads to the conclusion that diffusion is extremely rapid in highly cycled material. The liquid does not take part in any inherent kinetic process, in contrast to the previously studied absorption reaction. However, its presence is necessary to maintain isothermal conditions. DOE

N89-16967* National Aeronautics and Space Administration, Washington, DC.
COMBUSTIBILITY OF TITANIUM POWDERS
Ye. I. Popov, V. G. Poyarkov, and Yu. A. Finayev Feb. 1989 6 p Transl. into ENGLISH from Vosplamenyayemost Poroshkov Titana, Izvestiya Akademiyi Nauk BSSR, no. 2, 1975, p 91-92
(Contract NASw-4307)
(NASA-TT-20455; NAS 1.77:20455) Avail: Issuing Activity CSCL 21B

The combustion of compact samples was studied; the mechanism of autoignition is defined. Several studies are made of the combustibility of titanium using 50 samples. The data provide a clear idea of the combustibility of titanium powders. Author

26 METALLIC MATERIALS

Includes physical, chemical, and mechanical properties of metals, e.g., corrosion; and metallurgy.

N89-16968# Bhabha Atomic Research Centre, Bombay (India). Chemistry Div.
HYDROGEN DIFFUSION IN TANTALUM
M. S. Anand and D. D. Pruthi 1987 9 p
(DE88-704073; BARC-1379) Avail: NTIS (US Sales Only) HC A02/MF A01

Using resistivity technique, the diffusion of hydrogen in tantalum has been studied in the temperature range of 298-373 K. The diffusivity values obtained obey the following Arrhenius equation: D=4.38x10 to the -4 exp(-0.142/kT) sq cm /sec. The diffusion parameters agree with those obtained by others. The data has been interpreted in terms of modified over barrier diffusion mechanism. DOE

N89-16969# Japan Atomic Energy Research Inst., Tokyo. Dept. of Fuels and Materials Research.
INTERNAL STRESS DURING HIGH-TEMPERATURE CREEP AND ACTIVATION ENERGY FOR CREEP OF HASTELLOY XR
Yuji Kurata and Yutaka Ogawa Jul. 1988 18 p In JAPANESE; ENGLISH summary
(DE88-755231; JAERI-M-88-136) Avail: NTIS (US Sales Only) HC A03/MF A01

Creep tests and measurements of internal stress during creep and activation energy for creep were performed at 900 C for Hastelloy XR and XR-II developed as heat resistant alloys for high temperature gas cooled reactors. Creep rupture time and steady-state creep rate were influenced by the parameters of boron content, grain size and heat treatment temperature of the alloys. Although the internal stress during creep was also dependent on these parameters, the activation energy for creep was independent of them. It is shown that dependence of the steady-state creep rate on the parameters corresponds to the change in the internal stress. The fact shows the concept of the internal stress is effective to describe steady-state creep behavior of the alloys. DOE

N89-16970# California Univ., Santa Barbara. Dept. of Chemical and Nuclear Engineering.
KINETICS AND MECHANISMS OF HYDROGEN ATTACK IN 2.25Cr-1Mo STEEL
B. L. Chao, G. R. Odette, and G. E. Lucas Aug. 1988 294 p Prepared for Oak Ridge National Lab., TN
(Contract DE-AC05-84OR-21400)
(DE89-001381; ORNL/Sub-82-22276/01) Avail: NTIS HC A13/MF A01

It is the purpose of this study to understand the kinetics and mechanisms of the hydrogen attack process in a 2.25Cr-1Mo steel which is a candidate for the pressure vessel material for the coal liquefaction process. An SA387-G22-C2 2.25Cr-1Mo steel together with its heat affected zone and weld sections were used as the material for studying the kinetics and mechanisms of HA. These materials were exposed to 490 to 585 C and 16.2 to 20.7MPa hydrogen pressure for up to 9000 hours. The same materials were exposed to thermal control conditions (490 to 585 C and 0.35MPa helium) so that the difference in volume swelling and mechanical property change is defined as the net effect due to hydrogen alone. Tensile, Charpy impact, and creep/creep rupture properties were evaluated as a function of hydrogen damage. X-ray diffraction and transmission/analytical electron microscopy (TEM/AEM) techniques were used to study the carbide species and their chemical compositions. A two-stage replication/TEM technique was used to study the distribution and growth of methane cavities. Based on the concept of pre-existing cavities and a constrained cavity growth mechanism, a mathematical model is developed and calibrated with experimentally measured parameters. This model is used to predict the material response to temperatures and hydrogen pressures not tested in this study. DOE

N89-16971# California Univ., Berkeley. Dept. of Physics.
ELECTRONIC BEHAVIOR OF HIGHLY CORRELATED METALS Ph.D. Thesis
Ariel Reich Oct. 1988 120 p Prepared in cooperation with California Univ., Berkeley. Lawrence Berkeley Lab.
(Contract DE-AC03-76SF-00098)
(DE89-002492; LBL-26091) Avail: NTIS HC A06/MF A01

The question of the strongly interacting many-body problem ia addressed, i.e., systems where the interparticle correlations are so strong as to defy perturbative approaches. These subtle correlations occur in narrow band materials, such as the lanthanides and actinides, wherein the f-electrons are so localized that a variety of new phenomena, including intermediate-valence and heavy-fermionic behavior, may occur. As well, one has the alloying problem, where local interactions are paramount in determining the overall behavior. The technique employed in dealing with these systems is the Small Cluster method, wherein the full many-body Hamiltonian for a small grouping of atoms, coupled with periodic boundary conditions, is solved exactly. This is tantamount to solving a bulk crystal at the high points of symmetry in the Brillouin Zone. The mathematical overhead is further reduced by employing the full space group and spin symmetries. By its very nature, the Small Cluster method is well able to handle short-range interactions, as well as the combinatorial complexity of the many-body problem, on an equal footing. The nature of long-range order and phase transition behavior cannot be incorporated, but sometimes clues as to their origin can be discerned. The calculations presented include: a two-band Anderson model for an intermediate-valence system, wherein photoemission and fluctuation behavior is examined; a single-band Hubbard model for a ternary alloy system, such as copper-silver-gold; and a Hubbard model for a heavy-fermion system, wherein Fermi surface, transport, magnetic and superconducting properties are discussed. DOE

N89-16972# Sandia National Labs., Albuquerque, NM. Process Metallurgy Div.
THE EFFECT OF CHEMISTRY MODIFICATIONS ON THE SOLIDIFICATION BEHAVIOR AND WELDABILITY OF ALLOY 625
M. J. Cieslak 1988 7 p Presented at the JOWOG 22D Joining Subgroup, Aldermasten, England, 4 Oct. 1988
(Contract DE-AC04-76DP-00789)
(DE89-001046; SAND-88-0936C; CONF-8810176-1) Avail: NTIS HC A02/MF A01

The purpose of this study was to examine the effect of chemistry

variations on the solidification behavior and weldability of Alloy 625. As the effect of several tramp elements (i.e., S, P, etc.) could be predicted a priori, the experimental alloy design excluded these elements as factors. A 3-factor, 2-level, full fractorial experimental design was examined with the elements Nb(0 wt percent, 3.5 wt percent), C(0.005 wt. percent, 0.035 wt. percent), and Si(0.01 wt. percent, 0.40 wt. percent) being chosen to fill the design matrix. Compositions of the alloys studied are listed. These compositions were prepared using VIM/VAR techniques in the Sandia National Laboratories Melting and Solidification Facility. Conventional hot and cold working techniques were used to produce 3 mm thick sheet for Varestraint weldability testing. Differential thermal analysis (DTA) was used to establish significant solidification temperatures and reactions. Greater experimental detail has been given previously. DOE

N89-16973# State Univ. of New York, Buffalo. Dept. of Chemistry.
MOLECULAR SPECTROSCOPY AT CORRUGATED METAL SURFACES
P. T. Leung and Thomas F. George Oct. 1988 31 p
(Contract N00014-86-K-0043)
(AD-A200124; UBUFFALO/DC/88/TR-84) Avail: NTIS HC A03/MF A01 CSCL 07B

Spectroscopic properties for molecules in the vicinity of metal surfaces are usually determined by the energy transfer mechanisms between the molecules and the substrate, which can involve various collective excitations of the substrate electrons such as surface plasmons and excitons. A brief review of this subject, including various phenomena such as fluorescence and photoabsorption lineshapes, is presented. The review includes recent work of the authors, with emphasis on the effects due to surface corrugations. Examples which illustrate possible applications of such studies in the areas of surface photochemistry and heterogeneous catalysis are also discussed. GRA

N89-16974# State Univ. of New York at Buffalo, Amherst. Dept. of Chemistry.
EFFECT OF FINITE SIZE ON MAGNETORESISTANCE
H. R. Lee, H. G. Oh, and Thomas F. George Oct. 1988 11 p Submitted for publication
(Contract N00014-86-K-0043)
(AD-A200267; UBUFFALO/DC/88/TR-86) Avail: NTIS HC A03/MF A01 CSCL 20C

Finite size effects are studied for magnetoresistance in a disordered metallic system. Quantum corrections to the conductivity are strongly affected by the presence of an in-plane magnetic field in a thin film. They are also affected significantly by the boundaries of the finite quantum size. Expressions are obtained for the quantum correction to the conductivity due to both effects. The dephasing characteristic time scale due to the magnetic field is found by the exact eigenvalues of the system. One-, two- and three-dimensional results can be obtained with the proper limits. Some numerical results are presented for the given inelastic scattering length. GRA

N89-16975# Naval Postgraduate School, Monterey, CA.
PROCESSING OF 2090 ALUMINUM ALLOY FOR SUPERPLASTICITY M.S. Thesis
Henry C. Regis Jun. 1988 71 p
(AD-A200425) Avail: NTIS HC A04/MF A01 CSCL 11F

The applicability of a thermomechanical process, involving warm rolling to facilitate continuous recrystallization (CRX), to aluminum alloy 2090 was considered. The thermomechanical process has been shown to result in 2 to 5 mm grains and superplasticity at 300 C in Al-Mg and Al-Mg-Li alloys. In this study, the warm rolling temperature and the reheating time between consecutive rolling passes were varied. Superplastic ductility of 320 percent was obtained during tension testing at 350 C. Microstructural analysis of the structures produced during warm rolling indicates inadequate interaction between precipitating phases and dislocation structures. Thus, improved warm-temperature superplastic ductility may be obtained by initial precipitation treatments followed by warm rolling. GRA

N89-16976# Notre Dame Univ., IN. Dept. of Materials Science and Engineering.
MICROSTRUCTURAL EFFECTS IN ABRASIVE WEAR Final Report, 15 Sep. 1981 - 14 Mar. 1986
T. H. Kosel Mar. 1988 37 p
(Contract DE-AC02-81ER-10963)
(DE89-003032; DOE/ER-10963/8) Avail: NTIS HC A03/MF A01

This report summarizes research performed on abrasion of metallic alloys. The work was designed to improve our understanding of the factors affecting abrasion rates in two-phase alloys containing large, hard second-phase particles (SPPs) such as carbides, since this class of alloys generally has very high abrasion resistance owing to the presence of such carbides. The project was divided into sections dealing with material removal in the carbide and matrix phases. The materials studied included Stellite and high Cr-Mo white cast irons and a set of specially prepared model alloys containing one of six types of artificial SPPs dispersed in a sintered matrix of pure Cu. Scratch tests were employed to simulate abrasion mechanisms, and specially designed scratch test systems were fabricated to permit scratch testing in-situ in the scanning electron microscope (SEM) and to permit scratches to be made at fixed depths of cut rather than fixed loads. Three types of abrasion tests were employed; a dry-sand rubber wheel abrasion test; a low-speed gouging abrasion test employing a special low-speed Al2O3 grinding wheel; and a pin-on-disc abrasion test using abrasive paper. Abrasive type and size was varied in the rubber wheel and the pin-on-disc tests. DOE

N89-16977# Oak Ridge National Lab., TN.
THE ELECTRONIC STRUCTURE AND THE STATE OF COMPOSITIONAL ORDER IN METALLIC ALLOYS
B. L. Gyorffy, D. D. Johnson, F. J. Pinski (Cincinnati Univ., OH.), D. M. Nicholson, and G. M. Stocks 1987 49 p Presented at the NATO Advanced Study Inst. on Alloy Phase Stability, Crete, Greece, 14-17 Jun. 1987
(Contract DE-AC05-84OR-21400)
(DE89-003147; CONF-8706103-11) Avail: NTIS HC A03/MF A01

Many two-component (A,B) systems crystallize into a random solid solution. In such a state the atoms occupy a more or less regular array of lattice sites but each site can be A or B in a random fashion. Then, on lowering the temperature, the system will either phase separate or order, starting at some transition temperature T sub c. The aim of these lectures is to present a microscopic approach to the understanding of these scientifically interesting and technologically important processes. DOE

N89-16978# Allied-Signal Aerospace Co., Kansas City, MO.
ANALYSIS OF LOW ALLOY AND STAINLESS STEELS BY INDUCTIVELY COUPLED ARGON PLASMA SPECTROMETER Final Report
H. Reimer Nov. 1988 11 p
(Contract DE-AC04-76DP-00613)
(DE89-003227; KCP-613-4032) Avail: NTIS HC A03/MF A01

Eleven elements in low alloy and stainless steels were analyzed using separate sampling and excitation analysis (SSEA). This solid sampling device is used in conjunction with an inductively coupled argon plasma (ICAP) optical emission spectrometer. Samples are eroded by a controlled spark, and the metal aerosol caused by the erosion is swept into an argon plasma to be excited. This short study was undertaken to provide an alternate method of analysis in case of instrument failure during the usual procedure employed in the laboratory. Accuracy and precision studies also were performed. Precision was determined by analyzing the same sample 11 times. Five certified standards used as samples were analyzed to determine accuracy. The precision and confidence intervals were calculated. The precision as percent relative standard

deviation ranged from 8.4 percent for aluminum at a concentration of 0.008 percent to 0.48 percent at 27 percent for chromium. DOE

N89-16979# Oak Ridge National Lab., TN.
PROCUREMENT AND SCREENING TEST DATA FOR ADVANCED AUSTENITIC ALLOYS FOR 650 C STEAM SERVICE, PART 2 Final Report
R. W. Swindeman, G. M. Goodwin, P. J. Maziasz, and E. Bolling Aug. 1988 61 p
(Contract DE-AC05-84OR-21400)
(DE89-001331; ORNL/TM-10206/P2) Avail: NTIS HC A04/MF A01

The results of screening tests on alloys from three compositional groups are summarized and compared to the alloy design and performance criteria identified as needed for austenitic alloys suitable as superheater/reheater tubing in advanced heat recovery systems. The three alloy groups included lean (nominally 14 percent Cr and 16 percent Ni) austenitic stainless steels that were modifications of type 316 stainless steel, 20Cr-30Ni-Fe alloys that were modifications of alloy 800H, and Ni-Cr aluminides, (Ni,Cr)3Al. The screening tests covered fabricability, mechanical properties, weldability, and oxidation behavior. The lean stainless steels were found to possess excellent strength and ductility if cold-worked to an equivalent strain in the range 5 to 10 percent prior to testing. However, they possessed marginal weldability, poor oxidation resistance, and sensitivity to aging. The modified alloy 800H alloys also exhibited good strength and ductility in the cold-worked condition. The weldability was marginal, while the oxidation resistance was good. The aluminides were difficult to fabricate by methods typically used to produce superheater tubing alloys. The alloys that could be worked had marginal strength and ductility. An aluminide cast alloy, however, was found to be very strong and ductile. DOE

N89-16980 ESDU International Ltd., London (England).
SELECTION OF ALLOYS FOR HYDRODYNAMIC BEARINGS
Oct. 1988 26 p
(ESDU-88018; ISBN-0-85679-650-6; ISSN-0141-2590) Avail: ESDU

This Data Item 88018, an addition to the Sub-series on Tribology, provides a selection procedure for alloys for bearings operating in the hydrodynamic lubrication regime and only experiencing boundary lubrication at start-up or run-down or in unusual circumstances. The alloys treated are those used in industrial machinery (such as turbines, electric motors, marine gear boxes, rolling mills, gear pumps, hydraulic motors, low and medium speed diesels, and reciprocating compressors and pumps). The various alloys are identified and their available forms (for example, solid or thick- or thin-walled) are tabulated. A selection procedure identifies the alloy providing the best tribological properties while meeting the required loads at the expected working temperature. The chosen alloys, is then further studied to ensure it meets the need to avoid bearing failure due to embedded particles, incompatibility with the counterface and hence wear, mechanical stress and fatigue, elevated temperature and corrosion. ESDU

N89-16981 ESDU International Ltd., London (England).
EFFECT OF FRETTING ON FATIGUE STRENGTH OF TITANIUM ALLOYS
Nov. 1988 53 p
(ESDU-88027; ISBN-0-85679-659-X; ISSN-0141-4089; ISSN-0141-3996) Avail: ESDU

This Data Item 88027, an addition to the Sub-series on Stress and Strength and on Fatigue-Endurance Data, plots as stress versus endurance the results extracted from the literature of over 400 fretting fatigue tests carried out on five alloys. The results allow the detrimental effect of fretting and the effect of clamping pressure to be determined. Most of the tests were made in a normal temperature air environment, but the effect of salt water and elevated temperature is also shown. The effect of various surface coatings and treatments is presented so that their relative performance can be compared. The curves appear on 21 graphs, each accompanied by a table containing such information as the alloy composition, treatments applied, test arrangements and alloy tensile strength and proof stress. ESDU

N89-16982# Sandia National Labs., Albuquerque, NM.
TRIBOLOGY OF AMORPHOUS ALLOYS FORMED WITH ION BEAMS
D. M. Follstaedt, J. A. Knapp, and L. E. Pope 1988 23 p Presented at the Fall Meeting of the Materials Research Society, Boston, MA, 28 Nov. 1988
(Contract DE-AC04-76DP-00789)
(DE89-003274; SAND-88-1534C; CONF-881155-9) Avail: NTIS HC A03/MF A01

The changes in friction and wear properties (i.e., tribology) of steels due to thin surface alloys formed by ions beams are surveyed, and considered in light of their microstructure. Amorphous alloys containing both Ti and C are found to give superior performance in comparison to alloys with N, B, C, P or Ti. All the amorphous layers reduce friction, but the duration of benefits and wear resistance at high loads vary with composition. By examining similar amorphous alloys with Ti alone or C alone, the critical roles played by each in resisting wear are demonstrated. Amorphous alloys with Ti and C appear to be quite hard. DOE

N89-16983# Brookhaven National Lab., Upton, NY.
GLANCING ANGLE EXAFS STUDIES OF Cu-Al THIN FILM INTERFACES
H. Chen and S. M. Heald 1988 3 p Presented at the 5th International Conference on X-ray Absorption Fine Structure, Seattle, WA, 21 Aug. 1988
(Contracts DE-AC02-76CH-00016; DE-AS05-80ER-10742)
(DE89-003614; BNL-41815; CONF-8808149-5) Avail: NTIS HC A02/MF A01

The glancing angle EXAFS technique has been employed to study the initial reactions on Cu-Al thin film interfaces. Samples prepared under UHV and non-UHV conditions are compared. Preliminary data indicate that the UHV prepared interface has a larger amount of initial reaction than the non-UHV one. When annealed at 160 C, the resulting compound formation at the interfaces of the two samples are different. DOE

N89-16984# Argonne National Lab., IL. Materials and Components Technology Div.
NITRIDE AND CARBIDE COATINGS FOR HIGH SPEED STEEL CUTTING TOOLS
George R. Fenske 1988 22 p Presented at the Tribology Conference, Baltimore, MD, 16 Oct. 1988
(Contract W-31-109-eng-38)
(DE89-003623; CONF-8810213-1) Avail: NTIS HC A03/MF A01

Hard nitride and carbide coatings of Ti, Zr, and Hf were deposited by physical vapor deposition processes on high-speed steel cutting tools to determine their effectiveness in improving the wear properties of the inserts and increasing cutting-tool performance. A collaborative research program involving industrial, university, and government laboratories was established to develop coating processes and tool wear models, to characterize the coating properties and the effect of process parameters on the coating properties, and to evaluate the cutting performance of coated inserts. Two coating processes were selected for investigation: high-rate reactive sputtering and activated reactive evaporation. The lifetimes of coated inserts were extended 2 to 10 times, depending on the coating composition and process. Analysis of the wear modes that occurred during the cutting tests indicated that the coatings failed by fracture after plastic deformation of the underlying substrate occurred as a result of substrate softening at the high cutting speeds. DOE

N89-16985# Delaware Univ., Newark.
SELECTIVITY OF THE REACTIONS OF OXYGENATES ON TRANSITION METAL SURFACES Progress Report, 15 Dec. 1987 - 14 Dec. 1988
Mark A. Barteau 1988 5 p

(Contract DE-FG02-84ER-13290)
(DE89-003691; DOE/ER-13290/4) Avail: NTIS HC A02/MF A01

The goal of this research has been to understand, by means of surface science studies, the elementary processes involved in the synthesis of methanol and higher alcohols on transition metals, and the dependence of these processes upon the nature of the surface. To date we have completed TPD and HREELS studies of methanol, formaldehyde, formic acid, methyl formate, ethanol, acetaldehyde, acetic acid, 1-propanol, propanal, propionic acid, 2-propanol, acetone, allyl alcohol, acrolein, acrylic acid, and propylene on clean and oxygen-dosed Pd(111) surfaces. We have completed TPD, HREELS, and XPS studies of methanol, formaldehyde, and formic acid on clean and oxygen-dosed Rh(111) surfaces. DOE

N89-16986*# National Aeronautics and Space Administration. Lewis Research Center, Cleveland, OH.
REFRACTORY METAL ALLOYS AND COMPOSITES FOR SPACE NUCLEAR POWER SYSTEMS Final Report
Robert H. Titran, Joseph R. Stephens, and Donald W. Petrasek Sep. 1988 24 p Presented at the Metallurgical Society Fall Meeting, Chicago, IL, 27-29 Sep. 1988; sponsored in part by the Metallurgical Society of AIME and the American Society for Metals
(Contract DE-AI03-86SF-16310)
(NASA-TM-101364; E-4398; DOE/NASA/16310-8; NAS 1.15:101364) Avail: NTIS HC A03/MF A01 CSCL 11F

Space power requirements for future NASA and other U.S. missions will range from a few kilowatts to megawatts of electricity. Maximum efficiency is a key goal of any power system in order to minimize weight and size so that the Space Shuttle may be used a minimum number of times to put the power supply into orbit. Nuclear power has been identified as the primary power source to meet these high levels of electrical demand. One method to achieve maximum efficiency is to operate the power supply, energy conservation system, and related components at relatively high temperatures. For systems now in the planning stages, design temperatures range from 1300 K for the immediate future to as high as 1700 K for the advanced systems. NASA Lewis Research Center has undertaken a research program on advanced technology of refractory metal alloys and composites that will provide baseline information for space power systems in the 1900's and the 21st century. Special emphasis is focused on the refractory metal alloys of niobium and on the refractory metal composites which utilize tungsten alloy wires for reinforcement. Basic research on the creep and creep-rupture properties of wires, matrices, and composites are discussed. Author

N89-16987# Gosudarstvennyi Komitet po Ispolzovaniyu Atomnoi Energii, Moscow (USSR).
FRACTURE MODE OF METALS IN HEAVY ELECTRIC FIELDS
S. V. Zajtsev and A. L. Suvorov 1987 16 p In RUSSIAN
(DE88-704818; ITEF-154(1987)) Avail: NTIS (US Sales Only) HC A03/MF A01

Investigation into the character and micromechanism of fracture of point samples of refractory metals under strong electric field effect is conducted using auto-ion microscopy method. Fracture electric strain-finite point sample diameter (tungsten, molybdenum and some alloys: W-5 percent Re, W-1.5 percent ThO(sub 2) dependence as well as the shape (and microstructure) of fracture surface are studied. Based on analyzing the dependence of destructive potential-diameter at the point apex, the form and microstructure of fracture surface, a conclusion is drawn that the micromechanism of the given phenomenon consists in the melting of a thin presurface metal layer, its partial removal by means of electrical field and subsequent amorphization at the expense of fast cooling. The results obtained may be used when developing methods for increasing electrical device resistance to the action of strong electrical field. DOE

N89-16988# Oak Ridge National Lab., TN.
OXIDATION OF Ni3Al BELOW 850 C AND ITS EFFECT ON FRACTURE BEHAVIOR
J. H. DeVan and C. A. Hippsley (United Kingdom Atomic Energy Authority, Harwell, England) 1988 14 p Presented at the Workshop on the Oxidation of High-Temperature Intermetallics, Cleveland, OH, 20 Sep. 1988
(Contract DE-AC05-84OR-21400)
(DE89-002232; CONF-8809190-1) Avail: NTIS HC A03/MF A01

Studies were conducted to establish the oxidation kinetics and reaction products associated with exposure of Ni3Al to air at intermediate temperatures. A significant finding was the susceptibility of Ni3Al to internal oxidation at 600 to 825 C. Since oxygen embrittlement of Ni3Al is observed in the same temperature range, crack growth studies were subsequently conducted to examine a possible connection between the embrittlement and internal oxidation processes. Chemical analyses of the near-crack-tip region showed a periodicity in surface oxidation products symptomatic of a stepwise crack propagation process. A kinetic model is proposed in which oxygen diffuses along the grain boundary in front of a stationary crack tip until a critical oxygen inventory is achieved. The crack jumps forward by a small increment (approx 0.5 microns), and the process repeats. Surface analytical chemistry results and an Arrhenius analysis of crack rate vs temperature are presented as evidence for the proposed cracking model. DOE

N89-16989# Brookhaven National Lab., Upton, NY.
EXPERIMENTAL EVIDENCE FOR POSITRON TRAPPING AT DISLOCATIONS IN Ni3Al ALLOYS
S. G. Usmar and K. G. Lynn 1988 3 p Presented at the 8th International Conference on Positron Annihilation, Gent, Belgium, 29 Aug. 1988
(Contract DE-AC02-76CH-00016)
(DE89-004520; BNL-41322; CONF-8808122-13) Avail: NTIS HC A02/MF A01

Cold worked Ni3Al alloys were studied using positron lifetime spectroscopy. The isochronal annealing curves of Ni76Al24 + 0 and 500 at. ppM B were measured. In pure Ni76Al24 three annealing stages were identified while in the boron doped alloy only two were identified. Vacancy annealing (stage 3) was found to start at approximately 250 C in reasonable agreement with previously published data for both alloys. The high temperature annealing stage in boron doped Ni76Al24 starts between 750 and 800 C and is complete at 1000 C. This stage was attributed to migration of dislocations to various sinks. In pure Ni76Al24 the intermediate and high temperature annealing stages occur at 750 to 800 and 1050 C, respectively. These stages were attributed to the migration of dislocations (750 to 800 C) and recrystallization (approximately 1050 C). The nature of the dislocation trap will be discussed. DOE

N89-16990# Oregon Graduate Center for Study and Research, Beaverton.
QUANTITATIVE MEASUREMENT AND MODELING OF SENSITIZATION DEVELOPMENT IN STAINLESS STEELS
S. M. Bruemmer 1988 282 p
(Contract DE-AC06-86NE-37963)
(DE89-004646; DOE/NE-37963/7) Avail: NTIS HC A13/MF A01

The current state-of-the-art to quantitatively measure and model sensitization development in austenitic stainless steels is assessed and critically analyzed. A modeling capability is evolved and validated using a diverse experimental data base. Quantitative predictions are demonstrated for simple and complex thermal and thermomechanical treatments. Commercial stainless steel heats ranging from high-carbon Type 304 and 316 to low-carbon Type 304L and 316L have been examined including many heats which correspond to extra-low-carbon, nuclear-grade compositions. Within certain limits the electrochemical potentiokinetic reactivation (EPR) test was found to give accurate and reproducible measurements of the degree of sensitization (DOS) in Type 304 and 316 stainless

steels. EPR test results are used to develop the quantitative data base and evolve/validate the quantitative modeling capability. This thesis represents a first step to evolve methods for the quantitative assessment of structural reliability in stainless steel components and weldments. Assessments will be based on component-specific information concerning material characteristics, fabrication history and service exposure. DOE

N89-17282# Fraunhofer-Inst. fuer Betriebsfestigkeit, Darmstadt (Germany, F.R.).
FRETTING CORROSION FATIGUE [ERMUEDUNGSFESTIGKEIT BEI REIBKORROSION]
G. Fischer *In its* Papers of the 5th LBF Colloquium 1988 p 185-194 In GERMAN (For primary document see N89-17272 09-39)
Avail: NTIS HC A12/MF A01

N89-17324*# Cincinnati Univ., OH.
ANISOTROPIC CONSTITUTIVE MODELING FOR NICKEL BASE SINGLE CRYSTAL SUPERALLOY RENE N4 AT 982 C
D. C. Stouffer, N. Jayaraman, M. Y. Sheh, and D. Alden *In* NASA, Lewis Research Center, Turbine Engine Hot Section Technology, 1987 Oct. 1987 p 289-298 (For primary document see N89-17298 09-39)
Avail: NTIS HC A20/MF A01 CSCL 11F

N89-17325*# Engineering Science Software, Inc., Smithfield, RI.
CONSTITUTIVE MODELLING OF SINGLE CRYSTAL AND DIRECTIONALLY SOLIDIFIED SUPERALLOYS
Kevin P. Walker and Eric H. Jordan (Connecticut Univ., Storrs.) *In* NASA, Lewis Research Center, Turbine Engine Hot Section Technology, 1987 Oct. 1987 p 299-301 (For primary document see N89-17298 09-39)
(Grant NAG3-512)
Avail: NTIS HC A20/MF A01 CSCL 11F

27 NONMETALLIC MATERIALS

Includes physical, chemical, and mechanical properties of plastics, elastomers, lubricants, polymers, textiles, adhesives, and ceramic materials.

For composite materials see *24 Composite Materials.*

N89-16991 New South Wales Univ., Kensington (Australia). School of Chemical Engineering and Industrial Chemistry.
PROPERTIES AND PERFORMANCE OF POLYAMIDE MEMBRANES M.S. Thesis
Chen-Wu Yao Jan. 1988 3 p
Avail: Issuing Activity

The transport behavior of polymeric membranes is dependent upon their chemical composition and morphological structure. Modification of these factors can produce membranes with unique and useful transport properties. Polyamide 6 ultrafiltration (UF) membranes were prepared from a low-cost protic solvent and produced by the phase inversion process. These membranes were found to have low macromolecule rejection and low water fluxes due to their limited surface porosity and sponge-structured sublayer. Two methods of structural modification were examined to improve these properties: (1) relating to hydrolysis phenomena in the acidic casting solution, and (2) relating to the physico-chemical coagulation processes during membrane formation. These processes are discussed in detail. Author

N89-16992# Office of Naval Research, London (England).
ENGINEERING MATERIALS FOR VERY HIGH TEMPERATURES: AN ORNL WORKSHOP
Louis Cartz 1988 79 p Workshop held in Coventry, United Kingdom, 29 Aug. 1988
(ORNL-8-016-R) Avail: NTIS HC A05/MF A01

The limitations of present-day materials at high temperatures are reviewed. Silicon nitride based ceramics, silicon carbide, and carbon materials are discussed. Near-term and long-term studies are described to improve the performance at temperatures above 1400 C of monolithic ceramics, composites, and ceramic coatings. For individual titles, see N89-16993 through N89-16999.

N89-16993# Warwick Univ. Coventry (England). Centre for Advanced Materials Technology.
MICROSTRUCTURE OF HIGH-TEMPERATURE CERAMICS
M. H. Lewis *In* Office of Naval Research, Engineering Materials for Very High Temperatures. An ORNL Workshop 1988 p 2-12 (For primary document see N89-16992 09-27)
Avail: NTIS HC A05/MF A01

After more than a decade of intense activity in development of monolithic ceramics, they have limited application as engineering components at elevated temperatures. There is now a good understanding of deformation and fracture mechanisms and hence of the principles for design of ideal microstructures. This is rarely achievable in practice due to the conflicting requirement for ease of fabrication or the inability to tailor the geometrical or chemical characteristics of microstructure via natural reactions during sintering. The artificially produced microstructure of the ceramic composite is an alternative. High temperature properties of these varied microstructures are surveyed. Author

N89-16994# Office National d'Etudes et de Recherches Aeronautiques, Paris (France). Materials Dept.
CERAMIC-CERAMIC COMPOSITES FOR USE AT HIGH TEMPERATURE **c24**
J. F. Jamet *In* Office of Naval Research, Engineering Materials for Very High Temperatures. An ORNL Workshop 1988 p 13-25 (For primary document see N89-16992 09-27)
Avail: NTIS HC A05/MF A01

Ceramic-ceramic (C-C) composites can be used beyond 1600 C with efficient protection. Silicon compound protective systems have made great strides and this special class of C-C composites remains a very promising one. Nevertheless, beyond 1600 C in low pressure and dissociated environments, SiC composites have to be investigated in more detail. SiC Nicalon for long fibers and Si whiskers are the main ceramic reinforcements successfully used to date with various ceramic matrices. The first may be used up to 1350 C if its protection is insured. The second is very attractive for higher temperatures, and especially hot spots of engines. Fiber suppliers have recognized the need for more refractory products and are working toward improving them. Below 1000 C, ceramic composites are in progress and reinforced glass-ceramic composites presently show the most advantages in this range. Author

N89-16995# Technische Hogeschool, Eindhoven (Netherlands). Dept. of Physical Chemistry.
DEVELOPMENT OF COMPOSITE HIGH TEMPERATURE MATERIALS FOR FUTURE ENERGY CONVERSION APPLICATIONS **c24**
R. Metselaar and L. R. Wolff *In* Office of Naval Research, Engineering Materials for Very High Temperatures. An ORNL Workshop 1988 p 27-34 (For primary document see N89-16992 09-27)
Avail: NTIS HC A05/MF A01

At high temperatures monolithic materials can no longer fulfill all requirements posed by advanced energy conversion applications. It is shown how diffusion couples can be used to study metal-ceramic interactions and to develop composite materials. Attention is paid to the development of a hot shell for a combustion heated thermionic energy converter operating at 1450 C. It is shown how the combination of chemical and physical requirements leads to the design of a trilayer material consisting of a W emitter coated with a diffusion barrier of TiN and an outer protective shell of SiC. Author

N89-16996# Rolls-Royce Ltd., Derby (England). Non-Metal and Composite Manufacturing Technology.
LIMITATIONS AT HIGH TEMPERATURES OF PRESENT DAY ENGINEERING MATERIALS **c07**
G. W. Meetham *In* Office of Naval Research, Engineering

Materials for Very High Temperatures. An ORNL Workshop 1988 p 35-42 (For primary document see N89-16992 09-27)
Avail: NTIS HC A05/MF A01

The developments which have led to the current materials scene are discussed. Future requirements which cannot be met by current materials are highlighted. The discussion centers around three major engine components - turbine airfoils, discs and combustors. Author

N89-16997# Swedish Inst. for Silicate Research, Gotheborg.
THE SHAPING OF STRUCTURAL ENGINEERING CERAMICS
R. Carlsson *In* Office of Naval Research, Engineering Materials for Very High Temperatures. An ORNL Workshop 1988 p 43-51 (For primary document see N89-16992 09-27)
Avail: NTIS HC A05/MF A01

The main shape-forming methods for engineering ceramics, particularly for components of complicated shape, are compared with respect to technical and economical advantages and disadvantages. Different development trends are presented. Hot isostatic pressing (HIP) using the glass encapsulation technique offers a good way to avoid nonuniform deformation during sintering; this is important for complicated shapes. Combined efforts in these areas have made possible the development of a vehicle gas turbine rotor in HIP-ed silicon nitride. Some details of the performance of this component are given. Author

N89-16998# Army Materials Technology Lab., Watertown, MA.
TIME AND TEMPERATURE DEPENDENCE OF STRENGTH IN HIGH PERFORMANCE CERAMICS
R. N. Katz, G. D. Quinn, M. J. Slavin, and J. J. Swab *In* Office of Naval Research, Engineering Materials for Very High Temperatures. An ORNL Workshop 1988 p 53-62 (For primary document see N89-16992 09-27)
Avail: NTIS HC A05/MF A01

A hierarchical approach to time-temperature-strength evaluation based on stepped temperature stress rupture (STSR) testing, stress rupture (SR) testing, and the development of fracture mechanism maps are presented. Utilization of this hierarchical philosophy is illustrated with examples of data from materials at different levels of maturity, i.e., hot-pressed silicon nitride, Y-TZP, and toughened Al2O3. Author

N89-16999# Popper (P.), Newcastle-under-Lyme (England).
ENGINEERING CERAMICS IN WEST GERMANY
P. Popper *In* Office of Naval Research, Engineering Materials for Very High Temperatures. An ORNL Workshop 1988 p 63-68 (For primary document see N89-16992 09-27)
Avail: NTIS HC A05/MF A01

The development of engineering ceramics in the Federal Republic of Germany is described by stating the objectives and considering the achievements of three projects: ceramic components for vehicular gas turbines, a follow-on study with the stress on improving reproducibility and reliability and extension to other engines, and high performance structural ceramics. Author

N89-17000# Army Armament Research, Development and Engineering Center, Picatinny Arsenal, NJ. Armament Engineering Directorate.
PRESSURE/TEMPERATURE SENSITIVE INORGANIC PHOSPHORS Technical Report, Sep. 1987 - Feb. 1988
William O. Seals, Henry W. Offen, W. Dale Turley, and Henry M. Borella (EG and G Energy Measurements, Inc., Santa Barbara, CA.) Sep. 1988 27 p
(AD-A199716; ARAED-TR-88017) Avail: NTIS HC A03/MF A01 CSCL 07B

A class of inorganic phosphors, such as rare earth doped lanthinum oxy-sulfide and Yttrium oxy-sulfide, show spectral emission characteristics that are strongly pressure and temperature dependent. The relative intensity of the emission lines and the fluorescence decay time have indicated strong pressure dependence in the range of several kilobars. This property suggests that these inorganic phosphors could be applied as remotely operated pressure transducers. The intensity of the emissions has also been observed to show strong dependency upon temperature. Kistler gauges are presently used to monitor pressures. Prior vulnerability studies indicated that hydraulic pressures in excess of 100,000 psi were experienced when one gallon of stored liquid propellant was impacted by a shaped charge. These pressures exceed the upper limit of the Kistler gauges. In field use, large quantities will be housed in an armored or self-propelled howitzer. It is critical to measure the pressures developed in these larger quantities of stored propellant when impacted by a battlefield threat. The potential for using organic phosphors to measure high pressures and temperatures are discussed. GRA

N89-17001# Academy of Sciences of the Uzbek SSR, Tashkent.
ELECTRIC CONDUCTIVITY OF POLYMER COMPOSITE MATERIALS. COMPOSITE ON PROPYLENE AND SILICON BASE
K. K. Ametov, B. Kaipov, S. M. Zholdasova, A. G. Lavrushko, N. M. Galashina, B. S. Yakovlev, E. I. Ismatov, and A. M. Gamretskaya 1987 9 p In RUSSIAN; ENGLISH summary
(DE88-704293; IYF-R-9-308) Avail: NTIS (US Sales Only) HC A02/MF A01

Electric conductivity in polymer composites of the polypropylene-silicon type prepared by the method of polymerization filling is studied. The four-probe method is used to plot the dependence of electric resistance on silicon content and temperature in the 160 to 300 K range. The conclusion is made that the current value in composite is limited by resistance of insulating layers. DOE

N89-17002# Tennessee Univ., Knoxville. Dept. of Chemistry.
STATISTICAL MECHANICS OF POLYMER SYSTEMS Final Report
Jeffrey Kovac 15 Feb. 1988 13 p
(Contract DE-FG05-84ER-45114)
(DE89-002012; DOE/ER-45114/4) Avail: NTIS HC A03/MF A01

We have made major progress in the development of computer simulation methods for the study of lattice models of polymer chains and have applied those methods to several problems of current interest. Much of our effort has gone into development and testing of the models in order to be sure that the results are physically meaningful and not artifacts of the lattice model. In addition, we have expanded the scope of dynamic Monte Carlo lattice models by including a nearest neighbor interaction energy. This allows us to study solvent and temperature effects on the chain dynamics. The three major problems that we have studied include the motion of chains in dense systems and the validity of the model, the dynamics of chains in the theta region, and the dynamics of collasping polymer chains. DOE

N89-17003# Sandia National Labs., Albuquerque, NM.
PHOTODEFLECTION AND PHOTOCONDUCTIVITY STUDIES IN CERAMICS
C. H. Seager 1988 13 p Presented at the 41st Pacific Coast Regional Meet of American Ceramic Society, San Francisco, CA, 24 Oct. 1988
(Contract DE-AC04-76DP-00789)
(DE89-002186; SAND-88-2864C; CONF-8810195-3) Avail: NTIS HC A03/MF A01

Sensitive calorimetric techniques such as photothermal deflection spectroscopy (PDS) offer many advantages over conventional transmission spectroscopy for measuring the optical properties of ceramics. Insensitivity to light scattering is of particular importance for optical studies of these materials. The physics of the PDS method will be briefly reviewed as well as the experimental arrangement necessary to carry out sensitive (3 to 5 ppM) determinations of absorptance on ceramic specimens over a wide range of photon energies. Examples will be given of PDS studies on PLZT and doped ZnO ceramics. In the latter case coupled PDS/photoconductivity measurements have given new insights into the role of impurities added to optimize the electronic properties of ZnO varistors. DOE

N89-17004# Arizona Univ., Tucson.
CERAMICS DERIVED FROM ORGANO-METALLIC POLYMERS Final Technical Report, 1 Dec. 1986 - 30 Nov. 1987
D. R. Uhlmann Jul. 1988 20 p
(Grant AF-AFOSR-0107-87; AF Proj. 2303)
(AD-A200118; AFOSR-88-1069TR) Avail: NTIS HC A03/MF A01 CSCL 11B

Work carried out was directed to several areas. All involved the use of organo metallic precursors to produce novel ceramic and glass materials. The areas of principal activity included the following: (1) polytetrafluoroethylene-silicate composites via sol-gel processing; (2) fluoropolymer modified silicate glasses; (3) sintering behavior of sol-gel derived anorthite and cordierite glass powders; (4) coating pretreatment effects in thermally nitrided sol gel silica coatings; and (5) sol gel derived coatings. GRA

N89-17005# American Society for Engineering Education, Washington, DC.
ION ASSISTED DEPOSITION OF FIBER COATINGS FOR CERAMIC MATRIX COMPOSITES WTH LOW DIELECTRIC LOSS TANGENTS Final Report, 15 Oct. 1987 - 15 Oct. 1988
Alan Kahn 15 Oct. 1988 35 p Sponsored by Naval Research Lab., Washington, DC
(AD-A200162) Avail: NTIS HC A03/MF A01 CSCL 11C

The preliminary goal of achieving facility in the growth and characterization of thin amorphous silver nitride films was reached without difficulty. Thermal annealing studies resulted in the discovery of both bubble formation and crystallization in the film. This research can be divided into three segments. First is the fabrication of the amorphous films themselves. Second, the thermal stability of the films on various substrates would be investigated. Thirdly, the knowledge obtained about the structure and properties of the material would be utilized in understanding and further refining the science of thin film deposition. These divisions were reflected finally in the preparation of three publications: Near Infrared Rugate Filter Fabrication by Ion Beam Assisted Deposition of Si(1-x) N(x) Films - The major emphasis of this paper is on the optical properties of the films. Stability of Silicon Nitride Coatings Produced by Ion Assisted Deposition; Fractal and spherulitic Morphology of Silicon Nitride Crystallized from Amorphous Films. GRA

N89-17006# Michigan Univ., Ann Arbor.
MECHANISTIC STUDIES OF PRESSURE-ASSISTED SUPERPLASTICITY OF STRUCTURAL CERAMICS Annual Scientific Report, 15 Jun. 1987 - 14 Jun. 1988
I-Wei Chen 15 Jul. 1988 29 p
(Grant AF-AFOSR-0289-87; AF Proj. 2304)
(AD-A200202; UMSC-88-C-AF-2; AFOSR-88-0918TR) Avail: NTIS HC A03/MF A01 CSCL 07B

Superplastic flow in silicon nitride ceramics containing YAG was investigated. A low flow stress was found possible when the solid SIALON grains are included in the liquid phase YAG above a critical temperature. The mechanisms of grain growth and microstructural development in silicon nitride and zirconia were studied. The effect of Manganese addition on lowering the forming temperature of zirconia was demonstrated. GRA

N89-17007# Northwestern Univ., Evanston, IL. Dept. of Chemistry.
PBT,PBO-BASED HYBRID POLYMERS WITH NONLINEAR OPTICAL PROPERTIES OR HIGH ELECTRICAL CONDUCTIVITY Final Report, 15 Mar. 1986 - 15 Aug. 1988
Tobin J. Marks and Stephen H. Carr 29 Aug. 1988 29 p
(Grant AF-AFOSR-0105-86; AF Proj. 2303)
(AD-A200226; AFOSR-88-1023TR) Avail: NTIS HC A03/MF A01 CSCL 07F

This project involves a collaborative synthetic, polymer processing, and physicochemical program directed at exploiting the unique properties of the high modulus/high strength polymers poly(p-phenylenebenzobisthiazole) (PBT) and poly-(p-phenylenebenzobisoxazole) (PBO) for electronic charge transport and nonlinear optical (NLO) properties. In the former area, we have continued our successful studies of directly doping these polymers by electrochemical means and of processing phthalocyanine/polymer hybrid materials. In the NLO area, we have continued exploration of the properties of NLO chromophore/PBT hybrid materials and of glassy macromolecules with such chromophores covalently bonded to the backbone. Initial studies of oriented NLO chromophores embedded in crosslinkable matrices have also been carried out. Approaches to inorganic/organic hybrid NLO materials via intercalation processes are also under investigation. GRA

N89-17008# Cincinnati Univ., OH. Dept. of Materials Science and Engineering.
STRUCTURE AND PROPERTIES OF POLYMER INTERPHASES Annual Report No. 3, 1 Jul. 1987 - 30 Jun. 1988
F. James Boerio 30 Sep. 1988 38 p
(Contract N00014-85-K-0459)
(AD-A200238) Avail: NTIS HC A03/MF A01 CSCL 07F

The molecular structure of interphases between polymer systems and metal substrates was determined by using X-ray photoelectron spectroscopy (XPS), reflection-absorption infrared spectroscopy (RAIR), and attenuated total-reflection infrared spectroscopy (ATR) to characterize the failure surfaces of double cantilever beam adhesive joints prepared by curing beams of epoxies against metal beams. The structure of the interphases depended strongly on the curing agent, metal substrate, and use of a silane primer on the substrate. When joints were prepared by curing an epoxy with a tertiary amine curing agent at 75 C against a steel substrate primed with a dilute aqueous solution of gamma-aminopropyltriethoxy-silane, there was little reaction between the primer and adhesive and failure occurred near the primer/adhesive interface. The interphase consisted of low molecular weight siloxane oligomers in which the amino groups formed bicarbonates with water and carbon dioxide absorbed from the atmosphere. When similar joints were cured at 150 C, the bicarbonates dissociated, enabling the adhesive and primer to react, and shifting the locus of failure near the primer/adherend interface or into the epoxy. The use of surface-enhanced Raman scattering (sers) for non-destructive characterization of interphases between polymers and metals was demonstrated. GRA

N89-17009# University of Southern California, Los Angeles. Dept. of Chemistry.
DEVELOPMENT OF CONDUCTING POLYMERS OF HIGH STRUCTURAL STRENGTH Final Technical Report, 1 Jun. 1985 - 31 May 1988
Larry R. Dalton 31 May 1988 17 p
(Contract F49620-85-C-0096)
(AD-A200310; AFOSR-88-1043TR) Avail: NTIS HC A03/MF A01 CSCL 06G

Magnetic resonance measurements confirmed the fundamental pi-electron nature of the solitonic defect in polyacetylene. It is clear that the defect is delocalized with the exact extent and nature of delocalization dependent upon the lattice. For some polymer preparations, helium temperatures are required to freeze out dynamics and yield resolved ENDOR spectra. For these materials, the barriers to soliton delocalization must be small. Because of the dependence of ENDOR spectra upon polymer lattice, solliton concentration, temperature, it is clear that the intrinsic (isolated chain) soliton localization/delocalization length cannot be obtained from the experimental data. The ratio of positive to negative spin densities appears not to change with polymer lattice that these are likely determined by intramolecular electron coulomb interactions. Most theoretical calculations are in reasonable agreement with the experimental numbers. GRA

N89-17010# Sandia National Labs., Albuquerque, NM.
MAGNETIZATION, TRANSPORT AND STRUCTURAL STUDIES OF Tl-Ca-Ba-Cu-O: BULK CERAMICS, SINGLE CRYSTALS, AND POLYCRYSTALLINE THIN FILMS
E. L. Venturini, J. F. Kwak, D. S. Ginley, B. Morosin, and R. J. Baughman 1988 21 p Presented at the Workshop on the Materials Science of High T sub c Superconductors: Magnetic

Interactions, Gaithersburg, MD, 11-13 Oct. 1988
(Contract DE-AC04-76DP-00789)
(DE89-003264; SAND-88-2692C; CONF-8810147-1) Avail: NTIS HC A03/MF A01

A detailed investigation of the Tl-Ca-Ba-Cu-O system of high temperature superconductors is presented including static magnetization, electrical transport, structural and processing data for sintered and melted bulk ceramics, single crystals, and polycrystalline thin films. This system is shown by X-ray diffraction and energy dispersive X-ray analysis to have at least five distinct superconducting phase containing either two or three Cu-O sheets separated by one or two Tl-O planes. Bulk ceramic Tl-2223 has a Meissner effect up to 124 K and zero resistance up to 120 K, but transition temperatures are found to be a strong function of processing even for single crystals. Magnetization versus field data suggest weak flux pinning in all samples above 30 K. Melt processed bulk ceramics of Tl-2223 have transport critical current densities greater than 5000 A/sq cm at 76 K with modest magnetic field dependence, indicating strong intergranular links which are not present in Y-123. This is also observed for unoriented polycrystalline thin films. Tl-2223 films have critical current densities at 76 K up to 240,000 A/sq cm with a modest dependence on in-plane magnetic fields, implying negligible effects of grain boundary Josephson functions. DOE

N89-17011# Sandia National Labs., Albuquerque, NM.
COMPATIBILITY STUDY OF AN ABSORBER MATERIAL AND TWO SILICONE ADHESIVES
R. J. Martinez, T. R. Guess, and K. T. Gillen 1988 8 p Presented at the JOWOG-28 Meeting, Albuquerque, NM, 1 Oct. 1988
(Contract DE-AC04-76DP-00789)
(DE89-002361; SAND-88-2754C; CONF-8810151-7) Avail: NTIS HC A02/MF A01

A radar absorbing material, CMS-184, and assemblies bonded with two silicone based structural adhesives, DC-577 and RTV-630, were subjected to limited accelerated aging conditions and then evaluated for degradation of mechanical properties and adhesion, respectively. Aging conditions likely to be equivalent to 150 to 750 years at 72 degrees F and 100 percent RH only slightly changed the tensile strength and failure strain of CMS-184 (initial modulus remained unchanged). The RTV-630 adhesive performed better than DC-577 adhesive in butt tensile tests of unaged and aged specimens. Based on the results of these accelerated aging studies, both the CMS-184 absorber material and the RTV-630 adhesive should survive the expected life of current weapon systems. DOE

N89-17012# Pennsylvania Univ., Philadelphia. Dept. of Chemistry.
SYNTHESIS AND PROPERTIES OF NEW PRECERAMIC MATERIALS Progress Report, 1 Jun. 1987 - 30 Nov. 1988
Larry G. Sneddon Aug. 1988 10 p
(Contract DE-FG02-87ER-13732)
(DE89-003436; DOE/ER-13732/1) Avail: NTIS HC A02

The development of new methods for the production of complex materials is one of the most important problems in modern solid state chemistry and materials science. This project is attempting to apply the synthetic principles which have evolved in inorganic and organometallic chemistry to the production of important non-oxide ceramics, such as boron nitride, boron carbide and metal borides. The synthetic approach is focusing on the use of transition metal catalysts to induce transformations in molecular boron-hydrogen compounds leading to the formation of useful preceramic materials. Our recent work has now resulted in the production of several new polymer systems, including poly(vinylborazine) and poly(vinylpentaborane), which have proven to be high yield precursors to boron nitride and/or boron carbide. Current work is now directed toward the synthesis of new types of molecular and polymeric boron-containing species and an exploration of the solid state properties of the ceramics which have been produced in these studies. DOE

N89-17013# Los Alamos National Lab., NM. Theoretical Div.
THEORETICAL PREDICTIONS FOR SIDE-CHAIN LIQUID-CRYSTAL POLYMERS AND COMPARISON TO EXPERIMENT
F. Dowell 1988 7 p Presented at the Fall Meeting of the Materials Research Society, Boston, MA, 28 Nov. 1988 Submitted for publication
(Contract W-7405-eng-36)
(DE89-003578; LA-UR-88-3884; CONF-881155-12) Avail: NTIS HC A02/MF A01

This paper presents results from a new unique microscopic molecular theory for side-chain liquid-crystalline polymers (LCPs) in the nematic (N) and multiple smectic-A (SA) LC phases and the isotropic (I) liquid phase. There are no ad hoc or arbitrarily adjustable parameters in this theory. The agreement between the theoretical and experimental values for various properties (including transition temperatures and quadratic characteristic radii) is very good (relative deviations between 0 and less than 6.2 percent). The theoretical results also show--for the first time--that the N and I phases for these LCPs involve the packing of plate-like sections of backbones and side chains and that the local bilayer SA phase involves packing of side-chains within a plate-like section. This type of packing is predicted to be typical for side-chain LCPs. This theory can predict--for the first time--whether the side chains of a molecule pack on the same or alternating opposite sides of the backbone and whether side chains on different molecules interdigitate (overlap) with each other. DOE

N89-17014# Texas Univ., Austin. Dept. of Chemical Engineering.
SYNTHESIS AND ANALYSIS OF NOVEL POLYMERS WITH POTENTIAL FOR PROVIDING BOTH HIGH PERMSELECTIVITY AND PERMEABILITY IN GAS SEPARATION APPLICATIONS Summary Technical Report, Apr. 1986 - Dec. 1988
W. J. Koros and D. R. Paul Dec. 1988 17 p
(Contract DE-FG05-86ER-13507)
(DE89-004325; DOE/ER-13507/4) Avail: NTIS HC A03/MF A01

We have gained significant insights into the basic principles governing sorption and transport in glassy materials. The following three important areas can be identified in which advances in the basic science controlling gas separation membrane operations were made. Extremely attractive new membrane materials have been identified. These materials will be compared to conventional materials to illustrate the value of the systematic structure- property approach. Two basic rules were formulated that provide improved guidance in selecting candidate materials for gas separation membranes. The permeability and permselectivity parameters mentioned below determine the productivity and the product purity, respectively, that can be achieved using a membrane material. Important preliminary insights into the process of plasticization of a series of structurally-related glassy polymers were achieved. Extensive experimental work involving three classes of polymers, the polycarbonates, the polyimides and the polysulfones have proven that the more restricted glassy environment provides a greater ability than that in rubbery materials to regulate the relative permeation rates of passage of gaseous penetrants that have only subtly different molecular sizes or shapes. DOE

N89-17283# Fraunhofer-Inst. fuer Betriebsfestigkeit, Darmstadt (Germany, F.R.).
FATIGUE BEHAVIOR OF CERAMIC THERMAL BARRIER COATINGS [ZUM ERMUDUNGSVORGANG KERAMISCHER WAERMEDAEMMSCHICHTEN]
P. Pantucek *In its* Proceedings of the 5th LBF Colloquium 1988 p 195-206 In GERMAN (For primary document see N89-17272 09-39)
Avail: NTIS HC A12/MF A01

N89-17334*# Pratt and Whitney Aircraft, East Hartford, CT.
HIGH TEMPERATURE CONSTITUTIVE AND CRACK INITIATION MODELING OF COATED SINGLE CRYSTAL SUPERALLOYS

Thomas G. Meyer, David M. Nissley, and Gustav A. Swanson *In* NASA, Lewis Research Center, Turbine Engine Hot Section Technology, 1987 Oct. 1987 p 401-412 (For primary document see N89-17298 09-39)
(Contract NAS3-23939)
Avail: NTIS HC A20/MF A01 CSCL 11B

28 PROPELLANTS AND FUELS

Includes rocket propellants, igniters, and oxidizers; their storage and handling procedures; and aircraft fuels.

For related information see also *07 Aircraft Propulsion and Power, 20 Spacecraft Propulsion and Power,* and *44 Energy Production and Conversion.*

N89-17015# Southwest Research Inst., San Antonio, TX. Fuels and Lubricants Research Div.
FUEL PROPERTY AND ANTIOXIDANT EFFECTS ON ELASTOMER INTEGRITY, PHASE 2 Final Report, Sep. 1985 - Feb. 1988
J. P. Cuellar, Jr. Mar. 1988 33 p Original contains color illustrations
(Contract N00014-85-C-2520)
(AD-A200250; SwRI-8845-002) Avail: NTIS HC A03/MF A01 CSCL 21D

The program objective was to determine if typical antioxidants used in JP-5 turbine fuel could exhibit harmful effects on fuel system elastomers as a consequence of chemical change of the antioxidants during the inhibition process. One stable and one unstable fuel (relative to peroxidation tendency), with and without an antioxidant, were stored at 43C in contact with 14 elastomer materials. Storage periods ranged from 7 to 270 days. Post-storage elastomer results indicated no deleterious effect attributable to the antioxidants. Significant changes in elastomer properties were confined to the uninhibited, unstable fuel which developed appreciable levels of peroxides over the course of the study. GRA

N89-17016# Oak Ridge National Lab., TN.
RESULTS FROM THE FEDERAL METHANOL FLEET Progress Report
R. N. McGill and R. L. Graves 1988 7 p Presented at the 8th International Symposium on Alcohol Fuels, Tokyo, Japan, 13 Nov. 1988
(Contract DE-AC05-84OR-21400)
(DE88-015291; CONF-881138-1) Avail: NTIS HC A02

The Federal Methanol Fleet, initiated by the United States Congress in fiscal year 1985 and managed by the Oak Ridge National Laboratory (ORNL) for the Department of Energy (DOE), is a project to evaluate a variety of methanol vehicles with different engine/fuel systems and to gather information regarding their operation in typical fleet environments. Three different DOE laboratories serve as fleet sites for the project. Twenty vehicles of four different types have been retro-fitted for methanol and are being evaluated alongside nineteen comparable gasoline vehicles. Engine types in the project include four-cylinder engines, V-6s, V-8s; fuel system include carburetors, throttle-body fuel injection, and port fuel injection. Some of the methanol engines have increased compression ratios, while others utilize turbo-chargers. Results highlighted in this paper include emissions, lubricating oil analyses, and cold-weather performance. DOE

N89-17017*# National Aeronautics and Space Administration. Lewis Research Center, Cleveland, OH.
EXPERIMENTAL VERIFICATION OF THE THERMODYNAMIC PROPERTIES FOR A JET-A FUEL
Carmen M. GraciaSalcedo, Theodore A. Brabbs, and Bonnie J. McBride Sep. 1988 10 p Presented at the 196th National Meeting of the American Chemical Society, Los Angeles, CA, 25-30 Sep. 1988 Prepared in cooperation with Army Aviation Systems Command, Cleveland, OH; and Sverdrup Technology, Inc., Cleveland, OH
(NASA-TM-101475; E-4593; NAS 1.15:101475) Avail: NTIS HC A02/MF A01 CSCL 21D

Thermodynamic properties for a Jet-A fuel were determined by Shell Development Company in 1970 under a contract for NASA Lewis Research Center. The polynomial fit necessary to include Jet-A fuel (liquid and gaseous phases) in the library of thermodynamic properties of the NASA Lewis Chemical Equilibrium Program is calculated. To verify the thermodynamic data, the temperatures of mixtures of liquid Jet-A injected into a hot nitrogen stream were experimentally measured and compared to those calculated by the program. Iso-octane, a fuel for which the thermodynamic properties are well known, was used as a standard to calibrate the apparatus. The measured temperatures for the iso-octane/nitrogen mixtures reproduced the calculated temperatures except for a small loss due to the non-adiabatic behavior of the apparatus. The measurements for Jet-A were corrected for this heat loss and showed excellent agreement with the calculated temperatures. These experiments show that this process can be adequately described by the thermodynamic properties fitted for the Chemical Equilibrium Program. Author

N89-17018# Los Alamos National Lab., NM.
PREDICTION AND SYNTHESIS EFFORTS AT LOS ALAMOS
J. R. Stine and M. D. Coburn 1988 17 p Presented at the 7th Annual Working Group Meeting on Synthesis of High Energy Density Materials, Parsippany, NJ, 1 Jun. 1988
(Contract W-7405-eng-36)
(DE89-003605; LA-UR-88-3996; CONF-8806277-1) Avail: NTIS HC A03/MF A01

One important aspect of an organic synthesis effort related to the development of new explosives, is the ability to estimate the properties of proposed molecules. In most cases, the detonation velocity and C-J pressure are estimated for the proposed explosive using any number of existing predictive methods. Novel explosives are being proposed, at Los Alamos and elsewhere, that are qualitatively different in their molecular makeup than most of the existing conventional ones. These explosives include, highly strained cage molecules, heterocyclic molecules, low hydrogen-containing molecules, and high nitrogen-containing molecules. This paper describes alternate ways of viewing detonation velocities and a new method for estimating detonation velocity of a proposed compound. DOE

N89-16912# Bombrini Parodi-Delfino S.p.A., Colleferro (Italy). Defense and Space Div.
PROPELLANT GRAIN DESIGN
S. Scippa *In* AGARD, Design Methods in Solid Rocket Motors Apr. 1988 20 p Previously announced as N87-28595 (For primary document see N89-16906 09-20)
Copyright Avail: NTIS HC A11/MF A01

N89-16913# Societe Nationale des Poudres et Explosifs, Vert-Le-Petit (France). Direction Technique Autopropulsion.
SOLID PROPELLANT GRAIN DESIGN
Bernard Zeller *In* AGARD, Design Methods in Solid Rocket Motors Apr. 1988 29 p (For primary document see N89-16906 09-20)
Copyright Avail: NTIS HC A11/MF A01

N89-16914# Air Force Rocket Propulsion Lab., Edwards AFB, CA.
STATE OF THE ART OF SOLID PROPELLANT ROCKET MOTOR GRAIN DESIGN IN THE UNITED STATES
Durwood I. Thrasher *In* AGARD, Design Methods in Solid Rocket Motors Apr. 1988 21 p (For primary document see N89-16906 09-20)
Copyright Avail: NTIS HC A11/MF A01

29 MATERIALS PROCESSING

Includes space-based development of products and processes for commercial applications.
For biological materials see *55 Space Biology*.

N89-17019# National Research Council of Canada, Ottawa (Ontario).
WORKSHOP ON MICROGRAVITY EXPERIMENTATION IN AIRCRAFT AND ROCKETS
1988 129 p In ENGLISH and FRENCH Workshop held in Ottawa, Ontario, 5-6 May 1988
(NRCC-29151; NR15-33/1988; ISBN-0-660-12891-8) Avail: NTIS HC A07/MF A01; also available from Publication Sales and Distribution, National Research Council of Canada, Ottawa, ON, Canada K1A OR6

This Workshop was intended to bring together the existing and potential users of microgravity in the Canadian community to exchange ideas and report on work done to date. In view of the fact that no real space experimentation had been done in Canada since SPACEBOUND '87 (May 1987) the Organizing Committee decided that it would be worthwhile to bring together those who had already flown experiments on the NASA KC-135 and the MASER 1 rocket, in the interim, to disseminate their knowledge to those potential experimenters waiting their turn to fly. Brought together were just over one hundred microgravity experimenters, including a number from the U.S. The programs of Canada, Japan, the United States and Sweden were presented, as well as those ranging from Materials Science and Bio-satellites, to Life Sciences. The Workshops held in the two areas of Materials Science and Life Sciences were stimulating and a number of recommendations were made. For individual titles, see N89-17020 through N89-17044.

N89-17020# National Research Council of Canada, Ottawa (Ontario). Space Div.
PARABOLIC FLIGHT: A USEFUL TEST BED
Marc Garneau *In its* Workshop on Microgravity Experimentation in Aircraft and Rockets 1988 p 3-8 (For primary document see N89-17019 09-29)
Avail: NTIS HC A07/MF A01; also available from Publication Sales and Distribution, National Research Council of Canada, Ottawa, ON, Canada K1A OR6

Although parabolic flight aircraft such as NASA's KC-135 do not provide the quality of the duration of microgravity available on a sounding rocket, a space shuttle or a space station, the weightless environment which they provide is often acceptable for checking out the ideas, hardware and procedures which could one day be tested in space. Moreover, such aircraft offer quick and inexpensive access to the required environment at a time when spaceflights are at a premium. Canada is now flying aboard the KC-135 and the number of Canadian investigators making use of this service is growing. It is therefore worth examining parabolic flight in a little more detail and in particular the steps involved in getting an experiment manifested and flown under government sponsorship. Author

N89-17021# Swedish Space Corp., Solna.
MICROGRAVITY ROCKETS IN SWEDEN
L. Bjorn and J. Zaar *In* National Research Council of Canada, Workshop on Microgravity Experimentation in Aircraft and Rockets 1988 p 9-16 (For primary document see N89-17019 09-29)
Avail: NTIS HC A07/MF A01; also available from Publication Sales and Distribution, National Research Council of Canada, Ottawa, ON, Canada K1A OR6

The Swedish sounding rocket program MASER provides periodically recurring flight opportunities for experiments (approximately 1 per year) under microgravity conditions. Conducted by the Swedish Space Corporation MASER is a cost effective, easily accessible experiment facility giving 7 minutes of microgravity. Short campaign periods are guaranteed through the use of guided rockets, and fast land recovery is obtained at the well-equipped Esrange rocket range. The payload is modularized to provide simple interfaces, large flexibility and independence between experiment modules. All service systems which are necessary for telecommunication, payload control, recovery, and maintenance of the required low acceleration levels (10 to the -4g) during the flight are included in the system. Four to six 17 inch experiment modules can be flown totalling a maximum of 230 kg. High speed telemetry and uplink command control of experiments can be provided on request. The price for the flight ticket is derived from the weight of the experiment module and includes all services related to integration and testing of payload, transport in Sweden, launch campaign, data distribution and a final report. If required, the launch program will be increased. Author

N89-17022# National Space Development Agency, Tokyo (Japan). Space Experiment Group.
SPACE UTILIZATION PROMOTION PROGRAM OF NASDA
K. Yanagawa, R. Kanki, T. Amaike, and N. Takeda *In* National Research Council of Canada, Workshop on Microgravity Experimentation in Aircraft and Rockets 1988 p 17-23 (For primary document see N89-17019 09-29)
Avail: NTIS HC A07/MF A01; also available from Publication Sales and Distribution, National Research Council of Canada, Ottawa, ON, Canada K1A OR6

Current space research and development trends in Japan include: (1) Expectation of environment utilization like microgravity in space besides earth observation or communication terminal point; (2) Acquisition of new knowledge from space research and development; (3) Contribution to global social and economical development through the advancement of science and technology; (4) International cooperation based on peaceful purposes; and (5) Development of manned space activities for the next era. Japan has decided to participate in NASA's proposed international space station program with the Japanese Experiment Module (JEM) consisting of pressurized module, exposed facility, and logistic module. Author

N89-17023# National Research Council of Canada, Ottawa (Ontario). Space Div.
CANADIAN MICROGRAVITY RESEARCH USING AIRCRAFT AND ROCKETS
Glen S. Campbell and R. D. Hendry *In its* Workshop on Microgravity Experimentation in Aircraft and Rockets 1988 p 25-30 (For primary document see N89-17019 09-29)
Avail: NTIS HC A07/MF A01; also available from Publication Sales and Distribution, National Research Council of Canada, Ottawa, ON, Canada K1A OR6

The accident to the U.S. Space Shuttle has resulted in a large backlog of Shuttle secondary payloads, such as Hitchhikers and Get Away Specials. Consequently, rockets and parabolic aircraft provide a much quicker access to microgravity. For a rocket, the microgravity time is five to seven minutes, and the time from the initial concept of an experiment to flight is about 1 1/2 to two years. Parabolic aircraft give 15 to 20 seconds of zero-g per parabola, and an experiment can fly to eight months after acceptance of the experimenter's proposal. This paper summarizes Canadian microgravity experiments that have flown on rockets, the NASA KC-135 aircraft, and the NRC (National Research Council of Canada) T-33 aircraft. Author

N89-17024# Academy of Sciences (USSR), Moscow.
ON FUNDAMENTAL PROBLEMS OF SPACE MATERIALS SCIENCE (SMS)
L. L. Regel *In* National Research Council of Canada, Workshop on Microgravity Experimentation in Aircraft and Rockets 1988 p 31-37 (For primary document see N89-17019 09-29)
Avail: NTIS HC A07/MF A01; also available from Publication Sales and Distribution, National Research Council of Canada, Ottawa, ON, Canada K1A OR6

This paper is a review dealing with recent publications on theoretical and experimental investigations on space materials science under lower gravity. The importance of the results obtained

by the present time and the wide perspectives for future investigations in this field are outlined. Author

N89-17025# National Research Council of Canada, Ottawa (Ontario).
CANADIAN PARTICIPATION IN INTERNATIONAL BIOSATELLITE PROGRAMS Abstract Only
Alan J. Mortimer *In its* Workshop on Microgravity Experimentation in Aircraft and Rockets 1988 p 39 (For primary document see N89-17019 09-29)
Avail: NTIS HC A07/MF A01; also available from Publication Sales and Distribution, National Research Council of Canada, Ottawa, ON, Canada K1A OR6

In the era leading up to experimentation on the space station access to microgravity will be a very rare commodity. Even less common will be opportunities for long duration experiments in space. For many biological systems bio-satellites offer experiment duration in excess of normal shuttle flight length, simplified hardware requirements and a higher quality microgravity environment. Canada is currently discussing with the Soviet Union the possibility of including experiments on the 1989 and 1991 Cosmos bio-satellite flights. Canadian investigators have participated in the past as part of American investigator teams; however, there has never been official Canadian participation. Author

N89-17026*# National Aeronautics and Space Administration. Lyndon B. Johnson Space Center, Houston, TX.
NASA's ZERO-g AIRCRAFT OPERATIONS Abstract Only
R. K. Williams *In* National Research Council of Canada, Workshop on Microgravity Experimentation in Aircraft and Rockets 1988 p 41 (For primary document see N89-17019 09-29)
Avail: NTIS HC A07/MF A01; also available from Publication Sales and Distribution, National Research Council of Canada, Ottawa, ON, Canada K1A OR6 CSCL 22A

NASA's Zero-g aircraft, operated by the Johnson Space Center, provides the unique weightless or zero-g environment of space flight for hardware development and test and astronaut training purposes. The program, which began in 1959, uses a slightly modified Boeing KC-135A aircraft, flying a parabolic trajectory, to produce weightless periods of 20 to 25 seconds. The program has supported the Mercury, Gemini, Apollo, Skylab, Apollo-Soyuz and Shuttle programs as well as a number of unmanned space operations. Typical experiments for flight in the aircraft have included materials processing experiments, welding, fluid manipulation, cryogenics, propellant tankage, satellite deployment dynamics, planetary sciences research, crew training with weightless indoctrination, space suits, tethers, etc., and medical studies including vestibular research. The facility is available to microgravity research organizations on a cost-reimbursable basis, providing a large, hands-on test area for diagnostic and support equipment for the Principal Investigators and providing an iterative-type design approach to microgravity experiment development. The facility allows concepts to be proven and baseline experimentation to be accomplished relatively inexpensively prior to committing to the large expense of a space flight. Author

N89-17027*# McGill Univ., Montreal (Quebec).
LIFE SCIENCE EXPERIMENTS DURING PARABOLIC FLIGHT: THE MCGILL EXPERIENCE
D. G. D. Watt *In* National Research Council of Canada, Workshop on Microgravity Experimentation in Aircraft and Rockets 1988 p 43-46 Sponsored in part by NASA, and Medical Research Council of Canada (For primary document see N89-17019 09-29)
Avail: NTIS HC A07/MF A01; also available from Publication Sales and Distribution, National Research Council of Canada, Ottawa, ON, Canada K1A OR6 CSCL 22A

Over the past twelve years, members of the Aerospace Medical Research Unit of McGill University have carried out a wide variety of tests and experiments in the weightless condition created by parabolic flight. This paper discusses the pros and cons of that environment for the life scientist, and uses examples from the McGill program of the types of activities which can be carried out in a transport aircraft such as the NASA KC-135. Author

N89-17028# Conatec, Inc., Lanham, MD.
ADVANCED RESEARCH ROCKETS FOR LONG DURATION MICROGRAVITY SCIENCE
W. H. Montag and R. W. McIntyre *In* National Research Council of Canada, Workshop on Microgravity Experimentation in Aircraft and Rockets 1988 p 47-54 (For primary document see N89-17019 09-29)
Avail: NTIS HC A07/MF A01; also available from Publication Sales and Distribution, National Research Council of Canada, Ottawa, ON, Canada K1A OR6

The Challenger tragedy has resulted in the loss of reliable access to space for the small payload user. In particular, the microgravity science community which was to receive extensive access to the Shuttle has been forced to reevaluate alternative flight opportunities. Suborbital rockets have been widely utilized for microgravity experimentation in European, Japanese, USSR, and United States programs. Two of the most publicized programs are the NASA Space Processing Applications Rocket (SPAR) program (1975 to 1983) and the Federal Republic of Germany Technical Experiments Under Microgravity (TEXUS) program which is currently operational in Europe. The Black Brant and SKYLARK launch vehicles used for these programs provide 5 to 6 minutes of microgravity environment. Enhancements to these current systems can extend the useful microgravity time to seven minutes. Recently, interest has been expressed in using suborbital launch vehicles to achieve microgravity environment times of 15 to 20 minutes. Over the past 14 months, Conatec has been developing a series of launch vehicles based on flight proven solid rocket motors which will provide in excess of 15 minutes of microgravity. Current programs can be extended to seven minutes. Author

N89-17029# Comingo Ltd., Trail (British Columbia).
ANALYSIS OF Cd0.21Hg0.79Te QUENCHED IN 10(-4) g
A. B. Bollong and G. T. Proux *In* National Research Council of Canada, Workshop on Microgravity Experimentation in Aircraft and Rockets 1988 p 57-61 (For primary document see N89-17019 09-29)
Avail: NTIS HC A07/MF A01; also available from Publication Sales and Distribution, National Research Council of Canada, Ottawa, ON, Canada K1A OR6

A 95 gm sample of Cd sub 0.21 Hg sub 0.79 Te was solidified in 10 to the -4g. Infrared transmission analysis shows significant improvement in both radial and longitudinal uniformity when compared with baseline samples. This paper summarizes the experiment and results. Author

N89-17030*# National Aeronautics and Space Administration. Marshall Space Flight Center, Huntsville, AL.
HARDWARE FOR STUDYING THE DEMIXING OF AQUEOUS POLYMER TWO-PHASE SYSTEMS IN LOW GRAVITY Abstract Only
J. M. VanAlstine (Universities Space Research Association, Huntsville, AL.) *In* National Research Council of Canada, Workshop on Microgravity Experimentation in Aircraft and Rockets 1988 p 63 (For primary document see N89-17019 09-29)
Avail: NTIS HC A07/MF A01; also available from Publication Sales and Distribution, National Research Council of Canada, Ottawa, ON, Canada K1A OR6 CSCL 22A

The gravity-free demixing behavior of aqueous polymer two-phase systems (APTPS) has been studied on Earth, and onboard KC-135 aircraft and the Space Shuttle. Results suggest a good correlation between the demixing behavior of isopycnic systems on Earth and the low g behavior of systems exhibiting phase density differences. The short term (20 s) behavior of APTPS onboard KC-135 aircraft has been shown to mimic their initial demixing behavior in space. It appears that the few minutes of low g provided by parabolic rocket flight will be sufficient to study all but the later stages of demixing of APTPS. We are therefore

turning our attention toward the design and use of hardware for studying the demixing of APTPS onboard sounding rockets. This seminar will discuss the evolution of hardware and research from hand-held KC-135 and Shuttle hardware through to automated hardware designed for utilization of KC-135, sounding rocket, and Space Shuttle Mid-deck Locker flight opportunities. Author

N89-17031# Canadian Astronautics Ltd., Ottawa (Ontario). Space Systems Group.
DROPLET SEPARATION DYNAMICS AND KINEMATICS UNDER MICROGRAVITY
Richard Boudreault *In* National Research Council of Canada, Workshop on Microgravity Experimentation in Aircraft and Rockets 1988 p 65-73 (For primary document see N89-17019 09-29)
Avail: NTIS HC A07/MF A01; also available from Publication Sales and Distribution, National Research Council of Canada, Ottawa, ON, Canada K1A OR6

This paper summarizes the findings of experiments on the generation of free-falling millimetric droplets conducted during a series of KC-135 parabolic flights in March 1988. The separation of the alginate droplets is reviewed and accompanied by a discussion of the duration and morphology of droplet spherization and the separation process. Author

N89-17032# SED Systems, Inc., Saskatoon (Saskatchewan).
DESIGN CONSIDERATIONS FOR THE CLEM135 BUBBLE COALESCENCE EXPERIMENT
W. S. C. Brooks and B. G. Thompson (Alberta Research Council, Edmonton, Canada) *In* National Research Council of Canada, Workshop on Microgravity Experimentation in Aircraft and Rockets 1988 p 75-78 (For primary document see N89-17019 09-29)
Avail: NTIS HC A07/MF A01; also available from Publication Sales and Distribution, National Research Council of Canada, Ottawa, ON, Canada K1A OR6

The CLEM135 bubble coalescence experiment was designed for flight on the NASA KC135 low gravity aircraft. The objective of the experiment was to observe the coalescence of gas bubbles in a reduced gravity environment. This paper outlines the requirements for the experimental apparatus and identifies the design considerations under which the instrument was constructed. Experimental results are included as well and discussed as they pertain to the implementation the design in reduced gravity. Author

N89-17033# Ontario Research Foundation, Mississauga.
SYSTEM ENGINEERING AND LOGISTICS FOR KC-135 EXPERIMENTATION
B. G. Sellars *In* National Research Council of Canada, Workshop on Microgravity Experimentation in Aircraft and Rockets 1988 p 79-81 (For primary document see N89-17019 09-29)
Avail: NTIS HC A07/MF A01; also available from Publication Sales and Distribution, National Research Council of Canada, Ottawa, ON, Canada K1A OR6

This paper provides a generic overview of Ontario Research Foundation (ORF) experience for KC-135 experiment design, engineering and execution as affected by operational, safety and logistical factors. The ORF Sol/Spherol experiment flew on NASA's KC-135 in February and October 1987. Examples from this experiment are used to illustrate factors affecting system and experiment design. Author

N89-17034# Manitoba Univ., Winnipeg.
THE EFFECTS OF MICROGRAVITY AND LINEAR ACCELERATIONS ON CUTANEOMUSCULAR REFLEXES IN HUMAN LOWER LIMB MUSCULATURE **c52**
T. Szturm, R. M. Jell, D. Kriellaars, D. J. Ireland, and S. Lafortune *In* National Research Council of Canada, Workshop on Microgravity Experimentation in Aircraft and Rockets 1988 p 87-91 (For primary document see N89-17019 09-29)
Avail: NTIS HC A07/MF A01; also available from Publication Sales and Distribution, National Research Council of Canada, Ottawa, ON, Canada K1A OR6

Current knowledge of the otolith-spinal system is largely based on animal experiments. It is generally accepted that the otolith receptors behave as linear motion detectors and are sensitive to slow or maintained tilts relative to the gravity vector. It has been established from animal experiments that the coupling of the otolith and organs (otolith primary afferents) and motoneurons subserving lower limb extensors and flexors involve a multi-link pathway which is shared by Flexion Reflex Afferents (primary cutaneous afferents, joint afferents, and high threshold muscle afferents). In the development of a postural related test of human otolith function we have taken the approach to examine the convergent effects of static tilt (a practical and effective form of natural otolith stimulation) and the reflex action of cutaneous nerve stimulation in lower limb musculature. From the analysis of the reflex effects of sural nerve stimulation in normal human subjects during static tilt in pitch, we have demonstrated a highly significant tilt-dependent modulation of the magnitude of the initial component of cutaneomuscular test reflex in both lower limb flexors and extensors. The purpose of this study was to seek further evidence in support of the otolith dependence of the cutaneomuscular reflex response. Author

N89-17035# National Research Council of Canada, Ottawa (Ontario).
OCULAR TORSION IN THE WEIGHTLESSNESS OF PARABOLIC FLIGHT Abstract Only **c52**
K. E. Money, N. M. Kirienko, W. H. Johnson, D. G. D. Watt, C. H. Markham, and S. G. Diamond (California Univ., Los Angeles.) *In its* Workshop on Microgravity Experimentation in Aircraft and Rockets 1988 p 93 (For primary document see N89-17019 09-29)
Avail: NTIS HC A07/MF A01; also available from Publication Sales and Distribution, National Research Council of Canada, Ottawa, ON, Canada K1A OR6

Preliminary findings of torsional eyeball displacements (rotational displacements about the optic axis) in parabolic flight that were reported in Spacebound '87 have been confirmed. The more recent experiments have used photographs of both eyes, instead of only the right eye, and they show that both eyes generally (but not invariably) show torsional displacements in the same direction. Too few subjects have been tested to allow general conclusions, but it seems clear that the eyes do move torsionally in response to both hypogravity and hypergravity. It is reasonable to think that, in space flight, the torsional positions of the eyes are not the same as on Earth. Author

N89-17036# National Research Council of Canada, Ottawa (Ontario).
THE USE OF SOUNDING ROCKETS IN THE STUDY OF MICROGRAVITY CELL BIOLOGY **c51**
Alan J. Mortimer *In its* Workshop on Microgravity Experimentation in Aircraft and Rockets 1988 p 95-97 (For primary document see N89-17019 09-29)
Avail: NTIS HC A07/MF A01; also available from Publication Sales and Distribution, National Research Council of Canada, Ottawa, ON, Canada K1A OR6

Traditionally, sounding rockets have been used in the study of atmospheric physics, and to a lesser degree in materials science. During free fall a rocket payload may be exposed to very good microgravity conditions (of the order of 10 to the -5g). The short duration of the period of microgravity and the limited payload size available in a sounding rocket preclude the study of many, but not all, biological processes. Several classes of biological processes which occur at the cellular level occur within the time frame of several minutes, comparable with that available with typical sounding rockets. In addition single cells are small, thus the experimental volume may be adjusted to fit a rocket payload geometry. Two areas of particular experimental interest are cell fusion, which may be more readily controlled in microgravity, and cell transport. It is this latter phenomenon which is currently under investigation. Author

N89-17037# Canadian Astronautics Ltd., Ottawa (Ontario).
ENCAPSULATION PROCESS HARDWARE FOR A KC-135 AIRCRAFT
J. Bottrill, Richard Boudreault, J. Bradley, C. Choma, R. Escher, Z. Saghir, V. Willson, and D. Wilmut *In* National Research Council of Canada, Workshop on Microgravity Experimentation in Aircraft and Rockets 1988 p 103-112 (For primary document see N89-17019 09-29)
Avail: NTIS HC A07/MF A01; also available from Publication Sales and Distribution, National Research Council of Canada, Ottawa, ON, Canada K1A OR6

A total of four experiments were built and tested on board NASA's KC-135 Microgravity facility. The following paper outlines in detail the hardware in the final apparatus, observations on how the apparatus operated in microgravity, practical lessons learned which influenced the design of the next piece of flight hardware, and a scientific assessment of the data collected. Author

N89-17038# Payload Systems, Inc., Wellesley, MA.
PYTHON MICROGRAVITY ACCELEROMETER SYSTEM
V. Nijhawan and A. P. Arrott *In* National Research Council of Canada, Workshop on Microgravity Experimentation in Aircraft and Rockets 1988 p 113-117 (For primary document see N89-17019 09-29)
Avail: NTIS HC A07/MF A01; also available from Publication Sales and Distribution, National Research Council of Canada, Ottawa, ON, Canada K1A OR6

Scientists performing experiments in the unique microgravity environment of space frequently require an accurate and useful view of the acceleration at their experiment. Payload Systems has developed a Microgravity Accelerometer System for use in the Space Shuttle middeck locker. Known as PYTHON, this system has a detachable sensor head that can be mounted to individual experiments. Acceleration data is analyzed in real time and the resulting acceleration information is displayed. A non-space qualified version of PYTHON is used regularly in the simulated reduced gravity aboard the KC-135 aircraft. The acceleration data is analyzed and a parabola-by-parabola report is made available to investigators. Author

N89-17039# Blaber (A.) and Blaber (P.), Hamilton (Ontario).
A CANADIAN LOW EARTH ORBIT LAUNCH VEHICLE: LAUNCH VEHICLE PERFORMANCE ANALYSIS OF BLACK BRANT VC AND NIHKA ROCKET MOTOR CONFIGURATIONS **c15**
A. Blaber, J. S. Bullard (Bullard, J. S., Brandtford, Ontario), and P. Blaber *In* National Research Council of Canada, Workshop on Microgravity Experimentation in Aircraft and Rockets 1988 p 119-121 (For primary document see N89-17019 09-29)
Avail: NTIS HC A07/MF A01; also available from Publication Sales and Distribution, National Research Council of Canada, Ottawa, ON, Canada K1A OR6

A computer program was developed for IBM-PC and compatible computers to simulate the flight of sounding rockets and Low Earth Orbit launch vehicles. The program was designed to determine the capabilities of various configurations of clustered and staged rocket motors and can be used to predict apogee heights and durations in microgravity. The simulation was used to investigate the feasibility of a Canadian Low Earth Orbit launch vehicle. Author

N89-17040# BM Hi-Tech, Inc., Collingwood (Ontario).
HIGH TEMPERATURE MATERIAL PROCESSING SYSTEM FOR KC-135 MICROGRAVITY EXPERIMENTS
S. E. Prasad, N. Maffei, and D. R. Tansley *In* National Research Council of Canada, Workshop on Microgravity Experimentation in Aircraft and Rockets 1988 p 123-126 (For primary document see N89-17019 09-29)
Avail: NTIS HC A07/MF A01; also available from Publication Sales and Distribution, National Research Council of Canada, Ottawa, ON, Canada K1A OR6

The paper describes a system for processing high temperature materials. The apparatus consists of a magazine that can accommodate eight experimental specimens and a discharge shroud that can be used for either active or passive cooling. The furnace can operate up to 1000 C and can accommodate specimens up to 2mm dia and 50mm long. Other features of the system include an on board control module and support facilities. Author

N89-17041# National Aeronautical Establishment, Ottawa (Ontario).
PRELIMINARY RESULTS: FLIGHT TESTING THE NAE T-33 MICROGRAVITY FACILITY Abstract Only
J. F. Aitken *In* National Research Council of Canada, Workshop on Microgravity Experimentation in Aircraft and Rockets 1988 p 127 (For primary document see N89-17019 09-29)
Avail: NTIS HC A07/MF A01; also available from Publication Sales and Distribution, National Research Council of Canada, Ottawa, ON, Canada K1A OR6

Problems encountered in configuring the NAE T-33 C-FSKH for microgravity work have delayed operational availability of the facility from the fall of '87 to the spring of '88. At this time the aircraft is just completing a series of flight tests to develop a new instrumentation system and the piloting techniques necessary for microgravity flights. Thus only preliminary data is available to indicate the aircraft's performance capabilities as a microgravity platform. This paper provides a description of the facility itself and its performance capabilities based on those development tests. Author

N89-17042# Canadian Astronautics Ltd., Ottawa (Ontario).
CONCENTRICITY AND SPHERICITY OF COMPOSITE DROPS UNDER MICROGRAVITY Abstract Only
Z. Saghir, Richard Boudreault, and Y. Boudreault (Laval Univ., Quebec) *In* National Research Council of Canada, Workshop on Microgravity Experimentation in Aircraft and Rockets 1988 p 129 (For primary document see N89-17019 09-29)
Avail: NTIS HC A07/MF A01; also available from Publication Sales and Distribution, National Research Council of Canada, Ottawa, ON, Canada K1A OR6

A program dealing with the encapsulation of cells has been established by CAL and the National Research Council of Canada. This program produces ultraspherical microcapsules containing living cells. These microcapsules could then be injected in patients to start producing specific drugs. This technique would produce artificial organs of relatively small size (in the range of 250 to 500 microns). The program includes both planned space and parabolic aircraft flights. As a part of the program, a KC-135 parabolic flight was carried out in early February '87. The experiment dealt with the testing of the critical technology of concentric drop generation and dynamic under microgravity. An experimental hardware permitting the growth of composite drops of approximately 8 mm in diameter was produced. A concentric injector device was created and tested. In the apparatus the fluids are pushed through valves controlling their flow rates. The drops are then recorded on 8 mm video and 35 mm still cameras. The cameras are placed perpendicularly to each other in order to record specific dynamics modes. The still camera uses the black-lighting technology. An electronic circuit assists in controlling the experiment. The flight permitted a microgravity environment for a period of less than 20 seconds. Because the experimental hardware was secured to the deck of the aircraft during flight, more vibrations and g-jitter than anticipated were observed, although because of the nature of the experiment these induced motions did not have a significant effect on the results. Author

N89-17043# Electrofuels Mfg. Co., Toronto (Ontario).
THE DESIGN OF A HEAT-PIPE FURNACE FOR MICROGRAVITY
C. B. Alcock, S. DasGupta, J. K. Jacobs, and M. Machler *In* National Research Council of Canada, Workshop on Microgravity Experimentation in Aircraft and Rockets 1988 p 131-134 (For primary document see N89-17019 09-29)
Avail: NTIS HC A07/MF A01; also available from Publication

Sales and Distribution, National Research Council of Canada, Ottawa, ON, Canada K1A OR6

An industrially important measurement of the growth kinetics of iron sulphide particles in a molten salt matrix (LiCl/KCl) requires microgravity and extreme isothermality at 480 C. After review of a number of standard techniques for isothermal furnaces, a novel design based on the use of evapdration/condensation heat transport was developed and tested. Effective thermal equalization over the surface of a furnace requires high thermal conductivity. To evaporate a liquid, the heat of vaporization must be supplied; to condense a vapor, the heat of vaporization must be removed. A liquid with an appropriate vapor pressure over the required temperature range and a means of containing that liquid constitute a heat pipe. For the temperature range between 350 C and 1100 C, liquid alkali metals (sodium and potassium) in an inconel container are the best choice. Author

N89-17044# National Research Council of Canada, Ottawa (Ontario).
DEVELOPMENT OF A PORTABLE PHYSIOLOGICAL MONITORING SYSTEM FOR THE KC-135: THE S.F.U. BIOPACK Abstract Only **c52**
I. B. Mekjavic, M. Frank, P. J. Sullivan, B. Trygvasson, R. Thirsk, and R. Hesselgrave (Defence and Civil Inst. of Environmental Medicine, Downsview, Ontario) *In its* Workshop on Microgravity Experimentation in Aircraft and Rockets 1988 p 135 (For primary document see N89-17019 09-29)
Avail: NTIS HC A07/MF A01; also available from Publication Sales and Distribution, National Research Council of Canada, Ottawa, ON, Canada K1A OR6

Alterations in the magnitude and direction of the gravitational vector, as induced in the KC-135 aircraft during parabolic flight maneuvers, induces motion sickness, characterized by a number of physiological responses affecting mainly the cardiovascular, respiratory, gastrointestinal, renal, thermoregulatory, visual and behavioral systems. Despite extensive investigations in land-based laboratories to document the pattern of these responses and their interaction, the etiology of motion sickness remains unresolved. The physiological data available from astronauts during prolonged sojourns in space and during brief exposures to a microgravity environment as experienced on the KC-135, are unfortunately subjective, observational and rather sparse. Author

N89-17045*# National Aeronautics and Space Administration, Washington, DC.
MICROGRAVITY SCIENCE AND APPLICATIONS BIBLIOGRAPHY, 1988 REVISION
Jan. 1989 75 p Prepared in cooperation with USRA, Washington, DC
(Contract NASw-4174)
(NASA-TM-4098; NAS 1.15:4098) Avail: NTIS HC A04/MF A01 CSCL 22A

The Microgravity Science and Applications (MSA) Bibliography is a compilation of government reports, contractor reports, conference proceedings, and journal articles dealing with flight experiments utilizing a low-gravity environment to elucidate and control various processes or with ground-based activities that provide supporting research. It encompasses literature published but not cited in the 1984 Revision and the literature which was published in the past year. Subdivisions of the bibliography include: electronic materials; metals, alloys, and composites; fluid dynamics and transports; biotechnology; glass and ceramics; and combustion. Also included are publications from the European, Soviet, and Japanese MSA programs. In addition, there is a list of patents and appendices providing a compilation of anonymously authored collections of reports and a cross reference index. Author

N89-17046*# National Aeronautics and Space Administration. Lewis Research Center, Cleveland, OH.
BEHAVIOR IN NORMAL AND REDUCED GRAVITY OF AN ENCLOSED LIQUID/GAS SYSTEM WITH NONUNIFORM HEATING FROM ABOVE
H. D. Ross, D. N. Schiller, P. Disimile, and W. A. Sirignano Jan. 1989 12 p Presented at the 27th Aerospace Sciences Meeting, Reno, NV, 9-12 Jan. 1989; sponsored in part by AIAA Prepared in cooperation with California Univ., Irvine; and Cincinnati Univ., OH
(NASA-TM-101471; E-4585; NAS 1.15:101471) Avail: NTIS HC A03/MF A01 CSCL 12A

The temperature and velocity fields have been investigated for a single-phase gas system and a two-layer gas-and-liquid system enclosed in a circular cylinder being heated suddenly and nonuniformly from above. The transient response of the gas, liquid, and container walls was modelled numerically in normal and reduced gravity (10 to the -5 g). Verification of the model was accomplished via flow visualization experiments in 10 cm high by 10 cm diameter plexiglass cylinders. Author

31 ENGINEERING (GENERAL)

Includes vacuum technology; control engineering; display engineering; cryogenics; and fire prevention.

N89-17047# Joint Publications Research Service, Arlington, VA.
JPRS REPORT: SCIENCE AND TECHNOLOGY. JAPAN. DEVELOPMENTS IN MANUFACTURING PROCESS TECHNOLOGY
8 Jul. 1988 121 p Transl. into ENGLISH of Kikai To Kogu (Tokyo, Japan), Jan. 1988 78 p
(JPRS-JST-88-010) Avail: NTIS HC A06/MF A01

Topics addressed include: ceramics processing; fiber reinforced plastic cutting technology; hard material cutting technology; electric discharge method; brittle material processing; use of cataphoresis effect; ultrasonic vibration; laser beam heat method; and microdrilling using electron beams. For individual titles, see N89-17048 through N89-17055.

N89-17048# Joint Publications Research Service, Arlington, VA.
FRP (FIBER REINFORCED PLASTICS) CUTTING TECHNOLOGY REPORTED
Noboru Iijima *In its* JPRS Report: Science and Technology. Japan. Developments in Manufacturing Process Technology 8 Jul. 1988 p 21-31 Transl. into ENGLISH from Kikai To Kogu (Tokyo, Japan), Jan. 1988 p 26-31 (For primary document see N89-17047 09-31)
Avail: NTIS HC A06/MF A01

The effectiveness of the oscillating cutting method for fiber reinforced plastics (FRP) is described through a comparison of normal cutting and oscillation cutting from the standpoint of cutting properties, such as cutting resistance and finished surface roughness, based on the research applying oscillation cutting to FRP processing. Author

N89-17049# Joint Publications Research Service, Arlington, VA.
HARD MATERIAL CUTTING TECHNOLOGY DESCRIBED
Takeaki Kitagawa and Katsuhiro Maekawa *In its* JPRS Report: Science and Technology. Japan. Developments in Manufacturing Process Technology 8 Jul. 1988 p 32-45 Transl. into ENGLISH from Kikai To Kogu (Tokyo, Japan), Jan. 1988 p 32-39 (For primary document see N89-17047 09-31)
Avail: NTIS HC A06/MF A01

A description was given for modifying an argon gas arc welding machine into a plasma hot machining unit with relative ease. As application examples of this method, ultrahard cutting-resistant materials, such as high manganese steel and chilled cast iron and ceramics, and highly brittle cutting-resistant materials, especially silicon nitride, were electively taken up to study changes in their machining resistance, tool wear, chip configuration, and finished surface roughness in plasma hot machining. It was also shown that, in the machining of carbon steel, application under such machining conditions as those that produce a builtup edge is effective in improving tool wear. Author

N89-17050# Joint Publications Research Service, Arlington, VA.
ELECTRIC DISCHARGE METHOD FOR CERAMICS REPORTED

Masanori Yoshikawa *In its* JPRS Report: Science and Technology. Japan. Developments in Manufacturing Process Technology 8 Jul. 1988 p 46-61 Transl. into ENGLISH from Kikai To Kogu (Tokyo, Japan), Jan. 1988 p 40-47 (For primary document see N89-17047 09-31)
Avail: NTIS HC A06/MF A01

Reports were made that electric discharge grinding composite processing is effective not only for metallic materials but also for ceramics, which are bad conductors, but they tend to lack persuasive power because the mechanism is not clear. In studying the mechanism of this processing method, it is necessary to consider everything from the fact that the method uses an electrolytic solution as a processing fluid to the effects of the electric discharge processing phenomenon on ceramics in the electrolytic solution. In order to explain the mechanism of electric discharge grinding composite processing of fine ceramics, the electric discharge processing phenomenon was studied on alumina, silicon nitride, and zirconia using an acrylic resin rotational tool containing no abrasive and one using a nonconducting vitrified diamond grinder equipped with a discharge electrode. Based on these studies involving the mechanism of ceramics removal with electric discharge, the electric discharge grinding composite processing of ceramics is discussed. Author

N89-17051# Joint Publications Research Service, Arlington, VA.
BRITTLE MATERIAL PROCESSING REPORTED
Koichi Hatano *In its* JPRS Report: Science and Technology. Japan. Developments in Manufacturing Process Technology 8 Jul. 1988 p 62-70 Transl. into ENGLISH from Kikai To Kogu (Tokyo, Japan), Jan. 1988 p 48-53 (For primary document see N89-17047 09-31)
Avail: NTIS HC A06/MF A01

Currently there is a problem involving the processing of new materials, such as fine ceramics and composite materials. These materials have their own old and new histories. The materials are characterized as materials with super hardness that are extremely difficult to process. The development of a fine ceramic engine has triggered the advancement of the ultrasonic processing method, enabling the processing of ceramics. Shibayama Machinery Corporation handles the products of the international recognized Branson Sonic Power, Inc. The processing, examples, and machinery are discussed. Author

N89-17052# Joint Publications Research Service, Arlington, VA.
USE OF CATAPHORESIS EFFECTS DISCUSSED
Toshiji Kurobe *In its* JPRS Report: Science and Technology. Japan. Developments in Manufacturing Process Technology 8 Jul. 1988 p 71-85 Transl. into ENGLISH from Kikai To Kogu (Tokyo, Japan), Jan. 1988 p 54-60 (For primary document see N89-17047 09-31)
Avail: NTIS HC A06/MF A01

With the appearance of information machines and precision devices, higher processing accuracy of machinery parts accompanying such machines and devices was strongly demanded. Sometimes processing accuracy on the submicron order is demanded. In the case of materials used for electronic parts, not only must the geometric configurations, such as shape accuracy and surface accuracy, be perfect, but also the creation of an almost perfect face from a crystallographic viewpoint is demanded. In order to respond to diversified needs for the present processing techniques, processing methods free from traditional approaches originating from ideas are being pursued more and more. Among electric and magnetic field-assisted fine finishing techniques, a finishing technique utilizing a cataphoresis phenomenon which claims an electric field is going to be discussed. The finishing method utilizing a field is characterized by the finishing processing that can be electromagnetically controlled, and finishing processing for free surfaces is possible to a certain extent. Author

N89-17053# Joint Publications Research Service, Arlington, VA.
ULTRASONIC VIBRATION METHOD DISCUSSED
Nagao Saito *In its* JPRS Report: Science and Technology. Japan. Developments in Manufacturing Process Technology 8 Jul. 1988 p 86-94 Transl. into ENGLISH from Kikai To Kogu (Tokyo, Japan), Jan. 1988 p 61-65 (For primary document see N89-17047 09-31)
Avail: NTIS HC A06/MF A01

As a result of the discharge finishing processing test giving ultrasonic vibration to the electrode for discharge processing, the following was determined. The processing efficiency is improved by the scavenging effect of ultrasonic vibration, and it is futher improved since the electrode descending time, t sub D, during the discharge stabilizing action can be extended. It is also effective with an amplitude of + or - 1 micrometer. The roughness of the finished surface is slightly improved compared with that of the ordinary mirror finish processing when the bath servo voltage and ultrasonic vibration amplitude that do not produce ultrasonic hammering are selected. It is preferable to adequately control the distance between electrodes and the ultrasonic vibration amplitude utilizing the voltage current waveforms between electrodes. The problem in this processing method involves how to vibrate the electrode of an optimal shape, and work is being done to establish this method. Author

N89-17054# Joint Publications Research Service, Arlington, VA.
LASER BEAM HEAT METHOD REPORTED
Hachiro Tsuchiya and Hidekazu Goto *In its* JPRS Report: Science and Technology. Japan. Developments in Manufacturing Process Technology 8 Jul. 1988 p 95-103 Transl. into ENGLISH from Kikai To Kogu (Tokyo, Japan), Jan. 1988 p 66-70 (For primary document see N89-17047 09-31)
Avail: NTIS HC A06/MF A01

An outline of research involving the processing method utilizing laser-induced thermochemistry was presented, with the CO2 laser processing of ceramics in CF4 gas used as a practical processing example. It has become clear that it will be possible to conduct laser proccessing of ceramics with high efficiency and high precision by utilizing the thermochemical processes, but it is not believed that the present method is the best one and it is not clear that it can be applied to commercial processing. It is thought that the processing characteristics of this method will be greatly changed by the combination of the atmospheric gas and the material, and it is important to conduct tests on various combinations. However, it is believed that the improvement and development will become possible by theoretically confirming the basic process of the processing, especially of the the thermochemical process between the solid surface and the atmospheric gas molecule. Actually, it is believed that the thermochemical process on the solid surface is quite complicated. For example, it was confirmed that when thermochemical processing the Si monocrystal in the CF4 gas, the processing speed would change by at least 10 times through changing the gas pressure and the mixing O2 gas density. However, conversely speaking, it is believed that the fact that this method is complicated, with many unexplained points and room for research, conceals the possibility of its being applied to various fields, and also, in this sense, the quantitative confirmation of its basic process in an important problem to be solved in the future. Author

N89-17055# Joint Publications Research Service, Arlington, VA.
MICRODRILLING USING ELECTRON BEAMS REPORTED
Megumi Omine *In its* JPRS Report: Science and Technology. Japan. Developments in Manufacturing Process Technology 8 Jul. 1988 p 104-118 Transl. into ENGLISH from Kikai To Kogu (Tokyo, Japan), Jan. 1988 p 71-78 (For primary document see N89-17047 09-31)
Avail: NTIS HC A06/MF A01

The concept of pulsed electron beam working, specifically, drilling, an outline of the technique for such working, and examples of applications of the technique were described. The technique may soon be put to use for PC board drilling and other applications and it may possibly contribute toward innovating various manufacturing processes. The important targets to be achieved in the future utilizing this technique include developing measures to prevent the electron beam from being scattered by vapor and to prevent the vaporized material from being redeposited over the

area around the point of working. With regard to the hardware needed to practice this technique, it is considered necessary to develop electron gun systems which can converge beams into smaller spots than presently possible in order to meet the needs for increasingly fine fabrication processes. Author

N89-17056 ESDU International Ltd., London (England).
EFFECTIVENESS: N(SUB TU) RELATIONSHIPS FOR THE DESIGN AND PERFORMANCE EVALUATION OF ADDITIONAL SHELL-AND-TUBE HEAT EXCHANGER GEOMETRIES
Nov. 1988 106 p
(ESDU-88021; ISBN-0-85679-653-0; ISSN-0141-402X) Avail: ESDU

This Data Item 88021, an addition to the Sub-series on Heat Transfer, complements ESDU 86018 by extending the range of configurations covered there and in particular considering the effect of using small numbers of baffles for E- and J-shells and the use of J-shells in series. It also explores the limitations of the assumptions associated with the effectiveness - N(sub TU) method and shows where those assumptions break down. The curves presented for each exchanger geometry show the locus of designs for which a temperature cross may occur and the locus of 95 percent heat transfer effectiveness which indicates the region of uneconomic design. The method assumes a linear temperature/enthalpy relationship (constant specific heat capacity) for both streams. It applies to boiling or condensing flow of a single component with no temperature change, or boiling and condensing flow of a mixture that is always two-phase. It excludes conditions in which transition from single- to two-phase flow occurs. However, by use of average property values, it is possible to extend the method to apply to cases where there is some variation of physical and thermodynamic properties with temperature. ESDU

N89-17057 ESDU International Ltd., London (England).
FOULING IN COOLING WATER SYSTEMS
Nov. 1988 53 p
(ESDU-88024; ISBN-0-85679-656-5; ISSN-0141-4062) Avail: ESDU

This Data Item 88024, an addition to the Sub-series on Heat Transfer, considers scaling, corrosion, biofouling and particulate deposition and discusses the variables of importance for each. Advice is given on the design and subsequent operational management of a plant to minimize fouling. The importance of the water source, and hence its composition, is emphasised. Test equipment for assessing fouling is described. A table of heat transfer fouling resistances, showing their depemdence on temperature, water velocity, material and water treatment applied, will be of particular value. Various means of fouling control are considered, using chemicals and biocides as appropriate. The properties of biocides currently used in industrial applications are discussed. On-line mechanical cleaning methods are also considered. ESDU

N89-17058*# Texas A&M Univ., College Station. Dept. of Aerospace Engineering.
SUBSELENEAN TUNNELER MELTING HEAD DESIGN: A PRELIMINARY STUDY
Bill Engblom, Eric Graham, Jeevan Perera, Alan Strahan, and Ted Ro May 1988 129 p
(Grant NGT-21-002-080)
(NASA-CR-184750; NAS 1.26:184750) Avail: NTIS HC A07/MF A01 CSCL 13B

The placement of base facilities in subsurface tunnels created as a result of subsurface mining is described as an alternative to the establishing of a base on the lunar surface. Placement of the base facilities and operations in subselenean tunnels will allow personnel to live and work free from the problem of radiation and temperature variations. A conceptual design for a tunneling device applicable to such a lunar base application was performed to assess the feasibility of the concept. A tunneler was designed which would melt through the lunar material leaving behind glass lined tunnels for later development. The tunneler uses a nuclear generator which supplies the energy to thermally melt the regolith about the cone shaped head. Melted regolith is exacavated through intakes in the head and transferred to a truck which hauls it to the surface. The tunnel walls are solidified to provide support lining by using an active cooling system about the mid section of the tunneler. Also addressed is the rationale for a subselenean tunneler and the tunneler configuration and subsystems, as well as the reasoning behind the resulting design. Author

32 COMMUNICATIONS AND RADAR

Includes radar; land and global communications; communications theory; and optical communications.

For related information see also *04 Aircraft Communications and Navigation* and *17 Space Communications, Spacecraft Communications, Command and Tracking.* For search and rescue see *03 Air Transportation and Safety,* and *16 Space Transportation.*

N89-17059 New South Wales Univ., Kensington (Australia).
THE DESIGN, ANALYSIS, AND IMPLEMENTATION OF A FULLY DISTRIBUTED LOCAL AREA NETWORK FOR INTEGRATED VOICE AND DATA COMMUNICATIONS Ph.D. Thesis
Gary J. Anido Nov. 1987 2 p
Avail: Issuing Activity

A theoretical and experimental investigation into the integration of packetized voice and data onto a local area network is presented which concentrates on a class of LAN integrating voice and data by means of service cycles. Examples of such networks include Expressnet, Fasnet, the Zurich ring, and Welnet. Fundamental differences between these networks involve the way service cycles are controlled. In each case, however, cycles are initiated from a fixed location. One consequence is an inherent unfairness to both voice and data. Contrasted against these networks is XLNET, a distributed network designed for the purposes of the investigation. XLNET is novel in that cycles are initiated from a location which varies under the applied load. The performance of cyclic service networks, including XLNET, are compared. A simplified queuing model is solved exactly to yield closed form expressions for the transform of queue length distribution, and mean queue length. The results are compared with known exact solutions and good agreement is observed. Additionally, advantage is taken of the closed form nature by comparison with a number of approximation techniques. Author

N89-17060*# Westinghouse Electric Corp., Baltimore, MD.
PROPAGATION EFFECTS HANDBOOK FOR SATELLITE SYSTEMS DESIGN. A SUMMARY OF PROPAGATION IMPAIRMENTS ON 10 TO 100 GHz SATELLITE LINKS WITH TECHNIQUES FOR SYSTEM DESIGN
Louis J. Ippolito Washington, DC Feb. 1989 531 p
(Contracts NAS7-100; JPL-958178)
(NASA-RP-1082(04); NAS 1.61:1082(04)) Avail: NTIS HC A23/MF A01 CSCL 20N

The NASA Propagation Effects Handbook for Satellite Systems Design provides a systematic compilation of the major propagation effects experienced on space-Earth paths in the 10 to 100 GHz frequency band region. It provides both a detailed description of the propagation phenomenon and a summary of the impact of the effect on the communications system design and performance. Chapter 2 through 5 describe the propagation effects, prediction models, and available experimental data bases. In Chapter 6, design techniques and prediction methods available for evaluating propagation effects on space-Earth communication systems are presented. Chapter 7 addresses the system design process and how the effects of propagation on system design and performance should be considered and how that can be mitigated. Examples of operational and planned Ku, Ka, and EHF satellite communications systems are given. Author

N89-17061 British Broadcasting Corp., Kingswood (England). Engineering Div.
THE VISIBILITY OF NOISE IN SYSTEM 1 COLOUR TELEVISION
A. Oliphant, K. J. Taylor, and N. T. Misson Nov. 1988 19 p (BBC-RD-1988/12; EL-194) Avail: BBC. Kingswood Warren, Tadworth, Surrey, United Kingdom

A series of subjective tests was carried out in 1986 using various levels of white noise and de-emphasized triangular noise added to baseband video signals. It was later pointed out that the form of noise that is of interest in planning the service areas of transmitters arise from vestigial-sideband demodulation of a television signal (VSB noise). This form of noise has a spectrum which is flat above 1.25 MHz but is 3 dB lower at low frequencies. Because high frequency is less visible than low frequency noise, it would be expected that VSB noise would cause less impairment than white noise for the same signal-to-noise ratio. Previously published work has not considered VSB noise (its effects have been inferred from results for white noise by applying an assumed weighting factor); a second series of tests was therefore arranged to investigate VSB noise, with a few values of white noise and de-emphasized triangular noise included for comparison with the first series of tests. This comparison showed very close consistency between the two series of tests, allowing the results of the two series of test to be compared directly. The results of both series of tests are given and compared with previously published work. Author

N89-17062# Naval Ocean Systems Center, San Diego, CA.
ARRAY PROCESSING FOR A MULTIPLE-RANK SIGNAL Final Report, Oct. 1987 - Apr. 1988
David J. Edelblute May 1988 14 p
(AD-A197954; NOSC/TD-1262) Avail: NTIS HC A03/MF A01 CSCL 17H

Array processing is considered for a sensor array when the signal is composed of a superposition of wave fronts. The array processing requires a multiple-signal parameter formulation. Existing array processing theory is generalized. The required signal processing functions should not be referred to as beam forming, because a matrix estimation operator is required. The rank of the estimation operator is greater than 1. GRA

N89-17063# Mitre Corp., Bedford, MA.
VECTOR SPACE APPROACH TO NARROWBAND INTERFERENCE EXCISION Final Report
Ralph F. Guertin Jul. 1988 127 p
(Contract F19628-86-C-0001)
(AD-A199703; MTR-10289; ESD-TR-88-266) Avail: NTIS HC A07/MF A01 CSCL 25E

To realize the full performance advantage of a pseudonoise spread-spectrum communication system, a receiver must suppress strong narrowband interferers. Conventional frequency-domain excision techniques are complicated by spreading effects due to the sidelobes of the sin(x)/x function. This paper shows that such problems can be avoided by regarding the N samples of a band-limited times series and its finite Fourier transform as a vector in an N-dimensional space. Narrowband interference can be suppressed by projecting the data vector onto the subspace orthogonal to the one that best fits the interference. The theory developed here includes a least squares criterion for finding this subspace. GRA

N89-17064# Environmental Research Inst. of Michigan, Ann Arbor. Radar Science Lab.
INSTRUMENTATION FOR THE CHARACTERIZATION OF THE MICROWAVE PROPERTIES AT 18, 35 AND 94 GHz Final Report, Aug. 1985 - Jul. 1988
Robert G. Onstott and Richard W. Larson 1 Aug. 1988 34 p
(Contract N00014-81-C-0692)
(AD-A199741; ERIM-155900-65-F) Avail: NTIS HC A03/MF A01 CSCL 17I

The Earth Resources Millimeter-Wave Radar (ERMIR) has been developed to characterize the microwave properties of Earth scenes at 18, 35, and 94 GHz. This instrument operates in either the continuous-wave or frequency-modulated continuous-wave modes and may be used to measure reflectivity, transmissivity, backscatter, and bistatic scattering. The development and construction of this instrument was guided by the need to acquire these parameters in situ and in remote locations. GRA

N89-17065# Ecole Nationale Superieure des Telecommunications, Paris (France). Dept. Informatique.
APPLICATIONS OF CORRECTING CODING THEORY TO COMMUNICATION COMBINATORIAL PROBLEMS
Gerard D. Cohen Jul. 1988 19 p Revised Submitted for publication
(ENST-88C001; ISSN-0751-1337; ETN-89-93620) Copyright Avail: NTIS HC A03/MF A01

The use of techniques borrowed from coding theory for solving combinatorial questions originating in communication problems is reviewed. Conflict resolution with feedback in multiple access channels, coding for memories with defects, and writing on reluctant memories are discussed. ESA

N89-17066# Naval Postgraduate School, Monterey, CA.
EFFECTS OF IRREGULAR SEA SURFACE AND EVAPORATION DUCT ON RADAR DETECTION PERFORMANCE M.S. Thesis
Moshe Marom Jun. 1988 94 p
(AD-A200114) Avail: NTIS HC A05/MF A01 CSCL 17I

The detection performance of microwave search radars operating in close proximity to the sea surface is evaluated. The effects of media characteristics on the propagation of electromagnetic waves have been incorporated. Specular and diffused scattering from a rough surface, and the effects of the curvature of the earth's surface have been included in the study. Additionally, surface ducting effects caused by atmospheric anomalies are presented. Some design and operational considerations which can improve the detection performance of a surface search radar, are also presented. GRA

N89-17067# Defence Research Establishment Atlantic, Dartmouth (Nova Scotia).
FREQUENCY ESTIMATION OF RADAR SIGNALS USING AN ACOUSTO-OPTIC SPECTRUM ANALYZER AS AN RESM (RADAR ELECTRONIC SUPPORT MEASURES) RECEIVER
Guy Farley Jun. 1988 38 p
(AD-A200159; DREO-TN-88-19) Avail: NTIS HC A03/MF A01 CSCL 17I

In this report we present a statistical model for the signals of an acousto-optic spectrum analyzer (AOSA). Using the model, we calculate the Cramer-Rao bound for the estimation of the carrier frequency of radar signals and the performance of the peak detector estimator. We also present an algorithm for sidelobe rejection. GRA

N89-17068# Naval Research Lab., Washington, DC. Ionospheric Effects Branch.
A TECHNIQUE FOR RECORDING HF (HIGH FREQUENCY) OBLIQUE-INCIDENCE-SOUNDER DATA Interim Report
Mark Daehler 30 Aug. 1988 40 p
(AD-A200168; NRL-MR-6269) Avail: NTIS HC A03/MF A01 CSCL 20N

This report details the equipment, formats, and procedures developed for recording and displaying HF propagation data produced by the AN/TRQ-35 RCS-4B oblique-incidence sounder receiver. The information is being published in this form because of numerous requests regarding a means for using the large volume of sounder data accumulated by NRL in the course of its ionospheric effects studies. These techniques may ultimately be incorporated in a proposed worldwide database of ionospheric data. The AN/TRQ-35 sounder equipment is available to all branches of the DOD and is widely used for near-real-time HF frequency management. The data it produces, if properly recorded and stored, can also be used for numerous other purposes related to studies of ionospheric structure and HF skywave

communications. These include studies of the electron density versus height profile of the ionosphere; of forecasts of propagation conditions relevant to HF communications; of the geographical and temporal limitations of sounder data application; and of the effectiveness of frequency management techniques. Permanent records of ionospheric propagation have also proved valuable in evaluating tests of HF devices which are dependent on ionospheric propagation, such as communications transmitters and receivers, or direction finding equipment. GRA

N89-17069# Air Force Weapons Lab., Kirtland AFB, NM.
FIELD ENHANCEMENT OF UHF-VHF AIRCRAFT ANTENNAS Final Report, 16 Oct. - 18 Nov. 1986
Raymond W. Nethers, David W. Metzger, and Albert B. Griffin Aug. 1988 11 p
(AD-A200180; AFWL-TR-88-41) Avail: NTIS HC A03/MF A01 CSCL 09A

Results of high voltage electrical discharge tests of various electrode enhancement geometries are reported along with test conduct. Four antennas (collins, unknown 2- and 3-ft rods) were tested with both positive and negative voltages. It was found that on the negative electrode in large gaps, a large enhancement is needed to degrade the gap holdoff. GRA

N89-17070# Delaware Univ., Newark. Dept. of Mathematical Sciences.
FAR FIELD PATTERNS AND THE INVERSE SCATTERING PROBLEM FOR ELECTROMAGNETIC WAVES IN AN INHOMOGENEOUS MEDIUM
David Colton and Lassi Paivarinta 1988 16 p
(Grant AF-AFOSR-0087-86; AF Proj. 2304)
(AD-A200223; AFOSR-88-1132TR) Avail: NTIS HC A03/MF A01 CSCL 20N

We consider the scattering of time harmonic electromagnetic waves by an inhomogeneous medium of compact support. It is first shown that the set of far field patterns of the electric fields corresponding to incident plane waves propagating in arbitrary directions is complete in the space of square integrable tangential vector fields defined on the unit sphere. We then show that under certain conditions the electric far field patterns satisfy an integral identity involving the unique solution of a new class of boundary value problems for Maxwell's equations called the interior transmission problem for electromagnetic waves. Finally, it is indicated how this integral identity can be used to formulate an optimization scheme yielding an optimal solution of the inverse scattering problem for electromagnetic waves. GRA

N89-17071# Army Engineer Topographic Labs., Fort Belvoir, VA.
IMPROVING CLASSIFICATION ACCURACY OF RADAR IMAGES USING A MULTIPLE-STAGE CLASSIFIER Research Note, Jun. - Dec. 1984
Neil D. Fox and Pi-Fuay Chen Sep. 1988 25 p
(AD-A200291; ETL-0502) Avail: NTIS HC A03/MF A01 CSCL 17I

A simple method was introduced to classify radar image samples repeatedly for achieving a higher accuracy than by using a single-stage classifier. A Sobel edge operator was applied between the stages of classification to enhance the difference in texture between categories of radar image samples, thus reducing the overlap of image categories. GRA

N89-17072# Houston Univ., TX. Electromagnetics Lab.
JUNCTION CODE USER'S MANUAL. ELECTROMAGNETIC SCATTERING AND RADIATION BY ARBITRARY CONFIGURATIONS OF CONDUCTING BODIES AND WIRES Final Report, Oct. - Dec. 1987
D. R. Wilton and Shian-Uei Hwu Aug. 1988 202 p
(Contract N66001-85-D-0203)
(AD-A200315; TR-87-18; NOSC/TD-1324) Avail: NTIS HC A10/MF A01 CSCL 20N

The report gives a brief description of the computer program JUNCTION which results from the application of numerical procedures. The program invokes the method of moments to solve a coupled electric field integral equation for the currents induced on an arbitrary configuration of perfectly conducting bodies and wires. An important feature of the code is its ability to treat wire-to-wire, surface-to-surface, and wire-to-surface junctions. Wires may be connected to surfaces at essentially arbitrary angles and may be attached to surface edges or vertices. Results obtained using this algorithm are in the form of electric current and charge densities and far field patterns. This report gives a brief description of the computer program JUNCTION which results from application of numerical procedures. GRA

N89-17073# Michigan Univ., Ann Arbor. Communications and Signal Processing Lab.
CAPACITY OF FREQUENCY-HOP SPREAD-SPECTRUM MULTIPLE-ACCESS COMMUNICATION SYSTEMS
M. V. Hegde (Louisiana State Univ., Baton Rouge.) and W. E. Stark Oct. 1988 39 p
(Contract N00014-85-K-0545)
(AD-A200616; Rept-262) Avail: NTIS HC A03/MF A01 CSCL 25E

The information theoretic capacity of frequency-hop spread-spectrum multiple-access communication is considered. In order to account for independent encoding and decoding and private (to the sender and receiver) hopping patterns an interference channel model is adopted with K sender-receiver pairs with the i-th receiver only interested in the message transmitted by the i-th sender. Both synchronous and asynchronous hopping patterns are investigated. Although the channel exhibits memory in the case, we are able to compute the capacity region. The asymptotic normalized sum capacity is also computed. GRA

N89-17074# Ecole Nationale Superieure des Telecommunications, Paris (France).
STUDY OF ERROR CORRECTING CODES FOR HERTZIAN CHANNELS WITH A LARGE NUMBER OF STATES. APPLICATION TO QUADRATURE AMPLITUDE MODULATION (QAM) 64 Ph.D. Thesis [ETUDE DES CODES CORRECTEURS D'ERREURS POUR FAISCEAUX HERTZIENS A GRAND NOMBRE D'ETATS. APPLICATION AU MAQ 64]
Pierre-Francois Kamanou May 1988 166 p In FRENCH; ENGLISH summary
(ENST-88E007; ISSN-0751-1353; ETN-89-93626) Avail: NTIS HC A08/MF A01

Error correcting codes applicable to high reliability systems are studied. The main statistical characteristics of these codes are discussed. The analysis includes Ungerboeck, self orthogonal convolutive and Lee Nakamura block coding procedures. In all cases the choice of code and their parameters is guided by the available band width and by the conditions imposed by the frame structure. ESA

N89-17075# Army Tank-Automotive Command, Warren, MI.
ROBOTIC VEHICLE COMMUNICATIONS INTEROPERABILITY Final Report, Dec. 1987 - Aug. 1988
Daniele Mariani Aug. 1988 93 p
(TACOM-TR-13387) Avail: NTIS HC A05/MF A01 CSCL 17B

Communications Interoperability (CI) amongst different robotic vehicle systems would provide many benefits to the robotics development and user communities. This report takes a first step towards CI by proposing protocols for a communications interface standard for robotic vehicle communication systems. Author

N89-17076# Lawrence Livermore National Lab., CA.
MODELING THE PROPAGATION OF LONG INTENSE MICROWAVE PULSES IN MIXTURES OF AIR AND SF6
G. H. Khanaka, J. H. Yee, and D. J. Mayhall 14 Oct. 1988 13 p Presented at the 4th National High Power Microwave Conference, Monterey, CA, 9-12 May 1988 Submitted for publication
(Contract W-7405-eng-48)
(DE89-004787; UCRL-97840; CONF-8805132-12) Avail: NTIS HC A03/MF A01

We have used a set of self-consistent equations---Maxwell's equations and the electron fluid transport equations---to study the interaction of long intense microwave pulses with gases. In this interaction, the final shape of the transmitted pulse at breakdown is independent of the pulse length. We found that the threshold for breakdown is a factor of 7 higher in SF6 than in air. This difference we attribute to the fact that SF6 is an insulator. When SF6 was mixed with air, the breakdown threshold increased with the increase in the percentage of SF6. Introducing 5--10 percent of SF6 in air increased the breakdown threshold by a factor of 3--4. The electron density and conductivity and the plasma frequency increased as the pulse intensity increased. The growth rates of the electron density and conductivity were much higher in air than in SF6. DOE

N89-17077*# Michigan Univ., Ann Arbor. Dept. of Electrical Engineering and Computer Science.
SCATTERING BY A TWO DIMENSIONAL GROOVE IN A GROUND PLANE Technical Report, Sep. 1988 - Feb. 1989
K. Barkeshli and J. L. Volakis Feb. 1989 35 p
(Grant NAG2-541)
(NASA-CR-183087; NAS 1.26:183087; UM-Rept-025921-2-T)
Avail: NTIS HC A03/MF A01 CSCL 20N

Higher order boundary conditions involve derivatives of the fields beyond the first and were recently shown to be more effective than traditional first order conditions in modeling dielectric coatings and layers. In this report an application of a third order generalized boundary condition to scattering by a filled rectangular groove is presented. Deficiencies of such higher order boundary conditions are addressed and a correction is proposed for the present case. As part of the process of examining and improving the accuracy of the proposed generalized boundary conditions, an exact solution is developed and a comparison is provided with a solution based on the standard impedance boundary condition. Author

N89-17078*# Ford Aerospace and Communications Corp., Palo Alto, CA.
THE POTENTIAL IMPACT OF MMICS ON FUTURE SATELLITE COMMUNICATIONS Final Report, 1 Apr. 1987 - 31 Aug. 1988
Vernon E. Dunn Sep. 1988 133 p
(Contract NAS3-25077)
(NASA-CR-182227; NAS 1.26:182227) Avail: NTIS HC A07/MF A01 CSCL 17B

This is the Final Report representing the results of a 17-month study on the future trends and requirements of Monolithic Microwave Integrated Circuits (MMIC) for space communication applications. Specifically this report identifies potential space communication applications of MMICs, assesses the impact of MMIC on the classes of systems that were identified, determines the present status and probable 10-year growth in capability of required MMIC and competing technologies, identifies the applications most likely to benefit from further MMIC development and presents recommendations for NASA development activities to address the needs of these applications. Author

N89-17079*# Ford Aerospace and Communications Corp., Palo Alto, CA. Space Systems Div.
THE POTENTIAL IMPACT OF MMICS ON FUTURE SATELLITE COMMUNICATIONS: EXECUTIVE SUMMARY Final Report, 1 Apr. 1987 - 31 Aug. 1988
Vernon E. Dunn Sep. 1988 38 p
(Contract NAS3-25077)
(NASA-CR-182227-Exec-Summ; NAS 1.26:182227-Exec-Summ)
Avail: NTIS HC A03/MF A01 CSCL 17B

This Executive Summary presents the results of a 17-month study on the future trends and requirments for Monolithic Microwave Integrated circuits (MMIC) for space communication application. Specifically this report identifies potential space communication applications of MMICs, assesses the impact of MMIC on the classes of systems that were identified, determines the present status and probable 10-year growth in capability of required MMIC and competing technologies, identifies the applications most likely to benefit from further MMIC development, and presents recommendations for NASA development activities to address the needs of these applications. Author

33 ELECTRONICS AND ELECTRICAL ENGINEERING

Includes test equipment and maintainability; components, e.g., tunnel diodes and transistors; microminiaturization; and integrated circuitry.

For related information see also *60 Computer Operations and Hardware* and *76 Solid-State Physics.*

N89-17080# Optical Society of America, Washington, DC.
TOPICAL MEETING ON PICOSECOND ELECTRONICS AND OPTOELECTRONICS Final Report, 12 Jan. - 10 Oct. 1987
J. W. Quinn 10 Oct. 1987 213 p Meeting held in Incline Village, NV, 14-16 Jan. 1987; sponsored by AFOSR, IEEE, NSF, ONR, and Optical Society of America
(Grant AF-AFOSR-0181-87; AF Proj. 2306)
(AD-A189686; AFOSR-88-0152TR; IEEE-87TH0172-7; LC-86-063502; ISBN-0-936659-16-5) Avail: NTIS HC A10/MF A01 CSCL 09A

Topics addressed include: optoelectronic devices; semiconductor device physics; electronic devices; cryoelectronics; device fabrication technology; device characterization; and circuits and signal processing. For individual titles, see N89-17081 through N89-17139.

N89-17081# Bell Telephone Labs., Inc., Murray Hill, NJ.
A NON-CONTACT PICOSECOND PROBER FOR INTEGRATED CIRCUIT TESTING
J. A. Valdmanis and S. S. Pei *In* Optical Society of America, Topical Meeting on Picosecond Electronics and Optoelectronics 10 Oct. 1987 p 4-6 (For primary document see N89-17080 09-33)
Avail: NTIS HC A10/MF A01 CSCL 09A

A noncontact substrate-independent integrated circuit prober, based on electro-optic sampling, for internal node characterization of picosecond electrical waveforms at the water level, is described. Author

N89-17082# Stanford Univ., CA. Physics Lab.
PICOSECOND SAMPLING OF INTEGRATED CIRCUITS
M. J. W. Rodwell, K. J. Weingarten, and D. M. Bloom *In* Optical Society of America, Topical Meeting on Picosecond Electronics and Optoelectronics 10 Oct. 1987 p 7-9 (For primary document see N89-17080 09-33)
(Contract F49620-85-K-0016)
Avail: NTIS HC A10/MF A01 CSCL 09A

Electro-optic sampling provides wide bandwidth measurements of the internal voltages of GaAs ICs. The limitations to bandwidth and sensitivity are discussed, and the recent results presented. Author

N89-17083# IBM Watson Research Center, Yorktown Heights, NY.
PICOSECOND ELECTRICAL PULSES FOR VLSI ELECTRONICS CHARACTERIZATION
J.-M. Halbout, P. G. May, M. B. Ketchen, G. P. Li, C.-C. Chi, M. Scheuermann, and M. Smyth *In* Optical Society of America, Topical Meeting on Picosecond Electronics and Optoelectronics 10 Oct. 1987 p 10-1 (For primary document see N89-17080 09-33)
Avail: NTIS HC A10/MF A01 CSCL 09A

Picosecond electrical pulses are photoconductively generated and characterized on structures and materials compatible with silicon VLSI electronics. Author

N89-17084# Bell Telephone Labs., Inc., Holmdel, NJ.
ELECTRO-OPTIC SAMPLING OF HIGH-SPEED, InP-BASED INTEGRATED CIRCUITS

J. M. Wiesenfeld, R. S. Tucker, A. Antreasyan, C. A. Burrus, and A. J. Taylor (Los Alamos National Lab., NM.) *In* Optical Society of America, Topical Meeting on Picosecond Electronics and Optoelectronics 10 Oct. 1987 p 12-1 (For primary document see N89-17080 09-33)
Avail: NTIS HC A10/MF A01 CSCL 09A

Multigigahertz waveforms in an InGaAs/InP MISFET inverter circuit were samples noninvasively using pulses from a gain-switched InGaAsP laser. Propagation delays of 21 ps per MISFET stage were measured. Author

N89-17085# Bell Telephone Labs., Inc., Murray Hill, NJ.
MOLECULAR BEAM EPITAXY (MBE) FOR HIGH SPEED DEVICES
A. Y. Cho *In* Optical Society of America, Topical Meeting on Picosecond Electronics and Optoelectronics 10 Oct. 1987 p 16-1 (For primary document see N89-17080 09-33)
Avail: NTIS HC A10/MF A01 CSCL 09A

Recent development in molecular beam epitaxy pushes the frontier of devices to the ultimate imagination of device physicists and engineers. High-speed devices prepared with epitaxial superlattice structure or multiquantum wells and pseudomorphic strained layers are discussed. Author

N89-17086# Bell Telephone Labs., Inc., Murray Hill, NJ.
MULTIGIGAHERTZ LOGIC BASED ON InP-MISFET'S EXHIBITING EXTREMELY HIGH TRANSCONDUCTANCE
A. Antreasyan, P. A. Garbinski, V. D. Mattera, Jr., and H. Temkin *In* Optical Society of America, Topical Meeting on Picosecond Electronics and Optoelectronics 10 Oct. 1987 p 19-2 (For primary document see N89-17080 09-33)
Avail: NTIS HC A10/MF A01 CSCL 09A

High-speed logic at 5.0 GHz based on novel, enhancement mode InP metal-insulator-semiconductor field-effect transistors having a propagation delay of 25 ps/stage and transconductance of 320 mS/mm for agate length of 1 micrometer is reported. These measurements are the smallest propagation delay and the highest transconductance measured with a field-effect transistor or an InP substrate. Author

N89-17087# Lawrence Livermore National Lab., CA.
AN OPTICALLY STROBED SAMPLE AND HOLD CIRCUIT
Chuck McConaghy *In* Optical Society of America, Topical Meeting on Picosecond Electronics and Optoelectronics 10 Oct. 1987 p 22-2 (For primary document see N89-17080 09-33) (Contract W-7405-eng-48)
Avail: NTIS HC A10/MF A01 CSCL 09A

A GaAs sample and hold circuit with a 10 ps aperture time and 1 microsecond hold time was built and used to sample single shot signals. Author

N89-17088# Arizona Univ., Tucson. Optical Sciences Center.
HIGH-SPEED OPTICAL LOGIC USING GaAs
H. M. Gibbs, N. Peyghambarian, Y. H. Lee, J. L. Jewell, A. Migus, A. Antonetti, D. Hulin, and A. Mysyrowicz (Ecole Normale Superieure, Paris, France) *In* Optical Society of America, Topical Meeting on Picosecond Electronics and Optoelectronics 10 Oct. 1987 p 25-2 Sponsored in part by the Army Research Office, Washington, D.C. and NSF, Washington, D.C. (For primary document see N89-17080 09-33)
Avail: NTIS HC A10/MF A01 CSCL 09A

A bulk-GaAs nonlinear etalon can make a decision in approximately 1 ps and recover to make another in less than 100 ps, making possible high-speed optical logic. The status of bulk-GaAs etalons and their applications to high-speed optical logic is summarized. Author

N89-17089# Naval Research Lab., Washington, DC.
MILLIMETER-WAVE INTEGRATED CIRCUITS
Barry E. Spielman *In* Optical Society of America, Topical Meeting on Picosecond Electronics and Optoelectronics 10 Oct. 1987 p 30-3 (For primary document see N89-17080 09-33)
Avail: NTIS HC A10/MF A01 CSCL 09A

The technical issues, current research focal points, progress, and trends associated with GaAs and InP based monolithic millimeter-waves integrated circuit technology are summarized. Author

N89-17090# Varian Associates, Palo Alto, CA.
ENHANCED PERFORMANCE ULTRABROADBAND DISTRIBUTED AMPLIFIERS
G. Zdasiuk, M. Riaziat, R. LaRue, C. Yuen, and S. Bandy *In* Optical Society of America, Topical Meeting on Picosecond Electronics and Optoelectronics 10 Oct. 1987 p 33-3 (For primary document see N89-17080 09-33)
Avail: NTIS HC A10/MF A01 CSCL 09A

High-gain 2 to 20 GHz monolithic GaAs distributed amplifiers utilizing novel circuit approaches such as cascade-connected FETs and coplanar waveguide transmission lines are described. Preliminary results on a HEMT-based amplifier are also presented. Author

N89-17091# TRW Electronic Systems Group, Redondo Beach, CA.
HIGH PERFORMANCE QUARTER-MICRON-GATE MODFETS
John J. Berenz *In* Optical Society of America, Topical Meeting on Picosecond Electronics and Optoelectronics 10 Oct. 1987 p 37-3 (For primary document see N89-17080 09-33)
Avail: NTIS HC A10/MF A01 CSCL 09A

The latest results obtained with high performance quarter-micron-gate MODFETs used in RF applications are summarized. Results for both AlGaAs/GaAs and AlGaAs/InGaAs heterostructures are presented and compared. A projection of future performance achievements is given based on anticipated improvements in materials and fabrication technology. Author

N89-17092# Massachusetts Univ., Amherst. Dept. of Electrical and Computer Engineering.
PICOSECOND PHOTOCONDUCTIVE TRANSCEIVERS
Alfred P. DeFonzo, Charles Lutz, and Madhuri Jarwala *In* Optical Society of America, Topical Meeting on Picosecond Electronics and Optoelectronics 10 Oct. 1987 p 40-4 (For primary document see N89-17080 09-33)
Avail: NTIS HC A10/MF A01 CSCL 09A

The results of a study of picosecond electromagnetic transients generated and detected by photoconductivity in ion bombarded SOS, radiated and received by tapered slot traveling wave antennas are presented. Author

N89-17093# IBM Watson Research Center, Yorktown Heights, NY.
PHOTOCONDUCTIVE GENERATION OF SUB-PICOSECOND ELECTRICAL PULSES AND THEIR MEASUREMENT APPLICATIONS
D. Grischkowsky, C.-C. Chi, I. N. Duling, III, W. J. Gallagher, N. J. Halas (Bryn Mawr Coll., PA.), J.-M. Halbout, and M. B. Ketchen *In* Optical Society of America, Topical Meeting on Picosecond Electronics and Optoelectronics 10 Oct. 1987 p 44-4 Sponsored in part by ONR, Washington, D.C. (For primary document see N89-17080 09-33)
Avail: NTIS HC A10/MF A01 CSCL 09A

Experimental and theoretical results exploring the fundamanetal limits to the generation of ultrashort electrical pulses via photoconductive switching are discussed. Measurement applications demonstrating terahertz spectroscopy and sub-picosecond electronics with the subpicosecond electrical pulses are presented. Author

N89-17094# Fujitsu Ltd., Atsugi (Japan).
PROGRESS AND CHALLENGES IN HEMT LSI TECHNOLOGY
Masayuki Abe, Takashi Mimura, Kazuo Kondo, and Masaaki Kobayashi *In* Optical Society of America, Topical Meeting on Picosecond Electronics and Optoelectronics 10 Oct. 1987 p 46-4 Sponsored in part by Ministry of International Trade and Industry, Japan (For primary document see N89-17080 09-33)
Avail: NTIS HC A10/MF A01 CSCL 09A

A high electron mobility transistor is a promising device for ultrahigh speed LSI/VLSI, especially operating at 77 K. Recent progress and technical challenges in HEMT LSI technology are discussed. Author

N89-17095# Rochester Univ., NY. Dept. of Electrical Engineering.
PICOSECOND SWITCHING IN JOSEPHSON TUNNEL JUNCTIONS
R. Sobolewski, D. R. Dykaar, T. Y. Hsiang, and Gerard A. Mourou *In* Optical Society of America, Topical Meeting on Picosecond Electronics and Optoelectronics 10 Oct. 1987 p 49-5 Sponsored in part by NBS, Boulder, CO (For primary document see N89-17080 09-33)
(Grant NSF DMR-85-06689)
Avail: NTIS HC A10/MF A01 CSCL 09A
A superconducting electro-optic sampler was developed and used to probe the switching of a 30 x 30 micrometer Josephson tunnel junction. Author

N89-17096# Rochester Univ., NY. Lab. for Laser Energetics.
HIGH SPEED, HIGH REPETITION RATE, HIGH VOLTAGE PHOTOCONDUCTIVE SWITCHING
William R. Donaldson *In* Optical Society of America, Topical Meeting on Picosecond Electronics and Optoelectronics 10 Oct. 1987 p 54-5 (For primary document see N89-17080 09-33)
Avail: NTIS HC A10/MF A01 CSCL 09A
Robust silicon photoconductive switches which were operated for several million shots at 1 kHz switching 10 kV in 100 ps without failure are described. The switches are characterized to maintain the photoconductive state. Author

N89-17097# Maryland Univ., College Park. Dept. of Electrical Engineering.
GENERATION AND FORMING OF ULTRASHORT HIGH VOLTAGE PULSES
Hrayr A. Sayadian, S. T. Feng, J. Goldhar, and Chi H. Lee *In* Optical Society of America, Topical Meeting on Picosecond Electronics and Optoelectronics 10 Oct. 1987 p 57-5 (For primary document see N89-17080 09-33)
Avail: NTIS HC A10/MF A01 CSCL 09A
Picosecond multikilovolt pulses are generated using coaxial, microstrip, and coplanar pulse forming networks. A longitudinal Pockets effect is used to monitor the ultrashort pulses. Author

N89-17098# Maryland Univ., College Park. Dept. of Electrical Engineering.
GRAPHITE AS A PICOSECOND LASER ACTIVATED OPENING SWITCH
E. A. Chauchard, Chi H. Lee, C. Y. Huang, and A. M. Malvezzi (Harvard Univ., Cambridge, MA.) *In* Optical Society of America, Topical Meeting on Picosecond Electronics and Optoelectronics 10 Oct. 1987 p 60-6 Sponsored in part by DOE, Washington, DC (For primary document see N89-17080 09-33)
Avail: NTIS HC A10/MF A01 CSCL 09A
Highly oriented pyrolytic graphite exhibiting a high conductivity in the dark and a high resistivity when illuminated by intense laser light was used as an opening switch. Author

N89-17099# Royal Inst. of Tech., Stockholm (Sweden). Dept. of Applied Physics.
A SIMPLE TECHNIQUE TO GENERATE OR GATE MICROWAVE PULSES WITH PICOSECOND SPEEDS
W. Margulis, V. Grivitskas, E. Adomaitis, Z. Dobrovolskis, and A. Krotkus (Academy of Sciences of the Lithuanian SSR, Vilnius.) *In* Optical Society of America, Topical Meeting on Picosecond Electronics and Optoelectronics 10 Oct. 1987 p 63-6 (For primary document see N89-17080 09-33)
Avail: NTIS HC A10/MF A01 CSCL 09A
A simple ultrafast optoelectronic arrangement is decribed, enabling switching a number of cycles from a microwave generator, or shaping a microwave pulse with picosecond speed. Author

N89-17100# Texas Univ., Austin. Microelectronics Research Center.
A PROPOSED QUANTUM WELL INJECTION TRANSIT TIME (QWITT) DEVICE
Vijay P. Kesan, Dean P. Neikirk, and Ben G. Streetman *In* Optical Society of America, Topical Meeting on Picosecond Electronics and Optoelectronics 10 Oct. 1987 p 66-6 (For primary document see N89-17080 09-33)
(Contract F49620-86-C-0045)
Avail: NTIS HC A10/MF A01 CSCL 09A
A transit time device that uses resonant tunneling through a quantum well is proposed and analyzed. It permits varying injection phase delays, with a wide frequency range of operation and low noise performance. It also promises better output power than quantum-well oscillators. Author

N89-17101# Cornell Univ., Ithaca, NY. School of Electrical Engineering.
MODULATION EFFICIENCY LIMITED HIGH FREQUENCY PERFORMANCE OF THE MODFET
M. C. Foisy, J. C. Huang, P. J. Tasker, and L. F. Eastman *In* Optical Society of America, Topical Meeting on Picosecond Electronics and Optoelectronics 10 Oct. 1987 p 69-7 (For primary document see N89-17080 09-33)
Avail: NTIS HC A10/MF A01 CSCL 09A
Inefficient charge control is a primary degrading mechanism in high frequency MODFET operation. Numerical simulations illuminate the ramifications of varying each epilayer design parameter. Author

N89-17102# Illinois Univ., Urbana-Champaign. Coordinated Science Lab.
CHARACTERISTICS OF SHIELDED MICROSTRIP LINES ON GaAs-Si AT MILLIMETER-WAVE FREQUENCIES
M. I. Aksun and H. Morkoc *In* Optical Society of America, Topical Meeting on Picosecond Electronics and Optoelectronics 10 Oct. 1987 p 72-7 (For primary document see N89-17080 09-33)
Avail: NTIS HC A10/MF A01 CSCL 09A
GaAs on Si has attracted a great deal of interest. This is in part due to its potential use for microwave monolithic integration. The first theoretical study of dielectric losses of this composite material are reported. Author

N89-17103# IBM Watson Research Center, Yorktown Heights, NY.
NONEQUILIBRIUM PHONONS AND DISORDER IN Al(SUB x)Ga(SUB 1-x)As **c76**
J. A. Kash, J. C. Tsang, and S. S. Jha *In* Optical Society of America, Topical Meeting on Picosecond Electronics and Optoelectronics 10 Oct. 1987 p 76-7 (For primary document see N89-17080 09-33)
Avail: NTIS HC A10/MF A01 CSCL 20L
Despite alloy disorder, picosecond Raman measurements show significant nonequilibrium phonon effects in Al(sub x)Ga(sub 1-x)As. The virtual crystal approximation is shown to apply. Implications for heterojunction devices are considered. Author

N89-17104# Maryland Univ., College Park. Lab. for Physical Sciences.
INVESTIGATION OF PHOTOCONDUCTIVE PICOSECOND MICROSTRIPLINE SWITCHES ON SELF-IMPLANTED SILICON ON SAPPHIRE (SOS)
Alan Seabaugh, Geoffrey Burdge, Chi H. Lee, A. C. Seabaugh, Richard Brundage, Michael Bell, and John Albers (National Bureau of Standards, Gaithersburg, MD.) *In* Optical Society of America, Topical Meeting on Picosecond Electronics and Optoelectronics 10 Oct. 1987 p 79-8 (For primary document see N89-17080 09-33)
Avail: NTIS HC A10/MF A01 CSCL 09A
Picosecond photoconductivity on self-implanted SOS was measured over an implant fluence range of 10 to the 13th to 10 to the 15th sq cm. The photoconductive response time decreases

only slightly for implant fluences varying over three orders of magnitude. There is no change in the Raman spectrum up to implant fluences of 10 to the 15th sq cm, where there appears a small amorphous-like component to the optic phonon peak. The highest resistivity occurred at an implant fluence of 10 to the 14th sq cm. Work is now in progress on samples at a higher fluence level in order to determine the effect of amorphization on the photoconductive response. Author

N89-17105# Technische Hochschule, Aachen (Germany, F.R.). Inst. of Semiconductor Electronics.
FAST GaAs PHOTOCONDUCTIVE DETECTORS WITH HIGH SENSITIVITY INTEGRATED IN COPLANAR SYSTEMS ONTO GaAs SUBSTRATES
H. Schumacher, U. Salz, and H. Beneking *In* Optical Society of America, Topical Meeting on Picosecond Electronics and Optoelectronics 10 Oct. 1987 p 82-8 (For primary document see N89-17080 09-33)
Avail: NTIS HC A10/MF A01 CSCL 09A

An interdigitated photoconductive detector with fingers 1.5 micrometer wide was developed for optoelectronic correlation measurements. The very sensitive device fabricated onto s.i. GaAs and integrated in a coplanar line exhibits switching times of approximately 5 ps. Author

N89-17106# IBM Watson Research Center, Yorktown Heights, NY.
CARRIER LIFETIME VERSUS ION-IMPLANTATION DOSE IN SILICON ON SAPPHIRE **c76**
F. E. Doany, D. Grischkowsky, and C.-C. Chi *In* Optical Society of America, Topical Meeting on Picosecond Electronics and Optoelectronics 10 Oct. 1987 p 86-8 Sponsored in part by ONR, Washington, D.C. (For primary document see N89-17080 09-33)
Avail: NTIS HC A10/MF A01 CSCL 20L

Measurements of the carrier lifetime of a systematic series of silicon-on-sapphire samples is presented for a range of more than 4 orders of magnitude or O(+) ion implantation. Author

N89-17107# Maryland Univ., College Park. Dept. of Electrical Engineering.
PICOSECOND OPTOELECTRONIC SWITCHES USING COMPOSITE ELECTRONIC MATERIALS
E. A. Chauchard, Chi H. Lee, V. Diadiuk, and G. W. Turner (Massachusetts Inst. of Tech., Lexington.) *In* Optical Society of America, Topical Meeting on Picosecond Electronics and Optoelectronics 10 Oct. 1987 p 89-9 (For primary document see N89-17080 09-33)
Avail: NTIS HC A10/MF A01 CSCL 09A

Two composite picosecond optoelectronic switches were investigated. The GaAs on silicon-on-sapphire exhibits a 20 ps response while InGaAs on InP shows a strong dependence of its response time on bias voltage. Author

N89-17108# Picosecond Pulse Labs., Inc., Boulder, CO.
COMPARISON OF SAMPLING OSCILLOSCOPES WITH LESS THAN 35 ps TRANSITION DURATIONS
James R. Andrews *In* Optical Society of America, Topical Meeting on Picosecond Electronics and Optoelectronics 10 Oct. 1987 p 92-9 (For primary document see N89-17080 09-33)
Avail: NTIS HC A10/MF A01 CSCL 09A

A 17 ps tunnel diode pulser was used to measure the transient responses of HP 1430, Tek S4, Tek S6, PSPL S-1430D, and Iwatsu Sh-4B sampling oscilloscopes. Author

N89-17109# Rochester Univ., NY. Lab. for Laser Energetics.
A TECHNIQUE FOR WING SUPPRESSED IR SAMPLING **c76**
John Nees and Steve Williamson *In* Optical Society of America, Topical Meeting on Picosecond Electronics and Optoelectronics 10 Oct. 1987 p 95-9 (For primary document see N89-17080 09-33)
Avail: NTIS HC A10/MF A01 CSCL 20L

An experiment demonstrating the feasibility of using optical frequency doubling as a tool for wing suppression in infrared sampling experiments is described. Author

N89-17110# Sandia National Labs., Albuquerque, NM.
HIGH SPEED OPTO-ISOLATOR FOR RADAR APPLICATIONS
J. P. Anthes, P. Garcia, K. Y. Lau, and I. Ury (Ortel Corp., Alhambra, CA.) *In* Optical Society of America, Topical Meeting on Picosecond Electronics and Optoelectronics 10 Oct. 1987 p 97-9 Previously announced as N87-18714 (For primary document see N89-17080 09-33)
Avail: NTIS HC A10/MF A01 CSCL 09A

A high-speed unidirectional electronic coupler/switch that utilizes optoelectronic components is demonstrated. High attenuation of counter propagating radar signals offers improved radar performance. DOE

N89-17111# Tektronix, Inc., Beaverton, OR.
ENERGY VARIATIONS IN OPTICAL PULSES FROM GAIN-SWITCHED AlGaAs DIODE LASERS
R. T. Hawkins, J. H. Goll, and N. A. Anheier *In* Optical Society of America, Topical Meeting on Picosecond Electronics and Optoelectronics 10 Oct. 1987 p 100-102 (For primary document see N89-17080 09-33)
Avail: NTIS HC A10/MF A01 CSCL 09A

Optical pulses from gain-switched AlGaAs diode lasers, measured with a low noise CCD detector, are reported to have energy variations of less than 1 percent rms for pulse durations of less than 60 ps. Author

N89-17112# Bell Telephone Labs., Inc., Holmdel, NJ.
CHARACTERISTICS, PACKAGING AND PHYSICS OF ULTRA HIGH SPEED DIODE LASERS AND DETECTORS
J. E. Bowers and C. A. Burrus *In* Optical Society of America, Topical Meeting on Picosecond Electronics and Optoelectronics 10 Oct. 1987 p 104-106 (For primary document see N89-17080 09-33)
Avail: NTIS HC A10/MF A01 CSCL 09A

High-speed semiconductor lasers provide an efficient compact means of generating short tunable high power pulses. InGaAsP waveguide photodetectors have demonstrated high speed and high efficiency at zero bias. Author

N89-17113# Chalmers Univ. of Technology, Goeteborg (Sweden). Dept. of Electrical Measurements.
FREQUENCY CHIRPING IN PULSE MODULATED GAIN AND REAL INDEX GUIDED SINGLE QUANTUM WELL LASERS
A. Larsson, P. Andersson, and A. Yariv (California Inst. of Tech., Pasadena.) *In* Optical Society of America, Topical Meeting on Picosecond Electronics and Optoelectronics 10 Oct. 1987 p 107-109 (For primary document see N89-17080 09-33)
Avail: NTIS HC A10/MF A01 CSCL 09A

A small frequency chirp in pulse modulated real-index guided single quantum-well lasers and the strong influence of the guiding mechanism are examined. Author

N89-17114# Hewlett-Packard Co., Palo Alto, CA.
InP/GaInAs/InP PIN PHOTODIODE WITH FWHM LESS THAN 18 ps **c76**
S. Y. Wang, K. W. Carey, and B. H. Kolner *In* Optical Society of America, Topical Meeting on Picosecond Electronics and Optoelectronics 10 Oct. 1987 p 110-112 (For primary document see N89-17080 09-33)
Avail: NTIS HC A10/MF A01 CSCL 20L

High-speed front-side illuminated InP/GaInAs/InP PIN 1 to 1.6 micrometer photodetectors were fabricated from material grown by atmospheric pressure organometallic vapor-phase epitaxy. The devices have external quantum efficiencies of greater than 85 percent at 1.3 micrometer and the temporal response has a full width half maximum of less than 18 ps. Dark current density is 6 x 10 to the minus 6th A/sq cm at the operating bias of -4 V. The interface is abrupt to two monolayers at the InP (substrate) GaInAs

heterojunction and five monolayers at the GaInAs/InP p-layer heterojunction. Author

N89-17115# Bell Telephone Labs., Inc., Holmdel, NJ.
PICOSECOND MEASUREMENTS OF GAIN-SWITCHING IN A SEMICONDUCTOR LASER DRIVEN BY ULTRASHORT ELECTRICAL PULSES
P. M. Downey, J. E. Bowers, R. S. Tucker, and J. M. Wiesenfeld *In* Optical Society of America, Topical Meeting on Picosecond Electronics and Optoelectronics 10 Oct. 1987 p 113-115 (For primary document see N89-17080 09-33)
Avail: NTIS HC A10/MF A01 CSCL 09A

An InGaAsP laser, biased near threshold, is driven by 17 ps wide electrical pulses. Gain-switched pulses as short as 15 ps FWHM were observed. Author

N89-17116# IBM Watson Research Center, Yorktown Heights, NY.
MESFET COMPATIBLE IMSM DETECTORS
D. L. Rogers *In* Optical Society of America, Topical Meeting on Picosecond Electronics and Optoelectronics 10 Oct. 1987 p 116-120 (For primary document see N89-17080 09-33)
Avail: NTIS HC A10/MF A01 CSCL 09A

A type of interdigitated metal-semiconductor-metal detector is described using a shallow implant to limit surface trapping making it compatible with refractory gate MESFET processes. Author

N89-17117# Naval Research Lab., Washington, DC.
PICOSECOND OPTICAL AUTOCORRELATION EXPERIMENTS ON FAST PHOTODETECTORS
T. F. Carruthers and J. F. Weller *In* Optical Society of America, Topical Meeting on Picosecond Electronics and Optoelectronics 10 Oct. 1987 p 121-124 (For primary document see N89-17080 09-33)
Avail: NTIS HC A10/MF A01 CSCL 09A

The nonlinear component of the output of many picosecond photodetectors can be used to measure their intrinsic response times without resorting to cross-correlation circuits. Author

N89-17118# Bell Telephone Labs., Inc., Murray Hill, NJ.
DIRECT SUBPICOSECOND MEASUREMENT OF CARRIER MOBILITY OF PHOTOEXCITED ELECTRONS IN GaAs c76
M. C. Nuss and D. H. Auston *In* Optical Society of America, Topical Meeting on Picosecond Electronics and Optoelectronics 10 Oct. 1987 p 126-128 (For primary document see N89-17080 09-33)
Avail: NTIS HC A10/MF A01 CSCL 20L

The carrier mobility of photoexcited hot electrons is measured directly for the first time on a subpicosecond time scale using femtosecond electrical pulses. Author

N89-17119# Illinois Univ., Urbana. Dept. of Electrical and Computer Engineering.
NON-STATIONARY TRANSPORT IN MODFETS AND HETEROJUNCTION DEVICES Abstract Only c76
K. Hess *In* Optical Society of America, Topical Meeting on Picosecond Electronics and Optoelectronics 10 Oct. 1987 p 129 (For primary document see N89-17080 09-33)
Avail: NTIS HC A10/MF A01 CSCL 20L

New horizons have opened up in semiconductor research with the possibility of band gap engineering and the combination of signal transport by photons as well as electrons in new forms of ultrathin III-V compound layers. Self-consistent simulations of transient transport processes in single layer and single quantum-well modulation doped structures are reported. The simulations of picosecond and femtosecond thermalization after optical excitation are also reported and a comparison of the results with the experiments of Knox et al., is given. Author

N89-17120# Arizona State Univ., Tempe. Center for Solid State Electronics Research.
MONTE CARLO INVESTIGATION OF HOT PHOTOEXCITED ELECTRON RELAXATION IN GaAs c76
M. A. Osman, M. J. Kann, D. K. Ferry, and P. Lugli (Modena Univ., Italy) *In* Optical Society of America, Topical Meeting on Picosecond Electronics and Optoelectronics 10 Oct. 1987 p 133-135 Sponsored in part by ONR, Washington, D.C. (For primary document see N89-17080 09-33)
Avail: NTIS HC A10/MF A01 CSCL 20L

The relaxation of hot photoexcited electrons is investigated in GaAs using an ensemble Monte Carlo approach, taking into account both the electron-hole interaction and the hot photon effect. Immediately after exciation by a 568 nm laser pulse, a considerable fraction of electrons transfers to the upper valleys instead of cascading down the central valley. Author

N89-17121# Texas Univ., Austin. Dept. of Physics.
LONGITUDINALLY LOCALIZED OPTICAL CARRIER INJECTION FOR FEMTOSECOND TRANSPORT STUDIES c76
M. C. Downer, D. H. Reitze, and T. R. Zhang *In* Optical Society of America, Topical Meeting on Picosecond Electronics and Optoelectronics 10 Oct. 1987 p 133-135 Sponsored in part by the Joint Services Electronics Program and the Texas Advanced Technology Research Program (For primary document see N89-17080 09-33)
Avail: NTIS HC A10/MF A01 CSCL 20L

A technique for confining optical carrier excitation within a few hundred angstroms of a semiconductor surface opens possibilities for observing ballistic, quantum, and other femtosecond transport phenomenon. Author

N89-17122# Massachusetts Inst. of Tech., Cambridge. Dept. of Electrical Engineering.
FEMTOSECOND NONEQUILIBRIUM ELECTRONIC HEAT TRANSPORT IN THIN GOLD FILMS c76
S. D. Brorson, J. G. Fujimoto, and E. P. Ippen *In* Optical Society of America, Topical Meeting on Picosecond Electronics and Optoelectronics 10 Oct. 1987 p 136-138 (For primary document see N89-17080 09-33)
(Contract DAAL03-86-K-0002; AF-AFOSR-0213-85)
Avail: NTIS HC A10/MF A01 CSCL 20L

Using a front pump/back probe technique, ultrafast heat transport was observed through thin gold films. The results suggest transport occurs via nonequilibrium electrons. Author

N89-17123# IBM Watson Research Center, Yorktown Heights, NY.
BALLISTIC TRANSPORT AND HOT ELECTRON SPECTROSCOPY IN TUNNELLING HOT ELECTRON TRANSFER AMPLIFIER (THETA) c76
M. Heiblum *In* Optical Society of America, Topical Meeting on Picosecond Electronics and Optoelectronics 10 Oct. 1987 p 140-142 (For primary document see N89-17080 09-33)
Avail: NTIS HC A10/MF A01 CSCL 20L

An unambiguous demonstration of ballistic (collisionless) electron transport was done in GaAs with the aid of a Tunnelling Hot Electron Transfer Amplifier (THETA) device. Consequently, interesting quantum related phenomena were observed. Ballistic devices are potentially very fast; current gains as high as 10 were already measured at 77 K. Author

N89-17124*# Massachusetts Inst. of Tech., Lexington. Lincoln Lab.
MICROWAVE AND MILLIMETER-WAVE RESONANT TUNNELING DIODES c76
T. C. L. Gerhard Sollner, Elliott R. Brown, and W. D. Goodhue *In* Optical Society of America, Topical Meeting on Picosecond Electronics and Optoelectronics 10 Oct. 1987 p 143-145 Sponsored by the Army Research Office, Washington, D.C. and NASA, Washington, D.C. (For primary document see N89-17080 09-33)
Avail: NTIS HC A10/MF A01 CSCL 20L

Several demonstrated resonant tunneling devices including oscillators, mixers, multiplexers, and a variable negative resistance are discussed. Techniques of the millimeter/submillimeter regime are also discussed. Author

N89-17125# Texas Instruments, Inc., Dallas.
QUANTUM TRANSPORT CALCULATION OF RESONANT-TUNNELING RESPONSE TIME **c76**
William R. Frensley *In* Optical Society of America, Topical Meeting on Picosecond Electronics and Optoelectronics 10 Oct. 1987 p 146-148 Sponsored by ONR, Washington, D.C. and the Army Research Office, Washingtqn, D.C. (For primary document see N89-17080 09-33)
Avail: NTIS HC A10/MF A01 CSCL 20L

The transient response of a resonant tunneling diode is simulated by calculating the Wigner distribution. Switching times on the order of 100 ps are obtained. Author

N89-17126# Bell Telephone Labs., Inc., Murray Hill, NJ.
RESONANT TUNNELING ELECTRON SPECTROSCOPY **c76**
F. Capasso, S. Sen, A. Y. Cho, and A. L. Hutchinson *In* Optical Society of America, Topical Meeting on Picosecond Electronics and Optoelectronics 10 Oct. 1987 p 149-152 (For primary document see N89-17080 09-33)
Avail: NTIS HC A10/MF A01 CSCL 20L

An electron spectroscopy technique based on resonant tunneling is demonstrated. Direct information on the hot electron distribution function is obtained from the measured resonant tunneling collector current without requiring the use of derivative techniques. Author

N89-17127# Ecole Polytechnique, Palaiseau (France).
HIGH-SPEED PHENOMENA IN GaAs MULTIPLE-QUANTUM-WELLS **c76**
A. Mysyrowicz, D. Hulin, A. Migus, A. Antonetti, H. M. Gibbs, N. Peyghambarian, and H. Morkoc (Illinois Univ., Urbana-Champaign.) *In* Optical Society of America, Topical Meeting on Picosecond Electronics and Optoelectronics 10 Oct. 1987 p 156-158 (For primary document see N89-17080 09-33)
Avail: NTIS HC A10/MF A01 CSCL 20L

Different optical phenomena occurring within a few picoseconds after irradiation of GaAs multiple-quantum-well structures with femtosecond laser pulses are discussed. Author

N89-17128# Bell Telephone Labs., Inc., Holmdel, NJ.
PICOSECOND CARRIER TRANSPORT IN GaAs QUANTUM WELLS **c76**
Jagdeep Shah and R. A. Hopfel *In* Optical Society of America, Topical Meeting on Picosecond Electronics and Optoelectronics 10 Oct. 1987 p 159-161 (For primary document see N89-17080 09-33)
Avail: NTIS HC A10/MF A01 CSCL 20L

Recent experiments in picosecond optical pulses used to investigate the physics of high field transport in GaAs quantum wells are discussed. Author

N89-17129# Bell Telephone Labs., Inc., Holmdel, NJ.
QUANTUM-CONFINED STARK EFFECT IN InGaAs/InP QUANTUM WELLS GROWN BY METAL-ORGANIC CHEMICAL VAPOR DEPOSITION **c76**
I. Bar-Joseph, C. Klingshirn, D. A. B. Miller, D. S. Chemia, U. Koren, and B. I. Miller *In* Optical Society of America, Topical Meeting on Picosecond Electronics and Optoelectronics 10 Oct. 1987 p 162-165 (For primary document see N89-17080 09-33)
Avail: NTIS HC A10/MF A01 CSCL 20L

Large shifts of absorption spectra in InGaAs/InP multiple quantum wells with applied electric fields are reported. Applications for light modulators are discussed. Author

N89-17130# Bell Telephone Labs., Inc., Holmdel, NJ.
DYNAMICS OF BELOW-GAP PHOTOEXCITATION IN GaAs QUANTUM WELLS **c76**
J. E. Zucker, A. VonLehmen, D. S. Chemia, and J. P. Heritage (Bell Communications Research, Inc., Red Bank, NJ.) *In* Optical Society of America, Topical Meeting on Picosecond Electronics and Optoelectronics 10 Oct. 1987 p 166-168 (For primary document see N89-17080 09-33)
Avail: NTIS HC A10/MF A01 CSCL 20L

Time-resolved transmission experiments in GaAs quantum wells show that photoexcitation in the transparent region of the heterostructure can produce a striking variety of excitonic effects. Author

N89-17131# Texas A&M Univ., College Station. Dept. of Electrical Engineering.
RADAR AND EW APPLICATIONS OF MULTI-GIGAHERTZ OPTICAL COMPONENTS AND SYSTEMS
Henry F. Taylor *In* Optical Society of America, Topical Meeting on Picosecond Electronics and Optoelectronics 10 Oct. 1987 p 170-172 (For primary document see N89-17080 09-33)
Avail: NTIS HC A10/MF A01 CSCL 09A

Optical techniques for the generation, control, transmission, and processing of wideband signals in military systems are discussed. Author

N89-17132# Hughes Research Labs., Malibu, CA.
CHARACTERISTICS AND APPLICATIONS OF WIDEBAND GUIDED-WAVE DEVICES
C. M. Gee, G. D. Thurmond, and H. W. Yen *In* Optical Society of America, Topical Meeting on Picosecond Electronics and Optoelectronics 10 Oct. 1987 p 173-175 (For primary document see N89-17080 09-33)
Avail: NTIS HC A10/MF A01 CSCL 09A

Design and fabrication of wideband and high-speed guided-wave electro-optic and electroabsorption devices are reviewed. Their applications in RF fiber-optic links are presented. Author

N89-17133# Maryland Univ., College Park. Dept. of Electrical Engineering.
A NEW OPTOELECTRONIC CW MICROWAVE SOURCE
C. J. Clark, E. A. Chauchard, K. Webb, K. Zaki, Chi H. Lee, P. Polak-Dingles, H.-L. A. Hung, and Ho C. Huang (Communications Satellite Corp., Clarksburg, MD.) *In* Optical Society of America, Topical Meeting on Picosecond Electronics and Optoelectronics 10 Oct. 1987 p 176-178 (For primary document see N89-17080 09-33)
Avail: NTIS HC A10/MF A01 CSCL 09A

A continuous wave microwave source which can be time-synchronized with laser pulses is described. Its phase noise of 3.5 ps is attributed primarily to the laser time jitter. Author

N89-17134# Bell Telephone Labs., Inc., Holmdel, NJ.
OPTICAL MODULATION ABOVE 20 GHz USING A WAVEGUIDE ELECTRO-OPTIC SWITCH
S. K. Korotky, G. Eisenstein, R. S. Tucker, J. J. Veselka, and G. Raybon *In* Optical Society of America, Topical Meeting on Picosecond Electronics and Optoelectronics 10 Oct. 1987 p 179-181 (For primary document see N89-17080 09-33)
Avail: NTIS HC A10/MF A01 CSCL 09A

The intensity modulation of an optical carrier at frequencies above 20 GHz are reported using a Ti:LiNbO(sub 3), optical waveguide switch. A self electro-optic sampling technique is used to observe the modulation. Author

N89-17135# Texas Univ., Austin. Dept. of Electrical and Computer Engineering.
PICOSECOND RESPONSE OF AN OPTICALLY CONTROLLED MILLIMETER WAVE PHASE SHIFTER
C.-K. C. Tzuang, D. Miller, T.-H. Wang, T. Itoh, Dean P. Neikirk, P. Williams, and M. C. Downer *In* Optical Society of America, Topical Meeting on Picosecond Electronics and Optoelectronics 10 Oct. 1987 p 182-184 (For primary document see N89-17080 09-33)
(Grant AF-AFOSR-0036-86)
Avail: NTIS HC A10/MF A01 CSCL 09A

The dispersion of a picosecond pulse propagating along a coplanar waveguide on a semiconductor substrate is studied.

Numerical calculations are used to predict the pulse shape for varying carrier concentrations in a multilayer AlGaAs/GaAs/AlGaAs structure. Author

N89-17136# Rochester Univ., NY. Lab. for Laser Energetics.
ELECTRON DEVICE PROBING IN THE FEMTOSECOND TIME SCALE
Gerard A. Mourou *In* Optical Society of America, Topical Meeting on Picosecond Electronics and Optoelectronics 10 Oct. 1987 p 186-187 (For primary document see N89-17080 09-33)
Avail: NTIS HC A10/MF A01 CSCL 09A

Femtosecond optical techniques were used to time resolve electrical waveforms with femtosecond resolution or terahertz bandwidth. The techniques were used to study the response of ultrafast components such as MESFET, MODFET, permeable base device Josephson junction, and normal superconducting transmission lines and more recently transient transport in semiconductors such as velocity overshoot and resonant tunneling. Present and future roles of optical techniques in electronics from a device characterization and physics point of view are discussed. Author

N89-17137# Bell Telephone Labs., Inc., Murray Hill, NJ.
ELECTRICAL PULSE COMPRESSION BY TRAVELING-WAVE PHOTOCONDUCTIVITY
D. H. Auston, M. C. Nuss, and P. R. Smith *In* Optical Society of America, Topical Meeting on Picosecond Electronics and Optoelectronics 10 Oct. 1987 p 188-190 (For primary document see N89-17080 09-33)
Avail: NTIS HC A10/MF A01 CSCL 09A

A technique is described for compressing picosecond electrical pulses by reflecting them from a moving mirror produced by a traveling wave photoconductor having a velocity close to the eleictrical propagation velocity. Author

N89-17138# IBM Watson Research Center, Yorktown Heights, NY.
PICOSECOND OPTOELECTRONIC STUDY OF A THIN FILM TRANSMISSION LINE STRUCTURE
G. Arjavalingam, J.-M. Halbout, G. V. Kopcsay, and M. B. Ketchen *In* Optical Society of America, Topical Meeting on Picosecond Electronics and Optoelectronics 10 Oct. 1987 p 191-193 (For primary document see N89-17080 09-33)
Avail: NTIS HC A10/MF A01 CSCL 09A

Using photoconductively generated picosecond electrical pulses the properties of a transmission line structure consisting of coupled microstrip lines separated from a ground plane by a thin insulator layer are studied. In addition to the distortion of the transmitted pulses, the near- and far-end coupled noise are characterized with picosecond resolution. Author

N89-17139# Lawrence Livermore National Lab., CA.
SILICON PULSE SHARPENING DIODES: SWITCHING KILOVOLTS IN TENS OF PICOSECONDS
M. D. Pocha, J. D. Wiedwald, C. G. Dease, and M. M. Contreras *In* Optical Society of America, Topical Meeting on Picosecond Electronics and Optoelectronics 10 Oct. 1987 p 194-196 Previously announced as N87-22905 (For primary document see N89-17080 09-33)
(Contract W-7405-eng-48)
Avail: NTIS HC A10/MF A01 CSCL 09A

Numerical analysis was used to determine the physical mechanisms involved in silicon switching diodes. Plots of values for free carrier densities, current density, and electric field, were used in visualizing the operation of these devices. It is concluded tnat the large initial electic field present in the diode is responsible for its behavior. DOE

N89-17140# University of Southern California, Los Angeles. School of Engineering.
JOINT SERVICE ELECTRONICS PROGRAM: RESEARCH IN ELECTRONICS Final Report, 1 Apr. 1985 - 31 Mar. 1988
William H. Steier 1 Jun. 1988 16 p
(Contract F49620-85-C-0071)
(AD-A199659; AFOSR-88-0799TR) Avail: NTIS HC A03/MF A01 CSCL 09A

This final report summarizes the research units supported by Joint Services; the significant research accomplishments described in previous annual reports are listed; and publications and Ph.D Thesis are listed as well. GRA

N89-17141# Case Western Reserve Univ., Cleveland, OH.
ELECTROCHEMISTRY OF CARBON RELATIVE TO BATTERIES AND FUEL CELLS
Ernest Yeager and Donald Tryk 1 Sep. 1988 17 p Presented at the 33d International Power Sources Symposium, Cherry Hill, NJ, 13-16 Jun. 1988
(Contract N00014-83-K-0343)
(AD-A199698; TR-65) Avail: NTIS HC A03/MF A01 CSCL 10C

Carbon of various types are extensively used in battery and fuel cell applications as an electronic conductor, a catalyst for specific reactions, a support for other catalysts and as a high surface area electrode affording a large total capacity (capacitor batteries). This report considers the basic properties of carbons and graphites of importance to these applications including the electronic and solid state properties; pore structure of activated carbons; intrinsic surface electronic and electrochemical properties; surface chemical groups and acid/base properties; redox reactions on carbon/graphite surfaces; electrocatalytic properties of carbon surfaces for various electrode reactions; chemically modified carbon/graphite surfaces; electrochemical oxidation of carbon in battery and fuel cell applications. GRA

N89-17142# Arkansas Univ., Fayetteville. Dept. of Electrical Engineering.
ADAPTIVE HYBRID PICTURE CODING Ph.D. Thesis. Final Report, 30 Sep. 1984 - 30 Sep. 1988
Mark K. Cook Jul. 1988 157 p
(Grant AF-AFOSR-0322-84; AF Proj. 2305)
(AD-A200059; AFOSR-88-1011TR) Avail: NTIS HC A08/MF A01 CSCL 20C

A novel approach to quantize design through the employment of estimation theory techniques leads to a solution to the problem of quantizing noise corrupted sources. By viewing the quantizer as a general estimation device, a risk function can be defined for predetermined cost functions and minimized to realize a quantizer structure which counteracts the effects of the additive noise. GRA

N89-17143# Sandia National Labs., Albuquerque, NM.
NICKEL HYDROGEN BATTERY DEVELOPMENT Final Report
R. Beauchamp and J. Sindorf Aug. 1988 94 p Prepared in cooperation with Johnson Controls, Inc., Milwaukee, WI.
(Contract DE-AC04-76DP-00789)
(DE89-001063; SAND-88-7100) Avail: NTIS HC A05/MF A01

Development continued on a sealed nickel hydrogen battery for deep discharge, 20-year life, terrestrial energy storage applications that would be cost-competitive with a lead-acid battery. A 7 kWh battery was fabricated, tested, and delivered to Sandia. It consists of four battery modules, each with ten 150 Ah cells in series. These modules are assembled into pressure vessels. The modules are connected in a serials/parallel arrangement resulting in a nominal 300 Ah at 24 volts. During testing at JCI, the battery delivered 7.85 kWh with an energy efficiency of 84 percent. DOE

N89-17144# Sandia National Labs., Albuquerque, NM.
STRESS DRIVEN DIFFUSIVE VOIDING OF ALUMINUM CONDUCTOR LINES: A MODEL FOR TIME DEPENDENT FAILURE
F. G. Yost, A. D. Romig, Jr., and R. J. Bourcier 1988 16 p Presented at the Metallurgical Society Fall Meeting and American Society for Metals Materials Week, Chicago, IL, 24 Sep. 1988
(Contract DE-AC04-76DP-00789)

(DE89-001665; SAND-88-0946C; CONF-880901-8) Avail: NTIS HC A03/MF A01

Cracking or voiding of passivated aluminum conductor lines in integrated circuits has been observed by many workers since 1984. This problem has been brought on by the trend in the microelectronics industry to miniaturize circuitry. Most reports on the subject attribute the cause to diffusion creep. This report points out certain difficulties with this conclusion and presents the essential features of a related failure mechanism. A numerical stress analysis is presented to illustrate stress gradients in conductor lines. These stress gradients are known to drive mass transport which leads to void formation. Equations are presented which describe the growth rates of two void morphologies. A definition of failure is made and the time to failure is calculated and the relationship with line width and temperature is given. With properties of aluminum taken from the literature, it will be shown that the calculated failure time is in very good agreement with experimental data. DOE

N89-17145# Argonne National Lab., IL. Chemical Technology Div.

DEVELOPMENT OF OVERCHARGE TOLERANCE IN Li/FeS AND Li/FeS2 CELLS

T. D. Kaun, T. F. Holifield, M. Nigohosian, and P. A. Nelson 1988 12 p Presented at the Electrochemical Society Fall Meeting, Chicago, IL, 9 Oct. 1988

(Contract W-31-109-eng-38)
(DE89-003952; CONF-881061-10; CONF-881061-10) Avail: NTIS HC A03/MF A01

An innovative application of a self-discharge mechanism for molten-electrolyte Li-alloy/FeS(sub x) cells has led to the development of overcharge-tolerant cells. Conventional Li-alloy/FeS(sub x) battery cells require an electronic charger/equalizer. Two versions of the cell have been demonstrated: LiAl+10 mol percent Li5Al5Fe/LiCl-LiBr-KBr (BN, MgO)/FeS2 (operated at 400 C) and LiAl+10 mol percent Li2Fe2/LiF-LiCl-LiBr(MgO)/FeS (operated at 475 C). These cells exhibit a unique combination of overcharge capacity and extended trickle-charge tolerance at 2--5 mA/cm². The basis for the self-discharge is diffusion of reduced lithium species across the separator by a lithium-shuttle mechanism that is controlled by the Li-activity of the Li-alloy electrode. A bimodal self-discharge rate (a 20-fold increase toward the end of charge) results from a 150--250 mV step increase in Li-activity. Cells having overcharge tolerance have operated with stable performance for greater than 200 cycles. The overcharge tolerance rates are sufficient for battery cells to exhibit built-in charge/equalization capability. DOE

N89-17146*# Colorado State Univ., Fort Collins. Dept. of Mechanical Engineering.

CHARACTERIZATION OF HOLLOW CATHODE, RING CUSP DISCHARGE CHAMBERS M.S. Thesis

Jason A. Vaughn Jan. 1989 85 p

(Grant NGR-06-002-112)
(NASA-CR-182255; NAS 1.26:182255) Avail: NTIS HC A05/MF A01 CSCL 09C

An experimental study into the effects of changes in such physical design parameters as hollow cathode position, anode position and ring cusp magnetic field configuration and strength on discharge chamber performance, is described. The results are presented in terms of comparative plasma ion energy cost, extracted ion fraction and ion beam profile data. Such comparisons are used to demonstrate specific means by which changes in these design parameters induce changes in performance, i.e., through changes in the loss rates of primary electrons to the anode, of ions to discharge chamber walls or of ions to cathode and anode surfaces. Results show: (1) the rate of primary electron loss to the anode decreases as the anode is moved downstream of the ring cusp toward the screen grid, (2) the loss rate of ions to hollow cathode surfaces are excessive if the cathode is located upstream of a point of peak magnetic flux density on the discharge chamber centerline, and (3) the fraction of the ions produced that are lost to discharge chamber walls and ring magnet surfaces is reduced by positioning the magnet rings so the plasma density is uniform over the grid surface and so there are no steep magnetic flux density gradients near the walls through which ions can be lost by Bohm diffusion. The uniformity of the plasma density at the grids can also be improved by moving the point of primary electron injection into the discharge chamber off of the chamber centerline. Other results show the discharge chamber losses decrease when a filament cathode is substituted for a hollow cathode to the extent of the hollow cathode operating power. When plasma ion energy cost is determined in such a way that the cost of operating the hollow cathode is subtracted out, the performance using either electron source is similar. Author

N89-17147# Mission Research Corp., Albuquerque, NM.

PHOTOCURRENT MODELING OF MODERN MICROCIRCUIT PN JUNCTIONS

Edward E. Enlow and David R. Alexander 1988 37 p Presented at the 25th Annual Conference on Nuclear and Space Radiation Effects, Portland, OR, 12 Jul. 1988

(Contracts DE-AC04-76DP-00789; Sandia-95-4664)
(DE88-012860; SAND-88-7106C; CONF-880730-5-FP;
MRC/ARO-87-NSREC-028) Avail: NTIS HC A03/MF A01

Mathematical models have been developed for time dependent photocurrent prediction in modern microcircuit PN junctions. The enhanced photocurrent model addresses deficiencies in the Wirth-Rogers photocurrent model for the application to modern microcircuits. The enhanced model incorporates high injection effects on excess minority carrier lifetime and an electric field in the quasi-neutral regions. Both of these effects increase photocurrent production especially in high resistivity material. The enhanced model also includes the effect of the proximity of an ohmic contact or high/low junction. The addition of these variables adds complexity to the enhanced photocurrent model, which was constructed for use in computer simulation codes for analyzing dose rate effects on microcircuits. The enhanced photocurrent model has been successfully implemented in SPICE 2G. DOE

N89-17148*# Michigan Univ., Ann Arbor. Dept. of Electrical Engineering and Computer Science.

DERIVATION AND APPLICATION OF A CLASS OF GENERALIZED IMPEDANCE BOUNDARY CONDITIONS, PART 2 Technical Report, Sep. 1988 - Feb. 1989

J. L. Volakis, T. B. A. Senior, and J.-M. Jin Feb. 1989 53 p

(Grant NAG2-541)
(NASA-CR-183298; NAS 1.26:183298; UM-Rept-025921-T-1)
Avail: NTIS HC A04/MF A01 CSCL 09C

Boundary conditions involving higher order derivatives are presented by simulating surfaces whose reflection coefficients are known analytically, numerically, or experimentally. Procedures for determining the coefficients of the derivatives are discussed, along with the effect of displacing the surface where the boundary conditions are applied. Provided the coefficients satisfy a duality relation, equivalent forms of the boundary conditions involving tangential field components are deduced, and these provide the natural extension to non-planar surfaces. As an illustration, the simulation of metal-backed uniform and three-layer dielectric coatings is given. It is shown that fourth order conditions are capable of providing an accurate simulation for the uniform coating at least a quarter of a wavelength in thickness. Provided, though, some compromise in accuracy is acceptable, it is also shown that a third order condition may be sufficient for practical purposes when simulating uniform coatings. Author

N89-17149*# Texas A&M Univ., College Station. Dept. of Chemistry.

NEW SECONDARY BATTERIES UTILIZING ELECTRONICALLY CONDUCTIVE POLYMER CATHODES Final Report, 1 Feb. 1988 - 31 Jan. 1989

Charles R. Martin and Ralph E. White Feb. 1989 56 p

(Grant NAG9-173)
(NASA-CR-183248; NAS 1.26:183248) Avail: NTIS HC A04/MF A01 CSCL 09C

The objectives of this project are to optimize the transport

rates in electronically conductive polypyrrole films by controlling the morphology of the film and to assess the utility of these films as cathodes in a lithium/polypyrrole secondary battery. During this research period, progress has been made in improving the charge transport rate of the supermolecular-engineered polypyrrole electrode by eliminating the polypyrrole baselayer that hampered earlier work. Also, the fibril density of the polypyrrole electrode was increased, providing more electroactive sites per unit area.
Author

N89-17150# Technische Univ., Eindhoven (Netherlands).
ONE/f NOISE IN SILICON DEVICES Ph.D. Thesis
Rene Henricus Maria Clevers 1988 114 p
(ISBN-90-9002080-2; ETN-89-93339) Avail: NTIS HC A06/MF A01

Experimental data were obtained using a low noise preamplifier placed in a Faraday cage. The spectrum anayzer uses 42 parallel 1/3 octave filters with center frequencies ranging from 1.6 Hz to 20 KHz. The temperature dependence of the 1/f parameter is given for p Si samples. Data concerning the alpha noise parameters for p and n Si, and the same parameter for samples with doping concentrations between 10 to the 14th and 18th power/cc, and with various device geometries are also given. The main conclusion is that perfection of material and not device dimension, give rise to low alpha values.
ESA

N89-17151# Technische Univ., Berlin (Germany, F.R.). Fachbereich Elektrotechnik.
TEST-EFFICIENT DESIGN OF DIGITAL VLSI CIRCUITS Ph.D. Thesis [TEST-EFFIZIENTER ENTWURF VON DIGITALEN VLSI-SCHALTUNGEN]
Arnold Blum 1988 199 p In GERMAN
(ETN-89-93483) Avail: NTIS HC A09/MF A01

Starting from a conceptual analysis of the usual test aids for LSI circuits, test-accessible design were investigated for efficient VLSI-ULSI (Ultra Large Scale Integration) hardware test aids. The analytically deduced mathematical relations for the test circuit expenses were verified for industrial FET circuits. It is shown that test-accessible concepts lead to substantial reductions of the wiring expenses. The proposed high-speed testing method with self-adjusting continuous test sample ejections and injection mechanism allow an increase of the testing speed by up to two orders of magnitude compared to the level-sensitive concepts. Practical examples of implementation of the proposed test-efficient concepts are given.
ESA

34 FLUID MECHANICS AND HEAT TRANSFER

Includes boundary layers; hydrodynamics; fluidics; mass transfer; and ablation cooling.

For related information see also *02 Aerodynamics* and *77 Thermodynamics and Statistical Physics.*

N89-17152 New South Wales Univ., Kensington (Australia). School of Mechanical and Industrial Engineering.
EFFECT OF LEWIS NUMBER ON WET SURFACE HEAT EXCHANGERS M.S. Thesis
Mubashar Zafar Oct. 1987 3 p
Avail: Issuing Activity

A linearized approximate modified analogy theory of wet surface heat exchangers, was developed which predicts the effect of Lewis number more accurately, by introducing modified transfer coefficients, wet bulb depression and wet bulb temperature. A linear approximate model of wet surface heat exchangers is adopted and the equations of the model are rearranged with approximations to two independent sets of equations for modified wet bulb depression and temperature. Each set has been solved previously in published solutions for dry bulb temperature in dry surface heat exchangers, giving modified wet bulb and humidifying efficiencies. The humidifying and wet bulb efficiencies are then calculated using equations derived from the modified wet bulb depression and temperature definitions. An exact finite difference solution, of the basic equations has been used here and compared with the current theory. The comparison showed that for a cross-flow cooling tower and a evaporative cooler, the modified analogy theory is in better agreement for effective Lewis numbers between 0.50 and 3.0.
Author

N89-17153 Cranfield Inst. of Tech., Bedford (England).
A MODEL FOR TRANSITION BY ATTACHMENT LINE CONTAMINATION AND AN EXAMINATION OF CROSS-FLOW INSTABILITY IN THREE-DIMENSIONAL BOUNDARY LAYERS Ph.D. Thesis
I. R. Stewart 1987 165 p
Avail: Univ. Microfilms Order No. BRDX82172

A complete model for predicting the development of intermittent turbulence in a boundary layer flow downstream of a large two-dimensional circular trip on an attachment-line has been produced. This model gives good predictions of intermittency at any point in the flow and could form the basis of a useful design tool. The experimental work involved the development of a novel technique for data gathering which could be employed in other areas of interest. Stability calculations have been performed for the Falkner-Skan-Cooke family of boundary layers using linear stability theory. A relationship has been identified for the minimum critical Reynolds number and the height of the infection point in the profile. This correlation gives good agreement with the stability characteristics for boundary layer profiles typical of those occurring on suction wings. A discrepancy in previous empirical relations between skin friction and Reynolds number in fully developed turbulent flow on an attachment-line has been discovered.
Dissert. Abstr.

N89-17154# Lawrence Livermore National Lab., CA.
REMAPPING ON THE STAGGERED MESH
L. G. Margolin and C. W. Beason 26 Sep. 1988 10 p Presented at the Nuclear Explosives Code Developer's Conference, Boulder, CO, 11-14 Oct. 1988
(Contract W-7405-eng-48)
(DE89-002656; UCRL-99682; CONF-881093-9) Avail: NTIS HC A02/MF A01

The staggered mesh of von Neumann and Richtmyer provides a natural pattern of data storage for Lagrangian fluid dynamics. However, the solution of the advection equation, a necessary step for continuous rezone codes, leads to problems for fields stored on the nodes of the mesh, and in particular for the material velocities. In this paper, we describe a new scheme for advecting nodal quantities that is exactly conservative, computationally efficient and consistent in the sense of truncation error with the advection of cell-centered quantities.
DOE

N89-17155 Texas Univ., Austin.
INTERDEPENDENCE OF LARGE AND SMALL SCALE STRUCTURES IN A TURBULENT BOUNDARY LAYER Ph.D. Thesis
Mark Thomas Coughran 1988 199 p
Avail: Univ. Microfilms Order No. DA8816435

Research in the last twenty years has determined that the bursting process is responsible for much of the turbulence production in turbulent boundary layers and channel flows. The cause of the bursting is unknown. Some researchers have speculated on the possibility of interactions between the small scale, near-wall bursting process and the large scale motions in the outer part of the turbulent boundary layer. The major objective of the present study was to gain insight into the interaction mechanisms using drag reduction techniques. A Large Eddy Break Up (LEBU) device was installed in the outer part of the turbulent boundary layer in a water channel facility. The skin friction, integral length scales, and mean ejection frequency were altered simultaneously, indicating a link between the large and small scale motions. The alterations of mean streak spacing and mean burst frequency by the LEBU were less conclusive. Inner variables were found to be appropriate for scaling the mean ejection frequency

and mean burst frequency in the standard boundary layer flow. Flow visualization indicated that inclined structures may be associated with the ejections. Dissert. Abstr.

N89-17156# Naval Postgraduate School, Monterey, CA.
THE INTERACTION OF A FLUID INTERFACE WITH A VORTEX PAIR M.S. Thesis
Mark D. Petersen-Overton Jun. 1988 76 p
(AD-A200167) Avail: NTIS HC A05/MF A01 CSCL 20D

A detailed parametric study of the variables critical to a numerical model of the interaction of a free surface with an ascending vortex pair has been carried out. The model is based on a discrete vortex representation of the free surface and the use of the appropriate boundary conditions. A study was performed to minimize the numerical Helmholtz instabilities inherent in the numerical model for lower Froude numbers. A method of free-surface re-discretization was developed and implemented. Additionally, an investigation of the motion of vortex pair approaching and passing through a sharp salt/freshwater density interface was conducted. Experiments were performed in a large basin and the vortices were generated with two counter-rotating plates. The rise and intrusion of the Kelvin oval into the upper layer of lower density fluid was recorded on a video tape and then analyzed through the use of a motion analysis system. GRA

N89-17157# Naval Research Lab., Washington, DC. Lab. for Computational Physics and Fluid Dynamics.
APPROXIMATION OF VISCOELASTIC STRESSES FROM NEWTONIAN TURBULENT KINEMATICS Interim Report, Apr. 1986 - Apr. 1988
J. V. Lawler, E. W. Hendricks, R. A. Handler, and R. I. Leighton 1 Sep. 1988 56 p
(AD-A200188; NRL-MR-6272) Avail: NTIS HC A04/MF A01 CSCL 20D

A report is given on work conducted in the area of non-Newtonian turbulent kinematics. A summary of rheological measurements in turbulent non-Newtonian flows is given. A technique for approximating non-Newtonian viscoelastic stresses from Newtonian kinematics obtained by direct numerical simulation is presented. GRA

N89-17158# California Inst. of Tech., Pasadena. Graduate Aeronautical Labs.
INVESTIGATIONS OF THE MOTION OF DISCRETE-VELOCITY GASES BY CELLULAR AUTOMATA Final Technical Report, 1 Jan. - 31 Dec. 1987
Bradford Sturtevant and James E. Broadwell 2 Sep. 1988 42 p
(Grant AF-AFOSR-0155-87; AF Proj. 2307)
(AD-A200221; AFOSR-88-0934TR) Avail: NTIS HC A03/MF A01 CSCL 07D

A model of molecular gasdynamics with discrete components of molecular velocity has been implemented for parallel computation, and two test problems have been calculated. It is shown that fewer than ten values of each component of molecular velocity are necessary to produce accurate results in calculations by direct-simulation Monte-Carlo methods of rarefied-gas flows involving moderately strong shock waves. Thus significant savings in memory required to store the molecular velocities are realized. Most cellular automata intended to describe fluid motion simulate single-speed particles moving on square or hexagonal lattices. It is clear that with only one allowed molecular speed, temperature or energy cannot be specified independently of the velocity. The present paper describes the results of an exploratory investigation of heat conduction and shock wave formation with the two-dimentional model. The irreversible macroscopic behavior of this microscopically reversible system is also examined. GRA

N89-17159# Cornell Univ., Ithaca, NY.
UNSTEADY VISCOUS FLOWS OVER MOVING BODY Final Report, 1 Sep. 1986 - 30 Apr. 1988
S. F. Shen Aug. 1988 10 p
(Grant AF-AFOSR-0328-86; AF Proj. 2307)
(AD-A200269; AFOSR-88-1032TR) Avail: NTIS HC A02/MF A01 CSCL 20D

Unsteady separation was computed using Lagrangian body fixed coordinates. The boundary layer equations retain the usual form except for a Coriolis term which is absent in the two dimensional body fixed coordinate case. Results of unsteady separation over a circular cylinder impulsively started are presented. GRA

N89-17160# Naval Postgraduate School, Monterey, CA.
UNSTEADY FLOW ABOUT POROUS CAMBERED PLATES M.S. Thesis
Paul J. Lindsey Jun. 1988 63 p
(AD-A200282) Avail: NTIS HC A04/MF A01 CSCL 01C

The current parachute-canopy design methodology is mainly empirical. Under certain conditions, parachutes have been observed to collapse during periods of rapid deceleration, subsequent to the initial inflation of the canopy with a resulting loss of drag and ultimately the payload. Studies began with a two-dimensional model of flow about a rigid, nonporous camber. Even though highly idealized, the purpose of the investigation was not a solution of an immediate practical problem but to understand the physics of the problem. GRA

N89-17161# Academy of Sciences of the Ukrainian SSR, Kiev.
RELATIVISTICALLY-INVARIANT STATISTICAL HYDRODYNAMICS OF A NORMAL FLUID
A. D. Panferov, Yu. M. Sinyukov, and S. A. Smolyanskij 1987 27 p
(DE88-704370; ITP-87-33) Avail: NTIS (US Sales Only) HC A03/MF A01

Quasi-equilibrium statistical operators related to arbitrary space-like hypersurfaces are constructed for a normal relativistical fluid. The conditions under which local thermodynamic quantities are invariant with any choice of a hypersurface are found. The compatibility conditions for a quasi-equilibrium and a nonequilibrium description are obtained. The method of calculating the transport coefficients is demonstrated for the model of a relativistic self-interacting scalar field. DOE

N89-17162# Lawrence Livermore National Lab., CA.
IS THERE A STATISTICAL MECHANICS OF TURBULENCE
Robert H. Kraichnan and Shi-Yi Chen Sep. 1988 32 p Presented at the CNLS Conference on Advances in Fluid Turbulence, Los Alamos, NM, 16-20 May 1988 Submitted for publication
(Contract W-7405-eng-36)
(DE89-003471; LA-UR-88-3703; CONF-8805120-4) Avail: NTIS HC A03/MF A01

The statistical-mechanical treatment of turbulence is made questionable by strong nonlinearity and strong disequilibrium that result in the creation of ordered structures imbedded in disorder. Model systems are described which may provide some hope that a compact, yet faithful, statistical description of turbulence nevertheless is possible. Some essential dynamic features of the models are captured by low-order statistical approximations despite strongly non-Gaussian behavior. DOE

N89-17163# Lawrence Livermore National Lab., CA.
THE PROPERTIES OF TAGGED LATTICE FLUIDS. 2: VELOCITY CORRELATION FUNCTIONS
P. M. Binder, D. dHumieres, and L. Poujol 1988 7 p Presented at the Workshop in Discrete Kinetic Theory, Torino, Italy, 20 Sep. 1988 Submitted for publication
(Contract W-7405-eng-36)
(DE89-003475; LA-UR-88-3681; CONF-8809128-2) Avail: NTIS HC A02/MF A01

We report preliminary measurements of the velocity autocorrelation function for a tagged particle in a lattice gas. These measurements agree with the Boltzmann-level theory. The Green-Kubo integration of these measurements agrees with theoretical predictions for the diffusion coefficient. To within the error bars of the simulations (0.003) we observe no long-time tails. DOE

N89-17164 Georgia Inst. of Tech., Atlanta.
A COMPUTATIONAL METHOD FOR THREE DIMENSIONAL, INTERNAL VISCOUS FLOWS WITH SEPARATION AND SECONDARY FLOW PATTERNS Ph.D. Thesis
A. Hamid K. MazHer 1988 168 p
Avail: Univ. Microfilms Order No. DA8811340

A computational method to solve the 3-D Navier Stokes equations for internal, incompressible, Newtonian fluids is presented. Since these equations are difficult to solve analytically, a numerical approach is employed. To use this approach, a suitable treatment of the complex geometry is required, and a proper numerical technique to solve the flow equations is needed. A curvilinear coordinate system is employed to solve the problem of geometry, where an algebraic grid generation technique is used to generate the complex 3-D shape. A systematic algebraic procedure to construct grids for 2-D and 3-D internal flow geometries is presented. Dissert. Abstr.

N89-17165# Rensselaer Polytechnic Inst., Troy, NY.
AN ANALYSIS OF THE CLOSURE CONDITIONS FOR TWO-FLUID MODELS OF TWO-PHASE FLOW Progress Report No. 3
R. T. Lahey, Jr. and D. A. Drew 1988 73 p
(Contract DE-FG02-86ER-13489)
(DE89-003096; DOE/ER-13489/3) Avail: NTIS HC A04/MF A01

The third year of research was focused on the assessment of two-fluid models of two-phase flow. The purpose of this report is to highlight the salient findings made during the report period. Typical two-phase flow models were assessed against the Second Law of Thermodynamics. In addition, a novel new ensemble cell averaging technique was developed and applied to the derivation of interfacial forces and Reynolds stresses in two-phase flows. Finally, predictions from a typical 3-D two-fluid model were compared with phase separation data. DOE

N89-17166# Integral Technologies, Inc., Westmont, IL.
MULTIDIMENSIONAL MODELING OF CONVECTIVE HEAT TRANSFER WITH APPLICATION TO I. C. ENGINES Progress Report
Mark J. Jennings and Thomas Morel 30 Sep. 1988 32 p
(Contract DE-AC04-86AL-33183)
(DE89-004062; DOE/AL-33183/T9) Avail: NTIS HC A03/MF A01

The objective of this project is to develop a more comprehensive understanding of the convective heat transfer process in complex, unsteady turbulent reacting flows, typical of those which occur in internal combustion engines. The specific area of research is the representation of heat transfer in detailed multi-dimensional Navier-Stokes models, and modeling of turbulent transport mechanisms. The detailed tasks include a review of relevant prior work. Based on this review, and original work done under this contract, several modeling approaches will be formulated and further studied and tested. The tests will be carried out on flow cases which have relevance to engine flows, and for which reliable experimental data exist. Such data will be sought and identified. The analytical studies will lead to the determination of the best modeling approaches to be used for heat transfer simulation in internal combustion engines. Following that, a detailed study will be carried out of spatial and temporal heat flux distribution in a representative engine. This will be complemented by a parametric study of engine heat transfer dependence on intake flow details, combustion chamber geometry, engine speed and engine load. DOE

N89-17167# Von Karman Inst. for Fluid Dynamics, Rhode-Saint-Genese (Belgium).
MODELING AND APPLICATIONS OF TRANSPORT PHENOMENA IN POROUS MEDIA, VOLUME 2
1988 265 p Lecture series held in Rhode-Saint-Genese, Belgium, 30 Nov. - 3 Dec. 1987
(VKI-LS-1988-01-Vol-2; ISSN-0377-8312; ETN-89-93588) Avail: NTIS HC A12/MF A01

Porous media are defined, and models for transport in these media are reviewed. Stochastic description of porous media; multiphase flow in porous media; phase change phenomena in liquid saturated self heated particulate beds; heat transfer in self-heated particle beds submerged in liquid coolant; capillary pumping for a two phase heat transport system; and physical mechanisms during drying in porous media were discussed. For individual titles, see N89-17168 through N89-17173.

N89-17168# Ecole des Mines, Paris (France). Centre d'Information Geologique.
STOCHASTIC DESCRIPTION OF POROUS MEDIA
G. deMarsily *In* Von Karman Institute for Fluid Dynamics, Modeling and Applications of Transport Phenomena in Porous Media, Volume 2 1988 31 p (For primary document see N89-17167 09-34)
Avail: NTIS HC A12/MF A01

The properties of porous media in space are defined using the concept of random functions. This stochastic approach has two major advantages: to conceptually define the properties in space at a given point without having to define a volume over which these properties must be integrated; and to provide means to study the inherent heterogeneity and variability of these properties in space, and to evaluate the uncertainty of any method of estimation of their values. Examples of the use of these concepts in solving flow and transport problems, and the problem of estimation are discussed. ESA

N89-17169# Eidgenoessische Technische Hochschule, Zurich (Switzerland). Inst. for Hydromechanics and Water Resources Management.
MULTIPHASE FLOW IN POROUS MEDIA
Th. Dracos *In* Von Karman Institute for Fluid Dynamics, Modeling and Applications of Transport Phenomena in Porous Media, Volume 2 1988 23 p (For primary document see N89-17167 09-34)
Avail: NTIS HC A12/MF A01

The simultaneous flow of liquids and gases through porous media is introduced. It is assumed that cohesive forces in these fluids exceed the adhesion forces. In this case the fluids are not miscible, and stable interfaces form between the fluids. Air, water, and oils are not miscible under normal conditions (atm. pressure, room temperature, etc), however this does not mean that solubility or volatility is zero, but they are so small that a sharp interface forms and the physical properties of the fluids are not affected. Interfacial tension, contact angle, and wettability are considered. Interfacial curvature and capillary pressure are explained. Equilibrium and phase distribution are treated. ESA

N89-17170# Von Karman Inst. for Fluid Dynamics, Rhode-Saint-Genese (Belgium).
PHASE CHANGE PHENOMENA IN LIQUID SATURATED SELF HEATED PARTICULATE BED
J.-M. Buchlin and A. Stubos *In its* Modeling and Applications of Transport Phenomena in Porous Media, Volume 2 1988 80 p (For primary document see N89-17167 09-34)
Avail: NTIS HC A12/MF A01

Out-of-pile experiments in the laboratory on the thermohydraulic behavior of heated debris beds to support the in-pile Post Accident Heat Removal program are reviewed. The parameters controling the coolability of the particulate bed are identified. The dependence of the dryout heat flux on bed height, particle size, and bottom and top subcooling is emphasized. Attempts to model the bed structural changes are presented. Particle size has a strong effect on the value of the dryout heat flux. Shallow beds and deep beds do not exhibit the same behavior. Bottom cooling may induce downward boiling when internal capillary effect is significant. The simulation of the top-subcooling effect is difficult in out-of-pile experiments using ordinary liquids as water. Disturbances of bed structure have to be expected and further modeling is required. ESA

N89-17171# Joint Research Centre of the European Communities, Ispra (Italy).
HEAT TRANSFER IN SELF-HEATED PARTICLE BEDS SUBMERGED IN LIQUID COOLANT
Kent Mehr and Jorgen Wurtz *In* Von Karman Institute for Fluid Dynamics, Modeling and Applications of Transport Phenomena in Porous Media, Volume 2 1988 43 p (For primary document see N89-17167 09-34)
Avail: NTIS HC A12/MF A01

The Post Accident Heat Removal (PAHR) program for fast breeder reactors is outlined. In view of the high power density in the reactor core, the case of a local loss of cooling is considered as a severe hypothetical accident. The noncooled part of a reactor will heat up very fast and material may melt and be ejected from the core. When molten material comes into contact with liquid sodium, it freezes and fractures into particles of many different sizes. These particles, which mainly consist of UO2 and stainless steel, may settle on horizontal structures down in the lower plenum. Initially, the particles are very radioactive and the heating power due to self absorption is very high (up to 20 kW/liter of bed). The integrity of the supporting structure can only be maintained if the major part of the heat is evacuated through the upper bed surface to the overlaying sodium pool. The PAHR project studies the passive cooling of the self heated debris bed. The main goal is to investigate the partition of the total bed power into an upward and downward heat flow. ESA

N89-17172# Von Karman Inst. for Fluid Dynamics, Rhode-Saint-Genese (Belgium).
CAPILLARY PUMPING FOR A TWO PHASE HEAT TRANSPORT SYSTEM
J.-M. Buchlin and P. D. Tinari *In its* Modeling and Applications of Transport Phenomena in Porous Media, Volume 2 1988 45 p (For primary document see N89-17167 09-34)
Avail: NTIS HC A12/MF A01

It is suggested that capillary pumped heat transport loops could successfully meet the established criteria for at least one of the thermal control components in a man-tended, low Earth orbit, microgravity environment. The design and physics of the capillary pump are introduced. Problem areas such as the condensing radiator, startup/shutdown, noncondensable gas, and preflight testing are identified. An analytical model of the thermal capillary pumping loop is outlined. Experimental work on capillary pumping is reviewed. ESA

N89-17173# Ecole des Mines, Nancy (France). Lab. d'Energetique et de Mecanique Theorique et Appliquee.
PHYSICAL MECHANISMS DURING DRYING OF POROUS MEDIA
Christian Moyne, Christian Basilico, Jean-Christophe Batsale, and Alain DeGiovani *In* Von Karman Institute for Fluid Dynamics, Modeling and Applications of Transport Phenomena in Porous Media, Volume 2 1988 39 p (For primary document see N89-17167 09-34)
Avail: NTIS HC A12/MF A01

Drying of porous media is described from a chemical engineering point of view. Examination of the characteristic drying curve concept allows a general understanding of the phenomena. This method is useful for the design of dryers. A general model for the simultaneous heat and mass transfer in unsaturated porous media is derived, including heat transfer by conductive transport and phase change, mass transfer in liquid state by capillarity and filtration, and in gaseous phase by diffusion and convection. This model is compared with experimental results. Simplifications of this model are discussed, i.e., when is it possible to neglect the filtration terms; and whether it is possible to reduce it to a simple diffusion model or to a receding front one. ESA

N89-17174# Von Karman Inst. for Fluid Dynamics, Rhode-Saint-Genese (Belgium).
INTRODUCTION TO COMPUTATIONAL FLUID DYNAMICS
1988 450 p Lecture series held in Rhode-Saint-Genese, Belgium, 18-22 Jan. 1988
(VKI-LS-1988-02; ISSN-0377-8312; ETN-89-93589) Avail: NTIS HC A19/MF A01

Boundary layer equations and methods of solution; finite element techniques; and implicit time dependent methods for inviscid and viscous compressible flows were discussed. For individual titles, see N89-17175 through N89-17178.

N89-17175# Maryland Univ., College Park. Dept. of Aerospace Engineering.
INTRODUCTION TO COMPUTATIONAL FLUID DYNAMICS
J. D. Anderson, Jr. *In* Von Karman Institute for Fluid Dynamics, Introduction to Computational Fluid Dynamics 1988 269 p (For primary document see N89-17174 09-34)
Avail: NTIS HC A19/MF A01

The philosophy and power of computational fluid dynamics; the governing equations; solution techniques, and the working vocabulary in the discipline are introduced. ESA

N89-17176# Deutsche Forschungs- und Versuchsanstalt fuer Luft- und Raumfahrt, Goettingen (Germany, F.R.).
BOUNDARY LAYER EQUATIONS AND METHODS OF SOLUTION
R. Grundmann *In* Von Karman Institute for Fluid Dynamics, Introduction to Computational Fluid Dynamics 1988 31 p (For primary document see N89-17174 09-34)
Avail: NTIS HC A19/MF A01

Laminar boundary layer theory is introduced. Prandtl's idea is described. The hierarchy of the boundary layer equations is discussed; the relationship of the different types of boundary layer equations to the Navier-Stokes equations is demonstrated. It is pointed out that there are transformation techniques to reduce the problems of solution. A generalized discretization scheme is applied to a set of laminar compressible boundary layer equations and a numerical solution scheme for calculating the remaining tridiagonal linear difference equations is shown. A sample calculation of a laminar boundary layer along the symmetry line of a highly inclined ellipsoid is included. ESA

N89-17177# Ghent Univ. (Belgium).
INTRODUCTION TO FINITE ELEMENT TECHNIQUES IN FLUID MECHANICS
E. Dick *In* Von Karman Institute for Fluid Dynamics, Introduction to Computational Fluid Dynamics 1988 33 p (For primary document see N89-17174 09-34)
Avail: NTIS HC A19/MF A01

Strong and weak formulations of a boundary value problem used in a finite element approach are outlined. Piecewise defined shape functions are introduced. Implementation of the finite element method is explained. Examples of steady, incompressible potential flow; incompressible Navier-Stokes equations; and compressible Euler equations are given. ESA

N89-17178# Sherbrooke Univ. (Quebec). Faculte des Sciences Appliquees.
IMPLICIT TIME DEPENDENT METHODS FOR INVISCID AND VISCOUS COMPRESSIBLE METHODS
G. Degrez *In* Von Karman Institute for Fluid Dynamics, Introduction to Computational Fluid Dynamics 1988 100 p (For primary document see N89-17174 09-34)
Avail: NTIS HC A19/MF A01

Properties of inviscid and viscous compressible flow equations are reviewed. The stability of explicit and implicit time dependent methods are studied on simple test cases in ordinary differential equations in order to show the advantages of implicit methods with respect to explicit methods. It is shown how an implicit method can be constructed to solve partial differential equations such as the Euler or Navier-Stokes equations. Implicit time dependent methods for the solution of compressible Euler and Navier-Stokes equations are classified by the way they generate dissipation. Four classes of implicit method are presented: Linear multistep methods; predictor-corrector (MacCormack) methods; centered implicit dissipation schemes; and characteristic modeling schemes. ESA

N89-17179# Von Karman Inst. for Fluid Dynamics, Rhode-Saint-Genese (Belgium).
PARTICLE IMAGE DISPLACEMENT VELOCIMETRY
1988 496 p Lecture series held in Rhode-Saint-Genese, Belgium, 21-25 Mar. 1988
(VKI-LS-1988-06; ISSN-0377-8312; ETN-89-93596) Avail: NTIS HC A21/MF A01

Optical methods for measuring vector velocity fields; scattering power of seed materials; Mie scattering calculations; particle image displacement velocimetry (PIDV) processing techniques (image plane and Fourier plane); speckle velocimetry; application of PIDV to complex flows (resolution of the directional ambiguity, measurements of the third component); optical processing; probabilistic modeling of PIDV experiments; 3-D holographic interferometry; and PIDV equipment were discussed. For individual titles, see N89-17180 through N89-17201.

N89-17180# Illinois Univ., Urbana. Dept. of Theoretical and Applied Mechanics.
OPTICAL METHODS FOR MEASURING VECTOR VELOCITY FIELDS. 1: PRINCIPLES. 2: TECHNIQUES
Ronald J. Adrian *In* VKI, Particle Image Displacement Velocimetry 1988 41 p (For primary document see N89-17179 09-34)
(Grant NSF ATM-86-00509)
Avail: NTIS HC A21/MF A01

Principles of multipoint optical measurement are discussed, and options available for marking the fluid, illuminating the markers, recording the images, and analyzing the recordings are surveyed. Techniques that illustrate important approaches to multipoint measurement are described. Particle image displacement velocimetry and laser speckle velocimetry are introduced. ESA

N89-17181# Illinois Univ., Urbana. Dept. of Theoretical and Applied Mechanics.
SCATTERING POWER OF SEED MATERIALS: MIE SCATTERING CALCULATIONS
Ronald J. Adrian *In* VKI, Particle Image Displacement Velocimetry 1988 21 p (For primary document see N89-17179 09-34)
(Grant NSF ATM-86-00509)
Avail: NTIS HC A21/MF A01

The scattering properties of particles in relation to the two modes of pulsed laser velocimeter operation: particle image and speckle were investigated. Monodisperse particle populations (constant diameter) are assumed, and Mie's theory for scattering from spherical particles is used to evaluate the exposure produced on a photographic plate during a laser pulse. These results are used to determine the minimum particle diameter for particle image operation in water and air for various types of particles and various film properties. They also allow one to predict the minimum necessary particle concentrations for adequate speckle exposure, and to compare the detectability of light scattered from many fine particles, or a smaller number of larger particles. ESA

N89-17182# Illinois Univ., Urbana. Dept. of Theoretical and Applied Mechanics.
PROCESSING TECHNIQUES: IMAGE PLANE AND FOURIER PLANE
Ronald J. Adrian *In* VKI, Particle Image Displacement Velocimetry 1988 26 p (For primary document see N89-17179 09-34)
Avail: NTIS HC A21/MF A01

Full two-dimensional correlation of the interrogation spot images in the case of the image plane, and full two-dimensional spectrum analysis of the Young's fringe pattern in the case of analysis in the Fourier transform plane in particle image velocimetry (PIV) are introduced. The two-dimensional spatial correlation of the images of particles in high image density PIV produces a function that determines the mean displacement of the images in an interrogation spot, and hence the mean fluid velocity in the volume. Similar results can be obtained from the 2-D Fourier transform of the Young's fringe pattern. Alternatively one can deal with the fringes directly, and the method that extracts maximum information from the fringes is the Fourier transform approach. ESA

N89-17183# Illinois Univ., Urbana. Dept. of Theoretical and Applied Mechanics.
PROCESSING INFORMATION IN THE IMAGE PLANE
Ronald J. Adrian *In* VKI, Particle Image Displacement Velocimetry 1988 29 p (For primary document see N89-17179 09-34)
(Grant NSF ATM-86-00509)
Avail: NTIS HC A21/MF A01

Two image-plane techniques for interrogation of particle image velocimetry photographs are described. The orthogonal image compression technique works well provided that the image density is low. It is capable of accuracy better than 1 percent and it is very fast. Extrapolating the 1 sec per spot interrogation time from the DEC 11-23-Skymnk hardware to the Microvax 2 yields times of order 0.03 sec per point, without an array processor. At these speeds a 20 x 100 array would require only 1 min to analyze. The disadvantage is that low image density inevitably results in random locations of data and loss of data. Experience with the 2-D spatial correlation technique is very positive. It should be as accurate as orthogonal image compression, and it yields over 95 percent good data. The technique is very robust, and using an array processor that costs less than most image processors it is capable of analyzing an interrogation spot by correlation in less than 1 sec. This system is being modified to compute the correlation by FFT analysis of the Young's fringes, and speeds of order 0.28 per spot are achieved. ESA

N89-17184*# Florida State Univ., Tallahassee.
SOME COMMENTS ON PARTICLE IMAGE DISPLACEMENT VELOCIMETRY
L. M. Lourenco *In* VKI, Particle Image Displacement Velocimetry 1988 52 p (For primary document see N89-17179 09-34)
(Grant NAG2-314)
Avail: NTIS HC A21/MF A01

Laser speckle velocimetry (LSV) or particle image displacement velocimetry, is introduced. This technique provides the simultaneous visualization of the two-dimensional streamline pattern in unsteady flows as well as the quantification of the velocity field over an entire plane. The advantage of this technique is that the velocity field can be measured over an entire plane of the flow field simultaneously, with accuracy and spatial resolution. From this the instantaneous vorticity field can be easily obtained. This constitutes a great asset for the study of a variety of flows that evolve stochastically in both space and time. The basic concept of LSV; methods of data acquisition and reduction, examples of its use, and parameters that affect its utilization are described. ESA

N89-17185# Essen Univ. (Germany, F.R.).
PRACTICAL SYSTEMS FOR SPECKLE VELOCIMETRY
W. Merzkirch *In* VKI, Particle Image Displacement Velocimetry 1988 14 p (For primary document see N89-17179 09-34)
Avail: NTIS HC A21/MF A01

Light-sheet and light sources for flow visualization; length and number of exposures in laser flow photography are reviewed. Also reviewed are white light speckle patterns; influence of photographic film; and spatial filtering analysis. ESA

N89-17186# Essen Univ. (Germany, F.R.).
SPECKLE PHOTOGRAPHY OF FLOWS WITH VARYING FLUID DENSITY
W. Merzkirch *In* VKI, Particle Image Displacement Velocimetry 1988 5 p (For primary document see N89-17179 09-34)
Avail: NTIS HC A21/MF A01

A quantitative flow analysis method which relies on an arbitrarily oriented micro-sized pattern which is produced by the techniques of speckle photography is introduced. A microsized reference pattern is generated by a plate of ground glass in the light path. The recorded speckle pattern is determined by the scattering characteristics of the ground glass. After an exposure of this reference pattern is taken (in the absence of the flow), the refractively disturbing (compressible) flow is turned on, and a second exposure is taken on the same photographic plate. Due to the deflection of the light in the flow, this second pattern is

distorted with respect to the reference pattern, the displacement of individual speckles being a measure of the local deflection angle. ESA

N89-17187# Von Karman Inst. for Fluid Dynamics, Rhode-Saint-Genese (Belgium).
APPLICATION OF PARTICLE IMAGE DISPLACEMENT VELOCIMETRY (PIDV) TO COMPLEX FLOWS: RESOLUTION OF THE DIRECTIONAL AMBIGUITY
V. Gauthier and M. L. Riethmuller *In its* Particle Image Displacement Velocimetry 1988 48 p (For primary document see N89-17179 09-34)
Avail: NTIS HC A21/MF A01

A solution to the problem of indetermination of the direction of the velocity vectors in particle image displacement velocimetry (PIDV), which also eliminates the problem of measurement gap in the relatively low velocity area of the flow is proposed. An artificial velocity is superimposed to the whole field during the recording sequence, resulting in a shift of the measured velocity range which is then more adapted to the measurement with PIDV. This shifting technique is implemented successfully for measurements inside the front of a scaled heavy gas cloud by using a rotating mirror. The velocity field obtained reveals the details of the mixing motions in the heavy gas and in the air. The high resolution of the measurements allows the computation of the corresponding vorticity fields which visualize the dilution areas. The tests demonstrate the suitability of PIDV to resolve such flow, the implementation of the shifting technique being a determinant factor in the success. ESA

N89-17188# Von Karman Inst. for Fluid Dynamics, Rhode-Saint-Genese (Belgium).
APPLICATION OF PARTICLE IMAGE DISPLACEMENT VELOCIMETRY (PIDV) TO COMPLEX FLOWS: MEASUREMENTS OF THE THIRD COMPONENT
V. Gauthier and M. L. Riethmuller *In its* Particle Image Displacement Velocimetry 1988 44 p (For primary document see N89-17179 09-34)
Avail: NTIS HC A21/MF A01

The basis for the implementation of the particle image displacement velocimetry technique to 3-D flows is analyzed. Two stereoscopic methods are developed and tested. They retrieve the three components of the velocity through 2-D measurements. Their principle consists in recording the illuminated flow plane from two distinct directions. A system to perform 2-D measurements in the presence of a large out-of-plane component of the velocity is also proposed. Even though there are limitations in the photographic setup used, 3-D measurements are performed. Results confirm the theoretical predictions and show the feasibility of the technique in 3-D flows. ESA

N89-17189# Von Karman Inst. for Fluid Dynamics, Rhode-Saint-Genese (Belgium).
OPTICAL PROCESSING
C. S. Moraitis *In its* Particle Image Displacement Velocimetry 1988 29 p (For primary document see N89-17179 09-34)
Avail: NTIS HC A21/MF A01

The theory of optical Fourier transform formation applied in particle image displacement velocimetry through the formation and analysis of interference patterns containing information about the velocity of the flow field is introduced. The equations describing the formation of optical Fourier transforms are derived, starting from a general study of the diffraction from periodic and arbitrary objects. Optical specklegram analysis techniques alternative to the classical fringe formation are discussed. It is shown that the optical formation of the autocorrelation pattern of the probed region of the specklegrams presents considerable advantages over conventional methods, and configurations producing by optical means the autocorrelation function of an input transparency are described, along with the corresponding mathematical models. ESA

N89-17190# Von Karman Inst. for Fluid Dynamics, Rhode-Saint-Genese (Belgium).
PROBABILISTIC MODELING OF PARTICLE IMAGE DISPLACEMENT VELOCIMETRY (PIDV) EXPERIMENTS
C. S. Moraitis *In its* Particle Image Displacement Velocimetry 1988 24 p (For primary document see N89-17179 09-34)
(Grant EEC-ST2-0430)
Avail: NTIS HC A21/MF A01

A stochastic modeling procedure, that takes into account the parameters involved in a particle image displacement velocimetry (PIDV) experiment altogether is proposed. It is shown that the success of a PIDV experiment cannot be absolutely guaranteed, unless parameters actually escaping from the control of the experimenter are optimized. The model should be combined with scattering models and account should be taken of the photographic parameters, to allow for an overall optimization of an experiment. Computer simulations might be necessary, to allow for a better insight into the influence of certain parameters and to answer questions on the validity of the assumptions. ESA

N89-17191# Institut Franco-Allemand de Recherches, Saint-Louis (France).
FULL 3D MEASUREMENTS: THE HOLOGRAPHIC APPROACH
H. Royer *In* VKI, Particle Image Displacement Velocimetry 1988 10 p (For primary document see N89-17179 09-34)
Avail: NTIS HC A21/MF A01

Holography is shown to be a powerful and reliable method for the study of particle velocities. A volume a few hundred cc is easily recorded at a given time. The velocities can be measured directly in two dimensions and estimated in the third dimension. Lateral accelerations are also detected by the use of multiple exposures. The greatest difficulty concerns the exploration of the image field which is a tedious, time consuming operation. The use of Fourier techniques is the most promising way to fast global measurements. On the other hand, the automatic exploration of the whole volume provides more complete data than any other method. However, even with such improvements, holography will remain a delayed-action technique until an immediate-reconstruction process is invented. ESA

N89-17192# Stuttgart Univ. (Germany, F.R.). Inst. fuer Thermodynamik der Luft- und Raumfahrt.
SIMULTANEOUS MEASUREMENTS OF DROPLET SIZE AND DROPLET VELOCITY IN MONODISPERSE DROPLET STREAMS
K. Anders, N Roth,, and A. Frohn *In* VKI, Particle Image Displacement Velocimetry 1988 14 p (For primary document see N89-17179 09-34)
Avail: NTIS HC A21/MF A01

An instrument for simultaneous on-line measurements of droplet size and droplet velocity of periodically generated droplets is presented. Evaporation and combustion of small droplets, as well as the mutual interaction of neighboring droplets can be examined. Experiments can be carried out with monodisperse droplet streams. The droplets have the same size, the same spacing, and the same initial velocity. The droplet size is measured with a sizing method of very high accuracy, which evaluates the intensity distribution of the light scattered by the droplets. The droplet diameter ranges from 10 to 150 micrometer. Droplet velocity is measured by a particle image displacement velocimeter. Typical droplet velocities lie in the range from 10 to 20 m/sec. The results can be used to develop spray models. ESA

N89-17193# Technische Hochschule, Darmstadt (Germany, F.R.). Inst. for Aerodynamics and Measurement Techniques.
A PERSONAL COMPUTER BASED SYSTEM FOR THE EVALUATION OF MULTIPLE EXPOSED IMAGES IN LASER SPECKLE AND PARTICLE IMAGE DISPLACEMENT VELOCIMETRY **c61**
A. Bloch *In* VKI, Particle Image Displacement Velocimetry 1988 10 p (For primary document see N89-17179 09-34)
Avail: NTIS HC A21/MF A01

A low-cost system for the evaluation of slides obtained by

laser speckle and particle image displacement velocimetry was developed. The system is based on an IBM-AT personal computer and provides all useful features for this purpose, including a digital image processing system and a computer-driven support for the automatic point-by-point data reduction of the slides. The evaluation-time for a point is 2 min. This time seems to be unacceptable in industrial applications, so the setup may be of interest for tutorial and nonprofit research institutions. The setup was tested by examining the supersonic flow over a circular cone. Due to poor seeding conditions the results are not representative. ESA

N89-17194# Rome Univ. (Italy). Dipt. di Meccanica e Aeronautica.
DIGITAL DIRECT ANALYSIS OF A MULTIEXPOSED PHOTOGRAPH IN PARTICLE IMAGE DISPLACEMENT VELOCIMETRY (PIDV) **c35**
A. Cenedese and A. Paglialunga *In* VKI, Particle Image Displacement Velocimetry 1988 18 p (For primary document see N89-17179 09-34)
Avail: NTIS HC A21/MF A01

Direct analysis of the photographic plates used in particle image displacement velocimetry is reviewed. The image of each interrogation area, enlarged by a microscope, is recorded by a digital image acquisition system. After filtering, the digitized image can be analyzed with numerical tools. Bidimensional and monodimensional techniques are analyzed and the problems involved in their use are discussed. A technique based on image particle tracking is also presented. ESA

N89-17195# Arizona Univ., Tucson. Optical Sciences Center.
A NEW ALGORITHM FOR THE RAPID ANALYSIS OF PARTICLE IMAGE DISPLACEMENT DATA **c61**
Roy B. Frieden and Csaba K. Zoltani (Ballistic Research Labs., Aberdeen Proving Ground, MD.) *In* VKI, Particle Image Displacement Velocimetry 1988 8 p (For primary document see N89-17179 09-34)
Avail: NTIS HC A21/MF A01

An algorithm for the reduction of low density particle image velocimetry data is presented. Using cross correlation with fast Fourier transforms, it is possible to track and to obtain the velocities of several hundred particles in a minute or less on a Cray-XM-P computer. ESA

N89-17196# Edinburgh Univ. (Scotland).
A SCANNING LASER BEAM SYSTEM FOR TWO-DIMENSIONAL ILLUMINATION OF FLOW FIELDS **c36**
C. Gray and C. A. Greated *In* VKI, Particle Image Displacement Velocimetry 1988 10 p (For primary document see N89-17179 09-34)
Avail: NTIS HC A21/MF A01

A scanning continuous wave laser beam system for the efficient pulsed illumination of a planar region within a seeded flow is presented. This has a direct application in particle image displacement velocimetry where accurate and reliable recording of the flow field relies upon intense illumination of the measuring region for very short periods of time. The advantages of the arrangement over more conventional illumination systems are explained, and illustrated by the implementation of a working system for measurement of velocities over a 0.6 sq m area under water-waves generated within a laboratory wave flume. ESA

N89-17197# Essen Univ. (Germany, F.R.). Lehrstuhl fuer Stroemungslehre.
MEASUREMENT OF NATURAL CONVECTION BY WHITE LIGHT SPECKLE VELOCIMETRY
M. Grobel *In* VKI, Particle Image Displacement Velocimetry 1988 4 p (For primary document see N89-17179 09-34)
Avail: NTIS HC A21/MF A01

Application of a speckle velocimetric method to the natural convective flow along heated vertical wall contours of various shapes is discussed. Such flows are highly sensitive to possible disturbances produced by a mechanical probe, and, if investigated with tracer particles, they require the use of neutrally buoyant particles. The measurements are performed in water and the problem of particle selection is thus facilitated in comparison to air. The major aim is to determine whether for a specific configuration used in the studies the convective flow separates from the wall. The used configurations are plane (two-dimensional), so that speckle velocimetry can be applied in the foreward-scattering mode which is of advantage for reasons of light intensity. Results show that the seeding problem, which is extremely difficult in natural convective flow, is solved satisfactorily, so that reliable velocity measurements can be performed. The ability of the applied speckle technique to resolve very low absolute values of the flow velocity is stressed. ESA

N89-17198# Deutsche Forschungs- und Versuchsanstalt fuer Luft- und Raumfahrt, Goettingen (Germany, F.R.). Inst. fuer Experimentelle Stroemungsmechanik.
APPLICATION OF PARTICLE IMAGE VELOCITY TO HIGH SPEED FLOWS
J. Kompenhans and R. Hoecker *In* VKI, Particle Image Displacement Velocimetry 1988 17 p (For primary document see N89-17179 09-34)
Avail: NTIS HC A21/MF A01

A system was built to study the possibilities offered by particle image velocimetry (PIV) for aerodynamic research. The set-up was tested in high speed flows at Mach numbers up to Ma = 1. Results of the investigation of jet flows confirm the usefulness of PIV for the investigation of instantaneous flow velocity fields in wind tunnels. ESA

N89-17199# Gunma Univ., Maebashi (Japan).
APPLICATION OF A SPATIAL FILTER VELOCIMETER TO THE TWO PHASE FLOWS IN A SPARK IGNITION (SI)
Tomio Obokata *In* VKI, Particle Image Displacement Velocimetry 1988 20 p (For primary document see N89-17179 09-34)
Avail: NTIS HC A21/MF A01

Velocity measurements of two phase flows in the intake system of a spark ignition engine were performed using a spatial filter velocimeter (SFV). The SFV processor tracked the image displacement projected onto the spatial filter and yielded the object velocity signal in real time. Typical results consist of the velocity and droplets, steady and unsteady flow velocities in dense sprays, bubble slip velocity in fluid systems, and the velocity of propagating waves. ESA

N89-17200# Von Karman Inst. for Fluid Dynamics, Rhode-Saint-Genese (Belgium).
APPLICATION OF PARTICLE IMAGE DISPLACEMENT VELOCIMETRY TO A CENTRIFUGAL PUMP
N. Paone, M. L. Riethmuller, and R. A. VandenBraembussche *In its* Particle Image Displacement Velocimetry 1988 24 p (For primary document see N89-17179 09-34)
Avail: NTIS HC A21/MF A01

It is shown that particle image displacement velocimetry can be used for measurements in complex flows in difficult environments such as a centrifugal pump without increasing the complexity of the test setup. A careful selection of the tracers is necessary. Results show that commercially available films and particles can be used. An optical bench was designed to reduce the energy losses to a minimum without reducing basic performances. An electronic system was developed to synchronize the operations of the camera and the mechanical shutter with the impeller. This allows the choice of the blade over which the picture is taken. Two schemes of illumination were used; They allow the analysis of any circumferential position along the diffuser and of any radial tangential plane through it. The quality of the measured velocity fields is high enough to allow a further interpretation of the flow. Computations on the velocity field are possible and can extract more information; vorticity in particular is very suited to the study of wakes. ESA

N89-17201# Cambridge Univ. (England). Dept. of Engineering.
IN-SITU LASER MICROSCOPY FOR PARTICLE SIZING AND TRACKING
Y. Zhang, T. C. Chew, and K. N. C. Bray *In* VKI, Particle Image Displacement Velocimetry 1988 12 p (For primary document see N89-17179 09-34)
Avail: NTIS HC A21/MF A01

A particle sizing and tracking technique suitable for in situ measurements with high spatial resolution of both particle sizes and trajectories is described. The particles (oil droplets) are illuminated by a focused continuous wave laser and veiwed with a special microscope. In situ magnification provides details of particle trajectories and size distribution in the probe volume. Measurements of droplets with diameters in the range of 1 to 9 micrometer were made. The technique can be extended to cover particle diameters down to 0.5 micrometer. It is also a powerful means to study the microstructure of the flow field. ESA

N89-17202# Von Karman Inst. for Fluid Dynamics, Rhode-Saint-Genese (Belgium). Dept. of Civil Engineering.
MODELING AND APPLICATIONS OF TRANSPORT PHENOMENA IN POROUS MEDIA. VOLUME 1: MATHEMATICAL MODELING OF TRANSPORT IN POROUS MEDIA
J. Bear (Technion - Israel Inst. of Tech., Haifa.) 1988 105 p Lecture series held in Rhode-Saint-Genese, Belgium, 30 Nov. - 3 Dec. 1987
(VKS-LS-1988-01-Vol-1; ISSN-0377-8312; ETN-89-93587) Avail: NTIS HC A06/MF A01

Porous media are defined, and models for transport in these media are reviewed. Models that visualize a porous medium domain as a continuum, or as a set of overlapping continua, are considered. ESA

N89-17203# Centre d'Essais Aeronautique Toulouse (France). Groupe Aerodynamique.
FLOW VISUALIZATION BY THE PISTIL PROCEDURE (PRESENTATION OF WAKE IMAGES BY LOCAL COMPUTER PROCESSING). TEST REPORT 876/S-5 [VISUALISATION D'ECOULEMENTS PAR LE PROCEDE PISTIL. (PRESENTATION D'IMAGES DE SILLAGES PAR TRAITEMENT INFORMATIQUE LOCAL). PROCES-VERBAL 876/S-5]
18 May 1988 21 p In FRENCH
(Contract STPA/EG-35-CEAT/A/88)
(Rept-876/S-5; ETN-89-93608) Avail: NTIS HC A03/MF A01

A wake visualization procedure is presented. A total pressure sensor is used to scan the test zone. The pressure signal is treated by a microcomputer to create a map of the isopressure values in a color monitor. The results obtained in the wind tunnel concerning the wake of the Airbus 320 wing wake are presented. ESA

N89-17204# Centre d'Etudes et de Recherches, Toulouse (France). Dept. d'Etudes et de Recherches en Aerothermodynamique.
DECOUPLING OF IONIZATION IN THE HYPERSONIC BOUNDARY LIMIT [DECOUPLAGE DE L'IONISATION DANS LES COUCHES LIMITES HYPERSONIQUES]
J. Ph. Brazier and B. Aupoix Apr. 1988 59 p In FRENCH Sponsored by the Direction des Recherches Etudes et Techniques, Paris, France
(CERT-RT-OA-21/5005-AYD; DERAT-21/5005/13; ETN-89-93652) Avail: NTIS HC A04/MF A01

The validity of hypersonic flow calculation made first without considering ionization, and then computing the ionization without changing the velocity and temperature fields is studied. Hypersonic wind tunnel tests were carried out. The results show that the tested approximation is close to the direct approach. The ionization level is small in all cases, and has no influence on the flow. Catalytic effects due to the wall material are also observed. ESA

N89-17205# Lawrence Livermore National Lab., CA.
APPLICATION OF A TWO-EQUATION TURBULENCE MIX MODEL
W. Patrick Crowley 1988 19 p Presented at the Workshop on the Physics of Compressible Turbulent Mixing, Princeton, NJ, 23-27 Oct. 1988 Submitted for publication
(Contract W-7405-eng-48)
(DE89-004812; UCRL-98686; CONF-8810234-2) Avail: NTIS HC A03/MF A01

A mass averaged k-epsilon model was derived by Leith using a moment expansion and appropriate closure models. Moving the mesh with the mass averaged velocity results in a Lagrangian model with constant mass in each zone. In this paper Leith's model is transformed into an Almost Lagrangian model by taking the mesh velocity to be the ensemble averaged fluid velocity. Here the mass in each zone may change with time. The resulting 1-D model is used to simulate the Smits and Muck supersonic wind tunnel experiment in which pre- existing turbulence is amplified by a shock wave. From the model results we deduce a simplified k-epsilon model that is applicable to the Smits and Muck (S and M) experiment. In the analytic solution for the simplified model we find the shock thickness to be increased by a factor of 100,000; behind the shock the turbulent energy decays at t sup -1. DOE

N89-17206# Lawrence Livermore National Lab., CA.
TAILORING DOMAIN DECOMPOSITION TO THE NETWORK STRUCTURE FOR PARALLEL PROCESSING OF FLUID DYNAMICS
A. Louise Perkins Nov. 1988 21 p
(Contract W-7405-eng-48)
(DE89-005501; UCID-21609) Avail: NTIS HC A03/MF A01

We developed a biased domain decomposition clustering algorithm designed for use in our parallel processing program for the numerical solution of partial differential equations. The biased clustering algorithm is designed to work on a distributed memory parallel processor with a general network communication system connecting the individual processor units. To date, the algorithm has been simulated on the Cray-2 shared memory multiprocessor. DOE

N89-17303*# General Motors Corp., Indianapolis, IN. Gas Turbine Div.
AEROTHERMAL MODELING PROGRAM. PHASE 2, ELEMENT A: IMPROVED NUMERICAL METHODS FOR TURBULENT VISCOUS RECIRCULATING FLOWS
K. C. Karki, H. C. Mongia, Suhas V. Patankar, and A. K. Runchal (Analytic and Computational Research, Inc., Los Angeles, CA.) *In* NASA, Lewis Research Center, Turbine Engine Hot Section Technology, 1987 Oct. 1987 p 85-90 (For primary document see N89-17298 09-39)
Avail: NTIS HC A20/MF A01 CSCL 20D

N89-17304*# General Motors Corp., Indianapolis, IN. Gas Turbine Div.
AEROTHERMAL MODELING PROGRAM. PHASE 2, ELEMENT B: FLOW INTERACTION EXPERIMENT
M. Nikjooy, H. C. Mongia, S. N. B. Murthy, and J. P. Sullivan (Purdue Univ., West Lafayette, IN.) *In* NASA, Lewis Research Center, Turbine Engine Hot Section Technology, 1987 Oct. 1987 p 91-99 (For primary document see N89-17298 09-39)
(Contract NAS3-24350)
Avail: NTIS HC A20/MF A01 CSCL 20D

N89-17305*# General Motors Corp., Indianapolis, IN. Gas Turbine Div.
AEROTHERMAL MODELING PROGRAM, PHASE 2, ELEMENT C: FUEL INJECTOR-AIR SWIRL CHARACTERIZATION
A. A. Mostafa, H. C. Mongia, V. G. McDonnel, and G. S. Samuelsen (California Univ., Irvine.) *In its* Turbine Engine Hot Section Technology, 1987 Oct. 1987 p 101-110 (For primary document see N89-17298 09-39)
Avail: NTIS HC A20/MF A01 CSCL 20D

N89-17306*# United Technologies Research Center, East Hartford, CT.
APPLICATION OF ADVANCED DIAGNOSTICS TO AIRBLAST INJECTOR FLOWS
John B. McVey, Jan B. Kennedy, and Sid Russell *In* NASA, Lewis Research Center, Turbine Engine Hot Section Technology, 1987 Oct. 1987 p 111-118 (For primary document see N89-17298 09-39)
(Contract NAS3-24352)
Avail: NTIS HC A20/MF A01 CSCL 20D

N89-17307*# Minnesota Univ., Minneapolis.
DEVELOPMENT OF GENERALIZED BLOCK CORRECTION PROCEDURES FOR THE SOLUTION OF DISCRETIZED NAVIER-STOKES EQUATIONS
Kanchan M. Kelkar and Suhas V. Patankar *In* NASA, Lewis Research Center, Turbine Engine Hot Section Technology, 1987 Oct. 1987 p 119-128 (For primary document see N89-17298 09-39)
Avail: NTIS HC A20/MF A01 CSCL 20D

N89-17309*# Stanford Univ., CA.
HEAT TRANSFER WITH VERY HIGH FREE-STREAM TURBULENCE AND HEAT TRANSFER WITH STREAMWISE VORTICES
Robert J. Moffat, Paul Maciejewski, John K. Eaton, and Wayne Pauley *In* NASA, Lewis Research Center, Turbine Engine Hot Section Technology, 1987 Oct. 1987 p 131-154 (For primary document see N89-17298 09-39)
(Grant NAG3-522)
Avail: NTIS HC A20/MF A01 CSCL 20D

N89-17310*# Minnesota Univ., Minneapolis.
A LOW-REYNOLDS-NUMBER TWO-EQUATION TURBULENCE MODEL FOR PREDICTING HEAT TRANSFER ON TURBINE BLADES
Suhas V. Patankar and Rodney C. Schmidt *In* NASA, Lewis Research Center, Turbine Engine Hot Section Technology, 1987 Oct. 1987 p 155-167 (For primary document see N89-17298 09-39)
(Grant NAG3-579)
Avail: NTIS HC A20/MF A01 CSCL 20D

N89-17311*# United Technologies Research Center, East Hartford, CT.
MEASUREMENT OF AIRFOIL HEAT TRANSFER COEFFICIENTS ON A TURBINE STAGE
Robert P. Dring, Michael F. Blair, and H. David Joslyn *In* NASA, Lewis Research Center, Turbine Engine Hot Section Technology, 1987 Oct. 1987 p 169-179 (For primary document see N89-17298 09-39)
(Contract NAS3-23717)
Avail: NTIS HC A20/MF A01 CSCL 20D

N89-17312*# Arizona State Univ., Tempe.
HEAT TRANSFER IN THE TIP REGION OF A ROTOR BLADE SIMULATOR
M. K. Chyu and D. E. Metzger *In* NASA, Lewis Research Center, Turbine Engine Hot Section Technology, 1987 Oct. 1987 p 181-197 (For primary document see N89-17298 09-39)
(Grant NAG3-623)
Avail: NTIS HC A20/MF A01 CSCL 20D

N89-17313*# Scientific Research Associates, Inc., Glastonbury, CT.
TWO- AND THREE-DIMENSIONAL TURBINE BLADE ROW FLOW FIELD SIMULATIONS
R. C. Buggeln, W. R. Briley, H. McDonald, S. J. Shamroth, and B. C. Weinberg *In* NASA, Lewis Research Center, Turbine Engine Hot Section Technology, 1987 Oct. 1987 p 199-209 Prepared in cooperation with General Motors Corp., Indianapolis, IN (For primary document see N89-17298 09-39)
(Contracts NAS3-24358; NAS3-23695)
Avail: NTIS HC A20/MF A01 CSCL 20D

N89-17314*# Pratt and Whitney Aircraft, East Hartford, CT.
COOLANT PASSAGE HEAT TRANSFER WITH ROTATION
T. J. Hajek, J. H. Wagner, and B. V. Johnson (United Technologies Research Center, East Hartford, CT.) *In* NASA, Lewis Research Center, Turbine Engine Hot Section Technology, 1987 Oct. 1987 p 211-223 (For primary document see N89-17298 09-39)
(Contract NAS3-23691)
Avail: NTIS HC A20/MF A01 CSCL 20D

N89-17315*# General Motors Corp., Indianapolis, IN. Gas Turbine Div.
TURBINE AIRFOIL FILM COOLING
L. D. Hylton, V. Nirmalan, B. K. Sultanian, and R. M. Kaufman *In* NASA, Lewis Research Center, Turbine Engine Hot Section Technology, 1987 Oct. 1987 p 225-238 (For primary document see N89-17298 09-39)
(Contract NAS3-24619)
Avail: NTIS HC A20/MF A01 CSCL 20D

35 INSTRUMENTATION AND PHOTOGRAPHY

Includes remote sensors; measuring instruments and gages; detectors; cameras and photographic supplies; and holography.

For aerial photography see *43 Earth Resources and Remote Sensing.* For related information see also *06 Aircraft Instrumentation,* and *19 Spacecraft Instrumentation.*

N89-17207# Pacific Northwest Labs., Richland, WA.
PHOTOTYPE DESIGN AND TESTING OF TWO FIBER-OPTIC SPECTROCHEMICAL EMISSION SENSORS
Khris B. Olsen, Danny A. Nelson, Jeffrey W. Griffin, Bradley S. Matson, and Peter A. Eschbach (Washington State Univ., Pullman.) Sep. 1988 28 p Presented at 1st International Symposium on Field Screening Methods for Hazardous Waste Site Investigations, Las Vegas, NV, 11-13 Oct. 1988 Prepared in cooperation with Washington State Univ., Pullman
(Contract DE-AC06-76RL-01830)
(DE89-001741; PNL-SA-15916; CONF-8810133-2) Avail: NTIS HC A03/MF A01

A unique radio frequency-induced helium plasma (RFIHP) sensor and a spark discharge (SD) sensor were designed, and prototype units were developed and tested. Both sensors use an atomic excitation source coupled to a fiber-optic cable and optical spectrometer to monitor in situ the emission intensity of selected elements of interest in the ambient air. Potential applications include vadose zone monitoring of volatile species. The RFIHP sensor was designed to measure the total chlorine concentration from carbon tetrachloride (and other volatile chlorinated hydrocarbons), and the SD sensor was designed to measure in situ concentrations of chlorine-containing compounds. The results of this research demonstrate proof of concept of the theory, but suggest further refinements are necessary to achieve detection sensitivities sufficiently low to be useful for monitoring concentrations of selected elements in vadose zone air. DOE

N89-17208# Lawrence Livermore National Lab., CA.
A PHOTON-COUNTING, SUBNANOSECOND, IMAGING CAMERA FOR X-RAY DETECTION
M. R. Carter, D. F. Price, R. E. Stewart, and D. A. Whelan Sep. 1988 8 p Presented at the SPIE O-E Lase: International Symposium and Exhibition on Fiber Optics, Optoelectronics and Laser Applications, Boston, MA, 6-10 Sep. 1988
(Contract W-7405-eng-48)
(DE89-002874; UCRL-98505; CONF-8809105-9) Avail: NTIS HC A02/MF A01

We have developed a high-bandwidth, photon-counting, x-ray

detector for x-ray imaging experiments. It consists of an x-ray photocathode, an optional microchannel plate (MCP), optional electrostatic optics, and a subnanosecond phosphor. The detector can be used for 2-D imaging with a subnanosecond framing camera or 1-D imaging with a Reticon or streak-camera readout. Several versions of the 1-D detector have been developed. The MCP version employs a photocathode on the front surface of the MCP, and the transmission-photocathode version consists of a photocathode deposited on a thin polypropylene foil. The output electrons from the MCP or the transmission photocathode are accelerated into a fast phosphor deposited on a coherent fiber-optic faceplate. Both detectors can be enhanced with the use of electrostatic electron optics to compress the output electrons in one dimension. The best parameters achieved to date are a time resolution of 400 ps, spatial resolution of 100 microns, and electron compression of 10:1. Quantum efficiencies of 40 percent have been achieved. Effective quantum efficiencies greater then 100 percent have been achieved with the 1-D electrostatic optics. Data are presented on the efficiency, time response, at spatial resolution of the 1-D detectors. DOE

N89-17209# Ballistic Research Labs., Aberdeen Proving Ground, MD.
GYROSCOPIC TESTING OF ACCELEROMETERS TO DETERMINE CONING ANGLE
Nina Mishra, Jonathan A. Harrison, and David J. Hepner Nov. 1988 30 p
(AD-A200126; BRL-MR-3709) Avail: NTIS HC A03/MF A01 CSCL 14B

An experiment was performed to determine how accurately accelerometers could measure the coning angle of a spinning and coning laboratory gyroscope. Tests showed that coning angle measurements were well within expected results. The accelerometer can be used with or in place of the yawsonde for determination of flight stability of spin-stabilized projectiles. GRA

N89-17210# Utah Univ., Salt Lake City. Dept. of Chemistry.
ULTRAMICROELECTRODE SENSORS AND DETECTORS. CONSIDERATIONS OF THE STABILITY, SENSITIVITY, REPRODUCIBILITY AND MECHANISM OF ION TRANSPORT IN GAS PHASE CHROMATOGRAPHY AND IN HIGH PERFORMANCE LIQUID PHASE CHROMATOGRAPHY
Technical Report, Sep. 1987 - Jul. 1988
Rossella Brina, B. Stanley Pons, and Martin Fleischmann 15 Jul. 1988 16 p Submitted for publication
(Contract N00014-83-K-0470)
(AD-A200306; TR-103) Avail: NTIS HC A03/MF A01 CSCL 07D

We describe in this paper the use of ultramicroelectrodes as sensitive sensors and detectors in the gas phase and in liquid solutions of high resistance; particularly aspects regarding the sensitivity, stability, and reproducibility of the devices. The advantages of these detectors can be improved notably by appropriate choice of method of pretreatment of the electrode surface. The surface separating the working ultramicroelectrode from the secondary/reference electrode provides the medium for ionic conduction for the cell. The mechanism for ion conduction involves proton migration and diffusion across the surface of the separator. GRA

N89-17211*# National Aeronautics and Space Administration. Lewis Research Center, Cleveland, OH.
DEVELOPMENT OF AN INFRARED IMAGING SYSTEM FOR THE SURFACE TENSION DRIVEN CONVECTION EXPERIMENT
Alexander D. Pline Jan. 1989 12 p Presented at the Non-Contact Temperature Measurement Workshop, Pasadena, CA, 17-19 Jan. 1989; sponsored by JPL
(NASA-TM-101479; E-4605; NAS 1.15:101479) Avail: NTIS HC A03/MF A01 CSCL 14B

An infrared imaging system is used to quantify the imposed surface temperature distribution along a liquid/gas free surface in support of the Surface Tension Driven Convection Experiment, a planned Space Transportation System flight experiment. For ground-based work a commercially available instrument was used to determine the feasibility of using the type of imaging system for this experiment. The ground-based work was used as a baseline for compiling specifications for a flight qualified imager to be designed, fabricated, tested and qualified for flight. The requirements and specifications for the flight model are given along with the reasons for departures from the ground-based equipment. The flight qualification requirements discussed are a representative sample of the necessary procedures which must be followed to flight qualify diagnostic equipment for use aboard the STS. The potential problems and concerns associated with operating an imaging system in orbit are also discussed. Author

N89-17212*# Wisconsin Univ., Madison. Cooperative Inst. for Meteorological Satellite Studies.
HIGH-RESOLUTION INTERFEROMETER SOUNDER (HIS), PHASE 2 Final Report
Oct. 1988 35 p
(Contract NAS5-27608)
(NASA-CR-183414; NAS 1.26:183414) Avail: NTIS HC A03/MF A01 CSCL 14B

The High-resolution Interferometer Sounder (HIS) was successfully built, tested, and flight proven on the NASA U-2/ER-2 high altitude aircraft. The HIS demonstration has shown that, by using the technology of Fourier Transform Spectroscopy (FTS), it is possible to measure the spectrum of upwelling infrared radiance needed for temperature and humidity sounding with high spectral resolution and high radiometric precision. By resolving individual carbon dioxide lines, the retrieved temperature profiles have vertical resolutions of 1 to 2 km and RMS errors less than 1 C, about 2 to 4 times better than possible with current sounders. Implementing this capability on satellite sounders will greatly enhance the dynamical information content of temperature measurements from space. The aircraft model HIS is now a resource which should be used to support field experiments in mesoscale meteorology, to monitor trace gas concentrations and to better understand their effects on climate, to monitor the surface radiation budget and the radiative effects of clouds, and to collect data for research into retrieval techniques, especially under partially cloudy conditions. Author

N89-16841# Rolls-Royce Ltd., Derby (England). Advanced Research Lab.
HOLOGRAPHIC INTERFEROMETRY FOR FLOW VISUALIZATION STUDIES IN HIGH SPEED FANS
R. K. Parker *In* Von Karman Institute for Fluid Dynamics, Transonic Compressors, Volume 2 1988 45 p Previously announced as N88-28072 (For primary document see N89-16833 09-07)
Avail: NTIS HC A17/MF A01

N89-16842# Rolls-Royce Ltd., Derby (England).
USE OF HOLOGRAPHY IN VIBRATION AND FLUTTER STUDY OF FANS
R. J. Parker *In* Von Karman Institute for Fluid Dynamics, Transonic Compressors, Volume 2 1988 44 p Previously announced as N88-30098 (For primary document see N89-16833 09-07)
Avail: NTIS HC A17/MF A01

N89-16890# Deutsche Forschungs- und Versuchsanstalt fuer Luft- und Raumfahrt, Oberpfaffenhofen (West Germany).
STATUS OF SABREX
H. Goessl and W. Keydel *In its* Proceedings of the Colloquium about Joint Projects Within the DFVLR/ISRO Cooperation Jun. 1988 p 103-109 (For primary document see N89-16883 09-12)
Avail: NTIS HC A06/MF A01; DFVLR, VB-PL-DO, Postfach 90 60 58, 5000 Cologne, Fed. Republic of Germany, 34.50 Deutsche marks

N89-17194# Rome Univ. (Italy). Dipt. di Meccanica e Aeronautica.
DIGITAL DIRECT ANALYSIS OF A MULTIEXPOSED PHOTOGRAPH IN PARTICLE IMAGE DISPLACEMENT VELOCIMETRY (PIDV)
A. Cenedese and A. Paglialunga *In* VKI, Particle Image Displacement Velocimetry 1988 18 p (For primary document see N89-17179 09-34)
Avail: NTIS HC A21/MF A01

N89-17299*# United Technologies Research Center, East Hartford, CT.
DEVELOPMENT OF A HIGH TEMPERATURE THIN FILM STATIC STRAIN GAGE
Charles O. Hulse, Richard S. Bailey, Howard P. Grant, and John S. Przybyszewski (Pratt and Whitney Aircraft, East Hartford, CT.) *In* NASA, Lewis Research Center, Turbine Engine Hot Section Technology, 1987 Oct. 1987 p 43-51 (For primary document see N89-17298 09-39)
(Contract NAS3-23722)
Avail: NTIS HC A20/MF A01 CSCL 14B

N89-17300*# Northwestern Univ., Evanston, IL.
ELEVATED TEMPERATURE STRAIN GAGES
J. F. Lei, M. Shaarbaf, and J. O. Brittain *In* NASA, Lewis Research Center, Turbine Engine Hot Section Technology, 1987 Oct. 1987 p 53-75 (For primary document see N89-17298 09-39)
Avail: NTIS HC A20/MF A01 CSCL 14B

N89-17301*# National Aeronautics and Space Administration. Lewis Research Center, Cleveland, OH.
PROGRESS ON A PdCr WIRE STRAIN GAGE
David R. Englund *In its* Turbine Engine Hot Section Technology, 1987 Oct. 1987 p 77-79 (For primary document see N89-17298 09-39)
Avail: NTIS HC A20/MF A01 CSCL 14B

N89-17302*# National Aeronautics and Space Administration. Lewis Research Center, Cleveland, OH.
A COMPARISON OF TURBULENCE MEASUREMENT METHODS
Gustave C. Fralick *In its* Turbine Engine Hot Section Technology, 1987 Oct. 1987 p 81-84 (For primary document see N89-17298 09-39)
Avail: NTIS HC A20/MF A01 CSCL 14B

36 LASERS AND MASERS

Includes parametric amplifiers.
For related information see also *76 Solid-State Physics.*

N89-17213 New South Wales Univ., Kensington (Australia). School of Physics.
AN INVESTIGATION OF THE SPECTRAL CHARACTERISTICS OF A COMMERCIALLY AVAILABLE SEMICONDUCTOR LASER M.S. Thesis
M. W. Lawson Apr. 1986 2 p
Avail: Issuing Activity

The problem of determining semiconductor laser spectral linewidth is addressed. Spectral linewidth has important implications for high bit rate direct detection optical fiber communication systems and the future coherent optical systems being engineered for the 1990's. A theoretical analysis of the origin of the spectral linewidth and a calculated value for the laser used is given. A commercially available semiconductor laser was mounted on an optical bench and the spectral output was observed using a high resolution scanning Fabry Perot Interferometer. An automatic frequency control loop was developed using the Fabry Perot interferometer as a frequency discriminator. This circuit achieved laser frequency stability to within 100 MHz for several hours. Measurements of output power, frequency shift and spectral linewidth were taken for a range of laser drive currents. Characteristics due to unwanted optical feedback into the optical cavity are discussed. A 50 MHz laser current modulator was developed and its effects on the laser spectral output observed. A brief theoretical analysis of these effects are given. Author

N89-17214*# Old Dominion Univ., Norfolk, VA. Dept. of Mathematical Sciences.
THEORETICAL STUDIES OF SOLAR LASERS AND CONVERTERS Progress Report, 15 May - 31 Dec. 1988
John H. Heinbockel Dec. 1988 42 p
(Grant NAG1-757)
(NASA-CR-184589; NAS 1.26:184589) Avail: NTIS HC A03/MF A01 CSCL 20E

A second computer program was developed for the simulation of an n - C3F7I iodine laser. The computer program is given in Appendix A and a typical output from the computer program is illustrated in Appendix B. Author

N89-17215# Hughes Aircraft Co., El Segundo, CA. Electro-optical and Data Systems Group.
LASER COMMUNICATION TEST SYSTEM Final Report, Sep. 1986 - Sep. 1987
G. S. Mecherle, A. K. Rue, G. T. Pope, P. T. Benguhe, and M. A. Twete Jun. 1988 73 p
(Contract F33615-86-C-1073)
(AD-A199612; AFWAL-TR-88-1042) Avail: NTIS HC A04/MF A01 CSCL 25C

A Hughes-developed laser communication terminal related to aircraft applications was delivered for Air Force testing. The terminals employ laser diode transmitters, PIN diode receivers, and provide automatic tracking with a gimbal-mounted video camera and off-gimbal video tracker. The terminals are capable of 20 Kbps full duplex operation over 8 to 10 miles at sea level. Video tracking offers a legitimate alternative to quadrant tracking. The terminals were modified to provide performance monitors for transmitted signal, received signal, AGC voltage, tracking error, tracker status, and angular position. An automatic acquisition capability with spiral scans was implemented and performed well. GRA

N89-17216# Rochester Univ., NY. Inst. of Optics.
NONLINEAR OPTICS WITH BROAD-BAND LASERS Final Report, 15 Apr. - 31 Aug. 1988
Michael G. Raymer May 1988 7 p
(Contract DE-FG02-87ER-13761)
(DE89-002728; DOE/ER-13761/7) Avail: NTIS HC A02/MF A01

This project has focused on a number of related topics in nonlinear optics, unified by the theme of temporal fluctuations in the light field emitted by broad-band lasers. The following new results were obtained: the shot-to-shot statistics of multimode, pulsed dye lasers were measured, and cross correlations between mode energies were observed and explained; evidence for phase locking between the modes was also obtained; a new technique was demonstrated for smoothing the intensity fluctuations of the pulses emitted by multimode dye lasers; the influences of laser bandwidth in the stimulated Raman scattering process were studied experimentally and theoretically; a theoretical study was carried out to predict the effects of laser bandwidth in the spectrum of light scattered by atomic vapors; and fluctuation dynamics and instability behavior of multimode continuous-wave dye lasers were studied experimentally and theoretically. The mechanism for mode intensity fluctuations was found to be four-wave mixing, which is a deterministic process, not noise driven. DOE

N89-17217# Lawrence Livermore National Lab., CA.
INDUCTION-LINAC BASED FREE-ELECTRON LASER AMPLIFIER FOR FUSION APPLICATIONS
R. A. Jong and R. R. Stone 1 Aug. 1988 26 p Presented at the 10th International Free-Electron Laser Conference, Jerusalem, Israel, 29 Aug. - 2 Sep. 1988
(Contract W-7405-eng-48)

(DE89-001923; UCRL-98675; CONF-8808146-2) Avail: NTIS HC A03/MF A01

We describe an induction-linac based free-electron laser amplifier design for producing multi-megawatt levels of microwave power for electron cyclotron resonance heating of tokamak fusion devices such as the Compact Ignition Tokamak or the International Thermonuclear Experimental Reactor. The wiggler design strategy incorporates a tapering algorithm suitable for FEL systems with moderate space charge effects and minimizes spontaneous noise growth at frequencies below the fundamental, while enhancing the growth of the signal at the fundamental. In addition, engineering design considerations of the waveguide dimensions, the wiggler magnet gap spacing, the wiggler period, and the minimum magnetic field strength in the tapered region of the wiggler. This FEL is designed to produce an average power of about 10 MW at frequencies in the range from 380 GHz to 560 GHz. The achievement of this average power at a reasonable cost requires a high duty factor, which affects some component design. In addition, the desire to obtain a high extraction efficiency pushes the beam energy up and requires magnetic field strengths in the wiggler that are near or possibly larger than the Halbach limit. We used a methodology for our system study that had been developed earlier. We considered several FEL configurations and selected one that minimized total cost. DOE

N89-17218# Los Alamos National Lab., NM.
HIGH POWER KrF LASER DEVELOPMENT AT LOS ALAMOS
Thomas McDonald, David Cartwright, Charles Fenstermacher, Joseph Figueira, Philip Goldstone, David Harris, William Mead, and Louis Rosocha 1988 5 p Presented at the 19th European Conference on Laser Interation with Matter, Madrid, Spain, 3-7 Oct. 1988
(Contract W-7405-eng-36)
(DE89-002242; LA-UR-88-3382; CONF-881056-6) Avail: NTIS HC A02/MF A01

The objective of the high power laser development program at Los Alamos is to appraise the potential of the KrF laser as a driver for inertial confinement fusion (ICF), ultimately at energy levels that will produce high target gain (gain of order 100). A KrF laser system prototype, the 10-kJ Aurora laser, which is nearing initial system operation, will serve as a feasibility demonstration of KrF technology and system design concepts appropriate to large scale ICF driver systems. The issues of affordable cost, which is a major concern for all ICF drivers now under development, and technology scaling are also being examined. It is found that, through technology advances and component cost reductions, the potential exists for a KrF driver to achieve a cost goal in the neighborhood of 100 dollars per joule. The authors suggest that the next step toward a multimegajoule Laboratory Microfusion Facility (LMF) is an Intermediate Driver facility in the few hundred kilojoule to one megajoule range, which will help verify the scaling of driver technology and cost to an LMF size. An Intermediate Driver facility would also increase the confidence in the estimates of energy needed for an LMF and would reduce the risk in target performance. DOE

N89-17219# Lawrence Livermore National Lab., CA.
APPLICATIONS OF ION IMPLANTATION FOR MODIFYING THE INTERACTIONS BETWEEN METALS AND HYDROGEN GAS
R. G. Musket Sep. 1988 15 p Presented at the International Conference on the Application of Accelerators in Research and Industry, Denton, TX, 7-9 Nov. 1988
(Contract W-7405-eng-48)
(DE89-002877; UCRL-98998; CONF-881151-28) Avail: NTIS HC A03/MF A01

Ion implantations into metals have been shown recently to either reduce or enhance interactions with gaseous hydrogen. Published studies concerned with modifications of these interactions are reviewed and discussed in terms of the mechanisms postulated to explain the observed changes. The interactions are hydrogenation, hydrogen permeation, and hydrogen embrittlement. In particular, the results of the reviewed studies are: uranium hydriding suppressed by implantation of oxygen and carbon; hydrogen gettered in iron and nickel using implantation of titanium; hydriding of titanium catalyzed by implanted palladium; tritium permeation of 304L stainless steel reduced using selective oxidation of implanted aluminum; and hydrogen attack of a low-alloy steel accelerated by implantation of helium. These studies revealed ion implantation to be an effective method for modifying the interactions of hydrogen gas with metals. DOE

N89-17220# Lawrence Livermore National Lab., CA.
RECENT RESULTS FROM THE NOVA EXPERIMENTS PROGRAM
R. L. Kauffman, M. D. Cable, E. M. Campbell, S. G. Glendinning, C. W. Hatcher, S. P. Hatchett, D. R. Kania, J. D. Kilkenny, H. N. Kornblum, and D. T. Kyrazis Oct. 1988 4 p Presented at the 19th European Conference on Laser Interaction with Matter, Madrid, Spain, 3-7 Oct., 1988
(Contract W-7405-eng-48)
(DE89-002901; UCRL-99701; CONF-881056-7) Avail: NTIS HC A02/MF A01

Recent experimental results using the Nova laser are reviewed. The experiments primarily address the physics of indirect-drive ICF. These experiments include investigating high-Z plasmas and radiation production, hydrodynamic stability, and high convergence implosions. The high-Z plasma experiments used a variety of targets to study the complex dynamics and ionization physics of high-Z plasmas. In long pulse irradiations of Au disks with 0.35- micron light, X-ray conversion efficiencies greater than 70 percent have been demonstrated. In collaboration with AWE, we have quantitatively measured material mix at an unstable accelerated interface. In other experiments, we have observed growth of modulations due to Rayleigh-Taylor instabilities in accelerated samples. Radiation-driven implosions experiments have demonstrated radial convergences of 30 fold with good agreement with 1-D hydrodynamic simulations. Presently these experiments are limited to about 20 kJ of 0.35-micron light due to damage in the amplifier glass. We are presently installing new amplifier glass which will allow routine, operation at 120 kJ of 1 omega light in a 2.5-ns pulse. In addition, we are significantly increasing our ability to measure and control the laser pulse shape. With these improvements, we will be able to perform high-power pulse-shaped experiments needed for high density implosions. DOE

N89-17221# Lawrence Livermore National Lab., CA.
INDUCTION-LINAC BASED FREE-ELECTRON LASER AMPLIFIERS FOR PLASMA HEATING
R. A. Jong 22 Aug. 1988 4 p Presented at the 13th International Conference on Infrared and Millimeter Waves, Honolulu, HI, 5-9 Dec. 1988
(Contract W-7405-eng-48)
(DE88-017004; UCRL-99439; CONF-881226-1) Avail: NTIS HC A02/MF A01

We describe an induction-linac based free-electron laser amplifier that is presently under construction at the Lawrence Livermore National Laboratory. It is designed to produce up to 2 MW of average power at a frequency of 250 GHz for plasma heating experiments in the Microwave Tokamak Experiment. In addition, we shall describe a FEL amplifier design for plasma heating of advanced tokamak fusion devices. This system is designed to produce average power levels of about 10 MW at frequencies ranging from 280 to 560 GHz. DOE

N89-17222# Naval Research Lab., Washington, DC. Plasma Physics Div.
ANEURISMS IN LASER-DRIVEN BLAST WAVES Interim Report
J. A. Stamper, B. H. Ripin, R. E. Peterkin, Jr., and R. F. Stellingwerf (Mission Research Corp., Albuquerque, NM.) 25 Aug. 1988 45 p
(AD-A200189; NRL-MR-6184) Avail: NTIS HC A03/MF A01 CSCL 09C

When a short-pulse laser beam is focused onto a solid target in a few Torr ambient gas, the expanding target plasma couples

to the resulting ambient plasma. Dark-field shadowgrams show that a thin, nearly-spherical blast front is produced. These shadowgrams also show the certain regions of the blast front (called aneurisms) may project well ahead of the neighboring, spherical part. Several mechanisms for aneurisms are discussed. One class of aneurisms is consistently produced along the laser axis when the laser energy is greater than about 10 Joules. Two-dimensional, hydrodynamic computer simulations of these on-axis aneurisms show that they can be accounted for the laser heating of an on-axis channel. GRA

N89-17223# Texas Univ., Austin. Dept. of Chemistry.
IN-SITU SURFACE DURING LASER-CONTROLLED CHEMICAL PROCESSING OF SURFACES Final Report, May 1986 - Apr. 1988
Alan Campion 20 Jun. 1988 7 p
(Grant AF-AFOSR-0094-86; AF Proj. 2303)
(AD-A200206; AFOSR-88-0805TR) Avail: NTIS HC A02/MF A01 CSCL 07D

Experiments designed to assess the utility of several methods of surface analysis under reaction conditions are described. The goal of the research was to develop new methods with which to understand the mechanisms associated with the preparation of materials of electronic interest by chemical vapor deposition, with an emphasis on laser control of the reactions. The focus of the work was improve the sensitivity of unenhanced surface Raman spectroscopy through the combined use of ultraviolet lasers, Cassegrain optical systems and charge-coupled device detectors. Model systems to test these technical improvements were designed and an understanding of the factors that govern sensitivity has been achieved. Construction of a system for laser direct writing as well as the installation of a multipurpose surface analysis system are also described. GRA

N89-17224# Naval Weapons Center, China Lake, CA.
AN ACTIVE NITROGEN PLASMA ATOM RESERVOIR FOR LASER-INDUCED IONIZATION SPECTROMETRY
Michael D. Seltzer and Robert B. Green 12 Oct. 1988 109 p
(AD-A200544) Avail: NTIS HC A06/MF A01 CSCL 07B

A microwave induced, atmospheric pressure active nitrogen plasma has been investigated as an atom reservoir for laser induced ionization spectrometry. Discrete analytical samples were introduced into the active nitrogen plasma by a microarc atomizer. Both laser-enhanced ionization (LEI) and dual laser ionization (DLI) were carried out in the plasma plume that extended from the Beenakker cavity. GRA

N89-17225# Lawrence Livermore National Lab., CA.
LASER INTERACTIONS WITH AEROSOL AUREOLES
Leonard C. Rosen, John Creighton, Mary A. Mansigh, and James Ipser Aug. 1988 52 p Prepared in cooperation with Florida Univ., Gainesville
(Contract W-7405-eng-48)
(DE89-002824; UCID-21539) Avail: NTIS HC A04/MF A01

The interaction of laser beams with atmospheric aerosols creates non-uniformities in temperature in the medium surrounding the aerosol. These variations in temperature, and therefore in the index of refraction, termed aureoles, act as scattering centers for the propagating laser beam. The time scales for the formation of the aureoles are developed within this report. The basic equations of energy balance, mass conservation and thermodynamics are used to derive the equations representing a water-droplet aerosol heated by a pulsed laser beam. These equations are solved numerically to yield the variations in aerosol surface temperature and in the surrounding medium as a function of time. The laser beam scattering is calculated for a range of parameters through the Born approximation using the computed temperatures. The range of variables for which beam scattering by atmospheric aerosol aureoles may be important is discussed. DOE

N89-17226# Tennessee Univ. Space Inst., Tullahoma.
LASER THERMAL PROPULSION Annual Technical Report, 1 Sep. 1987 - 31 Aug. 1988
Dennis Keefer Sep. 1988 4 p
(Grant AF-AFOSR-0317-86; AF Proj. 2308)
(AD-A200558; AFOSR-88-1051TR) Avail: NTIS HC A02/MF A01 CSCL 09E

The objective of this research was to determine, experimentally and analytically, the physical mechanisms that determine the behavior of continuous and quasi-continuous, laser sustained plasmas (LSP). The principle questions involve the effects of a forced convection environment, optical geometry and pulse format on the stability, fractional power absorption, plasma structure, and fluid mixing. The future application of this technology to space propulsion rests on the availability of lasers with powers in the megawatt range. It now appears likely that lasers of this size will be free electron lasers that produce power as a series of pulses, rather than continuously. Transient argon plasmas were created using the 20 ns pulse from an excimer laser at a wavelength of 307 nm. Author

N89-17227# Lawrence Livermore National Lab., CA.
SELECTED TOPICS IN FELs
E. T. Scharlemann 1988 34 p Presented at the International School on Electromagnetic Radiation and Particle Beams: Physics and Applications, Varenna, Italy, 20 Jun. 1988
(Contract W-7405-eng-48)
(DE89-004022; UCRL-99922; CONF-8806263-2) Avail: NTIS HC A03/MF A01

A tutorial introduction to wiggler tapering, electron beam dynamics in the wiggler--with particular emphasis on focusing--and optical guiding is presented. DOE

N89-17228# Lawrence Livermore National Lab., CA.
MIX EXPERIMENTS WITH THE NOVA LASER
V. C. Rupert, J. D. Kilkenny, and P. G. Skokowski Oct. 1988 10 p Presented at the Workshop on the Physics of Compressible Turbulent Mixing, Princeton, NJ, 24-2 Oct. 1988 Submitted for publication
(Contract W-7405-eng-48)
(DE89-004775; UCRL-100056; CONF-8810234-3) Avail: NTIS HC A02/MF A01

The NOVA mix experiments are designed to study mix between two dissimilar materials subjected to strong (M approximately 50) shocks and variable accelerations in a direction normal to their common boundary. The main purpose of the experiments is to provide a data base with which predictive models can be compared and normalized. Together with shock tube experiments, which explore a different regime, the current NOVA tests investigate the shock induced source terms in our model and the evolution of both Rayleigh-Taylor stable and unstable interfaces. DOE

N89-17229# Lawrence Livermore National Lab., CA.
PROGRESS TOWARDS A 44-ANGSTROM X-RAY LASER
B. J. MacGowan, J. L. Bourgade, P. Combis, C. J. Keane, R. A. London, M. Louis-Jacquet, D. L. Matthews, S. Maxon, D. Naccache, and M. D. Rosen (California Univ., Berkeley. Lawrence Berkeley Lab.) Nov. 1988 9 p Presented at the 4th Topical Meeting on Short Wavelength Coherent Radiation: Generation and Applications, Cape Cod, MA, 26 Sep. 1988
(Contracts W-7405-eng-48; DE-AC03-76SF-00098; F49620-87-K-0001)
(DE89-004807; UCRL-99058; CONF-880904-5) Avail: NTIS HC A03/MF A01

Since 1984 when soft X-ray amplification was convincingly demonstrated at XUV wavelengths near 200 angstroms, much effort has gone into obtaining soft X-ray gain at shorter wavelengths. One motivation is the possibility of using a high brightness source of amplified spontaneous emission to perform holography of live biological specimens over short time scales. DOE

N89-17230# Lawrence Livermore National Lab., CA.
HIGH ENERGY LASER BEAM SCATTERING BY ATMOSPHERIC AEROSOL AUREOLES
Leonard C. Rosen and James Ipser (Florida Univ., Gainesville.) Dec. 1988 11 p Presented at the Symposium on Lasers and

Optics, Los Angeles, CA, 15-20 Jan. 1989 Submitted for publication
(Contract W-7405-eng-48)
(DE89-004811; UCRL-99232; CONF-890142-1) Avail: NTIS HC A03/MF A01

The interaction of high energy laser beams with aerosols in the atmosphere produces non-uniform temperature variations in the medium surrounding the aerosols. These non-uniformities in the ambient index of refraction act as scattering centers for the laser beam. The basic thermodynamics and conservation equations are solved numerically for pulsed high energy lasers interacting with aerosol water droplet systems. The resulting temperature variations at the surface of the aerosol and in the surrounding medium are found for a variety of input variables including absorbed laser intensity, pulse repetition rate, pulse time, and particle radius. The laser beam scattering is calculated through the Born approximation utilizing the computed temperatures. The range of variables for which laser beam scattering by aerosol aureole systems may be important is discussed. DOE

N89-17231# Lawrence Livermore National Lab., CA.
THE X-RAY LASER: REVIEW OF RECENT EXPERIMENTAL RESULTS AND OF FUTURE PROSPECTS
D. L. Matthews, C. J. Keane, B. J. MacGowan, and J. Trebes Oct. 1988 4 p Presented at the 19th European Conference on Laser Interaction With Matter, Madrid, Spain, 3-7 Oct. 1988 Submitted for publication
(Contract W-7405-eng-48)
(DE89-005096; UCRL-100109; CONF-881056-9) Avail: NTIS HC A02/MF A01

We report the status of X-ray laser development in terms of X-ray wavelengths and efficiencies achieved. We also will discuss the X-ray laser characteristics needed to develop X-ray holographic imaging of in vitro human cells as well as other interesting new applications. Finally, we will comment on the new schemes emerging which should lead to much shorter X-ray wavelengths, perhaps approaching 1 nm. DOE

N89-17232# Sandia National Labs., Albuquerque, NM.
LASER STUDIES OF THE SiH RADICAL/SURFACE INTERACTION DURING DEPOSITION OF A THIN FILM
Pauline Ho, Richard J. Buss, and William G. Breiland 1988 11 p Presented at the Fall Meeting of the Materials Research Society, Boston, MA, 28 Nov. 1988
(Contract DE-AC04-76DP-00789)
(DE89-003902; SAND-88-1641C; CONF-881155-15) Avail: NTIS HC A03/MF A01

This paper presents a new method for studying the interaction of radicals with the surface of a depositing film using a combination of laser spectroscopy and molecular beam techniques. The reactivity of SiH molecules with the surface of a depositing a-Si:H film is measured to be at least 0.95, with no significant dependence on rotational state. DOE

N89-17233# Lawrence Livermore National Lab., CA.
Ne-LIKE ION X-RAY LASER EXPERIMENTS IN PLASMAS PRODUCED BY 0.53 MICRONS AND 0.35 MICRONS LASER LIGHT
C. J. Keane, J. L. Bourgade, P. Combis, R. A. London, M. Louis-Jacquet, B. J. MacGowan, D. L. Matthews, D. Naccache, O. Peyrusse, and M. D. Rosen et al Nov. 1988 6 p Presented at the 4th Topical Meeting on Short Wavelength Coherent Radiation: Generation and Applications, Cape Cod, MA, 26 Sep. 1988
(Contract W-7405-eng-48)
(DE89-004827; UCRL-100001; CONF-880904-7) Avail: NTIS HC A02/MF A01

Recent Ne-like ion X-ray laser experiments carried out at the Centre d'Etudes de Limeil-Valenton (CEL-V) with both 0.53-micron and 0.35-micron laser light will be described. This paper will concentrate primarily on the observation of amplification in Ne-like Sr (Z = 38) in plasmas produced by 0.53-micron laser light. Small signal gains of 4.4/cm and 4.0/cm have been measured for the Ne-like Sr J = 2-1 transitions at 164.1 and 166.5 A, respectively. In addition, the effects of pumping the Ne-like Se laser with 0.35-micron light have been investigated. The resulting Se spectra do not differ significantly from those observed with 0.53-micron light. A brief summary of other experiments carried out at CEL-V will also be given. DOE

N89-17234# Edgerton, Germeshausen and Grier, Inc., Idaho Falls, ID.
NDE METHODS FOR HIGH-TEMPERATURE MATERIALS AND ENVIRONMENTS
B. A. Barna, R. T. Allemeier, N. M. Carlson, J. A. Johnson, J. G. Rodriguez, C. L. Shull, and D. M. Tow 1988 5 p Presented at the 6th International Congress on Experimental Mechanics, Portland, OR, 5 Jun. 1988
(Contract DE-AC07-76ID-01570)
(DE89-005195; EGG-M-26287; CONF-880691-3) Avail: NTIS HC A02

The application of acousto-optic or optic sensing techniques to three high-temperature materials or processes is described. Noncontacting, laser-based sensors are used to image high-luminosity processes, generate ultrasound in molten weld pools, and detect surface dynamics for vibrational analysis. The description of these distinct research efforts gives an overview of one potential approach for developing new capabilities for high-temperature environments. DOE

N89-17235# Edgerton, Germeshausen and Grier, Inc., Idaho Falls, ID. National Engineering Lab.
LASER DETECTION OF ACOUSTIC DISPLACEMENTS BY DESTABILIZING A FREQUENCY STABLIZED HELIUM NEON LASER
B. A. Barna, D. M. Tow, R. T. Allemeier, J. G. Rodriguez, and J. A. Johnson 1988 7 p Presented at the Review of Progress in Quantitative Nondestructive Evaluation, La Jolla, CA, 31 Jul. 1988
(Contract DE-AC07-76ID-01570)
(DE89-005282; EGG-M-88168; CONF-880760-7) Avail: NTIS HC A02/MF A01

A sensor for detecting low-amplitude acoustic displacements is described. This instrument is based on a stabilized helium-neon laser and is capable of measuring submicron displacements of diffuse surfaces at distances of up to 10 m and with a bandwidth between 0.2 and 100 kHz. The potential for extension of the technique to higher frequencies is discussed. The sensor uses the inherent sensitivity of an alternate-mode balanced, frequency-stabilized laser to small amounts of retroreflected light. Applications of the sensor include a study of bonding flaws in complex multilayer materials, such as the thermal protection tiles on the Space Shuttle Orbiter and in graphite epoxy laminar composites. DOE

N89-17196# Edinburgh Univ. (Scotland).
A SCANNING LASER BEAM SYSTEM FOR TWO-DIMENSIONAL ILLUMINATION OF FLOW FIELDS
C. Gray and C. A. Greated *In* VKI, Particle Image Displacement Velocimetry 1988 10 p (For primary document see N89-17179 09-34)
Avail: NTIS HC A21/MF A01

37 MECHANICAL ENGINEERING

Includes auxiliary systems (nonpower); machine elements and processes; and mechanical equipment.

N89-17236# Carnegie-Mellon Univ., Pittsburgh, PA. Robotics Inst.
3-D VISION TECHNIQUES FOR AUTONOMOUS VEHICLES
Martial Hebert, Takeo Kanade, and Inso Kweon Aug. 1988 68 p
(Contract DACA76-85-C-0003; NSF DCR-86-04199; ARPA Order 5351)

(AD-A199643; CMU-RI-TR-88-12) Avail: NTIS HC A04/MF A01 CSCL 17G

A mobile robot needs an internal representation of its environment in order to accomplish its mission. Building such a representation involves transforming raw data from sensors into a meaningful geometric representation. In this paper, we introduce techniques for building terrain representations from range data for an outdoor mobile robot. We introduce three levels of representations that correspond to levels of planning: obstacle maps, terrain patches, and high resolution elevation maps. Since terrain representations from individual locations are not sufficient for many navigation tasks, we also introduce techniques for combining multiple maps. Combining maps may be achieved either by using features or the raw elevation data. Finally, we introduce algorithms for combining 3-D descriptions with descriptions from other sensors, such as color cameras. We examine the need for this type of sensor fusion when some semantic information has to be extracted from an observed scene and provide an example application of outdoor scene analysis. Many of the techniques presented in this paper have been tested in the field on three mobile robot systems developed at CMU. GRA

N89-17237# Sandia National Labs., Albuquerque, NM. Applied Mechanics Div.

SURFACE DEFORMATIONS RESULTING FROM LASER SPOT WELDING

D. J. Segalman and R. D. Krieg 1988 8 p Presented at the ASME Winter Annual Meeting, Chicago, IL, 1 Dec. 1988

(Contract DE-AC04-76DP-00789)

(DE88-014964; SAND-88-2084C; CONF-881210-2) Avail: NTIS HC A02

A method is described for modeling a very simple welding problem, that of forming and resolidifying a melt pool with a laser on a plate of 99.999 percent purity aluminum. The details of the optics, chemistry, and heat transfer are not included so that a rather complete description of the solid mechanics model can be presented. A constitutive model is developed which includes a room temperature-to-melt isotropic/kinematic plasticity behavior. The model is exercised on the laser spot problem and the results presented. The very hot and compliant region in and around the melt zone is restrained from radial expansion by relatively cool and stiff surrounding material which extrudes the melt material toward the laser beam. Because of the small laser spot size and the high conductivity of aluminum, cooling is very rapid when the laser is extinguished. The plastic deformations during heating then dictate the residual stress and deformation states in the solidified plate. The final state has a region of high hydrostatic tensile stress directly beneath the solidified melt zone and a slight depression which remains at the weld site. DOE

N89-17238# Chi Associates, Inc., Arlington, VA.

THE RANKINE AUTOMOTIVE SYSTEM TECHNOLOGY ASSESSMENT REPORT Final Report

George M. Thur 25 Oct. 1988 79 p

(Contract DE-AC01-87CE-90002)

(DE89-002693; DOE/CE-90002/T1) Avail: NTIS HC A05/MF A01

The following major technology advancements developed by the program are described: significant improvements in Rankine component performance, efficiency, size, and weight in the following areas: vapor generator, feed pump, condensers, expanders, and burners; and advancement in the state-of-art for: high heat flux heat exchangers, low emission combustion, controls, once through boiling, and heat engine working fluids. The commercialization results presented in this study reflect a total industry initiative. In fact, the technology was used in fields other than the intended automotive field. The government policy after the termination of the Rankine program was to insure proper documentation of the results. No attempt was made to encourage technology transfer and commercialization of the basic technology. This study shows the societal and economical impacts that are possible when research technology is converted into products for the marketplace, and also the degree of difficulty associated with technology conversion. DOE

N89-17239# Oak Ridge National Lab., TN.

ELECTRON BEAM WELDING PRODUCES IMPROVED DUPLEX CRACK ARREST SPECIMENS

J. F. King, J. D. Hudson, E. A. Metzbower, ed., and D. Hauser, ed. 1988 6 p Presented at the ASM/EWI Power Beam Conference, San Diego, CA, 2-4 May 1988 Sponsored in part by ASM International; The Edison Vending Inst.; The Welding Inst.; The Inst. of Metals; The Laser Inst. of America; Culham Laser Appl. Group; and The Welding Inst. of Canada

(Contract DE-AC05-84OR-21400)

(DE88-003885; CONF-880547-3) Avail: NTIS HC A02/MF A01

The crack arrest toughness, K sub Ia, is generally determined using a monolithic compact type specimen which contains a brittle weld bead to act as a crack initiation site. To test at higher temperatures and toughnesses, electron beam (EB) welded duplex specimens were fabricated. These specimens required the joining of hardened 4340 steel, which acts as the crack initiator, to A533 grade B class 1 steel base material and submerged arc welds in this base metal. The successful fabrication of these specimens required the development of an EB welding procedure with a very narrow heat-affected zone (HAZ). A technique was also developed to eliminate the porosity which was always present in the EB welds through the submerged arc weld deposit region of the joint. The technique involved remelting the joint surface of the A533 steel containing the submerged arc weld to a controlled depth using an oscillated electron beam. This remelt in vacuum reduced the gaseous constituents to low levels and prevented porosity from forming in the deep penetration EB welds between this surface and the 4340 steel. DOE

N89-17240# Oak Ridge National Lab., TN. Instrumentation and Controls Div.

INTEGRATION OF ROBOTICS AND TELEOPERATION FOR THE ADVANCED SERVOMANIPULATOR: CONSOLIDATED FUEL REPROCESSING PROGRAM

G. K. Corbett, M. W. Noakes, and C. T. Kring 1988 11 p Presented at the 2nd International Symposium on Robotics and Manufacturing Research, Education and Applications, Albuquerque, NM, 16-18 Nov. 1988

(Contract DE-AC05-84OR-21400)

(DE88-015281; CONF-881140-6) Avail: NTIS HC A03/MF A01

A robotic mode has been added to the Advanced Servomanipulator (ASM), a six degree-of-freedom master/slave teleoperator. In order to understand the requirements for implementation of robotics on an arm designed for teleoperation, a dynamic simulation of the ASM slave arm was developed. The ASM model and modifications of the control system and interface software for robotic operation are presented, along with some preliminary robotic mode performance results. DOE

N89-17241 Wisconsin Univ., Madison.

ACTIVE VIBRATION SUPPRESSION FOR ROBOTIC MANIPULATORS Ph.D. Thesis

Sanh Le 1988 289 p

Avail: Univ. Microfilms Order No. DA8813145

An experimental modal analysis was performed and the modal properties identified from the T3 robot formed the basis of this study. The acceleration measurements, which included joint servo characterization, and modal analysis, suggest that further improvement in the performance of the robot is achievable. An adaptive prefiltering concept based on a Recursive Least Squares (RLS) identification algorithm incorporated with a variable forgetting factor was derived and simulated. The adaptive prefiltering concept required moderate computation for the continuous tuning of the band rejection filters. The filters are effective in eliminating joint motor excitations that cause structural vibrations. The method provides a wider servo bandwidth at minimal computational costs. It is also very easy to incorporate this control algorithm into an existing control strategy that deals mainly with gross motion or

trajectory controls. Finally, an active vibration suppressor is designed and implemented for the T3 robot. The active suppressor is a compliant structure with built-in actuators linking the end of a robot arm and its end effector. Dissert. Abstr.

N89-17242# Naval Postgraduate School, Monterey, CA.
PENETRATION EFFECTS OF THE COMPOUND VORTEX IN GAS METAL-ARC WELDING M.S. Thesis
John P. Spencer May 1988 102 p
(AD-A200585) Avail: NTIS HC A06/MF A01 CSCL 11F

Twenty-one constant current welds were made at DCRP currents from 204 to 358 A. Three experiments were conducted where the current was in the form of a very slow sawtooth waveform from 200 A to 380 A over a period of 50 seconds. Two low frequency pulsed current welds were made using a 650 A peak current and a Hz. All welds were made bead on mild steel plate using constant current GMAW equipment and argon + 2 percent oxygen shielding gas. After welding, the plates were cut, ground, polished and etched with 12 percent nital solution to show depth of penetration. The constant current welds showed that unlike its behavior in GTAW, penetration increases gradually over the current range tested. Also, the growth of the finger constituted nearly all of the total penetration increase indicating convective flows of increasing magnitude. The ramped current experiments reinforced the observation that penetration increases gradually over the current range examined. The weld pool was also observed to fluctuate, slightly depress and finally depress significantly as the compound vortex started to form, formed completely and then grew stronger. The low frequency pulsed gas metal arc welds realized very little penetration because the wire feed motor was not fast enough and the torch had to be raised causing severe arc spreading. GRA

N89-17243# Southern Univ., Baton Rouge, LA. Dept. of Mechanical Engineering.
EXPERIMENTAL VALIDATION OF A ZERO-DIMENSIONAL COMPUTER MODEL FOR SPARK-IGNITION ENGINES Final Report
R. L. Scott, Jr. 15 Nov. 1988 80 p
(Contract DE-AS04-86AL-38221)
(DE89-002848; DOE/AL-38221/T5) Avail: NTIS HC A05/MF A01

The objective of this work is to validate a computer code that simulates a spark ignited internal combustion engine. The code and a CFR engine are run for a set of similar conditions and the maximum combustion chamber pressures are compared in value and angular locations. The results indicate that the code generally predicts the engine performance. However, improvements are needed in the combustion submodel. Also, intake and exhaust submodels need to be added to the code. DOE

N89-17244# Oak Ridge National Lab., TN.
ASSESSMENT OF NONINTRUSIVE METHODS FOR MONITORING THE OPERATIONAL READINESS OF SOLENOID-OPERATED VALVES
Robert C. Kryter 1988 11 p Presented at the 16th Water Reactor Safety Information Meeting, Gaithersburg, MD, 24 Oct. 1988
(Contract DE-AC05-84OR-21400)
(DE89-002330; CONF-8810155-11) Avail: NTIS HC A03/MF A01

Solenoid-operated valves (SOVs) are being studied at Oak Ridge National Laboratory as part of the USNRC Nuclear Plant Aging Research (NPAR) Program. The primary objective of the study is to identify and recommend methods for inspection, surveillance, and maintenance of SOVs that can ensure their operational readiness - that is, their ability to perform required safety functions under all anticipated operating conditions. An earlier (Phase 1) study described SOV failure modes and causes and identified measurable parameters that might be used to monitor the various degradations that lead to functional failure. The present (Phase 2) study focuses on devising and then demonstrating the effectiveness of techniques and/or equipment with which to measure the previously identified performance parameters and thus detect and trend the progress of any degradation. Several nonintrusive techniques are currently under investigation. Recent experimental results which demonstrate the feasibility and practicality of the techniques being studied are presented. DOE

N89-17245# Los Alamos National Lab., NM. Materials Science and Technology Lab.
UNLUBRICATED SLIDING PROPERTIES OF ION BEAM AND EXCIMER LASER MIXED Fe-Ti-C MULTILAYERED FILMS
Juha-Pekka Hirvonen, Michael Nastasi, Thomas R. Jervis, and Joseph R. Tesmer 1988 7 p Presented at the Fall Meeting of the Materials Research Society, Boston, MA, 28 Nov. - 3 Dec. 1988
(Contract W-7405-eng-36)
(DE89-003470; LA-UR-88-3667; CONF-881155-10) Avail: NTIS HC A02/MF A01

Multilayered Fe-Ti-C films consisting of eleven sublayers were vacuum deposited onto an AISI 304 stainless steel substrate and subsequently mixed using either 400 keV Xe ions or an excimer laser, operating at a wavelength of 308 nm. Ion mixing was accomplished in a two step process: the multilayers were first irradiated with 1 times 10 to the 17th power Xe per sq cm at 520 C, after which half of the sample was irradiated with 5 times 10 to the 15th power Xe per sq cm at O C. Laser mixing was carried out at both 1.1 and 1.7 J per sq cm with the number of pulses varied between 1 and 10. Pin-on-disc studies revealed only slight differences between the two kinds of ion beam mixed samples, whereas the dry sliding properties of laser mixed samples were strongly dependent on the total fluence used. In the optimum conditions similar friction coefficients were obtained on both kinds of samples. DOE

N89-17246 ESDU International Ltd., London (England).
COMPUTER PROGRAM FOR THE PREDICTION OF AIR-LIFT PUMP PERFORMANCE
Sep. 1988 54 p
(ESDU-88014; ISBN-0-85679-646-8; ISSN-0141-4011) Avail: ESDU

This Data Item 88014, an addition to the Sub-series on Fluid Mechanics, gives a FORTRAN program listing that predicts the operating characteristics of air-lift pumps. Such pumps operate by injecting air near the bottom of the riser so creating a two-phase flow that rises due to its density difference from that of the surrounding liquid, or liquid in a downcomer. Because there are no moving parts the pumps are virtually maintenance free and so provide a reliable means of raising corrosive, hazardous or abrasive liquids. Operating characteristics and design features are briefly discussed. The program applies to isothermal flow of a Newtonian liquid. It is based on the drift-flux model, which is explained, and uses empirical correlations from the literature to predict the gravity and friction components of pressure loss. Comparison with experiment shows predictions are generally within 30 percent which compares favorably with two phase correlations. However, because of that limitation, the prime uses of the program are either to modify an existing design, when the program can first be calibrated against experiment and then used to predict the effect of design charges, or to carry out a sensitivity analysis of a basic pump design. Guidance is given on the format for the input data and typical values are provided for equivalent hydraulic roughness and pressure losses in pipe fittings, data for which are required by the program. Both uses of the program are illustrated in worked examples that include specimen print-outs, and the program is available on magnetic media as ESDUpac 8814. ESDU

N89-17247 ESDU International Ltd., London (England).
THE DESIGN OF SPUR AND HELICAL INVOLUTE GEARS. A PROCEDURE COMPATIBLE WITH BS 436:1986: METHOD FOR CALCULATION OF CONTACT AND ROOT BENDING STRESS LIMITATIONS FOR METALLIC INVOLUTE GEARS
Dec. 1988 61 p
(ESDU-88033; ISBN-0-85679-665-4; ISSN-0141-4046) Avail: ESDU

This Data Item 88033, an addition to the Sub-series on Mechanisms, is a guide to BS 436:Part 3:1986 which provides a rigorous analytical procedure for rating a gear of known size in terms of allowable stresses or maximum power capacity. The method quantifies all the factors known to affect gear performance, and it requires a major reappraisal of traditional methods of gear design. ESDU 88033 discusses the factors, introduced in the new Standard, that affect material strength and the stresses induced, and provides advice on the choice of materials and manufacturing processes. An approximate method, compatible with BS 436:Part 3:1986 enables the physical size of suitable gears to be determined from a known power transmission requirement. The method is summarized in a flowchart and illustrated by worked examples. A discussion of methods by which the new Standard may be used to generate gear design data for optimization is included. ESDU

N89-17248*# National Aeronautics and Space Administration. Lewis Research Center, Cleveland, OH.

COMPUTER-AIDED DESIGN OF BEVEL GEAR TOOTH SURFACES

Hung Chang Shuo, Ronald L. Huston (Cincinnati Univ., OH.), and John J. Coy 1989 19 p Prepared for presentation at the 5th International Power Transmission and Gearing Conference, Chicago, IL, 25-27 Apr. 1989; sponsored in part by ASME Prepared in cooperation with Army Aviation Systems Command, Cleveland, OH

(Grant NAG3-188; DA Proj. 1L1-62209-A-47-A)

(NASA-TM-101449; E-4558; NAS 1.15:101449; AVSCOM-TM-88-C-005) Avail: NTIS HC A03/MF A01 CSCL 13I

This paper presents a computer-aided design procedure for generating bevel gears. The development is based on examining a perfectly plastic, cone-shaped gear blank rolling over a cutting tooth on a plane crown rack. The resulting impression on the plastic gear blank is the envelope of the cutting tooth. This impression and envelope thus form a conjugate tooth surface. Equations are presented for the locus of points on the tooth surface. The same procedures are then extended to simulate the generation of a spiral bevel gear. The corresponding governing equations are presented. Author

N89-17249# Oak Ridge National Lab., TN. Center for Engineering Systems Advanced Research.

HERMIES-3: A STEP TOWARD AUTONOMOUS MOBILITY, MANIPULATION AND PERCEPTION

C. R. Weisbin, B. L. Burks, J. R. Einstein, R. R. Feezell, W. W. Manges, and D. H. Thompson 1989 22 p Presented at the NASA Conference on Space Telerobotics, Pasadena, CA, 31 Jan. - Feb. 1989

(Contract DE-AC05-84OR-21400)

(DE89-004932; CONF-890153-1) Avail: NTiS HC A03/MF A01

HERMIES-3 is an autonomous robot comprised of a seven degree-of-freedom (DOF) manipulator designed for human scale tasks, a laser range finder, a sonar array, an omnidirectional wheel-driven chassis, multiple cameras, and a dual computer system containing a 16-node hypercube expandable to 128 nodes. The current experimental program involves performance of human-scale tasks (e.g., valve manipulation, use of tools), integration of a dexterous manipulator and platform motion in geometrically complex environments, and effective use of multiple cooperating robots (HERMIES-2B and HERMIES-3). The environment in which the robots operate has been designed to include multiple valves, pipes, meters, obstacles on the floor, valves occluded from view, and multiple paths of differing navigation complexity. The ongoing research program supports the development of autonomous capability for HERMIES-2B and 3 to perform complex navigation and manipulation under time constraints, while dealing with imprecise sensory information. DOE

N89-17250# Department of Defense, Washington, DC. Heat Engine Propulsion Div.

REPORT TO CONGRESS ON THE AUTOMOTIVE TECHNOLOGY DEVELOPMENT PROGRAM Annual Report No. 10

Nov. 1988 38 p

(DE89-004977; DOE/CE-0240) Avail: NTIS HC A03/MF A01

This is the tenth annual report on the progress in implementing the Automotive Propulsion Research and Development Act of 1978 (Title 3 of Public Law 95-238). The Act provides for an expanded research and development (R and D) effort with respect to advanced automotive propulsion systems technology which would complement and stimulate corresponding efforts by the private sector. Implementation of the Act is the responsibility of the Department of Energy's (DOE) Office of Transportation Systems (OTS). The programmatic goals of OTS are to increase end-use efficiency of highway vehicles and other transportation modes and to substitute abundant domestic fuels for petroleum based fuels. The Lewis Research Center (LERC) of the National Aeronautics and Space Administration (NASA) is the Technical Project Manager for advanced materials and alternative fuels utilization R and D. The R and D projects in progress address the high-risk areas associated with the development of ceramic components for the gas turbine engine, improvement to the Stirling engine, heavy-duty adiabatic diesel engine technology, advanced materials technology, and alternative fuels utilization technology. DOE

N89-17251# Oak Ridge National Lab., TN.

SPATIAL REASONING IN THE TREATMENT OF SYSTEMATIC SENSOR ERRORS

Martin Beckerman, Judson P. Jones, Reinhold C. Mann, Leslie A. Farkas, and S. E. Johnston (Kentucky Univ., Lexington.) 1988 12 p Presented at the Conference on Sensor Fusion: Spatial Reasoning and Scene Interpretation, Cambridge, MA, 6 Nov. 1988

(Contract DE-AC05-84OR-21400)

(DE89-003244; CONF-8811132-1) Avail: NTIS HC A03/MF A01

In processing ultrasonic and visual sensor data acquired by mobile robots systematic errors can occur. The sonar errors include distortions in size and surface orientation due to the beam resolution, and false echoes. The vision errors include, among others, ambiguities in discriminating depth discontinuities from intensity gradients generated by variations in surface brightness. In this paper we present a methodology for the removal of systematic errors using data from the sonar sensor domain to guide the processing of information in the vision domain, and vice versa. During the sonar data processing some errors are removed from 2D navigation maps through pattern analyses and consistent-labelling conditions, using spatial reasoning about the sonar beam and object characteristics. Others are removed using visual information. In the vision data processing vertical edge segments are extracted using a Canny-like algorithm, and are labelled. Object edge features are then constructed from the segments using statistical and spatial analyses. A least-squares method is used during the statistical analysis, and sonar range data are used in the spatial analysis. DOE

N89-17252# Edgerton, Germeshausen and Grier, Inc., Idaho Falls, ID. National Engineering Lab.

COMPUTER CONTROL OF GAS METAL ARC WELDING

H. B. Smartt, C. J. Einerson, and A. D. Watkins 1988 13 p Presented at the Computer Technology in Welding, Cambridge, United Kingdom, 8 Jun. 1988

(Contract DE-AC07-76ID-01570)

(DE89-005188; EGG-M-00487; CONF-880686-2) Avail: NTIS HC A03/MF A01

The state of an arc weld is determined by the composition of the weld and base metal and its thermomechanical history. The composition of the deposited weld metal depends primarily on the amount of filler metal dilution which occurs. The heat input to the weld, comprising pre-heat and process heat, is the controlling factor in the thermal cycle to which the material responds

metallurgically, to produce a specific set of weld properties. Thus, control of the arc welding process should focus on rational specification and real-time control of the heat and mass input to the weld. A process control model has been developed for the gas metal arc welding (GMAW) process using the state variables, time-domain method. The governing equations have been solved for the process parameters as functions of the desired heat input (in terms of heat per unit length) and mass input (in terms of transverse reinforcement area) to the weld. The resulting nonlinear model has been used with a simple proportional controller with deadband and variable coefficients to control the weld heat input and reinforcement area independently. A welding machine has been developed for this work, consisting of a computer-controlled welding head, positioning table, and operator panel, which is the front end for a conventional 300 A constant voltage power supply. Software for the system is written in the HPL language. System components communicate over an IEEE-488 bus. DOE

38 QUALITY ASSURANCE AND RELIABILITY

Includes product sampling procedures and techniques; and quality control.

N89-17253# Advisory Group for Aerospace Research and Development, Neuilly-Sur-Seine (France). Structures and Materials Panel.

AGARD/SMP REVIEW: DAMAGE TOLERANCE FOR ENGINE STRUCTURES. 1: NON-DESTRUCTIVE EVALUATION

Nov. 1988 125 p In ENGLISH and FRENCH Meeting held in Luxembourg, 1-6 May 1988

(AGARD-R-768; ISBN-92-835-0484-4) Copyright Avail: NTIS HC A06/MF A01

The AGARD Structures and Materials Panel is coordinating a series of workshops within the framework of a review of damage tolerance for engine structures. The review aims to address the areas critical to the acceptance of an approach based on damage tolerance concepts as an alternative lifing philosophy to that of safe-life for the design of engine components. Engineering assumptions, component design, life prediction of turbine disks, and the need for common AGARD approaches to nondestructive evaluation are among the topics covered. For individual titles, see N89-17254 through N89-17261.

N89-17254# Rolls-Royce Ltd., Derby (England). Dept. of Materials and Mechanical Technology.

THE IMPACT OF ENGINEERING ASSUMPTIONS ON NDE REQUIREMENTS

R. H. Jeal *In* AGARD, AGARD/SMP Review: Damage Tolerance for Engine Structures. 1: Non-Destructive Evaluation Nov. 1988 6 p (For primary document see N89-17253 09-38)

Copyright Avail: NTIS HC A06/MF A01

Geometrical aspects - including surface finish - have the advantage that they can be directly measured on the individual parts for comparison with those originally set. The designer can calculate the size of acceptable deviations from the norm and production is accepted or rejected on the basis of these tolerances. Material condition is a more difficult concept to deal with. It covers a wide range of phenomena ranging from cracks, scratches and porosity to the details of material microstructure which represent a deviation from the designers' assumption of a material as a continuous, isotropic, homogeneous media free from defects. These deviations are both difficult to find and their effect on performance is difficult to assess. Designers in the past used to assume safety factors to account for the unseen presence of defects. As more efficient use of available materials has been sought, these factors have been reduced but at the price of greater perfection in the materials. This has led to increasing demands upon the ability of the designer to assess the behavior of discontinuities and set the defect standards, and for the inspection engineer to establish techniques that will find smaller and smaller defects in more and more difficult situations on ever increasing degree of certainty. The way these changing design requirements have impacted upon the problem presented to the inspection engineer is discussed. Author

N89-17255# University Coll., London (England). Dept. of Mechanical Engineering.

REVIEW OF EXISTING NDT TECHNOLOGIES AND THEIR CAPABILITIES

Leonard J. Bond *In* AGARD, AGARD/SMP Review: Damage Tolerance for Engine Structures. 1: Non-Destructive Evaluation Nov. 1988 16 p (For primary document see N89-17253 09-38)

Copyright Avail: NTIS HC A06/MF A01

A review of selected nondestructive test (NDT) technologies is presented with regard to their reliability and capability to detect and characterize defects in critical aero-engine components such as discs and blisks (integrally bladed discs), both in production and after service. The performance of non-destructive testing is considered both at the time of manufacture and after service for parts fabricated from powder metals including AP1 and with particular consideration given to the needs of the European Fighter Aircraft (EFA). Various NDT technologies have been considered with the aim of establishing the current capability of each technology in terms of defect detection capability and probability of detection rates. The cause of the limits on performance are reviewed and areas where development can be expected in these and other NDT technologies within the next 5 to 10 years have been identified. Author

N89-17256# Pratt and Whitney Aircraft, West Palm Beach, FL. Dept. of Materials Engineering.

RELATIONSHIPS OF NONDESTRUCTIVE EVALUATION NEEDS AND COMPONENT DESIGN

John A. Harris, Jr. and M. C. VanWanderham *In* AGARD, AGARD/SMP Review: Damage Tolerance for Engine Structures. 1: Non-Destructive Evaluation Nov. 1988 8 p (For primary document see N89-17253 09-38)

Copyright Avail: NTIS HC A06/MF A01

Several well publicized engine and airframe failures which occurred in the late 1960 to mid 1970's time frame resulted in emphasis on development, application and quantification of nondestructive evaluation (NDE) as opposed to reliance on a Zero Defects design philosophy. As the use of fracture mechanics as a basis for damage tolerance and retirement analysis of components became established, additional emphasis was placed on screened flaw sizes, NDE and quantification of reliability. In the late 1970's a structural assessment was conducted on the design of the F100 engine which resulted in a series of relatively sophisticated safety inspections for selected critical components. The Retirement for Cause philosophy also coupled NDE and component lifing analyses to enable return to service decisions for engine components. These activities were (and are) performed usually after the component designs have been finalized. The establishment of Engine Structural Integrity Programs (ENSIP) for new U.S. military engine systems has now made NDE considerations an integral part of the design process. Classification of components, fracture mechanics analyses, critical flaw sizes, material quality, NDE and quantification of inspection reliability are now incorporated in the initial design process and directly influence the resultant component designs. Statistically based probabilistic approaches are supplementing the deterministic methods previously used. The relationships of NDE needs and component design in light of the evolution of the ENSIP approach for gas turbine engine component designs are discussed. Author

N89-17257# National Research Council of Canada, Ottawa (Ontario). Structures and Materials Lab.

IMPORTANCE OF SENSITIVITY AND RELIABILITY OF NDI TECHNIQUES ON DAMAGE TOLERANCE BASED LIFE PREDICTION OF TURBINE DISCS

A. K. Koul, A. Fahr, G. Gould, and N. Bellinger (Carleton Univ., Ottawa, Ontario) *In* AGARD, AGARD/SMP Review: Damage Tolerance for Engine Structures. 1: Non-Destructive Evaluation

Nov. 1988 22 p (For primary document see N89-17253 09-38)
Copyright Avail: NTIS HC A06/MF A01

The results of a demonstration program carried out to determine the influence of the sensitivity and reliability of nondestructive inspection (NDI) techniques on the damage tolerance based life assessment of aero engine turbine discs are discussed. The program was carried out on the 5th stage compressor discs of the J85-CAN40 engine, made from the AM-355 stainless steel. The sensitivity and reliability of several NDI techniques, in detecting service induced low cycle fatigue (LCF) cracks in the disc bolt hole regions, are assessed on the basis of detectable crack sizes at 90 percent probability of detection (POD) and 90 percent POD with 95 percent confidence level. The NDI techniques examined are the liquid penetrant inspection (LPI) technique, a manual eddy current inspection (ECI) technique using two gain settings and an ultrasonic leaky wave (ULW) technique using an automated C-scan system. The safe inspection intervals (SIIs) for the 5th stage compressor disc are calculated using deterministic fracture mechanics (DFM) and probabilistic fracture mechanics (PFM) principles. These calculations involve the use of the NDI data, finite element analysis and the experimental fatigue crack growth rate (FCGR) data generated on compact tension specimens machined from discs. The results indicate that the manual ECI technique with a high gain setting and the automated ULW technique are the most sensitive and reliable in detecting LCF cracks. Author

N89-17258# Societe Nationale d'Etude et de Construction de Moteurs d'Aviation, Evry Cedex (France).
SHORT TERM DEVELOPMENTS IN NON-DESTRUCTIVE EVALUATION APPLICABLE TO TURBINE ENGINE PARTS [LES DEVELOPPEMENTS A COURT TERME DES CONTROLES NONDESTRUCTIFS APPLICABLES AUX PIECES DE TURBOMACHINES]
J. Vaerman *In* AGARD, AGARD/SMP Review: Damage Tolerance for Engine Structures. 1: Non-Destructive Evaluation Nov. 1988 29 p In FRENCH (For primary document see N89-17253 09-38)
Copyright Avail: NTIS HC A06/MF A01

An analysis of the principles forming the basis of non-destructive evaluation (NDE) techniques is presented. Excitation energy sources, medium interaction (perturbation), and sensors and signal processing are examined. Factors affecting the evolution and adaptation of NDE methods are discussed and recent developments in acoustic microscopy, ultrasonic techniques, Foucault current methods, and X-ray tomography are described. Author

N89-17259# Naval Air Development Center, Warminster, PA.
LONG TERM POSSIBILITIES FOR NONDESTRUCTIVE EVALUATION FOR US NAVY AIRCRAFT
W. R. Scott *In* AGARD, AGARD/SMP Review: Damage Tolerance for Engine Structures. 1: Non-Destructive Evaluation Nov. 1988 13 p (For primary document see N89-17253 09-38)
Copyright Avail: NTIS HC A06/MF A01

The majority of nondestructive inspection (NDI) techniques currently in use for U.S. Navy aircraft are labor intensive, operator dependent and result in excessive aircraft down-time. For this reason NDI R and D efforts currently are directed toward developing rapid automated systems capable of remote or unattended inspection of large areas and inaccessible structures. Ongoing programs of this type that are discussed include laser ultrasonics, acoustic emission, and quantitative imaging. The primary thrust of the presentation will cover the advantages of each technique and the technical obstacles preventing its implementation. Author

N89-17260# Rolls-Royce Ltd., Derby (England). Dept. of Non-Destructive Testing Applications.
NEED FOR COMMON AGARD APPROACH AND ACTIONS
R. G. Taylor *In* AGARD, AGARD/SMP Review: Damage Tolerance for Engine Structures. 1: Non-Destructive Evaluation Nov. 1988 3 p (For primary document see N89-17253 09-38)
Copyright Avail: NTIS HC A06/MF A01

While there is no direct evidence that the different approaches used in nondestructive tests (NDT) have affected airworthiness, there are many pressures, both technical and commercial, for requiring a common approach within the community in the future. The technical pressures arise from a need to achieve the same technical standard of product, irrespective of the place of manufacture, in order to meet the stringent damage tolerance requirements now being placed on NDE, while the commercial pressures arise from the need for industry to rationalize the methodolgy, so that components are processed in the same way, irrespective of the customer. An example of the problems associated with the lack of a common approach, is shown in the differing requirements of the major aero engine manufactures, for the ultrasonic inspection of turbine discs. A study of the physics of the different methods demanded by the engine companies, shows that the same technical standard cannot be achieved, and the commercial problems are obvious when it is recognized that these different techniques are imposed on a common forging supplier. As a result of recent collaboration activities with a number of other engine manufacturers, Rolls-Royce has carried out a survey of the differences that currently exist and these are summarized. Author

N89-17261# Societe Nationale d'Etude et de Construction de Moteurs d'Aviation, Evry Cedex (France).
STATE-OF-THE-ART IN NON-DESTRUCTIVE EVALUATION OF TURBINE ENGINE PARTS [L'ETAT DE L'ART EN CONTROLE NONDESTRUCTIF DES PIECES DE TURBOMACHINE]
J. L. Meiffren *In* AGARD, AGARD/SMP Review: Damage Tolerance for Engine Structures. 1: Non-Destructive Evaluation Nov. 1988 16 p In FRENCH (For primary document see N89-17253 09-38)
Copyright Avail: NTIS HC A06/MF A01

An overview of non-destructive evaluation (NDE) methods used in aeronautical engineering is presented. The use of NDE during the fabrication of turbine engine components is discussed with particular emphasis on the ultrasonic evaluation of compressor and turbine disks, thickness measurement of turbine blades, and the evaluation of welds in compressor rotors. In addition, the application of NDE techniques to the evaluation of in-service engines is discussed. The detection of fatigue cracks and ruptures in operational engine parts is addressed along with statistical approaches to NDE. Author

N89-17262# Grumman Aerospace Corp., Bethpage, NY. Aircraft Systems Div.
R/M/T (RELIABILITY/MAINTAINABILITY/TESTABILITY) DESIGN FOR FAULT TOLERANCE. VOLUME 1: PROGRAM MANAGER'S GUIDE Final Report, Oct. 1985 - May 1986
David J. Conroe and Stanley J. Murn, Jr. Mar. 1988 153 p (Contract F30602-85-C-0161)
(AD-A200204; RADC-TR-88-69-Vol-1) Avail: NTIS HC A08/MF A01 CSCL 13H

Fault tolerance has come into almost universal use in modern day systems of all types. This report contains design guidance and general information for Air Force and contractor program managers with respect to the nature and form of Reliability/Maintainability/Testability (R/M/T) tasks needed in the development of fault tolerant systems. This program managers guide contains instructions for tailoring the R/M/T programmatic standards (MIL-STDs 785, 470 and 2165) for fault tolerant systems development. Important fault tolerance design options and tradeoff analysis methods are discussed to aid the program manager in understanding and overseeing the entire fault tolerant system design process. This report is Volume 1 of 2. Volume 2 will be an R/M/T Fault Tolerant Design Implementation Guide available at a later date. GRA

39 STRUCTURAL MECHANICS

Includes structural element design and weight analysis; fatigue; and thermal stress.

For applications see *05 Aircraft Design, Testing and Performance* and *18 Spacecraft Design, Testing and Performance.*

N89-17263 Purdue Univ., West Lafayette, IN.
VIBRATION AND AEROELASTIC TAILORING OF ADVANCED COMPOSITE PLATE-LIKE LIFTING SURFACES Ph.D. Thesis
Richard Y. L. Liu 1987 199 p
Avail: Univ. Microfilms Order No. DA8814556

Modern flight vehicles are often designed to meet requirements of high structural and aerodynamic performance. One way to attain this objective is to implement the techniques of aeroelastic tailoring. In this work, the lifting surface of a fighter aircraft is structurally idealized as a composite laminated plate element. By modifying the interactions between the surface deformation modes (e.g., bending and twisting), the elastic properties of the anisotropic plate can be controlled to satisfy a specific design criterion. The study is aimed at the conceptual understanding of the effect of elastic coupling upon the dynamic and aeroelastic behavior of a wing. The structural analysis is performed using the Rayleigh-Ritz method. A group of five non-dimensional parameters is identified to characterize the stiffness properties of a laminated plate. Three of these parameters measure the amount of elastic coupling present in the plate, and their influences on the vibration modes (natural frequencies and mode shapes) are evaluated in the vibration analysis. Dissert. Abstr.

N89-17264 Illinois Univ., Urbana-Champaign.
THE EFFECTS OF STRAIN INDUCED SOFTENING ON THE LOAD CARRYING CAPABILITY OF COMPONENTS Ph.D. Thesis
James Lee Handrock 1988 269 p
Avail: Univ. Microfilms Order No. DA8815348

In this study the effect of material softening on the load carrying capability of components was investigated. An elevated temperature (565 C) experimental test program was conducted using smooth, Bridgman notched, and British Standard V-notched test specimens. The basis of this program had a matrix of creep, fatigue, notch acuity, and stress ratio effects. From these test results a first-order model of cyclic softening was developed in which the current strength was defined as a function of the load cycle number and frequency. This model was then used to predict the results of completely reversed load control tests on both the plain and notched bars. Observations were also made regarding strain rate, frequency, and hold time effects. A time independent uniaxial constitutive model was developed in which strain induced cyclic softening was defined as a function of accumulated plastic strain. Good predictions were made of both overall strength loss and hysteresis behavior under controlled strain range conditions. This constitutive model was then used to investigate the geometrical effects of softening in a two-bar structure. A finite element analysis was completed on the Bridgman notched specimen geometry using isocyclic cyclic stress-strain curves to represent material softening. These curves allowed static analyses to be completed to simulate results for cyclic loading conditions. Dissert. Abstr.

N89-17265 Illinois Univ., Urbana-Champaign.
NUMERICAL ANALYSIS OF THE EFFECTS OF VOID GROWTH AND CRACK TIP OPENING ON DUCTILE FRACTURE Ph.D. Thesis
Craig Lee Hom 1988 146 p
Avail: Univ. Microfilms Order No. DA8815356

First, the finite element technique was used to study the growth of initially spherical voids in a cubic array under remote uniform loads of uniaxial tension, pure shear and high triaxial stress. The results show that shape change has a strong effect on the material's behavior. Indeed, for low triaxial stress states, the effect of voids on the material response is stronger than expected due to void elongation. For higher triaxiality, the voids interact strongly to cause rapid drops in the material's load carrying capacity. The second problem examines the effects of tip blunting and differential thinning on a crack in a thin elastic-plastic sheet. The finite element results show that two shear bands at 45 degrees to the plane of the sheet develop. Also, the results indicate the stresses are significantly higher in the near tip region at the midplane of the sheet than predicted by plane stress theory. Finally, the growth and interaction of an array of initially spherical voids ahead of a blunting plane strain crack tip were studied. The finite element results show that spherical voids grow towards the crack tip and coalesce with the crack before they coalesce with each other. Increases in plastic strain were observed in the near tip region due to the presence of the voids. The results are used to discuss ductile crack growth in engineering alloys. Dissert. Abstr.

N89-17266# Air Force Systems Command, Wright-Patterson AFB, OH. Foreign Technology Div.
THE BEHAVIOR OF SHELLS MADE OF COMPOSITES DURING THE DYNAMIC APPLICATION OF AXIAN COMPRESSION
A. S. Volmir and L. N. Smetanina 10 Aug. 1988 9 p Transl. into ENGLISH from Stroitel'naya Makhanika i Raschet Sooruzheniy (USSR), no. 4(70), Jul. - Aug. 1970 p 34-37
(AD-A200244; FTD-ID(RS)T-0538-88) Avail: NTIS HC A02/MF A01 CSCL 11D

In nonlinear formulation we examine the problem of the dynamic stability of cylindrical shells made of composites, e.g., glass reinforced plastic, under dynamic axial compression. We assume as given the law of mutual displacement of the ends of the shell. Using the Bubnov-Galerkin method, the equations of the nonlinear theory of shells in partial derivatives are reduced to ordinary differential equations with aperiodic coefficients. The equations obtained were integrated numerically using a BESM-2M computer for various loading rates and shell parameters relative to certain brands of glass-reinforced plastics. Similar problems for isotropic metal shells have been examined previously 1, 2. The case of dynamic application of external pressure to an orthotropic shell was examined. GRA

N89-17267 ESDU International Ltd., London (England).
CALCULATION METHODS FOR ALONG-WIND LOADING. PART 3: RESPONSE OF BUILDINGS AND PLATE-LIKE STRUCTURES TO ATMOSPHERIC TURBULENCE
Oct. 1988 75 p
(ESDU-88019; ISBN-0-85679-651-4; ISSN-0143-2702) Avail: ESDU

This Data Item 88019, an addition to the Sub-series on Wind Engineering, provides a step-by-step calculation method for the loading, accelerations and deflections of buildings and plate-like structures. The loading is derived as the sum of a mean component together with background and resonant fluctuating components. Precalculated loading factors, based on the wind models in the Sub-series, are included in graphical and equation form for estimation of the fluctuating components. Load/velocity admittance factors, which made allowance for the distortion of turbulence by the presence of the structure, are also included. The input data necessary are discussed and, where appropriate, approximate values are provided. A calculation sheet for the method is included and its use illustrated with a worked example. ESDU 88036 provides a computer program for this method, and for the similar method applied to line-like structures in ESDU 87035. ESDU

N89-17268 ESDU International Ltd., London (England).
PIPELINE VIBRATIONS. UNDAMPED NATURAL VIBRATION OF PIPELINES
Oct. 1988 96 p
(ESDU-88022; ISBN-0-85679-654-9; ISSN-0141-4011) Avail: ESDU

This Data Item 88022, an addition to the Sub-series on Fluid Mechanics, provides graphical data and a program listing in FORTRAN for the estimation of the natural vibration characteristics of non-rigid planar piping systems, either empty or running full. The program calculates natural frequencies and corresponding mode shapes, and normal-mode generalized masses and

stiffnesses of the transverse bending and axial modes of vibration, up to a chosen cut-off frequency. Lumped masses, to model in-line valves for example, and externally-acting elastic restraints in the plane of the system may be treated. The effects of bend flexibility may be included. The pipes may vary in cross-section, or be of different materials, but the fluid is assumed of constant density. The graphical data allow the estimation of the fundamental frequency of a single pipe, or of configurations with up to three right angle bends, subject to additional idealizations over those imposed by the computer model. Worked examples illustrate the use of both methods. The program is available on magnetic media as ESDUpac 8822. ESDU

N89-17269 ESDU International Ltd., London (England).
AVOIDANCE OF BUCKLING OF SOME ENGINEERING ELEMENTS (STRUTS, PLATES AND GUSSETS)
Nov. 1988 31 p
(ESDU-88034; ISBN-0-85679-666-2; ISSN-0141-4089) Avail: ESDU

This Data Item 88034, an addition to the Sub-series on Stress and Strength, after a general introduction to buckling, provides data on the buckling stress for overall buckling of a strut with various end conditions and making allowance for initial imperfections. For open cross-section struts, the prediction of both torsional and torsional-flexural buckling is treated, together with local buckling. For tubular section struts, both local and torsional buckling are considered. Curves are provided for the prediction of buckling of a rectangular plate with various edge conditions under biaxial compression or combined biaxial compression and tension. Curves also provide estimates of the buckling stress for the plate under pure shear with any combination of clamped or simply-supported edges, and for the plate under uniaxial compression with in-plane bending. Buckling of the free edge of a triangular gusset plate is considered, and data are included on the lateral instability of a uniform beam or cantilever under various lateral loading conditions. All the data relate to the onset of buckling, but reference is made to other ESDU work that includes the effect of material plasticity. ESDU

N89-17270 ESDU International Ltd., London (England).
MAXIMUM INELASTIC BENDING MOMENTS AND FORM FACTORS FOR SYMMETRIC BENDING OF BEAMS
Dec. 1988 35 p
(ESDU-88035; ISBN-0-85679-667-0; ISSN-0141-4097) Avail: ESDU

This Data Item 88035, an addition to the Sub-series on Structures, gives a FORTRAN program listing that calculates the applied bending moment that gives a maximum allowable extreme fiber stress in a beam under symmetric loading. The program includes the non-linear elastic behavior beyond the limit of proportionality using the generalized stress-strain curve of ESDU 76016. A form factor based on a elastic stress equivalent to the 0.2 percent proof stress is also given. The beam section may be any multi-segment polygon provided its first and second moments of area are balanced about the neutral x-axis (the axis about which the moment is applied). Details of the input format, the output interpretation and special warnings are provided, and two practical worked examples illustrate the use of the program. It is also available on magnetic media as ESDUpac 88035. ESDU

N89-17271 ESDU International Ltd., London (England).
CALCULATION METHODS FOR ALONG-WIND LOADING. PART 4: COMPUTER PROGRAM FOR ESTIMATION OF RESPONSE
Dec. 1988 73 p Supersedes ESDU-84034
(ESDU-88036; ISBN-0-85679-668-0; ISSN-0143-2702) Avail: ESDU

This Data Item 88036, an addition to the Sub-series on Wind Engineering, provides the FORTRAN program listing for the methods of ESDU 87035 (for line-like structures) and ESDU 88019 (for plate-like structures). The program calculates loading, accelerations and deflections on, for example, buildings, chimneys, solid or lattice towers, pipelines, individual structural members, bridges, and cranes. The program allows the stiffness and mass to vary vertically (and horizontally for the wide structures) and the height (or width) need not be constant. Appropriate mode shapes and influence coefficients are required and are provided, or the user may input values of his own. The format of the input and output is explained, and information is included on warnings provided. Worked examples illustrate the use of the software. The program is available on magnetic media as ESDUpac 88036. ESDU

N89-17272# Fraunhofer-Inst. fuer Betriebsfestigkeit, Darmstadt (Germany, F.R.).
PAPERS OF THE 5TH LBF COLLOQUIUM [VORTRAEGE DES FUENFTEN LBF-KOLLOQUIUMS]
O. Buxbaum, ed. 1988 272 p In GERMAN Colloquium held in Darmstadt, Fed. Republic of Germany, 8-9 Mar. 1988
(LBF-TB-180; ISSN-0721-5320; ETN-89-93516) Avail: NTIS HC A12/MF A01

The influence of the load sequence on the fatigue life of fatigue-fracture-endangered components; experimental methods for the reduction of the duration of fatigue tests; and modal analysis methods for the reduction of system-conditioned dynamic loads are treated. A procedure for the generation of load sequences, the strength evaluation of fiber-reinforced composite leaf springs under operational conditions, and the damage tolerance behavior of fiber reinforced composite airframes were studied. A finite element method for the evaluation and optimization of fiber reinforced composite structural components; the low-cycle fatigue behavior of cyclic hardening and softening steels under multiaxial elastoplastic loading conditions; and the fatigue behavior of shrink-bonded shaft-hub steel assemblies are presented. Fretting corrosion fatigue and fatigue behavior of ceramic thermal barrier coatings are also treated. For individual titles, see N89-17273 through N89-17283.

N89-17273# Fraunhofer-Inst. fuer Betriebsfestigkeit, Darmstadt (Germany, F.R.).
THE INFLUENCE OF THE LOAD SEQUENCE ON THE FATIGUE LIFE OF FATIGUE FRACTURE ENDANGERED COMPONENTS [ZUM REIHENFOLGEEINFLUSS DER BELASTUNGEN AUF DIE LEBENSDAUER SCHWINGBRUCHGEFAEHRDETER BAUTEILE]
H. Klaetschke and H. Oppermann *In its* Papers of the 5th LBF Colloquium 1988 p 17-30 In GERMAN (For primary document see N89-17272 09-39)
Avail: NTIS HC A12/MF A01

The influence of the load sequence on the fatigue life of components is treated. Numerical fatigue life predictions show relatively large uncertainties, as demonstrated by examples. The deviations between calculated fatigue life and test results for noncontinuous load sequences are discussed. The difference between real load sequences and artificially produced random sequences is outlined with a view to the fatigue life of samples. The effects of ordering the loads in the sequence according to amplitude and average value are discussed. Advice is given in order to avoid or reduce systematic errors in numerical fatigue life estimates ESA

N89-17274# Fraunhofer-Inst. fuer Betriebsfestigkeit, Darmstadt (Germany, F.R.).
THE RELIABLE REDUCTION OF RANDOM LOCAL SEQUENCES FOR FATIGUE TESTS [ZULAESSIGE VERKUERZUNG ZUFALLSARTIGER LASTFOLGEN FUER BETRIEBSFESTIGKEITSVERSUCHE]
H. Oppermann *In its* Papers of the 5th LBF Colloquium 1988 p 31-49 In GERMAN (For primary document see N89-17272 09-39)
Avail: NTIS HC A12/MF A01

Experimental methods for the reduction of fatigue test duration are presented. The increase of test frequency, increase of loading intensity, the load sequence with fuller frequency distribution, and the omission of small loading variations are discussed. The problems of test duration reduction by omitting small load cycles

are outlined; this method of reduction is very efficient. Experiences with the reduction of random load sequences are presented. The use of numerical fatigue life predictions for the reduction of load sequences cannot be advised. A concept for the reliable reduction of random load sequences is proposed. ESA

N89-17275# Fraunhofer-Inst. fuer Betriebsfestigkeit, Darmstadt (Germany, F.R.).
MODAL ANALYSIS METHODS FOR THE REDUCTION OF SYSTEM-CONDITIONED LOADS [DIE MODALANALYSE ALS HILFSMITTEL ZUR BEEINFLUSSUNG SYSTEMBEDINGTER BEANSPRUCHUNGEN]
D. Flade and H. Steinhilber *In its* Papers of the 5th LBF Colloquium 1988 p 51-67 In GERMAN (For primary document see N89-17272 09-39)
Avail: NTIS HC A12/MF A01

Modal analysis methods were applied to reduce dynamic loads in mechanical systems, numerically as well as experimentally. A numerical simulation model using the finite element method was developed, based on experimental data from existing constructions and on well-tried modal analysis which describes the dynamic behavior by modal and hence interdependent parameters. The dynamic characteristics of the computer model agree largely with those of the construction. The simulation calculations determine the effects of changes of any physical parameter, leading to an improved construction as well as to a better knowledge of the dynamics of the applied construction principles. ESA

N89-17276# Fraunhofer-Inst. fuer Betriebsfestigkeit, Darmstadt (Germany, F.R.).
A PROCEDURE FOR THE GENERATION OF LOAD SEQUENCES [EIN VERFAHREN ZUR GENERIERUNG VON LASTFOLGEN]
H. Steinhilber and H. Klaetschke *In its* Papers of the 5th LBF Colloquium 1988 p 69-78 In GERMAN (For primary document see N89-17272 09-39)
Avail: NTIS HC A12/MF A01

A method for the generation of load-time functions which are coupled by arbitrary, even varying correlation conditions was developed. The information carrier for these correlations, which can only be determined statistically, is the so-called compound density matrix. Additional information about the time sequence of the momentary values of the time functions are provided by a counting procedure using a momentary value sequence Markov matrix. This matrix together with the compound density matrix allow the generation of statistically correlated time functions. The application of the procedure is demonstrated by two examples. The procedure is shown to be suitable for operational load simulation in the laboratory. ESA

N89-17277# Fraunhofer-Inst. fuer Betriebsfestigkeit, Darmstadt (Germany, F.R.).
STRENGTH EVALUATION FOR FIBER REINFORCED COMPOSITE LEAF SPRINGS UNDER MECHANICAL AND ENVIRONMENT CONDITIONED LOADS [FESTIGKEITSNACHWEIS FUER MECHANISCHE UND UMWELTBEDINGTE BEANSPRUCHUNGEN AN BLATTFEDERN AUS FASERVERBUNDWERKSTOFF]
D. Schuetz and H. Oppermann *In its* Papers of the 5th LBF Colloquium 1988 p 79-91 In GERMAN (For primary document see N89-17272 09-39)
Avail: NTIS HC A12/MF A01

The strength of composite leaf springs under operational conditions was evaluated. A sufficient strength has also to be guaranteed under environmental conditions with similar humidity and temperature, and preferably to be tested on samples before the construction of the components. The influence of impact damage on the statistical strength of fiber reinforced composites is discussed. As long as the damage mechanisms are not sufficiently known, loading conditions close to reality have to be assumed to determine the fatigue strength. ESA

N89-17278# Fraunhofer-Inst. fuer Betriebsfestigkeit, Darmstadt (Germany, F.R.).
DAMAGE TOLERANCE BEHAVIOR OF FIBER REINFORCED COMPOSITE AIRFRAMES [ZUM SCHADENSTOLERANZVERHALTEN VON LUFTFAHRZEUGKONSTRUKTIONEN AUS FASERVERBUNDWERKSTOFFEN] c05
J. J. Gerharz and H. Huth *In its* Papers of the 5th LBF Colloquium 1988 p 93-110 In GERMAN (For primary document see N89-17272 09-39)
Avail: NTIS HC A12/MF A01

The evaluation of the damage tolerance of fiber-reinforced composite aircraft constructions was investigated. An example shows which studies are needed to determine the effects of critical damage on the required properties and to determine how this damage is tolerated by the constructions. The smaller the impactor radius and the thinner the laminate, the lower the energy at which the impact damage is visible. Even at high impact energies, damage on nonhardened constructions is not visible. The importance and effect of damage depend on the impact location. The decrease of pressure strength of laminate plates depends on the relative damage size. The laminate structure in hardened laminates can affect the impact damage. ESA

N89-17279# Fraunhofer-Inst. fuer Betriebsfestigkeit, Darmstadt (Germany, F.R.).
FINITE ELEMENT ANALYSIS FOR THE EVALUATION AND OPTIMIZATION OF FIBER REINFORCED COMPOSITE STRUCTURAL COMPONENTS [ANWENDUNG DER FINITE-ELEMENTE-METHODE ZUR BEURTEILUNG UND OPTIMIERUNG VON FASERVERBUNDKONSTRUKTIONEN]
H. Idelberger and J. J. Gerharz *In its* Papers of the 5th LBF Colloquium 1988 p 111-128 In GERMAN (For primary document see N89-17272 09-39)
Avail: NTIS HC A12/MF A01

A finite element method for the analysis of impact tests on nonhardened fiber reinforced composite structural plates is presented. The method is suited to global quantities such as plate deflection of support reaction, and gives a first indication of damage development, it has however still to be extended to allow the prediction of damage propagation. It is shown that the combination of experimental and analytical analysis of components is an efficient method for the optimization of constructions. The experimental investigations can be limited to measurements on the basic and the optimized laminate due to the numerical stress analysis. The interactions for the dimensioning of the optimal laminate were performed using finite element stress analysis. ESA

N89-17280# Fraunhofer-Inst. fuer Betriebsfestigkeit, Darmstadt (Germany, F.R.).
LOW-CYCLE FATIGUE BEHAVIOR OF CYCLIC HARDENING AND SOFTENING STEELS UNDER MULTIAXIAL ELASTIC-PLASTIC LOADING CONDITIONS WITH CONSTANT AND VARIABLE AMPLITUDES [KURZZEITSCHWINGFESTIGKEITSVERHALTEN VON ZYKLISCH ENTFESTIGENDEN UND VERFESTIGENDEN STAEHLEN UNTER MEHRACHSIGER ELASTO-PLASTISCHER BEANSPRUCHUNG MIT KONSTANTEN UND VERAENDERLICHEN AMPLITUDEN]
C. M. Sonsino and V. Grubisic *In its* Papers of the 5th LBF Colloquium 1988 p 129-152 In GERMAN (For primary document see N89-17272 09-39)
Avail: NTIS HC A12/MF A01

The fatigue behavior of cyclic hardening and softening steels under multiaxial elastoplastic strain situations was investigated in order to deduce advice for measuring practice. Extension and shear tests were performed on the steels 30CrNiMo8 and X10 CrNiTi 18 9. The test results were compared with calculations. The low-cycle fatigue behavior under pure extension or shear loading cannot be transferred to combined loading. The crack lifetime decrease under combined phase-shifted loading can be determined. The fatigue behavior under single step combined loading cannot be transferred to the materials behavior under

combined loading with variable amplitudes. The reliable evaluation of multiaxial loading conditions is very important for the cumulative damage due to variable loading amplitudes. ESA

N89-17281# Fraunhofer-Inst. fuer Betriebsfestigkeit, Darmstadt (Germany, F.R.).
FATIGUE BEHAVIOR OF SHRINK-BONDED SHAFT-HUB STEEL ASSEMBLIES [ZUM FESTIGKEITSVERHALTEN SCHRUMPFGEKLEBTER WELLE-NABE-VERBINDUNGEN AUS STAHL]
M. Berg *In its* Papers of the 5th LBF Colloquium 1988 p 171-184 In GERMAN Sponsored by Verein Deutscher Eisenhuettenleute, Fed. Republic of Germany and Arbeitsgemeinschaft Industrieller Forschungsvereinigungen, Fed. Republic of Germany (For primary document see N89-17272 09-39)
Avail: NTIS HC A12/MF A01

The fatigue behavior of torsion-loaded shrink-bonded shaft-hub joints was investigated. Static as well as vibratory loading test were performed under different conditions. It is shown that the fit between shaft and hub has a large effect on the static strength. The Woehler and lifetime diagrams are found to be unexpectedly flat. The maximum shear stress is between 63 percent and 92 percent of the static torsional shear strength. For variable torsional loading the tolerable stresses are a factor of 1.4 higher than for the usual cross-pressed joints. ESA

N89-17282# Fraunhofer-Inst. fuer Betriebsfestigkeit, Darmstadt (Germany, F.R.).
FRETTING CORROSION FATIGUE [ERMUEDUNGSFESTIGKEIT BEI REIBKORROSION] **c26**
G. Fischer *In its* Papers of the 5th LBF Colloquium 1988 p 185-194 In GERMAN (For primary document see N89-17272 09-39)
Avail: NTIS HC A12/MF A01

Vibratory loading tests were performed on unnotched, axially loaded flat samples, made of the materials GGG40 and St34-2, in order to evaluate the fretting corrosion fatigue behavior. The damage due to fretting corrosion in GGG40 is larger in single-step tests than in operational strength tests. The effects of the parameters which influence fretting corrosion, such as surface pressure, shot peening, and material, are not the same in single-step tests and random loading. Shot peening and surface pressure reduction in operational fatigue tests do not increase the lifetime. The fatigue behavior of GGG40 is better than that of St34-2; hence, the pairing cast iron/steel has a better behavior than steel/steel under certain conditions. The results allow a relatively exact lifetime estimate under fretting corosion conditions, as well as successful measures to reduce fretting corrosion. ESA

N89-17283# Fraunhofer-Inst. fuer Betriebsfestigkeit, Darmstadt (Germany, F.R.).
FATIGUE BEHAVIOR OF CERAMIC THERMAL BARRIER COATINGS [ZUM ERMUDUNGSVORGANG KERAMISCHER WAERMEDAEMMSCHICHTEN] **c27**
P. Pantucek *In its* Proceedings of the 5th LBF Colloquium 1988 p 195-206 In GERMAN (For primary document see N89-17272 09-39)
Avail: NTIS HC A12/MF A01

Thermally induced dilation, production-induced dilation, as well as dilation under loading of ceramic thermal barrier coatings were investigated. Thermomechanical strength tests were performed on samples made of IM 617, a 1 MM NiGiAlY layer, and a superficial 0.2 mm ZnO2 layer. The results show that failure mechanisms with ceramic thermal barrier coatings depend on operational load and eigenstresses due to the production. Temperature control during the production process can change the eigenstresses and substantially increase the lifetime. The results form a basis for dimensioning data. ESA

N89-17284# Centre National de la Recherche Scientifique, Marseilles (France). Lab. de Mecanique et d'Acoustique.
NUMERICAL AND THEORETICAL STUDY OF ELASTOPLASTIC DYNAMIC BUCKLING Final Report [ETUDE NUMERIQUE ET THEORIQUE DU FLAMBEMENT ELASTOPLASTIQUE DYNAMIQUE]
O. Debordes and C. Do Apr. 1988 205 p In FRENCH
(Contract DRET-84-34-097-00-470-75-01)
(ETN-89-93614) Avail: NTIS HC A10/MF A01

A finite element modelling of elastoplastic bucking based on the analysis of wave propagation and buckling initiation is presented. A theoretical study to identify the essential buckling parameters is included. The numerical integration methods for purely elastic propagation equations were investigated. Methods give satisfactory results with minimum space and time discretizations. The analysis of wave propagation in a Hopkinson bar, elastoplastic bar, Hopkinson bar system shows that the wave propagation velocity depends on the elastic characteristics only, and that the elastoplastic character causes a limitation of the wave stress amplitude, which is found in the wave transmitted to the second Hopkinson bar. The theoretical study on dynamic buckling shows the existence of instabilities, and allows to define a critical impact velocity. ESA

N89-17285# Office National d'Etudes et de Recherches Aerospatiales, Paris (France). Direction Scientifique de la Resistance des Structures.
DEVELOPMENT OF A VISCOPLASTIC CYCLIC BEHAVIOR LAW TO ALLOW A CORRECT DESCRIPTION OF CREEP PHENOMENA Final Report [DEVELOPPEMENT D'UNE LOI DE COMPORTEMENT VISCOPLASTIQUE CYCLIQUE PERMETTENT UNE DESCRIPTION CORRECTE DES EFFETS DE ROCHET]
J. L. Chaboche, D. Nouailhas, P. Paulmier, and H. Policella Mar. 1988 54 p In FRENCH
(Contract DRET-84-34-001)
(ONERA-RT-67/1765-RY-078-R; ETN-89-93615) Avail: NTIS HC A04/MF A01

It is shown that the problems to describe creep are found in the monoaxial case, particularly when plasticity is time independent. Systematic numerical simulations allow to develop a set of models offering a good compromise to describe simultaneously the creep effects and the monotonous or cyclic classic loadings. ESA

N89-17286*# National Aeronautics and Space Administration. Lewis Research Center, Cleveland, OH.
STOCHASTIC MODELING OF CRACK INITIATION AND SHORT-CRACK GROWTH UNDER CREEP AND CREEP-FATIGUE CONDITIONS
Takayuki Kitamura, Louis J. Ghosn, and Ryuichi Ohtani Jan. 1989 20 p Prepared in cooperation with Cleveland State Univ., OH and Kyoto Univ. (Japan)

(NASA-TM-101358; E-4386; NAS 1.15:101358) Avail: NTIS HC A03/MF A01 CSCL 20K

A simplified stochastic model is proposed for crack initiation and short-crack growth under creep and creep-fatigue conditions. Material inhomogeneity provides the random nature of crack initiation and early growth. In the model, the influence of microstructure is introduced by the variability of: (1) damage accumulation along grain boundaries, (2) critical damage required for crack initiation or growth, and (3) the grain-boundary length. The probabilities of crack initiation and growth are derived by using convolution integrals. The model is calibrated and used to predict the crack density and crack-growth rate of short cracks of 304 stainless steel under creep and creep-fatigue conditions. The mean-crack initiation lives are predicted to be within an average deviation of about 10 percent from the experimental results. The predicted cumulative distributions of crack-growth rate follow the experimental data closely. The applicability of the simplified stochastic model is discussed and the future research direction is outlined. Author

N89-17287# Advisory Group for Aerospace Research and Development, Neuilly-Sur-Seine (France). Structures and Materials Panel.

SHORT-CRACK GROWTH BEHAVIOUR IN AN ALUMINUM ALLOY: AN AGARD COOPERATIVE TEST PROGRAMME

J. C. Newman, Jr. and P. R. Edwards (Royal Aerospace Establishment, Farnborough, England) Dec. 1988 106 p (AGARD-R-732; ISBN-92-835-0493-3) Copyright Avail: NTIS HC A06/MF A01

An AGARD test program on the growth of short fatigue cracks was conducted to define the significance of the short-crack effect, to compare test results from various laboratories and to evaluate an existing analytical model to predict the growth of such cracks. The first phase of this program, the Core Program was aimed at test procedure and specimen standardization and calibration of the various laboratories. A detailed working document has been prepared and is included in this report. It describes the testing fundamentals and procedures and includes the analysis procedures used for handling the test data. The results from the test program showed good agreement among the participants on short-crack growth rates, on fatigue life to various crack sizes and breakthrough (surface- or corner-crack became a through crack), and on crack shapes. For individual titles, see N89-17288 through N89-17297.

N89-17288*# National Aeronautics and Space Administration. Langley Research Center, Hampton, VA.

SHORT-CRACK GROWTH BEHAVIOUR IN AN ALUMINUM ALLOY: AN AGARD COOPERATIVE TEST PROGRAM

J. C. Newman, Jr. and P. R. Edwards (Royal Aircraft Establishment, Farnborough, England) *In* AGARD, Short-Crack Growth Behaviour in an Aluminum Alloy: An AGARD Cooperative Test Programme Dec. 1988 p 1-60 (For primary document see N89-17287 09-39)

Copyright Avail: NTIS HC A06/MF A01 CSCL 20K

An AGARD Cooperative Test Program on the growth of short fatigue cracks was conducted to define the significance of the short-crack effect, to compare test results from various laboratories, and to evaluate an existing analytical crack-growth prediction model. The initiation and growth of short fatigue cracks (5 micrometer to 2 mm) from the surface of a semi-circular notch in 2024-T3 aluminum alloy sheet material were monitored under various load histories. The cracks initiated from inclusion particle clusters or voids on the notch surface and generally grew as surface cracks. Tests were conducted under several constant-amplitude (stress ratios of -2, -1, 0, and 0.5) and spectrum (FALSTAFF and GAUSSIAN) loading conditions at 3 stress levels each. Short crack growth was recorded using a plastic-replica technique. Over 250 edge-notched specimens were fatigue tested and nearly 950 cracks monitored by 12 participants from 9 countries. Long crack-growth rate data for cracks greater than 2 mm in length were obtained over a wide range in rates (10 to the -8 to 10 to the -1 mm/cycle) for all constant-amplitude loading conditions. Long crack-growth rate data for the FALSTAFF and GAUSSIAN load sequences were also obtained. Author

N89-17289# National Aerospace Lab., Amsterdam (Netherlands).

MICROSTRUCTURAL EXAMINATION OF CORE-PROGRAMME MATERIAL

R. J. H. Wanhill *In* AGARD, Short-Crack Growth Behaviour in an Aluminum Alloy: An AGARD Cooperative Test Programme Dec. 1988 p 61-65 (For primary document see N89-17287 09-39)

Copyright Avail: NTIS HC A06/MF A01

This annex describes the microstructure of the 2.3 mm thick 2024-T3 aluminum alloy sheet used in the core program. The significance of microstructure for fatigue crack growth in the low stress intensity regime is briefly discussed. The results are based on an extensive compilation and analysis of data for five different batches of 2024-T3 and T351. Author

N89-17290*# National Aeronautics and Space Administration. Langley Research Center, Hampton, VA.

PRELIMINARY FATIGUE TESTS ON SHORT-CRACK SPECIMENS

J. C. Newman, Jr., E. P. Phillips, and M. H. Swain (Planning Research Corp., Hampton, VA.) *In* AGARD, Short-Crack Growth Behaviour in an Aluminum Alloy: An AGARD Cooperative Test Programme Dec. 1988 p 66-69 (For primary document see N89-17287 09-39)

Copyright Avail: NTIS HC A06/MF A01 CSCL 20K

The objective of the preliminary fatigue tests was to determine the stress levels to be used by the participants in the Cooperative Test Program. As previously mentioned, the United States Air Force Wright-Patterson Aeronautical Laboratory machined about 700 single-edge-notched tension (SENT) specimens from material supplied by the NASA Langley Research Center. In addition, NASA Langley machined about 50 SENT specimens from the same material. Comparison of fatigue tests conducted on the two sets of specimens indicated a large difference in fatigue behavior under constant-amplitude loading. A recovery program was initiated to resolve this difference before the specimens were distributed to participants. The following sections describe the recovery program and the preliminary fatigue tests and analyses conducted to determine stress levels for constant-amplitude, FALSTAFF, and GAUSSIAN loading. Author

N89-17291*# National Aeronautics and Space Administration. Langley Research Center, Hampton, VA.

ALIGNMENT VERIFICATION PROCEDURES

P. R. Edwards (Royal Aircraft Establishment, Farnborough, England), E. P. Phillips, and J. C. Newman, Jr. *In* AGARD, Short-Crack Growth Behaviour in an Aluminum Alloy: An AGARD Cooperative Test Programme Dec. 1988 p 70-71 (For primary document see N89-17287 09-39)

Copyright Avail: NTIS HC A06/MF A01 CSCL 20K

In alignment verification procedures each laboratory is required to align its test machines and gripping fixtures to produce a nearly uniform tensile stress field on an un-notched sheet specimen. The blank specimens (50 mm w X 305 mm l X 2.3 mm th) supplied by the coordinators were strain gauged. Strain gauge readings were taken at all gauges (n = 1 through 10). The alignment verification procedures are as follows: (1) zero all strain gauges while specimen is in a free-supported condition; (2) put strain-gauged specimen in the test machine so that specimen front face (face 1) is in contact with reference jaw (standard position of specimen), tighten grips, and at zero load measure strains on all gauges. (epsilon sub nS0 is strain at gauge n, standard position, zero load); (3) with specimen in machine and at a tensile load of 10 kN measure strains (specimen in standard position). (Strain = epsilon sub nS10); (4) remove specimen from machine. Put specimen in machine so that specimen back face (face 2) is in contact with reference jaw (reverse position of specimen), tighten grips, and at zero load measure strains on all gauges. (Strain - epsilon sub nR0); and (5) with specimen in machine and at tensile load of 10 kN measure strains (specimen in reverse position). (epsilon sub nR10 is strain at gauge n, reverse position, 10 kN load). Author

N89-17292# Royal Aircraft Establishment, Farnborough (England).

ON-LINE SPECTRUM LOADING ACCURACY VERIFICATION

P. R. Edwards *In* AGARD, Short-Crack Growth Behaviour in an Aluminum Alloy: An AGARD Cooperative Test Programme Dec. 1988 p 72-74 (For primary document see N89-17287 09-39)

Copyright Avail: NTIS HC A06/MF A01

Eight laboratories carrying out variable-amplitude load tests using the FALSTAFF spectrum were visited by one of the coordinators (P.R. Edwards) and measurements taken to assess the accuracy with which the loading sequences were being applied. The measurements were taken on a portable Rainflow counting device which had a resolution of 64 levels. Thus the device was able to measure 64 x 64 triangular Rainflow matrices. All measurements were made on an alignment specimen with central

strain gauges on each side of the specimen because these measurements would be more convincing than any taken from the load cell of the servohydraulic fatigue machine. The assessment of the accuracy of loading and whether the actual sequence of loads was correct was done initially by a comparison of Rainflow matrices. However, it was found that all of the conclusions that could be drawn from such comparisons could equally be drawn from simple measurements of peaks and troughs. These measurements were extracted from the Rainflow matrix and are presented. Author

N89-17293# Planning Research Corp., Hampton, VA.
SUGGESTED PLASTIC-REPLICA METHOD
M. H. Swain *In* AGARD, Short-Crack Growth Behaviour in an Aluminum Alloy: An AGARD Cooperative test Programme Dec. 1988 p 75 (For primary document see N89-17287 09-39)
Copyright Avail: NTIS HC A06/MF A01

The Cooperative Test Program participants received their test specimens in the chemically-polished condition. Prior to testing, the notch area was cleaned with acetone and then ethanlol was applied with a swab. It was then etched, which removed a very thin layer of material revealing the grain structure. A replica of the notch surface was made after each cyclic interval. The cyclic interval was selected so that some 25 to 30 replicas were taken during a test. Acetyl cellulose replica film was used. Author

N89-17294*# National Aeronautics and Space Administration. Langley Research Center, Hampton, VA.
APPROXIMATE STRESS-INTENSITY FACTORS FOR A SURFACE CRACK AND THROUGH CRACK AT A SEMI-CIRCULAR NOTCH
J. C. Newman, Jr. *In* AGARD, Short-Crack Growth Behaviour in an Aluminum Alloy: An AGARD Cooperative test Programme Dec. 1988 p 76-77 (For primary document see N89-17287 09-39)
Copyright Avail: NTIS HC A06/MF A01 CSCL 20K

An approximate stress-intensity factor equation for a semi-elliptical surface crack located at the center of a semi-circular edge notch subjected to remote uniform stress is given. Author

N89-17295*# National Aeronautics and Space Administration. Langley Research Center, Hampton, VA.
LONG-CRACK GROWTH RATE DATA: CONSTANT AMPLITUDE AND FALSTAFF LOADING
E. P. Phillips *In* AGARD, Short-Crack Growth Behaviour in an Aluminum Alloy: An AGARD Cooperative Test Programme Dec. 1988 p 78-83 (For primary document see N89-17287 09-39)
Copyright Avail: NTIS HC A06/MF A01 CSCL 20K

This annex describes test procedures and presents the results from the tests for conventional, long-crack growth rate data. These data were used for comparisons with the short-crack growth rate data. Data were generated in tests with constant stress ratio load sequences (R = -2, -1, 0, and 0.5) and with the FALSTAFF load sequence. Results for long-crack tests with the GAUSSIAN load sequence are discussed. The constant stress ratio tests included decreasing, increasing, and constant load amplitude sequences. All cracks exceeded 6 mm in length when data were taken. All tests were conducted on center-cracked specimens of 2024-T3 aluminum alloy sheet taken from a large stock of this material held at the NASA Langley Research Center for fatigue research programs. The baseline long-crack growth rate data for this AGARD program were generated using 50 mm wide, center-cracked specimens which were cut from some of the same sheets that were used to make the edge-notched, short-crack specimens. At growth rates below about 10 to the -5 mm/cycle, the baseline data were supplemented by data generated using 76 mm wide specimens made from sheets other than those used for the short-crack program. At growth rates above about 10 to the -5 mm/cycle, the baseline data were supplemented by data generated using 305 mm wide specimens made from sheets other than those used for the other two specimen sizes. The results from the 305 mm specimens were published in 1969. All specimen configurations are shown. Author

N89-17296# Industrieanlagen-Betriebsgesellschaft m.b.H., Ottobrunn (Germany, F.R.).
LONG-CRACK GROWTH RATE DATA: GAUSSIAN LOADING
P. Heuler *In* AGARD, Short-Crack Growth Behaviour in an Aluminum Alloy: An AGARD Cooperative Test Programme Dec. 1988 p 84-85 (For primary document see N89-17287 09-39)
Copyright Avail: NTIS HC A06/MF A01

Conventional long-crack growth rate data under GAUSSIAN loading were generated at IABG within the AGARD short crack program on 2024-T3 sheet specimens. Test procedures and results are briefly reviewed in the following. Tests were carried out on 50 mm wide center-cracked specimens of 2024-T3 aluminum alloy sheet obtained from NASA Langley Research Center. A central slot of 0.4 by 3 mm was used as the crack starter. Specimen dimensions are shown. Author

N89-17297# P. P. Data Ltd., Fleet (England).
DATABASE PROGRAM FOR CRACK PROPAGATION DATA ACQUIRED IN THE AGARD SHORT CRACKS COLLABORATIVE EFFORT
P. R. Edwards *In* AGARD, Short-Crack Growth Behaviour in an Aluminum Alloy: An AGARD Cooperative Test Programme Dec. 1988 p 86-96 (For primary document see N89-17287 09-39)
Copyright Avail: NTIS HC A06/MF A01

The operation of a database program developed for use in the AGARD short cracks collaborative effort is described. Data are stored as files of crack length against number of cycles. If desired, sets of polynomial coefficients describing curves fitted to the data in each file are available. Any of the sets of data can be plotted, either a plot of crack length against number of cycles or a log-log plot of delta K (alternating stress intensity factor) against da/dN (crack growth rate), with adjustable scales in both cases. The object of the program is to enable easy cross-plotting of different sets of data on the same graph. The plots can be output to an external plotter if required, either for incorporation into technical reports or to produce viewgraphs. These features have been extensively used in this report. Least squares fit straight lines on log-log plots can be calculated and plotted for any set or sets of data. Provision exists for the fitting of polynomials to each set of data. This can be carried out interactively, because polynomials are plotted quickly on the graphics screen, and different orders of polynomial curve fit compared. If a suitable digitizing tablet is available then additional points can be added to the length against cycle curves, so as to force the polynomial to follow a desired curve, in particular, to follow the correct slope at the beginning and end of defined crack propagation curves. The program will run on Hewlett-Packard 9836/9816 or 9817/217/310/320 computers with virtually any kind of disc storage. Author

N89-17298*# National Aeronautics and Space Administration. Lewis Research Center, Cleveland, OH.
TURBINE ENGINE HOT SECTION TECHNOLOGY, 1987
Oct. 1987 464 p Workshop held in Cleveland, OH, 20-21 Oct. 1987
(NASA-CP-2493; E-3745; NAS 1.55:2493) Avail: NTIS HC A20/MF A01 CSCL 20K

Presentations were made concerning the development of design analysis tools for combustor liners, turbine vanes, and turbine blades. Presentations were divided into six sections: instrumentation, combustion, turbine heat transfer, structural analysis, fatigue and fracture, surface protective coatings, constitutive behavior of materials, stress-strain response and life prediction methods. For individual titles, see N89-17299 through N89-17337.

N89-17299*# United Technologies Research Center, East Hartford, CT.
DEVELOPMENT OF A HIGH TEMPERATURE THIN FILM STATIC STRAIN GAGE c35
Charles O. Hulse, Richard S. Bailey, Howard P. Grant, and John S. Przybyszewski (Pratt and Whitney Aircraft, East Hartford, CT.) *In* NASA, Lewis Research Center, Turbine Engine Hot Section

Technology, 1987 Oct. 1987 p 43-51 (For primary document see N89-17298 09-39)
(Contract NAS3-23722)
Avail: NTIS HC A20/MF A01 CSCL 14B

The objective is to develop a new thin film resistance strain gage system which will be suitable for use inside gas turbine engines on blades or vanes at temperatures up to 1250 K. These gages are to be capable of making strain measurements to plus or minus 2000 microstrain with total errors of no more than plus or minus 10 percent during a 50 hour period. In addition to survival and stability in this hostile environment, attaining a low temperature coefficient of resistance, of the order of 20 ppm/K or less, is an important goal. This requirement arises from the presently unavoidable uncertainties in the measurement of exact temperatures inside gas turbine engines for use in making corrections for apparent strain. Author

N89-17300*# Northwestern Univ., Evanston, IL.
ELEVATED TEMPERATURE STRAIN GAGES **c35**
J. F. Lei, M. Shaarbaf, and J. O. Brittain *In* NASA, Lewis Research Center, Turbine Engine HotSection Technology, 1987 Oct. 1987 p 53-75 (For primary document see N89-17298 09-39)
Avail: NTIS HC A20/MF A01 CSCL 14B

The objective is to study the electrical resistance of materials that are potentially useful as resistance strain gages at 1000 C. A set of criteria were set and used to select strain gage candidate materials that are electrically stable and reproducible at all temperatures up to 1000 C. For the experimental phase of this research, the electrical resistance change with temperature of three groups of materials (solid solution alloys, transition metal carbides, and semiconductors) were studied with the intention of identifying materials with low temperature coefficient of resistance and low resistance drift rate at 1000 C. A preliminary study of the gage factor on one of the best candidate materials, B sub 4 C, was also undertaken. The results of these investigations are presented. Author

N89-17301*# National Aeronautics and Space Administration. Lewis Research Center, Cleveland, OH.
PROGRESS ON A PdCr WIRE STRAIN GAGE **c35**
David R. Englund *In its* Turbine Engine Hot Section Technology, 1987 Oct. 1987 p 77-79 (For primary document see N89-17298 09-39)
Avail: NTIS HC A20/MF A01 CSCL 14B

The principal activity under the HOST effort to improve the state of the art in high temperature static strain measurement has been a contract under which a palladium-chromium (PdCr) alloy was developed. The contract effort is continuing with the goal of developing a thin film high temperature static strain gage system. In addition to this effort, researchers contracted with Battelle-Columbus Laboratories to draw the PdCr allow into wire while researchers at Lewis worked to gain experience with this alloy as a wire strain gage. Author

N89-17302*# National Aeronautics and Space Administration. Lewis Research Center, Cleveland, OH.
A COMPARISON OF TURBULENCE MEASUREMENT METHODS **c35**
Gustave C. Fralick *In its* Turbine Engine Hot Section Technology, 1987 Oct. 1987 p 81-84 (For primary document see N89-17298 09-39)
Avail: NTIS HC A20/MF A01 CSCL 14B

An experiment is described in which temperature (density) and velocity are measured separately but simultaneously as functions of time so that it is possible to determine the relationships among velocity, density, and the product of density and velocity. Temperatures were measured with a dual-wire thermocouple probe. Velocity data were supplied by a fringe laser-Doppler anemometer. Signals from thermocouples and the laser were recorded on FM magnetic tape for later processing. Author

N89-17303*# General Motors Corp., Indianapolis, IN. Gas Turbine Div.
AEROTHERMAL MODELING PROGRAM. PHASE 2, ELEMENT A: IMPROVED NUMERICAL METHODS FOR TURBULENT VISCOUS RECIRCULATING FLOWS **c34**
K. C. Karki, H. C. Mongia, Suhas V. Patankar, and A. K. Runchal (Analytic and Computational Research, Inc., Los Angeles, CA.) *In* NASA, Lewis Research Center, Turbine Engine Hot Section Technology, 1987 Oct. 1987 p 85-90 (For primary document see N89-17298 09-39)
Avail: NTIS HC A20/MF A01 CSCL 20D

The objective of this effort is to develop improved numerical schemes for predicting combustor flow fields. Various candidate numerical schemes were evaluated, and promising schemes were selected for detailed assessment. The criteria for evaluation included accuracy, computational efficiency, stability, and ease of extension to multidimensions. The candidate schemes were assessed against a variety of simple one and two dimensional problems. These results led to the selection of the following schemes for further evaluation: flux spline schemes (linear and cubic) and controlled numerical diffusion with internal feedback (CONDIF). The incorporation of the flux spline scheme and direct solution strategy in a computer program for three dimensional flows is in progress. Author

N89-17304*# General Motors Corp., Indianapolis, IN. Gas Turbine Div.
AEROTHERMAL MODELING PROGRAM. PHASE 2, ELEMENT B: FLOW INTERACTION EXPERIMENT **c34**
M. Nikjooy, H. C. Mongia, S. N. B. Murthy, and J. P. Sullivan (Purdue Univ., West Lafayette, IN.) *In* NASA, Lewis Research Center, Turbine Engine Hot Section Technology, 1987 Oct. 1987 p 91-99 (For primary document see N89-17298 09-39)
(Contract NAS3-24350)
Avail: NTIS HC A20/MF A01 CSCL 20D

NASA has instituted an extensive effort to improve the design process and data base for the hot section components of gas turbine engines. The purpose of element B is to establish a benchmark quality data set that consists of measurements of the interaction of circular jets with swirling flow. Such flows are typical of those that occur in the primary zone of modern annular combustion liners. Extensive computations of the swirling flows are to be compared with the measurements for the purpose of assessing the accuracy of current physical models used to predict such flows. Author

N89-17305*# General Motors Corp., Indianapolis, IN. Gas Turbine Div.
AEROTHERMAL MODELING PROGRAM, PHASE 2, ELEMENT C: FUEL INJECTOR-AIR SWIRL CHARACTERIZATION **c34**
A. A. Mostafa, H. C. Mongia, V. G. McDonnel, and G. S. Samuelsen (California Univ., Irvine.) *In its* Turbine Engine Hot Section Technology, 1987 Oct. 1987 p 101-110 (For primary document see N89-17298 09-39)
Avail: NTIS HC A20/MF A01 CSCL 20D

The main objectives of the NASA sponsored Aerothermal Modeling Program, Phase 2, Element C, are to collect benchmark quality data to quantify the fuel spray interaction with the turbulent swirling flows and to validate current and advanced two phase flow models. The technical tasks involved in this effort are discussed. Author

N89-17306*# United Technologies Research Center, East Hartford, CT.
APPLICATION OF ADVANCED DIAGNOSTICS TO AIRBLAST INJECTOR FLOWS **c34**
John B. McVey, Jan B. Kennedy, and Sid Russell *In* NASA, Lewis Research Center, Turbine Engine Hot Section Technology, 1987 Oct. 1987 p 111-118 (For primary document see N89-17298 09-39)
(Contract NAS3-24352)
Avail: NTIS HC A20/MF A01 CSCL 20D

This effort is concerned with the application of both conventional

laser velocimetry and phase Doppler anemometry to the flow produced by an airblast nozzle. The emphasis is placed on the acquisition of data using actual engine injector/swirler components at (noncombusting) conditions simulating those encountered in the engine. The objective of the effort was to test the applicability of the instrumentation to real injector flows, to develop information on the behavior of injectors at high flow, and to provide data useful in the development of physical models of injector flows.
Author

N89-17307*# Minnesota Univ., Minneapolis.
DEVELOPMENT OF GENERALIZED BLOCK CORRECTION PROCEDURES FOR THE SOLUTION OF DISCRETIZED NAVIER-STOKES EQUATIONS **c34**
Kanchan M. Kelkar and Suhas V. Patankar *In* NASA, Lewis Research Center, Turbine Engine Hot Section Technology, 1987 Oct. 1987 p 119-128 (For primary document see N89-17298 09-39)
Avail: NTIS HC A20/MF A01 CSCL 20D

Effort is directed towards developing a solution method which combines advantages of both the iterative and the direct methods. It involves iterative solution on the fine grid, convergence of which is enhanced by a direct solution for correction quantities on a coarse grid. The proposed block correction procedure was applied to compute recirculating flow in a driven cavity. Author

N89-17308*# Sverdrup Technology, Inc., Cleveland, OH.
EVALUATION OF AEROTHERMAL MODELING COMPUTER PROGRAMS **c61**
K. C. Hsieh and S. T. Yu *In* NASA, Lewis Research Center, Turbine Engine Hot Section Technology, 1987 Oct. 1987 p 129-130 (For primary document see N89-17298 09-39)
Avail: NTIS HC A20/MF A01 CSCL 09B

Various computer programs based upon the SIMPLE or SIMPLER algorithm were studied and compared for numerical accuracy, efficiency, and grid dependency. Four two dimensional and one three dimensional code originally developed by a number of research groups were considered. In general, the accuracy and computational efficieny of these TEACH type programs were improved by modifying the differencing schemes and their solvers. A brief description of each program is given. Error reduction, spline flux and second upwind differencing programs are covered.
Author

N89-17309*# Stanford Univ., CA.
HEAT TRANSFER WITH VERY HIGH FREE-STREAM TURBULENCE AND HEAT TRANSFER WITH STREAMWISE VORTICES **c34**
Robert J. Moffat, Paul Maciejewski, John K. Eaton, and Wayne Pauley *In* NASA, Lewis Research Center, Turbine Engine Hot Section Technology, 1987 Oct. 1987 p 131-154 (For primary document see N89-17298 09-39)
(Grant NAG3-522)
Avail: NTIS HC A20/MF A01 CSCL 20D

Two experimental programs related to augmentation of heat transfer by complex flow characteristics are reviewed. The first program deals with very high turbulence (up to 63 percent) which was shown to result in Stanton numbers as much as five times the expected values. Results from a number of trials show that fixing the free stream velocity, x-Reynolds number, turbulence intensity and integral length scale does not fix the Stanton number. Two such cases were found in which the Stanton number of one was 40 percent larger than the other. Mean velocity and mean temperature profiles are presented, as well as profiles of turbulence intensity within the boundary layer. The second program deals with vortices originating at bluff bodies and traveling downstream embedded in the wall boundary layer. Velocity vector maps from the boundary layers and distributions of Stanton number on the wall are presented for three types of bodies: square, cylindrical and teardrop. The heat transfer and velocity maps do not show evidence of the expected horseshoe vortices but, instead, show a strong common flow up vortex pair. The fluid mechanic mechanism responsible for this secondary flow field has not yet been identified.
Author

N89-17310*# Minnesota Univ., Minneapolis.
A LOW-REYNOLDS-NUMBER TWO-EQUATION TURBULENCE MODEL FOR PREDICTING HEAT TRANSFER ON TURBINE BLADES **c34**
Suhas V. Patankar and Rodney C. Schmidt *In* NASA, Lewis Research Center, Turbine Engine Hot Section Technology, 1987 Oct. 1987 p 155-167 (For primary document see N89-17298 09-39)
(Grant NAG3-579)
Avail: NTIS HC A20/MF A01 CSCL 20D

A modified form of the Lam-Bremhorst low-Reynolds number kappa-epsilon turbulence model was developed for predicting transitional boundary layer flows under conditions characteristic of gas turbine blades. The application of the model to flows with pressure gradients is described. Tests against a number of turbine blade cascade data sets are included. Some additional refinements of the model that were made in recent months are explained.
Author

N89-17311*# United Technologies Research Center, East Hartford, CT.
MEASUREMENT OF AIRFOIL HEAT TRANSFER COEFFICIENTS ON A TURBINE STAGE **c34**
Robert P. Dring, Michael F. Blair, and H. David Joslyn *In* NASA, Lewis Research Center, Turbine Engine Hot Section Technology, 1987 Oct. 1987 p 169-179 (For primary document see N89-17298 09-39)
(Contract NAS3-23717)
Avail: NTIS HC A20/MF A01 CSCL 20D

A combined experimental and analytical program was conducted to examine the impact of a number of variables on the midspan heat transfer coefficients of the three airfoil rows in a one and one-half stage large scale turbine model. Variables included stator/rotor axial spacing, Reynolds number, turbine inlet turbulence, flow coefficient, relevant stator 1/stator 2 circumferential position, and rotation. Heat transfer data were acquired on the suction and pressure surfaces of the three airfoils. High density data were also acquired in the leading edge stagnation regions. Extensive documentation of the steady and unsteady aerodynamics was acquired. Finally, heat transfer data were compared with both a steady and an unsteady boundary layer analysis.
Author

N89-17312*# Arizona State Univ., Tempe.
HEAT TRANSFER IN THE TIP REGION OF A ROTOR BLADE SIMULATOR **c34**
M. K. Chyu and D. E. Metzger *In* NASA, Lewis Research Center, Turbine Engine Hot Section Technology, 1987 Oct. 1987 p 181-197 (For primary document see N89-17298 09-39)
(Grant NAG3-623)
Avail: NTIS HC A20/MF A01 CSCL 20D

The measurement of mass transfer from cavities is discussed with emphasis on the effect of cavity orientations relative to the main flow direction. A finite difference computation for turbulent air flow and heat transfer over a two dimensional shrouded rectangular cavity is discussed.
Author

N89-17313*# Scientific Research Associates, Inc., Glastonbury, CT.
TWO- AND THREE-DIMENSIONAL TURBINE BLADE ROW FLOW FIELD SIMULATIONS **c34**
R. C. Buggeln, W. R. Briley, H. McDonald, S. J. Shamroth, and B. C. Weinberg *In* NASA, Lewis Research Center, Turbine Engine Hot Section Technology, 1987 Oct. 1987 p 199-209 Prepared in cooperation with General Motors Corp., Indianapolis, IN (For primary document see N89-17298 09-39)
(Contracts NAS3-24358; NAS3-23695)
Avail: NTIS HC A20/MF A01 CSCL 20D

Work performed in the numerical simulation of turbine passage

flows via a Navier-Stokes approach is discussed. Both laminar and turbulent simulations in both two and three dimensions are discussed. An outline of the approach, background, and an overview of the results are given. Author

N89-17314*# Pratt and Whitney Aircraft, East Hartford, CT.
COOLANT PASSAGE HEAT TRANSFER WITH ROTATION **c34**
T. J. Hajek, J. H. Wagner, and B. V. Johnson (United Technologies Research Center, East Hartford, CT.) *In* NASA, Lewis Research Center, Turbine Engine Hot Section Technology, 1987 Oct. 1987 p 211-223 (For primary document see N89-17298 09-39)
(Contract NAS3-23691)
Avail: NTIS HC A20/MF A01 CSCL 20D

The objective is to develop a heat transfer and pressure drop data base, computational fluid dynamic techniques and heat transfer correlations for rotating multipass coolant passages, with and without flow tabulators. The experimental effort is focused on the simulation of configurations and conditions expected in the blades of advanced aircraft high pressure turbines. With the use of this data base, the effects of Coriolis and buoyancy forces on the coolant side flow can be included in the design of turbine blades. Author

N89-17315*# General Motors Corp., Indianapolis, IN. Gas Turbine Div.
TURBINE AIRFOIL FILM COOLING **c34**
L. D. Hylton, V. Nirmalan, B. K. Sultanian, and R. M. Kaufman *In* NASA, Lewis Research Center, Turbine Engine Hot Section Technology, 1987 Oct. 1987 p 225-238 (For primary document see N89-17298 09-39)
(Contract NAS3-24619)
Avail: NTIS HC A20/MF A01 CSCL 20D

The experimental data obtained in this program gives insight into the physical phenomena that occur on a film cooled airfoil, and should provide a relevant data base for verification of new design tools. Results indicate that the downstream film cooling process is a complex function of the thermal dilution and turbulence augmentation parameters with trends actually reversing as blowing strength and coolant-to-gas temperature ratio varied. The pressure surface of the airfoil is shown to exhibit a considerably higher degree of sensitivity to changes in the film cooling parameters and, consequently, should prove to be more of a challenge than the suction surface in accurately predicting heat transfer levels with downstream film cooling. Author

N89-17316*# Pratt and Whitney Aircraft, East Hartford, CT.
THREE-DIMENSIONAL INELASTIC ANALYSIS METHODS FOR HOT SECTION COMPONENTS
E. S. Todd *In* NASA, Lewis Research Center, Turbine Engine Hot Section Technology, 1987 Oct. 1987 p 239-240 (For primary document see N89-17298 09-39)
(Contract NAS3-23697)
Avail: NTIS HC A20/MF A01 CSCL 20K

The objective of this program is to produce a series of new computer codes that permit more accurate and efficient three-dimensional inelastic structural analysis of combustor liners, turbine blades, and turbine vanes. Each code embodies a progression of mathematical models for increasingly comprehensive representation of the geometrical features, loading conditions, and forms of nonlinear material response that distinguish these three groups of hot section components. Author

N89-17317*# Pratt and Whitney Aircraft, East Hartford, CT.
THREE-DIMENSIONAL INELASTIC ANALYSIS FOR HOT SECTION COMPONENTS, BEST 3D CODE
Raymond B. Wilson and Prasanta K. Banerjee (State Univ. of New York, Buffalo.) *In* NASA, Lewis Research Center, Turbine Engine Hot Section Technology, 1987 Oct. 1987 p 241-248 (For primary document see N89-17298 09-39)
(Contract NAS3-23697)
Avail: NTIS HC A20/MF A01 CSCL 20K

The goal is the development of an alternative stress analysis tool, distinct from the finite element method, applicable to the engineering analysis of gas turbine engine structures. The boundary element method was selected for this development effort on the basis of its already demonstrated applicability to a variety of geometries and problem types characteristic of gas turbine engine components. Major features of the BEST3D computer program are described, and some of the significant developments carried out as part of the Inelastic Methods Contract are outlined. Author

N89-17318*# Sverdrup Technology, Inc., Cleveland, OH.
RESPONSE CHARACTERISTICS OF MHOST (MARC HOT-SECTION TECHNOLOGY) FOR 3-D INELASTIC ANALYSIS OF HOT-SECTION COMPONENTS
Lawrence K. Shen *In* NASA, Lewis Research Center, Turbine Engine Hot Section Technology, 1987 Oct. 1987 p 249-254 (For primary document see N89-17298 09-39)
Avail: NTIS HC A20/MF A01 CSCL 20K

The advantages of a newly developed code are demonstrated by comparisons of the analysis with existing theoretical data as well as with other available finite element programs. The new program shows promise to significantly reduce the computer time. It also permits accurate and efficient structural analysis of engine hot section components. Author

N89-17319*# National Aeronautics and Space Administration. Lewis Research Center, Cleveland, OH.
MECHANICS OF MATERIALS MODEL
Jeffrey P. Meister *In its* Turbine Engine Hot Section Technology, 1987 Oct. 1987 p 255-257 (For primary document see N89-17298 09-39)
Avail: NTIS HC A20/MF A01 CSCL 20K

The Mechanics of Materials Model (MOMM) is a three-dimensional inelastic structural analysis code for use as an early design stage tool for hot section components. MOMM is a stiffness method finite element code that uses a network of beams to characterize component behavior. The MOMM contains three material models to account for inelastic material behavior. These include the simplified material model, which assumes a bilinear stress-strain response; the state-of-the-art model, which utilizes the classical elastic-plastic-creep strain decomposition; and Walker's viscoplastic model, which accounts for the interaction between creep and plasticity that occurs under cyclic loading conditions. Author

N89-17320*# General Electric Co., Cincinnati, OH. Aircraft Engines.
COMPONENT SPECIFIC MODELING
R. L. McKnight and M. T. Tipton *In* NASA, Lewis Research Center, Turbine Engine Hot Section Technology, 1987 Oct. 1987 p 259-265 (For primary document see N89-17298 09-39)
Avail: NTIS HC A20/MF A01 CSCL 20K

The objective was to develop and verify a series of interdisciplinary modeling and analysis techniques specialized to address hot section components. These techniques incorporate data as well as theoretical methods from many diverse areas, including cycle and performance analysis, heat transfer analysis, linear and nonlinear stress analysis, and mission analysis. Author

N89-17321*# National Aeronautics and Space Administration. Lewis Research Center, Cleveland, OH.
THREE-DIMENSIONAL INELASTIC ANALYSIS METHODS FOR HOT SECTION COMPONENTS
Joseph Lackney (Sverdrup Technology, Inc., Cleveland, OH.) and C. C. Chamis *In its* Turbine Engine Hot Section Technology, 1987 Oct. 1987 p 267-271 (For primary document see N89-17298 09-39)

(Contract NAS3-23698)
Avail: NTIS HC A20/MF A01 CSCL 20K

The objective was to develop analytical methods capable of evaluating the cyclic time dependent inelasticity which occurs in hot section engine components. Because of the large excursions in temperature associated with hot section engine components, the techniques developed must be able to accommodate large variations in material behavior including plasticity and creep. To meet this objective, a matrix consisting of three constitutive mode-element formulations was developed. A separate program for each combination of constitutive mode-element model was written. The source codes of the nine programs range in size from 7300 lines for the Bodner/twenty code to 19,000 lines for the Haisler and Allen/nine code. All the codes were given a stand alone capability of performing cyclic nonlinear analysis. Author

N89-17322*# Southwest Research Inst., San Antonio, TX.
CONSTITUTIVE MODELING FOR ISOTROPIC MATERIALS
Ulric S. Lindholm and Kwai S. Chan *In* NASA, Lewis Research Center, Turbine Engine Hot Section Technology, 1987 Oct. 1987 p 273-279 (For primary document see N89-17298 09-39)
Avail: NTIS HC A20/MF A01 CSCL 20K

The fourth and final year of the HOST project with the initial objective of developing a unified constitutive model for finite element structural analysis of turbine engine hot section components is discussed. The final year's work was primarily concerned with the study of nonisothermal problems and the potential for thermal history effects to occur explicitly in the constitutive equations. Author

N89-17323*# Akron Univ., OH.
A CONTINUUM DEFORMATION THEORY FOR METAL-MATRIX COMPOSITES AT HIGH TEMPERATURE
D. N. Robinson *In* NASA, Lewis Research Center, Turbine Engine Hot Section Technology, 1987 Oct. 1987 p 281-287 (For primary document see N89-17298 09-39)
Avail: NTIS HC A20/MF A01 CSCL 20K

A continuum theory is presented for representing the high temperature, time dependent, hereditary deformation behavior of metallic composites that can be idealized as pseudohomogeneous continua with locally definable directional characteristics. Homogenization of textured materials (molecular, granular, fibrous) and applicability of continuum mechanics in structural applications depends on characteristic body dimensions, the severity of gradients (stress, temperature, etc.) in the structure and the relative size of the internal structure (cell size) of the material. The point of view taken here is that the composite is a material in its own right, with its own properties that can be measured and specified for the composite as a whole. Author

N89-17324*# Cincinnati Univ., OH.
ANISOTROPIC CONSTITUTIVE MODELING FOR NICKEL BASE SINGLE CRYSTAL SUPERALLOY RENE N4 AT 982 C **c26**
D. C. Stouffer, N. Jayaraman, M. Y. Sheh, and D. Alden *In* NASA, Lewis Research Center, Turbine Engine Hot Section Technology, 1987 Oct. 1987 p 289-298 (For primary document see N89-17298 09-39)
Avail: NTIS HC A20/MF A01 CSCL 11F

A back stress/drag stress constitutive model based on a crystallographic approach to model single crystal anisotropy is presented. Experimental results demonstrated the need for the back stress variable in the inelastic flow equations. Experimental findings suggested that back stress is orientation dependent and controls both strain hardening and recovery characteristics. Due to the observed stable fatigue loops at 1800 F, drag stress is considered constant for this temperature. The constitutive model operated with constraints determined only from tensile data was extensively tested from simple tensile and fatigue to complicated strain hold tests. The model predicted very well under those conditions. Author

N89-17325*# Engineering Science Software, Inc., Smithfield, RI.
CONSTITUTIVE MODELLING OF SINGLE CRYSTAL AND DIRECTIONALLY SOLIDIFIED SUPERALLOYS **c26**
Kevin P. Walker and Eric H. Jordan (Connecticut Univ., Storrs.) *In* NASA, Lewis Research Center, Turbine Engine Hot Section Technology, 1987 Oct. 1987 p 299-301 (For primary document see N89-17298 09-39)
(Grant NAG3-512)
Avail: NTIS HC A20/MF A01 CSCL 11F

Successful attempts were made to model the deformation behavior of nickel base superalloys to be used in gas turbine engines based on both a macroscopic constitutive model and a micromechanical formulation based on crystallographic slip theory. These models were programmed as FORTRAN subroutines, are currently being used to simulate thermomechanical loading predictions expected at the fatigue critical locations on a single crystal turbine blade. Such analyses form a natural precursor to the application of life prediction methods to gas turbine airfoils. Author

N89-17326*# National Aeronautics and Space Administration. Lewis Research Center, Cleveland, OH.
USE OF INELASTIC STRAIN AS A BASIS FOR ANALYZING THERMOMECHANICAL TEST DATA
P. A. Bartolotta and J. R. Ellis *In its* Turbine Engine Hot Section Technology, 1987 Oct. 1987 p 303-315 (For primary document see N89-17298 09-39)
Avail: NTIS HC A20/MF A01 CSCL 20K

It was shown that the proposed data analysis method, based on inelastic strain-time response, can be used effectively to represent cyclic response at elevated temperatures for Hastelloy-X. A high level of confidence in this method was built by making comparisons of the experimental and fitted data in two forms. Because of this level of confidence, the analysis was taken one step further and inelastic strain rates were calculated from the derivatives of the fit equations. Author

N89-17327*# National Aeronautics and Space Administration. Lewis Research Center, Cleveland, OH.
PRELIMINARY STUDY OF CREEP THRESHOLDS AND THERMOMECHANICAL RESPONSE IN HAYNES 188 AT TEMPERATURES IN THE RANGE 649 TO 871 C
J. R. Ellis, P. A. Bartolotta, and S. W. Mladsi *In its* Turbine Engine Hot Section Technology, 1987 Oct. 1987 p 317-334 (For primary document see N89-17298 09-39)
Avail: NTIS HC A20/MF A01 CSCL 20K

The following conclusions were drawn from this study of creep thresholds and thermomechanical response: (1) creep threshold can be determined using the latest electrohydraulic test equipment, providing that test durations are short and relatively large accumulations of creep strain are used in defining the threshold; (2) significant creep strains were measured under monotonic loading as stress levels as low as 4 ksi at temperatures predicted for solar receiver service; and (3) the material exhibited creep ratchetting during simulated service cycles, a result not predicted by analysis using current constitutive models for Haynes 188. Author

N89-17328*# National Aeronautics and Space Administration. Lewis Research Center, Cleveland, OH.
FINITE ELEMENT IMPLEMENTATION OF VISCOPLASTIC MODELS
V. K. Arya *In its* Turbine Engine Hot Section Technology, 1987 Oct. 1987 p 335-348 (For primary document see N89-17298 09-39)
Avail: NTIS HC A20/MF A01 CSCL 20K

A brief description of the implementation in MARK, the general purpose finite element structural analysis code, of two viscoplastic models developed by Robinson is given. One model is for isotropic materials and the other is for metal matrix composites. Also presented are analytical results obtained for hot section components using these models. Author

N89-17329*# National Aeronautics and Space Administration. Lewis Research Center, Cleveland, OH.
STRUCTURAL RESPONSE OF AN ADVANCED COMBUSTOR LINER: TEST AND ANALYSIS
Paul E. Moorhead, Robert L. Thompson, M. Tong, and M. Higgins (Sverdrup Technology, Inc., Cleveland, OH.) *In its* Turbine Engine Hot Section Technology, 1987 Oct. 1987 p 349-356 (For primary document see N89-17298 09-39)
Avail: NTIS HC A20/MF A01 CSCL 20K

An advanced (segmented) combustor liner supplied by Pratt and Whitney Aircraft was tested in the structural component test rig at Lewis Research Center. It was found that the segmented liner operated at much lower temperatures than the conventional liner (about 400 F lower) for the same heat flux. At the lower temperatures and low thermal gradients, little distortion to the segments was observed. The operating conditions were not severe enough to distort or damage the segmented liner. Author

N89-17330*# National Aeronautics and Space Administration. Lewis Research Center, Cleveland, OH.
THERMAL EXPANSION MISMATCH AND PLASTICITY IN THERMAL BARRIER COATING
George C. Chang, Woraphat Phucharoen (Cleveland State Univ., OH.), and Robert A. Miller *In its* Turbine Engine Hot Section Technology, 1987 Oct. 1987 p 357-368 (For primary document see N89-17298 09-39)
Avail: NTIS HC A20/MF A01 CSCL 20K

The basic objective of this investigation is the quantitative determination of stress states in a model thermal barrier coating (TBC) as it cools in the air to 600 C from an assumed stress-free state at 700 C. This model is intended to represent a thin plasma-sprayed zirconia-yttria ceramic layer with a nickel chromium-aluminum-yttrium bond coat on a cylindrical substrate made of nickel-based superalloys typically found in gas turbines. Author

N89-17331*# Garrett Turbine Engine Co., Phoenix, AZ.
THERMAL BARRIER COATING LIFE-PREDICTION MODEL DEVELOPMENT
T. E. Strangman, J. F. Neumann, and A. Liu *In* NASA, Lewis Research Center, Turbine Engine Hot Section Technology, 1987 Oct. 1987 p 369-375 (For primary document see N89-17298 09-39)
(Contract NAS3-23945)
Avail: NTIS HC A20/MF A01 CSCL 20K

The primary objective of this program was to develop an operative thermal barrier coating (TBC) design model for life prediction. The objective was successfully accomplished with the development, calibration, and demonstration of a mechanistic thermochemical model which rapidly predicts TBC life as a function of engine, mission, and materials system parameters. This thermochemical design model accounts for the three operative TBC damage modes (bond coating oxidation, zirconia toughness reduction, and molten salt film damage), which all contribute to spalling of the insulating zirconia layer. Author

N89-17332*# General Electric Co., Cincinnati, OH. Aircraft Engines.
THERMAL BARRIER COATING LIFE PREDICTION MODEL
B. Pilsner, R. Hillery, R. L. McKnight, T. Cook, and M. Hartle *In* NASA, Lewis Research Center, Turbine Engine Hot Section Technology, 1987 Oct. 1987 p 377-393 (For primary document see N89-17298 09-39)
Avail: NTIS HC A20/MF A01 CSCL 20K

The objectives of this research were to determine the predominant modes of degradation of a plasma sprayed thermal barrier coating (TBC) system, and then to develop and verify life prediction models accounting for these degradation modes. The TBC system consists of a low pressure plasma sprayed (LPPS) bond coat layer of Ni-22Cr-10Al-O.3Y, an air plasma sprayed (APS) yttria partially stabilized zirconia (ZrO sub 2-8Y sub 2 O sub 3) top coat on a conventionally cast Rene 80 (Ni base) substrate. Thermal cycle testing of TBCs was employed to evaluate the effect of coating edges, bond coat oxidation, bond coat creep, top coat thickness, and bond coat thickness. Author

N89-17333*# Pratt and Whitney Aircraft, East Hartford, CT.
THERMAL BARRIER COATING LIFE PREDICTION MODEL DEVELOPMENT
J. T. DeMasi, S. L. Manning, M. Ortiz, and K. D. Sheffler *In* NASA, Lewis Research Center, Turbine Engine Hot Section Technology, 1987 Oct. 1987 p 385-399 (For primary document see N89-17298 09-39)
(Contract NAS3-23944)
Avail: NTIS HC A20/MF A01 CSCL 20K

The objectives of this program are to increase understanding of thermal barrier coating (TBC) degradation and failure modes, to generate quantitative ceramic failure life data under cyclic thermal conditions which simulate those encountered in gas turbine engine service, and to develop an analytical methodology for prediction of coating life in the engine. Observations of degradation and failure modes in plasma deposited ceramic indicate that spallation failure results from progressive cracking of the ceramic parallel to and adjacent to, but not coincident with the metal-ceramic interface. Author

N89-17334*# Pratt and Whitney Aircraft, East Hartford, CT.
HIGH TEMPERATURE CONSTITUTIVE AND CRACK INITIATION MODELING OF COATED SINGLE CRYSTAL SUPERALLOYS **c27**
Thomas G. Meyer, David M. Nissley, and Gustav A. Swanson *In* NASA, Lewis Research Center, Turbine Engine Hot Section Technology, 1987 Oct. 1987 p 401-412 (For primary document see N89-17298 09-39)
(Contract NAS3-23939)
Avail: NTIS HC A20/MF A01 CSCL 11B

The purpose of this program is to develop life prediction models for anisotropic materials used in gas turbine airfoils. In the base portion of the program, two coated single crystal alloys are being tested. They are PWA 286 overlay coated and PWA 273 aluminide coated PWA 1480 and PWA 286 overlay coated Alloy 185. Viscoplastic constitutive models for these materials are also being developed to predict the cyclic stress-strain histories required for life prediction of the lab specimens and actual airfoil designs. Author

N89-17335*# General Electric Co., Cincinnati, OH. Aircraft Engines.
ELEVATED TEMPERATURE CRACK GROWTH
K. S. Kim, R. H. VanStone, S. N. Malik, and J. H. Laflen *In* NASA, Lewis Research Center, Turbine Engine Hot Section Technology, 1987 Oct. 1987 p 413-422 (For primary document see N89-17298 09-39)
(Contract NAS3-23940)
Avail: NTIS HC A20/MF A01 CSCL 20K

The purpose is to determine the ability of currently available P-I integrals to correlate fatigue crack propagation under conditions that simulate the turbojet engine combustor liner environment. The utility of advanced fracture mechanics measurements will also be evaluated. Research showed that the experimentally measured displacements and loads can be accurately predicted by finite element analyses that consider the growth of the fatigue crack. These results are being used to evaluate nonlinear fracture mechanics parameters for correlating the observed fatigue crack growth rates for different strain ranges. Author

N89-17336*# Pratt and Whitney Aircraft, East Hartford, CT.
CREEP FATIGUE LIFE PREDICTION FOR ENGINE HOT SECTION MATERIALS (ISOTROPIC) FIFTH YEAR PROGRESS REVIEW
Richard S. Nelson and Peter R. Harvey *In* NASA, Lewis Research Center, Turbine Engine Hot Section Technology, 1987 Oct. 1987 p 423-434 (For primary document see N89-17298 09-39)

(Contract NAS3-23288)
Avail: NTIS HC A20/MF A01 CSCL 20K

The need for advanced life prediction methods for hot section components for gas turbine engines is becoming more and more evident. The complex local strain and temperature histories at critical locations must be accurately interpreted to account for the effects of various damage mechanisms and their possible interactions. This program is designed to investigate these fundamental damage processes, identify modeling strategies, and develop practical models which can be used to guide the early design and development of new engines and to increase the durability of existing engines. Author

N89-17337*# National Aeronautics and Space Administration. Lewis Research Center, Cleveland, OH.
TOTAL STRAIN VERSION OF STRAINRANGE PARTITIONING FOR THERMOMECHANICAL FATIGUE AT LOW STRAINS
G. R. Halford and J. F. Saltsman *In its* Turbine Engine Hot Section Technology, 1987 Oct. 1987 p 435-458 (For primary document see N89-17298 09-39)
Avail: NTIS HC A20/MF A01 CSCL 20K

A new method is proposed for characterizing and predicting the thermal fatigue behavior of materials. The method is based on three innovations in characterizing high temperature material behavior: (1) the bithermal concept of fatigue testing; (2) advanced, nonlinear, cyclic constitutive models; and (3) the total strain version of traditional strainrange partitioning. Author

42 GEOSCIENCES (GENERAL)

No abstracts in this category.

43 EARTH RESOURCES AND REMOTE SENSING

Includes remote sensing of earth resources by aircraft and spacecraft; photogrammetry; and aerial photography.

For instrumentation see *35 Instrumentation and Photography.*

N89-17338# Technische Univ., Delft (Netherlands). Dept. of Geodesy.
KINEMATIC LEVELING ADJUSTMENTS WITH POLYNOMIALS AND POLYNOMIAL SPLINES
Auke deHaan May 1988 108 p
(ETN-89-93328) Avail: NTIS HC A06/MF A01

Approximating functions are described which can be used for the modeling of benchmark movements in leveling networks used to monitor vertical movements of the Earth's surface over periods of few days to a century. Height, height shift, vertical velocity, and acceleration can be estimated for any time or time interval within the interval of the measurements. The computer programs for kinematic leveling adjustments with polynomials and polynomial splines are described. Kinematic adjustments made with 5599 height difference measurements from 68 campaigns for the monitoring of vertical movements in and around Milan cathedral are presented and compared to classic leveling adjustments. ESA

N89-17339*# National Aeronautics and Space Administration. Ames Research Center, Moffett Field, CA.
ACCURACY ASSESSMENT, USING STRATIFIED PLURALITY SAMPLING, OF PORTIONS OF A LANDSAT CLASSIFICATION OF THE ARCTIC NATIONAL WILDLIFE REFUGE COASTAL PLAIN
Don H. Card and Laurence L. Strong (TGS Technology, Inc., Moffett Field, CA.) Jan. 1989 48 p Sponsored by NASA
(Contract GSRN-1-7060-0450)
(NASA-TM-101042; A-88309; NAS 1.15:101042) Avail: NTIS HC A03/MF A01 CSCL 08B

An application of a classification accuracy assessment procedure is described for a vegetation and land cover map prepared by digital image processing of LANDSAT multispectral scanner data. A statistical sampling procedure called Stratified Plurality Sampling was used to assess the accuracy of portions of a map of the Arctic National Wildlife Refuge coastal plain. Results are tabulated as percent correct classification overall as well as per category with associated confidence intervals. Although values of percent correct were disappointingly low for most categories, the study was useful in highlighting sources of classification error and demonstrating shortcomings of the plurality sampling method. Author

N89-17340# World Meteorological Organization, Geneva (Switzerland).
HYDROLOGICAL ASPECTS OF COMBINED EFFECTS OF STORM SURGES AND HEAVY RAINFALL ON RIVER FLOW
1988 85 p
(WMO-704; OH-30; ISBN-92-63-10704; ETN-89-92880)
Copyright Avail: MF A01; print copy available at WMO, Case Postale no. 5, CH-1211 Geneva 20, Switzerland

Storm-surge data, stages and discharges in rivers, precipitation and its areal and temporal variation, and methods of observation are reviewed. The deterministic approach to flood modeling in tidal areas including model structure, open sea models, bays and estuaries, and river models is discussed. The empirical approach to flood modeling in tidal areas, empirical models for coastal surge calculation, river surges, physically based formulas, and regression formulas are considered. Risk evaluation of storm surges in rivers and surge frequency at an open coast, flood frequency in tidal rivers, probable maximum floods, damage assessment, and flood insurance are treated. Forecasting centers, their location, choice of model and communication equipment, and dissemination of forecasts and warnings are presented. Case studies are given. ESA

N89-16886# National Remote Sensing Agency, Hyderabad (India).
INDIAN ACTIVITIES IN REMOTE SENSING APPLICATIONS: MICROWAVE REMOTE SENSING
B. L. Deekshatulu *In* DFVLR, Proceedings of the Colloquium about Joint Projects Within the DFVLR/ISRO Cooperation Jun. 1988 p 39-56 (For primary document see N89-16883 09-12)
Avail: NTIS HC A06/MF A01; DFVLR, VB-PL-DO, Postfach 90 60 58, 5000 Cologne, Fed. Republic of Germany, 34.50 Deutsche marks

N89-16887# Deutsche Forschungs- und Versuchsanstalt fuer Luft- und Raumfahrt, Oberpfaffenhofen (West Germany).
GERMAN SPACEBORNE REMOTE SENSING ACTIVITIES
H. Oettl *In its* Proceedings of the Colloquium about Joint Projects Within the DFVLR-ISRO Cooperation Jun. 1988 p 57-67 (For primary document see N89-16883 09-12)
Avail: NTIS HC A06/MF A01; DFVLR, VB-PL-DO, Postfach 90 60 58, 5000 Cologne, Fed. Republic of Germany, 34.50 Deutsche marks

44 ENERGY PRODUCTION AND CONVERSION

Includes specific energy conversion systems, e.g., fuel cells; global sources of energy; geophysical conversion; and windpower.

For related information see also *07 Aircraft Propulsion and Power, 20 Spacecraft Propulsion and Power,* and *28 Propellants and Fuels.*

N89-17341# Midwest Research Inst., Golden, CO. Solar Energy Research Inst.

DEVICE PHYSICS RELATED TO THE GRANULAR NATURE OF CuInSe2 SOLAR CELLS Final Report, 1 Apr. 1986 - 31 Mar. 1988

J. R. Sites (Colorado State Univ., Fort Collins.) Sep. 1988 32 p

(Contract DE-AC02-83CH-10093)

(DE89-000810; SERI/STR-211-3395) Avail: NTIS HC A03/MF A01

This report attempts to integrate our collective knowledge about polycrystalline solar cells. The dominant loss mechanisms for both CuInSe2 and CdTe cells are shown graphically, scaled to their estimated magnitudes. There are major limitations due to polycrystalline related mechanisms such as compensation and recombination, but there are also straightforward efficiency improvements possible through reductions in reflection, window absorption, and series resistance. A physical model for polycrystalline semiconductor diodes is proposed and described in detail. The key features of the model are to restrict most defect states to granular surfaces and to require them to be of such a nature that passivation approaching 100 percent is practical. The fact that these conditions have been nearly achieved empirically is both the cause of past successes and the hope for future improvements. DOE

N89-17342# Midwest Research Inst., Golden, CO. Solar Energy Research Inst.

RESEARCH ON HIGH-EFFICIENCY, SINGLE-JUNCTION, MONOLITHIC, THIN-FILM AMORPHOUS SILICON SOLAR CELLS, PHASE 3 Semiannual Report, 1 Oct. 1985 - 31 Mar. 1986

A. E. Delahoy, E. Eser, and F. Kampas (Chronar Corp., Princeton, NJ.) Sep. 1988 72 p Prepared in cooperation with Chronar Corp., Princeton, NJ

(Contract DE-AC02-83CH-10093)

(DE89-000813; SERI/STR-211-3414) Avail: NTIS HC A04/MF A01

This report describes the research conducted during the first half of Phase 3 of a research program on high-efficiency, single-junction, monolithic, thin-film amorphous silicon solar cells. Important progress toward improving the thermal stability of a-Si:H solar cells and panels was made. A substantial amount of work was also performed in developing granular tin oxide from both tetramethyltin and tin chloride. Two chambers of the multichamber deposition system were made operational. A cell efficiency of 10.8 percent was achieved through the use of light trapping, improved p-layer control, and a graded affinity transitional i-layer. Cells that improve in efficiency upon light soaking (inverse Staebler-Wronski cells) were also prepared. DOE

N89-17343# Spire Corp., Bedford, MA.

THERMAL DEGRADATION MECHANISMS IN GaAs SOLAR CELLS WITH HIGH-TEMPERATURE CONTACTS

S. P. Tobin, C. Bajgar, S. M. Vernon, C. J. Keavney, M. A. Chung, and D. S. Ruby (Sandia National Labs., Albuquerque, NM.) 1988 12 p Presented at the 20th IEEE Photovoltaic Specialists Conference, Las Vegas, NV, 26 Sep. 1988 Prepared in cooperation with Spire Corp., Bedford, MA; Air Force Wright Aeronautical Labs., Wright-Patterson AFB, OH

(Contract DE-AC04-76DP-00789)

(DE89-001375; SAND-88-2498C; CONF-880965-20) Avail: NTIS HC A03/MF A01

This objective of this work was to characterize the thermal stability of GaAs solar cells with high-temperature contacts. High-temperature stability is important for threat environments in space, for compatibility with high-temperature assembly techniques, and for enhanced reliability of cells. Our contact system, described previously, relies on a Pt solid-phase ohmic contact, a TiN barrier layer, and an Au conductor, with contact to a heavily doped p-GaAs contact layer. The behavior of both flat-plate and concentrator cells has been characterized as a function of temperature (400 to 600 C) and time (5 to 15 minutes) of the anneal. We find that GaAs cells experience minimal electrical degradation up to 550 C for 5 minutes, or to 490 C for 15 minutes. Increases in the 2kT perimeter dark current are responsible for small decreases in Voc and FF up to these temperatures. At higher temperatures a drastic decrease in efficiency is caused by metallurgical reactions at isolated regions along the grid lines. The reaction, which appears to involve Au-Ga, is initiated at the edges of the grid lines. Away from edges, the contacts are metallurgically stable. DOE

N89-17344# Varian Associates, Palo Alto, CA.

CONCENTRATOR EFFICIENCIES OF 29.2 PERCENT FOR A GaAs CELL AND 24.8 PERCENT FOR A MOUNTED CELL-LENS ASSEMBLY

N. R. Kaminar, D. D. Liu, H. F. MacMillan, L. D. Partain, M. L. Ristow, G. F. Virshup, and James M. Gee (Sandia National Labs., Albuquerque, NM.) 1988 4 p Presented at the 20th IEEE Photovoltaic Specialists Conference, Las Vegas, NV, 26 Sep. 1988

(Contract DE-AC04-76DP-00789)

(DE89-001612; SAND-88-2832C; CONF-880965-22) Avail: NTIS HC A02/MF A01

A lens/cell efficiency of 24.8 percent has been obtained in an outdoor test using a single GaAs cell and a Fresnel lens. This is the highest efficiency ever reported for a lens/cell assembly. During the test, the cell was water cooled to a junction temperature of 45 C and the concentration ratio was 205:1. In a related test, a 29.2 percent cell efficiency was obtained using a GaAs concentrator cell and an Entech prismatic cover glass designed to reduce the effect of shadowing of the grid lines. This efficiency was measured in the flash tester at Sandia Laboratories. DOE

N89-17345# Varian Associates, Palo Alto, CA.

RECENT ADVANCES IN HIGH-EFFICIENCY InGaAs CONCENTRATOR CELLS

J. G. Werthen, B. A. Arau, C. W. Ford, N. R. Kaminar, M. S. Kuryla, M. L. Ristow, C. R. Lewis, H. F. MacMillan, G. F. Virshup, and James M. Gee (Sandia National Labs., Albuquerque, NM.) 1988 4 p Presented at the 20th IEEE Photovoltaic Specialists Conference, Las Vegas, NV, 26 Sep. 1988

(Contract DE-AC04-76DP-00789)

(DE89-001613; SAND-88-0632C; CONF-880965-21) Avail: NTIS HC A02/MF A01

InGaAs concentrator cells with bandgaps of 1.15 eV and 1.35 eV have been developed. These cells are intended for eventual use in dual- and triple-junction tandem solar cells, respectively. The InGaAs cell structures were grown by MOCVD on GaAs substrates with grading layers to accommodate lattice mismatch. Efficiencies greater than 24 percent at 400 suns (AM 1.5D, 100 mW/sq cm) have been demonstrated by InGaAs cells with either bandgap. Since the 1.15-eV InGaAs has a bandgap close to silicon, comparison of the photovoltaic effect in materials with direct and indirect bandgaps is possible. The InGaAs demonstrates open-circuit voltage up to 800 mW (130 mW higher than Si) under concentration. Conversely, Si demonstrates a one-sun short-circuit current of 42 mA/sq cm compared to 31 mA/sq cm for InGaAs. Possible reasons for the higher voltages will be given, and implications regarding projected tandem cell performance will be discussed. DOE

N89-17346# Sandia National Labs., Albuquerque, NM.

THERMALLY CONDUCTIVE ALUMINA/ORGANIC COMPOSITES FOR PHOTOVOLTAIC CONCENTRATOR CELL ISOLATION

L. C. Beavis, J. K. G. Panitz, and D. J. Sharp 1988 6 p Presented at the 20th IEEE Photovoltaic Specialists Conference, Las Vegas, NV, 26 Sep. 1988
(Contract DE-AC04-76DP-00789)
(DE89-001181; SAND-88-2624C; CONF-880965-11) Avail: NTIS HC A02/MF A01

Electrophoretically deposited styrene-acrylate films were studied. These yield marginally useful thermal conductivities of 0.1 to 0.2 watts/meter-Kelvin, but have useful dielectric strengths over 2500 volts for 40 micrometer thick coatings. Thin, 25 micrometer, coatings of anodically grown Al2O3 films were also investigated. These films have thermal conductivities of approximately 6 to 8 watts/meter-Kelvin. Although these Al2O3 films have greater thermal conductivity than the polymer films, they exhibit porosity which typically limits their dielectric strength to less than 1000 volts. In the current study we have determined that styrene-acrylate can be electrophoretically deposited in porous anodic aluminum oxide films to form an alumina-organic composite with improved electrical breakdown strengths as well as higher thermal conductivity than styrene-acrylate films. DOE

N89-17347# Black and Veatch Consulting Engineers, Kansas City, MO.
A PERFORMANCE MODEL FOR NONUNIFORMLY ILLUMINATED FRONT-GRIDDED CONCENTRATOR CELLS
Kevin A. Kerschen and Paul A. Basore (Sandia National Labs., Albuquerque, NM.) 1988 14 p Presented at the 20th IEEE Photovoltaic Specialists Conference, Las Vegas, NV, 26-30 Sep. 1988
(Contract DE-AC04-76DP-00789)
(DE89-001368; SAND-88-0687C; CONF-880965-19) Avail: NTIS HC A03/MF A01

The illumination profile produced by Fresnel concentrating PV module optics may deviate dramatically from the uniform illumination conditions under which cell performance is normally measured. Estimating the expected performance of concentrator cells under nonuniform illumination is a challenge that goes beyond simply aggregating the measured performance of cells exposed to a range of uniform illumination conditions. It requires the ability to simulate the nonuniform illumination profile of the module optics and to understand the impact that nonuniform illumination has on the cell's power conversion mechanisms. This paper presents these enhancements to an existing PV concentrator performance model that simulates the performance of front-gridded cells with parallel grid lines operating under expected illumination conditions. The model uses standard test data for a user-selected reference cell to estimate the performance of similar cells with different area, metallization coverage, and illumination profile. It also accommodates the application of a prismatic optical cover to eliminate grid-line obscuration. DOE

N89-17348# Naval Postgraduate School, Monterey, CA.
A MICROPROCESSOR-BASED, SOLAR CELL PARAMETER MEASUREMENT SYSTEM M.S. Thesis
Robert R. Oxborrow Jun. 1988 89 p
(AD-A200227) Avail: NTIS HC A05/MF A01 CSCL 10B

The effects of the space environment on solar cells has, to date, been largely modeled and approximated in the design of solar arrays. Restrictions such as weight and cost have precluded direct analysis of the long term effects of radiation in space. At the Naval Postgraduate School (NPS), a simple circuit has been devised which facilitates in situ data collection and analysis of these effects. The circuit includes an op-amp and a high beta transistor for cell voltage biasing. When coupled to a microprocessor-based controller system, this circuit has the capability to measure and store data pertaining to solar cell performance I-V curves. The complete system consists of an NSC 800 microprocessor, D/A and A/D components, analog multiplexers and demultiplexers, biasing transistors and op-amps. This design provides a compact, low power, accurate method for I-V measurement and data storage. Such a system may be used to observe and monitor an array of test cells and their performance degradation in both the space environment and terrestrial applications. GRA

N89-17349# Sandia National Labs., Albuquerque, NM.
PC-1D VERSION 2: ENHANCED NUMERICAL SOLAR CELL MODELING
Paul A. Basore, D. T. Rover, and A. W. Smith 1988 15 p Presented at the 20th IEEE Photovoltaic Specialists Conference, Las Vegas, NV, 26 Sep. 1988 Prepared in cooperation with Iowa State Univ. of Science and Technology, Ames; and Georgia Inst. of Technology, Atlanta
(Contract DE-AC04-76DP-00789)
(DE89-000302; SAND-88-0579C; CONF-880965-3) Avail: NTIS HC A03/MF A01

PC-1D is a finite-element program for modeling semiconductor devices in one-dimension on personal computers. A combination of convenient user interface, rapid convergence, and the ability to address complex issues associated with heavy doping, high-level injection, and transients has led to widespread use of the program by solar cell researchers. Significant improvements have been made to the program, resulting in a new version to be demonstrated at this conference. This paper describes the enhancements and their application to modern crystalline cells, including new provisions for heterostructures, anti-reflection coatings and light trapping, an upgraded user interface, and unattended operation for optimization studies. DOE

N89-17350# Midwest Research Inst., Golden, CO. Solar Energy Research Inst.
WIND ENERGY SYSTEMS: PROGRAM SUMMARY FOR FISCAL YEARS 1986 AND 1987
Oct. 1988 103 p
(Contract DE-AC02-83CH-10093)
(DE88-001188; DOE/CH-10093/26) Avail: NTIS HC A06/MF A01

This document summarizes the research and development activities sponsored by the DOE Wind/Ocean Technologies Division during fiscal years (FY) 1986 and 1987. The summary is organized into the following sections: An introduction to the Federal Wind Energy Program, its history, and current research directions; The program's organization for FY 1986 and 1987; The program's budget; The highlighted accomplishments of DOE's field laboratories; The program's future role; An index to and summaries of individual projects and contracts managed by each laboratory; A bibliography of major publications produced by DOE and its laboratories in FY 1986 and FY 1987. DOE

N89-17351# Sandia National Labs., Albuquerque, NM. Applied Mechanics Div.
SIMPLIFIED FATIGUE DAMAGE AND CRACK GROWTH CALCULATIONS FOR WIND TURBINES
Paul S. Veers 1988 21 p Presented at the ASME Energy-sources Technology Conference and Exhibition and 7th Intersociety Cryogenic Symposium, Houston, TX, 22 Jan. 1989
(Contract DE-AC04-76DP-00789)
(DE89-003132; SAND-88-1806C; CONF-890102-7) Avail: NTIS HC A03/MF A01

Estimating fatigue life of wind turbine components, where the loading and structural response are random, can be a difficult task. The life estimate is sensitive to rare large loads and can be influences by the sequence of load applications. Sequence effects in fatigue crack initiation and crack growth are outlines. A simplified model for sequence effects in crack growth is presented along the model predictions of an American Society for Testing and Materials (ASTM) crack growth test series. The relative importance of including these effects in fatigue calculations is discussed. Analytical solutions for the time to crack initiation and crack growth provide quick estimates of fatigue life by approximating the loading as a narrow-band Gaussian process and by neglecting sequence effects. This approximation is both conservative and within the usual scatter in fatigue life estimates due to material variability. It is therefore a useful tool in estimating fatigue life especially when turbine response data are limited. DOE

N89-17352# Sandia National Labs., Albuquerque, NM. Wind Energy Research Div.

INITIAL STRUCTURAL RESPONSE MEASUREMENTS FOR THE SANDIA 34-METER VAWT TEST BED

Thomas D. Ashwill 1988 22 p Presented at the ASME Energy-Sources Technology Conference and Exhibition and 7th Intersociety Cryogenic Symposium, Houston, TX, 22 Jan. 1989

(Contract DE-AC04-76DP-00789)

(DE89-003133; SAND-88-0633C; CONF-890102-6) Avail: NTIS HC A03/MF A01

Sandia National Laboratories (SNL) has designed and constructed a 34-meter diameter vertical axis wind turbine (VAWT) Test Bed. The machine will be used to advance research in aerodynamics and structural dynamics, improve fatigue life prediction capabilities, and investigate control algorithms and systems concepts. The Test Bed has extensive instrumentation including 70 strain gauges to measure blade and tower response. Immediately after the blades were mounted, blade gravity stresses were measured and a modal analysis on the stationary rotor was performed to determine zero rpm modal frequencies. Assembly and start-up tests have been completed, and testing is in the machine characterization phase. Resonance surveys are underway to fully characterize the modal frequencies and mode shapes of the rotor, drive train and support cables. Measured gravity stresses, centrifugal stresses, and modal frequencies are compared to predicted values. DOE

N89-17353# Argonne National Lab., IL.

FIRST PRODUCTION OF POTABLE WATER BY OTEC (OCEAN THERMAL ENERGY CONVERSION) AND ITS POTENTIAL APPLICATIONS

Anthony Thomas and David L. Hillis 1988 4 p Presented at the OCEANS '88, Baltimore, MD, 31 Oct. 1988

(Contract W-31-109-eng-38)

(DE89-003630; CONF-8810180-2) Avail: NTIS HC A02

An experiment--the Heat and Mass Transfer Scoping Test Apparatus--was built to obtain design data for a larger test that will assess the technical feasibility of the open-cycle OTEC process. (The closed-cycle concept was successfully demonstrated in 1979.) The DOE-funded project is a joint effort between Argonne National Laboratory (ANL) and the Solar Energy Research Institute (SERI). The apparatus was erected at the Natural Energy Laboratory of Hawaii and became operational in the summer of 1987. It is used by both ANL and SERI to conduct open-cycle OTEC experiments. After initial debugging, it produced 350 gallons per hour of potable water having a salinity of 86 ppM, one-fifth that of local tap water available at the test site. DOE

N89-17354# Midwest Research Inst., Golden, CO. Solar Energy Research Inst.

PREDICTION OF STOCHASTIC BLADE RESPONSES USING MEASURED WIND-SPEED DATA AS INPUT TO THE FLAP CODE

A. D. Wright and R. W. Thresher Nov. 1988 8 p Presented at the ASME Energy-Sources Technology Conference and Exhibition and 7th Intersociety Cryogenic Symposium, Houston, TX, 22 Jan. 1989

(Contract DE-AC02-83CH-10093)

(DE89-000834; SERI/TP-217-3394; CONF-890102-12) Avail: NTIS HC A02/MF A01

Accurately predicting wind turbine blade loads and response is important in predicting the fatigue life of wind turbines. The necessity of including turbulent wind effects in structural dynamics models has long been recognized. At SERI, the structural dynamics model, or FLAP (Force and Loads Analysis Program), is being modified to include turbulent wind fluctuations in predicting rotor blade forces and moments. The objective of this paper is to show FLAP code predictions compared to measured blade loads, using actual anemometer array data and a curve-fitting routine to form series expansion coefficients as the turbulence input to FLAP. The predictions are performed for a three-blade upwind field test turbine. An array of nine anemometers was located 0.8 rotor diameters (D) upwind of the turbine, and data from each anemometer are used in a least-squares curve-fitting routine to obtain a series expansion of the turbulence field over the rotor disk. Three 10-min data cases are used to compare FLAP predictions to measured results. Each case represents a different mean wind speed and turbulence intensity. The time series of coefficients in the expansion of the turbulent velocity field are input to the FLAP code. Time series of predicted flap-bending, moments at two blade radial stations are obtained, and power spectra of the predictions are then compared to power spectra of the measured blade bending moments. DOE

N89-17355# Technische Univ., Munich (Germany, F.R.). Inst. fuer Luft- und Raumfahrt.

SYSTEMS ANALYSIS AND DESIGN OF A LUNAR SOLAR POWER PLANT FOR THE SUPPLY OF A LUNAR BASE [SYSTEMANALYSE UND ENTWURF EINES LUNAREN SOLARKRAFTWERKS ZUR VERSORGUNG EINER MONDBASIS]

B. Johnenning, M. Britsch, R. Dust, M. Grade, M. Grasme, J. Greiner-Petter, W. Jacubiec, J. Leppich, B. Luebke-Ossenbeck, and J. Mayer et al 8 Jun. 1988 46 p In GERMAN; ENGLISH summary

(ILR-Mitt-198; ETN-89-93481) Avail: NTIS HC A03/MF A01

The preliminary design and cost estimates of a lunar solar power station for the supply of a lunar base were performed. A power demand during a lunar day of 7.5 MW and during a lunar night of 2.5 MW, as well as photovoltaic power conversion were assumed. The option with the minimum sum of procurement and space transportation costs was selected. The facility consists of 228 Sun-following solar generators equipped with GaAs cells with a concentration ratio of 10, and 15 units with electrolysis and fuel cells with cryogenic storage of hydrogen and oxygen. The total systems mass is 1170 metric tons; the power output of the solar generators is 17.8 MW; the overall power conversion efficiency 9.6 percent; acquisition costs 4.4 billion dollars (1987) assuming 2000 dollars/kg transportation costs to the Moon; and mean lunar energy cost 8.5 dollars/kWh. ESA

N89-17356*# National Aeronautics and Space Administration. Lewis Research Center, Cleveland, OH.

THE EFFECT OF DIFFERENT MODULE CONFIGURATIONS ON THE RADIATION TOLERANCE OF MULTIJUNCTION SOLAR CELLS

James M. Gee and Henry B. Curtis 1988 20 p Prepared in cooperation with Sandia National Labs., Albuquerque, NM Sponsored by NASA

(Contract DE-AC04-76DP-00789)

(NASA-TM-101251; NAS 1.15:101251; DE89-000304; SAND-88-0628C; CONF-880965-2) Avail: NTIS HC A03/MF A01 CSCL 10A

The effect of different module configurations on the performance of multijunction (MJ) solar cells in a radiation environment was investigated. Module configuration refers to the electrical circuit in which the subcells of the multijunction cell are wired. Experimental data for AlCaAs, GaAs, InGaAs, and silicon single-junction concentrator cells subjected to 1 MeV electron irradiation was used to calculate the expected performance of AlGaAs/InGaAs, AlGa/silicon, GaAs/InGaAs, and GaAs/silicon Mj concentrator cells. These calculations included independent, series, and voltage-matched configurations. The module configuration was found to have a significant impact on the radiation tolerance characteristic of the MJ cells. DOE

45 ENVIRONMENT POLLUTION

Includes atmospheric, noise, thermal, and water pollution.

N89-17357# Applied Science Associates, Inc., Narragansett, RI.
EVALUATION OF SATELLITE-TRACKED SURFACE DRIFTING BUOYS FOR SIMULATING THE MOVEMENT OF SPILLED OIL IN THE MARINE ENVIRONMENT. VOLUME 1: EXECUTIVE SUMMARY Report, 1986 - 1988
Mark Reed, Chris Turner, Malcolm Spaulding, Katherine Jayko, Donald Dorson, and Oistein Johansen (Oceanographic Center, Trondheim, Norway) 15 Mar. 1988 19 p
(Contract DI-14-12-0001-30340)
(PB88-226048; OCS/MMS-87/0071-Vol-1) Avail: NTIS HC A03/MF A01 CSCL 13B

Satellite tracked surface drifters were studied to evaluate the simulation of movememt of spilled crude oil and assessing the skill of the Oil Spill Risk Analysis model. Review of the oil spill literature since 1980 shows that the most significant advance relative to surface transport processes relates to the effect of temporary submergence and surface shear on the distribution of oil behind the downwind leading edge of a surface slick. Dynamic analyses of three basic buoy shapes, the sphere, the spar or cylinder, and the disk or flattened spheroid, were undertaken using a numerical model. Results are given. Author

N89-17358# Applied Science Associates, Inc., Narragansett, RI.
EVALUATION OF SATELLITE-TRACKED SURFACE DRIFTING BUOYS FOR SIMULATING THE MOVEMENT OF SPILLED OIL IN THE MARINE ENVIRONMENT, VOLUME 2 Final Report
Mark Reed, Chris Turner, Malcolm Spaulding, Katherine Jayko, Donald Dorson, and Oistein Johansen (Oceanographic Center, Trondheim, Norway) 15 Mar. 1988 166 p
(Contract DI-14-12-0001-30340)
(PB88-226055; OCS/MMS-87/0071-Vol-2) Avail: NTIS HC A08/MF A01 CSCL 13B

Satellite tracked surface drifters were evaluated for use in simulating the movement of spilled crude oil and assessing the skill of the Oil Spill Risk Analysis (OSRA) model. Review of the literature since 1980 shows that the most significant advance relative to surface transport processes relates to the effect of temporary submergence and surface shear on the distribution of oil behind the downwind leading edge of a surface slick. The results of dynamic analyses suggests that, two existing drifters, a sphere and a disk, represent the most promising available surface drifters for simulating the movement of spilled crude oil. Author

N89-17359# Argonne National Lab., IL. Energy and Environmental Systems Div.
EMISSION-REDUCTION EFFECTS OF METHANOL VEHICLES: STATE OF KNOWLEDGE
M. K. Singh and R. R. Sekar Jul. 1988 49 p
(Contract W-31-109-eng-38)
(DE89-001148; ANL/EES-TM-352) Avail: NTIS HC A03/MF A01

Methanol-fueled vehicles are currently the subject of considerable interest as various national and local options are being considered to address the country's air quality problems. This report evaluates the emissions from several types of methanol-fueled vehicles and qualitatively assesses the potential effects of methanol fuel use on ambient air quality. The evaluation is based on the results of more than 50 recent tests of methanol-fueled vehicles and the U.S. Environmental Protection Agency's (EPA's) most recent assessment of the emissions effects of these vehicles. The emissions from methanol use in three forms in spark-ignition engines and six potential applications in compression-ignition engines are reviewed. The greatest benefit from neat-methanol-fueled or flexible-fuel vehicles is the lower reactivity of their volatile organic compound emissions relative to gasoline-fueled vehicles, thus potentially reducing the contribution of mobile pollution sources to the formation of ozone. The primary advantage of methanol blends is the reduction in carbon monoxide emissions relative to gasoline-fueled vehicles. Finally, nitrogen oxide and particulate emissions are substantially reduced in the various neat methanol applications to heavy-duty diesel engines. Methanol may thus provide a means of meeting the EPA's stringent 1991 to 1994 particulate regulations for heavy-duty diesel engines and vehicles. DOE

N89-17360# Oak Ridge National Lab., TN. Environmental Sciences Div.
ATMOSPHERIC CARBON DIOXIDE, CLIMATE AND GLOBAL VEGETATION CHANGE
W. M. Post 1988 36 p Presented at the Global Vegetation Change: Considerations for Developing a Long-term Research Plan, Laxenburg, Austria, 16 Apr. 1988
(Contract DE-AC05-84OR-21400)
(DE89-002196; CONF-8804214-1) Avail: NTIS HC A03/MF A01

Over the past several decades, significant progress has been made in measuring and understanding the global carbon cycle and in developing methods for projecting future changes in the atmospheric CO2 concentration. During this time, a natural starting point was to check the balance sheet that accounts for all carbon as it exchanged between the major global carbon reservoirs. While it is possible to achieve a balance for a single instant in time, it is not possible with current information to balance carbon fluxes for decade or longer time periods. The inability to account for all carbon exchanges indicated an insufficient knowledge of global carbon cycle processes. In this paper, I outline the scale of the discrepancies involved and offer hypotheses concerning previously underappreciated carbon fluxes that suggest new research directions. These hypotheses postulate global vegetation change at several time scales as a plausible reason for our inability to balance the global carbon cycle over long time periods. DOE

N89-17361# Technology and Management Systems, Inc., Burlington, MA.
SOURCE CHARACTERIZATION OF HEAVY GAS DISPERSION MODELS FOR REACTIVE CHEMICALS, VOLUME 1 Final Report, 22 Jan. 1986 - 21 Dec. 1987
Phani K. Raj and John A. Morris 21 Dec. 1987 258 p
(Contract F19628-86-C-0036)
(AD-A200121; AFGL-TR-88-0003-Vol-1) Avail: NTIS HC A12/MF A01 CSCL 24A

The U.S. Air Force and other agencies which handle, store and transport chemicals, fuels and oxidizers are interested in determining the potential area of hazard posed by the dispersion of vapors generated by accidental spills. This report describes the mathematical models developed to describe a variety of source types and the dispersion of vapor clouds/plumes in the atmosphere. Sixteen different source types are modeled including pressurized liquid releases, flashing and aerosol formation, two phase jet releases, explosive releases and releases of high vapor pressure liquids, cryogenic liquids and gases. The dispersion model takes into account the differences in source characteristics, high-than-air density of clouds (due to aerosol presence, temperature or molecular weight). The water vapor in the air are modeled and considered in the dispersion model. Transition from heavy gas dispersion to near neutral density dispersion is modeled without abrupt changes in size or discontinuity in concentrations. GRA

N89-17362# Naval Research Lab., Washington, DC. Chemical Dynamics and Diagnostics Branch.
MATERIAL COMPATABILITY WITH THRESHOLD LIMIT VALUE LEVELS OF MONOMETHYL HYDRAZINE Final Report
P. A. Taffe, S. L. Rose-Pehrsson, and J. R. Wyat 26 Oct. 1988 33 p
(AD-A200294; NRL-MR-6291) Avail: NTIS HC A03/MF A01 CSCL 24A

Materials were evaluated for potential use as ambient air sample lines for hydrazines. Fluorinated polymers performed the best, metals the worst. Various sample lengths were investigated: increasing the length enhance the differences between samples, although the ranking of performance remained essentially unchanged. The effects of internal diameter (id) upon transport

ability was evaluated by testing samples with ids of 3/16, 1/4, and 3/8 inch. The 3/8 inch id tubing consistently transported a larger percentage of the contaminant. Additional areas examined for their effects on performance were: temperature, humidity, joining of segments, pushing the pulling of the gas stream, and conditioning of the sample tube. The only variable found to have a significant effect on the results was conditioning; indicating that all new tubing should be thoroughly rinsed prior to use as well as periodically between sampling to remove ambient contaminants. GRA

N89-17363# Department of Energy, Washington, DC. Carbon Dioxide Research Div.
CARBON DIOXIDE AND CLIMATE: SUMMARIES OF RESEARCH IN FY 1988
Oct. 1988 93 p
(DE89-002966; DOE/ER-0385) Avail: NTIS HC A05/MF A01

Detailed worldwide measurements indicate that the amount of carbon dioxide in the earth's atmosphere has increased about 25 percent during the past 188 years, primarily because of fossil-fuel combustion and deforestation. Carbon dioxide is one of several trace gases that can modify the earth's heat balance by absorbing outgoing radiation from the earth's surface, thereby increasing the amount of heat retained by the atmosphere--the so-called greenhouse effect. Scientific analyses suggest that this increase could substantially affect climate, agriculture, and other human endeavors. The Carbon Dioxide Research Program is aimed at improving the scientific knowledge base to enable researchers to project future atmospheric concentrations of carbon dioxide, to estimate carbon dioxide-induced global and regional climate changes, and to assess the responses of vegetation to higher concentrations of carbon dioxide and changing climate. The Department of Energy is the lead Federal agency for research related to atmospheric carbon dioxide. Its responsibility is to sponsor a program of directed research and to coordinate this research with relevant activities of other Federal agencies, private concerns, and international institutions. DOE

N89-17364*# Texas Univ., Austin. Dept. of Aerospace Engineering and Engineering Mechanics.
A FEASIBILITY STUDY OF METHODS FOR STOPPING THE DEPLETION OF OZONE OVER ANTARCTICA Final Report
6 May 1988 74 p
(Grant NGT-21-002-080)
(NASA-CR-184583; NAS 1.26:184583) Avail: NTIS HC A04/MF A01 CSCL 13B

Ways of stopping the ozone depletion in the ozone hole over Antarctica were studied. The basic objectives were: (1) to define and understand the phenomenon of the ozone hole; (2) to determine possible methods of stopping the ozone depletion; (3) to identify unknowns about the hole and possible solutions. Two basic ways of attacking the problem were identified. First is replenishment of ozone as it is being depleted. Second is elimination of ozone destroying agents from the atmosphere. The second method is a more permanent form of the solution. Elimination and replenishment methods are discussed in detail. Author

N89-17365# Lawrence Livermore National Lab., CA. Atmospheric and Geophysical Sciences Div.
GREENHOUSE WARMING: WHAT DO WE KNOW
Michael C. MacCracken 16 Nov. 1988 11 p Presented at the Conference on the Implications of Climatic Change for California, San Francisco, CA, 21 Nov. 1988 Submitted for publication
(Contract W-7405-eng-48)
(DE89-004780; UCRL-99998; CONF-8811126-1) Avail: NTIS HC A03/MF A01

The continuing emissions of gases that are able to increase the efficiency with which the atmosphere traps infrared radiation are beginning to alter the global climate. During the next century, theoretical simulations project that global average temperatures will rise by several degrees Celsius above their pre-industrial baseline and that precipitation patterns may shift seasonally and spatially. Although research is being intensified so that detailed regional estimates can be provided, projected increases in summer temperatures and the accompanying increased evaporation, especially during natural warm excursions such as the summer of 1988, appear to pose troubling conditions for water supplies, agriculture, transport, and other activities dependent on water resources. DOE

N89-17366# Oak Ridge National Lab., TN. Advanced Monitoring Development Group.
SCREENING ENVIRONMENTAL POLLUTANTS AND BIOMARKERS: THE ANALYTICAL CHALLENGE
Vo-Dinh Tuan 1988 12 p Presented at the 1st International Symposium on Field Screening Methods for Hazardous Waste Site Investigations, Las Vegas, NV, 11 Oct. 1988
(Contract DE-AC05-84OR-21400)
(DE89-004931; CONF-8810133-5) Avail: NTIS HC A03/MF A01

Detailed characterization of most chemical pollutants in environmental samples from industrial and waste sites is possible using analytical techniques such as liquid or gas chromatography and mass spectroscopy. But for many environmental monitoring programs and assessment applications, these analytical procedures would be needlessly time-consuming and expensive. It is often desirable to have a screening procedure to prioritize environmental samples before detailed analyses are conducted on a subset of samples to reduce the total cost of monitoring programs and environmental studies. This presentation describes various screening techniques, such as synchronous fluorescence (SF), and room temperature phosphorescence (RTP), and provides an overview of advanced analytical techniques and instrumentation, such as surface-enhanced Raman scattering (SERS) and antibody-based fiberoptics sensors, used to detect trace levels of chemical pollutants and related biomarkers in complex environmental samples. DOE

N89-17367# Duke Univ., Durham, NC. Dept. of Botany.
INTEGRATION OF EXPERIMENTAL AND MODELING APPROACHES IN THE UNMANAGED ECOSYSTEM RESEARCH PLAN Performance Report, 15 Sep. 1987 - 14 Sep. 1988
Boyd R. Strain 19 Dec. 1988 4 p
(Contract DE-FG05-87ER-60575)
(DE89-005230; DOE/ER-60575/1) Avail: NTIS HC A02/MF A01

In year 1 of this award three phases of research were initiated in an investigation of physiological adaptations in plants grown for long periods in enhanced CO2 levels. The objectives of this research are: to improve the empirical data base of the effect of CO2 and climate variables on plants and ecosystems, paying particular attention to mechanisms of photosynthetic decline and the physiological controls of whole-plant growth; and to contribute new information to an integrated modeling approach for examining the effects of different CO2 and multiple environmental factors on whole plants and ecosystems data will be provided to the PRECO and SERECO-type models. DOE

46 GEOPHYSICS

Includes aeronomy; upper and lower atmosphere studies; ionospheric and magnetospheric physics; and geomagnetism.

For space radiation see *93 Space Radiation.*

N89-17368*# International Council of Scientific Unions, Urbana, IL. Scientific Committee on Solar-Terrestrial Physics.
MIDDLE ATMOSPHERE PROGRAM: HANDBOOK FOR MAP, VOLUME 26
Belva Edwards, ed. Jun. 1988 79 p Sponsored by NASA, Washington, D.C.
(NASA-CR-183350; NAS 1.26:183350) Avail: SCOSTEP Secretariat, Univ. of Illinois, 1406 W. Green Street, Urbana CSCL 04A

Middle Atmosphere Program activites conducted during 1986

and 1987 were reported by the various committees. Topics addressed include: GLOBUS NOx; the Stratospheric Winter; MAC/SINE; Middle Atmospheric Electrodynamics; New International Equatorial Observatory; SUPERCAMP; MAP/MAC activities; and noctilucent clouds. B.G.

N89-17369*# California Inst. of Tech., Pasadena. Seismological Lab.
STRAIN ACCUMULATION IN THE SANTA BARBARA CHANNEL, 1971-1987
Shawn Larsen, Nancy King, Duncan Agnew (California Univ., La Jolla.), and Bradford Hager [1988] 15 p
(Grant NAG5-842)
(NASA-CR-183402; NAS 1.26:183402) Avail: NTIS HC A03/MF A01 CSCL 08G

Geophysical evidence suggests a significant amount of north-south convergence occurs across the Santa Barbara Channel. Tectonic studies indicate a discrepancy between observed fault slip in California and the North American-Pacific plate motion. Newer plate motion models (NUVEL-1) yield a lower rate of convergence. Global Positioning System (GPS) data collected in the Santa Barbara Channel in 1987, when combined with 1971 trilateration measurements, should be sufficient to resolve the present-day convergence rate. In early 1987. from January 3 to 7, GPS data were collected at 14 sites in California and at 5 additional stations throughout North America. The data can be used to estimate the rate of crustal deformation (convergence) ocurring across the Santa Barbara Channel. The GPS baselines were computed with the Bernese 2nd generation software. A comparison was made between baseline lengths obtained with the Burnese and MIT softwares. Baseline changes from 1971 to January, 1987 (GPS-Bernese) across the Santa Barbara Channel were computed. A uniform strain model was calculated from the baseline changes. The present-day rate of convergence across the Santa Barbara Channel was determined to be 8 to 10 mm/yr. This conclusion is obtained from changes in the baseline length measured with a 1971 trilateration survey and a January, 1987, GPS survey. The rapid convergence rate, in addition to the history of large seismic events, suggests this region is a prime target for future geodetic and geophysical studies. B.G.

N89-17370# Chemical Research and Development Center, Aberdeen Proving Ground, MD.
ELECTRICAL PROPERTIES OF ATMOSPHERIC MOIST AIR: A SYSTEMATIC, EXPERIMENTAL STUDY Technical Report, May 1986 - May 1987
Hugh R. Carlon Sep. 1988 32 p
(AD-A199599; CRDEC-TR-88059) Avail: NTIS HC A03/MF A01 CSCL 07B

Systematic new measurements of the electrical properties of atmospheric moist air in a closed container near sea level are presented. Data were taken using a vapor electrical conductivity cell of new design. The cell consisted of 40 parallel square plates, each 26.5 sq cm and separated by 0.66 cm. The cell insulators were isolated from the cell plates by use of a technique that completely eliminated insulator leakage as a source of experimental error. Thus, very sensitive measurements could be made in still or moving air even at near-saturation humidity. Measurements were made over a wide range of humidities and electric field strengths ranging from near zero to three kV per cm. GRA

N89-17371# Technische Univ., Delft (Netherlands). Dept. of Geodesy.
AN ALGORITHM FOR ANALYSIS OF PLATE MOTIONS IN CRUST DYNAMICS PROJECT (CDP) NETWORKS Thesis
R. vanGein May 1988 71 p
(B8821606; ETN-89-93326) Avail: NTIS HC A04/MF A01

An algorithm is developed to analyze the motion of rigid lithospheric plates. This algorithm is important for the analysis of the satellite laser ranging network in the east Mediterranean region. In a spherical representation, angular velocity vectors of plates are estimated using baseline extension rates derived from a kinematical plate motion model and baseline extension rates derived from satellite laser ranging observations. Both covariance matrices are singular due to a loss of rank. A least squares adjustment is used to obtain the angular velocity vectors. Based on the algorithm a program was developed and applied to a worldwide network. ESA

N89-17372# National Aeronautical Lab., Bangalore (India).
ENERGY EVENTS IN THE ATMOSPHERIC BOUNDARY LAYER
R. Narasimha and Sudarsh V. Kailas (Indian Inst. of Science, Bangalore.) Jan. 1987 36 p Presented at the International Symposium on Perspective in Turbulence Studies
(NAL-TM-DU-8701) Avail: NTIS HC A03/MF A01

Turbulent velocity fluctuations in the atmospheric boundary layer are analyzed using the VITA technique, with a view to understanding the relation of the special events detected by the technique with turbulent bursts at high Reynolds numbers. Utilizing data acquired under conditions of neutral stability at the Boulder Atmospheric Observatory, it is found that the 'energy events' so detected are qualitatively similar in many respects to the turbulent bursts observed at much lower Reynolds numbers in the laboratory, but last longer and occur less frequently, in a manner not inconsistent with outer scaling. It is concluded that high Reynolds number flows reveal bursts tending to scale on outer variables - a conclusion that is considered particularly significant as wall parameters are of the same order in the atmospheric boundary layer as in the laboratory flows that have been widely studied. Author

N89-17373# Geological Survey, Menlo Park, CA.
HIGH-PRECISION GRAVITY NETWORK TO MONITOR TEMPORAL VARIATIONS IN GRAVITY ACROSS YUCCA MOUNTAIN, NEVADA
R. N. Harris and D. A. Ponce 1988 19 p
(Contract DE-AI08-78ET-44802)
(DE89-005023; USGS-OFR-88-243) Avail: NTIS HC A03/MF A01

Repeatable high-precision gravity surveys provide a method of monitoring temporal variations in the gravity field. Fluctuations in the gravity field may indicate water table changes, crustal deformation, or precursors to volcanism and earthquakes. This report describes a high-precision gravity loop which has been established across Yucca Mountain, Nevada in support of the Nevada Nuclear Waste Storage Investigations (NNWSI) program. The purpose of this gravity loop is to monitor temporal variations in gravity across Yucca Mountain in an effort to interpret and predict the stability of the tectonic framework and changes in the subsurface density field. Studies of the tectonic framework which include volcanic hazard seismicity, and faulting studies are in progress. Repeat high-precision gravity surveys are less expensive and can be made more rapidly than a corresponding leveling survey. High-precision gravity surveys are capable of detecting elevation changes of 3 to 5 cm, and thus can be employed as an efficient tool for monitoring vertical crustal movements while supplementing or partially replacing leveling data. The Yucca Mountain gravity network has been tied to absolute gravity measurements established in southern Nevada. These ties provide an absolute datum for comparing repeat occupations of the gravity network, and provide a method of monitoring broad-scale changes in gravity. Absolute gravity measurements were also made at the bottom and top of the Charleston Peak calibration loop in southern Nevada. These absolute gravity measurements provide local control of calibrating gravity meters over the gravity ranges observed at Yucca Mountain. DOE

47 METEOROLOGY AND CLIMATOLOGY

Includes weather forecasting and modification.

N89-17374*# National Aeronautics and Space Administration. Langley Research Center, Hampton, VA.
LIMB-DARKENING FUNCTIONS AS DERIVED FROM ALONG-TRACK OPERATION OF THE ERBE SCANNING RADIOMETER FOR JANUARY 1985
G. Louis Smith, Natividad Manalo, John T. Suttles, and Ira Walker (Planning Research Corp., Hampton, VA.) Washington, DC Mar. 1989 26 p
(NASA-RP-1214; L-16487; NAS 1.61:1214) Avail: NTIS HC A03/MF A01 CSCL 04B

During January 1985, the scanning radiometer aboard the Earth Radiation Budget Satellite was operated to scan along-track. These data have been analyzed to produce limb-darkening functions for Earth emitted radiation, which relate the radiance in any given direction to the radiant exitance. Limb-darkening functions are presented in tabular form and shown as figures for 10 day cases and 12 night cases, corresponding to various scene types and latitude zones. The scene types were computed using measurements within 10 deg of zenith. The limb-darkening functions have values of 1.03 to 1.09 at zenith, with 1.06 being typical. It is found that latitude causes a variation on the order of 1 percent, except for zenith angles greater than 70 deg. These limb-darkening models are about 2 percent higher at zenith than the models derived from Nimbus 7 data. Author

N89-17375# Pacific Northwest Labs., Richland, WA.
APPLICATIONS OF DIGITAL IMAGE PROCESSING TO ONGOING RESEARCH IN COMPLEX TERRAIN METEOROLOGY
J. M. Hubbe, C. D. Whiteman, H. P. Foote, and L. G. McWethy Oct. 1988 7 p Presented at the Digital Image Processing and Visual Communications Technologies in Meteorology Conference, Cambridge, MA, 26 Oct. 1987
(Contract DE-AC06-76RL-01830)
(DE89-001749; PNL-SA-15073; CONF-8710161-2) Avail: NTIS HC A02/MF A01

Digital elevation models and LANDSAT 5 Thematic Mapper (TM) scenes constitute image resolution data over spatial domains of typical interest in complex terrain meteorology. Techniques in use and under development for applying these data to research problems are presented. Topics include decorrelation of topographic shading under direct beam illumination and investigation of nighttime surface temperature. DOE

N89-17376 Texas A&M Univ., College Station.
ON DERIVING THE THREE-DIMENSIONAL KINEMATIC STRUCTURE ON CONVECTIVE STORMS FROM A SINGLE RADAR Ph.D. Thesis
Robert Monroe Cox 1988 158 p
Avail: Univ. Microfilms Order No. DA8815856

The objectives of this investigation were to determine the feasibility of deriving vertical velocity patterns, the magnitudes of those patterns, and the three-dimensional wind field in severe convective storms. A technique called Tracking Radar Echoes by Correlation (TREC), also called the NEXRAD Transverse Wind algorithm, and data from a single radar were used to determine the internal storm motions. The radar Doppler data were collected on 19 June 1980. TREC used correlation analysis to determine motion within and around a given storm. TREC was used to determine the u and v wind components. These components were gridded using a standard objective analysis technique. It has been shown that in weak reflectivity regions, random pattern matching can occur, therefore in areas of reflectivity less that 10 dBZ TREC-derived data were viewed with caution. Important results of this study are: (1) there was good agreement in both areal extent and magnitude between the TREC-derived vertical velocities and the dual-Doppler velocities; (2) for time increments of 5 min or less between radar volume scand, the horizontal wind field derived by TREC agreed with the dual-Doppler wind field during the multicell and transition phases of the storm; (3) the effects of the generator level motions on the TREC derived wind field were evident only in the supercell phase; and (4) vertical cross sections indicated regions of updrafts, and storm-relative inflows. Dissert. Abstr.

N89-17377 Minnesota Univ., Minneapolis.
A NUMERICAL MODELING INVESTIGATION OF THE EFFECT OF CONVECTIVE-MESOSCALE INTERACTIONS ON THE SEA BREEZE CIRCULATION Ph.D. Thesis
Dennis Allan Moon 1988 274 p
Avail: Univ. Microfilms Order No. DA8815812

A numerical investigation was performed concerning the effects of non-precipitating convective clouds on the sea breeze circulation. Sea breeze simulations used the Colorado State University mesoscale model. The procedure for estimating subgrid scale convective transports of mass momentum, heat, and moisture was based on the Raymond-Blyth (1986) stochastic mixing model for non-precipitating cumulus. Fractional cloud coverage in a model grid cell was determined by assigning a convective relaxation time for the decay of available buoyant energy. Sensitivity studies on the effect of convective feedback on the sea breeze circulation used the mesoscale model in its 2D configuration. The land-water configuration was a north-south peninsula with a width of about 230 km. The most notable effect of the cumulus feedback was a general strengthening of the horizontal sea breeze flow perturbations due to pressure gradients associated with the presence of cumulus heat transports over the land cells. The vertical velocities in the sea breeze updrafts were increased due to strengthening of the horizontal flows and increases in their depth. The updraft velocity in the sea breeze front with the aiding large scale wind was especially enhanced. Dissert. Abstr.

N89-17378 Wisconsin Univ., Madison.
KINETIC ENERGY DIAGNOSTIC STUDIES OF EXTRATROPICAL CYCLONES BASED ON STORM RELATIVE MOTION Ph.D. Thesis
Paul Ernest Spaete 1988 300 p
Avail: Univ. Microfilms Order No. DA8813155

The kinetic energy equations for earth and storm relative motions and their radial and tangential components are derived. The equations are used to estimate quasi-Lagrangian kinetic energy budgets of two extratropical cyclones representing different types of development, one with strong latent heat release, the other with little latent heat release. The intensification of the circulation during the evolution of both storms is uniquely identified by the kinetic energy of storm relative motion, while the kinetic energy of earth relative motion fails to make a unique identification. Decomposition of the storm relative kinetic energy budget into tangential and radial components allows the evolution of the storm's cyclonic circulation to be distinguished from kinetic energy advection and mass-momentum adjustment associated with relative influence of the upstream and downstream jets. Composite budgets are constructed from four storms. The results reveal a strong production of radial storm relative kinetic energy by baroclinic processes, a substantial portion of which is transformed to tangential storm relative kinetic energy through inertial processes. Dissert. Abstr.

N89-17379# National Oceanic and Atmospheric Administration, Norman, OK. National Severe Storms Lab.
OBSERVATIONS OF A THUNDERSTORM GENERATED GUST COMPARED WITH SOLITARY WAVE THEORY Final Report
R. J. Doviak and S. Chen Jun. 1988 145 p
(Contract DTFA01-80-Y-10524)
(AD-A200087; DOT/FAA/SA-88/1) Avail: NTIS HC A07/MF A01 CSCL 04B

Observations suggest that solitary and other nonlinear waves might be a source of wind shear hazard to safe flight. A derivation of the Benjamin-Davis-Ono (BDO) equation by a perturbation method is reviewed and extended to the case in which the fluid is in sheared flow. For nonsheared flows, our solution for the upper layer differs markedly from Benjamin's, which doesn't satisfy his specified boundary conditions. The internal steady-state solitary wave, described by the solution of the BDO equation, is compared

with a boundary layer solitary wave observed with NSSL's Doppler radar, and a 444-m-tall instrumented tower. Wave-induced vertical transport of the horizontal momentum of the strongly sheared ambient air contributed much to the observed wind perturbations and horizontal wind shear. It is shown that agreement between the theoretical results of the weakly nonlinear theory of BDO and observations of wind and temperature at the surface is coincidental because wave advection and frictional drag markedly affect wave properties. Only tall tower and Doppler radar measurements above the ground provided the necessary data to determine that the observed solitary wave was strongly nonlinear, and that it trapped thunderstorm outflow, which leaked out the rear of the wave. Wave amplitude data, for above the ground, show fairly good agreement with numerical results from strongly nonlinear theory. GRA

N89-17380# Naval Postgraduate School, Monterey, CA. Dept. of Meteorology.
ONR (OFFICE OF NAVAL RESEARCH) TROPICAL CYCLONE MOTION RESEARCH INITIATIVE: MID-YEAR REVIEW, DISCUSSION AND WORKING GROUP REPORTS Interim Report, Oct. 1987 - Dec. 1988
Russell L. Elsberry Sep. 1988 112 p
(AD-A200286; NPS63-88-005) Avail: NTIS HC A06/MF A01 CSCL 04B

The Office of Naval Research Tropical Cyclone Motion initiative is a five-year program to improve basic understanding of tropical cyclone motion. On 29 June to 1 July 1988, a meeting was held near Brisbane, Australia to: (1) Review recent research activities; (2) Discuss issues and plan future research; (3) Discuss the hypotheses that might be explored in a field experiment in the western North Pacific region during summer 1990; and (4) Form working groups to begin planning for the field experiments. Each of these topics will be briefly discussed to indicate the progress and plans of the initiative. GRA

N89-17381# Army Cold Regions Research and Engineering Lab., Hanover, NH.
NEW ENGLAND MOUNTAIN ICING CLIMATOLOGY
Charles C. Ryerson Aug. 1988 44 p
(AD-A200287; CRREL-88-12) Avail: NTIS HC A03/MF A01 CSCL 04B

Statistics and weather maps are used to compare the atmospheric icing climatology of two New England mountains: Mount Mansfield in northern Vermont and Mount Washington in New Hampshire. Atmospheric icing, as measured with Rosemount ice detectors, is twice as frequent on Mount Washington, with about 12 to 20 times greater intensities and 25 to 50 times more accretion. Periods between icing events average 35 to 45 hours on the two peaks. Most Mount Mansfield icing events are of low intensity. Plots indicate the return probabilities of ice events by length, intensity and accretion magnitude. Approximately half of all severe icing on the two peaks occurs during and immediately after cold front passages. Icing is most intense when lows are about 450 km to the east of the mountains. High-pressure centers are never closer than about 450 km during intense icing. Prolonged accretion periods occur when coastal and inland storms merge or follow closely. GRA

N89-17382 ESDU International Ltd., London (England).
WORLD-WIDE EXTREME WIND SPEEDS. PART 2: EXAMPLES USING VARIOUS METHODS OF ANALYSIS
Dec. 1988 12 p
(ESDU-88037; ISBN-0-85679-669-7; ISSN-0143-2702) Avail: ESDU

This Data Item 88037, an addition to the Sub-series on Wind Engineering, provides two examples of the use of the methods of ESDU 87034 for the analysis of wind speed maxima: using data for a single dominant storm mechanism and using data where there are two dominant mechanisms. In the first example, the quantity of data to be considered is reduced by taking only those wind speeds above a certain threshold, and the procedure for calculating confidence limits on the variation of estimated extreme wind speed with mean recurrence interval is illustrated. For the other example, a Monte Carlo method is used to determine confidence intervals on the estimate of extreme wind speed by generating a sequence of simulated annual extreme storms having the required characteristics. The errors in estimated extreme wind speed if the wind speed maxima from the two mechanisms are not analysed separately are also shown. A third example is included, showing the inverse use of the method of ESDU 88038 by which the parameters of the Fisher Tippett Type 1 extreme value distribution are deduced from the Weibull parameters of the parent cumulative distribution (in this case a two-year continuous wind speed record). This approach is particularly useful where complex topographic effects on wind speed at a site cannot be determined so that extreme wind speed cannot be predicted using a design wind speed map. ESDU

N89-17383 ESDU International Ltd., London (England).
ESTIMATION OF HOURS PER YEAR WHEN MEAN WIND SPEED EXCEEDS SPECIFIED THRESHOLDS
Dec. 1988 17 p
(ESDU-88038; ISBN-0-85679-670-0; ISSN-0143-2702) Avail: ESDU

This Data Item 88038, an addition to the Sub-series on Wind Engineering, provides an estimation method for use when meteorological records are inadequate to provide the data directly, or when they are not readily corrected for differences between the terrain at the site and the measuring station, or when a rapid estimate of wind speed frequency of occurrence is required. It uses a theoretical approach, with some empirical factors, to relate the parameters of the Fisher-Tippett Type 1 extreme value distribution to the parameters of the parent Weibull cumulative distribution from which the number of hours when the mean wind speed exceeds specified thresholds can be calculated. In practice, the extreme value mode and dispersion parameters (or estimates) are more readily available for various regions of the world than the parent distribution data. The method may be used inversely, as illustrated in ESDU 87037, to estimate extreme wind speeds from relatively short records of the parent distribution. It applies to winds from any sector and to the case when all wind directions are combined. A method is also provided to estimate the proportion of hours in a year when the wind direction is from a particular 30 degree sector. Guidance is given on correction factors for changes from the conditions of the basic data in terrain roughness, height and simple topography. The method has been tested against data from 50 UK sites and is considered applicable to wind climates in middle to high latitudes. It has been tentatively extended to apply to a wind climate contributed by more than one mechanism (for example, frontal depressions and thunderstorms). ESDU

N89-17384*# Kansas State Univ., Manhattan. Evapotranspiration Lab.
MEASUREMENTS OF MICROMETEOROLOGICAL PARAMETERS FOR TESTING LARGE SCALE MODELS Annual Report
E. T. Kanemasu, Tanvir Demetriades-Shah, David Watts, Dalin Nie, Larry Ballou, and Galen Harbers Mar. 1989 84 p
(Grant NAG5-389)
(NASA-CR-184766; NAS 1.26:184766) Avail: NTIS HC A05/MF A01 CSCL 04B

This annual report discusses work accomplished on the FIFE (First International Satellite Land-Surface Climatology) Project. It contains manuscripts and reports during the past year of Grant NAG 5-389. Of its six chapters, three treat soil heat flux, and two deal with information about the FIFE sites. The first chapter on net radiation and the fourth chapter are to be presented at the Agricultural and Forest Meteorology Conference to be held in March 1989 in Charleston, South Carolina. Author

N89-17385*# Iowa State Univ. of Science and Technology, Ames. Dept. of Physics.
LOW FREQUENCY OSCILLATIONS IN TOTAL OZONE MEASUREMENTS
X. H. Gao and J. L. Stanford 1989 16 p

(Grant NAG5-1060)
(NASA-CR-184759; NAS 1.26:184759) Avail: NTIS HC A03/MF A01 CSCL 04B

Low frequency oscillations with periods of approximately one to two months are found in eight years of global grids of total ozone data from the Total Ozone Mapping Spectrometer (TOMS) satellite instrument. The low frequency oscillations corroborate earlier analyses based on four years of data. In addition, both annual and seasonal one-point correlation maps based on the 8-year TOMS data are presented. The results clearly show a standing dipole in ozone perturbations, oscillating with 35 to 50 day periods over the equatorial Indian Ocean-west Pacific region. This contrasts with the eastward moving dipole reported in other data sets. The standing ozone dipole appears to be a dynamical feature associated with vertical atmospheric motions. Consistent with prior analyses based on lower stratospheric temperature fields, large-scale standing patterns are also found in the extratropics of both hemispheres, correlated with ozone fluctuations over the equatorial west Pacific. In the Northern Hemisphere, a standing pattern is observed extending from the tropical Indian Ocean to the north Pacific, across North America, and down to the equatorial Atlantic Ocean region. This feature is most pronounced in the NH summer. Author

N89-17386*# Purdue Univ., West Lafayette, IN. Dept. of Earth and Atmospheric Sciences.
STUDY OF THE EFFECT OF CLOUD INHOMOGENEITY ON THE EARTH RADIATION BUDGET EXPERIMENT Final Report, 1 Jul. 1987 - 31 Aug. 1988
Phillip J. Smith Aug. 1988 112 p
(Grant NAG5-101)
(NASA-CR-182962; NAS 1.26:182962) Avail: NTIS HC A06/MF A01 CSCL 04B

The Earth Radiation Budget Experiment (ERBE) is the most recent and probably the most intensive mission designed to gather precise measurements of the Earth's radiation components. The data obtained from ERBE is of great importance for future climatological studies. A statistical study reveals that the ERBE scanner data are highly correlated and that instantaneous measurements corresponding to neighboring pixels contain almost the same information. Analyzing only a fraction of the data set when sampling is suggested and applications of this strategy are given in the calculation of the albedo of the Earth and of the cloud-forcing over ocean. Author

48 OCEANOGRAPHY

Includes biological, dynamic, and physical oceanography; and marine resources.

For related information see also *43 Earth Resources and Remote Sensing.*

N89-17387# Rhode Island Univ., Narragansett. Graduate School of Oceanography.
OBJECTIVE ANALYSIS OF THE GULF STREAM THERMAL FRONT: METHODS AND ACCURACY
Karen L. Tracey, Amy I. Friedlander, and Randolph Watts Dec. 1987 112 p
(Contract N00014-81-C-0062; NSF OCE-85-17746)
(AD-A199717; GSO-TR-87-2) Avail: NTIS HC A06/MF A01 CSCL 08C

The objective analysis (OA) technique was adapted by Watts and Tracey in order to map the thermal frontal zone of the Gulf Stream. Here, we test the robustness of the adapted OA technique to the selection of four control parameters: mean field, standard deviation field, correlation function, and decimation time. Output OA maps of the thermocline depth are most affected by the choice of mean field, with the most realistic results produced using a time-averaged mean. The choice of the space-time correlation function has a large influence on the size of the estimated error fields, which are associated with the OA maps. The smallest errors occur using the analytic function which is based on 4 years of inverted echo sounder data collected in the same region of the Gulf Stream. Variations in the selection of the standard deviation field and decimation time have little effect on the output OA maps. We determine the accuracy of the output OA maps by comparing them with independent measurements of the thermal field. Two cases are evaluated: standard maps and high temporal resolution maps, with decimation times of 2 days and 1 day, respectively. Standard deviations (STD) between the standard maps at the 15 percent estimated error level and the XBTs (AXBTs) are determined to be 47 to 53 m. Comparisons of the high temporal resolution maps at the 20 percent error level with the XBTs (AXBTs) give STD differences of 47 m. GRA

N89-17388# Army Cold Regions Research and Engineering Lab., Hanover, NH.
PROFILE PROPERTIES OF UNDEFORMED FIRST-YEAR SEA ICE
Gordon F. Cox and Wilford F. Weeks Sep. 1988 64 p
(AD-A200172; CRREL-88-13) Avail: NTIS HC A04/MF A01 CSCL 08L

In many sea ice engineering problems the ice sheet is assumed to be a homogeneous plate whose mechanical properties are estimated from the bulk salinity and average temperature of the ice sheet. Typically no regard has been given to the vertical variation of ice properties in the ice sheet or to time of ice formation. This paper reviews some of the mechanical properties of sea ice, including ice tensile, flexural and shear strengths, as well as the ice modulus. Equations for these properties are given as functions of the ice brine volume, which can be determined from ice salinity and temperature. A numerical, finite difference model is developed to predict salinity and temperature profiles of a growing ice sheet. In this model ice temperatures are calculated by performing an energy balance of the heat fluxes at the ice surface. The conductive heat flux obtained from the energy balance is then used to calculate the rate of ice growth and ice thickness by applying the Stefan ice growth equation. Ice salinities are determined by considering the amount of initial salt entrapment at the ice/water interface and the subsequent brine drainage due to brine expulsion and gravity drainage. Ice salinity and temperature profiles are then generated using climatological data for the Central Arctic Basin. The profiles appear to be realistic and agree reasonably well with field data. GRA

51 LIFE SCIENCES (GENERAL)

N89-17389# Chemical Research and Development Center, Aberdeen Proving Ground, MD.
USING THEORETICAL DESCRIPTORS IN STRUCTURAL ACTIVITY RELATIONSHIPS. PART 2: POLARIZABILITY INDEX Technical Report, Feb. - Jun. 1987
George R. Famini Sep. 1988 49 p
(AD-A199594; CRDEC-TR-88137) Avail: NTIS HC A03/MF A01 CSCL 07C

Quantitative structure activity relationships (QSAR) have been used successfully in the past to develop predictive equations for numerous biological and physicochemical properties. Kamlet and Taft used linear solvation energy relationships (LSER), a subset of QSAR, to correlate over 100 solute/solvent dependent interactions with a set of empirically derived descriptors. A major difficulty with this approach has been the use of these empirically determined parameters. A new approach based upon the generalized LSER approach has been developed. This technique, called Theoretical LSER, uses only structural and quantum chemically derived descriptors. The introduction of a new electronic term based upon polarizability will be described. GRA

N89-17390*# National Aeronautics and Space Administration. Ames Research Center, Moffett Field, CA.
PROCEEDINGS OF A WORKSHOP ON LIGHTING REQUIREMENTS IN MICROGRAVITY: RODENTS AND NONHUMAN PRIMATES
Daniel C. Holley, ed. (San Jose State Univ., CA.), Charles M. Winget, ed., and Henry A. Leon, ed. Dec. 1988 273 p Workshop held in San Jose, CA, 16-17 Jul. 1987
(NASA-TM-101077; A-88278; NAS 1.15:101077) Avail: NTIS HC A12/MF A01 CSCL 06P

A workshop, sponsored by Ames Research Center, was held at San Jose State University, San Jose, California, July 16-17, 1987, to discuss and correlate observations and theories relating to lighting requirements in animal habitats for rodents and nonhuman primates in microgravity (near space). This volume represents the results of the workshop. It contains a summary of the conclusions reached and recommendations for lighting animal housing modules used in microgravity related projects. The recommendations cover various aspects of habitat lighting including engineering standards for intensity, spectral properties, and light cycle controls. Author

N89-17036# National Research Council of Canada, Ottawa (Ontario).
THE USE OF SOUNDING ROCKETS IN THE STUDY OF MICROGRAVITY CELL BIOLOGY
Alan J. Mortimer *In its* Workshop on Microgravity Experimentation in Aircraft and Rockets 1988 p 95-97 (For primary document see N89-17019 09-29)
Avail: NTIS HC A07/MF A01; also available from Publication Sales and Distribution, National Research Council of Canada, Ottawa, ON, Canada K1A OR6

52 AEROSPACE MEDICINE

Includes physiological factors; biological effects of radiation; and effects of weightlessness on man and animals.

N89-17391*# National Aeronautics and Space Administration. Lyndon B. Johnson Space Center, Houston, TX.
BODY DISPLACEMENT MEASURED DURING SUSTAINED +Gz, -Gz AND + OR -Gy ACCELERATION USING A STEREOSCOPIC PHOTOGRAPHIC SYSTEM Final Report, Jun. - May 1983
John W. Frazier, Joe W. McDaniel, Vance D. Skowronski, Nilss M. Aume (Aerospace Medical Research Labs., Wright-Patterson AFB, OH.), and Donald F. Stewart Mar. 1988 18 p
(NASA-TM-101269; NAS 1.15:101269; AD-A197988; AAMRL-TR-88-015) Avail: NTIS HC A03/MF A01 CSCL 06S

Pilot performance may be adversely affected by G induced body displacement. Controls may be difficult to reach and activate. The use of a head up display may be rendered ineffective by excessive head movement. Also, measurement of body displacement can be useful in evaluating restraint systems. A technique has been devised to quantify body displacement during acceleration studies conducted on the Dynamic Environment Simulator (DES), a three axis centrifuge. A stereoscopic photographic system consisting of two motorized 35 mm SLR cameras, a microprocessor controller, and displays were used. Reference marks defining the DES can in 3 dimensions (3-D) and targets on the subject are recorded photographically. The film strips were then processed on an x-y plotter to digitize the target information. From these data, calculations were performed to compute the 3-D coordinates of the points of interest. Data collected when using the stereoscopic photographic systems are presented on eye and shoulder displacements during various acceleration and restraint conditions. Eye displacements of 3.95 cm at +4.0 Gz, 4.79 cm at -1.0 Gz, and 10.16 cm at 2 Gy are reported. Improving the restraint system by adding lateral shoulder supports reduced the eye displacement at 2 Gy to 3.96 cm (61 percent). The average lateral restraining force exerted on the shoulder pads at 2 Gy was 55.8 Kg (123 lbs). GRA

N89-17392*# Grumman Aerospace Corp., Bethpage, NY. Space Systems.
EXTRAVEHICULAR ACTIVITIES LIMITATIONS STUDY. VOLUME 1: PHYSIOLOGICAL LIMITATIONS TO EXTRAVEHICULAR ACTIVITY IN SPACE Final Report
Paul A. Furr, Conrad B. Monson, Robert L. Santoro, William J. Sears, Donald H. Peterson, and Malcolm Smith (ILC Space Systems, Dover, DE.) 1988 269 p
(Contract NAS9-17702)
(NASA-CR-172098; NAS 1.26:172098; AS-EVALS-FR-8701-Vol-1) Avail: NTIS HC A12/MF A01 CSCL 06S

This report contains the results of a comprehensive literature search on physiological aspects of EVA. Specifically, the topics covered are: (1) Oxygen levels; (2) Optimum EVA work; (3) Food and Water; (4) Carbon dioxide levels; (5) Repetitive decompressions; (6) Thermal, and (7) Urine collection. The literature was assessed on each of these topics, followed by statements on conclusions and recommended future research needs. Author

N89-17393*# Grumman Aerospace Corp., Bethpage, NY. Space Systems.
EXTRAVEHICULAR ACTIVITIES LIMITATIONS STUDY. VOLUME 2: ESTABLISHMENT OF PHYSIOLOGICAL AND PERFORMANCE CRITERIA FOR EVA GLOVES Final Report
John M. OHara, Michael Briganti, John Cleland, and Dan Winfield (Research Triangle Inst., Research Triangle Park, NC.) 1988 175 p
(Contract NAS9-17702)
(NASA-CR-172099; NAS 1.26:172099; AS-EVALS-FR-8701-Vol-2) Avail: NTIS HC A08/MF A01 CSCL 06S

One of the major probelms faced in Extravehicular Activity (EVA) glove development has been the absence of concise and reliable methods to measure the effects of EVA gloves on human hand capabilities. This report describes the development of a standardized set of tests designed to assess EVA-gloved hand capabilities in six measurement domains: Range of Motion, Strength, Tactile Perception, Dexterity, Fatigue, and Comfort. Based on an assessment of general human hand functioning and EVA task requirements several tests within each measurement domain were developed to provide a comprehensive evaluation. All tests were designed to be conducted in a glove box with the bare hand as a baseline and the EVA glove at operating pressure. A test program was conducted to evaluate the tests using a representative EVA glove. Eleven test subjects participated in a repeated-measures design. The report presents the results of the tests in each capability domain. Author

N89-17394# SRI International Corp., Menlo Park, CA.
ROLE OF RETINOCORTICAL PROCESSING IN SPATIAL VISION Annual Report No. 1, 1 May 1987 - 1 May 1988
Donald H. Kelly Jun. 1988 21 p
(Contract F49620-87-K-0009)
(AD-A200198; AFOSR-88-0806TR) Avail: NTIS HC A03/MF A01 CSCL 06D

Several important image-processing functions have been proposed for the geometric distortion known as cortical (or more precisely, retinocortical) magnification. This spatial distortion can convert the radial velocities projected on the retina by egocentric motion into uniform, rectilinear motion at the cortex. It can also convert changes of size and orientation in retinal coordinates into mere translation at the cortex. In both cases, an image-like property is converted into a map-like property. Thus cortical magnification must play an essential role in forming our stable precepts of the world around us, even as it vexes the question of how the information from different fixations within the same scene can be arranged into a single precept. The cortical image subsequently undistorted, just to facilitate the superposition of multiple fixations is questioned. An understanding of the image-coding functions of the primary visual cortex (V1) should help to unravel this paradox. Using the tools of computer vision (LISP algorithms developed on Symbolics networks), we are attempting to build a working model that includes such processes as: faxational eye movements, retinal

filtering and inhomogeneity, retinocortical mapping, cortical (Gabor) image-coding, and other processes involved in the coordinate shifts needed for mapping purposes. GRA

N89-17395# Medical Coll. of Virginia, Richmond. Dept. of Neurology.
THE EFFECTS OF HYDRAZINES ON NEURONAL EXCITABILITY Annual Report, 1 May 1987 - 31 May 1988
Robert J. DeLorenzo 10 Jun. 1988 17 p
(Grant AF-AFOSR-0235-87; AF Proj. 2312)
(AD-A200199; AFOSR-88-0929TR) Avail: NTIS HC A03/MF A01 CSCL 07B

Hydrazines are toxic compounds with military and industrial applications including use as missile propellants for aircraft (i.e., the F-16 and space vehicles). Recurrent exposure from routine storage, use, and disposal hydrazines makes their toxic effects on the nervous system important. Exposure to hydrazine can result in status epilepticus and eventual respiratory collapse. Acute exposure can produce repeated tonic-clonic seizures in both animal and man. This project has continued to direct its effort in understanding the molecular mechanism by which hydrazines may produce their neuronal excitatory effects. Our investigation focuses on the effects of hydrazine on electrophysiological properties of identified neurons in the invertebrate Hermissenda Crassicornis. We have documented that hydrazines increase neuronal excitability in the LP-1 neuron of this nudibranch mollusc. Hydrazines also increase the rate of sustained repetitive firing in this system. We will study molecular mechanism mediating the effects of hydrazine on increased neuronal firing in isolated neurons. Specific anticonvulsant drugs may have potential benefit in blocking the excitable effects of hydrazine on neuronal activity. GRA

N89-17396# Harvard Medical School, Boston, MA. Dept. of Physiology and Biophysics.
PHARMACOLOGICAL RESETTING OF THE CIRCADIAN SLEEP-WAKE CYCLE Final Report, 1 May 1986 - 30 Apr. 1988
M. C. Moore-Ede 30 Jun. 1988 9 p
(Grant AF-AFOSR-0187-86; AF Proj. 2312)
(AD-A200246; AFOSR-88-1045TR) Avail: NTIS HC A02/MF A01 CSCL 06D

Our research has seen the completion of several projects aimed at elucidating the chronopharmacological properties of benzodiazepines in rodents and monkeys, and at investigating the circadian and homeostatic mechanisms involved in the regulation of sleep in monkeys. We have also recently completed a series of studies on the neural control of circadian rhythms in the squirrel monkey. The results obtained thus far have several interesting implications, some of which are currently being tested. GRA

N89-17397# Army Aeromedical Research Lab., Fort Rucker, AL.
CONTRAST SENSITIVITY IN ARMY AVIATOR CANDIDATES: CYCLOPLEGIA EFFECTS AND POPULATION NORMS Final Report
Isaac Behar, William G. Bachman, and Walter Egenmaier Sep. 1988 29 p
(AD-A200433; USAARL-88-16) Avail: NTIS HC A03/MF A01 CSCL 06E

This study was designed to provide information regarding three aspects of contrast sensitivity testing aviator candidates: (1) To determine whether contrast sensitivity functions (CSFs) obtained with the VISTECH Visual Contrast Test System (VCTs) are affected by ocular cycloplegia; (2) Since Army aviator candidates differ from the general population by being more highly selected with respect to visual and refractive status, more homogenous in age and in an age bracket when vision is optimal, a second purpose was to obtain a large normative sample of CSFs for establishing future contrast sensitivity standards for this population; and (3) To determine whether the VCTS provides useful CSFs under clinical screening conditions in a timely and simple manner. Contrast sensitivity thresholds were obtained at 5 spatial frequencies from 106 aviator candidates, prior to and following the administration of a cycloplegic. Contrast sensitivity functions obtained under cycloplegia were reduced about 20 percent. The CSFs of the aviator candidates are much superior than the general population norms. The VCTS provides useful CSFs under military screening conditions. GRA

N89-17398# Centre de Recherches du Service de Sante des Armees, Clamart (France).
MULTIPARAMETRIC RESEARCH OF EARLY INDICATORS OF VASCULAR RISK IN FLYING PERSONNEL [RECHERCHE MULTIPARAMETRIQUE DE MARQUERS PRECOCES DE RISQUE VASCULAIRE CHEZ LE PERSONNEL NAVIGANT]
14 Sep. 1988 98 p In FRENCH
(Contract DRET-85-1051)
(ETN-89-93613) Avail: NTIS HC A05/MF A01

A multivariate analysis was carried out covering biochemical, hematological, hemoreological, and biophysical factors to identify a set of risk factors with a high joint probability to help in the selection of flying personnel. The population tested consisted of 184 men from 40 to 55 years old, all flying personnel free of clinical infections. Significant correlations at the 5 percent level are found. ESA

N89-17399# Advisory Group for Aerospace Research and Development, Neuilly-Sur-Seine (France). Panel de Medecine Aerospatiale de IAGARD.
SLEEP AND WAKEFULNESS: HANDBOOK FOR FLIGHT MEDICAL OFFICERS, 2ND EDITION
A. N. Nicholson and Barbara M. Stone (Royal Aircraft Establishment, Farnborough, England) 1987 92 p
(AGARD-AG-270(F)) Avail: NTIS HC A05/MF A01

The first edition of this handbook was published in 1982, and since then the understanding of sleep and wakefulness has advanced considerably. This new handbook emphasizes the mangagement of aircrew and the problems they experience in coping with irregularity of rest and activity. Author

N89-17034# Manitoba Univ., Winnipeg.
THE EFFECTS OF MICROGRAVITY AND LINEAR ACCELERATIONS ON CUTANEOMUSCULAR REFLEXES IN HUMAN LOWER LIMB MUSCULATURE
T. Szturm, R. M. Jell, D. Kriellaars, D. J. Ireland, and S. Lafortune *In* National Research Council of Canada, Workshop on Microgravity Experimentation in Aircraft and Rockets 1988 p 87-91 (For primary document see N89-17019 09-29)
Avail: NTIS HC A07/MF A01; also available from Publication Sales and Distribution, National Research Council of Canada, Ottawa, ON, Canada K1A OR6

N89-17035# National Research Council of Canada, Ottawa (Ontario).
OCULAR TORSION IN THE WEIGHTLESSNESS OF PARABOLIC FLIGHT Abstract Only
K. E. Money, N. M. Kirienko, W. H. Johnson, D. G. D. Watt, C. H. Markham, and S. G. Diamond (California Univ., Los Angeles.) *In its* Workshop on Microgravity Experimentation in Aircraft and Rockets 1988 p 93 (For primary document see N89-17019 09-29)
Avail: NTIS HC A07/MF A01; also available from Publication Sales and Distribution, National Research Council of Canada, Ottawa, ON, Canada K1A OR6

N89-17044# National Research Council of Canada, Ottawa (Ontario).
DEVELOPMENT OF A PORTABLE PHYSIOLOGICAL MONITORING SYSTEM FOR THE KC-135: THE S.F.U. BIOPACK Abstract Only
I. B. Mekjavic, M. Frank, P. J. Sullivan, B. Trygvasson, R. Thirsk, and R. Hesselgrave (Defence and Civil Inst. of Environmental Medicine, Downsview, Ontario) *In its* Workshop on Microgravity Experimentation in Aircraft and Rockets 1988 p 135 (For primary document see N89-17019 09-29)
Avail: NTIS HC A07/MF A01; also available from Publication

Sales and Distribution, National Research Council of Canada, Ottawa, ON, Canada K1A OR6

53 BEHAVIORAL SCIENCES

Includes psychological factors; individual and group behavior; crew training and evaluation; and psychiatric research.

N89-17400# California Univ., Irvine. Dept. of Information and Computer Science.
MODELS OF INCREMENTAL CONCEPT FORMATION Interim Report, Jul. 1987 - Jun. 1988
John Gennari, Pat Langley, and Douglas Fisher Aug. 1988 58 p
(Contract MDA903-85-C-0324)
(AD-A199617; TR-3; ARI-RN-88-79) Avail: NTIS HC A04/MF A01 CSCL 12I

Given a set of observations, humans acquire concepts which organize the observations, and use them to classify future experience. This type of concept formation can occur in the absence of a tutor, and it can take place despite irrelevant and incomplete information. A reasonable model of such concept learning should both be incremental and capable of handling the type of complex experiences that people encounter in the real world. This paper reviews three previous models in incremental concept formation, and then presents Classit, a model that extends the earlier systems. All of the models integrate the process of recognition and learning, and all can be viewed as carrying out searches through the space of possible concept hierarchies. We also present some empirical studies of its behavior under a variety of conditions, in an attempt to show that Classit is a robust concept formation system. GRA

N89-17401# Virginia Polytechnic Inst. and State Univ., Blacksburg. Displays and Controls Lab.
THE ROLE OF SHORT-TERM MEMORY IN OPERATOR WORKLOAD Final Report, Jan. 1987 - Apr. 1988
William F. Reinhart, Carita D. Glynn, Craig Dye, Mark Takahama, and Harry L. Snyder Apr. 1988 180 p Prepared for Southeastern Center for Electrical Engineering Education, Inc., St. Cloud, FL
(Contract F33615-85-D-0514)
(AD-A200252; AAMRL-TR-88-024) Avail: NTIS HC A09/MF A01 CSCL 05H

The role of flight crew number in the advanced conceptual bomber is likely to call for rapid management of complex information. The elevated workload associated with these new informational tasks may be alleviated in part by the reduction of short term memory demands. Literature reviews were conducted to described the concepts of short term memory and workload. An experiment was conducted to describe the contribution of short term memory demands to operator workload. The Sternberg scanning model was used in a secondary task paradigm with various performance and subjective measures recorded. Sternberg choice reaction time and subjective ratings of workload increased as a function of visual memory set size. It was concluded that short term memory may significantly contribute to operator workload. Therefore, strategies for the reduction of short term memory demands in crew station information display design should be investigated. GRA

54 MAN/SYSTEM TECHNOLOGY AND LIFE SUPPORT

Includes human engineering; biotechnology; and space suits and protective clothing.

For related information see also *16 Space Transportation.*

N89-17402# Army Aeromedical Research Lab., Fort Rucker, AL.
A COMPARISON OF TWO WHOLE-BODY VIBRATION STANDARDS AS APPLIED TO ROTARY-WING AIRCRAFT: ISO (INTERNATIONAL STANDARDS ORGANIZATION) 2631 VS ADS (AERONAUTICAL DESIGN STANDARDS) 27 Final Report
Dennis L. Breen and Barclay P. Butler Jul. 1988 35 p
(AD-A200430; USAARL-88-11) Avail: NTIS HC A03/MF A01 CSCL 14B

Two whole-body vibration (WBV) standards, International Standards Organization (ISO) 2631 and Aeronautical Design Standard 27 (ADS-27), were compared using vibration signatures from the UH-1 and UH-60 helicopters ISO 2631 is a widely used WBV standard which accounts for variables such as intensity, duration of exposure, frequency range, and vibration in all three orthogonal directions. ADS-27 is a newer standard developed at the U.S. Army Aviation Systems Command (AVSCOM) for measuring WBV producted by rotary-winged aircraft. An analysis of the two vibration signature types shows when vibration levels are measured on a pass/fail performance criteria, the ADS-27 becomes the more stringent standard; however, ADS-27 fails to answer the important health hazard questions that ISO 2631 attempts. ISO 2631 vibration acquisition techniques were found to be more scientifically sound than those proposed by the ADS-27. The use of both standards may prove to be a more complete method of helicopter WBV assessment. GRA

N89-17403*# Universities Space Research Association, Houston, TX. Dept. of Mechanical Engineering and Aerospace Sciences.
THE SPACE STATION INTEGRATED REFUSE MANAGEMENT SYSTEM
Loren A. Anderson May 1988 280 p
(Grants NGT-21-002-080; NGT-80001)
(NASA-CR-184722; NAS 1.26:184722) Avail: NTIS HC A13/MF A01 CSCL 06K

The design and development of an Integrated Refuse Management System for the proposed International Space Station was performed. The primary goal was to make use of any existing potential energy or material properties that refuse may possess. The secondary goal was based on the complete removal or disposal of those products that could not, in any way, benefit astronauts' needs aboard the Space Station. The design of a continuous living and experimental habitat in space has spawned the need for a highly efficient and effective refuse management system capable of managing nearly forty-thousand pounds of refuse annually. To satisfy this need, the following four integrable systems were researched and developed: collection and transfer; recycle and reuse; advance disposal; and propulsion assist in disposal. The design of a Space Station subsystem capable of collecting and transporting refuse from its generation site to its disposal and/or recycling site was accomplished. Several methods of recycling or reusing refuse in the space environment were researched. The optimal solution was determined to be the method of pyrolysis. The objective of removing refuse from the Space Station environment, subsequent to recycling, was fulfilled with the design of a jettison vehicle. A number of jettison vehicle launch scenarios were analyzed. Selection of a proper disposal site and the development of a system to propel the vehicle to that site were completed. Reentry into the earth atmosphere for the purpose of refuse incineration was determined to be the most attractive solution. Author

N89-17404*# Texas A&M Univ., College Station. The Regenerative Concepts Team.
REGENERATIVE LIFE SUPPORT SYSTEM RESEARCH AND CONCEPTS Progress Report, Apr. - Dec. 1988
Dec. 1988 234 p
(Grant NAG9-253)
(NASA-CR-184760; NAS 1.26:184760; SRC-5-5873-3) Avail: NTIS HC A11/MF A01 CSCL 06K

Life support systems that involve recycling of atmospheres, water, food and waste are so complex that models incorporating all the interactions and relationships are vital to design, development, simulations, and ultimately to control of space qualified systems. During early modeling studies, FORTRAN and BASIC programs were used to obtain numerical comparisons of the performance of different regenerative concepts. Recently, models were made by combining existing capabilities with expert systems to establish an Intelligent Design Support Environment for simplifying user interfaces and to address the need for the engineering aspects. Progress was also made toward modeling and evaluating the operational aspects of closed loop life support systems using Time-step and Dynamic simulations over a period of time. Example models are presented which show the status and potential of developed modeling techniques. For instance, closed loop systems involving algae systeMs for atmospheric purification and food supply augmentation, plus models employing high plants and solid waste electrolysis are described and results of initial evaluations are presented. Author

55 SPACE BIOLOGY

Includes exobiology; planetary biology; and extraterrestrial life.

No abstracts in this category.

59 MATHEMATICAL AND COMPUTER SCIENCES (GENERAL)

No abstracts in this category.

60 COMPUTER OPERATIONS AND HARDWARE

Includes hardware for computer graphics, firmware, and data processing.

For components see *33 Electronics and Electrical Engineering.*

N89-17405# . Stanford Linear Accelerator Center, CA.
IEEE P1596, A SCALABLE COHERENT INTERFACE FOR GIGABYTE/SEC MULTIPROCESSOR APPLICATIONS
D. B. Gustavson Nov. 1988 4 p Presented at the IEEE Nuclear Science Symposium, Orlando, FL, 9 Nov. 1988
(Contract DE-AC03-76SF-00515)
(DE89-002813; SU-SLAC-PUB-4781; CONF-881103-9) Avail: NTIS HC A02/MF A01

IEEE P1596, the Scalable Coherent Interface (formerly known as SuperBus) is based on experience gained during the development of Fastbus (IEEE 960), Futurebus (IEEE 896.1) and other modern 32-bit buses. SCI goals include a minimum bandwidth of 1 GByte/sec per processor; efficient support of a coherent distributed-cache image of shared memory; and support for segmentation, bus repeaters and general switched interconnections like Banyan, Omega, or full crossbar networks. To achieve these ambitious goals, SCI must sacrifice the immediate handshake characteristic of the present generation of buses in favor of a packet-like split-cycle protocol. Wire-ORs, broadcasts, and even ordinary passive bus structures are to be avoided. However, a lower performance (1 GByte/sec per backplane instead of per processor) implementation using a register insertion ring architecture on a passive backplane appears to be possible using the same interface as for the more costly switch networks. This paper presents a summary of current directions, and reports the status of the work in progress. DOE

N89-17406# Argonne National Lab., IL. Mathematics and Computer Science Div.
VECTORIZING COMPILERS: A TEST SUITE AND RESULTS
David Callahan, Jack Dongarra, and David Levine Nov. 1988 38 p
(Contract W-31-109-eng-38)
(DE89-005376; ANL-88-46) Avail: NTIS HC A03

The report describes a collection of 100 FORTRAN loops used to test the effectiveness of an automatic vectorizing compiler. We present the results of compiling these loops using commercially available, vectorizing FORTRAN compilers on a variety of supercomputers, minisupercomputers, and mainframes. DOE

N89-17407# Oak Ridge National Lab., TN. Engineering Physics and Mathematics Div.
PERFORMANCE OF A SECOND GENERATION HYPERCUBE
T. H. Dunigan Nov. 1988 22 p
(Contract DE-AC05-84OR-21400)
(DE89-005674; ORNL/TM-10881) Avail: NTIS HC A03/MF A01

The performance of four commercially available hypercube parallel processors is analyzed. Computation and communication performance for a number of low-level benchmarks are presented for the Ametek S14 hypercube, the Intel iPSC/1 hypercube, the Ncube hypercube, and the second generation Intel iPSC/2 hypercube. DOE

61 COMPUTER PROGRAMMING AND SOFTWARE

Includes computer programs, routines, alogorithms, and specific applications, e.g., CAD/CAM.

N89-17408# Army Concepts Analysis Agency, Bethesda, MD.
AN ALGORITHM FOR CALCULATING THE AREA OF OVERLAP OF AN ELLIPSE AND A CONVEX POLYGON Research Paper, Oct. - Nov. 1987
Robert L. Helmbold Nov. 1987 62 p
(AD-A199654; CAA-RP-87-4) Avail: NTIS HC A04/MF A01 CSCL 12D

This paper describes a new and improved algorithm for estimating in computer simulations the area of overlap of an ellipse and a convex polygon. The need for such algorithms arises frequently in military operations analysis, in particular in estimating the portion of a rectangular target overlapped by a disk-shaped nuclear coverage area. A detailed description of the algorithm and illustrations of its application are included. GRA

N89-17409# Tokyo Univ. (Japan). Inst. of Industrial Science.
RESEARCH ON AUTOMATIC EXTRACTION OF MAP INFORMATION AND ITS IMAGE REPRESENTATION
Satoshi Yanagida and Shunji Murai 29 Feb. 1988 46 p In JAPANESE
(DE88-754960; UTIIS-8801) Avail: NTIS (US Sales Only) HC A03/MF A01

Various softwares were developed to input or store map information in computers and to output printing films efficientlly. The automatic input system allowing to input closed area graphic

data with attribute information by the input of boundary charts with color symbols or painted charts using a drum scanner was developed; a system for extracting and vectorizing building profiles from city planning maps was developed. As for storage, the improved run length format achieving easily an efficient data compression ratio, rapid retrieval, data registration or data transfer to a raster type output device was developed. The output system generating digital dot patterns to output printing films by a laser printer was developed, thereby eliminating a vast amount of manual operation, These systems are capable of practical uses without any enhancements. DOE

N89-17410# Naval Postgraduate School, Monterey, CA.
THE SUITABILITY OF AN OBJECT-ORIENTED LANGUAGE FOR PROTOTYPING AND ABSTRACT DATA TYPES M.S. Thesis
Michael O. Rowell Jun. 1988 136 p
(AD-A200417) Avail: NTIS HC A07/MF A01 CSCL 12E

ACTOR, an object-oriented follow-on language to Smalltalk, is used in an implementation of a prototype video store management package and in the implementation of a tree abstract data type package. This high level language has high power, familiar syntax, portability, windowing and extensive development tools which make it an excellent choice for prototyping. The intuitive nature of the language and the close connection between modeling physical and logical entities are aptly demonstrated by detailed discussion of the design of the video management package. Implementation of binary search tree and AVL tree abstract data types demonstrate that coding of constructs which are procedural in nature does not exploit the strengths of an object-oriented language such as ACTOR. GRA

N89-17411# Naval Postgraduate School, Monterey, CA.
AN ABSTRACT INTERACTIVE GRAPHICS INTERFACE FOR THE IBM/PC AND MACINTOSH M.S. Thesis
Ko-Hsin Liang Jun. 1988 181 p
(AD-A200427) Avail: NTIS HC A09/MF A01 CSCL 12E

Different computer systems have different programming environments in spite of their similar capabilities. GEM and Macintosh software system both provide an operating environment in which the users can utilize all kinds of functions and routines to produce a user-friendly application program. Unfortunately, the programmers have to repeat the learning procedure and recode the source works if for some reason the application program is needed to run on both IBM PC and Macintosh microcomputers. In this thesis, a common interface is provided for programmers to reduce duplicated efforts and hopefully to get the same effects in both operating environments. GRA

N89-17412# Sandia National Labs., Albuquerque, NM.
IMPROVING SOFTWARE QUALITY THROUGH HIERARCHICAL DESIGN
S. L. Sardalos 1988 10 p Presented at the Structured Development Forum X, San Francisco, CA, 8 Aug. 1988
(Contract DE-AC04-76DP-00789)
(DE88-014919; SAND-88-1662C; CONF-880894) Avail: NTIS HC A02/MF A01

This paper discusses hierarchical software design through its application to an example software product. Decomposition of the software product into discrete functional software sub-products is addressed. Potential improvements in managing and performing software quality assurance activities, such as review, inspection and test, are presented. Resulting simplification of software configuration management, product definition, and reusability is discussed. Finally, the hierarchical approach to software design and production is extended to describe a possible software design environment of the future. DOE

N89-17413# Stanford Linear Accelerator Center, CA.
HANDYPAK: A HISTOGRAM AND DISPLAY PACKAGE
A. Boyarski Sep. 1988 136 p
(Contract DE-AC03-76SF-00515)
(DE89-002742; SU-SLAC-234-Rev-2) Avail: NTIS HC A07/MF A01

HANDYPAK is a set of FORTRAN subroutines which a user may call for defining, accumulating, and outputting histograms or scatter plots. Sliced projections and statistical means and variances can be generated. Smooth curves and user specified functions or contours may also be drawn. User blocks may also be defined and manipulated. Histograms and user blocks can be saved on disk, and can be retrieved from disk at a later time. Output can be directed to a line printer, or to a variety of graphic devices. Plotting formats may be changed by the user. Windowing features allow multiple plots per page on graphic devices. HANDYPAK also runs interactively with a conversational command language which allows histograms to be manipulated or displayed at a terminal. This code works on IBM VM/CMS and VAX/VMS operating systems. DOE

N89-17414# Instituto de Pesquisas Espaciais, Sao Jose dos Campos (Brazil).
AUTOMATIC REGISTRATION OF SATELLITE IMAGERY
Gilberto CamaraNeto Aug. 1988 5 p In PORTUGUESE; ENGLISH summary Presented at the Latin-American Symposium on Remote Sensing, 4th Brazilian Symposium on Remote Sensing, 6th Penary Meeting, SELPER, Gramado, Brazil, 10-15 Aug. 1986
(INPE-4637-PRE/1349) Avail: NTIS HC A02/MF A01

Registration of satellite imagery is an important need in various application areas in remote sensing. A method is presented for registration which reduces use work to a minimum, the control points being automatically chosen. The method tests in LANDSAT TM imagery with good results. Author

N89-17415# Argonne National Lab., IL.
ACCURATE AND EFFICIENT TESTING OF THE EXPONENTIAL AND LOGARITHM FUNCTIONS IN Ada
Ping Tak Peter Tang Nov. 1988 93 p
(Contract W-31-109-eng-38)
(DE89-004443; ANL-88-24) Avail: NTIS HC A05/MF A01

We illustrate how table-driven techniques can be used to test highly accurate implementations of EXP and LOG. Our tests report the largest error observed in EXP and LOG accurately to within 1/500 unit in the last place. Methods to verify the tests' reliability are discussed. Results of applying the tests to our own as well as to a number of other implementations of EXP and LOG are presented. DOE

N89-17416# Oak Ridge National Lab., TN.
FINDING EIGENVALUES AND EIGENVECTORS OF UNSYMMETRIC MATRICES USING A DISTRIBUTED-MEMORY MULTIPROCESSOR
G. A. Geist and G. J. Davis Nov. 1988 27 p
(Contract DE-AC05-84OR-21400)
(DE89-004731; ORNL/TM-10938) Avail: NTIS HC A03/MF A01

Distributed-memory parallel algorithms for finding the eigenvalues and eigenvectors of a dense unsymmetric matrix are given. While several parallel algorithms have been developed for symmetric matrices, little work has been done on the unsymmetric case. Our parallel implementation proceeds in three major steps: reduction of the original matrix to Hessenberg form, application of the implicit double-shift QR algorithm to compute the eigenvalues, and back transformations to compute the eigenvectors. Several modifications to our parallel QR algorithm, including ring communication, pipelining and delayed updating are discussed and compared. Results and timings are given. DOE

N89-17417*# National Aeronautics and Space Administration. Langley Research Center, Hampton, VA.
A MULTISTAGE LINEAR ARRAY ASSIGNMENT PROBLEM Final Report
David M. Nicol, D. R. Shier, R. K. Kincaid, and D. S. Richards (Virginia Univ., Charlottesville.) Nov. 1988 34 p Submitted for publication

(Contracts NAS1-18107; NAS1-18605; AF-AFOSR-0117-88)
(NASA-CR-181748; ICASE-88-57; NAS 1.26:181748) Avail: NTIS HC A03/MF A01 CSCL 09B

The implementation of certain algorithms on parallel processing computing architectures can involve partitioning contiguous elements into a fixed number of groups, each of which is to be handled by a single processor. It is desired to find an assignment of elements to processors that minimizes the sum of the maximum workloads experienced at each stage. This problem can be viewed as a multi-objective network optimization problem. Polynomially-bounded algorithms are developed for the case of two stages, whereas the associated decision problem (for an arbitrary number of stages) is shown to be NP-complete. Heuristic procedures are therefore proposed and analyzed for the general problem. Computational experience with one of the exact problems, incorporating certain pruning rules, is presented with one of the exact problems. Empirical results also demonstrate that one of the heuristic procedures is especially effective in practice.

Author

N89-17418*# National Aeronautics and Space Administration. Langley Research Center, Hampton, VA.
ACCURATE MODELING OF PARALLEL SCIENTIFIC COMPUTATIONS Final Report
David M. Nicol (College of William and Mary, Williamsburg, VA.) and James C. Townsend Nov. 1988 13 p Submitted for publication
(Contracts NAS1-18107; NAS1-18605; AF-AFOSR-0117-88)
(NASA-CR-181756; ICASE-88-58; NAS 1.26:181756) Avail: NTIS HC A03/MF A01 CSCL 09B

Scientific codes are usually parallelized by partitioning a grid among processors. To achieve top performance it is necessary to partition the grid so as to balance workload and minimize communication/synchronization costs. This problem is particularly acute when the grid is irregular, changes over the course of the computation, and is not known until load time. Critical mapping and remapping decisions rest on the ability to accurately predict performance, given a description of a grid and its partition. This paper discusses one approach to this problem, and illustrates its use on a one-dimensional fluids code. The models constructed are shown to be accurate, and are used to find optimal remapping schedules.

Author

N89-17419# Lawrence Livermore National Lab., CA.
KINETICS: A COMPUTER PROGRAM TO ANALYZE CHEMICAL REACTION DATA
Robert L. Braun and Alan K. Burnham Nov. 1988 10 p Submitted for publication
(Contract W-7405-eng-48)
(DE89-004602; UCID-21588) Avail: NTIS HC A03/MF A01

KINETICS (Version 2.0) is a copyrighted, user-friendly kinetics analysis computer program designed for reactions such as kerogen or polymer decomposition. It can fit rate parameters to chemical reaction data (rate or cumulative reacted) measured at a series of constant temperatures, constant heating rates, or arbitrary thermal histories. The program uses two models with conversion-dependent Arrhenius parameters and two models with activation energy distributions. The discrete distribution model fits an average frequency factor and relative fractions and activation energies for up to 25 parallel, first-order reactions. The Gaussian distribution model fits a frequency factor, activation energy, Gaussian distribution parameter, and reaction order for up to 3 parallel reactions. For both distribution models, if the experiments are at a series of constant heating rates, the program uses a very fast approximate fitting procedure to determine possible initial parameter estimates for the subsequent nonlinear regression analysis. This increases the probability that the regression analysis will properly converge with a minimum of computer time. Once convergence is reached by the discrete model, the parameter space is further systematically searched to achieve global convergence. With the Gaussian model, the calculated rates or integrals can be convoluted with an experimental tracer signal during the nonlinear regression to account for dispersion effects often found in real chemical reaction data. KINETICS can also be used in an application mode to calculate reaction rates and integrals for previously determined Gaussian or discrete parameters, using an arbitrary thermal history. It is available for PC, VAX, SUN, CRAY computers and can be run interactively or in a batch mode. An auxillary program, PLOTKIN, is available to generate a variety of plots from KINETICS output files.

DOE

N89-17420# Sandia National Labs., Albuquerque, NM. Numerical Mathematics Div.
THE PERFORMANCE OF ASYNCHRONOUS ALGORITHMS ON HYPERCUBES
David E. Womble Dec. 1988 22 p
(Contract DE-AC04-76DP-00789)
(DE89-005503; SAND-88-2714) Avail: NTIS HC A03/MF A01

Many asynchronous algorithms have been developed for parallel computers. Most implementations of asynchronous algorithms, however, have been for shared memory machines. In this paper, we study the implementation and performance of some common asynchronous algorithms on the NCUBE/ten, a 1024 node hypercube. In addition, we summarize existing theoretical work and discuss some classes of algorithms that can be made asynchronous and some that cannot.

DOE

N89-17421# Oak Ridge National Lab., TN.
A BIBLIOGRAPHY ON PARALLEL AND VECTOR NUMERICAL ALGORITHMS
J. M. Ortega, R. G. Voigt, and C. H. Romine Jan. 1989 94 p
(Contract DE-AC05-84OR-21400)
(DE89-005693; ORNL/TM-10998) Avail: NTIS HC A05/MF A01

This technical report contains a bibliography of the current and past research papers dealing with numerical algorithms on both parallel and vector computers.

DOE

N89-17193# Technische Hochschule, Darmstadt (Germany, F.R.). Inst. for Aerodynamics and Measurement Techniques.
A PERSONAL COMPUTER BASED SYSTEM FOR THE EVALUATION OF MULTIPLE EXPOSED IMAGES IN LASER SPECKLE AND PARTICLE IMAGE DISPLACEMENT VELOCIMETRY
A. Bloch *In* VKI, Particle Image Displacement Velocimetry 1988 10 p (For primary document see N89-17179 09-34)
Avail: NTIS HC A21/MF A01

N89-17195# Arizona Univ., Tucson. Optical Sciences Center.
A NEW ALGORITHM FOR THE RAPID ANALYSIS OF PARTICLE IMAGE DISPLACEMENT DATA
Roy B. Frieden and Csaba K. Zoltani (Ballistic Research Labs., Aberdeen Proving Ground, MD.) *In* VKI, Particle Image Displacement Velocimetry 1988 8 p (For primary document see N89-17179 09-34)
Avail: NTIS HC A21/MF A01

N89-17308*# Sverdrup Technology, Inc., Cleveland, OH.
EVALUATION OF AEROTHERMAL MODELING COMPUTER PROGRAMS
K. C. Hsieh and S. T. Yu *In* NASA, Lewis Research Center, Turbine Engine Hot Section Technology, 1987 Oct. 1987 p 129-130 (For primary document see N89-17298 09-39)
Avail: NTIS HC A20/MF A01 CSCL 09B

62 COMPUTER SYSTEMS

Includes computer networks and special application computer systems.

N89-17422*# National Aeronautics and Space Administration. Lewis Research Center, Cleveland, OH.
PARALLEL GAUSSIAN ELIMINATION OF A BLOCK TRIDIAGONAL MATRIX USING MULTIPLE MICROCOMPUTERS

Richard A. Blech Washington, DC Feb. 1989 35 p
(NASA-TP-2892; E-4199; NAS 1.60:2892) Avail: NTIS HC A03/MF A01 CSCL 09B

The solution of a block tridiagonal matrix using parallel processing is demonstrated. The multiprocessor system on which results were obtained and the software environment used to program that system are described. Theoretical partitioning and resource allocation for the Gaussian elimination method used to solve the matrix are discussed. The results obtained from running 1, 2 and 3 processor versions of the block tridiagonal solver are presented. The PASCAL source code for these solvers is given in the appendix, and may be transportable to other shared memory parallel processors provided that the synchronization outlines are reproduced on the target system. Author

N89-17423# Naval Postgraduate School, Monterey, CA.
INTERCONNECTING DIFFERENT TYPES OF LOCAL AREA COMPUTER NETWORKS M.S. Thesis
Daniel C. Malkie Jun. 1988 75 p
(AD-A200280) Avail: NTIS HC A04/MF A01 CSCL 12G

When interconnecting local area computer networks of various types there are many issues which the Information Systems manager must consider. This thesis will identify some of these issues as they pertain to the interconnection of four local area computer networks. Relevant information which results from this thesis will be used to enhance this internetting. Step taken in solving the issues of interconnecting different types of LANs included the following: Thorough examination of existing LANs hardware and software; What fundamental requirements and objectives were to be accomplished; What were the specific hardware objectives, i.e., to be able to use a laser printer on another LAN; What were the specific software objectives, i.e., to be able to share certain application programs from a server. What protocol conversion had to be accomplished and what degree of interconnection strategy should be pursued, i.e., full file transfer versus message passing. How friendly should the user interface be and how that impacts on performance; and Government regulations and their effect on compatibility. GRA

N89-17424*# National Aeronautics and Space Administration. Lewis Research Center, Cleveland, OH.
A DATA ACQUISITION AND STORAGE SYSTEM FOR THE ION AUXILIARY PROPULSION SYSTEM CYCLIC THRUSTER TEST
John A. Hamley Feb. 1989 15 p
(NASA-TM-101469; E-4583; NAS 1.15:101469) Avail: NTIS HC A03/MF A01 CSCL 09B

A nine-track tape drive interfaced to a standard personal computer was used to transport data from a remote test site to the NASA Lewis mainframe computer for analysis. The Cyclic Ground Test of the Ion Auxiliary Propulsion System (IAPS), which successfully achieved its goal of 2557 cycles and 7057 hr of thrusting beam on time generated several megabytes of test data over many months of continuous testing. A flight-like controller and power supply were used to control the thruster and acquire data. Thruster data was converted to RS232 format and transmitted to a personal computer, which stored the raw digital data on the nine-track tape. The tape format was such that with minor modifications, mainframe flight data analysis software could be used to analyze the Cyclic Ground Test data. The personal computer also converted the digital data to engineering units and displayed real time thruster parameters. Hardcopy data was printed at a rate dependent on thruster operating conditions. The tape drive provided a convenient means to transport the data to the mainframe for analysis, and avoided a development effort for new data analysis software for the Cyclic test. This paper describes the data system, interfacing and software requirements. Author

63 CYBERNETICS

Includes feedback and control theory, artificial intelligence, robotics and expert systems.

For related information see also *54 Man/System Technology and Life Support.*

N89-17425# Syracuse Univ., NY.
NORTHEAST ARTIFICIAL INTELLIGENCE CONSORTIUM ANNUAL REPORT 1986. VOLUME 5. BUILDING AN INTELLIGENT ASSISTANT: THE ACQUISITION, INTEGRATION, AND MAINTENANCE OF COMPLEX DISTRIBUTED TASKS Interim Technical Report, Jan. - Dec. 1986
Victor Lesser, W. B. Croft, and Beverly Woolf et al Jun. 1988 295 p Prepared in cooperation with Northeast Artificial Intelligence Consortium, Syracuse, NY
(Contract F30602-85-C-0008)
(AD-A199824; RADC-TR-88-11-Vol-5) Avail: NTIS HC A13/MF A01 CSCL 12I

The Northeast Artificial Intelligence Consortium (NAIC) was created by the Air Force Systems Command, Rome Air Development Center, and the Office of Scientific Research. Its purpose is to conduct pertinent research in artificial intelligence and to perform activities ancillary to this research. This report describes progress that has been made in the second year of the existence of the NAIC on the technical research tasks undertaken at the member universities. The topics covered in general are: versatile expert system for equipment maintenance, distributed AI for communications system control, automatic photo interpretation, time-oriented problem solving, speech understanding systems, knowledge base maintenance, hardware architectures for very large systems, knowledge-based reasoning and planning, and a knowledge acquisition, assistance, and explanation system. The specific topic for this volume is the development of intelligent interfaces to support cooperating computer users in their interactions with a computer. GRA

N89-17426# Naval Ocean Systems Center, San Diego, CA. Architecture and Applied Research Branch.
TEMPORAL PATTERN RECOGNITION
Carey E. Priebe and Chen-Han Sung (San Diego State Univ., CA.) Sep. 1988 7 p Prepared in cooperation with California Univ., San Diego, La Jolla
(AD-A200090; NOSC/TD-1332) Avail: NTIS HC A02/MF A01 CSCL 12I

A self-organizing network architecture for the learning of recognition codes corresponding to temporal patterns is described. The problem presents itself in many real-world situations. In any non-trivial environment in which a proposed system will function the spectre of temporal information (information coming into the system over a period of time) is evident. In many cases it is not sufficient to process the information independent of its relative time-order. Disciplines as diverse as speech recognition, robotics and data fusion/situation analysis require that temporal aspect of the data be considered. In temporal environments such as these the information lost when using a non-temporal approach can be prohibitive. This approach is formulated to make use of this important temporal information. The network described takes as its input individual incoming events. Sequences of these events (letters, phonemes, or, more abstractly, object sightings in a vision system), received by the system over time are categorized as specific sequences by the temporal system. The Temporal system produces Gaussian classifications that represent the statistics of the temporal data, and the system uses a noisy environment, giving as output a Gaussian distance from the stored sequence, thus providing an analog measure of closeness of fit to currently known patterns. GRA

N89-17427# Naval Ocean Systems Center, San Diego, CA.
MACHINE LEARNING OF PARAMETER CONTROL DOCTRINE FOR SENSOR AND COMMUNICATION SYSTEMS Final Report
R. B. Kamen and R. A. Dillard Jul. 1988 115 p
(AD-A200096; NOSC/TR-1220) Avail: NTIS HC A06/MF A01 CSCL 17I

Artificial intelligence approaches to learning were reviewed for their potential contributions to the construction of a system to learn parameter control doctrine. Separate learning tasks were isolated and several levels of related problems were distinguished. Formulas for providing the learning system with measures of its performance were derived for four kinds of targets. GRA

N89-17428# Rutgers - The State Univ., New Brunswick, NJ. Center for Expert Systems Research.
EMPIRICAL ANALYSIS AND REFINEMENT OF EXPERT SYSTEM KNOWLEDGE BASES Annual Report
Sholom M. Weiss and Casimir A. Kulikowski 31 Aug. 1988 12 p
(Contract N00014-87-K-0398)
(AD-A200146) Avail: NTIS HC A03/MF A01 CSCL 12I

Knowledge base refinement is the modification of an existing expert system knowledge base with the goals of localizing specific weaknesses in a knowledge base and improving an expert system's performance. Systems that automate some aspects of knowledge base refinement can have a significant impact on the related problems of knowledge base acquisition, maintenance, verification, and learning from experience. The SEEK system was the first expert system framework to integrate large-scale performance information into all phases of knowledge base development and to provide automatic information about rule refinement. A recently developed successor system, SEEK2, significantly expands the scope of the original system in terms of generality and automated capabilities. Based on promising results using the SEEK approach, significant progress can be made in expert system techniques for knowledge acquisition, knowledge base refinement, maintenance, and verification. GRA

64 NUMERICAL ANALYSIS

Includes iteration, difference equations, and numerical approximation.

N89-17429# International Centre for Theoretical Physics, Trieste (Italy).
ON 2-BANACH ALGEBRAS
Noor Mohammad and A. H. Siddiqui Nov. 1987 16 p
(DE88-704194; IC-87/351) Avail: NTIS (US Sales Only) HC A03/MF A01

The notion of a 2-Banach algebra is introduced and its structure is studied. After a short discussion of some fundamental properties of bivectors and tensor product, several classical results of Banach algebras are extended to the 2-Banach algebra case. A condition under which a 2-Banach algebra becomes a Banach algebra is obtained and the relation between algebra of bivectors and 2-normed algebra is discussed. DOE

N89-17430# Los Alamos National Lab., NM.
GENERALIZED FINITE STRAINS, GENERALIZED STRESSES, AND A HYBRID VARIATIONAL PRINCIPLE FOR FINITE-ELEMENT COMPUTER PROGRAMS
W. A. Cook Aug. 1988 25 p
(Contract W-7405-eng-36)
(DE89-002101; LA-11372-MS) Avail: NTIS HC A03/MF A01

A generalized hybrid variational principle is presented that includes, as special cases, hybrid variational principles for the Lagrangian and Eulerian formulations. This generalized hybrid principle approximates equilibrium and constitutive equations. This report is an extension of a similar report entitled Generalized Finite Strains, Generalized Stresses, and a Principle of Virtual Work for Finite-Element Computer Programs. Two approaches are presented for solving nonlinear stress analysis problems with this generalized hybrid variational principle. Both use the finite-element method: one interates the nodal displacements, and the other iterates the incremental displacements. DOE

N89-17431# Los Alamos National Lab., NM.
GENERALIZED FINITE STRAINS, GENERALIZED STRESSES, AND A PRINCIPLE OF VIRTUAL WORK FOR FINITE-ELEMENT COMPUTER PROGRAMS
W. A. Cook and J. Genin Aug. 1988 28 p
(Contract W-7405-eng-36)
(DE89-002102; LA-11371-MS) Avail: NTIS HC A03/MF A01

This report compares strain and stress tensors and virtual work principles of the Lagrangian and Eulerian formulations. A generalized formulation is presented that includes the Lagrangian and Eulerian formulations as special cases. This formulation uses a reference configuration that is a linear combination of the deformed and undeformed configurations. Generalized strain and stress tensors are presented that include, as special cases, Green strain and Piola--Kirchhoff stress tensors of the Lagrangian formulation and Almansi strain and Cauchy stress tensors of the Eulerian formulation. Similarly, a generalized virtual work principle is presented that includes, also as special cases, the principles of virtual work for the Lagrangian and Eulerian formulations. Two approaches are presented for solving nonlinear stress analysis problems with the generalized formulation. Both use the finite-element method to approximate equilibrium: one iterates the nodal displacements, and the other iterates the incremental displacements. DOE

N89-17432# Limit Point Systems, Fremont, CA.
A VISUALIZATION MODEL BASED ON THE MATHEMATICS OF FIBER BUNDLES
D. M. Butler and M. H. Pendley Sep. 1988 22 p Prepared in cooperation with Sandia National Labs., Albuquerque, NM
(Contract DE-AC04-76DR-00789)
(DE89-002537; SAND-88-8971) Avail: NTIS HC A03/MF A01

In this report, we describe a visualization model based on the mathematics of fiber bundles. In a companion report (SAND 88-8972), we introduced the Visualization Management System (ViMS), a new approach to the development of software for Visualization in Scientific Computing (ViSC). A visualization management system implements a visualization model which specifies the class of geometric objects, the graphic representations of the objects and the operations provided by the system. In the model described here, the geometric objects are sections of fiber bundles. We give a brief, intuitive description of the mathematics of fiber bundles, emphasizing aspects relevant to our visualization model. We describe three important classes of operations on fiber bundles. We develop a flexible scheme for constructing graphic representations of fiber bundles and a simple but useful visualization taxonomy. DOE

N89-17433# Illinois Univ., Urbana. Model Based Measurement Lab.
ASSESSMENT AND COMPARISON OF TECHNIQUES FOR TRANSFORMING PARAMETERS TO A COMMON METRIC IN ITEM RESPONSE THEORY Ph.D. Thesis
Daniel O. Segall 1988 151 p
(Contracts N00014-83-K-0397; N00014-86-K-0482; RR04204)
(AD-A200067; MEASUREMENT/SER-84-6) Avail: NTIS HC A08/MF A01 CSCL 05H

Seven different techniques for transforming two sets of parameters to a common metric in item response theory were evaluated. These techniques include three techniques that estimate the transformation by equating the first two moments of the distributions of estimated difficulty parameters. Another three techniques are included that estimate the transformation by minimizing sums of squares criteria. The remaining technique (MLE) finds the scale transformation that maximizes the likelihood of observing vectors of item parameter differences. Results indicate that for calibrations with a small number of items with extreme estimated difficulty values all techniques perform satisfactorily for moderate sample sizes (500 subjects) and test lengths (60 items). With a large number of extreme estimated difficulty values the three sums of squares and MLE techniques perform satisfactorily, while the difficulty parameter techniques do not. The MLE technique

appears poorly suited for smaller samples (500 subjects) and shorter tests (30 items). GRA

N89-17434# Columbia Univ., New York, NY.
MASSIVE SYMBOLIC MATHEMATICAL COMPUTATIONS AND THEIR APPLICATIONS Quarterly Report, 1 May - 31 Jul. 1988
David V. Chudnovsky, Gregory V. Chudnovsky, Morton B. Friedman, and K. Prendergast 16 Aug. 1988 5 p
(Contract F49620-87-C-0113)
(AD-A200253; TR-2; AFOSR-88-1112TR) Avail: NTIS HC A02/MF A01 CSCL 12E

The development is continued on codes solving large-scale realistic models of aero-, hydrodynamic and astrophysical problems on fast vector and parallel versions of three-dimensional of aero- and hydrodynamics codes, tested by us on a variety of two-dimensional problems. These codes are used now for solutions of astronomical, astrophysical and cosmological problems. The main part of the code development is the reduction of its computational complexity, to make it feasible to run in a moderate time (days of super-computers) large simulations of galaxy evolution over a large fraction of Hubble time. For this purpose we use symbolic computational methods and computer algebra programs and tools, developed by us. Particularly successful was the development of specialized fast (scalar, vector and parallel) subroutines of evaluation of special functions and their integrals in the astrophysical code (needed for computation of chemical, thermodynamical and gravitational effects), that consume most of the runtime of the programs. Our algorithms for special function evaluations are based on our fast methods of power series and rational approximation computations. GRA

N89-17435# Carnegie-Mellon Univ., Pittsburgh, PA. Dept. of Computer Science.
AXIOMS FOR CONCURRENT OBJECTS Interim Report
Maurice P. Herlihy and Jennette M. Wing Dec. 1987 26 p
(Contract F33615-84-K-1520)
(AD-A200584; CMU-CS-86-154; AFWAL-TR-87-1175) Avail: NTIS HC A03/MF A01 CSCL 12D

Specification and verification techniques for abstract data types that have been successful for sequential programs can be extended in a natural way to provide the same benefits for concurrent programs. An approach is proposed to specifying and verifying concurrent objects based on a novel correctness condition, which we call linearizability. Linearizability provides the illusion that each operation takes effect instantaneously at some point between its invocation and its response, implying that the meaning of a concurrent objects operations can still be given by pre- and post conditions. This paper defines and discusses linearizability, and then gives examples of how to reason about concurrent objects and verify their implementations based on their (sequential) axiomatic specifications. GRA

N89-17436# Gosudarstvennyi Komitet po Ispolzovaniyu Atomnoi Energii, Moscow (USSR).
CLUSTER EXPANSION FOR VACUUM CONFINING FIELDS
Yu. A. Simonov 1987 24 p
(DE88-704367; ITEP-211(1987)) Avail: NTIS (US Sales Only) HC A03/MF A01

Colored particle Green functions in vacuum background random fields are written as path integrals. Averaging over random fields is done using the cluster (cumulant) expansion. The existence of a finite correlation length for vacuum background fields is shown to produce the linear confinement, in agreement with the results, obtained with the help of averaged Hamiltonians. A modified form of cluster expansion for nonabelian fields is introduced using the path-ordered cumulants. DOE

N89-17437 ESDU International Ltd., London (England).
THE KALMAN FILTER
Dec. 1988 20 p
(ESDU-88039; ISBN-0-85679-671-9; ISSN-0141-3988) Avail: ESDU

This Data Item 88039, an addition to the Sub-series on Dynamics, derives the discrete and continuous forms of the Kalman filter equations for a first-order randomly-excited linear system. Equations for the multi-dimensional filter for a randomly-excited system are also stated by extension from the first-order form. The Kalman filter estimates the state variables of a system from a combination of measurement data corrupted by noise and predicted values of the states obtained from a mathematical model of the system. The Kalman gains are found to weight appropriately the combination of measurements and predictions so as to minimize the variance of the estimation error of the states of the system. The technique is optimal because that error variance is less than or equal to that found by any other unbiased estimate. An example illustrates the application of the method to a system, described by a first-order linear differential equation, driven by a combination of a known (deterministic) input and a random input, the output of which is known to be corrupted by measurement noise. ESDU

N89-17438# Oak Ridge National Lab., TN. Engineering Physics and Mathematics Div.
GLOBAL EXISTENCE FOR SYMMETRIC DISCRETE VELOCITY MODELS
V. Protopopescu 1988 11 p Presented at the Workshop on Discrete Models Lattice Gas Dynamics and Foundations of Hydrodynamics, Torino, Italy, 19 Sep. 1988
(Contract DE-AC05-84OR-21400)
(DE89-003102; CONF-8809191-1) Avail: NTIS HC A03/MF A01

For symmetric discrete velocity models, some generalizations of previous global existence proofs are given to include bounded geometries, continuous models, and stationary states with no momentum conservation. Additional results and simpler proofs are obtained for completely symmetric models. DOE

N89-17439# Argonne National Lab., IL. Mathematics and Computer Science Div.
FLOATING-POINT STANDARDS: THEORY AND PRACTICE
W. J. Cody 1987 9 p Presented at the International Workshop on the Role of Interval Methods in Scientific Computing, Columbus, OH, 8 Sep. 1987
(Contract W-31-109-eng-38)
(DE89-003598; CONF-8709382-1) Avail: NTIS HC A02/MF A01

ANSI/IEEE Std 754-1985, the IEEE Standard for Binary Floating-Point Arithmetic, has now been joined by IEEE Std 854-1987, A Radix- Independent Standard for Floating-Point Arithmetic. These standards specify floating-point arithmetic systems that are intended to simplify the preparation of high-quality numerical software. The success of these standards hinges on how well they are implemented and how well they are supported by enhancements to algebraic languages. This paper briefly outlines the arithmetic systems specified by the standards, and discusses some existing implementations. DOE

N89-17440# Argonne National Lab., IL.
A PRESENTATION FOR VIRASORO ALGEBRAS
C. K. Zachos 1988 4 p Presented at the 17th International Colloquium on Group Theoretical Methods in Physics, St. Adele, Quebec, 27 Jun. 1988
(Contract W-31-109-eng-38)
(DE89-003883; ANL-HEP-CP-88-49; CONF-8806105-2) Avail: NTIS HC A02/MF A01

The entire Virasoro, Ramond and Neveu-Schwarz algebras can each be constructed from a finite number of well-chosen generators satisfying a small number of conditions. Our most economical sets consist of just two starting generators in all cases, subject to no more than six conditions for the Virasoro case, five conditions for the Ramond case, and nine conditions for the Neveu-Schwarz case. Consequently, the Virasoro algebra simply amounts to 6 equations in two operator unknowns, and correspondingly 5 to 9 equations for the foregoing superalgebras. DOE

N89-17441*# Tennessee Univ., Knoxville. Dept. of Computer Science.
SPARSE MATRIX METHODS RESEARCH USING THE CSM TESTBED SOFTWARE SYSTEM
Eleanor Chu and J. Alan George Washington, DC Mar. 1989 137 p
(Grant NAG1-803)
(NASA-CR-4219; NAS 1.26:4219) Avail: NTIS HC A07/MF A01 CSCL 12A

Research is described on sparse matrix techniques for the Computational Structural Mechanics (CSM) Testbed. The primary objective was to compare the performance of state-of-the-art techniques for solving sparse systems with those that are currently available in the CSM Testbed. Thus, one of the first tasks was to become familiar with the structure of the testbed, and to install some or all of the SPARSPAK package in the testbed. A suite of subroutines to extract from the data base the relevant structural and numerical information about the matrix equations was written, and all the demonstration problems distributed with the testbed were successfully solved. These codes were documented, and performance studies comparing the SPARSPAK technology to the methods currently in the testbed were completed. In addition, some preliminary studies were done comparing some recently developed out-of-core techniques with the performance of the testbed processor INV. Author

N89-17442# Los Alamos National Lab., NM.
FORCE STATE MAPPING USING EXPERIMENTAL DATA
Norman F. Hunter, Jr., Thomas Paez, and Dan L. Gregory (Sandia National Labs., Albuquerque, NM.) 1989 19 p Presented at the International Modal Analysis Conference, Las Vegas, NV, 3 Feb. 1989
(Contract W-7405-eng-36)
(DE89-000351; LA-UR-88-3080; CONF-890225-1) Avail: NTIS HC A03/MF A01

Techniques for the characterization and analysis of linear systems are well developed. Many techniques applicable to linear systems have limited applicability for nonlinear systems. In dealing with nonlinear systems, numerous new techniques are under development. New methods which are specifically tailored for nonlinear systems include force state mapping, difference equation techniques, and higher order frequency response functions. The force state mapping technique was introduced by Tomlinson and Worden. Their work is in turn based on a system identification procedure introduced by Masri and Caughey. In this paper we apply the technique to a linear system and to several types of nonlinear second order systems. In particular, we emphasize application of the technique to motion across a nonlinear joint or interface. For second order systems, this approach is quite straightforward, and the major problem is the development and application of techniques for dealing with noisy data. Extension of the technique to multi-degree-of-freedom systems requires explicit computation of the mass associated with each measurement location. Possible techniques for determining the magnitude of these mass terms are introduced as extensions of the technique for multi-degree-of-freedom systems. Either local or global estimation schemes may be used to determine the shape of the fitted surfaces. We emphasize global parameter estimation techniques for surfaces and apply these global estimation techniques in the time and frequency domains. DOE

N89-17443# Rochester Univ., NY. Dept. of Physics and Astronomy.
THE INTEGRABILITY CONDITION FOR DYNAMICAL SYSTEMS
Ashok Das 3 Oct. 1988 5 p Presented at the Meeting of the Division of Particles and Fields of the American Physical Society (APS), Storrs, CT, 15 Aug. 1988
(Contract DE-AC02-76ER-13065)
(DE89-004124; DOE/ER-13065/558; UR-1091; CONF-8808145-23) Avail: NTIS HC A02/MF A01

We derive a geometric condition as the sufficient condition for the integrability of a dynamical system with two Poisson bracket structures. The geometrical meaning of various properties of such systems are also clarified. DOE

N89-17444*# Catholic Univ. of America, Washington, DC. Dept. of Electrical Engineering.
DEVELOPMENT OF KINEMATIC EQUATIONS AND DETERMINATION OF WORKSPACE OF A 6 DOF END-EFFECTOR WITH CLOSED-KINEMATIC CHAIN MECHANISM Interim Report, 1 Jul. 1988 - 1 Jan. 1989
Charles C. Nguyen and Farhad J. Pooran Feb. 1989 17 p
(Grant NAG5-780)
(NASA-CR-183241; NAS 1.26:183241) Avail: NTIS HC A03/MF A01 CSCL 12A

This report presents results from the research grant entitled Active Control of Robot Manipulators, funded by the Goddard Space Flight Center, under Grant NAG5-780, for the period July 1, 1988 to January 1, 1989. An analysis is presented of a 6 degree-of-freedom robot end-effector built to study telerobotic assembly of NASA hardware in space. Since the end-effector is required to perform high precision motion in a limited workspace, closed-kinematic mechanisms are chosen for its design. A closed-form solution is obtained for the inverse kinematic problem and an iterative procedure employing Newton-Raphson method is proposed to solve the forward kinematic problem. A study of the end-effector workspace results in a general procedure for the workspace determination based on link constraints. Computer simulation results are presented. Author

N89-17445*# Sterling Federal Systems, Inc., Palo Alto, CA.
FLUX JACOBIAN MATRICES AND GENERALED ROE AVERAGE FOR AN EQUILIBRIUM REAL GAS
Marcel Vinokur Dec. 1988 19 p
(Contract NAS2-11555)
(NASA-CR-177512; NAS 1.26:177512) Avail: NTIS HC A03/MF A01 CSCL 12A

Inviscid flux Jacobian matrices and their properties used in numerical solutions of conservation laws are extended to general, equilibrium gas laws. Exact and approximate generalizations of the Roe average are presented. Results are given for one-dimensional flow, and then extended to three-dimensional flow with time-varying grids. Author

65 STATISTICS AND PROBABILITY

Includes data sampling and smoothing; Monte Carlo method; and stochastic processes.

N89-17446# Naval Underwater Systems Center, New London, CT.
THE WIGNER DISTRIBUTION FUNCTION WITH MINIMUM SPREAD
Albert H. Nuttall 1 Jun. 1988 51 p
(AD-A199661; NUSC-TR-8317) Avail: NTIS HC A04/MF A01 CSCL 12C

The Wigner distribution function (WDF) with minimum quadratic spread corresponds to a Gaussian amplitude-modulated waveform with linear frequency-modulation. The optimum WDF is two-dimensional Gaussian and has contours of equal height which are identical to the penalty contours of the quadratic spread measure employed. An alternative measure of spread, involving an exponential reward for concentration, leads to identically the same optimum waveform and WDF. A generalization to a certain class of smoothed WDFs is also possible and is presented. The sensitivity of the effective area of a smoothed WDF, to mismatch in shape factor and tilt in the time-frequency plane, is evaluated quantitatively. GRA

N89-17447# Alphatech, Inc., Burlington, MA.
DISTRIBUTED ESTIMATION FOR LARGE-SCALE EVENT-DRIVEN SYSTEMS
Demosthenis Teneketzis, David A. Castanon, and Nils R. Sandell, Jr. 1988 83 p

(Contract DE-AC01-80RA-50418)
(DE89-002688; DOE/RA-50418/T2) Avail: NTIS HC A05/MF A01

This paper is concerned with distributed estimation theory for dynamic stochastic systems. To bring into mathematical focus the issues arising from the absence of centralized information, we shall consider the class of event-driven stochastic dynamic systems. These systems are hybrid state systems whose state consists of a discrete component and a continuous component, where the transitions between the discrete components of the state correspond to the occurrence of the events. The evolution of the events in time is modeled by a Markov chain; the states of the Markov chain influence the dynamics of a linear stochastic system which models the evolution of the continuous components of the state. The distributed estimation problem is to estimate the hybrid state using noise corrupted, distributed observations. DOE

N89-17448*# National Aeronautics and Space Administration. Langley Research Center, Hampton, VA.
ON A CLASS OF NONSTATIONARY STOCHASTIC PROCESSES
A. G. Miamee (Hampton Inst., VA.) and Jay C. Hardin [1989] 17 p
(Grant NAG1-768)
(NASA-TM-101195; NAS 1.15:101195) Avail: NTIS HC A03/MF A01 CSCL 12A

A new class of nonstationary stochastic processes is introduced and some of the essential properties of its members are investigated. This class is richer than the class of stationary processes and has the potential of modeling some nonstationary time series. The relation between these newly defined processes with other important classes of nonstationary processes is investigated. Several examples of linearly correlated processes which are not stationary, periodically correlated, or harmonizable are given. Author

N89-17449# Syracuse Univ., NY. Dept. of Electrical and Computer Engineering.
EXTENSIONS TO THE MATRIX PENCIL APPROACH FOR DIRECTION FINDING Final Report, May 1986 - May 1987
Braham Himed and Donald Weiner Jul. 1988 105 p
(Contract F30602-81-C-0169)
(AD-A200112; RADC-TR-88-149) Avail: NTIS HC A06/MF A01 CSCL 12E

This work deals with the problem of direction finding using the matrix-pencil approach. Consider a linear array of m sensor and assume there are d narrowband sources. Having collected the data at the m sensors, the problem is to estimate the direction of arrival of these sources. The matrix-pencil approach is a non-search procedure, thus very easy to use. In this study, a generalization of the method to a linear array of m identical sensors with some arbitrary beam pattern was performed. It is also shown that the method still works when using different windows. The only restriction is that at least d elements of the window be non-zero to ensure the validity of the algorithm. A perturbation analysis due to equal sensor spacing was also performed. The concept of the chordal metric was introduced. It is shown that the bound derived on the chordal metric is equivalent to the chordal metric itself. The problem of estimating both the angular frequencies and the angles of arrival of the sources was then posed. It is proven that the method still works; i.e., the angular frequencies and the locations of the sources were estimated using two matric pencils. The rank values of these matrices are shown to contain both the angles of arrival and the angular frequencies of the sources. A computer simulation was performed each time to ensure the effectiveness of the method. GRA

N89-17450# North Carolina Univ., Chapel Hill. Dept. of Statistics.
ON A WIDE RANGE EXCLUSION PROCESS IN RANDOM MEDIUM WITH LOCAL JUMP INTENSITY Technical Report No. 236, Sep. 1987 - Aug. 1988
E. Platen Aug. 1988 32 p
(Contract F49620-85-C-0144)
(AD-A200510; AFOSR-88-1058TR) Avail: NTIS HC A03/MF A01 CSCL 12C

The paper investigates the macroscopic nonequilibrium dynamics of a wide range exclusion process in random medium. Based on a law of large numbers and the specific properties of the exclusion dynamics it is shown under suitable assumptions that the particles concentration follows a nonlinear evolution equation. GRA

66 SYSTEMS ANALYSIS

Includes mathematical modeling; network analysis; and operations research.

N89-17451# Lawrence Livermore National Lab., CA.
THE SPACE-BASED INTERCEPTOR
Christopher T. Cunningham Oct. 1988 30 p Presented at the Nuclear Arms Technologies in the 1990's, Washington, DC, 16 Apr. 1988
(Contract W-7405-eng-48)
(DE89-002869; UCRL-99768; CONF-8804202-2) Avail: NTIS HC A03/MF A01

We calculate the effectiveness and marginal cost-effectiveness of SBI defenses against a variety of possible Soviet threats. Defense effectiveness is expressed in terms of participation fraction, which depends on SBI flyout distance and threat basing, and in terms of the number of interceptors needed to accomplish a given mission. Optimal interceptor sizing favors large high velocity rockets. With such optimal design, the defense appears marginally cost-effective with a 50 percent kill criterion against current or responsively modified large liquid boosters, although not against more stressing threats. Survivability of direct attack is not assessed, although survivability enhancement options are briefly discussed. DOE

N89-17452# Defense Science Board, Washington, DC.
REPORT OF THE DEFENSE SCIENCE BOARD TASK FORCE SUBGROUP ON STRATEGIC AIR DEFENSE (SDI MILESTONE PANEL) Final Report
May 1988 13 p
(AD-A200164) Avail: NTIS HC A03/MF A01 CSCL 15C

Conclusions of the Defense Science Board's Strategic Defense Milestone Panel include: (1) In view of the technical, budgetary, political, and arms control uncertainties surrounding the ballistic missile defense program, the Panel recommends planning a number of steps in the technical development and deployment of a system to meet the JCS requirements rather than a single major action. (2) From a development point of view, priority should be given to the sensors, processing and communications necessary to provide an adequate assessment of what is actually going on, the nature and extent of the attack, and the detection and tracking of boosters and reentry vehicles. This framework is needed whatever weapons are actually used, and the research, development, and experimentation required to provide it involves most of the critical technologies. This surveillance system should evolve as the supporting technology becomes available, allowing the inclusion of whatever weapons are available and wanted. This restructuring would help assure priority attention to critical technical problems despite budget uncertainties, and (3) Deployment should be in steps, each of which should provide some capability and have some value in itself. GRA

N89-17453*# National Aeronautics and Space Administration. Lewis Research Center, Cleveland, OH.
PARALLEL PROCESSING OF A ROTATING SHAFT SIMULATION
Dale J. Arpasi Feb. 1989 68 p
(NASA-TM-101462; E-4290; NAS 1.15:101462) Avail: NTIS HC A04/MF A01 CSCL 12B

A FORTRAN program describing the vibration modes of a rotor-bearing system is analyzed for parellelism in this simulation using a Pascal-like structured language. Potential vector operations are also identified. A critical path through the simulation is identified and used in conjunction with somewhat fictitious processor characteristics to determine the time to calculate the problem on a parallel processing system having those characteristics. A parallel processing overhead time is included as a parameter for proper evaluation of the gain over serial calculation. The serial calculation time is determined for the same fictitious system. An improvement of up to 640 percent is possible depending on the value of the overhead time. Based on the analysis, certain conclusions are drawn pertaining to the development needs of parallel processing technology, and to the specification of parallel processing systems to meet computational needs. Author

67 THEORETICAL MATHEMATICS

Includes topology and number theory.

N89-17454# International Centre for Theoretical Physics, Trieste (Italy).
SPHERICAL-TYPE HYPERSURFACES IN A RIEMANNIAN MANIFOLD
Jean Pierre Ezin and Marko Rigoli Jun. 1988 12 p
(DE88-704224; IC-88/118) Avail: NTIS (US Sales Only) HC A03/MF A01

Let M be a compact hypersurface immersed in R sup n and let K and L be its mean curvature function and scalar curvature respectively. A classical global problem concerning these two geometrical quantities is to find out if assuming that either K or L is constant and under some additional assumptions M is a sphere. It was demonstrated that assuming the immersion to be an embedding, the consistency of K implies M to be spherical. It was also demonstrated that the sphere is the only compact hypersurface with constant scalar curvature embedded in Euclidean space. In this paper we give a generalization of these results when the ambient space is an appropriate Riemannian manifold (N,h). DOE

N89-17455# Oak Ridge National Lab., TN. Mathematical Sciences Section.
FINDING EIGENVALUES AND EIGENVECTORS OF UNSYMMETRIC MATRICES USING A HYPERCUBE MULTIPROCESSOR
G. A. Geist, R. C. Ward, G. J. Davis, and R. E. Funderlic (North Carolina State Univ., Raleigh.) 1988 7 p Presented at the 3rd Conference on Hypercube Concurrent Computers and Applications, Pasadena, CA, 19 Jan. 1988
(Contract DE-AC05-84OR-21400)
(DE89-002311; CONF-880117-7) Avail: NTIS HC A02/MF A01

Distributed-memory algorithms for finding the eigenvalues and eigenvectors of a dense unsymmetric matrix are given. While several parallel algorithms have been developed for symmetric systems, little work has been done on the unsymmetric case. Our parallel implementation proceeds in three major steps: reduction of the original matrix to Hessenberg form, application of the implicit double-shift QR algorithm to compute the eigenvalues, and back transformations to compute the eigenvectors. Several modifications to our parallel QR algorithm, including ring communication and pipelining, are discussed and compared. Results and timings are given. DOE

70 PHYSICS (GENERAL)

For precision time and time interval (PTTI) see *35 Instrumentation and Photography;* for geophysics, astrophysics or solar physics see *46 Geophysics, 90 Astrophysics,* or *92 Solar Physics.*

N89-17456# Lawrence Livermore National Lab., CA. Chemistry and Materials Science Dept.
RADIATION IMPOSED LIMITS ON SUPERCONDUCTING MAGNETS: A DATA BASE FOR COPPER STABILIZERS
M. W. Guinan, P. A. Hahn, C. E. Klabunde, and R. R. Coltman, Jr. (Oak Ridge National Lab., TN.) 28 Oct. 1987 17 p Presented at the 3rd International Conference on Fusion Reactor Materials, Karlsruhe, Federal Rep. of Germany, 4-8 Oct. 1987
(Contract W-7405-eng-48)
(DE89-002875; UCRL-96200; CONF-871036-37) Avail: NTIS HC A03/MF A01

Two of eight differently prepared copper stabilizer samples, previously irradiated in the RTNS-2 at LLNL, the IPNS-1 and the BSR at ORNL, have been irradiated to a fluence of 1.33 X 10 to the 22nd n/sq m at RTNS-2. During the course of the irradiation the samples were periodically removed (without warming) for measurements of the transverse magnetoresistance and returned for continued irradiation. This experiment extends the range of neutron-irradiation-induced resistivity by a factor of five over the previous experiments. A simple model is developed which reproduces the magnetoresistance results of all the experiments to an accuracy of 2.5 percent. DOE

N89-17457# Los Alamos National Lab., NM. Center of Buoyancy Definition.
CENTER OF BUOYANCY DEFINITION
Vernon Sandberg Dec. 1988 8 p
(Contract W-7405-eng-36)
(DE89-003017; LA-11416-MS) Avail: NTIS HC A02/MF A01

The center of buoyancy of an arbitrary shaped body is defined in analogy to the center of gravity. The definitions of the buoyant force and center of buoyancy in terms of integrals over the area of the body are converted to volume integrals and shown to have simple intuitive interpretations. DOE

N89-17458# Air Force Systems Command, Wright-Patterson AFB, OH. Foreign Technology Div.
DEVELOPMENT OF FINITE LOCAL PERTURBATIONS OF ELECTRICAL CONDUCTIVITY IN THE FLOW OF A WEAKLY-CONDUCTING GAS WHEN A MAGNETIC FIELD IS PRESENT
L. A. Zaklyazminskiy, V. S. Sokolov, L. M. Degtyarev, S. P. Kurdyusov, A. A. Samarskiy, and A. P. Favorskiy 8 Aug. 1988 7 p Transl. into ENGLISH from Novosibirsk Aerofiz Issledovaniya (USSR), 1972 p 71
(AD-A200243; FTD-ID(RS)T-0526-88) Avail: NTIS HC A02/MF A01 CSCL 20D

A study has been made of the possibility of development of a T-layer from local finite perturbation of electrical conductivity, introduced artificially into a steady state flow of a weakly conducting gas. The analysis is made with the help of a numerical solution of equations of magnetic hydrodynamics, formulated in the assumption that the electron, ion and neutral components of the medium are found in thermodynamic equilibrium; the viscosity, Hall effect and transfer of energy by radiation are not taken into account. GRA

N89-17459# Lawrence Livermore National Lab., CA.
ENERGY AND TECHNOLOGY REVIEW
Andrew J. Poggio, ed. Oct. 1988 48 p
(Contract W-7405-eng-48)
(DE89-005308; UCRL-52000-88-10) Avail: NTIS HC A03/MF A01

This issue of Energy and Technology Review contains: Neutron Penumbral Imaging of Laser-Fusion Targets--using our new penumbral-imaging diagnostic, we have obtained the first images that can be used to measure directly the deuterium-tritium burn region in laser-driven fusion targets; Computed Tomography for

Nondestructive Evaluation--various computed tomography systems and computational techniques are used in nondestructive evaluation; Three-Dimensional Image Analysis for Studying Nuclear Chromatin Structure--we have developed an optic-electronic system for acquiring cross-sectional views of cell nuclei, and computer codes to analyze these images and reconstruct the three-dimensional structures they represent; Imaging in the Nuclear Test Program--advanced techniques produce images of unprecedented detail and resolution from Nevada Test Site data; and Computational X-Ray Holography--visible-light experiments and numerically simulated holograms test our ideas about an X-ray microscope for biological research. DOE

71 ACOUSTICS

Includes sound generation, transmission and attenuation. For noise pollution see *45 Environmental Pollution.*

N89-17460 North Carolina State Univ., Raleigh.
ACOUSTIC WAVE PROPAGATION BY FINITE ELEMENTS AND TIME STEP INTEGRATION Ph.D. Thesis
Charles Edouard Chassaing 1987 125 p
Avail: Univ. Microfilms Order No. DA8815476

The finite element method is used to model acoustic radiation from a vibrating surface. The media is treated as a stationary compressible fluid, equivalent to a solid that does not support shear. The wave propagates from a boundary with a prescribed force/acceleration time history. The acoustic problem thus is transformed to a structural dynamic problem for numerical solution. Issues that are considered include the type and order of the elements, the time step integration method, the effect of node spacing and time step size. Unconditionally stable implicit time step integration methods are shown not suitable for calculating wave propagation due to computational expense and inter-element resonances and/or high frequency error. Boundary conditions are prescribed at the source and by reflecting and non-reflecting surfaces. Non-reflecting surfaces are treated as infinite boundaries, because they behave as if the wave propagates through the boundary to infinity. In the development of the finite element method, it is discovered that 1,2,3-order Lagrangian elements give good results, whereas higher orders do not because of high frequency error. High frequency in this context means few nodes per wavelength. Dissert. Abstr.

N89-17461# Bolt, Beranek, and Newman, Inc., Canoga Park, CA.
A STRATEGY FOR UNDERSTANDING NOISE-INDUCED ANNOYANCE Final Report, 1 Jan. - 29 Sep. 1987
S. Fidell, D. M. Green, T. J. Schultz, and K. S. Pearsons Aug. 1988 121 p
(Contract F33615-86-C-0530)
(AD-A200125; BBN-6337; HSD-TR-87-013) Avail: NTIS HC A06/MF A01 CSCL 05H

This report provides a rationale for development of a systematic approach to understanding noise-induced annoyance. Two quantitative models are developed to explain: (1) the prevalence of annoyance due to residential exposure to community noise sources; and (2) the intrusiveness of individual noise events. Both models deal explicitly with the probabilistic nature of annoyance, and assign clear roles to acoustic and nonacoustic determinants of annoyance. The former model provides a theoretical foundation for empirical dosage-effect relationships between noise exposure and community response, while the latter model differentiates between the direct and immediate annoyance of noise intrusions and response bias factors that influence the reporting of annoyance. The assumptions of both models are identified, and the nature of the experimentation necessary to test hypotheses derived from the models is described. GRA

N89-17462# Naval Postgraduate School, Monterey, CA.
SIGNAL ACQUISITION AND PROCESSING FOR AUTONOMOUS SPACE SHUTTLE CARGO BAY ACOUSTIC MEASUREMENTS (NASA G-313) M.S. Thesis
David P. Kuebler Jun. 1988 107 p
(AD-A200426) Avail: NTIS HC A06/MF A01 CSCL 20A

A narrowband trigonal acoustic transducer array and digital signal processing software are described in support of Space Shuttle Vibroacoustic experiment (NASA G-313). The three co-planar, vibrationally isolated pressure-sensing microphones, the preamplifiers and the filters are designed to meet dynamic range and anti-aliasing requirements for the digitization and processing of recorded flight data with one Herty resolution within the 30 to 780 Hz baseband acoustic spectrum. The experiment is designed to operate in environments up to 160 dB SPL and provides model recognition and directional information to identify resonances and localize high intensity sound sources within the ambient launch environment of the Space Shuttle Cargo Bay. Also included in this thesis is a model of the empty Cargo Bay resonances and modal density calculations based on an adiabatic perturbations of a rigid, right circular cylindrical enclosure. GRA

N89-17463 ESDU International Ltd., London (England).
JET-BY-JET SHIELDING OF NOISE
Nov. 1988 21 p
(ESDU-88023; ISBN-0-85679-655-7; ISSN-0307-0115) Avail: ESDU

This Data Item 88023, an addition to the Sub-series on Noise, provides a computer program listing in FORTFAN 77 for the prediction of the natural sheilding effect of two parallel identical jets. The shielding levels are predicted in one-third octave frequency bands over a range specified by the user for an observer in the far-field at any distance and angle to the jets except in the 40 degree quandrant center on the downstream axis of the jet. The method takes account of the jet's velocity and temperature, their diameters and the ratio of jet density to ambient. It considers each jet in turn as a point noise source and the other as the shielding jet and superimposes the sound fields so obtained. The theory is outlined and comparison of predictions obtained with experimental results is made that shows a root mean square error between measurements and predictions of less than 0.5 dB. The method of providing the input data and the format of the output is illustrated with a worked example. The program is also available on magnetic media as ESDUpac 8823. ESDU

N89-17464 ESDU International Ltd., London (England).
FLOW INDUCED ACOUSTIC RESONANCE IN TUBULAR HEAT EXCHANGERS
Dec. 1988 35 p
(ESDU-88028; ISBN-0-85679-660-3; ISSN-0141-402X) Avail: ESDU

This Data Item 88028, an addition to the Sub-series on Heat Transfer, and complements ESDU 87019, which provides prediction methods for vibration of heat exchanger bundles. After outlining the nature of acoustic resonance, calculation methods are given for the acoustic frequency in both rectangular and cylindrical ducts. Procedures, based on a correlation of all the available acoustic data (all data on periodic wake shedding derived from measurements in the flow field were discarded because of their inapplicability), are given for the prediction of resonance. Possible damage caused by accoustic resonance is considered, and the means by which a design can be modified, before or after fabrication, are discussed. The methods apply to bundles in a rectangular cross-section duct, to shell-and-tube heat exchangers and to helical coil arrangements. ESDU

N89-17465# Universite de Technologie de Compiegne (France). Div. Acoustiques et Vibrations Industrielles.
CHARACTERIZATION AND MODELING OF ACOUSTIC BEAMS FROM ULTRASONIC TRANSDUCERS IN SOLID OR LIQUID MEDIA Final Report [CARACTERISATION ET MODELISATION DU FAISCEAU ACOUSTIQUE DE TRANSDUCTEURS ULTRASONORES EN MILIEU SOLIDE OU LIQUIDE]

J. F. deBelleval Aug. 1988 20 p In FRENCH
(Contract DRET-87-187)
(RF-DAVI-88-08; ETN-89-93653) Avail: NTIS HC A03/MF A01

The prediction of time or frequency response of transducers in all points of the acoustic field were studied. Measurements were carried out using a transducer immersed directly in a fluid or coupled with a plane or cylindrical solid interface. Computer programs were developed to describe these fields, with input either from models or measurements. The method allows one to detect a number of parasitic effects such as double beams and focusing errors.
ESA

N89-17466*# Massachusetts Inst. of Tech., Cambridge.
ROTATING HOT-WIRE INVESTIGATION OF THE VORTEX RESPONSIBLE FOR BLADE-VORTEX INTERACTION NOISE
Richard Remo Fontana Dec. 1988 240 p
(Grant NAG2-182)
(NASA-CR-177454; NAS 1.26:177454) Avail: NTIS HC A01/MF A01 CSCL 20A

This distribution of the circumferential velocity of the vortex responsible for blade-vortex interaction noise was measured using a rotating hot-wire rake synchronously meshed with a model helicopter rotor at the blade passage frequency. Simultaneous far-field acoustic data and blade differential pressure measurements were obtained. Results show that the shape of the measured far-field acoustic blade-vortex interaction signature depends on the blade-vortex interaction geometry. The experimental results are compared with the Widnall-Wolf model for blade-vortex interaction noise. Author

N89-17467*# National Aeronautics and Space Administration. Langley Research Center, Hampton, VA.
EQUIVALENT LINEARIZATION FOR FATIGUE LIFE ESTIMATES OF A NONLINEAR STRUCTURE
R. N. Miles Jan. 1989 21 p Prepared in cooperation with California Univ., Berkeley
(NASA-TM-101536; NAS 1.15:101536) Avail: NTIS HC A03/MF A01 CSCL 20A

An analysis is presented of the suitability of the method of equivalent linearization for estimating the fatigue life of a nonlinear structure. Comparisons are made of the fatigue life of a nonlinear plate as predicted using conventional equivalent linearization and three other more accurate methods. The excitation of the plate is assumed to be Gaussian white noise and the plate response is modeled using a single resonant mode. The methods used for comparison consist of numerical simulation, a probabalistic formulation, and a modification of equivalent linearization which avoids the usual assumption that the response process is Gaussian. Remarkably close agreement is obtained between all four methods, even for cases where the response is significantly linear. Author

72 ATOMIC AND MOLECULAR PHYSICS

Includes atomic structure, electron properties, and molecular spectra.

N89-17468 New South Wales Univ., Kensington (Australia).
COLLISION-INDUCED DECOMPOSITION OF MULTIATOMIC IONS Ph.D. Thesis
Margaret M. Sheil Dec. 1987 2 p
Avail: Issuing Activity

Collision-induced decomposition (CID) of multiatomic peptide ions was studied on a large double-focussing mass spectrometer by the mass-analyzed ion kinetic energy (MIKE) technique. Low-energy CID of peptide ions was investigated on a Fourier transform ion cyclotron resonance (FT/ICR) mass spectrometer. In the course of studies of the dynamics of CID, gaseous ions of beauvericin, valinomycin, valine-gramicidin A and bradykinin were examined in detail. Results of MIKE/CID experiments show that the translational energy losses and internal energy uptakes of the incident ions during collisions with helium atoms increase, when the translational energy of the ions is raised. The translational energy losses and fragment ion yields are higher when helium rather than argon is used as the collision gas. It is suggested that scattering during collision is an important source of ion loss in MIKE/CID experiments. Differences in the results with different collision gases are presumed to reflect differences in the proportions of ions scattered during collision. Differences were found in MIKE/CID spectra following ionization by field desorption (FD) and secondary ion mass spectrometry (SIMS). There is a remarkable degree of agreement between MIKE and FT/ICR CID spectra of (M+H) ions formed by SIMS and chemical ionization respectively. The intensities of fragment ions in FT/ICR/CID spectra are shown to increase with both increasing collision time and increasing translational energy of the ions, albeit the latter appears to be more significant. Author

N89-17469# Vanderbilt Univ., Nashville, TN.
ELECTRONIC INTERACTIONS OF ELECTRONS, PHOTONS, AND ATOMS WITH MATERIAL SURFACES Final Report, Apr. 1986 - Apr. 1988
Norman H. Tolk and Richard F. Haglund, Jr. 31 Aug. 1988 16 p
(Grant AF-AFOSR-0150-86; AF Proj. 2303)
(AD-A199626; AFOSR-88-1118TR) Avail: NTIS HC A03/MF A01 CSCL 07D

The microscopic mechanisms by which the energy of incoming beams of atoms, ions, electrons and photons is absorbed, localized and redirected to produce neutral-particle desorption from surfaces and subsequent surface modification of restructuring are studied. The model system LiF was used, and the results compared with measurements of electronically desorbed Li-atoms adsorbed on other substrates. This study explored how the degree of surface metallization influences the choice of the final excitation state of the desorbing particle. Measurements were made to compare the desorption of excited state neutral lithium from lithium fluoride by electron, photon and ion bombardment and from lithium-dosed tungsten and lithium-dosed glass by electron and photon bombardment. In the electron and photon desorption experiments, only the first lithium resonance line is observed. These results contrast with the ion sputtering results, where emissions from higher excited states were observed. This suggests that the presence of a metal rich surface provides a channel for de-excitation of excited lithium states which are above the lithium metal Fermi energy.
GRA

N89-17470# Oak Ridge National Lab., TN.
DEVELOPMENT OF AN OPTICAL DIGITAL IONIZATION CHAMBER
J. E. Turner, S. R. Hunter, R. N. Hamm, H. A. Wright, G. S. Hurst, and W. A. Gibson (Pellissippi International, Knoxville, TN.) 1988 17 p Presented at the Workshop on Implementation of Dose Equivalent Meters Based on Microdosimetric Techniques in Radiation Protection, Schloss Elmau, Federal Rep. of Germany, 18 Oct. 1988
(Contract DE-AC05-84OR-21400)
(DE89-002209; CONF-881022-1) Avail: NTIS HC A03/MF A01

We are developing a new device for optically detecting and imaging the track of a charged particle in a gas. The electrons in the particle track are made to oscillate rapidly by the application of an external, short-duration, high-voltage, RF electric field. The excited electrons produce additional ionization and electronic excitation of the gas molecules in their immediate vicinity, leading to copious light emission (fluorescence) from the selected gas, allowing the location of the electrons along the track to be determined. Two digital cameras simultaneously scan the emitted light across two perpendicular planes outside the chamber containing gas. The information thus obtained for a given track can be used to infer relevant quantities for microdosimetry and dosimetry, e.g., energy deposited, LET, and track structure in the gas. The design of such a device now being constructed and methods of obtaining the dosimetric data from the digital output will be described. DOE

N89-17471# Brookhaven National Lab., Upton, NY. Chemistry Dept.
NUCLEAR REORGANIZATION BARRIERS TO ELECTRON TRANSFER
Norman Sutin, Bruce S. Brunschwig, Carol Creutz, and Jay R. Winkler 1988 15 p Presented at the 19th International Conference on Solution Chemistry, Lund, Sweden, 15 Aug. 1988
(Contract DE-AC02-76CH-00016)
(DE88-016582; BNL-41602; CONF-8808130-1) Avail: NTIS HC A03

The nuclear barrier to electron transfer arises from the need for reorganization of intramolecular and solvent internuclear distances prior to electron transfer. For reactions with relatively small driving force (normal free-energy region) the nuclear factors and rates increase as intrinsic inner-shell and outer-shell barriers decrease; this is illustrated by data for transition metal complexes in their ground electronic states. By contrast, in the inverted free-energy region, rates and nuclear factors decrease with decreasing intrinsic barriers; this is illustrated by data for the decay of charge-transfer excited states. Several approaches to the evaluation of the outer-shell barrier are explored in an investigation of the distance dependence of the nuclear factor in intramolecular electron-transfer processes. DOE

N89-17472# Naval Research Lab., Washington, DC. Plasma Physics Div.
THE ELECTRON-WATER VAPOR (H2O) COLLISION CROSS SECTIONS Interim Report
A. W. Ali 26 Aug. 1988 37 p
(AD-A200187; NRL-MR-6268) Avail: NTIS HC A03/MF A01 CSCL 04A

Water vapor (H2O) is one of the minor constituents of the atmosphere and it plays an important role in the deionization processes of the partially ionized air. It controls the air conductivity, especially that of the unheated air. Therefore, the role of H2O in modifying the electron velocity distribution in wet air is required for characterizations of partially ionized wet air. This requires the solution of a Boltzmann equation with an appropriate set of electron-molecule scattering cross sections. This report, accordingly, presents a set of up to date cross sections for the electron - H2O collisions over a wide range of electron energies. The set comprises the total, ionization, dissociative ionization, dissociative excitation, electronic, vibrational, rotational, elastic and momentum transfer cross sections. GRA

N89-17473# National Academy of Sciences - National Research Council, Washington, DC.
PHOTONICS: MAINTAINING COMPETITIVENESS IN THE INFORMATION ERA
1988 107 p
(Contract N00014-88-J-1006; NSF DMR-85-01909)
(AD-A200230) Avail: NTIS HC A06/MF A01 CSCL 09E

Photonics concerns the use of photons to work with or to replace electrons in certain communications, computer, or control applications traditionally carried out by electronics. It is a key high-technology area, well established in long-distance fiber-optic telecommunications and rapidly growing in other areas of great importance to society. This report concentrates on technical areas where the overall worldwide market for equipment approaches $400 billion per year, i.e., Telecommunications; Information processing; Optical storage and display; Optical sensors; and Policy Issues. It is essential to increase our industrial competitiveness in product development, manufacturing skills, and marketing; There must be continuing industrial effort in long-range research and innovation; The photonics industry should consider the advantages of an industry association that could help organize consortia to conduct cooperative research and address technical problems and policy issues beyond the scope of any one organization; and Government contractors who receive a percentage of sales for their independent research should devote a sizable fraction to projects with a life span of 5 to 10 years. GRA

N89-17474# Naval Research Lab., Washington, DC. Plasma Radiation Branch.
ELECTRON COLLISION SHIFT OF THE LYMAN-ALPHA LINE IN H AND He+ Interim Report
M. Blaha (Maryland Univ., College Park.) and J. Davis 9 Sep. 1988 55 p
(AD-A200296; NRL-MR-6294) Avail: NTIS HC A04/MF A01 CSCL 20E

The interaction of plasma microfields with radiating atoms and ions causes a line broadening that governs both the half-width and shift of the spectral line, i.e., the intensity distribution in frequency is altered to reflect the presence of the plasma. The line shifts are of particular interest both for their intrinsic value in terms of providing insight into the fundamental nature of the underlying physical processes affecting the emission of radiation as well as its diagnostic value in the study of high density plasmas. In addition, exact wavelengths of spectral lines of highly charged ions are required in the determination of line opacities and level positions for X-ray laser transitions. The sensitivity of spectral line shift is investigated in the impact approximation for a variety of assumptions using the distorted-wave with exchange approach. The formalism is applied to the Lyman-alpha line of hydrogen and ionized helium to determine the influence of various assumptions on the line shift as well as identifying the differences between a neutral and ionized radiator. The results are compared and contrasted with a number of other calculations and experimental measurements. GRA

N89-17475# Natioanl Inst. of Standards and Technology, Boulder, CO. Time and Frequence Div.
COOLED ION FREQUENCY STANDARD Annual Report, Oct. 1987 - Sep. 1988
D. J. Wineland 27 Sep. 1988 11 p
(Contract N00014-88-F-0014)
(AD-A200373) Avail: NTIS HC A03/MF A01 CSCL 20E

The purpose of this work is to develop techniques to overcome the fundamental limits of present frequency standards--the second order and residual first-order Doppler shifts. To this end suitable frequency reference transitions are studied in ions which are stored on electromagnetic traps and cooled by radiation pressure to less than 1k. GRA

N89-17476# State Univ. of New York, Buffalo. Dept. of Chemistry.
NONLOCAL AND QUASILOCAL POTENTIALS IN THE SPONTANEOUS EMISSION OF MOLECULAR EXCIPLEXES COUPLED TO THE PHONON BATH OF A SOLID MATRIX
Kai-Shue Lam and Thomas F. George Oct. 1988 50 p Prepared in cooperation with California State Polytechnic Univ., Pomona
(Contract N00014-86-K-0043)
(AD-A200509; TR-87) Avail: NTIS HC A03/MF A01 CSCL 07D

Molecular Exciplexes coupled to the phonon bath of a solid matrix are treated by a two-state model allowing for radiative relaxation from the excited to ground state and thermal relaxation from each of the states to the phonon bath. Molecular dynamics is considerably simplified by a canonical (Duke-Soules) transformation on the model Hamiltonian. This transformation: (1) renormalizes the bath-free exciplex potential surfaces to phonon-dressed surfaces, and (2) combines the radiative and phonon couplings into a single effective coupling. This leads to an effective nonlocal potential whose kernel is a product of radiative and nonradiative parts, and which can be interpreted pictorially in an intuitive manner when individual terms in the Born series solution of the corresponding Schrodinger equation are linked to special Feynman diagrams. GRA

N89-17477# Gosudarstvennyi Komitet po Ispolzovaniyu Atomnoi Energii, Moscow (USSR).
ON THE EXPERIMENTAL BASIS OF THE PAULI EXCLUSIVE PRINCIPLE
L. B. Okun 1987 16 p

(DE88-704366; ITEP-209(1987)) Avail: NTIS (US Sales Only) HC A03/MF A01

The paper proposes and advocates quantitative tests of the Pauli principle in atoms using modern experimental techniques. At the same time it reminds and illustrates why it is so difficult to violate the Pauli principle on paper, in the framework of accepted fundamental theoretical ideas. DOE

N89-17478# Oak Ridge National Lab., TN.
PRODUCTION AND TRANSPORT OF CONVOY ELECTRONS IN AMORPHOUS CARBON FOILS

J. P. Gibbons, S. B. Elston, R. DeSerio, C. Biedermann, M. Breinig, C. E. Gonzalez-Lepera, O. Heil, H. P. Huelskoetter, H. Rothard, and I. A. Sellin et al 1988 11 p Presented at the International Conference on the Application of Accelerators in Research and Industry, Denton, TX, 7 Nov. 1988 Prepared in cooperation with Tennessee Univ., Knoxville.; Frankfurt Univ., Federal Rep. of Germany

(Contract DE-AC05-84OR-21400)

(DE89-002313; CONF-881151-32) Avail: NTIS HC A03/MF A01

The production of free convoy electrons, emitted with velocities near the ion velocity in ion-solid collisions, is not well understood. Experiments concerning thickness-dependent yields have suggested the dominant mechanism for convoy production is electron loss to the continuum (ELC) in the bulk of the solid. Free electrons created in the bulk are subject to multiple elastic and inelastic scattering during transport through remaining layers of the solid. We discuss doubly-differential measurements of convoy measurements of convoy electrons as a function of target thickness for fast O(5+) ion projectiles incident on carbon foils of varied thicknesses. Angular distributions confirm the ELC model for convoy production. From the radial broadening of the convoy cusps we have determined energy and angular spreading parameters due to post-collisional multiple scattering. DOE

N89-17479# Louisiana State Univ., Baton Rouge. Dept. of Chemistry.
THEORETICAL STUDIES OF ELECTRONS AND ELECTRON TRANSFER PROCESSES IN FLUIDS Progress Report, Aug. 1987 - Sep. 1988

N. R. Kestner 1988 19 p

(Contract DE-FG05-87ER-13674)

(DE89-003259; DOE/ER-13674/2) Avail: NTIS HC A03/MF A01

Research accomplished during the past year involved studies of interaction of hydrated metal ions. Studies with model potentials have demonstrated the distortion of hydration shells at high concentrations. We have also evaluated the radial distribution functions between interacting ions and have calculated the effect on electron transfer rates. It dramatically increased this rate. Research also involved studies of water-water interactions and weak intermolecular forces, in general. The role of Basis Set Superposition Error (BSSE) in limiting the accuracy of atom-atom and molecule-molecule interactions have been demonstrated. New techniques which remove the BSSE at the second order correlation level have been completed. In collaboration with Dr. S. Gupta we have studied the interaction of propane molecules and used these to evaluate liquid properties. Using Density Functional Theory a very large calculation on the iron dimer has been published; other work on the interaction of argon atoms has been completed. We have developed the pseudopotential for ammonia for Landman and Jortner and have collaborated on studies of negative ammonia clusters. We have also completed extensive work with negatively negatively charged water dimmers. Our work on sodium water clusters which have been observed experimentally in beams has been completed. These may also be involved in photobleaching hydrated electrons. Our work on the conformation of several conducting polymer fragments has been published. We show that some helical structure exists. DOE

N89-17480# Oak Ridge National Lab., TN.
A HIGH-INTENSITY PLASMA SPUTTER HEAVY NEGATIVE ION SOURCE

G. D. Alton, Y. Mori, A. Takagi, A. Ueno, and S. Fukumoto (National Lab. for High Energy Physics, Ibaraki, Japan) 1988 17 p Presented at the Symposium of Northeastern Accelerator Personnel, New Haven, CT, 24 Oct. 1988

(Contract DE-AC05-84OR-21400)

(DE89-003113; CONF-8810242-1) Avail: NTIS HC A03/MF A01

A high-intensity, pulsed-mode, plasma-sputter heavy negative ion source has been developed; this source holds promise for a number of uses, including tandem electrostatic accelerator/ synchrotron injection applications. To date, the source has been used to generate mA intensities from more than 18 sputter probes. A brief description of the source and typical performance data for a number of ion species are given. DOE

N89-17481# Argonne National Lab., IL. Materials Science Div.
COMPOSITIONAL CHANGES DURING ION BOMBARDMENT

L. E. Rehn Sep. 1988 23 p Presented at the Metallurgical Society Fall Meeting and American Society for Metals Materials Week, Chicago, IL, 24 Sep. 1988

(Contract W-31-109-eng-38)

(DE89-003974; CONF-880901-14) Avail: NTIS HC A03/MF A01

Ion irradiation initiates several processes that can alter the composition of the target. This presentation provides an overview of our current understanding of these kinetics processes, which include implantation, sputtering, displacement mixing, radiation-enhanced diffusion, and radiation-induced segregation. The latter two effects can alter the target composition to depths that are substantially greater than the projected ion range. DOE

N89-17482# Sandia National Labs., Albuquerque, NM.
ATOMIC-SCALE MODELING OF LOW-ENERGY ION-SOLID PROCESSES

Brian W. Dodson 1988 14 p Presented at the Fall Meeting of the Materials Research Society, Boston, MA, 28 Nov. 1988

(Contract DE-AC04-76DP-00789)

(DE89-004374; SAND-88-3144C; CONF-881155-18) Avail: NTIS HC A03/MF A01

Various techniques which have been applied to modeling low-energy (much less than 1 keV) ion-solid interactions on an atomistic scale are described. In addition to their individual strengths, all such methods also have a number of drawbacks, both fundamental and practical. The range of validity, and the problems encountered external to this range, will be outlined for the different approaches. Finally, examples of molecular dynamics simulations of low-energy ion-solid interactions will be presented. DOE

N89-17483*# Stanford Univ., CA. Dept. of Chemistry.
REACTION DYNAMICS OF H + O2 AT 1.6 eV COLLISION ENERGY

Michael J. Bronikowski, Zhang Rong, David J. Rakestraw, and Richard N. Zare 1 Mar. 1989 19 p

(Grant NAG2-472)

(NASA-CR-183182; NAS 1.26:183182) Avail: NTIS HC A03/MF A01 CSCL 20H

The hot hydrogen atom reaction, H + O2 yields OH + O, has been studied at a center of mass collision energy of 1.6 eV. H atoms were generated by 266 nm photolysis of HI in a mixture of HI and O2 at 293 K. The OH product was probed by laser induced fluorescence and the nascent OH vibrational, rotational, and fine structure distributions were determined. The OH(v=0/OH(v=1) vibrational branching ratio was measured to be 1.72 + or - 0.09. The data suggest that the H + O2 reaction at this collision energy proceeds via two competing mechanisms: reaction involving a long-lived complex and direct reaction. Author

73 NUCLEAR AND HIGH-ENERGY PHYSICS

Includes elementary and nuclear particles; and reactor theory.

For space radiation see *93 Space Radiation.*

N89-17484# International Atomic Energy Agency, Vienna (Austria).
SMALL REACTORS FOR LOW-TEMPERATURE NUCLEAR HEAT APPLICATIONS
Jun. 1988 58 p Presented at the Advisory Group Meeting on Small Reactors for Low-temperature Nuclear Heat Applications, Winnipeg, Manitoba, 8-12 Jun. 1987
(DE88-704336; IAEA-TECDOC-463; CONF-8706349) Avail: NTIS (US Sales Only) HC A04/MF A01

In accordance with the Member States' calls for information exchange in the field of nuclear heat application (NHA) two IAEA meetings were organized already in 1976 and 1977. After this promising period, the development of relevant programs in IAEA Member States was slowed down and therefore only after several years interruption a new Technical Committee Meeting with a Workshop was organized in late 1983, to review the status of NHA, after a few new specific plans appeared in some IAEA Member States in the early 1980's for the use of heat from existing or constructed NPPs and for developing nuclear heating plants (NHP). In June 1987 an Advisory Group Meeting was convened in Winnipeg, Canada, to discuss and formulate a state-of-the-art review on Small Reactors for Low Temperature Nuclear Heat Application. Information on this subject gained up to 1987 in the Member States whose experts attended this meeting is embodied in the present Technical Report. DOE

N89-17485# California Univ., Berkeley. Lawrence Berkeley Lab.
THE TWO-BEAM ACCELERATOR AND THE RELATIVISTIC KLYSTRON POWER SOURCE
Andrew M. Sessler Apr. 1988 40 p Presented at the Budker Memorial Seminar: International Seminar on Topics in High Energy Physics and Controlled Fusion, Novosibirsk, USSR, 26 Apr. 1988
(Contracts W-7405-eng-48; DE-AC03-76SF-00098)
(DE89-002673; LBL-25760; CONF-8804224-1) Avail: NTIS HC A03/MF A01

This paper discusses the concept of a two-beam accelerator. Two versions are discussed, one employing a free electron laser, the second employing a branched beam sent through transfer cavities as in a klystron. DOE

74 OPTICS

Includes light phenomena; and optical devices.

For lasers see *36 Lasers and Masers.*

N89-17486# Lawrence Livermore National Lab., CA.
REVIEW OF PRECISION SURFACE GENERATING PROCESSES AND THEIR POTENTIAL APPLICATION TO THE FABRICATION OF LARGE OPTICAL COMPONENTS
I. F. Stowers, R. Komanduri (National Science Foundation, Washington, DC.), and E. D. Baird 3 Oct. 1988 12 p Presented at the 32nd International Technical Symposium on Optical and Opto-Electronic Applied Sciences and Engineering, San Diego, CA, 14 Aug. 1988
(Contract W-7405-eng-48)
(DE89-001712; UCRL-99735; CONF-880887-26) Avail: NTIS HC A03/MF A01

Over the last decade a wide variety of processes applicable to ultraprecision contouring and polishing have evolved. Examples of these processes include float polishing, elastic emission machining, erosive jet, ion milling, plasma assisted chemical etching, and precision ductile grinding. These processes are reviewed with the intent of comparing their removal rates, resultant surface roughness, demonstrated contour accuracy, and applicability to the manufacture of large optical components. The incentive for this study is the evolution of a deterministic manufacturing process able to lower the cost of fabricating large precision optical components by an order of magnitude. DOE

N89-17487# State Univ. of New York, Buffalo. Dept. of Chemistry.
FRESNEL COEFFICIENTS FOR A PHASE CONJUGATOR
Henk F. Arnoldus and Thomas F. George Oct. 1988 33 p
(Contract N00014-86-K-0043)
(AD-A200123; UBUFFALO/DC/88/TR-85) Avail: NTIS HC A03/MF A01 CSCL 07D

Optical phase conjugation via four-wave mixing is examined in detail. The Fresnel coefficients for reflection and transmission of a plane wave irradiating the surface of the phase conjugator are calculated. It appears that for normal incidence and a weak nonlinear interaction the device produces the phase-conjugated beam with respect to the incoming beam. For finite angles of incidence or stronger nonlinearities in the crystal, the generated wave deviates from the ideal conjugated wave, and also a second reflected wave appears. It is pointed out how this could explain certain controversies regarding atomic lifetimes near the surface of a phase conjugator. GRA

N89-17488# Naval Research Lab., Washington, DC. Plasma Physics Div.
PRECISE INTERFEROMETRIC PHASE DETERMINATION Interim Report
J. A. Stamper 30 Aug. 1988 30 p
(AD-A200186; NRL-MR-6160) Avail: NTIS HC A03/MF A01 CSCL 20F

A precise determination of phase shifts from interferometric fringes is necessary to accurately determine density structure. This is accomplished by a careful comparison of the pair of interferograms representing the initial and final phases. A step-by-step procedure is given for determining the interpolated phase shift from fringes crossing a given axial position of a medium with axial symmetry. Non-uniform final fringe spacing is assumed and accounted for in the interpolation. An example is included, as well as a listing of the computer program. GRA

N89-17489# Brown Univ., Providence, RI. Div. of Engineering.
OPTICAL FIBER SCIENCE AND TECHNOLOGY: NOVEL FIBERS AND FIBER SENSORS Final Report, 1 Oct. 1986 - 29 Feb. 1988
T. F. Morse 29 Feb. 1988 5 p
(Grant AF-AFOSR-0020-87; AF Proj. 2917)
(AD-A200311; AFOSR-88-1121TR) Avail: NTIS HC A02/MF A01 CSCL 20F

This equipment grant has permitted the purchase of a complete optical fiber draw facility and auxilliary equipment for our fiber characterization laboratory. The draw tower has been erected in a specially prepared laboratory. It is a 7.8 m automated tower with a 20 kw carbon induction furnace, and sufficient room for two UV coating stages, or a UV coating stage, and a thermal curing stage. The tower installation took perhaps somewhat more time than initially anticipated, largely due to difficulties in the site preparation. The tower itself has been installed on a reinforced concrete pad, with appropriate vibration isolation. For about six months, we have been gaining experience in the use of the tower, and have been drawing kilometer lengths of fiber that range in diameter from 50 microns to 250 microns with a tolerance of the order of a few microns. In anticipation of expanding the coating capabilities of our draw tower, a vacuum system was purchased for use with radio frequency sputtering on-line on the tower. This will be particularly useful for ceramic coated fibers in the study of the behavior of fiber strengthened composite materials. GRA

N89-17490# Sandia National Labs., Albuquerque, NM.
AN OPTICAL MODULATOR/SWITCH USING THE REFLECTION FROM A TRANSLATED DEPLETION EDGE
T. C. Huang, K. W. Lee, T. Hausken, N. Dagli, L. A. Coldren, and D. Myers 1989 5 p Presented at the Conference on Integrated

and Guided-wave Optics, Houston, TX, 6 Feb. 1989 Prepared in cooperation with California Univ., Santa Barbara
(Contract DE-AC04-76DP-00789)
(DE89-001380; SAND-88-2675C; CONF-890226-1) Avail: NTIS HC A02/MF A01

An optical waveguide modulator/switch using the impedance discontinuity at a p-n junction across the guide has been demonstrated. From the calculated results, a high speed, small size, single mode modulator/switch is expected. A device with a y-branch was made and the on-off ratio in both the straight through guide and the reflection guide is more than 2:1 for a 1.15 micron lightwave. DOE

N89-17491# Lawrence Livermore National Lab., CA.
ANALYSIS OF INTERFEROMETER IMAGES WITH FOURIER DOMAIN TECHNIQUES
P. J. VanArsdall 1 May 1988 9 p
(Contract W-7405-eng-48)
(DE89-002927; UCID-21534) Avail: NTIS HC A02/MF A01

This article discusses our interactive analysis system for processing interferograms digitized from video images. The technique used is based on angle modulation theory, in which a large amount of tilt is introduced into one arm of the interferometer. The tilt component then serves as a spatial carrier to the modulating wave-front phase. Fourier-domain bandpass processing of the interference fringes effectively removes the adverse effects of irradiance variations and camera background signals. We describe this two-dimensional signal-processing technique and present wave-front measurements made during tests of the zig-zag amplifier for the High Average Power Program. DOE

N89-17492# Lawrence Livermore National Lab., CA.
PRECISION TRANSFER FUNCTION MEASUREMENTS OF INTEGRATED OPTICAL MODULATORS
Mark Lowry, Greg Lancaster, Richard T. Peterson, Glen McWright, Dan Nelson, and Bill Kidd Oct. 1988 7 p Presented at the SPIE O-E Lase: International Symposium and Exhibition on Fiber Optics, Optoelectronics and Laser Applications, Boston, MA, 6 Sep. 1988
(Contract W-7405-eng-48)
(DE89-004021; UCRL-99954; CONF-8809105-11) Avail: NTIS HC A02/MF A01

We present transfer function (TF) data from a Crystal Technology, Inc. 2 x 2 switch modulator. The data was obtained using an in-house designed and built automated measurement system that uses pulsed optical illumination at 840 nm and pulsed electrical modulation input, to simulate our actual operating conditions for the device. The precision of the TF system electronics is found to be better than 1 percent over most of the measurement range and approaching 0.1 percent at the midrange of the signals. The reproducibility of the transfer functions themselves was found to be better than 2.0 percent. The effects of photorefractive damage on the device transfer function were studied. For optical doses of approximately 12 mJ (device output) at 840 nm the photorefractively induced changes in the TF were less than 10 percent. The effects of temperature on the transfer function were studied over a temperature range of 23 C to 45 C and found to be quite significant for one of three devices measured. For two others the temperature effects were nearly negligible. DOE

N89-17493# Lawrence Livermore National Lab., CA.
X-RAY OPTICS FOR X-RAY LASER RESEARCH AND APPLICATIONS
N. M. Ceglio Nov. 1988 14 p Presented at the 4th Topical Meeting on Short Wavelength Coherent Radiation: Generation and Applications, Cape Cod, MA, 26-29 Sep. 1988
(Contract W-7405-eng-48)
(DE89-004026; UCRL-99946; CONF-880904-4) Avail: NTIS HC A03/MF A01

State of the art capabilities in soft X-ray lenses, multilayer mirrors, beamsplitters, and synthetically generated holograms are reviewed. Application of these capabilities in recent X-ray laser cavity experiments, and to the development of a soft X-ray interferometer and a high intensity soft X-ray laser are discussed. DOE

N89-17494# Centre National d'Etudes Spatiales, Toulouse (France).
EFFECTS OF DEPOLARIZATION OBTAINED BY SPECULAR REFLECTION ON METALLIC MIRRORS: APPLICATIONS TO LASER TELECOMMUNICATION AND TO EARTH OBSERVATION [EFFECTS DE DEPOLARISATION OBTENUS PAR REFLEXION SPECULAIRE SUR DES MIROIRS METALLIQUES: APPLICATIONS AUX TELECOMMUNICATIONS LASER ET A L'OBSERVATION DE LA TERRE]
G. Otrio 10 Jun. 1987 23 p In FRENCH; ENGLISH summary
(CNES-CT/DRT/TIT/IO-87/150; ETN-89-93616) Avail: NTIS HC A03/MF A01

A theoretical approach estimating the amount of depolarized light after reflection at 45 deg on an aluminum and silver mirror, for GaAlAs laser diodes is presented. The computations are done for different values of the polarization plane and for different wavelengths. The results show that if the reflection angle is limited to less than 30 deg the depolarization effect is negligible. ESA

N89-17495# Centre National d'Etudes Spatiales, Toulouse (France).
OPTICAL COMMUNICATION. FOUR QUADRANT AVALANCHE DETECTOR. MODELING, THEORETICAL RESULTS AND COMPARISON WITH EXPERIMENTAL VALUES [TELECOMMUNICATIONS OPTIQUES DETECTEUR 4 QUADRANTS A AVALANCHE: MODELISATION, PRESENTATION DE RESULTATS THEORIQUES ET COMPARAISON AVEC LES RESULTATS EXPERIMENTAUX]
E. Sein 2 Apr. 1987 53 p Partly in ENGLISH and FRENCH
(CNES-CT/DRT/TIT/IO-87/086; ETN-89-93618) Avail: NTIS HC A04/MF A01

An instrumental approach for the acquisition and tracking design in optical space communications is described. The instrument is based on 4 quadrant avalanche silicon detectors. The theoretical results derived from use of the components, giving the noise equivalent angle on GEO and LEO satellites in various working modes, are given. It is shown that the use of this type of detector is possible at a low frequency modulation of telecommunication beam in order to avoid stray light. ESA

N89-17496# Centre National d'Etudes Spatiales, Toulouse (France).
NON RETURN TO ZERO (NRZ) CLOCK RECOVERY BREADBOARD FOR 200 MB/S OPTICAL INTERSATELLITE LINK
L. Frecon and J. P. Lefevre 23 Jan. 1987 82 p In FRENCH; ENGLISH summary
(CNES-CT/DRT/TIT/TR-87/024; ETN-89-93619) Avail: NTIS HC A05/MF A01

A complete breadboard for the study of high data rate intersatellite links was developed and tested. The emitter is a laser diode, while the receiver is an avalanche photodiode. Other characteristics are wavelength multiplexer and NRZ 200 MB/s per channel. After theoretical analysis a detailed description of the clock recovery part of the breadboard is given including a three pole Butterworth filter. The performances are presented in terms of degradation of bit error rate. ESA

N89-17497# Lawrence Livermore National Lab., CA.
EXPLOSION OF INTEGRATED OPTIC DEVICES USED IN NEW GENERATION SYSTEMS
Frank Roeske 15 Nov. 1988 4 p Presented at the Military Fibre Optic Conference 1988, Los Angeles, CA, 5-8 Dec. 1988 Submitted for publication
(Contract W-7405-eng-48)
(DE89-004012; UCRL-99980; CONF-881247-1) Avail: NTIS HC A02/MF A01

Integrated optics, indeed shows great promise for improving the quality and quantity of data needed in nuclear test diagnostics

systems and other military systems. The systems described will give the testing program better than an order of magnitude increase in temporal response and dynamic range over the presently used counterparts, while also making it possible to increase the number of data channels by greater than an order of magnitude. Should these expectations reach fruition we should see a true explosion in the use of these devices in the near future. DOE

N89-16888# Deutsche Forschungs- und Versuchsanstalt fuer Luft- und Raumfahrt, Oberpfaffenhofen (West Germany).
PRESENTATION OF THE STATUS OF THE EXPERIMENT AND MISSION ACTIVITIES OF THE MONOCULAR ELECTRO-OPTICAL STEREO SCANNER (MEOSS)
F. Lanzl *In its* Proceedings of the Colloquium about Joint Projects Within the DFVLR/ISRO Cooperation Jun. 1988 p 69-79 (For primary document see N89-16883 09-12)
Avail: NTIS HC A06/MF A01; DFVLR, VB-PL-DO, Postfach 90 60 58, 5000 Cologne, Fed. Republic of Germany, 34.50 Deutsche marks

75 PLASMA PHYSICS

Includes magnetohydrodynamics and plasma fusion.
For ionospheric plasmas see *46 Geophysics*. For space plasmas see *90 Astrophysics*.

N89-17498# Los Alamos National Lab., NM.
FIELD-REVERSED CONFIGURATION (FRC) EXPERIMENTS
R. E. Siemon, R. E. Chrien, W. N. Hugrass, S. Okada, D. J. Rej, D. P. Taggart, M. Tuszewski, R. B. Webster, B. L. Wright, and J. T. Slough (Spectra Technology, Inc., Bellevue, WA.) et al 1988 15 p Presented at the 12th International Conference on Plasma Physics and Controlled Nuclear Fusion Research, Nice, France, 12 Oct. 1988 Prepared in cooperation with Seattle Univ., WA
(Contract W-7405-eng-36)
(DE89-000389; LA-UR-88-2878; IAEA-CN-50/C-4-1; CONF-881015-16) Avail: NTIS HC A03/MF A01

FRCs with equilibrium separatrix radii up to 0.18 m have been formed and studied in FRX-C/LSM. For best formation conditions at low fill pressure, the particle confinement exceeds the predictions of LHD transport calculations by up to a factor of two; however, the inferred flux confinement is more anomalous than in smaller FRCs. Higher bias field produces axial shocks and degradation in confinement, while higher fill pressure results in gross fluting during formation. FRCs have been formed in TRX with s from 2 to 6. These relatively collisional FRCs exhibit flux lifetimes of 10 yields 20 kinetic growth times for the internal tilt mode. The coaxial slow source has produced annular FRCs in a coaxial coil geometry on slow time scales using low voltages. DOE

N89-17499# Oak Ridge National Lab., TN.
HIGH POWER ION CYCLOTRON RESONANCE HEATING (ICRH) IN JET
J. Jacquinot 1988 13 p Presented at the 15th European Conference on Controlled Fusion and Plasma Heating, Dubrovnik, Yugoslavia, 16 May 1988 Prepared in cooperation with Joint European Torus Project, Abingdon (England)
(Contract DE-AC05-84OR-21400)
(DE89-002218; CONF-880534-14) Avail: NTIS HC A03/MF A01

Ion Cyclotron Resonance Heating (ICRH) powers of up to 17 MW have been coupled to JET limiter plasmas. The plasma stored energy has reached 7 MJ with 13 MW of RF in 5 MA discharges with Z(sub eff) = 2. When l(sub p)/B(sub phi) = 1 MA/T the stored energy can be 50 percent greater than the Goldston L mode scaling. This is due to transient stabilization of sawteeth (up to 3 s) and to a significant energy content in the minority particles accelerated by RF (up to 30 percent of the total stored energy). Central temperatures of T(sub e) - 11 keV and T(sub i) = 8 keV have been reached with RF alone. (He sup 3)D fusion experiments have given a 60 kW fusion yield (fusion rate of 2 x 10 to the 16th/s in the form of energetic fast particles (14.7 MeV(H), 3.6 MeV(He sup 4)) in agreement with modelling. When transposing the same calculation to a (D)T scenario, Q is predicted to be between 0.12 and 0.8 using plasma parameters already achieved. For the first time, a peaked density profile generated by pellet injection could be reheated and sustained by ICRF for 1.2 s. Electron heat transport in the central region is reduced by a factor 2 to 3. The fusion product n(sub io)tau(sub E)T(sub io) reaches 2.2 x 10 to the 20th/m/s/keV in in 3 MA discharges which is a factor of 2.3 times larger than with normal density profile. DOE

N89-17500# Oak Ridge National Lab., TN.
PLASMA PERFORMANCE IN JET: ACHIEVEMENTS AND PROJECTIONS
A. Gibson 1988 16 p Presented at the 15th European Conference on Controlled Fusion and Plasma Heating, Dubrovnik, Yugoslavia, 16 May 1988 Prepared in cooperation with Joint European Torus Project, Abingdon (England)
(Contract DE-AC05-84OR-21400)
(DE89-002219; CONF-880534-13) Avail: NTIS HC A03

An account is given of recent experimental advances on JET, especially as they relate to fusion performance. Scaling relations are used to identify the critical parameters which need to be optimized to secure the best fusion performance. Finally the established best performance of JET is used as a base to project the performance to be expected in future D-T operation. DOE

N89-17501# Lawrence Livermore National Lab., CA.
PROGRESS TOWARD HIGH-GAIN LASER FUSION
Erik Storm 28 Sep. 1988 5 p Presented at the 19th European Conference on Laser Interaction with Matter, Madrid, Spain, 3-7 Oct. 1988
(Contract W-7405-eng-48)
(DE89-002661; UCRL-98828; CONF-881056-5) Avail: NTIS HC A02/MF A01

A 1985 to 1986 Review of the U.S. inertial confinement fusion program by the National Academy of Sciences concluded that five more years might be required to obtain enough data to determine the future course of the program. Since then, data from the Nova laser and from the Halite/Centurion program have resolved most of the outstanding problems identified by the NAS review. In particular, we now believe that we can produce a sufficiently uniform target; that we can keep the energy content in hot electrons and high-energy photons low enough (approximately 1 to 10 percent of drive energy, depending on target design) and achieve enough pulse-shaping accuracy (approximately 10 percent, with a dynamic range of 100:1) to keep the fuel on a near-Fermi-degenerate adiabat; that we can produce an approximately 100-Mbar pressure pulse of sufficient uniformity (approximately 1 percent), and can control hydrodynamic instabilities so that the mix of the pusher into the hot spot is low enough to permit marginal ignition. These results are sufficiently encouraging that DOE is planning to complete a 10-MJ laboratory microfusion facility to demonstrate high-gain ICF in the laboratory within a decade. DOE

N89-17502# Lawrence Livermore National Lab., CA.
PROGRESS IN LABORATORY HIGH GAIN ICF (INERTIAL CONFINEMENT FUSION): PROSPECTS FOR THE FUTURE
Erik Storm, J. D. Lindl, E. M. Campbell, T. P. Bernat, L. W. Coleman, J. L. Emmett, W. J. Hogan, J. T. Hunt, W. F. Krupke, and W. H. Lowdermilk 1988 32 p Presented at the International Seminar on Nuclear War, Erice, Italy, 20-23 Aug. 1988
(Contract W-7405-eng-48)
(DE89-002664; UCRL-99427; CONF-8808101-3) Avail: NTIS HC A03/MF A01

Inertial Confinement Fusion (ICF), a thermonuclear reaction in a small (approximately 5 mm diameter) fuel capsule filled with a few milligrams of deuterium and tritium, has been the subject of very fruitful experimentation since the early 1970's. High gain ICF is now on the threshold of practical applications. With a Laboratory Microfusion Facility (LMF), these applications will have major implications for national defense, basic and applied science, and

power production. With a driver capable of delivering about 10 MJ in a 10-ns pulse at an intensity of approximately 3 X 10 to the 14th W/sq cm, an appropriately configured cryogenic capsule could be compressed to a density of about 200 g/ cu cm and a temperature of 3 to 5 keV. Under these conditions, up to 10 mg of DT could be ignited, and with a burn efficiency of about 30 percent, release up to 1000 MJ of fusion energy, an energy gain of about 100. A thousand megajoules is equivalent to about one quarter ton of TNT, or about 7 gallons of oil--an amount of energy tractable under laboratory conditions and potentially very useful for a variety of applications. DOE

N89-17503# Lawrence Livermore National Lab., CA.
MODEL MICROFIELD CALCULATIONS OF RADIATIVE AND TRANSPORT PROPERTIES OF IONS IN STRONGLY COUPLED PLASMAS
David B. Boercker 26 Aug. 1988 24 p Presented at the 9th International Conference on Spectral Line Shapes, Torun, Poland, 25-29 Jul. 1988
(Contract W-7405-eng-48)
(DE89-001244; UCRL-99437; CONF-8807121-1) Avail: NTIS HC A03/MF A01

The radiative and transport properties of a strongly coupled plasma are closely related because they are both determined by the behavior of the electric microfield seen by the ions. By focusing on the dynamics of the microfield, a simple, unified model of both types of properties has recently been developed. This model will be described here and shown to reproduce both the static and impact limits of ion Stark broadening. In between these extremes, comparisons with computer simulation data for both the electric field and the radiator dipole autocorrelation functions will be made. DOE

N89-17504# Toronto Univ. (Ontario). Inst. for Aerospace Studies.
HYDROGEN EROSION OF CARBON FOR FUSION APPLICATIONS
James William Davis Nov. 1988 150 p
(UTIAS-328; ISSN-0082-5255) Avail: NTIS HC A07/MF A01

Carbon is the most commonly-used material for plasma-fusion surfaces in current fusion devices, and is a leading contender for such surfaces in the next generation. This widespread use of carbon has resulted in the need for extensive characterization of carbon materials under conditions simulating a fusion reactor environment. Experiments are described which measure the erosion of carbon, mostly in the form of pyrolytic graphite, due to bombardment by energetic (H+) and thermal (H0) hydrogen species. Erosion yields have been measured as a function of sample temperature, H+ energy, H flux density, and in the case of multi-species bombardment, the (H+)/(H0) flux ratio. An analytic model for the synergistic effect which occurs during simultaneous H+ and H0 bombardment is also presented. Investigation of the flux dependence of the erosion yield, has indicated that for a constant graphite temperature, there is a strong effect of incident flux density. When the maximum erosion yield is considered (the temperature at which the maximum yield occurs shifts with flux density), the flux dependence is not as strong; however, there is still a drop-off in the erosion yield at high flux density. The H0 + H+ synergism has been carefully investigated as a function of the relative H0 and H+ fluxes; the primary result being that if the energetic H+ ions comprise greater than or equivalent to 10 percent of the incident flux, then the yield attributed to the H0 atoms becomes as large as that of the ions. The composition of the hydrocarbon spectrum produced varies substantially between the extremes of predominantly energetic ion bombardment - mostly CH4 produced - and predominantly sub-eV H0 atoms, where C2Hx and C3Hx species dominate the reaction. The overall result is that the maximum erosion yield remains less that or equivalent to 0.1 C/H. Author

N89-17505# Berkeley Research Association, Springfield, VA.
MODELING OF ATOMIC PROCESSES FOR X-RAY LASER PLASMAS Final Report, 15 Jun. 1986 - 14 Feb. 1988
Uday Gupta Jul. 1988 76 p
(Contract F49620-86-C-0076)
(AD-A200219; BRA-89-W010R; AFOSR-88-0977TR) Avail: NTIS HC A05/MF A01 CSCL 07E

This work dealt with the theoretical modeling and computation of photoionization, photoexcitation, radiative decay and radiative recombination processes for multielectron atoms and ions in plasmas. Such atomic processes lead to and influence lasing in X-ray lasers operating both in the soft and hard X-ray regions. This research utilized a two-component, finite temperature, self consistent density functional method and demonstrated that this method is applicable for arbitrary plasma density and temperature and is capable of accurately treating multielectron ions of arbitrary Z. Electron collisional ionization and excitation processes were investigated. These processes are an important mechanism through which population inversion of ionic energy levels lead to lasing in the soft X-ray region. Previously theoretical calculations utilizing a semi-classical impact approximation have been performed. In many cases such a method is inadequate. Computations were carried out by electron impact ionization and excitation cross-sections and rate coefficients utilizing the distorted wave with exchange method. GRA

N89-17506# Columbia Univ., New York, NY. School of Mines.
ALFVEN WAVES IN A COLD PLASMA WITH CURVED MAGNETIC FIELDS Final Report, 1 Jan. 1985 - 31 Dec. 1986
Philip M. Carrion, Akira Hasegawa, Waldo Patton, and Manju Prakash Jun. 1988 39 p
(Grant AF-AFOSR-0029-85; AF Proj. 2311)
(AD-A200312; AFOSR-88-1083TR) Avail: NTIS HC A03/MF A01 CSCL 04A

The set of linearized magnetohydrodynamic equations has been reduced to the reflectivity equation for the compressional magnetic perturbations in the framework of the Radoski model. It has been shown that the reflection coefficient is a function of the inhomogeneities of the magnetic field, and the inhomogeneities of the Alfven velocity. An interesting property of the reflectivity equation is that, near Alfven resonant magnetic force lines, this equation reduces to the curvature free Budden equation. Near Alfven resonances the curvature does not play a significant role and Budden's asymptotics in time can be applied to the wave field near the magnetic force lines where the Alfven dispersion relation holds. GRA

N89-17507# Naval Postgraduate School, Monterey, CA. Plasma Physics Div.
INVESTIGATION OF COLLISIONAL EFFECTS IN THE PLASMA EROSION OPENING SWITCH Interim Report
J. M. Grossmann, R. Kulsrud, J. M. Neri, and P. F. Ottinger 20 Sep. 1988 42 p
(AD-A200319; NRL-MR-6240; DE89-001396) Avail: NTIS HC A03/MF A01 CSCL 09A

During the conduction phase of the plasma erosion opening switch (PEOS), current channels in the main body of the plasma have been observed experimentally to be much wider than the collisionless skin depth. In addition, the maximum current carried by the switch before opening (the conduction current) seems to scale roughly linearly with plasma density, n, and switch length, 1. Collisionless PIC code simulations of the plasma switch show current conducted in skin-depth like channels, with the conduction current scaling close to 1 to the 2/5ths power and the fourth root of n. Here the effect of collisions on the behavior of the PEOS is investigated and shown to bring the PIC simulations and experimental results in closer agreement. In the collisional simulations, wider current channels are observed and the conduction current scales linearly with 1 and as sq root of n with density in anode dominated simulations. Linear scaling with length and density in the cathode dominated case can be inferred. GRA

N89-17508# Wisconsin Univ., Madison.
NEOCLASSICAL MHD DESCRIPTIONS OF TOKAMAK PLASMAS

J. D. Callen, Y. B. Kim, A. K. Sundaram, B. A. Carreras, L. Garcia, K. C. Shaing, D. A. Spong, H. Biglari, P. H. Diamond, and O. J. Kwon (California Univ., San Diego, La Jolla.) 1988 8 p Presented at the 12th International Conference on Plasma Physics and Controlled Nuclear Fusion Research, Nice, France, 12-19 Oct. 1988
(Contracts DE-AC05-84OR-21400; DE-FG02-86ER-53218; DE-FG03-88ER-53275)
(DE89-003117; IAEA-CN-50/D-II-1; CONF-881015-28) Avail: NTIS HC A02/MF A01

Considerable progress has been made in extending neoclassical MHD theory and in exploring the linear instabilities, nonlinear behavior and turbulence models it implies for tokamak plasmas. The areas highlighted in this paper include: extension of the neoclassical MHD equations to include temperature-gradient and heat flow effects; the free energy and entropy evolution implied by this more complete description; a proper ballooning mode formalism analysis of the linear instabilities; a new rippling mode type instability; numerical simulation of the linear instabilities which exhibit a smooth transition from resistive ballooning modes at high collisionality to neoclassical MHD modes at low collisionality; numerical simulation of the nonlinear growth of a single helicity tearing mode; and a Direct-Interaction-Approximation model of neoclassical MHD turbulence and the anomalous transport it induces which substantially improves upon previous mixing length model estimates. DOE

N89-17509# Wisconsin Univ., Madison. Dept. of Electrical and Computer Engineering.
FUSION PLASMA THEORY: TASK 3: AUXILIARY HEATING IN TOKAMAKS Final Report
J. E. Scharer Jul. 1988 14 p
(Contract DE-FG02-86ER-53218)
(DE89-003256; DOE/ER-53218/9) Avail: NTIS HC A03/MF A01

The research of the past three year period includes the topics of ICRF fast wave coupling to L- and H-mode edge profiles and coupled full wave ICRF field solutions for CIT and TFTR supershots. Also developed were Quasi-linear Fokker-Planck codes to model nonlocal wave reflection, mode conversion, wave deposition and simulation of core sawtooth phenomena for large tokamaks such as JET. Also examined were coupling between launched fast waves and ion Bernstein waves driven by density gradients near the plasma edge and the effects of known edge turbulence and ponderomotive effects on the direct launching of ion Bernstein waves. It is found that a Te10 ICRF fast mode waveguide launcher only has a moderate increase in its reflection coefficient when coupling into a model H-mode plasma density profile. Our full wave 1-D ICRF code results have corrected earlier formulations by other authors and described a method for calculation of wave fields with an evanescent ion Bernstein mode. The results show that wave reflections, minority and majority absorption and mode conversion are sensitive to plasma and wave parameters and yield stronger minority and majority than a WKB formulation would yield. The wave heating code is coupled to a Fokker-Planck code to model strong electron sawtooth phenomena occurring during minority hydrogen heating on JET. We find that fast ion tail formation and electron drag heating rather than direct electron heating or electron heating via mode conversion to ion Bernstein waves play an important role in core plasma sawtooth dynamics. We find that linear coupling from fast modes to ion Bernstein modes occurs due to larger density gradient scale lengths near the plasma edge. DOE

N89-17510# Bhabha Atomic Research Centre, Bombay (India). Plasma Physics Div.
SEEDED INERT GAS DRIVEN DISK GENERATOR
N. K. Joshi, N. Venkatramani, and V. K. Rohatgi 1987 42 p
(DE88-704083; BARC-1391) Avail: NTIS (US Sales Only) HC A03/MF A01

This report outlines the present status of work being carried out in closed cycle MHD and disk generators. It gives the basic principles and discusses a proposal for setting up an experimental facility to study nonequilibrium plasmas using an inert gas driven disk generator. Disk geometry is a near ideal geometry for plasma studies since it has single or few pair electrodes combined with near perfect insulating walls. The proposed outlay of facility with components and subsystem is given. The facility may also be used to study the concept of fully ionized seed and to develop advanced diagnostic techniques. The basic equation describing the working parameters of such a system is also given in the Appendix. DOE

N89-17511# Academy of Sciences of the Uzbek SSR, Tashkent.
ROLE OF CHARGE EXCHANGE PROCESS IN FORMING OF ION CHARGE AND ENERGY STATES IN MULTICOMPONENT LASER PLASMA PRODUCED FROM GAS-CONTENT SOLIDS
M. R. Bedilov, Yu. A. Bykovskij, Kh. B. Beisembaeva, and M. S. Sabitov 1987 12 p In RUSSIAN; ENGLISH summary
(DE88-704828; IYF-R-6-299) Avail: NTIS (US Sales Only) HC A03/MF A01

Experimental results obtained during the investigation into plasma produced under effect of laser irradiation with q=10 to the 9th to 10 to the 11th W/sq cm on a target comprising adopted gases are presented. It is shown that the process of multicharge ion recharging on the gas neutral atom produces a notable effect on the formation of charge and energy state of multicomponent laser plasma. DOE

N89-17512# Edgerton, Germeshausen and Grier, Inc., Idaho Falls, ID.
SAFETY COMPARISON OF FUSION FUEL CYCLES
Sandra J. Brereton, John E. Massidda, and Mujid S. Kazimi (Massachusetts Inst. of Tech., Cambridge.) 1988 7 p Presented at the 8th Topical Meeting on Technology of Fusion Energy, Salt Lake City, UT, 9 Oct. 1988
(Contract DE-AC07-76ID-01570)
(DE89-005200; EGG-M-88257; CONF-881031-54) Avail: NTIS HC A02/MF A01

Potential safety advantages are achievable through the use of advanced fuel cycles, which eliminate the need to breed and fuel tritium, and produce fewer neutrons. In this work, the operational radiological hazards associated with the deuterium-tritium (DT), deuterium-deuterium (DD) and deuterium-helium-3 (DHe) fusion fuel cycles have been compared. The advanced fuels have a clear advantage over the DT fuel cycle in terms of tritium hazard. In terms of activation and waste disposal hazards, the operational safety advantages of the advanced fuels are less clear, and appear to be strongly material dependent. DOE

N89-17513# Texas Univ., Austin. Inst. for Fusion Studies.
THEORY OF NEOCLASSICAL RESISTIVITY-GRADIENT-DRIVEN TURBULENCE
O. J. Kwon, P. H. Diamond, and T. S. Hahm (Princeton Univ., NJ.) Dec. 1988 30 p Prepared in cooperation with General Atomics Technologies Corp., San Diego, CA
(Contracts DE-FG05-80ET-53088; DE-FG03-88ER-53275)
(DE89-005391; DOE/ET-53088/356; IFSR-356) Avail: NTIS HC A03/MF A01

It is shown that rippling instabilities can tap the density gradient expansion free energy source through the density dependence of the neoclassical resistivity. Linear analyses show that the region where neoclassical rippling modes are significantly excited extends from the edge of the plasma to the region where Nu sub *e less than or equal to 1. Since these modes are non-dispersive, diamagnetic effects are negligible in comparison to the nonlinear decorrelation rate at saturation. Thus, the relevant regime is the strong turbulence regime. The turbulent radial diffusivities of the temperature and the density are obtained as eigenvalues of the renormalized eigenmode equations at steady state. The density gradient acts to enhance the level of turbulence, compared to that driven by the temperature gradient alone. The saturated turbulent state is characterized by: current decoupling, the breakdown of Boltzmann relation, a radial mode scale of density fluctuations exceeding that of temperature fluctuations, implying

that density diffusivity exceeds temperature diffusivity, and that density fluctuation levels exceed temperature fluctuation levels. Magnetic fluctuation levels are negligible. DOE

N89-17514# Wisconsin Univ., Madison. Dept. of Physics.
BEHAVIOR OF THE REVERSED FIELD PINCH WITH NONIDEAL BOUNDARY CONDITIONS Ph.D. Thesis
Yung-Lung Ho Nov. 1988 73 p
(Contract DE-FG02-85ER-53212)
(DE89-005497; DOE/ER-53212/131) Avail: NTIS HC A04/MF A01

The linear and nonlinear magnetohydrodynamic stability of current-driven modes are studied for a reversed field pinch with nonideal boundary conditions. The plasma is bounded by a thin resistive shell surrounded by a vacuum region out to a radius at which a perfectly conducting wall is situated. The distant wall and the thin shell problems are studied by removing either the resistive shell or the conducting wall. Linearly, growth rates of tearing modes and kink modes are calculated by analytical solutions based on the modified Bessel function model for the equilibrium. The effects of variation of the shell resistivity and wall proximity on the growth rates are investigated. The modes that may be important in different parameter regimes and with different boundary conditions are identified. The nonlinear behaviors are studied with a three-dimensional magnetohydrodynamics code. The fluctuations generally rise with increasing distance between the conducting wall and the plasma. The enhanced fluctuation induced v x b electric field primarily oppose toroidal current; hence, loop voltage must increase to sustain the constant. Quasilinear interaction between modes typically associated with the dynamo action is identified as the most probable nonlinear destabilization mechanism. The helicity and energy balance properties of the simulation results are discussed. The interruption of current density along field lines intersecting the resistive shell is shown to lead to surface helicity leakage. This effect is intimately tied to stability, as fluctuation induced v x b electric field is necessary to transport the helicity to the surface. In this manner, all aspects of helicity balance, i.e., injection, transport, and dissipation, are considered self-consistently. The importance of the helicity and energy dissipation by the mean components of the magnetic field and current density is discussed. DOE

N89-17515# Wisconsin Univ., Madison. Plasma Physics Research.
STUDIES OF A POLOIDAL DIVERTOR REVERSED FIELD PINCH Ph.D. Thesis
John Stephen Sarff Nov. 1988 95 p
(Contract DE-FG02-85ER-53198)
(DE89-005498; DOE/ER-53198/130) Avail: NTIS HC A04/MF A01

Several attempts have been made to form a reversed field pinch (RFP) in a four-node, poloidal divertor configuration which positions the plasma far from a conducting wall. In this configuration, the plasma is localized within a magnetic separatrix formed by the combination of toroidal currents in the plasma and four, internal, conducting rings. These experiments were conducted on three devices: Tokapole II, the Wisconsin Levitated Octupole, and the modified Octupole with smaller conducting rings. Transient, RFP-like equilibria were obtained on Tokapole II and the Wisconsin Levitated Octupole. RFP-like equilibria with field reversal duration approximately 1 msec were obtained in the small ring Octupole. None of these plasmas was sustained against resistive magnetic diffusion. Local, internal measurements of the magnetic field in Tokapole II plasmas indicated the plasma current and density were mostly confined to the region inside the magnetic separatrix. The sharp drop in plasma pressure near the separatrix generated a large diamagnetic current in that region. Large magnetic perturbations observed in the startup phase of these plasmas. On the small ring Octupole, the perturbation was measured to have a dominant poloidal mode number of m = 1 and toroidal mode numbers n is approximately -5, i.e., internally resonant or nonresonant modes. This perturbation was stationary and was phase-locked to a magnetic field error. If the tenuous plasma region outside the separatrix is vacuum-like, then this behavior might represent current-driven instability owing to the lack of nearly, stabilizing boundary. Such instability is consistent with linear magnetohydrodynamic stability calculations and nonlinear simulations of a cylindrical REP plasma bounded by a large vacuum region and a distant conducting wall. DOE

76 SOLID-STATE PHYSICS

Includes superconductivity.

For related information, see also *33 Electronics and Electrical Engineering* and *36 Lasers and Masers.*

N89-17516# Illinois Univ., Urbana. Coordinated Science Lab.
MONTE CARLO STUDIES OF NONLINEAR ELECTRON TRANSPORT IN 3-5 SEMICONDUCTORS Ph.D. Thesis
Ki W. Kim 1988 133 p
(Contract N00014-84-C-0149)
(AD-A199700; UILU-ENG-88-2246) Avail: NTIS HC A07/MF A01 CSCL 20L

Electron transport in 3-5 semiconductors, especially the Ga/As/AlGaAs material systems, is studied in various nonequilibrium situations. Throughout the study, a Monte Carlo simulation method is used for the analysis of transport properties in the semiclassical Boltzmann transport picture. The present work essentially consists of two aspects. The first topic is hot electron transport in GaAs, focusing on the electron impact ionization effects. The dependence of impact ionization rates on the details of the band structure is investigated by using two (local and nonlocal) pseudopotential methods. The spatial evolution of the ionization rate and the average electron energy are studied in nonuniform fields characteristic of p+-n junctions. The effects of field fluctuations due to the random distribution of dopants are studied as well. The possibility of new GaAs electron-emitting diodes is explored numerically and compared with the corresponding Si devices. The second aspect deals with the effects of conduction band discontinuities on the electron transport. In particular, one-dimensional heterostructures are modeled to study the nonlinear transport across heterointerfaces. GRA

N89-17517# Naval Postgraduate School, Monterey, CA.
MONTE CARLO CALCULATION OF ELECTRON MULTIPLE SCATTERING IN THIN FOILS M.S. Thesis
Daniel C. Jensen Jun. 1988 89 p
(AD-A199872) Avail: NTIS HC A05/MF A01 CSCL 20H

The electron photon transport code ITS has many applications in the physics and medical industries. The code was originally intended for the use in determining particle transport in think materials. The code breaks down for very thin targets because the multiple scattering approximation used to determine the electron deflection angles for thin steps is inadequate. A method of correction has been developed by Tom Jordan and Joseph Mack which combines a small angle approximation theory to the multiple scattering and an explicit large angle treatment based on a Poisson distribution. This method has been validated against several experiments with great success. The multiple scattering theory of Moliere has also been incorporated into a correction scheme and shows good agreement with experimental data. GRA

N89-17518# California Univ., Berkeley. Lawrence Berkeley Lab. Materials and Chemical Scirences Div.
BREAKDOWN VOLTAGE MAPPING OF IMPURITY CONCENTRATIONS IN GaAs WAFERS M.S. Thesis
David Emory Bliss Apr. 1988 62 p Prepared in cooperation with California Univ., Berkeley.
(Contract DE-AC03-76SF-00098)
(DE89-002489; LBL-26035) Avail: NTIS HC A04/MF A01

Using a modified x-y plotter, spatially resolved breakdown voltage measurements were obtained for a variety of GaAs materials. Breakdown voltage values were calibrated against net impurity concentration using C-V measurements. Spatially resolved

Hall effect measurements on GaAs doped with Si correlated well with a breakdown voltage map of the impurity concentration. The technique provides a quick means for determining doping uniformity in epitaxial films and implanted layers as well as dopant incorporation rates in bulk crystals. An inverse correlation between etch pit density and breakdown voltage is shown for LEC wafers. DOE

N89-17519# Oak Ridge National Lab., TN. Solid State Div.
THE ANNEALING BEHAVIOR OF ION-IMPLANTED SINGLE CRYSTALS OF THE TYPE YBa2Cu3O(SUB x)
J. C. McCallum, C. W. White, and L. A. Boatner Sep. 1988 14 p Presented at the International Conference on the Application of Accelerators in Research and Industry, Denton, TX, 7 Nov. 1988
(Contract DE-AC05-84OR-21400)
(DE89-002189; CONF-881151-24) Avail: NTIS HC A03/MF A01

Recent measurements have shown that the structural disorder induced by the implantation of ions into high-T sub c superconducting oxides of the type YBa2Cu3O sub chi can lead to significant decomposition of the implanted region during subsequent thermal processing. We have used Rutherford backscattering spectrometry and ion channeling to examine the effects of ion implantation and thermal annealing on the near-surface composition of these materials. Our results indicate that the decomposition of the implanted region of YBa2Cu3O sub chi single crystals is associated with Ba migration and occurs for ion doses above a definite threshold when thermal anneals are carried out at temperatures greater than 500 degrees C in a variety of atmospheres (O2, O2 + H2O, Ar). Importantly, we have also observed that the implanted crystals can be annealed in O2 at a temperature of 850 C with little decomposition of the implanted region occurring and that, under these conditions, the implantation-induced disorder is substantially removed. DOE

N89-17520# Brookhaven National Lab., Upton, NY.
ORIENTATION DEPENDENT X-RAY ABSORPTION IN HIGH T (SUB c) SUPERCONDUCTORS
S. M. Heald, J. M. Tranquada, C. Y. Yang, Youwen Xu, A. R. Moodenbaugh, M. A. Subramanian, and A. W. Sleight 1988 3 p Presented at the 5th International Conference on X-ray Absorption Fine Structure, Seattle, WA, 21 Aug. 1988 Prepared in cooperation with Du Pont de Nemours (E. I.) and Co., Wilmington, DE
(Contracts DE-AC02-76CH-00016; DE-AS05-80ER-10742)
(DE89-002910; BNL-41817; CONF-8808149-3) Avail: NTIS HC A02/MF A01

Orientation dependent X-ray absorption measurements have been on a number of high-T sub c superconductors using powders oriented in a magnetic field. Both the near edge and EXAFS show a strong orientation dependence which has proven very useful in understanding these anisotropic materials. DOE

N89-17521# Oak Ridge National Lab., TN.
HOPPING MODEL FOR THE NON-DEBYE DIELECTRIC RESPONSE IN IONIC CRYSTALS
J. C. Wang and J. B. Bates Oct. 1988 7 p Presented at the Fall Meeting of the Materials Research Society, Boston, MA, 28 Nov. 1988 Submitted for publication
(Contract DE-AC05-84OR-21400)
(DE89-003151; CONF-881155-7) Avail: NTIS HC A02/MF A01

A model based on ion hopping in potential double-wells is proposed to explain the non-Debye dielectric response in solids. Relying on some assumptions, an attempt is made to remove the average nature of previous diffusion theories. This results in a distribution of activation energies, G(E), which decays exponentially on both sides of some given value E(sub o). It is shown that the existence of a dielectric loss peak is a result of the decay of G(E) for E greater than E(sub o), the constant-phase-angle behavior above the loss peak is associated with the decay of G(E) for E less than E (sub o), and G(E) can produce all the main features of the empirical Havriliak-Negami function. An interesting property of this G(E) is that it broadens with increasing temperature, consistent with many experimental observations. DOE

N89-17522# Naval Research Lab., Washington, DC.
FRACTAL AND SPHERULITIC MORPHOLOGY OF SILICON NITRIDE CRYSTALLIZED FROM AMORPHOUS FILMS
A. D. Kahn, K. S. Grabowski, E. P. Donovan, C. A. Carosella, G. K. Hubler, and K. K. Christenson (Illinois Univ., Urbana.) 1988 16 p
(AD-A200158) Avail: NTIS HC A03/MF A01 CSCL 11B

Thin films of substoichiometric silicon nitride were grown by the use of ion beam assisted deposition. The amorphous films were annealed at high temperatures (1017 to 1200C) to produce crystalline alpha-Si3N4. Both highly symmetric spherulitic crystal morphologies and irregular fractal aggregates were seen. In the latter case, a fractal dimension of 1.2 was measured. These two macroscopically different forms possessed correspondingly different microstructures. The morphologies were found to be determined by the temperature of the anneal. GRA

N89-17523# EPI-Tech Corp., Paradise Valley, AZ.
GROWTH OF GALLIUM ARSENIDE USING ION CLUSTER BEAM TECHNOLOGY, VOLUME 1, PHASE 2 Final Report, Feb. 1984 - Nov. 1987
Robert L. Adams and James M. Bennett Sep. 1988 89 p
(Contract F33615-84-C-1562)
(AD-A200231; AFWAL-TR-88-1055-Vol-1) Avail: NTIS HC A05/MF A01 CSCL 07B

This program was designed to study the feasibility of growing epitaxial GaAs thin films for subsequent application in electronic devices. Due to mechanical difficulties and design problems the technique of deposition via ionized clusters was not realized. Data collected is somewhat inconclusive. To answer the feasibility question further, work including modification of the hardware needs to be performed. To this point the techniques have been shown to be capable of growing single crystal GaAs, but the required electrical characteristics of the film are not present. GRA

N89-17524# State Univ. of New York, Stony Brook. Dept. of Physics.
MILLIMETER WAVE GENERATION USING JOSEPHSON JUNCTION ARRAYS Final Scientific Report, 1 May 1985 - 30 Jun. 1988
James E. Lukens 31 Jul. 1988 8 p
(Grant AF-AFOSR-0205-85; AF Proj. 2305)
(AD-A200259; AFOSR-88-1052TR) Avail: NTIS HC A02/MF A01 CSCL 09A

Studies have been carried out to develop methods to couple Josephson junction oscillators at frequencies near 100 GHz so as to demonstrate the feasibility of Josephson effect sources of reasonable power and impedance. Phase-locking of junctions separated by greater than a wavelength and coupled through microstrip line has been demonstrated and found in accord with theory. Forty junction arrays operating at 100 GHz and 350 GHz using this phase-locking scheme have been tested. Both series and parallel biasing of the junctions have been tested. It has been established that a total critical current spread of less than 10 percent is required for complete phase-locking with series bias. For parallel biased arrays with a critical current spread of 20 percent, all junctions locked in-phase providing coherent addition of power to the 20 Ohm load. GRA

N89-17525# Massachusetts Inst. of Tech., Cambridge. Dept. of Materials Science and Engineering.
INVESTIGATION OF DEFECT AND ELECTRONIC INTERACTIONS ASSOCIATED WITH GaAs DEVICE PROCESSING Annual Report, 28 Feb. 1987 - 29 Feb. 1988
Jacek Lagowski and Harry C. Gatos 1 Aug. 1988 37 p
(Grant AF-AFOSR-0342-86; AF Proj. 2306)
(AD-A200541; AFOSR-88-1125TR) Avail: NTIS HC A03/MF A01 CSCL 07B

Our research in the period Feb. 28, 1987 to Feb. 29, 1988

resulted in five publications enclosed with this report and two completed Ph.D. theses. The research focussed on the properties of low diffusivity transition elements and their direct role (compensating levels) and indirect role (impurity gettering) in achieving semi-insulating III-V compounds. The results of our systematic study on optical and electronic properties of vanadium in GaAs were summarized in a detailed publication. A similar publication, dealing with properties of titanium, is under preparation. Our study established the positions of the energy levels of substitutional Vanadium and Titanium (both donor and acceptor states) and concluded that they are not suitable for achieving semi-insulating GaAs. In Inp, however, the deep Ti donor level (Ti4+/Ti3+) has an ideal location (0.63 eV below the conduction band) for producing a new type of semi-insulating Inp based on codoping with Ti and shallow acceptors. In spite of wrong energy level positions, the vanadium was found to be beneficial for obtaining semiinsulating GaAs. GRA

N89-17526# California Univ., Berkeley. Lawrence Berkeley Lab.
NEW Al-Ni-Ge CONTACTS ON GaAs: THEIR STRUCTURE AND ELECTRICAL PROPERTIES
Z. Liliental-Weber, J. Washburn, C. Musgrave, E. R. Weber, R. Zuleeg, W. V. Lampert, and T. W. Haas Mar. 1988 9 p Presented at the Spring Meeting of the Materials Research Society, Reno, NV, 4 Apr. 1988 Prepared in cooperation with California Univ., Berkeley; Air Force Wright Aeronautical Labs., Wright-Patterson AFB, OH
(Contract DE-AC03-76SF-00098)
(DE89-002918; LBL-25113; CONF-880408-41) Avail: NTIS HC A02/MF A01

The structure and composition of the recently developed Al-Ni-GE ohmic contacts to n-GaAs were investigated by transmission electron microscopy combined with secondary ion mass spectroscopy (SIMS) and Auger spectroscopy. The semiconductor/metal-alloy interface of these contacts remain very flat after annealing (500 C for 1 min - contact resistance 1.4 times 10 (-6) omega square cm), in contrast to the widely used Au-Ni-Ge contacts. The metal sequence during deposition is found to be a critical factor in determining the electrical contact properties and the dispersion of the oxide layer on the semiconductor surface after chemical cleaning. Ge doping of the GaAs beneath the contact layer was observed by SIMS, and a tunneling mechanism through the N+GaAs:Ge layer was proposed to explain the ohmic properties of the contacts. DOE

N89-17527# Salerno Univ. (Italy). Dipt. di Fisica.
A SIMPLE METHOD FOR PREPARING SUPERCONDUCTING HIGH T(SUB c) THIN FILMS
P. Romano, A. Nigro, R. Vaglio, E. Signorelli, and K. E. Gray Aug. 1988 4 p Presented at the Applied Superconductivity Conference, San Francisco, CA, 21-25 Aug. 1988 Prepared in cooperation with Consiglio Nazionale delle Ricerche, Cinisello Balsamo (Italy); Argonne National Lab., IL
(Contract W-31-109-eng-38)
(DE89-003663; CONF-880812-28) Avail: NTIS HC A02/MF A01

High quality superconducting thin films of the high Tc compound YBa2Cu3O7 have been prepared on sapphire using a new, simple method that combines d.c. magnetron sputtering from a single target and evaporation from a heated source. The method should be especially suitable for depositing thin films on complex surfaces. YBa2Cu3O7 (delta) films with Tc=92K (onset) were prepared using an YCu3 target and evaporating barium by a specially designed, feedback controlled, molybdenum heater using both pure barium or a barium-aluminum alloy. The films were characterized by X-rays, Electron Dispersion Spectroscopy and other techniques. DOE

N89-17528# Brookhaven National Lab., Upton, NY.
INTERACTION OF CO, CO2 AND H2O WITH Ba AND YBa2Cu3O7
S. L. Qiu, C. L. Lin, M. W. Ruckman, J. Chen, D. H. Chen, Y. W. Xu, A. R. Moodenbaugh, Myron Strongin, D. Nichols, and J. E. Crow (Temple Univ., Philadelphia, PA.) 1988 8 p Presented at the 35d National Vacuum Symposium and 4th International Laser Science Conference, Atlanta, GA, 2 Oct. 1988
(Contract DE-AC02-76CH-00016)
(DE89-003160; BNL-41917; CONF-881002-25) Avail: NTIS HC A02/MF A01

Photoemission from high Tc superconductors crucially depends on surface stoichiometry as well as the interaction of impurities with the reactive surface. In this paper we discuss the photoemission spectra of clean YBa2Cu3O7 and YBa2Cu3O sub 6.25 as well as the spectra after the interaction of CO, CO2 and H2O with both the high Tc 1-2-3 compound and Ba metal. DOE

N89-17529# Argonne National Lab., IL. Materials Science Div.
STUDIES OF NiO METAL INTERFACES
Karl L. Merkle and Beiling Shao May 1988 6 p Presented at the Spring Meeting of the Materials Research Society, Reno, NV, 4 Apr. 1988
(Contract W-31-109-eng-38)
(DE89-003634; CONF-880408-42) Avail: NTIS HC A02/MF A01

Transmission electron microscopy techniques were applied to investigate the structure of interfaces between noble metals and NiO. Interfaces between NiO and Pt or Cu were formed by diffusion bonding. NiO and Cu form aligned lattices, while no unique topotactical relationship was found for the NiO-Pt interfaces. Internal reduction of (Ni, Cu)O was also used to investigate NiO-Cu interfaces at polyhedral Cu precipitates in a NiO matrix. The morphology and compositions of precipitates was studied for several reduction treatments. The formation of largely (111) interfaces during solid state reduction suggests that these planes of densest packing are associated with the lowest interfacial free energy. The quite large lattice mismatch is accommodated by misfit dislocations as observed by HREM. DOE

N89-17530*# National Aeronautics and Space Administration. Marshall Space Flight Center, Huntsville, AL.
PROCESSING OF STRONG FLUX TRAPPING HIGH T(SUBc) OXIDE SUPERCONDUCTORS: CENTER DIRECTOR'S DISCRETIONARY FUND Final Report
M. K. Wu, C. A. Higgins, P. T. Leong, H. Chou, B. H. Loo, P. A. Curreri, P. N. Peters, R. C. Sisk, C. Y. Huang, and Y. Shapira (Massachusetts Inst. of Tech., Cambridge.) Jan. 1989 16 p
(NASA-TM-100350; NAS 1.15:100350) Avail: NTIS HC A03/MF A01 CSCL 20L

Magnetic suspension effect was first observed in samples of YBa2Cu3O7/AgO(Y-123/AgO) composites. Magnetization measurements of these samples show a much larger hysteresis which corresponds to a large critical current density. In addition to the Y-123AgO composites, recently similar suspension effects in other RE-123/AgO, where RE stands for rare-Earth elements, were also observed. Some samples exhibit even stronger flux pinning than that of the Y-123/AgO sample. An interesting observation was that in order to form the composite which exhibits strong flux trapping effect the sintering temperature depends on the particular RE-123 compound used. The paper presents the detailed processing conditions for the formation of these RE-123/AgO composites, as well as the magnetization and critical field data. Author

N89-17531# China Nuclear Information Centre, Beijing.
STUDY OF STRUCTURE OF HIGH-Tc SUPERCONDUCTOR Y(YV)Ba2Cu3O(SUB 9-x) AND ITS RESISTANCE SHARP DROP
Jiemo Tian, Baoqing Zhang, Lingling Wang, Xiaming Dai, Jialong Wang, and Guangguo Pan (Tsinghua Univ., Beijing, China) Dec. 1987 10 p In CHINESE
(DE88-704104; CNIC-00126; TSHUNE-0002) Avail: NTIS (US Sales Only) HC A02/MF A01

This paper describes the crysal structure of the high-Tc superconductor YBa(sub 2)Cu(sub 3)O(sub 9-x). X-ray diffraction spectra and transmission electron diffraction patterns show that single phase YBa(sub 2)Cu(sub 3)O(sub 9-x) (orthorhombic cell a = 382.95 pm; b = 388.22 pm; c = 1165.95 pm) can change

into the multiphase compound with oxygen content increase. The new high-Tc superconductor Ba(sub 2)(YV)(sub 1)Cu(sub 3)O(sub 9-x) was investigated. The resistance measurements show that its onset of transition is 118 K, the resistive midpoint of transition is 97 K, and there is zero resistance at 93 K with Tc = 2 K. And, superconductivities of Ba(sub 2)(YV)(sub 1)Cu(sub 3)O(sub 9-x) system were studied in detail. This paper gives the crystal structure of Ba(sub 2)(YV)(sub 1)Cu(sub 3)O(sub 9-x) with X-ray diffractions. The resistance sharp drops of YBa(sub 2)Cu(sub 3)O(sub 9-x) at 190 K and 240 K were found. The changes of transmission electron diffraction patterns indicate the phase change has occurred at about 220 K, and its crystal parameters change obviously. DOE

N89-17532# Sandia National Labs., Albuquerque, NM.
CHARACTERISTICS OF LIFT-OFF FABRICATED AlGaAs/InGaAs SINGLE-STRAINED-QUANTUM-WELL STRUCTURES ON GLASS AND SILICON SUBSTRATES
J. F. Klem, E. D. Jones, D. R. Myers, and J. A. Lott 1988 7 p Presented at the International Symposium on Gallium-Arsenide and Related Compounds, Atlanta, GA, 11 Sep. 1988
(Contract DE-AC04-76DP-00789)
(DE89-001374; SAND-88-2588C; CONF-8809152-4) Avail: NTIS HC A02/MF A01

A technique involving the liftoff of thin (approx 1 micron) III-V structures grown on GaAs substrates and subsequent bonding to glass or SiO2 -covered Si substrates has been investigated. AlGaAs/InGaAs/GaAs single-strained-quantum-well structures have been grown by molecular beam epitaxy and characterized before and after lift-off and bonding to foreign substrates. X-ray diffraction measurements were performed to determine the strain state of the films over a wide temperature range after bonding. Low-temperature photoluminescence measurements on 125-A-well undoped structures show that the narrow linewidths observed in the as-grown samples (approx 4 MeV) are not broadened by the lift-off and bonding process. Room- and low-temperature dc measurements made on modulation-doped field-effect transistors show that electronic transport properties are not adversely affected by this process. DOE

N89-17533# Sandia National Labs., Albuquerque, NM.
OXYGEN AND COPPER VALENCIES IN OXYGEN-DOPED SUPERCONDUCTING La2CuO(SUB 4.13)
N. D. Shinn, J. W. Rogers, Jr., J. E. Schirber, E. L. Venturini, D. S. Ginley, and B. Morosin 1988 8 p Presented at the 35th National Vacuum Symposium and 4th International Laser Science Conference, Atlanta, GA, 2 Oct. 1988
(Contract DE-AC04-76DP-00789)
(DE89-003265; SAND-88-2261C; CONF-881002-24) Avail: NTIS HC A02/MF A01

Oxygen enrichment of La2CuO4 by a high-temperature and high-pressure (1--3 kbar at 875K) treatment produces a stable, bulk superconductor, La2CuO(sub 4.13) (T sub c approx. 30K). Annealing in vacuum above 350K depletes the excess oxygen from La2CuO(sub 4.13) as O2(g), eliminates the superconductivity, and results in semiconducting La2CuO4. These annealed samples were subsequently recharged with oxygen, thereby reversibly restoring the bulk superconductivity. X-ray photoelectron spectroscopy has been used to identify the oxygen and copper valencies which correlate with the bulk superconductivity in this interstitially-oxygen-doped perovskite material. An XPS O(1s) binding energy of 532.1 eV is measured for the excess oxygen which, with additional analytical and quantitative magnetization data, indicates that the predominant excess oxygen species is a superoxide ion (O sup-2). The angular dependence of the O(1s) peak intensity indicates a near-surface concentration enrichment of the superoxide species. The majority copper valency is Cu(II) with a Cu(2p) binding energy of 933.0 + or - 0.1 eV; however, evidence for a minority Cu(III) species with a Cu(2p) binding energy of 934.4 + or - 0.2 eV is found only in the superconducting, oxygen-enriched material. DOE

N89-17534# Lawrence Livermore National Lab., CA.
PHASES AND MICROSTRUCTURES OF CARBON-IMPLANTED NIOBIUM
J. S. Huang, R. G. Musket, and M. A. Wall Nov. 1988 6 p Presented at the Fall Meeting of the Materials Research Society, Boston, MA, 28 Nov. 1988
(Contract W-7405-eng-48)
(DE89-004017; UCRL-99977; CONF-881155-14) Avail: NTIS HC A02/MF A01

Polycrystalline niobium was implanted with 200, 100, and 50 keV carbon ions to create a uniform distribution of carbon over a thickness of about 0.25 micron. Samples implanted with calculated carbon content of 0.6, 1.9, 5.8, and 16 atomic percent were prepared, and the uniformity of the carbon distribution with depth was confirmed by Auger electron spectroscopy analysis. Glancing-angle X-ray diffraction analysis and transmission electron microscopy were used to characterize the phases and microstructures formed. The results indicated that no detectable second phases were present except on the surfaces where an amorphous phase and many particles were formed from contamination. Despite the low equilibrium solubility limit of carbon in Nb, we have created metastable solid solutions of Nb and C with carbon contents as high as 16 at. percent. DOE

N89-17535*# National Aeronautics and Space Administration. Marshall Space Flight Center, Huntsville, AL.
PROTEIN CRYSTAL NUCLEATION KINETICS USING RELATIVE LIGHT-SCATTERING TECHNIQUES: CENTER DIRECTOR'S DISCRETIONARY FUND Final Report
Marc Lee Pusey Jan. 1989 15 p
(NASA-TM-100348; NAS 1.15:100348) Avail: NTIS HC A03/MF A01 CSCL 20L

Light-scattering intensity measurements are a sensitive method for following changes in the hydrodynamic radius of particles in solution. The approach used in this report utilizes the light-scattering intensity ratios of a polydisperse to a monodisperse system. By numerically modeling the process, and fitting the model curves to the data, estimates have been obtained for the dimerization equilibrium constant, the dimer + dimer yields tetramer equilibrium constant, and the association rate constant for the dimerization process. Author

N89-17103# IBM Watson Research Center, Yorktown Heights, NY.
NONEQUILIBRIUM PHONONS AND DISORDER IN Al(SUB x)Ga(SUB 1-x)As
J. A. Kash, J. C. Tsang, and S. S. Jha *In* Optical Society of America, Topical Meeting on Picosecond Electronics and Optoelectronics 10 Oct. 1987 p 76-7 (For primary document see N89-17080 09-33)
Avail: NTIS HC A10/MF A01 CSCL 20L

N89-17106# IBM Watson Research Center, Yorktown Heights, NY.
CARRIER LIFETIME VERSUS ION-IMPLANTATION DOSE IN SILICON ON SAPPHIRE
F. E. Doany, D. Grischkowsky, and C.-C. Chi *In* Optical Society of America, Topical Meeting on Picosecond Electronics and Optoelectronics 10 Oct. 1987 p 86-8 Sponsored in part by ONR, Washington, D.C. (For primary document see N89-17080 09-33)
Avail: NTIS HC A10/MF A01 CSCL 20L

N89-17109# Rochester Univ., NY. Lab. for Laser Energetics.
A TECHNIQUE FOR WING SUPPRESSED IR SAMPLING
John Nees and Steve Williamson *In* Optical Society of America, Topical Meeting on Picosecond Electronics and Optoelectronics 10 Oct. 1987 p 95-9 (For primary document see N89-17080 09-33)
Avail: NTIS HC A10/MF A01 CSCL 20L

N89-17114# Hewlett-Packard Co., Palo Alto, CA.
InP/GaInAs/InP PIN PHOTODIODE WITH FWHM LESS THAN 18 ps
S. Y. Wang, K. W. Carey, and B. H. Kolner *In* Optical Society of America, Topical Meeting on Picosecond Electronics and Optoelectronics 10 Oct. 1987 p 110-112 (For primary document see N89-17080 09-33)
Avail: NTIS HC A10/MF A01 CSCL 20L

N89-17118# Bell Telephone Labs., Inc., Murray Hill, NJ.
DIRECT SUBPICOSECOND MEASUREMENT OF CARRIER MOBILITY OF PHOTOEXCITED ELECTRONS IN GaAs
M. C. Nuss and D. H. Auston *In* Optical Society of America, Topical Meeting on Picosecond Electronics and Optoelectronics 10 Oct. 1987 p 126-128 (For primary document see N89-17080 09-33)
Avail: NTIS HC A10/MF A01 CSCL 20L

N89-17119# Illinois Univ., Urbana. Dept. of Electrical and Computer Engineering.
NON-STATIONARY TRANSPORT IN MODFETS AND HETEROJUNCTION DEVICES Abstract Only
K. Hess *In* Optical Society of America, Topical Meeting on Picosecond Electronics and Optoelectronics 10 Oct. 1987 p 129 (For primary document see N89-17080 09-33)
Avail: NTIS HC A10/MF A01 CSCL 20L

N89-17120# Arizona State Univ., Tempe. Center for Solid State Electronics Research.
MONTE CARLO INVESTIGATION OF HOT PHOTOEXCITED ELECTRON RELAXATION IN GaAs
M. A. Osman, M. J. Kann, D. K. Ferry, and P. Lugli (Modena Univ., Italy) *In* Optical Society of America, Topical Meeting on Picosecond Electronics and Optoelectronics 10 Oct. 1987 p 133-135 Sponsored in part by ONR, Washington, D.C. (For primary document see N89-17080 09-33)
Avail: NTIS HC A10/MF A01 CSCL 20L

N89-17121# Texas Univ., Austin. Dept. of Physics.
LONGITUDINALLY LOCALIZED OPTICAL CARRIER INJECTION FOR FEMTOSECOND TRANSPORT STUDIES
M. C. Downer, D. H. Reitze, and T. R. Zhang *In* Optical Society of America, Topical Meeting on Picosecond Electronics and Optoelectronics 10 Oct. 1987 p 133-135 Sponsored in part by the Joint Services Electronics Program and the Texas Advanced Technology Research Program (For primary document see N89-17080 09-33)
Avail: NTIS HC A10/MF A01 CSCL 20L

N89-17122# Massachusetts Inst. of Tech., Cambridge. Dept. of Electrical Engineering.
FEMTOSECOND NONEQUILIBRIUM ELECTRONIC HEAT TRANSPORT IN THIN GOLD FILMS
S. D. Brorson, J. G. Fujimoto, and E. P. Ippen *In* Optical Society of America, Topical Meeting on Picosecond Electronics and Optoelectronics 10 Oct. 1987 p 136-138 (For primary document see N89-17080 09-33)
(Contract DAAL03-86-K-0002; AF-AFOSR-0213-85)
Avail: NTIS HC A10/MF A01 CSCL 20L

N89-17123# IBM Watson Research Center, Yorktown Heights, NY.
BALLISTIC TRANSPORT AND HOT ELECTRON SPECTROSCOPY IN TUNNELLING HOT ELECTRON TRANSFER AMPLIFIER (THETA)
M. Heiblum *In* Optical Society of America, Topical Meeting on Picosecond Electronics and Optoelectronics 10 Oct. 1987 p 140-142 (For primary document see N89-17080 09-33)
Avail: NTIS HC A10/MF A01 CSCL 20L

N89-17124*# Massachusetts Inst. of Tech., Lexington. Lincoln Lab.
MICROWAVE AND MILLIMETER-WAVE RESONANT TUNNELING DIODES
T. C. L. Gerhard Sollner, Elliott R. Brown, and W. D. Goodhue *In* Optical Society of America, Topical Meeting on Picosecond Electronics and Optoelectronics 10 Oct. 1987 p 143-145 Sponsored by the Army Research Office, Washington, D.C. and NASA, Washington, D.C. (For primary document see N89-17080 09-33)
Avail: NTIS HC A10/MF A01 CSCL 20L

N89-17125# Texas Instruments, Inc., Dallas.
QUANTUM TRANSPORT CALCULATION OF RESONANT-TUNNELING RESPONSE TIME
William R. Frensley *In* Optical Society of America, Topical Meeting on Picosecond Electronics and Optoelectronics 10 Oct. 1987 p 146-148 Sponsored by ONR, Washington, D.C. and the Army Research Office, Washington, D.C. (For primary document see N89-17080 09-33)
Avail: NTIS HC A10/MF A01 CSCL 20L

N89-17126# Bell Telephone Labs., Inc., Murray Hill, NJ.
RESONANT TUNNELING ELECTRON SPECTROSCOPY
F. Capasso, S. Sen, A. Y. Cho, and A. L. Hutchinson *In* Optical Society of America, Topical Meeting on Picosecond Electronics and Optoelectronics 10 Oct. 1987 p 149-152 (For primary document see N89-17080 09-33)
Avail: NTIS HC A10/MF A01 CSCL 20L

N89-17127# Ecole Polytechnique, Palaiseau (France).
HIGH-SPEED PHENOMENA IN GaAs MULTIPLE-QUANTUM-WELLS
A. Mysyrowicz, D. Hulin, A. Migus, A. Antonetti, H. M. Gibbs, N. Peyghambarian, and H. Morkoc (Illinois Univ., Urbana-Champaign.) *In* Optical Society of America, Topical Meeting on Picosecond Electronics and Optoelectronics 10 Oct. 1987 p 156-158 (For primary document see N89-17080 09-33)
Avail: NTIS HC A10/MF A01 CSCL 20L

N89-17128# Bell Telephone Labs., Inc., Holmdel, NJ.
PICOSECOND CARRIER TRANSPORT IN GaAs QUANTUM WELLS
Jagdeep Shah and R. A. Hopfel *In* Optical Society of America, Topical Meeting on Picosecond Electronics and Optoelectronics 10 Oct. 1987 p 159-161 (For primary document see N89-17080 09-33)
Avail: NTIS HC A10/MF A01 CSCL 20L

N89-17129# Bell Telephone Labs., Inc., Holmdel, NJ.
QUANTUM-CONFINED STARK EFFECT IN InGaAs/InP QUANTUM WELLS GROWN BY METAL-ORGANIC CHEMICAL VAPOR DEPOSITION
I. Bar-Joseph, C. Klingshirn, D. A. B. Miller, D. S. Chemia, U. Koren, and B. I. Miller *In* Optical Society of America, Topical Meeting on Picosecond Electronics and Optoelectronics 10 Oct. 1987 p 162-165 (For primary document see N89-17080 09-33)
Avail: NTIS HC A10/MF A01 CSCL 20L

N89-17130# Bell Telephone Labs., Inc., Holmdel, NJ.
DYNAMICS OF BELOW-GAP PHOTOEXCITATION IN GaAs QUANTUM WELLS
J. E. Zucker, A. VonLehmen, D. S. Chemia, and J. P. Heritage (Bell Communications Research, Inc., Red Bank, NJ.) *In* Optical Society of America, Topical Meeting on Picosecond Electronics and Optoelectronics 10 Oct. 1987 p 166-168 (For primary document see N89-17080 09-33)
Avail: NTIS HC A10/MF A01 CSCL 20L

77 THERMODYNAMICS AND STATISTICAL PHYSICS

Includes quantum mechanics; theoretical physics; and Bose and Fermi statistics.

For related information see also *25 Inorganic and Physical Chemistry* and *34 Fluid Mechanics and Heat Transfer.*

N89-17536# International Centre for Theoretical Physics, Trieste (Italy).

SUPERSYMMETRIC INSTANTONS AND TOPOLOGICAL QUANTUM FIELD THEORY

Danny Birmingham, Mark Rakowski, and George Thompson May 1988 8 p

(DE88-704211; IC-88/100) Avail: NTIS (US Sales Only) HC A02/MF A01

We present an action which generates the supersymmetric self-dual equations corresponding to Euclidean super Yang-Mills theory in four dimensions. By adding additional constraint fields with new local symmetries, the classical equations of this system are the usual super self-dual equations when a gauge is chosen for the constraint fields. This construction is a supersymmetric generalization of the Labastida-Pernici action which corresponds to a gauge unfixed version of Witten's topological quantum field theory. We discuss some topological prospects for this model, and the role of supersymmetric instantons in Donaldson Theory. DOE

N89-17537# International Centre for Theoretical Physics, Trieste (Italy).

GEOMETRY ON THE SPACE OF GEOMETRIES

T. Christodoulakis and J. Zanelli Jun. 1988 20 p

(DE88-704214; IC-88/103) Avail: NTIS (US Sales Only) HC A03/MF A01

We discuss the geometric structure of the configuration space of pure gravity. This is an infinite dimensional manifold, M, where each point represents one spatial geometry g(sub ij) (x). The metric on M is dictated by geometrodynamics, and from it, the Christoffel symbols and Riemann tensor can be found. A free geometry tracing a geodesic on the manifold describes the time evolution of space in the strong gravity limit. In a regularization previously introduced by the authors, it is found that M does not have the same dimensionality, D, everywhere, and that D is not a scalar, although it is covariantly constant. In this regularization, it is seen that the path integral measure can be absorbed in a renormalization of the cosmological constant. DOE

N89-17538# Connecticut Univ., Storrs.

INVESTIGATIONS IN PARTICLE AND FIELD THEORY

Progress Report, 1 Dec. 1986 - 30 Nov. 1988

K. Haller, M. M. Islam, P. D. Mannheim, and D. G. Caldi 1988 17 p

(Contract DE-AC02-79ER-10336)

(DE89-003004; DOE/ER-10336/8) Avail: NTIS HC A03/MF A01

Progress for the period December 1, 1986 - November 30, 1988 is reported in various aspects of particle and field theory. The implications for future research are discussed. The work described includes investigations into topological features and the dynamics of gauge theory, lattice gauge theory, nucleon structure, novel spontaneous symmetry breaking modes, and general relativity and cosmology. DOE

N89-17539# Brookhaven National Lab., Upton, NY. Physics Dept.

LATTICE GAUGE THEORIES AND MONTE CARLO ALGORITHMS

Michael Creutz Oct. 1988 35 p Presented at the 14th GIFT International Seminar on Theoretical Physics, Jaca, Spain, 6 Jun. 1988

(Contract DE-AC02-76CH-00016)

(DE89-003569; BNL-42028; CONF-8806279-1) Avail: NTIS HC A03/MF A01

Lattice gauge theory has become the primary tool for non-perturbative calculations in quantum field theory. These lectures review some of the foundations of this subject. The first lecture reviews the basic definition of the theory in terms of invariant integrals over group elements on lattice bonds. The lattice represents an ultraviolet cutoff, and renormalization group arguments show how the bare coupling must be varied to obtain the continuum limit. Expansions in the inverse of the coupling constant demonstrate quark confinement in the strong coupling limit. The second lecture turns to numerical simulation, which has become an important approach to calculating hadronic properties. Here I discuss the basic algorithms for obtaining appropriately weighted gauge field configurations. The third lecture turns to algorithms for treating fermionic fields, which still require considerably more computer time than needed for purely bosonic simulations. Some particularly promising recent approaches are based on global accept-reject steps and should display a rather favorable dependence of computer time on the system volume. DOE

N89-17540*# California Univ., Santa Barbara. Inst. for Theoretical Physics.

IS THE GREAT ATTRACTOR REALLY A GREAT WALL

Albert Stebbins and Michael S. Turner Nov. 1988 8 p Sponsored by NASA, Washington, DC and DOE, Washington, DC Prepared in cooperation with Toronto Univ., Ontario, Chicago Univ., IL and Fermi National Accelerator Lab., Batavia, IL

(NASA-CR-184772; NAS 1.26:184772; FERMILAB-Pub-88/170-A) Avail: NTIS HC A02/MF A01 CSCL 20C

Some of the cosmological consequences are discussed of a late time phase transition which produces light domain walls. The observed peculiar velocity field of the Universe and the observed isotropy of the microwave background radiation severely constrain the wall surface density in such a scenario. The most interesting consequence of such a phase transition is the possibility that the local, coherent streaming motion reported by the Seven Samurai could be explained by the repulsive effect of a relic domain wall with the Hubble volume (the Great Wall). Author

N89-17541# Pacific Northwest Labs., Richland, WA.

A REVIEW OF SECOND LAW TECHNIQUES APPLICABLE TO BASIC THERMAL SCIENCE RESEARCH

M. Kevin Drost and Joseph R. Zamorski Nov. 1988 13 p Presented at the American Institute of Mechanical Engineers Meeting, Chicago, IL, 25 Sep. 1988

(Contract DE-AC06-76RL-01830)

(DE89-004356; PNL-SA-15524; CONF-8809201-1) Avail: NTIS HC A03/MF A01

This paper reports the results of a review of second law analysis techniques which can contribute to basic research in the thermal sciences. The review demonstrated that second law analysis has a role in basic thermal science research. Unlike traditional techniques, second law analysis accurately identifies the sources and location of thermodynamic losses. This allows the development of innovative solutions to thermal science problems by directing research to the key technical issues. Two classes of second law techniques were identified as being particularly useful. First, system and component investigations can provide information of the source and nature of irreversibilities on a macroscopic scale. This information will help to identify new research topics and will support the evaluation of current research efforts. Second, the differential approach can provide information on the causes and spatial and temporal distribution of local irreversibilities. This information enhances the understanding of fluid mechanics, thermodynamics, and heat and mass transfer, and may suggest innovative methods for reducing irreversibilities. DOE

80 SOCIAL SCIENCES (GENERAL)

Includes educational matters.

No abstracts in this category.

81 ADMINISTRATION AND MANAGEMENT

Includes management planning and research.

No abstracts in this category.

82 DOCUMENTATION AND INFORMATION SCIENCE

Includes information management; information storage and retrieval technology; technical writing; graphic arts; and micrography.

For computer documentation see *61 Computer Programming and Software.*

N89-17542 Polytechnic Univ., Brooklyn, NY.
MAINTENANCE OF DATABASE INTEGRITY IN A SCHEME-LESS DATABASE SYSTEM Ph.D. Thesis
Harry S. Goldberg 1988 125 p
Avail: Univ. Microfilms Order No. DA8809166

A database should accurately model the enterprise it represents. The problem of database integrity maintenance is the problem of ensuring that the data in the database is accurate. Semantic integrity refers to the compliance of the database with constraints that are derived from the knowledge about what is and is not allowed in that part of the universe that is represented by the data. The automatic maintenance of the database integrity is examined. It presents the results of an experiment in the area of automatic maintenance of database integrity. The goals of the experiment were: to develop an automatic database integrity constrain maintenance system for applications in the Directed Hypergraph Database Model to consist of two components (a constraint-descriptor database and a software system to enforce and/or verify the constraints specified in the constraint-descriptor database); and to develop the system so that the integrity constraints of the database are described using only the constructs of the Directed Hypergraph Database Model itself. A formalization of the notions of semantic intgrity constrints and completeness with respect to integrity control is developed. The methodology is evaluated using the criteria developed to determine what level of semantic integrity completeness it provides. The uniformity of the representation of the operational and the integrity constraint data results in a conceptually simple design. In addition, it achieves a high level of software reuse by utilizing existing database access routines to access the integrity constraint data. Dissert. Abstr.

N89-17543# Los Alamos National Lab., NM.
A DOCUMENT PREPARATION SYSTEM IN A LARGE NETWORK ENVIRONMENT
Manuel Vigil, Stephany Bouchier, Claudia Sanders, Steve Sydoriak, and Kyle Wheeler 1988 12 p Presented at the ACM Conference on Document Processing Systems, Santa Fe, NM, 5 Dec. 1988
(Contract W-7405-eng-36)
(DE88-014466; LA-UR-88-1792; CONF-881223-1) Avail: NTIS HC A03/MF A01

At Los Alamos National Laboratory, we have developed an integrated document preparation system that produces publication-quality documents. This system combines text formatters and computer graphics capabilities that have been adapted to meet the needs of users in a large scientific research laboratory. This paper describes the integration of document processing technology to develop a system architecture, based on a page description language, to provide network-wide capabilities in a distributed computing environment. We describe the Laboratory requirements, the integration and implementation issues, and the challenges we faced developing this system. DOE

N89-17544 Pittsburgh Univ., PA.
A FORMAL LANGUAGE MODEL FOR LOCAL AREA NETWORK CONFIGURATION Ph.D. Thesis
William Walter Oblitey 1988 125 p
Avail: Univ. Microfilms Order No. DA8817896

Current design of local area networks (LANs) is controlled by technology rather than the needs of organizations and manufacturing establishments. Thus, most common implementations of LANs in organizations are Ethernets and Token-rings. Research trends, however, indicate the marked differences between user expectations and LAN realities. The need to redirect research efforts towards the development of expert systems that enable organizations to design LANs that best meet their needs is the objective herein. In order to generate an expert system that designs LANs to suit specific user environments and requirements, a new expert system shell is required. This requirement calls for the formulation of a formal language that can be used to express the design of LANs. A model is presented for the formal specification of LANs that best suit the structural and operational characteristics of LAN user establishments. The establishment consists of a set of agents which interact with each other through electronic devices. The agents are considered as models of workstations. The interactions of agents determine the relationships among workstations with the establishment. Dissert. Abstr.

N89-17545# Oak Ridge National Lab., TN.
LIFE CYCLE MANAGEMENT HANDBOOK
C. E. Synder, T. D. Mott (Evaluation Research Corp., Vienna, VA.), and J. W. Crutcher Sep. 1988 118 p
(Contract DE-AC05-84OR-21400)
(DE89-004315; ORNL/DSRD-13) Avail: NTIS HC A06/MF A01

Life cycle management (LCM) is a standard management discipline for acquiring and using information system resources in a cost-effective manner throughout the life of an information system. Three life cycle management strategies are presented in this report. Section 2, which comprises most of the document, describes the full (five-phase) LCM strategy. The condensed LCM strategy and the one-phase LCM strategy are briefly discussed in Section 3. Appendix A gives examples of formats for system decision and project management documentation; Appendix B provides a list of defined acronyms; and an expanded contents, intended to serve as an index, appears in Appendix C. DOE

N89-17546# Oak Ridge National Lab., TN.
OPTICAL STORAGE: FINANCIAL MANAGEMENT AND BUDGET APPLICATIONS
John D. Morris and M. L. Emrich Oct. 1988 12 p Presented at the National Governor's Association Meeting: Finding the Future Conference, Washington, DC, 12 Dec. 1988
(Contract DE-AC05-84OR-21400)
(DE89-004916; CONF-881249-1) Avail: NTIS HC A03/MF A01

Recent optical storage technology advances have improved the micro-computer's ability to handle large quantities of data. This paper will explain the evolution of this technology including the state of the art. The factors involved in this evolution will be described, namely the division of research into three distinct areas: Compact Disk Read Only Memory (CD-ROM); Write Once Read Many (WORM); and Erasable Optical Storage (EOS). The future implications of these areas will be reported. In addition, practical applications that utilize optical media in the financial environment will be highlighted. DOE

83 ECONOMICS AND COST ANALYSIS

Includes cost effectiveness studies.

No abstracts in this category.

84 LAW, POLITICAL SCIENCE AND SPACE POLICY

Includes NASA appropriation hearings; aviation law; space law and policy; international law; international cooperation; and patent policy.

No abstracts in this category.

85 URBAN TECHNOLOGY AND TRANSPORTATION

Includes applications of space technology to urban problems; technology transfer; technology assessment; and surface and mass transportation.

For related information see also *03 Air Transportation and Safety, 16 Space Transportation,* and *44 Energy Production and Conversion.*

N89-17547# Pacific Northwest Labs., Richland, WA.
TECHNOLOGY TRANSFER FOR THE US DEPARTMENT OF ENERGY'S ENERGY STORAGE PROGRAM. VOLUME 1: RECOMMENDATIONS
C. L. Bruneau and L. L. Fassbender Oct. 1988 40 p
(Contract DE-AC06-76RL-01830)
(DE89-002806; PNL-6484-Vol-1) Avail: NTIS HC A03/MF A01

Technologies developed by the U.S. Department of Energy's (DOE) Energy Storage (STOR) Program must be converted into products, processes, or services that benefit the private sector. The process of technology transfer is the primary means of accomplishing this. The purpose of this report is to examine the technology transfer activities of the STOR Program and suggest mechanisms that might make the transfer of technologies from national laboratories and universities to the private sector more effective. A brief summary of recommendations that would improve the effectiveness of the transfer of energy storage technologies from the national laboratories to the private sector is discussed. DOE

N89-17548*# Southwest Research Inst., San Antonio, TX.
THE EFFECT OF INSULATED COMBUSTION CHAMBER SURFACES ON DIRECT-INJECTED DIESEL ENGINE PERFORMANCE, EMISSIONS, AND COMBUSTION
Daniel W. Dickey, Shannon Vinyard, and Rifat Keribar (Integral Technologies, Inc., Westmont, IL.) Sep. 1988 176 p
(Contract DEN3-330)
(NASA-CR-182204; NAS 1.26:182204; DOE/NASA/0330-3; SwRI-8966) Avail: NTIS HC A09/MF A01 CSCL 13B

The combustion chamber of a single-cylinder, direct-injected diesel engine was insulated with ceramic coatings to determine the effect of low heat rejection (LHR) operation on engine performance, emissions, and combustion. In comparison to the baseline cooled engine, the LHR engine had lower thermal efficiency, with higher smoke, particulate, and full load carbon monoxide emissions. The unburned hydrocarbon emissions were reduced across the load range. The nitrous oxide emissions increased at some part-load conditions and were reduced slightly at full loads. The poor LHR engine performance was attributed to degraded combustion characterized by less premixed burning, lower heat release rates, and longer combustion duration compared to the baseline cooled engine. Author

88 SPACE SCIENCES (GENERAL)

No abstracts in this category.

89 ASTRONOMY

Includes radio, gamma-ray, and infrared astronomy, and astrometry.

N89-17549 Clemson Univ., SC.
PHOTOELECTRIC PHOTOMETRY OF VERY SHORT PERIOD ECLIPSING BINARY SYSTEMS AND THEIR LIGHT CURVE SOLUTIONS Ph.D. Thesis
Ronald George Samec 1987 198 p
Avail: Univ. Microfilms Order No. DA8811906

Photoelectric observations were made during the nine month period between May 1986 and January 1987 of the very short period eclipsing binary systems V523 Cassiopeiae, TY Bootis, VZ Piscium, AD Cancri, BX Pegasi, and CE Leonis. The facilities of Kitt Peak National Observatory and Lowell Observatory were used on three separate observing runs. The first three respective systems were observed with B and V filters in the standard system. The remaining systems were observed in the newly standardized Cousins system (Bessell, 1976). Light curves with complete phase coverage were obtained for the first four respective systems. The observations of those systems are reported. The observations of TY Boo, AD Cnc, V523 Cas, and VZ Psc were subjected to synthetic light curve analysis using the Wilson-Devinney Code. Several solutions were obtained for each of the first three respective systems, which are all found to be partially eclipsing. Both AD Cnc and V523 Cas were modeled with subluminous regions and the resulting sunspot parameters are reported. A simultaneous modeling of the B, V light curves and the double line radial velocity curves of V523 Cas was performed. Absolute parameters were derived for V523 Cas. The Wilson-Devinney code was found incapable of modeling the asymmetric and near ellipsoidal system, VZ Psc. Resulting parameters of the best solutions are tabulated and discussed along with those of other systems which were modeled similarly. The two competing theories of contact structure are evaluated in the light of the results. Dissert. Abstr.

N89-17550 Leicester Univ. (England).
OPTICAL AND INFRARED STUDIES OF COMETARY DUST Ph.D. Thesis
C. M. Birkett 1987 206 p
Avail: Univ. Microfilms Order No. BRD-82617

In 1968, Finson and Probstein outlined a theory which could be used to analyze cometary dust tails. This theory is applied to a series of P/Halley images. The application of the theory is successful and shows P/Halley underwent a series of major outbursts during early 1986. The duration of the outbursts is approx. 2 days. This value coincides with the 2.2 day nuclear rotation period, estimated by other observers. The size of the dust grains varies from submicron to several hundred microns and their calculated orbital parameters indicate that a considerable fraction of the larger grains contribute to the Zodiacal Dust Cloud. A range of CCD and Schmidt Telescope images reveal dust features in the comae of comets P/Crommelin, P/Giacobini-Zinner and P/Halley. Mie (1908) developed a method by which the general properties of scattering and emission by dust grains, can be used to model cometary thermal spectra. Such a method is applied to several P/Halley spectra, taken during April 1986. The results indicate that the dust grains could be composed of both an

absorbing (magnetite) and a dielectric (silicate) material. The interrelations between decaying and Earth-crossing asteroids are discussed. Dissert. Abstr.

90 ASTROPHYSICS

Includes cosmology; celestial mechanics; space plasmas; and interstellar and interplanetary gases and dust.
For related information see also *75 Plasma Physics*.

N89-17551 Washington Univ., Seattle.
ION MICROPROBE MEASUREMENTS OF H, C, O, Mg, AND Si ISOTOPIC ABUNDANCES IN INDIVIDUAL INTERPLANETARY DUST PARTICLES Ph.D. Thesis
Kevin Daniel McKeegan 1987 201 p
Avail: Univ. Microfilms Order No. DA8802754

The isotopic abundances of H, C, O, Mg, and/or Si measured by means of secondary ion mass spectrometry in 48 individual approximately 10 micrometer diameter particles collected from Earth's stratosphere are reported. Thirty-one of these are chondritic interplanetary dust particles (IDPs). The results of a search for previously unrecognized types of IDPs are also reported. The results confirm that IDPs are among the most primitive samples available for laboratory study. However, is most IDPs are from comets, the data do not support a model of comet dust as unaltered interstellar core/mantle grains, unless the isotopic composition of the interstellar dust is homogeneous and similar to the Solar System composition. Dissert. Abstr.

N89-17552 Stanford Univ., CA.
A NEUTRAL HYDROGEN SURVEY OF GALAXIES IN THE CANCER REGION Ph.D. Thesis
Michael David Bicay 1988 318 p
Avail: Univ. Microfilms Order No. DA8808349

Results from a neutral hydrogen (H I) survey of over 1100 galaxies in the Cancer region are presented. These galaxies represent an unbiased subset selected from a sample of 1553 galaxies of type Sa or later. High-quality 21 cm measurements conducted with the 305 m telescope at Arecibo Observatory yield such integral properties as H I mass, inferred total mass, and optical luminosity. The surface density distribution of the sample galaxies is analyzed through use of the two-point angular correlation function. The 21 cm redshifts are supplemented with optical results to form a sample of over 3000 galaxies in order to determine the three-dimensional distribution of galaxies in this portion of the sky. A blue luminosity-H I linewidth correlation is found for a carefully selected subsample of 409 spiral galaxies. The slopes for this relation are analyzed in detail and are found to be shallower than the corresponding infrared relation. This Tully-Fisher relation provides the basis for computing redshift-independent distance moduli, and combined with the easily obtained H I redshifrs, permits estimation of the Hubble ratio. AS part of an ongoing investigation into the effect of environment on the integral properties of of galaxies, IRAS data was used to derive the far-infrared (FIR) properties of cluster galaxies. Dissert. Abstr.

N89-17553 Minnesota Univ., Minneapolis.
THE ROLE OF PRESOLAR DUST IN THE FORMATION OF THE SOLAR SYSTEM Ph.D. Thesis
Gary Robert Huss 1987 263 p
Avail: Univ. Microfilms Order No. DA8805713

Paradigms play an important role in directing scientific research and in interpreting scientific data. Over the last fifteen years, a large body of data was gathered that is at odds with standard paradigms that underlie research on meteorites and the origin of the solar system. An interpretive framework is being constructed to encompass all of the apparently contradictory data on meteorites and other solar system objects. The thrust is that the primary building material for meteorites and terrestrial planets was presolar dust which survived evaporation during the formation of the solar system. The problem is introduce and a history of the thought that led to the paradigm that is now popular is presented. The presently available data on interstellar dust; the conditions in interstellar space; star formation; chondritic meteorites and their potential as sources of information about the formation of the solar system; and the chemical, mineralogic, and isotopic data that was acquired from chondritic meteorites are discussed. The broad outlines of a model that seems to explain the chemical, isotopic, and textural information from meteorites in terms of the ability of various kinds of interstellar dust to survive the formation of the sun is sketched. An attempt to numerically model the chemical processing believed to have taken place in the accretion disk is described, and the implications of the results of that calculation discussed. Several potential avenues of additional work that can be undertaken to both improve the scope of the model and to test the general approach are summarized.
Dissert. Abstr.

N89-17554# Academy of Sciences of the Armenian SSR, Erivan.
WHAT TOPOLOGY COULD THE UNIVERSE BE CREATED WITH
V. G. Gurzadyan and A. A. Kocharyan 1987 24 p
(DE88-704321; EFI-968(18)-87) Avail: NTIS (US Sales Only) HC A03/MF A01

In the framework of Hawking quantum cosmology the topological and geometrical properties of a created Universe with cosmological constant are considered. Probabilities for the Universe creation with different topologies (including torus, sphere, hyperbolic space) are calculated. These topologies turned out to be equally probable for the case of inflationary Universe. For the considered model the probability for the quantum change of topology during the Universe evolution is calculated. DOE

N89-17555# Academy of Sciences of the Ukrainian SSR, Kiev.
ORIGIN AND DYNAMICS OF EXPANDING NEUTRAL HYDROGEN SUPERSHELLS
I. G. Kolesnik and S. A. Silich 1987 21 p
(DE88-704372; ITP-87-59) Avail: NTIS (US Sales Only) HC A03/MF A01

The evolutionary model of expanding supershells regulated by induced star formation is proposed. It is suggested that giant expanding shells are formed in superclouds at late evolutionary stage of star complexes. To understand the dynamics of the most huge supershells it is necessary to take into account that expanding shells can trigger star formation in cold dense pre-existing cloudlets. Efficiency of induced star formation must be less than one percent to fit observational properties of supershells. DOE

N89-17556# Stanford Linear Accelerator Center, CA.
AN ESSAY ON DISCRETE FOUNDATIONS FOR PHYSICS
H. Pierre Noyes and David O. McGoveran Jul. 1988 49 p Presented at the 9th Annual International Meeting of the Alternative Natural Philosophy Association, Cambridge, England, 23 Sep. 1987
(Contract DE-AC03-76SF-00515)
(DE89-002992; SU-SLAC-PUB-4528; CONF-8709318-4) Avail: NTIS HC A03

We base our theory of physics and cosmology on the five principles of finiteness, discreteness, finite computability, absolute non-uniqueness, and strict construction. Our modeling methodology starts from the current practice of physics, constructs a self-consistent representation based on the ordering operator calculus and provides rules of correspondence that allow us to test the theory by experiment. We use program universe to construct a growing collection of bit strings whose initial portions (labels) provide the quantum numbers that are conserved in the events defined by the construction. The labels are followed by content strings which are used to construct event-based finite and discrete coordinates. On general grounds such a theory has a limiting velocity, and positions and velocities do not commute. We therefore reconcile quantum mechanics with relativity at an appropriately fundamental stage in the construction. We show that events in different coordinate systems are connected by the appropriate finite and discrete version of the Lorentz transformation,

that 3-momentum is conserved in events, and that this conservation law is the same as the requirement that different paths can interfere only when they differ by an integral number of deBroglie wavelengths. DOE

N89-17557# Hiroshima Univ., Takehara (Japan). Research Inst. for Theoretical Physics.
MONOPOLES AND MAGNETIC FIELDS IN THE INFLATIONARY UNIVERSE
Misao Sasaki Apr. 1988 10 p
(DE88-755532; RRK-88-12) Avail: NTIS (US Sales Only) HC A02/MF A01

We discuss the cosmological implications of monopoles which have multiple units of the Dirac charge, are relatively light compared with the grand unified mass scale, and which do not catalyze nucleon decay. Combined with the inflationary universe scenario, though admittedly model-dependent, we find the monopole condensation can occur during the inflationary stage and these monopoles can excite the magnetic current on large spatial scales and give rise to primordial magnetic fields of an appreciable strength. We also find the present density of residual monopoles can be such that it gives the flux which is just below the bound based on the persistence of the galactic magnetic field. DOE

N89-17558*# National Aeronautics and Space Administration. Marshall Space Flight Center, Huntsville, AL.
IDEAL BLACK HOLE FLUID
Larry L. Smalley Jan. 1989 12 p Prepared in cooperation with Alabama Univ., Huntsville
(NASA-TM-100349; NAS 1.15:100349) Avail: NTIS HC A03/MF A01 CSCL 03B

The concept of a primordial black hole fluid is introduced and its consequence for supercluster-sized (i.e., large scale voids) and the missing mass question are discussed. Author

91 LUNAR AND PLANETARY EXPLORATION

Includes planetology; and manned and unmanned flights.

For spacecraft design or space stations see *18 Spacecraft Design, Testing and Performance.*

N89-17559 Arizona Univ., Tucson.
SODIUM IN Io'S EXTENDED ATMOSPHERE Ph.D. Thesis
Nicholas McCord Schneider 1988 219 p
Avail: Univ. Microfilms Order No. DA8814275

Several observations of the Io sodium cloud are combined to create a consistent picture of the extended Io atmosphere and its interaction with the Jovian plasma torus. The LPL echelle spectrograph was used to obtain three types of high-resolution spectra of the extended sodium cloud at the sodium D-lines. The first class of observations made use of the mutual satellite eclipses of 1985 to probe the density profile of the atmosphere in the range 1I4 to 10 Io radii, a previously unstudied region. The second type of observation examined the sodium emission in Io's immediate vicinity, allowing an accurate measurement of the velocity structure around Io. The final method employed a high-sensitivity detector to study faint jets of high-speed sodium farther out in the extended cloud. The synthesis of these three data sets results in a better understanding of how sodium is distributed about Io as a function of position and velocity. Dissert. Abstr.

N89-17560*# National Aeronautics and Space Administration, Washington, DC.
PLANETARY CARTOGRAPHY IN THE NEXT DECADE: DIGITAL CARTOGRAPHY AND EMERGING OPPORTUNITIES
Feb. 1989 24 p
(NASA-TM-4092; NAS 1.15:4092) Avail: NTIS HC A03/MF A01 CSCL 03B

Planetary maps being produced today will represent views of the solar system for many decades to come. The primary objective of the planetary cartography program is to produce the most complete and accurate maps from hundreds of thousands of planetary images in support of scientific studies and future missions. Here, the utilization of digital techniques and digital bases in response to recent advances in computer technology are emphasized. Author

N89-16885# Indian Space Research Organization, Ahmedabad.
METEORITES AND LUNAR SAMPLES AS SPACE PROBES
M. N. Rao *In* DFVLR, Proceedings of the Colloquium about Joint Projects Within the DFVLR/ISRO Cooperation Jun. 1988 p 27-38 (For primary document see N89-16883 09-12)
Avail: NTIS HC A06/MF A01; DFVLR, VB-PL-DO, Postfach 90 60 58, 5000 Cologne, Fed. Republic of Germany, 34.50 Deutsche marks

92 SOLAR PHYSICS

Includes solar activity, solar flares, solar radiation and sunspots.

For related information see *93 Space Radiation.*

N89-17561 Arizona Univ., Tucson.
THE VISUAL SHAPE AND MULTIPOLE MOMENTS OF THE SUN Ph.D. Thesis
Burt Jay Beardsley 1987 129 p
Avail: Univ. Microfilms Order No. DA8803247

The 1983 solar shape investigation performed at the Santa Catalina Laboratory for Experimental Relativity by Astrometry (SCLERA) is described. Solar diameter measurements, with the North Star defined as theta = 0 degree polar angle. Expressing the Sun's apparent shape in terms of a Legendre series, these diameters have enabled the calculation of the P2 (quadrupole) and P4 (hexadecapole) shape calculations. The theoretical framework used to provide a relationship between the observed shape of the Sun and the multiple moments of the solar gravitational potential field was improved to include, in general, the effect of differential rotation in both latitude and radius. Using the shape coefficients and the theoretical framework, the gravitational potential multipole moments, expressed as P2 and P4 coefficients of a Legendre series were found to be J2 = (3.4 + or - 1.3) E-6 and J4 = (1.7 + or - 1.1) E-6, respectively. It was found that the contribution to the perihelion precession of Mercury's orbit, caused by the combined effects from the gravitational quadrupole term and general relativity, was approximately 1 sigma different from the observed amount after all other known Newtonian contributions were removed from the observed precession. It was also shown that large changes in the apparent limb darkening functions were occurring near the equatorial regions of the Sun during the time of the observations. Evidence for periodic shape distortions near the equator were also found. Dissert. Abstr.

93 SPACE RADIATION

Includes cosmic radiation; and inner and outer earth's radiation belts.

For biological effects of radiation see *52 Aerospace Medicine.* For theory see *73 Nuclear and High-Energy Physics.*

N89-17562*# National Aeronautics and Space Administration. Langley Research Center, Hampton, VA.
BRYNTRN: A BARYON TRANSPORT MODEL
John W. Wilson, Lawrence W. Townsend, John E. Nealy, Sang Y. Chun, B. S. Hong, Warren W. Buck, S. L. Lamkin, Barry D. Ganapol, Ferdous Khan, and Francis A. Cucinotta (Old Dominion Univ., Norfolk, VA.) Washington, DC Mar. 1989 84 p
(NASA-TP-2887; L-16512; NAS 1.60:2887) Avail: NTIS HC A05/MF A01 CSCL 03B

The development of an interaction data base and a numerical solution to the transport of baryons through an arbitrary shield material based on a straight ahead approximation of the Boltzmann

equation are described. The code is most accurate for continuous energy boundary values, but gives reasonable results for discrete spectra at the boundary using even a relatively coarse energy grid (30 points) and large spatial increments (1 cm in H2O). The resulting computer code is self-contained, efficient and ready to use. The code requires only a very small fraction of the computer resources required for Monte Carlo codes. Author

N89-17563# Hiroshima Univ., Takehara (Japan). Research Inst. for Theoretical Physics.

ISOTROPIZATION OF THE COSMIC BACKGROUND RADIATION DUE TO GALACTIC GRAVITATIONAL SCREENING

Kenji Tomita Apr. 1988 12 p

(DE88-755533; RRK-88-13) Avail: NTIS (US Sales Only) HC A03/MF A01

The primordial objects with the masses of galaxies or their clusters formed at early stages such as z greater than 10 can play a powerful role of gravitational lenses and their random multiple scattering brings an effective screening for the cosmic background radiation. In a cold-dark-matter dominant model with the white-noise spectrum of initial density perturbations, it is shown that, if the primordial objects with the masses 10(sup 12)h(sup -1) (solar mass) are in the nonlinear stage at the epochs $1 + z = 10$ similar to 20, the objects with 6 x 10(sup 14)h(sup -1) (solar mass) are in the nonlinear stage at $1 + z = 6.3$ similar to 14, and accordingly the small-scale anisotropy of the radiation may be smoothed-out within 13 similar to 28 minutes by this gravitational screening, where the Hubble constant H(sub o) = 100 h km s(sup -1) Mpc(sup -1). DOE

99 GENERAL

No abstracts in this category.

Typical Subject Index Listing

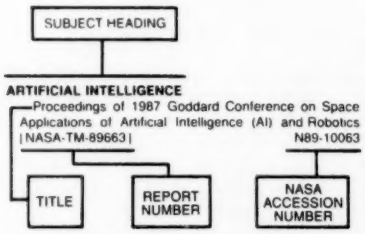

The subject heading is the key to the subject content of the document. Titles, report numbers, and accession numbers of pertinent documents are provided under each subject heading. When the title is insufficiently descriptive of the document content, a title extension has been added, separated from the title by three hyphens. The report number helps to indicate the type of document cited (e.g., NASA report, NASA translation, NASA contractor report). The NASA accession number is the number by which the document abstracts are arranged in this journal and by which the document is sold or requested. The titles, with title extensions if present, are arranged under each subject heading in ascending accession number order. The subject headings have been selected from the latest revision of the *NASA Thesaurus* (NASA SP-7064).

A

A-300 AIRCRAFT
Comparison of the results of tests on A300 aircraft in the RAE 5 metre and the ONERA F1 wind tunnels N89-16849

A-310 AIRCRAFT
The accurate measurement of drag in the 8 ft x 6 ft tunnel N89-16855

A-320 AIRCRAFT
The CFM 56-5 on the A-320 at Air France N89-16793

ABRASION
Microstructural effects in abrasive wear [DE89-003032] N89-16976

ABSORBENTS
Compatibility study of an absorber material and two silicone adhesives [DE89-002361] N89-17011

ABSORBERS (MATERIALS)
Compatibility study of an absorber material and two silicone adhesives [DE89-002361] N89-17011

ABSORPTION CROSS SECTIONS
Absolute absorption cross section measurements of ozone and the temperature dependence at four reference wavelengths leading to renormalization of the cross section between 240 and 350 nm [AD-A199737] N89-16942

ABUNDANCE
Ion microprobe measurements of H, C, O, Mg, and Si isotopic abundances in individual interplanetary dust particles N89-17551

ACCELERATED LIFE TESTS
Compatibility study of an absorber material and two silicone adhesives [DE89-002361] N89-17011

ACCELERATION STRESSES (PHYSIOLOGY)
The effects of microgravity and linear accelerations on cutaneomuscular reflexes in human lower limb musculature N89-17034
Body displacement measured during sustained +Gz, -Gz and + or -Gy acceleration using a stereoscopic photographic system [NASA-TM-101269] N89-17391

ACCELEROMETERS
PYTHON microgravity accelerometer system N89-17038
Gyroscopic testing of accelerometers to determine coning angle [AD-A200126] N89-17209

ACCIDENTS
Source characterization of heavy gas dispersion models for reactive chemicals, volume 1 [AD-A200121] N89-17361

ACCURACY
Aerodynamic Data Accuracy and Quality: Requirements and Capabilities in Wind Tunnel Testing [AGARD-CP-429] N89-16846
Hierarchy of uncertainty sources in transonic wind tunnel testing N89-16851
An overview of the application of standard measurement uncertainty methodology to propulsion testing N89-16854
On-line spectrum loading accuracy verification N89-17292
Accuracy assessment, using stratified plurality sampling, of portions of a LANDSAT classification of the Arctic National Wildlife Refuge Coastal Plain [NASA-TM-101042] N89-17339

ACETYLENE
Development of conducting polymers of high structural strength [AD-A200310] N89-17009

ACOUSTIC EMISSION
Long term possibilities for nondestructive evaluation for US Navy aircraft N89-17259

ACOUSTIC MEASUREMENT
Signal acquisition and processing for autonomous space shuttle cargo bay acoustic measurements (NASA G-313) [AD-A200426] N89-17462
Characterization and modeling of acoustic beams from ultrasonic transducers in solid or liquid media [RF-DAVI-88-08] N89-17465

ACOUSTICS
NASA powered lift facility internally generated noise and its transmission to the acoustic far field [NASA-CR-182217] N89-16882
A modified VAPEPS method for predicting vibroacoustic response of unreinforced mass loaded honeycomb panels [NASA-TM-101467] N89-16905

ACOUSTO-OPTICS
Frequency estimation of radar signals using an acousto-optic spectrum analyzer as an RESM (Radar Electronic Support Measures) receiver [AD-A200159] N89-17067

ACQUISITION
Aircraft airframe cost estimating relationships: Bombers and transports [AD-A200264] N89-16721
Aircraft airframe cost estimating relationships: Attack aircraft [AD-A200265] N89-16722

ACRYLATES
Isotropic kevlar and PBA (poly 1,4-benzamide) reinforcements for composites [AD-A200239] N89-16927

ACTIVATED CARBON
Electrochemistry of carbon relative to batteries and fuel cells [AD-A199698] N89-17141

ACTIVATION ENERGY
Internal stress during high-temperature creep and activation energy for creep of Hastelloy XR [DE88-755231] N89-16969

ACTIVE CONTROL
Spillover stabilization in the control of large flexible space structures N89-16902

ACTIVITY (BIOLOGY)
Using theoretical descriptors in structural activity relationships. Part 2: Polarizability index [AD-A199594] N89-17389

ACTUATORS
Active vibration suppression for robotic manipulators N89-17241

ADA (PROGRAMMING LANGUAGE)
Inertial navigation system simulator: Behavioral specification [AD-A200604] N89-16771
Inertial navigation system simulator program: Top-level design [AD-A200605] N89-16772
Functional performance specification for an external computer system simulator [AD-A200611] N89-16881
Accurate and efficient testing of the exponential and logarithm functions in Ada [DE89-004443] N89-17415

ADAPTIVE CONTROL
Adaptive control techniques for large space structures [AD-A200208] N89-16901

ADAPTIVE FILTERS
Study of error correcting codes for Hertzian channels with a large number of states. Application to Quadrature Amplitude Modulation (QAM) 64 [ENST-88E007] N89-17074
Active vibration suppression for robotic manipulators N89-17241

ADDITIVES
An investigation of the rechargeability of certain modified forms of MnO2 [AD-A199885] N89-16943
Investigation of fuel additive effects on sooting flames [AD-A200273] N89-16948
Oxygen and copper valencies in oxygen-doped superconducting La2CuO(sub 4.13) [DE89-003265] N89-17533

ADHESIVE BONDING
Adsorption of phosphorus acids on alumina [AD-A200548] N89-16957

ADHESIVES
Structure and properties of polymer interphases [AD-A200238] N89-17008
Compatibility study of an absorber material and two silicone adhesives [DE89-002361] N89-17011

ADSORPTION
Adsorption of phosphorus acids on alumina [AD-A200548] N89-16957
Studies of metal/carbon surface chemistry [DE88-011264] N89-16960

AEROACOUSTICS
On the aeroacoustics, aerodynamics and aeroelasticity of lifting surfaces N89-16724

AERODYNAMIC CHARACTERISTICS
An experimental investigation of the aerodynamic characteristics of slanted base ogive cylinders using magnetic suspension technology [NASA-CR-184624] N89-16758

AERODYNAMIC COEFFICIENTS
Yawing moment coefficient for plain ailerons at subonic speeds [ESDU-88029] N89-16734

AERODYNAMIC CONFIGURATIONS
Aerodynamic performance of wings of arbitrary planform in inviscid, incompressible, irrotational flow [AD-A200436] N89-16728
Estimation of drag arising from asymmetry in thrust or airframe configuration [ESDU-88006] N89-16730
Study of the aerodynamic situation along the C 160 aircraft in parachuting configuration [DAT-88-06] N89-16756
Development of a panel method for modeling configurations with unsteady component motions, phase 1 [AD-A200255] N89-16775

AERODYNAMIC DRAG
Estimation of drag arising from asymmetry in thrust or airframe configuration
[ESDU-88006] N89-16730
Intake drag N89-16747
Analytical and experimental methods used to resolve the aerodynamic results of tests conducted in three test facilities N89-16850
Development of testing techniques in a large transonic wind tunnel to achieve a required drag accuracy and flow standards for modern civil transports N89-16857
Precision improvement of transport aircraft drag measurements N89-16858

AERODYNAMIC FORCES
Instantaneous force measurement on a model subjected to rapid control variations N89-16872

AERODYNAMIC INTERFERENCE
Transonic wind tunnel boundary interference: A correction procedure N89-16861

AERODYNAMIC STABILITY
Transonic aeroelastic analysis of launch vehicle configurations N89-16723
Analytical and experimental methods used to resolve the aerodynamic results of tests conducted in three test facilities N89-16850

AERODYNAMICS
On the aeroacoustics, aerodynamics and aeroelasticity of lifting surfaces N89-16724
Turbulence effects on the high angle of attack aerodynamics of a vertically launched missile
[AD-A200418] N89-16727
Introduction to intake aerodynamics N89-16739
Intake Aerodynamics, volume 2 — conference
[VKI-LS-1988-04-VOL-2] N89-16748
Wind tunnel requirements for computational fluid dynamics code verification N89-16880

AEROELASTICITY
Transonic aeroelastic analysis of launch vehicle configurations N89-16723
On the aeroacoustics, aerodynamics and aeroelasticity of lifting surfaces N89-16724
Aeroelastic optimization of a helicopter rotor N89-16778
Requirements and capabilities in unsteady windtunnel testing N89-16878
Vibration and aeroelastic tailoring of advanced composite plate-like lifting surfaces N89-17263

AEROSOLS
Laser interactions with aerosol aureoles
[DE89-002824] N89-17225
High energy laser beam scattering by atmospheric aerosol aureoles
[DE89-004811] N89-17230
Source characterization of heavy gas dispersion models for reactive chemicals, volume 1
[AD-A200121] N89-17361

AEROSPACE ENVIRONMENTS
A microprocessor-based, solar cell parameter measurement system
[AD-A200227] N89-17348

AEROSPACE MEDICINE
Life science experiments during parabolic flight: The McGill experience N89-17027
Contrast sensitivity in Army aviator candidates: Cycloplegia effects and population norms
[AD-A200433] N89-17397

AEROTHERMODYNAMICS
Aerothermal modeling program. Phase 2, element A: Improved numerical methods for turbulent viscous recirculating flows N89-17303
Aerothermal modeling program. Phase 2, element B: Flow interaction experiment N89-17304
Aerothermal modeling program, Phase 2, Element C: Fuel injector-air swirl characterization N89-17305
Evaluation of aerothermal modeling computer programs N89-17308
Measurement of airfoil heat transfer coefficients on a turbine stage N89-17311
Two- and three-dimensional turbine blade row flow field simulations N89-17313

AFTERBODIES
Accurate drag estimation using a single component drag model technique N89-16856

AILERONS
Rolling moment derivative Lxi, for plain ailerons at subsonic speeds
[ESDU-88013] N89-16731
Yawing moment coefficient for plain ailerons at subonic speeds
[ESDU-88029] N89-16734

AIR BREATHING ENGINES
An overview of the application of standard measurement uncertainty methodology to propulsion testing N89-16854

AIR CONDUCTIVITY
The electron-water vapor (H2O) collision cross sections
[AD-A200187] N89-17472

AIR DEFENSE
Report of the Defense Science Board Task Force Subgroup on Strategic Air Defense (SDI Milestone Panel)
[AD-A200164] N89-17452

AIR PIRACY
Aviation security: A system's perspective
[DE89-002020] N89-16766

AIR POLLUTION
Material compatability with threshold limit value levels of monomethyl hydrazine
[AD-A200294] N89-17362
Carbon dioxide and climate: Summaries of research in FY 1988
[DE89-002966] N89-17363
A feasibility study of methods for stopping the depletion of ozone over Antarctica
[NASA-CR-184583] N89-17364

AIR QUALITY
Emission-reduction effects of methanol vehicles: State of knowledge
[DE89-001148] N89-17359

AIR SAMPLING
Material compatability with threshold limit value levels of monomethyl hydrazine
[AD-A200294] N89-17362

AIR TRAFFIC CONTROL
Human factors in aviation operations: The hearback problem
[NASA-CR-177398] N89-16769

AIR WATER INTERACTIONS
Evaluation of satellite-tracked surface drifting buoys for simulating the movement of spilled oil in the marine environment. Volume 1: Executive summary
[PB88-226048] N89-17357
Evaluation of satellite-tracked surface drifting buoys for simulating the movement of spilled oil in the marine environment, volume 2
[PB88-226055] N89-17358
A numerical modeling investigation of the effect of convective-mesoscale interactions on the sea breeze circulation N89-17377

AIRBORNE EQUIPMENT
Development of a portable physiological monitoring system for the KC-135: The S.F.U. biopack N89-17044

AIRCRAFT ACCIDENT INVESTIGATION
Aircraft accident/incident summary report, Travis Air Force Base, California, 8 April 1987
[PB88-910414] N89-16768

AIRCRAFT ANTENNAS
Field enhancement of UHF-VHF aircraft antennas
[AD-A200180] N89-17069

AIRCRAFT CONFIGURATIONS
Estimation of drag arising from asymmetry in thrust or airframe configuration
[ESDU-88006] N89-16730
Wind tunnel predicted air vehicle performance: A review of lessons learned N89-16852

AIRCRAFT CONTROL
Instantaneous force measurement on a model subjected to rapid control variations N89-16872

AIRCRAFT DESIGN
Intake-airframe integration N89-16744
Development of direct-inverse 3-D methods for applied transonic aerodynamic wing design and analysis
[NASA-CR-184788] N89-16761
The design, construction and test of a postbuckled, carbon fibre reinforced plastic wing box N89-16773
Wind tunnel predicted air vehicle performance: A review of lessons learned N89-16852
Requirements and capabilities in unsteady windtunnel testing N89-16878

AIRCRAFT ENGINES
Operational requirements for engine condition monitoring from the EFA viewpoint N89-16781
An overview of US Navy engine monitoring system programs and user experience N89-16782
Engine usage condition and maintenance management systems in the UK armed forces N89-16783
Canadian forces aircraft condition/health monitoring: Policy, plans and experience N89-16784
On board life monitoring system Tornado (OLMOS) N89-16785
Information management systems for on-board monitoring systems N89-16786
CF-18 engine performance monitoring N89-16787
B-1B CITS engine monitoring N89-16788
Engine life consumption monitoring program for RB199 integrated in the on-board life monitoring system N89-16789
Commercial engine monitoring status at GE Aircraft Engines, Cincinnati, Ohio N89-16799
Fault management in aircraft power plant controls N89-16809
Discrete operating conditions gas path analysis N89-16810
Need for common AGARD approach and actions N89-17260
State-of-the-art in non-destructive evaluation of turbine engine parts N89-17261
Turbine Engine Hot Section Technology, 1987
[NASA-CP-2493] N89-17298

AIRCRAFT EQUIPMENT
Laser communication test system
[AD-A199612] N89-17215

AIRCRAFT INDUSTRY
Need for common AGARD approach and actions N89-17260

AIRCRAFT MAINTENANCE
Maintenance aid system for wide body aircraft N89-16805

AIRCRAFT NOISE
A strategy for understanding noise-induced annoyance
[AD-A200125] N89-17461
Rotating hot-wire investigation of the vortex responsible for blade-vortex interaction noise
[NASA-CR-177454] N89-17466

AIRCRAFT PILOTS
Contrast sensitivity in Army aviator candidates: Cycloplegia effects and population norms
[AD-A200433] N89-17397

AIRCRAFT PRODUCTION COSTS
Aircraft airframe cost estimating relationships: All mission types
[AD-A200262] N89-16719

AIRCRAFT SAFETY
Aviation security: A system's perspective
[DE89-002020] N89-16766

AIRFOIL PROFILES
Reynolds number effects in transonic flow
[AGARD-AG-303] N89-16760
A critical assessment of wind tunnel results for the NACA 0012 airfoil N89-16847
Precision improvement of transport aircraft drag measurements N89-16858

AIRFOILS
Development of direct-inverse 3-D methods for applied transonic aerodynamic wing design and analysis
[NASA-CR-184788] N89-16761
Supercritical flow past a symmetrical bicircular arc airfoil
[NASA-CR-184787] N89-16762
Wind tunnel-sidewall-boundary-layer effects in transonic airfoil testing-some correctable, but some not N89-16864
Computerized thermographic technique for the detection of boundary layer separation N89-16876
Limitations at high temperatures of present day engineering materials N89-16996
Measurement of airfoil heat transfer coefficients on a turbine stage N89-17311
Turbine airfoil film cooling N89-17315
Thermal barrier coating life-prediction model development N89-17331
High temperature constitutive and crack initiation modeling of coated single crystal superalloys N89-17334

AIRFRAMES
Aircraft airframe cost estimating relationships: All mission types
[AD-A200262] N89-16719
Aircraft airframe cost estimating relationships: Fighters
[AD-A200263] N89-16720
Aircraft airframe cost estimating relationships: Bombers and transports
[AD-A200264] N89-16721
Aircraft airframe cost estimating relationships: Attack aircraft
[AD-A200265] N89-16722
Damage tolerance behavior of fiber reinforced composite airframes N89-17278

AIRPORT SECURITY
Aviation security: A system's perspective
[DE89-002020] N89-16766

AIRSPEED
Derivation of primary air-data parameters for hypersonic flight
[ESDU-88025] N89-16732

ALCOHOLS
Vapour pressures and critical points of liquids. C7 to C20 alkanols
[ESDU-88012] N89-16962

ALGEBRA
On 2-Banach algebras
[DE88-704194] N89-17429
Massive symbolic mathematical computations and their applications
[AD-A200253] N89-17434

A presentation for Virasoro algebras
[DE89-003883] N89-17440

ALGORITHMS
A new algorithm for the rapid analysis of particle image displacement data N89-17195
Evaluation of aerothermal modeling computer programs N89-17308
An algorithm for analysis of plate motions in Crust Dynamics Project (CDP) networks
[B8821606] N89-17371
An algorithm for calculating the area of overlap of an ellipse and a convex polygon
[AD-A199654] N89-17408
Finding Eigenvalues and Eigenvectors of unsymmetric matrices using a distributed-memory multiprocessor
[DE89-004731] N89-17416
The performance of asynchronous algorithms on hypercubes
[DE89-005503] N89-17420
A bibliography on parallel and vector numerical algorithms
[DE89-005693] N89-17421
Massive symbolic mathematical computations and their applications
[AD-A200253] N89-17434
Finding Eigenvalues and Eigenvectors of unsymmetric matrices using a hypercube multiprocessor
[DE89-002311] N89-17455
Behavior of the reversed field pinch with nonideal boundary conditions
[DE89-005497] N89-17514
Lattice gauge theories and Monte Carlo algorithms
[DE89-003569] N89-17539

ALIGNMENT
Alignment verification procedures N89-17291

ALKALI METALS
Studies of metal/carbon surface chemistry
[DE88-011264] N89-16960

ALKYL COMPOUNDS
Vapour pressures and critical points of liquids. C7 to C20 alkanols
[ESDU-88012] N89-16962

ALLOYS
Investigation of microstructural factors that cause low fracture toughness in silicon carbide whisker/Al alloy composites
[AD-A200147] N89-16925
Selection of alloys for hydrodynamic bearings
[ESDU-88018] N89-16980
Refractory metal alloys and composites for space nuclear power systems
[NASA-TM-101364] N89-16986
Progress on a PdCr wire strain gage N89-17301

ALUMINIDES
Oxidation of Ni3Al below 850 C and its effect on fracture behavior
[DE89-002232] N89-16988

ALUMINUM
Mechanical-chemical energy transfer observations of vaporific explosions
[AD-A200428] N89-16956
Stress driven diffusive voiding of aluminum conductor lines: A model for time dependent failure
[DE89-001665] N89-17144

ALUMINUM ALLOYS
Processing of 2090 aluminum alloy for superplasticity
[AD-A200425] N89-16975
Short-Crack Growth Behaviour in an Aluminum Alloy: An AGARD Cooperative Test Programme
[AGARD-R-732] N89-17287
Short-crack growth behaviour in an aluminum alloy: An AGARD cooperative test program N89-17288
Microstructural examination of core-programme material N89-17289
Long-crack growth rate data: Constant amplitude and FALSTAFF loading N89-17295
Long-crack growth rate data: Gaussian loading N89-17296

ALUMINUM GALLIUM ARSENIDES
Nonequilibrium phonons and disorder in Al(sub x)Ga(sub 1-x)As N89-17103
Energy variations in optical pulses from gain-switched AlGaAs diode lasers N89-17111

ALUMINUM OXIDES
Adsorption of phosphorus acids on alumina
[AD-A200548] N89-16957
Time and temperature dependence of strength in high performance ceramics N89-16998
Use of cataphoresis effects discussed N89-17052

AMIDES
The 15N CP/MAS NMR of aramids: A tool for characterization of the morphology of high modulus fibers for composites
[AD-A199656] N89-16921

AMINES
Structure and properties of polymer interphases
[AD-A200238] N89-17008

AMORPHOUS MATERIALS
Production and transport of convoy electrons in amorphous carbon foils
[DE89-002313] N89-17478
Fractal and spherulitic morphology of silicon nitride crystallized from amorphous films
[AD-A200158] N89-17522

AMORPHOUS SILICON
Research on high-efficiency, single-junction, monolithic, thin-film amorphous silicon solar cells, phase 3
[DE89-000813] N89-17342

AMPLIFIERS
Ballistic transport and hot electron spectroscopy in Tunnelling Hot Electron Transfer Amplifier (THETA) N89-17123

AMPLITUDE MODULATION
Study of error correcting codes for Hertzian channels with a large number of states. Application to Quadrature Amplitude Modulation (QAM) 64
[ENST-88E007] N89-17074
A technique for wing suppressed IR sampling N89-17109

ANEMOMETERS
Prediction of stochastic blade responses using measured wind-speed data as input to the FLAP code
[DE89-000834] N89-17354

ANGLE OF ATTACK
Turbulence effects on the high angle of attack aerodynamics of a vertically launched missile
[AD-A200418] N89-16727
Intakes for high angle of attack N89-16745

ANGLES (GEOMETRY)
Gyroscopic testing of accelerometers to determine coning angle
[AD-A200126] N89-17209

ANGULAR VELOCITY
Extensions to the matrix pencil approach for direction finding
[AD-A200112] N89-17449

ANISOTROPIC PLATES
Vibration and aeroelastic tailoring of advanced composite plate-like lifting surfaces N89-17263

ANISOTROPY
Anisotropic constitutive modeling for nickel base single crystal superalloy Rene N4 at 982 C N89-17324

ANNEALING
Procurement and screening test data for advanced austenitic alloys for 650 C steam service, part 2
[DE89-001331] N89-16979
Glancing angle EXAFS studies of Cu-Al thin film interfaces
[DE89-003614] N89-16983
The annealing behavior of ion-implanted single crystals of the type YBa2Cu3O(sub x)
[DE89-002189] N89-17519

ANOMALIES
Investigation of collisional effects in the plasma erosion opening switch
[AD-A200319] N89-17507
Ion microprobe measurements of H, C, O, Mg, and Si isotopic abundances in individual interplanetary dust particles N89-17551

ANTARCTIC REGIONS
A feasibility study of methods for stopping the depletion of ozone over Antarctica
[NASA-CR-184583] N89-17364

ANTENNA DESIGN
Field enhancement of UHF-VHF aircraft antennas
[AD-A200180] N89-17069
Picosecond photoconductive transceivers N89-17092

ANTENNAS
High power Ion Cyclotron Resonance Heating (ICRH) in JET
[DE89-002218] N89-17499

ANTIBODIES
Screening environmental pollutants and biomarkers: The analytical challenge
[DE89-004931] N89-17366

ANTIMISSILE DEFENSE
Report of the Defense Science Board Task Force Subgroup on Strategic Air Defense (SDI Milestone Panel)
[AD-A200164] N89-17452

ANTIOXIDANTS
Fuel property and antioxidant effects on elastomer integrity, phase 2
[AD-A200250] N89-17015

APPROXIMATION
Approximate stress-intensity factors for a surface crack and through crack at a semi-circular notch N89-17294

ARC WELDING
Penetration effects of the compound vortex in gas metal-arc welding
[AD-A200585] N89-17242
Computer control of gas metal arc welding
[DE89-005188] N89-17252

ARCHITECTURE (COMPUTERS)
Computer control of gas metal arc welding
[DE89-005188] N89-17252
Vectorizing compilers: A test suite and results
[DE89-005376] N89-17406
Improving software quality through hierarchical design
[DE88-014919] N89-17412
HANDYPAK: A histogram and display package
[DE89-002742] N89-17413
Accurate and efficient testing of the exponential and logarithm functions in Ada
[DE89-004443] N89-17415
Northeast Artificial Intelligence Consortium annual report 1986. Volume 5. Building an intelligent assistant: The acquisition, integration, and maintenance of complex distributed tasks
[AD-A199824] N89-17425
Temporal pattern recognition
[AD-A200090] N89-17426
Floating-point standards: Theory and practice
[DE89-003598] N89-17439

ARGON
Analysis of low alloy and stainless steels by inductively coupled argon plasma spectrometer
[DE89-003227] N89-16978

ARGON PLASMA
Analysis of low alloy and stainless steels by inductively coupled argon plasma spectrometer
[DE89-003227] N89-16978
Laser thermal propulsion
[AD-A200558] N89-17226

ARRAYS
Array processing for a multiple-rank signal
[AD-A197954] N89-17062

ARTIFICIAL INTELLIGENCE
HERMIES-3: A step toward autonomous mobility, manipulation and perception
[DE89-004932] N89-17249
Northeast Artificial Intelligence Consortium annual report 1986. Volume 5. Building an intelligent assistant: The acquisition, integration, and maintenance of complex distributed tasks
[AD-A199824] N89-17425
Temporal pattern recognition
[AD-A200090] N89-17426
Machine learning of parameter control doctrine for sensor and communication systems
[AD-A200096] N89-17427

ASTRONOMICAL MAPS
Planetary cartography in the next decade: Digital cartography and emerging opportunities
[NASA-TM-4092] N89-17560

ASTRONOMICAL MODELS
Photoelectric photometry of very short period eclipsing binary systems and their light curve solutions N89-17549
The role of presolar dust in the formation of the solar system N89-17553

ASTROPHYSICS
Ideal black hole fluid
[NASA-TM-100349] N89-17558

ATMOSPHERIC BOUNDARY LAYER
Energy events in the atmospheric boundary layer
[NAL-TM-DU-8701] N89-17372

ATMOSPHERIC CHEMISTRY
Greenhouse warming: What do we know
[DE89-004780] N89-17365

ATMOSPHERIC CIRCULATION
A numerical modeling investigation of the effect of convective-mesoscale interactions on the sea breeze circulation N89-17377
Kinetic energy diagnostic studies of extratropical cyclones based on storm relative motion N89-17378

ATMOSPHERIC COMPOSITION
Absolute absorption cross section measurements of ozone and the temperature dependence at four reference wavelengths leading to renormalization of the cross section between 240 and 350 nm
[AD-A199737] N89-16942
Atmospheric carbon dioxide, climate and global vegetation change
[DE89-002196] N89-17360
Carbon dioxide and climate: Summaries of research in FY 1988
[DE89-002966] N89-17363
Low frequency oscillations in total ozone measurements
[NASA-CR-184759] N89-17385
Sodium in Io's extended atmosphere N89-17559

ATMOSPHERIC ELECTRICITY
Electrical properties of atmospheric moist air: A systematic, experimental study
[AD-A199599] N89-17370
ATMOSPHERIC HEATING
Greenhouse warming: What do we know
[DE89-004780] N89-17365
ATMOSPHERIC IONIZATION
The electron-water vapor (H2O) collision cross sections
[AD-A200187] N89-17472
ATMOSPHERIC MOISTURE
Ion content of moist atmospheric air and the molecular structure of water vapor thus inferred
[AD-A199732] N89-16940
ATMOSPHERIC PRESSURE
Derivation of primary air-data parameters for hypersonic flight
[ESDU-88025] N89-16732
ATMOSPHERIC SOUNDING
High-resolution Interferometer Sounder (HIS), phase 2
[NASA-CR-183414] N89-17212
Middle Atmosphere Program: Handbook for MAP, volume 26
[NASA-CR-183350] N89-17368
ATMOSPHERIC TEMPERATURE
Derivation of primary air-data parameters for hypersonic flight
[ESDU-88025] N89-16732
Absolute absorption cross section measurements of ozone and the temperature dependence at four reference wavelengths leading to renormalization of the cross section between 240 and 350 nm
[AD-A199737] N89-16942
ATMOSPHERIC TURBULENCE
Calculation methods for along-wind loading. Part 3: Response of buildings and plate-like structures to atmospheric turbulence
[ESDU-88019] N89-17267
ATOMIC EXCITATIONS
Monte Carlo investigation of hot photoexcited electron relaxation in GaAs N89-17120
ATOMIC INTERACTIONS
Atomic-scale modeling of low-energy ion-solid processes
[DE89-004374] N89-17482
ATOMIC SPECTRA
Cooled ion frequency standard
[AD-A200373] N89-17475
ATOMIC STRUCTURE
The electronic structure and the state of compositional order in metallic alloys
[DE89-003147] N89-16977
ATOMIZING
Application of advanced diagnostics to airblast injector flows N89-17306
ATTENTION
Human factors in aviation operations: The hearback problem
[NASA-CR-177398] N89-16769
ATTENUATION
Propagation effects handbook for satellite systems design. A summary of propagation impairments on 10 to 100 GHz satellite links with techniques for system design
[NASA-RP-1082(04)] N89-17060
ATTITUDE CONTROL
Control of reaction wheels through digital techniques using reference models
[INPE-4618-TDL/335] N89-16903
ATTRACTION
Is the great attractor really a great wall
[NASA-CR-184772] N89-17540
AUDIO FREQUENCIES
Laser detection of acoustic displacements by destabilizing a frequency stabilized helium neon laser
[DE89-005282] N89-17235
AUGMENTATION
Field enhancement of UHF-VHF aircraft antennas
[AD-A200180] N89-17069
AUSTENITIC STAINLESS STEELS
Procurement and screening test data for advanced austenitic alloys for 650 C steam service, part 2
[DE89-001331] N89-16979
AUTOCORRELATION
Picosecond optical autocorrelation experiments on fast photodetectors N89-17117
Optical processing --- particle image displacement velocimetry N89-17189
AUTOMATA THEORY
Investigations of the motion of discrete-velocity gases by cellular automata
[AD-A200221] N89-17158
AUTOMATIC CONTROL
Research on automatic extraction of map information and its image representation
[DE88-754960] N89-17409
Automatic registration of satellite imagery
[INPE-4637-PRE/1349] N89-17414
AUTOMOBILES
The Rankine automotive system technology assessment report
[DE89-002693] N89-17238
Report to Congress on the Automotive Technology Development Program
[DE89-004977] N89-17250
AUTONOMOUS NAVIGATION
3-D vision techniques for autonomous vehicles
[AD-A199643] N89-17236
HERMIES-3: A step toward autonomous mobility, manipulation and perception
[DE89-004932] N89-17249
AUXILIARY PROPULSION
A data acquisition and storage system for the ion auxiliary propulsion system cyclic thruster test
[NASA-TM-101469] N89-17424
AVALANCHE DIODES
Optical communication. Four quadrant avalanche detector. Modeling, theoretical results and comparison with experimental values
[CNES-CT/DRT/TIT/IO-87/086] N89-17495
AXIAL FLOW
Axial velocity density ratio influence on exit flow angle in transonic/supersonic cascades N89-16830
AXIAL FLOW TURBINES
Heat transfer in the tip region of a rotor blade simulator N89-17312
AXIAL LOADS
Accurate drag estimation using a single component drag model technique N89-16856
AXIAL STRESS
A multiaxial strength criterion for composites
[AD-A199610] N89-16920
AXIOMS
Axioms for concurrent objects
[AD-A200584] N89-17435

B

B-1 AIRCRAFT
B-1B CITS engine monitoring N89-16788
BACKGROUND NOISE
A strategy for understanding noise-induced annoyance
[AD-A200125] N89-17461
BACKGROUND RADIATION
Isotropization of the cosmic background radiation due to galactic gravitational screening
[DE88-755533] N89-17563
BACKSCATTERING
Instrumentation for the characterization of the microwave properties at 18, 35 and 94 GHz
[AD-A199741] N89-17064
BALANCE
Balance accuracy and repeatability as a limiting parameter in aircraft development force measurements in conventional and cryogenic wind tunnels N89-16873
BALLISTICS
Finite element analysis of F-16 ballistic tests
[AD-A200289] N89-16776
Ballistic transport and hot electron spectroscopy in Tunnelling Hot Electron Transfer Amplifier (THETA) N89-17123
BALLOON SOUNDING
ISRO-DFVLR collaboration in space sciences N89-16884
BANACH SPACE
On 2-Banach algebras
[DE88-704194] N89-17429
BAND STRUCTURE OF SOLIDS
Molecular Beam Epitaxy (MBE) for high speed devices N89-17085
BARIUM
Interaction of CO, CO2 and H2O with Ba and YBa2Cu3O7
[DE89-003160] N89-17528
BARIUM COMPOUNDS
Study of structure of high-Tc superconductor Y(YV)Ba2Cu3O(sub 9-x) and its resistance sharp drop
[DE88-704104] N89-17531
BARIUM OXIDES
Magnetization, transport and structural studies of Tl-Ca-Ba-Cu-O: Bulk ceramics, single crystals, and polycrystalline thin films
[DE89-003264] N89-17010
Interaction of CO, CO2 and H2O with Ba and YBa2Cu3O7
[DE89-003160] N89-17528
BARRIER LAYERS
Nuclear reorganization barriers to electron transfer
[DE88-016582] N89-17471
BARYONS
BRYNTRN: A baryon transport model
[NASA-TP-2887] N89-17562
BATTERY CHARGERS
Development of overcharge tolerance in Li/FeS and Li/FeS2 cells
[DE89-003952] N89-17145
BAYS (STRUCTURAL UNITS)
Signal acquisition and processing for autonomous space shuttle cargo bay acoustic measurements (NASA G-313)
[AD-A200426] N89-17462
BEAM SPLITTERS
X-ray optics for X-ray laser research and applications
[DE89-004026] N89-17493
BEAMS (SUPPORTS)
Maximum inelastic bending moments and form factors for symmetric bending of beams
[ESDU-88035] N89-17270
BEARINGS
Selection of alloys for hydrodynamic bearings
[ESDU-88018] N89-16980
BEDS (PROCESS ENGINEERING)
Phase change phenomena in liquid saturated self heated particulate bed --- core meltdown N89-17170
Heat transfer in self-heated particle beds submerged in liquid coolant N89-17171
BEHAVIOR
The behavior of shells made of composites during the dynamic application of axian compression
[AD-A200244] N89-17266
BENDING MOMENTS
The design of spur and helical involute gears. A procedure compatible with BS 436:1986: Method for calculation of contact and root bending stress limitations for metallic involute gears
[ESDU-88033] N89-17247
Maximum inelastic bending moments and form factors for symmetric bending of beams
[ESDU-88035] N89-17270
BENZENE
Isotropic kevlar and PBA (poly 1,4-benzamide) reinforcements for composites
[AD-A200239] N89-16927
BIBLIOGRAPHIES
On fundamental problems of Space Materials Science (SMS) N89-17024
Microgravity science and applications bibliography, 1988 revision
[NASA-TM-4098] N89-17045
A bibliography on parallel and vector numerical algorithms
[DE89-005693] N89-17421
BINARY SYSTEMS (MATERIALS)
Hardware for studying the demixing of aqueous polymer two-phase systems in low gravity N89-17030
BIOLOGICAL EFFECTS
Encapsulation process hardware for a KC-135 aircraft N89-17037
BIOSATELLITES
Canadian participation in international biosatellite programs N89-17025
BISMUTH
An investigation of the rechargeability of certain modified forms of MnO2
[AD-A199885] N89-16943
BLACK HOLES (ASTRONOMY)
Ideal black hole fluid
[NASA-TM-100349] N89-17558
BLADE TIPS
Tip clearance signal processor development
[AD-A199830] N89-16822
Heat transfer in the tip region of a rotor blade simulator N89-17312
BLADE-VORTEX INTERACTION
Rotating hot-wire investigation of the vortex responsible for blade-vortex interaction noise
[NASA-CR-177454] N89-17466
BLUFF BODIES
Characterization of nonpremixed turbulent bluff-body burner flames
[PB89-100507] N89-16945
Heat transfer with very high free-stream turbulence and heat transfer with streamwise vortices N89-17309
BLUNT BODIES
Verification of a Navier-Stokes code for solving the hypersonic blunt body problem
[DE89-003169] N89-16737
An experimental investigation of the aerodynamic characteristics of slanted base ogive cylinders using magnetic suspension technology
[NASA-CR-184624] N89-16758

BODY KINEMATICS
Body displacement measured during sustained +Gz, -Gz and + or -Gy acceleration using a stereoscopic photographic system
[NASA-TM-101269] N89-17391
BODY-WING CONFIGURATIONS
Expriments on the DFVLR-F4 wing body configuration in several European windtunnels N89-16848
BOILING
Phase change phenomena in liquid saturated self heated particulate bed --- core meltdown N89-17170
BOLTZMANN DISTRIBUTION
Monte Carlo studies of nonlinear electron transport in 3-5 semiconductors
[AD-A199700] N89-17516
BOMBER AIRCRAFT
The role of short-term memory in operator workload
[AD-A200252] N89-17401
BONDING
High temperature properties of ceramic/carbon systems in an oxidizing environment
[AD-A200254] N89-16928
BORON CARBIDES
Synthesis and properties of low carbon boron carbides
[DE89-002184] N89-16923
Interfacial bonding in W/C and W/B4C multilayers
[DE89-002931] N89-16936
Synthesis and properties of new preceramic materials
[DE89-003436] N89-17012
BORON NITRIDES
Synthesis and properties of new preceramic materials
[DE89-003436] N89-17012
BOSONS
On the experimental basis of the Pauli exclusive principle
[DE88-704366] N89-17477
BOUNDARIES
Derivation and application of a class of generalized impedance boundary conditions, part 2
[NASA-CR-183298] N89-17148
BOUNDARY ELEMENT METHOD
Three-dimensional inelastic analysis for hot section components, BEST 3D code N89-17317
BOUNDARY LAYER CONTROL
Supersonic compressors N89-16836
Experiments on boundary layer transition tripping at low Reynolds numbers N89-16868
BOUNDARY LAYER FLOW
Transonic wind tunnel boundary interference: A correction procedure N89-16861
Wind tunnel-sidewall-boundary-layer effects in transonic airfoil testing-some correctable, but some not N89-16864
A model for transition by attachment line contamination and an examination of cross-flow instability in three-dimensional boundary layers N89-17153
Introduction to Computational Fluid Dynamics --- conference
[VKI-LS-1988-02] N89-17174
Boundary layer equations and methods of solution N89-17176
A low-Reynolds-number two-equation turbulence model for predicting heat transfer on turbine blades N89-17310
BOUNDARY LAYER SEPARATION
Physical aspects of viscous simulation and associated research requirements N89-16865
Computerized thermographic technique for the detection of boundary layer separation N89-16876
BOUNDARY LAYER STABILITY
A model for transition by attachment line contamination and an examination of cross-flow instability in three-dimensional boundary layers N89-17153
BOUNDARY LAYER TRANSITION
Physical aspects of viscous simulation and associated research requirements N89-16865
On Reynolds number effects and simulation N89-16866
Experiments on boundary layer transition tripping at low Reynolds numbers N89-16868
BOUNDARY LAYERS
A proposed boundary layer simulation methodology for wind tunnel testing N89-16867
Heat transfer with very high free-stream turbulence and heat transfer with streamwise vortices N89-17309
BOUNDARY VALUE PROBLEMS
Far field patterns and the inverse scattering problem for electromagnetic waves in an inhomogeneous medium
[AD-A200223] N89-17070
BREADBOARD MODELS
Non return to zero (NRZ) clock recovery breadboard for 200 MB/S optical intersatellite link
[CNES-CT/DRT/TIT/TR-87/024] N89-17496
BRIGHTNESS
Progress towards a 44-Angstrom X-ray laser
[DE89-004807] N89-17229
BRILLOUIN ZONES
Electronic behavior of highly correlated metals
[DE89-002492] N89-16971
The electronic structure and the state of compositional order in metallic alloys
[DE89-003147] N89-16977
BRITTLENESS
High temperature properties of ceramic/carbon systems in an oxidizing environment
[AD-A200254] N89-16928
Brittle material processing reported N89-17051
BROADBAND
Nonlinear optics with broad-band lasers
[DE89-002728] N89-17216
BUBBLES
Design considerations for the CLEM135 bubble coalescence experiment N89-17032
BUCKLING
The design, construction and test of a postbuckled, carbon fibre reinforced plastic wing box N89-16773
Avoidance of buckling of some engineering elements (struts, plates and gussets)
[ESDU-88034] N89-17269
BUDGETS
Optical storage: Financial management and budget applications
[DE89-004916] N89-17546
BUFFETING
Some difficulties in the wind tunnel prediction of modern civil aircraft buffeting: Proposed remedies N89-16869
BUNDLES
A visualization model based on the mathematics of fiber bundles
[DE89-002537] N89-17432
BUOYANCY
Center of buoyancy definition
[DE89-003017] N89-17457
BUOYS
Evaluation of satellite-tracked surface drifting buoys for simulating the movement of spilled oil in the marine environment. Volume 1: Executive summary
[PB88-226048] N89-17357
Evaluation of satellite-tracked surface drifting buoys for simulating the movement of spilled oil in the marine environment, volume 2
[PB88-226055] N89-17358

C

C-135 AIRCRAFT
Parabolic flight: A useful test bed N89-17020
Droplet separation dynamics and kinematics under microgravity N89-17031
System engineering and logistics for KC-135 experimentation N89-17033
High temperature material processing system for KC-135 microgravity experiments N89-17040
Development of a portable physiological monitoring system for the KC-135: The S.F.U. biopack N89-17044
C-160 AIRCRAFT
Study of the aerodynamic situation along the C 160 aircraft in parachuting configuration
[DAT-88-06] N89-16756
CADMIUM TELLURIDES
Device physics related to the granular nature of CuInSe2 solar cells
[DE89-000810] N89-17341
CALCIUM
The effects of hydrazines on neuronal excitability
[AD-A200199] N89-17395
CALCIUM OXIDES
Magnetization, transport and structural studies of Tl-Ca-Ba-Cu-O: Bulk ceramics, single crystals, and polycrystalline thin films
[DE89-003264] N89-17010
CALIBRATING
Engine simulator tests: Comparison of calibration and wind tunnel results N89-16871
CAMBER
Unsteady flow about porous cambered plates
[AD-A200282] N89-17160
CAMBERED WINGS
Boundaries of linear characteristics of cambered and twisted wings at subcritical Mach numbers
[ESDU-88030] N89-16735
CAMERAS
German spaceborne remote sensing activities N89-16887
CANADA
Canadian microgravity research using aircraft and rockets N89-17023
CANADIAN SPACE PROGRAM
Canadian participation in international biosatellite programs N89-17025
CAPILLARY FLOW
Capillary pumping for a two phase heat transport system --- space stations N89-17172
CARBIDES
Microstructural effects in abrasive wear
[DE89-003032] N89-16976
CARBON
Studies of metal/carbon surface chemistry
[DE88-011264] N89-16960
Electrochemistry of carbon relative to batteries and fuel cells
[AD-A199698] N89-17141
Hydrogen erosion of carbon for fusion applications
[UTIAS-328] N89-17504
Phases and microstructures of carbon-implanted niobium
[DE89-004017] N89-17534
CARBON DIOXIDE
Atmospheric carbon dioxide, climate and global vegetation change
[DE89-002196] N89-17360
Carbon dioxide and climate: Summaries of research in FY 1988
[DE89-002966] N89-17363
Greenhouse warming: What do we know
[DE89-004780] N89-17365
Integration of experimental and modeling approaches in the unmanaged ecosystem research plan
[DE89-005230] N89-17367
Interaction of CO, CO2 and H2O with Ba and YBa2Cu3O7
[DE89-003160] N89-17528
CARBON DIOXIDE CONCENTRATION
Atmospheric carbon dioxide, climate and global vegetation change
[DE89-002196] N89-17360
Carbon dioxide and climate: Summaries of research in FY 1988
[DE89-002966] N89-17363
CARBON FIBER REINFORCED PLASTICS
The design, construction and test of a postbuckled, carbon fibre reinforced plastic wing box N89-16773
Qualification tests of preimpregnated carbon epoxy T800H/DA 0506 from Structil. Test report M6-570500
[REPT-M6-570500] N89-16934
CARBON MONOXIDE
Interaction of CO, CO2 and H2O with Ba and YBa2Cu3O7
[DE89-003160] N89-17528
CARDIOVASCULAR SYSTEM
Multiparametric research of early indicators of vascular risk in flying personnel
[ETN-89-93613] N89-17398
CARRIER INJECTION
A proposed Quantum Well Injection Transit Time (QWITT) device N89-17100
Longitudinally localized optical carrier injection for femtosecond transport studies N89-17121
CARRIER LIFETIME
Carrier lifetime versus ion-implantation dose in silicon on sapphire N89-17106
CARRIER MOBILITY
Direct subpicosecond measurement of carrier mobility of photoexcited electrons in GaAs N89-17118
CARRIER TRANSPORT (SOLID STATE)
Picosecond carrier transport in GaAs quantum wells N89-17128
CASCADE FLOW
Transonic Compressors, volume 1 --- conference
[VKI-LS-1988-03-VOL-1] N89-16825
Loss development in transonic compressor cascades N89-16826
Incidence angle rules in supersonic cascades N89-16827
Exit angle rules in supersonic cascades N89-16828
Shock losses in transonic and supersonic compressor cascades N89-16829
Axial velocity density ratio influence on exit flow angle in transonic/supersonic cascades N89-16830
Inverse methods for blade design, controlled diffusion blading for supercritical compressor flow N89-16832
CASSEGRAIN OPTICS
In-situ surface during laser-controlled chemical processing of surfaces
[AD-A200206] N89-17223
CATALYSIS
The behavior of microdisks and micoring electrodes. Prediction of the amperometric response of microdisks and of the steady state for CE and EC Catalytic reactions by application of Neumann's integral theorem
[AD-A200415] N89-16952

CATALYSTS
Light-off temperature determination of oxidation catalyst using Fourier transform infrared technique
[AD-A199596] N89-16938
CAUCHY PROBLEM
Accuracy of various wall-correction methods for 3D subsonic wind-tunnel testing N89-16863
CAVITIES
Heat transfer in the tip region of a rotor blade simulator N89-17312
CELLS (BIOLOGY)
The use of sounding rockets in the study of microgravity cell biology N89-17036
Encapsulation process hardware for a KC-135 aircraft N89-17037
Concentricity and sphericity of composite drops under microgravity N89-17042
CENTAURUS CONSTELLATION
Project Longshot: An unmanned probe to Alpha Centauri
[NASA-CR-184718] N89-16904
CENTRIFUGAL PUMPS
Application of particle image displacement velocimetry to a centrifugal pump N89-17200
CERAMIC COATINGS
Papers of the 5th LBF Colloquium
[LBF-TB-180] N89-17272
Fatigue behavior of ceramic thermal barrier coatings N89-17283
Thermal expansion mismatch and plasticity in thermal barrier coating N89-17330
CERAMIC FIBERS
Optical fiber science and technology: Novel fibers and fiber sensors
[AD-A200311] N89-17489
CERAMIC MATRIX COMPOSITES
Ion assisted deposition of fiber coatings for ceramic matrix composites wth low dielectric loss tangents
[AD-A200162] N89-17005
CERAMICS
National Research Council Resident Research Associateship (NRC-RRA) Program
[AD-A200183] N89-16926
High temperature properties of ceramic/carbon systems in an oxidizing environment
[AD-A200254] N89-16928
Engineering Materials for Very High Temperatures: An ORNL Workshop
[ORNL-6-016-R] N89-16992
Microstructure of high-temperature ceramics N89-16993
Ceramic-ceramic composites for use at high temperature N89-16994
Development of composite high temperature materials for future energy conversion applications N89-16995
The shaping of structural engineering ceramics N89-16997
Time and temperature dependence of strength in high performance ceramics N89-16998
Engineering ceramics in West Germany N89-16999
Photodeflection and photoconductivity studies in ceramics
[DE89-002186] N89-17003
Ceramics derived from organo-metallic polymers
[AD-A200118] N89-17004
Ion assisted deposition of fiber coatings for ceramic matrix composites wth low dielectric loss tangents
[AD-A200162] N89-17005
Mechanistic studies of pressure-assisted superplasticity of structural ceramics
[AD-A200202] N89-17006
Magnetization, transport and structural studies of Tl-Ca-Ba-Cu-O: Bulk ceramics, single crystals, and polycrystalline thin films
[DE89-003264] N89-17010
Synthesis and properties of new preceramic materials
[DE89-003436] N89-17012
JPRS report: Science and technology. Japan. Developments in Manufacturing Process Technology
[JPRS-JST-88-010] N89-17047
Electric discharge method for ceramics reported N89-17050
Brittle material processing reported N89-17051
Laser beam heat method reported N89-17054
Thermal barrier coating life prediction model development N89-17333
The effect of insulated combustion chamber surfaces on direct-injected diesel engine performance, emissions, and combustion
[NASA-CR-182204] N89-17548
CEREBRAL CORTEX
Role of retinocortical processing in spatial vision
[AD-A200198] N89-17394
CHAINS
Development of kinematic equations and determination of workspace of a 6 DOF end-effector with closed-kinematic chain mechanism
[NASA-CR-183241] N89-17444
CHANNEL CAPACITY
Capacity of frequency-hop spread-spectrum multiple-access communication systems
[AD-A200616] N89-17073
CHANNEL FLOW
Interdependence of large and small scale structures in a turbulent boundary layer N89-17155
CHARACTERIZATION
Characterization of hypersonic wind tunnel flow fields for improved data accuracy N89-16874
Aerothermal modeling program, Phase 2, Element C: Fuel injector-air swirl characterization N89-17305
CHARGE EFFICIENCY
An investigation of the rechargeability of certain modified forms of MnO2
[AD-A199885] N89-16943
Nickel hydrogen battery development
[DE89-001063] N89-17143
Development of overcharge tolerance in Li/FeS and Li/FeS2 cells
[DE89-003952] N89-17145
CHARGE EXCHANGE
Role of charge exchange process in forming of ion charge and energy states in multicomponent laser plasma produced from gas-content solids
[DE88-704828] N89-17511
CHECKOUT
Sparse matrix methods research using the CSM testbed software system
[NASA-CR-4219] N89-17441
CHEMICAL ANALYSIS
The 15N CP/MAS NMR of aramids: A tool for characterization of the morphology of high modulus fibers for composites
[AD-A199656] N89-16921
CHEMICAL BONDS
Interfacial bonding in W/C and W/B4C multilayers
[DE89-002931] N89-16936
Studies of metal/carbon surface chemistry
[DE88-011264] N89-16960
Statistical mechanics of polymer systems
[DE89-002012] N89-17002
Development of conducting polymers of high structural strength
[AD-A200310] N89-17009
Theoretical predictions for side-chain liquid-crystal polymers and comparison to experiment
[DE89-003578] N89-17013
CHEMICAL COMPOSITION
The effect of chemistry modifications on the solidification behavior and weldability of Alloy 625
[DE89-001046] N89-16972
Properties and performance of polyamide membranes N89-16991
CHEMICAL EQUILIBRIUM
Experimental verification of the thermodynamic properties for a jet-A fuel
[NASA-TM-101475] N89-17017
CHEMICAL EXPLOSIONS
Mechanical-chemical energy transfer observations of vaporific explosions
[AD-A200428] N89-16956
CHEMICAL FUELS
Source characterization of heavy gas dispersion models for reactive chemicals, volume 1
[AD-A200121] N89-17361
CHEMICAL LASERS
The kinetics and dynamics of iodine monofluoride formation in gas-phase collisions
[AD-A199622] N89-16939
CHEMICAL PROPERTIES
Synthesis and properties of low carbon boron carbides
[DE89-002184] N89-16923
CHEMICAL REACTIONS
Light-off temperature determination of oxidation catalyst using Fourier transform infrared technique
[AD-A199596] N89-16938
The behavior of microdisk and microring electrodes. Mass transport to the disk in the unsteady state: Coupled chemical reactions
[AD-A200422] N89-16954
Selectivity of the reactions of oxygenates on transition metal surfaces
[DE89-003691] N89-16985
Synthesis and properties of new preceramic materials
[DE89-003436] N89-17012
In-situ surface during laser-controlled chemical processing of surfaces
[AD-A200206] N89-17223
Laser studies of the SiH radical/surface interaction during deposition of a thin film
[DE89-003902] N89-17232
KINETICS: A computer program to analyze chemical reaction data
[DE89-004602] N89-17419
Reaction dynamics of H + O2 at 1.6 eV collision energy
[NASA-CR-183182] N89-17483
CHEMILUMINESCENCE
The kinetics and dynamics of iodine monofluoride formation in gas-phase collisions
[AD-A199622] N89-16939
CHEMISORPTION
Adsorption of phosphorus acids on alumina
[AD-A200548] N89-16957
CHIRP
Frequency chirping in pulse modulated gain and real index guided single quantum well lasers N89-17113
CHROMATOGRAPHY
Evaluation of a supercritical fluid chromatograph coupled to a surface-wave-sustained microwave-induced plasma detector
[AD-A198728] N89-16937
CHROMIUM ALLOYS
Microstructural effects in abrasive wear
[DE89-003032] N89-16976
Procurement and screening test data for advanced austenitic alloys for 650 C steam service, part 2
[DE89-001331] N89-16979
CHROMIUM STEELS
The effects of strain induced softening on the load carrying capability of components N89-17264
CIRCADIAN RHYTHMS
Pharmacological resetting of the circadian sleep-wake cycle
[AD-A200246] N89-17396
Sleep and wakefulness: Handbook for flight medical officers, 2nd edition
[AGARD-AG-270(F)] N89-17399
CIRCULAR CYLINDERS
Supercritical flow past a symmetrical bicircular arc airfoil
[NASA-CR-184787] N89-16762
CIRCULAR POLARIZATION
Effects of depolarization obtained by specular reflection on metallic mirrors: Applications to laser telecommunication and to Earth observation
[CNES-CT/DRT/TIT/IO-87/150] N89-17494
CITIES
Research on automatic extraction of map information and its image representation
[DE88-754960] N89-17409
CLASSIFICATIONS
Improving classification accuracy of radar images using a multiple-stage classifier
[AD-A200291] N89-17071
Models of incremental concept formation
[AD-A199617] N89-17400
CLASSIFIERS
Improving classification accuracy of radar images using a multiple-stage classifier
[AD-A200291] N89-17071
CLEARANCES
Human factors in aviation operations: The hearback problem
[NASA-CR-177398] N89-16769
Tip clearance signal processor development
[AD-A199830] N89-16822
CLIMATE
New England mountain icing climatology
[AD-A200287] N89-17381
CLIMATE CHANGE
Atmospheric carbon dioxide, climate and global vegetation change
[DE89-002196] N89-17360
CLIMATOLOGY
New England mountain icing climatology
[AD-A200287] N89-17381
Estimation of hours per year when mean wind speed exceeds specified thresholds
[ESDU-88038] N89-17383
Measurements of micrometeorological parameters for testing large scale models
[NASA-CR-184766] N89-17384
Study of the effect of cloud inhomogeneity on the earth radiation budget experiment
[NASA-CR-182962] N89-17386
CLOCKS
Non return to zero (NRZ) clock recovery breadboard for 200 MB/S optical intersatellite link
[CNES-CT/DRT/TIT/TR-87/024] N89-17496
CLOSED CYCLES
Behavior in normal and reduced gravity of an enclosed liquid/gas system with nonuniform heating from above
[NASA-TM-101471] N89-17046

Seeded inert gas driven disk generator
[DE88-704083] N89-17510
CLOSED ECOLOGICAL SYSTEMS
Regenerative life support system research and concepts
[NASA-CR-184760] N89-17404
CLOSURE LAW
An analysis of the closure conditions for two-fluid models of two-phase flow
[DE89-003096] N89-17165
CLOUD COVER
Study of the effect of cloud inhomogeneity on the earth radiation budget experiment
[NASA-CR-182962] N89-17386
CLOUD DISPERSAL
Source characterization of heavy gas dispersion models for reactive chemicals, volume 1
[AD-A200121] N89-17361
CLUSTER ANALYSIS
Cluster expansion for vacuum confining fields
[DE88-704367] N89-17436
CLUSTERS
Theoretical studies of electrons and electron transfer processes in fluids
[DE89-003259] N89-17479
COAL GASIFICATION
Modern and prospective technologies for hydrogen production from fossil fuels
[DE89-001270] N89-16959
COALESCING
Design considerations for the CLEM135 bubble coalescence experiment N89-17032
COATINGS
Adsorption of phosphorus acids on alumina
[AD-A200548] N89-16957
Nitride and carbide coatings for high speed steel cutting tools
[DE89-003623] N89-16984
Engineering Materials for Very High Temperatures: An ORNL Workshop
[ORNL-8-016-R] N89-16992
Ion assisted deposition of fiber coatings for ceramic matrix composites wth low dielectric loss tangents
[AD-A200162] N89-17005
COBALT ALLOYS
Preliminary study of creep thresholds and thermomechanical response in Haynes 188 at temperatures in the range 649 to 871 C N89-17327
COCKPITS
COMPASS (Trademark): A generalized ground-based monitoring system N89-16819
CODING
Wind tunnel requirements for computational fluid dynamics code verification N89-16880
Applications of correcting coding theory to communication combinatorial problems
[ENST-88C001] N89-17065
JUNCTION code user's manual. Electromagnetic scattering and radiation by arbitrary configurations of conducting bodies and wires
[AD-A200315] N89-17072
Adaptive hybrid picture coding
[AD-A200059] N89-17142
COEFFICIENTS
Fresnel coefficients for a phase conjugator
[AD-A200123] N89-17487
COHERENT RADIATION
X-ray optics for X-ray laser research and applications
[DE89-004026] N89-17493
COLD FRONTS
New England mountain icing climatology
[AD-A200287] N89-17381
COLD PLASMAS
Alfven waves in a cold plasma with curved magnetic fields
[AD-A200312] N89-17506
COLD WORKING
Experimental evidence for positron trapping at dislocations in Ni3Al alloys
[DE89-004520] N89-16989
COLLISION PARAMETERS
Production and transport of convoy electrons in amorphous carbon foils
[DE89-002313] N89-17478
Reaction dynamics of H + O2 at 1.6 eV collision energy
[NASA-CR-183182] N89-17483
COLLISIONAL PLASMAS
Electron collision shift of the Lyman-alpha line in H and He+
[AD-A200296] N89-17474
Modeling of atomic processes for X-ray laser plasmas
[AD-A200219] N89-17505
Investigation of collisional effects in the plasma erosion opening switch
[AD-A200319] N89-17507
COLOR TELEVISION
The visibility of noise in system 1 colour television
[BBC-RD-1988/12] N89-17061
COMBINATORIAL ANALYSIS
Applications of correcting coding theory to communication combinatorial problems
[ENST-88C001] N89-17065
COMBUSTION
Laminar flame in a turbulent flow
[AD-A200241] N89-16947
Mechanical-chemical energy transfer observations of vaporific explosions
[AD-A200428] N89-16956
Development of a lattice gas model for the study of combustion
[ETN-89-93612] N89-16964
Combustibility of titanium powders
[NASA-TT-20455] N89-16967
Turbine Engine Hot Section Technology, 1987
[NASA-CP-2493] N89-17298
COMBUSTION CHAMBERS
Measurements of gas turbine combustor and engine augmentor tube sooting characteristics
[AD-A199768] N89-16821
Numerical study of two-stage light-gas hypervelocity projectile launchers
[UTIAS-327] N89-16894
Characterization of nonpremixed turbulent bluff-body burner flames
[PB89-100507] N89-16945
Limitations at high temperatures of present day engineering materials N89-16996
Aerothermal modeling program. Phase 2, element A: Improved numerical methods for turbulent viscous recirculating flows N89-17303
Application of advanced diagnostics to airblast injector flows N89-17306
Three-dimensional inelastic analysis methods for hot section components N89-17316
Structural response of an advanced combustor liner: Test and analysis N89-17329
Elevated temperature crack growth N89-17335
The effect of insulated combustion chamber surfaces on direct-injected diesel engine performance, emissions, and combustion
[NASA-CR-182204] N89-17548
COMBUSTION EFFICIENCY
Results from the Federal Methanol Fleet
[DE88-015291] N89-17016
COMBUSTION PRODUCTS
Emission-reduction effects of methanol vehicles: State of knowledge
[DE89-001148] N89-17359
The effect of insulated combustion chamber surfaces on direct-injected diesel engine performance, emissions, and combustion
[NASA-CR-182204] N89-17548
COMET TAILS
Optical and infrared studies of cometary dust N89-17550
COMETARY ATMOSPHERES
Optical and infrared studies of cometary dust N89-17550
COMMAND AND CONTROL
Temporal pattern recognition
[AD-A200090] N89-17426
COMMUNICATION
Robotic vehicle communications interoperability
[TACOM-TR-13387] N89-17075
COMMUNICATION THEORY
Applications of correcting coding theory to communication combinatorial problems
[ENST-88C001] N89-17065
COMMUNITIES
A strategy for understanding noise-induced annoyance
[AD-A200125] N89-17461
COMMUTATORS
A presentation for Virasoro algebras
[DE89-003883] N89-17440
The integrability condition for dynamical systems
[DE89-004124] N89-17443
COMPATIBILITY
Inlet-engine compatibility N89-16741
Compatibility study of an absorber material and two silicone adhesives
[DE89-002361] N89-17011
Fuel property and antioxidant effects on elastomer integrity, phase 2
[AD-A200250] N89-17015
COMPILERS
Vectorizing compilers: A test suite and results
[DE89-005376] N89-17406
COMPLEX COMPOUNDS
An in situ surface Fourier transform study of complexes of lithium, magnesium potassium and lanthanum ferrocyanide at platinum and gold electrodes
[AD-A200305] N89-16950
COMPONENT RELIABILITY
AGARD/SMP Review: Damage Tolerance for Engine Structures. 1: Non-Destructive Evaluation
[AGARD-R-768] N89-17253
The impact of engineering assumptions on NDE requirements N89-17254
Relationships of nondestructive evaluation needs and component design N89-17256
COMPOSITE MATERIALS
Nonlinear dynamic responses of composite rotor blades
[AD-A200145] N89-16774
Design of filament-wound rocket cases N89-16910
Investigation of microstructural factors that cause low fracture toughness in silicon carbide whisker/Al alloy composites
[AD-A200147] N89-16925
National Research Council Resident Research Associateship (NRC-RRA) Program
[AD-A200183] N89-16926
Refractory metal alloys and composites for space nuclear power systems
[NASA-TM-101364] N89-16986
Engineering Materials for Very High Temperatures: An ORNL Workshop
[ORNL-8-016-R] N89-16992
Development of composite high temperature materials for future energy conversion applications N89-16995
Electric conductivity of polymer composite materials. Composite on propylene and silicon base
[DE88-704293] N89-17001
Compatibility study of an absorber material and two silicone adhesives
[DE89-002361] N89-17011
FRP (Fiber Reinforced Plastics) cutting technology reported N89-17048
Brittle material processing reported N89-17051
Picosecond optoelectronic switches using composite electronic materials N89-17107
The behavior of shells made of composites during the dynamic application of axian compression
[AD-A200244] N89-17266
Thermally conductive alumina/organic composites for photovoltaic concentrator cell isolation
[DE89-001181] N89-17346
COMPOSITE STRUCTURES
Nonlinear dynamic responses of composite rotor blades
[AD-A200145] N89-16774
Composite motor case design N89-16909
Considerations for designers of cases for small solid propellant rocket motors N89-16911
A multiaxial strength criterion for composites
[AD-A199610] N89-16920
Hygrothermal deformations of laminated composite shells N89-16924
COMPRESSIBLE FLOW
Evaluation and application of a new interferometry technique for compressible flow research
[NASA-CR-177467] N89-16765
Introduction to Computational Fluid Dynamics --- conference
[VKI-LS-1988-02] N89-17174
Implicit time dependent methods for inviscid and viscous compressible methods N89-17178
COMPRESSING
Electrical pulse compression by traveling-wave photoconductivity N89-17137
COMPRESSOR BLADES
The effects of a compressor rebuild on gas turbine engine performance N89-16803
COMPRESSOR ROTORS
Axial supersonic inlet compound N89-16839
Design methodology for advanced High Pressure (HP) compressor first stage N89-16840
Holographic interferometry for flow visualization studies in high speed fans N89-16841
Use of holography in vibration and flutter study of fans N89-16842
COMPUTATION
Accurate modeling of parallel scientific computations
[NASA-CR-181756] N89-17418
COMPUTATIONAL FLUID DYNAMICS
Transonic aeroelastic analysis of launch vehicle configurations N89-16723
Aerodynamic performance of wings of arbitrary planform in inviscid, incompressible, irrotational flow
[AD-A200436] N89-16728
Verification of a Navier-Stokes code for solving the hypersonic blunt body problem
[DE89-003169] N89-16737

Intake Aerodynamics, volume 2 — conference
[VKI-LS-1988-04-VOL-2] N89-16748
Computational methods for inlet airframe integration N89-16752
CFD application to subsonic inlet airframe integration — computational fluid dynamics (CFD) N89-16753
CFD application to supersonic/hypersonic inlet airframe integration — computational fluid dynamics (CFD) N89-16754
A statistical theory for gas surface interactions in rarefied hypersonic flows
[IC-AERO-88-01] N89-16755
Transonic Compressors, volume 1 — conference
[VKI-LS-1988-03-VOL-1] N89-16825
Incidence angle rules in supersonic cascades N89-16827
Exit angle rules in supersonic cascades N89-16828
Analysis of 3D viscous flows in transonic compressors N89-16831
Transonic Compressors, volume 2 — conference
[VKI-LS-1988-03-VOL-2] N89-16833
The design and development of transonic multistage compressors N89-16834
Supersonic compressors N89-16836
Design methodology for advanced High Pressure (HP) compressor first stage N89-16840
Aerodynamic Data Accuracy and Quality: Requirements and Capabilities in Wind Tunnel Testing
[AGARD-CP-429] N89-16846
The accurate measurement of drag in the 8 ft x 8 ft tunnel N89-16855
The use of computational fluid dynamic methods to assess the effects of model support systems and working section modifications on the flow around wind tunnel models N89-16862
Physical aspects of viscous simulation and associated research requirements N89-16865
On Reynolds number effects and simulation N89-16866
A proposed boundary layer simulation methodology for wind tunnel testing N89-16867
Wind tunnel requirements for computational fluid dynamics code verification N89-16880
Modeling and Applications of Transport Phenomena in Porous Media, volume 2 — conference
[VKI-LS-1988-01-VOL-2] N89-17167
Stochastic description of porous media N89-17168
Multiphase flow in porous media N89-17169
Physical mechanisms during drying of porous media N89-17173
Introduction to Computational Fluid Dynamics — conference
[VKI-LS-1988-02] N89-17174
Introduction to computational fluid dynamics N89-17175
Boundary layer equations and methods of solution N89-17176
Introduction to finite element techniques in fluid mechanics N89-17177
Implicit time dependent methods for inviscid and viscous compressible methods N89-17178
Modeling and applications of transport phenomena in porous media. Volume 1: Mathematical modeling of transport in porous media
[VKS-LS-1988-01-VOL-1] N89-17202
Decoupling of ionization in the hypersonic boundary limit — computational fluid dynamics
[CERT-RT-OA-21/5005-AYD] N89-17204
Aerothermal modeling program. Phase 2, element A: Improved numerical methods for turbulent viscous recirculating flows N89-17303
Development of generalized block correction procedures for the solution of discretized Navier-Stokes equations N89-17307

COMPUTATIONAL GRIDS
Remapping on the staggered mesh
[DE89-002656] N89-17154
Development of generalized block correction procedures for the solution of discretized Navier-Stokes equations N89-17307

COMPUTER AIDED DESIGN
Overall optimization of solid rocket motor N89-16916
Computer-aided design of bevel gear tooth surfaces
[NASA-TM-101449] N89-17248
A formal language model for local area network configuration N89-17544

COMPUTER AIDED TOMOGRAPHY
Energy and Technology Review
[DE89-005306] N89-17459

COMPUTER ASSISTED INSTRUCTION
Northeast Artificial Intelligence Consortium annual report 1986. Volume 5. Building an intelligent assistant: The acquisition, integration, and maintenance of complex distributed tasks
[AD-A199624] N89-17425

COMPUTER GRAPHICS
An abstract interactive graphics interface for the IBM/PC and Macintosh
[AD-A200427] N89-17411
HANDYPAK: A histogram and display package
[DE89-002742] N89-17413
Automatic registration of satellite imagery
[INPE-4637-PRE/1349] N89-17414
A visualization model based on the mathematics of fiber bundles
[DE89-002537] N89-17432

COMPUTER NETWORKS
Temporal pattern recognition
[AD-A200090] N89-17426

COMPUTER PROGRAM INTEGRITY
Maintenance of database integrity in a scheme-less database system N89-17542

COMPUTER PROGRAMMING
JUNCTION code user's manual. Electromagnetic scattering and radiation by arbitrary configurations of conducting bodies and wires
[AD-A200315] N89-17072
An algorithm for analysis of plate motions in Crust Dynamics Project (CDP) networks
[88821606] N89-17371
An abstract interactive graphics interface for the IBM/PC and Macintosh
[AD-A200427] N89-17411

COMPUTER PROGRAMS
Event-centered scheduling program: The need for PERT (Program Evaluation Review Technique) in C-141 ISO inspection management
[AD-A200094] N89-16718
Development of direct-inverse 3-D methods for applied transonic aerodynamic wing design and analysis
[NASA-CR-184788] N89-16761
Inertial navigation system simulator program: Top-level design
[AD-A200605] N89-16772
An indirect method for numerical optimization using the Kreisselmeir-Steinhauser function
[NASA-CR-4220] N89-16779
A joint study on the computerisation of in-field aero engine vibration diagnosis N89-16808
Tip clearance signal processor development
[AD-A199830] N89-16822
The synchronous injection ignition valveless pulsejet N89-16823
The use of computational fluid dynamic methods to assess the effects of model support systems and working section modifications on the flow around wind tunnel models N89-16862
Accuracy of various wall-correction methods for 3D subsonic wind-tunnel testing N89-16863
Computerized thermographic technique for the detection of boundary layer separation N89-16876
User and technical documentation
[NASA-CR-172087] N89-16893
Design and analysis of solid rocket motor nozzle N89-16908
Overall optimization of solid rocket motor N89-16916
Elastic wrinkling of sandwich panels with laminated fibre reinforced face plates (face plates of AsBoDs, AsDIDs and AsBsDs types). (Computer program)
[ESDU-88015] N89-16930
A Canadian low earth orbit launch vehicle: Launch vehicle performance analysis of Black Brant VC and Nihka rocket motor configurations N89-17039
JUNCTION code user's manual. Electromagnetic scattering and radiation by arbitrary configurations of conducting bodies and wires
[AD-A200315] N89-17072
Theoretical studies of solar lasers and converters
[NASA-CR-184589] N89-17214
Computer program for the prediction of air-lift pump performance
[ESDU-88014] N89-17246
Pipeline vibrations. Undamped natural vibration of pipelines
[ESDU-88022] N89-17268
Maximum inelastic bending moments and form factors for symmetric bending of beams
[ESDU-88035] N89-17270
Calculation methods for along-wind loading. Part 4: Computer program for estimation of response
[ESDU-88036] N89-17271
Evaluation of aerothermal modeling computer programs N89-17308
Three-dimensional inelastic analysis for hot section components, BEST 3D code N89-17317
Three-dimensional inelastic analysis methods for hot section components N89-17321
Constitutive modeling for isotropic materials N89-17322
PC-1D Version 2: Enhanced numerical solar cell modeling
[DE89-000302] N89-17349
Prediction of stochastic blade responses using measured wind-speed data as input to the FLAP code
[DE89-000834] N89-17354
Strain accumulation in the Santa Barbara Channel, 1971-1987
[NASA-CR-183402] N89-17369
Regenerative life support system research and concepts
[NASA-CR-184760] N89-17404
The suitability of an object-oriented language for prototyping and abstract data types
[AD-A200417] N89-17410
KINETICS: A computer program to analyze chemical reaction data
[DE89-004602] N89-17419
Interconnecting different types of local area computer networks
[AD-A200280] N89-17423
Massive symbolic mathematical computations and their applications
[AD-A200253] N89-17434
Sparse matrix methods research using the CSM testbed software system
[NASA-CR-4219] N89-17441
Signal acquisition and processing for autonomous space shuttle cargo bay acoustic measurements (NASA G-313)
[AD-A200426] N89-17462
Jet-by-jet shielding of noise
[ESDU-88023] N89-17463
BRYNTRN: A baryon transport model
[NASA-TP-2887] N89-17562

COMPUTER STORAGE DEVICES
Optical storage: Financial management and budget applications
[DE89-004916] N89-17546

COMPUTER SYSTEMS DESIGN
A personal computer based system for the evaluation of multiple exposed images in laser speckle and particle image displacement velocimetry N89-17193
Initial structural response measurements for the Sandia 34-meter VAWT test bed
[DE89-003133] N89-17352
Empirical analysis and refinement of expert system knowledge bases
[AD-A200146] N89-17428

COMPUTER SYSTEMS PERFORMANCE
The design, analysis, and implementation of a fully distributed local area network for integrated voice and data communications N89-17059
Machine learning of parameter control doctrine for sensor and communication systems
[AD-A200096] N89-17427
Empirical analysis and refinement of expert system knowledge bases
[AD-A200146] N89-17428

COMPUTER TECHNIQUES
R/M/T (Reliability/Maintainability/Testability) design for fault tolerance. Volume 1: Program manager's guide
[AD-A200204] N89-17262
Development of generalized block correction procedures for the solution of discretized Navier-Stokes equations N89-17307
Planetary cartography in the next decade: Digital cartography and emerging opportunities
[NASA-TM-4092] N89-17560

COMPUTER VISION
3-D vision techniques for autonomous vehicles
[AD-A199643] N89-17236
Spatial reasoning in the treatment of systematic sensor errors
[DE89-003244] N89-17251
Role of retinocortical processing in spatial vision
[AD-A200198] N89-17394

COMPUTERIZED SIMULATION
Inertial navigation system simulator: Behavioral specification
[AD-A200604] N89-16771
Inertial navigation system simulator program: Top-level design
[AD-A200605] N89-16772
Analysis of 3D viscous flows in transonic compressors N89-16831
Wind tunnel predicted air vehicle performance: A review of lessons learned N89-16852
On Reynolds number effects and simulation N89-16866
A proposed boundary layer simulation methodology for wind tunnel testing N89-16867
Functional performance specification for an external computer system simulator
[AD-A200611] N89-16881
Statistical mechanics of polymer systems
[DE89-002012] N89-17002

Theoretical studies of solar lasers and converters
[NASA-CR-184589] N89-17214
Aneurisms in laser-driven blast waves
[AD-A200189] N89-17222
Experimental validation of a zero-dimensional computer model for spark-ignition engines
[DE89-002848] N89-17243
An algorithm for calculating the area of overlap of an ellipse and a convex polygon
[AD-A199654] N89-17408
Extensions to the matrix pencil approach for direction finding
[AD-A200112] N89-17449
Parallel processing of a rotating shaft simulation
[NASA-TM-101462] N89-17453
Atomic-scale modeling of low-energy ion-solid processes
[DE89-004374] N89-17482
Model microfield calculations of radiative and transport properties of ions in strongly coupled plasmas
[DE89-001244] N89-17503
Lattice gauge theories and Monte Carlo algorithms
[DE89-003569] N89-17539

CONCENTRATION (COMPOSITION)
An intelligent sensor for equipment health monitoring of ferromagnetic wear debris concentration in fluids N89-16818

CONCENTRATORS
Concentrator efficiencies of 29.2 percent for a GaAs cell and 24.8 percent for a mounted cell-lens assembly
[DE89-001612] N89-17344
Recent advances in high-efficiency InGaAs concentrator cells
[DE89-001613] N89-17345

CONCENTRICITY
Concentricity and sphericity of composite drops under microgravity N89-17042

CONDENSING
Adsorption of phosphorus acids on alumina
[AD-A200548] N89-16957

CONDUCTION BANDS
Longitudinally localized optical carrier injection for femtosecond transport studies N89-17121
Monte Carlo studies of nonlinear electron transport in 3-5 semiconductors
[AD-A199700] N89-17516

CONDUCTIVE HEAT TRANSFER
Profile properties of undeformed first-year sea ice
[AD-A200172] N89-17388

CONDUCTORS
Stress driven diffusive voiding of aluminum conductor lines: A model for time dependent failure
[DE89-001665] N89-17144

CONFERENCES
Intake Aerodynamics, volume 1 --- conference
[VKI-LS-1988-04-VOL-1] N89-16738
Intake Aerodynamics, volume 2 --- conference
[VKI-LS-1988-04-VOL-2] N89-16748
Transonic Compressors, volume 1 --- conference
[VKI-LS-1988-03-VOL-1] N89-16825
Transonic Compessors, volume 2 --- conference
[VKI-LS-1988-03-VOL-2] N89-16833
Proceedings of the Colloquium about Joint Projects Within the DFVLR/ISRO Cooperation
[DFVLR-MITT-88-19] N89-16883
Engineering Materials for Very High Temperatures: An ORNL Workshop
[ORNL-8-016-R] N89-16992
Microgravity science and applications bibliography, 1988 revision
[NASA-TM-4098] N89-17045
Topical Meeting on Picosecond Electronics and Optoelectronics
[AD-A189686] N89-17080
Modeling and Applications of Transport Phenomena in Porous Media, volume 2 --- conference
[VKI-LS-1988-01-VOL-2] N89-17167
Introduction to Computational Fluid Dynamics --- conference
[VKI-LS-1988-02] N89-17174
Particle Image Displacement Velocimetry --- conference
[VKI-LS-1988-06] N89-17179
AGARD/SMP Review: Damage Tolerance for Engine Structures. 1: Non-Destructive Evaluation
[AGARD-R-768] N89-17253
Turbine Engine Hot Section Technology, 1987
[NASA-CP-2493] N89-17298
Middle Atmosphere Program: Handbook for MAP, volume 26
[NASA-CR-183350] N89-17368
ONR (Office of Naval Research) tropical cyclone motion research initiative: Mid-year review, discussion and working group reports
[AD-A200286] N89-17380

CONFORMAL MAPPING
Spherical-type hypersurfaces in a Riemannian manifold
[DE88-704224] N89-17454

CONGRESSIONAL REPORTS
Report to Congress on the Automotive Technology Development Program
[DE89-004977] N89-17250

CONSTRAINTS
An indirect method for numerical optimization using the Kreisselmeir-Steinhauser function
[NASA-CR-4220] N89-16779
Extravehicular activities limitations study. Volume 1: Physiological limitations to extravehicular activity in space
[NASA-CR-172098] N89-17392
Extravehicular activities limitations study. Volume 2: Establishment of physiological and performance criteria for EVA gloves
[NASA-CR-172099] N89-17393

CONTACT LOADS
The design of spur and helical involute gears. A procedure compatible with BS 436:1986: Method for calculation of contact and root bending stress limitations for metallic involute gears
[ESDU-88033] N89-17247

CONTAMINANTS
Screening environmental pollutants and biomarkers: The analytical challenge
[DE89-004931] N89-17366

CONTINUOUS WAVE LASERS
A scanning laser beam system for two-dimensional illumination of flow fields N89-17196

CONTINUUM MODELING
Modeling and applications of transport phenomena in porous media. Volume 1: Mathematical modeling of transport in porous media
[VKS-LS-1988-01-VOL-1] N89-17202
A continuum deformation theory for metal-matrix composites at high temperature N89-17323

CONTRAST
Contrast sensitivity in Army aviator candidates: Cycloplegia effects and population norms
[AD-A200433] N89-17397

CONTROL SURFACES
Accuracy of lift and center-of-thrust measurements at missile control surfaces N89-16875

CONTROL SYSTEMS DESIGN
The advantage of a thrust rating concept used on the RB199 engine N89-16800
Adaptive control techniques for large space structures
[AD-A200208] N89-16901
Computer control of gas metal arc welding
[DE89-005188] N89-17252

CONTROLLERS
Controller-Programmer for telemetry systems
[DE89-002539] N89-16898
Spillover stabilization in the control of large flexible space structures N89-16902

CONVECTION
Development of an infrared imaging system for the surface tension driven convection experiment
[NASA-TM-101479] N89-17211
On deriving the three-dimensional kinematic structure on convective storms from a single radar N89-17376

CONVECTIVE FLOW
Measurement of natural convection by white light speckle velocimetry N89-17197
Penetration effects of the compound vortex in gas metal-arc welding
[AD-A200585] N89-17242

CONVECTIVE HEAT TRANSFER
Multidimensional modeling of convective heat transfer with application to I. C. engines
[DE89-004062] N89-17166
Phase change phenomena in liquid saturated self heated particulate bed --- core meltdown N89-17170
Heat transfer in self-heated particle beds submerged in liquid coolant N89-17171

CONVERGENCE
Strain accumulation in the Santa Barbara Channel, 1971-1987
[NASA-CR-183402] N89-17369

CONVEXITY
An algorithm for calculating the area of overlap of an ellipse and a convex polygon
[AD-A199654] N89-17408

COOLANTS
Coolant passage heat transfer with rotation N89-17314

COOLING
Effect of Lewis number on wet surface heat exchangers N89-17152
Thermal expansion mismatch and plasticity in thermal barrier coating N89-17330
Cooled ion frequency standard
[AD-A200373] N89-17475

COOLING SYSTEMS
Fouling in cooling water systems
[ESDU-88024] N89-17057

COOPERATION
Short-Crack Growth Behaviour in an Aluminum Alloy: An AGARD Cooperative Test Programme
[AGARD-R-732] N89-17287
Database program for crack propagation data acquired in the AGARD short cracks collaborative effort N89-17297

COPOLYMERS
The 15N CP/MAS NMR of aramids: A tool for characterization of the morphology of high modulus fibers for composites
[AD-A199656] N89-16921

COPPER
Oxygen and copper valencies in oxygen-doped superconducting La2CuO(sub 4.13)
[DE89-003265] N89-17533

COPPER COMPOUNDS
Study of structure of high-Tc superconductor Y(YV)Ba2Cu3O(sub 9-x) and its resistance sharp drop
[DE88-704104] N89-17531

COPPER SELENIDES
Device physics related to the granular nature of CuInSe2 solar cells
[DE89-000810] N89-17341

CORES
Microstructural examination of core-programme material N89-17289

CORRECTION
Wind tunnel-sidewall-boundary-layer effects in transonic airfoil testing-some correctable, but some not N89-16864

CORRELATION
A model for transition by attachment line contamination and an examination of cross-flow instability in three-dimensional boundary layers N89-17153
A comparison of turbulence measurement methods N89-17302
Multiparametric research of early indicators of vascular risk in flying personnel
[ETN-89-93613] N89-17398

CORRUGATING
Molecular spectroscopy at corrugated metal surfaces
[AD-A200124] N89-16973

COSMIC DUST
Optical and infrared studies of cometary dust N89-17550

COSMIC RAYS
Meteorites and lunar samples as space probes --- Indian/German space cooperation N89-16885
Isotropization of the cosmic background radiation due to galactic gravitational screening
[DE88-755533] N89-17563

COSMOLOGY
Geometry on the space of geometries
[DE88-704214] N89-17537
Investigations in particle and field theory
[DE89-003004] N89-17538
Is the great attractor really a great wall
[NASA-CR-184772] N89-17540
What topology could the universe be created with
[DE88-704321] N89-17554
An essay on discrete foundations for physics
[DE89-002992] N89-17556
Monopoles and magnetic fields in the inflationary universe
[DE88-755532] N89-17557
Isotropization of the cosmic background radiation due to galactic gravitational screening
[DE88-755533] N89-17563

COST ANALYSIS
Nickel hydrogen battery development
[DE89-001063] N89-17143

COST ESTIMATES
Aircraft airframe cost estimating relationships: All mission types
[AD-A200262] N89-16719
Aircraft airframe cost estimating relationships: Fighters
[AD-A200263] N89-16720
Aircraft airframe cost estimating relationships: Bombers and transports
[AD-A200264] N89-16721
Aircraft airframe cost estimating relationships: Attack aircraft
[AD-A200265] N89-16722
Systems analysis and design of a lunar solar power plant for the supply of a lunar base
[ILR-MITT-198] N89-17355

COWLINGS
Transonic cowl design N89-16746

CRACK ARREST
Electron beam welding produces improved duplex crack arrest specimens
[DE88-003885] N89-17239
CRACK CLOSURE
Elevated temperature crack growth N89-17335
CRACK INITIATION
Stochastic modeling of crack initiation and short-crack growth under creep and creep-fatigue conditions
[NASA-TM-101358] N89-17286
High temperature constitutive and crack initiation modeling of coated single crystal superalloys
N89-17334
CRACK PROPAGATION
Importance of sensitivity and reliability of NDI techniques on damage tolerance based life prediction of turbine discs N89-17257
Numerical analysis of the effects of void growth and crack tip opening on ductile fracture N89-17265
Stochastic modeling of crack initiation and short-crack growth under creep and creep-fatigue conditions
[NASA-TM-101358] N89-17286
Short-Crack Growth Behaviour in an Aluminum Alloy: An AGARD Cooperative Test Programme
[AGARD-R-732] N89-17287
Short-crack growth behaviour in an aluminum alloy: An AGARD cooperative test program N89-17288
Microstructural examination of core-programme material N89-17289
Preliminary fatigue tests on short-crack specimens
N89-17290
Long-crack growth rate data: Constant amplitude and FALSTAFF loading N89-17295
Long-crack growth rate data: Gaussian loading
N89-17296
Database program for crack propagation data acquired in the AGARD short cracks collaborative effort
N89-17297
Elevated temperature crack growth N89-17335
Simplified fatigue damage and crack growth calculations for wind turbines
[DE89-003132] N89-17351
CRACK TIPS
Numerical analysis of the effects of void growth and crack tip opening on ductile fracture N89-17265
Elevated temperature crack growth N89-17335
CRACKS
The effect of chemistry modifications on the solidification behavior and weldability of Alloy 625
[DE89-001046] N89-16972
Stress driven diffusive voiding of aluminum conductor lines: A model for time dependent failure
[DE89-001665] N89-17144
Total strain version of strainrange partitioning for thermomechanical fatigue at low strains N89-17337
CREEP ANALYSIS
Stochastic modeling of crack initiation and short-crack growth under creep and creep-fatigue conditions
[NASA-TM-101358] N89-17286
CREEP PROPERTIES
Internal stress during high-temperature creep and activation energy for creep of Hastelloy XR
[DE88-755231] N89-16969
Development of a viscoplastic cyclic behavior law to allow a correct description of creep phenomena
[ONERA-RT-67/1765-RY-078-R] N89-17285
Preliminary study of creep thresholds and thermomechanical response in Haynes 188 at temperatures in the range 649 to 871 C N89-17327
Total strain version of strainrange partitioning for thermomechanical fatigue at low strains N89-17337
CREEP STRENGTH
Stochastic modeling of crack initiation and short-crack growth under creep and creep-fatigue conditions
[NASA-TM-101358] N89-17286
CREEP TESTS
Preliminary study of creep thresholds and thermomechanical response in Haynes 188 at temperatures in the range 649 to 871 C N89-17327
CRITICAL POINT
Vapour pressures and critical points of liquids. C7 to C20 alkanols
[ESDU-88012] N89-16962
Vapour pressures and critical points of liquids. Organic oxygen compounds
[ESDU-88017] N89-16963
CRITICAL TEMPERATURE
The electronic structure and the state of compositional order in metallic alloys
[DE89-003147] N89-16977
A simple method for preparing superconducting high T(sub c) thin films
[DE89-003663] N89-17527
CROSS FLOW
Evaluation of aerothermal modeling computer programs N89-17308
CRUISING FLIGHT
Supersonic through-flow fan assessment
[NASA-CR-182202] N89-16843
CRYSTAL DEFECTS
High temperature constitutive and crack initiation modeling of coated single crystal superalloys
N89-17334
Compositional changes during ion bombardment
[DE89-003974] N89-17481
CRYSTAL DISLOCATIONS
Experimental evidence for positron trapping at dislocations in Ni3Al alloys
[DE89-004520] N89-16989
CRYSTAL LATTICES
InP/GainAs/InP PIN photodiode with FWHM less than 18 ps N89-17114
Studies of NiO metal interfaces
[DE89-003634] N89-17529
CRYSTAL STRUCTURE
Synthesis and properties of low carbon boron carbides
[DE89-002184] N89-16923
Electronic behavior of highly correlated metals
[DE89-002492] N89-16971
The electronic structure and the state of compositional order in metallic alloys
[DE89-003147] N89-16977
Nonequilibrium phonons and disorder in Al(sub x)Ga(sub 1-x)As N89-17103
New Al-Ni-Ge contacts on GaAs: Their structure and electrical properties
[DE89-002918] N89-17526
Study of structure of high-Tc superconductor Y(YV)Ba2Cu3O(sub 9-x) and its resistance sharp drop
[DE88-704104] N89-17531
CRYSTALLINITY
Manufacturing thermoplastic matrix composites
[AD-A199724] N89-16922
CRYSTALLOGRAPHY
Constitutive modelling of single crystal and directionally solidified superalloys N89-17325
CRYSTALS
Fractal and spherulitic morphology of silicon nitride crystallized from amorphous films
[AD-A200158] N89-17522
CUMULUS CLOUDS
A numerical modeling investigation of the effect of convective-mesoscale interactions on the sea breeze circulation N89-17377
CURING
Structure and properties of polymer interphases
[AD-A200238] N89-17008
CURVATURE
Alfven waves in a cold plasma with curved magnetic fields
[AD-A200312] N89-17506
CUTTERS
Nitride and carbide coatings for high speed steel cutting tools
[DE89-003623] N89-16984
CUTTING
FRP (Fiber Reinforced Plastics) cutting technology reported N89-17048
Hard material cutting technology described
N89-17049
CYCLIC LOADS
Low-cycle fatigue behavior of cyclic hardening and softening steels under multiaxial elastic-plastic loading conditions with constant and variable amplitudes
N89-17280
Development of a viscoplastic cyclic behavior law to allow a correct description of creep phenomena
[ONERA-RT-67/1765-RY-078-R] N89-17285
On-line spectrum loading accuracy verification
N89-17292
Long-crack growth rate data: Gaussian loading
N89-17296
CYCLONES
Kinetic energy diagnostic studies of extratropical cyclones based on storm relative motion N89-17378
ONR (Office of Naval Research) tropical cyclone motion research initiative: Mid-year review, discussion and working group reports
[AD-A200286] N89-17380
CYLINDERS
An experimental investigation of the aerodynamic characteristics of slanted base ogive cylinders using magnetic suspension technology
[NASA-CR-184824] N89-16758
CYLINDRICAL BODIES
Heat transfer with very high free-stream turbulence and heat transfer with streamwise vortices N89-17309
CYLINDRICAL SHELLS
The behavior of shells made of composites during the dynamic application of axian compression
[AD-A200244] N89-17286

D

DAMAGE
AGARD/SMP Review: Damage Tolerance for Engine Structures. 1: Non-Destructive Evaluation
[AGARD-R-768] N89-17253
Importance of sensitivity and reliability of NDI techniques on damage tolerance based life prediction of turbine discs N89-17257
DAMAGE ASSESSMENT
Microanalytical characterization of wear damage in an alumina-silicon carbide whisker composite
[DE89-003149] N89-16932
Damage tolerance behavior of fiber reinforced composite airframes N89-17278
DARK MATTER
Is the great attractor really a great wall
[NASA-CR-184772] N89-17540
DATA ACQUISITION
High-resolution Interferometer Sounder (HIS), phase 2
[NASA-CR-183414] N89-17212
Database program for crack propagation data acquired in the AGARD short cracks collaborative effort
N89-17297
A microprocessor-based, solar cell parameter measurement system
[AD-A200227] N89-17348
A data acquisition and storage system for the ion auxiliary propulsion system cyclic thruster test
[NASA-TM-101469] N89-17424
DATA BASE MANAGEMENT SYSTEMS
Database program for crack propagation data acquired in the AGARD short cracks collaborative effort
N89-17297
DATA BASES
Coolant passage heat transfer with rotation
N89-17314
Maintenance of database integrity in a scheme-less database system N89-17542
Planetary cartography in the next decade: Digital cartography and emerging opportunities
[NASA-TM-4092] N89-17560
BRYNTRN: A baryon transport model
[NASA-TP-2887] N89-17562
DATA COMPRESSION
COMPASS (Trademark): A generalized ground-based monitoring system N89-16819
DATA FLOW ANALYSIS
Event-centered scheduling program: The need for PERT (Program Evaluation Review Technique) in C-141 ISO inspection management
[AD-A200094] N89-16718
DATA LINKS
Non return to zero (NRZ) clock recovery breadboard for 200 MB/S optical intersatellite link
[CNES-CT/DRT/TIT/TR-87/024] N89-17496
DATA PROCESSING
CF-18/F404 transient performance trending
N89-16814
The design, analysis, and implementation of a fully distributed local area network for integrated voice and data communications N89-17059
DATA RECORDING
COMPASS (Trademark): A generalized ground-based monitoring system N89-16819
DATA REDUCTION
A new algorithm for the rapid analysis of particle image displacement data N89-17195
DATA SMOOTHING
COMPASS (Trademark): A generalized ground-based monitoring system N89-16819
DATA STORAGE
Remapping on the staggered mesh
[DE89-002656] N89-17154
A data acquisition and storage system for the ion auxiliary propulsion system cyclic thruster test
[NASA-TM-101469] N89-17424
DEBRIS
Gas path condition monitoring using electrostatic techniques N89-16817
An intelligent sensor for equipment health monitoring of ferromagnetic wear debris concentration in fluids
N89-16818
DEBYE-SCHERRER METHOD
Hopping model for the non-Debye dielectric response in ionic crystals
[DE89-003151] N89-17521
DECISION MAKING
A model of the effect of sparing and repair turnaround time of the inertial navigation system on aircraft readiness for the F/A-18
[AD-A200317] N89-16777

DECOMPOSITION
Kinetics of the isothermal decomposition of lanthanum nickel hydride
[DE89-002905] N89-16966
Tailoring domain decomposition to the network structure for parallel processing of fluid dynamics
[DE89-005501] N89-17206
Collision-induced decomposition of multiatomic ions N89-17468

DEFECTS
CF-18/F404 transient performance trending N89-16814
Review of existing NDT technologies and their capabilities N89-17255
Investigation of defect and electronic interactions associated with GaAs device processing
[AD-A200541] N89-17525

DEFENSE PROGRAM
The space-based interceptor
[DE89-002869] N89-17451

DEFLECTION
Speckle photography of flows with varying fluid density N89-17186
Monte Carlo calculation of electron multiple scattering in thin foils
[AD-A199872] N89-17517

DEFORMATION
Hygrothermal deformations of laminated composite shells N89-16924
Surface deformations resulting from laser spot welding
[DE88-014964] N89-17237
A continuum deformation theory for metal-matrix composites at high temperature N89-17323

DEGRADATION
A microprocessor-based, solar cell parameter measurement system
[AD-A200227] N89-17348

DEGREES OF FREEDOM
Development of kinematic equations and determination of workspace of a 6 DOF end-effector with closed-kinematic chain mechanism
[NASA-CR-183241] N89-17444

DEIONIZATION
The electron-water vapor (H2O) collision cross sections
[AD-A200187] N89-17472

DELAMINATING
Tensile strength of composite structures with internal ply drops and free-edge effects N89-16929

DELTA WINGS
Numerical solution of flow fields around Delta wings using Euler equations method
[NAL-TM-FM-8701] N89-16757

DEMODULATION
The visibility of noise in system 1 colour television
[BBC-RD-1988/12] N89-17061

DEMOGRAPHY
Contrast sensitivity in Army aviator candidates: Cyclopiegia effects and population norms
[AD-A200433] N89-17397

DENSITY DISTRIBUTION
Axial velocity density ratio influence on exit flow angle in transonic/supersonic cascades N89-16830
High power Ion Cyclotron Resonance Heating (ICRH) in JET
[DE89-002218] N89-17499

DENSITY MEASUREMENT
Development and application of oxygen flow tagging for velocity measurements and flow visualization in turbulent three-dimensional supersonic flows
[AD-A200119] N89-16725
Development of conducting polymers of high structural strength
[AD-A200310] N89-17009

DEPLETION
An optical modulator/switch using the reflection from a translated depletion edge
[DE89-001380] N89-17490

DEPOSITION
Gas jet deposition of multicomponent ultrafine microstructures
[AD-A200101] N89-16946
Ion assisted deposition of fiber coatings for ceramic matrix composites wth low dielectric loss tangents
[AD-A200162] N89-17005
Laser studies of the SiH radical/surface interaction during deposition of a thin film
[DE89-003902] N89-17232
Fractal and spherulitic morphology of silicon nitride crystallized from amorphous films
[AD-A200158] N89-17522
Growth of gallium arsenide using ion cluster beam technology, volume 1, phase 2
[AD-A200231] N89-17523

DEPTH
Gas jet deposition of multicomponent ultrafine microstructures
[AD-A200101] N89-16946

DERIVATION
Derivation and application of a class of generalized impedance boundary conditions, part 2
[NASA-CR-183298] N89-17148

DESIGN ANALYSIS
An indirect method for numerical optimization using the Kreisselmeir-Steinhauser function
[NASA-CR-4220] N89-16779
The design and development of transonic multistage compressors N89-16834
Advances in solid rocket nozzle design and analysis technology in the United States since 1970 N89-16907
Design and analysis of solid rocket motor nozzle N89-16908
Effectiveness: N(sub TU) relationships for the design and performance evaluation of additional shell-and-tube heat exchanger geometries
[ESDU-88021] N89-17056
Phototype design and testing of two fiber-optic spectrochemical emission sensors
[DE89-001741] N89-17207
Computer-aided design of bevel gear tooth surfaces
[NASA-TM-101449] N89-17248
The impact of engineering assumptions on NDE requirements N89-17254

DESTABILIZATION
Laser detection of acoustic displacements by destabilizing a frequency stablized helium neon laser
[DE89-005282] N89-17235

DETECTION
Gas path modelling, diagnosis and sensor fault detection N89-16811
Review of existing NDT technologies and their capabilities N89-17255
Material compatability with threshold limit value levels of monomethyl hydrazine
[AD-A200294] N89-17362
Explosion of integrated optic devices used in new generation systems
[DE89-004012] N89-17497

DETERIORATION
Adsorption of phosphorus acids on alumina
[AD-A200548] N89-16957

DETONATION
Prediction and synthesis efforts at Los Alamos
[DE89-003605] N89-17018

DIAGNOSIS
Getting more from vibration analysis N89-16807

DIAMETERS
Measurements of gas turbine combustor and engine augmentor tube sooting characteristics
[AD-A199768] N89-16821

DIELECTRIC PROPERTIES
Hopping model for the non-Debye dielectric response in ionic crystals
[DE89-003151] N89-17521

DIELECTRICS
Characteristics of shielded microstrip lines on GaAs-Si at millimeter-wave frequencies N89-17102

DIESEL ENGINES
Emission-reduction effects of methanol vehicles: State of knowledge
[DE89-001148] N89-17359
The effect of insulated combustion chamber surfaces on direct-injected diesel engine performance, emissions, and combustion
[NASA-CR-182204] N89-17548

DIFFRACTION PATTERNS
Processing techniques: Image plane and Fourier plane --- particle image velocimetry N89-17182

DIFFUSION
Hydrogen diffusion in tantalum
[DE88-704073] N89-16968
Stress driven diffusive voiding of aluminum conductor lines: A model for time dependent failure
[DE89-001665] N89-17144
Compositional changes during ion bombardment
[DE89-003974] N89-17481

DIFFUSION FLAMES
Characterization of nonpremixed turbulent bluff-body burner flames
[PB89-100507] N89-16945

DIFFUSIVITY
Stress driven diffusive voiding of aluminum conductor lines: A model for time dependent failure
[DE89-001665] N89-17144

DIGITAL COMMAND SYSTEMS
Control of reaction wheels through digital techniques using reference models
[INPE-4618-TDL/335] N89-16903

DIGITAL COMPUTERS
COMPASS (Trademark): A generalized ground-based monitoring system N89-16819

DIGITAL ELECTRONICS
Military engine condition monitoring systems: The UK experience N89-16797
Test-efficient design of digital VLSI circuits
[ETN-89-93483] N89-17151

DIGITAL SIMULATION
Modal analysis methods for the reduction of system-conditioned loads N89-17275

DIGITAL SYSTEMS
The advantage of a thrust rating concept used on the RB199 engine N89-16800
Multigigahertz logic based on InP-MISFET's exhibiting extremely high transconductance N89-17086
Signal acquisition and processing for autonomous space shuttle cargo bay acoustic measurements (NASA G-313)
[AD-A200426] N89-17462
Development of an optical digital ionization chamber
[DE89-002209] N89-17470

DIGITAL TECHNIQUES
Planetary cartography in the next decade: Digital cartography and emerging opportunities
[NASA-TM-4092] N89-17560

DIODES
Energy variations in optical pulses from gain-switched AlGaAs diode lasers N89-17111
Microwave and millimeter-wave resonant tunneling diodes N89-17124
Quantum transport calculation of resonant-tunneling response time N89-17125
Radar and EW applications of multi-gigahertz optical components and systems N89-17131
Silicon pulse sharpening diodes: Switching kilovolts in tens of picoseconds N89-17139
Laser communication test system
[AD-A199612] N89-17215

DIRECTION FINDING
Extensions to the matrix pencil approach for direction finding
[AD-A200112] N89-17449

DISCRETE FUNCTIONS
Discrete operating conditions gas path analysis N89-16810

DISCRIMINATION
Models of incremental concept formation
[AD-A199617] N89-17400

DISKS
Seeded inert gas driven disk generator
[DE88-704083] N89-17510

DISKS (SHAPES)
Review of existing NDT technologies and their capabilities N89-17255

DISORDERS
Nonequilibrium phonons and disorder in Al(sub x)Ga(sub 1-x)As N89-17103

DISPERSING
Droplet separation dynamics and kinematics under microgravity N89-17031

DISPLACEMENT
Laser detection of acoustic displacements by destabilizing a frequency stablized helium neon laser
[DE89-005282] N89-17235
Body displacement measured during sustained +Gz, -Gz and + or -Gy acceleration using a stereoscopic photographic system
[NASA-TM-101269] N89-17391

DISSOCIATION
The electron-water vapor (H2O) collision cross sections
[AD-A200187] N89-17472

DISTRIBUTED AMPLIFIERS
Enhanced performance ultrabroadband distributed amplifiers N89-17090

DISTRIBUTED PARAMETER SYSTEMS
The design, analysis, and implementation of a fully distributed local area network for integrated voice and data communications N89-17059

DISTRIBUTED PROCESSING
Finding Eigenvalues and Eigenvectors of unsymmetric matrices using a distributed-memory multiprocessor
[DE89-004731] N89-17416

DISTRIBUTION FUNCTIONS
Quantum transport calculation of resonant-tunneling response time N89-17125
Resonant tunneling electron spectroscopy N89-17126
Global existence for symmetric discrete velocity models
[DE89-003102] N89-17438
The Wigner distribution function with minimum spread
[AD-A199661] N89-17446
Distributed estimation for large-scale event-driven systems
[DE89-002688] N89-17447

DOCUMENTATION
JUNCTION code user's manual. Electromagnetic scattering and radiation by arbitrary configurations of conducting bodies and wires
[AD-A200315] N89-17072
DOCUMENTS
A document preparation system in a large network environment
[DE88-014466] N89-17543
DOPPLER EFFECT
Cooled ion frequency standard
[AD-A200373] N89-17475
DOWNTIME
A model of the effect of sparing and repair turnaround time of the inertial navigation system on aircraft readiness for the F/A-18
[AD-A200317] N89-16777
DRAG CHUTES
Unsteady flow about porous cambered plates
[AD-A200282] N89-17160
DRAG MEASUREMENT
Estimation of drag arising from asymmetry in thrust or airframe configuration
[ESDU-88006] N89-16730
The accurate measurement of drag in the 8 ft x 8 ft tunnel N89-16855
Accurate drag estimation using a single component drag model technique N89-16856
Precision improvement of transport aircraft drag measurements N89-16858
Balance accuracy and repeatability as a limiting parameter in aircraft development force measurements in conventional and cryogenic wind tunnels N89-16873
DRAG REDUCTION
Interdependence of large and small scale structures in a turbulent boundary layer N89-17155
Approximation of viscoelastic stresses from Newtonian turbulent kinematics
[AD-A200188] N89-17157
DRILLING
Microdrilling using electron beams reported N89-17055
DROPS (LIQUIDS)
Droplet separation dynamics and kinematics under microgravity N89-17031
Simultaneous measurements of droplet size and droplet velocity in monodisperse droplet streams N89-17192
DRYING
Physical mechanisms during drying of porous media N89-17173
DUCTED FLOW
CFD application to subsonic inlet airframe integration --- computational fluid dynamics (CFD) N89-16753
DUCTILITY
Numerical analysis of the effects of void growth and crack tip opening on ductile fracture N89-17265
DUST
The role of presolar dust in the formation of the solar system N89-17553
DYE LASERS
Nonlinear optics with broad-band lasers
[DE89-002728] N89-17216
DYNAMIC CHARACTERISTICS
GPS (Global Positioning System) user equipment evaluation techniques using a rotor mounted antenna
[AD-A200515] N89-16770
Development of a panel method for modeling configurations with unsteady component motions, phase 1
[AD-A200255] N89-16775
Identification of dynamic characteristics for fault isolation purposes in a gas turbine using closed-loop measurements N89-16813
On a wide range exclusion process in random medium with local jump intensity
[AD-A200510] N89-17450
DYNAMIC LOADS
Modal analysis methods for the reduction of system-conditioned loads N89-17275
A procedure for the generation of load sequences N89-17276
DYNAMIC MODELS
Nonlocal and quasilocal potentials in the spontaneous emission of molecular exciplexes coupled to the phonon bath of a solid matrix
[AD-A200509] N89-17476
DYNAMIC RESPONSE
Nonlinear dynamic responses of composite rotor blades
[AD-A200145] N89-16774
Calculation methods for along-wind loading. Part 3: Response of buildings and plate-like structures to atmospheric turbulence
[ESDU-88019] N89-17267
DYNAMIC STABILITY
The behavior of shells made of composites during the dynamic application of axian compression
[AD-A200244] N89-17266
Numerical and theoretical study of elastoplastic dynamic buckling
[ETN-89-93614] N89-17284
DYNAMIC STRUCTURAL ANALYSIS
Calculation methods for along-wind loading. Part 3: Response of buildings and plate-like structures to atmospheric turbulence
[ESDU-88019] N89-17267
Modal analysis methods for the reduction of system-conditioned loads N89-17275
Initial structural response measurements for the Sandia 34-meter VAWT test bed
[DE89-003133] N89-17352
Prediction of stochastic blade responses using measured wind-speed data as input to the FLAP code
[DE89-000834] N89-17354
DYNAMICAL SYSTEMS
The integrability condition for dynamical systems
[DE89-004124] N89-17443
DYNAMICS
Droplet separation dynamics and kinematics under microgravity N89-17031

E

EARTH ATMOSPHERE
Ion microprobe measurements of H, C, O, Mg, and Si isotopic abundances in individual interplanetary dust particles N89-17551
EARTH IONOSPHERE
A technique for recording HF (High Frequency) oblique-incidence-sounder data
[AD-A200168] N89-17068
EARTH MAGNETOSPHERE
Alfven waves in a cold plasma with curved magnetic fields
[AD-A200312] N89-17506
EARTH MOVEMENTS
Kinematic leveling adjustments with polynomials and polynomial splines
[ETN-89-93328] N89-17338
EARTH ORBITAL ENVIRONMENTS
A Canadian low earth orbit launch vehicle: Launch vehicle performance analysis of Black Brant VC and Nihka rocket motor configurations N89-17039
EARTH RADIATION BUDGET
Limb-darkening functions as derived from along-track operation of the ERBE scanning radiometer for January 1985
[NASA-RP-1214] N89-17374
EARTH RADIATION BUDGET EXPERIMENT
Study of the effect of cloud inhomogeneity on the earth radiation budget experiment
[NASA-CR-182962] N89-17386
ECLIPSING BINARY STARS
Photoelectric photometry of very short period eclipsing binary systems and their light curve solutions N89-17549
ECONOMICS
Modern and prospective technologies for hydrogen production from fossil fuels
[DE89-001270] N89-16959
Small reactors for low-temperature nuclear heat applications
[DE88-704336] N89-17484
ECOSYSTEMS
Integration of experimental and modeling approaches in the unmanaged ecosystem research plan
[DE89-005230] N89-17367
EDDY CURRENTS
Tip clearance signal processor development
[AD-A199830] N89-16822
EDGE LOADING
Tensile strength of composite structures with internal ply drops and free-edge effects N89-16929
EFFICIENCY
Technology transfer for the US Department of Energy's Energy Storage Program. Volume 1: Recommendations
[DE89-002806] N89-17547
EIGENVALUES
Finding Eigenvalues and Eigenvectors of unsymmetric matrices using a distributed-memory multiprocessor
[DE89-004731] N89-17416
Finding Eigenvalues and Eigenvectors of unsymmetric matrices using a hypercube multiprocessor
[DE89-002311] N89-17455
EIGENVECTORS
Finding Eigenvalues and Eigenvectors of unsymmetric matrices using a distributed-memory multiprocessor
[DE89-004731] N89-17416
Finding Eigenvalues and Eigenvectors of unsymmetric matrices using a hypercube multiprocessor
[DE89-002311] N89-17455
EINSTEIN EQUATIONS
What topology could the universe be created with
[DE88-704321] N89-17554
ELASTIC BENDING
Maximum inelastic bending moments and form factors for symmetric bending of beams
[ESDU-88035] N89-17270
ELASTIC BUCKLING
Numerical and theoretical study of elastoplastic dynamic buckling
[ETN-89-93614] N89-17284
ELASTIC DEFORMATION
Elastic wrinkling of sandwich panels with laminated fibre reinforced face plates (face plates of AsBoDs, AsDIDs and AsBsDs types). (Computer program)
[ESDU-88015] N89-16930
Active vibration suppression for robotic manipulators N89-17241
ELASTOMERS
Fuel property and antioxidant effects on elastomer integrity, phase 2
[AD-A200250] N89-17015
ELASTOPLASTICITY
Low-cycle fatigue behavior of cyclic hardening and softening steels under multiaxial elastic-plastic loading conditions with constant and variable amplitudes N89-17280
Numerical and theoretical study of elastoplastic dynamic buckling
[ETN-89-93614] N89-17284
ELECTRIC BATTERIES
Electrochemistry of carbon relative to batteries and fuel cells
[AD-A199698] N89-17141
New secondary batteries utilizing electronically conductive polymer cathodes
[NASA-CR-183248] N89-17149
ELECTRIC CURRENT
JUNCTION code user's manual. Electromagnetic scattering and radiation by arbitrary configurations of conducting bodies and wires
[AD-A200315] N89-17072
Photocurrent modeling of modern microcircuit PN junctions
[DE88-012860] N89-17147
ELECTRIC DISCHARGES
Electric discharge method for ceramics reported N89-17050
Ultrasonic vibration method discussed N89-17053
Development of overcharge tolerance in Li/FeS and Li/FeS2 cells
[DE89-003952] N89-17145
ELECTRIC FIELDS
Fracture mode of metals in heavy electric fields
[DE88-704818] N89-16987
Far field patterns and the inverse scattering problem for electromagnetic waves in an inhomogeneous medium
[AD-A200223] N89-17070
ELECTRIC POTENTIAL
Use of cataphoresis effects discussed N89-17052
Breakdown voltage mapping of impurity concentrations in GaAs wafers
[DE89-002489] N89-17518
ELECTRICAL PROPERTIES
Photodeflection and photoconductivity studies in ceramics
[DE89-002186] N89-17003
New Al-Ni-Ge contacts on GaAs: Their structure and electrical properties
[DE89-002918] N89-17526
ELECTRICAL RESISTANCE
Development of a high temperature thin film static strain gage N89-17299
Elevated temperature strain gages N89-17300
Study of structure of high-Tc superconductor Y(YV)Ba2Cu3O(sub 9-x) and its resistance sharp drop
[DE88-704104] N89-17531
ELECTRICAL RESISTIVITY
Electric conductivity of polymer composite materials. Composite on propylene and silicon base
[DE88-704293] N89-17001
PBT,PBO-based hybrid polymers with nonlinear optical properties or high electrical conductivity
[AD-A200226] N89-17007
Development of conducting polymers of high structural strength
[AD-A200310] N89-17009
Electrical properties of atmospheric moist air: A systematic, experimental study
[AD-A199599] N89-17370

Investigation of collisional effects in the plasma erosion opening switch
[AD-A200319] N89-17507
Theory of neoclassical resistivity-gradient-driven turbulence
[DE89-005391] N89-17513

ELECTRO-OPTICS
Topical Meeting on Picosecond Electronics and Optoelectronics
[AD-A189686] N89-17080
A non-contact picosecond prober for integrated circuit testing N89-17081
Electro-optic sampling of high-speed, InP-based integrated circuits N89-17084
Picosecond switching in Josephson tunnel junctions N89-17095
Generation and forming of ultrashort high voltage pulses N89-17097
Graphite as a picosecond laser activated opening switch N89-17098
Picosecond optoelectronic switches using composite electronic materials N89-17107
A new optoelectronic CW microwave source N89-17133
Optical modulation above 20 GHz using a waveguide electro-optic switch N89-17134
Picosecond response of an optically controlled millimeter wave phase shifter N89-17135
Electron device probing in the femtosecond time scale N89-17136
Picosecond optoelectronic study of a thin film transmission line structure N89-17138
Temporal pattern recognition
[AD-A200090] N89-17426
Development of an optical digital ionization chamber
[DE89-002209] N89-17470
Photonics: Maintaining competitiveness in the information era
[AD-A200230] N89-17473
Precision transfer function measurements of integrated optical modulators
[DE89-004021] N89-17492

ELECTROCATALYSTS
Electrochemistry of carbon relative to batteries and fuel cells
[AD-A199698] N89-17141

ELECTROCHEMICAL OXIDATION
Electrochemistry of carbon relative to batteries and fuel cells
[AD-A199698] N89-17141

ELECTROCHEMISTRY
In-situ vibrational spectroelectrochemistry
[AD-A200303] N89-16949
The behavior of microdisks and microring electrodes. Applications of Neumann's integral theorem
[AD-A200307] N89-16951
The behavior of microdisks and micoring electrodes. Prediction of the amperometric response of microdisks and of the steady state for CE and EC Catalytic reactions by application of Neumann's integral theorem
[AD-A200415] N89-16952

ELECTRODES
An in situ surface Fourier transform study of complexes of lithium, magnesium potassium and lanthanum ferrocyanide at platinum and gold electrodes
[AD-A200305] N89-16950
The behavior of microdisks and microring electrodes. Applications of Neumann's integral theorem
[AD-A200307] N89-16951
The behavior of microdisks and micoring electrodes. Prediction of the amperometric response of microdisks and of the steady state for CE and EC Catalytic reactions by application of Neumann's integral theorem
[AD-A200415] N89-16952
The behavior of microdisk and microring electrodes. Mass transport to the disk in the unsteady state: Chronopotentiometry
[AD-A200421] N89-16953
The behavior of microdisk and microring electrodes. Mass transport to the disk in the unsteady state: Coupled chemical reactions
[AD-A200422] N89-16954
The use of narrow gap line microelectrodes as sensitive and species selective gas chromatographic detectors
[AD-A200424] N89-16955
Field enhancement of UHF-VHF aircraft antennas
[AD-A200180] N89-17069
New secondary batteries utilizing electronically conductive polymer cathodes
[NASA-CR-183248] N89-17149
Ultramicroelectrode sensors and detectors. Considerations of the stability, sensitivity, reproducibility and mechanism of ion transport in gas phase chromatography and in high performance liquid phase chromatography
[AD-A200306] N89-17210

ELECTRODYNAMICS
Middle Atmosphere Program: Handbook for MAP, volume 26
[NASA-CR-183350] N89-17368

ELECTROLYTIC CELLS
A microprocessor-based, solar cell parameter measurement system
[AD-A200227] N89-17348

ELECTROMAGNETIC PROPERTIES
JUNCTION code user's manual. Electromagnetic scattering and radiation by arbitrary configurations of conducting bodies and wires
[AD-A200315] N89-17072

ELECTROMAGNETIC PULSES
Modeling the propagation of long intense microwave pulses in mixtures of air and SF6
[DE89-004787] N89-17076

ELECTROMAGNETIC RADIATION
Effects of irregular sea surface and evaporation duct on radar detection performance
[AD-A200114] N89-17066

ELECTROMAGNETIC SCATTERING
JUNCTION code user's manual. Electromagnetic scattering and radiation by arbitrary configurations of conducting bodies and wires
[AD-A200315] N89-17072

ELECTROMAGNETISM
Cooled ion frequency standard
[AD-A200373] N89-17475

ELECTRON BEAM WELDING
Electron beam welding produces improved duplex crack arrest specimens
[DE88-003885] N89-17239

ELECTRON BEAMS
Microdrilling using electron beams reported N89-17055
Selected topics in FELs
[DE89-004022] N89-17227

ELECTRON COUNTERS
Development of an optical digital ionization chamber
[DE89-002209] N89-17470

ELECTRON CYCLOTRON HEATING
Induction-linac based free-electron laser amplifier for fusion applications
[DE89-001923] N89-17217

ELECTRON DENSITY (CONCENTRATION)
Modeling the propagation of long intense microwave pulses in mixtures of air and SF6
[DE89-004787] N89-17076
High power Ion Cyclotron Resonance Heating (ICRH) in JET
[DE89-002218] N89-17499

ELECTRON DENSITY PROFILES
A technique for recording HF (High Frequency) oblique-incidence-sounder data
[AD-A200168] N89-17068

ELECTRON DISTRIBUTION
Electron collision shift of the Lyman-alpha line in H and He+
[AD-A200296] N89-17474

ELECTRON GUNS
Mechanical design of a RF electron gun
[DE89-004890] N89-16895

ELECTRON IMPACT
Modeling of atomic processes for X-ray laser plasmas
[AD-A200219] N89-17505

ELECTRON SCATTERING
The electron-water vapor (H2O) collision cross sections
[AD-A200187] N89-17472
Electron collision shift of the Lyman-alpha line in H and He+
[AD-A200296] N89-17474
Monte Carlo calculation of electron multiple scattering in thin foils
[AD-A199872] N89-17517

ELECTRON SPECTROSCOPY
Resonant tunneling electron spectroscopy N89-17126

ELECTRON TRANSFER
In-situ vibrational spectroelectrochemistry
[AD-A200303] N89-16949
Femtosecond nonequilibrium electronic heat transport in thin gold films N89-17122
Ballistic transport and hot electron spectroscopy in Tunnelling Hot Electron Transfer Amplifier (THETA) N89-17123
Nuclear reorganization barriers to electron transfer
[DE88-016582] N89-17471
Theoretical studies of electrons and electron transfer processes in fluids
[DE89-003259] N89-17479
Monte Carlo studies of nonlinear electron transport in 3-5 semiconductors
[AD-A199700] N89-17516

ELECTRON-HOLE DROPS
Monte Carlo investigation of hot photoexcited electron relaxation in GaAs N89-17120

ELECTRON-ION RECOMBINATION
Modeling of atomic processes for X-ray laser plasmas
[AD-A200219] N89-17505

ELECTRONIC CONTROL
Joint service electronics program: Research in electronics
[AD-A199659] N89-17140
In-situ surface during laser-controlled chemical processing of surfaces
[AD-A200206] N89-17223

ELECTRONIC EQUIPMENT
Characteristics and applications of wideband guided-wave devices N89-17132
Electron device probing in the femtosecond time scale N89-17136

ELECTRONIC EQUIPMENT TESTS
Test-efficient design of digital VLSI circuits
[ETN-89-93483] N89-17151

ELECTRONS
Molecular spectroscopy at corrugated metal surfaces
[AD-A200124] N89-16973
Electronic interactions of electrons, photons, and atoms with material surfaces
[AD-A199626] N89-17469
Production and transport of convoy electrons in amorphous carbon foils
[DE89-002313] N89-17478
Theoretical studies of electrons and electron transfer processes in fluids
[DE89-003259] N89-17479

ELECTROSTATIC CHARGE
Gas path condition monitoring using electrostatic techniques N89-16817

ELECTROSTATIC ENGINES
Characterization of hollow cathode, ring cusp discharge chambers
[NASA-CR-182255] N89-17146

ELLIPSES
An algorithm for calculating the area of overlap of an ellipse and a convex polygon
[AD-A199654] N89-17408

EMBEDDED COMPUTER SYSTEMS
Inertial navigation system simulator: Behavioral specification
[AD-A200604] N89-16771
Inertial navigation system simulator program: Top-level design
[AD-A200605] N89-16772
Functional performance specification for an external computer system simulator
[AD-A200611] N89-16881

EMERGENCIES
Technology assessment for aircraft command in emergency situations
[DOT/FAA/CT-88/20] N89-16767

EMISSION
Phototype design and testing of two fiber-optic spectrochemical emission sensors
[DE89-001741] N89-17207
Emission-reduction effects of methanol vehicles: State of knowledge
[DE89-001148] N89-17359

EMISSION SPECTRA
Phototype design and testing of two fiber-optic spectrochemical emission sensors
[DE89-001741] N89-17207
Interaction of CO, CO2 and H2O with Ba and YBa2Cu3O7
[DE89-003160] N89-17528

ENCAPSULATING
The shaping of structural engineering ceramics N89-16997
Encapsulation process hardware for a KC-135 aircraft N89-17037
Concentricity and sphericity of composite drops under microgravity N89-17042

END EFFECTORS
Development of kinematic equations and determination of workspace of a 6 DOF end-effector with closed-kinematic chain mechanism
[NASA-CR-183241] N89-17444

ENERGY CONSERVATION
A review of second law techniques applicable to basic thermal science research
[DE89-004356] N89-17541

ENERGY CONVERSION
Development of composite high temperature materials for future energy conversion applications N89-16995

ENERGY CONVERSION EFFICIENCY
Device physics related to the granular nature of CuInSe2 solar cells
[DE89-000810] N89-17341

Research on high-efficiency, single-junction, monolithic, thin-film amorphous silicon solar cells, phase 3 [DE89-000813] N89-17342
Thermal degradation mechanisms in GaAs solar cells with high-temperature contacts [DE89-001375] N89-17343
Concentrator efficiencies of 29.2 percent for a GaAs cell and 24.8 percent for a mounted cell-lens assembly [DE89-001612] N89-17344
Recent advances in high-efficiency InGaAs concentrator cells [DE89-001613] N89-17345

ENERGY GAPS (SOLID STATE)
Non-stationary transport in MODFETs and heterojunction devices N89-17119
Dynamics of below-gap photoexcitation in GaAs quantum wells N89-17130

ENERGY SPECTRA
Energy events in the atmospheric boundary layer [NAL-TM-DU-8701] N89-17372

ENERGY STORAGE
Nickel hydrogen battery development [DE89-001063] N89-17143

ENERGY TECHNOLOGY
Energy and Technology Review [DE89-005308] N89-17459
Technology transfer for the US Department of Energy's Energy Storage Program. Volume 1: Recommendations [DE89-002806] N89-17547

ENERGY TRANSFER
Mechanical-chemical energy transfer observations of vaporific explosions [AD-A200428] N89-16956
BRYNTRN: A baryon transport model [NASA-TP-2887] N89-17562

ENGINE AIRFRAME INTEGRATION
Intake Aerodynamics, volume 2 --- conference [VKI-LS-1988-04-VOL-2] N89-16748
Computational methods for inlet airframe integration N89-16752
CFD application to subsonic inlet airframe integration --- computational fluid dynamics (CFD) N89-16753
CFD application to supersonic/hypersonic inlet airframe integration --- computational fluid dynamics (CFD) N89-16754

ENGINE CONTROL
Engine condition monitoring: State-of-the-art civil application N89-16792
F100-PW-220 engine monitoring system N89-16795
Military engine monitoring status at GE Aircraft Engines, Cincinnati, Ohio N89-16798
Commercial engine monitoring status at GE Aircraft Engines, Cincinnati, Ohio N89-16799
The advantage of a thrust rating concept used on the RB199 engine N89-16800
Fault management in aircraft power plant controls N89-16809

ENGINE DESIGN
Intake Aerodynamics, volume 1 --- conference [VKI-LS-1988-04-VOL-1] N89-16738
Inlet-engine compatibility N89-16741
Intake swirl and simplified methods for dynamic pressure distortion assessment N89-16742
Jaguar/Tornado intake design N89-16743
Transonic cowl design N89-16746
Intake drag N89-16747
Intake Aerodynamics, volume 2 --- conference [VKI-LS-1988-04-VOL-2] N89-16748
Transport aircraft intake design N89-16749
Recent UK trials in engine health monitoring: Feedback and feedforward N89-16790
Implication of engine performance monitoring for the aircraft manufacturer N89-16794
Military engine monitoring status at GE Aircraft Engines, Cincinnati, Ohio N89-16798
Commercial engine monitoring status at GE Aircraft Engines, Cincinnati, Ohio N89-16799
The advantage of a thrust rating concept used on the RB199 engine N89-16800
Transonic Compressors, volume 2 --- conference [VKI-LS-1988-03-VOL-2] N89-16833
The design and development of transonic multistage compressors N89-16834
Design of critical compressor stages N89-16835
Supersonic compressors N89-16836
Supersonic throughflow fans N89-16837
Design methodology for advanced High Pressure (HP) compressor first stage N89-16840
Composite motor case design N89-16909
Design of filament-wound rocket cases N89-16910
State of the art of solid propellant rocket motor grain design in the United States N89-16914
Design and analysis of solid rocket motor internal insulation N89-16915
Overall optimization of solid rocket motor N89-16916
Multidimensional modeling of convective heat transfer with application to I. C. engines [DE89-004062] N89-17166
AGARD/SMP Review: Damage Tolerance for Engine Structures. 1: Non-Destructive Evaluation [AGARD-R-768] N89-17253
Relationships of nondestructive evaluation needs and component design N89-17256

ENGINE FAILURE
Recent UK trials in engine health monitoring: Feedback and feedforward N89-16790
F110 engine monitoring and maintenance management systems for F-16 C/D N89-16791
Engine condition monitoring: State-of-the-art civil application N89-16792
Implication of engine performance monitoring for the aircraft manufacturer N89-16794
F100-PW-220 engine monitoring system N89-16795
Military engine condition monitoring systems: The UK experience N89-16797
Military engine monitoring status at GE Aircraft Engines, Cincinnati, Ohio N89-16798

ENGINE INLETS
Intake Aerodynamics, volume 1 --- conference [VKI-LS-1988-04-VOL-1] N89-16738
Introduction to intake aerodynamics N89-16739
Tactical fighter inlets N89-16740
Inlet-engine compatibility N89-16741
Intake swirl and simplified methods for dynamic pressure distortion assessment N89-16742
Jaguar/Tornado intake design N89-16743
Intakes for high angle of attack N89-16745
Transonic cowl design N89-16746
Intake drag N89-16747
Intake Aerodynamics, volume 2 --- conference [VKI-LS-1988-04-VOL-2] N89-16748
Transport aircraft intake design N89-16749
Missile intakes N89-16750
Wind tunnel air intake test techniques N89-16751
CFD application to subsonic inlet airframe integration --- computational fluid dynamics (CFD) N89-16753
CFD application to supersonic/hypersonic inlet airframe integration --- computational fluid dynamics (CFD) N89-16754

ENGINE MONITORING INSTRUMENTS
Engine Condition Monitoring: Technology and Experience [AGARD-CP-448] N89-16780
Operational requirements for engine condition monitoring from the EFA viewpoint N89-16781
An overview of US Navy engine monitoring system programs and user experience N89-16782
Engine usage condition and maintenance management systems in the UK armed forces N89-16783
Canadian forces aircraft condition/health monitoring: Policy, plans and experience N89-16784
On board life monitoring system Tornado (OLMOS) N89-16785
Information management systems for on-board monitoring systems N89-16786
CF-18 engine performance monitoring N89-16787
B-1B CITS engine monitoring N89-16788
Engine life consumption monitoring program for RB199 integrated in the on-board life monitoring system N89-16789
Recent UK trials in engine health monitoring: Feedback and feedforward N89-16790
F110 engine monitoring and maintenance management systems for F-16 C/D N89-16791
Engine condition monitoring: State-of-the-art civil application N89-16792
The CFM 56-5 on the A-320 at Air France N89-16793
Implication of engine performance monitoring for the aircraft manufacturer N89-16794
F100-PW-220 engine monitoring system N89-16795
Service life calculator for the M53 turbofan engine N89-16796
Military engine condition monitoring systems: The UK experience N89-16797
Military engine monitoring status at GE Aircraft Engines, Cincinnati, Ohio N89-16798
Commercial engine monitoring status at GE Aircraft Engines, Cincinnati, Ohio N89-16799
The advantage of a thrust rating concept used on the RB199 engine N89-16800
Trend monitoring of a turboprop engine at low and mean power N89-16801
Gas path analysis and engine performance monitoring in a Chinook helicopter N89-16802
System considerations for integrated machinery health monitoring N89-16804
Maintenance aid system for wide body aircraft N89-16805
Getting more from vibration analysis N89-16807
A joint study on the computerisation of in-field aero engine vibration diagnosis N89-16808
Discrete operating conditions gas path analysis N89-16810
Gas path modelling, diagnosis and sensor fault detection N89-16811
System-theoretical method for dynamic on-condition monitoring of gas turbines N89-16812
Identification of dynamic characteristics for fault isolation purposes in a gas turbine using closed-loop measurements N89-16813
Space shuttle main engine monitoring experience and advanced monitoring systems development N89-16815
Plume spectrometry for liquid rocket engine health monitoring N89-16816
Gas path condition monitoring using electrostatic techniques N89-16817
An intelligent sensor for equipment health monitoring of ferromagnetic wear debris concentration in fluids N89-16818
COMPASS (Trademark): A generalized ground-based monitoring system N89-16819

ENGINE NOISE
NASA powered lift facility internally generated noise and its transmission to the acoustic far field [NASA-CR-182217] N89-16882

ENGINE PARTS
F100-PW-220 engine monitoring system N89-16795
An intelligent sensor for equipment health monitoring of ferromagnetic wear debris concentration in fluids N89-16818
Design Methods in Solid Rocket Motors [AGARD-LS-150-REV] N89-16906
Design and analysis of solid rocket motor internal insulation N89-16915
Overall optimization of solid rocket motor N89-16916
Limitations at high temperatures of present day engineering materials N89-16996
The impact of engineering assumptions on NDE requirements N89-17254
Relationships of nondestructive evaluation needs and component design N89-17256
Short term developments in non-destructive evaluation applicable to turbine engine parts N89-17258
State-of-the-art in non-destructive evaluation of turbine engine parts N89-17261
Finite element implementation of viscoplastic models N89-17328

ENGINE TESTS
Wind tunnel air intake test techniques N89-16751
Recent UK trials in engine health monitoring: Feedback and feedforward N89-16790
Implication of engine performance monitoring for the aircraft manufacturer N89-16794
System considerations for integrated machinery health monitoring N89-16804
Plume spectrometry for liquid rocket engine health monitoring N89-16816
Supersonic through-flow fan assessment [NASA-CR-182202] N89-16843
Measurement uncertainty of the AGARD/PEP uniform engine test program N89-16853
An overview of the application of standard measurement uncertainty methodology to propulsion testing N89-16854
Accuracy requirements for high-speed test with engine simulation on transport aircraft models in the NLR-HST N89-16870
Engine simulator tests: Comparison of calibration and wind tunnel results N89-16871
State of the art of solid propellant rocket motor grain design in the United States N89-16914
A data acquisition and storage system for the ion auxiliary propulsion system cyclic thruster test [NASA-TM-101469] N89-17424

ENGINES
Experimental validation of a zero-dimensional computer model for spark-ignition engines [DE89-002848] N89-17243

ENGRAVING
Microdrilling using electron beams reported N89-17055

ENVIRONMENT MODELS
Signal acquisition and processing for autonomous space shuttle cargo bay acoustic measurements (NASA G-313) [AD-A200426] N89-17462

ENVIRONMENTAL MONITORING
Screening environmental pollutants and biomarkers: The analytical challenge [DE89-004931] N89-17366

ENVIRONMENTS
Proceedings of a workshop on Lighting Requirements in Microgravity: Rodents and Nonhuman Primates [NASA-TM-101077] N89-17390
Hydrogen erosion of carbon for fusion applications [UTIAS-328] N89-17504

EPITAXY
Growth of gallium arsenide using ion cluster beam technology, volume 1, phase 2
[AD-A200231] N89-17523
EPOXY MATRIX COMPOSITES
Isotropic kevlar and PBA (poly 1,4-benzamide) reinforcements for composites
[AD-A200239] N89-16927
Qualification tests of preimpregnated carbon epoxy T800H/DA 0506 from Structil. Test report M6-570500
[REPT-M6-570500] N89-16934
Evaluation of physical chemical test methods for characterizing polymerized composites or polymerizing composites: Literature review
[REPT-49-438/F] N89-16935
EPOXY RESINS
A multiaxial strength criterion for composites
[AD-A199610] N89-16920
EQUATIONS OF MOTION
Is there a statistical mechanics of turbulence
[DE89-003471] N89-17162
EQUATIONS OF STATE
The Kalman filter
[ESDU-88039] N89-17437
EQUILIBRIUM EQUATIONS
Development of finite local perturbations of electrical conductivity in the flow of a weakly-conducting gas when a magnetic field is present
[AD-A200243] N89-17458
EQUILIBRIUM FLOW
Flux Jacobian matrices and generaled Roe average for an equilibrium real gas
[NASA-CR-177512] N89-17445
EQUIPMENT SPECIFICATIONS
Thermophysical property measurements in fluid mixtures
[DE89-003281] N89-16961
FRP (Fiber Reinforced Plastics) cutting technology reported N89-17048
Hard material cutting technology described N89-17049
Brittle material processing reported N89-17051
EROSION
Hydrogen erosion of carbon for fusion applications
[UTIAS-328] N89-17504
Investigation of collisional effects in the plasma erosion opening switch
[AD-A200319] N89-17507
ERROR ANALYSIS
B-1B CITS engine monitoring N89-16788
A critical assessment of wind tunnel results for the NACA 0012 airfoil N89-16847
Measurement uncertainty of the AGARD/PEP uniform engine test program N89-16853
An overview of the application of standard measurement uncertainty methodology to propulsion testing N89-16854
Objective analysis of the Gulf Stream thermal front: Methods and accuracy
[AD-A199717] N89-17387
Accurate and efficient testing of the exponential and logarithm functions in Ada
[DE89-004443] N89-17415
ERROR CORRECTING CODES
Study of error correcting codes for Hertzian channels with a large number of states. Application to Quadrature Amplitude Modulation (QAM) 64
[ENST-88E007] N89-17074
ERRORS
Spatial reasoning in the treatment of systematic sensor errors
[DE89-003244] N89-17251
ESTIMATES
Distributed estimation for large-scale event-driven systems
[DE89-002688] N89-17447
Equivalent linearization for fatigue life estimates of a nonlinear structure
[NASA-TM-101536] N89-17467
ETALONS
High-speed optical logic using GaAs N89-17088
ETCHING
Suggested plastic-replica method N89-17293
ETHYL ALCOHOL
Gas chromatographic method for the determination of trace quantities of diethyl malonate in ethanol
[AD-A199733] N89-16941
EULER EQUATIONS OF MOTION
Numerical solution of flow fields around Delta wings using Euler equations method
[NAL-TM-FM-8701] N89-16757
EUROPEAN SPACE PROGRAMS
German spaceborne remote sensing activities N89-16887
Status of Sabrex N89-16890
Autonomous payload control experiment on SROSS-3, a status review --- Indian/German space cooperation N89-16891
EVALUATION
Evaluation and application of a new interferometry technique for compressible flow research
[NASA-CR-177467] N89-16765
Assessment and comparison of techniques for transforming parameters to a common metric in item response theory
[AD-A200067] N89-17433
EVENTS
Distributed estimation for large-scale event-driven systems
[DE89-002688] N89-17447
EVOLUTION (DEVELOPMENT)
The role of presolar dust in the formation of the solar system N89-17553
EXCIMER LASERS
The kinetics and dynamics of iodine monofluoride formation in gas-phase collisions
[AD-A199622] N89-16939
EXCITATION
Direct subpicosecond measurement of carrier mobility of photoexcited electrons in GaAs N89-17118
Dynamics of below-gap photoexcitation in GaAs quantum wells N89-17130
Electronic interactions of electrons, photons, and atoms with material surfaces
[AD-A199626] N89-17469
Theoretical studies of electrons and electron transfer processes in fluids
[DE89-003259] N89-17479
EXHAUST GASES
Emission-reduction effects of methanol vehicles: State of knowledge
[DE89-001148] N89-17359
EXHAUST NOZZLES
Measurements of gas turbine combustor and engine augmentor tube sooting characteristics
[AD-A199768] N89-16821
EXPERIMENTATION
Wind tunnel requirements for computational fluid dynamics code verification N89-16880
EXPERT SYSTEMS
Regenerative life support system research and concepts
[NASA-CR-184760] N89-17404
Empirical analysis and refinement of expert system knowledge bases
[AD-A200146] N89-17428
A formal language model for local area network configuration N89-17544
EXPLOSIONS
Combustibility of titanium powders
[NASA-TT-20455] N89-16967
EXPLOSIVES
Prediction and synthesis efforts at Los Alamos
[DE89-003605] N89-17018
Source characterization of heavy gas dispersion models for reactive chemicals, volume 1
[AD-A200121] N89-17361
EXPONENTIAL FUNCTIONS
Accurate and efficient testing of the exponential and logarithm functions in Ada
[DE89-004443] N89-17415
EXPOSURE
A strategy for understanding noise-induced annoyance
[AD-A200125] N89-17461
EXTRACTION
Research on automatic extraction of map information and its image representation
[DE88-754960] N89-17409
EXTRAVEHICULAR ACTIVITY
Extravehicular activities limitations study. Volume 1: Physiological limitations to extravehicular activity in space
[NASA-CR-172098] N89-17392
Extravehicular activities limitations study. Volume 2: Establishment of physiological and performance criteria for EVA gloves
[NASA-CR-172099] N89-17393
EYE DISEASES
Contrast sensitivity in Army aviator candidates: Cyclopiegia effects and population norms
[AD-A200433] N89-17397
EYE MOVEMENTS
Ocular torsion in the weightlessness of parabolic flight N89-17035
Role of retinocortical processing in spatial vision
[AD-A200198] N89-17394

F

F-16 AIRCRAFT
Finite element analysis of F-16 ballistic tests
[AD-A200289] N89-16776
F-18 AIRCRAFT
A model of the effect of sparing and repair turnaround time of the inertial navigation system on aircraft readiness for the F/A-18
[AD-A200317] N89-16777
FABRICATION
The effects of a compressor rebuild on gas turbine engine performance N89-16803
Enhanced performance ultrabroadband distributed amplifiers N89-17090
Picosecond photoconductive transceivers N89-17092
Characteristics and applications of wideband guided-wave devices N89-17132
Review of precision surface generating processes and their potential application to the fabrication of large optical components
[DE89-001712] N89-17486
Optical fiber science and technology: Novel fibers and fiber sensors
[AD-A200311] N89-17489
Characteristics of lift-off fabricated AlGaAs/InGaAs single-strained-quantum-well structures on glass and silicon substrates
[DE89-001374] N89-17532
FAILURE
A multiaxial strength criterion for composites
[AD-A199610] N89-16920
Adsorption of phosphorus acids on alumina
[AD-A200548] N89-16957
Structure and properties of polymer interphases
[AD-A200238] N89-17008
FAILURE ANALYSIS
Maintenance aid system for wide body aircraft N89-16805
Getting more from vibration analysis N89-16807
Fault management in aircraft power plant controls N89-16809
Discrete operating conditions gas path analysis N89-16810
FAR FIELDS
Far field patterns and the inverse scattering problem for electromagnetic waves in an inhomogeneous medium
[AD-A200223] N89-17070
FATIGUE (MATERIALS)
On board life monitoring system Tornado (OLMOS) N89-16785
Information management systems for on-board monitoring systems N89-16786
Fatigue behavior of ceramic thermal barrier coatings N89-17283
FATIGUE LIFE
Papers of the 5th LBF Colloquium
[LBF-TB-180] N89-17272
The influence of the load sequence on the fatigue life of fatigue fracture endangered components N89-17273
Stochastic modeling of crack initiation and short-crack growth under creep and creep-fatigue conditions
[NASA-TM-101358] N89-17286
Short-crack growth behaviour in an aluminum alloy: An AGARD cooperative test program N89-17288
Simplified fatigue damage and crack growth calculations for wind turbines
[DE89-003132] N89-17351
Initial structural response measurements for the Sandia 34-meter VAWT test bed
[DE89-003133] N89-17352
Equivalent linearization for fatigue life estimates of a nonlinear structure
[NASA-TM-101536] N89-17467
FATIGUE TESTS
The reliable reduction of random local sequences for fatigue tests N89-17274
Preliminary fatigue tests on short-crack specimens N89-17290
FAULT TOLERANCE
F110 engine monitoring and maintenance management systems for F-16 C/D N89-16791
R/M/T (Reliability/Maintainability/Testability) design for fault tolerance. Volume 1: Program manager's guide
[AD-A200204] N89-17262
FEEDBACK
R-parametrization and its role in classification of linear multivariable feedback systems
[NASA-TM-101066] N89-16844
FERMI SURFACES
Electronic interactions of electrons, photons, and atoms with material surfaces
[AD-A199626] N89-17469

FERMIONS
On the experimental basis of the Pauli exclusive principle
[DE88-704366] N89-17477
Lattice gauge theories and Monte Carlo algorithms
[DE89-003569] N89-17539
FERROCENES
Investigation of fuel additive effects on sooting flames
[AD-A200273] N89-16948
FERROMAGNETIC MATERIALS
An intelligent sensor for equipment health monitoring of ferromagnetic wear debris concentration in fluids N89-16816
FEYNMAN DIAGRAMS
Cluster expansion for vacuum confining fields
[DE88-704367] N89-17436
FIBER COMPOSITES
Composite motor case design N89-16909
Elastic wrinkling of sandwich panels with laminated fibre reinforced face plates (face plates of AsBoDs, AsDlDs and AsBsDs types). (Computer program)
[ESDU-88015] N89-16930
Ion assisted deposition of fiber coatings for ceramic matrix composites wth low dielectric loss tangents
[AD-A200162] N89-17005
FRP (Fiber Reinforced Plastics) cutting technology reported N89-17048
Papers of the 5th LBF Colloquium
[LBF-TB-180] N89-17272
Strength evaluation for fiber reinforced composite leaf springs under mechanical and environment conditioned loads N89-17277
Damage tolerance behavior of fiber reinforced composite airframes N89-17278
Finite element analysis for the evaluation and optimization of fiber reinforced composite structural components N89-17279
Optical fiber science and technology: Novel fibers and fiber sensors
[AD-A200311] N89-17489
FIBER OPTICS
High speed opto-isolator for radar applications N89-17110
Radar and EW applications of multi-gigahertz optical components and systems N89-17131
Phototype design and testing of two fiber-optic spectrochemical emission sensors
[DE89-001741] N89-17207
FIBER STRENGTH
Optical fiber science and technology: Novel fibers and fiber sensors
[AD-A200311] N89-17489
FIBERS
Ceramic-ceramic composites for use at high temperature N89-16994
A visualization model based on the mathematics of fiber bundles
[DE89-002537] N89-17432
FIELD EFFECT TRANSISTORS
Multigigahertz logic based on InP-MISFET's exhibiting extremely high transconductance N89-17086
An optically strobed sample and hold circuit N89-17087
MESFET compatible IMSM detectors N89-17116
FIELD STRENGTH
Fracture mode of metals in heavy electric fields
[DE88-704818] N89-16987
Electrical properties of atmospheric moist air: A systematic, experimental study
[AD-A199599] N89-17370
FIELD THEORY (PHYSICS)
Relativistically-invariant statistical hydrodynamics of a normal fluid
[DE88-704370] N89-17161
Supersymmetric instantons and topological quantum field theory
[DE88-704211] N89-17536
Investigations in particle and field theory
[DE89-003004] N89-17538
FIGHTER AIRCRAFT
Aircraft airframe cost estimating relationships: Fighters
[AD-A200263] N89-16720
Tactical fighter inlets N89-16740
Inlet-engine compatibility N89-16741
Particular flight mechanics specifications related to wind tunnel test results N89-16879
Vibration and aeroelastic tailoring of advanced composite plate-like lifting surfaces N89-17263
FILAMENT WINDING
Composite motor case design N89-16909
Design of filament-wound rocket cases N89-16910
FILM COOLING
Turbine airfoil film cooling N89-17315
FILTERS
Properties and performance of polyamide membranes N89-16991
FINANCE
Optical storage: Financial management and budget applications
[DE89-004916] N89-17546
FINITE DIFFERENCE THEORY
Evaluation of aerothermal modeling computer programs N89-17308
Heat transfer in the tip region of a rotor blade simulator N89-17312
Profile properties of undeformed first-year sea ice
[AD-A200172] N89-17388
FINITE ELEMENT METHOD
The design, construction and test of a postbuckled, carbon fibre reinforced plastic wing box N89-16773
Finite element analysis of F-16 ballistic tests
[AD-A200289] N89-16776
Introduction to finite element techniques in fluid mechanics N89-17177
Numerical analysis of the effects of void growth and crack tip opening on ductile fracture N89-17265
Papers of the 5th LBF Colloquium
[LBF-TB-180] N89-17272
Finite element analysis for the evaluation and optimization of fiber reinforced composite structural components N89-17279
Turbine Engine Hot Section Technology, 1987
[NASA-CP-2493] N89-17296
Response characteristics of MHOST (MARC Hot-Section Technology) for 3-D inelastic analysis of hot-section components N89-17318
Mechanics of materials model N89-17319
Three-dimensional inelastic analysis methods for hot section components N89-17321
Constitutive modeling for isotropic materials N89-17322
Finite element implementation of viscoplastic models N89-17328
Structural response of an advanced combustor liner: Test and analysis N89-17329
Thermal expansion mismatch and plasticity in thermal barrier coating N89-17330
Thermal barrier coating life prediction model N89-17332
High temperature constitutive and crack initiation modeling of coated single crystal superalloys N89-17334
Elevated temperature crack growth N89-17335
PC-1D Version 2: Enhanced numerical solar cell modeling
[DE89-000302] N89-17349
Generalized finite strains, generalized stresses, and a hybrid variational principle for finite-element computer programs
[DE89-002101] N89-17430
Generalized finite strains, generalized stresses, and a principle of virtual work for finite-element computer programs
[DE89-002102] N89-17431
Sparse matrix methods research using the CSM testbed software system
[NASA-CR-4219] N89-17441
Acoustic wave propagation by finite elements and time step integration N89-17460
FIRE PREVENTION
Investigation of fuel additive effects on sooting flames
[AD-A200273] N89-16948
FLAME IONIZATION
Gas chromatographic method for the determination of trace quantities of diethyl malonate in ethanol
[AD-A199733] N89-16941
FLAME PROPAGATION
Development of a lattice gas model for the study of combustion
[ETN-89-93612] N89-16964
FLAME STABILITY
Characterization of nonpremixed turbulent bluff-body burner flames
[PB89-100507] N89-16945
FLAMES
Laminar flame in a turbulent flow
[AD-A200241] N89-16947
FLEXIBLE BODIES
Spillover stabilization in the control of large flexible space structures N89-16902
FLIGHT CONTROL
Modal control of an oblique wing aircraft
[NASA-TP-2898] N89-16845
FLIGHT CREWS
The role of short-term memory in operator workload
[AD-A200252] N89-17401
FLIGHT ENVELOPES
Accuracy of lift and center-of-thrust measurements at missile control surfaces N89-16875
FLIGHT HAZARDS
Piloted-simulation evaluation of escape guidance for microburst wind shear encounters
[NASA-TP-2886] N89-16820
FLIGHT MECHANICS
Particular flight mechanics specifications related to wind tunnel test results N89-16879
FLIGHT SAFETY
System considerations for integrated machinery health monitoring N89-16804
Observations of a thunderstorm generated gust compared with solitary wave theory
[AD-A200087] N89-17379
FLIGHT SIMULATION
Piloted-simulation evaluation of escape guidance for microburst wind shear encounters
[NASA-TP-2886] N89-16820
Modifications to the NASA Ames Space Station Proximity Operations (PROX OPS) Simulator
[NASA-CR-177510] N89-16896
A Canadian low earth orbit launch vehicle: Launch vehicle performance analysis of Black Brant VC and Nihka rocket motor configurations N89-17039
FLIGHT STRESS (BIOLOGY)
Sleep and wakefulness: Handbook for flight medical officers, 2nd edition
[AGARD-AG-270(F)] N89-17399
FLIGHT TESTS
Controller-Programmer for telemetry systems
[DE89-002539] N89-16898
Preliminary results: Flight testing the NAE T-33 microgravity facility N89-17041
Microgravity science and applications bibliography, 1988 revision
[NASA-TM-4098] N89-17045
FLOATING POINT ARITHMETIC
Floating-point standards: Theory and practice
[DE89-003598] N89-17439
FLOOD PREDICTIONS
Hydrological aspects of combined effects of storm surges and heavy rainfall on river flow
[WMO-704] N89-17340
FLOODS
Hydrological aspects of combined effects of storm surges and heavy rainfall on river flow
[WMO-704] N89-17340
FLOW CHARACTERISTICS
Intake-airframe integration N89-16744
Intakes for high angle of attack N89-16745
FLOW DISTRIBUTION
Vortex dynamics for rotorcraft interactional aerodynamics
[AD-A200128] N89-16726
Numerical solutions to three-dimensional shock wave/vortex interaction at hypersonic speeds N89-16729
Numerical solution of flow fields around Delta wings using Euler equations method
[NAL-TM-FM-8701] N89-16757
Reynolds number effects in transonic flow
[AGARD-AG-303] N89-16760
Propulsive-jet flow field analysis using the three-dimensional Navier-Stokes equations
[NASA-CR-177508] N89-16764
Evaluation and application of a new interferometry technique for compressible flow research
[NASA-CR-177467] N89-16765
Shock losses in transonic and supersonic compressor cascades N89-16829
Flow unsteadiness in three low-speed wind tunnels N89-16859
The use of computational fluid dynamic methods to assess the effects of model support systems and working section modifications on the flow around wind tunnel models N89-16862
Accuracy of various wall-correction methods for 3D subsonic wind-tunnel testing N89-16863
Physical aspects of viscous simulation and associated research requirements N89-16865
Characterization of hypersonic wind tunnel flow fields for improved data accuracy N89-16874
Accuracy problems in wind tunnels during transport aircraft development N89-16877
Wind tunnel requirements for computational fluid dynamics code verification N89-16880
Characterization of nonpremixed turbulent bluff-body burner flames
[PB89-100507] N89-16945
Unsteady viscous flows over moving body
[AD-A200269] N89-17159
A computational method for three dimensional, internal viscous flows with separation and secondary flow patterns N89-17164
A scanning laser beam system for two-dimensional illumination of flow fields N89-17196

Aerothermal modeling program. Phase 2, element A: Improved numerical methods for turbulent viscous recirculating flows N89-17303
Application of advanced diagnostics to airblast injector flows N89-17306
Measurement of airfoil heat transfer coefficients on a turbine stage N89-17311
Two- and three-dimensional turbine blade row flow field simulations N89-17313

FLOW EQUATIONS
Computational methods for inlet airframe integration N89-16752
Physical mechanisms during drying of porous media N89-17173
Introduction to Computational Fluid Dynamics --- conference [VKI-LS-1988-02] N89-17174
Introduction to computational fluid dynamics N89-17175
Introduction to finite element techniques in fluid mechanics N89-17177
Implicit time dependent methods for inviscid and viscous compressible methods N89-17178

FLOW MEASUREMENT
Particle Image Displacement Velocimetry --- conference [VKI-LS-1988-06] N89-17179
Optical methods for measuring vector velocity fields. 1: Principles. 2: Techniques N89-17180
Processing information in the image plane --- particle image velocimetry N89-17183
Some comments on particle image displacement velocimetry N89-17184
Practical systems for speckle velocimetry N89-17185
Speckle photography of flows with varying fluid density N89-17186
Application of Particle Image Displacement Velocimetry (PIDV) to complex flows: Resolution of the directional ambiguity N89-17187
Application of Particle Image Displacement Velocimetry (PIDV) to complex flows: Measurements of the third component N89-17188
Optical processing --- particle image displacement velocimetry N89-17189
Probabilistic modeling of Particle Image Displacement Velocimetry (PIDV) experiments N89-17190
Full 3D measurements: The holographic approach --- flow measurement N89-17191
A personal computer based system for the evaluation of multiple exposed images in laser speckle and particle image displacement velocimetry N89-17193
Digital direct analysis of a multiexposed photograph in Particle Image Displacement Velocimetry (PIDV) N89-17194
A new algorithm for the rapid analysis of particle image displacement data N89-17195
A scanning laser beam system for two-dimensional illumination of flow fields N89-17196
Measurement of natural convection by white light speckle velocimetry N89-17197
In-situ laser microscopy for particle sizing and tracking N89-17201

FLOW THEORY
Introduction to Computational Fluid Dynamics --- conference [VKI-LS-1988-02] N89-17174
Boundary layer equations and methods of solution N89-17176
Heat transfer with very high free-stream turbulence and heat transfer with streamwise vortices N89-17309

FLOW VELOCITY
Development and application of oxygen flow tagging for velocity measurements and flow visualization in turbulent three-dimensional supersonic flows [AD-A200119] N89-16725
Boundaries of linear characteristics of cambered and twisted wings at subcritical Mach numbers [ESDU-88030] N89-16735
Axial velocity density ratio influence on exit flow angle in transonic/supersonic cascades N89-16830
Supersonic through-flow fan assessment [NASA-CR-182202] N89-16843
Flow unsteadiness in three low-speed wind tunnels N89-16859
Particle Image Displacement Velocimetry --- conference [VKI-LS-1988-06] N89-17179
Processing techniques: Image plane and Fourier plane --- particle image velocimetry N89-17182
Some comments on particle image displacement velocimetry N89-17184
Practical systems for speckle velocimetry N89-17185
Application of Particle Image Displacement Velocimetry (PIDV) to complex flows: Resolution of the directional ambiguity N89-17187
Application of particle image velocity to high speed flows N89-17198
Application of a spatial filter velocimeter to the two phase flows in a Spark Ignition (SI) N89-17199
A comparison of turbulence measurement methods N89-17302
Flow induced acoustic resonance in tubular heat exchangers [ESDU-88028] N89-17464

FLOW VISUALIZATION
Development and application of oxygen flow tagging for velocity measurements and flow visualization in turbulent three-dimensional supersonic flows [AD-A200119] N89-16725
Holographic interferometry for flow visualization studies in high speed fans N89-16841
Use of holography in vibration and flutter study of fans N89-16842
Experiments on boundary layer transition tripping at low Reynolds numbers N89-16868
Particle Image Displacement Velocimetry --- conference [VKI-LS-1988-06] N89-17179
Optical methods for measuring vector velocity fields. 1: Principles. 2: Techniques N89-17180
Scattering power of seed materials: Mie scattering calculations N89-17181
Some comments on particle image displacement velocimetry N89-17184
Application of Particle Image Displacement Velocimetry (PIDV) to complex flows: Resolution of the directional ambiguity N89-17187
A scanning laser beam system for two-dimensional illumination of flow fields N89-17196
Flow visualization by the PISTIL procedure (presentation of wake images by local computer processing). Test report 876/S-5 --- wake image representation by local computer treatment (PISTIL) [REPT-876/S-5] N89-17203

FLUID BOUNDARIES
The interaction of a fluid interface with a vortex pair [AD-A200167] N89-17156

FLUID DYNAMICS
Tailoring domain decomposition to the network structure for parallel processing of fluid dynamics [DE89-005501] N89-17206
Heat transfer with very high free-stream turbulence and heat transfer with streamwise vortices N89-17309

FLUID FILMS
Thinning and rupture of a thin liquid film on a horizontal heated solid surface [DE89-001792] N89-16944

FLUID FLOW
An intelligent sensor for equipment health monitoring of ferromagnetic wear debris concentration in fluids N89-16818
Remapping on the staggered mesh [DE89-002656] N89-17154
Development of generalized block correction procedures for the solution of discretized Navier-Stokes equations N89-17307
Coolant passage heat transfer with rotation N89-17314

FLUID JETS
Evaluation of aerothermal modeling computer programs N89-17308

FLUID MECHANICS
Tailoring domain decomposition to the network structure for parallel processing of fluid dynamics [DE89-005501] N89-17206
Computer program for the prediction of air-lift pump performance [ESDU-88014] N89-17246
Pipeline vibrations. Undamped natural vibration of pipelines [ESDU-88022] N89-17268
A review of second law techniques applicable to basic thermal science research [DE89-004356] N89-17541

FLUIDS
Thermophysical property measurements in fluid mixtures [DE89-003281] N89-16961
Theoretical studies of electrons and electron transfer processes in fluids [DE89-003259] N89-17479
Ideal black hole fluid [NASA-TM-100349] N89-17558

FLUORESCENCE
Molecular spectroscopy at corrugated metal surfaces [AD-A200124] N89-16973
Pressure/temperature sensitive inorganic phosphors [AD-A199718] N89-17000

FLUORIDES
The kinetics and dynamics of iodine monofluoride formation in gas-phase collisions [AD-A199622] N89-16939

FLUOROPOLYMERS
Ceramics derived from organo-metallic polymers [AD-A200118] N89-17004
Material compatability with threshold limit value levels of monomethyl hydrazine [AD-A200294] N89-17362

FLUTTER ANALYSIS
Use of holography in vibration and flutter study of fans N89-16842

FLUX DENSITY
Microdrilling using electron beams reported N89-17055
Flux Jacobian matrices and generaled Roe average for an equilibrium real gas [NASA-CR-177512] N89-17445

FLUX PINNING
Processing of strong flux trapping high T(subc) oxide superconductors: Center director's discretionary fund [NASA-TM-100350] N89-17530

FLYING PERSONNEL
Multiparametric research of early indicators of vascular risk in flying personnel [ETN-89-93613] N89-17398

FOILS (MATERIALS)
Monte Carlo calculation of electron multiple scattering in thin foils [AD-A199872] N89-17517

FORCE DISTRIBUTION
Normal-force-curve and pitching-moment-curve slopes for tangent-ogive forebody-cyclinder combinations at zero angle of attack [ESDU-88026] N89-16733
Lift and longitudinal forces on propeller/nacelle/wing/flap systems [ESDU-88031] N89-16736
Expriments on the DFVLR-F4 wing body configuration in several European windtunnels N89-16848

FORCED CONVECTION
Laser thermal propulsion [AD-A200558] N89-17226

FORECASTING
Atmospheric carbon dioxide, climate and global vegetation change [DE89-002196] N89-17360

FORM FACTORS
Maximum inelastic bending moments and form factors for symmetric bending of beams [ESDU-88035] N89-17270

FORMING TECHNIQUES
The shaping of structural engineering ceramics N89-16997

FOSSIL FUELS
Modern and prospective technologies for hydrogen production from fossil fuels [DE89-001270] N89-16959

FOULING
Fouling in cooling water systems [ESDU-88024] N89-17057

FOURIER ANALYSIS
Analysis of interferometer images with Fourier domain techniques [DE89-002927] N89-17491

FOURIER TRANSFORMATION
Light-off temperature determination of oxidation catalyst using Fourier transform infrared technique [AD-A199596] N89-16938
An in situ surface Fourier transform study of complexes of lithium, magnesium potassium and lanthanum ferrocyanide at platinum and gold electrodes [AD-A200305] N89-16950
Vector space approach to narrowband interference excision [AD-A199703] N89-17063
Processing techniques: Image plane and Fourier plane --- particle image velocimetry N89-17182
Optical processing --- particle image displacement velocimetry N89-17189
High-resolution Interferometer Sounder (HIS), phase 2 [NASA-CR-183414] N89-17212
Analysis of interferometer images with Fourier domain techniques [DE89-002927] N89-17491

FRACTALS
Fractal and spherulitic morphology of silicon nitride crystallized from amorphous films [AD-A200158] N89-17522

FRACTURE MECHANICS
High temperature properties of ceramic/carbon systems in an oxidizing environment [AD-A200254] N89-16928

Oxidation of Ni3Al below 850 C and its effect on fracture behavior
[DE89-002232] N89-16988
Stress driven diffusive voiding of aluminum conductor lines: A model for time dependent failure
[DE89-001865] N89-17144
AGARD/SMP Review: Damage Tolerance for Engine Structures. 1: Non-Destructive Evaluation
[AGARD-R-768] N89-17253
The impact of engineering assumptions on NDE requirements N89-17254
Review of existing NDT technologies and their capabilities N89-17255
Relationships of nondestructive evaluation needs and component design N89-17256
Importance of sensitivity and reliability of NDI techniques on damage tolerance based life prediction of turbine discs N89-17257
Turbine Engine Hot Section Technology, 1987
[NASA-CP-2493] N89-17298

FRACTURE STRENGTH
Investigation of microstructural factors that cause low fracture toughness in silicon carbide whisker/Al alloy composites
[AD-A200147] N89-16925
Mechanical characterization of SiC whisker-reinforced MoSi
[DE89-003486] N89-16933
Electron beam welding produces improved duplex crack arrest specimens
[DE88-003885] N89-17239
Strength evaluation for fiber reinforced composite leaf springs under mechanical and environment conditioned loads N89-17277

FRACTURES (MATERIALS)
A multiaxial strength criterion for composites
[AD-A199610] N89-16920
Investigation of microstructural factors that cause low fracture toughness in silicon carbide whisker/Al alloy composites
[AD-A200147] N89-16925
Fracture mode of metals in heavy electric fields
[DE88-704818] N89-16987
The influence of the load sequence on the fatigue life of fatigue fracture endangered components N89-17273

FRACTURING
Numerical analysis of the effects of void growth and crack tip opening on ductile fracture N89-17265

FRAGMENTS
Mechanical-chemical energy transfer observations of vaporific explosions
[AD-A200428] N89-16956

FREE ELECTRON LASERS
Induction-linac based free-electron laser amplifier for fusion applications
[DE89-001923] N89-17217
Induction-linac based free-electron laser amplifiers for plasma heating
[DE88-017004] N89-17221
Laser thermal propulsion
[AD-A200558] N89-17226
Selected topics in FELs
[DE89-004022] N89-17227
The two-beam accelerator and the relativistic klystron power source
[DE89-002673] N89-17485

FREE FLOW
Heat transfer with very high free-stream turbulence and heat transfer with streamwise vortices N89-17309

FREQUENCY HOPPING
Capacity of frequency-hop spread-spectrum multiple-access communication systems
[AD-A200616] N89-17073

FREQUENCY MODULATION
Modulation efficiency limited high frequency performance of the MODFET N89-17101
A technique for wing suppressed IR sampling N89-17109

FREQUENCY STANDARDS
Cooled ion frequency standard
[AD-A200373] N89-17475

FRESNEL LENSES
Concentrator efficiencies of 29.2 percent for a GaAs cell and 24.8 percent for a mounted cell-lens assembly
[DE89-001612] N89-17344

FRETTING
Effect of fretting on fatigue strength of titanium alloys
[ESDU-88027] N89-16981

FRETTING CORROSION
Papers of the 5th LBF Colloquium
[LBF-TB-180] N89-17272
Fretting corrosion fatigue N89-17282

FRICTION
Tribology of amorphous alloys formed with ion beams
[DE89-003274] N89-16982

FRONTS (METEOROLOGY)
Objective analysis of the Gulf Stream thermal front: Methods and accuracy
[AD-A199717] N89-17367

FUEL CELLS
Electrochemistry of carbon relative to batteries and fuel cells
[AD-A199698] N89-17141

FUEL COMBUSTION
The synchronous injection ignition valveless pulsejet N89-16823

FUEL INJECTION
The synchronous injection ignition valveless pulsejet N89-16823
Application of advanced diagnostics to airblast injector flows N89-17306

FUEL SPRAYS
Aerothermal modeling program, Phase 2, Element C: Fuel injector-air swirl characterization N89-17305
Application of advanced diagnostics to airblast injector flows N89-17306

FUEL-AIR RATIO
Measurements of gas turbine combustor and engine augmentor tube sooting characteristics
[AD-A199768] N89-16821
Characterization of nonpremixed turbulent bluff-body burner flames
[PB89-100507] N89-16945

FUELS
Investigation of fuel additive effects on sooting flames
[AD-A200273] N89-16948
Results from the Federal Methanol Fleet
[DE88-015291] N89-17016

FURNACES
The design of a heat-pipe furnace for microgravity N89-17043

FUSION REACTORS
Hydrogen erosion of carbon for fusion applications
[UTIAS-328] N89-17504
Fusion plasma theory: Task 3: Auxiliary heating in tokamaks
[DE89-003256] N89-17509

G

GALACTIC CLUSTERS
A neutral hydrogen survey of galaxies in the Cancer region N89-17552

GALACTIC EVOLUTION
Ideal black hole fluid
[NASA-TM-100349] N89-17558

GALAXIES
A neutral hydrogen survey of galaxies in the Cancer region N89-17552

GALLIUM ARSENIDES
Molecular Beam Epitaxy (MBE) for high speed devices N89-17085
High-speed optical logic using GaAs N89-17088
Fast GaAs photoconductive detectors with high sensitivity integrated in coplanar systems onto GaAs substrates N89-17105
InP/GaInAs/InP PIN photodiode with FWHM less than 18 ps N89-17114
High-speed phenomena in GaAs multiple-quantum-wells N89-17127
Picosecond carrier transport in GaAs quantum wells N89-17128
Quantum-confined Stark effect in InGaAs/InP quantum wells grown by metal-organic chemical vapor deposition N89-17129
Dynamics of below-gap photoexcitation in GaAs quantum wells N89-17130
Thermal degradation mechanisms in GaAs solar cells with high-temperature contacts
[DE89-001375] N89-17343
Concentrator efficiencies of 29.2 percent for a GaAs cell and 24.8 percent for a mounted cell-lens assembly
[DE89-001612] N89-17344
Recent advances in high-efficiency InGaAs concentrator cells
[DE89-001613] N89-17345
Breakdown voltage mapping of impurity concentrations in GaAs wafers
[DE89-002489] N89-17518
Growth of gallium arsenide using ion cluster beam technology, volume 1, phase 2
[AD-A200231] N89-17523
Investigation of defect and electronic interactions associated with GaAs device processing
[AD-A200541] N89-17525
New Al-Ni-Ge contacts on GaAs: Their structure and electrical properties
[DE89-002918] N89-17526
Characteristics of lift-off fabricated AlGaAs/InGaAs single-strained-quantum-well structures on glass and silicon substrates
[DE89-001374] N89-17532

GAS CHROMATOGRAPHY
Gas chromatographic method for the determination of trace quantities of diethyl malonate in ethanol
[AD-A199733] N89-16941
The use of narrow gap line microelectrodes as sensitive and species selective gas chromatographic detectors
[AD-A200424] N89-16955
Ultramicroelectrode sensors and detectors. Considerations of the stability, sensitivity, reproducibility and mechanism of ion transport in gas phase chromatography and in high performance liquid phase chromatography
[AD-A200306] N89-17210

GAS DYNAMICS
Gas path modelling, diagnosis and sensor fault detection N89-16811
Investigations of the motion of discrete-velocity gases by cellular automata
[AD-A200221] N89-17158

GAS EXPANSION
Origin and dynamics of expanding neutral hydrogen supershells
[DE88-704372] N89-17555

GAS FLOW
Gas path modelling, diagnosis and sensor fault detection N89-16811
The properties of tagged lattice fluids. 2: Velocity correlation functions
[DE89-003475] N89-17163
Material compatability with threshold limit value levels of monomethyl hydrazine
[AD-A200294] N89-17362
Development of finite local perturbations of electrical conductivity in the flow of a weakly-conducting gas when a magnetic field is present
[AD-A200243] N89-17458

GAS JETS
Gas jet deposition of multicomponent ultrafine microstructures
[AD-A200101] N89-16946

GAS PATH ANALYSIS
Gas path analysis and engine performance monitoring in a Chinook helicopter N89-16802
Discrete operating conditions gas path analysis N89-16810
Gas path modelling, diagnosis and sensor fault detection N89-16811
Gas path condition monitoring using electrostatic techniques N89-16817

GAS TEMPERATURE
A comparison of turbulence measurement methods N89-17302

GAS TURBINE ENGINES
The effects of a compressor rebuild on gas turbine engine performance N89-16803
Getting more from vibration analysis N89-16807
System-theoretical method for dynamic on-condition monitoring of gas turbines N89-16812
Identification of dynamic characteristics for fault isolation purposes in a gas turbine using closed-loop measurements N89-16813
Gas path condition monitoring using electrostatic techniques N89-16817
An intelligent sensor for equipment health monitoring of ferromagnetic wear debris concentration in fluids N89-16818
Measurements of gas turbine combustor and engine augmentor tube sooting characteristics
[AD-A199768] N89-16821
Limitations at high temperatures of present day engineering materials N89-16998
Engineering ceramics in West Germany N89-16999
AGARD/SMP Review: Damage Tolerance for Engine Structures. 1: Non-Destructive Evaluation
[AGARD-R-768] N89-17253
The impact of engineering assumptions on NDE requirements N89-17254
Relationships of nondestructive evaluation needs and component design N89-17256
Importance of sensitivity and reliability of NDI techniques on damage tolerance based life prediction of turbine discs N89-17257
State-of-the-art in non-destructive evaluation of turbine engine parts N89-17261
Turbine Engine Hot Section Technology, 1987
[NASA-CP-2493] N89-17298
Development of a high temperature thin film static strain gage N89-17299
Aerothermal modeling program. Phase 2, element B: Flow interaction experiment N89-17304
Application of advanced diagnostics to airblast injector flows N89-17306

A low-Reynolds-number two-equation turbulence model for predicting heat transfer on turbine blades N89-17310
Measurement of airfoil heat transfer coefficients on a turbine stage N89-17311
Two- and three-dimensional turbine blade row flow field simulations N89-17313
Coolant passage heat transfer with rotation N89-17314
Turbine airfoil film cooling N89-17315
Three-dimensional inelastic analysis methods for hot section components N89-17316
Three-dimensional inelastic analysis for hot section components, BEST 3D code N89-17317
Response characteristics of MHOST (MARC Hot-Section Technology) for 3-D inelastic analysis of hot-section components N89-17318
Mechanics of materials model N89-17319
Component specific modeling N89-17320
Three-dimensional inelastic analysis methods for hot section components N89-17321
Constitutive modeling for isotropic materials N89-17322
Anisotropic constitutive modeling for nickel base single crystal superalloy Rene N4 at 982 C N89-17324
Constitutive modelling of single crystal and directionally solidified superalloys N89-17325
Finite element implementation of viscoplastic models N89-17328
Structural response of an advanced combustor liner: Test and analysis N89-17329
Thermal expansion mismatch and plasticity in thermal barrier coating N89-17330
Thermal barrier coating life-prediction model development N89-17331
Thermal barrier coating life prediction model development N89-17333
High temperature constitutive and crack initiation modeling of coated single crystal superalloys N89-17334
Creep fatigue life prediction for engine hot section materials (ISOTROPIC) fifth year progress review N89-17336

GAS TURBINES
Engine Condition Monitoring: Technology and Experience
[AGARD-CP-448] N89-16780

GAS WELDING
Penetration effects of the compound vortex in gas metal-arc welding
[AD-A200585] N89-17242

GAS-METAL INTERACTIONS
Applications of ion implantation for modifying the interactions between metals and hydrogen gas
[DE89-002877] N89-17219

GAS-SOLID INTERACTIONS
A statistical theory for gas surface interactions in rarefied hypersonic flows
[IC-AERO-88-01] N89-16755

GASEOUS FUELS
Source characterization of heavy gas dispersion models for reactive chemicals, volume 1
[AD-A200121] N89-17361

GASES
Behavior in normal and reduced gravity of an enclosed liquid/gas system with nonuniform heating from above
[NASA-TM-101471] N89-17046
The properties of tagged lattice fluids. 2: Velocity correlation functions
[DE89-003475] N89-17163

GATES (CIRCUITS)
High performance quarter-micron-gate MODFETs N89-17091
A simple technique to generate or gate microwave pulses with picosecond speeds N89-17099

GAUGE THEORY
Investigations in particle and field theory
[DE89-003004] N89-17538
Lattice gauge theories and Monte Carlo algorithms
[DE89-003569] N89-17539

GAUSS EQUATION
Long-crack growth rate data: Gaussian loading N89-17296

GAUSSIAN ELIMINATION
Parallel Gaussian elimination of a block tridiagonal matrix using multiple microcomputers
[NASA-TP-2892] N89-17422

GEAR TEETH
Computer-aided design of bevel gear tooth surfaces
[NASA-TM-101449] N89-17248

GEARS
An intelligent sensor for equipment health monitoring of ferromagnetic wear debris concentration in fluids N89-16818
The design of spur and helical involute gears. A procedure compatible with BS 436:1986: Method for calculation of contact and root bending stress limitations for metallic involute gears
[ESDU-88033] N89-17247
Computer-aided design of bevel gear tooth surfaces
[NASA-TM-101449] N89-17248

GELS
Ceramics derived from organo-metallic polymers
[AD-A200118] N89-17004

GEODESIC LINES
Geometry on the space of geometries
[DE88-704214] N89-17537

GEODETIC SATELLITES
An algorithm for analysis of plate motions in Crust Dynamics Project (CDP) networks
[B8821606] N89-17371

GEOMETRY
Effectiveness: N(sub TU) relationships for the design and performance evaluation of additional shell-and-tube heat exchanger geometries
[ESDU-88021] N89-17056
Center of buoyancy definition
[DE89-003017] N89-17457
Geometry on the space of geometries
[DE88-704214] N89-17537

GERMANIUM ALLOYS
New Al-Ni-Ge contacts on GaAs: Their structure and electrical properties
[DE89-002918] N89-17526

GLASS
Characteristics of lift-off fabricated AlGaAs/InGaAs single-strained-quantum-well structures on glass and silicon substrates
[DE89-001374] N89-17532

GLASS COATINGS
Ceramics derived from organo-metallic polymers
[AD-A200118] N89-17004

GLASS FIBER REINFORCED PLASTICS
Ceramic-ceramic composites for use at high temperature N89-16994
The behavior of shells made of composites during the dynamic application of axian compression
[AD-A200244] N89-17266

GLOBAL POSITIONING SYSTEM
GPS (Global Positioning System) user equipment evaluation techniques using a rotor mounted antenna
[AD-A200515] N89-16770

GLOVES
Extravehicular activities limitations study. Volume 2: Establishment of physiological and performance criteria for EVA gloves
[NASA-CR-172099] N89-17393

GOLD
Gas jet deposition of multicomponent ultrafine microstructures
[AD-A200101] N89-16946
Femtosecond nonequilibrium electronic heat transport in thin gold films N89-17122

GRAIN BOUNDARIES
Stress driven diffusive voiding of aluminum conductor lines: A model for time dependent failure
[DE89-001665] N89-17144
Suggested plastic-replica method N89-17293

GRAIN SIZE
Solid propellant grain design N89-16913

GRAVIMETRY
High-precision gravity network to monitor temporal variations in gravity across Yucca Mountain, Nevada
[DE89-005023] N89-17373

GRAVITATIONAL EFFECTS
Workshop on Microgravity Experimentation in Aircraft and Rockets
[NRCC-29151] N89-17019
On fundamental problems of Space Materials Science (SMS) N89-17024
The effects of microgravity and linear accelerations on cutaneomuscular reflexes in human lower limb musculature N89-17034
The use of sounding rockets in the study of microgravity cell biology N89-17036
Body displacement measured during sustained +Gz, -Gz and + or -Gy acceleration using a stereoscopic photographic system
[NASA-TM-101269] N89-17391

GRAVITATIONAL FIELDS
Behavior in normal and reduced gravity of an enclosed liquid/gas system with nonuniform heating from above
[NASA-TM-101471] N89-17046
Geometry on the space of geometries
[DE88-704214] N89-17537
Isotropization of the cosmic background radiation due to galactic gravitational screening
[DE88-755533] N89-17563

GREEN'S FUNCTIONS
Cluster expansion for vacuum confining fields
[DE88-704367] N89-17436

GREENHOUSE EFFECT
Atmospheric carbon dioxide, climate and global vegetation change
[DE89-002196] N89-17360
Carbon dioxide and climate: Summaries of research in FY 1988
[DE89-002966] N89-17363
Greenhouse warming: What do we know
[DE89-004780] N89-17365

GRID GENERATION (MATHEMATICS)
Generation of three-dimensional body-fitted grids by solving hyperbolic and parabolic partial differential equations
[NASA-TM-101069] N89-16763

GRINDING (MATERIAL REMOVAL)
Electric discharge method for ceramics reported N89-17050
Use of cataphoresis effects discussed N89-17052

GRINDING MACHINES
Electric discharge method for ceramics reported N89-17050

GROOVES
Scattering by a two dimensional groove in a ground plane
[NASA-CR-183087] N89-17077

GROWTH
Growth of gallium arsenide using ion cluster beam technology, volume 1, phase 2
[AD-A200231] N89-17523

GULF STREAM
Objective analysis of the Gulf Stream thermal front: Methods and accuracy
[AD-A199717] N89-17387

GUSTS
Observations of a thunderstorm generated gust compared with solitary wave theory
[AD-A200087] N89-17379

GYROSCOPIC STABILITY
Gyroscopic testing of accelerometers to determine coning angle
[AD-A200126] N89-17209

H

HABITATS
Proceedings of a workshop on Lighting Requirements in Microgravity: Rodents and Nonhuman Primates
[NASA-TM-101077] N89-17390

HAMILTONIAN FUNCTIONS
The integrability condition for dynamical systems
[DE89-004124] N89-17443

HAND (ANATOMY)
Extravehicular activities limitations study. Volume 2: Establishment of physiological and performance criteria for EVA gloves
[NASA-CR-172099] N89-17393

HANDBOOKS
Propagation effects handbook for satellite systems design. A summary of propagation impairments on 10 to 100 GHz satellite links with techniques for system design
[NASA-RP-1082(04)] N89-17060
Life cycle management handbook
[DE89-004315] N89-17545

HARDENING (MATERIALS)
Low-cycle fatigue behavior of cyclic hardening and softening steels under multiaxial elastic-plastic loading conditions with constant and variable amplitudes N89-17280

HARDNESS
Tribology of amorphous alloys formed with ion beams
[DE89-003274] N89-16982

HARMONICS
Far field patterns and the inverse scattering problem for electromagnetic waves in an inhomogeneous medium
[AD-A200223] N89-17070

HASTELLOY (TRADEMARK)
Internal stress during high-temperature creep and activation energy for creep of Hastelloy XR
[DE88-755231] N89-16969
Use of inelastic strain as a basis for analyzing thermomechanical test data N89-17326

HAZARDS
Source characterization of heavy gas dispersion models for reactive chemicals, volume 1
[AD-A200121] N89-17361

HEARING
Human factors in aviation operations: The hearback problem
[NASA-CR-177398] N89-16789

HEAT EXCHANGERS
Effect of Lewis number on wet surface heat exchangers N89-17152
HEAT FLUX
Structural response of an advanced combustor liner: Test and analysis N89-17329
Measurements of micrometeorological parameters for testing large scale models
[NASA-CR-184766] N89-17384
HEAT PIPES
The design of a heat-pipe furnace for microgravity N89-17043
HEAT PUMPS
Capillary pumping for a two phase heat transport system — space stations N89-17172
HEAT RESISTANT ALLOYS
Limitations at high temperatures of present day engineering materials N89-16996
Anisotropic constitutive modeling for nickel base single crystal superalloy Rene N4 at 982 C N89-17324
Constitutive modelling of single crystal and directionally solidified superalloys N89-17325
High temperature constitutive and crack initiation modeling of coated single crystal superalloys N89-17334
HEAT TRANSFER
Effectiveness: N(sub TU) relationships for the design and performance evaluation of additional shell-and-tube heat exchanger geometries
[ESDU-88021] N89-17056
Femtosecond nonequilibrium electronic heat transport in thin gold films N89-17122
Turbine Engine Hot Section Technology, 1987
[NASA-CP-2493] N89-17298
Aerothermal modeling program. Phase 2, element A: Improved numerical methods for turbulent viscous recirculating flows N89-17303
Heat transfer with very high free-stream turbulence and heat transfer with streamwise vortices N89-17309
A low-Reynolds-number two-equation turbulence model for predicting heat transfer on turbine blades N89-17310
Measurement of airfoil heat transfer coefficients on a turbine stage N89-17311
Heat transfer in the tip region of a rotor blade simulator N89-17312
Two- and three-dimensional turbine blade row flow field simulations N89-17313
Coolant passage heat transfer with rotation N89-17314
Turbine airfoil film cooling N89-17315
Component specific modeling N89-17320
First production of potable water by OTEC (Ocean Thermal Energy Conversion) and its potential applications
[DE89-003630] N89-17353
Flow induced acoustic resonance in tubular heat exchangers
[ESDU-88028] N89-17454
HEAT TRANSFER COEFFICIENTS
Effect of Lewis number on wet surface heat exchangers N89-17152
Measurement of airfoil heat transfer coefficients on a turbine stage N89-17311
Coolant passage heat transfer with rotation N89-17314
HEATING
Thinning and rupture of a thin liquid film on a horizontal heated solid surface
[DE89-001792] N89-16944
Behavior in normal and reduced gravity of an enclosed liquid/gas system with nonuniform heating from above
[NASA-TM-101471] N89-17046
Measurement of natural convection by white light speckle velocimetry N89-17197
HEATING EQUIPMENT
Procurement and screening test data for advanced austenitic alloys for 650 C steam service, part 2
[DE89-001331] N89-16979
HEAVY LIFT LAUNCH VEHICLES
Analysis and design of a universal shuttle for rockets
[ILR-MITT-199] N89-16897
HELICOPTER ENGINES
System-theoretical method for dynamic on-condition monitoring of gas turbines N89-16812
HELICOPTER WAKES
Development of a panel method for modeling configurations with unsteady component motions, phase 1
[AD-A200255] N89-16775
HELICOPTERS
Nonlinear dynamic responses of composite rotor blades
[AD-A200145] N89-16774
A comparison of two whole-body vibration standards as applied to rotary-wing aircraft: ISO (International Standards Organization) 2631 vs ADS (Aeronautical Design Standards) 27
[AD-A200430] N89-17402
HELIUM ATOMS
Electron collision shift of the Lyman-alpha line in H and He+
[AD-A200296] N89-17474
HELIUM IONS
Electron collision shift of the Lyman-alpha line in H and He+
[AD-A200296] N89-17474
HELIUM-NEON LASERS
Laser detection of acoustic displacements by destabilizing a frequency stablized helium neon laser
[DE89-005282] N89-17235
HETEROJUNCTION DEVICES
Non-stationary transport in MODFETs and heterojunction devices N89-17119
HIERARCHIES
Models of incremental concept formation
[AD-A199617] N89-17400
Improving software quality through hierarchical design
[DE88-014919] N89-17412
HIGH ELECTRON MOBILITY TRANSISTORS
Progress and challenges in HEMT LSI technology N89-17094
HIGH FREQUENCIES
Modulation efficiency limited high frequency performance of the MODFET N89-17101
HIGH GAIN
Progress toward high-gain laser fusion
[DE89-002661] N89-17501
Progress in laboratory high gain ICF (Inertial Confinement Fusion): Prospects for the future
[DE89-002664] N89-17502
HIGH LEVEL LANGUAGES
The suitability of an object-oriented language for prototyping and abstract data types
[AD-A200417] N89-17410
HIGH POLYMERS
Development of conducting polymers of high structural strength
[AD-A200310] N89-17009
HIGH POWER LASERS
The kinetics and dynamics of iodine monofluoride formation in gas-phase collisions
[AD-A199622] N89-16939
High power KrF laser development at Los Alamos
[DE89-002242] N89-17218
High energy laser beam scattering by atmospheric aerosol aureoles
[DE89-004811] N89-17230
HIGH PRESSURE
Gas jet deposition of multicomponent ultrafine microstructures
[AD-A200101] N89-16948
HIGH RESOLUTION
High-resolution Interferometer Sounder (HIS), phase 2
[NASA-CR-183414] N89-17212
HIGH REYNOLDS NUMBER
Energy events in the atmospheric boundary layer
[NAL-TM-DU-8701] N89-17372
HIGH SPEED
Multigigahertz logic based on InP-MISFET's exhibiting extremely high transconductance N89-17086
High-speed optical logic using GaAs N89-17088
High speed, high repetition rate, high voltage photoconductive switching N89-17096
High speed opto-isolator for radar applications N89-17110
InP/GaInAs/InP PIN photodiode with FWHM less than 18 ps N89-17114
HIGH TEMPERATURE
Internal stress during high-temperature creep and activation energy for creep of Hastelloy XR
[DE88-755231] N89-16969
Engineering Materials for Very High Temperatures: An ORNL Workshop
[ORNL-8-016-R] N89-16992
Microstructure of high-temperature ceramics N89-16993
High temperature material processing system for KC-135 microgravity experiments N89-17040
A continuum deformation theory for metal-matrix composites at high temperature N89-17323
HIGH TEMPERATURE ENVIRONMENTS
High temperature properties of ceramic/carbon systems in an oxidizing environment
[AD-A200254] N89-16928
Ceramic-ceramic composites for use at high temperature N89-16994
NDE methods for high-temperature materials and environments
[DE89-005195] N89-17234
Development of a high temperature thin film static strain gage N89-17299
Elevated temperature strain gages N89-17300
Thermal barrier coating life prediction model development N89-17333
High temperature constitutive and crack initiation modeling of coated single crystal superalloys N89-17334
Elevated temperature crack growth N89-17335
Total strain version of strainrange partitioning for thermomechanical fatigue at low strains N89-17337
Thermal degradation mechanisms in GaAs solar cells with high-temperature contacts
[DE89-001375] N89-17343
HIGH TEMPERATURE SUPERCONDUCTORS
Orientation dependent X-ray absorption in high T (sub c) superconductors
[DE89-002910] N89-17520
Study of structure of high-Tc superconductor Y(YV)Ba2Cu3O(sub 9-x) and its resistance sharp drop
[DE88-704104] N89-17531
HIGH TEMPERATURE TESTS
The effects of strain induced softening on the load carrying capability of components N89-17264
HISTOGRAMS
HANDYPAK: A histogram and display package
[DE89-002742] N89-17413
HOLLOW CATHODES
Characterization of hollow cathode, ring cusp discharge chambers
[NASA-CR-182255] N89-17146
HOLOGRAPHIC INTERFEROMETRY
Holographic interferometry for flow visualization studies in high speed fans N89-16841
Use of holography in vibration and flutter study of fans N89-16842
Full 3D measurements: The holographic approach — flow measurement N89-17191
HOLOGRAPHY
Progress towards a 44-Angstrom X-ray laser
[DE89-004807] N89-17229
Energy and Technology Review
[DE89-005308] N89-17459
X-ray optics for X-ray laser research and applications
[DE89-004026] N89-17493
HOMEOSTASIS
Pharmacological resetting of the circadian sleep-wake cycle
[AD-A200246] N89-17396
HONEYCOMB STRUCTURES
A modified VAPEPS method for predicting vibroacoustic response of unreinforced mass loaded honeycomb panels
[NASA-TM-101467] N89-16905
Hygrothermal deformations of laminated composite shells N89-16924
HOT ELECTRONS
Direct subpicosecond measurement of carrier mobility of photoexcited electrons in GaAs N89-17118
Monte Carlo investigation of hot photoexcited electron relaxation in GaAs N89-17120
Ballistic transport and hot electron spectroscopy in Tunnelling Hot Electron Transfer Amplifier (THETA) N89-17123
HOT ISOSTATIC PRESSING
The shaping of structural engineering ceramics N89-16997
HOT WORKING
Hard material cutting technology described N89-17049
HUBBLE CONSTANT
Is the great attractor really a great wall
[NASA-CR-184772] N89-17540
HUMAN BEINGS
The effects of microgravity and linear accelerations on cutaneomuscular reflexes in human lower limb musculature N89-17034
HUMAN FACTORS ENGINEERING
Human factors in aviation operations: The hearback problem
[NASA-CR-177398] N89-16769
HUMAN PERFORMANCE
Extravehicular activities limitations study. Volume 2: Establishment of physiological and performance criteria for EVA gloves
[NASA-CR-172099] N89-17393
HYDRAZINES
Material compatability with threshold limit value levels of monomethyl hydrazine
[AD-A200294] N89-17362
The effects of hydrazines on neuronal excitability
[AD-A200199] N89-17395
HYDRODYNAMIC EQUATIONS
Laminar flame in a turbulent flow
[AD-A200241] N89-16947

HYDRODYNAMICS
Selection of alloys for hydrodynamic bearings [ESDU-88018] N89-16980
Relativistically-invariant statistical hydrodynamics of a normal fluid [DE88-704370] N89-17161
HYDROGEN
Hydrogen diffusion in tantalum [DE88-704073] N89-16968
Kinetics and mechanisms of hydrogen attack in 2.25Cr-1Mo steel [DE89-001381] N89-16970
Applications of ion implantation for modifying the interactions between metals and hydrogen gas [DE89-002877] N89-17219
Reaction dynamics of H + O2 at 1.6 eV collision energy [NASA-CR-183182] N89-17483
Hydrogen erosion of carbon for fusion applications [UTIAS-328] N89-17504
A neutral hydrogen survey of galaxies in the Cancer region N89-17552
Origin and dynamics of expanding neutral hydrogen supershells [DE88-704372] N89-17555
HYDROGEN BONDS
Ion content of moist atmospheric air and the molecular structure of water vapor thus inferred [AD-A199732] N89-16940
HYDROGEN IONS
Ion content of moist atmospheric air and the molecular structure of water vapor thus inferred [AD-A199732] N89-16940
Electron collision shift of the Lyman-alpha line in H and He+ [AD-A200296] N89-17474
HYDROGEN PRODUCTION
Modern and prospective technologies for hydrogen production from fossil fuels [DE89-001270] N89-16959
HYDROTHERMAL STRESS ANALYSIS
Hygrothermal deformations of laminated composite shells N89-16924
HYPERBOLIC FUNCTIONS
Generation of three-dimensional body-fitted grids by solving hyperbolic and parabolic partial differential equations [NASA-TM-101069] N89-16763
HYPERCUBE MULTIPROCESSORS
Performance of a second generation hypercube [DE89-005674] N89-17407
The performance of asynchronous algorithms on hypercubes [DE89-005503] N89-17420
Finding Eigenvalues and Eigenvectors of unsymmetric matrices using a hypercube multiprocessor [DE89-002311] N89-17455
HYPERSONIC BOUNDARY LAYER
Decoupling of ionization in the hypersonic boundary limit --- computational fluid dynamics [CERT-RT-OA-21/5005-AYD] N89-17204
HYPERSONIC FLIGHT
Derivation of primary air-data parameters for hypersonic flight [ESDU-88025] N89-16732
HYPERSONIC FLOW
Verification of a Navier-Stokes code for solving the hypersonic blunt body problem [DE89-003169] N89-16737
A statistical theory for gas surface interactions in rarefied hypersonic flows [IC-AERO-88-01] N89-16755
Three dimensional viscous analysis of a hypersonic inlet [NASA-TM-101474] N89-16759
Inviscid flow field analysis of complex reentry vehicles. Volume 1: Description of numerical methods [DE89-002814] N89-16900
Decoupling of ionization in the hypersonic boundary limit --- computational fluid dynamics [CERT-RT-OA-21/5005-AYD] N89-17204
HYPERSONIC INLETS
CFD application to supersonic/hypersonic inlet airframe integration --- computational fluid dynamics (CFD) N89-16754
HYPERSONIC SPEED
Numerical solutions to three-dimensional shock wave/vortex interaction at hypersonic speeds N89-16729
HYPERSONIC WIND TUNNELS
Characterization of hypersonic wind tunnel flow fields for improved data accuracy N89-16874
HYPERSPHERES
Spherical-type hypersurfaces in a Riemannian manifold [DE88-704224] N89-17454
HYPERVELOCITY LAUNCHERS
Numerical study of two-stage light-gas hypervelocity projectile launchers [UTIAS-327] N89-16894

I

ICE FORMATION
New England mountain icing climatology [AD-A200287] N89-17381
Profile properties of undeformed first-year sea ice [AD-A200172] N89-17388
IGNITION
The synchronous injection ignition valveless pulsejet N89-16823
Combustibility of titanium powders [NASA-TT-20455] N89-16967
ILLUMINATING
A scanning laser beam system for two-dimensional illumination of flow fields N89-17196
A performance model for nonuniformly illuminated front-gridded concentrator cells [DE89-001368] N89-17347
ILLUMINATION
Proceedings of a workshop on Lighting Requirements in Microgravity: Rodents and Nonhuman Primates [NASA-TM-101077] N89-17390
IMAGE ANALYSIS
Digital direct analysis of a multiexposed photograph in Particle Image Displacement Velocimetry (PIDV) N89-17194
Energy and Technology Review [DE89-005308] N89-17459
IMAGE PROCESSING
Adaptive hybrid picture coding [AD-A200059] N89-17142
Processing techniques: Image plane and Fourier plane --- particle image velocimetry N89-17182
Processing information in the image plane --- particle image velocimetry N89-17183
Optical processing --- particle image displacement velocimetry N89-17189
Probabilistic modeling of Particle Image Displacement Velocimetry (PIDV) experiments N89-17190
A personal computer based system for the evaluation of multiple exposed images in laser speckle and particle image displacement velocimetry N89-17193
A new algorithm for the rapid analysis of particle image displacement data N89-17195
NDE methods for high-temperature materials and environments [DE89-005195] N89-17234
3-D vision techniques for autonomous vehicles [AD-A199643] N89-17236
Applications of digital image processing to ongoing research in complex terrain meteorology [DE89-001749] N89-17375
Role of retinocortical processing in spatial vision [AD-A200198] N89-17394
Research on automatic extraction of map information and its image representation [DE88-754960] N89-17409
Automatic registration of satellite imagery [INPE-4637-PRE/1349] N89-17414
Analysis of interferometer images with Fourier domain techniques [DE89-002927] N89-17491
IMAGE VELOCITY SENSORS
Optical methods for measuring vector velocity fields. 1: Principles. 2: Techniques N89-17180
IMAGES
Improving classification accuracy of radar images using a multiple-stage classifier [AD-A200291] N89-17071
Adaptive hybrid picture coding [AD-A200059] N89-17142
IMAGING TECHNIQUES
Optical methods for measuring vector velocity fields. 1: Principles. 2: Techniques N89-17180
Application of Particle Image Displacement Velocimetry (PIDV) to complex flows: Resolution of the directional ambiguity N89-17187
Application of Particle Image Displacement Velocimetry (PIDV) to complex flows: Measurements of the third component N89-17188
Probabilistic modeling of Particle Image Displacement Velocimetry (PIDV) experiments N89-17190
Application of particle image velocity to high speed flows N89-17198
Application of particle image displacement velocimetry to a centrifugal pump N89-17200
A photon-counting, subnanosecond, imaging camera for X-ray detection [DE89-002874] N89-17208
Long term possibilities for nondestructive evaluation for US Navy aircraft N89-17259
IMPACT DAMAGE
Damage tolerance behavior of fiber reinforced composite airframes N89-17278
IMPACT LOADS
Mix experiments with the NOVA laser [DE89-004775] N89-17228
IMPACT TOLERANCES
Damage tolerance behavior of fiber reinforced composite airframes N89-17278
IMPEDANCE
Derivation and application of a class of generalized impedance boundary conditions, part 2 [NASA-CR-183298] N89-17148
IMPURITIES
Breakdown voltage mapping of impurity concentrations in GaAs wafers [DE89-002489] N89-17518
IN-FLIGHT MONITORING
Technology assessment for aircraft command in emergency situations [DOT/FAA/CT-88/20] N89-16767
Engine Condition Monitoring: Technology and Experience [AGARD-CP-448] N89-16780
Operational requirements for engine condition monitoring from the EFA viewpoint N89-16781
An overview of US Navy engine monitoring system programs and user experience N89-16782
Engine usage condition and maintenance management systems in the UK armed forces N89-16783
On board life monitoring system Tornado (OLMOS) N89-16785
Information management systems for on-board monitoring systems N89-16786
CF-18 engine performance monitoring N89-16787
B-1B CITS engine monitoring N89-16788
Engine life consumption monitoring program for RB199 integrated in the on-board life monitoring system N89-16789
Recent UK trials in engine health monitoring: Feedback and feedforward N89-16790
F110 engine monitoring and maintenance management systems for F-16 C/D N89-16791
Engine condition monitoring: State-of-the-art civil application N89-16792
The CFM 56-5 on the A-320 at Air France N89-16793
Implication of engine performance monitoring for the aircraft manufacturer N89-16794
F100-PW-220 engine monitoring system N89-16795
Service life calculator for the M53 turbofan engine N89-16796
Military engine condition monitoring systems: The UK experience N89-16797
Military engine monitoring status at GE Aircraft Engines, Cincinnati, Ohio N89-16798
Gas path analysis and engine performance monitoring in a Chinook helicopter N89-16802
System considerations for integrated machinery health monitoring N89-16804
Maintenance aid system for wide body aircraft N89-16805
Identification of dynamic characteristics for fault isolation purposes in a gas turbine using closed-loop measurements N89-16813
Space shuttle main engine monitoring experience and advanced monitoring systems development N89-16815
Gas path condition monitoring using electrostatic techniques N89-16817
COMPASS (Trademark): A generalized ground-based monitoring system N89-16819
INCIDENCE
Incidence angle rules in supersonic cascades N89-16827
Fresnel coefficients for a phase conjugator [AD-A200123] N89-17487
INCOMPRESSIBLE FLOW
Aerodynamic performance of wings of arbitrary planform in inviscid, incompressible, irrotational flow [AD-A200436] N89-16728
A computational method for three dimensional, internal viscous flows with separation and secondary flow patterns N89-17164
INDIAN SPACE PROGRAM
Proceedings of the Colloquium about Joint Projects Within the DFVLR/ISRO Cooperation [DFVLR-MITT-88-19] N89-16883
ISRO-DFVLR collaboration in space sciences N89-16884
Indian activities in remote sensing applications: Microwave remote sensing N89-16886

Presentation of the status of the experiment and mission activities of the Monocular Electro-Optical Stereo Scanner (MEOSS) — Indian/German space cooperation N89-16888

Mission under SROSS program and position paper on SROSS-2 with MEOSS payload — Indian/German space cooperation N89-16889

INDIAN SPACECRAFT

Indian activities in remote sensing applications: Microwave remote sensing N89-16886

INDIUM ARSENIDES

InP/GaInAs/InP PIN photodiode with FWHM less than 18 ps N89-17114

Quantum-confined Stark effect in InGaAs/InP quantum wells grown by metal-organic chemical vapor deposition N89-17129

Recent advances in high-efficiency InGaAs concentrator cells

[DE89-001613] N89-17345

INDIUM PHOSPHIDES

InP/GaInAs/InP PIN photodiode with FWHM less than 18 ps N89-17114

Quantum-confined Stark effect in InGaAs/InP quantum wells grown by metal-organic chemical vapor deposition N89-17129

INDUSTRIES

Report to Congress on the Automotive Technology Development Program

[DE89-004977] N89-17250

INELASTIC SCATTERING

Effect of finite size on magnetoresistance

[AD-A200267] N89-16974

Production and transport of convoy electrons in amorphous carbon foils

[DE89-002313] N89-17478

INELASTIC STRESS

Use of inelastic strain as a basis for analyzing thermomechanical test data N89-17326

INERTIAL CONFINEMENT FUSION

High power KrF laser development at Los Alamos

[DE89-002242] N89-17218

Plasma performance in JET: Achievements and projections

[DE89-002219] N89-17500

Progress toward high-gain laser fusion

[DE89-002661] N89-17501

Progress in laboratory high gain ICF (Inertial Confinement Fusion): Prospects for the future

[DE89-002664] N89-17502

INERTIAL NAVIGATION

Inertial navigation system simulator: Behavioral specification

[AD-A200604] N89-16771

Inertial navigation system simulator program: Top-level design

[AD-A200605] N89-16772

Functional performance specification for an external computer system simulator

[AD-A200611] N89-16881

INFORMATION MANAGEMENT

Life cycle management handbook

[DE89-004315] N89-17545

INFORMATION RETRIEVAL

Research on automatic extraction of map information and its image representation

[DE88-754960] N89-17409

INFORMATION SYSTEMS

Information management systems for on-board monitoring systems N89-16786

A document preparation system in a large network environment

[DE88-014466] N89-17543

Life cycle management handbook

[DE89-004315] N89-17545

INFORMATION THEORY

Models of incremental concept formation

[AD-A199617] N89-17400

INFRARED IMAGERY

Development of an infrared imaging system for the surface tension driven convection experiment

[NASA-TM-101479] N89-17211

INFRARED RADIATION

Light-off temperature determination of oxidation catalyst using Fourier transform infrared technique

[AD-A199596] N89-16938

A technique for wing suppressed IR sampling N89-17109

INFRARED SPECTRA

Absolute absorption cross section measurements of ozone and the temperature dependence at four reference wavelengths leading to renormalization of the cross section between 240 and 350 nm

[AD-A199737] N89-16942

In-situ vibrational spectroelectrochemistry

[AD-A200303] N89-16949

Optical and infrared studies of cometary dust N89-17550

INFRARED SPECTROSCOPY

Structure and properties of polymer interphases

[AD-A200238] N89-17008

INHOMOGENEITY

Study of the effect of cloud inhomogeneity on the earth radiation budget experiment

[NASA-CR-182962] N89-17386

INJECTORS

Application of advanced diagnostics to airblast injector flows N89-17306

INLET AIRFRAME CONFIGURATIONS

Intake Aerodynamics, volume 1 — conference

[VKI-LS-1988-04-VOL-1] N89-16736

Tactical fighter inlets N89-15740

Inlet-engine compatibility N89-16741

Intake swirl and simplified methods for dynamic pressure distortion assessment N89-16742

Intake-airframe integration N89-16744

Intakes for high angle of attack N89-16745

Intake Aerodynamics, volume 2 — conference

[VKI-LS-1988-04-VOL-2] N89-16748

Computational methods for inlet airframe integration N89-16752

CFD application to subsonic inlet airframe integration — computational fluid dynamics (CFD) N89-16753

CFD application to supersonic/hypersonic inlet airframe integration — computational fluid dynamics (CFD) N89-16754

INLET FLOW

Intake swirl and simplified methods for dynamic pressure distortion assessment N89-16742

Intake-airframe integration N89-16744

Incidence angle rules in supersonic cascades N89-16827

Measurement of airfoil heat transfer coefficients on a turbine stage N89-17311

INSPECTION

Event-centered scheduling program: The need for PERT (Program Evaluation Review Technique) in C-141 ISO inspection management

[AD-A200094] N89-16718

Assessment of nonintrusive methods for monitoring the operational readiness of solenoid-operated valves

[DE89-002330] N89-17244

The impact of engineering assumptions on NDE requirements N89-17254

Relationships of nondestructive evaluation needs and component design N89-17256

Importance of sensitivity and reliability of NDI techniques on damage tolerance based life prediction of turbine discs N89-17257

Long term possibilities for nondestructive evaluation for US Navy aircraft N89-17259

Need for common AGARD approach and actions N89-17260

INSTALLING

Installed thrust as a predictor of engine health for jet engines N89-16806

INSTANTONS

Supersymmetric instantons and topological quantum field theory

[DE88-704211] N89-17536

INSTRUMENT LANDING SYSTEMS

Aircraft accident/incident summary report, Travis Air Force Base, California, 8 April 1987

[PB88-910414] N89-16768

INSULATION

Design and analysis of solid rocket motor internal insulation N89-16915

Investigation of defect and electronic interactions associated with GaAs device processing

[AD-A200541] N89-17525

The effect of insulated combustion chamber surfaces on direct-injected diesel engine performance, emissions, and combustion

[NASA-CR-182204] N89-17548

INTAKE SYSTEMS

Three dimensional viscous analysis of a hypersonic inlet

[NASA-TM-101474] N89-16759

INTEGRAL EQUATIONS

Center of buoyancy definition

[DE89-003017] N89-17457

INTEGRALS

The behavior of microdisks and microring electrodes. Applications of Neumann's integral theorem

[AD-A200307] N89-16951

Elevated temperature crack growth N89-17335

INTEGRATED CIRCUITS

The potential impact of MMICs on future satellite communications

[NASA-CR-182227] N89-17078

The potential impact of MMICs on future satellite communications: Executive summary

[NASA-CR-182227-EXEC-SUMM] N89-17079

Topical Meeting on Picosecond Electronics and Optoelectronics

[AD-A189686] N89-17080

A non-contact picosecond prober for integrated circuit testing N89-17081

Picosecond sampling of integrated circuits N89-17082

Electro-optic sampling of high-speed, InP-based integrated circuits N89-17084

Multigigahertz logic based on InP-MISFET's exhibiting extremely high transconductance N89-17086

Millimeter-wave integrated circuits N89-17089

Enhanced performance ultrabroadband distributed amplifiers N89-17090

Characteristics of shielded microstrip lines on GaAs-Si at millimeter-wave frequencies N89-17102

INTERACTIONAL AERODYNAMICS

Vortex dynamics for rotorcraft interactional aerodynamics

[AD-A200128] N89-16726

INTERCEPTION

The space-based interceptor

[DE89-002869] N89-17451

INTERFACES

Interfacial bonding in W/C and W/B4C multilayers

[DE89-002931] N89-16936

Glancing angle EXAFS studies of Cu-Al thin film interfaces

[DE89-003614] N89-16983

Robotic vehicle communications interoperability

[TACOM-TR-13387] N89-17075

The interaction of a fluid interface with a vortex pair

[AD-A200167] N89-17156

IEEE P1596, a scalable coherent interface for gigabyte/sec multiprocessor applications

[DE89-002813] N89-17405

An abstract interactive graphics interface for the IBM/PC and Macintosh

[AD-A200427] N89-17411

Studies of NiO metal interfaces

[DE89-003634] N89-17529

INTERFACIAL TENSION

Development of an infrared imaging system for the surface tension driven convection experiment

[NASA-TM-101479] N89-17211

INTERFEROMETERS

High-resolution Interferometer Sounder (HIS), phase 2

[NASA-CR-183414] N89-17212

Analysis of interferometer images with Fourier domain techniques

[DE89-002927] N89-17491

INTERFEROMETRY

Evaluation and application of a new interferometry technique for compressible flow research

[NASA-CR-177467] N89-16765

Precise interferometric phase determination

[AD-A200186] N89-17488

Analysis of interferometer images with Fourier domain techniques

[DE89-002927] N89-17491

INTERIOR BALLISTICS

Propellant grain design N89-16912

INTERNAL COMBUSTION ENGINES

Results from the Federal Methanol Fleet

[DE88-015291] N89-17016

Multidimensional modeling of convective heat transfer with application to I. C. engines

[DE89-004062] N89-17166

Application of a spatial filter velocimeter to the two phase flows in a Spark Ignition (SI) N89-17199

Emission-reduction effects of methanol vehicles: State of knowledge

[DE89-001148] N89-17359

INTERNATIONAL COOPERATION

Proceedings of the Colloquium about Joint Projects Within the DFVLR/ISRO Cooperation

[DFVLR-MITT-88-19] N89-16883

ISRO-DFVLR collaboration in space sciences N89-16884

Space utilization promotion program of NASDA N89-17022

Canadian participation in international biosatellite programs N89-17025

Microgravity science and applications bibliography, 1988 revision

[NASA-TM-4098] N89-17045

INTERNATIONAL SYSTEM OF UNITS

Assessment and comparison of techniques for transforming parameters to a common metric in item response theory

[AD-A200067] N89-17433

INTERPLANETARY DUST
Ion microprobe measurements of H, C, O, Mg, and Si isotopic abundances in individual interplanetary dust particles N89-17551
INTERPOLATION
Precise interferometric phase determination
[AD-A200186] N89-17488
INTERPROCESSOR COMMUNICATION
Interconnecting different types of local area computer networks
[AD-A200280] N89-17423
INTERSTELLAR MATTER
Photoabsorption and photodissociation of molecules important in the interstellar medium
[NASA-CR-184771] N89-16965
The role of presolar dust in the formation of the solar system N89-17553
INTERSTELLAR RADIATION
Photoabsorption and photodissociation of molecules important in the interstellar medium
[NASA-CR-184771] N89-16965
INTERSTELLAR TRAVEL
Project Longshot: An unmanned probe to Alpha Centauri
[NASA-CR-184718] N89-16904
INTRAMOLECULAR STRUCTURES
Nuclear reorganization barriers to electron transfer
[DE88-016582] N89-17471
INTRUSION
The interaction of a fluid interface with a vortex pair
[AD-A200167] N89-17156
INVERSE SCATTERING
Far field patterns and the inverse scattering problem for electromagnetic waves in an inhomogeneous medium
[AD-A200223] N89-17070
INVISCID FLOW
Aerodynamic performance of wings of arbitrary planform in inviscid, incompressible, irrotational flow
[AD-A200436] N89-16728
Physical aspects of viscous simulation and associated research requirements N89-16865
Inviscid flow field analysis of complex reentry vehicles. Volume 1: Description of numerical methods
[DE89-002814] N89-16900
Implicit time dependent methods for inviscid and viscous compressible methods N89-17178
IO
Sodium in Io's extended atmosphere N89-17559
IODINE LASERS
The kinetics and dynamics of iodine monofluoride formation in gas-phase collisions
[AD-A199622] N89-16939
Theoretical studies of solar lasers and converters
[NASA-CR-184589] N89-17214
ION ATOM INTERACTIONS
Atomic-scale modeling of low-energy ion-solid processes
[DE89-004374] N89-17482
ION BEAMS
Tribology of amorphous alloys formed with ion beams
[DE89-003274] N89-16982
Unlubricated sliding properties of ion beam and excimer laser mixed Fe-Ti-C multilayered films
[DE89-003470] N89-17245
A high-intensity plasma sputter heavy negative ion source
[DE89-003113] N89-17480
Atomic-scale modeling of low-energy ion-solid processes
[DE89-004374] N89-17482
Growth of gallium arsenide using ion cluster beam technology, volume 1, phase 2
[AD-A200231] N89-17523
ION CHARGE
Role of charge exchange process in forming of ion charge and energy states in multicomponent laser plasma produced from gas-content solids
[DE88-704828] N89-17511
ION CURRENTS
Ultramicroelectrode sensors and detectors. Considerations of the stability, sensitivity, reproducibility and mechanism of ion transport in gas phase chromatography and in high performance liquid phase chromatography
[AD-A200306] N89-17210
ION CYCLOTRON RADIATION
High power Ion Cyclotron Resonance Heating (ICRH) in JET
[DE89-002218] N89-17499
ION DENSITY (CONCENTRATION)
Ion content of moist atmospheric air and the molecular structure of water vapor thus inferred
[AD-A199732] N89-16940
ION EMISSION
Electronic interactions of electrons, photons, and atoms with material surfaces
[AD-A199626] N89-17469
ION ENGINES
Characterization of hollow cathode, ring cusp discharge chambers
[NASA-CR-182255] N89-17146
ION EXCHANGING
Ultramicroelectrode sensors and detectors. Considerations of the stability, sensitivity, reproducibility and mechanism of ion transport in gas phase chromatography and in high performance liquid phase chromatography
[AD-A200306] N89-17210
ION IMPACT
Modeling of atomic processes for X-ray laser plasmas
[AD-A200219] N89-17505
ION IMPLANTATION
Tribology of amorphous alloys formed with ion beams
[DE89-003274] N89-16982
Carrier lifetime versus ion-implantation dose in silicon on sapphire N89-17106
Applications of ion implantation for modifying the interactions between metals and hydrogen gas
[DE89-002877] N89-17219
Compositional changes during ion bombardment
[DE89-003974] N89-17481
The annealing behavior of ion-implanted single crystals of the type YBa2Cu3O(sub x)
[DE89-002189] N89-17519
Phases and microstructures of carbon-implanted niobium
[DE89-004017] N89-17534
ION IRRADIATION
Electronic interactions of electrons, photons, and atoms with material surfaces
[AD-A199626] N89-17469
ION PROPULSION
A data acquisition and storage system for the ion auxiliary propulsion system cyclic thruster test
[NASA-TM-101469] N89-17424
IONIC COLLISIONS
Collision-induced decomposition of multiatomic ions N89-17468
IONIC CRYSTALS
Hopping model for the non-Debye dielectric response in ionic crystals
[DE89-003151] N89-17521
IONIZATION
Decoupling of ionization in the hypersonic boundary limit --- computational fluid dynamics
[CERT-RT-OA-21/5005-AYD] N89-17204
An active nitrogen plasma atom reservoir for laser-induced ionization spectrometry
[AD-A200544] N89-17224
Collision-induced decomposition of multiatomic ions N89-17468
IONIZATION CHAMBERS
Development of an optical digital ionization chamber
[DE89-002209] N89-17470
IONIZATION CROSS SECTIONS
The electron-water vapor (H2O) collision cross sections
[AD-A200187] N89-17472
IONIZED GASES
Development of finite local perturbations of electrical conductivity in the flow of a weakly-conducting gas when a magnetic field is present
[AD-A200243] N89-17458
IONOSPHERIC PROPAGATION
A technique for recording HF (High Frequency) oblique-incidence-sounder data
[AD-A200168] N89-17068
IRRADIATION
High-speed phenomena in GaAs multiple-quantum-wells N89-17127
IRRITATION
A strategy for understanding noise-induced annoyance
[AD-A200125] N89-17461
ISOLATORS
High speed opto-isolator for radar applications N89-17110
ISOTHERMAL PROCESSES
The design of a heat-pipe furnace for microgravity N89-17043
Constitutive modeling for isotropic materials N89-17322
Use of inelastic strain as a basis for analyzing thermomechanical test data N89-17326
ISOTOPES
Ion microprobe measurements of H, C, O, Mg, and Si isotopic abundances in individual interplanetary dust particles N89-17551
ISOTROPISM
A multiaxial strength criterion for composites
[AD-A199610] N89-16920
The behavior of shells made of composites during the dynamic application of axian compression
[AD-A200244] N89-17266
ISOTROPY
Creep fatigue life prediction for engine hot section materials (ISOTROPIC) fifth year progress review N89-17336
Isotropization of the cosmic background radiation due to galactic gravitational screening
[DE88-755533] N89-17563
ITERATION
Development of generalized block correction procedures for the solution of discretized Navier-Stokes equations N89-17307

J

JACOBI MATRIX METHOD
Flux Jacobian matrices and generaled Roe average for an equilibrium real gas
[NASA-CR-177512] N89-17445
JAGUAR AIRCRAFT
Jaguar/Tornado intake design N89-16743
JAPANESE SPACE PROGRAM
Space utilization promotion program of NASDA N89-17022
JET BLAST EFFECTS
Jet-by-jet shielding of noise
[ESDU-88023] N89-17463
JET ENGINE FUELS
Experimental verification of the thermodynamic properties for a jet-A fuel
[NASA-TM-101475] N89-17017
JET ENGINES
Gas path modelling, diagnosis and sensor fault detection N89-16811
Review of existing NDT technologies and their capabilities N89-17255
JET FLOW
Aerothermal modeling program. Phase 2, element B: Flow interaction experiment N89-17304
Jet-by-jet shielding of noise
[ESDU-88023] N89-17463
JET MIXING FLOW
The synchronous injection ignition valveless pulsejet N89-16823
JET VANES
Variable geometry in supersonic compressors N89-16838
JOINTS (JUNCTIONS)
Adsorption of phosphorus acids on alumina
[AD-A200548] N89-16957
Structure and properties of polymer interphases
[AD-A200238] N89-17008
JOSEPHSON JUNCTIONS
Picosecond switching in Josephson tunnel junctions N89-17095
Millimeter wave generation using Josephson junction arrays
[AD-A200259] N89-17524
JP-5 JET FUEL
Fuel property and antioxidant effects on elastomer integrity, phase 2
[AD-A200250] N89-17015

K

K-EPSILON TURBULENCE MODEL
Application of a two-equation turbulence mix model
[DE89-004812] N89-17205
KALMAN FILTERS
The Kalman filter
[ESDU-88039] N89-17437
KERNEL FUNCTIONS
The Wigner distribution function with minimum spread
[AD-A199661] N89-17446
KEVLAR (TRADEMARK)
Isotropic kevlar and PBA (poly 1,4-benzamide) reinforcements for composites
[AD-A200239] N89-16927
KINEMATIC EQUATIONS
Development of kinematic equations and determination of workspace of a 6 DOF end-effector with closed-kinematic chain mechanism
[NASA-CR-183241] N89-17444
KINEMATICS
Droplet separation dynamics and kinematics under microgravity N89-17031
Approximation of viscoelastic stresses from Newtonian turbulent kinematics
[AD-A200188] N89-17157

On deriving the three-dimensional kinematic structure on convective storms from a single radar N89-17376
KINETIC ENERGY
Kinetic energy diagnostic studies of extratropical cyclones based on storm relative motion N89-17378
Collision-induced decomposition of multiatomic ions N89-17468
KINETIC EQUATIONS
Kinematic leveling adjustments with polynomials and polynomial splines
[ETN-89-93328] N89-17338
KINETICS
Protein crystal nucleation kinetics using relative light-scattering techniques: Center director's discretionary fund
[NASA-TM-100348] N89-17535
KNOWLEDGE BASES (ARTIFICIAL INTELLIGENCE)
Empirical analysis and refinement of expert system knowledge bases
[AD-A200146] N89-17428
KRYPTON FLUORIDE LASERS
High power KrF laser development at Los Alamos
[DE89-002242] N89-17218

L

LABORATORIES
Progress in laboratory high gain ICF (Inertial Confinement Fusion): Prospects for the future
[DE89-002664] N89-17502
LAMINAR BOUNDARY LAYER
Boundary layer equations and methods of solution N89-17176
LAMINAR FLOW
Laminar flame in a turbulent flow
[AD-A200241] N89-16947
Aerothermal modeling program. Phase 2, element A: Improved numerical methods for turbulent viscous recirculating flows N89-17303
Two- and three-dimensional turbine blade row flow field simulations N89-17313
LAMINAR HEAT TRANSFER
Verification of a Navier-Stokes code for solving the hypersonic blunt body problem
[DE89-003169] N89-16737
LAMINATES
Tensile strength of composite structures with internal ply drops and free-edge effects N89-16929
Elastic wrinkling of sandwich panels with laminated fibre reinforced face plates (face plates of AsBoDs, AsDIDs and AsBsDs types). (Computer program)
[ESDU-88015] N89-16930
Vibration and aeroelastic tailoring of advanced composite plate-like lifting surfaces N89-17263
LANDING
Human factors in aviation operations: The hearback problem
[NASA-CR-177398] N89-16769
LANDSAT SATELLITES
Accuracy assessment, using stratified plurality sampling, of portions of a LANDSAT classification of the Arctic National Wildlife Refuge Coastal Plain
[NASA-TM-101042] N89-17339
LANTHANUM
Kinetics of the isothermal decomposition of lanthanum nickel hydride
[DE89-002905] N89-16966
Oxygen and copper valencies in oxygen-doped superconducting La2CuO(sub 4.13)
[DE89-003265] N89-17533
LANTHANUM COMPOUNDS
An in situ surface Fourier transform study of complexes of lithium, magnesium potassium and lanthanum ferrocyanide at platinum and gold electrodes
[AD-A200305] N89-16950
LARGE SCALE INTEGRATION
Progress and challenges in HEMT LSI technology N89-17094
LARGE SPACE STRUCTURES
Adaptive control techniques for large space structures
[AD-A200208] N89-16901
Spillover stabilization in the control of large flexible space structures N89-16902
LASER APPLICATIONS
JPRS report: Science and technology. Japan. Developments in Manufacturing Process Technology
[JPRS-JST-88-010] N89-17047
Graphite as a picosecond laser activated opening switch N89-17098
In-situ surface during laser-controlled chemical processing of surfaces
[AD-A200206] N89-17223
The X-ray laser: Review of recent experimental results and of future prospects
[DE89-005096] N89-17231
Long term possibilities for nondestructive evaluation for US Navy aircraft N89-17259
X-ray optics for X-ray laser research and applications
[DE89-004026] N89-17493
LASER BEAMS
Laser beam heat method reported N89-17054
Laser interactions with aerosol aureoles
[DE89-002824] N89-17225
High energy laser beam scattering by atmospheric aerosol aureoles
[DE89-004811] N89-17230
LASER DOPPLER VELOCIMETERS
Particle Image Displacement Velocimetry — conference
[VKI-LS-1988-06] N89-17179
Optical methods for measuring vector velocity fields. 1: Principles. 2: Techniques N89-17180
Scattering power of seed materials: Mie scattering calculations N89-17181
Processing techniques: Image plane and Fourier plane — particle image velocimetry N89-17182
Processing information in the image plane — particle image velocimetry N89-17183
Some comments on particle image displacement velocimetry N89-17184
Practical systems for speckle velocimetry N89-17185
Application of Particle Image Displacement Velocimetry (PIDV) to complex flows: Resolution of the directional ambiguity N89-17187
Application of Particle Image Displacement Velocimetry (PIDV) to complex flows: Measurements of the third component N89-17188
Probabilistic modeling of Particle Image Displacement Velocimetry (PIDV) experiments N89-17190
Digital direct analysis of a multiexposed photograph in Particle Image Displacement Velocimetry (PIDV) N89-17194
A new algorithm for the rapid analysis of particle image displacement data N89-17195
Application of particle image velocity to high speed flows N89-17198
Application of particle image displacement velocimetry to a centrifugal pump N89-17200
A comparison of turbulence measurement methods N89-17302
LASER FUSION
Recent results from the Nova experiments program
[DE89-002901] N89-17220
Energy and Technology Review
[DE89-005308] N89-17459
Progress toward high-gain laser fusion
[DE89-002661] N89-17501
LASER MICROSCOPY
In-situ laser microscopy for particle sizing and tracking N89-17201
LASER OUTPUTS
Aneurisms in laser-driven blast waves
[AD-A200189] N89-17222
LASER PLASMA INTERACTIONS
Laser interactions with aerosol aureoles
[DE89-002824] N89-17225
LASER PLASMAS
An active nitrogen plasma atom reservoir for laser-induced ionization spectrometry
[AD-A200544] N89-17224
Laser thermal propulsion
[AD-A200558] N89-17226
Ne-like ion X-ray laser experiments in plasmas produced by 0.53 microns and 0.35 microns laser light
[DE89-004827] N89-17233
Electron collision shift of the Lyman-alpha line in H and He+
[AD-A200296] N89-17474
Modeling of atomic processes for X-ray laser plasmas
[AD-A200219] N89-17505
Role of charge exchange process in forming of ion charge and energy states in multicomponent laser plasma produced from gas-content solids
[DE88-704828] N89-17511
LASER PROPULSION
Laser thermal propulsion
[AD-A200558] N89-17226
LASER RANGER/TRACKER
An algorithm for analysis of plate motions in Crust Dynamics Project (CDP) networks
[88821606] N89-17371
LASER SPECTROMETERS
An active nitrogen plasma atom reservoir for laser-induced ionization spectrometry
[AD-A200544] N89-17224
LASER SPECTROSCOPY
Laser studies of the SiH radical/surface interaction during deposition of a thin film
[DE89-003902] N89-17232
LASER TARGET INTERACTIONS
Aneurisms in laser-driven blast waves
[AD-A200189] N89-17222
LASER TARGETS
High power KrF laser development at Los Alamos
[DE89-002242] N89-17218
LASER WEAPONS
Report of the Defense Science Board Task Force Subgroup on Strategic Air Defense (SDI Milestone Panel)
[AD-A200164] N89-17452
LASER WELDING
Surface deformations resulting from laser spot welding
[DE88-014964] N89-17237
LASERS
Laser communication test system
[AD-A199612] N89-17215
Mix experiments with the NOVA laser
[DE89-004775] N89-17228
LASING
Characteristics, packaging and physics of ultra high speed diode lasers and detectors N89-17112
LATTICES (MATHEMATICS)
Development of a lattice gas model for the study of combustion
[ETN-89-93612] N89-16964
LAUNCH VEHICLES
Transonic aeroelastic analysis of launch vehicle configurations N89-16723
Mission under SROSS program and position paper on SROSS-2 with MEOSS payload — Indian/German space cooperation N89-16889
A Canadian low earth orbit launch vehicle: Launch vehicle performance analysis of Black Brant VC and Nihka rocket motor configurations N89-17039
LAUNCHING
Turbulence effects on the high angle of attack aerodynamics of a vertically launched missile
[AD-A200418] N89-16727
LEAD (METAL)
An investigation of the rechargeability of certain modified forms of MnO2
[AD-A199885] N89-16943
LEARNING
Models of incremental concept formation
[AD-A199617] N89-17400
An abstract interactive graphics interface for the IBM/PC and Macintosh
[AD-A200427] N89-17411
Machine learning of parameter control doctrine for sensor and communication systems
[AD-A200096] N89-17427
LEGENDRE FUNCTIONS
The visual shape and multipole moments of the sun N89-17561
LENSES
Explosion of integrated optic devices used in new generation systems
[DE89-004012] N89-17497
LEVELING
Kinematic leveling adjustments with polynomials and polynomial splines
[ETN-89-93328] N89-17338
LEWIS NUMBERS
Effect of Lewis number on wet surface heat exchangers N89-17152
LIBRATION
User and technical documentation
[NASA-CR-172087] N89-16893
LIFE (DURABILITY)
Engine life consumption monitoring program for RB199 integrated in the on-board life monitoring system N89-16789
Installed thrust as a predictor of engine health for jet engines N89-16806
AGARD/SMP Review: Damage Tolerance for Engine Structures. 1: Non-Destructive Evaluation
[AGARD-R-768] N89-17253
Relationships of nondestructive evaluation needs and component design N89-17256
Fretting corrosion fatigue N89-17282
Thermal barrier coating life-prediction model development N89-17331
Thermal barrier coating life prediction model N89-17332
Thermal barrier coating life prediction model development N89-17333
High temperature constitutive and crack initiation modeling of coated single crystal superalloys N89-17334
Creep fatigue life prediction for engine hot section materials (ISOTROPIC) fifth year progress review N89-17336
LIFE SCIENCES
Life science experiments during parabolic flight: The McGill experience N89-17027

LIFT
Rolling moment derivative Lxi, for plain ailerons at subsonic speeds
[ESDU-88013] N89-16731
Lift and longitudinal forces on propeller/nacelle/wing/flap systems
[ESDU-88031] N89-16736
Comparison of the results of tests on A300 aircraft in the RAE 5 metre and the ONERA F1 wind tunnels N89-16849
Accuracy of lift and center-of-thrust measurements at missile control surfaces N89-16875
Computer program for the prediction of air-lift pump performance
[ESDU-88014] N89-17246
LIFT DEVICES
On the aeroacoustics, aerodynamics and aeroelasticity of lifting surfaces N89-16724
Vibration and aeroelastic tailoring of advanced composite plate-like lifting surfaces N89-17263
LIGHT AMPLIFIERS
Induction-linac based free-electron laser amplifier for fusion applications
[DE89-001923] N89-17217
Induction-linac based free-electron laser amplifiers for plasma heating
[DE88-017004] N89-17221
LIGHT CURVE
Photoelectric photometry of very short period eclipsing binary systems and their light curve solutions N89-17549
LIGHT GAS GUNS
Numerical study of two-stage light-gas hypervelocity projectile launchers
[UTIAS-327] N89-16894
LIGHT MODULATION
An optical modulator/switch using the reflection from a transiated depletion edge
[DE89-001380] N89-17490
LIGHT SCATTERING
Measurement of natural convection by white light speckle velocimetry N89-17197
Nonlinear optics with broad-band lasers
[DE89-002728] N89-17216
Protein crystal nucleation kinetics using relative light-scattering techniques: Center director's discretionary fund
[NASA-TM-100348] N89-17535
LIMB DARKENING
Limb-darkening functions as derived from along-track operation of the ERBE scanning radiometer for January 1985
[NASA-RP-1214] N89-17374
LIMBS (ANATOMY)
The effects of microgravity and linear accelerations on cutaneomuscular reflexes in human lower limb musculature N89-17034
LINE SPECTRA
Absolute absorption cross section measurements of ozone and the temperature dependence at four reference wavelengths leading to renormalization of the cross section between 240 and 350 nm
[AD-A199737] N89-16942
An investigation of the spectral characteristics of a commercially available semiconductor laser N89-17213
LINEAR ACCELERATORS
Induction-linac based free-electron laser amplifiers for plasma heating
[DE88-017004] N89-17221
LINEAR ARRAYS
A multistage linear array assignment problem
[NASA-CR-181748] N89-17417
Extensions to the matrix pencil approach for direction finding
[AD-A200112] N89-17449
LINEAR PROGRAMMING
The performance of asynchronous algorithms on hypercubes
[DE89-005503] N89-17420
LINEAR SYSTEMS
R-parametrization and its role in classification of linear multivariable feedback systems
[NASA-TM-101066] N89-16844
Adaptive control techniques for large space structures
[AD-A200208] N89-16901
The Kalman filter
[ESDU-88039] N89-17437
Force state mapping using experimental data
[DE89-000351] N89-17442
LININGS
Design and analysis of solid rocket motor internal insulation N89-16915
Three-dimensional inelastic analysis methods for hot section components N89-17316
Structural response of an advanced combustor liner: Test and analysis N89-17329
Elevated temperature crack growth N89-17335
Hydrogen erosion of carbon for fusion applications
[UTIAS-328] N89-17504
LIQUID CHROMATOGRAPHY
Ultramicroelectrode sensors and detectors. Considerations of the stability, sensitivity, reproducibility and mechanism of ion transport in gas phase chromatography and in high performance liquid phase chromatography
[AD-A200306] N89-17210
LIQUID COOLING
Fouling in cooling water systems
[ESDU-88024] N89-17057
Heat transfer in self-heated particle beds submerged in liquid coolant N89-17171
LIQUID CRYSTALS
Theoretical predictions for side-chain liquid-crystal polymers and comparison to experiment
[DE89-003578] N89-17013
LIQUID SLOSHING
Investigation of liquid sloshing in spin-stabilized satellites
[AD-A199629] N89-16899
LIQUIDS
Thinning and rupture of a thin liquid film on a horizontal heated solid surface
[DE89-001792] N89-16944
Behavior in normal and reduced gravity of an enclosed liquid/gas system with nonuniform heating from above
[NASA-TM-101471] N89-17046
Characterization and modeling of acoustic beams from ultrasonic transducers in solid or liquid media
[RF-DAVI-88-08] N89-17465
LITHIUM COMPOUNDS
An in situ surface Fourier transform study of complexes of lithium, magnesium potassium and lanthanum ferrocyanide at platinum and gold electrodes
[AD-A200305] N89-16950
LITHIUM SULFUR BATTERIES
Development of overcharge tolerance in Li/FeS and Li/FeS2 cells
[DE89-003952] N89-17145
LITTORAL DRIFT
Evaluation of satellite-tracked surface drifting buoys for simulating the movement of spilled oil in the marine environment. Volume 1: Executive summary
[PB88-226048] N89-17357
Evaluation of satellite-tracked surface drifting buoys for simulating the movement of spilled oil in the marine environment, volume 2
[PB88-226055] N89-17358
LOAD DISTRIBUTION (FORCES)
Comparison of the results of tests on A300 aircraft in the RAE 5 metre and the ONERA F1 wind tunnels N89-16849
LOAD TESTS
Strength evaluation for fiber reinforced composite leaf springs under mechanical and environment conditioned loads N89-17277
Finite element analysis for the evaluation and optimization of fiber reinforced composite structural components N89-17279
LOADING
The reliable reduction of random local sequences for fatigue tests N89-17274
LOADS (FORCES)
A modified VAPEPS method for predicting vibroacoustic response of unreinforced mass loaded honeycomb panels
[NASA-TM-101467] N89-16905
Calculation methods for along-wind loading. Part 3: Response of buildings and plate-like structures to atmospheric turbulence
[ESDU-88019] N89-17267
Calculation methods for along-wind loading. Part 4: Computer program for estimation of response
[ESDU-88036] N89-17271
The influence of the load sequence on the fatigue life of fatigue fracture endangered components N89-17273
Prediction of stochastic blade responses using measured wind-speed data as input to the FLAP code
[DE89-000834] N89-17354
LOCAL AREA NETWORKS
The design, analysis, and implementation of a fully distributed local area network for integrated voice and data communications N89-17059
Interconnecting different types of local area computer networks
[AD-A200280] N89-17423
A formal language model for local area network configuration N89-17544
LOGARITHMS
Accurate and efficient testing of the exponential and logarithm functions in Ada
[DE89-004443] N89-17415
LOGIC CIRCUITS
High-speed optical logic using GaAs N89-17088
Test-efficient design of digital VLSI circuits
[ETN-89-93483] N89-17151
LOGISTICS
System engineering and logistics for KC-135 experimentation N89-17033
LONG DURATION SPACE FLIGHT
Advanced research rockets for long duration microgravity science N89-17028
LORENTZ TRANSFORMATIONS
An essay on discrete foundations for physics
[DE89-002992] N89-17556
LOSS OF COOLANT
Phase change phenomena in liquid saturated self heated particulate bed --- core meltdown N89-17170
Heat transfer in self-heated particle beds submerged in liquid coolant N89-17171
LOSSES
Loss development in transonic compressor cascades N89-16826
Shock losses in transonic and supersonic compressor cascades N89-16829
LOW ASPECT RATIO WINGS
Turbulence effects on the high angle of attack aerodynamics of a vertically launched missile
[AD-A200418] N89-16727
LOW FREQUENCIES
Low frequency oscillations in total ozone measurements
[NASA-CR-184759] N89-17385
LOW NOISE
Tip sensor development
[AD-A200080] N89-16824
LOW REYNOLDS NUMBER
Experiments on boundary layer transition tripping at low Reynolds numbers N89-16868
LOW SPEED WIND TUNNELS
Flow unsteadiness in three low-speed wind tunnels N89-16859
LOW TEMPERATURE
Gas jet deposition of multicomponent ultrafine microstructures
[AD-A200101] N89-16946
LUBRICATION
Selection of alloys for hydrodynamic bearings
[ESDU-88018] N89-16980
LUMINOSITY
A neutral hydrogen survey of galaxies in the Cancer region N89-17552
LUNAR BASES
Subselenean tunneler melting head design: A preliminary study
[NASA-CR-184750] N89-17058
Systems analysis and design of a lunar solar power plant for the supply of a lunar base
[ILR-MITT-198] N89-17355
LUNAR SOIL
Meteorites and lunar samples as space probes --- Indian/German space cooperation N89-16885
LUNAR SURFACE
Subselenean tunneler melting head design: A preliminary study
[NASA-CR-184750] N89-17058
LYMAN ALPHA RADIATION
Electron collision shift of the Lyman-alpha line in H and He+
[AD-A200296] N89-17474

M

MACH NUMBER
Derivation of primary air-data parameters for hypersonic flight
[ESDU-88025] N89-16732
Boundaries of linear characteristics of cambered and twisted wings at subcritical Mach numbers
[ESDU-88030] N89-16735
Loss development in transonic compressor cascades N89-16826
MACHINING
Nitride and carbide coatings for high speed steel cutting tools
[DE89-003623] N89-16984
JPRS report: Science and technology. Japan. Developments in Manufacturing Process Technology
[JPRS-JST-88-010] N89-17047
Hard material cutting technology described N89-17049
Brittle material processing reported N89-17051
Laser beam heat method reported N89-17054
Review of precision surface generating processes and their potential application to the fabrication of large optical components
[DE89-001712] N89-17486

MAGNESIUM COMPOUNDS
An in situ surface Fourier transform study of complexes of lithium, magnesium potassium and lanthanum ferrocyanide at platinum and gold electrodes
[AD-A200305] N89-16950
MAGNETIC DISTURBANCES
Alfven waves in a cold plasma with curved magnetic fields
[AD-A200312] N89-17506
MAGNETIC FIELD CONFIGURATIONS
Field-reversed configuration (FRC) experiments
[DE89-000389] N89-17498
Studies of a poloidal divertor reversed field pinch
[DE89-005498] N89-17515
MAGNETIC FIELDS
Effect of finite size on magnetoresistance
[AD-A200267] N89-16974
Alfven waves in a cold plasma with curved magnetic fields
[AD-A200312] N89-17506
Behavior of the reversed field pinch with nonideal boundary conditions
[DE89-005497] N89-17514
Orientation dependent X-ray absorption in high T (sub c) superconductors
[DE89-002910] N89-17520
Monopoles and magnetic fields in the inflationary universe
[DE88-755532] N89-17557
MAGNETIC FLUX
Radiation imposed limits on superconducting magnets: A data base for copper stabilizers
[DE89-002875] N89-17456
MAGNETIC SUSPENSION
An experimental investigation of the aerodynamic characteristics of slanted base ogive cylinders using magnetic suspension technology
[NASA-CR-184624] N89-16758
MAGNETIZATION
Magnetization, transport and structural studies of Tl-Ca-Ba-Cu-O: Bulk ceramics, single crystals, and polycrystalline thin films
[DE89-003264] N89-17010
Processing of strong flux trapping high T(subc) oxide superconductors: Center director's discretionary fund
[NASA-TM-100350] N89-17530
MAGNETOHYDRODYNAMIC GENERATORS
Seeded inert gas driven disk generator
[DE88-704083] N89-17510
MAGNETOHYDRODYNAMIC STABILITY
Behavior of the reversed field pinch with nonideal boundary conditions
[DE89-005497] N89-17514
MAGNETOHYDRODYNAMIC WAVES
Alfven waves in a cold plasma with curved magnetic fields
[AD-A200312] N89-17506
MAGNETOHYDRODYNAMICS
Development of finite local perturbations of electrical conductivity in the flow of a weakly-conducting gas when a magnetic field is present
[AD-A200243] N89-17458
Field-reversed configuration (FRC) experiments
[DE89-000389] N89-17498
Alfven waves in a cold plasma with curved magnetic fields
[AD-A200312] N89-17506
Neoclassical MHD descriptions of tokamak plasmas
[DE89-003117] N89-17508
MAGNETORESISTIVITY
Effect of finite size on magnetoresistance
[AD-A200267] N89-16974
Radiation imposed limits on superconducting magnets: A data base for copper stabilizers
[DE89-002875] N89-17456
MAGNETS
An intelligent sensor for equipment health monitoring of ferromagnetic wear debris concentration in fluids N89-16818
MAINTAINABILITY
A model of the effect of sparing and repair turnaround time of the inertial navigation system on aircraft readiness for the F/A-18
[AD-A200317] N89-16777
R/M/T (Reliability/Maintainability/Testability) design for fault tolerance. Volume 1: Program manager's guide
[AD-A200204] N89-17262
MAINTENANCE
Aircraft accident/incident summary report, Travis Air Force Base, California, 8 April 1987
[PB88-910414] N89-16768
A model of the effect of sparing and repair turnaround time of the inertial navigation system on aircraft readiness for the F/A-18
[AD-A200317] N89-16777
Operational requirements for engine condition monitoring from the EFA viewpoint N89-16781
Engine usage condition and maintenance management systems in the UK armed forces N89-16783
Canadian forces aircraft condition/health monitoring: Policy, plans and experience N89-16784
On board life monitoring system Tornado (OLMOS) N89-16785
Information management systems for on-board monitoring systems N89-16786
CF-18 engine performance monitoring N89-16787
F110 engine monitoring and maintenance management systems for F-16 C/D N89-16791
Engine condition monitoring: State-of-the-art civil application N89-16792
F100-PW-220 engine monitoring system N89-16795
The effects of a compressor rebuild on gas turbine engine performance N89-16803
CF-18/F404 transient performance trending N89-16814
Assessment of nonintrusive methods for monitoring the operational readiness of solenoid-operated valves
[DE89-002330] N89-17244
MAN-COMPUTER INTERFACE
Northeast Artificial Intelligence Consortium annual report 1986. Volume 5. Building an intelligent assistant: The acquisition, integration, and maintenance of complex distributed tasks
[AD-A199824] N89-17425
MANAGEMENT
Optical storage: Financial management and budget applications
[DE89-004916] N89-17546
MANAGEMENT METHODS
Event-centered scheduling program: The need for PERT (Program Evaluation Review Technique) in C-141 ISO inspection management
[AD-A200094] N89-16718
The space station integrated refuse management system
[NASA-CR-184722] N89-17403
MANAGEMENT SYSTEMS
F110 engine monitoring and maintenance management systems for F-16 C/D N89-16791
MANGANESE OXIDES
An investigation of the rechargeability of certain modified forms of MnO2
[AD-A199885] N89-16943
MANIPULATORS
Active vibration suppression for robotic manipulators N89-17241
HERMIES-3: A step toward autonomous mobility, manipulation and perception
[DE89-004932] N89-17249
Development of kinematic equations and determination of workspace of a 6 DOF end-effector with closed-kinematic chain mechanism
[NASA-CR-183241] N89-17444
MANUALS
JUNCTION code user's manual. Electromagnetic scattering and radiation by arbitrary configurations of conducting bodies and wires
[AD-A200315] N89-17072
Life cycle management handbook
[DE89-004315] N89-17545
MANUFACTURING
Manufacturing thermoplastic matrix composites
[AD-A199724] N89-16922
JPRS report: Science and technology. Japan. Developments in Manufacturing Process Technology
[JPRS-JST-88-010] N89-17047
Computer-aided design of bevel gear tooth surfaces
[NASA-TM-101449] N89-17248
MAPPING
Remapping on the staggered mesh
[DE89-002656] N89-17154
Force state mapping using experimental data
[DE89-000351] N89-17442
MAPS
Research on automatic extraction of map information and its image representation
[DE88-754960] N89-17409
MARKETING
Photonics: Maintaining competitiveness in the information era
[AD-A200230] N89-17473
MARKING
Development and application of oxygen flow tagging for velocity measurements and flow visualization in turbulent three-dimensional supersonic flows
[AD-A200119] N89-16725
MASS DISTRIBUTION
A modified VAPEPS method for predicting vibroacoustic response of unreinforced mass loaded honeycomb panels
[NASA-TM-101467] N89-16905
MASS FLOW
The synchronous injection ignition valveless pulsejet N89-16823
MASS TRANSFER
The behavior of microdisks and microring electrodes. Applications of Neumann's integral theorem
[AD-A200307] N89-16951
The behavior of microdisks and microring electrodes. Prediction of the amperometric response of microdisks and of the steady state for CE and EC Catalytic reactions by application of Neumann's integral theorem
[AD-A200415] N89-16952
The behavior of microdisk and microring electrodes. Mass transport to the disk in the unsteady state: Chronopotentiometry
[AD-A200421] N89-16953
The behavior of microdisk and microring electrodes. Mass transport to the disk in the unsteady state: Coupled chemical reactions
[AD-A200422] N89-16954
Application of a two-equation turbulence mix model
[DE89-004812] N89-17205
First production of potable water by OTEC (Ocean Thermal Energy Conversion) and its potential applications
[DE89-003630] N89-17353
MATHEMATICAL LOGIC
Axioms for concurrent objects
[AD-A200584] N89-17435
MATHEMATICAL MODELS
Vortex dynamics for rotorcraft interactional aerodynamics
[AD-A200128] N89-16726
Development of a panel method for modeling configurations with unsteady component motions, phase 1
[AD-A200255] N89-16775
System-theoretical method for dynamic on-condition monitoring of gas turbines N89-16812
Tip sensor development
[AD-A200080] N89-16824
Accuracy of various wall-correction methods for 3D subsonic wind-tunnel testing N89-16863
Some difficulties in the wind tunnel prediction of modern civil aircraft buffeting: Proposed remedies N89-16869
Requirements and capabilities in unsteady windtunnel testing N89-16878
Development of a lattice gas model for the study of combustion
[ETN-89-93612] N89-16964
Frequency estimation of radar signals using an acousto-optic spectrum analyzer as an RESM (Radar Electronic Support Measures) receiver
[AD-A200159] N89-17067
Modulation efficiency limited high frequency performance of the MODFET N89-17101
Monte Carlo investigation of hot photoexcited electron relaxation in GaAs N89-17120
Quantum transport calculation of resonant-tunneling response time N89-17125
Photocurrent modeling of modern microcircuit PN junctions
[DE88-012860] N89-17147
A model for transition by attachment line contamination and an examination of cross-flow instability in three-dimensional boundary layers N89-17153
The interaction of a fluid interface with a vortex pair
[AD-A200167] N89-17156
An analysis of the closure conditions for two-fluid models of two-phase flow
[DE89-003098] N89-17165
Modeling and Applications of Transport Phenomena in Porous Media, volume 2 --- conference
[VKI-LS-1988-01-VOL-2] N89-17167
Physical mechanisms during drying of porous media N89-17173
Modeling and applications of transport phenomena in porous media. Volume 1: Mathematical modeling of transport in porous media
[VKS-LS-1988-01-VOL-1] N89-17202
Development of a viscoplastic cyclic behavior law to allow a correct description of creep phenomena
[ONERA-RT-67/1765-RY-078-R] N89-17285
Mechanics of materials model N89-17319
Component specific modeling N89-17320
Constitutive modeling for isotrupic materials N89-17322
Anisotropic constitutive modeling for nickel base single crystal superalloy Rene N4 at 982 C N89-17324
Thermal barrier coating life-prediction model development N89-17331
A performance model for nonuniformly illuminated front-gridded concentrator cells
[DE89-001368] N89-17347

PC-1D Version 2: Enhanced numerical solar cell modeling
[DE89-000302] N89-17349
Simplified fatigue damage and crack growth calculations for wind turbines
[DE89-003132] N89-17351
Source characterization of heavy gas dispersion models for reactive chemicals, volume 1
[AD-A200121] N89-17361
Integration of experimental and modeling approaches in the unmanaged ecosystem research plan
[DE89-005230] N89-17367
Strain accumulation in the Santa Barbara Channel, 1971-1987
[NASA-CR-183402] N89-17369
A numerical modeling investigation of the effect of convective-mesoscale interactions on the sea breeze circulation N89-17377
Profile properties of undeformed first-year sea ice
[AD-A200172] N89-17388
Regenerative life support system research and concepts
[NASA-CR-184760] N89-17404
A visualization model based on the mathematics of fiber bundles
[DE89-002537] N89-17432
Global existence for symmetric discrete velocity models
[DE89-003102] N89-17438
Acoustic wave propagation by finite elements and time step integration N89-17460
A strategy for understanding noise-induced annoyance
[AD-A200125] N89-17461
Characterization and modeling of acoustic beams from ultrasonic transducers in solid or liquid media
[RF-DAVI-88-08] N89-17465
High power Ion Cyclotron Resonance Heating (ICRH) in JET
[DE89-002218] N89-17499
Model microfield calculations of radiative and transport properties of ions in strongly coupled plasmas
[DE89-001244] N89-17503
The role of presolar dust in the formation of the solar system N89-17553

MATRICES (MATHEMATICS)
Parallel Gaussian elimination of a block tridiagonal matrix using multiple microcomputers
[NASA-TP-2892] N89-17422
Finding Eigenvalues and Eigenvectors of unsymmetric matrices using a hypercube multiprocessor
[DE89-002311] N89-17455

MATRIX MATERIALS
Manufacturing thermoplastic matrix composites
[AD-A199724] N89-16922
Mechanical characterization of SiC whisker-reinforced MoSi
[DE89-003486] N89-16933
Ion assisted deposition of fiber coatings for ceramic matrix composites wth low dielectric loss tangents
[AD-A200162] N89-17005

MATRIX METHODS
Sparse matrix methods research using the CSM testbed software system
[NASA-CR-4219] N89-17441

MAXWELL EQUATION
Far field patterns and the inverse scattering problem for electromagnetic waves in an inhomogeneous medium
[AD-A200223] N89-17070
Modeling the propagation of long intense microwave pulses in mixtures of air and SF6
[DE89-004787] N89-17076

MEASURING INSTRUMENTS
Accurate drag estimation using a single component drag model technique N89-16856
Thermophysical property measurements in fluid mixtures
[DE89-003281] N89-16961
A non-contact picosecond prober for integrated circuit testing N89-17081
Fast GaAs photoconductive detectors with high sensitivity integrated in coplanar systems onto GaAs substrates N89-17105

MECHANICAL DRIVES
Development of kinematic equations and determination of workspace of a 6 DOF end-effector with closed-kinematic chain mechanism
[NASA-CR-183241] N89-17444

MECHANICAL ENGINEERING
The design and development of transonic multistage compressors N89-16834
Mechanical design of a RF electron gun
[DE89-004890] N89-16895

MECHANICAL PROPERTIES
Qualification tests of preimpregnated carbon epoxy T800H/DA 0506 from Structil. Test report M6-570500
[REPT-M6-570500] N89-16934
Microstructure of high-temperature ceramics N89-16993
Mechanistic studies of pressure-assisted superplasticity of structural ceramics
[AD-A200202] N89-17006
Profile properties of undeformed first-year sea ice
[AD-A200172] N89-17388

MELTING
Subselenean tunneler melting head design: A preliminary study
[NASA-CR-184750] N89-17058

MEMBRANES
Properties and performance of polyamide membranes N89-16991
Synthesis and analysis of novel polymers with potential for providing both high permselectivity and permeability in gas separation applications
[DE89-004325] N89-17014

MEMORY
The role of short-term memory in operator workload
[AD-A200252] N89-17401

MENTAL PERFORMANCE
The role of short-term memory in operator workload
[AD-A200252] N89-17401

MERCURY CADMIUM TELLURIDES
Analysis of Cd0.21Hg0.79Te quenched in 10(-4) g N89-17029

MESOSCALE PHENOMENA
A numerical modeling investigation of the effect of convective-mesoscale interactions on the sea breeze circulation N89-17377

METAL BONDING
Fatigue behavior of shrink-bonded shaft-hub steel assemblies N89-17281

METAL FATIGUE
Effect of fretting on fatigue strength of titanium alloys
[ESDU-88027] N89-16981
Importance of sensitivity and reliability of NDI techniques on damage tolerance based life prediction of turbine discs N89-17257
The effects of strain induced softening on the load carrying capability of components N89-17264
Papers of the 5th LBF Colloquium
[LBF-TB-180] N89-17272
Low-cycle fatigue behavior of cyclic hardening and softening steels under multiaxial elastic-plastic loading conditions with constant and variable amplitudes N89-17280
Fatigue behavior of shrink-bonded shaft-hub steel assemblies N89-17281
Fretting corrosion fatigue N89-17282
Constitutive modelling of single crystal and directionally solidified superalloys N89-17325

METAL FILMS
Glancing angle EXAFS studies of Cu-Al thin film interfaces
[DE89-003614] N89-16983
Femtosecond nonequilibrium electronic heat transport in thin gold films N89-17122

METAL HYDRIDES
Kinetics of the isothermal decomposition of lanthanum nickel hydride
[DE89-002905] N89-16966

METAL IONS
Electronic interactions of electrons, photons, and atoms with material surfaces
[AD-A199626] N89-17469

METAL MATRIX COMPOSITES
A multiaxial strength criterion for composites
[AD-A199610] N89-16920
A continuum deformation theory for metal-matrix composites at high temperature N89-17323
Finite element implementation of viscoplastic models N89-17328

METAL POWDER
Combustibility of titanium powders
[NASA-TT-20455] N89-16967

METAL SHELLS
Considerations for designers of cases for small solid propellant rocket motors N89-16911

METAL SURFACES
Studies of metal/carbon surface chemistry
[DE88-011264] N89-16960
Molecular spectroscopy at corrugated metal surfaces
[AD-A200124] N89-16973
Selectivity of the reactions of oxygenates on transition metal surfaces
[DE89-003691] N89-16985
Structure and properties of polymer interphases
[AD-A200238] N89-17008

METAL-GAS SYSTEMS
Hydrogen diffusion in tantalum
[DE88-704073] N89-16968

METALS
Electronic behavior of highly correlated metals
[DE89-002492] N89-16971
Effect of finite size on magnetoresistance
[AD-A200267] N89-16974
Numerical analysis of the effects of void growth and crack tip opening on ductile fracture N89-17265
Compositional changes during ion bombardment
[DE89-003974] N89-17481

METEOROIDS
Meteorites and lunar samples as space probes --- Indian/German space cooperation N89-16885

METEOROLOGICAL PARAMETERS
Measurements of micrometeorological parameters for testing large scale models
[NASA-CR-184766] N89-17384

METEOROLOGY
Applications of digital image processing to ongoing research in complex terrain meteorology
[DE89-001749] N89-17375

METHYL ALCOHOL
Conversion of natural gas to methanol
[DE89-001088] N89-16958
Results from the Federal Methanol Fleet
[DE88-015291] N89-17016

METHYLHYDRAZINE
Material compatability with threshold limit value levels of monomethyl hydrazine
[AD-A200294] N89-17362

MICROBURSTS (METEOROLOGY)
Piloted-simulation evaluation of escape guidance for microburst wind shear encounters
[NASA-TP-2886] N89-16820

MICROCOMPUTERS
Flow visualization by the PISTIL procedure (presentation of wake images by local computer processing). Test report 876/S-5 --- wake image representation by local computer treatment (PISTIL)
[REPT-876/S-5] N89-17203
An abstract interactive graphics interface for the IBM/PC and Macintosh
[AD-A200427] N89-17411
Parallel Gaussian elimination of a block tridiagonal matrix using multiple microcomputers
[NASA-TP-2892] N89-17422

MICROELECTRONICS
The behavior of microdisk and microring electrodes. Mass transport to the disk in the unsteady state: Chronopotentiometry
[AD-A200421] N89-16953
The behavior of microdisk and microring electrodes. Mass transport to the disk in the unsteady state: Coupled chemical reactions
[AD-A200422] N89-16954
Photocurrent modeling of modern microcircuit PN junctions
[DE88-012860] N89-17147

MICROGRAVITY APPLICATIONS
Microgravity science and applications bibliography, 1988 revision
[NASA-TM-4098] N89-17045

MICROPROCESSORS
A microprocessor-based, solar cell parameter measurement system
[AD-A200227] N89-17348

MICROSTRIP TRANSMISSION LINES
Characteristics of shielded microstrip lines on GaAs-Si at millimeter-wave frequencies N89-17102
Investigation of photoconductive picosecond microstripline switches on self-implanted Silicon On Sapphire (SOS) N89-17104

MICROSTRUCTURE
Investigation of microstructural factors that cause low fracture toughness in silicon carbide whisker/Al alloy composites
[AD-A200147] N89-16925
Microanalytical characterization of wear damage in an alumina-silicon carbide whisker composite
[DE89-003149] N89-16932
Gas jet deposition of multicomponent ultrafine microstructures
[AD-A200101] N89-16946
Processing of 2090 aluminum alloy for superplasticity
[AD-A200425] N89-16975
Tribology of amorphous alloys formed with ion beams
[DE89-003274] N89-16982
Fracture mode of metals in heavy electric fields
[DE88-704818] N89-16987
Microstructure of high-temperature ceramics N89-16993
Microstructural examination of core-programme material N89-17289
Suggested plastic-replica method N89-17293

Studies of NiO metal interfaces
[DE89-003634] N89-17529
Phases and microstructures of carbon-implanted niobium
[DE89-004017] N89-17534

MICROWAVE ANTENNAS
Millimeter wave generation using Josephson junction arrays
[AD-A200259] N89-17524

MICROWAVE CIRCUITS
The potential impact of MMICs on future satellite communications
[NASA-CR-182227] N89-17078
The potential impact of MMICs on future satellite communications: Executive summary
[NASA-CR-182227-EXEC-SUMM] N89-17079

MICROWAVE EMISSION
Propagation effects handbook for satellite systems design. A summary of propagation impairments on 10 to 100 GHz satellite links with techniques for system design
[NASA-RP-1082(04)] N89-17060

MICROWAVE EQUIPMENT
Effects of irregular sea surface and evaporation duct on radar detection performance
[AD-A200114] N89-17066
Radar and EW applications of multi-gigahertz optical components and systems N89-17131

MICROWAVE PHOTOGRAPHY
Indian activities in remote sensing applications: Microwave remote sensing N89-16886

MICROWAVE RADIOMETERS
Status of Sabrex N89-16890

MICROWAVES
Instrumentation for the characterization of the microwave properties at 18, 35 and 94 GHz
[AD-A199741] N89-17064
Modeling the propagation of long intense microwave pulses in mixtures of air and SF6
[DE89-004787] N89-17076
Picosecond sampling of integrated circuits N89-17082
A simple technique to generate or gate microwave pulses with picosecond speeds N89-17099
Microwave and millimeter-wave resonant tunneling diodes N89-17124
A new optoelectronic CW microwave source N89-17133

MIDDLE ATMOSPHERE
Middle Atmosphere Program: Handbook for MAP, volume 26
[NASA-CR-183350] N89-17368

MIE SCATTERING
Scattering power of seed materials: Mie scattering calculations N89-17181
Optical and infrared studies of cometary dust N89-17550

MILITARY HELICOPTERS
Gas path analysis and engine performance monitoring in a Chinook helicopter N89-16802

MILITARY OPERATIONS
Engine Condition Monitoring: Technology and Experience
[AGARD-CP-448] N89-16780
A joint study on the computerisation of in-field aero engine vibration diagnosis N89-16808

MILITARY TECHNOLOGY
Operational requirements for engine condition monitoring from the EFA viewpoint N89-16781
An overview of US Navy engine monitoring system programs and user experience N89-16782
Engine usage condition and maintenance management systems in the UK armed forces N89-16783
Canadian forces aircraft condition/health monitoring: Policy, plans and experience N89-16784

MILLIMETER WAVES
Millimeter-wave integrated circuits N89-17089
Picosecond photoconductive transceivers N89-17092
Characteristics of shielded microstrip lines on GaAs-Si at millimeter-wave frequencies N89-17102
Microwave and millimeter-wave resonant tunneling diodes N89-17124
Picosecond response of an optically controlled millimeter wave phase shifter N89-17135
Millimeter wave generation using Josephson junction arrays
[AD-A200259] N89-17524

MINICOMPUTERS
Military engine condition monitoring systems: The UK experience N89-16797

MINORITY CARRIERS
Picosecond optical autocorrelation experiments on fast photodetectors N89-17117

MIRRORS
Effects of depolarization obtained by specular reflection on metallic mirrors: Applications to laser telecommunication and to Earth observation
[CNES-CT/DRT/TIT/IO-87/150] N89-17494

MISSILE CONTROL
Accuracy of lift and center-of-thrust measurements at missile control surfaces N89-16875

MISSILE DETECTION
Report of the Defense Science Board Task Force Subgroup on Strategic Air Defense (SDI Milestone Panel)
[AD-A200164] N89-17452

MISSILES
Turbulence effects on the high angle of attack aerodynamics of a vertically launched missile
[AD-A200418] N89-16727

MIXING
Hardware for studying the demixing of aqueous polymer two-phase systems in low gravity N89-17030
Mix experiments with the NOVA laser
[DE89-004775] N89-17228

MIXTURES
Thermophysical property measurements in fluid mixtures
[DE89-003281] N89-16961

MOBILITY
HERMIES-3: A step toward autonomous mobility, manipulation and perception
[DE89-004932] N89-17249

MODAL RESPONSE
Modal control of an oblique wing aircraft
[NASA-TP-2898] N89-16845
Active vibration suppression for robotic manipulators N89-17241
Papers of the 5th LBF Colloquium
[LBF-TB-180] N89-17272
Modal analysis methods for the reduction of system-conditioned loads N89-17275
Initial structural response measurements for the Sandia 34-meter VAWT test bed
[DE89-003133] N89-17352

MODELS
Capacity of frequency-hop spread-spectrum multiple-access communication systems
[AD-A200616] N89-17073
Unsteady flow about porous cambered plates
[AD-A200282] N89-17160
In-situ surface during laser-controlled chemical processing of surfaces
[AD-A200206] N89-17223
Stochastic modeling of crack initiation and short-crack growth under creep and creep-fatigue conditions
[NASA-TM-101358] N89-17286
Accurate modeling of parallel scientific computations
[NASA-CR-181756] N89-17418

MODFETS
High performance quarter-micron-gate MODFETs N89-17091
Modulation efficiency limited high frequency performance of the MODFET N89-17101
Non-stationary transport in MODFETs and heterojunction devices N89-17119

MODULATION TRANSFER FUNCTION
Precision transfer function measurements of integrated optical modulators
[DE89-004021] N89-17492

MODULATORS
Optical modulation above 20 GHz using a waveguide electro-optic switch N89-17134
An optical modulator/switch using the reflection from a translated depletion edge
[DE89-001380] N89-17490
Precision transfer function measurements of integrated optical modulators
[DE89-004021] N89-17492

MOISTURE
Adsorption of phosphorus acids on alumina
[AD-A200548] N89-16957

MOISTURE CONTENT
Synthesis and analysis of epichlorohydrin based wet strength resins for paper N89-16919
Hygrothermal deformations of laminated composite shells N89-16924
Electrical properties of atmospheric moist air: A systematic, experimental study
[AD-A199599] N89-17370

MOLECULAR BEAM EPITAXY
Molecular Beam Epitaxy (MBE) for high speed devices N89-17085

MOLECULAR BEAMS
Laser studies of the SiH radical/surface interaction during deposition of a thin film
[DE89-003902] N89-17232

MOLECULAR CLOUDS
Photoabsorption and photodissociation of molecules important in the interstellar medium
[NASA-CR-184771] N89-16965

MOLECULAR COLLISIONS
The kinetics and dynamics of iodine monofluoride formation in gas-phase collisions
[AD-A199622] N89-16939

MOLECULAR EXCITATION
The effects of hydrazines on neuronal excitability
[AD-A200199] N89-17395

MOLECULAR RELAXATION
Monte Carlo investigation of hot photoexcited electron relaxation in GaAs N89-17120

MOLECULAR SPECTROSCOPY
Molecular spectroscopy at corrugated metal surfaces
[AD-A200124] N89-16973

MOLECULAR STRUCTURE
The 15N CP/MAS NMR of aramids: A tool for characterization of the morphology of high modulus fibers for composites
[AD-A199656] N89-16921
Ion content of moist atmospheric air and the molecular structure of water vapor thus inferred
[AD-A199732] N89-16940
Statistical mechanics of polymer systems
[DE89-002012] N89-17002
Structure and properties of polymer interphases
[AD-A200238] N89-17008
Synthesis and analysis of novel polymers with potential for providing both high permselectivity and permeability in gas separation applications
[DE89-004325] N89-17014

MOLECULES
Gas jet deposition of multicomponent ultrafine microstructures
[AD-A200101] N89-16946
Molecular spectroscopy at corrugated metal surfaces
[AD-A200124] N89-16973
Investigations of the motion of discrete-velocity gases by cellular automata
[AD-A200221] N89-17158

MOLYBDENUM
The effects of strain induced softening on the load carrying capability of components N89-17264

MOLYBDENUM ALLOYS
Microstructural effects in abrasive wear
[DE89-003032] N89-16976

MOLYBDENUM COMPOUNDS
Mechanical characterization of SiC whisker-reinforced MoSi
[DE89-003486] N89-16933

MOMENT DISTRIBUTION
Expriments on the DFVLR-F4 wing body configuration in several European windtunnels N89-16848

MOMENTS
The visual shape and multipole moments of the sun N89-17561

MOMENTUM TRANSFER
The electronic structure and the state of compositional order in metallic alloys
[DE89-003147] N89-16977
The electron-water vapor (H2O) collision cross sections
[AD-A200187] N89-17472

MONITORS
High-precision gravity network to monitor temporal variations in gravity across Yucca Mountain, Nevada
[DE89-005023] N89-17373

MONOPOLES
Monopoles and magnetic fields in the inflationary universe
[DE88-755532] N89-17557

MONTE CARLO METHOD
Statistical mechanics of polymer systems
[DE89-002012] N89-17002
Monte Carlo investigation of hot photoexcited electron relaxation in GaAs N89-17120
Investigations of the motion of discrete-velocity gases by cellular automata
[AD-A200221] N89-17158
Monte Carlo studies of nonlinear electron transport in 3-5 semiconductors
[AD-A199700] N89-17516
Monte Carlo calculation of electron multiple scattering in thin foils
[AD-A199872] N89-17517
Lattice gauge theories and Monte Carlo algorithms
[DE89-003589] N89-17539

MORPHOLOGY
Properties and performance of polyamide membranes N89-16991
Ion assisted deposition of fiber coatings for ceramic matrix composites wth low dielectric loss tangents
[AD-A200162] N89-17005

Fractal and spherulitic morphology of silicon nitride crystallized from amorphous films
[AD-A200158] N89-17522
Studies of NiO metal interfaces
[DE89-003634] N89-17529

MOTION SIMULATION
Investigations of the motion of discrete-velocity gases by cellular automata
[AD-A200221] N89-17158

MOTOR VEHICLES
Engineering ceramics in West Germany N89-16999

MOUNTAINS
High-precision gravity network to monitor temporal variations in gravity across Yucca Mountain, Nevada
[DE89-005023] N89-17373
New England mountain icing climatology
[AD-A200287] N89-17381

MRCA AIRCRAFT
Jaguar/Tornado intake design N89-16743
Intake-airframe integration N89-16744

MSM (SEMICONDUCTORS)
MESFET compatible IMSM detectors N89-17116

MULTIPHASE FLOW
Multiphase flow in porous media N89-17169

MULTIPLEXING
A microprocessor-based, solar cell parameter measurement system
[AD-A200227] N89-17348

MULTIPROCESSING (COMPUTERS)
IEEE P1596, a scalable coherent interface for gigabyte/sec multiprocessor applications
[DE89-002813] N89-17405
Finding Eigenvalues and Eigenvectors of unsymmetric matrices using a distributed-memory multiprocessor
[DE89-004731] N89-17416
Parallel Gaussian elimination of a block tridiagonal matrix using multiple microcomputers
[NASA-TP-2892] N89-17422

MULTISPECTRAL BAND SCANNERS
German spaceborne remote sensing activities N89-16887
Accuracy assessment, using stratified plurality sampling, of portions of a LANDSAT classification of the Arctic National Wildlife Refuge Coastal Plain
[NASA-TM-101042] N89-17339

MULTISTATIC RADAR
Instrumentation for the characterization of the microwave properties at 18, 35 and 94 GHz
[AD-A199741] N89-17064

MULTIVARIATE STATISTICAL ANALYSIS
Multiparametric research of early indicators of vascular risk in flying personnel
[ETN-89-93613] N89-17398

MUSCULAR TONUS
The effects of microgravity and linear accelerations on cutaneomuscular reflexes in human lower limb musculature N89-17034

N

NACELLES
Lift and longitudinal forces on propeller/nacelle/wing/flap systems
[ESDU-88031] N89-16736

NARROWBAND
Vector space approach to narrowband interference excision
[AD-A199703] N89-17063
Extensions to the matrix pencil approach for direction finding
[AD-A200112] N89-17449

NASA SPACE PROGRAMS
NASA photovoltaic research and technology
[NASA-TM-101422] N89-16917
NASA's Zero-g aircraft operations N89-17026

NATURAL GAS
Conversion of natural gas to methanol
[DE89-001088] N89-16958

NAVIER-STOKES EQUATION
Verification of a Navier-Stokes code for solving the hypersonic blunt body problem
[DE89-003169] N89-16737
Propulsive-jet flow field analysis using the three-dimensional Navier-Stokes equations
[NASA-CR-177508] N89-16764
Accuracy problems in wind tunnels during transport aircraft development N89-16877
Development of generalized block correction procedures for the solution of discretized Navier-Stokes equations N89-17307

NEGATIVE IONS
A high-intensity plasma sputter heavy negative ion source
[DE89-003113] N89-17480

NEON
Ne-like ion X-ray laser experiments in plasmas produced by 0.53 microns and 0.35 microns laser light
[DE89-004827] N89-17233

NETWORK ANALYSIS
The design, analysis, and implementation of a fully distributed local area network for integrated voice and data communications N89-17059
A formal language model for local area network configuration N89-17544

NEUMANN PROBLEM
The behavior of microdisks and micoring electrodes. Prediction of the amperometric response of microdisks and of the steady state for CE and EC Catalytic reactions by application of Neumann's integral theorem
[AD-A200415] N89-16952

NEURONS
The effects of hydrazines on neuronal excitability
[AD-A200199] N89-17395

NEUROPHYSIOLOGY
The effects of hydrazines on neuronal excitability
[AD-A200199] N89-17395

NEUTRAL ATOMS
Electronic interactions of electrons, photons, and atoms with material surfaces
[AD-A199626] N89-17469
A neutral hydrogen survey of galaxies in the Cancer region N89-17552

NEUTRAL GASES
Role of charge exchange process in forming of ion charge and energy states in multicomponent laser plasma produced from gas-content solids
[DE88-704828] N89-17511
Origin and dynamics of expanding neutral hydrogen supershells
[DE88-704372] N89-17555

NEUTRAL PARTICLES
Electronic interactions of electrons, photons, and atoms with material surfaces
[AD-A199626] N89-17469

NEVADA
High-precision gravity network to monitor temporal variations in gravity across Yucca Mountain, Nevada
[DE89-005023] N89-17373

NEW ENGLAND (US)
New England mountain icing climatology
[AD-A200287] N89-17381

NEWTONIAN FLUIDS
A computational method for three dimensional, internal viscous flows with separation and secondary flow patterns N89-17164

NICKEL ALLOYS
Procurement and screening test data for advanced austenitic alloys for 650 C steam service, part 2
[DE89-001331] N89-16979
Oxidation of Ni3Al below 850 C and its effect on fracture behavior
[DE89-002232] N89-16988
Experimental evidence for positron trapping at dislocations in Ni3Al alloys
[DE89-004520] N89-16989
Limitations at high temperatures of present day engineering materials N89-16996
Anisotropic constitutive modeling for nickel base single crystal superalloy Rene N4 at 982 C N89-17324
Constitutive modelling of single crystal and directionally solidified superalloys N89-17325
New Al-Ni-Ge contacts on GaAs: Their structure and electrical properties
[DE89-002918] N89-17526

NICKEL COMPOUNDS
Kinetics of the isothermal decomposition of lanthanum nickel hydride
[DE89-002905] N89-16966

NICKEL HYDROGEN BATTERIES
Nickel hydrogen battery development
[DE89-001063] N89-17143

NIGHT
Applications of digital image processing to ongoing research in complex terrain meteorology
[DE89-001749] N89-17375

NIOBIUM
Design and analysis report for the flight weight 20-inch Columbium secondary nozzle for the RL10 engine
[NASA-CR-179612] N89-16918
Phases and microstructures of carbon-implanted niobium
[DE89-004017] N89-17534

NITRO COMPOUNDS
Prediction and synthesis efforts at Los Alamos
[DE89-003605] N89-17018

NITROGEN PLASMA
An active nitrogen plasma atom reservoir for laser-induced ionization spectrometry
[AD-A200544] N89-17224

NOBLE METALS
Studies of NiO metal interfaces
[DE89-003634] N89-17529

NOCTILUCENT CLOUDS
Middle Atmosphere Program: Handbook for MAP, volume 26
[NASA-CR-183350] N89-17368

NOISE MEASUREMENT
GPS (Global Positioning System) user equipment evaluation techniques using a rotor mounted antenna
[AD-A200515] N89-16770

NOISE POLLUTION
A strategy for understanding noise-induced annoyance
[AD-A200125] N89-17461

NOISE PREDICTION
One/f noise in silicon devices
[ISBN-90-9002080-2] N89-17150

NOISE REDUCTION
NASA powered lift facility internally generated noise and its transmission to the acoustic far field
[NASA-CR-182217] N89-16882
Picosecond sampling of integrated circuits N89-17082
MESFET compatible IMSM detectors N89-17116
Jet-by-jet shielding of noise
[ESDU-88023] N89-17463

NOISE SPECTRA
One/f noise in silicon devices
[ISBN-90-9002080-2] N89-17150

NONDESTRUCTIVE TESTS
NDE methods for high-temperature materials and environments
[DE89-005195] N89-17234
AGARD/SMP Review: Damage Tolerance for Engine Structures. 1: Non-Destructive Evaluation
[AGARD-R-768] N89-17253
The impact of engineering assumptions on NDE requirements N89-17254
Review of existing NDT technologies and their capabilities N89-17255
Relationships of nondestructive evaluation needs and component design N89-17256
Importance of sensitivity and reliability of NDI techniques on damage tolerance based life prediction of turbine discs N89-17257
Short term developments in non-destructive evaluation applicable to turbine engine parts N89-17258
Long term possibilities for nondestructive evaluation for US Navy aircraft N89-17259
Need for common AGARD approach and actions N89-17260
State-of-the-art in non-destructive evaluation of turbine engine parts N89-17261

NONEQUILIBRIUM FLOW
On a wide range exclusion process in random medium with local jump intensity
[AD-A200510] N89-17450

NONEQUILIBRIUM IONIZATION
Monte Carlo studies of nonlinear electron transport in 3-5 semiconductors
[AD-A199700] N89-17516

NONLINEAR EVOLUTION EQUATIONS
On a wide range exclusion process in random medium with local jump intensity
[AD-A200510] N89-17450

NONLINEAR OPTICS
Electrical pulse compression by traveling-wave photoconductivity N89-17137
Nonlinear optics with broad-band lasers
[DE89-002728] N89-17216
Fresnel coefficients for a phase conjugator
[AD-A200123] N89-17487

NONLINEAR SYSTEMS
Nonlinear dynamic responses of composite rotor blades
[AD-A200145] N89-16774
A model of the effect of sparing and repair turnaround time of the inertial navigation system on aircraft readiness for the F/A-18
[AD-A200317] N89-16777
PBT,PBO-based hybrid polymers with nonlinear optical properties or high electrical conductivity
[AD-A200226] N89-17007
The behavior of shells made of composites during the dynamic application of axian compression
[AD-A200244] N89-17266

NONLINEARITY
PBT,PBO-based hybrid polymers with nonlinear optical properties or high electrical conductivity
[AD-A200226] N89-17007
Equivalent linearization for fatigue life estimates of a nonlinear structure
[NASA-TM-101536] N89-17467

NONNEWTONIAN FLUIDS
Approximation of viscoelastic stresses from Newtonian turbulent kinematics
[AD-A200188] N89-17157
NONUNIFORMITY
Behavior in normal and reduced gravity of an enclosed liquid/gas system with nonuniform heating from above
[NASA-TM-101471] N89-17046
NOTCH TESTS
The effects of strain induced softening on the load carrying capability of components N89-17264
Approximate stress-intensity factors for a surface crack and through crack at a semi-circular notch N89-17294
NOVA LASER SYSTEM
Recent results from the Nova experiments program
[DE89-002901] N89-17220
Mix experiments with the NOVA laser
[DE89-004775] N89-17228
NOZZLE DESIGN
Impact of nozzle design constraints on test section flow quality N89-16860
Engine simulator tests: Comparison of calibration and wind tunnel results N89-16871
Advances in solid rocket nozzle design and analysis technology in the United States since 1970 N89-16907
Design and analysis of solid rocket motor nozzle N89-16906
NOZZLE FLOW
Impact of nozzle design constraints on test section flow quality N89-16860
NOZZLE GEOMETRY
Impact of nozzle design constraints on test section flow quality N89-16860
NOZZLE THRUST COEFFICIENTS
Design and analysis of solid rocket motor nozzle N89-16908
NOZZLES
Design and analysis report for the flight weight 20-inch Columbium secondary nozzle for the RL10 engine
[NASA-CR-179612] N89-16918
NUCLEAR EXPLOSIONS
Explosion of integrated optic devices used in new generation systems
[DE89-004012] N89-17497
NUCLEAR FUELS
Safety comparison of fusion fuel cycles
[DE89-005200] N89-17512
NUCLEAR FUSION
Induction-linac based free-electron laser amplifier for fusion applications
[DE89-001923] N89-17217
Safety comparison of fusion fuel cycles
[DE89-005200] N89-17512
NUCLEAR MAGNETIC RESONANCE
The 15N CP/MAS NMR of aramids: A tool for characterization of the morphology of high modulus fibers for composites
[AD-A199656] N89-16921
NUCLEAR POWER PLANTS
Assessment of nonintrusive methods for monitoring the operational readiness of solenoid-operated valves
[DE89-002330] N89-17244
Small reactors for low-temperature nuclear heat applications
[DE88-704336] N89-17484
NUCLEATION
Protein crystal nucleation kinetics using relative light-scattering techniques: Center director's discretionary fund
[NASA-TM-100348] N89-17535
NUMERICAL ANALYSIS
Numerical solution of flow fields around Delta wings using Euler equations method
[NAL-TM-FM-8701] N89-16757
Accuracy of lift and center-of-thrust measurements at missile control surfaces N89-16875
A bibliography on parallel and vector numerical algorithms
[DE89-005693] N89-17421
Development of finite local perturbations of electrical conductivity in the flow of a weakly-conducting gas when a magnetic field is present
[AD-A200243] N89-17458
NUMERICAL CONTROL
Computer control of gas metal arc welding
[DE89-005188] N89-17252
NUMERICAL INTEGRATION
Acoustic wave propagation by finite elements and time step integration N89-17460

O

OBLIQUE SHOCK WAVES
Numerical solutions to three-dimensional shock wave/vortex interaction at hypersonic speeds N89-16729
OBLIQUE WINGS
Modal control of an oblique wing aircraft
[NASA-TP-2898] N89-16845
OCEAN CURRENTS
Evaluation of satellite-tracked surface drifting buoys for simulating the movement of spilled oil in the marine environment. Volume 1: Executive summary
[PB88-226048] N89-17357
Evaluation of satellite-tracked surface drifting buoys for simulating the movement of spilled oil in the marine environment, volume 2
[PB88-226055] N89-17358
OCEAN SURFACE
Effects of irregular sea surface and evaporation duct on radar detection performance
[AD-A200114] N89-17066
OCEANOGRAPHIC PARAMETERS
Objective analysis of the Gulf Stream thermal front: Methods and accuracy
[AD-A199717] N89-17387
OCEANS
First production of potable water by OTEC (Ocean Thermal Energy Conversion) and its potential applications
[DE89-003630] N89-17353
OGIVES
An experimental investigation of the aerodynamic characteristics of slanted base ogive cylinders using magnetic suspension technology
[NASA-CR-184624] N89-16758
OIL SLICKS
Evaluation of satellite-tracked surface drifting buoys for simulating the movement of spilled oil in the marine environment. Volume 1: Executive summary
[PB88-226048] N89-17357
Evaluation of satellite-tracked surface drifting buoys for simulating the movement of spilled oil in the marine environment, volume 2
[PB88-226055] N89-17358
ON-LINE SYSTEMS
On-line spectrum loading accuracy verification N89-17292
Optical fiber science and technology: Novel fibers and fiber sensors
[AD-A200311] N89-17489
ONBOARD EQUIPMENT
Satellite-ground dating and synchronization technique
[CNES-CT/DRT/TIT/TB-040-T] N89-16892
OPENINGS
Investigation of collisional effects in the plasma erosion opening switch
[AD-A200319] N89-17507
OPERATIONS RESEARCH
An algorithm for calculating the area of overlap of an ellipse and a convex polygon
[AD-A199654] N89-17408
OPTICAL COMMUNICATION
MESFET compatible IMSM detectors N89-17116
An investigation of the spectral characteristics of a commercially available semiconductor laser N89-17213
Laser communication test system
[AD-A199612] N89-17215
Effects of depolarization obtained by specular reflection on metallic mirrors: Applications to laser telecommunication and to Earth observation
[CNES-CT/DRT/TIT/IO-87/150] N89-17494
Optical communication. Four quadrant avalanche detector. Modeling, theoretical results and comparison with experimental values
[CNES-CT/DRT/TIT/IO-87/086] N89-17495
Non return to zero (NRZ) clock recovery breadboard for 200 MB/S optical intersatellite link
[CNES-CT/DRT/TIT/TR-87/024] N89-17496
OPTICAL EQUIPMENT
Photonics: Maintaining competitiveness in the information era
[AD-A200230] N89-17473
Review of precision surface generating processes and their potential application to the fabrication of large optical components
[DE89-001712] N89-17486
An optical modulator/switch using the reflection from a translated depletion edge
[DE89-001380] N89-17490
Explosion of integrated optic devices used in new generation systems
[DE89-004012] N89-17497
OPTICAL FIBERS
An investigation of the spectral characteristics of a commercially available semiconductor laser N89-17213
Optical fiber science and technology: Novel fibers and fiber sensors
[AD-A200311] N89-17489
OPTICAL MEMORY (DATA STORAGE)
Optical storage: Financial management and budget applications
[DE89-004916] N89-17546
OPTICAL PROPERTIES
Photodeflection and photoconductivity studies in ceramics
[DE89-002186] N89-17003
PBT,PBO-based hybrid polymers with nonlinear optical properties or high electrical conductivity
[AD-A200226] N89-17007
OPTICAL PUMPING
Ne-like ion X-ray laser experiments in plasmas produced by 0.53 microns and 0.35 microns laser light
[DE89-004827] N89-17233
OPTICAL RADAR
German spaceborne remote sensing activities N89-16887
High speed opto-isolator for radar applications N89-17110
OPTICAL REFLECTION
Fresnel coefficients for a phase conjugator
[AD-A200123] N89-17487
An optical modulator/switch using the reflection from a translated depletion edge
[DE89-001380] N89-17490
OPTICAL TRANSFER FUNCTION
Optical processing --- particle image displacement velocimetry N89-17189
OPTICAL WAVEGUIDES
Optical modulation above 20 GHz using a waveguide electro-optic switch N89-17134
OPTIMIZATION
Aeroelastic optimization of a helicopter rotor N89-16778
An indirect method for numerical optimization using the Kreisselmeir-Steinhauser function
[NASA-CR-4220] N89-16779
Field enhancement of UHF-VHF aircraft antennas
[AD-A200180] N89-17069
Finite element analysis for the evaluation and optimization of fiber reinforced composite structural components N89-17279
ORBITAL MECHANICS
User and technical documentation
[NASA-CR-172087] N89-16893
ORBITAL SERVICING
Modifications to the NASA Ames Space Station Proximity Operations (PROX OPS) Simulator
[NASA-CR-177510] N89-16896
ORGANIC COMPOUNDS
Vapour pressures and critical points of liquids. Organic oxygen compounds
[ESDU-88017] N89-16963
ORGANOMETALLIC POLYMERS
Ceramics derived from organo-metallic polymers
[AD-A200118] N89-17004
OSCILLATIONS
FRP (Fiber Reinforced Plastics) cutting technology reported N89-17048
Low frequency oscillations in total ozone measurements
[NASA-CR-184759] N89-17385
OSCILLOSCOPES
Comparison of sampling oscilloscopes with less than 35 ps transition durations N89-17108
OUTLET FLOW
Exit angle rules in supersonic cascades N89-16828
OXIDATION
Light-off temperature determination of oxidation catalyst using Fourier transform infrared technique
[AD-A199596] N89-16938
Oxidation of Ni3Al below 850 C and its effect on fracture behavior
[DE89-002232] N89-16988
OXIDES
Processing of strong flux trapping high T(subc) oxide superconductors: Center director's discretionary fund
[NASA-TM-100350] N89-17530
OXYGEN
Development and application of oxygen flow tagging for velocity measurements and flow visualization in turbulent three-dimensional supersonic flows
[AD-A200119] N89-16725
Reaction dynamics of H + O2 at 1.6 eV collision energy
[NASA-CR-183182] N89-17483
Oxygen and copper valencies in oxygen-doped superconducting La2CuO(sub 4.13)
[DE89-003265] N89-17533

OXYGEN COMPOUNDS
Vapour pressures and critical points of liquids. Organic oxygen compounds
[ESDU-88017] N89-16963
OZONE
Absolute absorption cross section measurements of ozone and the temperature dependence at four reference wavelengths leading to renormalization of the cross section between 240 and 350 nm
[AD-A199737] N89-16942
Low frequency oscillations in total ozone measurements
[NASA-CR-184759] N89-17385
OZONE DEPLETION
A feasibility study of methods for stopping the depletion of ozone over Antarctica
[NASA-CR-184583] N89-17364

P

P-N JUNCTIONS
Photocurrent modeling of modern microcircuit PN junctions
[DE88-012860] N89-17147
PACIFIC OCEAN
ONR (Office of Naval Research) tropical cyclone motion research initiative: Mid-year review, discussion and working group reports
[AD-A200286] N89-17380
PANEL METHOD (FLUID DYNAMICS)
Development of a panel method for modeling configurations with unsteady component motions, phase 1
[AD-A200255] N89-16775
PANELS
A modified VAPEPS method for predicting vibroacoustic response of unreinforced mass loaded honeycomb panels
[NASA-TM-101467] N89-16905
Wrinkling of sandwich panel face plates (isotropic face plates on orthotropic cores, in-plane loading or bending)
[ESDU-88032] N89-16931
PAPERS
Synthesis and analysis of epichlorohydrin based wet strength resins for paper N89-16919
PARABOLIC FLIGHT
Workshop on Microgravity Experimentation in Aircraft and Rockets
[NRCC-29151] N89-17019
Parabolic flight: A useful test bed N89-17020
Canadian microgravity research using aircraft and rockets N89-17023
NASA's Zero-g aircraft operations N89-17026
Life science experiments during parabolic flight: The McGill experience N89-17027
System engineering and logistics for KC-135 experimentation N89-17033
Ocular torsion in the weightlessness of parabolic flight N89-17035
Preliminary results: Flight testing the NAE T-33 microgravity facility N89-17041
Development of a portable physiological monitoring system for the KC-135: The S.F.U. biopack N89-17044
PARACHUTE DESCENT
Study of the aerodynamic situation along the C 160 aircraft in parachuting configuration
[DAT-88-06] N89-16756
PARACHUTES
Study of the aerodynamic situation along the C 160 aircraft in parachuting configuration
[DAT-88-06] N89-16756
PARALLEL COMPUTERS
A bibliography on parallel and vector numerical algorithms
[DE89-005693] N89-17421
PARALLEL PROCESSING (COMPUTERS)
Tailoring domain decomposition to the network structure for parallel processing of fluid dynamics
[DE89-005501] N89-17206
Performance of a second generation hypercube
[DE89-005674] N89-17407
A multistage linear array assignment problem
[NASA-CR-181748] N89-17417
Accurate modeling of parallel scientific computations
[NASA-CR-181756] N89-17418
Axioms for concurrent objects
[AD-A200584] N89-17435
Parallel processing of a rotating shaft simulation
[NASA-TM-101462] N89-17453
Finding Eigenvalues and Eigenvectors of unsymmetric matrices using a hypercube multiprocessor
[DE89-002311] N89-17455
PARALLEL PROGRAMMING
Parallel Gaussian elimination of a block tridiagonal matrix using multiple microcomputers
[NASA-TP-2892] N89-17422
Massive symbolic mathematical computations and their applications
[AD-A200253] N89-17434
PARAMETER IDENTIFICATION
Machine learning of parameter control doctrine for sensor and communication systems
[AD-A200096] N89-17427
PARAMETERIZATION
R-parametrization and its role in classification of linear multivariable feedback systems
[NASA-TM-101066] N89-16844
Probabilistic modeling of Particle Image Displacement Velocimetry (PIDV) experiments N89-17190
Using theoretical descriptors in structural activity relationships. Part 2: Polarizability index
[AD-A199594] N89-17389
Assessment and comparison of techniques for transforming parameters to a common metric in item response theory
[AD-A200067] N89-17433
PARTIAL DIFFERENTIAL EQUATIONS
Generation of three-dimensional body-fitted grids by solving hyperbolic and parabolic partial differential equations
[NASA-TM-101069] N89-16763
PARTICLE ACCELERATORS
A high-intensity plasma sputter heavy negative ion source
[DE89-003113] N89-17480
PARTICLE COLLISIONS
The electron-water vapor (H2O) collision cross sections
[AD-A200187] N89-17472
PARTICLE ENERGY
Electronic interactions of electrons, photons, and atoms with material surfaces
[AD-A199626] N89-17469
PARTICLE INTERACTIONS
Electronic interactions of electrons, photons, and atoms with material surfaces
[AD-A199626] N89-17469
Production and transport of convoy electrons in amorphous carbon foils
[DE89-002313] N89-17478
PARTICLE PRODUCTION
Gas jet deposition of multicomponent ultrafine microstructures
[AD-A200101] N89-16946
PARTICLE SIZE DISTRIBUTION
In-situ laser microscopy for particle sizing and tracking N89-17201
PARTICLE THEORY
Investigations in particle and field theory
[DE89-003004] N89-17538
PARTICLES
Scattering power of seed materials: Mie scattering calculations N89-17181
PASSIVITY
Device physics related to the granular nature of CuInSe2 solar cells
[DE89-000810] N89-17341
PATTERN RECOGNITION
Improving classification accuracy of radar images using a multiple-stage classifier
[AD-A200291] N89-17071
Temporal pattern recognition
[AD-A200090] N89-17426
PAULI EXCLUSION PRINCIPLE
On the experimental basis of the Pauli exclusive principle
[DE88-704366] N89-17477
PAYLOADS
Mission under SROSS program and position paper on SROSS-2 with MEOSS payload --- Indian/German space cooperation N89-16889
Autonomous payload control experiment on SROSS-3, a status review --- Indian/German space cooperation N89-16891
PENETRATION
Penetration effects of the compound vortex in gas metal-arc welding
[AD-A200585] N89-17242
PEPTIDES
Collision-induced decomposition of multiatomic ions N89-17468
PERCEPTION
Spatial reasoning in the treatment of systematic sensor errors
[DE89-003244] N89-17251
PERFORMANCE PREDICTION
Trend monitoring of a turboprop engine at low and mean power N89-16801
Wind tunnel predicted air vehicle performance: A review of lessons learned N89-16852
A performance model for nonuniformly illuminated front-gridded concentrator cells
[DE89-001368] N89-17347
Plasma performance in JET: Achievements and projections
[DE89-002219] N89-17500
PERFORMANCE TESTS
GPS (Global Positioning System) user equipment evaluation techniques using a rotor mounted antenna
[AD-A200515] N89-16770
Results from the Federal Methanol Fleet
[DE88-015291] N89-17016
A non-contact picosecond prober for integrated circuit testing N89-17081
High performance quarter-micron-gate MODFETs N89-17091
The effect of different module configurations on the radiation tolerance of multijunction solar cells
[NASA-TM-101251] N89-17356
Extravehicular activities limitations study. Volume 2: Establishment of physiological and performance criteria for EVA gloves
[NASA-CR-172099] N89-17393
Performance of a second generation hypercube
[DE89-005674] N89-17407
Plasma performance in JET: Achievements and projections
[DE89-002219] N89-17500
PERMEABILITY
Synthesis and analysis of novel polymers with potential for providing both high permselectivity and permeability in gas separation applications
[DE89-004325] N89-17014
PERT
Event-centered scheduling program: The need for PERT (Program Evaluation Review Technique) in C-141 ISO inspection management
[AD-A200094] N89-16718
PERTURBATION
Extensions to the matrix pencil approach for direction finding
[AD-A200112] N89-17449
PERTURBATION THEORY
Hierarchy of uncertainty sources in transonic wind tunnel testing N89-16851
Observations of a thunderstorm generated gust compared with solitary wave theory
[AD-A200087] N89-17379
PHARMACOLOGY
Pharmacological resetting of the circadian sleep-wake cycle
[AD-A200246] N89-17396
PHASE CHANGE MATERIALS
Preliminary study of creep thresholds and thermomechanical response in Haynes 188 at temperatures in the range 649 to 871 C N89-17327
PHASE LOCKED SYSTEMS
Nonlinear optics with broad-band lasers
[DE89-002728] N89-17216
PHASE SHIFT
Picosecond response of an optically controlled millimeter wave phase shifter N89-17135
Precise interferometric phase determination
[AD-A200186] N89-17488
PHASE TRANSFORMATIONS
The effect of chemistry modifications on the solidification behavior and weldability of Alloy 625
[DE89-001046] N89-16972
The electronic structure and the state of compositional order in metallic alloys
[DE89-003147] N89-16977
Study of structure of high-Tc superconductor Y(YV)Ba2Cu3O(sub 9-x) and its resistance sharp drop
[DE88-704104] N89-17531
Is the great attractor really a great wall
[NASA-CR-184772] N89-17540
PHONONS
Nonequilibrium phonons and disorder in Al(sub x)Ga(sub 1-x)As N89-17103
Nonlocal and quasilocal potentials in the spontaneous emission of molecular exciplexes coupled to the phonon bath of a solid matrix
[AD-A200509] N89-17476
PHOSPHORS
Pressure/temperature sensitive inorganic phosphors
[AD-A199718] N89-17000
PHOTOABSORPTION
Photoabsorption and photodissociation of molecules important in the interstellar medium
[NASA-CR-184771] N89-16965
PHOTOCHEMICAL REACTIONS
Molecular spectroscopy at corrugated metal surfaces
[AD-A200124] N89-16973

PHOTOCONDUCTIVITY
Photodeflection and photoconductivity studies in ceramics
[DE89-002186] N89-17003
Picosecond electrical pulses for VLSI electronics characterization N89-17083
Picosecond photoconductive transceivers N89-17092
Photoconductive generation of sub-picosecond electrical pulses and their measurement applications N89-17093
High speed, high repetition rate, high voltage photoconductive switching N89-17096
Generation and forming of ultrashort high voltage pulses N89-17097
Investigation of photoconductive picosecond microstripline switches on self-implanted Silicon On Sapphire (SOS) N89-17104
Fast GaAs photoconductive detectors with high sensitivity integrated in coplanar systems onto GaAs substrates N89-17105
Carrier lifetime versus ion-implantation dose in silicon on sapphire N89-17106
Characteristics, packaging and physics of ultra high speed diode lasers and detectors N89-17112
Picosecond measurements of gain-switching in a semiconductor laser driven by ultrashort electrical pulses N89-17115
Picosecond optical autocorrelation experiments on fast photodetectors N89-17117
Electrical pulse compression by traveling-wave photoconductivity N89-17137
Picosecond optoelectronic study of a thin film transmission line structure N89-17138
PHOTOCONDUCTORS
An optically strobed sample and hold circuit N89-17087
PHOTODIODES
High speed opto-isolator for radar applications N89-17110
InP/GaInAs/InP PIN photodiode with FWHM less than 18 ps N89-17114
PHOTODISSOCIATION
Photoabsorption and photodissociation of molecules important in the interstellar medium
[NASA-CR-184771] N89-16965
PHOTOELECTRON SPECTROSCOPY
Structure and properties of polymer interphases
[AD-A200238] N89-17008
PHOTOGRAPHIC MEASUREMENT
Processing information in the image plane --- particle image velocimetry N89-17183
Practical systems for speckle velocimetry N89-17185
Speckle photography of flows with varying fluid density N89-17186
A personal computer based system for the evaluation of multiple exposed images in laser speckle and particle image displacement velocimetry N89-17193
Digital direct analysis of a multiexposed photograph in Particle Image Displacement Velocimetry (PIDV) N89-17194
PHOTOINTERPRETATION
A personal computer based system for the evaluation of multiple exposed images in laser speckle and particle image displacement velocimetry N89-17193
Northeast Artificial Intelligence Consortium annual report 1986. Volume 5. Building an intelligent assistant: The acquisition, integration, and maintenance of complex distributed tasks
[AD-A199824] N89-17425
PHOTOIONIZATION
Modeling of atomic processes for X-ray laser plasmas
[AD-A200219] N89-17505
PHOTOLYSIS
The kinetics and dynamics of iodine monofluoride formation in gas-phase collisions
[AD-A199622] N89-16939
PHOTOMETERS
Picosecond optical autocorrelation experiments on fast photodetectors N89-17117
A photon-counting, subnanosecond, imaging camera for X-ray detection
[DE89-002874] N89-17208
PHOTOMETRY
Optical and infrared studies of cometary dust N89-17550
PHOTONICS
Photonics: Maintaining competitiveness in the information era
[AD-A200230] N89-17473
PHOTONS
A photon-counting, subnanosecond, imaging camera for X-ray detection
[DE89-002874] N89-17208
Electronic interactions of electrons, photons, and atoms with material surfaces
[AD-A199626] N89-17489
Monte Carlo calculation of electron multiple scattering in thin foils
[AD-A199872] N89-17517
PHOTOVOLTAIC CELLS
NASA photovoltaic research and technology
[NASA-TM-101422] N89-16917
Thermally conductive alumina/organic composites for photovoltaic concentrator cell isolation
[DE89-001181] N89-17346
PHOTOVOLTAIC EFFECT
Recent advances in high-efficiency InGaAs concentrator cells
[DE89-001613] N89-17345
PHTHALOCYANIN
PBT,PBO-based hybrid polymers with nonlinear optical properties or high electrical conductivity
[AD-A200226] N89-17007
PHYSICAL CHEMISTRY
Using theoretical descriptors in structural activity relationships. Part 2: Polarizability index
[AD-A199594] N89-17389
PHYSIOLOGICAL EFFECTS
The effects of microgravity and linear accelerations on cutaneomuscular reflexes in human lower limb musculature N89-17034
Development of a portable physiological monitoring system for the KC-135: The S.F.U. biopack N89-17044
Extravehicular activities limitations study. Volume 1: Physiological limitations to extravehicular activity in space
[NASA-CR-172098] N89-17392
PICOSECOND PULSES
A non-contact picosecond prober for integrated circuit testing N89-17081
Picosecond sampling of integrated circuits N89-17082
Picosecond electrical pulses for VLSI electronics characterization N89-17083
Picosecond photoconductive transceivers N89-17092
Photoconductive generation of sub-picosecond electrical pulses and their measurement applications N89-17093
Generation and forming of ultrashort high voltage pulses N89-17097
Graphite as a picosecond laser activated opening switch N89-17098
A simple technique to generate or gate microwave pulses with picosecond speeds N89-17099
Nonequilibrium phonons and disorder in Al(sub x)Ga(sub 1-x)As N89-17103
Investigation of photoconductive picosecond microstripline switches on self-implanted Silicon On Sapphire (SOS) N89-17104
Carrier lifetime versus ion-implantation dose in silicon on sapphire N89-17106
Picosecond optoelectronic switches using composite electronic materials N89-17107
Comparison of sampling oscilloscopes with less than 35 ps transition durations N89-17108
Picosecond measurements of gain-switching in a semiconductor laser driven by ultrashort electrical pulses N89-17115
Picosecond optical autocorrelation experiments on fast photodetectors N89-17117
High-speed phenomena in GaAs multiple-quantum-wells N89-17127
Picosecond carrier transport in GaAs quantum wells N89-17128
Picosecond response of an optically controlled millimeter wave phase shifter N89-17135
Electron device probing in the femtosecond time scale N89-17136
Electrical pulse compression by traveling-wave photoconductivity N89-17137
Picosecond optoelectronic study of a thin film transmission line structure N89-17138
Silicon pulse sharpening diodes: Switching kilovolts in tens of picoseconds N89-17139
PILOT PERFORMANCE
Piloted-simulation evaluation of escape guidance for microburst wind shear encounters
[NASA-TP-2886] N89-16820
Body displacement measured during sustained +Gz, -Gz and + or -Gy acceleration using a stereoscopic photographic system
[NASA-TM-101269] N89-17391
PILOT SELECTION
Multiparametric research of early indicators of vascular risk in flying personnel
[ETN-89-93613] N89-17398
PILOT TRAINING
Aircraft accident/incident summary report, Travis Air Force Base, California, 8 April 1987
[PB88-910414] N89-16768
PIPE FLOW
Pipeline vibrations. Undamped natural vibration of pipelines
[ESDU-88022] N89-17268
PIPELINES
Pipeline vibrations. Undamped natural vibration of pipelines
[ESDU-88022] N89-17268
PITCHING MOMENTS
Normal-force-curve and pitching-moment-curve slopes for tangent-ogive forebody-cyclinder combinations at zero angle of attack
[ESDU-88026] N89-16733
PLANE WAVES
Fresnel coefficients for a phase conjugator
[AD-A200123] N89-17487
PLANETARY MAPPING
Planetary cartography in the next decade: Digital cartography and emerging opportunities
[NASA-TM-4092] N89-17560
PLANFORMS
Aerodynamic performance of wings of arbitrary planform in inviscid, incompressible, irrotational flow
[AD-A200436] N89-16728
PLANNING
Canadian forces aircraft condition/health monitoring: Policy, plans and experience N89-16784
PLASMA CONTROL
Field-reversed configuration (FRC) experiments
[DE89-000389] N89-17498
Plasma performance in JET: Achievements and projections
[DE89-002219] N89-17500
Studies of a poloidal divertor reversed field pinch
[DE89-005498] N89-17515
PLASMA DIAGNOSTICS
Studies of a poloidal divertor reversed field pinch
[DE89-005498] N89-17515
PLASMA HEATING
Induction-linac based free-electron laser amplifiers for plasma heating
[DE88-017004] N89-17221
Aneurisms in laser-driven blast waves
[AD-A200189] N89-17222
High power Ion Cyclotron Resonance Heating (ICRH) in JET
[DE89-002218] N89-17499
PLASMA PHYSICS
Fusion plasma theory: Task 3: Auxiliary heating in tokamaks
[DE89-003256] N89-17509
PLASMA PROBES
Phototype design and testing of two fiber-optic spectrochemical emission sensors
[DE89-001741] N89-17207
PLASMA SPECTRA
Laser thermal propulsion
[AD-A200558] N89-17226
PLASMA SPRAYING
Thermal barrier coating life-prediction model development N89-17331
Thermal barrier coating life prediction model N89-17332
Thermal barrier coating life prediction model development N89-17333
PLASMAS (PHYSICS)
A high-intensity plasma sputter heavy negative ion source
[DE89-003113] N89-17480
Plasma performance in JET: Achievements and projections
[DE89-002219] N89-17500
Neoclassical MHD descriptions of tokamak plasmas
[DE89-003117] N89-17508
Sodium in Io's extended atmosphere N89-17559
PLASMONS
Molecular spectroscopy at corrugated metal surfaces
[AD-A200124] N89-16973
PLASTIC DEFORMATION
The effects of strain induced softening on the load carrying capability of components N89-17264
PLASTIC FLOW
Numerical analysis of the effects of void growth and crack tip opening on ductile fracture N89-17265
PLASTIC PROPERTIES
Processing of 2090 aluminum alloy for superplasticity
[AD-A200425] N89-16975
Three-dimensional inelastic analysis methods for hot section components N89-17321
Thermal expansion mismatch and plasticity in thermal barrier coating N89-17330
PLASTICS
The behavior of shells made of composites during the dynamic application of axian compression
[AD-A200244] N89-17266
Suggested plastic-replica method N89-17293

PLATES (STRUCTURAL MEMBERS)
Wrinkling of sandwich panel face plates (isotropic face plates on orthotropic cores, in-plane loading or bending) [ESDU-88032] N89-16931
Avoidance of buckling of some engineering elements (struts, plates and gussets) [ESDU-88034] N89-17269
Finite element analysis for the evaluation and optimization of fiber reinforced composite structural components N89-17279
PLATES (TECTONICS)
Strain accumulation in the Santa Barbara Channel, 1971-1987 [NASA-CR-183402] N89-17369
An algorithm for analysis of plate motions in Crust Dynamics Project (CDP) networks [B8821606] N89-17371
PLUMES
Source characterization of heavy gas dispersion models for reactive chemicals, volume 1 [AD-A200121] N89-17361
PLY ORIENTATION
Tensile strength of composite structures with internal ply drops and free-edge effects N89-16929
POLICIES
Canadian forces aircraft condition/health monitoring: Policy, plans and experience N89-16784
POLISHING
Review of precision surface generating processes and their potential application to the fabrication of large optical components [DE89-001712] N89-17486
POLOIDAL FLUX
Studies of a poloidal divertor reversed field pinch [DE89-005498] N89-17515
POLYAMIDE RESINS
Synthesis and analysis of epichlorohydrin based wet strength resins for paper N89-16919
Properties and performance of polyamide membranes N89-16991
POLYCARBONATES
Synthesis and analysis of novel polymers with potential for providing both high permselectivity and permeability in gas separation applications [DE89-004325] N89-17014
POLYCRYSTALS
Magnetization, transport and structural studies of Tl-Ca-Ba-Cu-O: Bulk ceramics, single crystals, and polycrystalline thin films [DE89-003264] N89-17010
Device physics related to the granular nature of CuInSe2 solar cells [DE89-000810] N89-17341
POLYGONS
An algorithm for calculating the area of overlap of an ellipse and a convex polygon [AD-A199654] N89-17408
POLYIMIDES
Synthesis and analysis of novel polymers with potential for providing both high permselectivity and permeability in gas separation applications [DE89-004325] N89-17014
POLYMER CHEMISTRY
Hardware for studying the demixing of aqueous polymer two-phase systems in low gravity N89-17030
POLYMER PHYSICS
Theoretical studies of electrons and electron transfer processes in fluids [DE89-003259] N89-17479
POLYMERIC FILMS
New secondary batteries utilizing electronically conductive polymer cathodes [NASA-CR-183248] N89-17149
POLYMERIZATION
Evaluation of physical chemical test methods for characterizing polymerized composites or polymerizing composites: Literature review [REPT-49-438/F] N89-16935
Theoretical predictions for side-chain liquid-crystal polymers and comparison to experiment [DE89-003578] N89-17013
POLYNOMIALS
Kinematic leveling adjustments with polynomials and polynomial splines [ETN-89-93328] N89-17338
POLYPROPYLENE
Electric conductivity of polymer composite materials. Composite on propylene and silicon base [DE88-704293] N89-17001
POLYSULFIDES
Synthesis and analysis of novel polymers with potential for providing both high permselectivity and permeability in gas separation applications [DE89-004325] N89-17014
POROSITY
Modeling and Applications of Transport Phenomena in Porous Media, volume 2 --- conference [VKI-LS-1988-01-VOL-2] N89-17167
Stochastic description of porous media N89-17168
Multiphase flow in porous media N89-17169
Physical mechanisms during drying of porous media N89-17173
Modeling and applications of transport phenomena in porous media. Volume 1: Mathematical modeling of transport in porous media [VKS-LS-1988-01-VOL-1] N89-17202
Electron beam welding produces improved duplex crack arrest specimens [DE88-003685] N89-17239
POROUS PLATES
Unsteady flow about porous cambered plates [AD-A200282] N89-17160
POSITION (LOCATION)
Extensions to the matrix pencil approach for direction finding [AD-A200112] N89-17449
Precise interferometric phase determination [AD-A200186] N89-17488
POSITRONS
Experimental evidence for positron trapping at dislocations in Ni3Al alloys [DE89-004520] N89-16989
POTASSIUM COMPOUNDS
An in situ surface Fourier transform study of complexes of lithium, magnesium potassium and lanthanum ferrocyanide at platinum and gold electrodes [AD-A200305] N89-16950
POTENTIAL FIELDS
The visual shape and multipole moments of the sun N89-17561
POTENTIAL FLOW
Aerodynamic performance of wings of arbitrary planform in inviscid, incompressible, irrotational flow [AD-A200436] N89-16728
POWDER METALLURGY
Review of existing NDT technologies and their capabilities N89-17255
POWER CONDITIONING
Penetration effects of the compound vortex in gas metal-arc welding [AD-A200585] N89-17242
POWER EFFICIENCY
A proposed Quantum Well Injection Transit Time (QWITT) device N89-17100
POWERED LIFT AIRCRAFT
NASA powered lift facility internally generated noise and its transmission to the acoustic far field [NASA-CR-182217] N89-16882
PRECISION
Review of precision surface generating processes and their potential application to the fabrication of large optical components [DE89-001712] N89-17486
PREDICTION ANALYSIS TECHNIQUES
Vortex dynamics for rotorcraft interactional aerodynamics [AD-A200128] N89-16726
Tip sensor development [AD-A200080] N89-16824
Some difficulties in the wind tunnel prediction of modern civil aircraft buffeting: Proposed remedies N89-16869
Prediction and synthesis efforts at Los Alamos [DE89-003605] N89-17018
An analysis of the closure conditions for two-fluid models of two-phase flow [DE89-003096] N89-17165
The reliable reduction of random local sequences for fatigue tests N89-17274
Fretting corrosion fatigue N89-17282
Profile properties of undeformed first-year sea ice [AD-A200172] N89-17388
Using theoretical descriptors in structural activity relationships. Part 2: Polarizability index [AD-A199594] N89-17389
A strategy for understanding noise-induced annoyance [AD-A200125] N89-17461
PREDICTIONS
A modified VAPEPS method for predicting vibroacoustic response of unreinforced mass loaded honeycomb panels [NASA-TM-101467] N89-16905
Theoretical predictions for side-chain liquid-crystal polymers and comparison to experiment [DE89-003578] N89-17013
The influence of the load sequence on the fatigue life of fatigue fracture endangered components N89-17273
Short-crack growth behaviour in an aluminum alloy: An AGARD cooperative test program N89-17288
Development of generalized block correction procedures for the solution of discretized Navier-Stokes equations N89-17307
Thermal barrier coating life-prediction model development N89-17331
Thermal barrier coating life prediction model N89-17332
Thermal barrier coating life prediction model development N89-17333
Prediction of stochastic blade responses using measured wind-speed data as input to the FLAP code [DE89-000834] N89-17354
World-wide extreme wind speeds. Part 2: Examples using various methods of analysis [ESDU-88037] N89-17382
Progress in laboratory high gain ICF (Inertial Confinement Fusion): Prospects for the future [DE89-002664] N89-17502
PREPARATION
A document preparation system in a large network environment [DE88-014466] N89-17543
PRESSURE
Mechanistic studies of pressure-assisted superplasticity of structural ceramics [AD-A200202] N89-17006
PRESSURE DEPENDENCE
Pressure/temperature sensitive inorganic phosphors [AD-A199718] N89-17000
PRESSURE DISTRIBUTION
On the aeroacoustics, aerodynamics and aeroelasticity of lifting surfaces N89-16724
Intake swirl and simplified methods for dynamic pressure distortion assessment N89-16742
Expriments on the DFVLR-F4 wing body configuration in several European windtunnels N89-16848
PRESSURE EFFECTS
Loss development in transonic compressor cascades N89-16826
Manufacturing thermoplastic matrix composites [AD-A199724] N89-16922
PRESSURE MEASUREMENT
Flow visualization by the PISTIL procedure (presentation of wake images by local computer processing). Test report 876/S-5 --- wake image representation by local computer treatment (PISTIL) [REPT-876/S-5] N89-17203
PRESSURE REDUCTION
Coolant passage heat transfer with rotation N89-17314
PRESSURE SENSORS
Pressure/temperature sensitive inorganic phosphors [AD-A199718] N89-17000
PRESSURE VESSELS
Kinetics and mechanisms of hydrogen attack in 2.25Cr-1Mo steel [DE89-001381] N89-16970
The effects of strain induced softening on the load carrying capability of components N89-17264
Total strain version of strainrange partitioning for thermomechanical fatigue at low strains N89-17337
PRIMATES
Proceedings of a workshop on Lighting Requirements in Microgravity: Rodents and Nonhuman Primates [NASA-TM-101077] N89-17390
PRINTED CIRCUITS
Stress driven diffusive voiding of aluminum conductor lines: A model for time dependent failure [DE89-001665] N89-17144
PROBLEM SOLVING
Accuracy problems in wind tunnels during transport aircraft development N89-16877
Applications of correcting coding theory to communication combinatorial problems [ENST-88C001] N89-17065
Development of generalized block correction procedures for the solution of discretized Navier-Stokes equations N89-17307
A multistage linear array assignment problem [NASA-CR-181748] N89-17417
PROCEDURES
Alignment verification procedures N89-17291
PROCESS CONTROL (INDUSTRY)
Computer control of gas metal arc welding [DE89-005188] N89-17252
PROCUREMENT
Aircraft airframe cost estimating relationships: All mission types [AD-A200262] N89-16719
Aircraft airframe cost estimating relationships: Fighters [AD-A200263] N89-16720
Aircraft airframe cost estimating relationships: Bombers and transports [AD-A200264] N89-16721

Procurement and screening test data for advanced austenitic alloys for 650 C steam service, part 2
[DE89-001331] N89-16979
PRODUCT DEVELOPMENT
The design and development of transonic multistage compressors N89-16834
PRODUCTION ENGINEERING
JPRS report: Science and technology. Japan. Developments in Manufacturing Process Technology
[JPRS-JST-88-010] N89-17047
PROGRAMMING LANGUAGES
A formal language model for local area network configuration N89-17544
PROJECT MANAGEMENT
Life cycle management handbook
[DE89-004315] N89-17545
PROPELLANT COMBUSTION
Design and analysis of solid rocket motor internal insulation N89-16915
PROPELLANT GRAINS
Propellant grain design N89-16912
Solid propellant grain design N89-16913
State of the art of solid propellant rocket motor grain design in the United States N89-16914
PROPELLANT PROPERTIES
Solid propellant grain design N89-16913
PROPELLERS
Lift and longitudinal forces on propeller/nacelle/wing/flap systems
[ESDU-88031] N89-16736
PROPULSION SYSTEM CONFIGURATIONS
Design and analysis report for the flight weight 20-inch Columbium secondary nozzle for the RL10 engine
[NASA-CR-179612] N89-16918
PROPULSION SYSTEM PERFORMANCE
Space shuttle main engine monitoring experience and advanced monitoring systems development N89-16815
Supersonic throughflow fans N89-16837
PROPYLENE
Electric conductivity of polymer composite materials. Composite on propylene and silicon base
[DE88-704293] N89-17001
PROTECTIVE COATINGS
The effects of a compressor rebuild on gas turbine engine performance N89-16803
The effect of insulated combustion chamber surfaces on direct-injected diesel engine performance, emissions, and combustion
[NASA-CR-182204] N89-17548
PROTEIN SYNTHESIS
Protein crystal nucleation kinetics using relative light-scattering techniques: Center director's discretionary fund
[NASA-TM-100348] N89-17535
PROTOCOL (COMPUTERS)
A formal language model for local area network configuration N89-17544
PROTOTYPES
Phototype design and testing of two fiber-optic spectrochemical emission sensors
[DE89-001741] N89-17207
The suitability of an object-oriented language for prototyping and abstract data types
[AD-A200417] N89-17410
PROVING
Wind tunnel requirements for computational fluid dynamics code verification N89-16880
Experimental verification of the thermodynamic properties for a jet-A fuel
[NASA-TM-101475] N89-17017
Alignment verification procedures N89-17291
On-line spectrum loading accuracy verification N89-17292
PROXIMITY
Modifications to the NASA Ames Space Station Proximity Operations (PROX OPS) Simulator
[NASA-CR-177510] N89-16896
PSYCHOACOUSTICS
A strategy for understanding noise-induced annoyance
[AD-A200125] N89-17481
PULSE DURATION
Microdrilling using electron beams reported N89-17055
PULSE GENERATORS
Generation and forming of ultrashort high voltage pulses N89-17097
A simple technique to generate or gate microwave pulses with picosecond speeds N89-17099
PULSE MODULATION
Frequency chirping in pulse modulated gain and real index guided single quantum well lasers N89-17113
PULSE REPETITION RATE
High speed, high repetition rate, high voltage photoconductive switching N89-17096
PULSES
The synchronous injection ignition valveless pulsejet N89-16823
PUMPS
Computer program for the prediction of air-lift pump performance
[ESDU-88014] N89-17246
PURIFICATION
Fouling in cooling water systems
[ESDU-88024] N89-17057
PYROLYSIS
Graphite as a picosecond laser activated opening switch N89-17098
The space station integrated refuse management system
[NASA-CR-184722] N89-17403
PYRROLES
New secondary batteries utilizing electronically conductive polymer cathodes
[NASA-CR-183248] N89-17149

Q

QUALITY CONTROL
AGARD/SMP Review: Damage Tolerance for Engine Structures. 1: Non-Destructive Evaluation
[AGARD-R-766] N89-17253
The impact of engineering assumptions on NDE requirements N89-17254
Improving software quality through hierarchical design
[DE88-014919] N89-17412
QUANTUM CHEMISTRY
Using theoretical descriptors in structural activity relationships. Part 2: Polarizability index
[AD-A199594] N89-17389
QUANTUM CHROMODYNAMICS
Cluster expansion for vacuum confining fields
[DE88-704367] N89-17436
QUANTUM ELECTRONICS
Joint service electronics program: Research in electronics
[AD-A199659] N89-17140
Adaptive hybrid picture coding
[AD-A200059] N89-17142
QUANTUM MECHANICS
A proposed Quantum Well Injection Transit Time (QWITT) device N89-17100
Modulation efficiency limited high frequency performance of the MODFET N89-17101
Electron device probing in the femtosecond time scale N89-17136
The Wigner distribution function with minimum spread
[AD-A199661] N89-17446
On the experimental basis of the Pauli exclusive principle
[DE88-704366] N89-17477
An essay on discrete foundations for physics
[DE89-002992] N89-17556
QUANTUM NUMBERS
Effect of finite size on magnetoresistance
[AD-A200267] N89-16974
QUANTUM THEORY
Quantum transport calculation of resonant-tunneling response time N89-17125
Supersymmetric instantons and topological quantum field theory
[DE88-704211] N89-17536
QUANTUM WELLS
Topical Meeting on Picosecond Electronics and Optoelectronics
[AD-A189686] N89-17080
A proposed Quantum Well Injection Transit Time (QWITT) device N89-17100
Frequency chirping in pulse modulated gain and real index guided single quantum well lasers N89-17113
Resonant tunneling electron spectroscopy N89-17126
High-speed phenomena in GaAs multiple-quantum-wells N89-17127
Picosecond carrier transport in GaAs quantum wells N89-17128
Quantum-confined Stark effect in InGaAs/InP quantum wells grown by metal-organic chemical vapor deposition N89-17129
Dynamics of below-gap photoexcitation in GaAs quantum wells N89-17130
QUARKS
An essay on discrete foundations for physics
[DE89-002992] N89-17556
QUENCHING (COOLING)
Analysis of Cd0.21Hg0.79Te quenched in 10(-4) g N89-17029
The effects of strain induced softening on the load carrying capability of components N89-17264

R

RADAR DETECTION
Effects of irregular sea surface and evaporation duct on radar detection performance
[AD-A200114] N89-17066
RADAR ECHOES
On deriving the three-dimensional kinematic structure on convective storms from a single radar N89-17376
RADAR IMAGERY
Improving classification accuracy of radar images using a multiple-stage classifier
[AD-A200291] N89-17071
RADAR MEASUREMENT
Instrumentation for the characterization of the microwave properties at 18, 35 and 94 GHz
[AD-A199741] N89-17064
RADAR RECEIVERS
Frequency estimation of radar signals using an acousto-optic spectrum analyzer as an RESM (Radar Electronic Support Measures) receiver
[AD-A200159] N89-17067
RADIANT FLUX DENSITY
Electron collision shift of the Lyman-alpha line in H and He+
[AD-A200296] N89-17474
RADIATION COUNTERS
Evaluation of a supercritical fluid chromatograph coupled to a surface-wave-sustained microwave-induced plasma detector
[AD-A198728] N89-16937
RADIATION DOSAGE
Radiation imposed limits on superconducting magnets: A data base for copper stabilizers
[DE89-002875] N89-17456
RADIATION EFFECTS
The effect of different module configurations on the radiation tolerance of multijunction solar cells
[NASA-TM-101251] N89-17356
Compositional changes during ion bombardment
[DE89-003974] N89-17481
RADIATION HAZARDS
Safety comparison of fusion fuel cycles
[DE89-005200] N89-17512
RADIATION MEASUREMENT
Electron collision shift of the Lyman-alpha line in H and He+
[AD-A200296] N89-17474
RADIO COMMUNICATION
Study of error correcting codes for Hertzian channels with a large number of states. Application to Quadrature Amplitude Modulation (QAM) 64
[ENST-88E007] N89-17074
RADIO FREQUENCIES
Mechanical design of a RF electron gun
[DE89-004890] N89-16895
RADIO FREQUENCY INTERFERENCE
Vector space approach to narrowband interference excision
[AD-A199703] N89-17063
RADIOACTIVE DECAY
Modeling of atomic processes for X-ray laser plasmas
[AD-A200219] N89-17505
RADIOMETERS
Limb-darkening functions as derived from along-track operation of the ERBE scanning radiometer for January 1985
[NASA-RP-1214] N89-17374
RAIN
Propagation effects handbook for satellite systems design. A summary of propagation impairments on 10 to 100 GHz satellite links with techniques for system design
[NASA-RP-1082(04)] N89-17060
Hydrological aspects of combined effects of storm surges and heavy rainfall on river flow
[WMO-704] N89-17340
RAMAN SPECTRA
In-situ vibrational spectroelectrochemistry
[AD-A200303] N89-16949
RAMJET MISSILES
Missile intakes N89-16750
RANKINE CYCLE
The Rankine automotive system technology assessment report
[DE89-002693] N89-17238
RARE GASES
Seeded inert gas driven disk generator
[DE88-704083] N89-17510
RAREFIED GAS DYNAMICS
A statistical theory for gas surface interactions in rarefied hypersonic flows
[IC-AERO-88-01] N89-16755

RATIOS
Axial velocity density ratio influence on exit flow angle in transonic/supersonic cascades N89-16830
RAYLEIGH SCATTERING
GPS (Global Positioning System) user equipment evaluation techniques using a rotor mounted antenna [AD-A200515] N89-16770
REACTION KINETICS
The kinetics and dynamics of iodine monofluoride formation in gas-phase collisions [AD-A199622] N89-16939
The behavior of microdisks and microring electrodes. Applications of Neumann's integral theorem [AD-A200307] N89-16951
Kinetics of the isothermal decomposition of lanthanum nickel hydride [DE89-002905] N89-16966
Kinetics and mechanisms of hydrogen attack in 2.25Cr-1Mo steel [DE89-001381] N89-16970
Selectivity of the reactions of oxygenates on transition metal surfaces [DE89-003691] N89-16985
Oxidation of Ni3Al below 850 C and its effect on fracture behavior [DE89-002232] N89-16988
KINETICS: A computer program to analyze chemical reaction data [DE89-004602] N89-17419
Reaction dynamics of H + O2 at 1.6 eV collision energy [NASA-CR-183182] N89-17483
REACTION WHEELS
Control of reaction wheels through digital techniques using reference models [INPE-4618-TDL/335] N89-16903
REACTIVITY
Gas jet deposition of multicomponent ultrafine microstructures [AD-A200101] N89-16946
REACTOR DESIGN
The two-beam accelerator and the relativistic klystron power source [DE89-002673] N89-17485
REACTOR SAFETY
Phase change phenomena in liquid saturated self heated particulate bed --- core meltdown N89-17170
Safety comparison of fusion fuel cycles [DE89-005200] N89-17512
REACTOR TECHNOLOGY
Small reactors for low-temperature nuclear heat applications [DE88-704336] N89-17484
Field-reversed configuration (FRC) experiments [DE89-000389] N89-17498
REAL GASES
Flux Jacobian matrices and generaled Roe average for an equilibrium real gas [NASA-CR-177512] N89-17445
REAL TIME OPERATION
Evaluation and application of a new interferometry technique for compressible flow research [NASA-CR-177467] N89-16765
RECEIVERS
Laser communication test system [AD-A199612] N89-17215
RECORDING
A technique for recording HF (High Frequency) oblique-incidence-sounder data [AD-A200168] N89-17068
RECRYSTALLIZATION
Processing of 2090 aluminum alloy for superplasticity [AD-A200425] N89-16975
RECTANGULAR PLATES
Scattering by a two dimensional groove in a ground plane [NASA-CR-183087] N89-17077
REDUCED GRAVITY
Workshop on Microgravity Experimentation in Aircraft and Rockets [NRCC-29151] N89-17019
Parabolic flight: A useful test bed N89-17020
On fundamental problems of Space Materials Science (SMS) N89-17024
Advanced research rockets for long duration microgravity science N89-17028
Analysis of Cd0.21Hg0.79Te quenched in 10(-4) g N89-17029
Hardware for studying the demixing of aqueous polymer two-phase systems in low gravity N89-17030
Droplet separation dynamics and kinematics under microgravity N89-17031
Design considerations for the CLEM135 bubble coalescence experiment N89-17032
System engineering and logistics for KC-135 experimentation N89-17033
The effects of microgravity and linear accelerations on cutaneomuscular reflexes in human lower limb musculature N89-17034
The use of sounding rockets in the study of microgravity cell biology N89-17036
Encapsulation process hardware for a KC-135 aircraft N89-17037
PYTHON microgravity accelerometer system N89-17038
High temperature material processing system for KC-135 microgravity experiments N89-17040
Concentricity and sphericity of composite drops under microgravity N89-17042
The design of a heat-pipe furnace for microgravity N89-17043
Behavior in normal and reduced gravity of an enclosed liquid/gas system with nonuniform heating from above [NASA-TM-101471] N89-17046
Proceedings of a workshop on Lighting Requirements in Microgravity: Rodents and Nonhuman Primates [NASA-TM-101077] N89-17390
REDUNDANCY ENCODING
Study of error correcting codes for Hertzian channels with a large number of states. Application to Quadrature Amplitude Modulation (QAM) 64 [ENST-88E007] N89-17074
REENTRY VEHICLES
Inviscid flow field analysis of complex reentry vehicles. Volume 1: Description of numerical methods [DE89-002814] N89-16900
REFLECTANCE
Interfacial bonding in W/C and W/B4C multilayers [DE89-002931] N89-16936
Glancing angle EXAFS studies of Cu-Al thin film interfaces [DE89-003614] N89-16983
Instrumentation for the characterization of the microwave properties at 18, 35 and 94 GHz [AD-A199741] N89-17064
REFRACTORY MATERIALS
Development of composite high temperature materials for future energy conversion applications N89-16995
NDE methods for high-temperature materials and environments [DE89-005195] N89-17234
REFRACTORY METALS
Refractory metal alloys and composites for space nuclear power systems [NASA-TM-101364] N89-16986
REGENERATION (ENGINEERING)
Regenerative life support system research and concepts [NASA-CR-184760] N89-17404
REGRESSION ANALYSIS
The effect of chemistry modifications on the solidification behavior and weldability of Alloy 625 [DE89-001046] N89-16972
KINETICS: A computer program to analyze chemical reaction data [DE89-004602] N89-17419
REINFORCING MATERIALS
Isotropic kevlar and PBA (poly 1,4-benzamide) reinforcements for composites [AD-A200239] N89-16927
RELATIVISTIC EFFECTS
Relativistically-invariant statistical hydrodynamics of a normal fluid [DE88-704370] N89-17161
RELATIVITY
Geometry on the space of geometries [DE88-704214] N89-17537
Investigations in particle and field theory [DE89-003004] N89-17538
An essay on discrete foundations for physics [DE89-002992] N89-17556
RELEASING
Source characterization of heavy gas dispersion models for reactive chemicals, volume 1 [AD-A200121] N89-17361
RELIABILITY
Importance of sensitivity and reliability of NDI techniques on damage tolerance based life prediction of turbine discs N89-17257
R/M/T (Reliability/Maintainability/Testability) design for fault tolerance. Volume 1: Program manager's guide [AD-A200204] N89-17262
The reliable reduction of random local sequences for fatigue tests N89-17274
RELIABILITY ENGINEERING
Fault management in aircraft power plant controls N89-16809
REMOTE CONTROL
Robotic vehicle communications interoperability [TACOM-TR-13387] N89-17075
REMOTE MANIPULATOR SYSTEM
Integration of robotics and teleoperation for the advanced servomanipulator: Consolidated fuel reprocessing program [DE88-015281] N89-17240
REMOTE SENSING
Proceedings of the Colloquium about Joint Projects Within the DFVLR/ISRO Cooperation [DFVLR-MITT-88-19] N89-16883
Indian activities in remote sensing applications: Microwave remote sensing N89-16886
Spatial reasoning in the treatment of systematic sensor errors [DE89-003244] N89-17251
Accuracy assessment, using stratified plurality sampling, of portions of a LANDSAT classification of the Arctic National Wildlife Refuge Coastal Plain [NASA-TM-101042] N89-17339
Limb-darkening functions as derived from along-track operation of the ERBE scanning radiometer for January 1985 [NASA-RP-1214] N89-17374
Study of the effect of cloud inhomogeneity on the earth radiation budget experiment [NASA-CR-182962] N89-17386
REMOVAL
Microstructural effects in abrasive wear [DE89-003032] N89-16976
REPLICAS
Suggested plastic-replica method N89-17293
REQUIREMENTS
Operational requirements for engine condition monitoring from the EFA viewpoint N89-16781
An overview of US Navy engine monitoring system programs and user experience N89-16782
Requirements and capabilities in unsteady windtunnel testing N89-16878
RESEARCH AIRCRAFT
Modal control of an oblique wing aircraft [NASA-TP-2898] N89-16845
RESEARCH AND DEVELOPMENT
NASA photovoltaic research and technology [NASA-TM-101422] N89-16917
Space utilization promotion program of NASDA N89-17022
Report to Congress on the Automotive Technology Development Program [DE89-004977] N89-17250
RESEARCH FACILITIES
NASA powered lift facility internally generated noise and its transmission to the acoustic far field [NASA-CR-182217] N89-16882
Proceedings of a workshop on Lighting Requirements in Microgravity: Rodents and Nonhuman Primates [NASA-TM-101077] N89-17390
RESEARCH MANAGEMENT
National Research Council Resident Research Associateship (NRC-RRA) Program [AD-A200183] N89-16926
Short-Crack Growth Behaviour in an Aluminum Alloy: An AGARD Cooperative Test Programme [AGARD-R-732] N89-17287
Report of the Defense Science Board Task Force Subgroup on Strategic Air Defense (SDI Milestone Panel) [AD-A200164] N89-17452
Photonics: Maintaining competitiveness in the information era [AD-A200230] N89-17473
RESIDENTIAL AREAS
A strategy for understanding noise-induced annoyance [AD-A200125] N89-17461
RESIDUAL STRESS
Internal stress during high-temperature creep and activation energy for creep of Hastelloy XR [DE88-755231] N89-16969
RESIN MATRIX COMPOSITES
Manufacturing thermoplastic matrix composites [AD-A199724] N89-16922
RESONANT FREQUENCIES
Pipeline vibrations. Undamped natural vibration of pipelines [ESDU-88022] N89-17268
RESONANT TUNNELING
A proposed Quantum Well Injection Transit Time (QWITT) device N89-17100
Microwave and millimeter-wave resonant tunneling diodes N89-17124
Quantum transport calculation of resonant-tunneling response time N89-17125
Resonant tunneling electron spectroscopy N89-17126
RESONANT VIBRATION
Pipeline vibrations. Undamped natural vibration of pipelines [ESDU-88022] N89-17268

Flow induced acoustic resonance in tubular heat exchangers
[ESDU-88028] N89-17464

RESPONSES
Assessment and comparison of techniques for transforming parameters to a common metric in item response theory
[AD-A200067] N89-17433

RETINA
Role of retinocortical processing in spatial vision
[AD-A200198] N89-17394

REUSABLE LAUNCH VEHICLES
Analysis and design of a universal shuttle for rockets
[ILR-MITT-199] N89-16897

REVERSE FIELD PINCH
Field-reversed configuration (FRC) experiments
[DE89-000389] N89-17496
Behavior of the reversed field pinch with nonideal boundary conditions
[DE89-005497] N89-17514
Studies of a poloidal divertor reversed field pinch
[DE89-005498] N89-17515

REYNOLDS NUMBER
Reynolds number effects in transonic flow
[AGARD-AG-303] N89-16760
On Reynolds number effects and simulation N89-16866
A low-Reynolds-number two-equation turbulence model for predicting heat transfer on turbine blades N89-17310

RHEOLOGY
Approximation of viscoelastic stresses from Newtonian turbulent kinematics
[AD-A200188] N89-17157

RIEMANN MANIFOLD
Spherical-type hypersurfaces in a Riemannian manifold
[DE88-704224] N89-17454

RIGID ROTORS
Aeroelastic optimization of a helicopter rotor N89-16778

RING CURRENTS
Characterization of hollow cathode, ring cusp discharge chambers
[NASA-CR-182255] N89-17146

RISK
Multiparametric research of early indicators of vascular risk in flying personnel
[ETN-89-93613] N89-17398

RIVERS
Hydrological aspects of combined effects of storm surges and heavy rainfall on river flow
[WMO-704] N89-17340

ROBOTICS
Integration of robotics and teleoperation for the advanced servomanipulator: Consolidated fuel reprocessing program
[DE88-015281] N89-17240
Active vibration suppression for robotic manipulators N89-17241

ROBOTS
Robotic vehicle communications interoperability
[TACOM-TR-13387] N89-17075
3-D vision techniques for autonomous vehicles
[AD-A199643] N89-17236
Active vibration suppression for robotic manipulators N89-17241
HERMIES-3: A step toward autonomous mobility, manipulation and perception
[DE89-004932] N89-17249
Spatial reasoning in the treatment of systematic sensor errors
[DE89-003244] N89-17251
Development of kinematic equations and determination of workspace of a 6 DOF end-effector with closed-kinematic chain mechanism
[NASA-CR-183241] N89-17444

ROCKET ENGINE CASES
Composite motor case design N89-16909
Design of filament-wound rocket cases N89-16910
Considerations for designers of cases for small solid propellant rocket motors N89-16911
Design and analysis of solid rocket motor internal insulation N89-16915

ROCKET ENGINE DESIGN
Missile intakes N89-16750
Design Methods in Solid Rocket Motors
[AGARD-LS-150-REV] N89-16906
Considerations for designers of cases for small solid propellant rocket motors N89-16911
Propellant grain design N89-16912

ROCKET EXHAUST
Plume spectrometry for liquid rocket engine health monitoring N89-16816

ROCKET NOZZLES
Advances in solid rocket nozzle design and analysis technology in the United States since 1970 N89-16907
Design and analysis of solid rocket motor nozzle N89-16908

ROCKET VEHICLES
The space-based interceptor
[DE89-002869] N89-17451

ROLL FORMING
Processing of 2090 aluminum alloy for superplasticity
[AD-A200425] N89-16975

ROLLING MOMENTS
Rolling moment derivative Lxi, for plain ailerons at subsonic speeds
[ESDU-88013] N89-16731

ROTARY WING AIRCRAFT
Vortex dynamics for rotorcraft interactional aerodynamics
[AD-A200128] N89-16726

ROTARY WINGS
Vortex dynamics for rotorcraft interactional aerodynamics
[AD-A200128] N89-16726
Aeroelastic optimization of a helicopter rotor N89-16778

ROTATING LIQUIDS
Investigation of liquid sloshing in spin-stabilized satellites
[AD-A199629] N89-16899

ROTATING SHAFTS
Parallel processing of a rotating shaft simulation
[NASA-TM-101462] N89-17453

ROTOR BLADES (TURBOMACHINERY)
Tip sensor development
[AD-A200080] N89-16824
Rotating hot-wire investigation of the vortex responsible for blade-vortex interaction noise
[NASA-CR-177454] N89-17466

RUN TIME (COMPUTERS)
Massive symbolic mathematical computations and their applications
[AD-A200253] N89-17434

RUPTURING
Thinning and rupture of a thin liquid film on a horizontal heated solid surface
[DE89-001792] N89-16944
Time and temperature dependence of strength in high performance ceramics N89-16998

S

SABOTAGE
Aviation security: A system's perspective
[DE89-002020] N89-16766

SAMPLING
Picosecond sampling of integrated circuits N89-17082
Electro-optic sampling of high-speed, InP-based integrated circuits N89-17084
An optically strobed sample and hold circuit N89-17087
Photoconductive generation of sub-picosecond electrical pulses and their measurement applications N89-17093
Comparison of sampling oscilloscopes with less than 35 ps transition durations N89-17108
A technique for wing suppressed IR sampling N89-17109
Accuracy assessment, using stratified plurality sampling, of portions of a LANDSAT classification of the Arctic National Wildlife Refuge Coastal Plain
[NASA-TM-101042] N89-17339

SANDWICH STRUCTURES
Elastic wrinkling of sandwich panels with laminated fibre reinforced face plates (face plates of AsBoDs, AsDIDs and AsBsDs types). (Computer program)
[ESDU-88015] N89-16930
Wrinkling of sandwich panel face plates (isotropic face plates on orthotropic cores, in-plane loading or bending)
[ESDU-88032] N89-16931

SATELLITE ATMOSPHERES
Sodium in Io's extended atmosphere N89-17559

SATELLITE COMMUNICATION
Propagation effects handbook for satellite systems design. A summary of propagation impairments on 10 to 100 GHz satellite links with techniques for system design
[NASA-RP-1082(04)] N89-17060
The potential impact of MMICs on future satellite communications
[NASA-CR-182227] N89-17078
The potential impact of MMICs on future satellite communications: Executive summary
[NASA-CR-182227-EXEC-SUMM] N89-17079

SATELLITE CONTROL
Control of reaction wheels through digital techniques using reference models
[INPE-4618-TDL/335] N89-16903

SATELLITE IMAGERY
Automatic registration of satellite imagery
[INPE-4637-PRE/1349] N89-17414

SATELLITE OBSERVATION
Presentation of the status of the experiment and mission activities of the Monocular Electro-Optical Stereo Scanner (MEOSS) --- Indian/German space cooperation N89-16888
Evaluation of satellite-tracked surface drifting buoys for simulating the movement of spilled oil in the marine environment. Volume 1: Executive summary
[PB88-226048] N89-17357
Evaluation of satellite-tracked surface drifting buoys for simulating the movement of spilled oil in the marine environment, volume 2
[PB88-226055] N89-17358
Limb-darkening functions as derived from along-track operation of the ERBE scanning radiometer for January 1985
[NASA-RP-1214] N89-17374

SATELLITE ORIENTATION
Investigation of liquid sloshing in spin-stabilized satellites
[AD-A199629] N89-16899

SATELLITE SOUNDING
High-resolution Interferometer Sounder (HIS), phase 2
[NASA-CR-183414] N89-17212

SATELLITE TRANSMISSION
Non return to zero (NRZ) clock recovery breadboard for 200 MB/S optical intersatellite link
[CNES-CT/DRT/TIT/TR-87/024] N89-17496

SATELLITE-BORNE PHOTOGRAPHY
German spaceborne remote sensing activities N89-16887

SAWTOOTH WAVEFORMS
Penetration effects of the compound vortex in gas metal-arc welding
[AD-A200585] N89-17242

SCALE EFFECT
On Reynolds number effects and simulation N89-16866

SCALING LAWS
IEEE P1596, a scalable coherent interface for gigabyte/sec multiprocessor applications
[DE89-002813] N89-17405
Investigation of collisional effects in the plasma erosion opening switch
[AD-A200319] N89-17507

SCANNERS
Presentation of the status of the experiment and mission activities of the Monocular Electro-Optical Stereo Scanner (MEOSS) --- Indian/German space cooperation N89-16888
Flow visualization by the PISTIL procedure (presentation of wake images by local computer processing). Test report 876/S-5 --- wake image representation by local computer treatment (PISTIL)
[REPT-876/S-5] N89-17203
Limb-darkening functions as derived from along-track operation of the ERBE scanning radiometer for January 1985
[NASA-RP-1214] N89-17374

SCATTERING
Effects of irregular sea surface and evaporation duct on radar detection performance
[AD-A200114] N89-17066
Scattering by a two dimensional groove in a ground plane
[NASA-CR-183087] N89-17077

SCATTERING CROSS SECTIONS
High energy laser beam scattering by atmospheric aerosol aureoles
[DE89-004811] N89-17230

SCHEDULING
Event-centered scheduling program: The need for PERT (Program Evaluation Review Technique) in C-141 ISO inspection management
[AD-A200094] N89-16718

SCHOTTKY DIODES
Characteristics, packaging and physics of ultra high speed diode lasers and detectors N89-17112

SCHROEDINGER EQUATION
Nonlocal and quasilocal potentials in the spontaneous emission of molecular exciplexes coupled to the phonon bath of a solid matrix
[AD-A200509] N89-17476

SEA BREEZE
A numerical modeling investigation of the effect of convective-mesoscale interactions on the sea breeze circulation N89-17377

SEA ICE
Profile properties of undeformed first-year sea ice
[AD-A200172] N89-17388
SEARCH RADAR
Effects of irregular sea surface and evaporation duct on radar detection performance
[AD-A200114] N89-17066
Machine learning of parameter control doctrine for sensor and communication systems
[AD-A200096] N89-17427
SECONDARY INJECTION
Design and analysis report for the flight weight 20-inch Columbium secondary nozzle for the RL10 engine
[NASA-CR-179612] N89-16918
SEDATIVES
Pharmacological resetting of the circadian sleep-wake cycle
[AD-A200246] N89-17396
SEGMENTS
Structural response of an advanced combustor liner: Test and analysis N89-17329
SEISMOLOGY
Strain accumulation in the Santa Barbara Channel, 1971-1987
[NASA-CR-183402] N89-17369
SELECTIVITY
Synthesis and analysis of novel polymers with potential for providing both high permselectivity and permeability in gas separation applications
[DE89-004325] N89-17014
SEMANTICS
3-D vision techniques for autonomous vehicles
[AD-A199643] N89-17236
Maintenance of database integrity in a scheme-less database system N89-17542
SEMICONDUCTOR DEVICES
Topical Meeting on Picosecond Electronics and Optoelectronics
[AD-A189686] N89-17080
PC-1D Version 2: Enhanced numerical solar cell modeling
[DE89-000302] N89-17349
Investigation of defect and electronic interactions associated with GaAs device processing
[AD-A200541] N89-17525
New Al-Ni-Ge contacts on GaAs: Their structure and electrical properties
[DE89-002918] N89-17526
SEMICONDUCTOR JUNCTIONS
Research on high-efficiency, single-junction, monolithic, thin-film amorphous silicon solar cells, phase 3
[DE89-000813] N89-17342
SEMICONDUCTOR LASERS
Characteristics, packaging and physics of ultra high speed diode lasers and detectors N89-17112
Frequency chirping in pulse modulated gain and real index guided single quantum well lasers N89-17113
Picosecond measurements of gain-switching in a semiconductor laser driven by ultrashort electrical pulses N89-17115
An investigation of the spectral characteristics of a commercially available semiconductor laser N89-17213
Precision transfer function measurements of integrated optical modulators
[DE89-004021] N89-17492
SEMICONDUCTORS (MATERIALS)
Direct subpicosecond measurement of carrier mobility of photoexcited electrons in GaAs N89-17118
Monte Carlo investigation of hot photoexcited electron relaxation in GaAs N89-17120
Longitudinally localized optical carrier injection for femtosecond transport studies N89-17121
Picosecond response of an optically controlled millimeter wave phase shifter N89-17135
Joint service electronics program: Research in electronics
[AD-A199659] N89-17140
Monte Carlo studies of nonlinear electron transport in 3-5 semiconductors
[AD-A199700] N89-17516
SENSITIVITY
The use of narrow gap line microelectrodes as sensitive and species selective gas chromatographic detectors
[AD-A200424] N89-16955
Pressure/temperature sensitive inorganic phosphors
[AD-A199718] N89-17000
Importance of sensitivity and reliability of NDI techniques on damage tolerance based life prediction of turbine discs N89-17257
Contrast sensitivity in Army aviator candidates: Cycloplegia effects and population norms
[AD-A200433] N89-17397
SEPARATED FLOW
Unsteady viscous flows over moving body
[AD-A200269] N89-17159
A computational method for three dimensional, internal viscous flows with separation and secondary flow patterns N89-17164
SEQUENCING
The reliable reduction of random local sequences for fatigue tests N89-17274
A procedure for the generation of load sequences N89-17276
Axioms for concurrent objects
[AD-A200584] N89-17435
SERVICE LIFE
Service life calculator for the M53 turbofan engine N89-16796
SERVOMECHANISMS
Integration of robotics and teleoperation for the advanced servomanipulator: Consolidated fuel reprocessing program
[DE88-015281] N89-17240
SHADOWGRAPH PHOTOGRAPHY
Aneurisms in laser-driven blast waves
[AD-A200189] N89-17222
SHAFTS (MACHINE ELEMENTS)
Fatigue behavior of shrink-bonded shaft-hub steel assemblies N89-17281
SHAPES
Center of buoyancy definition
[DE89-003017] N89-17457
The visual shape and multipole moments of the sun N89-17561
SHEAR STRESS
Approximation of viscoelastic stresses from Newtonian turbulent kinematics
[AD-A200188] N89-17157
SHELL STABILITY
The behavior of shells made of composites during the dynamic application of axian compression
[AD-A200244] N89-17266
SHELL THEORY
Origin and dynamics of expanding neutral hydrogen supershells
[DE88-704372] N89-17555
SHELLS (STRUCTURAL FORMS)
Hygrothermal deformations of laminated composite shells N89-16924
SHIELDING
Intake-airframe integration N89-16744
SHOCK LAYERS
Physical aspects of viscous simulation and associated research requirements N89-16865
SHOCK WAVE INTERACTION
Shock losses in transonic and supersonic compressor cascades N89-16829
SHOCK WAVES
Inviscid flow field analysis of complex reentry vehicles. Volume 1: Description of numerical methods
[DE89-002814] N89-16900
Investigations of the motion of discrete-velocity gases by cellular automata
[AD-A200221] N89-17158
Application of a two-equation turbulence mix model
[DE89-004812] N89-17205
Mix experiments with the NOVA laser
[DE89-004775] N89-17228
SIGNAL DETECTION
Picosecond optical autocorrelation experiments on fast photodetectors N89-17117
SIGNAL DETECTORS
Tip sensor development
[AD-A200080] N89-16824
Array processing for a multiple-rank signal
[AD-A197954] N89-17062
SIGNAL PROCESSING
Gas path condition monitoring using electrostatic techniques N89-16817
Tip clearance signal processor development
[AD-A199830] N89-16822
Array processing for a multiple-rank signal
[AD-A197954] N89-17062
Topical Meeting on Picosecond Electronics and Optoelectronics
[AD-A189686] N89-17080
Picosecond electrical pulses for VLSI electronics characterization N89-17083
An optically strobed sample and hold circuit N89-17087
Millimeter-wave integrated circuits N89-17089
Photoconductive generation of sub-picosecond electrical pulses and their measurement applications N89-17093
Picosecond switching in Josephson tunnel junctions N89-17095
High speed, high repetition rate, high voltage photoconductive switching N89-17096
A simple technique to generate or gate microwave pulses with picosecond speeds N89-17099
Comparison of sampling oscilloscopes with less than 35 ps transition durations N89-17108
MESFET compatible IMSM detectors N89-17116
Dynamics of below-gap photoexcitation in GaAs quantum wells N89-17130
Radar and EW applications of multi-gigahertz optical components and systems N89-17131
Characteristics and applications of wideband guided-wave devices N89-17132
A new optoelectronic CW microwave source N89-17133
Optical modulation above 20 GHz using a waveguide electro-optic switch N89-17134
Joint service electronics program: Research in electronics
[AD-A199659] N89-17140
Signal acquisition and processing for autonomous space shuttle cargo bay acoustic measurements (NASA G-313)
[AD-A200426] N89-17462
SIGNAL TRANSMISSION
Radar and EW applications of multi-gigahertz optical components and systems N89-17131
SILANES
Structure and properties of polymer interphases
[AD-A200238] N89-17008
SILICIDES
Mechanical characterization of SiC whisker-reinforced MoSi
[DE89-003486] N89-16933
SILICON
Electric conductivity of polymer composite materials. Composite on propylene and silicon base
[DE88-704293] N89-17001
Silicon pulse sharpening diodes: Switching kilovolts in tens of picoseconds N89-17139
Characteristics of lift-off fabricated AlGaAs/InGaAs single-strained-quantum-well structures on glass and silicon substrates
[DE89-001374] N89-17532
SILICON CARBIDES
Investigation of microstructural factors that cause low fracture toughness in silicon carbide whisker/Al alloy composites
[AD-A200147] N89-16925
Microanalytical characterization of wear damage in an alumina-silicon carbide whisker composite
[DE89-003149] N89-16932
Mechanical characterization of SiC whisker-reinforced MoSi
[DE89-003486] N89-16933
Ceramic-ceramic composites for use at high temperature N89-16994
Development of composite high temperature materials for future energy conversion applications N89-16995
SILICON FILMS
Characteristics of lift-off fabricated AlGaAs/InGaAs single-strained-quantum-well structures on glass and silicon substrates
[DE89-001374] N89-17532
SILICON JUNCTIONS
One/f noise in silicon devices
[ISBN-90-9002080-2] N89-17150
SILICON NITRIDES
Time and temperature dependence of strength in high performance ceramics N89-16998
Fractal and spherulitic morphology of silicon nitride crystallized from amorphous films
[AD-A200158] N89-17522
SIMULATION
Accuracy requirements for high-speed test with engine simulation on transport aircraft models in the NLR-HST N89-16870
Numerical study of two-stage light-gas hypervelocity projectile launchers
[UTIAS-327] N89-16894
Investigation of collisional effects in the plasma erosion opening switch
[AD-A200319] N89-17507
SIMULATORS
Inertial navigation system simulator: Behavioral specification
[AD-A200604] N89-16771
Engine simulator tests: Comparison of calibration and wind tunnel results N89-16871
Functional performance specification for an external computer system simulator
[AD-A200611] N89-16881
Heat transfer in the tip region of a rotor blade simulator N89-17312
SINE WAVES
The interaction of a fluid interface with a vortex pair
[AD-A200167] N89-17156

SINGLE CRYSTALS
Magnetization, transport and structural studies of Tl-Ca-Ba-Cu-O: Bulk ceramics, single crystals, and polycrystalline thin films
[DE89-003264] N89-17010
Anisotropic constitutive modeling for nickel base single crystal superalloy Rene N4 at 982 C N89-17324
Constitutive modelling of single crystal and directionally solidified superalloys N89-17325
High temperature constitutive and crack initiation modeling of coated single crystal superalloys N89-17334
The annealing behavior of ion-implanted single crystals of the type YBa2Cu3O(sub x)
[DE89-002189] N89-17519
SIZE DISTRIBUTION
Simultaneous measurements of droplet size and droplet velocity in monodisperse droplet streams N89-17192
SKIN FRICTION
A model for transition by attachment line contamination and an examination of cross-flow instability in three-dimensional boundary layers N89-17153
SKY WAVES
A technique for recording HF (High Frequency) oblique-incidence-sounder data
[AD-A200168] N89-17068
SLEEP
Sleep and wakefulness: Handbook for flight medical officers, 2nd edition
[AGARD-AG-270(F)] N89-17399
SLEEP DEPRIVATION
Pharmacological resetting of the circadian sleep-wake cycle
[AD-A200246] N89-17396
Sleep and wakefulness: Handbook for flight medical officers, 2nd edition
[AGARD-AG-270(F)] N89-17399
SLIDING FRICTION
Microanalytical characterization of wear damage in an alumina-silicon carbide whisker composite
[DE89-003149] N89-16932
Unlubricated sliding properties of ion beam and excimer laser mixed Fe-Ti-C multilayered films
[DE89-003470] N89-17245
SLOPES
Normal-force-curve and pitching-moment-curve slopes for tangent-ogive forebody-cylinder combinations at zero angle of attack
[ESDU-88026] N89-16733
An experimental investigation of the aerodynamic characteristics of slanted base ogive cylinders using magnetic suspension technology
[NASA-CR-184624] N89-16758
SODIUM
Sodium in Io's extended atmosphere N89-17559
SOFTENING
The effects of strain induced softening on the load carrying capability of components N89-17264
SOFTWARE ENGINEERING
Improving software quality through hierarchical design
[DE88-014919] N89-17412
Maintenance of database integrity in a scheme-less database system N89-17542
SOFTWARE TOOLS
Massive symbolic mathematical computations and their applications
[AD-A200253] N89-17434
SOILS
Measurements of micrometeorological parameters for testing large scale models
[NASA-CR-184766] N89-17384
SOLAR CELLS
Device physics related to the granular nature of CuInSe2 solar cells
[DE89-000810] N89-17341
Research on high-efficiency, single-junction, monolithic, thin-film amorphous silicon solar cells, phase 3
[DE89-000813] N89-17342
Thermal degradation mechanisms in GaAs solar cells with high-temperature contacts
[DE89-001375] N89-17343
Concentrator efficiencies of 29.2 percent for a GaAs cell and 24.8 percent for a mounted cell-lens assembly
[DE89-001612] N89-17344
Recent advances in high-efficiency InGaAs concentrator cells
[DE89-001613] N89-17345
Thermally conductive alumina/organic composites for photovoltaic concentrator cell isolation
[DE89-001181] N89-17346
A performance model for nonuniformly illuminated front-gridded concentrator cells
[DE89-001368] N89-17347
A microprocessor-based, solar cell parameter measurement system
[AD-A200227] N89-17348
PC-1D Version 2: Enhanced numerical solar cell modeling
[DE89-000302] N89-17349
The effect of different module configurations on the radiation tolerance of multijunction solar cells
[NASA-TM-101251] N89-17356
SOLAR COLLECTORS
Preliminary study of creep thresholds and thermomechanical response in Haynes 188 at temperatures in the range 649 to 871 C N89-17327
Thermally conductive alumina/organic composites for photovoltaic concentrator cell isolation
[DE89-001181] N89-17346
A performance model for nonuniformly illuminated front-gridded concentrator cells
[DE89-001368] N89-17347
The effect of different module configurations on the radiation tolerance of multijunction solar cells
[NASA-TM-101251] N89-17356
SOLAR FLARES
Meteorites and lunar samples as space probes --- Indian/German space cooperation N89-16885
SOLAR GENERATORS
Systems analysis and design of a lunar solar power plant for the supply of a lunar base
[ILR-MITT-198] N89-17355
SOLAR SYSTEM
The role of presolar dust in the formation of the solar system N89-17553
SOLENOIDS
Assessment of nonintrusive methods for monitoring the operational readiness of solenoid-operated valves
[DE89-002330] N89-17244
SOLID NITROGEN
The 15N CP/MAS NMR of aramids: A tool for characterization of the morphology of high modulus fibers for composites
[AD-A199656] N89-16921
SOLID PROPELLANT ROCKET ENGINES
Design Methods in Solid Rocket Motors
[AGARD-LS-150-REV] N89-16906
Advances in solid rocket nozzle design and analysis technology in the United States since 1970 N89-16907
Design and analysis of solid rocket motor nozzle N89-16908
Composite motor case design N89-16909
Considerations for designers of cases for small solid propellant rocket motors N89-16911
Propellant grain design N89-16912
Overall optimization of solid rocket motor N89-16916
SOLID PROPELLANTS
Numerical study of two-stage light-gas hypervelocity projectile launchers
[UTIAS-327] N89-16894
SOLID ROCKET PROPELLANTS
Design Methods in Solid Rocket Motors
[AGARD-LS-150-REV] N89-16906
Propellant grain design N89-16912
Solid propellant grain design N89-16913
State of the art of solid propellant rocket motor grain design in the United States N89-16914
SOLID STATE
Synthesis and properties of new preceramic materials
[DE89-003436] N89-17012
SOLID STATE DEVICES
Topical Meeting on Picosecond Electronics and Optoelectronics
[AD-A189686] N89-17080
SOLID SURFACES
Thinning and rupture of a thin liquid film on a horizontal heated solid surface
[DE89-001792] N89-16944
SOLIDIFICATION
The effect of chemistry modifications on the solidification behavior and weldability of Alloy 625
[DE89-001046] N89-16972
SOLIDS
Role of charge exchange process in forming of ion charge and energy states in multicomponent laser plasma produced from gas-content solids
[DE88-704828] N89-17511
SOLITARY WAVES
Observations of a thunderstorm generated gust compared with solitary wave theory
[AD-A200087] N89-17379
SONDES
Gyroscopic testing of accelerometers to determine coning angle
[AD-A200126] N89-17209
SOOT
Measurements of gas turbine combustor and engine augmentor tube sooting characteristics
[AD-A199768] N89-16821
Investigation of fuel additive effects on sooting flames
[AD-A200273] N89-16948
SOS (SEMICONDUCTORS)
Investigation of photoconductive picosecond microstripline switches on self-implanted Silicon On Sapphire (SOS) N89-17104
Carrier lifetime versus ion-implantation dose in silicon on sapphire N89-17106
SOUND GENERATORS
Signal acquisition and processing for autonomous space shuttle cargo bay acoustic measurements (NASA G-313)
[AD-A200426] N89-17462
SOUND WAVES
Acoustic wave propagation by finite elements and time step integration N89-17460
Signal acquisition and processing for autonomous space shuttle cargo bay acoustic measurements (NASA G-313)
[AD-A200426] N89-17462
SOUNDING
A technique for recording HF (High Frequency) oblique-incidence-sounder data
[AD-A200168] N89-17068
SOUNDING ROCKETS
Microgravity rockets in Sweden N89-17021
Advanced research rockets for long duration microgravity science N89-17026
The use of sounding rockets in the study of microgravity cell biology N89-17036
A Canadian low earth orbit launch vehicle: Launch vehicle performance analysis of Black Brant VC and Nihka rocket motor configurations N89-17039
SPACE CHARGE
Induction-linac based free-electron laser amplifier for fusion applications
[DE89-001923] N89-17217
SPACE EXPLORATION
Project Longshot: An unmanned probe to Alpha Centauri
[NASA-CR-184718] N89-16904
SPACE MISSIONS
Mission under SROSS program and position paper on SROSS-2 with MEOSS payload --- Indian/German space cooperation N89-16889
Status of Sabrex N89-16890
Autonomous payload control experiment on SROSS-3, a status review --- Indian/German space cooperation N89-16891
SPACE POWER REACTORS
Refractory metal alloys and composites for space nuclear power systems
[NASA-TM-101364] N89-16986
SPACE PROBES
Project Longshot: An unmanned probe to Alpha Centauri
[NASA-CR-184718] N89-16904
SPACE PROCESSING
High temperature material processing system for KC-135 microgravity experiments N89-17040
SPACE SHUTTLE MAIN ENGINE
Engine Condition Monitoring: Technology and Experience
[AGARD-CP-448] N89-16780
Space shuttle main engine monitoring experience and advanced monitoring systems development N89-16815
Plume spectrometry for liquid rocket engine health monitoring N89-16816
SPACE SHUTTLE PAYLOADS
Development of an infrared imaging system for the surface tension driven convection experiment
[NASA-TM-101479] N89-17211
SPACE SHUTTLES
Analysis and design of a universal shuttle for rockets
[ILR-MITT-199] N89-16897
Signal acquisition and processing for autonomous space shuttle cargo bay acoustic measurements (NASA G-313)
[AD-A200426] N89-17462
SPACE STATIONS
Modifications to the NASA Ames Space Station Proximity Operations (PROX OPS) Simulator
[NASA-CR-177510] N89-16896
The space station integrated refuse management system
[NASA-CR-184722] N89-17403
SPACE TRANSPORTATION SYSTEM
Analysis and design of a universal shuttle for rockets
[ILR-MITT-199] N89-16897
SPACE WEAPONS
The space-based interceptor
[DE89-002869] N89-17451
Report of the Defense Science Board Task Force Subgroup on Strategic Air Defense (SDI Milestone Panel)
[AD-A200164] N89-17452
SPACEBORNE EXPERIMENTS
Workshop on Microgravity Experimentation in Aircraft and Rockets
[NRCC-29151] N89-17019

Development of an infrared imaging system for the surface tension driven convection experiment
[NASA-TM-101479] N89-17211

SPACECRAFT COMMUNICATION
Effects of depolarization obtained by specular reflection on metallic mirrors: Applications to laser telecommunication and to Earth observation
[CNES-CT/DRT/TIT/IO-87/150] N89-17494
Optical communication. Four quadrant avalanche detector. Modeling, theoretical results and comparison with experimental values
[CNES-CT/DRT/TIT/IO-87/086] N89-17495

SPACECRAFT COMPONENTS
Capillary pumping for a two phase heat transport system --- space stations N89-17172

SPACECRAFT EQUIPMENT
Autonomous payload control experiment on SROSS-3, a status review --- Indian/German space cooperation N89-16891

SPACECRAFT POWER SUPPLIES
NASA photovoltaic research and technology
[NASA-TM-101422] N89-16917
The two-beam accelerator and the relativistic klystron power source
[DE89-002673] N89-17485

SPACECRAFT PROPULSION
Laser thermal propulsion
[AD-A200558] N89-17226

SPACECRAFT TEMPERATURE
Capillary pumping for a two phase heat transport system --- space stations N89-17172

SPACECRAFT TRAJECTORIES
User and technical documentation
[NASA-CR-172087] N89-16893

SPARE PARTS
A model of the effect of sparing and repair turnaround time of the inertial navigation system on aircraft readiness for the F/A-18
[AD-A200317] N89-16777

SPARK IGNITION
Experimental validation of a zero-dimensional computer model for spark-ignition engines
[DE89-002848] N89-17243
Emission-reduction effects of methanol vehicles: State of knowledge
[DE89-001148] N89-17359

SPATIAL DISTRIBUTION
Role of retinocortical processing in spatial vision
[AD-A200198] N89-17394
Origin and dynamics of expanding neutral hydrogen supershells
[DE88-704372] N89-17555

SPATIAL FILTERING
Application of a spatial filter velocimeter to the two phase flows in a Spark Ignition (SI) N89-17199

SPATIAL RESOLUTION
Spatial reasoning in the treatment of systematic sensor errors
[DE89-003244] N89-17251

SPECIFICATIONS
Small reactors for low-temperature nuclear heat applications
[DE88-704336] N89-17484

SPECKLE PATTERNS
Particle Image Displacement Velocimetry --- conference
[VKI-LS-1988-06] N89-17179
Practical systems for speckle velocimetry N89-17185
Speckle photography of flows with varying fluid density N89-17186
Digital direct analysis of a multiexposed photograph in Particle Image Displacement Velocimetry (PIDV) N89-17194
Measurement of natural convection by white light speckle velocimetry N89-17197

SPECTRAL EMISSION
Pressure/temperature sensitive inorganic phosphors
[AD-A199718] N89-17000

SPECTRAL LINE WIDTH
An investigation of the spectral characteristics of a commercially available semiconductor laser N89-17213

SPECTRAL METHODS
On-line spectrum loading accuracy verification N89-17292

SPECTRAL REFLECTANCE
An in situ surface Fourier transform study of complexes of lithium, magnesium potassium and lanthanum ferrocyanide at platinum and gold electrodes
[AD-A200305] N89-16950

SPECTROMETERS
Analysis of low alloy and stainless steels by inductively coupled argon plasma spectrometer
[DE89-003227] N89-16978
Phototype design and testing of two fiber-optic spectrochemical emission sensors
[DE89-001741] N89-17207

SPECTROSCOPY
Plume spectrometry for liquid rocket engine health monitoring N89-16816
Molecular spectroscopy at corrugated metal surfaces
[AD-A200124] N89-16973
Photodeflection and photoconductivity studies in ceramics
[DE89-002186] N89-17003

SPECTRUM ANALYSIS
Frequency estimation of radar signals using an acousto-optic spectrum analyzer as an RESM (Radar Electronic Support Measures) receiver
[AD-A200159] N89-17067

SPECULAR REFLECTION
Effects of depolarization obtained by specular reflection on metallic mirrors: Applications to laser telecommunication and to Earth observation
[CNES-CT/DRT/TIT/IO-87/150] N89-17494

SPHERES
Concentricity and sphericity of composite drops under microgravity N89-17042

SPHEROIDS
Scattering power of seed materials: Mie scattering calculations N89-17181

SPHERULITES
Fractal and spherulitic morphology of silicon nitride crystallized from amorphous films
[AD-A200158] N89-17522

SPILLING
Source characterization of heavy gas dispersion models for reactive chemicals, volume 1
[AD-A200121] N89-17361

SPIN DYNAMICS
Gyroscopic testing of accelerometers to determine coning angle
[AD-A200126] N89-17209
On the experimental basis of the Pauli exclusive principle
[DE88-704366] N89-17477

SPIN STABILIZATION
Investigation of liquid sloshing in spin-stabilized satellites
[AD-A199629] N89-16899
Gyroscopic testing of accelerometers to determine coning angle
[AD-A200126] N89-17209

SPONTANEOUS EMISSION
Nonlocal and quasilocal potentials in the spontaneous emission of molecular exciplexes coupled to the phonon bath of a solid matrix
[AD-A200509] N89-17476

SPOT WELDS
Surface deformations resulting from laser spot welding
[DE88-014964] N89-17237

SPRAY CHARACTERISTICS
Simultaneous measurements of droplet size and droplet velocity in monodisperse droplet streams N89-17192

SPRAYED COATINGS
Thermal barrier coating life-prediction model development N89-17331
Thermal barrier coating life prediction model N89-17332
Thermal barrier coating life prediction model development N89-17333

SPREAD SPECTRUM TRANSMISSION
Vector space approach to narrowband interference excision
[AD-A199703] N89-17063
Capacity of frequency-hop spread-spectrum multiple-access communication systems
[AD-A200616] N89-17073

SPRINGS (ELASTIC)
Strength evaluation for fiber reinforced composite leaf springs under mechanical and environment conditioned loads N89-17277

SPUTTERING
A high-intensity plasma sputter heavy negative ion source
[DE89-003113] N89-17480
Optical fiber science and technology: Novel fibers and fiber sensors
[AD-A200311] N89-17489

STAINLESS STEELS
Analysis of low alloy and stainless steels by inductively coupled argon plasma spectrometer
[DE89-003227] N89-16978
Quantitative measurement and modeling of sensitization development in stainless steels
[DE89-004646] N89-16990
Unlubricated sliding properties of ion beam and excimer laser mixed Fe-Ti-C multilayered films
[DE89-003470] N89-17245

STANDARDS
Thermophysical property measurements in fluid mixtures
[DE89-003281] N89-16961
Need for common AGARD approach and actions N89-17260
R/M/T (Reliability/Maintainability/Testability) design for fault tolerance. Volume 1: Program manager's guide
[AD-A200204] N89-17262
A comparison of two whole-body vibration standards as applied to rotary-wing aircraft: ISO (International Standards Organization) 2631 vs ADS (Aeronautical Design Standards) 27
[AD-A200430] N89-17402
Floating-point standards: Theory and practice
[DE89-003598] N89-17439

STAR FORMATION
Origin and dynamics of expanding neutral hydrogen supershells
[DE88-704372] N89-17555

STARK EFFECT
Quantum-confined Stark effect in InGaAs/InP quantum wells grown by metal-organic chemical vapor deposition N89-17129

STATE ESTIMATION
The Kalman filter
[ESDU-88039] N89-17437
Force state mapping using experimental data
[DE89-000351] N89-17442

STATIC ELECTRICITY
Electrical properties of atmospheric moist air: A systematic, experimental study
[AD-A199599] N89-17370

STATISTICAL ANALYSIS
CF-18/F404 transient performance trending N89-16814
Frequency estimation of radar signals using an acousto-optic spectrum analyzer as an RESM (Radar Electronic Support Measures) receiver
[AD-A200159] N89-17067
HANDYPAK: A histogram and display package
[DE89-002742] N89-17413

STATISTICAL CORRELATION
A procedure for the generation of load sequences N89-17276

STATISTICAL DISTRIBUTIONS
Distributed estimation for large-scale event-driven systems
[DE89-002688] N89-17447

STATISTICAL MECHANICS
A statistical theory for gas surface interactions in rarefied hypersonic flows
[IC-AERO-88-01] N89-16755
The electronic structure and the state of compositional order in metallic alloys
[DE89-003147] N89-16977
Statistical mechanics of polymer systems
[DE89-002012] N89-17002
Relativistically-invariant statistical hydrodynamics of a normal fluid
[DE88-704370] N89-17161
Is there a statistical mechanics of turbulence
[DE89-003471] N89-17162

STEADY STATE
The behavior of microdisks and microring electrodes. Applications of Neumann's integral theorem
[AD-A200307] N89-16951
The behavior of microdisks and micoring electrodes. Prediction of the amperometric response of microdisks and of the steady state for CE and EC Catalytic reactions by application of Neumann's integral theorem
[AD-A200415] N89-16952

STEEL STRUCTURES
Fatigue behavior of shrink-bonded shaft-hub steel assemblies N89-17281

STEELS
Kinetics and mechanisms of hydrogen attack in 2.25Cr-1Mo steel
[DE89-001381] N89-16970
Nitride and carbide coatings for high speed steel cutting tools
[DE89-003623] N89-16984
Structure and properties of polymer interphases
[AD-A200238] N89-17008

STEREOPHOTOGRAPHY
Application of Particle Image Displacement Velocimetry (PIDV) to complex flows: Measurements of the third component N89-17188
Digital direct analysis of a multiexposed photograph in Particle Image Displacement Velocimetry (PIDV) N89-17194

STEREOSCOPY
Presentation of the status of the experiment and mission activities of the Monocular Electro-Optical Stereo Scanner (MEOSS) --- Indian/German space cooperation N89-16888

STOCHASTIC PROCESSES
Stochastic description of porous media N89-17168
Probabilistic modeling of Particle Image Displacement Velocimetry (PIDV) experiments N89-17190

Stochastic modeling of crack initiation and short-crack growth under creep and creep-fatigue conditions [NASA-TM-101358] N89-17286
Prediction of stochastic blade responses using measured wind-speed data as input to the FLAP code [DE89-000834] N89-17354
On a class of nonstationary stochastic processes [NASA-TM-101195] N89-17448

STOICHIOMETRY
The annealing behavior of ion-implanted single crystals of the type YBa2Cu3O(sub x) [DE89-002189] N89-17519

STORAGE BATTERIES
An investigation of the rechargeability of certain modified forms of MnO2 [AD-A199885] N89-16943
New secondary batteries utilizing electronically conductive polymer cathodes [NASA-CR-183248] N89-17149

STORMS
On deriving the three-dimensional kinematic structure on convective storms from a single radar N89-17376
New England mountain icing climatology [AD-A200267] N89-17381
World-wide extreme wind speeds. Part 2: Examples using various methods of analysis [ESDU-88037] N89-17382

STRAIN GAGES
Development of a high temperature thin film static strain gage N89-17299
Elevated temperature strain gages N89-17300
Progress on a PdCr wire strain gage N89-17301

STRAIN MEASUREMENT
Progress on a PdCr wire strain gage N89-17301

STRAIN RATE
Use of inelastic strain as a basis for analyzing thermomechanical test data N89-17326

STREAK CAMERAS
A photon-counting, subnanosecond, imaging camera for X-ray detection [DE89-002874] N89-17208

STRESS (PSYCHOLOGY)
A strategy for understanding noise-induced annoyance [AD-A200125] N89-17461

STRESS ANALYSIS
A multiaxial strength criterion for composites [AD-A199610] N89-16920
Wrinkling of sandwich panel face plates (isotropic face plates on orthotropic cores, in-plane loading or bending) [ESDU-88032] N89-16931
Effect of fretting on fatigue strength of titanium alloys [ESDU-88027] N89-16981
Stress driven diffusive voiding of aluminum conductor lines: A model for time dependent failure [DE89-001665] N89-17144
The design of spur and helical involute gears. A procedure compatible with BS 436:1986: Method for calculation of contact and root bending stress limitations for metallic involute gears [ESDU-88033] N89-17247
Numerical and theoretical study of elastoplastic dynamic buckling [ETN-89-93614] N89-17284
Preliminary fatigue tests on short-crack specimens N89-17290
Three-dimensional inelastic analysis for hot section components, BEST 3D code N89-17317
Component specific modeling N89-17320
Generalized finite strains, generalized stresses, and a hybrid variational principle for finite-element computer programs [DE89-002101] N89-17430
Generalized finite strains, generalized stresses, and a principle of virtual work for finite-element computer programs [DE89-002102] N89-17431

STRESS CORROSION CRACKING
Quantitative measurement and modeling of sensitization development in stainless steels [DE89-004646] N89-16990

STRESS INTENSITY FACTORS
Approximate stress-intensity factors for a surface crack and through crack at a semi-circular notch N89-17294
Long-crack growth rate data: Constant amplitude and FALSTAFF loading N89-17295

STRESS TENSORS
A multiaxial strength criterion for composites [AD-A199610] N89-16920
Generalized finite strains, generalized stresses, and a principle of virtual work for finite-element computer programs [DE89-002102] N89-17431

STRESS-STRAIN RELATIONSHIPS
Total strain version of strainrange partitioning for thermomechanical fatigue at low strains N89-17337

STRESSES
Time and temperature dependence of strength in high performance ceramics N89-16998
Avoidance of buckling of some engineering elements (struts, plates and gussets) [ESDU-88034] N89-17269
Initial structural response measurements for the Sandia 34-meter VAWT test bed [DE89-003133] N89-17352
Generalized finite strains, generalized stresses, and a hybrid variational principle for finite-element computer programs [DE89-002101] N89-17430
Generalized finite strains, generalized stresses, and a principle of virtual work for finite-element computer programs [DE89-002102] N89-17431

STRING THEORY
An essay on discrete foundations for physics [DE89-002992] N89-17556

STRIP TRANSMISSION LINES
Millimeter wave generation using Josephson junction arrays [AD-A200259] N89-17524

STROBOSCOPES
An optically strobed sample and hold circuit N89-17087

STRONGLY COUPLED PLASMAS
Aneurisms in laser-driven blast waves [AD-A200189] N89-17222
Model microfield calculations of radiative and transport properties of ions in strongly coupled plasmas [DE89-001244] N89-17503

STRUCTURAL ANALYSIS
Processing of 2090 aluminum alloy for superplasticity [AD-A200425] N89-16975
Development of conducting polymers of high structural strength [AD-A200310] N89-17009
Vibration and aeroelastic tailoring of advanced composite plate-like lifting surfaces N89-17263
Turbine Engine Hot Section Technology, 1987 [NASA-CP-2493] N89-17298
Three-dimensional inelastic analysis methods for hot section components N89-17316
Three-dimensional inelastic analysis for hot section components, BEST 3D code N89-17317
Response characteristics of MHOST (MARC Hot-Section Technology) for 3-D inelastic analysis of hot-section components N89-17318
Mechanics of materials model N89-17319
Three-dimensional inelastic analysis methods for hot section components N89-17321
Constitutive modeling for isotropic materials N89-17322
A continuum deformation theory for metal-matrix composites at high temperature N89-17323
Use of inelastic strain as a basis for analyzing thermomechanical test data N89-17326
Structural response of an advanced combustor liner: Test and analysis N89-17329
Equivalent linearization for fatigue life estimates of a nonlinear structure [NASA-TM-101536] N89-17467

STRUCTURAL DESIGN
Mechanical design of a RF electron gun [DE89-004890] N89-16895
Characteristics and applications of wideband guided-wave devices N89-17132
AGARD/SMP Review: Damage Tolerance for Engine Structures. 1: Non-Destructive Evaluation [AGARD-R-768] N89-17253
The impact of engineering assumptions on NDE requirements N89-17254

STRUCTURAL MEMBERS
Mechanistic studies of pressure-assisted superplasticity of structural ceramics [AD-A200202] N89-17006

STRUCTURAL STABILITY
Aeroelastic optimization of a helicopter rotor N89-16778
Spillover stabilization in the control of large flexible space structures N89-16902
High-precision gravity network to monitor temporal variations in gravity across Yucca Mountain, Nevada [DE89-005023] N89-17373

STRUCTURAL VIBRATION
Vibration and aeroelastic tailoring of advanced composite plate-like lifting surfaces N89-17263

STRUTS
Avoidance of buckling of some engineering elements (struts, plates and gussets) [ESDU-88034] N89-17269

SUBCRITICAL FLOW
Boundaries of linear characteristics of cambered and twisted wings at subcritical Mach numbers [ESDU-88030] N89-16735

SUBROUTINES
User and technical documentation [NASA-CR-172087] N89-16893

SUBSONIC FLOW
CFD application to subsonic inlet airframe integration --- computational fluid dynamics (CFD) N89-16753

SUBSONIC SPEED
Rolling moment derivative Lxi, for plain ailerons at subsonic speeds [ESDU-88013] N89-16731
Yawing moment coefficient for plain ailerons at subonic speeds [ESDU-88029] N89-16734

SUBSTRATES
Gas jet deposition of multicomponent ultrafine microstructures [AD-A200101] N89-16946
Characteristics of lift-off fabricated AlGaAs/InGaAs single-strained-quantum-well structures on glass and silicon substrates [DE89-001374] N89-17532

SULFUR FLUORIDES
Modeling the propagation of long intense microwave pulses in mixtures of air and SF6 [DE89-004787] N89-17076

SUN
The visual shape and multipole moments of the sun N89-17561

SUPERCONDUCTING MAGNETS
Radiation imposed limits on superconducting magnets: A data base for copper stabilizers [DE89-002875] N89-17456

SUPERCONDUCTIVITY
Electronic behavior of highly correlated metals [DE89-002492] N89-16971
Magnetization, transport and structural studies of Tl-Ca-Ba-Cu-O: Bulk ceramics, single crystals, and polycrystalline thin films [DE89-003264] N89-17010
The annealing behavior of ion-implanted single crystals of the type YBa2Cu3O(sub x) [DE89-002189] N89-17519
A simple method for preparing superconducting high T(sub c) thin films [DE89-003663] N89-17527
Oxygen and copper valencies in oxygen-doped superconducting La2CuO(sub 4.13) [DE89-003265] N89-17533

SUPERCONDUCTORS
Interaction of CO, CO2 and H2O with Ba and YBa2Cu3O7 [DE89-003160] N89-17528
Processing of strong flux trapping high T(subc) oxide superconductors: Center director's discretionary fund [NASA-TM-100350] N89-17530

SUPERCRITICAL FLOW
Supercritical flow past a symmetrical bicircular arc airfoil [NASA-CR-184787] N89-16762
Inverse methods for blade design, controlled diffusion blading for supercritical compressor flow N89-16832
Evaluation of a supercritical fluid chromatograph coupled to a surface-wave-sustained microwave-induced plasma detector [AD-A198728] N89-16937

SUPERCRITICAL FLUIDS
Evaluation of a supercritical fluid chromatograph coupled to a surface-wave-sustained microwave-induced plasma detector [AD-A198728] N89-16937

SUPERLATTICES
High temperature properties of ceramic/carbon systems in an oxidizing environment [AD-A200254] N89-16928
Molecular Beam Epitaxy (MBE) for high speed devices N89-17085

SUPERPLASTICITY
Mechanistic studies of pressure-assisted superplasticity of structural ceramics [AD-A200202] N89-17006

SUPERSONIC AIRCRAFT
Supersonic through-flow fan assessment [NASA-CR-182202] N89-16843
Instantaneous force measurement on a model subjected to rapid control variations N89-16872

SUPERSONIC COMPRESSORS
Incidence angle rules in supersonic cascades N89-16827
Exit angle rules in supersonic cascades N89-16828
Shock losses in transonic and supersonic compressor cascades N89-16829

Axial velocity density ratio influence on exit flow angle in transonic/supersonic cascades N89-16830
Supersonic compressors N89-16836
Supersonic throughflow fans N89-16837
Variable geometry in supersonic compressors N89-16838

SUPERSONIC FLIGHT
Inlet-engine compatibility N89-16741
Supersonic throughflow fans N89-16837

SUPERSONIC FLOW
Development and application of oxygen flow tagging for velocity measurements and flow visualization in turbulent three-dimensional supersonic flows [AD-A200119] N89-16725
Inviscid flow field analysis of complex reentry vehicles. Volume 1: Description of numerical methods [DE89-002814] N89-16900

SUPERSONIC FLUTTER
Use of holography in vibration and flutter study of fans N89-16842

SUPERSONIC INLETS
Intake Aerodynamics, volume 1 --- conference [VKI-LS-1988-04-VOL-1] N89-16738
Intake swirl and simplified methods for dynamic pressure distortion assessment N89-16742
Jaguar/Tornado intake design N89-16743
Intakes for high angle of attack N89-16745
Transonic cowl design N89-16746
CFD application to supersonic/hypersonic inlet airframe integration --- computational fluid dynamics (CFD) N89-16754
Variable geometry in supersonic compressors N89-16838
Axial supersonic inlet compound N89-16839

SUPERSONIC JET FLOW
Propulsive-jet flow field analysis using the three-dimensional Navier-Stokes equations [NASA-CR-177508] N89-16764

SUPERSONIC SPEED
Development and application of oxygen flow tagging for velocity measurements and flow visualization in turbulent three-dimensional supersonic flows [AD-A200119] N89-16725

SUPERSYMMETRY
Supersymmetric instantons and topological quantum field theory [DE88-704211] N89-17536

SUPPORTS
The use of computational fluid dynamic methods to assess the effects of model support systems and working section modifications on the flow around wind tunnel models N89-16862

SURFACE CRACKS
Approximate stress-intensity factors for a surface crack and through crack at a semi-circular notch N89-17294

SURFACE FINISHING
Hard material cutting technology described N89-17049
Use of cataphoresis effects discussed N89-17052
Ultrasonic vibration method discussed N89-17053
Review of precision surface generating processes and their potential application to the fabrication of large optical components [DE89-001712] N89-17486

SURFACE PROPERTIES
Selectivity of the reactions of oxygenates on transition metal surfaces [DE89-003691] N89-16985
Derivation and application of a class of generalized impedance boundary conditions, part 2 [NASA-CR-183298] N89-17148
Laser studies of the SiH radical/surface interaction during deposition of a thin film [DE89-003902] N89-17232
Surface deformations resulting from laser spot welding [DE88-014964] N89-17237
Approximate stress-intensity factors for a surface crack and through crack at a semi-circular notch N89-17294

SURFACE REACTIONS
Studies of metal/carbon surface chemistry [DE88-011264] N89-16960
In-situ surface during laser-controlled chemical processing of surfaces [AD-A200206] N89-17223

SURFACE ROUGHNESS
Experiments on boundary layer transition tripping at low Reynolds numbers N89-16868
Interfacial bonding in W/C and W/B4C multilayers [DE89-002931] N89-16936

SURFACE TEMPERATURE
Applications of digital image processing to ongoing research in complex terrain meteorology [DE89-001749] N89-17375

SURFACE VEHICLES
3-D vision techniques for autonomous vehicles [AD-A199643] N89-17236

SURFACES
On the aeroacoustics, aerodynamics and aeroelasticity of lifting surfaces N89-16724
Acoustic wave propagation by finite elements and time step integration N89-17460

SURGES
Hydrological aspects of combined effects of storm surges and heavy rainfall on river flow [WMO-704] N89-17340

SWEDEN
Microgravity rockets in Sweden N89-17021

SWIRLING
Intake swirl and simplified methods for dynamic pressure distortion assessment N89-16742
Aerothermal modeling program. Phase 2, element B: Flow interaction experiment N89-17304
Aerothermal modeling program, Phase 2, Element C: Fuel injector-air swirl characterization N89-17305

SWITCHES
Picosecond electrical pulses for VLSI electronics characterization N89-17083
Photoconductive generation of sub-picosecond electrical pulses and their measurement applications N89-17093
High speed, high repetition rate, high voltage photoconductive switching N89-17096
Generation and forming of ultrashort high voltage pulses N89-17097
Graphite as a picosecond laser activated opening switch N89-17098
Investigation of photoconductive picosecond microstripline switches on self-implanted Silicon On Sapphire (SOS) N89-17104
Picosecond optoelectronic switches using composite electronic materials N89-17107
Picosecond measurements of gain-switching in a semiconductor laser driven by ultrashort electrical pulses N89-17115
Optical modulation above 20 GHz using a waveguide electro-optic switch N89-17134
An optical modulator/switch using the reflection from a translated depletion edge [DE89-001380] N89-17490

SWITCHING
A simple technique to generate or gate microwave pulses with picosecond speeds N89-17099
A new optoelectronic CW microwave source N89-17133

SWITCHING CIRCUITS
High speed opto-isolator for radar applications N89-17110
Energy variations in optical pulses from gain-switched AlGaAs diode lasers N89-17111
Silicon pulse sharpening diodes: Switching kilovolts in tens of picoseconds N89-17139

SYMBOLIC PROGRAMMING
Massive symbolic mathematical computations and their applications [AD-A200253] N89-17434

SYMMETRY
Supercritical flow past a symmetrical bicircular arc airfoil [NASA-CR-184787] N89-16762
GPS (Global Positioning System) user equipment evaluation techniques using a rotor mounted antenna [AD-A200515] N89-16770
Global existence for symmetric discrete velocity models [DE89-003102] N89-17438

SYNCHRONISM
Satellite-ground dating and synchronization technique [CNES-CT/DRT/TIT/TB-040-T] N89-16892
The performance of asynchronous algorithms on hypercubes [DE89-005503] N89-17420

SYNTAX
The suitability of an object-oriented language for prototyping and abstract data types [AD-A200417] N89-17410

SYNTHESIS (CHEMISTRY)
Synthesis and properties of low carbon boron carbides [DE89-002184] N89-16923
Conversion of natural gas to methanol [DE89-001088] N89-16958
Synthesis and properties of new precerarnic materials [DE89-003436] N89-17012
Prediction and synthesis efforts at Los Alamos [DE89-003605] N89-17018

SYNTHETIC FUELS
Conversion of natural gas to methanol [DE89-001088] N89-16958

SYSTEMS ANALYSIS
GPS (Global Positioning System) user equipment evaluation techniques using a rotor mounted antenna [AD-A200515] N89-16770
Engine Condition Monitoring: Technology and Experience [AGARD-CP-448] N89-16780
Operational requirements for engine condition monitoring from the EFA viewpoint N89-16781
Analysis and design of a universal shuttle for rockets [ILR-MITT-199] N89-16897
Systems analysis and design of a lunar solar power plant for the supply of a lunar base [ILR-MITT-198] N89-17355

SYSTEMS ENGINEERING
Inverse methods for blade design, controlled diffusion blading for supercritical compressor flow N89-16832
Design of critical compressor stages N89-16835
Analysis and design of a universal shuttle for rockets [ILR-MITT-199] N89-16897
System engineering and logistics for KC-135 experimentation N89-17033
Application of particle image displacement velocimetry to a centrifugal pump N89-17200
Systems analysis and design of a lunar solar power plant for the supply of a lunar base [ILR-MITT-198] N89-17355

SYSTEMS INTEGRATION
System considerations for integrated machinery health monitoring N89-16804
Fast GaAs photoconductive detectors with high sensitivity integrated in coplanar systems onto GaAs substrates N89-17105
The space station integrated refuse management system [NASA-CR-184722] N89-17403
Explosion of integrated optic devices used in new generation systems [DE89-004012] N89-17497
A document preparation system in a large network environment [DE88-014466] N89-17543

SYSTEMS MANAGEMENT
R/M/T (Reliability/Maintainability/Testability) design for fault tolerance. Volume 1: Program manager's guide [AD-A200204] N89-17262

T

T-33 AIRCRAFT
Preliminary results: Flight testing the NAE T-33 microgravity facility N89-17041

TAKEOFF
Human factors in aviation operations: The hearback problem [NASA-CR-177398] N89-16769

TANTALUM
Hydrogen diffusion in tantalum [DE88-704073] N89-16968

TARGETS
Monte Carlo calculation of electron multiple scattering in thin foils [AD-A199872] N89-17517

TASKS
Screening environmental pollutants and biomarkers: The analytical challenge [DE89-004931] N89-17366

TECHNOLOGY ASSESSMENT
Technology assessment for aircraft command in emergency situations [DOT/FAA/CT-88/20] N89-16767
NASA photovoltaic research and technology [NASA-TM-101422] N89-16917
Modern and prospective technologies for hydrogen production from fossil fuels [DE89-001270] N89-16959
The potential impact of MMICs on future satellite communications: Executive summary [NASA-CR-182227-EXEC-SUMM] N89-17079
The Rankine automotive system technology assessment report [DE89-002693] N89-17238
Report to Congress on the Automotive Technology Development Program [DE89-004977] N89-17250
Applications of digital image processing to ongoing research in complex terrain meteorology [DE89-001749] N89-17375

TECHNOLOGY TRANSFER
The Rankine automotive system technology assessment report [DE89-002693] N89-17238
Technology transfer for the US Department of Energy's Energy Storage Program. Volume 1: Recommendations [DE89-002806] N89-17547

TELECOMMUNICATION
Capacity of frequency-hop spread-spectrum multiple-access communication systems [AD-A200616] N89-17073

Laser communication test system
[AD-A199612] N89-17215
TELEMETRY
Controller-Programmer for telemetry systems
[DE89-002539] N89-16898
TELEOPERATORS
Integration of robotics and teleoperation for the advanced servomanipulator: Consolidated fuel reprocessing program
[DE88-015281] N89-17240
TEMPERATURE CONTROL
Capillary pumping for a two phase heat transport system --- space stations N89-17172
TEMPERATURE DEPENDENCE
Absolute absorption cross section measurements of ozone and the temperature dependence at four reference wavelengths leading to renormalization of the cross section between 240 and 350 nm
[AD-A199737] N89-16942
Time and temperature dependence of strength in high performance ceramics N89-16998
Pressure/temperature sensitive inorganic phosphors
[AD-A199718] N89-17000
TEMPERATURE EFFECTS
Manufacturing thermoplastic matrix composites
[AD-A199724] N89-16922
Hygrothermal deformations of laminated composite shells N89-16924
One/f noise in silicon devices
[ISBN-90-9002060-2] N89-17150
Precision transfer function measurements of integrated optical modulators
[DE89-004021] N89-17492
TEMPERATURE GRADIENTS
High energy laser beam scattering by atmospheric aerosol aureoles
[DE89-004811] N89-17230
Theory of neoclassical resistivity-gradient-driven turbulence
[DE89-005391] N89-17513
TEMPERATURE MEASUREMENT
Development and application of oxygen flow tagging for velocity measurements and flow visualization in turbulent three-dimensional supersonic flows
[AD-A200119] N89-16725
Development of a high temperature thin film static strain gage N89-17299
TEMPERATURE PROFILES
Development and application of oxygen flow tagging for velocity measurements and flow visualization in turbulent three-dimensional supersonic flows
[AD-A200119] N89-16725
TEMPERATURE RATIO
Development of conducting polymers of high structural strength
[AD-A200310] N89-17009
TEMPERING
The effects of strain induced softening on the load carrying capability of components N89-17264
TEMPORAL DISTRIBUTION
High-precision gravity network to monitor temporal variations in gravity across Yucca Mountain, Nevada
[DE89-005023] N89-17373
TENSILE PROPERTIES
Compatibility study of an absorber material and two silicone adhesives
[DE89-002361] N89-17011
TENSILE STRENGTH
Tensile strength of composite structures with internal ply drops and free-edge effects N89-16929
TENSORS
On 2-Banach algebras
[DE88-704194] N89-17429
TERRAIN
Applications of digital image processing to ongoing research in complex terrain meteorology
[DE89-001749] N89-17375
TERRAIN ANALYSIS
Applications of digital image processing to ongoing research in complex terrain meteorology
[DE89-001749] N89-17375
TERRESTRIAL RADIATION
Measurements of micrometeorological parameters for testing large scale models
[NASA-CR-184766] N89-17384
TEST EQUIPMENT
Evaluation of physical chemical test methods for characterizing polymerized composites or polymerizing composites: Literature review
[REPT-49-438/F] N89-16935
TEST FIRING
Finite element analysis of F-16 ballistic tests
[AD-A200289] N89-16776
THEMATIC MAPPING
Applications of digital image processing to ongoing research in complex terrain meteorology
[DE89-001749] N89-17375
THERMAL CONDUCTIVITY
Investigations of the motion of discrete-velocity gases by cellular automata
[AD-A200221] N89-17158
Thermally conductive alumina/organic composites for photovoltaic concentrator cell isolation
[DE89-001181] N89-17346
THERMAL CONTROL COATINGS
Turbine Engine Hot Section Technology, 1987
[NASA-CP-2493] N89-17298
Thermal expansion mismatch and plasticity in thermal barrier coating N89-17330
Thermal barrier coating life-prediction model development N89-17331
Thermal barrier coating life prediction model N89-17332
Thermal barrier coating life prediction model development N89-17333
High temperature constitutive and crack initiation modeling of coated single crystal superalloys N89-17334
THERMAL CYCLING TESTS
Structural response of an advanced combustor liner: Test and analysis N89-17329
Thermal barrier coating life prediction model N89-17332
Creep fatigue life prediction for engine hot section materials (ISOTROPIC) fifth year progress review N89-17336
THERMAL DEGRADATION
Kinetics and mechanisms of hydrogen attack in 2.25Cr-1Mo steel
[DE89-001381] N89-16970
Thermal degradation mechanisms in GaAs solar cells with high-temperature contacts
[DE89-001375] N89-17343
THERMAL DIFFUSIVITY
Theory of neoclassical resistivity-gradient-driven turbulence
[DE89-005391] N89-17513
THERMAL ENERGY
First production of potable water by OTEC (Ocean Thermal Energy Conversion) and its potential applications
[DE89-003630] N89-17353
THERMAL EXPANSION
Thermal expansion mismatch and plasticity in thermal barrier coating N89-17330
THERMAL FATIGUE
Turbine Engine Hot Section Technology, 1987
[NASA-CP-2493] N89-17298
Elevated temperature crack growth N89-17335
Creep fatigue life prediction for engine hot section materials (ISOTROPIC) fifth year progress review N89-17336
Total strain version of strainrange partitioning for thermomechanical fatigue at low strains N89-17337
THERMAL INSULATION
Fatigue behavior of ceramic thermal barrier coatings N89-17283
THERMAL STABILITY
Thermal degradation mechanisms in GaAs solar cells with high-temperature contacts
[DE89-001375] N89-17343
THERMAL STRESSES
Thermal expansion mismatch and plasticity in thermal barrier coating N89-17330
Total strain version of strainrange partitioning for thermomechanical fatigue at low strains N89-17337
THERMIONIC CONVERTERS
Development of composite high temperature materials for future energy conversion applications N89-16995
THERMOCHEMISTRY
Laser beam heat method reported N89-17054
THERMOCLINES
Objective analysis of the Gulf Stream thermal front: Methods and accuracy
[AD-A199717] N89-17387
THERMODYNAMIC EQUILIBRIUM
Development of finite local perturbations of electrical conductivity in the flow of a weakly-conducting gas when a magnetic field is present
[AD-A200243] N89-17458
THERMODYNAMIC PROPERTIES
Ceramic-ceramic composites for use at high temperature N89-16994
Experimental verification of the thermodynamic properties for a jet-A fuel
[NASA-TM-101475] N89-17017
Preliminary study of creep thresholds and thermomechanical response in Haynes 188 at temperatures in the range 649 to 871 C N89-17327
Optical fiber science and technology: Novel fibers and fiber sensors
[AD-A200311] N89-17489
THERMODYNAMICS
Quantitative measurement and modeling of sensitization development in stainless steels
[DE89-004646] N89-16990
An analysis of the closure conditions for two-fluid models of two-phase flow
[DE89-003096] N89-17165
A review of second law techniques applicable to basic thermal science research
[DE89-004356] N89-17541
THERMOGRAPHY
Computerized thermographic technique for the detection of boundary layer separation N89-16876
THERMOHYDRAULICS
Phase change phenomena in liquid saturated self heated particulate bed --- core meltdown N89-17170
THERMOPLASTIC RESINS
Manufacturing thermoplastic matrix composites
[AD-A199724] N89-16922
THIN FILMS
Thinning and rupture of a thin liquid film on a horizontal heated solid surface
[DE89-001792] N89-16944
Gas jet deposition of multicomponent ultrafine microstructures
[AD-A200101] N89-16946
Effect of finite size on magnetoresistance
[AD-A200267] N89-16974
Glancing angle EXAFS studies of Cu-Al thin film interfaces
[DE89-003614] N89-16983
Magnetization, transport and structural studies of Tl-Ca-Ba-Cu-O: Bulk ceramics, single crystals, and polycrystalline thin films
[DE89-003264] N89-17010
Femtosecond nonequilibrium electronic heat transport in thin gold films N89-17122
Picosecond optoelectronic study of a thin film transmission line structure N89-17138
Laser studies of the SiH radical/surface interaction during deposition of a thin film
[DE89-003902] N89-17232
Unlubricated sliding properties of ion beam and excimer laser mixed Fe-Ti-C multilayered films
[DE89-003470] N89-17245
Development of a high temperature thin film static strain gage N89-17299
Progress on a PdCr wire strain gage N89-17301
Research on high-efficiency, single-junction, monolithic, thin-film amorphous silicon solar cells, phase 3
[DE89-000813] N89-17342
Fractal and spherulitic morphology of silicon nitride crystallized from amorphous films
[AD-A200158] N89-17522
A simple method for preparing superconducting high T(sub c) thin films
[DE89-003663] N89-17527
THREE DIMENSIONAL BOUNDARY LAYER
A model for transition by attachment line contamination and an examination of cross-flow instability in three-dimensional boundary layers N89-17153
THREE DIMENSIONAL FLOW
Development and application of oxygen flow tagging for velocity measurements and flow visualization in turbulent three-dimensional supersonic flows
[AD-A200119] N89-16725
Three dimensional viscous analysis of a hypersonic inlet
[NASA-TM-101474] N89-16759
Propulsive-jet flow field analysis using the three-dimensional Navier-Stokes equations
[NASA-CR-177508] N89-16764
Analysis of 3D viscous flows in transonic compressors N89-16831
A computational method for three dimensional, internal viscous flows with separation and secondary flow patterns N89-17164
Application of Particle Image Displacement Velocimetry (PIDV) to complex flows: Measurements of the third component N89-17188
Full 3D measurements: The holographic approach --- flow measurement N89-17191
Two- and three-dimensional turbine blade row flow field simulations N89-17313
THREE DIMENSIONAL MODELS
Generation of three-dimensional body-fitted grids by solving hyperbolic and parabolic partial differential equations
[NASA-TM-101069] N89-16763
THRUST
Estimation of drag arising from asymmetry in thrust or airframe configuration
[ESDU-88006] N89-16730

The advantage of a thrust rating concept used on the RB199 engine N89-16800
Installed thrust as a predictor of engine health for jet engines N89-16806
Accuracy of lift and center-of-thrust measurements at missile control surfaces N89-16875

THRUST MEASUREMENT
A data acquisition and storage system for the ion auxiliary propulsion system cyclic thruster test [NASA-TM-101469] N89-17424

THUNDERSTORMS
Observations of a thunderstorm generated gust compared with solitary wave theory [AD-A200087] N89-17379

TIME DEPENDENCE
Implicit time dependent methods for inviscid and viscous compressible methods N89-17178

TIME MEASUREMENT
Satellite-ground dating and synchronization technique [CNES-CT/DRT/TIT/TB-040-T] N89-16892

TIME SERIES ANALYSIS
On a class of nonstationary stochastic processes [NASA-TM-101195] N89-17448

TITANIUM
Combustibility of titanium powders [NASA-TT-20455] N89-16967

TITANIUM ALLOYS
Effect of fretting on fatigue strength of titanium alloys [ESDU-88027] N89-16981

TOKAMAK DEVICES
Induction-linac based free-electron laser amplifier for fusion applications [DE89-001923] N89-17217
Plasma performance in JET: Achievements and projections [DE89-002219] N89-17500
Neoclassical MHD descriptions of tokamak plasmas [DE89-003117] N89-17508
Fusion plasma theory: Task 3: Auxiliary heating in tokamaks [DE89-003256] N89-17509

TOLERANCES (MECHANICS)
Development of overcharge tolerance in Li/FeS and Li/FeS2 cells [DE89-003952] N89-17145
AGARD/SMP Review: Damage Tolerance for Engine Structures. 1: Non-Destructive Evaluation [AGARD-R-768] N89-17253
Importance of sensitivity and reliability of NDI techniques on damage tolerance based life prediction of turbine discs N89-17257

TOMOGRAPHY
Short term developments in non-destructive evaluation applicable to turbine engine parts N89-17258

TOPOGRAPHY
World-wide extreme wind speeds. Part 2: Examples using various methods of analysis [ESDU-88037] N89-17382

TOPOLOGY
Enhanced performance ultrabroadband distributed amplifiers N89-17090
Supersymmetric instantons and topological quantum field theory [DE88-704211] N89-17536
What topology could the universe be created with [DE88-704321] N89-17554

TOROIDAL PLASMAS
Behavior of the reversed field pinch with nonideal boundary conditions [DE89-005497] N89-17514

TORSIONAL STRESS
Finite element analysis of F-16 ballistic tests [AD-A200289] N89-16776
Ocular torsion in the weightlessness of parabolic flight N89-17035

TOWERS
Optical fiber science and technology: Novel fibers and fiber sensors [AD-A200311] N89-17489

TOXICITY
The effects of hydrazines on neuronal excitability [AD-A200199] N89-17395

TRACE ELEMENTS
Gas chromatographic method for the determination of trace quantities of diethyl malonate in ethanol [AD-A199733] N89-16941

TRACKING (POSITION)
The synchronous injection ignition valveless pulsejet N89-16823

TRACKING RADAR
On deriving the three-dimensional kinematic structure on convective storms from a single radar N89-17376

TRANQUILIZERS
Pharmacological resetting of the circadian sleep-wake cycle [AD-A200246] N89-17396

TRANSCONDUCTANCE
Multigigahertz logic based on InP-MISFET's exhibiting extremely high transconductance N89-17086

TRANSFORMATIONS (MATHEMATICS)
Electrical pulse compression by traveling-wave photoconductivity N89-17137
Assessment and comparison of techniques for transforming parameters to a common metric in item response theory [AD-A200067] N89-17433

TRANSIENT RESPONSE
Comparison of sampling oscilloscopes with less than 35 ps transition durations N89-17108

TRANSITION TEMPERATURE
Processing of strong flux trapping high T(subc) oxide superconductors: Center director's discretionary fund [NASA-TM-100350] N89-17530

TRANSMISSION LINES
Picosecond optoelectronic study of a thin film transmission line structure N89-17138

TRANSMISSIVITY
Instrumentation for the characterization of the microwave properties at 18, 35 and 94 GHz [AD-A199741] N89-17064

TRANSMITTER RECEIVERS
Picosecond photoconductive transceivers N89-17092

TRANSMITTERS
A technique for recording HF (High Frequency) oblique-incidence-sounder data [AD-A200168] N89-17068
Laser communication test system [AD-A199612] N89-17215

TRANSONIC COMPRESSORS
Transonic Compressors, volume 1 --- conference [VKI-LS-1988-03-VOL-1] N89-16825
Loss development in transonic compressor cascades N89-16826
Shock losses in transonic and supersonic compressor cascades N89-16829
Axial velocity density ratio influence on exit flow angle in transonic/supersonic cascades N89-16830
Analysis of 3D viscous flows in transonic compressors N89-16831
Inverse methods for blade design, controlled diffusion blading for supercritical compressor flow N89-16832
Transonic Compressors, volume 2 --- conference [VKI-LS-1988-03-VOL-2] N89-16833
The design and development of transonic multistage compressors N89-16834
Design of critical compressor stages N89-16835
Design methodology for advanced High Pressure (HP) compressor first stage N89-16840
Holographic interferometry for flow visualization studies in high speed fans N89-16841

TRANSONIC FLIGHT
Transonic cowl design N89-16746

TRANSONIC FLOW
Reynolds number effects in transonic flow [AGARD-AG-303] N89-16760
Expriments on the DFVLR-F4 wing body configuration in several European windtunnels N89-16848
A proposed boundary layer simulation methodology for wind tunnel testing N89-16867

TRANSONIC SPEED
Development of direct-inverse 3-D methods for applied transonic aerodynamic wing design and analysis [NASA-CR-184788] N89-16761

TRANSONIC WIND TUNNELS
Hierarchy of uncertainty sources in transonic wind tunnel testing N89-16851
Development of testing techniques in a large transonic wind tunnel to achieve a required drag accuracy and flow standards for modern civil transports N89-16857
Transonic wind tunnel boundary interference: A correction procedure N89-16861

TRANSPORT AIRCRAFT
Transport aircraft intake design N89-16749
Development of testing techniques in a large transonic wind tunnel to achieve a required drag accuracy and flow standards for modern civil transports N89-16857
Precision improvement of transport aircraft drag measurements N89-16858
Accuracy of various wall-correction methods for 3D subsonic wind-tunnel testing N89-16863
Accuracy requirements for high-speed test with engine simulation on transport aircraft models in the NLR-HST N89-16870
Balance accuracy and repeatability as a limiting parameter in aircraft development force measurements in conventional and cryogenic wind tunnels N89-16873
Accuracy problems in wind tunnels during transport aircraft development N89-16877
Particular flight mechanics specifications related to wind tunnel test results N89-16879

TRANSPORT PROPERTIES
Properties and performance of polyamide membranes N89-16991
Direct subpicosecond measurement of carrier mobility of photoexcited electrons in GaAs N89-17118
Non-stationary transport in MODFETs and heterojunction devices N89-17119
Longitudinally localized optical carrier injection for femtosecond transport studies N89-17121
Microwave and millimeter-wave resonant tunneling diodes N89-17124
Quantum transport calculation of resonant-tunneling response time N89-17125
Production and transport of convoy electrons in amorphous carbon foils [DE89-002313] N89-17478
Model microfield calculations of radiative and transport properties of ions in strongly coupled plasmas [DE89-001244] N89-17503
Monte Carlo studies of nonlinear electron transport in 3-5 semiconductors [AD-A199700] N89-17516
BRYNTRN: A baryon transport model [NASA-TP-2887] N89-17562

TRANSPORT THEORY
Multidimensional modeling of convective heat transfer with application to I. C. engines [DE89-004062] N89-17166
Modeling and Applications of Transport Phenomena in Porous Media, volume 2 --- conference [VKI-LS-1988-01-VOL-2] N89-17167
Modeling and applications of transport phenomena in porous media. Volume 1: Mathematical modeling of transport in porous media [VKS-LS-1988-01-VOL-1] N89-17202
Theory of neoclassical resistivity-gradient-driven turbulence [DE89-005391] N89-17513

TRAPPING
Experimental evidence for positron trapping at dislocations in Ni3Al alloys [DE89-004520] N89-16989

TRAVELING WAVES
Electrical pulse compression by traveling-wave photoconductivity N89-17137

TRENDS
Trend monitoring of a turboprop engine at low and mean power N89-16801

TRIBOLOGY
Tribology of amorphous alloys formed with ion beams [DE89-003274] N89-16982

TROPICAL STORMS
ONR (Office of Naval Research) tropical cyclone motion research initiative: Mid-year review, discussion and working group reports [AD-A200286] N89-17380

TUBE HEAT EXCHANGERS
Effectiveness: N(sub TU) relationships for the design and performance evaluation of additional shell-and-tube heat exchanger geometries [ESDU-88021] N89-17056
Flow induced acoustic resonance in tubular heat exchangers [ESDU-88028] N89-17464

TUNGSTEN CARBIDES
Interfacial bonding in W/C and W/B4C multilayers [DE89-002931] N89-16936

TUNNELING (EXCAVATION)
Subselenean tunneler melting head design: A preliminary study [NASA-CR-184750] N89-17058

TURBINE BLADES
Limitations at high temperatures of present day engineering materials N89-16996
Review of existing NDT technologies and their capabilities N89-17255
Turbine Engine Hot Section Technology, 1987 [NASA-CP-2493] N89-17298
Development of a high temperature thin film static strain gage N89-17299
A low-Reynolds-number two-equation turbulence model for predicting heat transfer on turbine blades N89-17310
Measurement of airfoil heat transfer coefficients on a turbine stage N89-17311
Heat transfer in the tip region of a rotor blade simulator N89-17312
Two- and three-dimensional turbine blade row flow field simulations N89-17313
Coolant passage heat transfer with rotation N89-17314
Three-dimensional inelastic analysis methods for hot section components N89-17316
Constitutive modelling of single crystal and directionally solidified superalloys N89-17325

Prediction of stochastic blade responses using measured wind-speed data as input to the FLAP code [DE89-000834] N89-17354

TURBOCOMPRESSORS
Design of critical compressor stages N89-16835
Axial supersonic inlet compound N89-16839

TURBOFAN ENGINES
The CFM 56-5 on the A-320 at Air France N89-16793
Service life calculator for the M53 turbofan engine N89-16796
CF-18/F404 transient performance trending N89-16814
COMPASS (Trademark): A generalized ground-based monitoring system N89-16819
Supersonic through-flow fan assessment [NASA-CR-182202] N89-16843

TURBOFANS
Supersonic throughflow fans N89-16837

TURBOJET ENGINES
Installed thrust as a predictor of engine health for jet engines N89-16806
Elevated temperature crack growth N89-17335

TURBOPROP ENGINES
Trend monitoring of a turboprop engine at low and mean power N89-16801

TURBULENCE
Interdependence of large and small scale structures in a turbulent boundary layer N89-17155
Is there a statistical mechanics of turbulence [DE89-003471] N89-17162
Heat transfer with very high free-stream turbulence and heat transfer with streamwise vortices N89-17309
Prediction of stochastic blade responses using measured wind-speed data as input to the FLAP code [DE89-000834] N89-17354
Theory of neoclassical resistivity-gradient-driven turbulence [DE89-005391] N89-17513

TURBULENCE EFFECTS
Turbulence effects on the high angle of attack aerodynamics of a vertically launched missile [AD-A200418] N89-16727

TURBULENCE MODELS
A low-Reynolds-number two-equation turbulence model for predicting heat transfer on turbine blades N89-17310

TURBULENT BOUNDARY LAYER
Interdependence of large and small scale structures in a turbulent boundary layer N89-17155

TURBULENT DIFFUSION
Interdependence of large and small scale structures in a turbulent boundary layer N89-17155

TURBULENT FLOW
Development and application of oxygen flow tagging for velocity measurements and flow visualization in turbulent three-dimensional supersonic flows [AD-A200119] N89-16725
Laminar flame in a turbulent flow [AD-A200241] N89-16947
A model for transition by attachment line contamination and an examination of cross-flow instability in three-dimensional boundary layers N89-17153
Approximation of viscoelastic stresses from Newtonian turbulent kinematics [AD-A200188] N89-17157
Multidimensional modeling of convective heat transfer with application to I. C. engines [DE89-004062] N89-17166
Mix experiments with the NOVA laser [DE89-004775] N89-17228
A comparison of turbulence measurement methods N89-17302
Aerothermal modeling program. Phase 2, element A: Improved numerical methods for turbulent viscous recirculating flows N89-17303
Aerothermal modeling program. Phase 2, element B: Flow interaction experiment N89-17304
Aerothermal modeling program, Phase 2, Element C: Fuel injector-air swirl characterization N89-17305
A low-Reynolds-number two-equation turbulence model for predicting heat transfer on turbine blades N89-17310
Measurement of airfoil heat transfer coefficients on a turbine stage N89-17311

TURBULENT MIXING
The synchronous injection ignition valveless pulsejet N89-16823

TWISTED WINGS
Boundaries of linear characteristics of cambered and twisted wings at subcritical Mach numbers [ESDU-88030] N89-16735

TWO DIMENSIONAL BODIES
A critical assessment of wind tunnel results for the NACA 0012 airfoil N89-16847
Scattering by a two dimensional groove in a ground plane [NASA-CR-183087] N89-17077

TWO DIMENSIONAL FLOW
Two- and three-dimensional turbine blade row flow field simulations N89-17313

TWO PHASE FLOW
Effectiveness: N(sub TU) relationships for the design and performance evaluation of additional shell-and-tube heat exchanger geometries [ESDU-88021] N89-17056
An analysis of the closure conditions for two-fluid models of two-phase flow [DE89-003096] N89-17165
Capillary pumping for a two phase heat transport system — space stations N89-17172
Application of a spatial filter velocimeter to the two phase flows in a Spark Ignition (SI) N89-17199
Computer program for the prediction of air-lift pump performance [ESDU-88014] N89-17246

U

U.S.S.R. SPACE PROGRAM
Canadian participation in international biosatellite programs N89-17025

ULTRASONIC RADIATION
Characterization and modeling of acoustic beams from ultrasonic transducers in solid or liquid media [RF-DAVI-88-08] N89-17465

ULTRASONIC TESTS
Short term developments in non-destructive evaluation applicable to turbine engine parts N89-17258

ULTRASONIC WAVE TRANSDUCERS
Characterization and modeling of acoustic beams from ultrasonic transducers in solid or liquid media [RF-DAVI-88-08] N89-17465

ULTRASONICS
Brittle material processing reported N89-17051
Ultrasonic vibration method discussed N89-17053
Long term possibilities for nondestructive evaluation for US Navy aircraft N89-17259

UNDERGROUND STRUCTURES
Subselenean tunneler melting head design: A preliminary study [NASA-CR-184750] N89-17058

UNIVERSE
What topology could the universe be created with [DE88-704321] N89-17554
An essay on discrete foundations for physics [DE89-002992] N89-17556
Monopoles and magnetic fields in the inflationary universe [DE88-755532] N89-17557

UNSTEADY AERODYNAMICS
Flow unsteadiness in three low-speed wind tunnels N89-16859
Requirements and capabilities in unsteady windtunnel testing N89-16878
Unsteady viscous flows over moving body [AD-A200269] N89-17159

UNSTEADY FLOW
Unsteady viscous flows over moving body [AD-A200269] N89-17159
Unsteady flow about porous cambered plates [AD-A200282] N89-17160

UNSTEADY STATE
The behavior of microdisk and microring electrodes. Mass transport to the disk in the unsteady state: Chronopotentiometry [AD-A200421] N89-16953
The behavior of microdisk and microring electrodes. Mass transport to the disk in the unsteady state: Coupled chemical reactions [AD-A200422] N89-16954

UPPER ATMOSPHERE
National Research Council Resident Research Associateship (NRC-RRA) Program [AD-A200183] N89-16926

V

VACUUM
Cluster expansion for vacuum confining fields [DE88-704367] N89-17436

VACUUM ARC SWITCHES
Investigation of collisional effects in the plasma erosion opening switch [AD-A200319] N89-17507

VACUUM DEPOSITION
Unlubricated sliding properties of ion beam and excimer laser mixed Fe-Ti-C multilayered films [DE89-003470] N89-17245

VACUUM SYSTEMS
Mechanical design of a RF electron gun [DE89-004890] N89-16895

VALENCE
Oxygen and copper valencies in oxygen-doped superconducting La2CuO(sub 4.13) [DE89-003265] N89-17533

VALVES
Assessment of nonintrusive methods for monitoring the operational readiness of solenoid-operated valves [DE89-002330] N89-17244

VANELESS DIFFUSERS
Application of particle image displacement velocimetry to a centrifugal pump N89-17200

VANES
Three-dimensional inelastic analysis methods for hot section components N89-17316

VAPOR DEPOSITION
Quantum-confined Stark effect in InGaAs/InP quantum wells grown by metal-organic chemical vapor deposition N89-17129
Thermal barrier coating life prediction model development N89-17333

VAPOR PHASES
The kinetics and dynamics of iodine monofluoride formation in gas-phase collisions [AD-A199622] N89-16939

VAPOR PRESSURE
Vapour pressures and critical points of liquids. C7 to C20 alkanols [ESDU-88012] N89-16962
Vapour pressures and critical points of liquids. Organic oxygen compounds [ESDU-88017] N89-16963

VAPORIZING
Mechanical-chemical energy transfer observations of vaporific explosions [AD-A200428] N89-16956

VARIABLE GEOMETRY STRUCTURES
Variable geometry in supersonic compressors N89-16838

VARIATIONAL PRINCIPLES
Generalized finite strains, generalized stresses, and a hybrid variational principle for finite-element computer programs [DE89-002101] N89-17430

VECTOR SPACES
Vector space approach to narrowband interference excision [AD-A199703] N89-17063
On 2-Banach algebras [DE88-704194] N89-17429

VECTORS (MATHEMATICS)
Vectorizing compilers: A test suite and results [DE89-005376] N89-17406
A bibliography on parallel and vector numerical algorithms [DE89-005693] N89-17421

VEGETATION
Atmospheric carbon dioxide, climate and global vegetation change [DE89-002196] N89-17360

VELOCITY
Prediction and synthesis efforts at Los Alamos [DE89-003605] N89-17018

VELOCITY DISTRIBUTION
Application of Particle Image Displacement Velocimetry (PIDV) to complex flows: Resolution of the directional ambiguity N89-17187
Application of particle image velocity to high speed flows N89-17198

VELOCITY MEASUREMENT
Development and application of oxygen flow tagging for velocity measurements and flow visualization in turbulent three-dimensional supersonic flows [AD-A200119] N89-16725
The properties of tagged lattice fluids. 2: Velocity correlation functions [DE89-003475] N89-17163
Particle Image Displacement Velocimetry — conference [VKI-LS-1988-06] N89-17179
Some comments on particle image displacement velocimetry N89-17184
Practical systems for speckle velocimetry N89-17185
Simultaneous measurements of droplet size and droplet velocity in monodisperse droplet streams N89-17192
A new algorithm for the rapid analysis of particle image displacement data N89-17195
Application of particle image velocity to high speed flows N89-17198
Application of a spatial filter velocimeter to the two phase flows in a Spark Ignition (SI) N89-17199
Application of particle image displacement velocimetry to a centrifugal pump N89-17200

A comparison of turbulence measurement methods N89-17302

VERTICAL MOTION
Kinematic leveling adjustments with polynomials and polynomial splines
[ETN-89-93328] N89-17338

VERY LARGE SCALE INTEGRATION
Picosecond electrical pulses for VLSI electronics characterization N89-17083
Progress and challenges in HEMT LSI technology N89-17094
Test-efficient design of digital VLSI circuits
[ETN-89-93483] N89-17151

VIBRATION
Transonic aeroelastic analysis of launch vehicle configurations N89-16723
Engine Condition Monitoring: Technology and Experience
[AGARD-CP-448] N89-16780
Ultrasonic vibration method discussed N89-17053
A comparison of two whole-body vibration standards as applied to rotary-wing aircraft: ISO (International Standards Organization) 2631 vs ADS (Aeronautical Design Standards) 27
[AD-A200430] N89-17402
Acoustic wave propagation by finite elements and time step integration N89-17460

VIBRATION DAMPING
Active vibration suppression for robotic manipulators N89-17241

VIBRATION MEASUREMENT
Getting more from vibration analysis N89-16807

VIBRATION MODE
Spillover stabilization in the control of large flexible space structures N89-16902

VIBRATION TESTS
A joint study on the computerisation of in-field aero engine vibration diagnosis N89-16808
A modified VAPEPS method for predicting vibroacoustic response of unreinforced mass loaded honeycomb panels
[NASA-TM-101467] N89-16905

VIBRATIONAL SPECTRA
In-situ vibrational spectroelectrochemistry
[AD-A200303] N89-16949
A comparison of two whole-body vibration standards as applied to rotary-wing aircraft: ISO (International Standards Organization) 2631 vs ADS (Aeronautical Design Standards) 27
[AD-A200430] N89-17402

VIBRATORY LOADS
The influence of the load sequence on the fatigue life of fatigue fracture endangered components N89-17273
Numerical and theoretical study of elastoplastic dynamic buckling
[ETN-89-93614] N89-17284

VIDEO DATA
The visibility of noise in system 1 colour television
[BBC-RD-1988/12] N89-17061

VISCOELASTICITY
Approximation of viscoelastic stresses from Newtonian turbulent kinematics
[AD-A200188] N89-17157

VISCOPLASTICITY
Development of a viscoplastic cyclic behavior law to allow a correct description of creep phenomena
[ONERA-RT-67/1765-RY-078-R] N89-17285
Finite element implementation of viscoplastic models N89-17328

VISCOSITY
Thinning and rupture of a thin liquid film on a horizontal heated solid surface
[DE89-001792] N89-16944

VISCOUS FLOW
Three dimensional viscous analysis of a hypersonic inlet
[NASA-TM-101474] N89-16759
Analysis of 3D viscous flows in transonic compressors N89-16831
Physical aspects of viscous simulation and associated research requirements N89-16865
Unsteady viscous flows over moving body
[AD-A200269] N89-17159
Is there a statistical mechanics of turbulence
[DE89-003471] N89-17162
Implicit time dependent methods for inviscid and viscous compressible methods N89-17178
Aerothermal modeling program. Phase 2, element A: Improved numerical methods for turbulent viscous recirculating flows N89-17303

VISCOUS FLUIDS
Investigation of liquid sloshing in spin-stabilized satellites
[AD-A199629] N89-16899

VISIBILITY
The visibility of noise in system 1 colour television
[BBC-RD-1988/12] N89-17061

VISION
Contrast sensitivity in Army aviator candidates: Cycloplegia effects and population norms
[AD-A200433] N89-17397

VISUAL PERCEPTION
A visualization model based on the mathematics of fiber bundles
[DE89-002537] N89-17432

VOICE COMMUNICATION
The design, analysis, and implementation of a fully distributed local area network for integrated voice and data communications N89-17059

VOIDS
Stress driven diffusive voiding of aluminum conductor lines: A model for time dependent failure
[DE89-001665] N89-17144
Numerical analysis of the effects of void growth and crack tip opening on ductile fracture N89-17265

VORTICES
Vortex dynamics for rotorcraft interactional aerodynamics
[AD-A200128] N89-16726
Numerical solutions to three-dimensional shock wave/vortex interaction at hypersonic speeds N89-16729
Interdependence of large and small scale structures in a turbulent boundary layer N89-17155
The interaction of a fluid interface with a vortex pair
[AD-A200167] N89-17156
Heat transfer with very high free-stream turbulence and heat transfer with streamwise vortices N89-17309
A low-Reynolds-number two-equation turbulence model for predicting heat transfer on turbine blades N89-17310
Rotating hot-wire investigation of the vortex responsible for blade-vortex interaction noise
[NASA-CR-177454] N89-17466

VULNERABILITY
Finite element analysis of F-16 ballistic tests
[AD-A200289] N89-16776

W

WAFERS
Molecular Beam Epitaxy (MBE) for high speed devices N89-17085
Breakdown voltage mapping of impurity concentrations in GaAs wafers
[DE89-002489] N89-17518

WAKEFULNESS
Sleep and wakefulness: Handbook for flight medical officers, 2nd edition
[AGARD-AG-270(F)] N89-17399

WAKES
Vortex dynamics for rotorcraft interactional aerodynamics
[AD-A200128] N89-16726
Flow visualization by the PISTIL procedure (presentation of wake images by local computer processing). Test report 876/S-5 — wake image representation by local computer treatment (PISTIL)
[REPT-876/S-5] N89-17203

WALL FLOW
Wind tunnel-sidewall-boundary-layer effects in transonic airfoil testing-some correctable, but some not N89-16864
Measurement of natural convection by white light speckle velocimetry N89-17197

WALLS
Heat transfer with very high free-stream turbulence and heat transfer with streamwise vortices N89-17309

WAR GAMES
An algorithm for calculating the area of overlap of an ellipse and a convex polygon
[AD-A199654] N89-17408

WARNING SYSTEMS
An intelligent sensor for equipment health monitoring of ferromagnetic wear debris concentration in fluids N89-16818

WASTE DISPOSAL
The space station integrated refuse management system
[NASA-CR-184722] N89-17403

WATER POLLUTION
Screening environmental pollutants and biomarkers: The analytical challenge
[DE89-004931] N89-17366

WATER TREATMENT
Fouling in cooling water systems
[ESDU-88024] N89-17057

WATER VAPOR
Ion content of moist atmospheric air and the molecular structure of water vapor thus inferred
[AD-A199732] N89-16940
The electron-water vapor (H2O) collision cross sections
[AD-A200187] N89-17472

WAVE EXCITATION
Modeling of atomic processes for X-ray laser plasmas
[AD-A200219] N89-17505

WAVE FRONTS
Array processing for a multiple-rank signal
[AD-A197954] N89-17062

WAVE GENERATION
Millimeter wave generation using Josephson junction arrays
[AD-A200259] N89-17524

WAVE PROPAGATION
Propagation effects handbook for satellite systems design. A summary of propagation impairments on 10 to 100 GHz satellite links with techniques for system design
[NASA-RP-1082(04)] N89-17060
Effects of irregular sea surface and evaporation duct on radar detection performance
[AD-A200114] N89-17066
Acoustic wave propagation by finite elements and time step integration N89-17460

WAVEFORMS
Electron device probing in the femtosecond time scale N89-17136

WAVEGUIDES
Frequency chirping in pulse modulated gain and real index guided single quantum well lasers N89-17113
Characteristics and applications of wideband guided-wave devices N89-17132
Fusion plasma theory: Task 3: Auxiliary heating in tokamaks
[DE89-003256] N89-17509

WAVELENGTHS
The X-ray laser: Review of recent experimental results and of future prospects
[DE89-005096] N89-17231

WEAR
An intelligent sensor for equipment health monitoring of ferromagnetic wear debris concentration in fluids N89-16818
Microanalytical characterization of wear damage in an alumina-silicon carbide whisker composite
[DE89-003149] N89-16932
Microstructural effects in abrasive wear
[DE89-003032] N89-16976
Tribology of amorphous alloys formed with ion beams
[DE89-003274] N89-16982

WEAR RESISTANCE
Nitride and carbide coatings for high speed steel cutting tools
[DE89-003623] N89-16984

WEIGHTLESSNESS
Ocular torsion in the weightlessness of parabolic flight N89-17035

WEIGHTLESSNESS SIMULATION
Workshop on Microgravity Experimentation in Aircraft and Rockets
[NRCC-29151] N89-17019
Parabolic flight: A useful test bed N89-17020
Microgravity rockets in Sweden N89-17021
Space utilization promotion program of NASDA N89-17022
Canadian microgravity research using aircraft and rockets N89-17023
NASA's Zero-g aircraft operations N89-17026
Life science experiments during parabolic flight: The McGill experience N89-17027
Droplet separation dynamics and kinematics under microgravity N89-17031
Encapsulation process hardware for a KC-135 aircraft N89-17037
PYTHON microgravity accelerometer system N89-17038
High temperature material processing system for KC-135 microgravity experiments N89-17040
Preliminary results: Flight testing the NAE T-33 microgravity facility N89-17041

WELDABILITY
The effect of chemistry modifications on the solidification behavior and weldability of Alloy 625
[DE89-001046] N89-16972
Procurement and screening test data for advanced austenitic alloys for 650 C steam service, part 2
[DE89-001331] N89-16979

WELDED JOINTS
Electron beam welding produces improved duplex crack arrest specimens
[DE88-003885] N89-17239

Penetration effects of the compound vortex in gas metal-arc welding
[AD-A200585] N89-17242

WELDING
Quantitative measurement and modeling of sensitization development in stainless steels
[DE89-004646] N89-16990
Penetration effects of the compound vortex in gas metal-arc welding
[AD-A200585] N89-17242

WEST GERMANY
Proceedings of the Colloquium about Joint Projects Within the DFVLR/ISRO Cooperation
[DFVLR-MITT-88-19] N89-16883
ISRO-DFVLR collaboration in space sciences N89-16884

WHISKER COMPOSITES
Microanalytical characterization of wear damage in an alumina-silicon carbide whisker composite
[DE89-003149] N89-16932
Mechanical characterization of SiC whisker-reinforced MoSi
[DE89-003486] N89-16933

WHITE LIGHT HOLOGRAPHY
Measurement of natural convection by white light speckle velocimetry N89-17197

WHITE NOISE
The visibility of noise in system 1 colour television
[BBC-RD-1988/12] N89-17061

WIGGLER MAGNETS
Induction-linac based free-electron laser amplifier for fusion applications
[DE89-001923] N89-17217
Selected topics in FELs
[DE89-004022] N89-17227

WIGNER COEFFICIENT
Quantum transport calculation of resonant-tunneling response time N89-17125
The Wigner distribution function with minimum spread
[AD-A199661] N89-17446

WIND PRESSURE
Calculation methods for along-wind loading. Part 3: Response of buildings and plate-like structures to atmospheric turbulence
[ESDU-88019] N89-17267
Calculation methods for along-wind loading. Part 4: Computer program for estimation of response
[ESDU-88036] N89-17271
Simplified fatigue damage and crack growth calculations for wind turbines
[DE89-003132] N89-17351

WIND SHEAR
Piloted-simulation evaluation of escape guidance for microburst wind shear encounters
[NASA-TP-2886] N89-16820
Observations of a thunderstorm generated gust compared with solitary wave theory
[AD-A200087] N89-17379

WIND TUNNEL CALIBRATION
Aerodynamic Data Accuracy and Quality: Requirements and Capabilities in Wind Tunnel Testing
[AGARD-CP-429] N89-16846
A critical assessment of wind tunnel results for the NACA 0012 airfoil N89-16847
Comparison of the results of tests on A300 aircraft in the RAE 5 metre and the ONERA F1 wind tunnels N89-16849
Analytical and experimental methods used to resolve the aerodynamic results of tests conducted in three test facilities N89-16850
Hierarchy of uncertainty sources in transonic wind tunnel testing N89-16851
Wind tunnel predicted air vehicle performance: A review of lessons learned N89-16852
Measurement uncertainty of the AGARD/PEP uniform engine test program N89-16853
Development of testing techniques in a large transonic wind tunnel to achieve a required drag accuracy and flow standards for modern civil transports N89-16857
Transonic wind tunnel boundary interference: A correction procedure N89-16861

WIND TUNNEL MODELS
An experimental investigation of the aerodynamic characteristics of slanted base ogive cylinders using magnetic suspension technology
[NASA-CR-184624] N89-16758
The accurate measurement of drag in the 8 ft x 8 ft tunnel N89-16855
The use of computational fluid dynamic methods to assess the effects of model support systems and working section modifications on the flow around wind tunnel models N89-16862

WIND TUNNEL TESTS
Wind tunnel air intake test techniques N89-16751
Study of the aerodynamic situation along the C 160 aircraft in parachuting configuration
[DAT-88-06] N89-16756
An experimental investigation of the aerodynamic characteristics of slanted base ogive cylinders using magnetic suspension technology
[NASA-CR-184624] N89-16758
Reynolds number effects in transonic flow
[AGARD-AG-303] N89-16760
Aerodynamic Data Accuracy and Quality: Requirements and Capabilities in Wind Tunnel Testing
[AGARD-CP-429] N89-16846
A critical assessment of wind tunnel results for the NACA 0012 airfoil N89-16847
Expriments on the DFVLR-F4 wing body configuration in several European windtunnels N89-16848
Comparison of the results of tests on A300 aircraft in the RAE 5 metre and the ONERA F1 wind tunnels N89-16849
Analytical and experimental methods used to resolve the aerodynamic results of tests conducted in three test facilities N89-16850
Hierarchy of uncertainty sources in transonic wind tunnel testing N89-16851
Wind tunnel predicted air vehicle performance: A review of lessons learned N89-16852
Measurement uncertainty of the AGARD/PEP uniform engine test program N89-16853
An overview of the application of standard measurement uncertainty methodology to propulsion testing N89-16854
The accurate measurement of drag in the 8 ft x 8 ft tunnel N89-16855
Accurate drag estimation using a single component drag model technique N89-16856
Development of testing techniques in a large transonic wind tunnel to achieve a required drag accuracy and flow standards for modern civil transports N89-16857
Precision improvement of transport aircraft drag measurements N89-16858
Flow unsteadiness in three low-speed wind tunnels N89-16859
Impact of nozzle design constraints on test section flow quality N89-16860
Transonic wind tunnel boundary interference: A correction procedure N89-16861
The use of computational fluid dynamic methods to assess the effects of model support systems and working section modifications on the flow around wind tunnel models N89-16862
Accuracy of various-wall-correction methods for 3D subsonic wind-tunnel testing N89-16863
Wind tunnel-sidewall-boundary-layer effects in transonic airfoil testing-some correctable, but some not N89-16864
On Reynolds number effects and simulation N89-16866
A proposed boundary layer simulation methodology for wind tunnel testing N89-16867
Experiments on boundary layer transition tripping at low Reynolds numbers N89-16868
Some difficulties in the wind tunnel prediction of modern civil aircraft buffeting: Proposed remedies N89-16869
Accuracy requirements for high-speed test with engine simulation on transport aircraft models in the NLR-HST N89-16870
Engine simulator tests: Comparison of calibration and wind tunnel results N89-16871
Instantaneous force measurement on a model subjected to rapid control variations N89-16872
Balance accuracy and repeatability as a limiting parameter in aircraft development force measurements in conventional and cryogenic wind tunnels N89-16873
Characterization of hypersonic wind tunnel flow fields for improved data accuracy N89-16874
Accuracy of lift and center-of-thrust measurements at missile control surfaces N89-16875
Computerized thermographic technique for the detection of boundary layer separation N89-16876
Accuracy problems in wind tunnels during transport aircraft development N89-16877
Requirements and capabilities in unsteady windtunnel testing N89-16878
Particular flight mechanics specifications related to wind tunnel test results N89-16879
Application of particle image velocity to high speed flows N89-17198
Decoupling of ionization in the hypersonic boundary limit --- computational fluid dynamics
[CERT-RT-OA-21/5005-AYD] N89-17204

WIND TUNNEL WALLS
Wind tunnel-sidewall-boundary-layer effects in transonic airfoil testing-some correctable, but some not N89-16864

WIND TURBINES
Wind energy systems: Program summary for fiscal years 1986 and 1987
[DE88-001188] N89-17350
Simplified fatigue damage and crack growth calculations for wind turbines
[DE89-003132] N89-17351
Initial structural reaponse measurements for the Sandia 34-meter VAWT test bed
[DE89-003133] N89-17352

WIND VELOCITY
World-wide extreme wind speeds. Part 2: Examples using various methods of analysis
[ESDU-88037] N89-17382
Estimation of hours per year when mean wind speed exceeds specified thresholds
[ESDU-88038] N89-17383

WIND VELOCITY MEASUREMENT
Estimation of hours per year when mean wind speed exceeds specified thresholds
[ESDU-88038] N89-17383

WINDPOWER UTILIZATION
Wind energy systems: Program summary for fiscal years 1986 and 1987
[DE88-001188] N89-17350

WINDPOWERED GENERATORS
Wind energy systems: Program summary for fiscal years 1986 and 1987
[DE88-001188] N89-17350

WING CAMBER
Aerodynamic performance of wings of arbitrary planform in inviscid, incompressible, irrotational flow
[AD-A200436] N89-16728

WING FLAPS
Lift and longitudinal forces on propeller/nacelle/wing/flap systems
[ESDU-88031] N89-16736

WING LOADING
Aeroelastic optimization of a helicopter rotor N89-16778

WING PANELS
The design, construction and test of a postbuckled, carbon fibre reinforced plastic wing box N89-16773

WING PROFILES
Rolling moment derivative Lxi, for plain ailerons at subsonic speeds
[ESDU-88013] N89-16731

WINGS
Aerodynamic performance of wings of arbitrary planform in inviscid, incompressible, irrotational flow
[AD-A200436] N89-16728
Development of direct-inverse 3-D methods for applied transonic aerodynamic wing design and analysis
[NASA-CR-184788] N89-16761
Finite element analysis of F-16 ballistic tests
[AD-A200289] N89-16776
A technique for wing suppressed IR sampling N89-17109
Vibration and aeroelastic tailoring of advanced composite plate-like lifting surfaces N89-17263

WIRE
Progress on a PdCr wire strain gage N89-17301

WORK SOFTENING
Low-cycle fatigue behavior of cyclic hardening and softening steels under multiaxial elastic-plastic loading conditions with constant and variable amplitudes N89-17280

WORKLOADS (PSYCHOPHYSIOLOGY)
Technology assessment for aircraft command in emergency situations
[DOT/FAA/CT-88/20] N89-16767
The role of short-term memory in operator workload
[AD-A200252] N89-17401

WRINKLING
Elastic wrinkling of sandwich panels with laminated fibre reinforced face plates (face plates of AsBoDs, AsDIDs and AsBsDs types). (Computer program)
[ESDU-88015] N89-16930
Wrinkling of sandwich panel face plates (isotropic face plates on orthotropic cores, in-plane loading or bending)
[ESDU-88032] N89-16931

X

X RAY ABSORPTION
Orientation dependent X-ray absorption in high T (sub c) superconductors
[DE89-002910] N89-17520

X RAY INSPECTION
Short term developments in non-destructive evaluation applicable to turbine engine parts N89-17258

X RAY LASERS
Progress towards a 44-Angstrom X-ray laser
[DE89-004807] N89-17229

The X-ray laser: Review of recent experimental results and of future prospects
[DE89-005096] N89-17231
Ne-like ion X-ray laser experiments in plasmas produced by 0.53 microns and 0.35 microns laser light
[DE89-004827] N89-17233
X-ray optics for X-ray laser research and applications
[DE89-004026] N89-17493
Modeling of atomic processes for X-ray laser plasmas
[AD-A200219] N89-17505

X RAY SOURCES
Progress towards a 44-Angstrom X-ray laser
[DE89-004807] N89-17229

X RAY SPECTROSCOPY
Structure and properties of polymer interphases
[AD-A200238] N89-17008

X RAYS
A photon-counting, subnanosecond, imaging camera for X-ray detection
[DE89-002874] N89-17208
Modeling of atomic processes for X-ray laser plasmas
[AD-A200219] N89-17505

Y

YAWING MOMENTS
Yawing moment coefficient for plain ailerons at subonic speeds
[ESDU-88029] N89-16734

YIELD STRENGTH
Synthesis and analysis of epichlorohydrin based wet strength resins for paper N89-16919
Procurement and screening test data for advanced austenitic alloys for 650 C steam service, part 2
[DE89-001331] N89-16979
Effect of fretting on fatigue strength of titanium alloys
[ESDU-88027] N89-16981

YTTRIUM COMPOUNDS
Study of structure of high-Tc superconductor Y(YV)Ba2Cu3O(sub 9-x) and its resistance sharp drop
[DE88-704104] N89-17531

YTTRIUM OXIDES
A simple method for preparing superconducting high T(sub c) thin films
[DE89-003663] N89-17527
Interaction of CO, CO2 and H2O with Ba and YBa2Cu3O7
[DE89-003160] N89-17528

Z

ZERO ANGLE OF ATTACK
Normal-force-curve and pitching-moment-curve slopes for tangent-ogive forebody-cyclinder combinations at zero angle of attack
[ESDU-88026] N89-16733

ZERO FORCE CURVES
Normal-force-curve and pitching-moment-curve slopes for tangent-ogive forebody-cyclinder combinations at zero angle of attack
[ESDU-88026] N89-16733

ZETA PINCH
Recent results from the Nova experiments program
[DE89-002901] N89-17220

ZINC ALLOYS
The electronic structure and the state of compositional order in metallic alloys
[DE89-003147] N89-16977

Typical Personal Author Index Listing

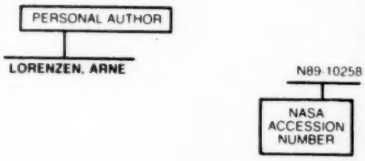

Listings in this index are arranged alphabetically by personal author. The NASA accession number denotes the number by which the citation is identified.

A

ABE, MASAYUKI N89-17094
ABJEAN, P. N89-16935
ADAMS, ROBERT L. N89-17523
ADKINS, C. L. J. N89-16923
ADOMAITIS, E. N89-17099
ADRIAN, RONALD J. N89-17180
N89-17181
N89-17182
N89-17183
AGBORMBAI, A. A. N89-16755
AGNEW, DUNCAN N89-17369
AITKEN, J. F. N89-17041
AKSUN, M. I. N89-17102
ALBERS, JOHN N89-17104
ALCOCK, C. B. N89-17043
ALCORN, CHARLES W. N89-16758
ALDEN, D. N89-17324
ALEXANDER, DAVID R. N89-17147
ALGUN, F. N89-16791
ALI, A. W. N89-17472
ALLARD, L. F. N89-16932
ALLEMEIER, R. T. N89-17234
N89-17235
ALONSO, MARIA A. N89-16927
ALTON, G. D. N89-17480
AMAIKE, T. N89-17022
AMETOV, K. K. N89-17001
ANAND, M. S. N89-16968
ANDERS, K. N89-17192
ANDERSON, BERNHARD H. N89-16753
ANDERSON, J. D., JR. N89-17175
ANDERSON, LOREN A. N89-17403
ANDERSSON, P. N89-17113
ANDREWS, JAMES R. N89-17108
ANHEIER, N. A. N89-17111
ANIDO, GARY J. N89-17059
ANTHES, J. P. N89-17110
ANTONETTI, A. N89-17088
N89-17127
ANTREASYAN, A. N89-17084
N89-17086
ARAU, B. A. N89-17345
ARJAVALINGAM, G. N89-17138
ARMAND, C. N89-16858
N89-16867
ARNESON, M. C. N89-16818
ARNOLDUS, HENK F. N89-17487
ARPASI, DALE J. N89-17453
ARROTT, A. P. N89-17038
ARYA, V. K. N89-17328
ASHBY, M. J. N89-16798
ASHILL, P. R. N89-16848
ASHWILL, THOMAS D. N89-17352
AULEHLA, F. N89-16742
AUME, NILSS M. N89-17391
AUPOIX, B. N89-17204
AUSTON, D. H. N89-17118
N89-17137

B

BACHALO, WILLIAM D. N89-16765
BACHMAN, WILLIAM G. N89-17397
BADHAM, H. N89-16911
BAILEY, RICHARD S. N89-17299
BAIRD, E. D. N89-17486
BAIRSTO, N. A. N89-16783
BAJGAR, C. N89-17343
BALL, C. L. N89-16834
N89-16837
BALLOU, LARRY N89-17384
BANDY, S. N89-17090
BANERJEE, PRASANTA K. N89-17317
BANKOFF, S. G. N89-16944
BAR-JOSEPH, I. N89-17129
BARKESHLI, K. N89-17077
BARNA, B. A. N89-17234
N89-17235
BARREAU, R. N89-16869
BARTEAU, MARK A. N89-16985
BARTOLOTTA, P. A. N89-17326
N89-17327
BASILICO, CHRISTIAN N89-17173
BASORE, PAUL A. N89-17347
N89-17349
BATCHELOR, K. N89-16895
BATES, J. B. N89-17521
BATSALE, JEAN-CHRISTOPHE N89-17173
BAUGHMAN, R. J. N89-17010
BAUMERT, W. N89-16871
BEALS, KEITH A. N89-16904
BEAR, J. N89-17202
BEARDSLEY, BURT JAY N89-17561
BEASON, C. W. N89-17154
BEAUCHAMP, R. N89-17143
BEAULIEU, MARTIN N89-16904
BEAVIS, L. C. N89-17346
BECK, J. N89-16891
BECKERMAN, MARTIN N89-17251
BEDILOV, M. R. N89-17511
BEHAR, ISAAC N89-17397
BEISEMBAEVA, KH. B. N89-17511
BELL, MICHAEL N89-17104
BELLINGER, N. N89-17257
BENEKING, H. N89-17105
BENGUHE, P. T. N89-17215
BENNETT, JAMES M. N89-17523
BENSON, THOMAS J. N89-16754
N89-16759
BERENZ, JOHN J. N89-17091
BERG, M. N89-17281
BERGER, J. N89-16869
BERNAT, T. P. N89-17502
BICAY, MICHAEL DAVID N89-17552
BIEDERMANN, C. N89-17478
BIGLARI, H. N89-17508
BINDER, B. N89-16871
BINDER, P. M. N89-17163
BINION, T. W., JR. N89-16760
BIRKETT, C. M. N89-17550
BIRMINGHAM, DANNY N89-17536
BISHOP, EDWARD W. N89-16767
BJORN, L. N89-17021
BLABER, A. N89-17039
BLABER, P. N89-17039
BLACKWOOD, D. J. N89-16950
BLAHA, M. N89-17474
BLAIR, MICHAEL F. N89-17311
BLECH, RICHARD A. N89-17422
BLISS, DAVID EMORY N89-17518
BLISS, DONALD B. N89-16726
BLOCH, A. N89-17193
BLOMBERG, RICHARD D. N89-16767
BLOOM, D. M. N89-17082
BLOTTNER, FREDERICK G. N89-16737
BLUM, ARNOLD N89-17151
BOALS, W. O., JR. N89-16854
BOATNER, L. A. N89-17519
BOERCKER, DAVID B. N89-17503
BOERIO, F. JAMES N89-17008
BOLLING, E. N89-16979
BOLLONG, A. B. N89-17029
BONCZYK, PAUL A. N89-16948
BOND, LEONARD J. N89-17255
BORELLA, HENRY M. N89-17000
BOTTRILL, J. N89-17037
BOUCHIER, STEPHANY N89-17543
BOUDREAU, ALBERT H. N89-16874
BOUDREAULT, RICHARD N89-17031
N89-17037
N89-17042
BOUDREAULT, Y. N89-17042
BOURCIER, R. J. N89-17144
BOURGADE, J. L. N89-17229
N89-17233
BOWERS, J. E. N89-17112
N89-17115
BOYARSKI, A. N89-17413
BRABBS, THEODORE A. N89-17017
BRADLEY, J. N89-17037
BRANDAO, MAURICIO PAZINI N89-16724
BRATCHER, T. W. N89-16816
BRAUN, ROBERT L. N89-17419
BRAY, K. N. C. N89-17201
BRAZIER, J. PH. N89-17204
BREEN, DENNIS L. N89-17402
BREILAND, WILLIAM G. N89-17232
BREINIG, M. N89-17478
BRERETON, SANDRA J. N89-17512
BREUGELMANS, F. A. E. N89-16838
N89-16839
BRIDGES, J. H., III N89-16816
BRIGANTI, MICHAEL N89-17393
BRILEY, W. R. N89-17313
BRINA, ROSSELLA N89-16955
N89-17210
BRITCHER, COLIN N89-16758
BRITSCH, M. N89-17355
BRITTAIN, J. O. N89-17300
BROADWELL, JAMES E. N89-17158
BROCKRIS, JOHN O. N89-16943
BRODY, ADAM N89-16896
BROEDE, J. N89-16789
BRONIKOWSKI, MICHAEL J. N89-17483
BROOKS, W. G. N89-16773
BROOKS, W. S. C. N89-17032
BRORSON, S. D. N89-17122
BROWN, ELLIOTT R. N89-17124
BRUEMMER, S. M. N89-16990
BRUNDAGE, RICHARD N89-17104
BRUNEAU, C. L. N89-17547
BRUNSCHWIG, BRUCE S. N89-17471
BUCHLIN, J.-M. N89-17170
N89-17172
BUCK, WARREN W. N89-17562
BUGGELN, R. C. N89-17313
BULLARD, J. S. N89-17039
BURDGE, GEOFFREY N89-17104
BURGSMUELLER, W. N89-16870
BURKS, B. L. N89-17249
BURNHAM, ALAN K. N89-17419
BURRUS, C. A. N89-17084
N89-17112
BUSS, RICHARD J. N89-17232
BUTLER, BARCLAY P. N89-17402
BUTLER, D. M. N89-17432
BUXBAUM, O. N89-17272
BYKOVSKIJ, YU. A. N89-17511

C

CABLE, M. D. N89-17220
CALDI, D. G. N89-17538
CALLAHAN, DAVID N89-17406
CALLEN, J. D. N89-17508
CAMARANETO, GILBERTO N89-17414
CAMPBELL, A. N. N89-16923
CAMPBELL, E. M. N89-17220
N89-17502
CAMPBELL, GLEN S. N89-17023
CAMPION, ALAN N89-17223
CAPASSO, F. N89-17126
CAPPS, D. S. N89-16855
CARD, DON H. N89-17339
CAREY, K. W. N89-17114

CARLON, HUGH R. N89-16940
N89-17370
CARLSON, LELAND A. N89-16761
CARLSON, N. M. N89-17234
CARLSSON, R. N89-16997
CAROL, M. N89-16756
CAROSELLA, C. A. N89-17522
CARR, H. R. N89-16808
CARR, STEPHEN H. N89-17007
CARRERAS, B. A. N89-17508
CARRION, PHILIP M. N89-17506
CARRUTHERS, T. F. N89-17117
CARTER, DAVID H. N89-16933
CARTER, E. C. N89-16857
CARTER, M. R. N89-17208
CARTWRIGHT, DAVID N89-17218
CARTZ, LOUIS N89-16992
CASSIE, A. M. N89-16856
CASTANON, DAVID A. N89-17447
CASTRO, J. H. N89-16918
CEGLIO, N. M. N89-17493
CENEDESE, A. N89-17194
CHABOCHE, J. L. N89-17285
CHAMBERS, K. W. N89-16818
CHAMIS, C. C. N89-17321
CHAMPAGNE, G. A. N89-16843
CHAN, KWAI S. N89-17322
CHAN, Y. Y. N89-16867
CHANG, GEORGE C. N89-17330
CHAO, B. L. N89-16970
CHASSAING, CHARLES EDOUARD N89-17460
CHAUCHARD, E. A. N89-17096
N89-17107
N89-17133
CHEESEMAN, I. C. N89-16807
CHEMIA, D. S. N89-17129
N89-17130
CHEN, D. H. N89-17528
CHEN, H. N89-16983
CHEN, I-WEI N89-17006
CHEN, J. N89-17528
CHEN, PI-FUAY N89-17071
CHEN, ROBERT T. N. N89-16844
CHEN, S. N89-17379
CHEN, SHI-YI N89-17162
CHENG, HSING C. N89-16959
CHETAIL, P. N89-16793
CHEW, T. C. N89-17201
CHI, C.-C. N89-17083
N89-17093
N89-17106
CHO, A. Y. N89-17085
N89-17126
CHOMA, C. N89-17037
CHOU, H. N89-17530
CHRIEN, R. E. N89-17498
CHRISTENSON, K. K. N89-17522
CHRISTODOULAKIS, T. N89-17537
CHU, ELEANOR N89-17441
CHUDNOVSKY, DAVID V. N89-17434
CHUDNOVSKY, GREGORY V. N89-17434
CHUN, SANG Y. N89-17562
CHUNG, M. A. N89-17343
CHYU, M. K. N89-17312
CIESLAK, M. J. N89-16972
CIKANEK, HARRY A. N89-16815
CLARK, C. J. N89-17133
CLARK, DAVID R. N89-16775
CLARK, ROSS D. N89-16850
CLELAND, JOHN N89-17393
CLEVERS, RENE HENRICUS MARIA N89-17150
COBURN, M. D. N89-17018
CODY, W. J. N89-17439
COHEN, GERARD D. N89-17065
COLDREN, L. A. N89-17490
COLEMAN, L. W. N89-17502
COLTMAN, R. R., JR. N89-17456
COLTON, DAVID N89-17070
COMBIS, P. N89-17229
N89-17233
CONNER, H. N89-16821
CONROE, DAVID J. N89-17262
CONTRERAS, M. M. N89-17139
COOK, MARK K. N89-17142
COOK, T. N89-17332
COOK, W. A. N89-17430
N89-17431
COOPER, BERNARD R. N89-16928
CORBETT, G. K. N89-17240
CORPENING, GRIFFIN PAT N89-16729
COSTES, B. N89-16935
COUGHRAN, MARK THOMAS N89-17155
COX, GORDON F. N89-17388
COX, ROBERT MONROE N89-17376
COY, JOHN J. N89-17248
CRAIG, W. W. N89-16936
CREIGHTON, JOHN N89-17225
CREUTZ, CAROL N89-17471
CREUTZ, MICHAEL N89-17539
CRITES, R. C. N89-16861
CROFT, W. B. N89-17425
CROW, J. E. N89-17528
CROWLEY, W. PATRICK N89-17205
CRUTCHER, J. W. N89-17545
CUCINOTTA, FRANCIS A. N89-17582
CUE, ROBERT W. N89-16784
N89-16787
CUELLAR, J. P., JR. N89-17015
CUNNINGHAM, CHRISTOPHER T. N89-17451
CURRERI, P. A. N89-17530
CURTIS, HENRY B. N89-17356
CUSTER, RICHARD L. P. N89-16767
CZAJKOWSKI, EVA A. N89-16902

D

DACUNHATRIVELATO, GILBERTO N89-16903
DAEHLER, MARK N89-17068
DAGLI, N. N89-17490
DAI, XIAMING N89-17531
DALTON, LARRY R. N89-17009
DANIELS, R. MICHAEL N89-16898
DAS, A. N89-16757
DAS, ASHOK N89-17443
DASCHBACH, JOHN N89-16951
N89-16952
DASGUPTA, S. N89-17043
DAVID, PAUL A. N89-16937
DAVIS, G. J. N89-17416
N89-17455
DAVIS, J. N89-17474
DAVIS, JAMES WILLIAM N89-17504
DAVIS, S. H. N89-16944
DAWES, W. N. N89-16831
DEASE, C. G. N89-17139
DEAZEVEDO, JOAO LUIZ FILGUEIRAS N89-16723
DEBELLEVAL, J. F. N89-17465
DEBORDES, O. N89-17284
DEEKSHATULU, B. L. N89-16886
DEFONZO, ALFRED P. N89-17092
DEGIOVANI, ALAIN N89-17173
DEGREZ, G. N89-17178
DEGTYAREV, L. M. N89-17458
DEHAAN, AUKE N89-17338
DELAHOY, A. E. N89-17342
DELORENZO, ROBERT J. N89-17395
DEMARSILY, G. N89-17168
DEMASI, J. T. N89-17333
DEMBIA, FRANK J. N89-16904
DEMETRIADES-SHAH, TANVIR N89-17384
DENAULT, GUY N89-16952
DENBOER, R. D. N89-16878
DENOST, J. P. N89-16910
DERBYSHIRE, K. N89-16788
DESERIO, R. N89-17478
DESTUYNDER, R. N89-16869
DEVAN, J. H. N89-16988
DHUMIERES, D. N89-17163
DIADIUK, V. N89-17107
DIAMOND, P. H. N89-17508
N89-17513
DIAMOND, S. G. N89-17035
DICK, E. N89-17177
DICKEY, DANIEL W. N89-17548
DILLARD, R. A. N89-17427
DISIMILE, P. N89-17046
DO, C. N89-17284
DOANY, F. E. N89-17106
DOBROVOLSKIS, Z. N89-17099
DODSON, BRIAN W. N89-17482
DONALDSON, WILLIAM R. N89-17096
DONGARRA, JACK N89-17406
DONOVAN, E. P. N89-17522
DORSON, DONALD N89-17357
N89-17358
DOVIAK, R. J. N89-17379
DOWELL, F. N89-17013
DOWNER, M. C. N89-17121
N89-17135
DOWNEY, P. M. N89-17115
DOXSEE, LAWRENCE EDWARD, JR. N89-16924
DRACOS, TH. N89-17169
DREVER, J. P. N89-16872
DREW, D. A. N89-17165
DRING, ROBERT P. N89-17311
DROST, M. KEVIN N89-17541
DUBE, FRANCOIS N89-16784
DUECK, W. N89-16818
DULING, I. N., III N89-17093
DUMAS, M. RIBADEAU N89-16875
DUNIGAN, T. H. N89-17407
DUNN, VERNON E. N89-17078
N89-17079
DUST, R. N89-17355
DYE, CRAIG N89-17401
DYKAAR, D. R. N89-17095
DYSON, R. J. E. N89-16798
N89-16799

E

EARNSHAW, P. B. N89-16849
EASTMAN, L. F. N89-17101
EATON, JOHN K. N89-17309
EDELBLUTE, DAVID J. N89-17062
EDWARDS, BELVA N89-17368
EDWARDS, P. R. N89-17287
N89-17288
N89-17291
N89-17292
N89-17297
EGENMAIER, WALTER N89-17397
EINERSON, C. J. N89-17252
EINSTEIN, J. R. N89-17249
EISENSTEIN, G. N89-17134
ELFSTROM, G. M. N89-16860
ELLIS, J. R. N89-17326
N89-17327
ELSBERRY, RUSSELL L. N89-17380
ELSENAAR, A. N89-16760
N89-16848
N89-16866
N89-16867
ELSTON, S. B. N89-17478
EMMETT, J. L. N89-17502
EMRICH, M. L. N89-17548
ENGBLOM, BILL N89-17058
ENGBLOM, JOHN J. N89-16774
ENGLUND, DAVID R. N89-17301
ENLOW, EDWARD E. N89-17147
ESCHBACH, PETER A. N89-17207
ESCHER, R. N89-17037
ESER, E. N89-17342
EVANS, P. R. N89-16909
EWALD, B. N89-16873
EZIN, JEAN PIERRE N89-17454

F

FAHR, A. N89-17257
FAMINI, GEORGE R. N89-17389
FARKAS, LESLIE A. N89-17251
FARLEY, GUY N89-17067
FASSBENDER, L. L. N89-17547
FAVORSKIY, A. P. N89-17458
FEEZELL, R. R. N89-17249
FENG, S. T. N89-17097
FENSKE, GEORGE R. N89-16984
FENSTERMACHER, CHARLES N89-17218
FERRY, D. K. N89-17120
FIDELL, S. N89-17461
FIEDLER, K. N89-16811
FIGUEIRA, JOSEPH N89-17218
FINAYEV, YU. A. N89-16967
FISCHER, G. N89-17282
FISH, JOHN CRISTOPHER N89-16929
FISHER, CELIA N89-16817
FISHER, DOUGLAS N89-17400
FLADE, D. N89-17275
FLEISCHMANN, MARTIN N89-16951
N89-16952
N89-16953
N89-16954
N89-17210
FLETCHER, W. D. M. N89-16783
FLOOD, DENNIS J. N89-16917
FOISY, M. C. N89-17101
FOLLSTAEDT, D. M. N89-16982
FONTANA, RICHARD REMO N89-17466
FOOTE, H. P. N89-17375
FORD, C. W. N89-17345
FOX, NEIL D. N89-17071
FRALICK, GUSTAVE C. N89-17302
FRANK, M. N89-17044
FRAZIER, JOHN W. N89-17391
FRECON, L. N89-17496
FREEMAN, D. E. N89-16942
FRENSLEY, WILLIAM R. N89-17125
FRIEDEN, ROY B. N89-17195
FRIEDLANDER, AMY I. N89-17387
FRIEDMAN, MORTON B. N89-17434
FROEBEL, E. N89-16859
FROHN, A. N89-17192
FUJIMARA, CLAY N89-16741
FUJIMOTO, J. G. N89-17122

FUKUMOTO, S. N89-17480
FUNDERLIC, R. E. N89-17455
FURR, PAUL A. N89-17392

G

GALANTE, LEONARD J. N89-16937
GALASHINA, N. M. N89-17001
GALLAGHER, W. J. N89-17093
GAMRETSKAYA, A. M. N89-17001
GANAPOL, BARRY D. N89-17562
GAO, X. H. N89-17385
GARBINSKI, P. A. N89-17086
GARCIA, L. N89-17508
GARCIA, P. N89-17110
GARNEAU, MARC N89-17020
GATOS, HARRY C. N89-17525
GAUTHIER, V. N89-17187
N89-17188
GEE, C. M. N89-17132
GEE, JAMES M. N89-17344
N89-17345
N89-17356
GEIST, G. A. N89-17416
N89-17455
GENIN, J. N89-17431
GENNARI, JOHN N89-17400
GENT, A. N. N89-16957
GEORGE, J. ALAN N89-17441
GEORGE, THOMAS F. N89-16973
N89-16974
N89-17476
N89-17487
GERHARZ, J. J. N89-17278
N89-17279
GHOSN, LOUIS J. N89-17286
GIBBONS, J. P. N89-17478
GIBBS, H. M. N89-17088
N89-17127
GIBBS, W. SCOTT N89-16933
GIBSON, A. N89-17500
GIBSON, W. A. N89-17470
GILLEN, K. T. N89-17011
GINLEY, D. S. N89-17010
N89-17533
GLENDINNING, S. G. N89-17220
GLENNY, D. E. N89-16802
GLYNN, CARITA D. N89-17401
GOESSL, H. N89-16890
GOLDBERG, HARRY S. N89-17542
GOLDHAR, J. N89-17097
GOLDSTONE, PHILIP N89-17218
GOLL, J. H. N89-17111
GONZALEZ-LEPERA, C. E. N89-17478
GOODFELLOW, J. V. N89-16781
GOODHUE, W. D. N89-17124
GOODWIN, G. M. N89-16979
GOTO, HIDEKAZU N89-17054
GOTTLIEB, J. J. N89-16894
GOULD, G. N89-17257
GOUTINES, MARIUS N89-16840
GRABOWSKI, K. S. N89-17522
GRACIASALCEDO, CARMEN M. N89-17017
GRADE, M. N89-17355
GRAFTON, T. A. N89-16821
GRAHAM, ERIC N89-17058
GRANT, HOWARD P. N89-17299
GRASME, M. N89-17355
GRAVES, R. L. N89-17016
GRAY, C. N89-17196
GRAY, K. E. N89-17527
GREATED, C. A. N89-17196
GREEN, D. M. N89-17461
GREEN, ROBERT B. N89-17224
GREGORY, DAN L. N89-17442
GREINER-PETTER, J. N89-17355
GRIFFIN, ALBERT B. N89-17069
GRIFFIN, JEFFREY W. N89-17207
GRISCHKOWSKY, D. N89-17093
N89-17106
GRIVITSKAS, V. N89-17099
GROBEL, M. N89-17197
GROSSMANN, J. M. N89-17507
GROTH, C. P. T. N89-16894
GRUBISIC, V. N89-17280
GRUNDMANN, R. N89-17176
GUBBAY, J. S. N89-16770
GUERTIN, RALPH F. N89-17063
GUESS, T. R. N89-17011
GUINAN, M. W. N89-17456
GUPTA, UDAY N89-17505
GURZADYAN, V. G. N89-17554
GUSTAVSON, D. B. N89-17405
GYORFFY, B. L. N89-16977

H

HAAS, T. W. N89-17526
HAGER, BRADFORD N89-17369
HAGLUND, RICHARD F., JR. N89-17469
HAHM, T. S. N89-17513
HAHN, P. A. N89-17456
HAINES, A. B. N89-16867
HAJEK, T. J. N89-17314
HALAS, N. J. N89-17093
HALBOUT, J.-M. N89-17083
N89-17093
N89-17138
HALFORD, G. R. N89-17337
HALLER, K. N89-17538
HALPERN, BRET L. N89-16946
HAMER, M. J. N89-16806
HAMILTON, JOHN W. N89-16767
HAMLEY, JOHN A. N89-17424
HAMM, R. N. N89-17470
HANDLER, R. A. N89-17157
HANDROCK, JAMES LEE N89-17264
HARBERS, GALEN N89-17384
HARDIN, JAY C. N89-17448
HARRIS, DAVID N89-17218
HARRIS, JOHN A., JR. N89-17256
HARRIS, R. N. N89-17373
HARRIS, THOMAS N89-16784
HARRISON, JONATHAN A. N89-17209
HARTLE, M. N89-17332
HARVEY, PETER R. N89-17336
HASE, CHRISTOPHER A. N89-16777
HASEGAWA, AKIRA N89-17506
HATANO, KOICHI N89-17051
HATCHER, C. W. N89-17220
HATCHETT, S. P. N89-17220
HAUSER, D. N89-17239
HAUSKEN, T. N89-17490
HAWKINS, R. T. N89-17111
HEADLEY, T. J. N89-16923
HEALD, S. M. N89-16983
N89-17520
HEBERT, MARTIAL N89-17236
HEGDE, M. V. N89-17073
HEIBLUM, M. N89-17123
HEIL, O. N89-17478
HEINBOCKEL, JOHN H. N89-17214
HELMBOLD, ROBERT L. N89-17408
HENDRICKS, E. W. N89-17157
HENDRY, R. D. N89-17023
HENRIKSEN, P. N. N89-16957
HENRY, J. R. N89-16814
HEPNER, DAVID J. N89-17209
HERITAGE, J. P. N89-17130
HERLIHY, MAURICE P. N89-17435
HESS, ANDREW J. N89-16782
HESS, K. N89-17119
HESS, R. W. N89-16719
N89-16720
N89-16721
N89-16722
HESSELGRAVE, R. N89-17044
HEULER, P. N89-17296
HIEFTJE, GARY M. N89-16937
HIGGINS, C. A. N89-17530
HIGGINS, M. N89-17329
HILAIRE, B. N89-16935
HILDRATH, JOSEPH H. N89-16907
HILLERY, R. N89-17332
HILLIS, DAVID L. N89-17353
HIMED, BRAHAM N89-17449
HINTON, DAVID A. N89-16820
HIPPSLEY, C. A. N89-16988
HIRVONEN, JUHA-PEKKA N89-17245
HO, PAULINE N89-17232
HO, YUNG-LUNG N89-17514
HOBBS, RANDY W. N89-16851
HOECKER, R. N89-17198
HOERL, F. N89-16812
HOGAN, W. J. N89-17502
HOGG, G. WILLIAM N89-16795
HOLIFIELD, T. F. N89-17145
HOLLEY, DANIEL C. N89-17390
HOLM, CHRIS L. N89-16728
HOLT, MAURICE N89-16762
HOM, CRAIG LEE N89-17265
HONG, B. S. N89-17562
HOPFEL, R. A. N89-17128
HORNUNG, H. C. N89-16760
HOUSER, MICHAEL C. N89-16765
HOUWINK, R. N89-16878
HSIANG, T. Y. N89-17095
HSIEH, K. C. N89-17308
HSU, CHEN C. N89-16938
HUANG, C. Y. N89-17098
N89-17530
HUANG, HO C. N89-17133
HUANG, J. C. N89-17101
HUANG, J. S. N89-17534
HUANG, T. C. N89-17490
HUBBE, J. M. N89-17375
HUBLER, G. K. N89-17522
HUDSON, J. D. N89-17239
HUELSKOETTER, H. P. N89-17478
HUFF, RONALD G. N89-16882
HUGRASS, W. N. N89-17498
HULIN, D. N89-17088
N89-17127
HULSE, CHARLES O. N89-17299
HUNG, H.-L. A. N89-17133
HUNT, J. T. N89-17502
HUNTER, NORMAN F., JR. N89-17442
HUNTER, S. R. N89-17470
HURST, G. S. N89-17470
HUSS, GARY ROBERT N89-17553
HUSTON, RONALD L. N89-17248
HUTCHINSON, A. L. N89-17126
HUTH, H. N89-17278
HWU, SHIAN-UEI N89-17072
HYLTON, L. D. N89-17315

I

IDELBERGER, H. N89-17279
IIJIMA, NOBORU N89-17048
IPPEN, E. P. N89-17122
IPPOLITO, LOUIS J. N89-17060
IPSER, JAMES N89-17225
N89-17230
IRELAND, D. J. N89-17034
ISLAM, M. M. N89-17538
ISMATOV, E. I. N89-17001
ITOH, T. N89-17135
IVES, G. J. N89-16808

J

JACOBS, J. K. N89-17043
JACQUINOT, J. N89-17499
JACUBIEC, W. N89-17355
JAMET, J. F. N89-16994
JANKOWSKI, A. F. N89-16936
JARWALA, MADHURI N89-17092
JAYARAMAN, N. N89-17324
JAYKO, KATHERINE N89-17357
N89-17358
JEAL, R. H. N89-17254
JELL, R. M. N89-17034
JENKINS, P. N89-16808
JENKINS, P. J. N89-16786
JENNINGS, MARK J. N89-17166
JENSEN, DANIEL C. N89-17517
JERVIS, THOMAS R. N89-17245
JEWELL, J. L. N89-17088
JHA, S. S. N89-17103
JIN, J.-M. N89-17148
JOHANSEN, OISTEIN N89-17357
N89-17358
JOHNENNING, B. N89-17355
JOHNSON, B. V. N89-17314
JOHNSON, C. B. N89-16864
JOHNSON, D. D. N89-16977
JOHNSON, J. A. N89-17234
N89-17235
JOHNSON, J. R. N89-16966
JOHNSON, W. H. N89-17035
JOHNSTON, S. E. N89-17251
JONES, E. D. N89-17532
JONES, JUDSON P. N89-17251
JONG, R. A. N89-17217
N89-17221
JORDAN, ERIC H. N89-17325
JOSEPHY, Y. N89-16966
JOSHI, N. K. N89-17510
JOSLYN, H. DAVID N89-17311

K

KAHN, A. D. N89-17522
KAHN, ALAN N89-17005
KAILAS, SUDARSH V. N89-17372
KAIPOV, B. N89-17001
KAMANOU, PIERRE-FRANCOIS N89-17074
KAMEN, R. B. N89-17427
KAMINAR, N. R. N89-17344
N89-17345
KAMPAS, F. N89-17342
KANADE, TAKEO N89-17236
KANEMASU, E. T. N89-17384
KANIA, D. R. N89-17220

KANKI, R. N89-17022
KANN, M. J. N89-17120
KAPPLER, G. N89-16812
KARKI, K. C. N89-17303
KASH, J. A. N89-17103
KATZ, R. N. N89-16996
KAUFFMAN, R. L. N89-17220
KAUFMAN, R. M. N89-17315
KAUN, T. D. N89-17145
KAZIMI, MUJID S. N89-17512
KEANE, C. J. N89-17229
N89-17231
N89-17233
KEAVNEY, C. J. N89-17343
KEEFER, DENNIS N89-17226
KELKAR, KANCHAN M. N89-17307
KELLY, DONALD H. N89-17394
KELLY, J. N89-16945
KENNEDY, JAN B. N89-17306
KEPLER, C. E. N89-16843
KERIBAR, RIFAT N89-17548
KERSCHEN, KEVIN A. N89-17347
KERSTIENS, JOSEPH N89-16904
KESAN, VIJAY P. N89-17100
KESTNER, N. R. N89-17479
KETCHEN, M. B. N89-17083
N89-17093
N89-17138
KEYDEL, W. N89-16890
KHAN, FERDOUS N89-17562
KHANAKA, G. H. N89-17076
KIDD, BILL N89-17492
KILKENNY, J. D. N89-17220
N89-17228
KIM, K. S. N89-17335
KIM, KI W. N89-17516
KIM, Y. B. N89-17508
KIMZEY, W. F. N89-16854
KINCAID, R. K. N89-17417
KING, J. F. N89-17239
KING, NANCY N89-17369
KIRIENKO, N. M. N89-17035
KITAGAWA, TAKEAKI N89-17049
KITAMURA, TAKAYUKI N89-17286
KLABUNDE, C. E. N89-17456
KLAETSCHKE, H. N89-17273
N89-17276
KLEIN, MARK H. N89-16771
N89-16772
KLEM, J. F. N89-17532
KLIMOV, A. M. N89-16947
KLINGSHIRN, C. N89-17129
KNAPP, J. A. N89-16962
KOBAYASHI, MASAAKI N89-17094
KOCHARYAN, A. A. N89-17554
KOEL, BRUCE E. N89-16960
KOLESNIK, I. G. N89-17555
KOLNER, B. H. N89-17114
KOMANDURI, R. N89-17486
KOMPENHANS, J. N89-17198
KONDO, KAZUO N89-17094
KOOI, J. W. N89-16870
KOPCSAY, G. V. N89-17138
KOREN, U. N89-17129
KORNBLUM, H. N. N89-17220
KOROS, W. J. N89-17014
KOROTKY, S. K. N89-17134
KOSEL, T. H. N89-16976
KOSUT, ROBERT L. N89-16901
KOUL, A. K. N89-17257
KOVAC, JEFFREY N89-17002
KRAICHNAN, ROBERT H. N89-17162
KRAMER, DANIEL L. N89-16904
KRENZ, GUENTER N89-16877
KRIEG, R. D. N89-17237
KRIELLAARS, D. N89-17034
KRING, C. T. N89-17240
KROTKUS, A. N89-17099
KRUPKE, W. F. N89-17502
KRYTER, ROBERT C. N89-17244
KUEBLER, DAVID P. N89-17462
KULIKOWSKI, CASIMIR A. N89-17428
KULSRUD, R. N89-17507
KUMAR, ANAND N89-16757
KUNZ, J. H. N89-16785
KURATA, YUJI N89-16969
KURDYUSOV, S. P. N89-17456
KUROBE, TOSHIJI N89-17052
KURYLA, M. S. N89-17345
KWAK, J. F. N89-17010
KWEON, INSO N89-17236
KWON, O. J. N89-17508
N89-17513
KYRAZIS, D. T. N89-17220

L

LABRUJERE, TH. E. N89-16863
LACKNEY, JOSEPH N89-17321
LAFLAMME, J. C. G. N89-16803
LAFLEN, J. H. N89-17335
LAFORTUNE, S. N89-17034
LAGOWSKI, JACEK N89-17525
LAGRANDEUR, ROSS N89-16784
LAHEY, R. T., JR. N89-17165
LAINE, B. N89-16788
LAIREZ, D. N89-16935
LAM, KAI-SHUE N89-17476
LAMKIN, S. L. N89-17562
LAMPERT, W. V. N89-17526
LANCASTER, GREG N89-17492
LANDHERR, STEFAN F. N89-16771
N89-16772
LANGLEY, LAWRENCE W. N89-16822
N89-16824
LANGLEY, PAT N89-17400
LANZL, F. N89-16888
LARSEN, SHAWN N89-17369
LARSON, RICHARD W. N89-17064
LARSSON, A. N89-17113
LARUE, R. N89-17090
LARUELLE, GERARD N89-16750
LAU, K. Y. N89-17110
LAUER, R. F., JR. N89-16852
LAVRUSHKO, A. G. N89-17001
LAWLER, J. V. N89-17157
LAWSON, M. W. N89-17213
LE, SANH N89-17241
LEBLANC, ALAIN N89-16784
LEE, CHI H. N89-17097
N89-17098
N89-17104
N89-17107
N89-17133
LEE, H. R. N89-16974
LEE, K. W. N89-17490
LEE, LONG C. N89-16965
LEE, Y. H. N89-17088
LEFEVRE, J. P. N89-17496
LEI, J. F. N89-17300
LEIGHTON, R. I. N89-17157
LEON, HENRY A. N89-17390
LEONG, P. T. N89-17530
LEPPICH, J. N89-17355
LESSER, VICTOR N89-17425
LEUNG, P. T. N89-16973
LEVINE, DAVID N89-17406
LEVIONNOIS, ALBERT N89-16805
LEWIS, C. R. N89-17345
LEWIS, M. H. N89-16993
LEYLAND, D. C. N89-16743
N89-16745
N89-16747
LEYNAERT, JACKY N89-16749
N89-16751
LI, G. P. N89-17083
LIANG, KO-HSIN N89-17411
LIBROWSKI, K. N89-16807
LILIENTAL-WEBER, Z. N89-17526
LIM, JOON WON N89-16778
LIN, C. L. N89-17528
LINDHOLM, ULRIC S. N89-17322
LINDL, J. D. N89-17502
LINDSEY, PAUL J. N89-17160
LIOU, M.-F. N89-16759
LIU, A. N89-17331
LIU, D. D. N89-17344
LIU, RICHARD Y. L. N89-17263
LONDON, R. A. N89-17229
N89-17233
LOO, B. H. N89-17530
LOPEZ, A. R. N89-16900
LOPEZ, JUAN D. N89-16941
LORIOT, M. N89-16934
LOTT, J. A. N89-17532
LOUIS-JACQUET, M. N89-17229
N89-17233
LOURENCO, L. M. N89-17184
LOWDERMILK, W. H. N89-17502
LOWRY, MARK N89-17492
LUCAS, G. E. N89-16970
LUEBKE-OSSENBECK, B. N89-17355
LUFFER, DEBRA R. N89-16937
LUGLI, P. N89-17120
LUKENS, JAMES E. N89-17524
LUNDERSTAEDT, R. N89-16811
LUTZ, CHARLES N89-17092
LYNCH, F. T. N89-16864
LYNN, K. G. N89-16989

M

MAARSINGH, R. A. N89-16863
MACCRACKEN, MICHAEL C. N89-17365
MACGOWAN, B. J. N89-17229
N89-17231
N89-17233
MACHLER, M. N89-17043
MACIEJEWSKI, PAUL N89-17309
MACKINTOSH, G. B. N89-16806
MACLEOD, J. D. N89-16803
MACMILLAN, H. F. N89-17344
N89-17345
MAEKAWA, KATSUHIRO N89-17049
MAFFEI, N. N89-17040
MAHAJAN, D. N89-16958
MAKOWIECKI, D. M. N89-16936
MALIK, S. N. N89-17335
MALKIE, DANIEL C. N89-17423
MALVEZZI, A. M. N89-17098
MANALO, NATIVIDAD N89-17374
MANGES, W. W. N89-17249
MANN, REINHOLD C. N89-17251
MANNHEIM, P. D. N89-17538
MANNING, S. L. N89-17333
MANSIGH, MARY A. N89-17225
MARGOLIN, L. G. N89-17154
MARGULIS, W. N89-17099
MARIANI, DANIELE N89-17075
MARKHAM, C. H. N89-17035
MARKS, TOBIN J. N89-17007
MAROM, MOSHE N89-17066
MARTIN, CHARLES R. N89-17149
MARTIN, JAMES P. N89-16766
MARTINEZ, R. J. N89-17011
MARVIN, JOSEPH G. N89-16880
MASKEW, BRIAN N89-16775
MASSIDDA, JOHN E. N89-17512
MATHIAS, LON J. N89-16921
MATIJEVIC, ZELJKO N89-16897
MATSON, BRADLEY S. N89-17207
MATTERA, V. D., JR. N89-17086
MATTHEWS, D. L. N89-17229
N89-17231
N89-17233
MAXON, S. N89-17229
MAY, P. G. N89-17083
MAYER, G. N89-16891
MAYER, J. N89-17355
MAYHALL, D. J. N89-17076
MAZAREANU, S. N89-16809
MAZHER, A. HAMID K. N89-17164
MAZIASZ, P. J. N89-16979
MCBRIDE, BONNIE J. N89-17017
MCCALLUM, J. C. N89-17519
MCCONAGHY, CHUCK N89-17087
MCCROSKEY, W. J. N89-16847
MCDANIEL, JOE W. N89-17391
MCDONALD, H. N89-17313
MCDONALD, THOMAS N89-17218
MCDONNEL, V. G. N89-17305
MCGILL, R. N. N89-17016
MCGOVERAN, DAVID O. N89-17556
MCINTYRE, R. W. N89-17028
MCKEEGAN, KEVIN DANIEL N89-17551
MCKNIGHT, R. L. N89-17320
N89-17332
MCNELIS, MARK E. N89-16905
MCVEY, JOHN B. N89-17306
MCWETHY, L. G. N89-17375
MCWRIGHT, GLEN N89-17492
MEAD, WILLIAM N89-17218
MECHERLE, G. S. N89-17215
MEETHAM, G. W. N89-16996
MEHR, KENT N89-17171
MEIFFREN, J. L. N89-17261
MEISTER, JEFFREY P. N89-17319
MEKJAVIC, I. B. N89-17044
MERKLE, KARL L. N89-17529
MERRINGTON, G. L. N89-16813
MERZKIRCH, W. N89-17185
N89-17186
METSELAAR, R. N89-16995
METZBOWER, E. A. N89-17239
METZGER, D. E. N89-17312
METZGER, DAVID W. N89-17069
MEYER, THOMAS G. N89-17334
MEYERS, B. C. N89-16881
MIAMEE, A. G. N89-17448
MICHEL, U. N89-16859
MIGUS, A. N89-17088
N89-17127
MILES, R. N. N89-17467
MILES, RICHARD B. N89-16725
MILLER, B. I. N89-17129

MILLER, D. N89-17135
MILLER, D. A. B. N89-17129
MILLER, ROBERT A. N89-17330
MIMURA, TAKASHI N89-17094
MISHRA, NINA N89-17209
MISSON, N. T. N89-17061
MLADSI, S. W. N89-17327
MOELLER, K. W. N89-16870
MOFFAT, ROBERT J. N89-17309
MOHAMMAD, NOOR N89-17429
MONAN, WILLIAM P. N89-16769
MONEY, K. E. N89-17035
MONGIA, H. C. N89-17303
N89-17304
N89-17305
MONSON, CONRAD B. N89-17392
MONTAG, W. H. N89-17028
MONTANO, PEDRO A. N89-16928
MONTI, R. N89-16876
MONTIN, J. L. N89-16818
MOODENBAUGH, A. R. N89-17520
N89-17528
MOON, DENNIS ALLAN N89-17377
MOORE-EDE, M. C. N89-17396
MOORE, R. D. N89-16837
MOORHEAD, PAUL E. N89-17329
MORAITIS, C. S. N89-17189
N89-17190
MORALES, R. I. N89-16936
MOREL, THOMAS N89-17166
MORI, Y. N89-17480
MORKOC, H. N89-17102
N89-17127
MOROSIN, B. N89-17010
N89-17533
MORRIS, JOHN A. N89-17361
MORRIS, JOHN D. N89-17546
MORSE, T. F. N89-17489
MORTIMER, ALAN J. N89-17025
N89-17036
MOSTAFA, A. A. N89-17305
MOTT, T. D. N89-17545
MOUROU, GERARD A. N89-17095
N89-17136
MOYNE, CHRISTIAN N89-17173
MUELLER, KENT A. N89-16718
MUELLER, R. N89-16848
MUIR, D. E. N89-16787
MUIR, T. F. N89-16919
MUMM, HANS N89-16881
MURAI, SHUNJI N89-17409
MURN, STANLEY J., JR. N89-17262
MURTHY, S. N. B. N89-17304
MUSGRAVE, C. N89-17526
MUSKET, R. G. N89-17219
N89-17534
MYERS, D. N89-17490
MYERS, D. R. N89-17532
MYERS, DENNIS A. N89-16795
MYSYROWICZ, A. N89-17088
N89-17127

N

NACCACHE, D. N89-17229
N89-17233
NAMAZIAN, M. N89-16945
NARASIMHA, R. N89-17372
NASTASI, MICHAEL N89-17245
NEALY, JOHN E. N89-17562
NEES, JOHN N89-17109
NEGAARD, GORDON R. N89-16776
NEIKIRK, DEAN P. N89-17100
N89-17135
NELSON, DAN N89-17492
NELSON, DANNY A. N89-17207
NELSON, P. A. N89-17145
NELSON, RICHARD S. N89-17336
NERI, J. M. N89-17507
NETHERS, RAYMOND W. N89-17069
NETZER, DAVID W. N89-16821
NEUMANN, J. F. N89-17331
NEWMAN, F. A. N89-16834
NEWMAN, J. C., JR. N89-17287
N89-17288
N89-17290
N89-17291
N89-17294
NGUYEN, CHARLES C. N89-17444
NICHOLS, D. N89-17528
NICHOLSON, A. N. N89-17399
NICHOLSON, D. M. N89-16977
NICOL, DAVID M. N89-17417
N89-17418
NIE, DALIN N89-17384
NIGOHOSIAN, M. N89-17145
NIGRO, A. N89-17527
NIJHAWAN, V. N89-17038
NIKJOOY, M. N89-17304
NIRMALAN, V. N89-17315
NISSLEY, DAVID M. N89-17334
NOACK, R. W. N89-16900
NOAKES, M. W. N89-17240
NOBRE, A. N89-16809
NOUAILHAS, D. N89-17285
NOVOTNY, MILOS N89-16937
NOYES, H. PIERRE N89-17556
NUMBERS, KEITH E. N89-16740
NUSS, M. C. N89-17118
N89-17137
NUTTALL, ALBERT H. N89-17446

O

OBLITEY, WILLIAM WALTER N89-17544
OBOKATA, TOMIO N89-17199
OCHOA, OZDEN O. N89-16774
OCONNOR, C. M. N89-16797
ODETTE, G. R. N89-16970
OETTL, H. N89-16887
OFFEN, HENRY W. N89-17000
OGAWA, YUTAKA N89-16969
OH, H. G. N89-16974
OHARA, JOHN M. N89-17393
OHARE, T. E. N89-16958
OHTANI, RYUICHI N89-17286
OKADA, S. N89-17498
OKUN, L. B. N89-17477
OLIPHANT, A. N89-17061
OLSEN, KHRIS B. N89-17207
OMINE, MEGUMI N89-17055
ONSTOTT, ROBERT G. N89-17064
OPPERMANN, H. N89-17273
N89-17274
N89-17277
ORTEGA, J. M. N89-17421
ORTIZ, M. N89-17333
OSMAN, M. A. N89-17120
OTRIO, G. N89-17494
OTTINGER, P. F. N89-17507
OXBORROW, ROBERT R. N89-17348

P

PAAS, J. E. N89-16799
PAEZ, THOMAS N89-17442
PAGLIALUNGA, A. N89-17194
PAIVARINTA, LASSI N89-17070
PALLISTER, K. C. N89-16857
PAN, GUANGGUO N89-17531
PANFEROV, A. D. N89-17161
PANITZ, J. K. G. N89-17346
PANTUCEK, P. N89-17283
PAONE, N. N89-17200
PAPAILIOU, K. D. N89-16810
PARKER, R. J. N89-16842
PARKER, R. K. N89-16841
PARKINSON, W. H. N89-16942
PARTAIN, L. D. N89-17344
PATANKAR, SUHAS V. N89-17303
N89-17307
N89-17310
PATTON, WALDO N89-17506
PAUL, D. R. N89-17014
PAULEY, WAYNE N89-17309
PAULMIER, P. N89-17285
PEARSONS, K. S. N89-17461
PEI, S. S. N89-17081
PENDLEY, M. H. N89-17432
PERERA, JEEVAN N89-17058
PERINELLE, J. N89-16875
PERKINS, A. LOUISE N89-17206
PETERKIN, R. E., JR. N89-17222
PETERS, P. N. N89-17530
PETERSEN-OVERTON, MARK D. N89-17156
PETERSON, DONALD H. N89-17392
PETERSON, RICHARD T. N89-17492
PETRASEK, DONALD W. N89-16986
PETROVIC, JOHN J. N89-16933
PEYGHAMBARIAN, N. N89-17088
N89-17127
PEYRUSSE, O. N89-17233
PHILLIPS, E. P. N89-17290
N89-17291
N89-17295
PHILLIPS, JAMES D. N89-16845
PHUCHAROEN, WORAPHAT N89-17330
PIANKO, MARC N89-16879
PILSNER, B. N89-17332
PINSKI, F. J. N89-16977
PLATEN, E. N89-17450
PLETCHER, DEREK N89-16952
PLINE, ALEXANDER D. N89-17211
POCHA, M. D. N89-17139
POGGIO, ANDREW J. N89-17459
POLAK-DINGLES, P. N89-17133
POLICELLA, H. N89-17285
PONCE, D. A. N89-17373
PONS, B. STANLEY N89-16949
N89-16950
N89-16951
N89-16952
N89-16953
N89-16954
N89-16955
N89-17210
POORAN, FARHAD J. N89-17444
POPE, G. T. N89-17215
POPE, L. E. N89-16982
POPOV, YE. I. N89-16967
POPPER, P. N89-16999
POST, W. M. N89-17360
POTTER, J. L. N89-16867
POUJOL, L. N89-17163
POWELL, DOUGLAS G. N89-16921
POWERS, WILLIAM T. N89-16816
POYARKOV, V. G. N89-16987
PRAKASH, MANJU N89-17506
PRASAD, S. E. N89-17040
PRENDERGAST, K. N89-17434
PRICE, D. F. N89-17208
PRIEBE, CAREY E. N89-17426
PROTOPOPESCU, V. N89-17438
PROUX, G. T. N89-17029
PROVOST, M. J. N89-16819
PRUTHI, D. D. N89-16968
PRZYBYSZEWSKI, JOHN S. N89-17299
PUJOL, C. N89-16858
PUSEY, MARC LEE N89-17535

Q

QIU, S. L. N89-17528
QUACKENBUSH, TODD R. N89-16726
QUEMARD, C. N89-16849
QUINN, G. D. N89-16998
QUINN, J. W. N89-17080

R

RABANG, M. PETER N89-16727
RAIMONDO, S. N89-16860
RAJ, PHANI K. N89-17361
RAKESTRAW, DAVID J. N89-17483
RAKOWSKI, MARK N89-17536
RAMSIER, R. D. N89-16957
RAO, M. N. N89-16885
RAYBON, G. N89-17134
RAYMER, MICHAEL G. N89-17216
REDDY, D. R. N89-16759
REDEKER, G. N89-16848
REED, C. L. N89-16764
REED, MARK N89-17357
N89-17358
REGEL, L. L. N89-17024
REGIS, HENRY C. N89-16975
REHN, L. E. N89-17481
REICH, ARIEL N89-16971
REILLY, J. J. N89-16966
REIMER, H. N89-16978
REINHART, WILLIAM F. N89-17401
REITZE, D. H. N89-17121
REJ, D. J. N89-17498
RESHOTKO, ELI N89-16867
RIAZIAT, M. N89-17090
RICHARDS, D. S. N89-17417
RICK, H. N89-16812
RIETHMULLER, M. L. N89-17187
N89-17188
N89-17200
RIGOLI, MARKO N89-17454
RIPIN, B. H. N89-17222
RISTOW, M. L. N89-17344
N89-17345
RO, TED N89-17058
ROBERT, M. N89-16872
ROBINSON, D. N. N89-17323
RODRIGUEZ, GILBERTO N89-16956
RODRIGUEZ, J. G. N89-17234
N89-17235
RODWELL, M. J. W. N89-17082
ROESKE, FRANK N89-17497
ROGERS, D. L. N89-17116

ROGERS, J. W., JR. N89-17533
ROHATGI, V. K. N89-17510
ROMANO, P. N89-17527
ROMANOFF, H. P. N89-16719
N89-16720
N89-16721
N89-16722
ROMIG, A. D., JR. N89-17144
ROMINE, C. H. N89-17421
RONG, ZHANG N89-17483
ROONEY, E. C. N89-16852
ROSE-PEHRSSON, S. L. N89-17362
ROSEN, LEONARD C. N89-17225
N89-17230
ROSEN, M. D. N89-17229
N89-17233
ROSENSTEIN, H. J. N89-16850
ROSOCHA, LOUIS N89-17218
ROSS, H. D. N89-17046
ROTH, N. N89-17192
ROTHARD, H. N89-17478
ROVER, D. T. N89-17349
ROWELL, MICHAEL O. N89-17410
ROYER, H. N89-17191
RUBY, D. S. N89-17343
RUCKMAN, M. W. N89-17528
RUDNITSKI, D. M. N89-16787
RUE, A. K. N89-17215
RUNCHAL, A. K. N89-17303
RUPERT, V. C. N89-17228
RUSSELL, SID N89-17306
RUSSO, GIUSEPPE P. N89-16867
N89-16868
RYERSON, CHARLES C. N89-17381

S

SABITOV, M. S. N89-17511
SAGHIR, Z. N89-17037
N89-17042
SAITO, HAGAO N89-17053
SALTSMAN, J. F. N89-17337
SALZ, U. N89-17105
SAMARSKIY, A. A. N89-17458
SAMEC, RONALD GEORGE N89-17549
SAMUELSEN, G. S. N89-17305
SANDBERG, VERNON N89-17457
SANDELL, NILS R., JR. N89-17447
SANDERS, CLAUDIA N89-17543
SANTORO, ROBERT L. N89-17392
SAPIENZA, R. S. N89-16958
SAPSARD, M. J. N89-16790
SARDALOS, S. L. N89-17412
SARFF, JOHN STEPHEN N89-17515
SASAKI, MISAO N89-17557
SAYADIAN, HRAYR A. N89-17097
SCHARER, J. E. N89-17509
SCHARLEMANN, E. T. N89-17227
SCHEFER, R. N89-16945
SCHEUERMANN, M. N89-17083
SCHILLER, D. N. N89-17046
SCHIRBER, J. E. N89-17533
SCHLUETER, HEINRICH N89-16792
SCHMIDT, E. N89-16832
SCHMIDT, RODNEY C. N89-17310
SCHMITT, JEROME J. N89-16946
SCHMITT, V. N89-16848
N89-16869
SCHMITZ, D. M. N89-16742
SCHNEIDER, NICHOLAS MCCORD N89-17559
SCHOEDDERT, ROLF N89-16792
SCHOFIELD, CHRISTOPHER N89-16784
SCHRAWYER, L. R. N89-16936
SCHREIBER, H. A. N89-16829
N89-16830
SCHUELLER, R. D. N89-16925
SCHUETZ, D. N89-17277
SCHULTZ, T. J. N89-17461
SCHULZ, U. N89-16785
SCHUMACHER, H. N89-17105
SCIPPA, S. N89-16912
SCOTT, R. L., JR. N89-17243
SCOTT, W. R. N89-17259
SEABAUGH, A. C. N89-17104
SEABAUGH, ALAN N89-17104
SEAGER, C. H. N89-17003
SEALS, WILLIAM O. N89-17000
SEARBY, G. N89-16964
SEARS, WILLIAM J. N89-17392
SEDDON, J. N89-16739
N89-16746
SEGALL, DANIEL O. N89-17433
SEGALMAN, D. J. N89-17237
SEIN, E. N89-17495
SEKAR, R. R. N89-17359
SELLARS, B. G. N89-17033
SELLIN, I. A. N89-17478
SELTZER, MICHAEL D. N89-17224
SEN, S. N89-17126
SENIOR, T. B. A. N89-17148
SESSLER, ANDREW M. N89-17485
SHAARBAF, M. N89-17300
SHAH, JAGDEEP N89-17128
SHAING, K. C. N89-17508
SHAMROTH, S. J. N89-17313
SHAO, BEILING N89-17529
SHAPIRA, Y. N89-17530
SHARP, D. J. N89-17346
SHAW, M. T. N89-16927
SHEEHAN, J. N89-16895
SHEFFLER, K. D. N89-17333
SHEH, M. Y. N89-17324
SHEIL, MARGARET M. N89-17468
SHEN, LAWRENCE K. N89-17318
SHEN, S. F. N89-17159
SHERRELL, F. G. N89-16816
SHIER, D. R. N89-17417
SHINN, N. D. N89-17533
SHULL, C. L. N89-17234
SHUO, HUNG CHANG N89-17248
SIDDIQUI, A. H. N89-17429
SIEMON, R. E. N89-17498
SIGNORELLI, E. N89-17527
SILICH, S. A. N89-17555
SIMONOV, YU. A. N89-17436
SINDORF, J. N89-17143
SINGH, M. K. N89-17359
SINGH, TARSEM N89-16889
SINYUKOV, YU. M. N89-17161
SIRIGNANO, W. A. N89-17046
SISK, R. C. N89-17530
SITES, J. R. N89-17341
SKAPERDAS, G. T. N89-16958
SKOKOWSKI, P. G. N89-17228
SKOWRONSKI, VANCE D. N89-17391
SLAVIN, M. J. N89-16998
SLEIGHT, A. W. N89-17520
SLOUGH, J. T. N89-17498
SMALLEY, LARRY L. N89-17558
SMARTT, H. B. N89-17252
SMETANINA, L. N. N89-17266
SMITH, A. W. N89-17349
SMITH, DUDLEY EDINGTON N89-16823
SMITH, G. E. N89-16759
SMITH, G. LOUIS N89-17374
SMITH, J. N89-16863
SMITH, MALCOLM N89-17392
SMITH, P. R. N89-17137
SMITH, PHILLIP J. N89-17386
SMOLYANSKIJ, S. A. N89-17161
SMYTH, M. N89-17083
SNEDDON, LARRY G. N89-17012
SNYDER, HARRY L. N89-17401
SOBOLEWSKI, R. N89-17095
SOKOLOV, V. S. N89-17458
SOLLNER, T. C. L. GERHARD N89-17124
SONSINO, C. M. N89-17280
SPAETE, PAUL ERNEST N89-17378
SPAULDING, MALCOLM N89-17357
N89-17358
SPENCER, JOHN P. N89-17242
SPIELMAN, BARRY E. N89-17089
SPONG, D. A. N89-17508
SPRINGER, GEORGE S. N89-16922
SPRUNG, CLAUDE N89-16796
STAEGER, W. N89-16871
STAMATIS, A. N89-16810
STAMPER, J. A. N89-17222
N89-17488
STANEWSKY, E. N89-16760
N89-16865
STANFORD, J. L. N89-17365
STANNILAND, D. R. N89-16862
STARK, W. E. N89-17073
STARKEN, HANS N89-16826
N89-16827
N89-16828
STEBBINS, ALBERT N89-17540
STEGER, JOSEPH L. N89-16763
STEIER, WILLIAM H. N89-17140
STEINBERG, M. N89-16959
STEINHILBER, H. N89-17275
N89-17276
STEINKE, R. J. N89-16834
STELLINGWERF, R. F. N89-17222
STEPHENS, JOSEPH R. N89-16986
STEWART, DONALD F. N89-17391
STEWART, I. R. N89-17153
STEWART, R. E. N89-17208
STEWART, R. M. N89-16807
STINE, J. R. N89-17018
STOCKS, G. M. N89-16977
STONE, BARBARA M. N89-17399
STONE, R. R. N89-17217
STORM, ERIK N89-17501
N89-17502
STOUFFER, D. C. N89-17324
STOWERS, I. F. N89-17486
STRAHAN, ALAN N89-17058
STRAIN, BOYD R. N89-17367
STRANGMAN, T. E. N89-17331
STREETMAN, BEN G. N89-17100
STRONG, LAURENCE L. N89-17339
STRONGIN, MYRON N89-17528
STUBOS, A. N89-17170
STURTEVANT, BRADFORD N89-17158
SUBBARAYA, B. H. N89-16884
SUBRAMANIAN, M. A. N89-17520
SULLIVAN, J. P. N89-17304
SULLIVAN, P. J. N89-17044
SULTANIAN, B. K. N89-17315
SUNDARAM, A. K. N89-17508
SUNG, CHEN-HAN N89-17426
SURBER, LEWIS E. N89-16740
N89-16741
N89-16744
SUTIN, NORMAN N89-17471
SUTO, MASAKO N89-16965
SUTTLES, JOHN T. N89-17374
SUVOROV, A. L. N89-16987
SWAB, J. J. N89-16998
SWAIN, M. H. N89-17290
N89-17293
SWANSON, GUSTAV A. N89-17334
SWINDEMAN, R. W. N89-16979
SYDORIAK, STEVE N89-17543
SYNDER, C. E. N89-17545
SZTURM, T. N89-17034

T

TAFFE, P. A. N89-17362
TAGGART, D. P. N89-17498
TAKAGI, A. N89-17480
TAKAHAMA, MARK N89-17401
TAKEDA, N. N89-17022
TANG, P. Y. N89-16920
TANG, PING TAK PETER N89-17415
TANSLEY, D. R. N89-17040
TASKER, P. J. N89-17101
TAYLOR, A. J. N89-17084
TAYLOR, HENRY F. N89-17131
TAYLOR, K. J. N89-17061
TAYLOR, R. G. N89-17260
TEMKIN, H. N89-17086
TENEKETZIS, DEMOSTHENIS N89-17447
TESMER, JOSEPH R. N89-17245
TESTER, R. M. N89-16804
THEIMER, P. N89-16800
THIRSK, R. N89-17044
THOMAS, ANTHONY N89-17353
THOMPSON, B. G. N89-17032
THOMPSON, D. H. N89-17249
THOMPSON, GEORGE N89-17536
THOMPSON, J. W., JR. N89-16854
THOMPSON, ROBERT L. N89-17329
THORP, G. P. N89-16911
THRASHER, DURWOOD I. N89-16914
THRESHER, R. W. N89-17354
THUR, GEORGE M. N89-17238
THURMOND, G. D. N89-17132
TIAN, JIEMO N89-17531
TINARI, P. D. N89-17172
TIPTON, M. T. N89-17320
TITRAN, ROBERT H. N89-16986
TOBIN, S. P. N89-17343
TODD, E. S. N89-17316
TOLK, NORMAN H. N89-17489
TOMITA, KENJI N89-17563
TONG, M. N89-17329
TOW, D. M. N89-17234
N89-17235
TOWNE, CHARLES E. N89-16752
TOWNSEND, JAMES C. N89-17418
TOWNSEND, LAWRENCE W. N89-17562
TRACEY, KAREN L. N89-17387
TRANQUADA, J. M. N89-17520
TREBES, J. N89-17231
TRUCHOT, A. N89-16908
N89-16915
N89-16916
TRYGVASSON, B. N89-17044
TRYK, DONALD N89-17141
TSANG, J. C. N89-17103
TSUCHIYA, HACHIRO N89-17054
TUAN, VO-DINH N89-17366

TUCKER, R. S. N89-17084
N89-17115
N89-17134
TURLEY, W. DALE N89-17000
TURNER, CHRIS N89-17357
N89-17358
TURNER, G. W. N89-17107
TURNER, J. E. N89-17470
TURNER, MICHAEL S. N89-17540
TUSZEWSKI, M. N89-17498
TWETE, M. A. N89-17215
TZUANG, C.-K. C. N89-17135

U

UENO, A. N89-17480
UHLMANN, D. R. N89-17004
URY, I. N89-17110
USMAR, S. G. N89-16989

V

VAERMAN, J. N89-17258
VAGLIO, R. N89-17527
VALDMANIS, J. A. N89-17081
VANALSTINE, J. M. N89-17030
VANARSDALL, P. J. N89-17491
VANDENBRAEMBUSSCHE, R. A. N89-17200
VANEVERY, D. N89-16860
VANGEIN, R. N89-17371
VANSTONE, R. H. N89-17335
VANWANDERHAM, M. C. N89-17256
VAQUEZ, PHILIPPE N89-16801
VAUGHN, JASON A. N89-17146
VEERS, PAUL S. N89-17351
VENKATRAMANI, N. N89-17510
VENTURINI, E. L. N89-17010
N89-17533
VERNON, S. M. N89-17343
VESELKA, J. J. N89-17134
VIEILLARD, A. N89-16794
VIGIL, MANUEL N89-17543
VINOKUR, MARCEL N89-17445
VINYARD, SHANNON N89-17548
VIRLOGEUX, PIERRE N89-16892
VIRSHUP, G. F. N89-17344
N89-17345
VLEGHERT, J. P. K. N89-16853
VOIGT, R. G. N89-17421
VOLAKIS, J. L. N89-17077
N89-17148
VOLMIR, A. S. N89-17266
VONLEHMEN, A. N89-17130

W

WAGGONER, C. A. N89-16818
WAGNER, J. H. N89-17314
WALKER, IRA N89-17374
WALKER, KEVIN P. N89-17325
WALL, M. A. N89-16936
N89-17534
WANG, J. C. N89-17521
WANG, JIALONG N89-17531
WANG, LINGLING N89-17531
WANG, S. Y. N89-17114
WANG, T.-H. N89-17135
WANHILL, R. J. H. N89-17289
WARD, R. C. N89-17455
WASHBURN, J. N89-17526
WATKINS, A. D. N89-17252
WATT, D. G. D. N89-17027
N89-17035
WATTS, DAVID N89-17384
WATTS, RANDOLPH N89-17387
WAWNER, F. E. N89-16925
WEBB, K. N89-17133
WEBER, E. R. N89-17526
WEBSTER, R. B. N89-17498
WEEKS, WILFORD F. N89-17388
WEINBERG, B. C. N89-17313
WEINER, DONALD N89-17449
WEINGARTEN, K. J. N89-17082
WEISBIN, C. R. N89-17249
WEISS, SHOLOM M. N89-17428
WELLER, J. F. N89-17117
WENNERSTROM, A. J. N89-16835
N89-16836
WERTHEN, J. G. N89-17345
WEST, JEFFREY R. N89-16904
WHEELER, KYLE N89-17543
WHELAN, D. A. N89-17208
WHITE, C. W. N89-17519
WHITE, RALPH E. N89-17149
WHITEHEAD, J. C. N89-16939
WHITEMAN, C. D. N89-17375
WHORIC, JAMES M. N89-16851
WIEDWALD, J. D. N89-17139
WIESENFELD, J. M. N89-17084
N89-17115
WILLIAMS, P. N89-17135
WILLIAMS, R. K. N89-17026
WILLIAMSON, STEVE N89-17109
WILLSON, V. N89-17037
WILMUT, D. N89-17037
WILSON, JOHN W. N89-17562
WILSON, RAYMOND B. N89-17317
WILTON, D. R. N89-17072
WINELAND, D. J. N89-17475
WINFIELD, DAN N89-17393
WING, JENNETTE M. N89-17435
WINGET, CHARLES M. N89-17390
WINKLER, JAY R. N89-17471
WOLFF, L. R. N89-16995
WOMBLE, DAVID E. N89-17420
WOOD, M. N. N89-16855
WOODLE, M. H. N89-16895
WOOLF, BEVERLY N89-17425
WRENN, GREGORY A. N89-16779
WRIGHT, A. D. N89-17354
WRIGHT, B. L. N89-17498
WRIGHT, H. A. N89-17470
WU, M. K. N89-17530
WURTZ, JORGEN N89-17171
WYAT, J. R. N89-17362

X

XU, Y. W. N89-17528
XU, YOUWEN N89-17520

Y

YAKOVLEV, B. S. N89-17001
YANAGAWA, K. N89-17022
YANAGIDA, SATOSHI N89-17409
YANG, C. Y. N89-17520
YAO, CHEN-WU N89-16991
YARIV, A. N89-17113
YEAGER, ERNEST N89-17141
YEE, J. H. N89-17076
YEN, H. W. N89-17132
YEW, KHOY CHUAH N89-16762
YOSHIKAWA, MASANORI N89-17050
YOSHINO, K. N89-16942
YOST, F. G. N89-17144
YOUNG, M. F. N89-16821
YU, S. T. N89-17308
YUEN, C. N89-17090
YUST, C. S. N89-16932

Z

ZAAR, J. N89-17021
ZACHOS, C. K. N89-17440
ZAFAR, MUBASHAR N89-17152
ZAJTSEV, S. V. N89-16987
ZAKI, K. N89-17133
ZAKLYAZMINSKIY, L. A. N89-17458
ZAMORSKI, JOSEPH R. N89-17541
ZANELLI, J. N89-17537
ZARE, RICHARD N. N89-17483
ZDASIUK, G. N89-17090
ZELLER, BERNARD N89-16913
ZHANG, BAOQING N89-17531
ZHANG, T. R. N89-17121
ZHANG, Y. N89-17201
ZHOLDASOVA, S. M. N89-17001
ZITO, JAMES A. N89-16904
ZOLTANI, CSABA K. N89-17195
ZUCKER, J. E. N89-17130
ZULEEG, R. N89-17526
ZUPPARDI, G. N89-16876
ZWAAN, R. J. N89-16878

Typical Corporate Source Index Listing

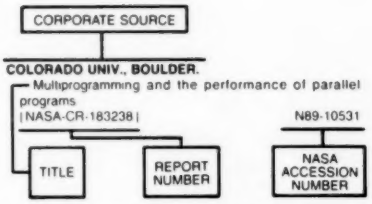

Listings in this index are arranged alphabetically by corporate source. The title of the document provides the user with a brief description of the subject matter. The report number helps to indicate the type of document cited (e.g., NASA report, translation, NASA contractor report). The NASA accession number denotes the number by which the citation is identified. The titles are arranged under each corporate source in ascending accession number order.

A

ACADEMY OF SCIENCES OF THE ARMENIAN SSR, ERIVAN.
What topology could the universe be created with
[DE88-704321] N89-17554

ACADEMY OF SCIENCES OF THE UKRAINIAN SSR, KIEV.
Relativistically-invariant statistical hydrodynamics of a normal fluid
[DE88-704370] N89-17161
Origin and dynamics of expanding neutral hydrogen supershells
[DE88-704372] N89-17555

ACADEMY OF SCIENCES OF THE UZBEK SSR, TASHKENT.
Electric conductivity of polymer composite materials. Composite on propylene and silicon base
[DE88-704293] N89-17001
Role of charge exchange process in forming of ion charge and energy states in multicomponent laser plasma produced from gas-content solids
[DE88-704828] N89-17511

ACADEMY OF SCIENCES (USSR), MOSCOW.
On fundamental problems of Space Materials Science (SMS) N89-17024

ADVISORY GROUP FOR AEROSPACE RESEARCH AND DEVELOPMENT, NEUILLY-SUR-SEINE (FRANCE).
Reynolds number effects in transonic flow
[AGARD-AG-303] N89-16760
Engine Condition Monitoring: Technology and Experience
[AGARD-CP-448] N89-16780
Aerodynamic Data Accuracy and Quality: Requirements and Capabilities in Wind Tunnel Testing
[AGARD-CP-429] N89-16846
Design Methods in Solid Rocket Motors
[AGARD-LS-150-REV] N89-16906
AGARD/SMP Review: Damage Tolerance for Engine Structures. 1: Non-Destructive Evaluation
[AGARD-R-768] N89-17253
Short-Crack Growth Behaviour in an Aluminum Alloy: An AGARD Cooperative Test Programme
[AGARD-R-732] N89-17287
Sleep and wakefulness: Handbook for flight medical officers, 2nd edition
[AGARD-AG-270(F)] N89-17399

AEROMETRICS, INC., SUNNYVALE, CA.
Evaluation and application of a new interferometry technique for compressible flow research
[NASA-CR-177467] N89-16765

AERONAUTICAL RESEARCH LABS., MELBOURNE (AUSTRALIA).
Gas path analysis and engine performance monitoring in a Chinook helicopter N89-16802
Identification of dynamic characteristics for fault isolation purposes in a gas turbine using closed-loop measurements N89-16813

AEROSPATIALE, SURESNES (FRANCE).
Evaluation of physical chemical test methods for characterizing polymerized composites or polymerizing composites: Literature review
[REPT-49-438/F] N89-16935

AEROSPATIALE USINES DE TOULOUSE (FRANCE).
Implication of engine performance monitoring for the aircraft manufacturer N89-16794

AIR COMMAND AND STAFF COLL., MAXWELL AFB, AL.
Event-centered scheduling program: The need for PERT (Program Evaluation Review Technique) in C-141 ISO inspection management
[AD-A200094] N89-16718

AIR FORCE ROCKET PROPULSION LAB., EDWARDS AFB, CA.
Advances in solid rocket nozzle design and analysis technology in the United States since 1970 N89-16907
State of the art of solid propellant rocket motor grain design in the United States N89-16914

AIR FORCE SYSTEMS COMMAND, WRIGHT-PATTERSON AFB, OH.
Laminar flame in a turbulent flow
[AD-A200241] N89-16947
The behavior of shells made of composites during the dynamic application of axian compression
[AD-A200244] N89-17266
Development of finite local perturbations of electrical conductivity in the flow of a weakly-conducting gas when a magnetic field is present
[AD-A200243] N89-17458

AIR FORCE WEAPONS LAB., KIRTLAND AFB, NM.
Field enhancement of UHF-VHF aircraft antennas
[AD-A200180] N89-17069

AIR FORCE WRIGHT AERONAUTICAL LABS., WRIGHT-PATTERSON AFB, OH.
Tactical fighter inlets N89-16740
Inlet-engine compatibility N89-16741
Intake-airframe integration N89-16744
Design of critical compressor stages N89-16835
Supersonic compressors N89-16836
New Al-Ni-Ge contacts on GaAs: Their structure and electrical properties
[DE89-002918] N89-17526

AIR FRANCE, PARIS.
The CFM 56-5 on the A-320 at Air France N89-16793

AIRCRAFT RESEARCH ASSOCIATION LTD., BEDFORD (ENGLAND).
Development of testing techniques in a large transonic wind tunnel to achieve a required drag accuracy and flow standards for modern civil transports N89-16857
The use of computational fluid dynamic methods to assess the effects of model support systems and working section modifications on the flow around wind tunnel models N89-16862

AKRON UNIV., OH.
Adsorption of phosphorus acids on alumina
[AD-A200548] N89-16957
A continuum deformation theory for metal-matrix composites at high temperature N89-17323

ALABAMA UNIV., HUNTSVILLE.
Ideal black hole fluid
[NASA-TM-100349] N89-17558

ALLIED-SIGNAL AEROSPACE CO., KANSAS CITY, MO.
Analysis of low alloy and stainless steels by inductively coupled argon plasma spectrometer
[DE89-003227] N89-16978

ALPHATECH, INC., BURLINGTON, MA.
Distributed estimation for large-scale event-driven systems
[DE89-002688] N89-17447

ALTEX TECHNOLOGIES CORP., LOS GATOS, CA.
Characterization of nonpremixed turbulent bluff-body burner flames
[PB89-100507] N89-16945

AMERICAN SOCIETY FOR ENGINEERING EDUCATION, WASHINGTON, DC.
Ion assisted deposition of fiber coatings for ceramic matrix composites wth low dielectric loss tangents
[AD-A200162] N89-17005

ANALYTICAL METHODS, INC., REDMOND, WA.
Development of a panel method for modeling configurations with unsteady component motions, phase 1
[AD-A200255] N89-16775

ANAMET LABS., INC., HAYWARD, CA.
Finite element analysis of F-16 ballistic tests
[AD-A200289] N89-16776

APPLIED SCIENCE ASSOCIATES, INC., NARRAGANSETT, RI.
Evaluation of satellite-tracked surface drifting buoys for simulating the movement of spilled oil in the marine environment. Volume 1: Executive summary
[PB88-226048] N89-17357
Evaluation of satellite-tracked surface drifting buoys for simulating the movement of spilled oil in the marine environment, volume 2
[PB88-226055] N89-17358

ARGONNE NATIONAL LAB., IL.
Nitride and carbide coatings for high speed steel cutting tools
[DE89-003623] N89-16984
Development of overcharge tolerance in Li/FeS and Li/FeS2 cells
[DE89-003952] N89-17145
First production of potable water by OTEC (Ocean Thermal Energy Conversion) and its potential applications
[DE89-003630] N89-17353
Emission-reduction effects of methanol vehicles: State of knowledge
[DE89-001148] N89-17359
Vectorizing compilers: A test suite and results
[DE89-005376] N89-17406
Accurate and efficient testing of the exponential and logarithm functions in Ada
[DE89-004443] N89-17415
Floating-point standards: Theory and practice
[DE89-003598] N89-17439
A presentation for Virasoro algebras
[DE89-003883] N89-17440
Compositional changes during ion bombardment
[DE89-003974] N89-17481
A simple method for preparing superconducting high T(sub c) thin films
[DE89-003663] N89-17527
Studies of NiO metal interfaces
[DE89-003634] N89-17529

ARIZONA STATE UNIV., TEMPE.
Monte Carlo investigation of hot photoexcited electron relaxation in GaAs N89-17120
Heat transfer in the tip region of a rotor blade simulator N89-17312

ARIZONA UNIV., TUCSON.
Ceramics derived from organo-metallic polymers
[AD-A200118] N89-17004
High-speed optical logic using GaAs N89-17088
A new algorithm for the rapid analysis of particle image displacement data N89-17195
Sodium in Io's extended atmosphere N89-17559
The visual shape and multipole moments of the sun N89-17561

ARKANSAS UNIV., FAYETTEVILLE.
Adaptive hybrid picture coding
[AD-A200059] N89-17142

ARMY AEROMEDICAL RESEARCH LAB., FORT RUCKER, AL.
Contrast sensitivity in Army aviator candidates: Cycloplegia effects and population norms
[AD-A200433] N89-17397
A comparison of two whole-body vibration standards as applied to rotary-wing aircraft: ISO (International Standards Organization) 2631 vs ADS (Aeronautical Design Standards) 27
[AD-A200430] N89-17402

ARMY ARMAMENT RESEARCH, DEVELOPMENT AND ENGINEERING CENTER, PICATINNY ARSENAL, NJ.
Pressure/temperature sensitive inorganic phosphors
[AD-A199718] N89-17000
ARMY AVIATION SYSTEMS COMMAND, CLEVELAND, OH.
Experimental verification of the thermodynamic properties for a jet-A fuel
[NASA-TM-101475] N89-17017
Computer-aided design of bevel gear tooth surfaces
[NASA-TM-101449] N89-17248
ARMY AVIATION SYSTEMS COMMAND, MOFFETT FIELD, CA.
A critical assesment of wind tunnel results for the NACA 0012 airfoil N89-16847
ARMY COLD REGIONS RESEARCH AND ENGINEERING LAB., HANOVER, NH.
New England mountain icing climatology
[AD-A200287] N89-17381
Profile properties of undeformed first-year sea ice
[AD-A200172] N89-17398
ARMY CONCEPTS ANALYSIS AGENCY, BETHESDA, MD.
An algorithm for calculating the area of overlap of an ellipse and a convex polygon
[AD-A199654] N89-17408
ARMY ENGINEER TOPOGRAPHIC LABS., FORT BELVOIR, VA.
Improving classification accuracy of radar images using a multiple-stage classifier
[AD-A200291] N89-17071
ARMY MATERIALS TECHNOLOGY LAB., WATERTOWN, MA.
Time and temperature dependence of strength in high performance ceramics N89-16998
ARMY TANK-AUTOMOTIVE COMMAND, WARREN, MI.
Robotic vehicle communications interoperability
[TACOM-TR-13387] N89-17075
ARNOLD ENGINEERING DEVELOPMENT CENTER, ARNOLD AIR FORCE STATION, TN.
Hierarchy of uncertainty sources in transonic wind tunnel testing N89-16851
An overview of the application of standard measurement uncertainty methodology to propulsion testing N89-16854
Characterization of hypersonic wind tunnel flow fields for improved data accuracy N89-16874
ATOMIC ENERGY OF CANADA LTD., PINAWA (MANITOBA).
An intelligent sensor for equipment health monitoring of ferromagnetic wear debris concentration in fluids N89-16818

B

BALLISTIC RESEARCH LABS., ABERDEEN PROVING GROUND, MD.
Gyroscopic testing of accelerometers to determine coning angle
[AD-A200126] N89-17209
BATTELLE COLUMBUS LABS., MOUNTAIN VIEW, CA.
Human factors in aviation operations: The hearback problem
[NASA-CR-177398] N89-16769
BELL TELEPHONE LABS., INC., HOLMDEL, NJ.
Electro-optic sampling of high-speed, InP-based integrated circuits N89-17064
Characteristics, packaging and physics of ultra high speed diode lasers and detectors N89-17112
Picosecond measurements of gain-switching in a semiconductor laser driven by ultrashort electrical pulses N89-17115
Picosecond carrier transport in GaAs quantum wells N89-17128
Quantum-confined Stark effect in InGaAs/InP quantum wells grown by metal-organic chemical vapor deposition N89-17129
Dynamics of below-gap photoexcitation in GaAs quantum wells N89-17130
Optical modulation above 20 GHz using a waveguide electro-optic switch N89-17134
BELL TELEPHONE LABS., INC., MURRAY HILL, NJ.
A non-contact picosecond prober for integrated circuit testing N89-17081
Molecular Beam Epitaxy (MBE) for high speed devices N89-17085
Multigigahertz logic based on InP-MISFET's exhibiting extremely high transconductance N89-17086
Direct subpicosecond measurement of carrier mobility of photoexcited electrons in GaAs N89-17118
Resonant tunneling electron spectroscopy N89-17126
Electrical pulse compression by traveling-wave photoconductivity N89-17137
BERKELEY RESEARCH ASSOCIATION, SPRINGFIELD, VA.
Modeling of atomic processes for X-ray laser plasmas
[AD-A200219] N89-17505
BHABHA ATOMIC RESEARCH CENTRE, BOMBAY (INDIA).
Hydrogen diffusion in tantalum
[DE88-704073] N89-16968
Seeded inert gas driven disk generator
[DE88-704083] N89-17510
BLABER (A.) AND BLABER (P.), HAMILTON (ONTARIO).
A Canadian low earth orbit launch vehicle: Launch vehicle performance analysis of Black Brant VC and Nihka rocket motor configurations N89-17039
BLACK AND VEATCH CONSULTING ENGINEERS, KANSAS CITY, MO.
A performance model for nonuniformly illuminated front-gridded concentrator cells
[DE89-001368] N89-17347
BM HI-TECH, INC., COLLINGWOOD (ONTARIO).
High temperature material processing system for KC-135 microgravity experiments N89-17040
BOEING VERTOL CO., PHILADELPHIA, PA.
Analytical and experimental methods used to resolve the aerodynamic results of tests conducted in three test facilities N89-16850
BOLT, BERANEK, AND NEWMAN, INC., CANOGA PARK, CA.
A strategy for understanding noise-induced annoyance
[AD-A200125] N89-17461
BOMBRINI PARODI-DELFINO S.P.A., COLLEFERRO (ITALY).
Propellant grain design N89-16912
BRITISH AEROSPACE AIRCRAFT GROUP, PRESTON (ENGLAND).
Jaguar/Tornado intake design N89-16743
Intakes for high angle of attack N89-16745
Intake drag N89-16747
BRITISH AEROSPACE PUBLIC LTD. CO., PRESTON (ENGLAND).
Accurate drag estimation using a single component drag model technique N89-16856
BRITISH BROADCASTING CORP., KINGSWOOD (ENGLAND).
The visibility of noise in system 1 colour television
[BBC-RD-1988/12] N89-17061
BROOKHAVEN NATIONAL LAB., UPTON, NY.
Mechanical design of a RF electron gun
[DE89-004890] N89-16895
Conversion of natural gas to methanol
[DE89-001088] N89-16958
Modern and prospective technologies for hydrogen production from fossil fuels
[DE89-001270] N89-16959
Kinetics of the isothermal decomposition of lanthanum nickel hydride
[DE89-002905] N89-16966
Glancing angle EXAFS studies of Cu-Al thin film interfaces
[DE89-003614] N89-16983
Experimental evidence for positron trapping at dislocations in Ni3Al alloys
[DE89-004520] N89-16989
Nuclear reorganization barriers to electron transfer
[DE88-016582] N89-17471
Orientation dependent X-ray absorption in high T (sub c) superconductors
[DE89-002910] N89-17520
Interaction of CO, CO2 and H2O with Ba and YBa2Cu3O7
[DE89-003160] N89-17528
Lattice gauge theories and Monte Carlo algorithms
[DE89-003569] N89-17539
BROWN UNIV., PROVIDENCE, RI.
Optical fiber science and technology: Novel fibers and fiber sensors
[AD-A200311] N89-17489
BUREAU VERITAS, PARIS (FRANCE).
Trend monitoring of a turboprop engine at low and mean power N89-16801

C

CALIFORNIA INST. OF TECH., PASADENA.
Investigations of the motion of discrete-velocity gases by cellular automata
[AD-A200221] N89-17158
Strain accumulation in the Santa Barbara Channel, 1971-1987
[NASA-CR-183402] N89-17369
CALIFORNIA STATE POLYTECHNIC UNIV., POMONA.
Nonlocal and quasilocal potentials in the spontaneous emission of molecular exciplexes coupled to the phonon bath of a solid matrix
[AD-A200509] N89-17476
CALIFORNIA UNIV., BERKELEY.
Supercritical flow past a symmetrical bicircular arc airfoil
[NASA-CR-184787] N89-16762
Electronic behavior of highly correlated metals
[DE89-002492] N89-16971
Equivalent linearization for fatigue life estimates of a nonlinear structure
[NASA-TM-101536] N89-17467
Breakdown voltage mapping of impurity concentrations in GaAs wafers
[DE89-002489] N89-17518
New Al-Ni-Ge contacts on GaAs: Their structure and electrical properties
[DE89-002918] N89-17526
CALIFORNIA UNIV., BERKELEY. LAWRENCE BERKELEY LAB.
Electronic behavior of highly correlated metals
[DE89-002492] N89-16971
The two-beam accelerator and the relativistic klystron power source
[DE89-002673] N89-17485
Breakdown voltage mapping of impurity concentrations in GaAs wafers
[DE89-002489] N89-17518
New Al-Ni-Ge contacts on GaAs: Their structure and electrical properties
[DE89-002918] N89-17526
CALIFORNIA UNIV., IRVINE.
Behavior in normal and reduced gravity of an enclosed liquid/gas system with nonuniform heating from above
[NASA-TM-101471] N89-17046
Models of incremental concept formation
[AD-A199617] N89-17400
CALIFORNIA UNIV., SAN DIEGO, LA JOLLA.
Temporal pattern recognition
[AD-A200090] N89-17426
CALIFORNIA UNIV., SANTA BARBARA.
Kinetics and mechanisms of hydrogen attack in 2.25Cr-1Mo steel
[DE89-001381] N89-16970
An optical modulator/switch using the reflection from a translated depletion edge
[DE89-001380] N89-17490
Is the great attractor really a great wall
[NASA-CR-184772] N89-17540
CALSPAN FIELD SERVICES, INC., ARNOLD AFS, TN.
Hierarchy of uncertainty sources in transonic wind tunnel testing N89-16851
CAMBRIDGE UNIV. (ENGLAND).
Analysis of 3D viscous flows in transonic compressors N89-16831
In-situ laser microscopy for particle sizing and tracking N89-17201
CANADIAN ASTRONAUTICS LTD., OTTAWA (ONTARIO).
Droplet separation dynamics and kinematics under microgravity N89-17031
Encapsulation process hardware for a KC-135 aircraft N89-17037
Concentricity and sphericity of composite drops under microgravity N89-17042
CANADIAN FORCES BASE TRENTON, ASTRA (ONTARIO).
CF-18/F404 transient performance trending N89-16814
CARNEGIE-MELLON UNIV., PITTSBURGH, PA.
Inertial navigation system simulator: Behavioral specification
[AD-A200604] N89-16771
Inertial navigation system simulator program: Top-level design
[AD-A200605] N89-16772
Functional performance specification for an external computer system simulator
[AD-A200611] N89-16881
3-D vision techniques for autonomous vehicles
[AD-A199643] N89-17236
Axioms for concurrent objects
[AD-A200584] N89-17435
CASE WESTERN RESERVE UNIV., CLEVELAND, OH.
A proposed boundary layer simulation methodology for wind tunnel testing N89-16867
Electrochemistry of carbon relative to batteries and fuel cells
[AD-A199698] N89-17141
CATHOLIC UNIV. OF AMERICA, WASHINGTON, DC.
Development of kinematic equations and determination of workspace of a 6 DOF end-effector with closed-kinematic chain mechanism
[NASA-CR-183241] N89-17444

CENTRE AEROPORTE DE TOULOUSE (FRANCE).
Study of the aerodynamic situation along the C 160 aircraft in parachuting configuration
[DAT-88-06] N89-16756
CENTRE D'ESSAIS AERONAUTIQUE TOULOUSE (FRANCE).
Qualification tests of preimpregnated carbon epoxy T800H/DA 0506 from Structil. Test report M6-570500
[REPT-M6-570500] N89-16934
Flow visualization by the PISTIL procedure (presentation of wake images by local computer processing). Test report 876/S-5
[REPT-876/S-5] N89-17203
CENTRE D'ETUDES ET DE RECHERCHES, TOULOUSE (FRANCE).
Decoupling of ionization in the hypersonic boundary limit
[CERT-RT-OA-21/5005-AYD] N89-17204
CENTRE DE RECHERCHES DU SERVICE DE SANTE DES ARMEES, CLAMART (FRANCE).
Multiparametric research of early indicators of vascular risk in flying personnel
[ETN-89-93613] N89-17398
CENTRE NATIONAL D'ETUDES SPATIALES, TOULOUSE (FRANCE).
Satellite-ground dating and synchronization technique
[CNES-CT/DRT/TIT/TB-040-T] N89-16892
Effects of depolarization obtained by specular reflection on metallic mirrors: Applications to laser telecommunication and to Earth observation
[CNES-CT/DRT/TIT/IO-87/150] N89-17494
Optical communication. Four quadrant avalanche detector. Modeling, theoretical results and comparison with experimental values
[CNES-CT/DRT/TIT/IO-87/086] N89-17495
Non return to zero (NRZ) clock recovery breadboard for 200 MB/S optical intersatellite link
[CNES-CT/DRT/TIT/TR-87/024] N89-17496
CENTRE NATIONAL DE LA RECHERCHE SCIENTIFIQUE, MARSEILLES (FRANCE).
Numerical and theoretical study of elastoplastic dynamic buckling
[ETN-89-93614] N89-17284
CHALMERS UNIV. OF TECHNOLOGY, GOETEBORG (SWEDEN).
Frequency chirping in pulse modulated gain and real index guided single quantum well lasers N89-17113
CHEMICAL RESEARCH AND DEVELOPMENT CENTER, ABERDEEN PROVING GROUND, MD.
Light-off temperature determination of oxidation catalyst using Fourier transform infrared technique
[AD-A199596] N89-16938
Ion content of moist atmospheric air and the molecular structure of water vapor thus inferred
[AD-A199732] N89-16940
Gas chromatographic method for the determination of trace quantities of diethyl malonate in ethanol
[AD-A199733] N89-16941
Electrical properties of atmospheric moist air: A systematic, experimental study
[AD-A199599] N89-17370
Using theoretical descriptors in structural activity relationships. Part 2: Polarizability index
[AD-A199594] N89-17389
CHI ASSOCIATES, INC., ARLINGTON, VA.
The Rankine automotive system technology assessment report
[DE89-002693] N89-17238
CHICAGO UNIV., IL.
Is the great attractor really a great wall
[NASA-CR-184772] N89-17540
CHINA NUCLEAR INFORMATION CENTRE, BEIJING.
Study of structure of high-Tc superconductor Y(YV)Ba2Cu3O(sub 9-x) and its resistance sharp drop
[DE88-704104] N89-17531
CINCINNATI UNIV., OH.
Structure and properties of polymer interphases
[AD-A200238] N89-17008
Behavior in normal and reduced gravity of an enclosed liquid/gas system with nonuniform heating from above
[NASA-TM-101471] N89-17046
Anisotropic constitutive modeling for nickel base single crystal superalloy Rene N4 at 982 C N89-17324
CLEMSON UNIV., SC.
Photoelectric photometry of very short period eclipsing binary systems and their light curve solutions N89-17549
CLEVELAND STATE UNIV., OH.
Stochastic modeling of crack initiation and short-crack growth under creep and creep-fatigue conditions
[NASA-TM-101358] N89-17286
COLORADO STATE UNIV., FORT COLLINS.
Characterization of hollow cathode, ring cusp discharge chambers
[NASA-CR-182255] N89-17146
COLORADO UNIV., BOULDER.
Studies of metal/carbon surface chemistry
[DE88-011264] N89-16960
COLUMBIA UNIV., NEW YORK, NY.
Massive symbolic mathematical computations and their applications
[AD-A200253] N89-17434
Alfven waves in a cold plasma with curved magnetic fields
[AD-A200312] N89-17506
COMINGO LTD., TRAIL (BRITISH COLUMBIA).
Analysis of Cd0.21Hg0.79Te quenched in 10(-4) g N89-17029
COMPUTING DEVICES CO., OTTAWA (ONTARIO).
Installed thrust as a predictor of engine health for jet engines N89-16806
CONATEC, INC., LANHAM, MD.
Advanced research rockets for long duration microgravity science N89-17028
CONNECTICUT UNIV., STORRS.
Isotropic kevlar and PBA (poly 1,4-benzamide) reinforcements for composites
[AD-A200239] N89-16927
Investigations in particle and field theory
[DE89-003004] N89-17538
CONSIGLIO NAZIONALE DELLE RICERCHE, CINISELLO BALSAMO (ITALY).
A simple method for preparing superconducting high T(sub c) thin films
[DE89-003663] N89-17527
CONTINUUM DYNAMICS, INC., PRINCETON, NJ.
Vortex dynamics for rotorcraft interactional aerodynamics
[AD-A200128] N89-16726
CORNELL UNIV., ITHACA, NY.
Modulation efficiency limited high frequency performance of the MODFET N89-17101
Unsteady viscous flows over moving body
[AD-A200269] N89-17159
CRANFIELD INST. OF TECH., BEDFORD (ENGLAND).
The design, construction and test of a postbuckled, carbon fibre reinforced plastic wing box N89-16773
A model for transition by attachment line contamination and an examination of cross-flow instability in three-dimensional boundary layers N89-17153

D

DEFENCE RESEARCH ESTABLISHMENT ATLANTIC, DARTMOUTH (NOVA SCOTIA).
Frequency estimation of radar signals using an acousto-optic spectrum analyzer as an RESM (Radar Electronic Support Measures) receiver
[AD-A200159] N89-17067
DEFENCE SCIENCE AND TECHNOLOGY ORGANIZATION, SALISBURY (AUSTRALIA).
GPS (Global Positioning System) user equipment evaluation techniques using a rotor mounted antenna
[AD-A200515] N89-16770
DEFENSE SCIENCE BOARD, WASHINGTON, DC.
Report of the Defense Science Board Task Force Subgroup on Strategic Air Defense (SDI Milestone Panel)
[AD-A200164] N89-17452
DELAWARE UNIV., NEWARK.
Selectivity of the reactions of oxygenates on transition metal surfaces
[DE89-003691] N89-16985
Far field patterns and the inverse scattering problem for electromagnetic waves in an inhomogeneous medium
[AD-A200223] N89-17070
DEPARTMENT OF DEFENSE, WASHINGTON, DC.
Report to Congress on the Automotive Technology Development Program
[DE89-004977] N89-17250
DEPARTMENT OF ENERGY, WASHINGTON, DC.
Carbon dioxide and climate: Summaries of research in FY 1988
[DE89-002966] N89-17363
DEUTSCHE FORSCHUNGS- UND VERSUCHSANSTALT FUER LUFT- UND RAUMFAHRT, BERLIN (GERMANY, F.R.).
Flow unsteadiness in three low-speed wind tunnels N89-16859
DEUTSCHE FORSCHUNGS- UND VERSUCHSANSTALT FUER LUFT- UND RAUMFAHRT, BRUNSWICK (GERMANY, F.R.).
Expriments on the DFVLR-F4 wing body configuration in several European windtunnels N89-16848
DEUTSCHE FORSCHUNGS- UND VERSUCHSANSTALT FUER LUFT- UND RAUMFAHRT, GOETTINGEN (GERMANY, F.R.).
Physical aspects of viscous simulation and associated research requirements N89-16865
Engine simulator tests: Comparison of calibration and wind tunnel results N89-16871
Boundary layer equations and methods of solution N89-17176
Application of particle image velocity to high speed flows N89-17198
DEUTSCHE FORSCHUNGS- UND VERSUCHSANSTALT FUER LUFT- UND RAUMFAHRT, OBERPFAFFENHOFEN (WEST GERMANY).
Proceedings of the Colloquium about Joint Projects Within the DFVLR/ISRO Cooperation
[DFVLR-MITT-88-19] N89-16883
German spaceborne remote sensing activities N89-16887
Presentation of the status of the experiment and mission activities of the Monocular Electro-Optical Stereo Scanner (MEOSS) N89-16888
Status of Sabrex N89-16890
Autonomous payload control experiment on SROSS-3, a status review N89-16891
DEUTSCHE FORSCHUNGS- UND VERSUCHSANSTALT FUER LUFT- UND RAUMFAHRT, PORZ (GERMANY, F.R.).
Loss development in transonic compressor cascades N89-16826
Incidence angle rules in supersonic cascades N89-16827
Exit angle rules in supersonic cascades N89-16828
Shock losses in transonic and supersonic compressor cascades N89-16829
Axial velocity density ratio influence on exit flow angle in transonic/supersonic cascades N89-16830
DEUTSCHE LUFTHANSA A.G., HAMBURG (GERMANY, F.R.).
Engine condition monitoring: State-of-the-art civil application N89-16792
DIRECTION DES RECHERCHES ETUDES ET TECHNIQUES, PARIS (FRANCE).
Development of a lattice gas model for the study of combustion
[ETN-89-93612] N89-16964
DSMA INTERNATIONAL, INC., TORONTO (ONTARIO).
Impact of nozzle design constraints on test section flow quality N89-16860
DU PONT DE NEMOURS (E. I.) AND CO., WILMINGTON, DE.
Orientation dependent X-ray absorption in high T (sub c) superconductors
[DE89-002910] N89-17520
DUKE UNIV., DURHAM, NC.
Integration of experimental and modeling approaches in the unmanaged ecosystem research plan
[DE89-005230] N89-17367
DUNLAP AND ASSOCIATES, INC., NORWALK, CT.
Technology assessment for aircraft command in emergency situations
[DOT/FAA/CT-88/20] N89-16767

E

EAGLE ENGINEERING, INC., HOUSTON, TX.
User and technical documentation
[NASA-CR-172087] N89-16893
ECOLE DES MINES, NANCY (FRANCE).
Physical mechanisms during drying of porous media N89-17173
ECOLE DES MINES, PARIS (FRANCE).
Stochastic description of porous media N89-17168
ECOLE NATIONALE SUPERIEURE DES TELECOMMUNICATIONS, PARIS (FRANCE).
Applications of correcting coding theory to communication combinatorial problems
[ENST-88C001] N89-17065
Study of error correcting codes for Hertzian channels with a large number of states. Application to Quadrature Amplitude Modulation (QAM) 64
[ENST-88E007] N89-17074
ECOLE POLYTECHNIQUE, PALAISEAU (FRANCE).
High-speed phenomena in GaAs multiple-quantum-wells N89-17127
EDGERTON, GERMESHAUSEN AND GRIER, INC., IDAHO FALLS, ID.
NDE methods for high-temperature materials and environments
[DE89-005195] N89-17234
Laser detection of acoustic displacements by destabilizing a frequency stablized helium neon laser
[DE89-005282] N89-17235
Computer control of gas metal arc welding
[DE89-005188] N89-17252
Safety comparison of fusion fuel cycles
[DE89-005200] N89-17512
EDINBURGH UNIV. (SCOTLAND).
A scanning laser beam system for two-dimensional illumination of flow fields N89-17196

EIDGENOESSISCHE TECHNISCHE HOCHSCHULE, ZURICH (SWITZERLAND).
Multiphase flow in porous media N89-17169
ELECTROFUELS MFG. CO., TORONTO (ONTARIO).
The design of a heat-pipe furnace for microgravity N89-17043
EMENTECK, INC., COLLEGE STATION, TX.
An investigation of the rechargeability of certain modified forms of MnO2
[AD-A199685] N89-16943
ENGINEERING SCIENCE SOFTWARE, INC., SMITHFIELD, RI.
Constitutive modelling of single crystal and directionally solidified superalloys N89-17325
ENVIRONMENTAL RESEARCH INST. OF MICHIGAN, ANN ARBOR.
Instrumentation for the characterization of the microwave properties at 18, 35 and 94 GHz
[AD-A199741] N89-17064
EPI-TECH CORP., PARADISE VALLEY, AZ.
Growth of gallium arsenide using ion cluster beam technology, volume 1, phase 2
[AD-A200231] N89-17523
ESDU INTERNATIONAL LTD., LONDON (ENGLAND).
Estimation of drag arising from asymmetry in thrust or airframe configuration
[ESDU-88006] N89-16730
Rolling moment derivative Lxi, for plain ailerons at subsonic speeds
[ESDU-88013] N89-16731
Derivation of primary air-data parameters for hypersonic flight
[ESDU-88025] N89-16732
Normal-force-curve and pitching-moment-curve slopes for tangent-ogive forebody-cyclinder combinations at zero angle of attack
[ESDU-88026] N89-16733
Yawing moment coefficient for plain ailerons at subonic speeds
[ESDU-88029] N89-16734
Boundaries of linear characteristics of cambered and twisted wings at subcritical Mach numbers
[ESDU-88030] N89-16735
Lift and longitudinal forces on propeller/nacelle/wing/flap systems
[ESDU-88031] N89-16736
Elastic wrinkling of sandwich panels with laminated fibre reinforced face plates (face plates of AsBoDs, AsDIDs and AsBsDs types). (Computer program)
[ESDU-88015] N89-16930
Wrinkling of sandwich panel face plates (isotropic face plates on orthotropic cores, in-plane loading or bending)
[ESDU-88032] N89-16931
Vapour pressures and critical points of liquids. C7 to C20 alkanols
[ESDU-88012] N89-16962
Vapour pressures and critical points of liquids. Organic oxygen compounds
[ESDU-88017] N89-16963
Selection of alloys for hydrodynamic bearings
[ESDU-88018] N89-16980
Effect of fretting on fatigue strength of titanium alloys
[ESDU-88027] N89-16981
Effectiveness: N(sub TU) relationships for the design and performance evaluation of additional shell-and-tube heat exchanger geometries
[ESDU-88021] N89-17056
Fouling in cooling water systems
[ESDU-88024] N89-17057
Computer program for the prediction of air-lift pump performance
[ESDU-88014] N89-17246
The design of spur and helical involute gears. A procedure compatible with BS 436:1986: Method for calculation of contact and root bending stress limitations for metallic involute gears
[ESDU-88033] N89-17247
Calculation methods for along-wind loading. Part 3: Response of buildings and plate-like structures to atmospheric turbulence
[ESDU-88019] N89-17267
Pipeline vibrations. Undamped natural vibration of pipelines
[ESDU-88022] N89-17268
Avoidance of buckling of some engineering elements (struts, plates and gussets)
[ESDU-88034] N89-17269
Maximum inelastic bending moments and form factors for symmetric bending of beams
[ESDU-88035] N89-17270
Calculation methods for along-wind loading. Part 4: Computer program for estimation of response
[ESDU-88036] N89-17271
World-wide extreme wind speeds. Part 2: Examples using various methods of analysis
[ESDU-88037] N89-17382
Estimation of hours per year when mean wind speed exceeds specified thresholds
[ESDU-88038] N89-17383
The Kalman filter
[ESDU-88039] N89-17437
Jet-by-jet shielding of noise
[ESDU-88023] N89-17463
Flow induced acoustic resonance in tubular heat exchangers
[ESDU-88028] N89-17464
ESSEN UNIV. (GERMANY, F.R.).
Practical systems for speckle velocimetry N89-17185
Speckle photography of flows with varying fluid density N89-17186
Measurement of natural convection by white light speckle velocimetry N89-17197
EUROPEAN SPACE AGENCY, PARIS (FRANCE).
Design and analysis of solid rocket motor nozzle N89-16908
Design and analysis of solid rocket motor internal insulation N89-16915
Overall optimization of solid rocket motor N89-16916

F

FEDERAL AVIATION AGENCY, ATLANTIC CITY, NJ.
Technology assessment for aircraft command in emergency situations
[DOT/FAA/CT-88/20] N89-16767
FERMI NATIONAL ACCELERATOR LAB., BATAVIA, IL.
Is the great attractor really a great wall
[NASA-CR-184772] N89-17540
FLORIDA STATE UNIV., TALLAHASSEE.
Some comments on particle image displacement velocimetry N89-17184
FLORIDA UNIV., GAINESVILLE.
Laser interactions with aerosol aureoles
[DE89-002824] N89-17225
FORD AEROSPACE AND COMMUNICATIONS CORP., PALO ALTO, CA.
The potential impact of MMICs on future satellite communications
[NASA-CR-182227] N89-17078
The potential impact of MMICs on future satellite communications: Executive summary
[NASA-CR-182227-EXEC-SUMM] N89-17079
FRAUNHOFER-INST. FUER BETRIEBSFESTIGKEIT, DARMSTADT (GERMANY, F.R.).
Papers of the 5th LBF Colloquium
[LBF-TB-180] N89-17272
The influence of the load sequence on the fatigue life of fatigue fracture endangered components N89-17273
The reliable reduction of random local sequences for fatigue tests N89-17274
Modal analysis methods for the reduction of system-conditioned loads N89-17275
A procedure for the generation of load sequences N89-17276
Strength evaluation for fiber reinforced composite leaf springs under mechanical and environment conditioned loads N89-17277
Damage tolerance behavior of fiber reinforced composite airframes N89-17278
Finite element analysis for the evaluation and optimization of fiber reinforced composite structural components N89-17279
Low-cycle fatigue behavior of cyclic hardening and softening steels under multiaxial elastic-plastic loading conditions with constant and variable amplitudes N89-17280
Fatigue behavior of shrink-bonded shaft-hub steel assemblies N89-17281
Fretting corrosion fatigue N89-17282
Fatigue behavior of ceramic thermal barrier coatings N89-17283
FUJITSU LTD., ATSUGI (JAPAN).
Progress and challenges in HEMT LSI technology N89-17094

G

GARRETT TURBINE ENGINE CO., PHOENIX, AZ.
Thermal barrier coating life-prediction model development N89-17331
GASTOPS LTD., OTTAWA (ONTARIO).
CF-18 engine performance monitoring N89-16787
GEC AVIONICS LTD., ROCHESTER (ENGLAND).
System considerations for integrated machinery health monitoring N89-16804
GENERAL ATOMICS TECHNOLOGIES CORP., SAN DIEGO, CA.
Theory of neoclassical resistivity-gradient-driven turbulence
[DE89-005391] N89-17513
GENERAL DYNAMICS CORP., FORT WORTH, TX.
Propulsive-jet flow field analysis using the three-dimensional Navier-Stokes equations
[NASA-CR-177508] N89-16764
GENERAL ELECTRIC CO., CINCINNATI, OH.
Military engine monitoring status at GE Aircraft Engines, Cincinnati, Ohio N89-16798
Commercial engine monitoring status at GE Aircraft Engines, Cincinnati, Ohio N89-16799
Component specific modeling N89-17320
Thermal barrier coating life prediction model N89-17332
Elevated temperature crack growth N89-17335
GENERAL MOTORS CORP., INDIANAPOLIS, IN.
Aerothermal modeling program. Phase 2, element A: Improved numerical methods for turbulent viscous recirculating flows N89-17303
Aerothermal modeling program. Phase 2, element B: Flow interaction experiment N89-17304
Aerothermal modeling program, Phase 2, Element C: Fuel injector-air swirl characterization N89-17305
Two- and three-dimensional turbine blade row flow field simulations N89-17313
Turbine airfoil film cooling N89-17315
GEOLOGICAL SURVEY, MENLO PARK, CA.
High-precision gravity network to monitor temporal variations in gravity across Yucca Mountain, Nevada
[DE89-005023] N89-17373
GEORGIA INST. OF TECH., ATLANTA.
A computational method for three dimensional, internal viscous flows with separation and secondary flow patterns N89-17164
PC-1D Version 2: Enhanced numerical solar cell modeling
[DE89-000302] N89-17349
GERMAN AIR FORCE AIR ARMAMENT DIRECTORATE, COLOGNE (GERMANY, F.R.).
On board life monitoring system Tornado (OLMOS) N89-16785
GHENT UNIV. (BELGIUM).
Introduction to finite element techniques in fluid mechanics N89-17177
GOSUDARSTVENNYI KOMITET PO ISPOLZOVANIYU ATOMNOI ENERGII, MOSCOW (USSR).
Fracture mode of metals in heavy electric fields
[DE88-704818] N89-16987
Cluster expansion for vacuum confining fields
[DE88-704367] N89-17436
On the experimental basis of the Pauli exclusive principle
[DE88-704366] N89-17477
GRUMMAN AEROSPACE CORP., BETHPAGE, NY.
R/M/T (Reliability/Maintainability/Testability) design for fault tolerance. Volume 1: Program manager's guide
[AD-A200204] N89-17262
Extravehicular activities limitations study. Volume 1: Physiological limitations to extravehicular activity in space
[NASA-CR-172098] N89-17392
Extravehicular activities limitations study. Volume 2: Establishment of physiological and performance criteria for EVA gloves
[NASA-CR-172099] N89-17393
GUNMA UNIV., MAEBASHI (JAPAN).
Application of a spatial filter velocimeter to the two phase flows in a Spark Ignition (SI) N89-17199

H

HARVARD MEDICAL SCHOOL, BOSTON, MA.
Pharmacological resetting of the circadian sleep-wake cycle
[AD-A200246] N89-17396
HERCULES, INC., ROCKET CENTER, WV.
Composite motor case design N89-16909
HEWLETT-PACKARD CO., PALO ALTO, CA.
InP/GaInAs/InP PIN photodiode with FWHM less than 18 ps N89-17114
HIROSHIMA UNIV., TAKEHARA (JAPAN).
Monopoles and magnetic fields in the inflationary universe
[DE88-755532] N89-17557
Isotropization of the cosmic background radiation due to galactic gravitational screening
[DE88-755533] N89-17563
HOCHSCHULE DER BUNDESWEHR, HAMBURG (GERMANY, F.R.).
Gas path modelling, diagnosis and sensor fault detection N89-16811
HOUSTON UNIV., TX.
JUNCTION code user's manual. Electromagnetic scattering and radiation by arbitrary configurations of conducting bodies and wires
[AD-A200315] N89-17072

HUGHES AIRCRAFT CO., EL SEGUNDO, CA.
Laser communication test system
[AD-A199612] N89-17215
HUGHES RESEARCH LABS., MALIBU, CA.
Characteristics and applications of wideband guided-wave devices N89-17132

I

IBM WATSON RESEARCH CENTER, YORKTOWN HEIGHTS, NY.
Picosecond electrical pulses for VLSI electronics characterization N89-17083
Photoconductive generation of sub-picosecond electrical pulses and their measurement applications N89-17093
Nonequilibrium phonons and disorder in Al(sub x)Ga(sub 1-x)As N89-17103
Carrier lifetime versus ion-implantation dose in silicon on sapphire N89-17106
MESFET compatible IMSM detectors N89-17116
Ballistic transport and hot electron spectroscopy in Tunnelling Hot Electron Transfer Amplifier (THETA) N89-17123
Picosecond optoelectronic study of a thin film transmission line structure N89-17138
ILLINOIS UNIV., URBANA.
Non-stationary transport in MODFETs and heterojunction devices N89-17119
Optical methods for measuring vector velocity fields. 1: Principles. 2: Techniques N89-17180
Scattering power of seed materials: Mie scattering calculations N89-17181
Processing techniques: Image plane and Fourier plane N89-17182
Processing information in the image plane N89-17183
Assessment and comparison of techniques for transforming parameters to a common metric in item response theory
[AD-A200067] N89-17433
Monte Carlo studies of nonlinear electron transport in 3-5 semiconductors
[AD-A199700] N89-17516
ILLINOIS UNIV., URBANA-CHAMPAIGN.
Characteristics of shielded microstrip lines on GaAs-Si at millimeter-wave frequencies N89-17102
The effects of strain induced softening on the load carrying capability of components N89-17264
Numerical analysis of the effects of void growth and crack tip opening on ductile fracture N89-17265
IMI SUMMERFIELD, KIDDERMINSTER (ENGLAND).
Considerations for designers of cases for small solid propellant rocket motors N89-16911
IMPERIAL COLL. OF SCIENCE AND TECHNOLOGY, LONDON (ENGLAND).
A statistical theory for gas surface interactions in rarefied hypersonic flows
[IC-AERO-88-01] N89-16755
INDIAN SPACE RESEARCH ORGANIZATION, AHMEDABAD.
ISRO-DFVLR collaboration in space sciences N89-16884
Meteorites and lunar samples as space probes N89-16885
INDIAN SPACE RESEARCH ORGANIZATION, BANGALORE.
Mission under SROSS program and position paper on SROSS-2 with MEOSS payload N89-16889
INDIANA UNIV., BLOOMINGTON.
Evaluation of a supercritical fluid chromatograph coupled to a surface-wave-sustained microwave-induced plasma detector
[AD-A198728] N89-16937
INDUSTRIEANLAGEN-BETRIEBSGESELLSCHAFT M.B.H., OTTOBRUNN (GERMANY, F.R.).
Long-crack growth rate data: Gaussian loading N89-17296
INSTITUT DE MECANIQUE DES FLUIDES DE LILLE (FRANCE).
Particular flight mechanics specifications related to wind tunnel test results N89-16879
INSTITUT FRANCO-ALLEMAND DE RECHERCHES, SAINT-LOUIS (FRANCE).
Full 3D measurements: The holographic approach N89-17191
INSTITUTO DE PESQUISAS ESPACIAIS, SAO JOSE DOS CAMPOS (BRAZIL).
Control of reaction wheels through digital techniques using reference models
[INPE-4618-TDL/335] N89-16903
Automatic registration of satellite imagery
[INPE-4637-PRE/1349] N89-17414
INTEGRAL TECHNOLOGIES, INC., WESTMONT, IL.
Multidimensional modeling of convective heat transfer with application to I. C. engines
[DE89-004062] N89-17166
INTEGRATED SYSTEMS, INC., SANTA CLARA, CA.
Adaptive control techniques for large space structures
[AD-A200208] N89-16901
INTERNATIONAL ATOMIC ENERGY AGENCY, VIENNA (AUSTRIA).
Small reactors for low-temperature nuclear heat applications
[DE88-704336] N89-17484
INTERNATIONAL CENTRE FOR THEORETICAL PHYSICS, TRIESTE (ITALY).
On 2-Banach algebras
[DE88-704194] N89-17429
Spherical-type hypersurfaces in a Riemannian manifold
[DE88-704224] N89-17454
Supersymmetric instantons and topological quantum field theory
[DE88-704211] N89-17536
Geometry on the space of geometries
[DE88-704214] N89-17537
INTERNATIONAL COUNCIL OF SCIENTIFIC UNIONS, URBANA, IL.
Middle Atmosphere Program: Handbook for MAP, volume 26
[NASA-CR-183350] N89-17368
IOWA STATE UNIV. OF SCIENCE AND TECHNOLOGY, AMES.
Investigation of liquid sloshing in spin-stabilized satellites
[AD-A199629] N89-16899
PC-1D Version 2: Enhanced numerical solar cell modeling
[DE89-000302] N89-17349
Low frequency oscillations in total ozone measurements
[NASA-CR-184759] N89-17385

J

JAPAN ATOMIC ENERGY RESEARCH INST., TOKYO.
Internal stress during high-temperature creep and activation energy for creep of Hastelloy XR
[DE88-755231] N89-16969
JAYCOR, VIENNA, VA.
Investigation of collisional effects in the plasma erosion opening switch
[AD-A200319] N89-17507
JOHANN-WOLFGANG-GOETHE-UNIV., FRANKFURT AM MAIN (GERMANY, F.R.).
Production and transport of convoy electrons in amorphous carbon foils
[DE89-002313] N89-17478
JOHNSON CONTROLS, INC., MILWAUKEE, WI.
Nickel hydrogen battery development
[DE89-001063] N89-17143
JOINT EUROPEAN TORUS PROJECT, ABINGDON (ENGLAND).
High power Ion Cyclotron Resonance Heating (ICRH) in JET
[DE89-002218] N89-17499
Plasma performance in JET: Achievements and projections
[DE89-002219] N89-17500
JOINT PUBLICATIONS RESEARCH SERVICE, ARLINGTON, VA.
JPRS report: Science and technology. Japan. Developments in Manufacturing Process Technology
[JPRS-JST-88-010] N89-17047
FRP (Fiber Reinforced Plastics) cutting technology reported N89-17048
Hard material cutting technology described N89-17049
Electric discharge method for ceramics reported N89-17050
Brittle material processing reported N89-17051
Use of cataphoresis effects discussed N89-17052
Ultrasonic vibration method discussed N89-17053
Laser beam heat method reported N89-17054
Microdrilling using electron beams reported N89-17055
JOINT RESEARCH CENTRE OF THE EUROPEAN COMMUNITIES, ISPRA (ITALY).
Heat transfer in self-heated particle beds submerged in liquid coolant N89-17171

K

KANSAS STATE UNIV., MANHATTAN.
Measurements of micrometeorological parameters for testing large scale models
[NASA-CR-184766] N89-17384
KYOTO UNIV. (JAPAN).
Stochastic modeling of crack initiation and short-crack growth under creep and creep-fatigue conditions
[NASA-TM-101358] N89-17286

L

LAWRENCE LIVERMORE NATIONAL LAB., CA.
Interfacial bonding in W/C and W/B4C multilayers
[DE89-002931] N89-16936
Modeling the propagation of long intense microwave pulses in mixtures of air and SF6
[DE89-004787] N89-17076
An optically strobed sample and hold circuit N89-17087
Silicon pulse sharpening diodes: Switching kilovolts in tens of picoseconds N89-17139
Remapping on the staggered mesh
[DE89-002656] N89-17154
Is there a statistical mechanics of turbulence
[DE89-003471] N89-17162
The properties of tagged lattice fluids. 2: Velocity correlation functions
[DE89-003475] N89-17163
Application of a two-equation turbulence mix model
[DE89-004812] N89-17205
Tailoring domain decomposition to the network structure for parallel processing of fluid dynamics
[DE89-005501] N89-17206
A photon-counting, subnanosecond, imaging camera for X-ray detection
[DE89-002874] N89-17208
Induction-linac based free-electron laser amplifier for fusion applications
[DE89-001923] N89-17217
Applications of ion implantation for modifying the interactions between metals and hydrogen gas
[DE89-002877] N89-17219
Recent results from the Nova experiments program
[DE89-002901] N89-17220
Induction-linac based free-electron laser amplifiers for plasma heating
[DE88-017004] N89-17221
Laser interactions with aerosol aureoles
[DE89-002824] N89-17225
Selected topics in FELs
[DE89-004022] N89-17227
Mix experiments with the NOVA laser
[DE89-004775] N89-17228
Progress towards a 44-Angstrom X-ray laser
[DE89-004807] N89-17229
High energy laser beam scattering by atmospheric aerosol aureoles
[DE89-004811] N89-17230
The X-ray laser: Review of recent experimental results and of future prospects
[DE89-005096] N89-17231
Ne-like ion X-ray laser experiments in plasmas produced by 0.53 microns and 0.35 microns laser light
[DE89-004827] N89-17233
Greenhouse warming: What do we know
[DE89-004780] N89-17365
KINETICS: A computer program to analyze chemical reaction data
[DE89-004602] N89-17419
The space-based interceptor
[DE89-002869] N89-17451
Radiation imposed limits on superconducting magnets: A data base for copper stabilizers
[DE89-002875] N89-17456
Energy and Technology Review
[DE89-005308] N89-17459
Review of precision surface generating processes and their potential application to the fabrication of large optical components
[DE89-001712] N89-17486
Analysis of interferometer images with Fourier domain techniques
[DE89-002927] N89-17491
Precision transfer function measurements of integrated optical modulators
[DE89-004021] N89-17492
X-ray optics for X-ray laser research and applications
[DE89-004026] N89-17493
Explosion of integrated optic devices used in new generation systems
[DE89-004012] N89-17497

Progress toward high-gain laser fusion
[DE89-002681] N89-17501
Progress in laboratory high gain ICF (Inertial Confinement Fusion): Prospects for the future
[DE89-002564] N89-17502
Model microfield calculations of radiative and transport properties of ions in strongly coupled plasmas
[DE89-001244] N89-17503
Phases and microstructures of carbon-implanted niobium
[DE89-004017] N89-17534

LEICESTER UNIV. (ENGLAND).
Optical and infrared studies of cometary dust N89-17550

LIMIT POINT SYSTEMS, FREMONT, CA.
A visualization model based on the mathematics of fiber bundles
[DE89-002537] N89-17432

LOS ALAMOS NATIONAL LAB., NM.
Mechanical characterization of SiC whisker-reinforced MoSi
[DE89-003486] N89-16933
Theoretical predictions for side-chain liquid-crystal polymers and comparison to experiment
[DE89-003578] N89-17013
Prediction and synthesis efforts at Los Alamos
[DE89-003605] N89-17018
High power KrF laser development at Los Alamos
[DE89-002242] N89-17218
Unlubricated sliding properties of ion beam and excimer laser mixed Fe-Ti-C multilayered films
[DE89-003470] N89-17245
Generalized finite strains, generalized stresses, and a hybrid variational principle for finite-element computer programs
[DE89-002101] N89-17430
Generalized finite strains, generalized stresses, and a principle of virtual work for finite-element computer programs
[DE89-002102] N89-17431
Force state mapping using experimental data
[DE89-000351] N89-17442
Center of buoyancy definition
[DE89-003017] N89-17457
Field-reversed configuration (FRC) experiments
[DE89-000389] N89-17498
A document preparation system in a large network environment
[DE88-014466] N89-17543

LOUISIANA STATE UNIV., BATON ROUGE.
Theoretical studies of electrons and electron transfer processes in fluids
[DE89-003259] N89-17479

M

MANCHESTER COLL. OF SCIENCE AND TECHNOLOGY (ENGLAND).
The kinetics and dynamics of iodine monofluoride formation in gas-phase collisions
[AD-A199622] N89-16939

MANITOBA UNIV., WINNIPEG.
The effects of microgravity and linear accelerations on cutaneomuscular reflexes in human lower limb musculature N89-17034

MARYLAND UNIV., COLLEGE PARK.
Numerical solutions to three-dimensional shock wave/vortex interaction at hypersonic speeds N89-16729
Aeroelastic optimization of a helicopter rotor N89-16778
Tensile strength of composite structures with internal ply drops and free-edge effects N89-16929
Generation and forming of ultrashort high voltage pulses N89-17097
Graphite as a picosecond laser activated opening switch N89-17098
Investigation of photoconductive picosecond microstripline switches on self-implanted Silicon On Sapphire (SOS) N89-17104
Picosecond optoelectronic switches using composite electronic materials N89-17107
A new optoelectronic CW microwave source N89-17133
Introduction to computational fluid dynamics N89-17175

MASSACHUSETTS INST. OF TECH., CAMBRIDGE.
Femtosecond nonequilibrium electronic heat transport in thin gold films N89-17122
Rotating hot-wire investigation of the vortex responsible for blade-vortex interaction noise
[NASA-CR-177454] N89-17466
Investigation of defect and electronic interactions associated with GaAs device processing
[AD-A200541] N89-17525

MASSACHUSETTS INST. OF TECH., LEXINGTON.
Microwave and millimeter-wave resonant tunneling diodes N89-17124

MASSACHUSETTS UNIV., AMHERST.
Picosecond photoconductive transceivers N89-17092

MATRA SERVICE AERODYNAMIQUE, VELIZY-VILLACOUBLAY (FRANCE).
Accuracy of lift and center-of-thrust measurements at missile control surfaces N89-16875

MCDONNELL AIRCRAFT CO., ST. LOUIS, MO.
Transonic wind tunnel boundary interference: A correction procedure N89-16861

MCGILL UNIV., MONTREAL (QUEBEC).
Life science experiments during parabolic flight: The McGill experience N89-17027

MEDICAL COLL. OF VIRGINIA, RICHMOND.
The effects of hydrazines on neuronal excitability
[AD-A200199] N89-17395

MESSERSCHMITT-BOELKOW-BLOHM G.M.B.H., BREMEN (GERMANY, F.R.).
Accuracy requirements for high-speed test with engine simulation on transport aircraft models in the NLR-HST N89-16870
Accuracy problems in wind tunnels during transport aircraft development N89-16877

MESSERSCHMITT-BOELKOW-BLOHM G.M.B.H., MUNICH (GERMANY, F.R.).
Intake swirl and simplified methods for dynamic pressure distortion assessment N89-16742

MICHIGAN UNIV., ANN ARBOR.
Mechanistic studies of pressure-assisted superplasticity of structural ceramics
[AD-A200202] N89-17006
Capacity of frequency-hop spread-spectrum multiple-access communication systems
[AD-A200616] N89-17073
Scattering by a two dimensional groove in a ground plane
[NASA-CR-183087] N89-17077
Derivation and application of a class of generalized impedance boundary conditions, part 2
[NASA-CR-183298] N89-17148

MIDWEST RESEARCH INST., GOLDEN, CO.
Device physics related to the granular nature of CuInSe2 solar cells
[DE89-000810] N89-17341
Research on high-efficiency, single-junction, monolithic, thin-film amorphous silicon solar cells, phase 3
[DE89-000813] N89-17342
Wind energy systems: Program summary for fiscal years 1986 and 1987
[DE88-001188] N89-17350
Prediction of stochastic blade responses using measured wind-speed data as input to the FLAP code
[DE89-000834] N89-17354

MINISTRY OF DEFENCE, LONDON (ENGLAND).
Recent UK trials in engine health monitoring: Feedback and feedforward N89-16790

MINNESOTA UNIV., MINNEAPOLIS.
Development of generalized block correction procedures for the solution of discretized Navier-Stokes equations N89-17307
A low-Reynolds-number two-equation turbulence model for predicting heat transfer on turbine blades N89-17310
A numerical modeling investigation of the effect of convective-mesoscale interactions on the sea breeze circulation N89-17377
The role of presolar dust in the formation of the solar system N89-17553

MISSION RESEARCH CORP., ALBUQUERQUE, NM.
Photocurrent modeling of modern microcircuit PN junctions
[DE88-012860] N89-17147

MITRE CORP., BEDFORD, MA.
Vector space approach to narrowband interference excision
[AD-A199703] N89-17063

MOTOREN- UND TURBINEN-UNION MUENCHEN G.M.B.H. (GERMANY, F.R.).
Engine life consumption monitoring program for RB199 integrated in the on-board life monitoring system N89-16789
The advantage of a thrust rating concept used on the RB199 engine N89-16800

N

NAPLES UNIV. (ITALY).
Experiments on boundary layer transition tripping at low Reynolds numbers N89-16868
Computerized thermographic technique for the detection of boundary layer separation N89-16876

NATIONAL ACADEMY OF SCIENCES - NATIONAL RESEARCH COUNCIL, WASHINGTON, DC.
National Research Council Resident Research Associateship (NRC-RRA) Program
[AD-A200183] N89-16926
Photonics: Maintaining competitiveness in the information era
[AD-A200230] N89-17473

NATIONAL AERONAUTICAL ESTABLISHMENT, OTTAWA (ONTARIO).
Preliminary results: Flight testing the NAE T-33 microgravity facility N89-17041

NATIONAL AERONAUTICAL LAB., BANGALORE (INDIA).
Numerical solution of flow fields around Delta wings using Euler equations method
[NAL-TM-FM-8701] N89-16757
Energy events in the atmospheric boundary layer
[NAL-TM-DU-8701] N89-17372

NATIONAL AERONAUTICS AND SPACE ADMINISTRATION, WASHINGTON, DC.
Combustibility of titanium powders
[NASA-TT-20455] N89-16967
Microgravity science and applications bibliography, 1988 revision
[NASA-TM-4098] N89-17045
Planetary cartography in the next decade: Digital cartography and emerging opportunities
[NASA-TM-4092] N89-17560

NATIONAL AERONAUTICS AND SPACE ADMINISTRATION. AMES RESEARCH CENTER, MOFFETT FIELD, CA.
Generation of three-dimensional body-fitted grids by solving hyperbolic and parabolic partial differential equations
[NASA-TM-101069] N89-16763
R-parametrization and its role in classification of linear multivariable feedback systems
[NASA-TM-101066] N89-16844
Modal control of an oblique wing aircraft
[NASA-TP-2898] N89-16845
Wind tunnel requirements for computational fluid dynamics code verification N89-16880
Accuracy assessment, using stratified plurality sampling, of portions of a LANDSAT classification of the Arctic National Wildlife Refuge Coastal Plain
[NASA-TM-101042] N89-17339
Proceedings of a workshop on Lighting Requirements in Microgravity: Rodents and Nonhuman Primates
[NASA-TM-101077] N89-17390

NATIONAL AERONAUTICS AND SPACE ADMINISTRATION. LYNDON B. JOHNSON SPACE CENTER, HOUSTON, TX.
NASA's Zero-g aircraft operations N89-17026
Body displacement measured during sustained +Gz, -Gz and + or -Gy acceleration using a stereoscopic photographic system
[NASA-TM-101269] N89-17391

NATIONAL AERONAUTICS AND SPACE ADMINISTRATION. LANGLEY RESEARCH CENTER, HAMPTON, VA.
Piloted-simulation evaluation of escape guidance for microburst wind shear encounters
[NASA-TP-2886] N89-16820
Wind tunnel-sidewall-boundary-layer effects in transonic airfoil testing-some correctable, but some not N89-16864
Short-crack growth behaviour in an aluminum alloy: An AGARD cooperative test program N89-17288
Preliminary fatigue tests on short-crack specimens N89-17290
Alignment verification procedures N89-17291
Approximate stress-intensity factors for a surface crack and through crack at a semi-circular notch N89-17294
Long-crack growth rate data: Constant amplitude and FALSTAFF loading N89-17295
Limb-darkening functions as derived from along-track operation of the ERBE scanning radiometer for January 1985
[NASA-RP-1214] N89-17374
A multistage linear array assignment problem
[NASA-CR-181748] N89-17417
Accurate modeling of parallel scientific computations
[NASA-CR-181756] N89-17418
On a class of nonstationary stochastic processes
[NASA-TM-101195] N89-17448
Equivalent linearization for fatigue life estimates of a nonlinear structure
[NASA-TM-101536] N89-17467
BRYNTRN: A baryon transport model
[NASA-TP-2887] N89-17562

NATIONAL AERONAUTICS AND SPACE ADMINISTRATION. LEWIS RESEARCH CENTER, CLEVELAND, OH.
Computational methods for inlet airframe integration N89-16752

CFD application to subsonic inlet airframe integration N89-16753
CFD application to supersonic/hypersonic inlet airframe integration N89-16754
Three dimensional viscous analysis of a hypersonic inlet
[NASA-TM-101474] N89-16759
The design and development of transonic multistage compressors N89-16834
Supersonic throughflow fans N89-16837
A modified VAPEPS method for predicting vibroacoustic response of unreinforced mass loaded honeycomb panels
[NASA-TM-101467] N89-16905
NASA photovoltaic research and technology
[NASA-TM-101422] N89-16917
Refractory metal alloys and composites for space nuclear power systems
[NASA-TM-101364] N89-16986
Experimental verification of the thermodynamic properties for a jet-A fuel
[NASA-TM-101475] N89-17017
Behavior in normal and reduced gravity of an enclosed liquid/gas system with nonuniform heating from above
[NASA-TM-101471] N89-17046
Development of an infrared imaging system for the surface tension driven convection experiment
[NASA-TM-101479] N89-17211
Computer-aided design of bevel gear tooth surfaces
[NASA-TM-101449] N89-17248
Stochastic modeling of crack initiation and short-crack growth under creep and creep-fatigue conditions
[NASA-TM-101358] N89-17286
Turbine Engine Hot Section Technology, 1987
[NASA-CP-2493] N89-17298
Progress on a PdCr wire strain gage N89-17301
A comparison of turbulence measurement methods N89-17302
Mechanics of materials model N89-17319
Three-dimensional inelastic analysis methods for hot section components N89-17321
Use of inelastic strain as a basis for analyzing thermomechanical test data N89-17326
Preliminary study of creep thresholds and thermomechanical response in Haynes 188 at temperatures in the range 649 to 871 C N89-17327
Finite element implementation of viscoplastic models N89-17328
Structural response of an advanced combustor liner: Test and analysis N89-17329
Thermal expansion mismatch and plasticity in thermal barrier coating N89-17330
Total strain version of strainrange partitioning for thermomechanical fatigue at low strains N89-17337
The effect of different module configurations on the radiation tolerance of multijunction solar cells
[NASA-TM-101251] N89-17356
Parallel Gaussian elimination of a block tridiagonal matrix using multiple microcomputers
[NASA-TP-2892] N89-17422
A data acquisition and storage system for the ion auxiliary propulsion system cyclic thruster test
[NASA-TM-101469] N89-17424
Parallel processing of a rotating shaft simulation
[NASA-TM-101462] N89-17453

NATIONAL AERONAUTICS AND SPACE ADMINISTRATION. MARSHALL SPACE FLIGHT CENTER, HUNTSVILLE, AL.
Space shuttle main engine monitoring experience and advanced monitoring systems development N89-16815
Plume spectrometry for liquid rocket engine health monitoring N89-16816
Hardware for studying the demixing of aqueous polymer two-phase systems in low gravity N89-17030
Processing of strong flux trapping high T(subc) oxide superconductors: Center director's discretionary fund
[NASA-TM-100350] N89-17530
Protein crystal nucleation kinetics using relative light-scattering techniques: Center director's discretionary fund
[NASA-TM-100348] N89-17535
Ideal black hole fluid
[NASA-TM-100349] N89-17558

NATIONAL AEROSPACE LAB., AMSTERDAM (NETHERLANDS).
Measurement uncertainty of the AGARD/PEP uniform engine test program N89-16853
Accuracy of various wall-correction methods for 3D subsonic wind-tunnel testing N89-16863
On Reynolds number effects and simulation N89-16866
Requirements and capabilities in unsteady windtunnel testing N89-16878
Microstructural examination of core-programme material N89-17289

NATIONAL DEFENCE HEADQUARTERS, OTTAWA (ONTARIO).
Canadian forces aircraft condition/health monitoring: Policy, plans and experience N89-16784

NATIOANL INST. OF STANDARDS AND TECHNOLOGY, BOULDER, CO.
Cooled ion frequency standard
[AD-A200373] N89-17475

NATIONAL INST. OF STANDARDS AND TECHNOLOGY, GAITHERSBURG, MD.
Thermophysical property measurements in fluid mixtures
[DE89-003281] N89-16961

NATIONAL OCEANIC AND ATMOSPHERIC ADMINISTRATION, NORMAN, OK.
Observations of a thunderstorm generated gust compared with solitary wave theory
[AD-A200087] N89-17379

NATIONAL REMOTE SENSING AGENCY, HYDERABAD (INDIA).
Indian activities in remote sensing applications: Microwave remote sensing N89-16886

NATIONAL RESEARCH COUNCIL OF CANADA, OTTAWA (ONTARIO).
The effects of a compressor rebuild on gas turbine engine performance N89-16803
Workshop on Microgravity Experimentation in Aircraft and Rockets
[NRCC-29151] N89-17019
Parabolic flight: A useful test bed N89-17020
Canadian microgravity research using aircraft and rockets N89-17023
Canadian participation in international biosatellite programs N89-17025
Ocular torsion in the weightlessness of parabolic flight N89-17035
The use of sounding rockets in the study of microgravity cell biology N89-17036
Development of a portable physiological monitoring system for the KC-135: The S.F.U. biopack N89-17044
Importance of sensitivity and reliability of NDI techniques on damage tolerance based life prediction of turbine discs N89-17257

NATIONAL SPACE DEVELOPMENT AGENCY, TOKYO (JAPAN).
Space utilization promotion program of NASDA N89-17022

NATIONAL TECHNICAL UNIV., ATHENS (GREECE).
Discrete operating conditions gas path analysis N89-16810

NATIONAL TRANSPORTATION SAFETY BOARD, WASHINGTON, DC.
Aircraft accident/incident summary report, Travis Air Force Base, California, 8 April 1987
[PB88-910414] N89-16768

NATO EUROPEAN FIGHTER MANAGEMENT AGENCY, MUNICH (GERMANY, F.R.).
Operational requirements for engine condition monitoring from the EFA viewpoint N89-16781

NAVAL ACADEMY, ANNAPOLIS, MD.
Project Longshot: An unmanned probe to Alpha Centauri
[NASA-CR-184718] N89-16904

NAVAL AIR DEVELOPMENT CENTER, WARMINSTER, PA.
Long term possibilities for nondestructive evaluation for US Navy aircraft N89-17259

NAVAL AIR SYSTEMS COMMAND, WASHINGTON, DC.
An overview of US Navy engine monitoring system programs and user experience N89-16782
Wind tunnel predicted air vehicle performance: A review of lessons learned N89-16852

NAVAL OCEAN SYSTEMS CENTER, SAN DIEGO, CA.
A multiaxial strength criterion for composites
[AD-A199610] N89-16920
Array processing for a multiple-rank signal
[AD-A197954] N89-17062
Temporal pattern recognition
[AD-A200090] N89-17426
Machine learning of parameter control doctrine for sensor and communication systems
[AD-A200096] N89-17427

NAVAL POSTGRADUATE SCHOOL, MONTEREY, CA.
Turbulence effects on the high angle of attack aerodynamics of a vertically launched missile
[AD-A200418] N89-16727
Aerodynamic performance of wings of arbitrary planform in inviscid, incompressible, irrotational flow
[AD-A200436] N89-16728
A model of the effect of sparing and repair turnaround time of the inertial navigation system on aircraft readiness for the F/A-18
[AD-A200317] N89-16777
Measurements of gas turbine combustor and engine augmentor tube sooting characteristics
[AD-A199768] N89-16821
Mechanical-chemical energy transfer observations of vaporific explosions
[AD-A200428] N89-16956
Processing of 2090 aluminum alloy for superplasticity
[AD-A200425] N89-16975
Effects of irregular sea surface and evaporation duct on radar detection performance
[AD-A200114] N89-17066
The interaction of a fluid interface with a vortex pair
[AD-A200167] N89-17156
Unsteady flow about porous cambered plates
[AD-A200282] N89-17160
Penetration effects of the compound vortex in gas metal-arc welding
[AD-A200585] N89-17242
A microprocessor-based, solar cell parameter measurement system
[AD-A200227] N89-17348
ONR (Office of Naval Research) tropical cyclone motion research initiative: Mid-year review, discussion and working group reports
[AD-A200286] N89-17380
The suitability of an object-oriented language for prototyping and abstract data types
[AD-A200417] N89-17410
An abstract interactive graphics interface for the IBM/PC and Macintosh
[AD-A200427] N89-17411
Interconnecting different types of local area computer networks
[AD-A200280] N89-17423
Signal acquisition and processing for autonomous space shuttle cargo bay acoustic measurements (NASA G-313)
[AD-A200426] N89-17462
Investigation of collisional effects in the plasma erosion opening switch
[AD-A200319] N89-17507
Monte Carlo calculation of electron multiple scattering in thin foils
[AD-A199872] N89-17517

NAVAL RESEARCH LAB., WASHINGTON, DC.
A technique for recording HF (High Frequency) oblique-incidence-sounder data
[AD-A200168] N89-17068
Millimeter-wave integrated circuits N89-17089
Picosecond optical autocorrelation experiments on fast photodetectors N89-17117
Approximation of viscoelastic stresses from Newtonian turbulent kinematics
[AD-A200188] N89-17157
Aneurisms in laser-driven blast waves
[AD-A200189] N89-17222
Material compatability with threshold limit value levels of monomethyl hydrazine
[AD-A200294] N89-17362
The electron-water vapor (H2O) collision cross sections
[AD-A200187] N89-17472
Electron collision shift of the Lyman-alpha line in H and He+
[AD-A200296] N89-17474
Precise interferometric phase determination
[AD-A200186] N89-17488
Fractal and spherulitic morphology of silicon nitride crystallized from amorphous films
[AD-A200158] N89-17522

NAVAL UNDERWATER SYSTEMS CENTER, NEW LONDON, CT.
The Wigner distribution function with minimum spread
[AD-A199661] N89-17446

NAVAL WEAPONS CENTER, CHINA LAKE, CA.
An active nitrogen plasma atom reservoir for laser-induced ionization spectrometry
[AD-A200544] N89-17224

NEW SOUTH WALES UNIV., KENSINGTON (AUSTRALIA).
Synthesis and analysis of epichlorohydrin based wet strength resins for paper N89-16919
Properties and performance of polyamide membranes N89-16991
The design, analysis, and implementation of a fully distributed local area network for integrated voice and data communications N89-17059
Effect of Lewis number on wet surface heat exchangers N89-17152
An investigation of the spectral characteristics of a commercially available semiconductor laser N89-17213
Collision-induced decomposition of multiatomic ions N89-17468

NORTH CAROLINA STATE UNIV., RALEIGH.
Acoustic wave propagation by finite elements and time step integration N89-17460

NORTH CAROLINA UNIV., CHAPEL HILL.
On a wide range exclusion process in random medium with local jump intensity
[AD-A200510] N89-17450

NORTHEAST ARTIFICIAL INTELLIGENCE CONSORTIUM, SYRACUSE, NY.
Northeast Artificial Intelligence Consortium annual report 1986. Volume 5. Building an intelligent assistant: The acquisition, integration, and maintenance of complex distributed tasks
[AD-A199824] N89-17425

NORTHWESTERN UNIV., EVANSTON, IL.
Thinning and rupture of a thin liquid film on a horizontal heated solid surface
[DE89-001792] N89-16944
PBT,PBO-based hybrid polymers with nonlinear optical properties or high electrical conductivity
[AD-A200226] N89-17007
Elevated temperature strain gages N89-17300

NOTRE DAME UNIV., IN.
Microstructural effects in abrasive wear
[DE89-003032] N89-16976

O

OAK RIDGE NATIONAL LAB., TN.
Microanalytical characterization of wear damage in an alumina-silicon carbide whisker composite
[DE89-003149] N89-16932
The electronic structure and the state of compositional order in metallic alloys
[DE89-003147] N89-16977
Procurement and screening test data for advanced austenitic alloys for 650 C steam service, part 2
[DE89-001331] N89-16979
Oxidation of N3Al below 850 C and its effect on fracture behavior
[DE89-002232] N89-16988
Results from the Federal Methanol Fleet
[DE88-015291] N89-17016
Electron beam welding produces improved duplex crack arrest specimens
[DE88-003885] N89-17239
Integration of robotics and teleoperation for the advanced servomanipulator: Consolidated fuel reprocessing program
[DE88-015281] N89-17240
Assessment of nonintrusive methods for monitoring the operational readiness of solenoid-operated valves
[DE89-002330] N89-17244
HERMIES-3: A step toward autonomous mobility, manipulation and perception
[DE89-004932] N89-17249
Spatial reasoning in the treatment of systematic sensor errors
[DE89-003244] N89-17251
Atmospheric carbon dioxide, climate and global vegetation change
[DE89-002196] N89-17360
Screening environmental pollutants and biomarkers: The analytical challenge
[DE89-004931] N89-17366
Performance of a second generation hypercube
[DE89-005674] N89-17407
Finding Eigenvalues and Eigenvectors of unsymmetric matrices using a distributed-memory multiprocessor
[DE89-004731] N89-17416
A bibliography on parallel and vector numerical algorithms
[DE89-005693] N89-17421
Global existence for symmetric discrete velocity models
[DE89-003102] N89-17438
Finding Eigenvalues and Eigenvectors of unsymmetric matrices using a hypercube multiprocessor
[DE89-002311] N89-17455
Development of an optical digital ionization chamber
[DE89-002209] N89-17470
Production and transport of convoy electrons in amorphous carbon foils
[DE89-002313] N89-17478
A high-intensity plasma sputter heavy negative ion source
[DE89-003113] N89-17480
High power Ion Cyclotron Resonance Heating (ICRH) in JET
[DE89-002218] N89-17499
Plasma performance in JET: Achievements and projections
[DE89-002219] N89-17500
The annealing behavior of ion-implanted single crystals of the type YBa2Cu3O(sub x)
[DE89-002189] N89-17519
Hopping model for the non-Debye dielectric response in ionic crystals
[DE89-003151] N89-17521
Life cycle management handbook
[DE89-004315] N89-17545
Optical storage: Financial management and budget applications
[DE89-004916] N89-17546

OFFICE NATIONAL D'ETUDES ET DE RECHERCHES AERONAUTIQUES, PARIS (FRANCE).
Comparison of the results of tests on A300 aircraft in the RAE 5 metre and the ONERA F1 wind tunnels N89-16849
Some difficulties in the wind tunnel prediction of modern civil aircraft buffeting: Proposed remedies N89-16869
Ceramic-ceramic composites for use at high temperature N89-16994

OFFICE NATIONAL D'ETUDES ET DE RECHERCHES AEROSPATIALES, MODANE (FRANCE).
Precision improvement of transport aircraft drag measurements N89-16858
Instantaneous force measurement on a model subjected to rapid control variations N89-16872

OFFICE NATIONAL D'ETUDES ET DE RECHERCHES AEROSPATIALES, PARIS (FRANCE).
Transport aircraft intake design N89-16749
Missile intakes N89-16750
Wind tunnel air intake test techniques N89-16751
Development of a viscoplastic cyclic behavior law to allow a correct description of creep phenomena
[ONERA-RT-67/1765-RY-078-R] N89-17285

OFFICE OF NAVAL RESEARCH, LONDON (ENGLAND).
Engineering Materials for Very High Temperatures: An ORNL Workshop
[ORNL-8-016-R] N89-16992

OLD DOMINION UNIV., NORFOLK, VA.
An experimental investigation of the aerodynamic characteristics of slanted base ogive cylinders using magnetic suspension technology
[NASA-CR-184624] N89-16758
Theoretical studies of solar lasers and converters
[NASA-CR-184589] N89-17214

ONTARIO RESEARCH FOUNDATION, MISSISSAUGA.
System engineering and logistics for KC-135 experimentation N89-17033

OPTICAL SOCIETY OF AMERICA, WASHINGTON, DC.
Topical Meeting on Picosecond Electronics and Optoelectronics
[AD-A189686] N89-17080

OREGON GRADUATE CENTER FOR STUDY AND RESEARCH, BEAVERTON.
Quantitative measurement and modeling of sensitization development in stainless steels
[DE89-004646] N89-16990

P

P. P. DATA LTD., FLEET (ENGLAND).
Database program for crack propagation data acquired in the AGARD short cracks collaborative effort N89-17297

PACIFIC NORTHWEST LABS., RICHLAND, WA.
Phototype design and testing of two fiber-optic spectrochemical emission sensors
[DE89-001741] N89-17207
Applications of digital image processing to ongoing research in complex terrain meteorology
[DE89-001749] N89-17375
A review of second law techniques applicable to basic thermal science research
[DE89-004356] N89-17541
Technology transfer for the US Department of Energy's Energy Storage Program. Volume 1: Recommendations
[DE89-002806] N89-17547

PAYLOAD SYSTEMS, INC., WELLESLEY, MA.
PYTHON microgravity accelerometer system N89-17038

PENNSYLVANIA UNIV., PHILADELPHIA.
Synthesis and properties of new preceramic materials
[DE89-003436] N89-17012

PICOSECOND PULSE LABS., INC., BOULDER, CO.
Comparison of sampling oscilloscopes with less than 35 ps transition durations N89-17108

PITTSBURGH UNIV., PA.
A formal language model for local area network configuration N89-17544

PLANNING RESEARCH CORP., HAMPTON, VA.
An indirect method for numerical optimization using the Kreisselmeir-Steinhauser function
[NASA-CR-4220] N89-16779
Suggested plastic-replica method N89-17293

POLYTECHNIC UNIV., BROOKLYN, NY.
Maintenance of database integrity in a scheme-less database system N89-17542

POPPER (P.), NEWCASTLE-UNDER-LYME (ENGLAND).
Engineering ceramics in West Germany N89-16999

PRATT AND WHITNEY AIRCRAFT, EAST HARTFORD, CT.
Coolant passage heat transfer with rotation N89-17314
Three-dimensional inelastic analysis methods for hot section components N89-17316
Three-dimensional inelastic analysis for hot section components, BEST 3D code N89-17317
Thermal barrier coating life prediction model development N89-17333
High temperature constitutive and crack initiation modeling of coated single crystal superalloys N89-17334
Creep fatigue life prediction for engine hot section materials (ISOTROPIC) fifth year progress review N89-17336

PRATT AND WHITNEY AIRCRAFT, WEST PALM BEACH, FL.
F100-PW-220 engine monitoring system N89-16795
Design and analysis report for the flight weight 20-inch Columbium secondary nozzle for the RL10 engine
[NASA-CR-179612] N89-16918
Relationships of nondestructive evaluation needs and component design N89-17256

PRATT AND WHITNEY AIRCRAFT OF CANADA LTD., LONGUEUIL (QUEBEC).
Fault management in aircraft power plant controls N89-16809

PRINCETON UNIV., NJ.
Development and application of oxygen flow tagging for velocity measurements and flow visualization in turbulent three-dimensional supersonic flows
[AD-A200119] N89-16725

PURDUE UNIV., WEST LAFAYETTE, IN.
Vibration and aeroelastic tailoring of advanced composite plate-like lifting surfaces N89-17263
Study of the effect of cloud inhomogeneity on the earth radiation budget experiment
[NASA-CR-182962] N89-17386

R

RAND CORP., SANTA MONICA, CA.
Aircraft airframe cost estimating relationships: All mission types
[AD-A200262] N89-16719
Aircraft airframe cost estimating relationships: Fighters
[AD-A200263] N89-16720
Aircraft airframe cost estimating relationships: Bombers and transports
[AD-A200264] N89-16721
Aircraft airframe cost estimating relationships: Attack aircraft
[AD-A200265] N89-16722

RENSSELAER POLYTECHNIC INST., TROY, NY.
An analysis of the closure conditions for two-fluid models of two-phase flow
[DE89-003096] N89-17165

RHODE ISLAND UNIV., NARRAGANSETT.
Objective analysis of the Gulf Stream thermal front: Methods and accuracy
[AD-A199717] N89-17387

ROCHESTER UNIV., NY.
Picosecond switching in Josephson tunnel junctions N89-17095
High speed, high repetition rate, high voltage photoconductive switching N89-17096
A technique for wing suppressed IR sampling N89-17109
Electron device probing in the femtosecond time scale N89-17136
Nonlinear optics with broad-band lasers
[DE89-002728] N89-17216
The integrability condition for dynamical systems
[DE89-004124] N89-17443

ROCKWELL INTERNATIONAL CORP., LAKEWOOD, CA.
B-1B CITS engine monitoring N89-16788

ROLLS-ROYCE LTD., BRISTOL (ENGLAND).
Military engine condition monitoring systems: The UK experience N89-16797
A joint study on the computerisation of in-field aero engine vibration diagnosis N89-16808

ROLLS-ROYCE LTD., DERBY (ENGLAND).
COMPASS (Trademark): A generalized ground-based monitoring system N89-16819
Holographic interferometry for flow visualization studies in high speed fans N89-16841
Use of holography in vibration and flutter study of fans N89-16842
Limitations at high temperatures of present day engineering materials N89-16996
The impact of engineering assumptions on NDE requirements N89-17254
Need for common AGARD approach and actions N89-17260

ROME UNIV. (ITALY).
Digital direct analysis of a multiexposed photograph in Particle Image Displacement Velocimetry (PIDV) N89-17194

ROYAL AIR FORCE, LONDON (ENGLAND).
Engine usage condition and maintenance management systems in the UK armed forces N89-16783
Information management systems for on-board monitoring systems N89-16786
ROYAL AIRCRAFT ESTABLISHMENT, BEDFORD (ENGLAND).
The accurate measurement of drag in the 8 ft x 8 ft tunnel N89-16855
ROYAL AIRCRAFT ESTABLISHMENT, FARNBOROUGH (ENGLAND).
On-line spectrum loading accuracy verification N89-17292
ROYAL INST. OF TECH., STOCKHOLM (SWEDEN).
A simple technique to generate or gate microwave pulses with picosecond speeds N89-17099
RUTGERS - THE STATE UNIV., NEW BRUNSWICK, NJ.
Empirical analysis and refinement of expert system knowledge bases
[AD-A200146] N89-17428

S

SALERNO UNIV. (ITALY).
A simple method for preparing superconducting high T(sub c) thin films
[DE89-003663] N89-17527
SAN DIEGO STATE UNIV., CA.
Photoabsorption and photodissociation of molecules important in the interstellar medium
[NASA-CR-184771] N89-16965
SANDIA NATIONAL LABS., ALBUQUERQUE, NM.
Verification of a Navier-Stokes code for solving the hypersonic blunt body problem
[DE89-003169] N89-16737
Aviation security: A system's perspective
[DE89-002020] N89-16766
Controller-Programmer for telemetry systems
[DE89-002539] N89-16898
Inviscid flow field analysis of complex reentry vehicles. Volume 1: Description of numerical methods
[DE89-002814] N89-16900
Synthesis and properties of low carbon boron carbides
[DE89-002184] N89-16923
The effect of chemistry modifications on the solidification behavior and weldability of Alloy 625
[DE89-001046] N89-16972
Tribology of amorphous alloys formed with ion beams
[DE89-003274] N89-16982
Photodeflection and photoconductivity studies in ceramics
[DE89-002186] N89-17003
Magnetization, transport and structural studies of Tl-Ca-Ba-Cu-O: Bulk ceramics, single crystals, and polycrystalline thin films
[DE89-003264] N89-17010
Compatibility study of an absorber material and two silicone adhesives
[DE89-002361] N89-17011
High speed opto-isolator for radar applications N89-17110
Nickel hydrogen battery development
[DE89-001063] N89-17143
Stress driven diffusive voiding of aluminum conductor lines: A model for time dependent failure
[DE89-001665] N89-17144
Laser studies of the SiH radical/surface interaction during deposition of a thin film
[DE89-003902] N89-17232
Surface deformations resulting from laser spot welding
[DE88-014964] N89-17237
Thermally conductive alumina/organic composites for photovoltaic concentrator cell isolation
[DE89-001181] N89-17346
PC-1D Version 2: Enhanced numerical solar cell modeling
[DE89-000302] N89-17349
Simplified fatigue damage and crack growth calculations for wind turbines
[DE89-003132] N89-17351
Initial structural response measurements for the Sandia 34-meter VAWT test bed
[DE89-003133] N89-17352
The effect of different module configurations on the radiation tolerance of multijunction solar cells
[NASA-TM-101251] N89-17356
Improving software quality through hierarchical design
[DE88-014919] N89-17412
The performance of asynchronous algorithms on hypercubes
[DE89-005503] N89-17420
A visualization model based on the mathematics of fiber bundles
[DE89-002537] N89-17432
Atomic-scale modeling of low-energy ion-solid processes
[DE89-004374] N89-17482
An optical modulator/switch using the reflection from a translated depletion edge
[DE89-001380] N89-17490
Characteristics of lift-off fabricated AlGaAs/InGaAs single-strained-quantum-well structures on glass and silicon substrates
[DE89-001374] N89-17532
Oxygen and copper valencies in oxygen-doped superconducting La2CuO(sub 4.13)
[DE89-003265] N89-17533
SCHMITT TECHNOLOGY ASSOCIATES, NEW HAVEN, CT.
Gas jet deposition of multicomponent ultrafine microstructures
[AD-A200101] N89-16946
SCIENTIFIC RESEARCH ASSOCIATES, INC., GLASTONBURY, CT.
Two- and three-dimensional turbine blade row flow field simulations N89-17313
SEATTLE UNIV., WA.
Field-reversed configuration (FRC) experiments
[DE89-000389] N89-17498
SED SYSTEMS, INC., SASKATOON (SASKATCHEWAN).
Design considerations for the CLEM135 bubble coalescence experiment N89-17032
SHERBROOKE UNIV. (QUEBEC).
Implicit time dependent methods for inviscid and viscous compressible methods N89-17178
SMITHSONIAN ASTROPHYSICAL OBSERVATORY, CAMBRIDGE, MA.
Absolute absorption cross section measurements of ozone and the temperature dependence at four reference wavelengths leading to renormalization of the cross section between 240 and 350 nm
[AD-A199737] N89-16942
SOCIETE DE FABRICATION D'INSTRUMENTS DE MESURE, MASSY (FRANCE).
Maintenance aid system for wide body aircraft N89-16805
SOCIETE NATIONALE D'ETUDE ET DE CONSTRUCTION DE MOTEURS D'AVIATION, EVRY CEDEX (FRANCE).
Service life calculator for the M53 turbofan engine N89-16796
Short term developments in non-destructive evaluation applicable to turbine engine parts N89-17258
State-of-the-art in non-destructive evaluation of turbine engine parts N89-17261
SOCIETE NATIONALE D'ETUDE ET DE CONSTRUCTION DE MOTEURS D'AVIATION, VILLAROCHE (FRANCE).
Design methodology for advanced High Pressure (HP) compressor first stage N89-16840
SOCIETE NATIONALE DES POUDRES ET EXPLOSIFS, VERT-LE-PETIT (FRANCE).
Solid propellant grain design N89-16913
SOCIETE NATIONALE INDUSTRIELLE AEROSPATIALE, SAINT-MEDARD-EN-JALLES (FRANCE).
Design of filament-wound rocket cases N89-16910
SOUTHEASTERN CENTER FOR ELECTRICAL ENGINEERING EDUCATION, INC., ST. CLOUD, FL.
The role of short-term memory in operator workload
[AD-A200252] N89-17401
SOUTHERN UNIV., BATON ROUGE, LA.
Experimental validation of a zero-dimensional computer model for spark-ignition engines
[DE89-002848] N89-17243
SOUTHWEST RESEARCH INST., SAN ANTONIO, TX.
Fuel property and antioxidant effects on elastomer integrity, phase 2
[AD-A200250] N89-17015
Constitutive modeling for isotropic materials N89-17322
The effect of insulated combustion chamber surfaces on direct-injected diesel engine performance, emissions, and combustion
[NASA-CR-182204] N89-17548
SPIRE CORP., BEDFORD, MA.
Thermal degradation mechanisms in GaAs solar cells with high-temperature contacts
[DE89-001375] N89-17343
SRI INTERNATIONAL CORP., MENLO PARK, CA.
Role of retinocortical processing in spatial vision
[AD-A200198] N89-17394
STANFORD LINEAR ACCELERATOR CENTER, CA.
IEEE P1596, a scalable coherent interface for gigabyte/sec multiprocessor applications
[DE89-002813] N89-17405
HANDYPAK: A histogram and display package
[DE89-002742] N89-17413
An essay on discrete foundations for physics
[DE89-002992] N89-17556
STANFORD UNIV., CA.
Transonic aeroelastic analysis of launch vehicle configurations N89-16723
On the aeroacoustics, aerodynamics and aeroelasticity of lifting surfaces N89-16724
Manufacturing thermoplastic matrix composites
[AD-A199724] N89-16922
Hygrothermal deformations of laminated composite shells N89-16924
Picosecond sampling of integrated circuits N89-17082
Heat transfer with very high free-stream turbulence and heat transfer with streamwise vortices N89-17309
Reaction dynamics of H + O2 at 1.6 eV collision energy
[NASA-CR-183182] N89-17483
A neutral hydrogen survey of galaxies in the Cancer region N89-17552
STATE UNIV. OF NEW YORK, BUFFALO.
Molecular spectroscopy at corrugated metal surfaces
[AD-A200124] N89-16973
Nonlocal and quasilocal potentials in the spontaneous emission of molecular exciplexes coupled to the phonon bath of a solid matrix
[AD-A200509] N89-17476
Fresnel coefficients for a phase conjugator
[AD-A200123] N89-17487
STATE UNIV. OF NEW YORK, STONY BROOK.
Millimeter wave generation using Josephson junction arrays
[AD-A200259] N89-17524
STATE UNIV. OF NEW YORK AT BUFFALO, AMHERST.
Effect of finite size on magnetoresistance
[AD-A200267] N89-16974
STERLING FEDERAL SYSTEMS, INC., PALO ALTO, CA.
Modifications to the NASA Ames Space Station Proximity Operations (PROX OPS) Simulator
[NASA-CR-177510] N89-16896
Flux Jacobian matrices and generaled Roe average for an equilibrium real gas
[NASA-CR-177512] N89-17445
STEWART HUGHES LTD., SOUTHHAMPTON (ENGLAND).
Getting more from vibration analysis N89-16807
Gas path condition monitoring using electrostatic techniques N89-16817
STUTTGART UNIV. (GERMANY, F.R.).
Inverse methods for blade design, controlled diffusion blading for supercritical compressor flow N89-16832
Simultaneous measurements of droplet size and droplet velocity in monodisperse droplet streams N89-17192
SVERDRUP TECHNOLOGY, INC., ARNOLD AIR FORCE STATION, TN.
An overview of the application of standard measurement uncertainty methodology to propulsion testing N89-16854
SVERDRUP TECHNOLOGY, INC., CLEVELAND, OH.
Three dimensional viscous analysis of a hypersonic inlet
[NASA-TM-101474] N89-16759
NASA powered lift facility internally generated noise and its transmission to the acoustic far field
[NASA-CR-182217] N89-16882
Experimental verification of the thermodynamic properties for a jet-A fuel
[NASA-TM-101475] N89-17017
Evaluation of aerothermal modeling computer programs N89-17308
Response characteristics of MHOST (MARC Hot-Section Technology) for 3-D inelastic analysis of hot-section components N89-17318
SWEDISH INST. FOR SILICATE RESEARCH, GOTHEBORG.
The shaping of structural engineering ceramics N89-16997
SWEDISH SPACE CORP., SOLNA.
Microgravity rockets in Sweden N89-17021
SYRACUSE UNIV., NY.
Northeast Artificial Intelligence Consortium annual report 1986. Volume 5. Building an intelligent assistant: The acquisition, integration, and maintenance of complex distributed tasks
[AD-A199824] N89-17425
Extensions to the matrix pencil approach for direction finding
[AD-A200112] N89-17449

T

TECHNISCHE HOCHSCHULE, AACHEN (GERMANY, F.R.).
Fast GaAs photoconductive detectors with high sensitivity integrated in coplanar systems onto GaAs substrates N89-17105

TECHNISCHE HOCHSCHULE, DARMSTADT (GERMANY, F.R.).
A personal computer based system for the evaluation of multiple exposed images in laser speckle and particle image displacement velocimetry N89-17193
TECHNISCHE HOGESCHOOL, EINDHOVEN (NETHERLANDS).
Development of composite high temperature materials for future energy conversion applications N89-16905
TECHNISCHE UNIV., BERLIN (GERMANY, F.R.).
Analysis and design of a universal shuttle for rockets [ILR-MITT-199] N89-16897
Test-efficient design of digital VLSI circuits [ETN-89-93483] N89-17151
TECHNISCHE UNIV., DARMSTADT (GERMANY, F.R.).
Balance accuracy and repeatability as a limiting parameter in aircraft development force measurements in conventional and cryogenic wind tunnels N89-16873
TECHNISCHE UNIV., DELFT (NETHERLANDS).
Kinematic leveling adjustments with polynomials and polynomial splines [ETN-89-93328] N89-17338
An algorithm for analysis of plate motions in Crust Dynamics Project (CDP) networks [B8821606] N89-17371
TECHNISCHE UNIV., EINDHOVEN (NETHERLANDS).
One/f noise in silicon devices [ISBN-90-9002060-2] N89-17150
TECHNISCHE UNIV., MUNICH (GERMANY, F.R.).
System-theoretical method for dynamic on-condition monitoring of gas turbines N89-16812
Systems analysis and design of a lunar solar power plant for the supply of a lunar base [ILR-MITT-198] N89-17355
TECHNOLOGY AND MANAGEMENT SYSTEMS, INC., BURLINGTON, MA.
Source characterization of heavy gas dispersion models for reactive chemicals, volume 1 [AD-A200121] N89-17351
TEKTRONIX, INC., BEAVERTON, OR.
Energy variations in optical pulses from gain-switched AlGaAs diode lasers N89-17111
TENNESSEE UNIV., KNOXVILLE.
Statistical mechanics of polymer systems [DE89-002012] N89-17002
Sparse matrix methods research using the CSM testbed software system [NASA-CR-4219] N89-17441
Production and transport of convoy electrons in amorphous carbon foils [DE89-002313] N89-17478
TENNESSEE UNIV. SPACE INST., TULLAHOMA.
Laser thermal propulsion [AD-A200558] N89-17226
TEXAS A&M UNIV., COLLEGE STATION.
Development of direct-inverse 3-D methods for applied transonic aerodynamic wing design and analysis [NASA-CR-184788] N89-16761
Nonlinear dynamic responses of composite rotor blades [AD-A200145] N89-16774
Subseleneon tunneler melting head design: A preliminary study [NASA-CR-184750] N89-17058
Radar and EW applications of multi-gigahertz optical components and systems N89-17131
New secondary batteries utilizing electronically conductive polymer cathodes [NASA-CR-183248] N89-17149
On deriving the three-dimensional kinematic structure on convective storms from a single radar N89-17376
Regenerative life support system research and concepts [NASA-CR-184760] N89-17404
TEXAS INSTRUMENTS, INC., DALLAS.
Quantum transport calculation of resonant-tunneling response time N89-17125
TEXAS UNIV., ARLINGTON.
The synchronous injection ignition valveless pulsejet N89-16823
TEXAS UNIV., AUSTIN.
Synthesis and analysis of novel polymers with potential for providing both high permselectivity and permeability in gas separation applications [DE89-004325] N89-17014
A proposed Quantum Well Injection Transit Time (QWITT) device N89-17100
Longitudinally localized optical carrier injection for femtosecond transport studies N89-17121
Picosecond response of an optically controlled millimeter wave phase shifter N89-17135
Interdependence of large and small scale structures in a turbulent boundary layer N89-17155
In-situ surface during laser-controlled chemical processing of surfaces [AD-A200206] N89-17223
A feasibility study of methods for stopping the depletion of ozone over Antarctica [NASA-CR-184583] N89-17364
Theory of neoclassical resistivity-gradient-driven turbulence [DE89-005391] N89-17513
TOKYO UNIV. (JAPAN).
Research on automatic extraction of map information and its image representation [DE88-754960] N89-17409
TORONTO UNIV. (ONTARIO).
Numerical study of two-stage light-gas hypervelocity projectile launchers [UTIAS-327] N89-16894
Hydrogen erosion of carbon for fusion applications [UTIAS-328] N89-17504
Is the great attractor really a great wall [NASA-CR-184772] N89-17540
TRW ELECTRONIC SYSTEMS GROUP, REDONDO BEACH, CA.
High performance quarter-micron-gate MODFETs N89-17091
TURKISH AIR FORCE, ANKARA.
F110 engine monitoring and maintenance management systems for F-16 C/D N89-16791

U

UNITED TECHNOLOGIES RESEARCH CENTER, EAST HARTFORD, CT.
Supersonic through-flow fan assessment [NASA-CR-182202] N89-16843
Investigation of fuel additive effects on sooting flames [AD-A200273] N89-16948
Development of a high temperature thin film static strain gage N89-17299
Application of advanced diagnostics to airblast injector flows N89-17306
Measurement of airfoil heat transfer coefficients on a turbine stage N89-17311
UNIVERSITE DE TECHNOLOGIE DE COMPIEGNE (FRANCE).
Characterization and modeling of acoustic beams from ultrasonic transducers in solid or liquid media [RF-DAVI-88-08] N89-17465
UNIVERSITIES SPACE RESEARCH ASSOCIATION, HOUSTON, TX.
The space station integrated refuse management system [NASA-CR-184722] N89-17403
UNIVERSITIES SPACE RESEARCH ASSOCIATION, WASHINGTON, DC.
Microgravity science and applications bibliography, 1988 revision [NASA-TM-4096] N89-17045
UNIVERSITY COLL., LONDON (ENGLAND).
Review of existing NDT technologies and their capabilities N89-17255
UNIVERSITY OF SOUTHERN CALIFORNIA, LOS ANGELES.
Development of conducting polymers of high structural strength [AD-A200310] N89-17009
Joint service electronics program: Research in electronics [AD-A199659] N89-17140
UNIVERSITY OF SOUTHERN MISSISSIPPI, HATTIESBURG.
The 15N CP/MAS NMR of aramids: A tool for characterization of the morphology of high modulus fibers for composites [AD-A199656] N89-16921
UTAH UNIV., SALT LAKE CITY.
In-situ vibrational spectroelectrochemistry [AD-A200303] N89-16949
An in situ surface Fourier transform study of complexes of lithium, magnesium potassium and lanthanum ferrocyanide at platinum and gold electrodes [AD-A200305] N89-16950
The behavior of microdisks and microring electrodes. Applications of Neumann's integral theorem [AD-A200307] N89-16951
The behavior of microdisks and micoring electrodes. Prediction of the amperometric response of microdieks and of the steady state for CE and EC Catalytic reactions by application of Neumann's integral theorem [AD-A200415] N89-16952
The behavior of microdisk and microring electrodes. Mass transport to the disk in the unsteady stale: Chronopotentiometry [AD-A200421] N89-16953
The behavior of microdisk and microring electrodes. Mass transport to the disk in the unsteady state: Coupled chemical reactions [AD-A200422] N89-16954
The use of narrow gap line microelectrodes as sensitive and species selective gas chromatographic detectors [AD-A200424] N89-16955
Ultramicroelectrode sensors and detectors. Considerations of the stability, sensitivity, reproducibility and mechanism of ion transport in gas phase chromatography and in high performance liquid phase chromatography [AD-A200306] N89-17210

V

VANDERBILT UNIV., NASHVILLE, TN.
Electronic interactions of electrons, photons, and atoms with material surfaces [AD-A199626] N89-17469
VARIAN ASSOCIATES, PALO ALTO, CA.
Enhanced performance ultrabroadband distributed amplifiers N89-17090
Concentrator efficiencies of 29.2 percent for a GaAs cell and 24.8 percent for a mounted cell-lens assembly [DE89-001612] N89-17344
Recent advances in high-efficiency InGaAs concentrator cells [DE89-001613] N89-17345
VATELL CORP., CHRISTIANSBURG, VA.
Tip clearance signal processor development [AD-A199830] N89-16822
Tip sensor development [AD-A200080] N89-16824
VIRGINIA POLYTECHNIC INST. AND STATE UNIV., BLACKSBURG.
Spillover stabilization in the control of large flexible space structures N89-16902
The role of short-term memory in operator workload [AD-A200252] N89-17401
VIRGINIA UNIV., CHARLOTTESVILLE.
Investigation of microstructural factors that cause low fracture toughness in silicon carbide whisker/Al alloy composites [AD-A200147] N89-16925
VON KARMAN INST. FOR FLUID DYNAMICS, RHODE-SAINT-GENESE (BELGIUM).
Intake Aerodynamics, volume 1 [VKI-LS-1988-04-VOL-1] N89-16738
Introduction to intake aerodynamics N89-16739
Transonic cowl design N89-16746
Intake Aerodynamics, volume 2 [VKI-LS-1988-04-VOL-2] N89-16748
Transonic Compressors, volume 1 [VKI-LS-1988-03-VOL-1] N89-16825
Transonic Compessors, volume 2 [VKI-LS-1988-03-VOL-2] N89-16833
Variable geometry in supersonic compressors N89-16838
Axial supersonic inlet compound N89-16839
Modeling and Applications of Transport Phenomena in Porous Media, volume 2 [VKI-LS-1988-01-VOL-2] N89-17167
Phase change phenomena in liquid saturated self heated particulate bed N89-17170
Capillary pumping for a two phase heat transport system N89-17172
Introduction to Computational Fluid Dynamics [VKI-LS-1988-02] N89-17174
Particle Image Displacement Velocimetry [VKI-LS-1988-06] N89-17179
Application of Particle Image Displacement Velocimetry (PIDV) to complex flows: Resolution of the directional ambiguity N89-17187
Application of Particle Image Displacement Velocimetry (PIDV) to complex flows: Measurements of the third component N89-17188
Optical processing N89-17189
Probabilistic modeling of Particle Image Displacement Velocimetry (PIDV) experiments N89-17190
Application of particle image displacement velocimetry to a centrifugal pump N89-17200
Modeling and applications of transport phenomena in porous media. Volume 1: Mathematical modeling of transport in porous media [VKS-LS-1988-01-VOL-1] N89-17202

W

WARWICK UNIV. COVENTRY (ENGLAND).
Microstructure of high-temperature ceramics N89-16993
WASHINGTON UNIV., SEATTLE.
Ion microprobe measurements of H, C, O, Mg, and Si isotopic abundances in individual interplanetary dust particles N89-17551

WEST VIRGINIA UNIV., MORGANTOWN.
High temperature properties of ceramic/carbon systems in an oxidizing environment
[AD-A200254] N89-16928
WESTINGHOUSE ELECTRIC CORP., BALTIMORE, MD.
Propagation effects handbook for satellite systems design. A summary of propagation impairments on 10 to 100 GHz satellite links with techniques for system design
[NASA-RP-1082(04)] N89-17060
WISCONSIN UNIV., MADISON.
High-resolution Interferometer Sounder (HIS), phase 2
[NASA-CR-183414] N89-17212
Active vibration suppression for robotic manipulators N89-17241
Kinetic energy diagnostic studies of extratropical cyclones based on storm relative motion N89-17378
Neoclassical MHD descriptions of tokamak plasmas
[DE89-003117] N89-17508
Fusion plasma theory: Task 3: Auxiliary heating in tokamaks
[DE89-003256] N89-17509
Behavior of the reversed field pinch with nonideal boundary conditions
[DE89-005497] N89-17514
Studies of a poloidal divertor reversed field pinch
[DE89-005498] N89-17515
WORLD METEOROLOGICAL ORGANIZATION, GENEVA (SWITZERLAND).
Hydrological aspects of combined effects of storm surges and heavy rainfall on river flow
[WMO-704] N89-17340

Typical Contract Number Index Listing

Listings in this index are arranged alphanumerically by contract number. Under each contract number the NASA accession numbers denoting documents that have been produced as a result of research done under that contract are arranged in ascending order. The NASA accession number denotes the number by which the citation is identified.

AF PROJ. 2302 ..... N89-16899
AF PROJ. 2303 ..... N89-16939
N89-17004
N89-17007
N89-17223
N89-17469
AF PROJ. 2304 ..... N89-17006
N89-17070
AF PROJ. 2305 ..... N89-17142
N89-17524
AF PROJ. 2306 ..... N89-16928
N89-17080
N89-17525
AF PROJ. 2307 ..... N89-16725
N89-17158
N89-17159
AF PROJ. 2308 ..... N89-17226
AF PROJ. 2311 ..... N89-17506
AF PROJ. 2312 ..... N89-17395
N89-17396
AF PROJ. 2917 ..... N89-17489
AF-AFOSR-0020-87 ..... N89-17489
AF-AFOSR-0029-85 ..... N89-17506
AF-AFOSR-0036-86 ..... N89-17135
AF-AFOSR-0039-85 ..... N89-16939
AF-AFOSR-0080-86 ..... N89-16899
AF-AFOSR-0087-86 ..... N89-17070
AF-AFOSR-0094-86 ..... N89-17223
AF-AFOSR-0105-86 ..... N89-17007
AF-AFOSR-0107-87 ..... N89-17004
AF-AFOSR-0117-88 ..... N89-17417
N89-17418
AF-AFOSR-0150-86 ..... N89-17469
AF-AFOSR-0155-87 ..... N89-17158
AF-AFOSR-0181-87 ..... N89-17080
AF-AFOSR-0187-86 ..... N89-17396
AF-AFOSR-0191-86 ..... N89-16725
AF-AFOSR-0205-85 ..... N89-17524
AF-AFOSR-0213-85 ..... N89-17122
AF-AFOSR-0235-87 ..... N89-17395
AF-AFOSR-0251-87 ..... N89-16928
AF-AFOSR-0289-87 ..... N89-17006
AF-AFOSR-0317-86 ..... N89-17226
AF-AFOSR-0322-84 ..... N89-17142
AF-AFOSR-0328-86 ..... N89-17159
AF-AFOSR-0342-86 ..... N89-17525
ARP-3610-147 ..... N89-16814
ARPA ORDER 5351 ..... N89-17236
DA PROJ. 1L1-62209-A-47-A N89-17248
DAAL03-86-K-0002 ..... N89-17122
DAAL03-87-C-0011 ..... N89-16775
DAAL03-87-C-0013 ..... N89-16726
DACA76-85-C-0003 ..... N89-17236
DE-AC01-80RA-50418 ..... N89-17447
DE-AC01-87CE-90002 ..... N89-17238
DE-AC02-76CH-00016 ..... N89-16895
N89-16958
N89-16959
N89-16966
N89-16983
N89-16989
N89-17471
N89-17520
N89-17528
N89-17539
DE-AC02-76ER-13065 ..... N89-17443
DE-AC02-79ER-10336 ..... N89-17538
DE-AC02-81ER-10963 ..... N89-16976
DE-AC02-83CH-10093 ..... N89-17341
N89-17342
N89-17350
N89-17354
DE-AC03-76SF-00098 ..... N89-16971
N89-17229
N89-17485
N89-17518
N89-17526
DE-AC03-76SF-00515 ..... N89-17405
N89-17413
N89-17556
DE-AC04-76DP-00613 ..... N89-16978
DE-AC04-76DP-00789 ..... N89-16737
N89-16766
N89-16898
N89-16900
N89-16923
N89-16972
N89-16982
N89-17003
N89-17010
N89-17011
N89-17143
N89-17144
N89-17147
N89-17232
N89-17237
N89-17343
N89-17344
N89-17345
N89-17346
N89-17347
N89-17349
N89-17351
N89-17352
N89-17356
N89-17412
N89-17420
N89-17482
N89-17490
N89-17532
N89-17533
DE-AC04-76DR-00789 ..... N89-17432
DE-AC04-86AL-33183 ..... N89-17166
DE-AC05-84OR-21400 ..... N89-16932
N89-16970
N89-16977
N89-16979
N89-16988
N89-17016
N89-17239
N89-17240
N89-17244
N89-17249
N89-17251
N89-17360
N89-17366
N89-17407
N89-17416
N89-17421
N89-17438
N89-17455
N89-17470
N89-17478
N89-17480
N89-17499
N89-17500
N89-17508
N89-17519
N89-17521
N89-17545
N89-17546
DE-AC06-76RL-01830 ..... N89-17207
N89-17375
N89-17541
N89-17547
DE-AC06-86NE-37963 ..... N89-16990
DE-AC07-76ID-01570 ..... N89-17234
N89-17235
N89-17252
N89-17512
DE-AI01-76PR-06010 ..... N89-16961
DE-AI03-86SF-16310 ..... N89-16986
DE-AI08-78ET-44802 ..... N89-17373
DE-AS04-86AL-38221 ..... N89-17243
DE-AS05-80ER-10742 ..... N89-16983
N89-17520
DE-AT01-82ER-12045 ..... N89-16961
DE-FG02-84ER-13290 ..... N89-16985
DE-FG02-85ER-53198 ..... N89-17515
DE-FG02-85ER-53212 ..... N89-17514
DE-FG02-86ER-13489 ..... N89-17165
DE-FG02-86ER-13641 ..... N89-16944
DE-FG02-86ER-53218 ..... N89-17508
N89-17509
DE-FG02-87ER-13732 ..... N89-17012
DE-FG02-87ER-13761 ..... N89-17216
DE-FG03-88ER-53275 ..... N89-17508
N89-17513
DE-FG05-80ET-53088 ..... N89-17513
DE-FG05-84ER-45114 ..... N89-17002
DE-FG05-86ER-13507 ..... N89-17014
DE-FG05-87ER-13674 ..... N89-17479
DE-FG05-87ER-60575 ..... N89-17367
DE-FG22-84PC-70779 ..... N89-16960
DEN3-330 ..... N89-17548
DI-14-12-0001-30340 ..... N89-17357
N89-17358
DRET-84-34-001 ..... N89-17285
DRET-84-34-097-00-470-75-01 ..... N89-17284
DRET-85-1051 ..... N89-17398
DRET-87-187 ..... N89-17465
DTFA01-80-Y-10524 ..... N89-17379
DTFA03-87-C-00020 ..... N89-16767
EEC-ST2-0430 ..... N89-17190
FE220786FRMC4 ..... N89-16814
F19628-85-C-0003 ..... N89-16771
N89-16772
N89-16881
F19628-85-K-0049 ..... N89-16942
F19628-86-C-0001 ..... N89-17063
F19628-86-C-0036 ..... N89-17361
F30602-81-C-0169 ..... N89-17449
F30602-85-C-0008 ..... N89-17425
F30602-85-C-0161 ..... N89-17262
F33615-84-C-1562 ..... N89-17523
F33615-84-C-3216 ..... N89-16776
F33615-84-C-5049 ..... N89-16922
F33615-84-K-1520 ..... N89-17435
F33615-85-D-0514 ..... N89-17401
F33615-86-C-0530 ..... N89-17461
F33615-86-C-1073 ..... N89-17215
F33615-87-C-2801 ..... N89-16824
F33615-87-C-2802 ..... N89-16822
F49620-85-C-0071 ..... N89-17140
F49620-85-C-0094 ..... N89-16901
F49620-85-C-0096 ..... N89-17009
F49620-85-C-0124 ..... N89-16926
F49620-85-C-0144 ..... N89-17450
F49620-85-K-0016 ..... N89-17082
F49620-86-C-0008 ..... N89-16719
N89-16720
N89-16721
N89-16722
F49620-86-C-0045 ..... N89-17100
F49620-86-C-0054 ..... N89-16948
F49620-86-C-0076 ..... N89-17505
F49620-86-K-0003 ..... N89-16774
F49620-87-C-0113 ..... N89-17434
F49620-87-K-0001 ..... N89-17229
F49620-87-K-0009 ..... N89-17394
GRI-5086-260-1250 ..... N89-16945
GSRN-1-7060-0450 ..... N89-17339
JPL-958178 ..... N89-17060
MDA903-85-C-0324 ..... N89-17400
NAGW-319 ..... N89-16985
NAG1-619 ..... N89-16761
NAG1-716 ..... N89-16758

NAG1-725 ..... N89-16762
NAG1-757 ..... N89-17214
NAG1-768 ..... N89-17448
NAG1-803 ..... N89-17441
NAG2-182 ..... N89-17466
NAG2-314 ..... N89-17184
NAG2-472 ..... N89-17483
NAG2-541 ..... N89-17077
N89-17148
NAG3-188 ..... N89-17248
NAG3-512 ..... N89-17325
NAG3-522 ..... N89-17309
NAG3-579 ..... N89-17310
NAG3-623 ..... N89-17312
NAG5-101 ..... N89-17386
NAG5-389 ..... N89-17384
NAG5-780 ..... N89-17444
NAG5-842 ..... N89-17369
NAG5-1060 ..... N89-17385
NAG9-173 ..... N89-17149
NAG9-253 ..... N89-17404
NASA ORDER A-30142-C N89-16764
NASW-4174 ..... N89-17045
NASW-4307 ..... N89-16967
NAS1-18000 ..... N89-16779
NAS1-18107 ..... N89-17417
N89-17418
NAS1-18605 ..... N89-17417
N89-17418
NAS2-11555 ..... N89-16896
N89-17445
NAS2-11575 ..... N89-16765
NAS2-11934 ..... N89-16769
NAS3-23268 ..... N89-17336
NAS3-23691 ..... N89-17314
NAS3-23695 ..... N89-17313
NAS3-23697 ..... N89-17316
N89-17317
NAS3-23698 ..... N89-17321
NAS3-23717 ..... N89-17311
NAS3-23722 ..... N89-17299
NAS3-23939 ..... N89-17334
NAS3-23940 ..... N89-17335
NAS3-23944 ..... N89-17333
NAS3-23945 ..... N89-17331
NAS3-24238 ..... N89-16918
NAS3-24350 ..... N89-17304
NAS3-24352 ..... N89-17306
NAS3-24358 ..... N89-17313
NAS3-24619 ..... N89-17315
NAS3-24843 ..... N89-16843
NAS3-25077 ..... N89-17078
N89-17079
NAS3-25266 ..... N89-16882
NAS5-27608 ..... N89-17212
NAS7-100 ..... N89-17060
NAS9-17702 ..... N89-17392
N89-17393
NAS9-17878 ..... N89-16893
NGR-06-002-112 ..... N89-17146
NGT-21-002-080 ..... N89-16904
N89-17058
N89-17364
N89-17403
NGT-80001 ..... N89-17403
NSF ATM-86-00509 ..... N89-17180
N89-17181
N89-17183
NSF DCR-86-04199 ..... N89-17236
NSF DMR-85-01909 ..... N89-17473
NSF DMR-85-06689 ..... N89-17095
NSF OCE-85-17746 ..... N89-17387
N00014-81-C-0062 ..... N89-17387
N00014-81-C-0692 ..... N89-17064
N00014-83-K-0343 ..... N89-17141
N00014-83-K-0397 ..... N89-17433
N00014-83-K-0470 ..... N89-16949
N89-16950
N89-16951
N89-16952
N89-16953
N89-16954
N89-16955
N89-17210
N00014-84-C-0149 ..... N89-17516
N00014-85-C-2520 ..... N89-17015
N00014-85-K-0179 ..... N89-16925
N00014-85-K-0222 ..... N89-16957
N00014-85-K-0459 ..... N89-17008
N00014-85-K-0545 ..... N89-17073
N00014-86-K-0043 ..... N89-16973
N89-16974
N89-17476
N89-17487
N00014-86-K-0366 ..... N89-16937
N00014-86-K-0482 ..... N89-17433
N00014-86-K-0659 ..... N89-16921
N00014-86-K-0772 ..... N89-16927
N00014-87-C-0662 ..... N89-16943
N00014-87-C-0840 ..... N89-16946
N00014-87-K-0398 ..... N89-17428
N00014-88-F-0014 ..... N89-17475
N00014-88-J-1006 ..... N89-17473
N66001-85-D-0203 ..... N89-17072
PES-86/1359/DRET/DS/SR2 ..... N89-16964
RR04204 ..... N89-17433
SANDIA-95-4664 ..... N89-17147
STPA-83-96-003 ..... N89-16934
STPA-86-96-031-00-471-75-86 ..... N89-16935
STPA/EG-35-CEAT/A/88 ..... N89-17203
W-31-109-ENG-38 ..... N89-16984
N89-17145
N89-17353
N89-17359
N89-17406
N89-17415
N89-17439
N89-17440
N89-17481
N89-17527
N89-17529
W-7405-ENG-36 ..... N89-16933
N89-17013
N89-17018
N89-17162
N89-17163
N89-17218
N89-17245
N89-17430
N89-17431
N89-17442
N89-17457
N89-17498
N89-17543
W-7405-ENG-48 ..... N89-16936
N89-17076
N89-17087
N89-17139
N89-17154
N89-17205
N89-17206
N89-17208
N89-17217
N89-17219
N89-17220
N89-17221
N89-17225
N89-17227
N89-17228
N89-17229
N89-17230
N89-17231
N89-17233
N89-17365
N89-17419
N89-17451
N89-17456
N89-17459
N89-17485
N89-17486
N89-17491
N89-17492
N89-17493
N89-17497
N89-17501
N89-17502
N89-17503
N89-17534
199-22-76-01 ..... N89-17562
474-12-10 ..... N89-16905
505-61-51 ..... N89-16844
N89-17466
505-61-71 ..... N89-16764
505-62-21 ..... N89-17017
N89-17422
N89-17453
505-63-1B N89-17286
505-63-01-10 ..... N89-17441
505-63-51 ..... N89-17248
505-66-41 ..... N89-16820
505-67-71 ..... N89-16769
505-90-21-01 ..... N89-17417
N89-17418
506-40-11 ..... N89-16765
506-41-11 ..... N89-16917
506-43-41-01 ..... N89-16779
506-47-31 ..... N89-16896
N89-17445
506-48-91 ..... N89-17424
506-49-21 ..... N89-17079
506-80-31-02 ..... N89-17467
533-04-11 ..... N89-17298
586-01-11 ..... N89-16986
672-40-05-70 ..... N89-17374
674-22-05 ..... N89-17046
694-03-03 ..... N89-17211
763-01-21 ..... N89-16759
805-95-00-02 ..... N89-17390

REPORT/ACCESSION NUMBER INDEX

Typical Report Number Index Listing

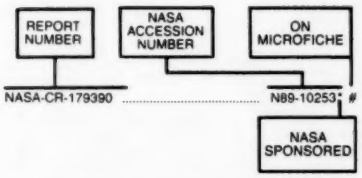

Listings in this index are arranged alphanumerically by report number. The NASA accession number denotes the number by which the citation is identified. An asterisk (*) indicates that the item is a NASA report. A pound sign (#) indicates that the item is available on microfiche.

A-88250 ..... N89-16845* #
A-88278 ..... N89-17390* #
A-88309 ..... N89-17339* #
A-89022 ..... N89-16763* #
A-89030 ..... N89-16844* #
A-89108 ..... N89-16769* #

AAMRL-TR-88-015 ..... N89-17391* #
AAMRL-TR-88-024 ..... N89-17401 #

ACSC-88-1925 ..... N89-16718 #

AD-A189686 ..... N89-17080 #
AD-A197954 ..... N89-17062 #
AD-A197988 ..... N89-17391* #
AD-A198728 ..... N89-16937 #
AD-A199594 ..... N89-17389 #
AD-A199596 ..... N89-16938 #
AD-A199599 ..... N89-17370 #
AD-A199610 ..... N89-16920 #
AD-A199612 ..... N89-17215 #
AD-A199617 ..... N89-17400 #
AD-A199622 ..... N89-16939 #
AD-A199626 ..... N89-17469 #
AD-A199629 ..... N89-16899 #
AD-A199643 ..... N89-17236 #
AD-A199654 ..... N89-17408 #
AD-A199656 ..... N89-16921 #
AD-A199659 ..... N89-17140 #
AD-A199661 ..... N89-17446 #
AD-A199698 ..... N89-17141 #
AD-A199700 ..... N89-17516 #
AD-A199703 ..... N89-17063 #
AD-A199717 ..... N89-17387 #
AD-A199718 ..... N89-17000 #
AD-A199724 ..... N89-16922 #
AD-A199732 ..... N89-16940 #
AD-A199733 ..... N89-16941 #
AD-A199737 ..... N89-16942 #
AD-A199741 ..... N89-17064 #
AD-A199768 ..... N89-16821 #
AD-A199824 ..... N89-17425 #
AD-A199830 ..... N89-16822 #
AD-A199872 ..... N89-17517 #
AD-A199885 ..... N89-16943 #
AD-A200059 ..... N89-17142 #
AD-A200067 ..... N89-17433 #
AD-A200080 ..... N89-16824 #
AD-A200087 ..... N89-17379 #
AD-A200090 ..... N89-17426 #
AD-A200094 ..... N89-16718 #
AD-A200096 ..... N89-17427 #
AD-A200101 ..... N89-16946 #
AD-A200112 ..... N89-17449 #
AD-A200114 ..... N89-17066 #
AD-A200118 ..... N89-17004 #
AD-A200119 ..... N89-16725 #
AD-A200121 ..... N89-17361 #
AD-A200123 ..... N89-17487 #
AD-A200124 ..... N89-16973 #
AD-A200125 ..... N89-17461 #
AD-A200126 ..... N89-17209 #
AD-A200128 ..... N89-16726 #
AD-A200145 ..... N89-16774 #
AD-A200146 ..... N89-17428 #
AD-A200147 ..... N89-16925 #
AD-A200158 ..... N89-17522 #
AD-A200159 ..... N89-17067 #
AD-A200162 ..... N89-17005 #
AD-A200164 ..... N89-17452 #
AD-A200167 ..... N89-17156 #
AD-A200168 ..... N89-17068 #
AD-A200172 ..... N89-17388 #
AD-A200180 ..... N89-17069 #
AD-A200183 ..... N89-16926 #
AD-A200186 ..... N89-17488 #
AD-A200187 ..... N89-17472 #
AD-A200188 ..... N89-17157 #
AD-A200189 ..... N89-17222 #
AD-A200198 ..... N89-17394 #
AD-A200199 ..... N89-17395 #
AD-A200202 ..... N89-17006 #
AD-A200204 ..... N89-17262 #
AD-A200206 ..... N89-17223 #
AD-A200208 ..... N89-16901 #
AD-A200219 ..... N89-17505 #
AD-A200221 ..... N89-17158 #
AD-A200223 ..... N89-17070 #
AD-A200226 ..... N89-17007 #
AD-A200227 ..... N89-17348 #
AD-A200230 ..... N89-17473 #
AD-A200231 ..... N89-17523 #
AD-A200238 ..... N89-17008 #
AD-A200239 ..... N89-16927 #
AD-A200241 ..... N89-16947 #
AD-A200243 ..... N89-17458 #
AD-A200244 ..... N89-17266 #
AD-A200246 ..... N89-17396 #
AD-A200250 ..... N89-17015 #
AD-A200252 ..... N89-17401 #
AD-A200253 ..... N89-17434 #
AD-A200254 ..... N89-16928 #
AD-A200255 ..... N89-16775 #
AD-A200259 ..... N89-17524 #
AD-A200262 ..... N89-16719 #
AD-A200263 ..... N89-16720 #
AD-A200264 ..... N89-16721 #
AD-A200265 ..... N89-16722 #
AD-A200267 ..... N89-16974 #
AD-A200269 ..... N89-17159 #
AD-A200273 ..... N89-16948 #
AD-A200280 ..... N89-17423 #
AD-A200282 ..... N89-17160 #
AD-A200286 ..... N89-17380 #
AD-A200287 ..... N89-17381 #
AD-A200289 ..... N89-16776 #
AD-A200291 ..... N89-17071 #
AD-A200294 ..... N89-17362 #
AD-A200296 ..... N89-17474 #
AD-A200303 ..... N89-16949 #
AD-A200305 ..... N89-16950 #
AD-A200306 ..... N89-17210 #
AD-A200307 ..... N89-16951 #
AD-A200310 ..... N89-17009 #
AD-A200311 ..... N89-17489 #
AD-A200312 ..... N89-17506 #
AD-A200315 ..... N89-17072 #
AD-A200317 ..... N89-16777 #
AD-A200319 ..... N89-17507 #
AD-A200373 ..... N89-17475 #
AD-A200415 ..... N89-16952 #
AD-A200417 ..... N89-17410 #
AD-A200418 ..... N89-16727 #
AD-A200421 ..... N89-16953 #
AD-A200422 ..... N89-16954 #
AD-A200424 ..... N89-16955 #
AD-A200425 ..... N89-16975 #
AD-A200426 ..... N89-17462 #
AD-A200427 ..... N89-17411 #
AD-A200428 ..... N89-16956 #
AD-A200430 ..... N89-17402 #
AD-A200433 ..... N89-17397 #
AD-A200436 ..... N89-16728 #
AD-A200509 ..... N89-17476 #
AD-A200510 ..... N89-17450 #
AD-A200515 ..... N89-16770 #
AD-A200541 ..... N89-17525 #
AD-A200544 ..... N89-17224 #
AD-A200548 ..... N89-16957 #
AD-A200558 ..... N89-17226 #
AD-A200584 ..... N89-17435 #
AD-A200585 ..... N89-17242 #
AD-A200604 ..... N89-16771 #
AD-A200605 ..... N89-16772 #
AD-A200611 ..... N89-16881 #
AD-A200616 ..... N89-17073 #

AFGL-TR-88-0003-VOL-1 ..... N89-17361 #
AFGL-TR-88-0161 ..... N89-16942 #

AFOSR-88-0152TR ..... N89-17080 #
AFOSR-88-0799TR ..... N89-17140 #
AFOSR-88-0801TR ..... N89-16948 #
AFOSR-88-0805TR ..... N89-17223 #
AFOSR-88-0806TR ..... N89-17394 #
AFOSR-88-0848TR ..... N89-16901 #
AFOSR-88-0918TR ..... N89-17006 #
AFOSR-88-0929TR ..... N89-17395 #
AFOSR-88-0934TR ..... N89-17158 #
AFOSR-88-0977TR ..... N89-17505 #
AFOSR-88-1011TR ..... N89-17142 #
AFOSR-88-1018TR ..... N89-16774 #
AFOSR-88-1023TR ..... N89-17007 #
AFOSR-88-1032TR ..... N89-17159 #
AFOSR-88-1034TR ..... N89-16939 #
AFOSR-88-1043TR ..... N89-17009 #
AFOSR-88-1045TR ..... N89-17396 #
AFOSR-88-1051TR ..... N89-17226 #
AFOSR-88-1052TR ..... N89-17524 #
AFOSR-88-1058TR ..... N89-17450 #
AFOSR-88-1069TR ..... N89-17004 #
AFOSR-88-1078TR ..... N89-16928 #
AFOSR-88-1083TR ..... N89-17506 #
AFOSR-88-1112TR ..... N89-17434 #
AFOSR-88-1118TR ..... N89-17469 #
AFOSR-88-1121TR ..... N89-17489 #
AFOSR-88-1125TR ..... N89-17525 #
AFOSR-88-1132TR ..... N89-17070 #
AFOSR-88-1141TR ..... N89-16899 #
AFOSR-88-1142TR ..... N89-16926 #
AFOSR-88-1153TR ..... N89-16725 #

AFWAL-TR-87-1175 ..... N89-17435 #
AFWAL-TR-88-1042 ..... N89-17215 #
AFWAL-TR-88-1055-VOL-1 ..... N89-17523 #
AFWAL-TR-88-2088 ..... N89-16824 #
AFWAL-TR-88-2089 ..... N89-16822 #
AFWAL-TR-88-3041 ..... N89-16776 #
AFWAL-TR-88-4115 ..... N89-16922 #

AFWL-TR-88-41 ..... N89-17069 #

AGARD-AG-270(F) ..... N89-17399 #
AGARD-AG-303 ..... N89-16760 #

AGARD-CP-429 ..... N89-16846 #
AGARD-CP-448 ..... N89-16780 #

AGARD-LS-150-REV ..... N89-16906 #

AGARD-R-732 ..... N89-17287 #
AGARD-R-768 ..... N89-17253 #

AIAA-89-0004 ..... N89-16759* #

AMI-8801 ..... N89-16775 #

ANL-HEP-CP-88-49 ..... N89-17440 #

ANL-88-24 ..... N89-17415 #
ANL-88-46 ..... N89-17406 #

ANL/EES-TM-352 ..... N89-17359 #

ARAED-TR-88017 ..... N89-17000 #

ARI-RN-88-79 ..... N89-17400 #

REPORT

ARO-25090.1-EG-SBI ..... N89-16775 #
ARO-25093.1-EG-SBI ..... N89-16726 #

AS-EVALS-FR-8701-VOL-1 ..... N89-17392* #
AS-EVALS-FR-8701-VOL-2 ..... N89-17393* #

AVSCOM-TM-88-C-005 ..... N89-17248* #

BARC-1379 ..... N89-16968 #
BARC-1391 ..... N89-17510 #

BBC-RD-1988/12 ..... N89-17061

BBN-6337 ..... N89-17461 #

BNL-41322 ..... N89-16989 #
BNL-41602 ..... N89-17471 #
BNL-41633 ..... N89-16959 #
BNL-41701 ..... N89-16958 #
BNL-41784 ..... N89-16966 #
BNL-41815 ..... N89-16983 #
BNL-41817 ..... N89-17520 #
BNL-41917 ..... N89-17528 #
BNL-42001 ..... N89-16895 #
BNL-42028 ..... N89-17539 #

BRA-89-W010R ..... N89-17505 #

BRL-MR-3709 ..... N89-17209 #

B8821606 ..... N89-17371 #

CAA-RP-87-4 ..... N89-17408 #

CERT-RT-OA-21/5005-AYD ..... N89-17204 #

CMU-CS-86-154 ..... N89-17435 #

CMU-RI-TR-88-12 ..... N89-17236 #

CMU/SEI-87-TR-33 ..... N89-16771 #
CMU/SEI-87-TR-34 ..... N89-16772 #
CMU/SEI-88-TR-25 ..... N89-16881 #

CNES-CT/DRT/TIT/IO-87/086 ..... N89-17495 #
CNES-CT/DRT/TIT/IO-87/150 ..... N89-17494 #

CNES-CT/DRT/TIT/TB-040-T ..... N89-16892 #

CNES-CT/DRT/TIT/TR-87/024 ..... N89-17496 #

CNIC-00126 ..... N89-17531 #

CONF-871036-37 ..... N89-17456 #
CONF-880117-7 ..... N89-17455 #
CONF-880406-41 ..... N89-17526 #
CONF-880406-42 ..... N89-17529 #
CONF-880534-13 ..... N89-17500 #
CONF-880534-14 ..... N89-17499 #
CONF-880547-3 ..... N89-17239 #
CONF-880686-2 ..... N89-17252 #
CONF-880691-3 ..... N89-17234 #
CONF-880730-5-FP ..... N89-17147 #
CONF-880760-7 ..... N89-17235 #
CONF-880812-28 ..... N89-17527 #
CONF-880887-26 ..... N89-17486 #
CONF-880894 ..... N89-17412 #
CONF-880901-8 ..... N89-17144 #
CONF-880901-14 ..... N89-17481 #
CONF-880904-4 ..... N89-17493 #
CONF-880904-5 ..... N89-17229 #
CONF-880904-7 ..... N89-17233 #
CONF-880925-2 ..... N89-16959 #
CONF-880965-2 ..... N89-17356* #
CONF-880965-3 ..... N89-17349 #
CONF-880965-11 ..... N89-17346 #
CONF-880965-19 ..... N89-17347 #
CONF-880965-20 ..... N89-17343 #
CONF-880965-21 ..... N89-17345 #
CONF-880965-22 ..... N89-17344 #
CONF-880969-5 ..... N89-16966 #
CONF-881002-24 ..... N89-17533 #
CONF-881002-25 ..... N89-17526 #
CONF-881015-16 ..... N89-17498 #
CONF-881015-28 ..... N89-17508 #
CONF-881022-1 ..... N89-17470 #
CONF-881031-54 ..... N89-17512 #
CONF-881049-52 ..... N89-16895 #
CONF-881056-5 ..... N89-17501 #
CONF-881056-6 ..... N89-17218 #
CONF-881056-7 ..... N89-17220 #
CONF-881056-9 ..... N89-17231 #
CONF-881061-10 ..... N89-17145 #
CONF-881061-10 ..... N89-17145 #
CONF-881093-9 ..... N89-17154 #
CONF-881103-9 ..... N89-17405 #

CONF-881125-2 ..... N89-16932 #
CONF-881125-3 ..... N89-16933 #
CONF-881138-1 ..... N89-17016 #
CONF-881140-6 ..... N89-17240 #
CONF-881151-24 ..... N89-17519 #
CONF-881151-28 ..... N89-17219 #
CONF-881151-32 ..... N89-17478 #
CONF-881155-7 ..... N89-17521 #
CONF-881155-9 ..... N89-16982 #
CONF-881155-10 ..... N89-17245 #
CONF-881155-12 ..... N89-17013 #
CONF-881155-14 ..... N89-17534 #
CONF-881155-15 ..... N89-17232 #
CONF-881155-18 ..... N89-17482 #
CONF-881210-2 ..... N89-17237 #
CONF-881223-1 ..... N89-17543 #
CONF-881226-1 ..... N89-17221 #
CONF-881247-1 ..... N89-17497 #
CONF-881249-1 ..... N89-17546 #
CONF-890102-6 ..... N89-17352 #
CONF-890102-7 ..... N89-17351 #
CONF-890102-12 ..... N89-17354 #
CONF-890142-1 ..... N89-17230 #
CONF-890151-1 ..... N89-16737 #
CONF-890153-1 ..... N89-17249 #
CONF-890225-1 ..... N89-17442 #
CONF-890226-1 ..... N89-17490 #
CONF-8706103-11 ..... N89-16977 #
CONF-8706349 ..... N89-17484 #
CONF-8709318-4 ..... N89-17556 #
CONF-8709382-1 ..... N89-17439 #
CONF-8710161-2 ..... N89-17375 #
CONF-8804202-2 ..... N89-17451 #
CONF-8804214-1 ..... N89-17360 #
CONF-8804224-1 ..... N89-17485 #
CONF-8805120-4 ..... N89-17162 #
CONF-8805132-12 ..... N89-17076 #
CONF-8806105-2 ..... N89-17440 #
CONF-8806263-2 ..... N89-17227 #
CONF-8806277-1 ..... N89-17018 #
CONF-8806279-1 ..... N89-17539 #
CONF-8807121-1 ..... N89-17503 #
CONF-8808101-3 ..... N89-17502 #
CONF-8808122-13 ..... N89-16989 #
CONF-8808130-1 ..... N89-17471 #
CONF-8808145-23 ..... N89-17443 #
CONF-8808146-2 ..... N89-17217 #
CONF-8808149-3 ..... N89-17520 #
CONF-8808149-5 ..... N89-16983 #
CONF-8808151-1 ..... N89-16956 #
CONF-8809105-9 ..... N89-17206 #
CONF-8809105-11 ..... N89-17492 #
CONF-8809128-2 ..... N89-17163 #
CONF-8809152-4 ..... N89-17532 #
CONF-8809190-1 ..... N89-16988 #
CONF-8809191-1 ..... N89-17438 #
CONF-8809201-1 ..... N89-17541 #
CONF-8810133-2 ..... N89-17207 #
CONF-8810133-5 ..... N89-17366 #
CONF-8810147-1 ..... N89-17010 #
CONF-8810151-7 ..... N89-17011 #
CONF-8810155-11 ..... N89-17244 #
CONF-8810176-1 ..... N89-16972 #
CONF-8810180-2 ..... N89-17353 #
CONF-8810195-2 ..... N89-16923 #
CONF-8810195-3 ..... N89-17003 #
CONF-8810213-1 ..... N89-16984 #
CONF-8810219-1 ..... N89-16766 #
CONF-8810230-1 ..... N89-16936 #
CONF-8810234-2 ..... N89-17205 #
CONF-8810234-3 ..... N89-17228 #
CONF-8810242-1 ..... N89-17480 #
CONF-8811126-1 ..... N89-17365 #
CONF-8811132-1 ..... N89-17251 #

CRDEC-TR-88059 ..... N89-17370 #
CRDEC-TR-88088 ..... N89-16940 #
CRDEC-TR-88117 ..... N89-16941 #
CRDEC-TR-88137 ..... N89-17389 #
CRDEC-TR-88160 ..... N89-16938 #

CRREL-88-12 ..... N89-17381 #
CRREL-88-13 ..... N89-17388 #

DAT-88-06 ..... N89-16756 #

DA88-1 ..... N89-16767 #

DERAT-21/5005/13 ..... N89-17204 #

DE88-001188 ..... N89-17350 #
DE88-003885 ..... N89-17239 #
DE88-011264 ..... N89-16960 #
DE88-012860 ..... N89-17147 #
DE88-014466 ..... N89-17543 #
DE88-014919 ..... N89-17412 #

DE88-014964 ..... N89-17237 #
DE88-015281 ..... N89-17240 #
DE88-015291 ..... N89-17016 #
DE88-016582 ..... N89-17471 #
DE88-017004 ..... N89-17221 #
DE88-704073 ..... N89-16968 #
DE88-704083 ..... N89-17510 #
DE88-704104 ..... N89-17531 #
DE88-704194 ..... N89-17429 #
DE88-704211 ..... N89-17536 #
DE88-704214 ..... N89-17537 #
DE88-704224 ..... N89-17454 #
DE88-704293 ..... N89-17001 #
DE88-704321 ..... N89-17554 #
DE88-704336 ..... N89-17484 #
DE88-704366 ..... N89-17477 #
DE88-704367 ..... N89-17436 #
DE88-704370 ..... N89-17161 #
DE88-704372 ..... N89-17555 #
DE88-704818 ..... N89-16987 #
DE88-704828 ..... N89-17511 #
DE88-754960 ..... N89-17409 #
DE88-755231 ..... N89-16969 #
DE88-755532 ..... N89-17557 #
DE88-755533 ..... N89-17563 #
DE89-000302 ..... N89-17349 #
DE89-000304 ..... N89-17356* #
DE89-000351 ..... N89-17442 #
DE89-000389 ..... N89-17498 #
DE89-000810 ..... N89-17341 #
DE89-000813 ..... N89-17342 #
DE89-000834 ..... N89-17354 #
DE89-001046 ..... N89-16972 #
DE89-001063 ..... N89-17143 #
DE89-001088 ..... N89-16958 #
DE89-001148 ..... N89-17359 #
DE89-001181 ..... N89-17346 #
DE89-001244 ..... N89-17503 #
DE89-001270 ..... N89-16959 #
DE89-001331 ..... N89-16979 #
DE89-001368 ..... N89-17347 #
DE89-001374 ..... N89-17532 #
DE89-001375 ..... N89-17343 #
DE89-001380 ..... N89-17490 #
DE89-001381 ..... N89-16970 #
DE89-001396 ..... N89-17507 #
DE89-001612 ..... N89-17344 #
DE89-001613 ..... N89-17345 #
DE89-001665 ..... N89-17144 #
DE89-001712 ..... N89-17486 #
DE89-001741 ..... N89-17207 #
DE89-001749 ..... N89-17375 #
DE89-001792 ..... N89-16944 #
DE89-001923 ..... N89-17217 #
DE89-002012 ..... N89-17002 #
DE89-002020 ..... N89-16766 #
DE89-002101 ..... N89-17430 #
DE89-002102 ..... N89-17431 #
DE89-002184 ..... N89-16923 #
DE89-002186 ..... N89-17003 #
DE89-002189 ..... N89-17519 #
DE89-002196 ..... N89-17360 #
DE89-002209 ..... N89-17470 #
DE89-002218 ..... N89-17499 #
DE89-002219 ..... N89-17500 #
DE89-002232 ..... N89-16988 #
DE89-002242 ..... N89-17218 #
DE89-002311 ..... N89-17455 #
DE89-002313 ..... N89-17478 #
DE89-002330 ..... N89-17244 #
DE89-002361 ..... N89-17011 #
DE89-002489 ..... N89-17518 #
DE89-002492 ..... N89-16971 #
DE89-002537 ..... N89-17432 #
DE89-002539 ..... N89-16898 #
DE89-002656 ..... N89-17154 #
DE89-002661 ..... N89-17501 #
DE89-002664 ..... N89-17502 #
DE89-002673 ..... N89-17485 #
DE89-002688 ..... N89-17447 #
DE89-002693 ..... N89-17238 #
DE89-002728 ..... N89-17216 #
DE89-002742 ..... N89-17413 #
DE89-002806 ..... N89-17547 #
DE89-002813 ..... N89-17405 #
DE89-002814 ..... N89-16900 #
DE89-002824 ..... N89-17225 #
DE89-002848 ..... N89-17243 #
DE89-002869 ..... N89-17451 #
DE89-002874 ..... N89-17208 #
DE89-002875 ..... N89-17456 #
DE89-002877 ..... N89-17219 #
DE89-002901 ..... N89-17220 #
DE89-002905 ..... N89-16966 #
DE89-002910 ..... N89-17520 #
DE89-002918 ..... N89-17526 #

ISBN-0-85679-651-4

DE89-002927 ..... N89-17491 #
DE89-002931 ..... N89-16936 #
DE89-002966 ..... N89-17363 #
DE89-002992 ..... N89-17556 #
DE89-003004 ..... N89-17538 #
DE89-003017 ..... N89-17457 #
DE89-003032 ..... N89-16976 #
DE89-003096 ..... N89-17165 #
DE89-003102 ..... N89-17438 #
DE89-003113 ..... N89-17480 #
DE89-003117 ..... N89-17508 #
DE89-003132 ..... N89-17351 #
DE89-003133 ..... N89-17352 #
DE89-003147 ..... N89-16977 #
DE89-003149 ..... N89-16932 #
DE89-003151 ..... N89-17521 #
DE89-003160 ..... N89-17528 #
DE89-003169 ..... N89-16737 #
DE89-003227 ..... N89-16978 #
DE89-003244 ..... N89-17251 #
DE89-003256 ..... N89-17509 #
DE89-003259 ..... N89-17479 #
DE89-003264 ..... N89-17010 #
DE89-003265 ..... N89-17533 #
DE89-003274 ..... N89-16982 #
DE89-003281 ..... N89-16961 #
DE89-003438 ..... N89-17012 #
DE89-003470 ..... N89-17245 #
DE89-003471 ..... N89-17162 #
DE89-003475 ..... N89-17163 #
DE89-003486 ..... N89-16933 #
DE89-003569 ..... N89-17539 #
DE89-003578 ..... N89-17013 #
DE89-003598 ..... N89-17439 #
DE89-003605 ..... N89-17018 #
DE89-003614 ..... N89-16983 #
DE89-003623 ..... N89-16984 #
DE89-003630 ..... N89-17353 #
DE89-003634 ..... N89-17529 #
DE89-003663 ..... N89-17527 #
DE89-003691 ..... N89-16985 #
DE89-003883 ..... N89-17440 #
DE89-003902 ..... N89-17232 #
DE89-003952 ..... N89-17145 #
DE89-003974 ..... N89-17481 #
DE89-004012 ..... N89-17497 #
DE89-004017 ..... N89-17534 #
DE89-004021 ..... N89-17492 #
DE89-004022 ..... N89-17227 #
DE89-004026 ..... N89-17493 #
DE89-004062 ..... N89-17166 #
DE89-004124 ..... N89-17443 #
DE89-004315 ..... N89-17545 #
DE89-004325 ..... N89-17014 #
DE89-004356 ..... N89-17541 #
DE89-004374 ..... N89-17482 #
DE89-004443 ..... N89-17415 #
DE89-004520 ..... N89-16989 #
DE89-004602 ..... N89-17419 #
DE89-004646 ..... N89-16990 #
DE89-004731 ..... N89-17416 #
DE89-004775 ..... N89-17228 #
DE89-004780 ..... N89-17365 #
DE89-004787 ..... N89-17076 #
DE89-004807 ..... N89-17229 #
DE89-004811 ..... N89-17230 #
DE89-004812 ..... N89-17205 #
DE89-004827 ..... N89-17233 #
DE89-004890 ..... N89-16895 #
DE89-004916 ..... N89-17546 #
DE89-004931 ..... N89-17366 #
DE89-004932 ..... N89-17249 #
DE89-004977 ..... N89-17250 #
DE89-005023 ..... N89-17373 #
DE89-005096 ..... N89-17231 #
DE89-005188 ..... N89-17252 #
DE89-005195 ..... N89-17234 #
DE89-005200 ..... N89-17512 #
DE89-005230 ..... N89-17367 #
DE89-005282 ..... N89-17235 #
DE89-005308 ..... N89-17459 #
DE89-005376 ..... N89-17406 #
DE89-005391 ..... N89-17513 #
DE89-005497 ..... N89-17514 #
DE89-005498 ..... N89-17515 #
DE89-005501 ..... N89-17206 #
DE89-005503 ..... N89-17420 #
DE89-005674 ..... N89-17407 #
DE89-005693 ..... N89-17421 #

DFVLR-MITT-88-19 ..... N89-16883 #

DODA-AR-005-416 ..... N89-16770 #

DOE/AL-33183/T9 ..... N89-17166 #
DOE/AL-38221/T5 ..... N89-17243 #

DOE/CE-0240 ..... N89-17250 #
DOE/CE-90002/T1 ..... N89-17238 #

DOE/CH-10093/26 ..... N89-17350 #

DOE/ER-0385 ..... N89-17363 #
DOE/ER-10336/8 ..... N89-17538 #
DOE/ER-10963/8 ..... N89-16976 #
DOE/ER-13065/558 ..... N89-17443 #
DOE/ER-13290/4 ..... N89-16985 #
DOE/ER-13489/3 ..... N89-17165 #
DOE/ER-13507/4 ..... N89-17014 #
DOE/ER-13641/1 ..... N89-16944 #
DOE/ER-13674/2 ..... N89-17479 #
DOE/ER-13732/1 ..... N89-17012 #
DOE/ER-13761/7 ..... N89-17216 #
DOE/ER-45114/4 ..... N89-17002 #
DOE/ER-53198/130 ..... N89-17515 #
DOE/ER-53212/131 ..... N89-17514 #
DOE/ER-53218/9 ..... N89-17509 #
DOE/ER-60575/1 ..... N89-17367 #

DOE/ET-53088/356 ..... N89-17513 #

DOE/NASA/0330-3 ..... N89-17548* #
DOE/NASA/16310-8 ..... N89-16986* #

DOE/NE-37963/7 ..... N89-16990 #

DOE/PC-70779/16 ..... N89-16960 #

DOE/PR-06010/T37 ..... N89-16961 #

DOE/RA-50418/T2 ..... N89-17447 #

DOT/FAA/CT-88/20 ..... N89-16767 #

DOT/FAA/DS-89/06 ..... N89-16820* #

DOT/FAA/SA-88/1 ..... N89-17379 #

DREO-TN-88-19 ..... N89-17067 #

E-3745 ..... N89-17298* #
E-4199 ..... N89-17422* #
E-4290 ..... N89-17453* #
E-4386 ..... N89-17286* #
E-4398 ..... N89-16986* #
E-4474 ..... N89-16882* #
E-4522 ..... N89-16917* #
E-4558 ..... N89-17248* #
E-4579 ..... N89-16905* #
E-4583 ..... N89-17424* #
E-4585 ..... N89-17046* #
E-4592 ..... N89-16759* #
E-4593 ..... N89-17017* #
E-4605 ..... N89-17211* #

EEI-88-208 ..... N89-16893* #

EFI-968(18)-87 ..... N89-17554 #

EGG-M-00487 ..... N89-17252 #
EGG-M-26287 ..... N89-17234 #
EGG-M-88168 ..... N89-17235 #
EGG-M-88257 ..... N89-17512 #

EL-194 ..... N89-17061

ENST-88C001 ..... N89-17065 #
ENST-88E007 ..... N89-17074 #

ERIM-155900-65-F ..... N89-17064 #

ESD-TR-87-196 ..... N89-16771 #
ESD-TR-87-197 ..... N89-16772 #
ESD-TR-88-026 ..... N89-16881 #
ESD-TR-88-266 ..... N89-17063 #

ESDU-88006 ..... N89-16730
ESDU-88012 ..... N89-16962
ESDU-88013 ..... N89-16731
ESDU-88014 ..... N89-17246
ESDU-88015 ..... N89-16930
ESDU-88017 ..... N89-16963
ESDU-88018 ..... N89-16980
ESDU-88019 ..... N89-17267
ESDU-88021 ..... N89-17056
ESDU-88022 ..... N89-17268
ESDU-88023 ..... N89-17463
ESDU-88024 ..... N89-17057
ESDU-88025 ..... N89-16732
ESDU-88026 ..... N89-16733
ESDU-88027 ..... N89-16981
ESDU-88028 ..... N89-17464
ESDU-88029 ..... N89-16734
ESDU-88030 ..... N89-16735
ESDU-88031 ..... N89-16736
ESDU-88032 ..... N89-16931
ESDU-88033 ..... N89-17247
ESDU-88034 ..... N89-17269
ESDU-88035 ..... N89-17270
ESDU-88036 ..... N89-17271
ESDU-88037 ..... N89-17382
ESDU-88038 ..... N89-17383
ESDU-88039 ..... N89-17437

ETL-0502 ..... N89-17071 #

ETN-89-92880 ..... N89-17340 #
ETN-89-93297 ..... N89-16755 #
ETN-89-93326 ..... N89-17371 #
ETN-89-93328 ..... N89-17338 #
ETN-89-93339 ..... N89-17150 #
ETN-89-93481 ..... N89-17355 #
ETN-89-93482 ..... N89-16897 #
ETN-89-93483 ..... N89-17151 #
ETN-89-93516 ..... N89-17272 #
ETN-89-93522 ..... N89-16883 #
ETN-89-93587 ..... N89-17202 #
ETN-89-93588 ..... N89-17167 #
ETN-89-93589 ..... N89-17174 #
ETN-89-93590 ..... N89-16825 #
ETN-89-93591 ..... N89-16833 #
ETN-89-93592 ..... N89-16738 #
ETN-89-93593 ..... N89-16748 #
ETN-89-93596 ..... N89-17179 #
ETN-89-93608 ..... N89-17203 #
ETN-89-93610 ..... N89-16756 #
ETN-89-93611 ..... N89-16934 #
ETN-89-93612 ..... N89-16964 #
ETN-89-93613 ..... N89-17398 #
ETN-89-93614 ..... N89-17284 #
ETN-89-93615 ..... N89-17285 #
ETN-89-93616 ..... N89-17494 #
ETN-89-93617 ..... N89-16892 #
ETN-89-93618 ..... N89-17495 #
ETN-89-93619 ..... N89-17496 #
ETN-89-93620 ..... N89-17065 #
ETN-89-93626 ..... N89-17074 #
ETN-89-93651 ..... N89-16935 #
ETN-89-93652 ..... N89-17204 #
ETN-89-93653 ..... N89-17465 #

FERMILAB-PUB-88/170-A ..... N89-17540* #

FTD-ID(RS)T-0526-88 ..... N89-17458 #
FTD-ID(RS)T-0538-88 ..... N89-17266 #
FTD-ID(RS)T-0642-88 ..... N89-16947 #

GRI-88/0168 ..... N89-16945 #

GSO-TR-87-2 ..... N89-17387 #

HSD-TR-87-013 ..... N89-17461 #

IAEA-CN-50/C-4-1 ..... N89-17498 #
IAEA-CN-50/D-II-1 ..... N89-17508 #

IAEA-TECDOC-463 ..... N89-17484 #

IC-AERO-88-01 ..... N89-16755 #

IC-87/351 ..... N89-17429 #
IC-88/100 ..... N89-17536 #
IC-88/103 ..... N89-17537 #
IC-88/118 ..... N89-17454 #

ICASE-88-57 ..... N89-17417* #
ICASE-88-58 ..... N89-17418* #

IEEE-87TH0172-7 ..... N89-17080 #

IFSR-356 ..... N89-17513 #

ILR-MITT-198 ..... N89-17355 #
ILR-MITT-199 ..... N89-16897 #

INDU/DC/GMH/TR-88-31 ..... N89-16937 #

INPE-4618-TDL/335 ..... N89-16903 #
INPE-4637-PRE/1349 ..... N89-17414 #

ISBN-0-660-12891-8 ..... N89-17019 #
ISBN-0-85679-638-7 ..... N89-16730
ISBN-0-85679-644-1 ..... N89-16962
ISBN-0-85679-645-X N89-16731
ISBN-0-85679-646-8 ..... N89-17246
ISBN-0-85679-647-6 ..... N89-16930
ISBN-0-85679-649-2 ..... N89-16963
ISBN-0-85679-650-6 ..... N89-16980
ISBN-0-85679-651-4 ..... N89-17267

ISBN-0-85679-653-0 ..... N89-17056
ISBN-0-85679-654-9 ..... N89-17268
ISBN-0-85679-655-7 ..... N89-17463
ISBN-0-85679-656-5 ..... N89-17057
ISBN-0-85679-657-3 ..... N89-16732
ISBN-0-85679-658-1 ..... N89-16733
ISBN-0-85679-659-X N89-16981
ISBN-0-85679-660-3 ..... N89-17464
ISBN-0-85679-661-1 ..... N89-16734
ISBN-0-85679-662-X N89-16735
ISBN-0-85679-663-8 ..... N89-16736
ISBN-0-85679-664-6 ..... N89-16931
ISBN-0-85679-665-4 ..... N89-17247
ISBN-0-85679-666-2 ..... N89-17269
ISBN-0-85679-667-0 ..... N89-17270
ISBN-0-85679-668-0 ..... N89-17271
ISBN-0-85679-669-7 ..... N89-17382
ISBN-0-85679-670-0 ..... N89-17383
ISBN-0-85679-671-9 ..... N89-17437
ISBN-0-936659-16-5 ..... N89-17080 #
ISBN-90-9002080-2 ..... N89-17150 #
ISBN-92-63-10704 ..... N89-17340 #
ISBN-92-835-0454-2 ..... N89-16906 #
ISBN-92-835-0469-0 ..... N89-16846 #
ISBN-92-835-0481 ..... N89-16780 #
ISBN-92-835-0484-4 ..... N89-17253 #
ISBN-92-835-0493-3 ..... N89-17287 #

ISI-110 ..... N89-16901 #

ISSN-0082-5255 ..... N89-16894 #
ISSN-0082-5255 ..... N89-17504 #
ISSN-0141-397X N89-16731
ISSN-0141-397X N89-16733
ISSN-0141-397X N89-16734
ISSN-0141-397X N89-16735
ISSN-0141-397X N89-16736
ISSN-0141-402X N89-17056
ISSN-0141-402X N89-17464
ISSN-0141-2590 ..... N89-16960
ISSN-0141-3988 ..... N89-17437
ISSN-0141-3996 ..... N89-16981
ISSN-0141-4011 ..... N89-17246
ISSN-0141-4011 ..... N89-17268
ISSN-0141-4046 ..... N89-17247
ISSN-0141-4054 ..... N89-16730
ISSN-0141-4054 ..... N89-16732
ISSN-0141-4062 ..... N89-16962
ISSN-0141-4062 ..... N89-16963
ISSN-0141-4062 ..... N89-17057
ISSN-0141-4089 ..... N89-16981
ISSN-0141-4089 ..... N89-17269
ISSN-0141-4097 ..... N89-16930
ISSN-0141-4097 ..... N89-16931
ISSN-0141-4097 ..... N89-17270
ISSN-0143-2702 ..... N89-17267
ISSN-0143-2702 ..... N89-17271
ISSN-0143-2702 ..... N89-17382
ISSN-0143-2702 ..... N89-17383
ISSN-0176-7739 ..... N89-16883 #
ISSN-0307-0115 ..... N89-17463
ISSN-0308-7247 ..... N89-16755 #
ISSN-0377-8312 ..... N89-16738 #
ISSN-0377-8312 ..... N89-16748 #
ISSN-0377-8312 ..... N89-16825 #
ISSN-0377-8312 ..... N89-16833 #
ISSN-0377-8312 ..... N89-17167 #
ISSN-0377-8312 ..... N89-17174 #
ISSN-0377-8312 ..... N89-17179 #
ISSN-0377-8312 ..... N89-17202 #
ISSN-0721-5320 ..... N89-17272 #
ISSN-0751-1337 ..... N89-17065 #
ISSN-0751-1353 ..... N89-17074 #

ISU-ERI-AMES-88175 ..... N89-16899 #

ITEF-154(1987) ..... N89-16987 #

ITEP-209(1987) ..... N89-17477 #
ITEP-211(1987) ..... N89-17436 #

ITP-87-33 ..... N89-17161 #
ITP-87-59 ..... N89-17555 #

IYF-R-6-299 ..... N89-17511 #
IYF-R-9-308 ..... N89-17001 #

JAERI-M-88-136 ..... N89-16969 #

JPRS-JST-88-010 ..... N89-17047 #

KCP-613-4032 ..... N89-16978 #

L-16487 ..... N89-17374* #
L-16496 ..... N89-16820* #
L-16512 ..... N89-17562* #

LA-UR-88-1792 ..... N89-17543 #
LA-UR-88-2878 ..... N89-17498 #
LA-UR-88-3080 ..... N89-17442 #
LA-UR-88-3382 ..... N89-17218 #
LA-UR-88-3667 ..... N89-17245 #
LA-UR-88-3681 ..... N89-17163 #
LA-UR-88-3703 ..... N89-17162 #
LA-UR-88-3776 ..... N89-16933 #
LA-UR-88-3884 ..... N89-17013 #
LA-UR-88-3996 ..... N89-17018 #

LA-11371-MS ..... N89-17431 #
LA-11372-MS ..... N89-17430 #
LA-11416-MS ..... N89-17457 #

LBF-TB-180 ..... N89-17272 #

LBL-25113 ..... N89-17526 #
LBL-25760 ..... N89-17485 #
LBL-26035 ..... N89-17518 #
LBL-26091 ..... N89-16971 #

LC-86-063502 ..... N89-17080 #

ME-5375-86 ..... N89-16774 #

MEASUREMENT/SER-84-6 ..... N89-17433 #

MRC/ARO-87-NSREC-028 ..... N89-17147 #

MTR-10289 ..... N89-17063 #

NAL-TM-DU-8701 ..... N89-17372 #

NAL-TM-FM-8701 ..... N89-16757 #

NAS 1.15:4002 ..... N89-17560* #
NAS 1.15:4098 ..... N89-17045* #
NAS 1.15:100348 ..... N89-17535* #
NAS 1.15:100349 ..... N89-17558* #
NAS 1.15:100350 ..... N89-17530* #
NAS 1.15:101042 ..... N89-17339* #
NAS 1.15:101066 ..... N89-16844* #
NAS 1.15:101069 ..... N89-16763* #
NAS 1.15:101077 ..... N89-17390* #
NAS 1.15:101195 ..... N89-17448* #
NAS 1.15:101251 ..... N89-17356* #
NAS 1.15:101269 ..... N89-17391* #
NAS 1.15:101358 ..... N89-17286* #
NAS 1.15:101364 ..... N89-16986* #
NAS 1.15:101422 ..... N89-16917* #
NAS 1.15:101449 ..... N89-17248* #
NAS 1.15:101462 ..... N89-17453* #
NAS 1.15:101467 ..... N89-16905* #
NAS 1.15:101469 ..... N89-17424* #
NAS 1.15:101471 ..... N89-17046* #
NAS 1.15:101474 ..... N89-16759* #
NAS 1.15:101475 ..... N89-17017* #
NAS 1.15:101479 ..... N89-17211* #
NAS 1.15:101536 ..... N89-17467* #
NAS 1.26:4219 ..... N89-17441* #
NAS 1.26:4220 ..... N89-16779* #
NAS 1.26:172087 ..... N89-16893* #
NAS 1.26:172098 ..... N89-17392* #
NAS 1.26:172099 ..... N89-17393* #
NAS 1.26:177398 ..... N89-16769* #
NAS 1.26:177454 ..... N89-17466* #
NAS 1.26:177467 ..... N89-16765* #
NAS 1.26:177508 ..... N89-16764* #
NAS 1.26:177510 ..... N89-16896* #
NAS 1.26:177512 ..... N89-17445* #
NAS 1.26:179612 ..... N89-16918* #
NAS 1.26:181748 ..... N89-17417* #
NAS 1.26:181756 ..... N89-17418* #
NAS 1.26:182202 ..... N89-16843* #
NAS 1.26:182204 ..... N89-17548* #
NAS 1.26:182217 ..... N89-16882* #
NAS 1.26:182227 ..... N89-17078* #
NAS 1.26:182227-EXEC-SUMM ..... N89-17079* #
NAS 1.26:182255 ..... N89-17146* #
NAS 1.26:182962 ..... N89-17386* #
NAS 1.26:183087 ..... N89-17077* #
NAS 1.26:183182 ..... N89-17483* #
NAS 1.26:183241 ..... N89-17444* #
NAS 1.26:183248 ..... N89-17149* #
NAS 1.26:183298 ..... N89-17148* #
NAS 1.26:183350 ..... N89-17368* #
NAS 1.26:183402 ..... N89-17369* #
NAS 1.26:183414 ..... N89-17212* #
NAS 1.26:184583 ..... N89-17364* #
NAS 1.26:184589 ..... N89-17214* #
NAS 1.26:184624 ..... N89-16758* #
NAS 1.26:184718 ..... N89-16904* #
NAS 1.26:184722 ..... N89-17403* #
NAS 1.26:184750 ..... N89-17058* #
NAS 1.26:184759 ..... N89-17385* #
NAS 1.26:184760 ..... N89-17404* #
NAS 1.26:184766 ..... N89-17384* #
NAS 1.26:184771 ..... N89-16965* #
NAS 1.26:184772 ..... N89-17540* #
NAS 1.26:184787 ..... N89-16762* #
NAS 1.26:184788 ..... N89-16761* #
NAS 1.55:2493 ..... N89-17298* #
NAS 1.60:2886 ..... N89-16820* #
NAS 1.60:2887 ..... N89-17562* #
NAS 1.60:2892 ..... N89-17422* #
NAS 1.60:2898 ..... N89-16845* #
NAS 1.61:1082(04) ..... N89-17060* #
NAS 1.61:1214 ..... N89-17374* #
NAS 1.77:20455 ..... N89-16967*

NASA-CP-2493 ..... N89-17298* #

NASA-CR-4219 ..... N89-17441* #
NASA-CR-4220 ..... N89-16779* #
NASA-CR-172087 ..... N89-16893* #
NASA-CR-172098 ..... N89-17392* #
NASA-CR-172099 ..... N89-17393* #
NASA-CR-177398 ..... N89-16769* #
NASA-CR-177454 ..... N89-17466* #
NASA-CR-177467 ..... N89-16765* #
NASA-CR-177508 ..... N89-16764* #
NASA-CR-177510 ..... N89-16896* #
NASA-CR-177512 ..... N89-17445* #
NASA-CR-179612 ..... N89-16918* #
NASA-CR-181748 ..... N89-17417* #
NASA-CR-181756 ..... N89-17418* #
NASA-CR-182202 ..... N89-16843* #
NASA-CR-182204 ..... N89-17548* #
NASA-CR-182217 ..... N89-16882* #
NASA-CR-182227 ..... N89-17078* #
NASA-CR-182227-EXEC-SUMM ..... N89-17079* #
NASA-CR-182255 ..... N89-17146* #
NASA-CR-182962 ..... N89-17386* #
NASA-CR-183087 ..... N89-17077* #
NASA-CR-183182 ..... N89-17483* #
NASA-CR-183241 ..... N89-17444* #
NASA-CR-183248 ..... N89-17149* #
NASA-CR-183298 ..... N89-17148* #
NASA-CR-183350 ..... N89-17368* #
NASA-CR-183402 ..... N89-17369* #
NASA-CR-183414 ..... N89-17212* #
NASA-CR-184583 ..... N89-17364* #
NASA-CR-184589 ..... N89-17214* #
NASA-CR-184624 ..... N89-16758* #
NASA-CR-184718 ..... N89-16904* #
NASA-CR-184722 ..... N89-17403* #
NASA-CR-184750 ..... N89-17058* #
NASA-CR-184759 ..... N89-17385* #
NASA-CR-184760 ..... N89-17404* #
NASA-CR-184766 ..... N89-17384* #
NASA-CR-184771 ..... N89-16965* #
NASA-CR-184772 ..... N89-17540* #
NASA-CR-184787 ..... N89-16762* #
NASA-CR-184788 ..... N89-16761* #

NASA-RP-1082(04) ..... N89-17060* #
NASA-RP-1214 ..... N89-17374* #

NASA-TM-4092 ..... N89-17560* #
NASA-TM-4098 ..... N89-17045* #
NASA-TM-100348 ..... N89-17535* #
NASA-TM-100349 ..... N89-17558* #
NASA-TM-100350 ..... N89-17530* #
NASA-TM-101042 ..... N89-17339* #
NASA-TM-101066 ..... N89-16844* #
NASA-TM-101069 ..... N89-16763* #
NASA-TM-101077 ..... N89-17390* #
NASA-TM-101195 ..... N89-17448* #
NASA-TM-101251 ..... N89-17356* #
NASA-TM-101269 ..... N89-17391* #
NASA-TM-101358 ..... N89-17286* #
NASA-TM-101364 ..... N89-16986* #
NASA-TM-101422 ..... N89-16917* #
NASA-TM-101449 ..... N89-17248* #
NASA-TM-101462 ..... N89-17453* #
NASA-TM-101467 ..... N89-16905* #
NASA-TM-101469 ..... N89-17424* #
NASA-TM-101471 ..... N89-17046* #
NASA-TM-101474 ..... N89-16759* #
NASA-TM-101475 ..... N89-17017* #
NASA-TM-101479 ..... N89-17211* #
NASA-TM-101536 ..... N89-17467* #

NASA-TP-2886 ..... N89-16820* #
NASA-TP-2887 ..... N89-17562* #
NASA-TP-2892 ..... N89-17422* #
NASA-TP-2898 ..... N89-16845* #

NASA-TT-20455 ..... N89-16967*

NOSC/TD-1262 ..... N89-17062 #

NOSC/TD-1295 ..... N89-16920 #
NOSC/TD-1324 ..... N89-17072 #
NOSC/TD-1332 ..... N89-17426 #

NOSC/TR-1220 ..... N89-17427 #

NPS63-88-005 ..... N89-17380 #
NPS67-88-002 ..... N89-16821 #

NRCC-29151 ..... N89-17019 #

NRL-MR-6160 ..... N89-17488 #
NRL-MR-6184 ..... N89-17222 #
NRL-MR-6240 ..... N89-17507 #
NRL-MR-6268 ..... N89-17472 #
NRL-MR-6269 ..... N89-17068 #
NRL-MR-6272 ..... N89-17157 #
NRL-MR-6291 ..... N89-17362 #
NRL-MR-6294 ..... N89-17474 #

NR15-33/1988 ..... N89-17019 #

NTSB-AAR-88-03-SUM ..... N89-16768 #

NUSC-TR-8317 ..... N89-17446 #

OCS/MMS-87/0071-VOL-1 ..... N89-17357 #
OCS/MMS-87/0071-VOL-2 ..... N89-17358 #

OH-30 ..... N89-17340 #

ONERA-RT-67/1765-RY-078-R ..... N89-17285 #

ORNL-8-016-R ..... N89-16992 #

ORNL/DSRD-13 ..... N89-17545 #

ORNL/SUB-82-22276/01 ..... N89-16970 #

ORNL/TM-10206/P2 ..... N89-16979 #
ORNL/TM-10881 ..... N89-17407 #
ORNL/TM-10938 ..... N89-17416 #
ORNL/TM-10998 ..... N89-17421 #

PB88-226048 ..... N89-17357 #
PB88-226055 ..... N89-17358 #
PB88-910414 ..... N89-16768 #
PB89-100507 ..... N89-16945 #

PNL-SA-15073 ..... N89-17375 #
PNL-SA-15524 ..... N89-17541 #
PNL-SA-15916 ..... N89-17207 #

PNL-6484-VOL-1 ..... N89-17547 #

RADC-TR-88-11-VOL-5 ..... N89-17425 #
RADC-TR-88-69-VOL-1 ..... N89-17262 #
RADC-TR-88-149 ..... N89-17449 #

RAND/N-2283/1-AF ..... N89-16719 #
RAND/N-2283/2-AF ..... N89-16720 #
RAND/N-2283/3-AF ..... N89-16721 #
RAND/N-2283/4-AF ..... N89-16722 #

REPT-M6-570500 ..... N89-16934 #

REPT-03/ONR-F1 ..... N89-16946 #
REPT-49-438/F ..... N89-16935 #
REPT-262 ..... N89-17073 #
REPT-876/S-5 ..... N89-17203 #
REPT-887.1C ..... N89-16776 #

RF-DAVI-88-08 ..... N89-17465 #

RRK-88-12 ..... N89-17557 #
RRK-88-13 ..... N89-17563 #

SAND-87-0776/1 ..... N89-16900 #
SAND-88-0579C ..... N89-17349 #
SAND-88-0628C ..... N89-17356* #
SAND-88-0632C ..... N89-17345 #
SAND-88-0633C ..... N89-17352 #
SAND-88-0687C ..... N89-17347 #
SAND-88-0917C ..... N89-16737 #
SAND-88-0936C ..... N89-16972 #
SAND-88-0946C ..... N89-17144 #
SAND-88-1534C ..... N89-16982 #
SAND-88-1641C ..... N89-17232 #
SAND-88-1662C ..... N89-17412 #
SAND-88-1806C ..... N89-17351 #
SAND-88-2084C ..... N89-17237 #
SAND-88-2261C ..... N89-17533 #
SAND-88-2498C ..... N89-17343 #
SAND-88-2588C ..... N89-17532 #
SAND-88-2624C ..... N89-17346 #
SAND-88-2629C ..... N89-16766 #
SAND-88-2675C ..... N89-17490 #
SAND-88-2692C ..... N89-17010 #
SAND-88-2714 ..... N89-17420 #
SAND-88-2754C ..... N89-17011 #
SAND-88-2832C ..... N89-17344 #
SAND-88-2864C ..... N89-17003 #
SAND-88-2976C ..... N89-16923 #
SAND-88-3144C ..... N89-17482 #
SAND-88-7100 ..... N89-17143 #
SAND-88-7106C ..... N89-17147 #
SAND-88-8971 ..... N89-17432 #
SAND-88-9003 ..... N89-16898 #

SERI/STR-211-3395 ..... N89-17341 #
SERI/STR-211-3414 ..... N89-17342 #

SERI/TP-217-3394 ..... N89-17354 #

SRC-5-5873-3 ..... N89-17404* #

SRL-0018-TM ..... N89-16770 #

SU-SLAC-PUB-4528 ..... N89-17556 #
SU-SLAC-PUB-4781 ..... N89-17405 #

SU-SLAC-234-REV-2 ..... N89-17413 #

SWRI-8845-002 ..... N89-17015 #
SWRI-8966 ..... N89-17548* #

TACOM-TR-13387 ..... N89-17075 #

TAMRF-5373-89-01 ..... N89-16761* #

TR-2 ..... N89-17434 #
TR-3 ..... N89-17400 #
TR-17 ..... N89-16957 #
TR-25 ..... N89-16927 #
TR-65 ..... N89-17141 #
TR-87 ..... N89-17476 #
TR-87-18 ..... N89-17072 #
TR-103 ..... N89-17210 #
TR-110 ..... N89-16953 #
TR-113 ..... N89-16954 #
TR-116 ..... N89-16955 #
TR-129 ..... N89-16951 #

TSHUNE-0002 ..... N89-17531 #

UBUFFALO/DC/88/TR-84 ..... N89-16973 #
UBUFFALO/DC/88/TR-85 ..... N89-17487 #
UBUFFALO/DC/88/TR-86 ..... N89-16974 #

UCID-21534 ..... N89-17491 #
UCID-21539 ..... N89-17225 #
UCID-21588 ..... N89-17419 #
UCID-21609 ..... N89-17206 #

UCRL-52000-88-10 ..... N89-17459 #
UCRL-96200 ..... N89-17456 #
UCRL-97840 ..... N89-17076 #
UCRL-98505 ..... N89-17208 #
UCRL-98675 ..... N89-17217 #
UCRL-98686 ..... N89-17205 #
UCRL-98828 ..... N89-17501 #
UCRL-98998 ..... N89-17219 #
UCRL-99058 ..... N89-17229 #
UCRL-99232 ..... N89-17230 #
UCRL-99378 ..... N89-16936 #
UCRL-99427 ..... N89-17502 #
UCRL-99437 ..... N89-17503 #
UCRL-99439 ..... N89-17221 #
UCRL-99682 ..... N89-17154 #
UCRL-99701 ..... N89-17220 #
UCRL-99735 ..... N89-17486 #
UCRL-99768 ..... N89-17451 #
UCRL-99922 ..... N89-17227 #
UCRL-99946 ..... N89-17493 #
UCRL-99954 ..... N89-17492 #
UCRL-99977 ..... N89-17534 #
UCRL-99980 ..... N89-17497 #
UCRL-99998 ..... N89-17365 #
UCRL-100001 ..... N89-17233 #
UCRL-100056 ..... N89-17228 #
UCRL-100109 ..... N89-17231 #

UILU-ENG-88-2246 ..... N89-17516 #

UM-REPT-025921-T-1 ..... N89-17148* #
UM-REPT-025921-2-T ..... N89-17077* #

UMSC-88-C-AF-2 ..... N89-17006 #

UR-1091 ..... N89-17443 #

USAARL-88-11 ..... N89-17402 #
USAARL-88-16 ..... N89-17397 #

USGS-OFR-88-243 ..... N89-17373 #

UTIAS-327 ..... N89-16894 #
UTIAS-328 ..... N89-17504 #

UTIIS-8801 ..... N89-17409 #

UTRC-R88-957367-31 ..... N89-16843* #
UTRC-R88-957464-A ..... N89-16948 #

UVA/525398/MS89/103 ..... N89-16925 #

VKI-LS-1988-01-VOL-2 ..... N89-17167 #
VKI-LS-1988-02 ..... N89-17174 #
VKI-LS-1988-03-VOL-1 ..... N89-16825 #
VKI-LS-1988-03-VOL-2 ..... N89-16833 #
VKI-LS-1988-04-VOL-1 ..... N89-16738 #
VKI-LS-1988-04-VOL-2 ..... N89-16748 #
VKI-LS-1988-06 ..... N89-17179 #

VKS-LS-1988-01-VOL-1 ..... N89-17202 #

VTR-88-01 ..... N89-16824 #

WMO-704 ..... N89-17340 #

FEDERAL REGIONAL DEPOSITORY LIBRARIES

ALABAMA

AUBURN UNIV. AT MONTGOMERY LIBRARY
Documents Department
Montgomery, AL 36193
(205) 271-9650

UNIV. OF ALABAMA LIBRARY
Documents Dept.-Box S
University, AL 35486
(205) 348-6046

ARIZONA

DEPT. OF LIBRARY, ARCHIVES AND PUBLIC RECORDS
Third Floor—State Cap.
1700 West Washington
Phoenix, AZ 85007
(602) 255-4121

UNIVERSITY OF ARIZONA LIB.
Government Documents Dept.
Tucson, AZ 85721
(602) 621-6433

ARKANSAS

ARKANSAS STATE LIBRARY
One Capitol Mall
Little Rock, AR 72201
(501) 371-2326

CALIFORNIA

CALIFORNIA STATE LIBRARY
Govt. Publications Section
P.O. Box 2037
Sacramento, CA 95809
(916) 324-4863

COLORADO

UNIV OF COLORADO LIB.
Government Pub. Division
Campus Box 184
Boulder, CO 80309
(303) 492-8834

DENVER PUBLIC LIBRARY
Govt. Pub. Department
1357 Broadway
Denver, CO 80203
(303) 571-2131

CONNECTICUT

CONNECTICUT STATE LIBRARY
Government Documents Unit
231 Capitol Avenue
Hartford, CT 06106
(203) 566-7029

FLORIDA

UNIV. OF FLORIDA LIBRARIES
Library West
Documents Department
Gainesville, FL 32611
(904) 392-0367

GEORGIA

UNIV. OF GEORGIA LIBRARIES
Government Reference Dept.
Athens, GA 30602
(404) 542-8949

HAWAII

UNIV. OF HAWAII LIBRARY
Govt. Documents Collection
2550 The Mall
Honolulu, HI 96822
(808) 948-8230

IDAHO

UNIV. OF IDAHO LIBRARY
Documents Section
Moscow, ID 83843
(208) 885-6344

ILLINOIS

ILLINOIS STATE LIBRARY
Information Services Branch
Centennial Building
Springfield, IL 62756
(217) 782-5185

INDIANA

INDIANA STATE LIBRARY
Serials Documents Section
140 North Senate Avenue
Indianapolis, IN 46204
(317) 232-3686

IOWA

UNIV. OF IOWA LIBRARIES
Govt. Documents Department
Iowa City, IA 52242
(319) 353-3318

KANSAS

UNIVERSITY OF KANSAS
Doc. Collect—Spencer Lib.
Lawrence, KS 66045-2800
(913) 864-4662

KENTUCKY

UNIV. OF KENTUCKY LIBRARIES
Govt. Pub. Department
Lexington, KY 40506-0039
(606) 257-3139

LOUISIANA

LOUISIANA STATE UNIVERSITY
Middleton Library
Govt. Docs. Dept.
Baton Rouge, LA 70803
(504) 388-2570

LOUISIANA TECHNICAL UNIV. LIBRARY
Documents Department
Ruston, LA 71272-0046
(318) 257-4962

MAINE

UNIVERSITY OF MAINE
Raymond H. Fogler Library
Tri-State Regional Documents Depository
Orono, ME 04469
(207) 581-1680

MARYLAND

UNIVERSITY OF MARYLAND
McKeldin Lib.—Doc. Div.
College Park, MD 20742
(301) 454-3034

MASSACHUSETTS

BOSTON PUBLIC LIBRARY
Government Docs. Dept.
Boston, MA 02117
(617) 536-5400 ext.226

MICHIGAN

DETROIT PUBLIC LIBRARY
Sociology Department
5201 Woodward Avenue
Detroit, MI 48202-4093
(313) 833-1409

MICHIGAN STATE LIBRARY
P.O. Box 30007
Lansing, MI 48909
(517) 373-1593

MINNESOTA

UNIVERSITY OF MINNESOTA
Government Pubs. Division
409 Wilson Library
309 19th Avenue South
Minneapolis, MN 55455
(612) 373-7870

MISSISSIPPI

UNIV. OF MISSISSIPPI LIB.
Documents Department
University, MS 38677
(601) 232-5857

MONTANA

UNIV. OF MONTANA
Mansfield Library
Documents Division
Missoula, MT 59812
(406) 243-6700

NEBRASKA

UNIVERSITY OF NEBRASKA - LINCOLN
Love Library
Documents Department
Lincoln, NE 68588-0410
(402) 472-2562

NEVADA

UNIVERSITY OF NEVADA LIB.
Govt. Pub. Department
Reno, NV 89557-0044
(702) 784-6579

NEW JERSEY

NEWARK PUBLIC LIBRARY
5 Washington Street
Newark, NJ 07101-0630
(201) 733-7812

NEW MEXICO

UNIVERSITY OF NEW MEXICO
Zimmerman Library
Government Pub. Dept.
Albuquerque, NM 87131
(505) 277-5441

NEW MEXICO STATE LIBRARY
Reference Department
325 Don Gaspar Avenue
Santa Fe, NM 87503
(505) 827-3826

NEW YORK

NEW YORK STATE LIBRARY
Empire State Plaza
Albany, NY 12230
(518) 474-5563

NORTH CAROLINA

UNIVERSITY OF NORTH CAROLINA AT CHAPEL HILL
Davis Library
BA/SS Documents Division
Chapel Hill, NC 27515
(919) 962-1151

NORTH DAKOTA

UNIVERSITY OF NORTH DAKOTA
Chester Fritz Library
Documents Department
Grand Forks, ND 58202
(701) 777-4629
In cooperation with North Dakota State Univ. Library

OHIO

STATE LIBRARY OF OHIO
Documents Department
65 South Front Street
Columbus, OH 43266-0334
(614) 462-7051

OKLAHOMA

OKLAHOMA DEPT. OF LIB.
Government Documents
200 NE 18th Street
Oklahoma City, OK 73105
(405) 521-2502, ext. 252

OKLAHOMA STATE UNIV. LIB.
Documents Department
Stillwater, OK 74078
(405) 624-6546

OREGON

PORTLAND STATE UNIV. LIB.
Documents Department
P.O. Box 1151
Portland, OR 97207
(503) 229-3673

PENNSYLVANIA

STATE LIBRARY OF PENN.
Government Pub. Section
P.O. Box 1601
Harrisburg, PA 17105
(717) 787-3752

TEXAS

TEXAS STATE LIBRARY
Public Services Department
P.O. Box 12927—Cap. Sta.
Austin, TX 78711
(512) 475-2996

TEXAS TECH. UNIV. LIBRARY
Govt. Documents Department
Lubbock, TX 79409
(806) 742-2268

UTAH

UTAH STATE UNIVERSITY
Merrill Library, U.M.C. 30
Logan, UT 84322
(801) 750-2682

VIRGINIA

UNIVERSITY OF VIRGINIA
Alderman Lib.—Public Doc.
Charlottesville, VA 22903-2498
(804) 924-3133

WASHINGTON

WASHINGTON STATE LIBRARY
Documents Section
Olympia, WA 98504
(206) 753-4027

WEST VIRGINIA

WEST VIRGINIA UNIV. LIB.
Documents Department
Morgantown, WV 26506-6069
(304) 293-3640

WISCONSIN

MILWAUKEE PUBLIC LIBRARY
814 West Wisconsin Avenue
Milwaukee, WI 53233
(414) 278-3065

ST. HIST LIB. OF WISCONSIN
Government Pub. Section
816 State Street
Madison, WI 53706
(608) 262-4347

WYOMING

WYOMING STATE LIBRARY
Supreme Ct. & Library Bld.
Cheyenne, WY 82002
(307) 777-5919

National Aeronautics and
Space Administration
Code NTT-4
Washington, D.C.
20546

Official Business

Penalty for Private Use, $300

SPECIAL FOURTH-CLASS RATE
POSTAGE & FEES PAID
NASA
PERMIT No. G 27

POSTMASTER: If Undeliverable (Section 158
Postal Manual) Do Not Return